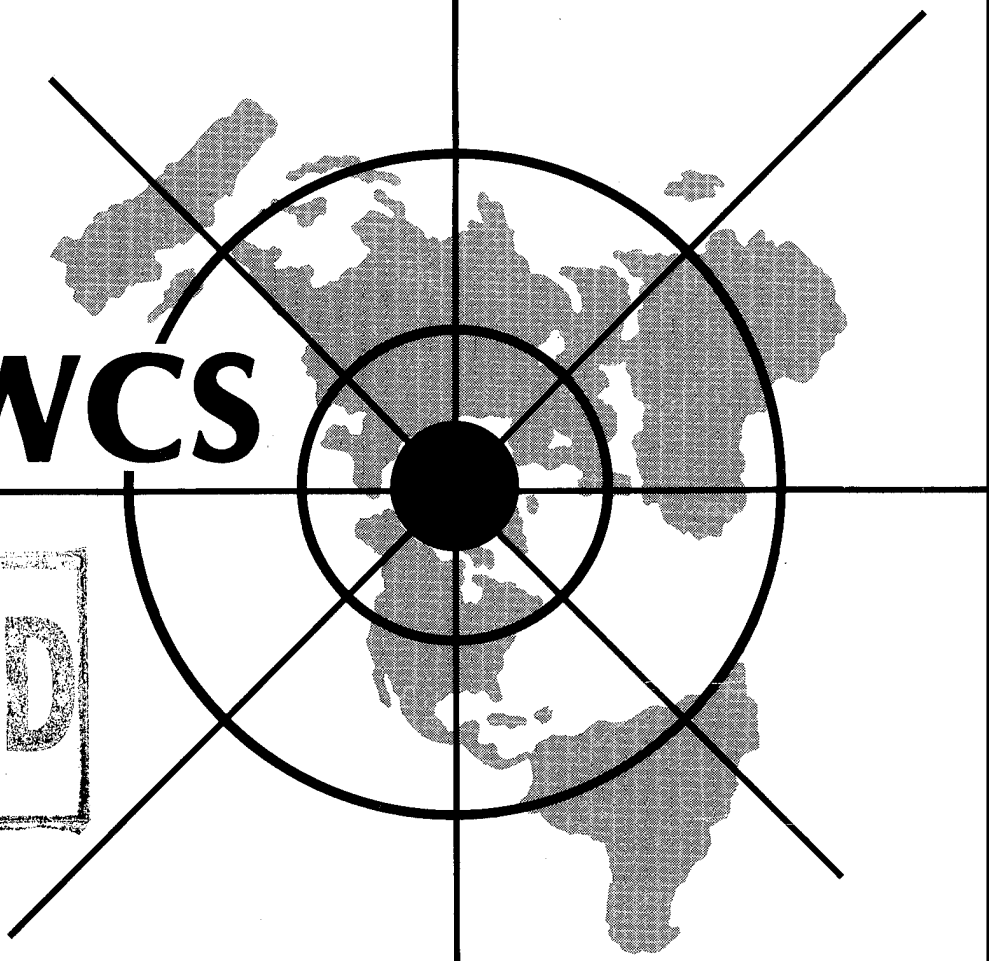
Proceedings of the
Thirty-Fourth

# IWCS



DTIC
ELECTE
DEC 1 2 1995
F

DISTRIBUTION STATEMENT A
Approved for public release;
Distribution Unlimited

# INTERNATIONAL WIRE AND CABLE SYMPOSIUM

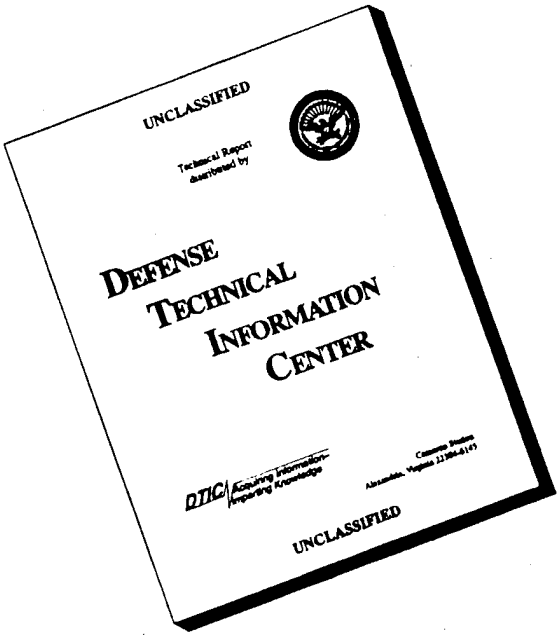
## November 19 thru 21, 1985

19951128 164

PUBLISHED
49884
91619

SPONSORED
BY THE U.S. ARMY
ELECTRONICS COMMAND FORT MONMOUTH, N.J.

# DISCLAIMER NOTICE




**THIS DOCUMENT IS BEST QUALITY AVAILABLE. THE COPY FURNISHED TO DTIC CONTAINED A SIGNIFICANT NUMBER OF PAGES WHICH DO NOT REPRODUCE LEGIBLY.**

Art Readdy
Grant Wilson
Courtyard Sharon Motel -

Accesion For
NTIS CRA&I ☑
DTIC TAB ☐
Unannounced ☐
Justification .....
By .....
Distribution /
Availability Codes
Dist | Avail and / or Special
A-1

# PROCEEDINGS OF 34TH INTERNATIONAL WIRE AND CABLE SYMPOSIUM

Sponsored by
US Army Communications-Electronics Command
(CECOM)
Fort Monmouth, New Jersey

HYATT CHERRY HILL, CHERRY HILL, NEW JERSEY
NOVEMBER 19, 20 and 21, 1985

APPROVED FOR PUBLIC RELEASE: DISTRIBUTION UNLIMITED

DTIC QUALITY INSPECTED 5

F49620-86-C-0088-1

# 34TH INTERNATIONAL WIRE AND CABLE SYMPOSIUM

## SYMPOSIUM COMMITTEE

Elmer F. Godwin, Director, GEF Associates (201) 741-8864
Susan Burgher, Assistant, US Army CECOM (201) 544-2770
Robert Depp, Defense Electronics Supply Center
Alan G. Dwyer, GTE Service Corporation
Raymond E. Jaeger, Spectran
Thomas Jones, Wyrough & Loser, Inc.
Vieney Mascarenhas, Canada Wire & Cable Ltd.
Joseph P. McCann, US Army CECOM
Kazuo Nomura, Sumitomo Electric, USA, Inc.
Eugene Riley, Ericsson, Inc.
John Thompson, Nokia, Inc.
George Webster, AT&T Bell Laboratories
Austin D. Wetherell, Underwriters Laboratories

## ADVISORY

Leo Chattler, DCM Industries, Inc.
Michael A. DeLucia, David W. Taylor Naval Ship R&D Center
Marta Farago, Northern Telecom Canada Ltd.
Irving Kolodny, Network Laboratories, Inc.
Joe Neigh, AMP, Inc.
Frank Short, R. T. Vanderbilt Company, Inc.

## CONSULTANT

William Chervenak, Corning Glass Works

### TECHNICAL SESSIONS

**Tuesday, 19 November 1985**

| | | |
|---|---|---|
| 9:30 a.m. | SESSION I | Panel Discussion—The TELCO Explosion How Far and How Fast |
| 2:00 p.m. | SESSION II | Fiber Optic Cable Design I |
| 2:00 p.m. | SESSION III | Materials |

**Wednesday, 20 November 1985**

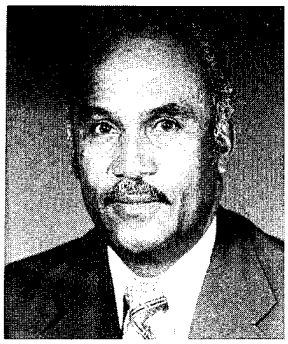
| | | |
|---|---|---|
| 9:00 a.m. | SESSION IV | Fiber Optic Cable Design II |
| 9:00 a.m. | SESSION V | Design/Testing I |
| 2:00 p.m. | SESSION VI | Design/Testing II |
| 2:00 p.m. | SESSION VII | Fire, Smoke, and Toxicity Technology |

**Thursday, 21 November 1985**

| | | |
|---|---|---|
| 9:00 a.m. | SESSION VIII | Splicing/Enclosure/Connector I |
| 9:00 a.m. | SESSION IX | Fiber Optic Application/Installation |
| 2:00 p.m. | SESSION X | Fiber Optic Systems/Networks |
| 2:00 p.m. | SESSION XI | Splicing/Enclosure/Connector II |

## PAPERS

Responsibility for contents rests upon the authors and not the symposium committee or its members. After the symposium, all the publication rights of each paper are reserved by their authors, and requests for republication of a paper should be addressed to the appropriate author. Abstracting is permitted, and it would be appreciated if the symposium is credited when abstracts or papers are republished. Requests for individual copies of papers should be addressed to the authors.



**Message From the Director**

On behalf of the U.S. Army Communications-Electronics Command (CECOM) and the Symposium Committee, welcome to the 34th International Wire and Cable Symposium (IWCS). Last year's Symposium in Reno was quite successful. The attendance at the technical sessions was excellent with many attendees expressing special interest in many of the papers presented. The number of foreign attendees (243) from 31 countries was the largest attendance to date. In addition, many new companies were represented at the Symposium.

The committee is looking forward to this year's Symposium and a return to Cherry Hill. A technical program beginning with a tutorial session on **"The Telco Explosion: How Far and How Fast,"** followed by ten technical sessions on various wire/cable systems, components, and their development, use and evaluation, should provide the interest and enthusiasm for a productive meeting.

The comment received most often during last year's Symposium and is of major concern to the committee, was the small attendance in the hospitality suites. It appears that many suites were located in remote areas of the MGM Grand Hotel and, as a result, they were not visited by many of the attendees. For the 1986 Symposium, consideration will be given to locating most, if not all, of the suites on one floor or in one wing of the hotel.

Committee members Eugene Riley of Ericsson, Inc., Austin D. Wetherell of Underwriters Laboratories, and Robert Depp of the Defense Electronics Supply Center, are retiring from the committee. Each member was extremely dedicated and contributed significantly to the success of the Symposium and the committee's objectives. On behalf of the committee, I extend to each a very special thanks for their sincere dedication, cooperation, and support of the Symposium activities. I wish them success in their future endeavors.

To ensure continued success in years to come, the committee solicits the support of all members of the wire and cable industry. Therefore, comments and suggestions are solicited and warranted from all attendees of the Symposium.

The 1986 Symposium (35th) will return to the MGM Grand Hotel in Reno, Nevada.

ELMER F. GODWIN
Director, IWCS

# PROCEEDINGS
# INTERNATIONAL WIRE & CABLE SYMPOSIUM

## BOUND—AVAILABLE AT FORT MONMOUTH

28th International Wire & Cable Symposium Proceedings—1979—$8.00
29th International Wire & Cable Symposium Proceedings—Not Avail
30th International Wire & Cable Symposium Proceedings—1981—$8.00
31st International Wire & Cable Symposium Proceedings—1982—$8.00
32nd International Wire & Cable Symposium Proceedings—1983—$10.00
33rd International Wire & Cable Symposium Proceedings—1984—$15.00
*34th International Wire & Cable Symposium Proceedings—1985—$20.00

*Extra copies: 1-3 $20.00; next 4-10 $15.00; next 11 & above $10.00 each

Make check or bank draft payable in US dollars to the INTERNATIONAL WIRE & CABLE SYMPOSIUM and forward request to:

International Wire & Cable Symposium
US Army Communications-Electronics Command
ATTN: AMSEL-COM-D-4
Fort Monmouth, NJ 07703-5202
USA

## PHOTOCOPIES—AVAILABLE AT DEPARTMENT OF COMMERCE

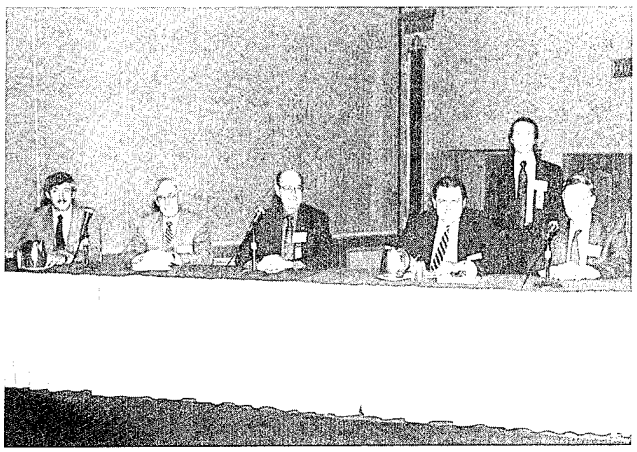
Photocopies are available for complete sets of papers for 1964 and 1966 thru 1984. Information on prices and shipping charges should be requested from the:

US Department of Commerce
National Technical Information Service
Springfield, Virginia 22151
USA

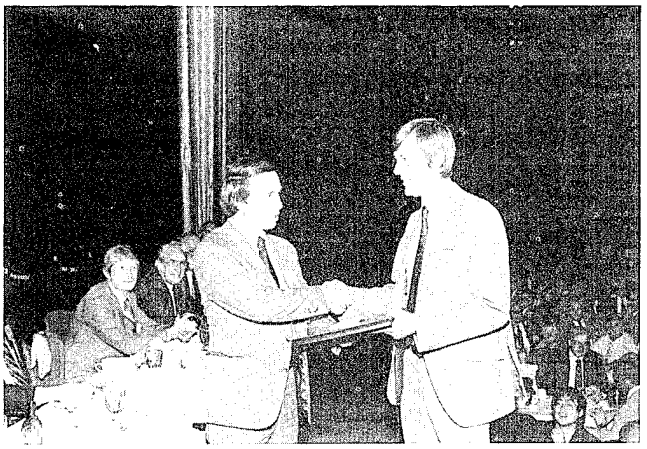
Include Title, Year and "AD" Number

| | |
|---|---|
| 13th Annual Wire & Cable Symposium (1964) | —AD 787164 |
| 15th Annual Wire & Cable Symposium (1966) | —AD A006601 |
| 16th International Wire & Cable Symposium (1967) | —AD 787165 |
| 17th International Wire & Cable Symposium (1968) | —AD 787166 |
| 18th International Wire & Cable Symposium (1969) | —AD 787167 |
| 19th International Wire & Cable Symposium Proceedings 1970 | —AD 714985 |
| 20th International Wire & Cable Symposium Proceedings 1971 | —AD 733399 |
| 21st International Wire & Cable Symposium Proceedings 1972 | —AD 752908 |
| 22nd International Wire & Cable Symposium Proceedings 1973 | —AD 772914 |
| 23rd International Wire & Cable Symposium Proceedings 1974 | —AD A003251 |
| 24th International Wire & Cable Symposium Proceedings 1975 | —AD A017787 |
| 25th International Wire & Cable Symposium Proceedings 1976 | —AD A032801 |
| 26th International Wire & Cable Symposium Proceedings 1977 | —AD A047609 |
| 27th International Wire & Cable Symposium Proceedings 1978 | —AD A062322 |
| 28th International Wire & Cable Symposium Proceedings 1979 | —AD A081428 |
| 29th International Wire & Cable Symposium Proceedings 1980 | —AD A096308 |
| 30th International Wire & Cable Symposium Proceedings 1981 | —AD A110859 |
| 31st International Wire & Cable Symposium Proceedings 1982 | —AD A125662 |
| 32nd International Wire & Cable Symposium Proceedings 1983 | —AD A136749 |
| 33rd International Wire & Cable Symposium Proceedings 1984 | —AD A152119 |
| Kwic Index of Technical Papers, International Wire & Cable Symposium (1952-1975) | —AD A027558 |

# Highlights of the 33rd International Wire and Cable Symposium November 13, 14, and 15, 1985 MGM Grand Hotel, Reno, Nevada



Panel Members—Tutorial Session:
(left to right) Mr. Roger Cole, Pacific Bell; Mr. Joseph Hull, U.S. Department of Commerce, Institute for Telecommunications Sciences; Mr. Ed Cohen, Rural Electrification Administration; Mr. O. J. Gasella, Exchange Carriers Standards Association; and Mr. Fred Andrews, Bellcore; (standing) Dr. James Tyler, Essex Group.



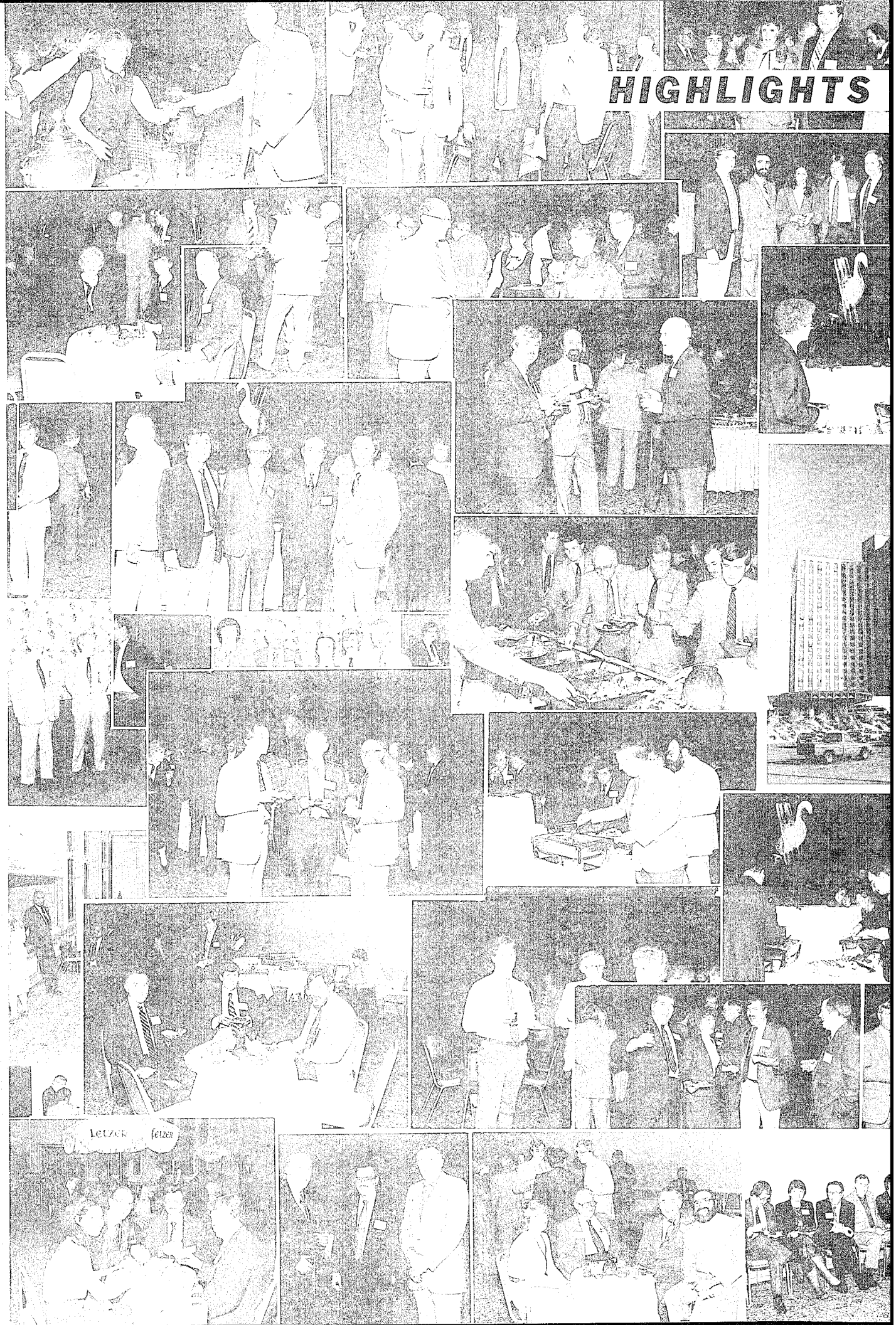
Committee Member Dr. James Tyler, Essex Group presenting the award for best technical presentation. Accepting the award for Mr. J. R. Bury, Standard Telecommunication Laboratories, Harlow, England is a colleague from the United Kingdom.



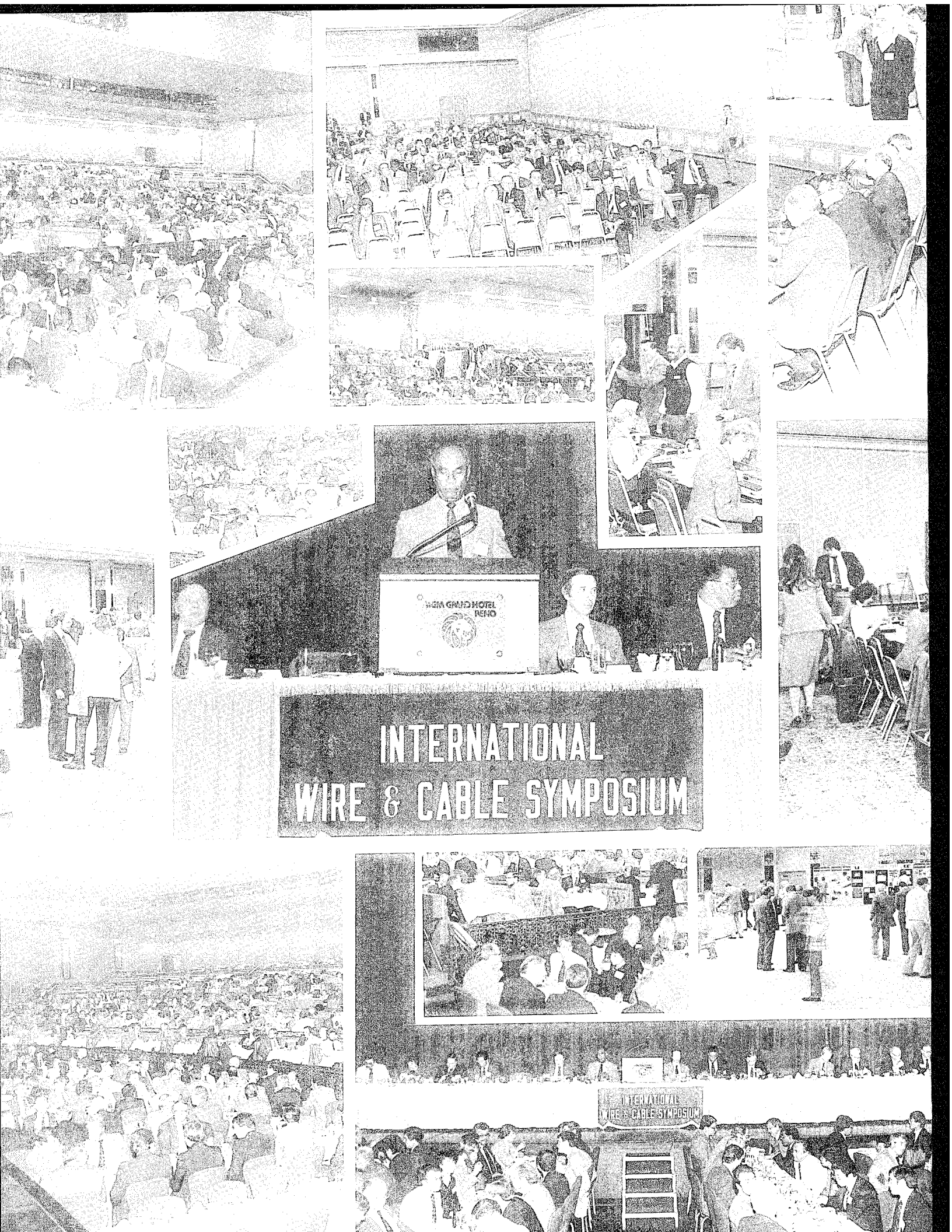
Committee Member Dr. James Tyler, Essex Group, presenting the award for Outstanding Technical Paper to (left) Mr. V. A. Fentress, Raychem Corp. and (right) Dr. D. V. Nelson, Stanford University.



Advisory Committee Member Joe Neigh, AMP, Inc. presenting Retirement Certificates to committee members (left) Drs. William Chervenak, Corning Glass Works and James Tyler (center) Essex Group. Mr. Andrew Dunin, DuPont Canada, Inc. is not included in the picture.

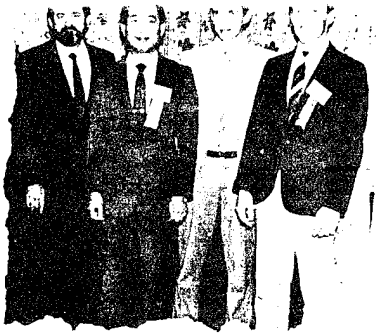

HIGHLIGHTS

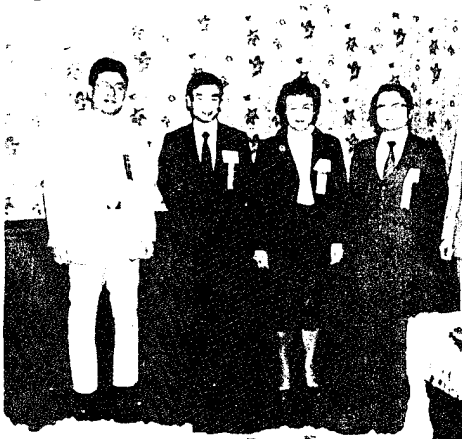

of 33rd IWCS

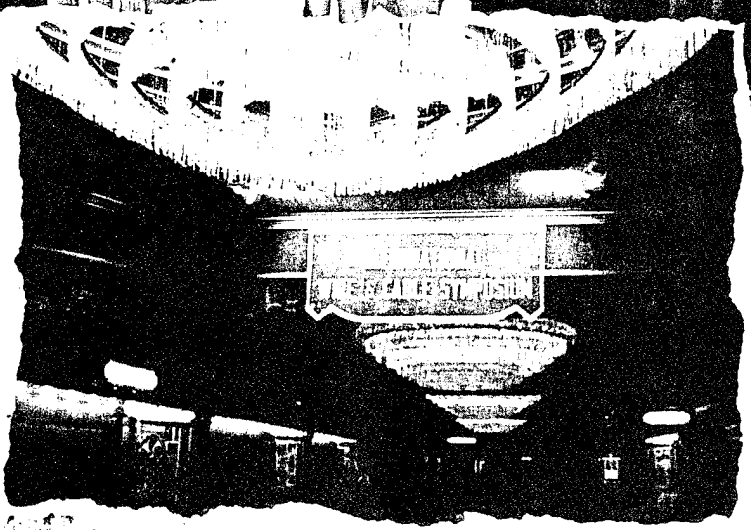

INTERNATIONAL
WIRE & CABLE SYMPOSIUM

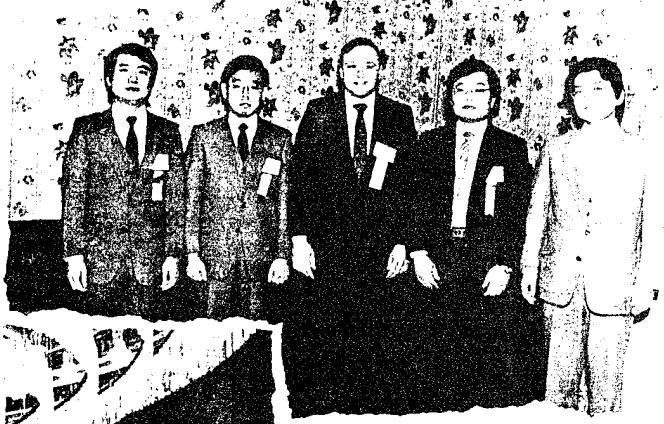












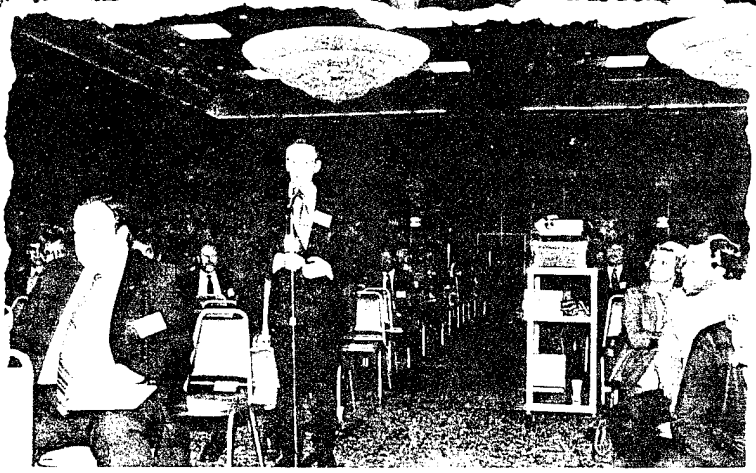














# AWARDS

| | *Outstanding Technical Paper* | *Best Presentation* |
|---|---|---|
| 1968 | H. Lubars and J. A. Olszewski, General Cable Corp.—"Analysis of Structural Return Loss in CATV Coaxial Cable" | N. Dean, B.I.C.C.—"The Development of Fully Filled Cables for Distribution Network" |
| 1969 | J. P. McCann, R. Sabia and B. Wargotz, Bell Laboratories—"Characterization of Filler and Insulation in Waterproof Cable" | J. D. Kirk, Alberta Government Telephones—"Progress and Pitfalls of Rural Buried Cable" |
| 1970 | D. E. Setzer and A. S. Windeler, Bell Laboratories—"A Low Capacitance Cable for the T2 Digital Transmission Line" | Dr. O. Leuchs, Kable and Metalwerke—"A New Self-Extinguishing Hydrogen Chloride Binding PVC Jacketing Compound for Cables" |
| 1971 | R. Lyenger, R. McClean and T. McManus, Bell Northern Research—"An Advanced Multi-Unit Coaxial Cable for Toll PCM Systems" | S. Nordblad, Telefonaktiebolaget L. M. Ericsson—"Multi-Paired Cable of Nonlayer Design for Low Capacitance Unbalance Telecommunications Network<br>N. Kojima, Nippon Telegraph and Telephone—"New Type Paired Cable for High Speed PCM Transmission" |
| 1972 | J. B. Howard, Bell Laboratories—"Stabilization Problems with Low Density Polyethylene Insulations" | S. Kaufman, Bell Laboratories—"Reclamation of Water-Logged Buried PIC Telephone Cable" |
| 1973 | Dr. H. Margin, Kabelmetal—"High Power Radio Frequency Coaxial Cables, Their Design and Rating" | R. J. Oakley, Northern Electric Co., Ltd.—"A Study Into Paired Cable Crosstalk" |
| 1974 | D. Doty, AMP Inc.—"Mass Wire Insulation Displacing Termination of Flat Cable" | G. H. Webster, Bell Laboratories—"Material Savings by Design in Exchange and Trunk Telephone Cable" |
| 1975 | T. S. Choo, Dow Chemical U.S.A.—"Corrosion Studies on Shielding Materials for Underground Telephone Cables" | J. E. Wimsey, United States Air Force—"The Bare Base Electrical Systems" |
| 1976 | N. J. Cogelia, Bell Telephone Laboratories and G. K. Lavoie and J. F. Glahn, US Department of Interior—"Rodent Biting Pressure and Chemical Action and Their Effects on Wire and Cable Sheath" | Michael DeLucia, Naval Ship Research and Development Center—"Highly Fire-Retardant Navy Shipboard Cable" |
| 1977 | Thomas K. McManus, Northern Telecom Canada Ltd. and R. Beveridge, Saskatchewan Telecommunications, Canada—"A New Generation of Filled Core Cable" | William L. Schmacher, AMP Inc.—"Design Considerations for Single Fiber Connector" |
| 1978 | Fumio Suzuki, Shizuyoshi Sato, Akinori Mori and Yoichi Suzuki; Sumitomo Electric Industries, Ltd., Japan—"Microcoaxial Cables Insulated with Highly Expanded Polyethylene By Chemical Blowing Method" | Richard C. Mondello, Bell Labs.—"Design and Manufacture of an Experimental Lightguide Cable For Undersea Transmission Systems" |
| 1979 | S. Masaki, Y. Yamazaki and T. Ideguchi, Nippon Telegraph and Telephone Public Corporation, Japan—"New Aluminum Sheath Cable Used for Electromagnetic Shielding" | I. Wadehra, IBM Corporation—"Performance of Polyvinyl Chloride Communication Cables in Modified Steiner Tunnel Test" |
| 1980 | P. Kish and Y. BeBorgne, Northern Telecom Canada Limited, Montreal, Canada—"General Crosstalk Model For Paired Communication Cables" | J. J. Refi, Bell Laboratories—"Mean Power Sum Far-End Crosstalk of PIC Cables as a Function of Average Twist Helix Angle" |
| 1981 | C. J. Arroyo, N. J. Cogelia, Bell Laboratories, and B. J. Darsey, Western Electric—"Thermal Behavior of Experimental Plenum Cable Sheaths Determined in a Radiant Heat Chamber" | G. S. Anderson, Belden Corporation—"Installation of Fiber Optic Cable on 457 Meter Tower" |
| 1982 | R. H. Whiteley, Raychem Ltd.—"A Comprehensive Small Scale Smoke Test" | A. Yoshizawa, The Furukawa Electric Co., Ltd.—"Structure and Characteristics of Cables for Robots" |
| 1983 | V. A. Fentress, Raychem Corp. and D. V. Nelson, Stanford University—"Fracture Mechanics Evaluation of the Static Fatigue Life of Optical Fibers in Bending" | J. R. Bury, Standard Telecommunication Laboratories, Ltd., Hailow, England—"Development of Flame Retardant, Low Aggressivitiy Cables" |
| 1984 | M. Fujise and Y. Iwamoto, KDD Research & Development Laboratories, 1-23 Nakameguro, 2-Chrome, Meguro-Ku, Tokyo, Japan—"Self-Core-Alignment Arc-Fusion Splicer Based on a Simple Local Monitoring Method" | William E. Dennis, Dow Corning Corporation, Midland, Michigan-"Hydrogen Evolving Tendancies of Cable Fillers and Optical Fiber Coatings" |

# CONTRIBUTORS

**AEG Kabel AG**
Monchengladbach, Germany
**AEG-Telefunken Kabelwerke Aktiengesellschaft, Rheydt**
West Germany
**AFA Industries**
Garfield, NJ
**Alcave**
Caracas, Venezuela
**Alcoa Fujikura Ltd.**
Pittsburgh, PA
**Allied Corporation**
Morristown, NJ
**American Hoechst Corp.**
Somerville, NJ
**Amoco Chemicals Corp.**
Chicago, IL
**Anzon America, Inc.**
Freehold, NJ
**ARCO Specialty Chemical**
Newtown Square, PA
**Arvey Corporation**
Cedar Grove, NJ
**AT&T Network Systems**
Gateway II, Newark, NJ
**Austral Standard Cables, Ltd.**
Victoria, Australia
**Badische Corp.**
Williamsburg, VA
**Barcel Wire & Cable Corp.**
Irvine, CA
**Baychem International, Inc.**
Houston, TX
**Beacon Reel Company**
Beacon Falls, CT
**Belding Corticelli Thread Co.**
New York, NY
**Belding Corticelli Thread Co.**
Putnam, CT
**Bell Canada**
Montreal, Quebec, Canada
**Berkshire Electric Cable Co.**
Leeds, MA
**BICC Telecommunication Cables**
Prescot, England
**Borden Chemical**
Columbus, Ohio
**Boston Insulated Wire & Cable**
Hamilton, Canada
**Breen Color Concentrates, Inc.**
Lambertville, NJ
**Burgess Pigment Company**
Sandersville, GA
**Cabot Corporation**
Boston, MA
**Cabot Corporation/Special Blacks Division**
Boston, MA
**Camden Wire Company, Inc.**
Camden, NY
**Capscan Cable Company**
Adelphia, NJ
**Carlew Chemicals Ltd.**
Montreal, Quebec, Canada
**R. E. Carroll, Inc.**
Trenton, NJ
**Cary Chemicals Inc.**
Farmingdale, NJ
**Celwave Systems, Inc.**
Claremont, NC
**Chase & Sons, Inc.**
Randolph, MA
**Ciba-Geigy Corporation**
Hawthorne, NY
**Collyer Insulated Wire**
Lincoln, RI
**Colorant/Chromatics Group**
Danbury, CT
**Colorite Plastics Company**
Ridgefield, NJ
**Communications Technology Corp.**
Los Angeles, CA
**Control Data Corporation**
Washington, DC
**Copperweld Bimetallics Group**
Pittsburgh, PA
**Corning Glass Works**
Corning, NY
**Crellin, Inc.**
Chatham, NY
**Davis-Standard Division of Crompton & Knowles**
Pawcatuck, CT
**DCM International Corp.**
**DCM Industries, Inc.**
San Leandro, CA
**Dow Chemical U.S.A.**
Midland, MI
**Dow Corning Corporation**
Midland, MI
**Duncan M. Gillies Co., Inc.**
West Boylston, MA
**DuPont Company**
Wilmington, DE
**Dussek Campbell Limited**
Belleville, Ontario, Canada
**Dussek Campbell Ltd.**
Crayford, Kent, England
**Eagle-Picher Industries, Inc.**
Cincinnati, OH
**Eastman Chemical Products, Inc.**
Kingsport, TN
**The Electric Wire & Cable Co.**
Haifa, Israel
**Electrolock, Inc.**
Chagrin Falls, OH
**Essex Group**
Decatur, IL
**Ethyl Corporation**
Sayreville, NJ
**Facile Technologies Inc.**
Paterson, NJ
**Fujikura, Ltd.**
Tokyo, Japan
**Gary Chemical Corp.**
Leominster, MA
**Gavitt Wire & Cable Co.**
Brookfield, MA
**Gem Gravure Company, Inc.**
West Hanover, MA
**General Cable Company**
Greenwich, CT
**Global Products Corporation**
Leominster, MA
**BF Goodrich Chemical Group**
Cleveland, Ohio
**Harbour Industries, Inc.**
Shelburne, VT
**Harwick Chemical Corp.**
Trenton, NJ

**Hindustan Cables Limited**
Calcutta, India
**HiTemp Wires, Div. of Ericsson**
Bohemia, NY
**ICI Americas Inc.**
Wilmington, DE
**International Wire Products, Co.**
Wyckoff, NJ
**ITT Surprenant**
Clinton, MA
**Judd Wire Division, HVE**
Turners Falls, MA
**Jutland Telephone**
Denmark
**Kable Tapes Limited**
Winnipeg, Monitoba, Canada
**Kenrich Petrochemicals, Inc.**
Bayonne, NJ
**Lamart Corporation**
Clifton, NJ
**Laribee Wire Mfg. Co. Inc.**
Jordan, NY
**LNP Corporation**
Malvern, PA
**Lowe Associates JJ**
**Reels, Tapes & Machinery Div.**
Bedford Hills, NY
**Lynn Plastics Corp.**
Lynn, MA
**Mach-1 Division, Burton Rubber**
Proc. Inc., Macedonia, OH
**Maillifer Co.**
South Hadley, MA
**Manning Paper Company**
Green Island, NY
**Manuli Cari S.p.A.**
Cologno Monzese (Milan), Italy
**Micro-Tek Corporation**
Cinnaminson, NJ
**K. Miller Tool & Mfg. Co., Inc.**
West Springfield, MA
**Mohawk Wire and Cable Co.**
Leominster, MA
**Monsanto Polymer Products**
St. Louis, MO
**Montgomery Co.**
Windsor Locks, CT
**Neptco Incorporated**
Pawtucket, RI
**Nesor Alloy Corporation**
West Caldwell, NJ
**New Brunswick Telephone Co., Ltd.**
Saint John, NB
**Nokia, Inc.**
Atlanta, GA
**North Anson Reel Company**
North Anson, ME
**Norchem, Inc.**
(formerly Northern Petrochemical)
Rolling Meadows, IL
**Northern Telecom Canada Ltd.**
Quebec, Canada
**NTT Ibaraki Electrical Comm. Lab.**
Tokai, Ibaraki, Japan
**Occidental Chemical Corp**
Niagara Falls, NY
**OKI Electric Cable Co., Ltd.**
Kawasaki-shi, Japan
**The Okonite Company**
Ramsey, NJ
**The Okonite Company**
Rumford, RI
**Olex Cables—Melbourne**
Victoria, Australia
**Omega Wire Inc.**
Camden, NY
**Omya, Inc.**
Proctor, VT
**Pantasote Inc.**
Passaic, NJ
**Pennwalt Corporation**
Philadelphia, PA
**Penreco**
Butler, PA
**Philips Kommunikations Ind. AG**
Koln, Schanzensti, West Germany
**Phillips Cables Ltd.**
Vancouver, B.C. Canada
**Photodyne, Inc.**
Newbury Park, CA
**Pirelli Cable Corporation**
Union, NJ
**Pirelli Cables Inc.**
Surrey, B.C., Canada
**Radiation Dynamics, Inc.**
Melville, L.I., NY
**Radiation Dynamics, Inc.**
Ronkonkoma, NY
**Raychem Corporation**
Menlo Park, CA
**Reichhold Chemicals, Inc.**
Hackettstown, NJ
**Reliance Comm/Tec.**
Franklin Park, IL
**David W. Riley, Consultant**
Extrusion Engineers
Plainfield, NJ
**H. M. Royal Incorporated**
Trenton, NJ
**Santech Inc.**
Toronto, Ontario, Canada
**S.A.T. Societe Anonyme De Telecommunications**
Paris, France
**Shell Chemical Company**
Houston, Texas
**Siecor Corporation**
Hickory, NC
**Siemens Aktiengesellschaft**
Munich, Germany
**Soltex Polymer Corp.**
Houston, TX
**Southwest Chemical Services Inc.**
Houston, TX
**SpecTran Corporation**
Sturbridge, MA
**Sterling Davis Electric**
Wallingford, CT
**Sumitomo Electric Industries, Ltd.**
Yokohama, Japan
**Sumitomo Electric Interconnect**
Fremont, CA
**Sumitomo Electric Research Triangle, Inc.**
Research Triangle Park, NC
**Sun Refining & Marketing Co.**
Philadelphia, PA
**The Swiss Insulating Works Comp.**
Breitenbach, Switzerland
**Syncro Machine Company**
Perth Amboy, NJ
**Taconic Plastics, Ltd.**
Petersbury, NY
**Tamaqua Cable Products Corp.**
Schuylkill Haven, PA

**Teknor Apex Company**
Pawtucket, RI
**Telcom Department of Malaysia**
Kuala Lumpur, W. Malaysia
**Telecom Australia**
Melbourne, Australia
**Teledyne Thermatics**
Elm City, NC
**Telephone Cables Ltd.**
Essex, England
**Tenneco Oil Processing & Marketing**
Houston, TX
**Thermax Wire Corporation**
Flushing, NY
**3M**
St. Paul, MI
**Torpedo Wire & Strip, Inc.**
Pittsfield, PA
**Trea Industries, Inc.**
North Kingstown, Inc.
**TRW, Inc.**
Redondo Beach, CA
**Union Carbide Corp.**
Danbury, CT
**Uniroyal Chemical Company**
Naugatuck, CT
**US Industrial Chemicals Co.**
Cincinnati, OH
**R. T. Vanderbilt Co., Inc.**
Norwalk, CT
**Videx Equipment Corp.**
Paterson, NJ
**VISTA Polymers, Inc.**
Houston, Texas
**Weber & Scher Mfg. Co. Inc.**
Newark, NJ
**Whitmor Plastic Wire & Cable**
North Hollywood, CA
**Wilson Fiberfill International**
Neshanic Station, NJ
**W. L. Gore & Associates, Inc.**
Newark, DE
**Wyre Wynd**
Jewett City, CT
**Wyrough and Loser, Inc.**
Trenton, NJ
**Zumbach Electronics Corp.**
Mount Kisco, NY

# TABLE OF CONTENTS


**TUESDAY, NOVEMBER 19, 1985—9:30 AM-12:00 PM**

**Hunterdon and Cumberland Rooms**

Greeting: Mr. Theodore A. Pfeiffer, Technical Director, US Army Communications-Electronics Command, Fort Monmouth, New Jersey

SESSION I: THE TELECO EXPLOSION: HOW FAR AND HOW FAST

*Chairperson:* Dr. Raymond E. Jaeger, Spectran

*Panel Members:*

Dr. Naoya Uchida, Deputy Director of the Outside Plant Development Division, Nippon Telegraph and Telephone Ibaraki, Electrical Communications Laboratory, Japan.

Mr. Christopher Todd, Head of Optical Communications, British Telecom Research Laboratories, United Kingdom.

Mr. Frank E. Wollensack, President, Lightnet, New Haven, Connecticut.

Mr. Egar L. Brown, Jr., Vice President, Network Planning Management Services Inc., Bell Atlantic, Alexandria, Virginia.

Mr. David J. Meskell, Jr., Head of Cable and Wire Department, AT&T Bell Laboratories, Norcross, Georgia.

**TUESDAY, NOVEMBER 19, 1985—2:00-5:00 PM**

**Gloucester Room**

SESSION II: FIBER OPTIC CABLE DESIGN I

*Chairperson:* Robert Depp, Defense Electronics Supply Center

Light Weight, High Tensile Strength and High Mobility Optical Cable—*N. Sato, Y. Sugawara, H. Yokosuka, K. Seto,* and *H. Katayose,* Fujikura Ltd., Chiba, Japan..... 1

Single Fibre Cables for Military Applications—*M. M. Ramsay, P. G. Hale,* and *R. Sutehall,* Standard Telecommunication Laboratories, Essex, UK..... 9

Development of Optical Curl Cord Cable Using Glass Fiber—*H. Horima, M. Dazai,* and *M. Hamaguchi,* Sumitomo Electric Industries, Ltd., Yokohama, Japan..... 16

Compact Lightguide Cable Design—*P. D. Patel* and *C. H. Gartside, III,* AT&T Bell Laboratories, Norcross, Georgia..... 21

Optical Fiber Cable for Special Circumstance—*N. Akasaka, F. Suzuki,* and *T. Aoki,* Sumitomo Electric Industries, Ltd., Yokohama, Japan..... 28

**TUESDAY, NOVEMBER 19, 1985—2:00-5:00 PM**

**Hunterdon Room**

SESSION III: MATERIALS

*Chairperson:* Vieney Mascarenhas, Canada Wire and Cable Limited

A New Coloring System by Liquid Pigment Injection Method—*S. Yamamoto, K. Mirua, M. Seto, K. Fuse,* and *M. Kajiwara,* The Furukawa Electric Co., Ltd., Tokyo, Japan.. 33

Versatile High Performance Filling Compounds for Telecoms Cable Applications—*J. R. Bury,* Standard Telecommunication Laboratories Ltd., Essex, England and *D. A. Joiner,* Synthetic Technology Ltd., Tunbridge Wells, Kent, England..... 38

Polyimide Film Insulation for Aerospace Wire and Cable: Why Long-Term Performance Exceeds Some Limited Laboratory Projections—*J. O. Punderson* and *J. F. Heacock,* E. I. DuPont de Nemours & Co., Inc., Wilmington, Delaware..... 44

Coated Copper Shielding Tapes for the Wire and Cable Industry—*K. E. Bow, B. K. Grosser,* and *D. G. Pikula,* Dow Chemical U.S.A., Granville, Ohio..... 51

Corrosion Performance of a Sheath with Plastic Coated Stainless Steel for Fiber Optic Cable—*P. U. Bakhru* and *K. E. Bow,* Dow Chemical U.S.A., Granville, Ohio, *P. L. Hagans* and *L. Shadoff,* Dow Chemical U.S.A., Midland, Michigan..... 61

Newly Developed UV Curable Polybutadiene Acrylate as a Primary Coating for Optical Fibers—*R. Ohno, T. Kikuchi,* and *Y. Matsumura,* Japan Synthetic Rubber Co., Ltd., Kawasaki, Japan..... 76

**WEDNESDAY, NOVEMBER 20, 1985—9:00 AM-12:00 PM**

**Gloucester Room**

SESSION IV: FIBER OPTIC CABLE DESIGN II

*Chairperson:* George Webster, AT&T Bell Laboratories

A Tactical Fiber Optic Cable—*A. C. Jenkins, C. R. Lovelace,* and *M. R. Reynolds,* AT&T Bell Laboratories, Norcross, Georgia, *V. E. Kalomiris,* U.S. Army Communications—Electronics Command, Fort Monmouth, New Jersey..... 82

Low Temperature Fiber Optic Tactical Cable Without the Use of Antibuckling Members—*J. Chamberlain* and *T. Clarke,* Siecor Corporation, Hickory, North Carolina 88

Long-Term Reliability of Optical Fiber Composite Ground Wire—*M. Ogai, H. Hiramatsu, M. Oda, Y. Kamata, Y. Miyajima,* and *M. Ieshige,* The Furukawa Electric Co., Ltd., Chiba, Japan 92

Optical Stability of Single Mode Fiber in Loose-Tube Cable Designs—*K. A. Emig, R. A. Modavis, J. R. Sicotte,* Corning Glass Works, Corning, New York, and *D. O. Bostrom, E. W. Riley, D. W. Williams,* Ericsson, Inc., Overland Park, Kansas 97

Prediction of Optical Cable Losses Due to Hydrogen—*S. R. Barnes, N. J. Pitt,* Standard Telecommunication Labs., Essex, England, and *S. Hornung,* British Telecom Research Labs., Suffolk, England 102

Overcoming the Hydrogen Problem in Optical Fibers—*P. Anelli, G. Grasso,* Società Cavi Pirelli, Milano, Italy, *E. Modone, B. Sordo,* Cselt Centro Studi Laboratori Comunicazioni, Torino, Italy, and *F. Esposto,* SIP D. G., Roma, Italy 107

**WEDNESDAY, NOVEMBER 20, 1985—9:00 AM-12:00 PM**

**Hunterdon Room**

SESSION V: DESIGN/TESTING I

*Chairperson:* Eugene Riley, Ericsson, Inc.

Evaluation of Temperature Conductivity in Optical Fiber Cables—*S. Mochizuki* and *T. Yashiro,* NTT Ibaraki Electrical Communication Laboratories, Tokai, Japan, *K. Arakawa,* NTT Musashino Electrical Communication Laboratories, Tokyo, Japan 119

The Future of Optical Time Domain Reflectometry: Utilization of the Coherent Detection Technique—*S. Heckmann, J. Rybach,* Philips Kommunikations Industrie AG Cologne, West Germany, *E. Brinkmeyer,* Technische Universität Hamburg-Harburg, Hamburg, West Germany, and *R. Knoechel,* Philips GmbH Forschungslaboratorium Hamburg, Hamburg, West Germany 125

Automated Multi Fiber Attenuation Change Measurement System—*K. Hafemeister, A. Garg, B. Hellmann, D. Schicketanz,* and *D. Vokey,* Siecor Corporation, Hickory, North Carolina 135

High Accuracy Measurement of Optical Fibre Length—*O. R. Andersen,* NKT Elektronik, Denmark 138

New Field Measurement System for Single Mode Fiber Dispersion Utilizing Wavelength Division Multiplexing Technique—*W. H. Hatton, M. Nishimura,* Sumitomo Electric Research Triangle Inc., Research Triangle Park, North Carolina and *W. Haltiwanger,* South Carolina Electric and Gas, Columbia, South Carolina 142

**WEDNESDAY, NOVEMBER 20, 1985—2:00-5:00 PM**

**Hunterdon Room**

SESSION VI: DESIGN/TESTING II

*Chairperson:* Tom Jones, Wyrough and Loser, Inc.

Insertion Loss and VSWR Analysis of Coaxial Cable—*A. J. Daniels,* TRW Inc., Redondo Beach, California 150

Quality Assurance Approach for Fiber Optic Cable—*B. R. Rapacki* and *P. A. Link,* Bell Communications Research, Holmdel, New Jersey 155

Advances in the Optimization of Multi-Layer Shield Designs—*J. W. Kincaid Jr.* and *J. A. Krabec,* Belden Technical Research Center, Geneva, Illinois 162

Crushing Metallic Shielded Telecommunications Cables with Dynamic Magnetic Fields—*P. U. Bakhru, K. E. Bow,* Dow Chemical USA, Granville, Ohio, *D. Fischer,* Superior Cable Corporation, Atlanta, Georgia, and *E. Schrom,* Consultant, Valatie, New York 173

An Initial Investigation on the Accelerated Aging and Lifetime Predictions of Wire and Cable Insulations Used for Local Network Installations—*G. L. Grune* and *T. L. Talarico,* IBM Corporation, Research Triangle Park, North Carolina 187

**WEDNESDAY, NOVEMBER 20, 1985—2:00-5:00 PM**

**Gloucester Room**

SESSION VII: FIRE, SMOKE, AND TOXICITY TECHNOLOGY

*Chairperson:* Austin D. Wetherell, Underwriters Laboratories

Full-Scale Fire Tests to Simulate an Electrical Cable Fire in the Control Room of an Industrial Plant—*R. M. Eichhorn* and *J. J. Pickering,* Union Carbide Corporation, Bound Brook, New Jersey 213

Development of Low Smoke, Halogen Free, Flame Retardant Cables for Ships—*Y. Shingo, T. Mathuda, M. Murayama, S. Yoshikawa, M. Hasegawa,* and *A. Yoshino,* Fujikura Ltd., Tokyo, Japan 220

A New Non-Halogenated Flame Retardant Compound and Its Jacketed Telecommunication Cables—*K. Nakano, T. Ishikawa, H. Suzuki, M. Sakasai,* and *N. Sato,* Fujikura Ltd., Chiba-ken, Japan ..... 227

Fire-Resistant Characteristics of Aerial Optical Cables—*T. Konno, S. Hasegawa, K. Sugawara, Y. Tabata,* Tohoku Electric Power Co., Inc., Sendai, Japan, *K. Niikura, H. Horima,* Sumitomo Electric Industries, Ltd., Yokohama, Japan, *Y. Yamada,* and *A. Kurosawa,* Kitanihon Electric Wire Co., Ltd., Sendai, Japan ..... 233

The Overall Safety of Wire and Cable Materials IV: A Test Regimen for Measuring Cable Fire and Hazard—*F. B. Clarke and I. A. Benjamin,* Benjamin/Clarke Associates, Inc., Kensington, Maryland ..... 241

Light Weight Polyimide Film/Mica Marine Cable—*C. D. Palmer, D. B. Allen,* and *W. J. Kopish,* E. I. Du Pont de Nemours & Co. Inc., Wilmington, Delaware ..... 250

**THURSDAY, NOVEMBER 21, 1985—9:00 AM-12:00 PM**

**Hunterdon Room**

SESSION VIII: SPLICING/ENCLOSURES/ CONNECTORS I

*Chairperson:* Alan G. Dwyer, GTE Service Corporation

Rapid Ribbon Splice for Optical Fiber Field Splicing—*N. E. Hardwick, III* and *S. T. Davies,* AT&T Bell Laboratories, Norcross, Georgia ..... 255

Field Molded Splice Closure System for Copper and Fiber Cables Using Low Pressure Molding—*I. H. Miller* and *J. L. Horton,* Bell Canada, Toronto, Ontario, Canada, *J. R. Scott* and *L. J. Charlebois,* Bell Northern Research, Ottawa, Ontario, Canada .... 260

Optical Fiber Cable with Premounted Multi-Fiber Connector—*S. Tachigami, A. Ohtake, Y. Obara, S. Nakai, R. Yuguchi,* and *Y. Kamata,* The Furukawa Electric Co., Ltd., Chiba, Japan ..... 267

High Strength Splice with Restoration Coat of Optical Fiber for Cabling—*T. Kakii, Y. Suetsugu,* and *S. Tanaka,* Sumitomo Electric Industries, Ltd., Yokohama, Japan ..... 275

A Two-Fiber Tactical Fiber-Optic Connector—*J. M. Anderson, B. V. Darden, B. G. LeFevre,* AT&T Bell Laboratories, Norcross, Georgia and *V. E. Kalomiris,* US Army Communications-Elec. Com., Fort Monmouth, New Jersey ..... 286

An Update on Practical Fusion Splicing of Multimode and Single-Mode Fibers—*S. L. Saikkonen* and *M. J. Hackert,* Corning Glass Works, Corning, New York ..... 293

**THURSDAY, NOVEMBER 21, 1985—9:00 AM-12:00 PM**

**Gloucester Room**

SESSION IX: FIBER OPTIC APPLICATION/ INSTALLATION

*Chairperson:* Kazuo Nomura, Sumitomo Electric USA, Inc.

Power and Communication Cables Designed for Later Insertion of Optical Fibers—*A. Gyger,* Cablex S.A., Morges, Switzerland ..... 300

Ethernet and Thinnet Undercarpet Compatible Local Area Network Wiring System—*K. P. Blum* and *C. W. Ponder,* Thomas & Betts Corporation, Raritan, New Jersey ..... 305

Very Light-Weight, Field-Use Portable Fiber Optic Cable with Connector—*T. Ohsugi, T. Yamazaki, Y. Kitayama,* and *T. Kakii,* Sumitomo Electric Industries, Ltd., Yokohama, Japan ..... 313

Underground Fiber Optic Cable Placement—Cable Pulling Tensions Helically Wrapped Cables in Straight and Curved Conduit Sections—*P. B. Grimado,* Bell Communications Research, Whippany, New Jersey ..... 320

Optical Fibre/Copper Conductor Composite LAN Cable for Mining Application—*P. Gregor, G. F. Hög, W. Gläsel,* and *H. G. Haag,* AEG Kabel Aktiengesellschaft, Mönchengladbach, Fed. Rep. of Germany .. 332

Manufacture and Performance of Fibre Units for Installation by the Viscous Drag of Air—*S. Hornung, S. A. Cassidy, P. Yennadhiou,* and *M. H. Reeve,* British Telecom Research Laboratories, Ipswich, UK ..... 342

**THURSDAY, NOVEMBER 21, 1985—2:00-5:00 PM**

**Gloucester Room**

SESSION X: FIBER OPTIC SYSTEMS/ NETWORKS

*Chairperson:* John Thompson, Nokia, Inc.

Mechanical Architecture of a 147 Kilometer Repeaterless Fiber Optic Undersea Cable System—*Tek-Che Chu, L. J. Marra,* and *R. K. Stix,* AT&T Bell Laboratories, Holmdel, New Jersey ..... 346

Optical Fibre and System Considerations for a Broadband Subscriber Network—*H. G. Haag, G. F. Hog,* and *P. E. Zamzow,* AEG Kabel Aktiengesellschaft, Federal Republic of Germany ..... 355

Design and Installation of an Optical Fibre Local Wideband Distribution System in an Urban Environment—*J. W. Reilly,* Mercury Communications Ltd., London, England, and *G. Holden,* BICC Telecommunication Cables Ltd., Prescot, England ..... 364

Cost Effective Optical Systems for UK Junction Network—*C. H. Robbins,* British Telecom, London, UK ..... 370

High-Performance Optical Fiber Cable Coverage Throughout Japan—*I. Yamanouchi,* Nippon Telegraph & Telephone Corporation, New York, New York 379

Cable Design and Installation Technique for Direct Buried Non-Metallic Optical Cables—*B. T. de Boer, R. W. A. Ayre,* and *R. B. Schuster,* Telecom Australia, Melbourne, Australia ..... 385

**THURSDAY, NOVEMBER 21, 1985—2:00-5:00 PM**

**Hunterdon Room**

SESSION XI: SPLICING/ENCLOSURE/CONNECTORS II

*Chairperson:* Joseph McCann, U.S. Army Communications-Electronics Command

A New Wire Connector Joins a Pair with a Pinch—*T. C. Cannon* and *D. T. Smith,* AT&T Bell Laboratories, Norcross, Georgia ..... 393

Local Launch and Monitor for Single-Mode Splicing—*R. Hughes, V. So,* and *P. J. Vella,* Bell Northern Research, Alberta, Canada ... 397

The Role of Re-Enterable Encapsulants in Waterproof Closures on Metallic Telecommunications Cables—*K. Dawes,* Raychem Manufacturing Corp., Fuquay-Varina, North Carolina and *T. E. McNeal,* Bell South Services, Birmingham, Alabama ..... 402

A Forced Encapsulation System for Splice Closures—*C. E. Angel, F. J. Mullin,* and *W. C. Reed,* AT&T Bell Laboratories, Norcross, Georgia ..... 407

Laboratory Performance Tests and Criteria for Reenterable Encapsulants—*J. T. Chapin* and *R. Sabia,* AT&T Bell Laboratories, Norcross, Georgia ..... 418

# LIGHT WEIGHT, HIGH TENSILE STRENGTH AND HIGH MOBILITY OPTICAL CABLE

N. Sato Y. Sugawara H. Yokosuka K. Seto H. Katayose

Fujikura Ltd. 1440 Mutsuzaki, Sakura, Chiba, Japan

## Abstract

A small diameter, light weight, high tensile and compressive strength, and flexible optical fiber cable has been developed. This cable is suitable for emergency cables, military communication systems, and indoor cables because of its high mobility and space saving.
The cable is totally composed of non-metallic material and has a plastic center core which has a Kevlar FRP center strength member and four spiral grooves on the surface : two smaller grooves for optical fibers and two larger grooves for the Kevlar tension members.
High density Kevlar bunches are so tightly housed in two grooves of the core that the cable has very high tensile strength, light weight and flexibility.

This paper also describes a connector and a mobile light weight reel which have developed to make handling and reeling much easier.

## 1. Introduction

Now optical fiber cables are expanding their application fields replacing existing metallic conductor cables because of its superior characteristics.
Besides its lower transmition loss and larger capacity, the properties such as smaller diameter, stronger mechanical strength,and more flexibility are always required.
Especially the outdoor mobile transmission system, such as, the moving TV camera system, emergency restoration system, and military communication system, is required more strict properties.
Moreover,the followings are added : reliability in a wide range of temperature, free from electromagnetic inflence, and flame retardant.
In these applications the cable is usually winded in a light and movable reel and repeated the installation and rereeling many times.
For this purpose, the cable and reel have to be tough enough and easy to handle.

To satisfy these requirements a number of cable configurations has been studied. Consequently, a very high tensile strength cable for its small diameter and light weight has been developed.
The cable has a slotted center core which has two sizes of spiral grooves : larger grooves for the stranded Kevlar tension member and smaller grooves for optical fibers. The cable is composed of non-metallic materials to prevent a device and a man from electric damages.
Connectors and light reels for this cable have also developed and a whole weight including 1km long cable, connectors at both end and reel is less than 20kg.

## 2. Cable design

### 2-1. Requirements

#### 1). Optical fiber

Transmission and optical characteristics shall be decided, based on the system requirments.
High and low temperature characteristics and screening levels have to have better characteristics than the characteristics for general purposes.

#### 2). Small diameter and light weight

When a 1km length cable with connectors at both ends is winded in a reel, the weight of the whole kit shall be less than 20kg so that the kit will be moved easily even by one or two persons.
Because the cable occupies the major part of the weight of the kit, the weight of the cable must be reduced about 15kg/km by making the diameter small and using light weight materials.

3). High tensile strength

If the cable is installed by one or two persons, a maximum pulling force will be approximately 50kg.
But sometimes much larger unexpected power can be loaded during the installation or after the installation outside.

It can be said that the stronger the better without increasing weight and diameter.
The most important thing is to house a light and small but very strong tension member into a small diameter of the cable well.

And breakage elongation of the TM should be less than that of optical fiber.

4). Side pressure characteristics

The cable is usually laid down on the ground and sometimes it can be pulled with side pressure during installation and be pressed by a heavy vehicle after installation.
The cable structure must be studied to be endurable to these conditions.

5). Flexibility

Flexibility is one of the important characteristics for the movable cable which is winded in a small reel and happens to be bent at very small radius.
Generally from the viewpoint of a cable structure, flexibility is an opposite characteristic to high tensile and side pressure strength.
In the cable design, especially in configuration and TM material, great efforts should be made to satisfy both characteristics.

6). Non-inductive

The induction free cable is appropriate to use in a field.
The non-metallic cable replaced for a steel tension member by FRP rod is usually used.
But Glass FRP may deteriorate the flexibility and tensile strength in such a small cable.
Therefore, some countermeasure shall be devised to solve this problem.

7). Stability over a wide range of temperatures

When the cable is applied for emergency restoration or military use, it must perform consistently over a wide range of temperatures, -40°C～+80°C.
And the cable has to be able to endure several times of installations and rewinding without any attenuation increase and any mechanical breakage even in such circumstances.

8). Flame retardant

The cable can be used in many kinds of environments such as disastrous or dangerous area so that it is preferable to be flame retardant.
But in general adding flame retardation makes some other properties worse ; therefore, the grade of retardation should be considered.

9). Specification

The following specification shown in table 1 was a target to be overcome at the designing stage.

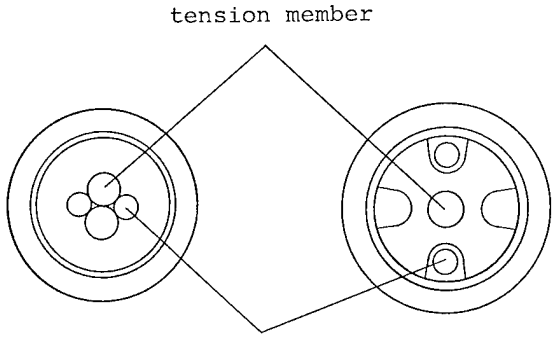
Table 1. Specification of a cable

| Item | | Specification |
|---|---|---|
| Optical fiber | Type | GI |
| | core/clad(μm) | 50/125 |
| Cable | dia. (mm) | 4.5> |
| | weight (kg/km) | 15> |
| Allowable tension (kgf) | | 100< |
| Breakage tensile strength (kgf) | | 250< |
| Compression resistance (kg/50mm) | | 300< |
| Bending radius (mm) | | 50> |
| Non-inductive | | Non-metallic |
| Temperature charscteristics | | -40°C～+80°C |
| Flame retardant | | self-extinguished |

## 2-2. Existing Cables

### 1). Cable configurations

Typical existing cables for the same purpose are shown in Fig. 1 and the example data of each cable is shown in table 2.




(A) stranded core (B) sloted core

Fig. 1 Existing cables

Table 2. Comparison between the two

| type | A | B |
|---|---|---|
| Cable outer dia.(mm) | 4.0 | 4.5 |
| Cable weight (kg/km) | 20 | 25 |
| Allowable tension (kg) | 60 | 50 |
| Compression resistance (kg/50mm) | 100 | 300 |

Small diameter, light weight, and high tensile strength are features of the stranded core type.
The best feature of the sloted core type is in a side pressure property.
The result of the squeezing test, illustrated in Fig. 2, which is tensile and bending test, is shown in Fig. 3.
Since the side pressure property was the most important thing to use in a field, slotted core type has been adopted.

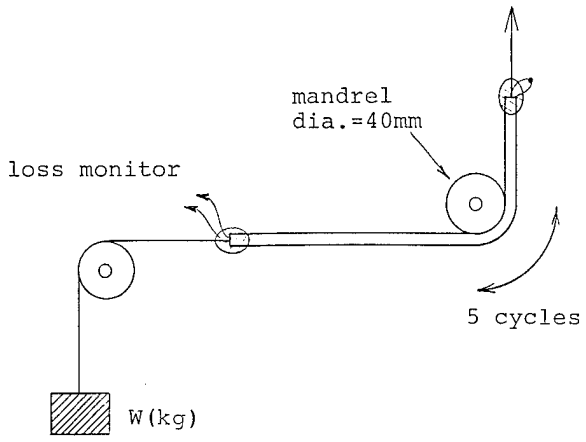



Fig. 2 Method of squeezing test

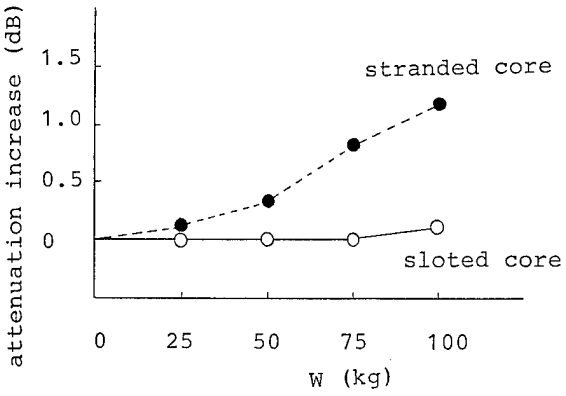



Fig. 3 Result of squeezing test

### 2). Tension member

A tension member is usually used in a optical fiber cable to provide tensile strength to installation elongation and compressive strength to thermal shrinkage. Tension member materials used in general are shown in table 3.
The Kevlar and the Kevlar FRP were studied and adopted as a tension member due to a small diameter, flexibility, light weight, non-metallic composition.

Table 3. Comparison of tension member

| | Steel wire | GFRP | Kevlar FRP | Kevlar |
|---|---|---|---|---|
| Tensile strength ($kg/mm^2$) | 150-200 | 120-150 | 120-150 | 141 |
| Modulus of elasticity ($kg/mm^2$) | 21000 | 3000-5000 | 6000-8000 | 7700 |
| Modulus of thermal expansion($X10^{-6}/°C$) | 11 | 6-8 | about -4 | about -4 |
| Specific gravity | 7.8 | 2.0-2.2 | 1.2-1.3 | 1.38 |
| Flexibility | ——— | bad | good | better |

## 3. Cable structure

A cable structure which is adopted as an optimum configuration for a small diameter, light weight, and high strength cable, is shown in Fig. 4 and its outline is in table 4.

Table 4. Cable specification

| item | | Specification |
|---|---|---|
| Optical fiber | Type | GI |
| | core/clad ($\mu m$) | 50/125 |
| | dia. (mm) | 0.6 |
| Cable | dia. (mm) | 4.3 |
| | weight (kg/km) | 15 |

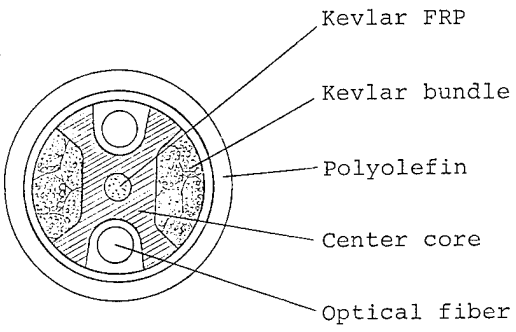



Fig. 4 Cable structure

The optical fiber used here is the tricoated, primary, buffer and secondary coating. The outer diameter of polyamide secondary coating is 0.6mm.
The fiber is prooftested with the load which is more than 1% elongation strain.

The cable is composed of non-metalic materials.
The best feature of this cable is in a slotted polyolefin center core. It has a Kevlar FRP tension member which is expected to mainly work as the compressive strength to thermal shrinkage, and two kinds of spiral grooves.
Smaller grooves for optical fibers and larger grooves for a high density Kevlar bundle which is stranded and tightly inserted.
The Kevlar bundle can change its shape to be housed fully in the grooves so the tensile strength is stronger than that of steel wire in a same cable diameter.
The center core and sheath are made of the frame retardant polyolefin.

Table 5. Tests and results

| Item | Test condition | Result |
|---|---|---|
| Temperature characteristics | measuring length :100m<br>temperature :from -60°C to 80°C | The maximum attenuation increase was less than 0.1dB/km. |
| Bending | bending diameter :100,90,80,70,60 50,40,30 mm<br>bending angle : 360° | The attenuation increase was not recognized over 70mm. |
| Cyclic-bending | bending diameter :70mm<br>bending angle :±360°<br>bending cycle :30cycles | The attenuation increase was not recognized. |
| Tensile-strength | measuring length :2m | The tensile load corresponding to 0.5% cable elongation was 100kg.<br>The breakage tensile strength was more than 250kgf. |
| Compression | compression board :50mm square metal plate | The attenuation increase was not recognized under 200kg. |
| Impact | impact load :1kg weight 25mm diameter column | The attenuation increase was not recognized under 0.25kg m.<br>No residual attenuation was recognized under 2kg m. |
| Squeezing | bending length :2m<br>bending diameter :40mm<br>bending cycle :5 cycle | The attenuation increase was less than 0.02dB under 50kg.<br>No residual attenuation was recognized under 80kg. |
| Flexibility | See Fig. 10. | See Fig. 11. |
| Flame test | horizontal specimen flame test | self-extinguished |

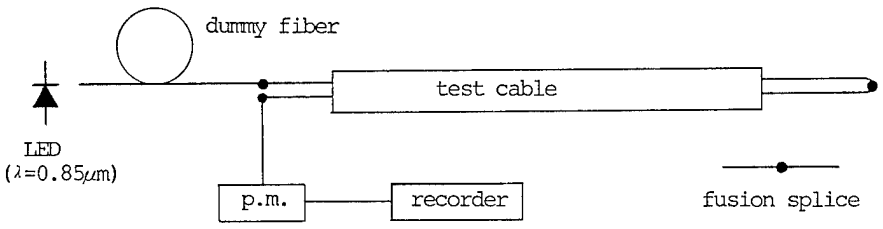



Fig. 5 Setup for measuring attenuation

## 4. Tests and results

Many kinds of tests were conducted for this cable. Testing methods and results obtained are listed in Table 5. The measuring method of attenuation change is shown in Fig 5.

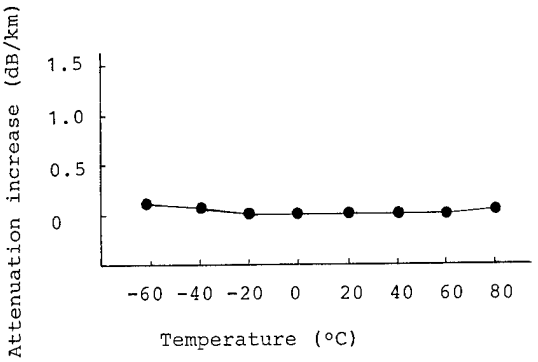



Fig. 6 Temperature characteristics

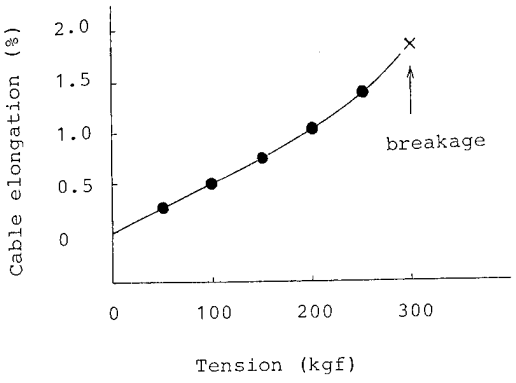



Fig. 7 Tensile strength test

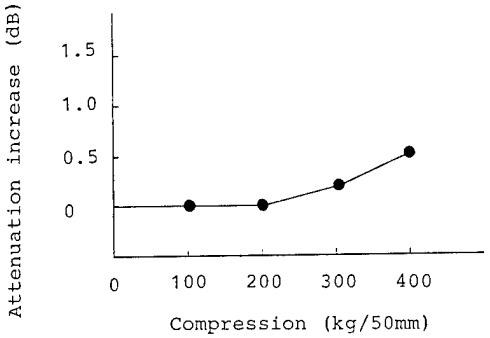



Fig. 8 Compression test

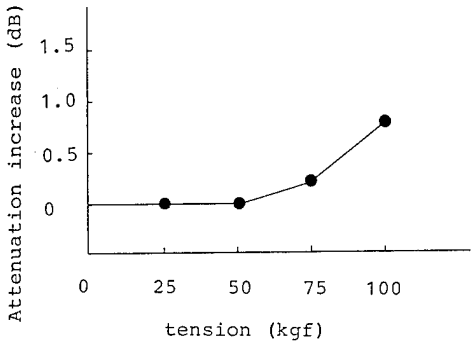



Fig. 9 Squeezing test

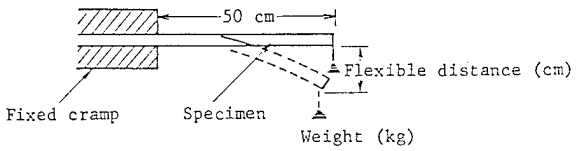



Fig. 10 Method of flexibility test

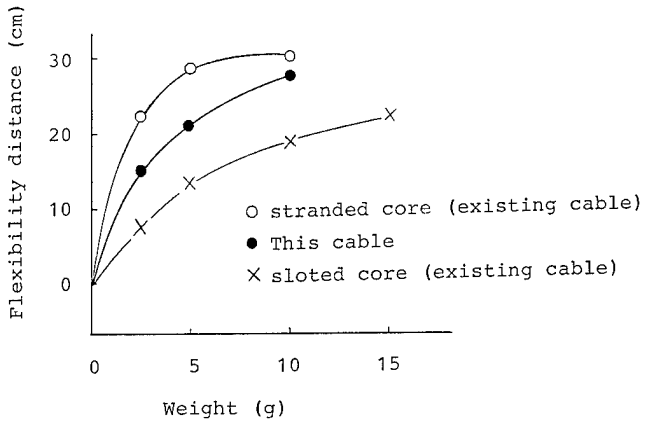



Fig. 11 Flexibility test

## 5. Connector and Reel

### 1). Connector

Generally the cable is connected to a cable or an optical device. A multi-connector shown in Fig. 12 was used for this cable because it can easily become a pulling cable end and can connect and disconnect.
In the whole line the weakness often appears around a connector, especially in the joint of a cable tension member and a connector.
After several trials the good Kevlar fixing method was developed and gained very strong connection which is more than 200kg.
The connector is water proof and easily becomes a pulling end by screwing a pulling eye into a connector.

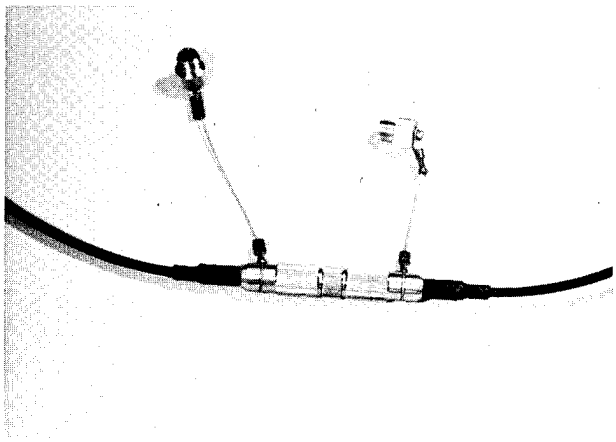


Fig. 12 Connector

### 2). Reel

To accomplish a high mobility cable system, it is very important to make an extremely light weight reel and it has to be easy to handle.
A light and movable reel which is specially designed is shown in Fig. 13.
This reel can house the 1km long cable and the total weight is less than 20kg including the connectors at both ends and the reel.

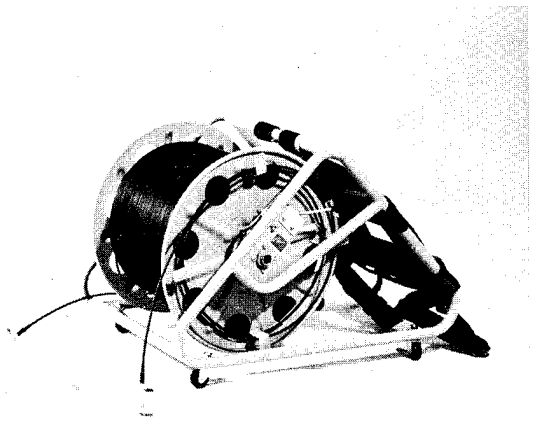
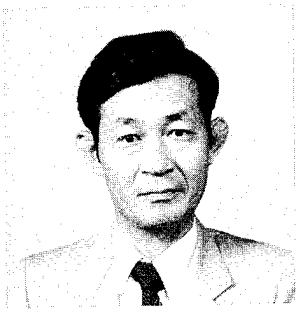


Fig. 13 Reel

## 6. Conclusion

A small diameter, light weight, high tensile and compressive strength, and flexible optical fiber cable has been developed with a higher tensile strength connector and a light reel.
The central plastic slotted core and outer cable sheath are made of flame retardant and the cable is totally composed of non-metallic material.
Housing Kevlar bundles fully in a slotted core enables the cable to have a very high tensile strength and a small diameter.
As nylon coated fibers are loosely housed in grooves, the mechanical properties such as compression, impact, bending and squeezing are satisfactory and the optical attenuation change is minimal between -60°C to +80°C.
This cable is very advantageous for using outdoor such as emergency cables, militaly communicaiton systems and, so on.

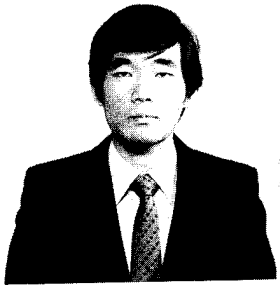


Nobuyasu Sato

Fujikura Ltd.

1440 Mutsuzaki,
Sakura, Chiba, 285,
Japan

Mr. Sato received the B.S. degree in Telecommunication Engineering from Tohoku University in 1966 and has been engaged in development of telecommunication cables. He is now a chief of telecommunication cable section and member of IECE of Japan.

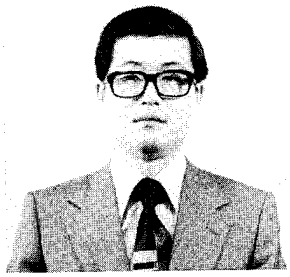


Katsuyuki Seto

Fujikura Ltd.

1440 Mutsuzaki,
Sakura, Chiba, 285,
Japan

Mr. Seto received the B.S. degree in Electronic Engineering from Yokohama National University in 1980 and has been engaged in development of telecommunication cables. He is now an engineer of telecommunicaiton cable section and a member of IECE of Japan.

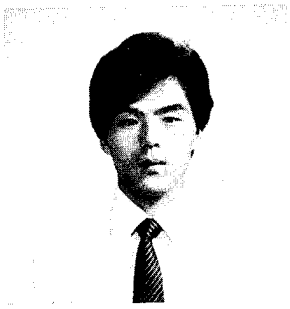


Yasuyuki Sugawara

Fujikura Ltd.

1440 Mutsuzaki,
Sakura, Chiba, 285
Japan

Mr. Sugawara received the B.S. degree in Telecommunication Engineering from Tohoku University in 1969 and has been engaged in development of telecommunication cables. He is now a chief of optical cable section and member of IECE of Japan.

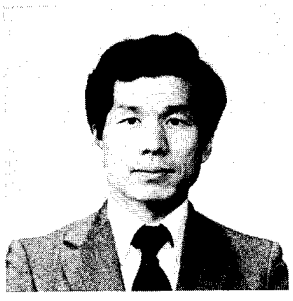


Hiroichi Katayose

Fujikura Ltd.

1440 Mutsuzaki,
Sakura, Chiba, 285,
Japan

Mr. Katayose received B.S. degree in Electronic Engineering from Nagaoka Technological University in 1983 and has been engaged in development of telecommunication cables. He is now an engineer of telecommunication section and a member of IECE of Japan.



Hiroshi Yokosuka

Fujikura Ltd.

1440 Mutsuzaki,
Sakura, Chiba, 285,
Japan

Mr. Yokosuka graduated in Mechanical Engineering Course from Tokyo metropolitan Technical junior College in 1967 and has been engaged in development of telecommunication cables. He is now an assistant cheif of telecommunication cable section.

# SINGLE FIBRE CABLES FOR MILITARY APPLICATIONS

M.M. Ramsay, P.G. Hale, R. Sutehall

Standard Telecommunication Laboratories,
Harlow, Essex, CM17 9NA, UK.

## Abstract

A family of cables are described, that have been designed at STL, to meet a wide range of military applications. The methods of manufacture and details of performance are given. The cables all have one feature of their manufacture in common in that all have a single dual or triple coated fibre, surrounded by straight or double contra-helical strands of Kevlar 49 held in close register by a binding of polyester yarn. Four variants illustrate the versatility of this manufacturing method and include single mode and a wide variety of multimode fibres.

## Introduction

Several cables have been designed using either graded index multimode or single mode optical fibres. Conventional single fibre cables generally comprise a central (neutral axis) fibre, which can be loose or tight buffered, surrounded by a helically laid strength member, commonly Kevlar 49, and an outer extruded sheath. Such cables suffer several disadvantages where high strength-to-weight or strength-to-size ratios are required. The disadvantages arise principally from any air gaps in the cable. These lead to an unnecessarily thick sheath, to an increased overall weight and diameter and to poor low-temperature performance. Obviously, tight fibre packaging and well compacted Kevlar 49 are indicated for minimum cable diameter. The philosophy adopted in the design of this family of cables has been to place Kevlar 49 yarns as strength members around a central tight buffered fibre and to bind this structure together with a polyester wrap. This procedure minimises dead weight and overall diameter. The wrap only adds a few tens of grams per kilometer and less than 100 μm to the overall diameter, in marked contrast to a conventional polymer sheath. A typical cross-section is shown in Fig. 1.

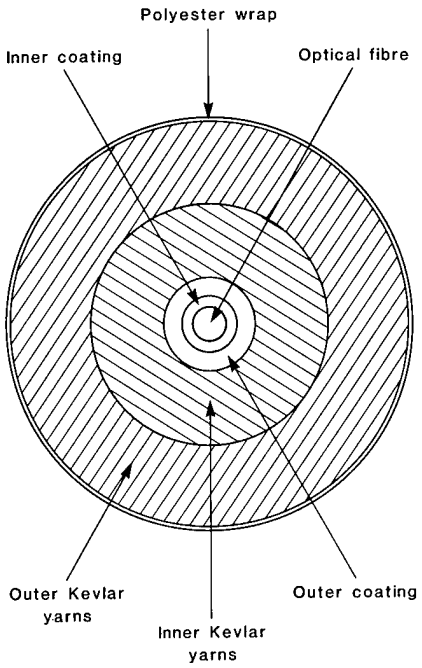



Fig. 1 Typical cable cross-section

## Applications

Variants of the generic cable design could meet performance requirements in a variety of both military and civil applications where the transmission properties of optical fibre offer significant advantages over existing techniques or where no other method is currently available. Particular benefit can be gained in systems requiring high information rates over long distances or where wavelength multiplexing allows simultaneous two-way transmission of, for example, command signals and return data. Specific applications of interest at present are in air-to-surface deployment, missile payout, underwater vehicles, sonobuoys and aerial tether cables. Although cable and fibre parameters will need to be matched to the application, the flexibility of the basic design is illustrated by the examples in the following sections.

## Cable Fabrication

All the cables have been constructed in the purpose built vertical strander shown schematically in Fig. 2, with the optical fibre passing up the axis of the machine. Two separate turntables, each accepting up to eight bobbins of yarn, can each be held stationary or rotated in either direction with individual closed loop speed controllers; this configuration allows straight, helical or contrahelical laid cables to be manufactured with any desired lay-length and Tex count. Back tension of each Kevlar yarn is individually maintained at a constant value using mechanical tensioning devices. The Kevlar stranded fibre is then passed up through the axis of a high speed rotating bobbin which applies the wrapping material, around a capstan and finally on to a take up drum. The tightness of the wrap is determined by the windage effect of the rotating bobbin, with increased speed tightening the wrap. If additional tension is required, the wrapping material can be passed through a flyer, the windage effect of which can be altered suitably. Crimped polyester wrapping material has been used on all cable to date.

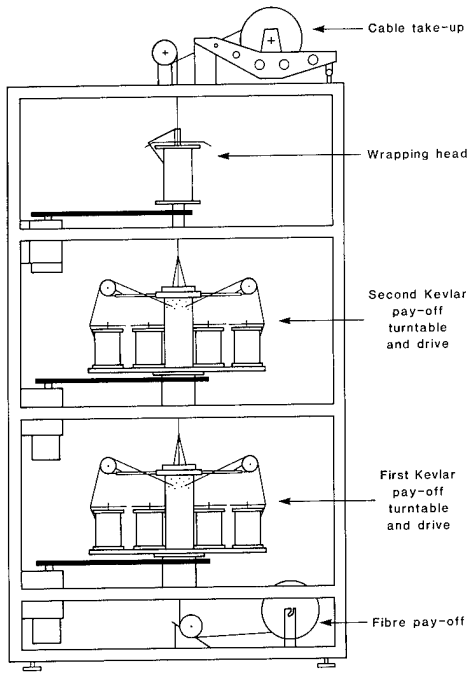



Fig. 2 Cable strander - schematic

The machine has proved very reliable in use, any imperfections in the cable being attributable solely to setting up errors by the operator. Line speed is generally limited by the wrapping head speed. For instance the 0.84 mm diameter cable used as an example below is made with a wrapping head speed of 7000 rev/min. dictated by the desired wrap tension, giving a line speed of 4.2 m/min. This may appear slow, but in a production environment the technique lends itself to a parallel process whereby a common drive system could be used to service multiple strander turntables and wrapping heads. Operator intervention is minimal. Once the machine is loaded it is left to run unattended, and can be switched off automatically as the fibre runs out, or after a predetermined time.

The maximum length of cable made has been 5 km. This, however, is only indicative of the fibre lengths that have been used, the machine itself having a much greater capacity. The maximum continous length of cable that can be made is limited currently by its size. For instance, in the 0.84 mm diameter cable example below a continuous length of approximately 18 km of cable can be made. Multiple wrapping heads could double or further increase cable length.

## High Speed Deployable Cable

For high speed pay-off applications a design target requires proof-test strains of about 2%. The use of tensile reinforcement reduces this level significantly and a proof strain of 1% becomes acceptable. The contribution of the fibre towards overall cable strength reduces as more tensile reinforcement is added until, in the extreme, the additional strength member only supports its own weight. In some intermediate situation, any axial load is taken jointly by the strength member and fibre, and the fibre is required to withstand the strain seen at this load

Since the time of application of the load is extremely short, a high probability of survival will be found close to the inert strength of the fibre[1]. It can therefore be argued that the fibres can be used up to the proof-test level. In practice however it would be prudent to ensure that the strain corresponding to the peak load is between 50% and 75% of the proof strain.

For example a typical cable consists of a 0.2 NA, 30/125 μm fibre with protective coatings 0.3 mm O.D., proof-tested at 1% strain, surrounded by three 217 dTex Kevlar yarns parallel laid, held by the polyester wrap. This gives an overall diameter of 0.55 mm. This version of the cable has been tested in simulated high speed payout conditions. Attenuation on a 50 mm diameter former was 4 dB/km at 850 nm and transmission of color video signals down a 2 km path length was unimpaired at pay-off speeds approaching Mach 1.

## Free-flooding Cables

For undersea applications at depth and consequently high hydrostatic pressure, it is important to avoid the generation of localised forces on the fibre as these will cause excess attenuation. Conventional cables are generally prone to such losses unless a pressure tube approach is used, which adds bulk to the structure. The wrapped cable design gives a free flooding capability which allows fluid to reach the surface of the coated fibre. This gives inherently good pressure performance.

For applications where the wrap alone does not provide sufficient handling or surface strength, a polymer sheath can be extruded over the cable core. Because the wrap constrains the Kevlar yarns, the cable core has a well defined and essentially constant diameter, and this allows a minimal sheath thickness to be applied: as low as 130 μm has been achieved. Sheathed versions of the cable, however, exhibit worse hydrostatic pressure performance.

## Fibre Packaging

The types of coating applied to an optical fibre influence both mechanical and optical performance and the requirements are conflicting. In general, for small overall package diameters a hard coating affords better mechanical protection to a silica fibre but a soft coating is desirable to buffer against microbend effects. Given the cable size, microbending under radial pressure is expected to be more severe than, say, in conventional landline telecommunications cable. Therefore, following the design principles laid down by Gloge[2], a twin-coat package consisting of a soft inner silicone resin layer with a hard shell uv-cured acrylate coating was developed. This package is predicted to have an upper service temperature above 100°C.
A cross-section of the package and cable is shown in Fig. 1.

## Fibre Designs

Multimode: It would be very attractive to use industry standard 50/125 0.20 NA multimode fibre, but in practice, significant attenuation increments are found when the cable is wound onto small diameter formers under high loads. Consideration of generalised microbend models such as that developed by Olshansky[3] leads the designer towards a reduced core/cladding diameter aspect ratio and increased NA. Some advantage can also be gained by increasing fibre diameter but size constraints, bend radius, cost considerations and the desire for compatibility with off-the-shelf connector technology led to diameter being fixed at 125 μm from the outset. Early trials with fibres having reduced core diameters showed minimal microbend and winding increments for a 30/125 design. Subsequent consideration of launch efficiency from LED sources led to the final design being fixed as 35 μm core diameter and up to 0.25 NA - well within the fabrication capability of conventional vapour deposition processes.

Fibre performance for the chosen design has been excellent, with negligible attenuation increments through processing to cable wound on 50 mm diameter formers, and with absolute attenuation levels of 4 dB/km at 0.85 μm wavelength being readily and repeatably achieved.

Single Mode: For future applications requiring higher bandwidth over longer distances, the use of single mode fibre becomes attractive. The factors affecting performance of single mode fibre are somewhat different. Accordingly, an empirical study of cable performance has also been undertaken to give a qualitative assessment of potential using telecom-standard 8 μm core, 0.05% refractive index difference, single mode fibre.

## 0.84 mm Diameter Cable

Most experience to date has been obtained on a cable designed for a particular stringent requirement, the target and achieved parameters of which are listed in Table 1.

Table 1

| Parameter | Target | Achieved |
|---|---|---|
| Diameter: | 1 mm (max.) | 0.84 ± 0.04 mm |
| Tensile strength: | 180 N break load<br>60 N service load | 181 N @ 0.6% strain |
| Minimum bend radius: | 25 mm | 25 mm |
| Crush resistance: | 1000 N: applied between a 25 mm radius mandrel and a flat plate. | Cable integrity unaffected |
| Weight: | 1 kg/km (max.) | 0.6 kg/km |
| Attenuation: | 4 dB/km @ 850 nm | 3.6 dB/km achieved on dispenser simulator |
| Temperature Performance: | Unspecified | 4.5 dB/km max. total loss (-40°C to +70°C) |
| Torsional Loading: | To withstand 360 deg. twist over 100 mm | Cable integrity and optical performance unaffected |

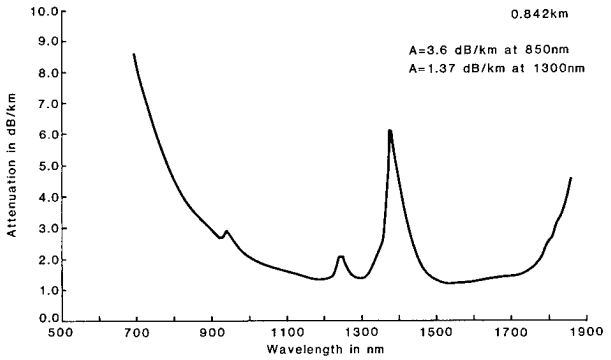



Fig.3 Multimode cable attenuation

The multimode cable consists of a 35/125 fibre package as previously described, 16 x 217 dTex Kevlar yarns contra-helically laid with lay length 60 mm, and continuous 150 dTex 30 strand polyester wrap with 1667 turns/m. As previously mentioned, cable production speed is 4.2 m/min. A number of cables have been produced and further performance data is given below.

Performance testing of cables in pseudo-service conditions was achieved by dispensing down a flooded mine-shaft and in deployment at sea. In both cases the depth achieved was monitored using data output from a pressure transducer in the falling body, and optical signal levels were continuously measured to allow calculation of fibre attenuation changes. Table 2 shows average attenuation levels for five recent 1150 m lengths of 35/125 fibre cable. In winding and subsequent dispensing to a depth of 1000 m, similar cables have shown attenuation changes of less that 1 dB/km. Figure 3 shows the spectral attenuation curve of a typical cabled fibre - note that the fibre design allows use at the 1300 nm window. The most recently produced fibres and cables have a lower average loss at 1300 nm of 1.1 dB/km.

Table 2

| | |
|---|---|
| Numerical aperture: | 0.228 ± 0.005 |
| Core diameter: | 34.9 ± 1.3 μm |
| Fibre attenuation @ 850 nm: | 3.45 ± 0.25 dB/km |
| Cable attenuation @ 850 nm: | 3.4 ± 0.3 dB/km |

Monomode cables with the same mechanical characteristics have been fabricated with fibres having single hard coatings and the dual package as described to simulate practical extremes. The single coating fibre showed significant cabling increments at 1.3 μm whereas the dual package had stable performance. Figure 4 depicts the spectral attenuation of a dual package cable, and spot attenuation values of 0.41 dB/km at 1300 nm and 0.23 dB/km at 1550 nm show that cabling losses are negligible.

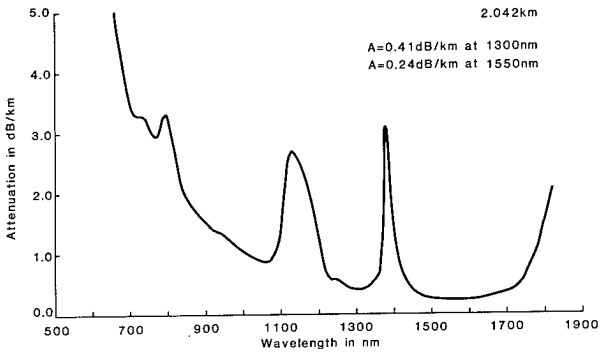



Fig.4 Single mode cable attenuation

## Wide Temperature Range Cables

Although performance at low temperatures was not specified for any of the above cables, it was found that the 0.84 mm cable showed virtually no attenuation increment at -40°C. A similar cable was tested at -70°C and again showed a negligible attenuation increment. There were therefore grounds for assuming that this type of construction would form a useful basis on which to develop a single fibre cable suitable for avionic applications.

## Design Requirements

The cable to be developed had to operate over an extended avionic temperature range of -65°C to +155°C. This necessitated the use of high temperature polymers, which in turn can only be extruded over primary coatings that will withstand the extrusion temperatures these require. Since, in this type of application, many connectors are used in comparatively short runs, a large core, high NA fibre is required.

## Fibre

The fibre developed for this cable has an overall diameter of 300 μm ± 5 μm and a core diameter of 200 μm ± 5 μm; the N.A. falls in the range 0.3 to 0.35 with a quasi-step index profile. The fibre is radiation hard within the short term recovery requirements of avionic specifications.

## Coatings

This fibre is coated with a thermally cured silicone resin applied on-line with fibre pulling. Thermogravimetric analysis of this coating has shown that with proper control of the constituents and care over the final state of cure, negligible weight loss can be achieved at temperatures up to 400°C. Such coatings are suitable for subsequent extrusion of high temperature fluorinated polymers. After trials the polymer selected for this application was ethylene-tetrafluoroethylene (Tefzel 200 $^{R}$ ) which is extruded to a final diameter of 1 mm overall.

## Cable Construction

The developed cable follows the construction shown in Fig. 1 but with the addition of a polymer sheath. The coated fibre is surrounded with double contra-helically stranded layers of Kevlar 49, each layer consisting of 5 strands of 1580 dTex yarn. The cable sheath is also ethylene-tetrafluoroethylene and gives a final diameter of 2.5 mm.

## Testing

A typical avionic test plan was prepared for this cable. The requirements of this specification have been satisfied in all tests. The following points are worth noting:

1. In the tensile test the load on the cable was increased to 250 N and held at that value for 1 minute. The corresponding extension was about 0.2%.

2. With a tensile load of 50 N, the cable withstood a total torsion corresponding to 10 turns per metre.

3. In the flammability test, it was demonstrated that the cable sheath is self extinguishing.

4. If the cable were to kink under bending stresses the resulting low bend radius could snap the fibre. This cable structure has passed the kink test proposed by the British Standards Institute[4].

5. Cable with 0.3 NA, quasi-step-index fibre, was temperature cycled between -65°C and +155°C for ten cycles and then between -65°C and +25°C for a further 20 cycles. After six cycles between -65°C and +155°C the cable demonstrated a stable response with consistent variation in attenuation of less than ±1 dB/km between high and low temperatures on successive cycles. On the reduced temperature range the variations were less than ±0.25 dB/km.

6. The thermal shock test was carried out by rapidly immersing the cable in a bath of isopropyl alcohol cooled with dry ice to -65°C. Later the cable was transferred from this cold bath to a water bath at +25°C. No perceptible change in attenuation was observed during either part of this test.

7. Other tests specified are cyclic flexing, bend, crush, impact, static cut-through, air ageing and tear resistance. A wide variety of contaminating fluid and solvent tests are also included. Cables passed all these tests.

Most of the cables produced to date have shown an attenuation at 850 nm below 5.0 dB/km and at 1300 nm approximately 1 dB/km.

## Sheathed Cable for Use at High Hydrostatic Pressures

For certain applications it is necessary to both operate in a high pressure environment and provide good abrasion resistance. A single mode, single fibre cable of this type has been supplied to the US Navy for testing. The cable is to be used at 1.3 μm and 1.55 μm and must have an attenuation no greater than 0.5 dB/km at either wavelength at pressures up to 10 kpsi. The cable was designed to have an axial working load of 900 N and a breaking load greater than 3.5 kN.

### Cable Design

Two cable types were developed to meet this specification, cross-sections of which are shown in Fig. 5.

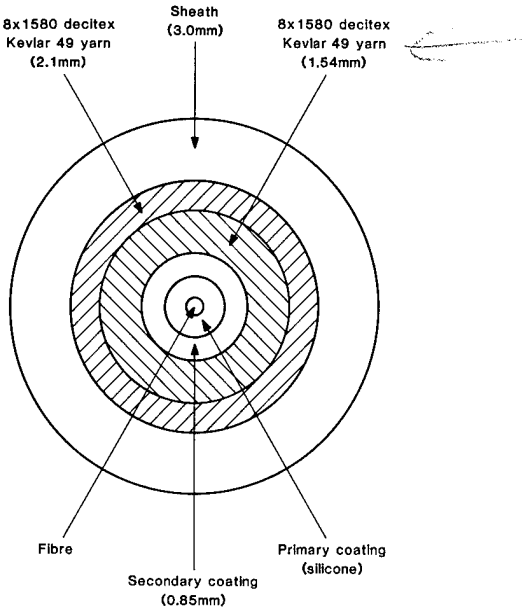



Fig. 5 Kevlar cable cross-section (served and parallel designs)

A design study and mechanical model showed that the tensile strength could be achieved by using 16 strands of 1580 dTex Kevlar 49.

Both cable types employed silicone resin buffered, nylon 12 coated single mode fibres with an overall diameter of 0.85 mm. The nylon coating process induces a guaranteed compression of 0.2%. Therefore, at a cable strain of 0.45%, fibre strain is only 0.25%. The stranded package with a diameter of approximately 2.1 mm was oversheathed to a diameter of 3 mm with Hytrel 7246, a polyester elastomer chosen for its wear resistance and flexibility, and which consistently gave minimal attenuation increments to the completed cable.

The straight laid version of the cable kept the same format, and in this case the polyester wrap is particularly important as it holds the entire Kevlar/fibre assembly together and maintains fibre centrality prior to sheathing.

Cable prototypes were constructed which showed excellent optical performance. However, when subjected to hydrostatic pressure, intrinsic cable attenuation increased dramatically above 5,000 psi, which was attributed to non-uniform radial collapse of the cable. This was overcome by development of a filling technique using thixotropic material which eliminated voids and irregularities within the Kevlar filaments. The wrapping technique is again important here, as this process forces and distributes the thixotropic material through the structure. The use of filling material allows an even distribution of pressure over the secondary coated fibre which is known to give good optical performance under hydrostatic pressure.

## Performance

Optical performance has generally been excellent with near zero cabling attenuation increments at both 1300 nm and 1550 nm. Figures 6 and 7 show spectral attenuation curves for each type of cable.

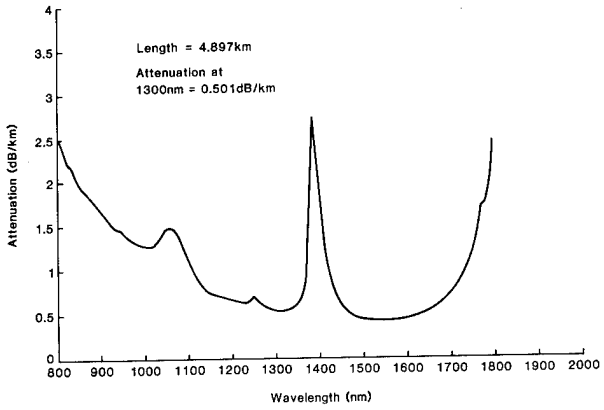



Fig. 6 Spectral attenuation – served Kevlar cable

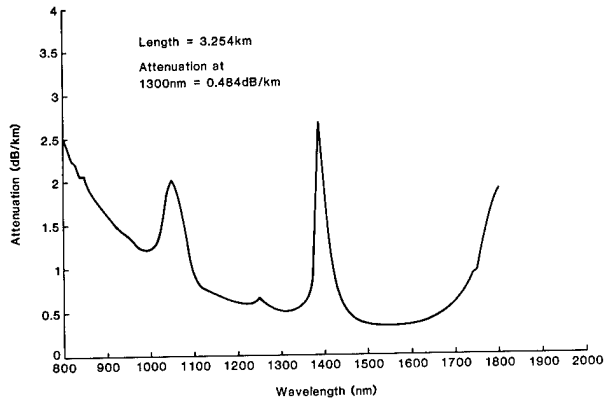



Fig. 7 Spectral attenuation – parallel Kevlar cable

Attenuation measurements have been conducted on served cable samples at high hydrostatic pressures, and Fig. 8 shows a plot of incremental attenuation versus pressure for the filled type. The reason for the transient increments in this experiment is not understood, but in each case the loss recovered, and showed no overall increase at 10,000 psi.

Tensile properties have been measured on several samples and typical results are shown in Fig. 9. The diagram consists of the average of three measurements made on an Instron machine over a short, 500 mm, gauge length. Note that there is a low modulus at low strains which is probably due to sheath contraction during manufacture, and that with the low strain knee removed, the cable has a strain of 0.4% – and hence the fibre a strain of 0.2% – at the working load of 900 N, within the design target of 0.45%.

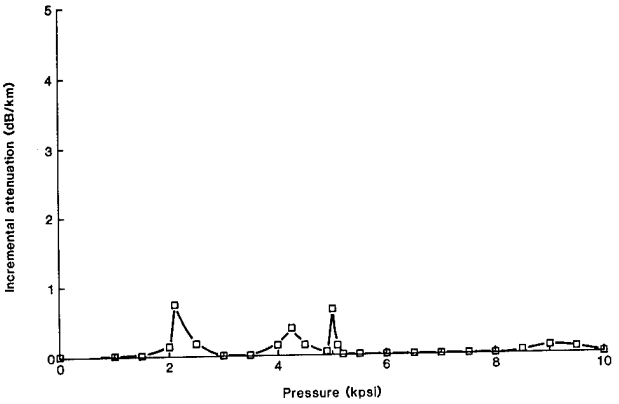



Fig. 8 Attenuation of Kevlar cable with respect to hydrostatic pressure

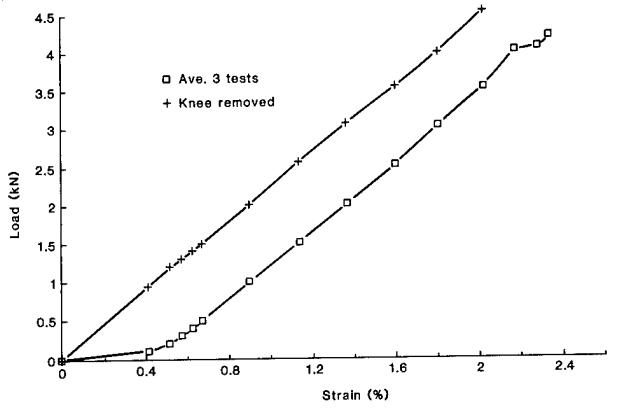



Fig. 9 Kevlar cable load-strain diagram

Tests are planned on 150 m lengths of cable when optical measurements will be made to determine fibre elongation and show whether fibre elongation occurs before the Kevlar is taking its share of the load. This effect is common with Kevlar-reinforced cables as the material has a very small compressive modulus and therefore does not counteract sheath retraction effects. With other cables it has been shown that the fibre does not see longitudinal strain during the low modulus portion of the curve.

## Conclusion

A versatile method of manufacturing single fibre cables has been described. The versatility has been demonstrated by describing four cables for very different applications that have been produced on the same machine.

Acknowledgements

A major part of this work has been supported by the Procurement Executive, Ministry of Defence (Directorate of Components, Valves and Devices) and sponsored from the Admiralty Research Establishment, Portland, the Royal Aircraft Establishment, Farnborough and the Royal Armaments Research and Development Establishment, Sevenoaks. The authors are grateful for the contributions from many colleagues within the Ministry of Defence, Standard Telecommunication Laboratories, Defence Systems Division and Component Division of STC plc. They also thank the Directors of Standard Telecommunication Laboratories for permission to publish this paper.

References

1 I.F. Scanlan, J.G. Lamb, W.J. Duncan, "Optical fibre under static strain: establishing the survival probability in service from tensile tests data", IEE Colloquium on the Implementation and Reliability of Optical Fibre Cable Links, London, June 1984

2 D. Gloge, "Optical-fiber packaging and its influence on fiber straitness and loss", Bell Syst. Tech. Jour. Feb.'75, 54, 2, pp.265-262

3 R. Olshansky, "Distortion losses in cabled optical fibers", App. Optics 1975, 14, pp.20-21

4 British Standard Institute, Test proposed for optical cables, 1984



M. Murray Ramsay obtained a B.Sc. from University College, London in 1952. He is a Chartered Physicist and Fellow of the Institute of Physics. He joined STL after graduating in 1952 and was a founder member of the team set up in 1958 to study optical communication systems. He acted as consultant to ITT-EOPD Roanoke in 1973 when work on optical communication systems was started there. He later returned to STL and is currently Chief Research Engineer for Optical fibre cables.



Dr. P.G. Hale graduated with an honours degree in Engineering Science and Economics from the University of Oxford in 1973. After a short period with Instron Limited he returned to the University of Oxford where he gained a D.Phil. on the subject of the metal coating of optical fibres in 1979. He joined STL in 1980 as a Research Fellow in the Optical Fibre Cable Group and currently manages the Sensor Engineering Laboratory.



R. Sutehall joined STL in 1971 to work on extrusion techniques. In 1979 he obtained a full certificate in the City and Guilds Plastics Technicians course. He is currently a Senior Research Engineer investigating all aspects of extrusion technology applied to optical fibre cables.

# DEVELOPMENT OF OPTICAL CURL CORD CABLE USING GLASS FIBER

H. HORIMA, M. DAZAI AND M. HAMAGUCHI

SUMITOMO ELECTRIC INDUSTRIES, LTD.
1, TAYA, TOTSUKA-KU, YOKOHAMA 244, JAPAN

## Abstract

We have developed optical curl cord cable, using silica type glass fiber, similar to the curl cord with regular telephones.
This cable is sufficiently flexible to freely expand and contract and possesses sufficient mechanical strength to withstand long-term use for the same expansion/contraction repeated motion.
The optical curl cord cable is very suitable for use in controlling such mobile devices as robots, cranes, and other devices which operate under high voltage or high noise conditions.
This paper describes the manufacture, transmission characteristics and physical properties of the newly developed optical curl cord cable using silica glass fiber.

## 1. Introduction

Recently, optical fibers are coming to be widely used not only for public telecommunication systems but also for data transmission, LAN (Local Area Network) systems, and so on. And according to the requirements of those systems, suitable types of optical fibers, cables and equipments have been developed.

Moreover, because of their excellent characteristics such as small size, light weight and immunity from electro-magnetic interference, optical fibers are to be considered for use in controlling such mobile devices as robots, cranes, and other devices which operate under high voltage or high noise conditions.

However, optical cables in such mobile devices must be sufficiently flexible to freely expand and contract in conjunction with the movements of the device, and must have sufficient mechanical strength to withstand long-term use for the same repeated motion.

For that purpose we have developed optical curl cord cable, using silica type glass fiber, similar to the curl cord with regular telephones.

This paper reports on the design, manufacture, results of evaluation on the characteristics of the newly developed optical curl cord cable, and the prospect of practically using this cable.

## 2. Outline of optical curl cord cable

### 2.1 Requirements for cable characteristics

The characteristic requirements for the optical curl cord cable from the use and environmental conditions are summarized below.

(1) Easy to expand and contract repeatedly and no change of transmission characteristics during those motions.

(2) No deterioration of transmission characteristics before and after the repeated expansion/contraction of $10^5$ times.

(3) Almost the same size, compared with the conventional telephone curl cord.

(4) Stable characteristics for a wide temperature range.

(5) Mechanically strong enough.

To meet these requirements, we set the target to develop optical curl cord cable.

### 2.2 Bending characteristics for various types of optical fibers

The bending test was first investigated in order to find the promising fiber structure for optical curl cord cable.

Five kinds of fibers as shown in Table 1 were selected as the test samples, and the relationship between loss increase and winding times was examined when wound on mandrels with 10 mm, 20 mm and 30 mm in diameter.

Table 1 Test Fibers

| No. | Fiber Type | Abbrebiation | Core/cladding Diameter (μm) | NA | Protective Coating |
|---|---|---|---|---|---|
| 1 | Silica Glass Fiber | GI-50/125 | 50/125 GI(Graded Index) Type | 0.2 | Silicone and Nylon |
| 2 | | SI-80/125 | 80/125 SI(Step Index) Type | 0.25 | |
| 3 | | SI-100/140 | 100/140 SI Type | 0.30 | |
| 4 | PCF(Plastic Cladding Fiber) | PCF | 200/300 | 0.35 | Nylon |
| 5 | APF(All Plastic Fiber) | APF | 720/750 | 0.5 | Special Coating |

The test result is shown in Fig. 1.
From the figure the fiber structures of SI-80/125, SI-100/140 and PCF are found to be prospective as optical curl cord cable, because a preferable curl diameter of the cable is thought to be 10~20 mm taking the handling into consideration.

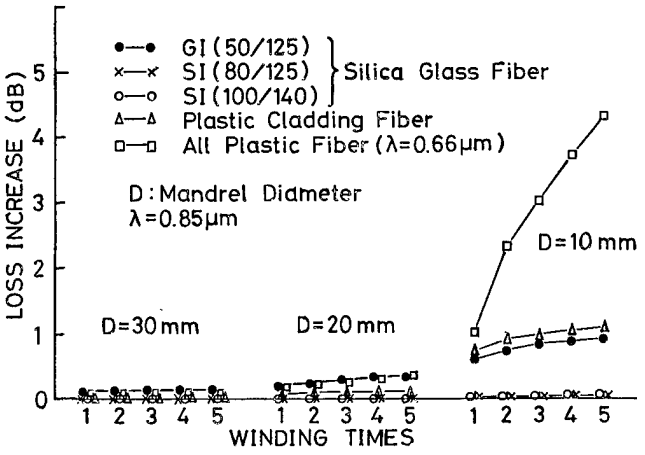



Fig. 1 Measurement result of bending characteristics for various types of optical fibers

## 2.3 Lifetime design of optical curl cord

As the fiber in optical curl cord cable is operated under small curled condition, the stress in the fiber is expected to become extremely large, compared with the fiber in ordinary optical cable.

For instance, when glass fiber of 125 μm cladding diameter is bent with the mandrel of 20 mmϕ, the bending stress of approximate 0.6 % is applied.

Consequently, the fiber lifetime design of optical curl cord cable must be treated carefully.

The lifetime of fiber $t_s$ is easily calculated by the following well-known equation. (1)

$$t_s = t_p \left(\frac{Ep}{Es}\right)^n \left[\left(1 - \frac{\ell n(1-F)}{NpL}\right)^{\frac{n-2}{m}} - 1\right]$$

where, L : Fiber system length (km)
F : Fiber failure probability
n : Stress corrosion parameter
m : Initial strength distribution parameter
$N_p$: Fiber failure probability on proof test (1/km)
$t_p$: Proof test time (sec.)
Ep: Proof test strain (%)
Es: Maximum service strain (%)

Although the system scale using this kind of optical curl cord cable seems to be small, the proof test level should be increased to a extent of 1.1% to guarantee the lifeteme of more than 10 years for the above-mentioned bending stress, using the parameters of NpL=0.01, F=0.01, n=22 and m=2.

## 2.4 Preliminary evaluation on manufacture and expansion/contraction characteristics

The transmission loss variation during the manufacturing process as shown in Table 2 and at expansion and contraction situation were also examined preliminarily in order to grasp the fiber suitability for optical curl cord cable using various kinds of fibers listed in Table 1.

The result is shown in Table 3. It is found that silica type fiber of SI-100/140 and PCF showed extremely stable characteristics for the cabling and expansion/contraction motion.

However, though the PCF showed the transmission loss recovery to the initial loss level, the remarkable loss increase of about 1 dB arised during curling process due to the occurrence of surface unevenness between glass core and plastic cladding. Therefore it is considered that the application area of the PCF curl cord cable might be limited.

Table 2 Cabling process of optical curl cord

| No. | Process | Content |
|---|---|---|
| 1 | Winding | Winding on to a mandrel |
| 2 | Heating | Heat treatment at 110°C for 5 minutes |
| 3 | Cooling | Plunging in water |
| 4 | Releasing | Release from the mandrel |
| 5 | Reverse winding | Reverse winding of heat-treated optical cable |

Table 3 Evaluation result of optical curl cord cable using various fibers

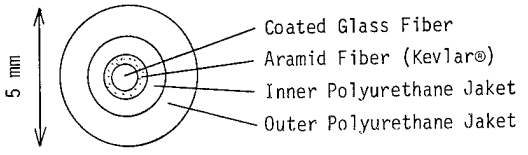
| Fiber Type | Loss Variation at 0.85 μm (dB) | | Remark |
|---|---|---|---|
| | Before and after manufacture | At the expansion of 6 times the initial curl length | |
| GI-50/125 | + 1.5 | + 1.0 | Curl cord length: 300 mm Curl diameter: 20 mm |
| SI-80/125 | + 0.7 | - 0.2 | |
| SI-100/140 | 0 | 0 | |
| PCF | + 0.1 | ~ 0 | |
| APF | + 14 | + 1 | |

## 3. Characteristics of optical curl cord

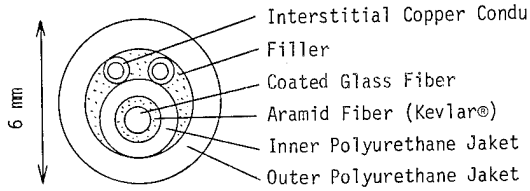
### 3.1 Structure of optical curl cord

According to the aforementioned investigation results, we designed and manufactured optical curl cord using silica glass fiber of SI-100/140, which is considered to be most suitable for it, and investigated the various characteristics in detail.

Cross-sectional view and the appearance of the prototype optical curl cord cables are shown in Fig. 2 and Photo 1, respectively.




(a) Non-Metallic Type




(b) Composite Type

Fig. 2 Cross-sectional view of optical curl cord cable

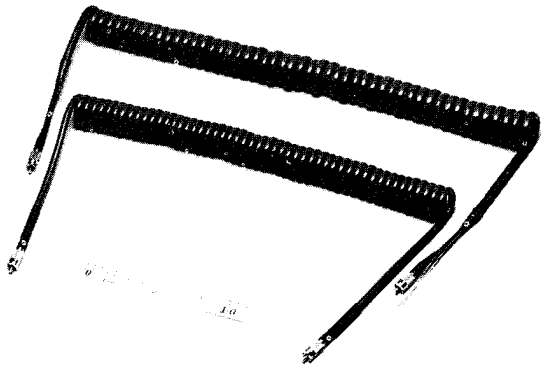


Photo 1 Appearance of optical curl cord cable

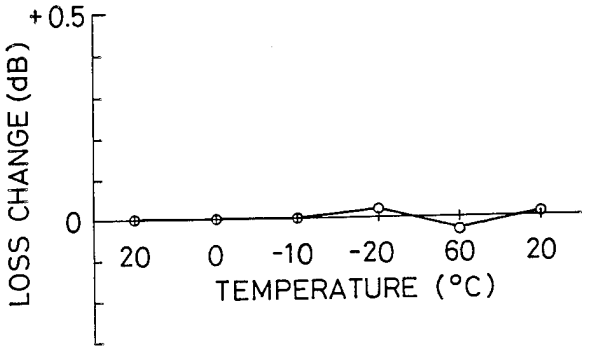
Both a non-metallic structure and a metallic structure comprising copper conductors were fabricated with curling diameter of about 20 mm and were mounted with optical connectors of Mini-BNC type at both ends.

### 3.2 Temperature characteristics

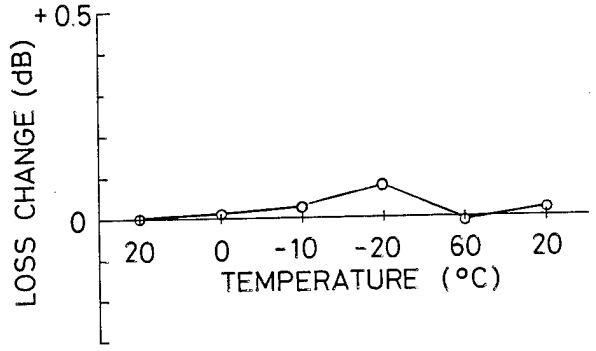
To examine temperature characteristics of optical curl cord cable, we carried out both heat cyclic test and heat shock test with the prototype cables shown in Fig. 2.

#### 3.2.1 Heat cyclic test

In the temperature range from -20°C to +60°C, we measured transmission loss change of optical curl cord both on initial contracted condition and on expanded condition at 6 times the initial contracted length. Fig. 3 shows the measurement result for nonmetallic type one. The maximum loss change was less than 0.1 dB at -20°C. Also in the case of metallic type, the similar measurement result was obtained. From these results, it appeared that the optical curl cord has stable characteristics against temperature change.




(a) At the initial length




(b) At 6 times the initial length

Fig. 3 Measurement result of heat cycle test for optical curl cord (nonmetallic type)

#### 3.2.2 Heat shock test

Next we conducted ten cycles of heat shock test in the temperature range from -20°C to +60°C, and loss change during the test was measured. We also checked fiber protrusion at Mimi-BNC type optical connector end surfaces.

As the result, as shown in Table 4 the transmission loss (including connector coupling loss) changes were almost 0, and fiber end surfaces showed no movement from connector end surfaces.

Table 4 Result of heat shock test

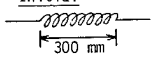
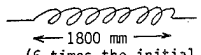
| Cable Type | Loss Change | Fiber Protrusion |
|---|---|---|
| Nonmetallic Type | 0 dB (N=8) | ~ 0 μm (N=2) |
| Metallic Type | - 0.06 dB (N=8) | ~ 0 μm (N=2) |

## 3.3 Mechanical characteristics

In order to grasp the mechanical characteristics of optical curl cord cable, we made expansion/contraction test of up to 6 times the initial length in some temperature conditions. The test conditions and results are shown in Table 5. Photo 2 shows the test view in temperature controlled chamber.

Even in the temperature conditions of -20°C and 60°C, the transmission loss variation was within ± 0.15 dB. And by the check of connector end faces after the test, no deterioration such as fiber protrusion was found.

Table 5 Result of expansion/contraction test for optical curl cord cable

| Test Condition | Temperature (°C) | Repeated Times (Times) | Loss Variation at 0.85 μm (dB) | |
|---|---|---|---|---|
| | | | Nonmetallic Type | Composite Type |
| 1 Initial   2 Expansion  ← 1800 mm → (6 times the initial length) | 20 | $10^5$ | ~ 0 | ~ 0 |
| 3 Contraction (Initial length) | - 20 | 1000 | + 0.10 | - 0.14 |
| 4 Expansion (Repeated) | + 60 | 1400 | - 0.04 | + 0.01 |

From these result, it was confirmed that the newly developed optical curl cord cable has good performance for expansion/contraction motion not only in normal condition but also in low and high temperature conditions.

Furthermore to know the mechanical strength of the cable against external forces, we did the mechanical test for impact and compression. The result was sufficient for practical use as shown in Table 6.

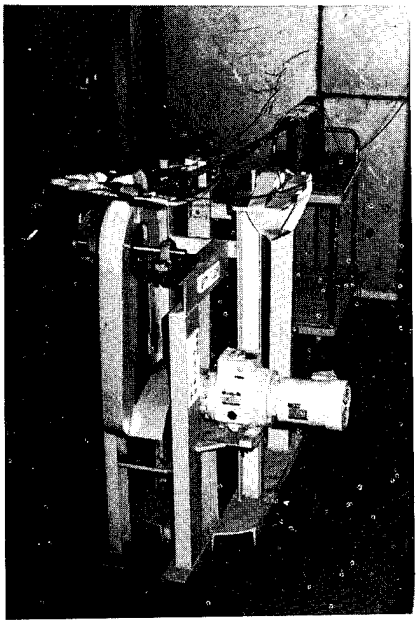
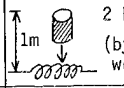
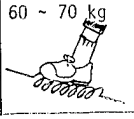


Photo 2 View of expansion/contraction test for optical curl cord cable in temperature controlled champer

Table 6 Impact and compression test of optical curl cord

| Item | Test Condition | Result |
|---|---|---|
| Impact |   2 kg ~ 1 m, 3 times (by a cylindrical weight of 25 mmφ) | No loss change |
| Compression |  60 ~ 70 kg Compression by a shoe heel | Maximum loss increase during compression: 1dB Loss change before and after test: 0dB |

## 4. Conclusion

We investigated the characteristics of many types of fibers to determine the most suitable fiber structure for the optical curl cord cable. According to the investigation results, we manufactured the prototype optical curl cord cable using silica glass SI fiber with 100 μmφ core and 140 μmφ cladding, and confirmed that the optical curl cord cable has very stable transmission, temperature and mechanical characteristics enough for practical use. This newly developed optical curl cord cable has the following features.

(1) Use of a low loss, silica-based fiber provides a transmission loss (exclusive of the loss through connectors at both ends) of 0 dB per 3 meters of optical curl cord.

(2) No deterioration in transmission characteristics was observed in expansion/contraction tests even in low and high temperature conditions.

(3) Transmission characteristics remain stable in compression and shock conditions which are expected under normal use.

(4) The curl radius is about 10 mm, allowing for easy handling and installation.

In order to guarantee long lifetime of optical curl cord cable of more than 10 years even at this bending stress, however, a little higher level of proof test should be needed, compared with the fiber in ordinary optical cable.

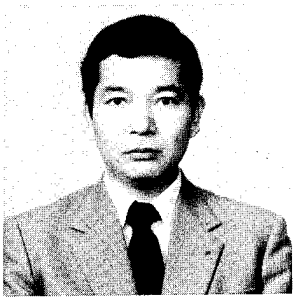
Accordingly, applications are seen in process control equipment, machine tools and robotics, mobile communications, test cables in noisy environments, keyboard links with computers and optical fiber patch panels.

Acknowledgement

The authors deeply acknowledge Mr. T. Takahashi and Mr. Y. Yumoto of Toyokuni-Sasaki Electric Wire and Cable Co., Ltd. and other persons for cooperation in developing the cable.

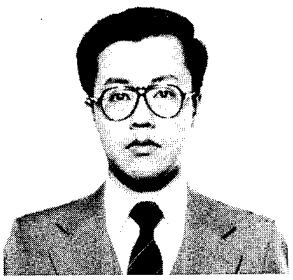
Reference

(1) Y. Mitsunaga et al., Electron. Lett., Vol. 17, No. 16, pp. 567, 1981.



Hiroaki Horima
Sumitomo Electric Industries, Ltd.
1, Taya-cho,
Totsuka-ku, Yokohama
Japan

Hiroaki Horima was born in 1947. He received the M.S. degree for engineering from Osaka University in 1972.
He joined Sumitomo Electric Industries Ltd. and worked on the development of CATV coaxial cables, multi-pair PEF-insulated junction cables and low loss unbalanced type cables.
Thereafter he concentrated on the development of optical fiber cables. He is a section manager of Fiber Optics Division in Sumitomo Electric Industries Ltd. He is a member of the Institute of Electronics and Communication Engineers of Japan.



Masahiko Dazai
Sumitomo Electric Industries, Ltd.
1, Taya-cho,
Totsuka-ku, Yokohama
Japan

Masahiko Dazai was born in 1955 and received the M.S. degree for engineering from Tohoku University in 1982. He joined Sumitomo Electric Industries, Ltd. in 1982, and has been engaged in development and design of optical fiber cables. He is a member of Fiber Optics Division in Sumitomo Electric Industries Ltd., and is a member of the Institute of Electronics and Communication Engineers of Japan.



Munehisa Hamaguchi
Sumitomo Electric Industries, Ltd.
1, Taya-cho,
Totsuka-ku, Yokohama
Japan

Munehisa Hamaguchi received a B.S. degree in Mechanical Engineering from Kyoto University in 1982. He joined Sumitomo Electric Industries, Ltd. in 1982, and has been engaged in development of optical connectors. He is a member of Fiber Optics Division in Sumitomo Electric Industries, Ltd., and is a member of the Japan Society of Precision Engineering.

# COMPACT LIGHTGUIDE CABLE DESIGN

P. D. Patel and C. H. Gartside, III

AT&T Bell Laboratories
Norcross, Georgia

## Abstract

A novel concept in lightguide cable design is presented. Fibers are packaged in bundles which are identified with color-coded binders. Several bundles are laid in a single large diameter filled tube forming the cable core. The cable is completed with the application of a reinforced polyethylene sheath. The design results in an extremely compact cable with excellent optical and mechanical performance. This cable will form the backbone of the nationwide AT&T Communications long-haul network. It is also recommended for interoffice trunking and subscriber loop applications.

## Introduction

During the past decade, a large variety of lightguide cable designs have been developed. Those used in the largest volume of applications are the ribbon[1-3], loose-tube[4-6] and slotted core[7-9] cable designs. Each design has its own unique advantages and disadvantages. In the ribbon cable, the cable core is formed by packaging the fibers into ribbons with adhesive-backed polyester tapes, assembling the ribbons into a rectangular stack and extruding a filled loose tube over the ribbon stack. The cable is completed with a reinforced polyethylene sheath. The primary advantages of ribbon cable are the option of factory installed connectors, greatly simplifying splicing in the field, and its compactness, allowing for up to 144 fibers in a cable of about one half inch in diameter. The compact structure and reinforced sheath also facilitate installation, particularly during difficult duct pulls.

With the loose-tube design, a filled loose tube is extruded over a fiber bundle, with typically up to twelve fibers per tube. Multiple tubes are stranded around a center strength member forming the cable core and the cable is completed with a polyethylene sheath. For rodent and lightning protection, a corrugated steel layer can be included in the sheath. However, the sheath is generally not reinforced for tensile loading. The major distinguishing features of this construction are the loose structure minimizing fiber microbending and the possibility of large fiber strain relief under tensile loads.

In the slotted-core design, multiple fibers are laid into grooves of a slotted core. The grooves are cut or extruded into the core with an oscillatory lay to a depth adequate to permit free fiber movement. The core is reinforced with either a steel wire or a fiberglass strength member. As in the loose-tube design, the cable is completed with the appropriate sheath. The major advantages of the slotted core design are the mechanical protection provided by the cable structure and the ability to fabricate the entire core in a single manufacturing operation. In the ribbon and loose-tube designs, multiple operations are necessary to fabricate the individual fiber units forming the core.

In all three designs, the fibers are loosely contained within the cable structure, resulting in excellent optical and mechanical performance. With proper design and manufacture, all three designs result in no increase in the optical attenuation. The loose structures allow for fiber movement and strain relief for a variety of loading conditions, i.e., tension, bending, crush, impact. etc.

Early this year, AT&T began production of a new lightguide cable design, designated as Lightpack™ Cable. The design incorporates the advantages of the three leading cable designs. Its primary features are: a compact lightweight cable, low optical loss, a reinforced low-friction sheath, simplified cable stripping and splicing, and a robust mechanical design. The design consists of multiple fiber bundles within a large-diameter filled tube and a steel reinforced polyethylene sheath. The cable has undergone extensive optical and mechanical testing, including: environmental cycling, EIA and specialized mechanical testing, duct installation tests and a plowing trial. AT&T Communications has successfully installed several thousand

kilometers of the cable, forming the backbone of its long-haul network.

## Cable Design

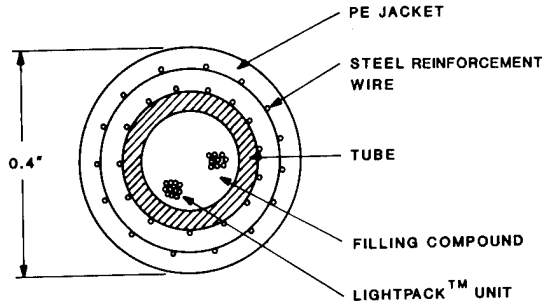
The basic Lightpack cable construction is illustrated in Figure 1a. Up to twelve fibers are assembled in a lightpack unit or bundle which is identified with a color-coded binder. Several units are then assembled into a cable core. A large diameter tube is extruded over the core which is filled with a soft waterblocking compound. The cable is completed with the application of a steel-reinforced polyethylene sheath. The reinforcing wires are applied in a crossply construction resulting in a torque-balanced cable with a 2,700 N (600 lb) load rating. The cable is compact with a nominal outer diameter of 10 mm (0.4 inch) and weight of 120 kg/km (0.080 lb/ft). The design also provides excellent mechanical protection against impact, crush and abrasion. For installations requiring a nonmetallic construction, the steel wires are replaced with nonmetallic elements. A cutaway view of the cable is shown in Figure 2.

For certain buried plant installations, additional protection is required against lightning and rodent attack. For these applications, an optional oversheath is provided in addition to the basic steel reinforced crossply sheath.[10] As illustrated in Figure 1b, it consists of corrugated layers of copper and stainless steel and an adhesively bonded polyethylene jacket. The sheath has survived simulated lightning tests with peak discharge currents up to 195 kA without fiber damage. The sheath has also been tested for rodent resistance and in 60 individual experiments, no failures were observed.

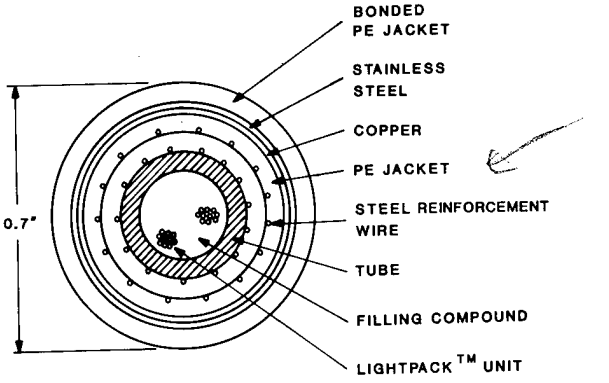
Another important consideration in material selection and cable design is hydrogen gas generation.[11] Hydrogen gas generated by aging or corrosion of lightguide cable materials may enter the optical fibers causing an increase in attenuation. In both the basic steel reinforced sheath and the oversheath, the selection of materials and their construction eliminate the possibility of hydrogen generation. This has been verified by accelerated aging tests and actual field experience.

## Optical Performance

Experimental cables containing between 4 and 48 fibers have been manufactured and optically characterized. The fiber used was the standard AT&T Technologies




(a) STEEL REINFORCED CROSSPLY SHEATH




(b) CROSSPLY SHEATH WITH RODENT AND LIGHTNING PROTECTION

FIGURE 1. LIGHTPACK™ CABLE

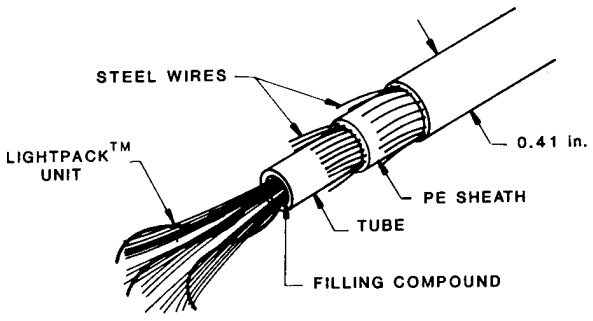



FIGURE 2. LIGHTPACK™ CABLE

depressed-cladding single-mode fiber with core and cladding diameters of 8.3 and 125 μm, respectively. The fibers are dual coated with an outer diameter of 245 μm. Figure 3 shows optical loss histograms at 1310 nm and 1550 nm for a typical 24-fiber

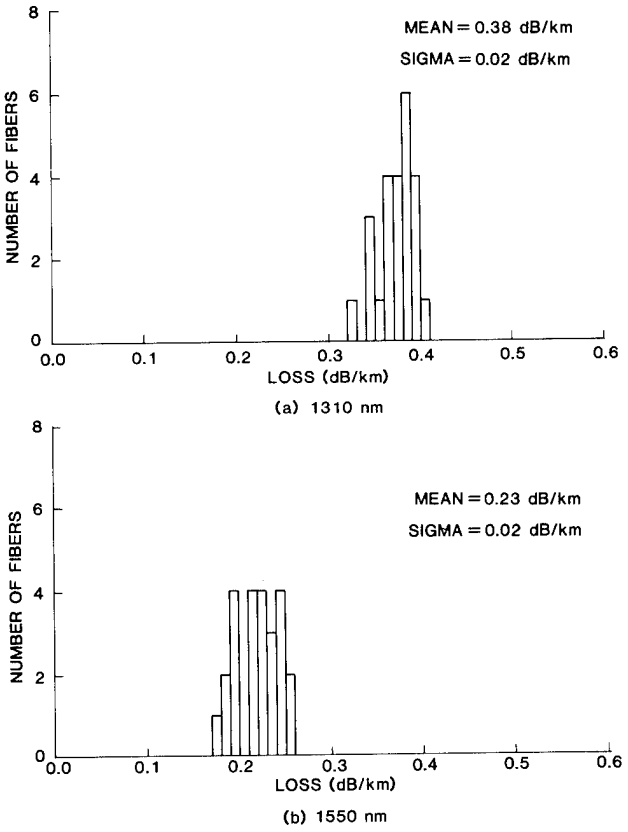



FIGURE 3. LIGHTPACK™ CABLE OPTICAL PERFORMANCE (24-FIBER CABLE)

cable consisting of two 12-fiber Lightpack units. At 1310 nm, the mean loss and standard deviation were 0.38 dB/km and 0.02 dB/km, respectively. The mean cable loss at 1550 nm was 0.23 dB/km with a standard deviation of 0.02 dB/km, indicating excellent upgrade capability at the longer wavelength. As illustrated in Figure 3, the final cable loss distributions were tight. The maximum individual fiber losses were 0.41 and 0.26 dB/km at 1310 and 1550 nm, respectively. Cabling resulted in no increase in the loss at either wavelength. This cable was also environmentally tested. After a five day exposure to 88°C (190°F), loss measurements were made at temperatures as low as -29°C (-20°F). The results at 1310 and 1550 nm are shown in Figure 4. Over the entire temperature range the maximum loss increase was less than 0.05 dB/km, demonstrating excellent thermal stability.

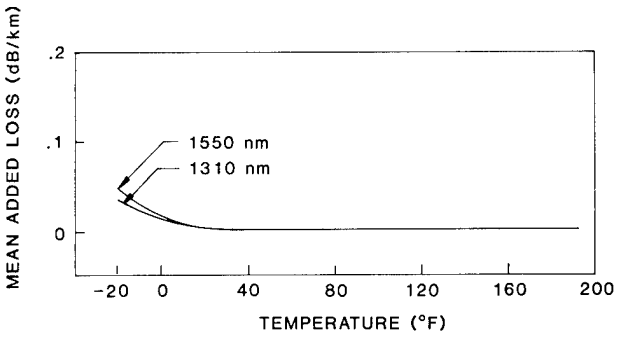



FIGURE 4. ENVIRONMENTAL RESULTS AT 1310 AND 1550 nm

## Mechanical Performance

The Lightpack cable has undergone extensive testing to evaluate its mechanical performance. The testing included both industry standard EIA Tests as well as three specialized tests developed by AT&T Bell Laboratories to evaluate design limits. The EIA Tests included: combined tension and bending, cyclic flex, cyclic impact, twist, compression loading and bending at hot and cold temperatures. In the tension and bend test, a 150-meter (490 feet) length of a one kilometer (3280 feet) long test cable is looped around sheaves and subjected to a 2,700 N (600 lb) load. The sheave diameter is equal to 20 times the cable diameter. In the cyclic bend test, the cable sample is bent around a mandrel with a diameter equal to 10 times the cable diameter. The test is performed at a rate of 30 cycles per minute for a total of 25 cycles. The impact test is performed on a cable sample at the rate of 30 impacts per minute with a total of 25 impacts. In the compression test, a 4,450-Newton (1000 pound) force is applied over a 100 mm (4 inch) cable length for a ten minute period. In the twist test, a cable sample with a four-meter (13 feet) length is rotated ± 180° about its axis. The cable must endure a minimum of ten cycles lasting a total time of ten minutes. In the bending test, the capability of the cable to endure bending at various temperatures is evaluated. A cable sample is wrapped four times on a mandrel whose radius is ten times the diameter of cable at -29°C (-20°F) and 60°C (140°F). In all of these EIA tests, testing should result in no sheath failure and a maximum added loss of less than 0.2 dB. Cable samples with twenty-four fibers were tested with the two sheath options. Test samples were evaluated for both sheath damage and loss increases. The standard EIA Test procedures were used and in all cases, no sheath damage was observed. The loss results are

TABLE 1

QUALIFICATION TESTS*

(Max loss increase on any tested fiber (dB)
at 1310/1550 nm)

| Cable/EIA Tests | Tension/Bend FOTP-33 | Cyclic Flex FOTP-104 | Cyclic Impact FOTP-25 | Twist FOTP-85 | Compressive Load FOTP-41 | Environmental Bend FOTP-37 | |
|---|---|---|---|---|---|---|---|
| | | | | | | Hot | Cold |
| 2 x 12 Cable X-ply Sheath | .02/.02 | .06/.10 | .05/.03 | .03/.05 | .03/.06 | .02/.05 | .02/.06 |
| 2 x 12 Cable B-Oversheath | .03/.03 | .03/.03 | .01/.05 | .01/.06 | .03/.02 | .03/.03 | .03/.03 |

*This data is a courtesy of S. C. Davis of AT&T Technologies, Inc. Atlanta.

listed in Table 1. In all cases, no appreciable loss increases were observed at either 1310 or 1550 nm.

The specialized tests were devised to determine the limits of the design and also simulate extreme conditions which could occur if the cable is mishandled during installation. These tests are mandrel wrap, plow chute simulation, and dynamic squeeze.

Although, the recommended minimum bending cable radius is about four inches (10x diameter), a much more severe bending condition is imposed in the mandrel wrap test. This test is designed to determine if the fibers experience strain when the cable is bent to an extremely small radius. A cable sample was prepared and wrapped on a 50-mm (2 inch) radius mandrel (half the recommended minimum bend radius) as shown in Figure 5. The sample contained 48 fibers and was 70 meters (230 feet) long. Fiber lengths are measured, initially on a 91-cm (36 inch) diameter cable reel and after wrapping the cable on the mandrel, using an optical method.[12] In Figure 6, the percent change in length is plotted for each fiber. No appreciable strain is imposed on the fibers, as indicated by measured values which are less than the measurement uncertainty of 0.04%. The large radial clearance in the tube and the soft filling compound allow the fibers to adjust their position in the tube to avoid high bending strains.

Two simulation tests were developed to evaluate the ability of various cable structures to withstand abuse during plowing. During cable plowing, a rapid acceleration of the plow can result in large cable tensions. With rapid vertical plow

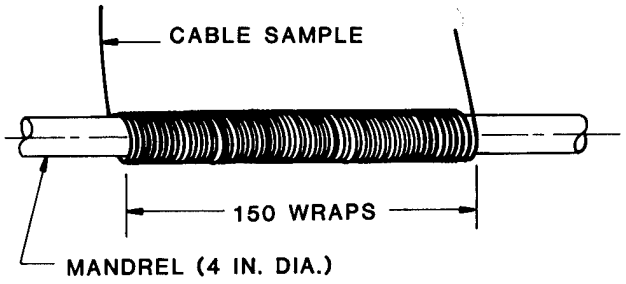



FIGURE 5. MANDREL WRAP TEST

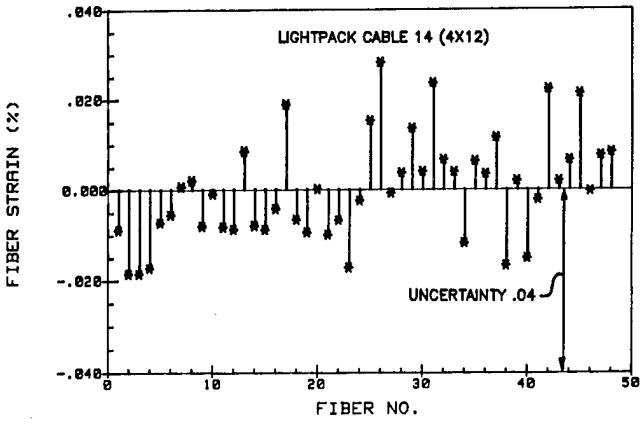



FIGURE 6. FIBER STRAIN AFTER MANDREL WRAP (4" DIA.)

motion, the cable can be severely deformed by concentrated lateral loading at the trailing edge of the plow chute. The complex loading, resulting from simultaneous plow acceleration and vertical motion, can cause cable damage and fiber breakage. The passage of a cable through a plow chute under tension is simulated in the first test. A cable sample is tensioned around a 17.8-cm (7 inch) diameter pulley with a discontinuous ramp as shown in Figure 7. The ramp simulates the trailing edge of the plow. The springs on one end of test setup allow the cable to slide past the sharp (~3 mm (0.12 inch) radius) ramp discontinuity while under tension. Cable tension and fiber continuity are recorded during the test as the load is increased. This being a destructive test, loading progresses until all the fibers are broken. A typical plot of the percentage of broken fibers versus sheath load is shown in Figure 8. Results are presented for the ribbon, loose-tube and Lightpack cable designs. Even though the loading conditions are very severe, all fibers remain continuous until the sheath load reaches about 4,450 N (1000 lb) for the Lightpack cable. Above 4,450 N (1000 lb), the sheath begins to collapse as the cable passes over the sharp edge under the combination of tensile and lateral loads. For the loose-tube design, the unit tubes are crushed between the central strength member and the sheath, resulting in fiber breakage at about 2,200 N (500 lb). For the ribbon cable, no fibers break, even for loads up to 8,900 N (2000 lb). This test demonstrates the advantage of strength member placement in the sheath, rather than in the core. It should be noted, however, that the objective of this test is to determine failure limits and all three cables perform very well in the field.

In the dynamic squeeze test, a cable sample is repeatedly pulled through rollers over a ten-foot test length. Rapid downward movement of a plow chute into rock or compacted soil, combined with tractor acceleration can result in cable squeezing. This problem has also been encountered in certain aerial installations.[13] The purpose of this test is to quantitatively evaluate the susceptibility of various cable structures to dynamic squeezing loads. Figure 9 shows a schematic of the test apparatus with a cable sample squeezed between movable and guide rollers. The roller separation is expressed in % squeeze (or % of the cable diameter). Cable pulling tension and fiber continuity are recorded during each segment of a test, lasting about 600 seconds at a given reduction in cable diameter. The cable diameter is progressively reduced and cumulative fiber breakage is recorded. The test is concluded when all the fibers have been

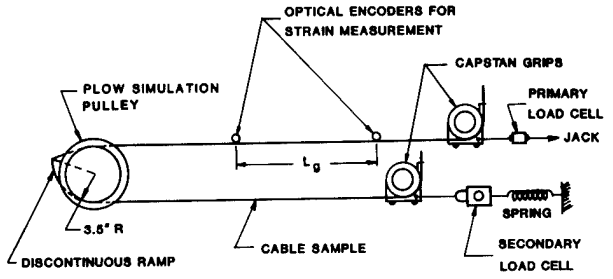



FIGURE 7. PLOW SIMULATION TEST

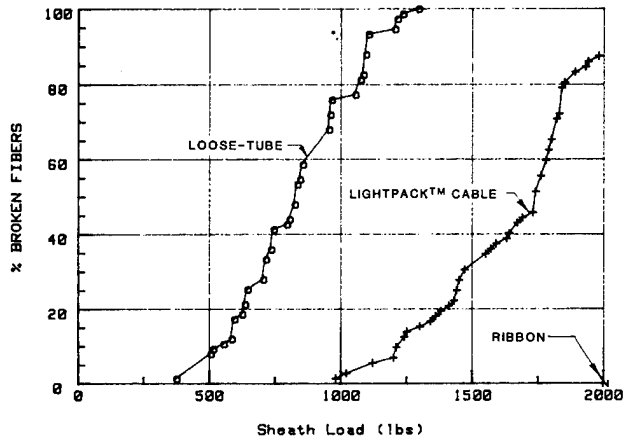



FIGURE 8. PLOW SIMULATION RESULTS

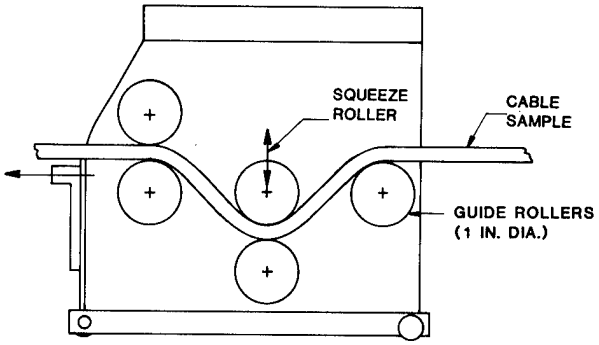



FIGURE 9. DYNAMIC SQUEEZE TEST

broken. The percentage of broken fibers as a function of cumulative squeeze time or diameter reduction is shown in Figure 10. All three designs can survive considerable abuse. In the Lightpack cable, the diameter must be reduced by more than 50% before any fibers are broken. The loose-tube cable exhibits comparable performance and the ribbon cable performance is exceptional.

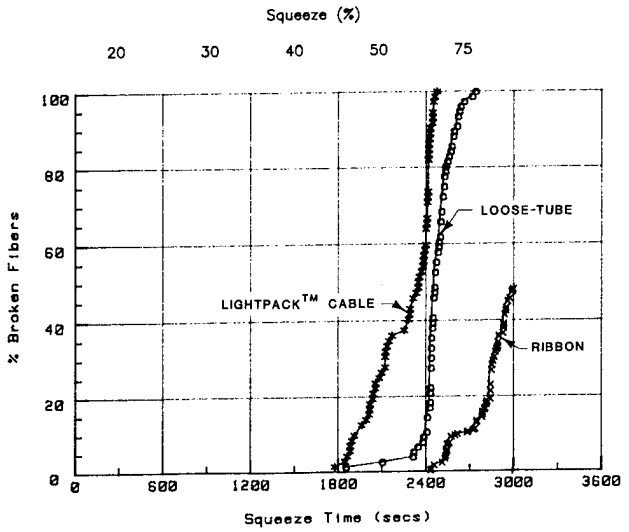



FIGURE 10. DYNAMIC SQUEEZE RESULTS

## Duct Test

In this experiment, the effect of tensile loads during duct pulling on the cable loss was determined. An experimental underground conduit run at the AT&T Bell Laboratories Atlanta facility was used for this test. A cable sample was pulled from a laboratory into the conduit, looped around a 61-cm (24 inch) diameter sheave in a manhole about 500 meters (1640 feet) away and pulled back into the laboratory, making the two ends accessible in an optical measurements laboratory. The cable had a steel reinforced crossply sheath and was one kilometer (3280 feet) in length. During the installation pull, the maximum recorded tension was less than 1,100 N (250 lb). Spectral loss measurements were made before and after installation and no loss increases were observed at either 1310 or 1550 nm. For 24 fibers, the mean installed losses at 1310 and 1550 nm were 0.36 dB/km and 0.22 dB/km, respectively. After installation an additional test was run. One end of the cable was anchored and the other end was gradually loaded to its rated load of 2,700 N (600 lb) and held for 30 minutes. After unloading, the loss was again measured with no increase observed.

## Plowing Trial

A 24-fiber cable with the rodent-lightning oversheath was tested for plowability at the AT&T Bell Laboratories Chester Laboratory. An ordinary static D5 Kelley plow was used. The cable was deliberately mishandled. Conditions included rapid jump starts of the plow, rapid up and down plow chute movement and sharp turns. Throughout the trial, no fiber was broken or experienced a measurable change in loss.

## Conclusions

The Lightpack design results in an extremely compact and simple cable structure. The optical performance after manufacture and during environmental exposure is excellent. Mechanical testing and installation trials have shown the cable to be very rugged - even with severe mishandling. The cable also simplifies stripping during splicing in the field.

## Acknowledgements

The authors would like to thank all members of AT&T Technologies and AT&T Bell Laboratories who have contributed to this development. Our special thanks to A. J. Panuska for coordinating cable manufacture and L. C. Hotchkiss for coordinating the optical loss measurements.

## References

1. P. F. Gagen and M. R. Santana, "Design and Performance of a Crossply Lightguide Cable Sheath," IWCS 1979.

2. B. R. Eichenbaum and M. R. Santana, "Design and Performance of a Filled High Fiber Count, Multi-Mode Optical Cable," IWCS 1982.

3. C. H. Gartside, III and J. L. Baden, "Single-Mode Ribbon Cable and Array Splicing," Telephony, p. 80, June 17, 1985.

4. P. R. Bark, et al., "High Fiber Count Cables of the Mini-Bundle Design," IWCS, 1981.

5. P. S. Venkatesan and K. Korbelak, "Characterization of Ruggedized Fiber Optic Dual Wavelength Cables," IWCS 1982.

6. M. H. Reeve and C. A. Millar, "An Initial Fibre and Cable Specification for Monomode Trunk Systems," ICC, Amsterdam, 1984.

7. T. S. Hope et al., "Developments in Slotted Core Optical Fibre Cables," IWCS 1981.

8. K. Abe, "Manufacturing of Optical Cables for the Telecommunications Industry," OFC, 1984

9. M. de Vecchis et al., "Cylindrical V-Grooved Non-Metallic Optical Fibre Cable," IWCS 1983.

10. W. C. L. Weinraub, D. D. Davis and M. D. Kinard, "A Rodent and Lightning Protection Sheath for Fiber Optic Cables," IWCS, 1983.

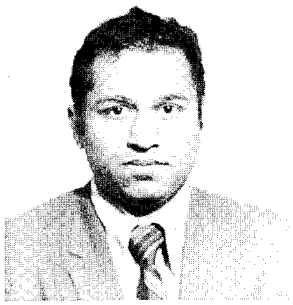
11. D. L. Philen and C. H. Gartside, III, "Prevention of Hydrogen Gas Induced Loss In Optical Fibers by Proper Lightguide Cable Design," IWCS, 1984.

12. D. L. Philen and P. D. Patel, "Measurements of Strain in Optical Fiber Cables Using a Commercial Distance Meter," ECOC, 1982.

13. Y. Kameo et al., "Jelly-Filled Optical Fiber Cables," IWCS 1981.



Charles Gartside is a Member of the Technical Staff of AT&T Bell Laboratories. Prior to joining AT&T Bell Labs in 1980, he has held engineering positions with Argonne National Laboratory and Westinghouse Electric Corporation. He received his undergraduate education at Widener College and holds a PhD in Mechanical Engineering from Carnegie-Mellon University. Dr. Gartside is a member of the American Society of Mechanical Engineers, Sigma Xi and Sigma Pi Sigma, and is a Registered Professional Engineer.



P. D. Patel received his B.E. Degree (6/62) in Mechanical Engineering from the M.S. University in India and his M.S. Degree (6/63) and Engr. Sc. D. Degree (6/68) in Mechanical Engineering from Columbia University. He joined AT&T Bell Laboratories in 1969 and has been working in Lightguide Cable design and development area since 1979.

# OPTICAL FIBER CABLE FOR SPECIAL CIRCUMSTANCE

Nobuhiro Akasaka, Fumio Suzuki, Tetsuji Aoki

Sumitomo Electric Industries, Ltd.
1, Taya-cho, Totsuka-ku, Yokohama, Japan

## Summary

Optical fiber cord's light weight, non-induction and small diameter have made it attractive for utilization in aircraft, space satellites and other special uses. However, quality specifications for the cord are generally so severe in regard to wide temperature range that the conventional cord especially its jacketing material is not suitable for these special uses. Therefore, several engineering plastics recently developed for special use were extruded as a jacket for optical fiber of loose tube structure. The newly developed cord showed excellent temperature characteristics of mechanical strength and optical transmission in a wide temperature range.

## 1. Introduction

The manufacturing process and quality of optical fiber cables have been improving continuously and the demand for the cables for standard uses has been rapidly growing.

However, the history of the cables is very short compared with that of metal cables, and optical cables for special use require further improvement. For example, development of special optical fiber cords for aircraft, space satellites and nuclear reactors has been a high priority because optical fiber is superior to metal cable because of its light weight, non-induction, small diameter and other characteristics. However, quality specifications for such special cords are generally so severe that the conventional cord is not suitable for special use.

This paper describes the development of a special cord fulfilling these quality requirement. In developing the cord, selection of the jacketing material and the cord structure for the optical fiber were most important. To find a suitable jacketing material, several engineering plastics which were developed recently were evaluated. Tight and loose tube structure were also compared. Characteristics of the newly developed cord are also described below.

## 2. Preliminary Study on Material and Structure

### 2.1 Material

(1) In general, UV-cured resin or heat-cured silicone rubber is used as the primary coating of optical fiber. For the special use cord, however, heat-cured silicone rubber is better than UV-cured resin because of its heat resistivity.

(2) As a secondary coating material, polyamide is used for standard cord, but for special use cord its heat resistivity is not adequate as its melting temperature is below 200 °C. Fluoroplastic, on the other hand, is well known as a heat resistant material but has drawbacks in terms of heat shrinkage. Given these circumstances it was decided that a new material for the inner jacket must be selected.
Table 1 shows the properties of several plastics which were developed recently for special use. Of these materials, thermoplastic polyimide seems to be the best.

(3) For the outer jacket, a softer material is preferable because the cord is bent or wound in small diameter and must be easy to handle. Fluororubber was judged best for these purposes.

### 2.2 Structure

As is well known, there are two types of jackets for optical fiber: loose tube structure and tight structure. For the special use cord, loose tube structure seems to be better-suited than tight structure for the following reasons.

(1) The cord must be mechanically strong.

(2) Young's modulus of the jacketing material must be high.

(3) Material of mechanically strong and high Young's modulus is difficult to extrude for tight structure.

Table 1 Comparison of Special Thermoplastics

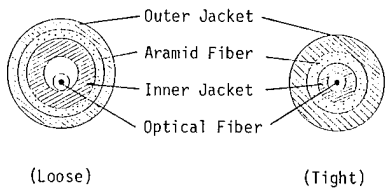
| | | | Modified Thermoplastic Polyimide | Polyether Plastic A | Polyether Plastic B | Fluoroplastic A | Fluoroplastic B |
|---|---|---|---|---|---|---|---|
| Heat Distortion Temperature | °C | | 200 | 205 | 150 | 50 | 76 |
| Maximum Service Temperature | °C | | 170 | 180 | 240 | 200 | 150 |
| Oxgen Index | % | | 45 | 36 | 24 | | 48 |
| Young's Modulus | $kg/mm^2$ | 23°C | 239 | 165 | 263 | 35 | 55 |
| | | 100°C | 183 | 171 | 216 | 15 | 20 |
| | | 200°C | 127 | 142 | 17 | | |
| Coefficient of Thermal Expansion | $1x10^{-5}$/°C | | 4.6 | 5.0 | 4.1 | 9.0 | 8.0 |
| Shrinkage at 200°C x 48Hr | % | | 0.4 | 0.2 | 1.2 | 3.3 | 2.5 |
| Extrudability | | | Superior | Poor | Good | Superior | Superior |

## 3. Experimental Result and Discussion

### 3.1 Material and Structure

The structure of the newly developed optical fiber cord is shown in Table 2. The inner jacket for silicone coated optical fiber has a loose tube structure and modified thermoplastic polyimide (MTPI) is used as the tube material. The cord consists of a loose tube unit, tension members of aramid fiber attached to the tube and an outer jacket of fluororubber.

Table 2 Cord Structure

| | | | New Cord | Conventional Cord |
|---|---|---|---|---|
| Optical Fiber | Dia. Core/Cladding | μm | 100 / 140 | |
| | Δ n | % | 2 | |
| | Coating Dia. | mm φ | 0.4 | |
| | Coating Material | | Heat-cured Silicone Rubber | |
| Inner Jacket | Dia. Inner/Outer | mm φ | 0.8 / 1.6 | 0.4 / 0.9 |
| | Material | | Modified Thermoplastic Polyimide | Fluoroplastic |
| Tension Member | | | Aramid Fiber | |
| Outer Jacket | Dia. Inner/outer | mm φ | 2.0 / 2.5 | 1.4 / 2.2 |
| | Material | | Fluororubber | Fluoroplastic |
| Structure | | |  | |

### 3.2 Temperature Dependence of Optical Transmission Loss

One of the most important characteristics of the newly developed cord is its temperature dependence of optical transmission loss.

Figure 1 shows transmission loss variation of the cord in the temperature range from -65 °C to 200 °C.

According to the figure, the temperature dependence of transmission loss of the new cord was lower than that of conventional cord. The difference was particularly great after the cord passed through high temperatures.

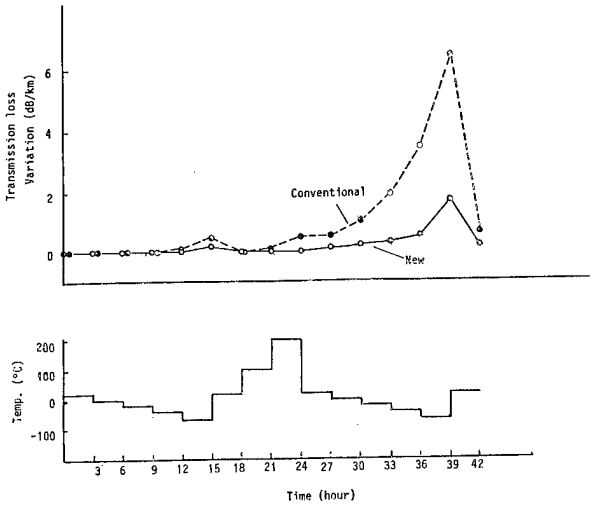



Figure 1 Temperature Dependence of Transmission Loss Variation

### 3.3 Mechanical Characteristics

Cords for short-distance transmission must be mechanically strong and easy to handle because they are small in diameter and are densely installed in narrow spaces. Test results of the mechanical characteristics of the cord are as follows:

(1) Tension property

Figure 2 shows the transmission loss variation of the cord and the elongation of the cord when tensile load was applied to both sides of the cord. No significant increase of transmission loss of the new cord was observed and elongation was 8.5 % at 100 Kgf tensile load. The conventional cord broke under at 18 Kgf load.

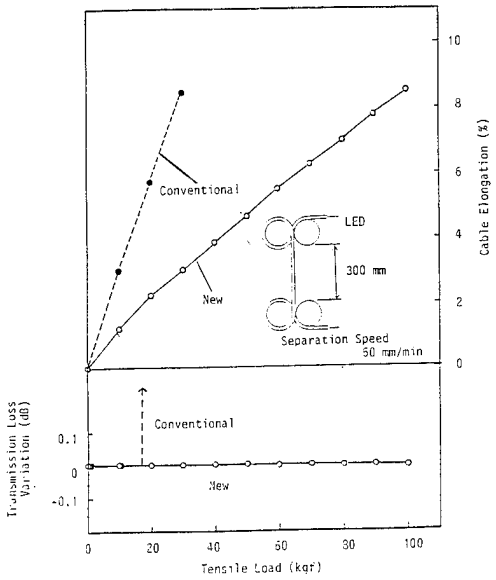



Figure 2 Tension Property

(2) Compression property

Figure 3 shows transmission loss variation of the cord when compressive load was applied on the cord between two 50 mm metal plates. No significant increase in transmission loss was observed up to 180 Kgf/50mm compressive load. On the other hand, for conventional cord transmission loss increased by 0.83 dB under 180 Kgf/50mm compressive load.

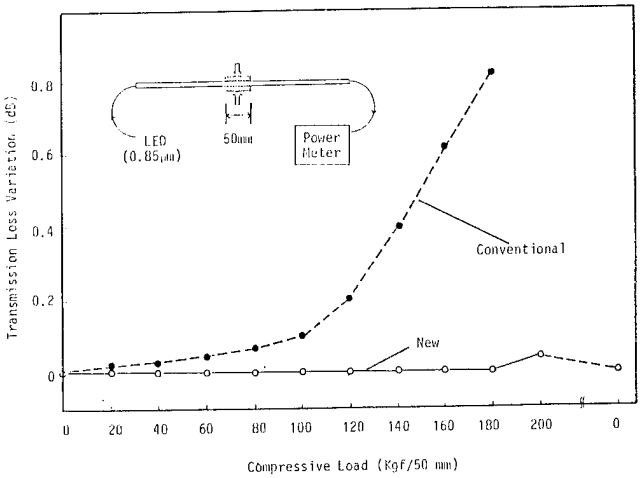



Figure 3 Compression Property

(3) Bending and winding properties

Figure 4 shows the relationship between bending diameter and transmission loss variation of the cord. No transmission loss variation of the new cord was observed at 5 mmϕ bending diameter and 1 turn. It increased by 0.04 dB at 10 turns. On the other hand, the increase of the conventional cord reached 0.05 dB at only 1 turn.

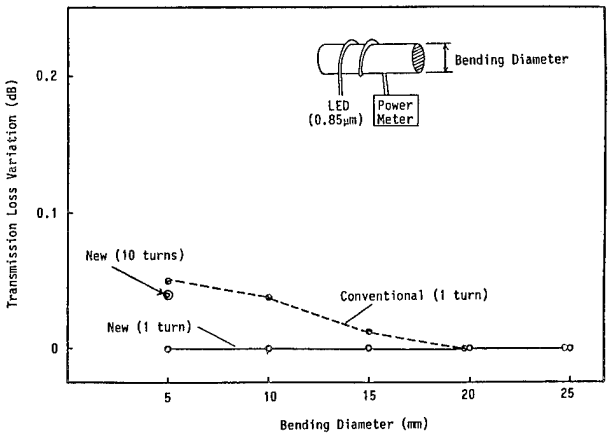



Figure 4 Bending and Winding Properties

3.4 Others

(1) Tension test of MTPI tube at high temperature

Figure 5 shows the relationship between Young's modulus and temperature of MTPI tube. The Young's modulus of MTPI tube at 200 °C was 125 Kgf/mm$^2$, which is almost the same as that of fluoroplastic at normal temperature. The result suggests that the new cord can be used up to 200 °C without any problem, at least in terms of mechanical strength.

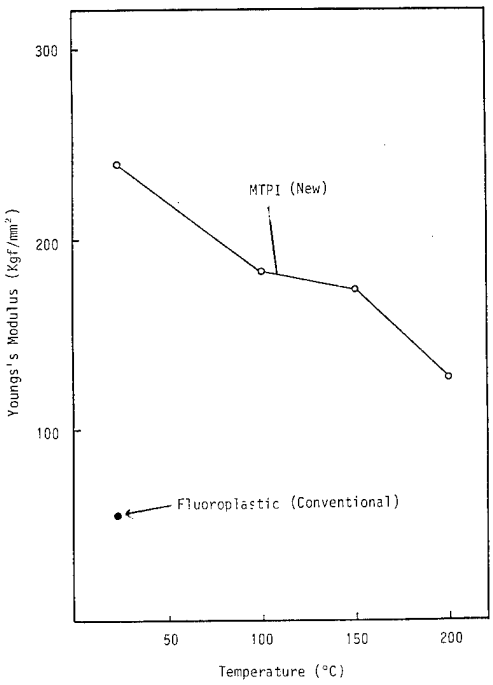



Figure 5 Temperature Dependence of Young's Modulus

(2) Heat shrinkage of MTPI tube

Figure 6 shows the relationship between shrinkage and temperature for MTPI tube. Shrinkage of MTPI tube is very low compared with the conventional fluoroplastic tube. This is the main reason why the temperature dependence of transmission loss of the new cord is lower than that of the conventional cord.

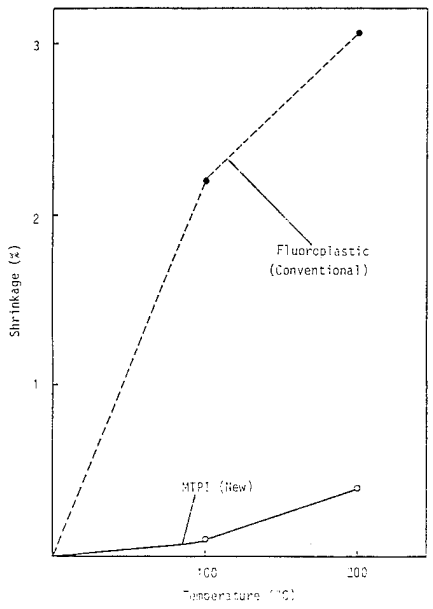



Figure 6 Shrinkage of Jacketing

## 4. Conclusion

A new cord having a loose tube of modified thermoplastic polyimide was developed. The cord showed excellent temperature characteristics of optical transmission and mechanical strength in a wide temperature range. The cord is suitable for preferably use in conditions of severe temperature change such as those facing aircraft and satellites.



Tetsuji Aoki

Sumitomo Electric
Industries, Ltd.
1, Taya-cho,
Totsuka-ku,
Yokohama,
Japan

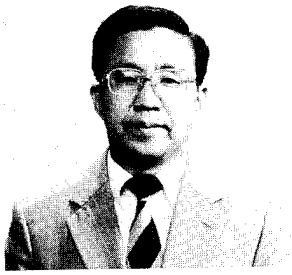
Tetsuji Aoki received his M.S. degree in Synthetic Chemistry from Nagoya Institute of Technology in 1975. He then joined Sumitomo Electric Industries and has been engaged in research and development of optical fiber and cables. Mr. Aoki is a senior engineer of Transmission Media R & D Dept. Yokohama Research Laboratories, and is a member of the Institute of Electronics & Communication Engineers of Japan.



Nobuhiro Akasaka

Sumitomo Electric
Industries, Ltd.
1. Taya-cho,
Totsuka-ku,
Yokohama,
Japan

Nobuhiro Akasaka recieved the M.S. degree in Chemical Engineering from Tokyo University in 1983. He joined Sumitomo Electirc Industries, Ltd. in 1983, and has been engaged in research and development of optical fiber and cables. Mr. Akasaka is a member of Transmission Media R & D Dept. Yokohama Research Laboratories.



Fumio Suzuki

Sumitomo Electric
Industries, Ltd.
1, Taya-cho,
Totsuka-ku,
Yokohama,
Japan

Fumio Suzuki finished the Chemical Engineering Course of Arai High School in Niigata Prefecture in 1958. He joined the Research Division of Sumitomo Electric Industries, Ltd. in 1958, and worked on application research of high polymers for wire and cables. Mr. Suzuki is now Cheef Research Associate of Transmission Media R & D Dept. Yokohama Research Laboratories, and a member of the Society of Polymer Science, Japan.

# A NEW COLORING SYSTEM BY LIQUID PIGMENT INJECTION METHOD

S. Yamamoto, K. Miura, M. Seto, K. Fuse, M. Kajiwara

The Furukawa Electric Co., Ltd.
2-6-1, Marunouchi, Chiyoda-ku, Tokyo Japan

## Summary

As in the field of electronic appliance wire and cable production, the size of one manufacturing lot is becoming smaller and smaller, the material loss when changing color is increasing. So, we have developed an epoch-making manufacturing method including a process of changing color of insulated wires with high efficiency productivity.

A new liquid pigment injection method thus developed need not change the material in the extruder as conventional coloring systems do. The new system worked with about one-fifth of loss in operation time and quantity of raw-material.

The new coloring system is applicable to electronic appliance wire processes for various types of materials such as normal and flame retardant PE, PVC, XL-PE, XL-PVC and high heat resistant XL-PE.

## 1. Introduction

Electronic appliance wires and cables are intended for many unspecified customers and include ones composed of diversified conductors and insulation materials. These requirements naturally result in extremely short length of products when they are brought in the insulated process, a disadvantage of these products.

The average continuous extrusion time per product in our plant is approximately 20 minutes. Change of the color of insulated wires or cables takes 10 minutes and causes a material loss of approximately 3 kg, a great loss in the production time and material.

As for changing the conductor and the size as well as centering adjustment, the fixed die and nipple which have become widely used have caused time-saving to a great degree. However, no attempt has yet been made to examine the possibility of changing the material and color while a wire or a cable is in process in the extruder. We then gave attention to the problem of color change, studied the subject, developed and put into use the liquid pigment injection method.

Following points were taken into account to develop the method.

1) Development of a liquid pigment vehicle which does not impair (mechanical, electric and thermal) properties of the insulation material.
2) Development of a compact size and inexpensive coloring system which can constantly feed the liquid pigment with a high viscosity used together with a highly densed filler material to the crosshead section of extrusion.

## 2. Properties of Liquid Pigment

We developed two kinds of liquid pigments, those for PE and PVC, and also these color pigments can be used in applications subjected to electron irradiation cure.

The vehicle for the pigment for the PE consists of a surface-active agent and a special anti-oxidizing agent. The same pigment as that for ordinary color master batches can be used. However, as high a degree of dilution as 50:1 can be adopted compared with 30:1 for ordinary color master batches because a higher pigment content is possible, resulting in a little cost reduction.

Table 1 shows comparison of properties obtained from sheet specimens of the natural PE specimens colored by the conventional color master batch and the liquid pigment. All materials were cross-linked by ray. These data show that the properties of specimens colored by liquid pigment are same as conventional color batch. Fig. 1 shows thermal aging characteristics of the same specimens as those in Table 1. Data at a point where specimens had an elongated retention of 50% of the original elongation at temperatures 180°C, 160°C, and 136°C were collected and plotted. The liquid pigment, as seen in the figure, has a little bit less advantage over the others, but to a degree of no problem in practical uses.

Fig. 2 shows results of thermal aging characteristics according to Beamex ER of our company, where wires were aged for a specified period of time at specified temperatures, then taken out, and wound 6 turns around a mandrel with the same diameter as wires. Evaluation of the result was based on whether cracks were found or not.

Table 1 Properties of Colored XL-PE by Liquid Pigment

| Test | Unit | Method | Natural | Color batch (Red) | Liquid pigment (Red) |
|---|---|---|---|---|---|
| Mechanical properties | | | | | |
| Tensile strength | $Kg/mm^2$ | JIS K 6723 | 2.04 | 2.30 | 2.38 |
| Elongation at rupture | % | | 610 | 650 | 600 |
| Modulus at 100% | $kg/mm^2$ | | 1.01 | 1.02 | 1.03 |
| Electric properties | | | | | |
| $\varepsilon$ | | JIS K 6760 | 2.29 | 2.29 | 2.30 |
| tan $\delta$ | | | $3.5\times10^{-4}$ | $2.9\times10^{-4}$ | $2\times10^{-3}$ |
| $\rho$ | $\Omega\cdot cm$ | | $7\times10^{15}$ | $1.6\times10^{16}$ | $3.4\times10^{16}$ |
| Brittleness temperature | °C | JIS K 6723 | -50> | -50> | -50> |
| Weatherability | | | | | |
| 200 hrs. T.S., retention | % | | 1.89 | 1.83 | 2.10 |
| EL., retention | % | Weather meter | 540 | 550 | 540 |
| Color | | | No change | No change | No change |
| 400 hrs. T.S., retention | % | | 1.04 | 1.98 | 1.68 |
| EL., retention | % | | 180 | 600 | 480 |
| Color | | | No change | No change | No change |
| 800 hrs. T.S., retention | % | | 1.35 | 1.87 | 1.50 |
| EL., retention | % | | 180 | 620 | 400 |
| Color | | | No change | No change | No change |

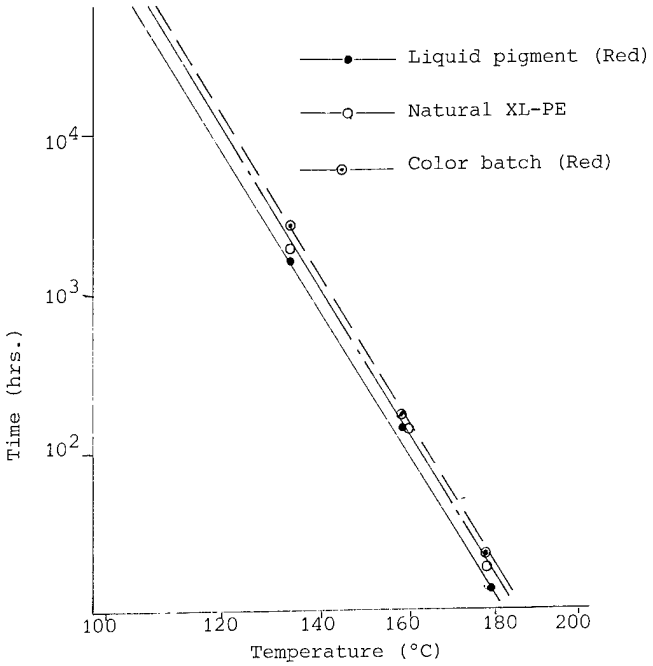



Fig. 1 Thermal Aging Property of Std. XL-PE vs. Liquid (Elongation, 50% retention)

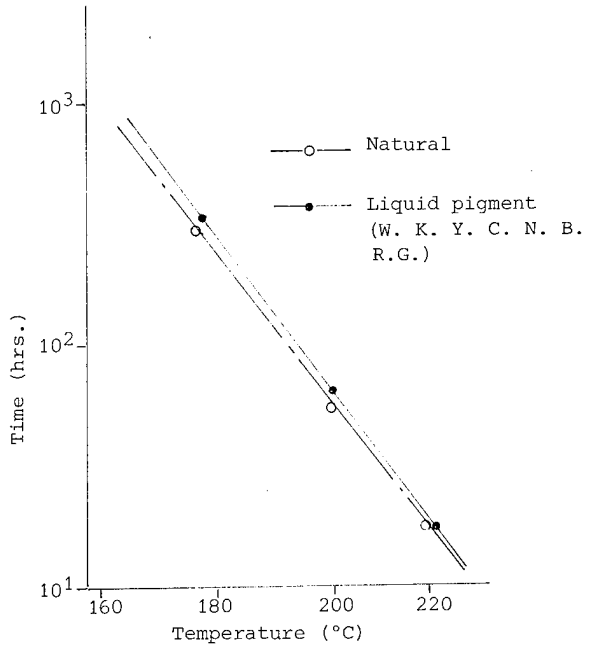



Fig. 2 Thermal Aging Property of Beamex ER* (Method: Wire wrapped around a same diameter mardrel after aging)

*: Beamex ER is trade name of high heat resistance-flame retardant XL PE insulated wire.

Beamex ER colored by the liquid pigment showed a better result than the non-colorded one. The vehicle for the pigment for the PVC consists of ordinary plasticizers. The same high degree of dilution of 50:1 as that for the pigment for the PE was possible because of a high pigment content.

Table 2 shows comparison of properties obtained from sheet specimens of the natural PVC, ones colored by the conventional color master batch and the liquid pigment. All materials were cross-linked by electron irradiation. The results show that the properties of specimens colored by the liquid pigment are equal to the conventional color batch.

Table 2 Properties of Colored XL-PVC by Liquid Pigment

| Test | Unit | Method | Natural | Color batch (Yellow) | Liquid pigment (Yellow) |
|---|---|---|---|---|---|
| Mechanical properties | | | | | |
| Tensile strength | $kg/mm^2$ | JIS K 6723 | 2.13 | 2.05 | 2.07 |
| Elongation at rupture | % | | 230 | 240 | 230 |
| Modulus at 100% | $kg/mm^2$ | | 1.64 | 1.53 | 1.56 |
| Oil resistance | | | | | |
| T.S., retention | % | JIS K 6723 | 93.0 | 100.5 | 100 |
| EL., retention | % | ASTM No. 2 oil 70°Cx2 hrs. | 82.6 | 79.2 | 76.1 |
| Thermal aging | | | | | |
| T.S., retention | % | 136°Cx7 days | 95.2 | 96.5 | 92.5 |
| EL., retention | % | | 85.0 | 80.0 | 78.8 |
| Weatherability | | | | | |
| 200 hrs. T.S., retention | % | Weather meter | 99.5 | 105.9 | 104.8 |
| El., retention | % | | 82.6 | 85.4 | 95.7 |
| Color | | | No change | No change | No change |
| 500 hrs. T.S., retention | % | | 99.5 | 108.3 | 102.9 |
| El., retention | % | | 78.3 | 79.2 | 82.6 |
| Color | | | No change | No change | No change |
| 1000 hrs. T.S., retention | % | | 93.4 | 103.9 | 101.0 |
| El., retention | % | | 82.6 | 91.7 | 82.6 |
| Color | | | No change | No change | No change |
| Oxygen index | | JIS K 7201 | 28.5 | 28.5 | 28.9 |
| Brittleness temperature | °C | JIS K 6723 | -27.5 | -27.5 | -27.5 |
| Volume resistivity | Ω·cm | JIS K 6760 | $1.3x10^{14}$ | $9.4x10^{13}$ | $5.5x10^{13}$ |

## 3. Manufacturing System

Conventional systems using the color master batch requires change of materials when they are in the hopper, the extruder and the cross-head. Because of the injection of the liquid pigment into the cross-head of the extrusion, on the other hand, the liquid pigment system eliminates the loss of time and material due to no change of the material required when it is in the hopper and the extruder.

Fig. 3 shows the outline of the system which is composed of the liquid color pumping equipment, liquid pigment injection inlet, an extruder screw rotation control unit to keep a constant pressure in the liquid pigment injection section, a newly designed gear pump to feed the polymer, and a special static mixer.

### 3.1 Liquid Pigment Pumping Equipment

The gear pump for feeding liquid pigment is provided with special disposable tanks made of paper for the liquid pigment, two tanks for each color.

The liquid pigment has as high a viscosity as 500 to 1000 poise and contains a highly densed filler material. Therefore, the gear pump is most suitable for supplying the liquid color at a constant.
A pump is required for each color used, normally 12 pumps in total. Each pump is provided with an electromagnetic clutch. Setting at an appropriate position the selector switch in the extruder control panel turns on one of these clutches to operate a gear pump for feeding a specified liquid pigment.

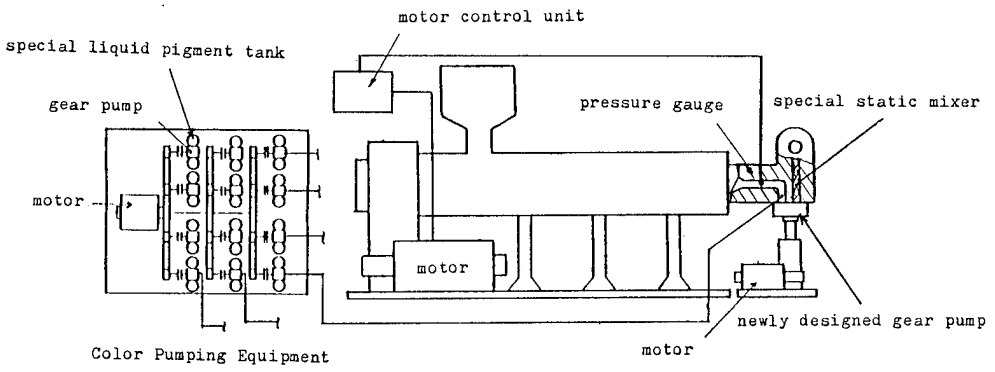



Fig. 3 Outline of Liquid Pigment Injection System

As many pipings up to the color injection inlet as colors used should be arranged.

### 3.2 Color Injection Inlet

The color injection inlet is mounted through a quick connector, which can be attached and detached with a single action, permitting the replacement of the port within 5 seconds.

### 3.3 Screw Rotation Control Unit

The liquid pigment cannot be injected at 50 $kg/cm^2$ or higher pressure. 10 $kg/cm^2$ or higher variation in the pressure at the injection inlet will cause color shading. A newly designed gear pump for polymer and the screw rotation control unit to keep a constant pressure in the injection section help to prevent this color shading.

### 3.4 Newly Designed Gear Pump

This gear pump is necessary to the polymer from the extruder to the cross-head and decrease the pressure in the liquid pigment injection section. It was newly designed to work against a differential pressure of some hundreds kilograms per square centi-meter to feed a highly viscous polymer with a viscosity of tens of thousand poise.

### 3.5 Special Static Mixer

This is used to disperse the liquid pigment in the polymer within a short term at the samll area (or section). It is a static mixer with a special configuration which enables a small pressure drop and prevents stagnation of the liquid pigment and materials.

A special static mixer measuring ϕ30 mm x 150 mmL can well cover the output rate of 1000 $cm^3/min$ of the ϕ65 extruder.

## 4. Effect of New Coloring System

Table 3 shows data related to color change of the polyethylene delivered from the ϕ65 extruder at a screw rotation speed of 10 rpm. Compared with the conventional color batch system, the new coloring system requires one fifth times as long color change time and has as many times less material loss. Of course, raising the rotation speed of the screw and output rate of the gear pump for the polymer during the color change process saves the time required for color change in proportion to the raising rate.

40 color changes per extruder at a day, that is, 1200 changes per month, for example, produce 160 hours of extra productivity and reduce the material loss by 2.9 tons.

Table 3 Effect of New Coloring System

| | Color | New system | Color batch method |
|---|---|---|---|
| Time (min) | W → R | 1.5 | 10 |
| | R → W | 3 | 30< |
| Material loss (kg) | W → R | 0.4 | 2.5 |
| | R → W | 0.8 | 7.5< |

## 5. Application

The new coloring system is applicable to insulating and jacketing processes in the electronic appliance wire production using different types of materials such as normal or flame retardant PE, PVC, XL-PE and XL-PVC and high heat resistant XL-PE.

## 6. Properties of Insulation or Jacket Colored by the New System

As mentioned above in Section 2 Properties of Liquid Pigment, the new coloring system showed better or at least equal performance in the physical, electrical and mechanical properties than the conventional system. Photo 1 shows the cross-sectional view of the polyethylene colored by the liquid pigment.




Photo 1 Cross-sectional View of the Polyethylene Colored by the Liquid Pigment

## 7. Conclusion

In a new manufacturing process including the above-mentioned coloring system, insulated wires can easily colored by the injection of liquid pigment using a newly developed system. Compared with the conventional coloring system, the new system can work with one fifth of loss in operation time and quantity of raw-material.

It has been made clear that normal PE, flame retardant PE, PVC, XL-PE, and high heat resistant XL-PE colored by the here introduced coloring system proved to have properties at a similar level to those colored by the conventional coloring system, and so can be put in the practical use. It will bring about a little bit cost reduction thanks to the high degree of dilution compared with conventional coloring system.



SHOJI YAMAMOTO
The Furukawa Electric
Co., Ltd.
6-Yawata-Kaigandori,
Ichihara, Chiba
Japan

Mr. Yamamoto graduated from Hakodate Technical College in 1972, where he majored in Industrial Chemistry. Then he joined The Furukawa Electric Co., Ltd. and has been engaged in research and development of flame reterdant plastics and manufacturing methods for foamed plastic insulation.

Mr. Yamamoto is now a member of the Electronic Appliance Wire Production Section.



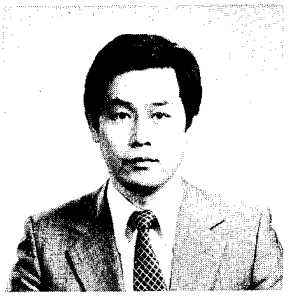
MASARU SETO
The Furukawa Electric
Co., Ltd.
6-Yawata-Kaigandori,
Ichihara, Chiba
Japan

Mr. Masaru Seto graduated from Yokohama National University in 1981 where he majored in applied chemistry. Then he joined The Furukawa Electric Co., Ltd. to be a member of the Electronic Appliance Wire Production Section.



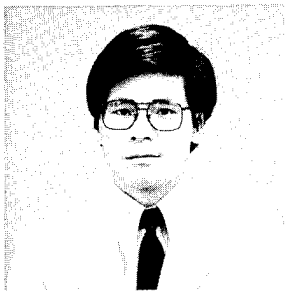
SHIN KAJIWARA
The Furukawa Electric
Co., Ltd.
6-Yawata-Kaigandori,
Ichihara, Chiba
Japan

Mr. Shin Kajiwara graduated from Sizuoka University in 1968, and then studied the organometallic complex as senior student of Tokyo Institute of Technology. He joined The Furukawa Electric Co., Ltd. and was involved in the study of insulation materials. He is now the section manager of Communication Products Production Section.



KAZUO MIURA
The Furukawa Electric
Co., Ltd.
6-Yawata-Kaigandori,
Ichihara, Chiba
Japan

Mr. Kazuo Miura joined The Furukawa Electric Co., Ltd. in 1962. He graduated from Nihon University, where he majored in mechanical engineering. After working for Communication Cable Production Engineering Section, he is now a member of the Electronic Appliance Wire Production Engineering Section.



KENICHI FUSE
The Furukawa Electric
Co., Ltd.
6-Yawata-Kaigandori,
Ichihara, Chiba
Japan

Mr. Fuse graduated from Keio Univ. 1971 with a M. Sc. degree in mechanical engineering. Then he joined The Furukawa Electric Co., Ltd. and has been engaged in research and development of plastic material and manufacturing methods for telephone cables.

Mr. Fuse is now manager of Research & Development Division at The Furukawa Electric Co., Ltd. and a member of the Society of Rheology, Japan.

# VERSATILE HIGH PERFORMANCE FILLING COMPOUNDS FOR TELECOMS CABLE APPLICATIONS

J.R. Bury

Standard Telecommunication Laboratories Limited
Harlow, Essex, CM17 9NA, England, UK.

D.A. Joiner

Synthetic Technology Limited
Tunbridge Wells, Kent, TN2 3EF, England, UK.

## Summary

A new range of thixotropic waterblocking compounds has been developed for use with all types of telecoms cables; conventional copper and fibre optic. They are also effective as corrosion protection for armour wires and power conductors. They are room temperature processable using simple pumping equipment yet operate over a wide temperature range.

## Introduction

Waterblocking of communication cables is a well established method of preventing water ingress into the cable and consequent adverse effects on its performance. The main types of filling compounds used for this purpose differ essentially in chemical nature, rheology, melting characteristics and other relevant physical properties. An alternative process using swellable powders and tapes has so far found only very limited application.

Methods of application of the filling compound to the cable fall into three main categories:

i) Room temperature pumping e.g. drum pumping of relatively low drop point petroleum jelly.
ii) Pumping of a partially molten slurry at elevated temperature.
iii) High temperature liquid filling using a completely molten compound and highly sophisticated applicators.

All three methods impose limitations on cable processing and on the range of acceptable filling compounds. More demanding requirements have resulted from an increasing need for waterblocked cables to operate under extremes of temperature e.g. when installed in tropical or sub-tropical climates or in sub-zero conditions. Specifications for such cables may require the use of high temperature compounds which are non-draining at up to 80°C while retaining satisfactory low temperature properties. The formulation of such materials has presented a serious challenge to suppliers of conventional types of filling compound.

In fibre optic cables the need for waterblocking is often coupled with a fibre buffering requirement as in loose tube and slotted core constructions. This requires a filling compound with stable viscosity characteristics over a wide temperature range and with favourable application characteristics to reduce the risk of fibre damage.

There is thus a need for a range of compounds with improved temperature performance and stable viscosity characteristics coupled with simple application techniques.

The use of thixotropic filling compounds eliminates the need for high temperature filling. The materials rely on shear forces to reduce viscosity for application. They are applied at room temperature and, unlike molten compounds which start to thicken on contact with the cold cable, they retain their low viscosity while flowing, thereby enabling better penetration of high pairage cables. Also thixotropic filling compounds exhibit stable viscosity/temperature characteristics and with suitable choice of base fluid can remain stable over the temperature range -60°C to +160°C.

## Materials Development

At the outset of this development a comprehensive list of objectives was defined for two main cable applications.

A. High Performance Conventional Cables

i) Cold pumping capability.
ii) Non-melting.
iii) Non-draining at elevated temperatures.
iv) Flexible at sub-zero temperatures.
v) Compatible with a wide range of cable polymers.
vi) Water resistant.
vii) Easily removed from cable cores.

B. Optical Cables

i) Non-melting, with no phase or structural changes over a broad temperature range.
ii) Soft and flexible down to below -40°C.
iii) Substantially constant viscosity over a broad temperature range.

iv) Non-draining or slumping at temperatures up to at least 100°C.
v) Compound homogeneity with no particulate fillers which could cause microbending losses.
vi) Easy to apply by pumping at ambient temperature.
vii) Compatible with cable polymers.
ix) Low hydrogen generation.
x) Good buffering properties.

To achieve these objectives, compounds were developed which use the phenomenon of thixotropy. The unique rheological properties of thixotropes allow the compound to flow when subjected to pumping shear. The compound will remain 'thinned' until the cable is filled, after which it rapidly regenerates to the original viscosity. Figure 1 shows the effect of shear on compound viscosity using a Haake Viscometer.

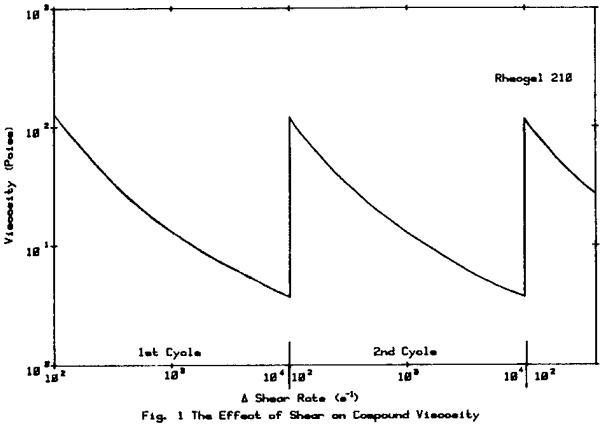


Fig. 1 The Effect of Shear on Compound Viscosity

The compounds consist of a base fluid which is specifically chosen for the particular application and is thickened by means of an ultra-fine, surface active, mineral. Other additives may include various gel stabilizers, viscosity modifiers, coupling agents and antioxidants.

All compounds are soft gels which are hydrophobic in nature. A typical formulation is given in Table 1.

Table 1 - Typical Formulation

| Constituent | Addition rate (%) |
|---|---|
| Base fluid | 83 |
| Mineral filler | 14 |
| Gel stabilizer | 1 |
| Viscosity modifier | 1 |
| Antioxidant | 1 |

These compounds can be pumped at room temperature under relatively low pressure using simple and inexpensive equipment.

## Compounds and Related Applications

The compounds are of two types:

i) Those based on fluids with superior dielectric properties suitable for use with metal conductor cables. These compounds have been designated Rheogel 85 and have a range of properties tailored to particular specifications. Due consideration has also been given to prevailing economic factors.
ii) Gels suitable for fibre optic cable applications. These have been coded Rheogel 210 and exhibit excellent stability over a very wide temperature range. Special attention is paid to the high quality requirement of the buffering medium to minimize the risk of microbending problems.

A number of compounds have been produced or are under active development for specific applications.

### A. High Performance Conventional Cables

Rheogel 85 has been developed as a high performance filling compound for conventional cables for use in extreme temperature environments. Typically cables to Rural Electrification Administration (REA) type specifications fall into this category which calls for resistance to compound drainage at elevated temperatures.

### B. Optical Cables

Rheogel 210 is a soft gel suitable for use in all types of fibre optic cable constructions. The compound is based on a synthetic fluid which is compatible with most cable materials, and is stable over a wide temperature range from -55°C to +160°C. It is especially suitable as a buffering medium for loose tube and slotted core designs.

### C. Conventional Cables

A low cost reduced performance version of Rheogel 85 is under development. This is aimed at the requirements currently met by high drop point petroleum jellies. A major consideration will be materials cost but there are also savings that can be made because of the simplified processing characteristics.

### D. Improved Dielectric Material

Another version of Rheogel 85 is under development which incorporates a small percentage of hollow plastic microspheres. This material will give greatly improved electrical characteristics without loss of thixotropic properties.

### E. Hydrogen Barrier for Optical Cables

Rheogel 210Z is a new grade which contains an additive to 'mop-up' any hydrogen produced during the operating life of the cable. This will allow the cable designer to concentrate

Table 2 - Properties of the Compounds

| Properties | Method | Rheogel 85 | Rheogel 210 |
|---|---|---|---|
| Density (g/ml) | Density column | 0.950 | 0.892 |
| Drop point (°C) | BS 5087 | >180* | >180* |
| Slump at 65°C (%) | After 120 hours | 0.3 | - |
| Slump at 80°C (%) | After 120 hours | 0.4 | 0.3 |
| Cone penetration at 23°C (dmm) | BS 2000 Part 179 | 185 | 280 |
| " " 0°C (dmm) | " " | 170 | 230 |
| " " -20°C (dmm) | " " | - | 200 |
| " " -40°C (dmm) | " " | - | 170 |
| Low temperature flexibility (°C) | Thin film bend test | Passed -45† | Passed -45† |
| Permittivity at 23°C | Tinsley Cell-type 4536 | 2.0Φ | 1.9 |
| " 100°C | " " " | 1.9Φ | 1.9 |
| Volume resistivity at 23°C (ohm.cm) | " " " | 1 x $10^{17}$Φ | 1 x $10^{17}$ |
| " " 100°C (ohm.cm) | " " " | 8 x $10^{13}$Φ | 1 x $10^{17}$ |
| Hydrogen generation ($cm^3/g$) | 2000 hours at 23°C | - | 0.0005 |
| " " ($cm^3/g$) | " 80°C | - | 0.002 |

* Compounds are non-melting † Lowest obtainable test temperature Φ Tests carried out on base fluid

on the more important design parameters without concern for the problems of hydrogen generation.

F. Corrosion Protection for Power Conductors and Armour Wires

These compounds can be used to penetrate the interstices of tightly packed conductors or armour wires. Because of their thixotropic nature they shear-thin to low viscosity for application and then quickly thicken to remain in place to provide excellent environmental protection. A semi-conductive version is under development.

Compound Properties

Table 2 details the materials' properties.

As well as measuring these properties compatibility tests have been carried out in combination with commonly used cable materials.

Dumb-bell test specimens in accordance with BS 2782, Method 320A were prepared from a typical MDPE and HDPE insulation polymer and immersed in the filling compounds for 14 days at 70°C. Also for Rheogel 210, dumb-bells were prepared from a Nylon 12 widely used for secondary coating of optical fibres. The resulting absorption of the compound by the polymer was determined together with its effect on polymer tensile properties.

Tables 3 and 4 summarize the results of these tests.

Table 3 - Compatibility Results for Rheogel 85

| Polymer | Sample | Weight Increase (%) | Yield Stress (MPa) | UTS (MPa) | EB (%) |
|---|---|---|---|---|---|
| MDPE | Unaged control | - | 18 | 14 | 490 |
| | Aged control | -0.1 | 20 | 13 | 440 |
| | Gel pretreated | 3.0 | 17 | 13 | 410 |
| HDPE | Unaged control | - | 24 | 13 | 210 |
| | Aged control | -0.2 | 24 | 13 | 170 |
| | Gel pretreated | 2.0 | 21 | 12 | 300 |

Table 4 - Compatibility Results for Rheogel 210

| Polymer | Sample | Weight Increase (%) | Yield Stress (MPa) | UTS (MPa) | EB (%) |
|---|---|---|---|---|---|
| MDPE | Unaged control | - | 18 | 13 | 460 |
| | Aged control | -0.2 | 18 | 13 | 260 |
| | Gel pretreated | 3.2 | 17 | 13 | 400 |
| HDPE | Unaged control | - | 24 | 13 | 210 |
| | Aged control | -0.2 | 24 | 13 | 270 |
| | Gel pretreated | 1.6 | 23 | 13 | 220 |
| PA 12 | Unaged control | - | 41 | 46 | 230 |
| | Aged control | -0.4 | 46 | 49 | 250 |
| | Gel pretreated | 0.1 | 46 | 47 | 260 |

Oxidative induction time (OIT) has been determined on 0.5/0.9 mm extruded insulation using the test procedure given in Section 3.10 of REA specification PE-39. This requires that the

insulation is conditioned in the filling compound for 8 hours at 68°C prior to a Differential Scanning Calorimetry (DSC) measurement of OIT on a sample in a copper pan at 199°C, using in this case a DuPont 1090 Thermal Analyzer. The results are summarized in Table 5.

Table 5 - Oxidative Induction Time

| Filling Compound | Oxidative Induction Time (minutes) | |
|---|---|---|
| | MDPE | HDPE |
| Control | 60 | 43 |
| Rheogel 85 | 46 | 43 |
| Rheogel 210 | 23 | 35 |

Resistance to thermal ageing of MDPE and HDPE insulation after immersion in the filling compounds has been determined using the test method described in Appendix E of British Telecom specification M142. This involves immersion of the insulated conductor (0.5/0.9 mm) in the filling compound for 14 days at 60°C prior to oven ageing at 105°C, in this case for a period of 1000 hours. The "wrap test" as specified in M142 was then carried out on the aged insulation, and in no case was there any evidence of cracking.

Phase or structural changes in the compound which could adversely affect its performance within the required operating temperature range or with respect to specified test requirements were investigated by DSC. The scans were carried out over the temperature range -60°C to +170°C using a DuPont 1090 Thermal Analyzer. The thermograms thus obtained are reproduced in Fig. 2, which also shows a typical thermogram for a compound having endothermic melting peaks.

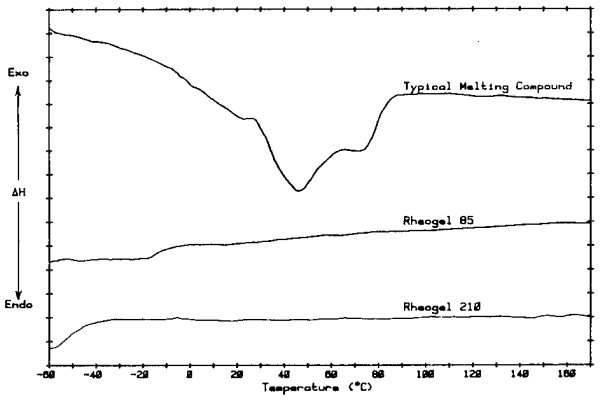



Fig. 2 DSC Thermograms

Tests have also been carried out with Rheogel 210 to confirm that viscosity is relatively independent of temperature. Figure 3 shows the results of these tests in comparison with the viscosity of a typical melting compound, using a Rheometrics Dynamic Spectrometer.

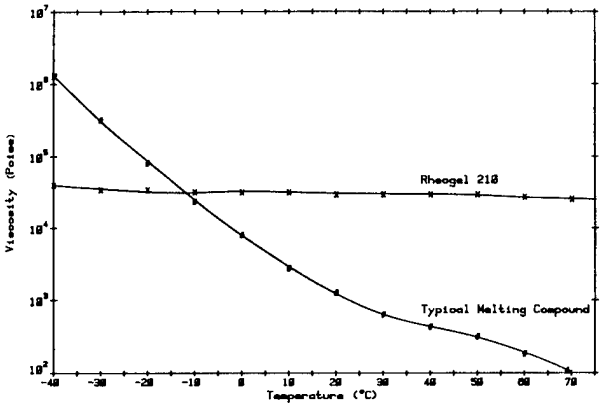



Fig. 3 Viscosity v. Temperature Using Rheometrics Dynamic Spectrometer

## Cable Filling

The cold pumping capability of these compounds has enabled the successful filling of a wide range of cable types and constructions. The ability to pump material at room temperature directly from the supply drum enables the cable-manufacturer to make economic use of simple, inexpensive equipment.

The filling apparatus consists of a simple drum pumping facility acting through a follow-on plate fitted to the supply drum. The shearing action of the pump reduces the viscosity of the compound so that it can pass along the delivery pipe into the applicator head. The compound is forced into the cable under pumping pressure and any excess is returned for reuse. A schematic of this equipment is shown in Fig. 4.

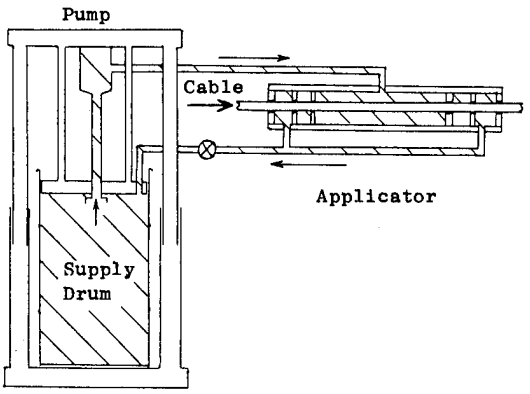


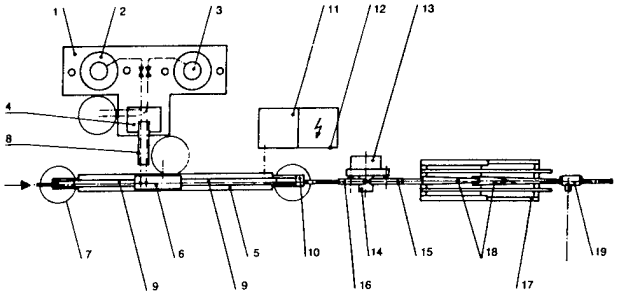

Fig. 4 Schematic of Cable Filling Equipment

The applicator head can be a very simple tube with end seals for small cables or a sophisticated chamber with pressure reduction dies and sizing units for larger high pairage cables.

As previously mentioned no heat is necessary at any stage of the operation and start-up or shut-down is simply a matter of switching the pump on or off.

Application pressures as low as 2 lb/in$^2$ have been used to fill slotted core fibre optic cables with Rheogel 210. Also high pairage cables, up to 1600 pairs in 100 pair units have been successfully filled with Rheogel 85 in one operation.

Equipment of the type manufactured by Kabelmetal Electro, in West Germany has proved ideal for filling conventional cables although the heating elements are not required. See Fig. 5.




1 Petro-Jelly ram press unit
2 follow-plate in the Petro-Jelly barrel
3 Petro-Jelly pump
4 hydraulic unit
5 basic frame
6 filling head
7 collecting barrels
8 flow-through heater above 40 to 80 mm core diameter
9 filling tool (tool housing and tool set)
10 stripping nipple
11 switch cabinet with hot water supply system
12 switch panel
13 strip pay-off support
14 Co/Al-foil pay-off
15 paper strip pay-off
16 length measuring strip pay-off
17 forming tool table
18 forming tool
19 extruder

Fig. 5 Plan of Kabelmetal Filling Equipment

## Cable Testing

### Conventional Cables

The most severe tests on filled cables are:

a) Tests to establish waterblocking characteristics.
b) Compound stability tests at elevated temperatures.

Many other aspects of testing, such as the electrical characteristics of the cable and compatibility and ageing, are carried out on sample cores or materials taken from cables. Where appropriate these have been dealt with under the heading "Compound Properties". This section is primarily concerned with water penetration and drainage tests.

Water Penetration One of the more severe water penetration tests currently used is required by the Indian PTT specification XNKH which calls for end-on application of a metre head of water for 14 days duration. Cables filled with Rheogel 85 have successfully passed this test.

Drainage Testing This test is found in REA specification PE-39 and is widely specified in various forms for cables required to operate in many tropical and sub-tropical environments. The test involves taking a length of cable with the lower section of sheath removed, flaring the cores into a fan and hanging the cable in an oven at temperatures up to 80$^o$C for up to 24 hours duration. No dripping of compound from the cable is normally allowed.

This is a particularly severe test for the more conventional melting types of compound as very high drop point materials are required. It is generally accepted that a drop point approximately 15$^o$C higher than the testing temperature is a minimum safety margin. However, this gives rise to cable production problems as the processing temperatures of these high drop point materials are very close to the softening temperature of the polyethylene insulations.

This test can be passed easily by the thixotropic materials, and compounds have been formulated to give minimal or no drainage from cables at 80$^o$C.

### Fibre Optic Cables

Water and Gas Blocking Various water blocking tests are specified for fibre optic cables but they are generally less severe than for conventional cables, and filling optical cables to pass these specifications is a relatively simple task. It is important to prevent water penetration from contacting the fibres which can lead to loss of optical performance. A more severe requirement is the gas blocking of military optical cables, and Rheogels have been used successfully for this application.

Buffering Another major use for these compounds is in the buffering of optical fibres in loose tube and slotted core/open channel cable designs. The compound is generally used in conjunction with acrylate coated fibres with which it must be compatible, and fills the remainder of the tube or open channel. Attenuation measurements will be carried out on a filled slotted core cable over the temperature range -40$^o$C to +70$^o$C and the results obtained will be given at the presentation.

Rheogel 210 has been specifically formulated for this application and is currently used in several production types of telecommunication cables.

## Conclusions

A range of thixotropic filling compounds has been developed for use in telecommunication cables. The materials are soft, hydrophobic gels which can be easily pumped at room temperature using simple equipment.

Various cable constructions, conventional copper and optical, have been successfully filled and tested to severe high performance specifications.

These compounds are commercially available and have been formulated with both performance and economics factors in mind.

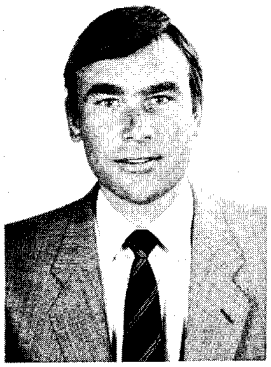
Further developments include work on a lower cost version of Rheogel 85 for regular PTT cables, an improved dielectric version and the new grade Rheogel 210Z for hydrogen protection.


## Acknowledgements

The authors thank STL Ltd. and Synthetic Technology Ltd. for permission to publish this paper. Thanks are also due to STC Technology Limited, STC Cable Products Division, STC Submarine Systems Limited and Kabelmetal Electro, for permission to use information contained in this paper. Contributions from J.S. Ragg and W.E. Simpson are acknowledged.




J.R. Bury joined STL in 1967 and until recently was Manager of the Polymer Technology Laboratory working on the development of new materials and techniques for wire and cable applications. In September, 1985 he joined Synthetic Technology Ltd. as Technical Director.He is a member of the Royal Society of Chemistry and the Plastics and Rubber Institute.



Dudley Joiner has spent many years working and researching with international companies specialising in lubrication and tribology. In 1977 he founded a company to manufacture and market synthetic lubricant compounds for industrial, marine and automotive applications. In 1982 this activity was extended to the production of synthetic gels for insulation and sealing purposes and subsequently embraced a joint venture project between Synthetic Technology and STC to perfect a range of thixotropic gels for filling and waterblocking telecommunication

# POLYIMIDE FILM INSULATION FOR AEROSPACE WIRE AND CABLE: WHY LONG-TERM PERFORMANCE EXCEEDS SOME LIMITED LABORATORY PROJECTIONS

John O. Punderson, Ph.D., Consultant
James F. Heacock, Ph.D., Research Associate

E.I. DuPont de Nemours & Co., Inc.
Wilmington, Delaware

It has been a point of technical interest to find out why recently reported laboratory studies on immersion of polyimide film insulations in hot or boiling water gave results which were grossly at odds with what we know from more than two decades of actual field experience. Differences between laboratory and field results have been made understandable by extending laboratory studies to a wider range of conditions and by defining the fundamental physical and chemical processes involved. Contrary to previous speculations, the polyimide-water interaction is not a simple linear function of relative humidity (RH). Below 100% RH, the reaction rate drops off as the fifth power of RH. Thus, at 50% RH the rate is only 3% of its value at 100% RH. In addition, it appears that insulation failures are not a problem in real-life exposure to humid conditions because molecular weight degradation is limited by the fundamental equilibrium (reversible) nature of the polyimide-water interaction.

## INTRODUCTION

A recent paper titled "Temperature Dependence of Hydrolysis of Polyimide Wire Insulation"[1] presented Arrhenius plots of time to failure data for polyimide wire insulations under a specific set of "accelerated" laboratory conditions. Speculative statements were made, without supporting data, implying a connection between these laboratory projections and field service problems. This prompted two studies:

(1) An extensive field examination of installed wiring in a variety of military and commercial aircraft.

(2) A series of controlled experiments on the effects of long exposures of polyimide films to various humidities and temperatures.

The objective was to find out why the Arrhenius plots of Reference 1 have not correctly projected the actual long-term field performance.

## BACKGROUND

### AROMATIC POLYIMIDES

The chemist who first synthesized an aromatic polyimide at the DuPont Experimental Station in the early 1950's was so impressed by its properties that he designated it by the code name Polymer "SP" - meaning "superlative properties." In film form this remarkable material had mechanical and electrical properties much like those of a polyester film, but in addition, it offered extremely advantageous retention of properties at high temperatures and resistance to ignition.

An organic polymer that could be heated essentially to red heat without melting was indeed novel, and specialized fabrication processes were developed. A film form became commercially available in 1966 under the trade name KAPTON®. Cable manufacturers were quick to provide a range of tape-wrapped wire constructions, and commercial and military specifications were adopted. Mechanical toughness of thin-walled insulations gave aerospace users significant savings in space and weight. More than 2.5 billion feet of polyimide film insulated wire is now in service in commercial and military aircraft. This represents a greater database of experience than exists for any other type of aerospace wiring.

### POLYIMIDE WATER EXPOSURE

A great deal has been known about the water resistance of polyimides since the earliest days of polyimide development. The situation for polyimides has some similarities to that for the proteins in our bodies. Theoretically, the connecting links in both proteins and polyimides could be totally broken down by reaction with water. In practice, however, we know that this does not happen for either proteins or polyimides - except in the presence of strongly alkaline (caustic) solutions.

In acids the polyimide is so stable that it can be dissolved in strong sulfuric

acid with little effect on the polymer chain length. Hot water immersion of polyimide films is known to cause some decrease in physical properties[2], but, more importantly, the effect is known to be limited in degree and to be reversible. Thus, properties can be regenerated by heating the exposed film to elevated temperatures.[3]

## FIELD EXPERIENCE

### FIELD EXPERIENCE EXAMINED

Field service failures in wiring can result from a number of causes. Simple mechanical abuse is an ever-present hazard. Polyimide insulations have gained wide acceptance in aerospace use because of their ability to provide substantial resistance to mechanical abuse while maintaining minimum weight and bulk.

Although the laboratory Arrhenius projections noted above[1] provided no actual data linking any field failure to polyimide hydrolysis, they did provide incentive for a thorough field inspection of installed wiring. The role of hydrolysis should not be a matter of speculation. If ten to twenty years of exposure to a wide spectrum of service conditions including high humidities has, indeed, resulted in a significant number of degraded specimens, this should be verifiable. If significant field failures are due to hydrolysis, rather than mechanical abuse, the failed specimens should show reduced physical properties and significantly reduced molecular weights. If field failures due to hydrolysis are indeed frequent, then it should not take long to find examples for public examination and impartial scientfic peer review.

In 1982 an extensive series of field inspections was undertaken. Among those participating in the inspections were three airframe manufacturers, three commercial airlines, two branches of military service, one standards organization, and one materials manufacturer. Hundreds of aircraft representing seven different types were inspected. Not a single specimen of aromatic polyimide insulation could be found that had failed or cracked in service due to humidity exposure!

### FIELD EXPERIENCE IN PERSPECTIVE

Obviously there is a substantial discrepancy between actual documented field experience and speculations based on Arrhenius plots from a limited range of laboratory test conditions. The remainder of this paper is devoted to examining some of the chemical and physical factors contributing to this discrepancy.

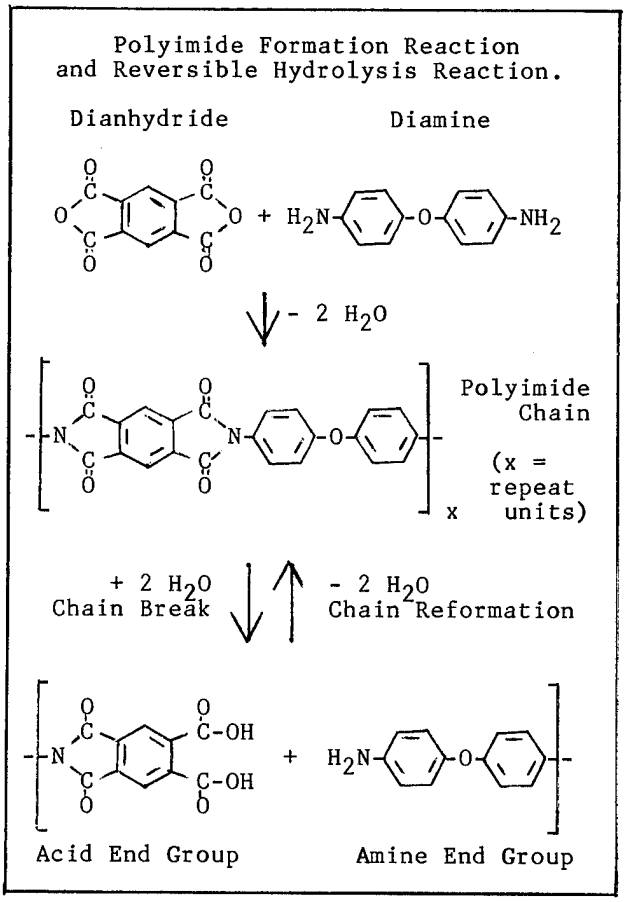
Our purpose is not to "justify" the long-term field performance of polyimide wire insulations. It should be axiomatic that no line of laboratory experimentation can predict field performance as accurately as field performance itself! Our purpose in reporting additional laboratory studies is to provide technical insights which may identify the reasons that the Arrhenius projections have failed to correspond to actual field experience.

## DUPONT HUMIDITY STUDIES

### BASIC POLYIMIDE REACTIONS

Figure 1 shows the basic chemical reactions by which polyimide polymer chains are formed and by which they can potentially be cleaved by reaction with water. (Both of these reactions go stepwise through an intermediate polyamide-acid form not shown. Note also that this discussion concerns aromatic polyimides, as distinguished from straight-chain aliphatic polyimides.)

FIGURE 1



Most importantly, Figure 1 shows that chain breaks are not necessarily permanent. The reaction is reversible, and chains can be reconnected at the break points, thus limiting the reduction of molecular weight and properties.

## MEASURING EXTENT OF REACTION

In order to study the effect of humidity on polyimide film, a measure of the average chain length (or molecular weight) of the polymer is needed before and after exposure. Fortunately, this can be determined quite accurately by dissolving a small amount (0.5%) of the polymer film in surfuric acid and measuring the viscosity (inherent viscosity) of the resulting solution.

From basic principles of polymer science the number average molecular weight can be estimated as:

$$M_n = 3.366 \times 10^4 \text{ (inh. visc.)}^{1.89}$$

## EFFECT ON MECHANICAL PROPERTIES

From tests on many film samples we have a practical correlation between inherent viscosity and tensile elongation:

$$\text{Elong. (\%)} = 113.3(\text{inh. visc.}) - 78.0$$

Thus, for example, a film with an inherent viscosity of 0.85 would be expected to break at an elongation of about 18.3%. This relationship serves as a guide in interpretting the practical significance of the experimental inherent viscosity data.

## HUMIDITY EXPOSURE EXPERIMENTS

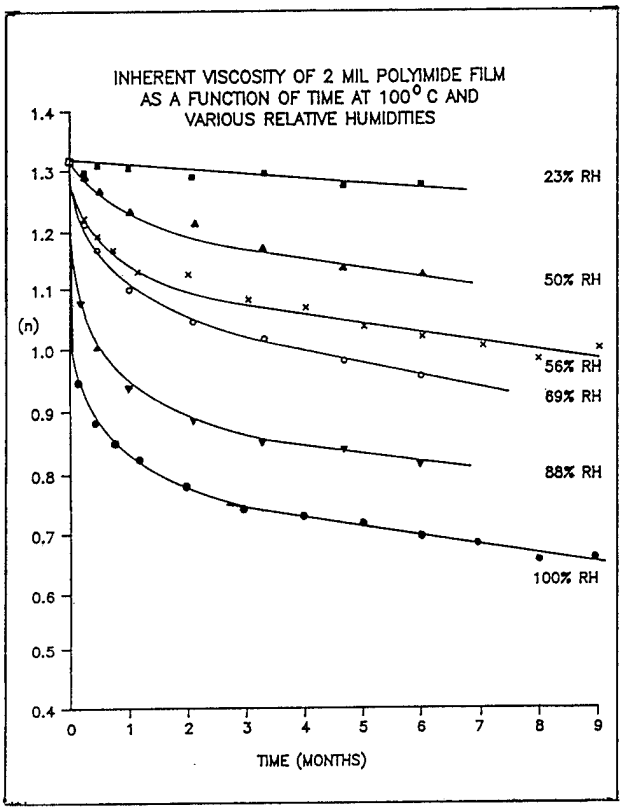
As a point of reference, the Arrhenius plots reported in the paper noted above[1] were based on a specific set of "accelerated" conditions. These included 1/2" mandrel wrap of AWG 22 insulated wires to produce strain in the insulations and immersion of the specimens in hot or boiling water (60-100°C) in lieu of humidity. Insulation life was projected to be about one year at room temperature.

To find the underlying reasons for the discrepancy between the above Arrhenius projections and real-life experience a controlled set of humidity exposure experiments was carried out. Polyimide film specimens (2 mil thickness) were exposed to humidity in closed containers over a period of months. Ranges of varibles studied were:

Humidity: 23-100%
Temperature: 70-100°C
Stress: Unstretched and stretched (17% residual strain)

Film specimens were removed at regular intervals and tested for inherent viscosity. Results are shown in Figures 2, 4, and 5.

FIGURE 2




## DISCUSSION OF RESULTS

### EFFECT OF HUMIDITY ON RATE OF REACTION

The inherent viscosity curves during the first few months at 70 to 100°C (Figure 2) show mainly the effects of chain breaks due to the reaction with water (Figure 1). This reaction appears to have a definite stopping point, however, depending on the humidity. A slight residual slope is also detectible indicating a much slower side-reaction, possibly involving end-groups[2].

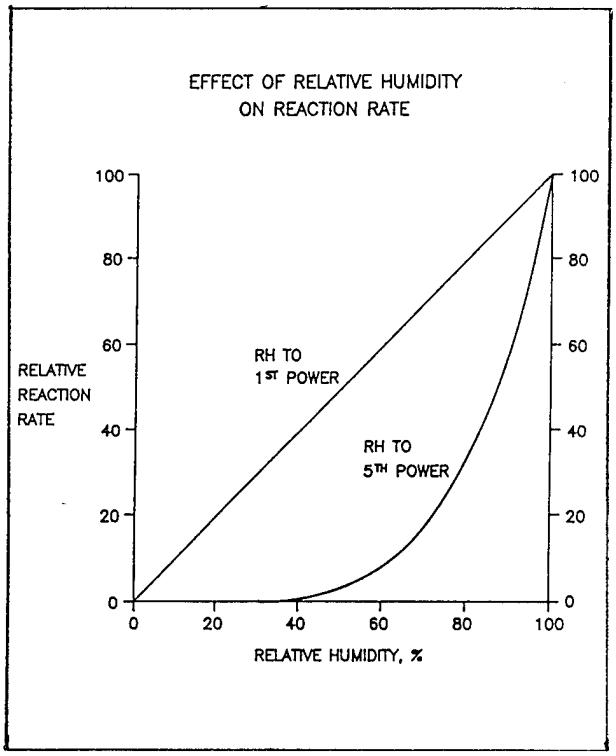
### FIFTH POWER DEPENDENCE ON RELATIVE HUMIDITY

One of the most striking and unexpected findings of this study was the high order (fifth power) dependence of the water reaction rate on relative humidity! This was determined by analysis of the rate curves using standard procedures of chemical kinetics as reported elsewhere[5].

The practical significance of this finding is illustrated by Figure 3. Below 100% relative humidity (RH) the rate of reac-

tion with water does not drop off linearly but rather on a fifth power curve. Thus, at 50% RH the rate is only 3% of its value at 100% RH, and at lower humidities the rate goes essentially to zero.

FIGURE 3




Since no climate on earth has 100% RH all the time and aircraft fly in atmospheres of low humidity, the service life of any aircraft is represented by a spectrum of humidities. The use of liquid water for Arrhenius projections is not a scientific acceleration but a point condition unrealistic to service life prediction. The best that can be said is that the actual service life will be substantially above the Arrhenius plot - and we know this to be true from experience of the past two decades.

REVERSIBLE REACTION - CHEMICAL EQUILIBRIUM

The above discussion concerned the rate at which a reaction might proceed toward an an endpoint. There are also chemical forces which can slow or even reverse such a course - so the endpoint or failure may never be reached.

Note that the chain breaking reaction shown in Figure 1 is accompanied by a reverse reaction which joins and reforms the broken chains. We can now examine the evidence that the reverse reaction exists and is of sufficient magnitude to be a significant factor in service performance:

(1) The high order dependence (fifth power) of rate on one of the reactants (water) is described in the chemical literature as indicative of an equilibrium reaction.

(2) The water reaction curves (e.g., Figure 2) do not stop at the same level. At low humidities the reaction does not go as far - as would be expected for a chemical equilibrium.

(3) The mathematics fit, i.e., the calculated "equilibrium constants" from the various experiments are, indeed, constant[5].

(4) At lower temperatures the reaction does not go as far (Figure 4). This is typical of a reversible reaction in which the equilibrium shifts with temperature.

(5) Delasi[3] found that the physical properties and molecular weight of hydrolyzed film could be regenerated by simple heating. This is absolute proof of the reverse reaction.

Papers on heat aging[4] contain well-known cautions about a number of chemical circumstances under which the basic Arrhenius theory may not be applicable. The existence of a reverse reaction is one such circumstance.

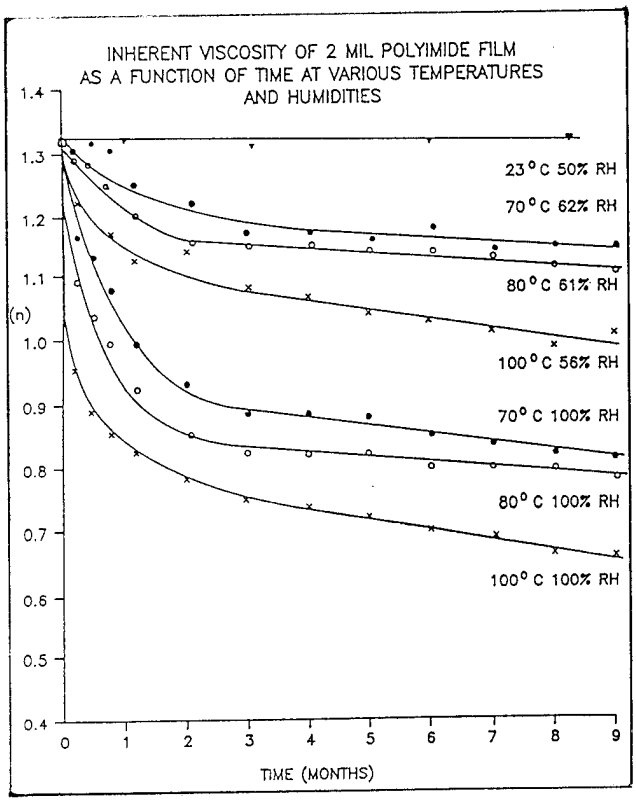
EFFECT OF TEMPERATURE

Arrhenius plots provide a way of dealing with the effect of temperature on reaction rate for a single chemical reaction. From a few experiments at high temperatures (short time to failure) we establish a slope which we project to lower temperatures (long time to failure) for purposes of predicting what we cannot measure in a short time. When more than one reaction is involved, however, a straight line projection may be in error.

Note in Figure 1 that the effect of water on the chain length of polyimide is controlled by two reactions, chain breaking and chain reformation. As temperature is decreased from 100° to 70°C, the chain break reaction slows more than the chain reformation reaction. In other words, the equilibrium of the two reactions shifts in the direction of fewer chain breaks. This effect is shown in the data of Figure 4. Note that, for a given RH, the reactions at lower temperatures are not only slower but they cause fewer chain breaks. The practical effects of the reverse reaction

and shift in equilibrium are that a failure point may be reached much slower than projected, or, under many conditions, never reached.

FIGURE 4




Also note that, in the normal spectrum of use conditions, high temperatures can have a favorable effect in that they speed the rate of the chain reformation reaction during periods of lower humidity. The net effect can be quite different from that obtained from a single set of exaggerated conditions.

## EFFECT OF STRESS

Mechanical stress, when combined with elevated temperatures and humidity, can be used in laboratory demonstrations to shift the equilibrium in the direction of more chain breaks. This effect is seen in Figure 5 where the lower curve was obtained by pre-stretching films to 40% elongation. After release, they recovered to a value of 17% residual strain before being submitted to humidity exposure.

The 1/2" mandrel wraps used for the Arrhenius plots of Reference 1 correspond to a strain of about 9% in the insulation. While this value is not as high as the 14% which is permitted in aircraft wiring at points of termination, it is nearly twice as high as the maximum allowable (4.7%) by radius of curvature specifications for the main body of wiring. Points of termination are not expected to be a problem because wires are held in place by the termination itself. More importantly, the extensive field inspection described above did not reveal cracks at any point in the wiring.

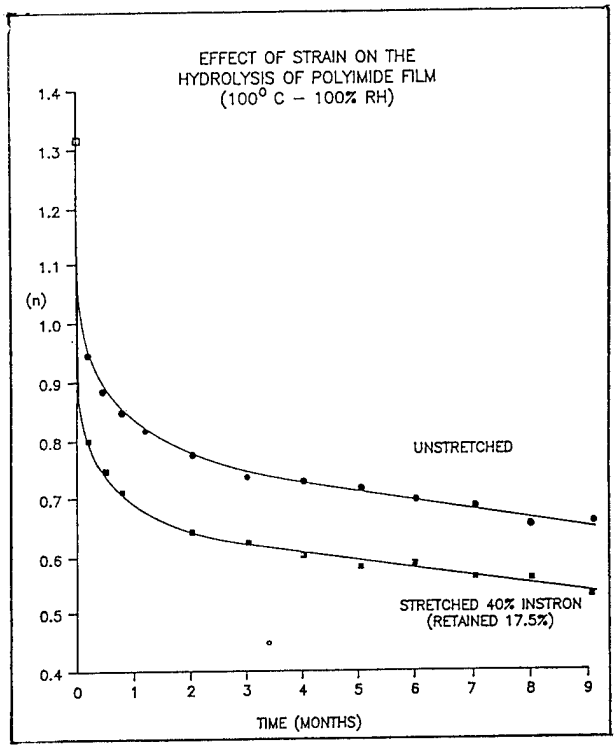
The actual stress in installed wiring is probably much less than would be expected from the allowable radius of curvature (4.7% strain). There are two reasons for this:

First, the normal stress relaxation which occurs in any polymer will cause a significant decay in stress with aging of the wire bundle.

Second, normal use of the wiring for electrical conduction causes heating which accelerates the stress relaxation. This "annealing" reaction has been experimentally observed[6].

In short, the effect of stress is not a large one, but this, together with other factors, illustrates an important point. A laboratory exaggeration of many conditions simultaneously is not a scientific "acceleration" if this leads to failure modes which do not actually occur in the spectrum of conditions encountered in real-life field service.

FIGURE 5



## OTHER ISSUES

### ARCING AND ARC TRACKING

Although this paper is primarily a review of research on resistance of aromatic polyimides to humidity effects, recent speculations implying a connection between hydrolysis, arc tracking, and field problems require some examination.

Shortcircuiting is a very common cause of destructive arcing, which can result from any type of insulation abuse or failure. Generally, high voltages increase the likelihood that arcs will occur, and high current capability of a circuit increases the power and destructiveness of the resulting arc. Any substantial power arc can destroy many conductors in a wire bundle. Mechanical cut-through and abrasion of insulations followed by shortcircuiting is the common cause of arcing.

"Arc tracking" is a special type of shortcircuit failure and is a rare phenomenon compared with arcing itself. We are aware of only three known cases of "arc tracking" in commercial aircraft over the past 13 years. It is not hard to see why there have been so few actual cases of "arc tracking" in field experience. At least five conditions must exist simultaneously for "arc tracking" to occur - with any insulation:

(1) A fault or crack to bare conductor must exist.

(2) The faulted conductor must be on an energized wire.

(3) Substantial voltage and current must be available.

(4) A conductive solution must exist dripping on or near the fault.

(5) A specific geometry of wire layout must exist which permits a completed electrical circuit, typically a return path to ground.

The three known cases of "arc tracking" were not common to one type of insulation but involved two different commercially used wires. All were traced to mechanical damage during wire installation. All were located under lavatories, and all were caused by the dripping of sanitary fluid on the fault.

It is important to note that faults are minimized by use of insulations having high resistance to mechanical damage. Recently, even this minimal risk has been virtually eliminated by wiring designs which do not route wire bundles directly under the flushing mechanisms.

Again, we must distinguish between actual field experience and laboratory tests. It is quite feasible to devise a laboratory setup with specific geometries of damaged wire and specific conditions of dripping electrolyte which "demonstrate" so-called degrees of arc tracking among materials. The practical significance of such testing must be questioned, however, when it is realized that even a slight change in the conditions - such as contamination of the electrolyte with oil or glycol - can result in arc tracking with any insulation.

To sum up, "arc tracking" has been observed only three times in the past 13 years, and it was not specific to one type of insulation. By no stretch of the imagination could it be termed a major cause of wiring problems. We would agree, however, that it is worthwhile to use some forethought in the routing of wire bundles under lavatories for ultimate risk reduction with any insulation.

### HYDROLYSIS AND ARC TRACKING

From the information now in hand it is clear that:

(1) Not a single case of wire failure has been identified due to humidity exposure of polyimide film insulations, and

(2) From the first of the five required conditions for arc tracking - undamaged wire does not arc track!

Thus, speculations about a connection between hydrolysis, arc tracking, and field problems are not consistent with the facts.

## SUMMARY AND CONCLUSIONS

Examination of the pertinent facts has revealed a considerable list of factors which might account for the failure of simple, single dimension Arrhenius plots to project correctly the actual long-term field performance of polyimide wire insulations. A combination of these factors is probably involved.

High on the list of significant factors is the fifth power drop off in reaction rate below 100% relative humidity and the existence of a reverse reaction which limits the extent of reaction with water over a wide range of service conditions.

It must be noted that a laboratory exaggeration of many conditions simultaneously is not a scientific "acceleration" if this leads to failure modes which do not actually occur in the spectrum of conditions encountered in real-life field service.

Shortcircuiting is a common cause of destructive arcing, but "arc tracking" has been a statistical rarity in aircraft wiring. Neither arcing nor arc tracking occurs in the absence of some prior wire damage. We are not aware of any wire damage from field service humidity exposure of aromatic polyimide insulations in aircraft.

REFERENCES


1. Campbell, F. J., IEEE Trans. on Electrical Insulation, Vol. EI-20, No. 1, 111-116 (1985).
2. DeIasi, R., and Russell, J., J. Appl. Polymer Sci., 15, 2965-2974 (1971).
3. DeIasi, R., J. Appl. Polymer Sci., 16, 2909-2919, (1972).
4. Daikin, T. W., AIEE Transactions, 67, 113-122 (1948).
5. Heacock, J. F., "A Kinetic Study of the Hydrolysis of Polyimide Film," to be published.
6. Wolf, C. J., and Soloman, R. S., paper presented at the Fifteenth National Technical Conference of the Society for the Advancement of Materials and Process Engineering (SAMPE), Cincinnati, Ohio, 4-6 Nov. 1983.


**********




James F. Heacock, Ph.D.
E.I. DuPont de Nemours & Co., Inc.
Circleville, Ohio


James F. Heacock, is a Research Associate in the Circleville Research Laboratory of DuPont's Polymer Products Department. His current research is concerned with improved polyimide and polyester films for industrial use. Prior to his present position, he worked at the DuPont Experimental Station, Wilmington, Delaware, and at the DuPont Yerkes Research Laboratory, Buffalo, New York.

Dr. Heacock received the B.S. degree in Chemistry from Morningside College, Sioux City, Iowa, in 1951 and the M.S. degree (1953) and Ph.D. degree (1959) in Organic Chemistry at Oklahoma State University.




John O. Punderson, Ph.D.
Punderson Consulting, Inc.
Marietta, Ohio


John O. Punderson is President of Punderson Consulting, Inc., following his retirement from the DuPont Company in 1982. He received the B.S. degree from the University of Chicago and the Ph.D. in Organic Chemistry from the University of Minnesota. During WW II he served at the Naval Research Laboratory, Washington, DC, and on an electronics repair ship.

At DuPont his activities included research and development on polymers for electrical applications under extreme conditions and fire safety standards for wire and cable. He has 17 patents and more than 25 publications.

Dr. Punderson is a member of the IEEE Power Engineering Society, the Electrical Insulation Society, and the Computer Society. He is active in the IEEE Insulated Conductors Committee and in fire safety commitees of the IEC, ISO, ASTM, NFPA, and the Society of the Plastics Industry. He serves on the Advisory Board of the Journal of Fire Sciences.

# COATED COPPER SHIELDING TAPES FOR THE WIRE AND CABLE INDUSTRY

K. E. Bow, B. K. Grosser, D. G. Pikula

Dow Chemical U.S.A., Granville, Ohio

Plastic coated copper tape shields have been developed for the wire and cable industry. When such shields are bonded to a polyethylene outer jacket, the bond is stable in the presence of moisture, thereby protecting the cable core. If combined with a recently developed ignition resistant chlorinated polyethylene jacket, a sheath is created that can be utilized in cables requiring flame resistance. The physical properties of the tape shield, combined properties of the shield and jacket, and properties of various cable designs are all discussed. Specifically, the development of such coated copper tapes and chlorinated polyethylene jackets provides wire and cable users with additional sheath designs which can be used to reduce expensive maintenance and extend cable service life.

## Introduction

The need to protect the working core of a cable from damage and environmentally caused degradation is vital to preserve the integrity of a communications system. A cable sheath is the first line of protection for a cable. The composite or bonded sheath in which the metallic shield or armor is adhesively bonded to the outer jacket has been shown to provide superior protection to the cable core. The properties of cables with bonded sheaths with coated steel have been described in several recent wire and cable symposium papers for telephone cable[1,2,3] and fiber optical cable[4,5,6,7]. Bonded sheaths with coated aluminum have been described in numerous symposium papers for many types of cable[8,9,10]. However, there have been relatively few papers describing the use of coated copper since it is more difficult to obtain a bond of a coating to copper which is stable in warm, moist environments[11]. This paper will describe a plastic coated copper which has bond stability in moist environments.

Bonded sheaths are useful for cables requiring ignition suppressant properties. Some previous work with adhesive coatings compatible with PVC jacketing compounds has been reported[12]. However, the conventional types of coatings used for bonding to polyethylene jackets are generally adhesively incompatible with PVC. A newly developed chlorinated polyethylene (CPE) jacket having ignition suppressance will form exceptional bonds to coated metals having such conventional coatings. This paper will also describe the properties of a bonded sheath consisting of a CPE jacket and coated copper.

Finally, the use of bonded sheaths with filled, waterblocked cables is considerably more difficult because the fillers and floodants can contaminate the coated metal and interfere with the bond. Often the shield or armor of a filled cable is completely flooded as well. Recent technological advances have led to the development of waterblocking materials which can be used over the core, between the core and shield, in a dry form[13]. This in turn allows the coated metal and jacket to be applied to the cable core without contamination from the filler and floodants. As a consequence, a filled, bonded sheath can be obtained which has resistance to water penetration and exceptional mechanical properties. This paper will also describe how the use of this technology in combination with the polyethylene or CPE jackets and coated copper can give the wire and cable industry new cable options for various applications.

## Material Developments

Plastic Coated Copper: Previous attempts to develop a coated copper with adhesive properties comparable to the coated aluminum currently used by the industry were not successful. In warm, moist environments, the bond of the coating would degrade, leading to greatly reduced levels of bond strength[14]. Intensive investigation of the phenomena indicated that copper ions were complexing with the functional groups of the coating resulting in a reduced level of bond[15]. The process was irreversible.

A new coated copper product has been developed which utilizes a modified copolymer coating. Jacket bond data was gathered by adhering a plaque of jacketing resin to the coated copper or coated aluminum in a platen press heated to 235°C. The data of Table 1 indicates that the bond of the coating to the copper is stable through 70 days of aging in 60°C water. There is a slight decrease in bond for the coated copper over the initial value. This decrease appears to be characteristic of the modified copolymer. However, the bond then stabilizes. The copolymer coated aluminum is

showing its characteristic increase in bond strength with aging. The levels of bond strength are comparable between the two coated metals.

Table 2 shows that the coated copper forms moisture resistant bonds with various jacketing resins such as chlorinated polyethylene, linear low, medium and high density polyethylenes. Bond strength varies somewhat between compounds due to the differences in physical properties between the resins and their influence on the bond test.

Another important property is for the coated metal to seal itself at the overlap of a cable. As the data of Table 3 indicate, the coated copper is again comparable to coated aluminum.

Chlorinated Polyethylene: Two chlorinated polyethylene compounds have been developed which are adhesively compatible with copolymer coated metals. The properties of these jacketing compound are shown in Table 4. The additional factor of ignition suppressance allows a cable with this jacket to be used in buildings or as a below or above ground cable connecting to buildings. These CPE compounds are commercially available or, optionally, they can be compounded by the user.

Waterblocking Tapes: A water barrier in the form of a water swellable tape has been previously introduced to the industry[16]. These waterblocking materials consist of nonwoven mats which encapsulate water swellable powders. Upon exposure to water, the powder swells to such a degree that a dam is created to the flow of water preventing further longitudinal flow. The physical and water swellable properties of the tapes utilized in this study are given in Table 5.

## Preparation of Test Cables

Purpose: Experimental tapes of various thicknesses in two types of copper alloys were coated on both sides with modified copolymer in a pilot coater. The 110 alloy was chosen for its general utility while the 194 alloy was chosen for its higher tensile strength and rodent resistance. These tapes were then formed over various core constructions and bonded sheath cables prepared with various jacketing compounds. These cables were then tested for selected properties in order to present to potential cable users what property ranges and levels of performance might be expected from copper shields or armors and CPE jackets. In particular, the bonded sheath with coated copper would benefit from excellent mechanical properties. So, it was felt important to illustrate that the ability now exists to achieve an excellent bonded sheath over a jelly filled and waterblocked cable core. Thus, a potential solution to a problem which has challenged the industry for many years could be implemented through the use of water swellable tapes. Obviously, this technology is appropriate for cables using other types of coated metals.

Specific applications may require further targeting of the type and thickness of the copper alloy. Experience so far indicates that the modified copolymer forms sufficient and moisture resistant bonds with a wide variety of copper alloys.

Equipment: An experimental sheathing line was used for the preparation of cable samples for testing. This line utilized a corrugator which imparted 14 corrugations to the inch to the shielding or armoring tape. The corrugation depth was 32 mils (0.8 mm). After corrugating, the tape was longitudinally formed about the cable core by means of a cone former. The jacket was then applied using pressure extrusion to force the jacketing resin down into the corrugations. Some tapes were formed smooth by means of a tray former.

Test Samples: The samples prepared are shown in Table 6. Cable samples having bonded sheaths with copper or copper alloy tapes of various thicknesses were prepared to demonstrate the properties of these sheaths for various applications. The run conditions are shown in Table 7. The CPE jacketing compound is best applied using a conventional polyethylene screw without a mixing screw without a mixing zone. The melt temperatures are slightly lower than those for polyethylene and pressures are higher. Overall, the CPE material processes very well in conventional equipment designed for polyethylene.

## Performance Testing of Bonded Sheath Cables with Coated Copper

Mechanical Properties: A most important advantage of the bonded sheath is that it combines the strength of the metal with the flexibility of the jacket to yield improved mechanical properties over unbonded sheaths. The most important area where this is manifested is in bend performance. Figure 1 compares the bend performance of cables with 5 mil copper bonded to a CPE jacket with both smooth and corrugated shields. The ratio of mandrel diameter to cable diameter was used as the parameter in this test while evidence of tearing of the copper was taken as failure. It can be seen that the bend performance of corrugated shield is improved over a smooth shield but the level of performance with smooth tapes should not be a hindrance to the practical use.

Figure 2 compares the bend performance of bonded sheath cables with different thicknesses of corrugated copper. The bend performance decreases as copper thickness increases. It appears, however, that there is sufficient bend performance for practical use at the 10 mil thickness.

A puncture test was run on the sheaths using a 12 penny nail. This nail was forced into the sheath at 0.5 inches/minute (1.2 cm/minute) using a tensile tester. The results of the test are

shown in Table 8. As expected, puncture resistance generally increases as the thickness of the armor increases.

Crush resistance was measured by recording the force required in compressing the sheath to 25% of its diameter in a tensile tester. A sample 4 inches (1.6 cm) long was used and the test speed was 0.5 inches/minute (1.2 cm/min). The results shown in Table 8 indicate that crush resistance also increases as the thickness of the copper increases.

Thermal Cycling: Another important property of the bonded sheath is that it resists jacket shrinkback because the bond between the jacket and metallic tape allows the shrinkage forces to be countered by the rigidity of the metallic component. To test for shrinkback, samples of sheath approximately 12 inches (30.5 cm) long were placed in an oven capable of automatically cycling from -40° to +60°C. An 8 hour cycle was used with 4 hours at each temperature and a 20 minute transition time. The amount of shrinkage was measured as a percentage of the initial length. The results are shown in Figure 3. The bonded sheath with a corrugated tape is showing very little shrinkage while the unbonded sheath is showing significant shrinkback. The sheath with a smooth tape did not exhibit shrinkback.

Adhesive Properties: Samples for bond tests were cut circumferentially from the sheath and tested for adhesion using a tensile tester and a 2 inch/minute (5.08 cm) test speed. The samples were then placed in 60°C water and aged for 24 days and retested. The results are shown in Table 9. The bond stability of the coated coppers are comparable to coated aluminum. There is a small decrease in bond strength initially for some samples but then the bond stabilizes. This pattern has been noted previously for the laboratory prepared samples. It should be noted that when corrugated samples are cut from a cable and tested, the bond strengths are much higher than the laboratory data (Table 2) due to the influence of the corrugations at the bond line. This effect has been previously studied by Levy, et al[17].

Fire Test: Samples of cable with the chlorinated polyethylene jacket were submitted to an outside laboratory for fire testing according to IEEE 383 Vertical Tray Flame Test. The cables tested and the results of the test measuring both char height and circuit integrity are shown in Table 10. The char height is slightly greater for the cables containing the coated copper versus cables without the metallic shield; however, the circuit integrity is increased by 25-40%. Maintaining circuit integrity longer in a real fire situation can have the benefit of extending the time over which control is exercised over the electrical functions of the system.

Water Resistance: Cable samples were prepared with a jelly filled core, a water swellable tape over the core (between the core and shield), and a bonded sheath of shield and jacket. These cables were subjected to a water resistance test based on the REA Specifications PE-39 and PE-89. In these tests, 6 foot samples of experimental cable were first sectioned in the center down to the core to expose the core-shield and shield-jacket interfaces. A 3 foot head of water was then applied to the exposed interfaces using a "T" fixture. Care was exercised to make sure the sheath layers were not compressed at the fixture. Failure was indicated if water persistently leaked from the cable ends. The test was run for 24 hours and then the cable samples were dissected to observe the degree of waterblocking.

The results of the tests are shown in Table 11. The water swellable tape formed a gel which acted as a dam to the flow of water in the core-shield interface while the bond between the shield and jacket effectively blocked this interface. For the conventional cable sample without an unbonded sheath, water flowed immediately between the shield and jacket leading to failure in this test. One sample with a more loosely fitting water swellable tape also leaked after one hour. This indicates that there is a critical amount of fit required when using such tapes. If the fit is too loose, not enough pressure will be developed to form a gelled mass with enough gel strength to resist the pressure of the flow. Additional work will need to be done with these tapes to quantify this effect.

Termination Considerations: The bond of shield to jacket is extremely good with the coated copper such that stripping for purposes of termination will be most difficult. There are many termination devices currently available which can be used for terminating without need for stripping of the jacket. Several of these devices were applied to several samples of bonded sheath and tested following some of the procedures outlined in REA Specification PE-33. These samples were tested by measuring the electrical resistance of two connectors applied to a 12 inch (9 centimeter) length of cable before and after thermally cycling for 25 cycles between -40° to +60°C. As the data of Table 12 show, terminations made with connectors which pierce the coatings of the shield are electrically stable. Use of such devices will greatly facilitate the termination of cables in the field.

## Suggested Cable Applications with Coated Copper

Buried Service Wire: Various commercial buried service wires (BSW) utilize copper alloys for armoring. The use of a coated copper alloy can bring benefits to these designs. The first is a water blocked shield jacket interface. Experimental Cable Sample A of Table 6 represents a new concept in buried service wire. Bonding between the copper shield and CPE jacket and the use of a water swellable tape between core and shield effectively blocks these interfaces from the flow of water. By eliminating these major paths for water flow, the incidence of water

ingress into underground splices and closures should be greatly reduced. This in turn will greatly reduce the incidence of corrosion and electrical problems within the telephone system.

The use of the CPE jacket will allow requirements for ignition suppressance to be met while the bonded sheath will increase the mechanical performance of the cable. The bend data of Table 13 shows how the bonded sheath outperforms a commercially available buried service wire with an unbonded sheath. It was noted that the unbonded sheath kinks after only one-half of a bend cycle at the 6x mandrel.

By choosing a copper alloy of sufficient thickness, the buried service wire can be designed for resistance to gophers and other rodents. In combination with the bonded sheath, these cables will have all the aforementioned benefits.

Signal/Indoor Cables: The use of the coated copper/CPE bonded sheath with signal or indoor telephone cable such as terminating cable brings new benefits to these cables as well. The major benefit in signal cables is ease of terminating. The major benefit for terminating cables is that they will be galvanically compatible with other copper sheathed cables in the outside plant. The CPE jacket has excellent ignition suppressance with lower levels of smoke generation than the conventional jackets. The mechanical performance is excellent due to the high level of bond between the coated copper and CPE jacket. The improved mechanical performance over conventional designs can greatly reduce the incidence of damage during installation and use.

Fiber Optical Cables: In combination with either a polyethylene jacket or a CPE jacket, the coated copper or copper alloys can bring benefits to these designs. The CPE jacket can be used in local area networks (LANs) allowing a cable to go between buildings, for example, without the need to change cable designs to achieve ignition suppressance when the cable enters and is terminated inside the buildings. The significant benefit of the copper armor in LANs is that the armor is galvanically compatible with other buried structures such as water pipes or ground beds.

By choosing a suitable thickness of copper alloy, a rodent resistant armor can be obtained. In combination with a bonded sheath and a polyethylene jacket, this cable design can be used to implement fiber optical cables into telephone systems where copper pair cable sheathed with various coppers are prevalent. The major benefit again of the copper armor is that it allows the fiber optical cables to be galvanically compatible with copper shielded and/or armored copper pair cables currently in use in the outside plant.

The benefits of the bonded sheath on fiber optical cable are many. The mechanical properties of the cable which are most importantly improved over unbonded sheaths are bend performance and reduced shrinkback (resistance to thermal cycling). Both improvements serve to greatly reduce the amount of mechanical stress which might be imposed on the fibers. The bond to the jacket effectively serves to integrate the armor into acting as a moisture barrier to the core, again helping to preserve the integrity of fibers and maintain cable reliability.

Coated copper shows a reduced propensity to hydrogen generation in corrosive environments, also increasing the reliability of the telephone system by preserving the integrity of the fibers.

A paper also presented at this symposium will show that the use of two-side coated metals in fiber optical cables will lead to cable designs which are significantly more resistant to lightning currents[18]. This allows the benefits which only metals can provide to fiber optical cable to be achieved while maximizing the benefit of immunity to electromagnetic interference possessed by optical fibers.

Telephone Cables: The use of bonded sheaths with coated copper or copper alloy shields and polyethylene jackets can be used to advantage in conventional copper pair telephone cable as well. The major benefit is that the bonded sheath will provide the cable with superior mechanical properties over unbonded sheaths. The use of a water swellable tape over the core will allow the bonded sheath to be achieved and, at the same time, significantly improves the resistance to water penetration. As previously mentioned, the use of coated copper either flooded or as a bonded sheath will also lead to cables with improved resistance to lightning.

## Conclusions

A plastic coated copper has been developed which has bond stability in the presence of heat and moisture. The coated copper is adhesively compatible with polyethylene jackets. This new coated copper can be utilized in cable designs requiring ignition suppressance by bonding the copper to newly developed thermoplastic jacketing resins formulated from chlorinated polyethylene.

Experimental cables were prepared utilizing a dry water swellable tape over a filled cable core. As a result, a bonded jacket, fully filled cable was achieved which has extremely good resistance to moisture penetration.

Various types of cables which can benefit from these three technologies either separately or in combination with each other are buried service wire, signal and/or indoor cable, fiber optical cable, and conventional copper conductor telephone cable.

Various alloys and thicknesses of coated copper have been developed for a wide variety of applications, including those requiring rodent resistance.

## References


[1] GM Yanizeski, EL Johnson, RG Schneider, "Cable Sheath Buckling Studies and the Development of a Bonded Stalpeth Sheath", International Wire & Cable Symposium Proceedings, 1980, p. 48-58.

[2] AC Levy, BJ Overton, "Evaluation of Adhesive Materials for Bonded Sheath Cable Designs", International Wire & Cable Symposium Proceedings, 1983, p. 88-92.

[3] DM Mitchell, RP Collins, DE West, MD Kinard, "Bonded ASP: A Superior Sheath for Buried and Underground Filled Cables", International Wire & Cable Symposium Proceedings, 1984, p. 207-212.

[4] JR Osterfield, SR Norman, DN McIntosch, AJ Rogers, R Castelli, M Tamburello, "An Optical Fibre Link in a Mountainous Environment", International Wire & Cable Symposium Proceedings, 1980, p. 202-211.

[5] TS Hope, RJ Williams, K Abe, "Developments in Slotted Core Optical Fiber Cables", International Wire & Cable Symposium Proceedings, 1981, p. 220-227.

[6] PS Venkatesan, K Korbelak, "Characterization of Ruggedized Fiber Optic Dual Wavelength Cables", International Wire & Cable Symposium Proceedings, 1982, p. 358-370.

[7] MM Rahman, GM Davidson, "Design Consideration for Jacketing Fiber Optic Cable", International Wire & Cable Symposium Proceedings, 1982, p. 377-380.

[8] GE Clock, GA Klumb, RC Mildner, "Adhesive Thermoplastic Copolymers for the Wire and Cable Industry", International Wire & Cable Symposium Proceedings, 1963.

[9] RC Mildner, WE Ropp, JH Snow, "The Evolution of Sheath Constructions for Communications Cable", International Wire & Cable Symposium Proceedings, 1966.

[10] ED Metcalf, "A Bonded, Non-Corrugated Aluminum/Polyethylene Sheathing System for Telephone Cable", International Wire & Cable Symposium Proceedings, 1972, p. 235-239.

[11] HG Frank, MC McGaugh, WE Ropp, "A Study of the Effect of Time, Temperature, and Moisture on Bonded Interfaces in 'Bonded Jacket' Cable Construction", International Wire & Cable Symposium Proceedings, 1968.

[12] W Purkert, MR Dembiak, "The Evolution of an Improved Sheath Design for Terminating Cable", International Wire & Cable Symposium Proceedings, 1967.

[13] BJ Nieuwhof, R de Vrieze, "Longitudinal Waterblocking Performance of Conductive and Non-conductive Waterswellable Nonwovens", International Wire & Cable Symposium Proceedings, 1983, p. 83-87.

[14] HG Frank, MC McGaugh, WE Ropp, "A Study of the Effect of Time, Temperature, and Moisture on Bonded Interfaces in 'Bonded Jacket' Cable Construction", International Wire & Cable Symposium Proceedings, 1968.

[15] B Wargotz, "Environmental Stability of Ethylene-Acrylic Acid Adhesive Copolymers Bonded to Metal Substrates", Journal of Applied Polymer Science, Volume 12, p. 1873-1888 (1968).

[16] BJ Nieuwhof, R de Vrieze, "Longitudinal Waterblocking Performance of Conductive and Non-conductive Waterswellable Nonwovens", International Wire & Cable Symposium Proceedings, 1983, p. 83-87.

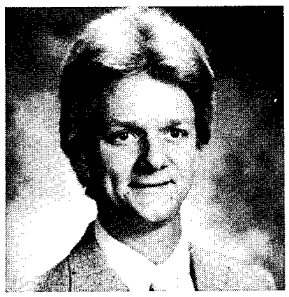
[17] AC Levy, BJ Overton, "Evaluation of Adhesive Materials for Bonded Sheath Cable Designs", International Wire & Cable Symposium Proceedings, 1983, p. 88-92.

[18] D Fischer, PU Bakhru, E Schrom, KE Bow, "Crushing Metallic Shielded Communications Cables With Dynamic Magnetic Fields", International Wire & Cable Symposium Proceedings, 1985.

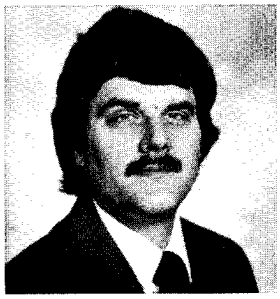

## Biography



Kenneth E. Bow is an Associate Development Scientist with Dow Chemical USA, Granville, Ohio. He has been involved in the research and development of materials for the wire and cable industry for over 20 years. He is currently responsible for the development of coated metal shielding and armoring tapes for applications in cables. Mr. Bow graduated with a B.S. E.E. degree from Michigan State University in 1962.



Brian K. Grosser is currently a Development Engineer for Dow Chemical USA at the Granville Research Center in Granville, Ohio. His current responsibilities include the development of new coated copper products for the wire and cable industry. Mr. Grosser graduated with a B.S.C.hE, M ENG ChE from the University of Louisville, Louisville, Kentucky, in 1983. He is actively involved in IEEE and the ICC.



Daniel G. Pikula is an Upper Level Research Technician with Dow Chemical USA in Granville, Ohio. He is currently engaged in activities associated with the technical service and development of coated metal shielding and armoring tapes for the wire and cable industry. Mr. Pikula is pursuing a B.S. in chemistry from Otterbein College.

Figure 1. Comparative Bend Performance of Bonded Sheaths with 5 mil (0.125 mm) Copper

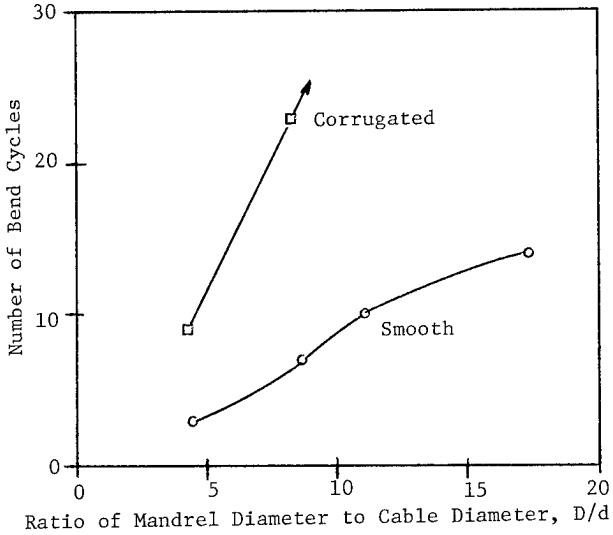



Figure 2. Comparative Bend Performance of Bonded Sheaths with Corrugated Coated Copper Alloy of Various Thicknesses

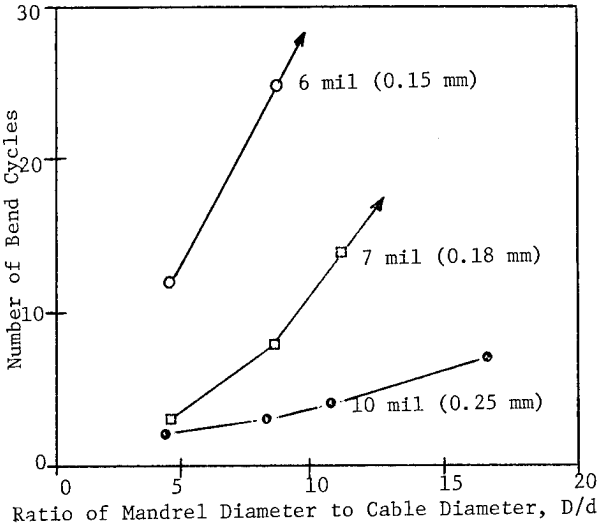



Figure 3. Effects of Thermal Cycling on Jacket Shrinkback

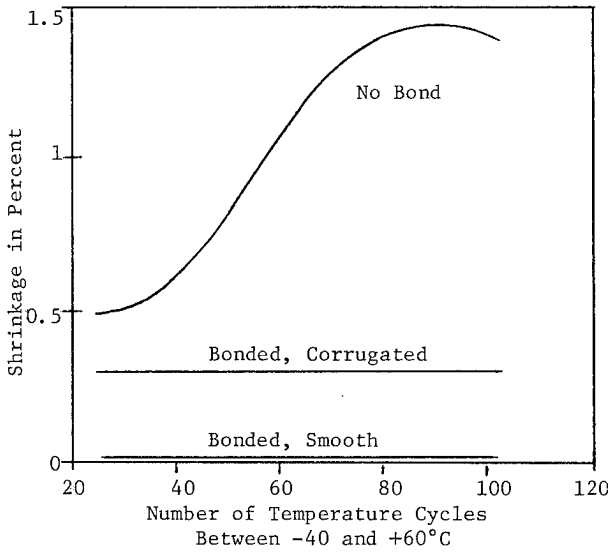


Table 1. Jacket Bond of Coated Copper and Coated Aluminum to LLDPE[1] Jacket

| Metals | Bond Strength[2] in g/mm (lb/in) Versus Time of Aging in 60°C Water, Days | | | |
|---|---|---|---|---|
| | Initial | 14 | 35 | 70 |
| Coated Copper[3] | 182.2 (10.2) | 167.9 ( 9.4) | 151.8 ( 8.5) | 164.3 ( 9.2) |
| Coated Aluminum[4] | 160.7 ( 9.0) | 184.0 (10.3) | 201.8 (11.3) | 214.3 (12.0) |

[1]Linear Low Density Polyethylene (No. 880).
[2]Metal/Coating Separation. Test Conditions: Peel Angle of 90°, Test Speed of 50.8 mm/minute.
[3]Experimental Plastic Coated Copper (No. XP 61000.05). Metal Thickness -- 0.125 mm (0.005 in); Type 110 Alloy.
[4]Copolymer Coated Aluminum (Type A282). Metal Thickness -- 0.20 mm (0.008 in).

Table 2. Jacket Bond of Coated Copper[1] to Various Jacketing Resins

| Jacketing Resin | Bond Strength[2] in g/mm (lb/in) Versus Time of Aging in 60°C Water, Days | | | | | |
|---|---|---|---|---|---|---|
| | Initial | 7 | 30 | 60 | 90 | 120 |
| LLDPE[3] | 137.8 (7.7) | 134.3 (7.5) | 137.8 ( 7.7) | 134.3 ( 7.5) | 134.3 (7.5) | 132.5 (7.4) |
| CPE[4] | 137.8 (7.7) | 111.0 (6.2) | 112.8 ( 6.3) | 114.6 ( 6.4) | 107.4 (6.0) | 103.8 (5.8) |
| MDPE[5] | 153.9 (8.6) | 137.8 (7.7) | 136.0 ( 7.6) | 137.8 ( 7.7) | 134.3 (7.5) | 132.5 (7.4) |
| HDPE[6] | 162.9 (9.1) | 139.6 (7.8) | 207.6 (11.6) | 202.3 (11.3) | --- | --- |

[1]Experimental Plastic Coated Copper (No. XP 61000.05). Metal Thickness -- 0.125 mm (0.005 in); Type 110 Alloy.
[2]Metal Coating Separation. Test Conditions: Peel Angle of 90°, Test Speed of 50.8 mm/minute.
[3]Linear Low Density Polyethylene (Type 880).
[4]Chlorinated Polyethylene (Formulation 546-82038-24).
[5]Medium Density Polyethylene (No. XP 60622.00).
[6]High Density Polyethylene.

Table 3. Heat Seal Characteristics of Coated Copper and Coated Aluminum

| | Heat Seal Strength[1] in g/mm (lbs/in) | |
|---|---|---|
| Copper[2] | Coating-Coating | 214.3 (12.0) |
| Aluminum[3] | Coating-Coating | 303.6 (17.0) |

[1]Dwell Time of 2 Seconds, 0.28 mPa (40 psig), 150°C (300°F) on Heat Seal Bars.
[2]Experimental Plastic Coated Copper (No. XP 61000.08).
[3]Copolymer Coated Aluminum (Type A282).

Table 4. Properties of Chlorinated Polyethylene Jacketing Compounds

| Property | Test Method | Value | |
|---|---|---|---|
| | | Formulation #54682038-24-2 | Formulation #54684026-30-2 |
| 100% Modulus MPa (psi) | ASTM D-412-75 | 9.52 (1,354) | 7.56 (1,075) |
| Ultimate Tensile MPa (psi) | ASTM D-412-75 | 10.96 (1,559) | 10.48 (1,490) |
| Elongation, % | ASTM D-412-75 | 420 | 465 |
| Hardness, Shore A | ASTM D-412-75 | 93 | 95 |
| Oxygen Index (LOI), %[1] | ASTM D-2863-77 | 31 | 32.5 |
| Heat Distortion @ 121°C, % | ICEA 6.4.14.2 | 0 | 3 |
| Low Temperature Brittleness, °C | ASTM D-746 | -29 | -35 |

[1]As specifically stated in the "LOI" test method, ASTM D-2863 is a small scale test to provide the laboratory rating of the relative flammability of products under controlled conditions of ignition and oxygen concentration. It is not designed to measure flammability under an actual fire situation. Note: Results of small scale tests are not intended to reflect behavior of this or any other material under actual fire conditions.

Table 5. Properties of Water Swellable Tapes

| Property | Test Method | Value | |
|---|---|---|---|
| | | Experimental[1] | Commercial |
| Wicking, mm/in (in/minute) | Dow | 10.2 (0.4) | 2.54 (0.1) |
| Immersion Capacity, g water/g sample | Dow | 70 | 26 |
| Ultimate Tensile (MD), $Kg/cm^2$ (psi) | ASTM D882 | 87.9 (1,250) | 67.5 (960) |
| Tape Thickness, mm (in) | ASTM D374C | 0.20 (0.008) | 0.41 (0.016) |

[1]XDR-0555-B-20377

Table 6. Test Samples Prepared on Experimental Jacketing Line

| Cable Type | Run/ Sample ID | Cable O.D., mm (in) | Coated Metal Designation Number | Metal Alloy | Metal Thickness, mm (in) | Jacketing Resin Formulation | Shield Configuration |
|---|---|---|---|---|---|---|---|
| F/O | A | 13.7 (.54) | XU 61000.11 | Copper 194 | .152 (.006) | 54684026-30-2 | Corrugated |
| F/O | B | 14.0 (.55) | XU 61000.12 | Copper 194 | .178 (.007) | 54684026-30-2 | Corrugated |
| F/O | C | 14.5 (.57) | XU 61000.13 | Copper 194 | .254 (.010) | 54684026-30-2 | Corrugated |
| BSW[1] | D | 13.7 (.54) | XU 61000.11 | Copper 194 | .152 (.006) | 54684026-30-2 | Corrugated |
| BSW[1] | E | 13.7 (.54) | XU 61000.12 | Copper 194 | .178 (.007) | 54684026-30-2 | Corrugated |
| BSW[1] | F | 14.0 (.55) | XU 61000.13 | Copper 194 | .254 (.010) | 54684026-30-2 | Corrugated |
| BSW[1] | G | 10.9 (.43) | XP 61000.08 | Copper 110 | .127 (.005) | 54684026-30-2 | Corrugated |
| Signal | H | 20.3 (.80) | A282 | Aluminum 1100 | .203 (.008) | 54682038-24-2 | Smooth |
| Signal | I | 20.3 (.80) | A282 | Aluminum 1100 | .203 (.008) | 54682038-24-2 | Corrugated |
| Signal | J | 20.6 (.81) | XP 61000.08 | Copper 110 | .127 (.005) | 54682038-24-2 | Smooth |
| Signal | K | 20.6 (.81) | XP 61000.08 | Copper 110 | .127 (.005) | 54682038-24-2 | Corrugated |
| Signal | L | 19.8 (.78) | A282 | Aluminum 1100 | .203 (.008) | 54684026-30-2 | Smooth |
| Signal | M | 20.1 (.79) | A282 | Aluminum 1100 | .203 (.008) | 54684026-30-2 | Corrugated |
| Signal | N | 20.1 (.79) | XP 61000.08 | Copper 110 | .127 (.005) | 54684026-30-2 | Smooth |
| Signal | O | 20.3 (.80) | XP 61000.08 | Copper 110 | .127 (.005) | 54684026-30-2 | Corrugated |
| Signal | P | 20.8 (.82) | XU 61000.11 | Copper 194 | .152 (.006) | 54684026-30-2 | Corrugated |
| Signal | Q | 20.8 (.82) | XU 61000.12 | Copper 194 | .178 (.007) | 54684026-30-2 | Corrugated |
| Signal | R | 20.8 (.82) | XU 61000.13 | Copper 194 | .254 (.010) | 54684026-30-2 | Corrugated |

[1]These samples contain a water swellable tape layer between the core and shield as described in Table 5.

Table 7. Run Conditions For Sample Preparation

| Cable Type | Run/ Sample ID | Extruder RPM | Line Speed, m/min (ft/min) | Jacket Melt Temperature, °C | Crosshead Pressure, kPA (psig) | Breaker Plate Pressure, kPA (psig) |
|---|---|---|---|---|---|---|
| F/O | A,B,C | 40 | 10.1 (33) | 185 | 17,530 (2,540) | 22,360 (3,240) |
| BSW | D,E,F | 40 | 10.1 (33) | 185 | 17,530 (2,540) | 22,360 (3,240) |
| BSW | G | 25 | 9.8 (32) | 177 | 15,590 (2,260) | 20,010 (2,900) |
| Signal | H-R | 65 | 9.8 (32) | 177 | 16,220 (2,350) | 19,320 (2,800) |

[1]Water bath temperature for all samples was 26°C. A paraffinic based mineral oil was used to lubricate all corrugated samples.

Table 8. Mechanical Properties of Bonded Sheath with Corrugated Coated Aluminum and Copper

| Sheath I.D. | Metal Thickness, mm (in) | Shield Configuration | Puncture Resistance[1] Through Shield, kg (lbs) | Crush Resistance[2] @ 25% of Initial Diameter/Unit Length, N/mm (lb/in) |
|---|---|---|---|---|
| No Armor | --- | --- | 6.8 (15) | 4.7 (26) |
| XP 61000.08 | .127 (.005) | Copper | 21.3 (47) | 12.0 (67) |
| XU 61000.11 | .152 (.006) | Copper Alloy | 19.5 (43) | 12.4 (69) |
| XU 61000.12 | .178 (.007) | Copper Alloy | 20.4 (45) | 12.9 (72) |
| XU 61000.13 | .254 (.010) | Copper Alloy | 26.8 (59) | 16.5 (92) |

[1]With Core.
[2]Without Core.

Table 9. Adhesive Properties with Bonded Sheath Cables

| Metals | Jacket Resin Formulation | Bond Strength[1] in g/mm (lb/in) Versus Time of Aging in 60°C Water, Days | | |
|---|---|---|---|---|
| | | Initial | 7 | 24 |
| 8 mil Aluminum (A282) | | | | |
| Smooth | 24-2 | 254.2 (14.2) | 218.4 (12.2) | 220.2 (12.3) |
| Corrugated | 24-2 | 388.4 (21.7) | Exceeds Jacket Tensile | Exceeds Jacket Tensile |
| 5 mil Copper (XP 61000.08) | | | | |
| Smooth | 24-2 | 209.4 (11.7) | 202.3 (11.3) | 182.6 (10.2) |
| Corrugated | 24-2 | 495.8 (27.7) | 447.5 (25.0) | 456.5 (25.5) |
| 8 mil Aluminum (A282) | | | | |
| Smooth | 30-2 | 222.0 (12.4) | 205.9 (11.5) | 193.3 (10.8) |
| Corrugated | 30-2 | 424.2 (23.7) | 399.2 (22.3) | 381.3 (21.3) |
| 5 mil Copper (XP 61000.08) | | | | |
| Smooth | 30-2 | 533.4 (29.8) | 264.9 (14.8) | 263.1 (14.7) |
| Corrugated | 30-2 | 513.7 (28.7) | 465.4 (26.0) | 449.3 (25.1) |
| 6 mil Copper Alloy (XU 61000.11) | | | | |
| Corrugated | 30-2 | 415.3 (23.2) | 469.0 (26.2) | 451.1 (25.2) |
| 7 mil Copper Alloy (XU 61000.12) | | | | |
| Corrugated | 30-2 | 481.5 (26.9) | 531.6 (29.7) | 546.0 (30.5) |
| 10 mil Copper Alloy (XU 61000.13) | | | | |
| Corrugated | 30-2 | 361.6 (20.2) | 408.1 (22.8) | 404.5 (22.6) |

[1]Metal/Coating Separation, Peel Angle @ 180°, Test Speed of 50.8 mm/min (2 in/min).

Table 10. Results of IEEE 383 Vertical Tray Flame Test[1]

| Cable Sheath | Char Height, Ft | Circuit Integrity, min |
|---|---|---|
| No Armor, PVC Jacket | 2.6 | 2.0 |
| 8 mil Aluminum/CPE Jacket | 3.0 | 5.6 |
| 5 mil Copper/CPE Jacket | 3.0 | 6.2 |
| 8 mil Copper Alloy/CPE Jacket | 3.0 | 7.1 |
| 10 mil Copper Alloy/CPE Jacket | 3.0 | 8.2 |

[1]Note: Results of Small Scale Tests are not Intended to Reflect Behavior of This or Any Other Material Under Actual Fire Conditions.

Table 11. Results of Water Penetration Test

| Cable Description | REA PE-39 - 1 Hour | French EDF/Dow - 24 Hours | Remarks |
|---|---|---|---|
| BSW (Bonded Sheath) | Pass | Pass | Water Was Effectively Blocked Within 25 cm (9.8 in) of Fault |
| BSW (Unbonded Sheath) | Fail | Fail | Leaked After 6 minutes |

Table 12. Connector Stability Data on Bonded Sheath With Coated Copper

| Cable Sheath | Initial Resistance (milliohms) | Resistance After 25 Cycles (milliohms) | Is Change In Resistance Less Than 5 Milliohms? |
|---|---|---|---|
| 5 mil Copper (XP 61000.08) | | | |
| Smooth | .69 | .93 | Yes |
| Corrugated | .75 | .82 | Yes |
| 6 mil Copper Alloy (XU 61000.11) | | | |
| Corrugated | .97 | 1.08 | Yes |
| 7 mil Copper Alloy (XU 61000.12) | | | |
| Corrugated | .87 | .91 | Yes |
| 10 mil Copper Alloy (XU 61000.13) | | | |
| Corrugated | 1.12 | 1.31 | Yes |

Note: Commercially Available Connector.

Table 13. Bend Performance of Buried Service Wire With Bonded Sheath Versus Unbonded Sheath

| Cable Type | Approximate Mandrel Diameter/Cable Diameter Ratio, D/d | | | |
|---|---|---|---|---|
| | 6 | 9 | 16 | 22 |
| Bonded Sheath[1] | 11.0 | 13 | 19 | 25+ |
| Unbonded Sheath[2] | 0.5 | 4 | 7 | 10 |

[1]CPE Bonded to Coated Copper XP 61000.08.
[2]PVC Unbonded to Copper Alloy.

# CORROSION PERFORMANCE OF A SHEATH WITH PLASTIC COATED STAINLESS STEEL FOR FIBER OPTIC CABLE

Prakash U. Bakhru
Dow Chemical U.S.A.
Granville, Ohio

Kenneth E. Bow
Dow Chemical U.S.A.
Granville, Ohio

Patrick L. Hagans
Dow Chemical U.S.A.
Midland, Michigan

Lewis Shadoff
Dow Chemical U.S.A.
Midland, Michigan

The properties of a bonded sheath based on plastic coated stainless steel are described for use in fiber optical cable. Overviews of mechanical properties, rodent resistance, lightning resistance and economics are presented. Detailed information on resistance to corrosion is given using an electrochemical polarization technique, an ac impedance technique, galvanic couples and a review of soil burial tests. Mass spectrometry is used to quantify the hydrogen evolution from bare and coated metals.

These data are useful in the selection of applications for sheaths with plastic coated stainless steel.

## Introduction

The key objective of any sheath design for a fiber optical cable is to protect the mechanical and optical properties of the glass fibers from the stresses associated with cable installation and the effects of environment after installation.

The use of coated metals in a bonded sheath provides numerous advantages as a package for a fiber optical cable. These advantages, along with comparative performance of various sheath designs, have been described in several previous International Wire and Cable Symposium papers[1,2,3,4,5]. Among them are moisture barrier, improved mechanical performance such as bend and flex strength and resistance to axial compression (crush strength), resistance to thermal cycling, rodent resistance, and the ability to locate buried cables. The disadvantages often cited are possible susceptibility to lightning and possible corrosion which could liberate hydrogen or allow moisture to eventually penetrate into the core of the cable and adversely affect the transmission characteristics of the fibers.

A 1983 symposium paper described a sheath design based on a dual shield of stainless steel and either a copper or coated aluminum which was recommended for buried or aerial applications where rodent and lightning resistance was essential[6]. Later, the design was firmed up around stainless steel and copper to minimize the effects associated with the liberation of hydrogen in case of exposure of the metallic members of the sheath to a corrosive environment[7]. Subsequently, this sheath design was utilized in a telephone plant because the sheath design could provide protection from a variety of severe environments encountered in the outside plant[8]. Continued research led to the development of a bonded sheath with plastic coated stainless steel which was recommended to fill the need for a standard sheath design for all cable applications whether aerial, duct or direct burial[9].

Various totally dielectric cable configurations have now been proposed to protect fiber optical cable from lightning and rodents. These cables have several disadvantages. One disadvantage is a need for a large diameter package necessitating large reel diameters. Another is that enclosing the cable in a pipe creates the potential for the pipe to fill with water thereby channeling water within the telephone system. Finally, such cables cannot be easily located once buried.

The use of metallic sheaths for fiber optical cables continues on an evolutionary process as well with the use of a single shield/armor of plastic coated stainless steel in a bonded sheath offering an economical alternative for environments where rodents, lightning and corrosive soil conditions are of concern.

## Cable Performance of Bonded Sheath with Coated Stainless Steel

Mechanical Properties: The improvement in mechanical properties of bonding a corrugated stainless steel to the cable jacket is shown in Figure 1. The sheath with the coated stainless steel has greater bend performance than standard sheaths with smooth coated aluminum.

Another mechanical property which is improved by the bonded sheath is the resistance to shrinkage due to thermal cycling. A bonded sheath with coated stainless steel showed no shrinkback of the jacket after 100 temperature cycles from -40 to +60°C. This resistance to shrinkage will help to minimize stress on the fibers during service.

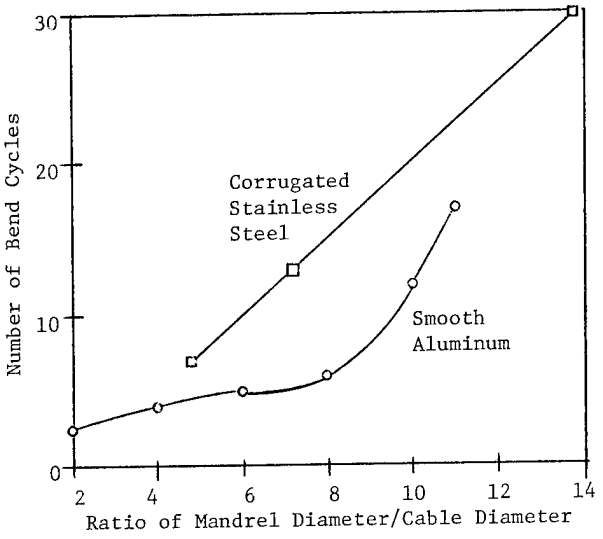



Figure 1. Bend Performance of Bonded Sheaths with Coated Aluminum or Stainless Steel

Rodent Resistance: Two samples of a fiber optical cable, one consisting of a 0.75" (19 mm) diameter bonded sheath with corrugated coated stainless steel and the second of a 1.125" (29 mm) diameter smooth high density polyethylene duct with a cable core inside, were sent to the Denver Wildlife Research Center for gopher testing. The results of the test are shown in Table 1. In no instance was the stainless steel armor penetrated by the gophers. The jacket was removed on every sample, however.

The all dielectric design based on a polyethylene pipe with core inserted showed an interesting pattern of behavior which requires interpretation for understanding. First of all, 3 of 10 samples sustained no damage or only slight damage. For whatever reason, the gopher chose not to attack these three samples. For the seven remaining samples, the gopher penetrated through the jacket into the interior of the pipe. In only one instance, however, was the core damaged. Using the rating system, the data gives one a good rating for this system -- 2.2. This rating is deceptive and not commensurate with the potential for failure which become evident by examination of the samples as follows:

1. The cable fit loosely in the interior of the pipe. It was not locked in place allowing it to move. Because it moved inside the pipe, it probably did not make a good target for the gopher and he left it alone.

2. The test configuration allows the gopher to approach the sample from one side. The pipe samples had 40-50% of their diameter removed but only on one side. In the gopher's habitat this will not be the case. It will be possible for the gopher to attack the pipe from all sides. Field experience indicates this is indeed the case. The loose soil from burial forms a "highway" for the gopher along and around the cable.

3. In the actual environment, once the pipe is penetrated, the enclosed fiber optical cable will now be continuous and susceptible to the gopher's bite. Since it is of a diameter which is easily attacked by the gopher, it is probable that an extremely high level of damage to the cable will be encountered.

Data from rodent tests of cable indicate that at least a 2.1" or greater diameter is required to prevent the gophers from biting on the cable[10]. This same study indicated that the gophers were still active 6 years after burial. A very comprehensive study by Sask-tel showed that gophers are active and continue to chew on buried facilities for 8 years[11]. The conclusion of these studies was that the cable protection must last the life of the cable not just the first 5 years.

The corrosion and rodent resistance data on stainless steel reported in this paper indicates that this armor fits the long term requirements as an armor for cable protection. In addition, the bonded sheath serves to improve gopher resistance by making it more difficult for the gopher to remove the cable jacket. All these factors coupled with smaller cable diameters make coated stainless steel a most desirable armor for fiber optical cable.

Lightning Protection: An area where all dielectric fiber optical cables are thought to be superior to fiber optical cables containing metals is in the area of lightning protection. Much work has been done to quantify the lightning performance of fiber optical cables containing a metallic armor of coated steel.

A recent study has shown that fiber optical cables with metallic members can withstand high impulse voltages within the application environment[12]. In this study, 31 samples from 6 different cable designs were subjected to 1.2 x 50 microsecond voltage wave form (IEEE Standard 4-1978). No sample failed below 55,000 volts. Some cable samples withstood a breakdown voltage of 90 kv. This study clearly demonstrated that susceptibility to lightning of optical cable containing metallic components is far less than perceived by users and such cable is likely to withstand voltages most often encountered in the field.

A paper also given at this symposium will show that the use of plastic coated metals greatly reduces the susceptibility of fiber optical cable to lightning[13]. The authors will show that magnetic crush is a cause for cable failure from lightning currents passing near the cable. To prevent this crushing effect, one needs to insure that the cable armor has no circumferential conductivity. This is accomplished through the use of plastic coated metals which break the circumferential conductivity at the overlap of the armor. Work by these authors will also show that stainless steel can handle the longitudinal current flow associated with most lightning strokes.

One important area is termination of the armor to some grounding point. A variety of commercially available connectors are available which can be used to electrically terminate the armor without need to strip the cable jacket.

Economics: Fiber optical cables are the most critical element of the broadband network since they concentrate a very large volume of messages, data and video under one cable sheath. System economics must take into consideration reliability, safeguarding of capital investment, revenue loss and high repair costs. In one economic study concerned with protection of fiber optical cable, Sask-Tel of Canada justified the cost of the armor by just preventing one cable outage over each 38 km of cable[14]. This economic study also noted that the intangible cost of poor public relations caused by service outages of high capacity fiber optical cable could be an even bigger business loss.

A way to look at the value of a sheath with coated stainless steel is to translate the system cost into the cost per channel. Figure 2 shows how the cost of the system is an extremely small factor versus the benefits provided.

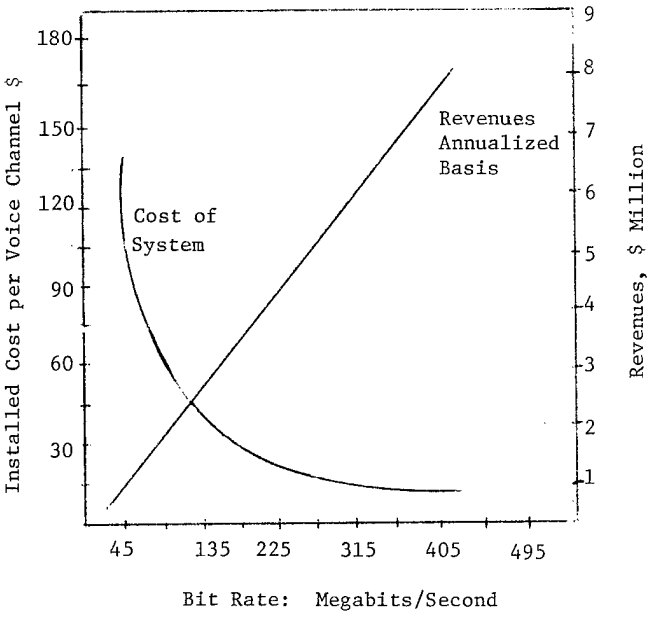


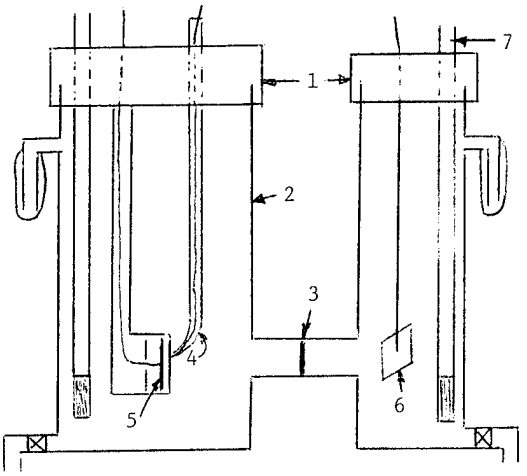

Figure 2. Relationship of Cost of System to Bit Rate and Value of Revenues.

## Electrochemical Corrosion Measurements of Bare Metals

Experimental: Linear sweep polarization is often used to electrochemically observe metal passivation and dissolution phenomenon[15,16]. The technique consists of ramping the potential at a fixed sweep rate (1 mV/sec in this work) anodically (positive direction) from the electrode rest or open circuit potential. The open circuit potential is defined as the potential at which the rate of the cathodic reaction (here, either reduction of water or dissolved oxygen) equals the rate of the anodic reaction which, for corrosion studies, is generally oxidation of the metal to form metal ions in solution. There is no net current flow at the open circuit potential. While the potential is being swept, the resultant current density is measured. The data are plotted as current density versus potential using an X-Y recorder.

The electrochemical cell used in these studies is shown in Figure 3. The cell is constructed entirely of glass and PTFE. The cell is composed of two compartments separated by a medium course glass frit. One side houses a platinum foil counter electrode attached to a platinum wire while the other contains the working (i.e. the metal being studied) and reference electrodes. The working electrode is mounted in a PTFE holder onto which is put a PTFE screw cap. The screw cap contains a hole which exposes 1.0 $cm^2$ of the working electrode's surface to the electrolyte. There is a small PTFE insert between the cap and electrode to prevent solution leakage. Electrical contact is made through a copper wire soldered to a spring. The reference electrode consists of a palladium bead formed from 0.2 mm diameter palladium wire (purity 99.995, Alfa Products) which has been sealed in a glass capillary tube. The bead is approximately 0.5 mm in diameter and is placed about 1-2 mm away from the electrode surface. The reference potential is established by "charging" the bead with hydrogen. This is accomplished by evolving hydrogen at approximately 0.5 mA for approximately 1 hour in a 0.1N sulfuric acid solution followed by oxygen evolution at approximately 1 mA for approximately 1 minute to activate the electrode. The resultant alpha hydrogen phase formed from hydrogen absorption by the palladium provides a good reversible hydrogen electrode. The potential is 50 mV more positive than a reversible hydrogen electrode on platinum. Equipment used consisted of a Princeton Applied Research Potentiostat (Model 173) and Universal Programmer (Model 175) with a Houston X-Y Recorder (Model 2000).

The metals studied are shown in Table 2 and include copper, aluminum, electrolytically chrome coated steel (ECCS) and 304 stainless steel. Each sample was solvent cleaned before being placed in the cell holder. The composition of each metal was checked with energy dispersive spectroscopy (EDS) contained on a scanning electron microscope (SEM).




1. PTFE Caps
2. Glass
3. Frit
4. Pd-H Reference Electrode
5. Working Electrode
6. Pt Counter Electrode
7. Glass Dearator

Figure 3. Electrochemical Cell

The composition of the electrolytes chosen for study are shown in Table 3. All chemicals were reagent grade or better. These electrolytes are thought to be descriptive of acidic, basic and neutral soils found in various parts of the United States. A fourth electrolyte consisting of 3.5% sodium chloride was also used. This particular electrolyte is often employed in salt spray chambers. The electrolytes were not deaerated before the electrochemistry was begun and they were continuously stirred with a PTFE coated stirring bar during the experiment.

Results: Metals used for shielding and armoring of cables may be exposed to wet soil because of sheath damage. Therefore, it is very important to be able to determine which metal would be the best to use under a given soil condition. The most direct way to assess the corrosion resistance of various metals is to determine the pitting or breakdown potential for each metal. In solutions containing large concentrations of aggressive anions such as $Cl^-$ and $SO_4^{2-}$, the principal mode of failure of most metals will be through pitting attack. Uniform or generalized corrosion will not be nearly as severe as pitting. Pitting potential is obtained using electrochemical polarization techniques by ramping the potential anodic (positive) until a very sharp rise in current is observed. The point at which this current begins to rise is known as the pitting potential. The more positive the pitting potential, the more resistant is the metal to pitting attack.

Polarization curves for bare copper, aluminum, ECCS steel and 304 stainless steel in the solutions described in Table 2 and in 3.5% NaCl are shown in Figures 4-7. All the curves show an initial flat region where the current only undergoes a small increase. This portion of the curve is known as the passivation region and presumably is where a protective oxide and/or hydroxide film is formed. This passivation film is, however, eventually broken down by the aggressive electrolyte as indicated by a sharp, steep rise in the current density. The point at which this occurs is known as the pitting potential.

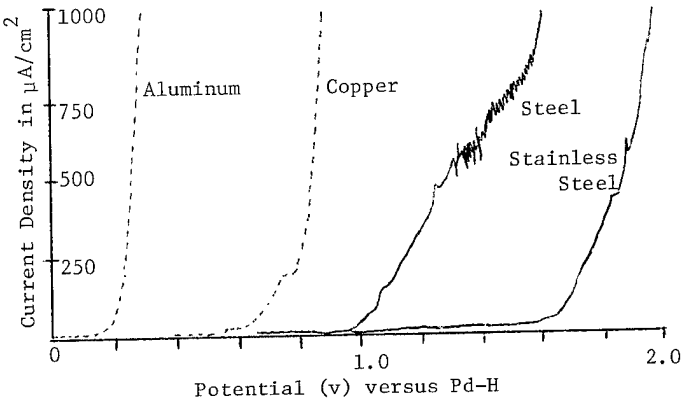



Figure 4. Polarization Curves for Various Metals in Solution A (pH=8.8)

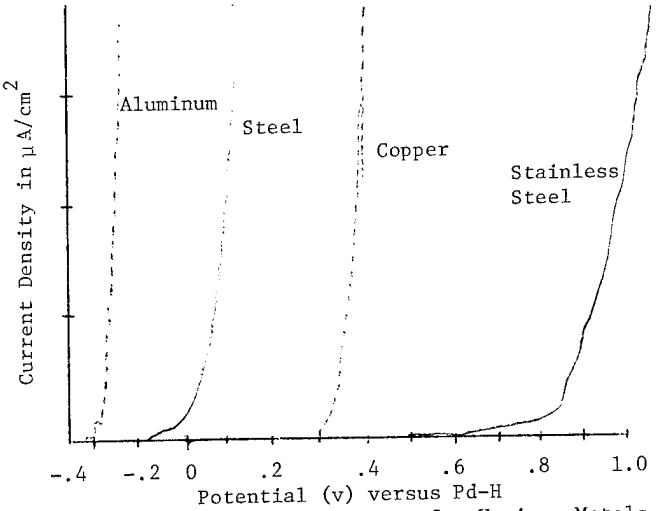



Figure 5. Polarization Curves for Various Metals in Solution C (pH=4.4)

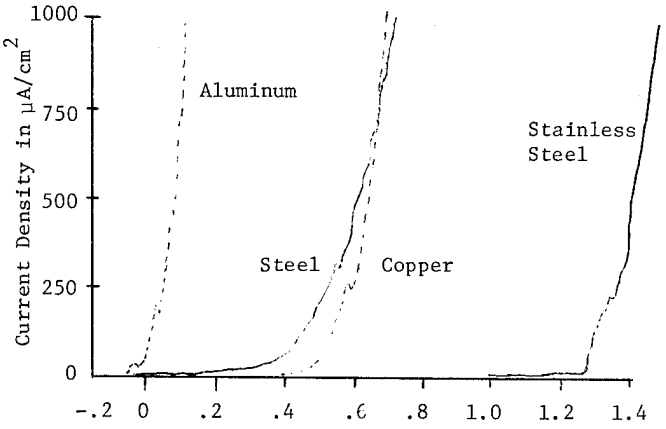



Figure 6. Polarization Curves for Various Metals in Solution G (pH=7.1)

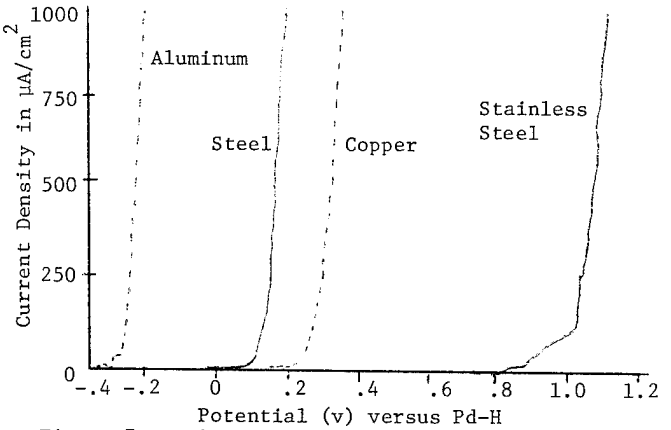



Figure 7. Polarization Curves for Various Metals in 3.5% Sodium Chloride Solution (pH=6.1)

In every electrolyte, 304 stainless steel is the most corrosion resistant as indicated by the large positive shift of the polarization curve and pitting potential compared to the other metals. Clearly this metal would be the first choice from a corrosion standpoint as a substrate for plastic coatings no matter what type of soil the cable was to be buried in.

The least corrosion resistant metal in every solution is bare aluminum. In each solution, experiments with aluminum had to be discontinued since aluminum had pits completely through its 8 mil thickness after only a 1 to 4 day exposure time. All the other metals lasted the full 2 weeks without complete pit penetration. In this test, 304 stainless steel showed no pitting attack as evidenced by SEM analysis and no change in the impedance. Copper was observed to have reasonably good pit performance with a pitting potential generally about midway between that for aluminum and stainless steel.

## AC Impedance Studies of Coated Metals

Background: The corrosion of plastic coated metals was examined with a technique known as ac impedance. This technique consists of perturbing the electrochemical interface by superimposing a low amplitude sine wave (typically a few millivolts peak to peak) $E \sin \omega t$ ($E$ = voltage, $\omega = 2\pi f$, $f$ = frequency, $t$ = time) on the dc polarization voltage. The dc current will then have superimposed on it a low amplitude sine wave $\Delta I \sin (\omega t - \phi)$ ($I$ = current, $\phi$ = phase shift). The impedance $Z(\omega)$ is then defined as the ratio of $\Delta E \sin \omega t$ to $\Delta I \sin (\omega t - \phi)$. Thus, by scanning frequency and measuring the voltage and current responses, the electrochemical interface can be characterized and kinetic and mechanistic information can be obtained.

Impedance data are plotted in two forms. In polar coordinates either $Z(\omega)$ or $\phi$ is plotted versus log $f$ (Bode plot) or in rectangular coordinates the real part of the impedance is plotted versus the imaginary part. For studying electrochemical reactions such as corrosion impedance, data can best be understood by representing the reaction with an equivalent circuit. A very simple example for an ideal one-step electron transfer reaction (with no diffusion or absorption effects) is shown in Figure 8. Here the resistance $R_r$ includes the resistance of the electrolyte, circuit leads and surface films while $R_{ct}$ represent the charge transfer resistance. $C_{dl}$ is the double layer capacitance created at the charged electrode-electrolyte interface. For more thorough reviews of utilizing the ac impedance technique for studying corrosion phenomenon, see references 17, 18, and 19.

The advantages of using ac impedance for studying electrochemical phenomena are the following.

1. Small signals are used which do not disturb the electrode properties.

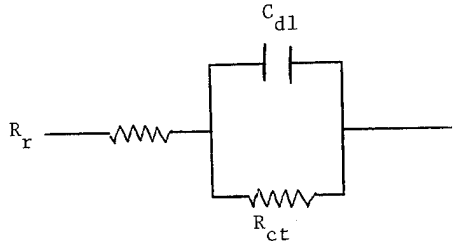
2. Corrosion on surfaces having low conductivity (e.g. painted, plastic coated or heavily oxided metals) can be studied since, as shown in Figure 8, the ohmic resistance, $R_r$, due to these surfaces can be separated from the circuit components directly. Most dc methods would fail in this case.

3. Studies in low conductivity media can be performed for the same reasons as in No. 2 above.

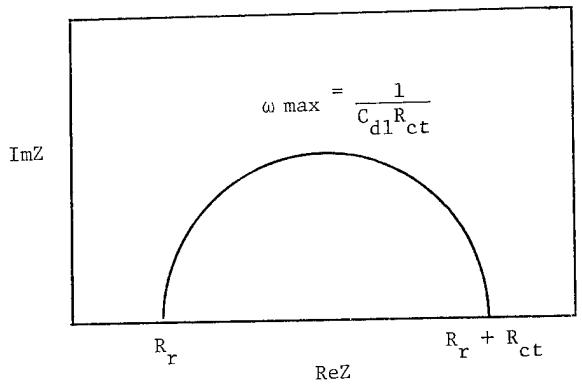
4. For many reactions, $R_r$, $R_{ct}$ and $C_{dl}$ can be obtained in the same measurement. In corrosion measurements, $R_{ct}$ is, in most cases, directly related to the polarization resistance $R_p$ which is a measure of the corrosion rate.

5. Mechanistic information can also be obtained since each rate determining step has its own time constant.

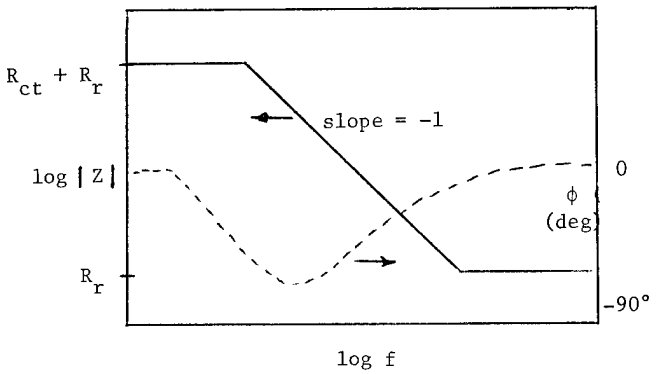
6. For corrosion processes, reactions can be observed long before visual changes occur on the sample surface. This extreme sensitivity is especially important when examining the corrosion resistance of coated metals.




A. Equivalent Circuit of an Ideal, One Step Reaction: $M = m^+ + e^-$




B. Nyquist Plot




C. Bode Plot

Figure 8. Equivalent Circuit and Impedence Plots for an Ideal, One-Step Electron Transfer Reaction.

Experimental: For the data reported in this section, measurements were taken with a Solartion 1174 Frequency Response Analyzer which was interfaced along a Solartion 1186 Electrochemical Interface to an Apple II+ computer. The analyzed data could be outputted to an Integral Data Systems 445 Printer or plotted as a Bode and/or Nyquist plot on a Hewlett-Packard 7225B Plotter. All experiments were conducted by potentiostating the electrode to the open circuit or rest potential. Frequency scans typically were from 5 mHz to 100 kHz and a 5 mV peak to peak amplitude was normally used for the perturbing voltage.

The cell used for the experiments is shown in Figure 9. The working elecrode for this study was the plastic coated steel described in Table 2. Approximately a 5 $cm^2$ area was marked off by sealing a glass tube to the surface with silicon rubber adhesive (Dow Corning, 732 RTV adhesive). A 3.5% sodium chloride solution was poured into the tube to which was put a platinum mesh counter electrode. The lead to the working electrode was made by scraping off some of the plastic coating on an edge outside of the area enclosed by the tube. No reference electrode was used for these studies.

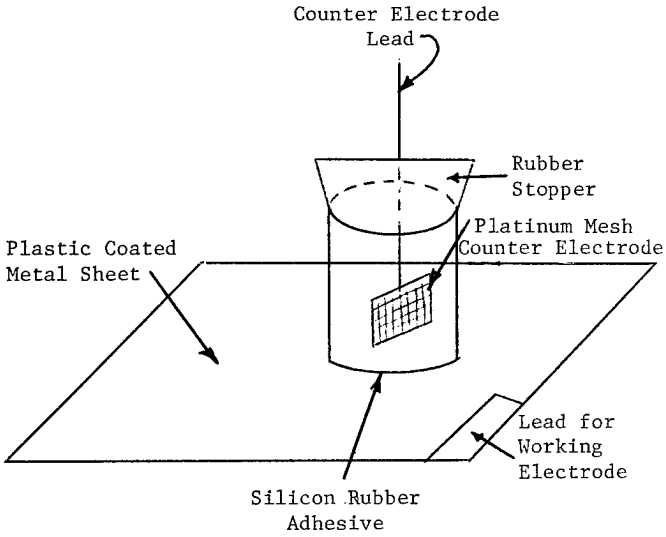
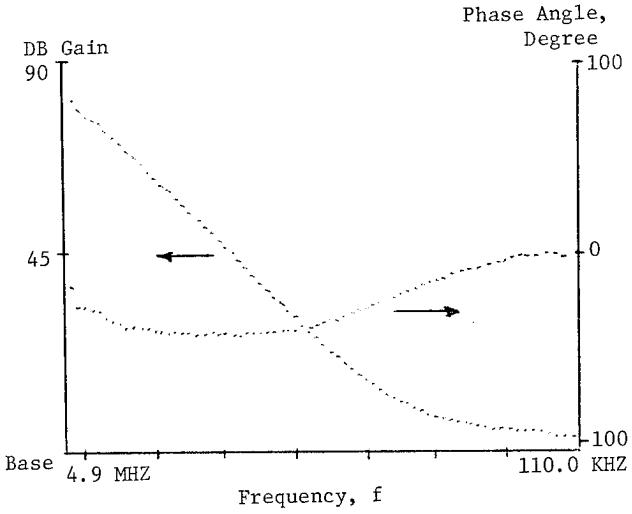



Figure 9. Electrochemical Cell for Impedence Measurements

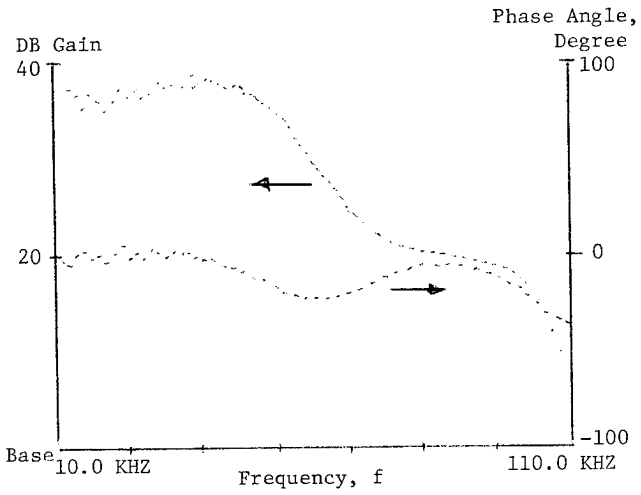
In order to study the effect of penetration of the electrolyte through the coating, controlled defects in the plastic coating were introduced in two ways. First, a Tukon 300 microhardness tester equipped with a Vickers indenter was used to introduce from one up to five defects in the 5 $cm^2$ area of analysis. These indents, only a few microns in size, were pyramid in shape. For the 2 mil coating on the coated steel, at least a 1,000 g load was required to produce an indent that would break down (as measured by ac impedance analysis) within 1 day after immersion in electrolyte. Defects were also produced by laser irradiation utilizing the 350 nm krypton fluoride line of a Lumonius 860 Eximer laser. The focused spot produced an affected area of approximately 0.5 mm as indicated by discoloration of the film. The area that showed direct penetration to the metal, however, was much smaller (approximately 100 microns). Multiple shots were usually required to produce a defect that would begin to corrode within 1 day after immersion.

Results: Impedance analysis of a 2 mil plastic ethylene acrylic acid copolymer coating on 6 mil steel demonstrated that this coating is extremely corrosion resistant and that there is no penetration of aggressive species through the coating. After a 4 month immersion in 3.5% NaCl, the impedance spectra indicated that the purely capacitive behavior was being observed. Other impedance studies on acrylic coatings[20,21] and paint coatings[22] of similar thickness on steel indicate that electrolyte penetration occurs almost immediately after immersion in an aggressive electrolyte. As long as the plastic coatings remain undamaged and contain no defects, they would be expected to remain corrosion resistant for a very extended period of time under these conditions.

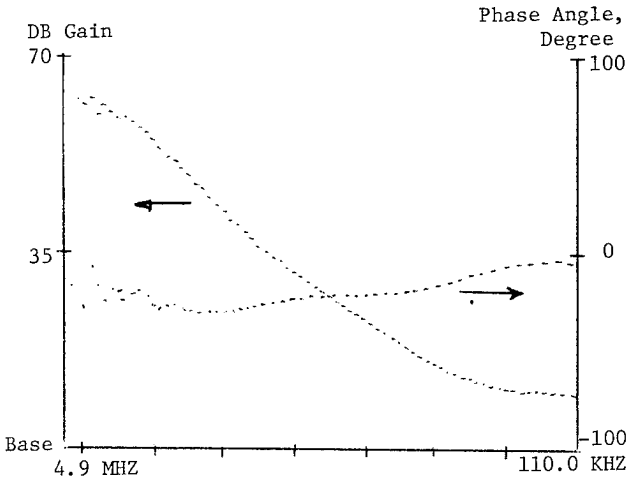
Because there are a number of ways damage may occur to a finished cable, it is important to understand how damaged plastic coatings will behave in soils containing aggressive ionic species. In order to obtain more mechanistic information on the corrosion of these plastic coated metals, defects were introduced into the coating to the metal in a very controlled manner rather than by scribing as is often done in salt spray tests. Both a microhardness indenter and a laser were used to introduce defects in the coating. Although these studies have just begun, some preliminary data were obtained. Figure 10 shows Bode plots for bare ECCS steel and coated ECCS steel damaged with the Vickers indenter and laser damaged coated steel after 1 day immersion in 3.5% NaCl. Although no definite conclusions can be drawn from these spectra, it is clear that the damaged samples corrode much differently than the bare substrate and that the way that the defect is introduced also affects the kinetics of corrosion. Measurements on the bare metal substrate reveal that capacitive-like behavior over a large frequency range is occurring as indicated by the broad minima in the phase angle. The damaged surfaces, however, show two sharp minima indicating that the presence of the plastic coating has complicated the corrosion process. Interestingly, the minima occur at much different frequencies and are of different values for the two types of damaged samples indicating that the kinetics of corrosion may be very much different in the two cases. For the case of the sample with 5 indentations, after a 5 day immersion, not all the indentations were observed to corrode equally. Only one showed severe corrosion as indicated by a thick oxide film and some undercutting under the coating (as observed with a light microscope). The other indents were much less corroded with two showing only negligible effects. Impedance spectra for the samples with a single indent in the coating show similar behavior to that for the samples with 5 indents. More data need to be obtained in order to understand the details of how these coatings so effectively protect the bare metallic substrate.




A. Bare Steel




B. Copolymer Coated Steel with 5 Indentations Using a Vickers Indenter.




C. Copolymer Coated Steel with Single Defect Provided by an Eximer Laser

Figure 10. Bode Plots Obtained from AC Impedence Measurements of Bare Steel and Coated Steel with Defects in the Coating After 1 Day Immersion in 3.5% NaCl Solution

## Galvanic Corrosion Studies

Background: The use of both a shield and armor is commonly practiced in the sheathing of telecommunications cable. A sheath design commonly used in copper pair telephone cable consists of an aluminum shield, a steel armor and a plastic jacket of polyethylene (ASP). A previous study on galvanic corrosion indicated that the use of plastic coatings on both the aluminum and steel effectively controlled the potential for galvanic corrosion between these two metals (the CACSP or coated ASP sheath)[23]. More recently, a dual shield/armor design has been developed for fiber optical cable consisting of a copper shield and a stainless steel armor[24]. Generally, these two metals are quite close together on the galvanic series and the possibility of galvanic corrosion should be minimized. However, galvanic studies were conducted to quantify the nature of this galvanic couple.

Experimental: The galvanic cell in Figure 11 was assembled. A modular current meter (Model PEC-AMD, Floyd Bell Associates) was used to record the galvanic current flowing in the cell on a weekly basis. After 26 weeks, the cell was disassembled and observations on corrosion recorded for the metals in the cell.

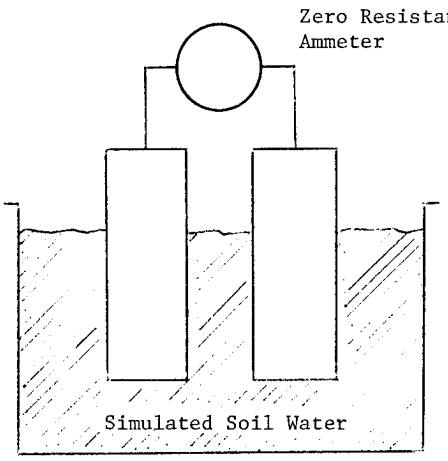



Figure 11. Test Apparatus for Measuring Galvanic Corrosion Currents

Results: Table 4 shows that protecting both the metals in a galvanic couple of copper and stainless steel with plastic coatings has the effect of greatly reducing the corrosive attack of the copper member of the couple. Note in the acidic clay soil water that the bare copper was greatly thinned by corrosion, ultimately resulting in a break in the electrical continuity of the metal. By coating both metals tightly with adherent plastic coatings, the galvanic couple is controlled, and the integrity of the copper is preserved. The magnitude of the improvement is shown by the galvanic current data of Figure 12. The couple with bare metals has a large negative current flow which after 18 weeks begins to drop due to consumption of the copper. By coating the stainless steel, the current flow is significantly reduced and turns positive. By coating both the copper and stainless steel with tightly adherent plastic coatings, the current flow in the cell becomes significantly less and slightly negative. The couple is under control and the integrity of the metals is preserved.

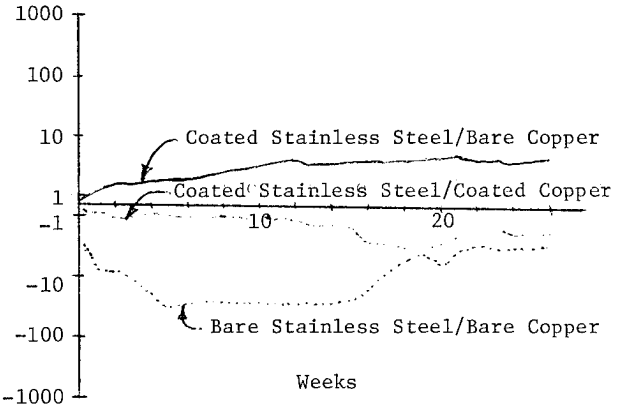



Figure 12. Galvanic Currents Between 110 Copper and 304 Stainless Steel in Solution C (pH=4.4)

The data in Table 4 on galvanic corrosion in the salt water marsh solution indicates that the magnitude of the galvanic effect is much less in this solution than the acidic clay. Again, the plastic coatings on both metals reduce the corrosive attack of the copper. The galvanic current data plotted in Figure 13 further substantiates the reduced aggressiveness of the galvanic couple of stainless and copper in this solution. It was also found that the couple in Solution A, the simulated alkaline soil water, also was not aggressive. The results were similar, however, in that the copper sustained the greatest corrosive attack.

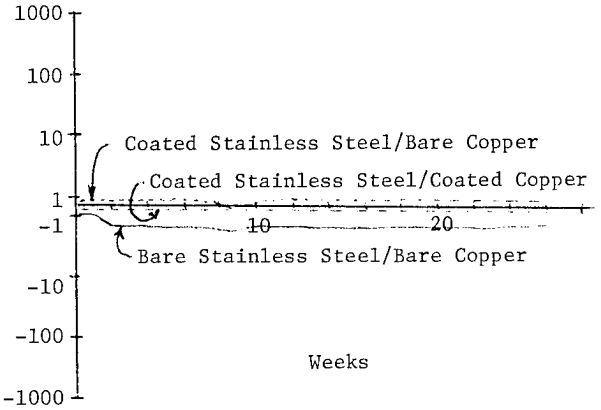



Figure 13. Galvanic Currents Between 110 Copper and 304 Stainless Steel in Solution G (pH=7.1)

## Soil Burial Corrosion Tests

The Type 304 stainless steel was studied as part of a soil burial evaluation of telephone cable shielding materials by the National Bureau of Standards (NBS) in conjunction with the Rural Electrification Administration (REA)[25]. In this study, a cable with a 5 mil (0.125 mm) thick corrugated 304 stainless steel armor was buried in 6 soils which differed widely in compositions and physical conditions. These widely different soil environments allowed for a comprehensive test program (three of the more aggressive soils are simulated as test solutions for purposes of this study and are described in Table 3). The jackets on the cable test samples were cut circumferentially in such a fashion as to expose a ring of shield to the soil. The ring was 0.5" (12.7 cm) wide. A "window" was also cut in the jacket. It was 0.5 (12.7 mm) wide and 2" (50.8 mm) in length. The samples were approximately 14" (36 cm) long and the ends were sealed with vinyl tape and sealing compound. Twelve samples were buried in each site (6 as is and 6 coupled to a copper cathode) and one sample of each type was recovered each year and a rating assigned commensurate with the degree of corrosion. The results of the tests of the Type 304 armor are shown in Table 5. The data show that after burial for up to 6 years, the Type 304 stainless steel shield, whether coupled to copper or not, provided excellent protection

in all of the soils. There were indications that in the case of cable samples with stainless coupled to copper, the copper was anodic to the stainless. These data collaborate the data from the laboratory studies reported herein.

## Hydrogen Evolution Studies

Experimental: An apparatus was designed and constructed to study the hydrogen generated by metals and coated metals in contact with various aqueous solutions. The requirements for the apparatus are to minimize the permeation of hydrogen and allow sampling at intervals over a one week period. A closed glass cylinder was designed which could be split and sealed circumferentially with an o-ring seal and a septum port at one end. The large opening at the o-ring was required in order to load the sample and the septum port was needed for syringe sampling. Normally, the septum port was facing down so that the solution covered the o-ring seal and the septum such that the head space did not contact the seal. This minimized the possibility of permeation through the seal and septum. The apparatus was inverted and 0.1 cc of gas withdrawn into a gas-tight syringe for injection in the the gas chromatograph.

The determination of hydrogen was accomplished by gas chromatography/mass spectrometry (gc/ms). The mass spectrometer used was a ZAB-HS (Zero - aberration, High - sensitivity, from Vg Analytical, Manchester, England) set to monitor molecular hydrogen during elution of the sample from the gas chromatograph. The column used was a 6 foot long 13X molecular sieve at 50°C which separates hydrogen from nitrogen and oxygen. This was necessary since these major air components affected the spectrometer sensitivity.

Standardization was done by injecting a known quantity of hydrogen into a sampling apparatus loaded with the solution but without metal present. This was employed as the reference during all the determinations. Also, one apparatus was used as a blank by filling with solution with no metal and sampling this during the experiment. This was done to ensure that no hydrogen was permeating from outside and that hydrogen was not being lost or generated by anything but the metal during the experiment.

The apparatus is capable of containing hydrogen without detectable loss for two weeks. No detectable hydrogen increase occurred in the control during this time. The sensitivity of the system was approximately 5-10 ppm, volume of hydrogen/volume of container (partial pressure of $5 \times 10^{-6}$ to $1 \times 10^{-5}$ atm).

The surface area was measured and the sample coiled around a 0.5" mandrel before inserting into the apparatus. Approximately 200 $cm^2$ of material was used. The materials tested were: coated and uncoated aluminum, steel, copper and stainless steel. All were exposed to synthetic sea water (ASTM D1141) at room temperature. In addition, copper was exposed to simulated acidic soil water (Solution C of Table 3).

Results: Of the samples exposed to synthetic sea water at ambient temperature, aluminum and steel showed detectable hydrogen evolution and copper and stainless steel did not. The results are shown in Figure 14. Quantitatively, the bare metals evolved hydrogen about 10 times faster than the plastic coated. When bare and plastic coated coppers were exposed to the acidic soil water solution, hydrogen was detected as shown in Figure 15. In this case, about 3-4 times as much hydrogen was given off by the bare copper versus the plastic coated. No detectable hydrogen was given off at ambient temperature by the bare or coated stainless steel. Comparing the metals for hydrogen evolution rate, it was found that bare aluminum was greater than steel was greater than copper while stainless steel did not give off detectable amounts of hydrogen.

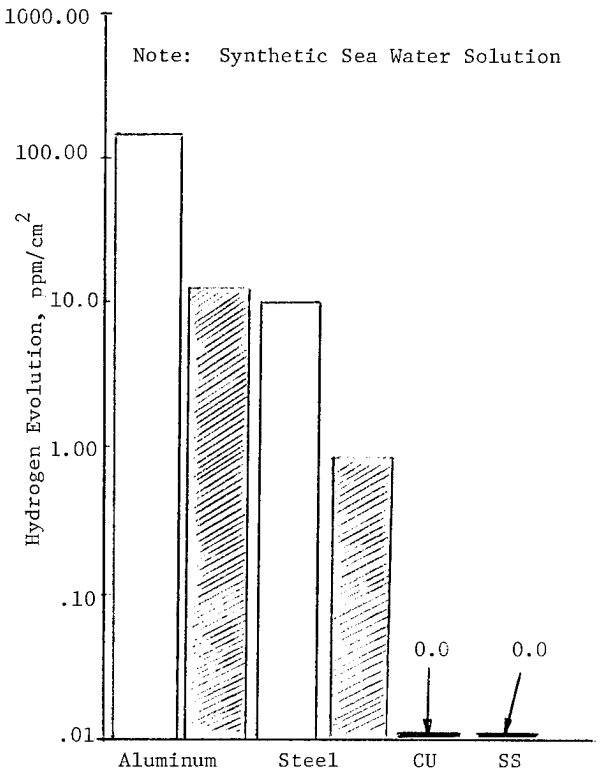



Figure 14. Hydrogen Evolution From Various Bare and Coated Metals.

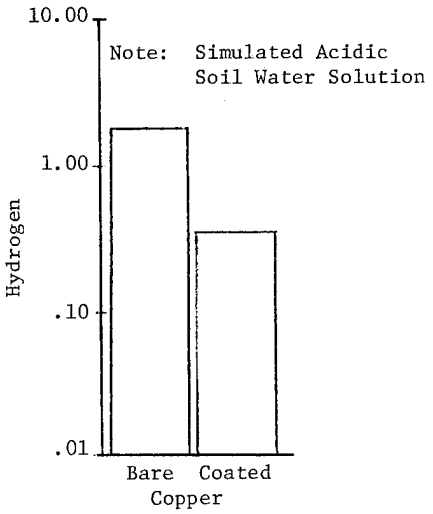



Figure 15. Hydrogen Evolution From Various Bare Metals.

## Conclusions

The use of plastic coated stainless steel leads to a sheath design for fiber optical cable which has the benefits of inherent corrosion resistance. In the event of sheath damage which exposes the armor, there is little probability that corrosion will proceed to weaken the armor and allow moisture to penetrate into the fibers. Another advantage of the plastic coated stainless steel is that it allows armored fiber optical cables to be used in highly corrosive soil environments where there is high probability of sheath damage from lightning. Economics are favorable over more expensive alternatives such as all dielectric cable or use of special protective systems for conventional armors.

The corrosion performance of plastic coated stainless steel is excellent. The material has been shown to be unaffected by corrosion in a wide variety of soil environments using electrochemical corrosion measurements, galvanic corrosion studies and soil burial test data.

Data are presented which show that the generation of hydrogen by coated stainless steel is virtually non-existent. Therefore, the adverse effects associated with hydrogenation of the glass fibers are prevented.

The plastic coatings enhance the mechanical performance of a fiber optical cable by allowing a bonded sheath to be obtained. Rodent resistance of the stainless steel is excellent. The use of single armor of two-side coated stainless steel has been shown to result in a sheath with immunity to the ground currents associated with lightning. The use of coated stainless steel will allow the benefits associated with immunity of lightwave transmission to electromagnetic interference to be obtained at the same time as the benefits associated with a metallic sheath: moisture protection, rodent resistance, and the ability to be located as a buried cable.

An ac impedance technique has been described which shows promise in understanding the corrosion performance of plastic coated metals.

Acknowledgement: The authors would like to thank Charles Langhoff, Jackie Raymond, Dan Pikula, Don Gromacki, Mike Schulz and Donna Shoults for their help in preparing samples, gathering data, and the preparation of this paper for publication.

## References

[1] JR Osterfield, SR Norman, DN McIntosch, AJ Rogers, R Castelli, M Tamburello, "An Optical Fibre Link in a Mountainous Environment", International Wire & Cable Symposium Proceedings, 1980, p. 202-211.

[2] TS Hope, RJ Williams, K Able, "Developments in Slotted Core Optical Fiber Cables", International Wire & Cable Symposium Proceedings, 1981, p. 220-227.

[3] PS Venkatesan, K Korbelak, "Characterization of Ruggedized Fiber Optic Dual Wavelength Cables", International Wire & Cable Symposium Proceedings, 1982, p. 358-370.

[4] MM Rahman, GM Davidson, "Design Consideration for Jacketing Fiber Optic Cable", International Wire & Cable Symposium Proceedings, 1982, p. 377-380.

[5] K Cornelison, M Fleck, "Applications and Comparative Performance of Lightwave Cable Sheaths", International Wire & Cable Symposium Proceedings, 1984, p. 130-140.

[6] WCL Weinraub, DD Davis, MD Kinard, "A Rodent and Lightning Protective Sheath for Fiber Optic Cables", International Wire & Cable Symposium Proceedings, 1983, p. 243-249.

[7] EW Mies, DL Philen, WD Reents, DA Meade, "Hydrogen Susceptibility Studies Pertaining to Optical Fiber Cables", Presented at the Optical Fiber Communication Conference, January 23-25, 1984, New Orleans, Louisiana, USA.

[8] J Durr, M Fournet, "Fiber Is The Future", Telephone Engineer & Management, August 15, 1984, p. 108-117.

[9] PU Bakhru, KE Bow, JW Smith, "New Plastic-Metal Laminate Sheaths for Fiber Optic Cable", ECOC '84 Conference Proceedings, 10th European Conference on Optical Communication, p. 288-289.

[10] RA Connolly, NJ Cogelia, "Can Any Cable Armor Stop A Gopher?", Telephony, June 27, 1970.

[11]Saskatchewan Telecommunications: Internal Report.

[12]HL Blumsack, DE Fischer, "High Voltage Impulse Breakdown Between Metallic Central Strength Member and Metallic Armor of Valtec Fiber Optic Cables", Special Technical Report.

[13]D Fischer, PU Bakhru, KE Bow, E Schrom, "Crushing Metallic Shielded Telecommunications Cables with Dynamic Magnetic Fields", 34th International Wire & Cable Symposium, 1985.

[14]Private discussion with Roy Hill, Outside Plant Engineer at Sask-Tel, Regina, Saskatchewan, Canada.

[15]M Pourbaix, Corrosion, 14, 25 (1974).

[16]R Baboian, GS Haynes, "Electrochemical Corrosion Testing", Mansfeld/Bertocci, Eds., ASTM STP 727, Philadelphia (1981).

[17]K Hladky, LM Callow, JL Dawson, Corrosion J, 15, 20 (1980).

[18]F Mansfeld, Corrosion - NACE, 36, 301 (1981).

[19]F Mansfeld, MW Kendig, S Tsai, Corrosion - NACE, 38, 570 (1982).

[20]LM Callow, JD Scatlebury, J. Oil Colour Chemist Association, 64, 83 (1981); Ibid. 119 (1981); Ibid. 140 (1981); Ibid. 65, 11 (1982).

[21]J Hubrecht, J Vereecken, M Piens, J. Electrochem. Society, 131, 2010 (1984).

[22]GW Walter, J. Electroanal. Chem. and Interfac. Electrochem., 118, 259 (1981).

[23]GD Schwank, KE Bow, "Galvanic Corrosion Studies of Aluminum and Steel Shielding Materials for Armored Telephone Cables", Materials Performance, Vol. 17, No. 9, September 1978, p. 25-30.

[24]WCL Weinraub, DD Davis, MD Kinard, "A Rodent and Lightning Protective Sheath for Fiber Optic Cables", International Wire & Cable Symposium Proceedings, 1983, p. 243-249.

[25]WF Gerhold, JP McCann, "Corrosion Evaluation of Underground Telephone Cable Shielding Matierals", Paper no. 31, Corrosion/76.

Biography



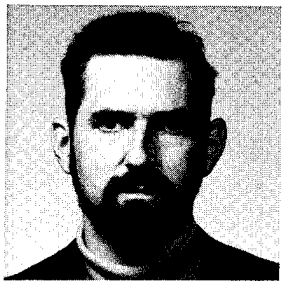
Prakash (Buck) U. Bakhru is a Development Leader with Dow Chemical USA in Granville, Ohio. He joined Dow in 1973, working on magnesium process research. He is currently engaged in the application development of coated metals for the Fiber Optical Cable Industry. Mr. Bakhru holds a Bachelors degree in Metallurgical Engineering from Nagpur University, India, and a Master's degree from the University of Missouri-Rolla.



Patrick L. Hagans is a Research Leader in the Central Research, Inorganic Materials and Catalysis, Laboratory, The Dow Chemical Company, Midland, Michigan. His research responsibilities include electrochemistry, surface physics and corrosion of metals. Dr. Hagans has B.S. and M.S. degrees in chemistry from Kent State University and received a Ph.D. from Case Western Reserve University in 1979.



Kenneth E. Bow is an Associate Development Scientist with Dow Chemical USA, Granville, Ohio. He has been involved in the research and development of materials for the Wire and Cable Industry for over 20 years. He is currently responsible for the development of coated metal shielding and armoring tapes for applications in cables. Mr. Bow graduated with a B.S. E.E. degree from Michigan State University in 1962.



Lewis A. Shadoff is a Research Associate with the Instrument Group, Dow Analytical Laboratory, The Dow Chemical Company, Midland, Michigan. Dr. Shadoff has been involved in analytical technologies for over 19 years. He received his B.S. in chemistry from the Polytechnic Institute of Brooklyn and his Ph.D. in chemistry from Kansas State University in 1966.

Table 1. Gopher Evaluations of Cable Samples

| Sheath | Diameter | Damage Index[1], Number of Samples | | | | | | |
|---|---|---|---|---|---|---|---|---|
| | | 0 | 1 | 2 | 3 | 4 | 5 | X |
| Bonded Sheath With Stainless Steel | 0.75" (19 mm) | - | - | 10 | - | - | - | 2.0 |
| Plastic Pipe With Cable Inside | Pipe: 1.125" (29 mm) Cable: 0.65" (16 mm) | 2 | 1 | 1 | 5 | 1 | - | 2.2 |

[1]Damage Index Code:
0 = No Attack
1 = Slight Damage
2 = Jacket Penetrated
3 = Armor Penetrated
4 = Fibers Damaged
5 = Cable Severed

Table 2. Description of Metals Used for Corrosion Resistance Testing

| Metal | Type of Alloy | Thickness of Metal | Code | Coating Type | Coating Thickness | Total Thickness |
|---|---|---|---|---|---|---|
| Aluminum | 1100 | 7.5 mil (0.19 mm) | -- | -- | -- | 7.5 mil (0.19 mm) |
| Coated Aluminum | 1100 | 7.5 mil (0.19 mm) | A282 | Copolymer[2] | 2.3 mil (0.058 mm) | 12.1 mil (0.31 mm) |
| Steel | 1010 ECCS | 6.1 mil (0.155 mm) | -- | -- | -- | 6.1 mil (0.155 mm) |
| Coated Steel | 1010 ECCS | 6.1 mil (0.155 mm) | S262 | Copolymer | 2.3 mil (0.058 mm) | 10.7 mil (0.27 mm) |
| Copper | 110 | 5.0 mil (0.125 mm) | -- | -- | -- | 5.0 mil (0.125 mm) |
| Coated Copper | 110 | 5.0 mil (0.125 mm) | XP 61000.08 | Modified Copolymer | 2.3 mil (0.058 mm) | 9.6 mil (0.24 mm) |
| Stainless Steel | 304 | 5.0 mil (0.125 mm) | -- | -- | -- | 5.0 mil (0.125 mm) |
| Coated Stainless Steel | 304 | 5.0 mil (0.125 mm) | XU 61001.03 | Copolymer | -- | 9.6 mil (0.24 mm) |

[1]ECCS - Electrolytic Chrome Coated Steel.
[2]Copolymer - Ethylene Acrylic Acid Copolymer.

Table 3. Formulations of Solutions Used in Electrochemical and Hydrogen Evolution Experiments

| Ingredient | Quantity, Grams for 5 Gallons of Solution | | |
|---|---|---|---|
| | Solution A | Solution C | Solution G |
| $CaCl_2 \cdot 2H_2O$ | 7.0828 | 38.7338 | -- |
| $MgSO_4$ (anh) | 2.0407 | 66.8992 | 14.6398 |
| $NaHCO_3$ | 123.3963 | -- | -- |
| $KNO_3$ | 0.1754 | -- | -- |
| $K_2SO_4$ | 2.9160 | -- | -- |
| 1.0N $H_2SO_4$ | 13.7415 | -- | -- |
| 1.0N HCl | 71.3872 | 973.1672 | 59.0674 |
| $NaNO_3$ | -- | 2.8997 | 0.9093 |
| $Na_2SO_4$ | -- | 100.4547 | 19.1103 |
| NaCl | -- | 17.4491 | 92.6211 |
| $CaSO_4 \cdot 2H_2O$ | -- | -- | 10.7799 |
| $H_2O$ | Balance | Balance | Balance |
| pH (Adjust with Acetic Acid or $NH_4OH$) | 8.8 | 4.0 | 7.1 |

Table 4. Effect of Plastic Coatings on the Control of Corrosion in a Galvanic Couple

| Galvanic Couple | | Soil Solution | pH of Solution | | Observations | |
|---|---|---|---|---|---|---|
| Stainless Steel | Copper | | Initial | Final | Stainless Steel | Copper |
| Bare | Bare | Acidic Clay[1] | 4.0 | 8.3 | No Corrosive Attack Plated with Patina | Corroded in Half; Thickness Reduced 50% |
| Plastic Coated | Bare | Acidic Clay | 4.0 | 8.08 | No Corrosive Attack Plated with Patina | Corroded in Half; Thickness Reduced 50% |
| Plastic Coated | Plastic Coated | Acidic Clay | 4.0 | 6.75 | No Corrosive Attack | No Surface Attack; Uniform Edge Attack |
| Bare | Bare | Salt Water Marsh[2] | 7.0 | 7.39 | No Corrosive Attack | Covered with Patina |
| Plastic Coated | Bare | Salt Water Marsh | 7.0 | 7.09 | No Corrosive Attack | Plated with Patina |
| Plastic Coated | Plastic Coated | Salt Water Marsh | 7.0 | 7.15 | No Corrosive Attack | No Surface Attack; Minor Edge Attack |

[1]Solution C of Table 3.
[2]Solution G of Table 3.

Table 5. Exposure of Type 304 Stainless Steel Armor[1] to Various Soils for Six Years

| Exposure Time, Years | Corrosion Rating[2] at Exposed Ring Versus Soil Types[3] | | | | | |
|---|---|---|---|---|---|---|
| | A | B | C | D | E | G |
| 1 | 10 | 10 | 10 | 10 | 10 | 10 |
| 2 | 10 | 10 | 10 | 10 | 10 | 10 |
| 3 | 10 | 10 | 10 | 10 | 10 | 10 |
| 4 | 10 | 10 | 10 | 10 | -- | 10 |
| 5 | 10 | 10 | 10 | 10 | 10 | 10 |
| 6 | 10 | 10 | 10 | 10 | -- | 10 |

[1]System No. 17, 5 mil Corrugated Type 304 Stainless Steel Shield
System No. 18, the same as No. 17 except the shield was coupled to copper

[2]10 Rating -- Unaffected, No Indication of Corrosion

[3]Soil Type A -- Sagemoor Sandy Loam; well drained alkaline soil
Soil Type B -- Hagerstown Loam; well drained
Soil Type C -- Clay Soil; poorly drained acidic clay
Soil Type D -- Lakewood Sand; white, loose sand with good drainage
Soil Type E -- Coastal Sand; white, coastal beach sand with poor drainage
Soil Type G -- Tidal Marsh; poorly drained marsh soil

# Newly Developed UV Curable Polybutadiene Acrylate as a Primary Coating for Optical Fibers

R. Ohno, T. Kikuchi and Y. Matsumura

Japan Synthetic Rubber Co., Ltd.
Kawasaki, Japan

## Abstract

UV curable polybutadiene acrylate has been proposed as a primary coating for optical fiber, to provide low excess losses over a wide temperature range. UV curable polybutadiene acrylate, however, has been understood to have poor thermal stability and slow cure rate, which prevents commercial usage. In this report, we will present a newly developed modified polybutadiene acrylate which shows minimal change in modulus at high temperature (80°C) for long-term service life and faster cure rate.

## Introduction

The most important role played by a polymer coating for optical fibers is to prevent optical losses due to microbending. Furthermore, it must be advantageous to use in a production mode, because optical fibers are coated in a fiber drawing process.

Optical fibers which possess a two coating structure consisting of a low modulus primary buffer surrounded by a high modulus secondary jacket are widely utilized to provide low excess optical losses due to microbending. Among these material systems much attention has been paid to dual coatings in which both layers are UV curable acrylates. UV curable coatings are covenient for processing at high draw rates owing to their rapid curing (1) as well as for in-line coating application. However, use of currently available UV curable acrylate primary coatings result in excess optical losses at -40°C because these coatings undergo an increase in modulus at very low temperature.

Recently, UV curable polybutadiene acrylates (PBA) have been proposed as a primary coating for optical fibers to provide low excess losses over a wide temperature range. These coatings are particulary effective because of their low modulus even at -40°C (2). However, increases in modulus of PBA are marked at high temperature after prolonged exposure (3) which results in a gradual increase in excess losses of coated fibers. Furthermore, its slow cure rate is not suitable for high speed drawing. These defects have prevented PBA from commercial usage, so far.

Here we present a newly developed modified polybutadiene acrylate (M-PBA) which has improved thermal stability as well as faster cure rate.

## Coating Materials

According to the method reported by T. Kimura et al. (2), a polybutadiene acrylate (PBA) coating was obtained by mixing an acrylic oligomer prepared from hydroxy-terminated 1,4-polybutadiene, diisocyanate and hydroxyethyl acrylate with low-viscosity acrylates,photoinitiators and antioxidants. This PBA was used as a standard for thermal stability and cure rate measurements.

A modified polybutadiene acrylate (M-PBA) coating was prepared by using an acrylic oligomer modified by selective hydrogenation of 1,4-polybutadiene structure as well as incorporation of polar groups. In this experiment, twenty percent of pendant vinyl groups in 1,4-polybutadiene were selectively hydrogenated.

## Properties

Thermal stability is evaluated by measuring Young's modulus increases of cured film which induce excess loss increase of coated fibers.

Fig. 1(A) shows Young's modulus increase of cured PBA and M-PBA in air at 80°C. Young's modulus of M-PBA is almost constant, at least within thirty days, while that of PBA increases in a shorter period.

Fig. 1(B) shows Young's modulus increase of cured PBA and M-PBA in water at 80°C. Young's modulus increase of PBA is more rapid in hot water than in air, while that of M-PBA is still constant even under this condition.

From these results, it is clear that M-PBA is substantially improved in thermal stability. Such an improvement is achieved by selective hydrogenation of pendant vinyl groups in 1,4-polybutadiene structure of acrylic oligomer.

Fig. 2(A) shows UV dosage dependency of Young's moduli of M-PBA and PBA.

Young's modulus of M-PBA becomes constant at more than 0.2 $J/cm^2$, which indicates that minimal UV dosage for complete cure of M-PBA is 0.2 $J/cm^2$. On the other hand, minimal UV dosage for complete cure of PBA is unable to be obtained from Fig. 2(A), because its Young's modulus continues to increase with UV dosage. Such behavior of Young's modulus of PBA can be explained in terms of crosslinking caused by carbon-carbon double bonds after complete cure of acryl groups of PBA, because hydroxy-terminated 1,4-polybutadiene with no acryl groups can be crosslinked in the presence of photoinitiators by UV irradiation. No increase in Young's modulus of M-PBA by excess UV dosage is due to selective hydrogenation.

Fig. 2(B) shows UV dosage dependecy of gel fraction of M-PBA and PBA.

Gel fraction of PBA, different from Young's modulus behavior, becomes constant at more than 1.5 $J/cm^2$, because crosslinking caused by carbon-carbon double bonds does not influence gel fraction after cure of acryl groups. On the other hand, gel fraction of M-PBA becomes constant above 0.2 $J/cm^2$, where Young's modulus is saturated.

These findings suggest that M-PBA is curable faster than PBA by about seven times, and hence allows high speed drawing. The improvement in cure rate of M-PBA is mainly due to the incorporation of polar groups into acrylic oligomer.

Temperature dependency of Young's modulus of M-PBA is shown in Fig. 3. It is almost as low as that of original PBA in the range of -40°C to room temperature in spite of chemical modifications of acrylic oligomer.

From such a property, low excess loss is expected for M-PBA coated fibers over a wide temperature range.

Other properties of M-PBA are shown in Table 1.

Low moisture absorption is one of the characteristic features of M-PBA among these properties.

## Conclusions

UV curable polybutadiene acrylate coatings, which provide optical fibers with low excess loss over a wide temperature range due to its low modulus, are improved in thermal stability and faster cure rate with the preservation of low modulus by chemical modification.

The modified polybutadiene acrylate is expected to have practical use as a primary coating for optical fibers.

## Acknowledgment

The authors are indebted to Dr. S. Yamakawa and Mr. T. Kimura, NTT Ibaraki Electrical Communication Laboratories, Nippon Telegraph and Telephone Corporation for their guidance to this work.

## References

(1) S.Sakaguchi and T.Kimura, Conference Proceedings OFC (1985), San Diego

(2) T.Kimura and S.Yamakawa, Electron Lett., 20, 201 (1984)

(3) Orvid R.Cutler, Conference Proceedings RADCURE (1984), Atlanta

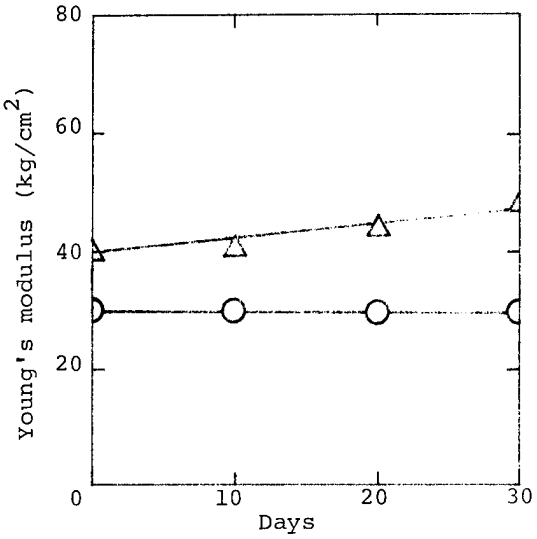



Fig. 1(A) Thermal stability of cured PBA in air at 80°C
○; M-PBA, △; PBA

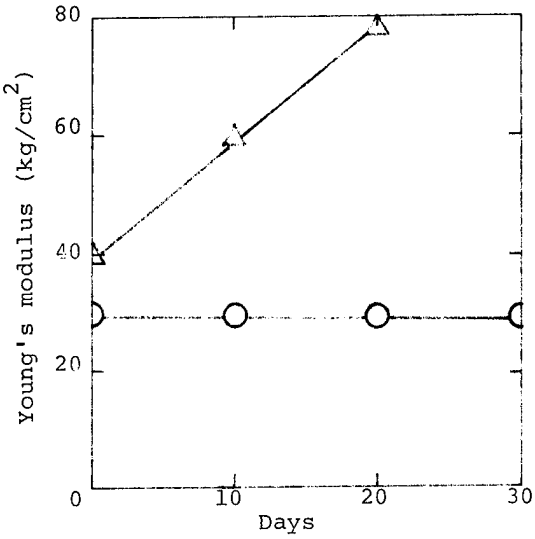



Fig. 1(B) Thermal stability of cured PBA in water at 80°C
○; M-PBA, △; PBA

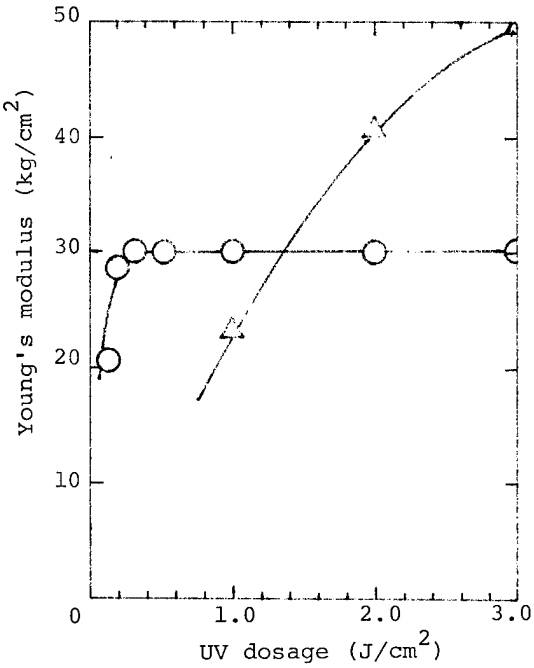



Fig. 2(A) UV dosage dependency of Young's modulus of PBA
○; M-PBA, △; PBA

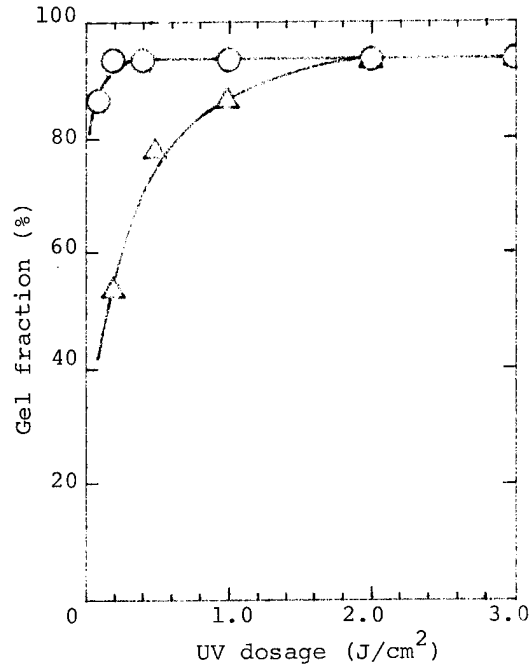



Fig. 2(B) UV dosage dependency of gel fraction of PBA
○; M-PBA, △; PBA

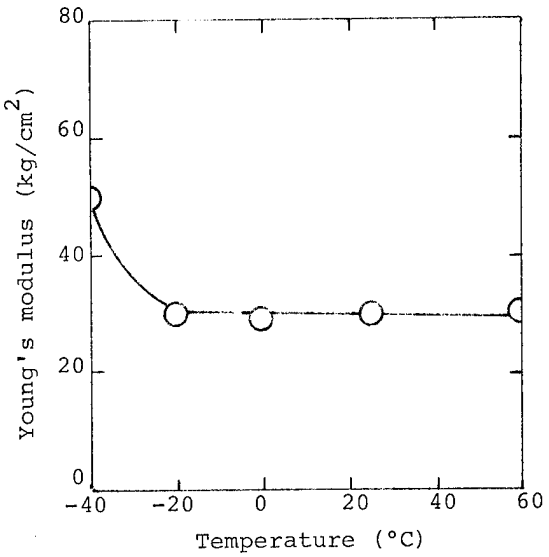
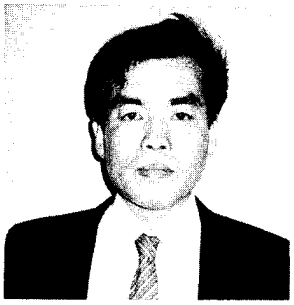



Fig. 3 Temperature dependency of Young's modulus of cured M-PBA

Table 1 Properties of M-PBA and cured M-PBA

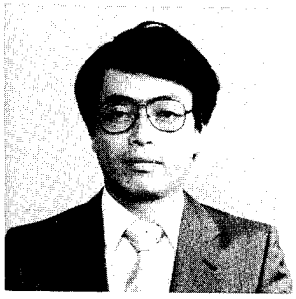
| Properties | Value |
|---|---|
| Density (g/cc) | 0.989 (25°C) |
| Viscosity (cps) | 5,300(25°C), 2,200(40°C), 900(55°C) |
| Shrinkage (%) | 4.5 |
| Refractive index | 1.496 (25°C) |
| Thermal expansion coefficient ($°C^{-1}$) | $3.1 \times 10^{-4}$ (-40~60°C) |
| Young's modulus ($kg/cm^2$) | 30 |
| Tensile strength ($kg/cm^2$) | 24 |
| Tensile elongation (%) | 110 |
| Moisture absorption (%) | 0.62 (60%RH) |



R. Ohno joined Japan Synthetic Rubber receiving both a B.S. and M.S. degree in Polymer Chemistry from Osaka University in 1967 and has worked on polymerization and organic synthetic research and application. He has spent the past three years working on the development of radiation curable resins.



Y. Matsumura is Manager of Radiation Curable Resin Section of Japan Synthetic Rubber. He obtained his Ph. D. in 1971 from Osaka University and joined Japan Synthetic Rubber in 1975. Since then, he has worked in the field of polymer chemistry and its application.



T. Kikuchi has worked on the development of radiation curable resins. He joined Japan Synthetic Rubber in 1969. He worked in technical section of a synthetic rubber plant before he was involved in the present work.

# A TACTICAL FIBER OPTIC CABLE

*A. C. Jenkins, C. R. Lovelace, and M. R. Reynolds*

AT&T Bell Laboratories
Norcross, Georgia 30071

*V. E. Kalomiris*

U.S. Army Communications - Electronics Command
Fort Monmouth, NJ 07703-5202

*ABSTRACT*

A ruggedized all-dielectric cable with two tightly-buffered dual-wavelength multimode fibers was designed to meet the rigors of tactical deployment. A polyester-elastomer fiber-buffering material was selected for its excellent temperature extreme performance. The cable was designed against specific requirements to achieve desirable features. Testing included environmental attenuation performance over a -46 °C to 71 °C temperature cycle and mechanical-durability tests of cyclic impact, cyclic flex, radial compression, knot test, cold bending and tensile strength as specified by DoD and EIA standards. The selected design surpasses both the environmental and mechanical requirements, exhibiting less than 0.2 dB/km added loss over the temperature range and showing no measurable attenuation after completion of mechanical durability testing. The final design is 6 mm (0.24 in.) in diameter, has a tensile load rating of 2200 Newtons (495 lbf), with mean 1300-nm attenuation about 1.0 dB/km and bandwidth product greater than 400 MHz-km.

## *1. INTRODUCTION*

AT&T Bell Laboratories has completed the development on *T*actical *F*iber *O*ptic *C*able *A*ssemblies (TFOCA) designed for use in the rugged tactical field environment. The TFOCA development effort was guided by detailed design criteria supplied by the contracting organization, the U.S. Army CECOM. The tactical fiber optic cable assemblies are for use in tactical *T*ime *D*ivision *M*ultiplex (TDM) communication systems for distances from one to eight kilometers without repeaters.

Each tactical fiber optic cable assembly includes two multimode fibers in a 1 km cable. Principal features of the TFOCA cable design are:

- Buffered fibers which operate over both the 800 to 900 nm and 1200 to 1300 nm wavelength regions and provide 400 MHz-km bandwidth product at 1300 nm.
- A rugged all-dielectric construction with a 2200-newton load rating.
- A diameter of only 6 mm, weighing under 30 kg/km.
- Cabled fiber loss averaging about 1.0 dB/km at 1300 nm.
- Less than 0.2 dB/km added loss over the temperature extremes -46 °C to +71 °C.

The design of the cable is described in the following sections, along with required performance and current testing results.

## *2. CABLE DESIGN REQUIREMENTS*

Several requirements were set to ensure that the TFOCA cable could operate in the tactical field environment. These requirements as well as the pertinent specifications are shown in Table 2-1.

The impact requirement is somewhat more severe than normally specified by the DoD. DoD-STD-1678 specifies impact testing with a mass dropped from 152 mm; the amount of mass depends on the cable diameter under test. Figure 2.1 shows the DoD requirement in graphical form. Two least-squares-fit lines describe a performance trend of mass versus cable diameter for the DoD specification. For a 6 mm cable, the mass is 1.5 kg yielding a 14.7 newton load. The TFOCA cable is required to withstand a 2 kg mass (yielding a load of 19.6 newtons), a 25% increase over the DoD requirement, but falling well within the performance trend. This requirement enforces the use of a jacketing material that has high tear and abrasion resistance.

The temperature performance requirement is also a difficult one. The -46 °C extreme enforces a need for cable materials which do not exhibit a rapid increase in elastic modulus as the temperature is lowered. Such materials keep the contractive forces on the optical fiber to a minimum. In addition, these materials must not degrade over the required temperature range.

## *3. CABLE DESIGN*

The TFOCA design evolved through a program of prototyping and testing in which key parameters were varied in order to surpass the requirements of Table 2-1. Figure 3.1 shows a cross-sectional view of the cable.

The cable construction begins with two fibers buffered to a diameter of 1.0 mm, as shown in Figure 3.2. The buffering material is a polyester-elastomer. The two buffered fibers are twisted together, forming the center of the cable. Around the two fibers, two layers of aramid yarn are stranded with opposite lays. The jacket is formed directly over the yarn from two extrusions of polyurethane which sandwich four stranded epoxy-glass rods. This jacket completes the cable and brings the diameter to 6.0 mm. An economic advantage is realized by manufacturing the cable in a single pass operation.

### *3.1 Thermoplastics*

The polyester-elastomer fiber-buffering material selection was based on processing ease and the attenuation performance of buffered fibers over the desired temperature range, -46 °C to 71 °C (see Table 2-1). Figure 3.3 shows typical differential-attenuation performance for a fiber buffered with this material. This figure represents performance outside the cable structure and illustrates the low levels of compressive-strain-induced microbending exerted by this material. The material continues to remain dimensionally stable over even wider non-operational temperature extremes. Such performance outside the cable structure aids in meeting the environmental and storage temperature performance criteria in the completed cable. The polyester material is preferred for its low room temperature modulus and relatively low hardness as well as its temperature performance, providing good protection to the fiber from microbending loss induced by lateral loading.

The choice of material for the cable jacket was influenced by several factors. Polyurethane is known for durability and has been

**Table 2-1. Cable Design Requirements**

| Test | Specification | Requirement |
|---|---|---|
| Temperature Performance | AT&T Bell Labs | Less than 0.2 dB/km increase in attenuation during temperature cycling between -46 ° C and 71 ° C |
| Impact | DoD-STD-1678 Method 2030 | No attenuation increase or damage after 100 impacts at 3 N-m |
| Tensile Strength | AT&T Bell Labs | Verify 2200-newton rating |
| Operating Tensile Load | EIA-FOTP-33 | No attenuation increase at 300 newtons |
| Flammability | DoD-STD-1678 Method 5010 | Continued burn $\leq$ 30 sec. on removal of flame; failure to ignite underlying tissue |
| Freezing Water Immersion | DoD-STD-1678 Method 4050 | No attenuation increase or damage while immersed in freezing water at 2 ° C |
| Cyclic Flex | EIA-FOTP-104 | No attenuation increase or damage after 2000 cycles over a 60-mm dia. mandrel |
| Knot | AT&T Bell Labs | No attenuation increase or damage while tied in 30-mm dia. knot |
| Cold Bend | DoD-STD-1678 Method 2020 | No attenuation increase or damage after wrapping 3 times around 30-mm dia. mandrel at -46 ° C |
| Radial Compression | DoD-STD-1678 Method 2040 | No attenuation increase or damage after radial loading of 2000 newtons |

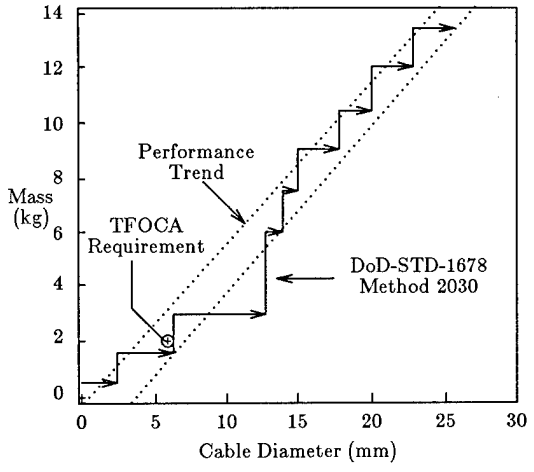



**Figure 2.1. Impact Test Requirements**

commonly used in military applications. Processing requirements are therefore well known and understood. One reason polyurethane has found common usage for such applications is the relatively slow change in modulus the material exhibits over a wide temperature range, -40 ° C to 80 ° C. It is also resistant to petroleum-based chemicals and oxidation. Thus, the material retains the flexibility and integrity required to survive the outdoor environment. An additional requirement listed in Table 2-1, flame retardance, is more difficult for polyurethanes as a family; however, flame-retardant versions exist which provide adequate performance while minimally affecting the other desirable properties. The polyurethane material is an off-the-shelf product to improve cost-effectiveness for the customer. Only more exotic and costly materials can provide the combination of performance offered by polyurethane. Two layers are used in the cable design, the first extruded directly over the yarn-covered fibers, and the second sandwiching four epoxy-glass rods.

*3.2 Strength Members*

Both the aramid yarns and the epoxy-glass rods contribute to the design's tensile-load rating. Current connectorization techniques attach to the yarn only, thereby defining a minimum load capacity from the yarn. The aramid yarns were selected to meet a tensile strength requirement of 1780 newtons for connectorization and to cushion the buffered fibers during impact and compressive loading.

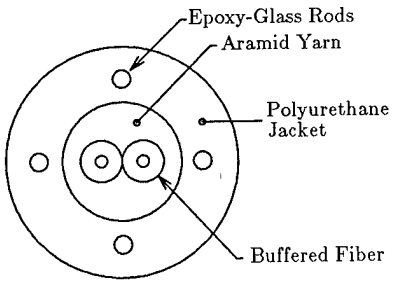



**Figure 3.1. Tactical Fiber Optic Cable**

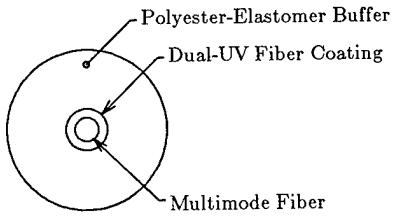



**Figure 3.2. Buffered Fiber**

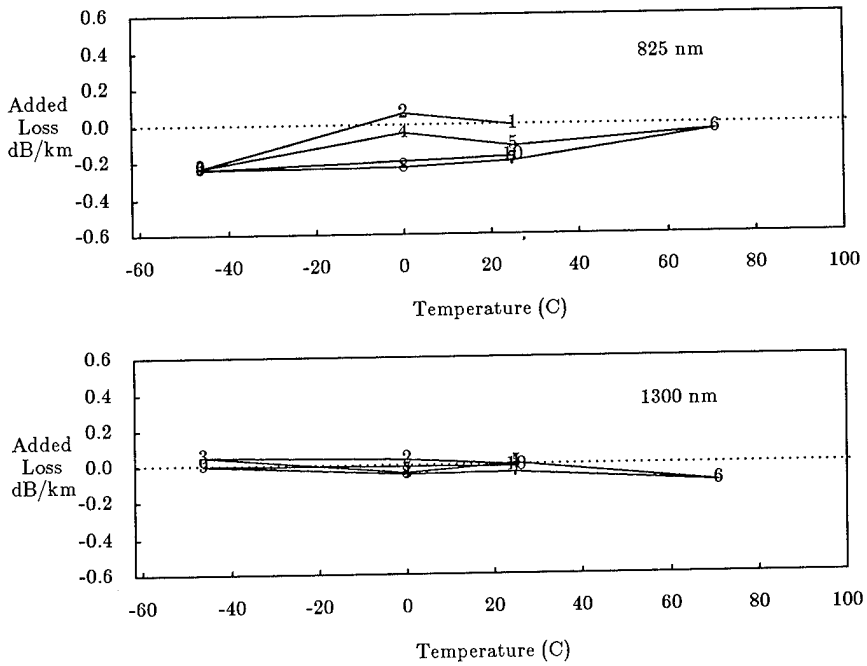



**Figure 3.3. Buffered Fiber Temperature Cycle Performance**

The yarn requires about 3120 newtons to elongate by 1%; therefore, at 1780 newtons, the cable will be elongated at most by about 0.6%. This guarantees that the 1% proof-tested fiber will survive during installation. The yarns are stranded around the fibers in two opposing layers to provide a torque-balanced design.

The yarns provide 80% of the tensile load capacity, leaving the remainder of the 2200 newton rating to the four epoxy-glass rods embedded in the polyurethane jacket. As shown in Figure 3.1, the rods are spaced equally within the jacket with a helical lay. In addition to the tensile load carrying capacity, the rods inhibit the axial contraction of the cable as the polyurethane cools immediately after extrusion and when the cable is operated at low-temperature extremes minimizing compressive fiber strain. The rods thus maintain minimal microbending effects, minimizing added loss. They also reinforce the jacket, helping to protect the underlying buffered fibers from mechanical abuse.

*3.3 Cable Manufacture*

Twenty-four one kilometer cables were manufactured with the TFOCA design using a single-pass cabling operation. These cables were taken up on 180 mm diameter military reels. Tolerances were tightly held yielding a maximum cable weight of 30 kg/km and an average diameter of 6 mm (0.24 in.). Figure 3.4 shows a histogram of loss performance at 1300 nm for the 24 cables. As shown, the average loss is 1.05 dB/km at 1300 nm and 3.57 dB/km at 825 nm. The bandwidth at 1300 nm is greater than 400 MHz-km for all 24 cables.

The glass rods provide an additional benefit during takeup on the small diameter military reel. The rods eliminate compressive strain due to bending which would contribute to cumulative microbending losses. The maximum cable loss after cable manufacture was under 1.5 dB/km at 1300 nm with one exception.

*4. CABLE PERFORMANCE*

The cable design was tested to determine its mechanical and environmental integrity for military applications. These tests included impact, knot, radial compression, cyclic flexing, operating cable tensile load, cable tensile strength, cold bend and freezing-water immersion. These tests are listed in Table 2-1 along with requirements and were performed in accordance with DoD-STD-1678 except where noted. All tests were conducted at 25 $\pm 5^{\circ}$C except the freezing water immersion and cold bend and environmental tests.

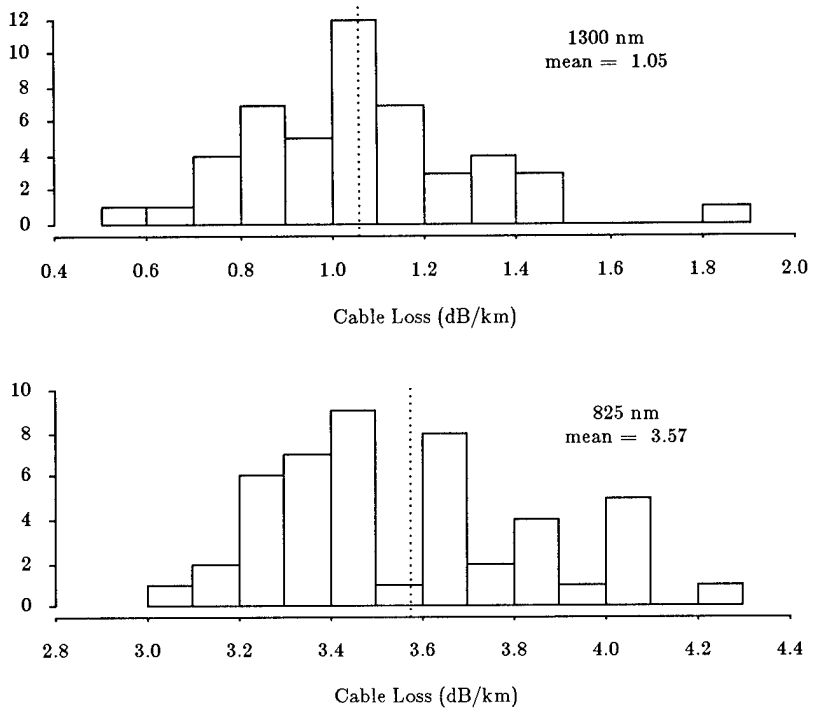



**Figure 3.4. TFOCA Cable Loss Performance for 24 Cables**

*4.1 Temperature Performance*

A key performance criterion for tactical cable is stable attenuation behavior over a wide range of temperatures. As noted in Table 2-1, the cable was designed to operate over the range -46 ° C to 71 ° C with less than 0.2 dB/km increase in attenuation at either 825 or 1300 nm. This performance was verified by cycling three 1 km cables over the required temperature range using the temperature cycle shown in Figure 4.1a.

Figure 4.1b shows the average performance of the three cables. As the figure shows, the average change in attenuation at -46 ° C was 0.03 dB/km at 825 nm and 0.06 dB/km at 1300 nm. The average change in attenuation at 71 ° C was 0.08 dB/km at 825 nm and 0.04 dB/km at 1300 nm. All variations of the final design performed well in the temperature cycle at both wavelengths. The following section highlights the mechanical performance of the TFOCA cable design.

*4.2 Mechanical Testing*

Three cable samples were used in each test. The samples were selected from different cable runs. Each sample used in the mechanical tests (except for the operating tensile test) consisted of a 20-meter length of cable with each fiber individually connectorized with biconic connectors. For most of the mechanical tests, the cables were connected to portable field-loss test sets before the start of the test and remained connected throughout. Any initial cable loss was zeroed out with the loss set so that loss measured during testing constituted added loss due to the test. The test sets use LED sources at both 825 and 1300 nm with measurement accuracy of $\pm 0.1$ dB. The freezing water immersion test and the operating tensile test, which required several hours to run, required a more accurate measurement of loss. A stable white-light source and monochromator were used to make comparative absolute loss measurements. Passing performance was defined as less than 0.2 dB increase in attenuation and no observed damage to the cable.

The TFOCA cable passed all mechanical requirements shown in Table 2-1 with no measurable change in attenuation or observed damage. Note especially the use of a 25% greater energy level in the impact test than normally required by DoD-STD-1678 Method 2030. The normal level is 100 cycles at 2.2 N-m; yet the cable was developed to withstand 3 N-m. In fact, one cable sample was tested beyond the requirement and withstood 500 cycles at 3 N-m.

The knot test was devised by AT&T Bell Laboratories for this application. In the knot test, a simple overhand knot was made in the cable at a large diameter ($\geq$ 300 mm) before connecting the cable to the test set and zeroing. The knot was then pulled down to a diameter of 30 mm and any increase in attenuation recorded. Once again, no measurable increase in attenuation occurred.

The tensile strength test, although an AT&T Bell Laboratories developed procedure, employed the same test set-up as the operational tensile test which is conducted per EIA-FOTP-33. A 150 meter sample is looped through several mandrels and then stretched to the appropriate load level. The sample was held at this load level for 5 minutes and then released. Three cable samples showed no increase in attenuation even when loaded to $\geq$ 2670 newtons, well beyond the required tensile strength. In addition there was no measurable increase in attenuation at the 300-newton requirement.

The remaining mechanical tests, cold bend, cyclic flex, radial compression and freezing water immersion were all conducted according to their respective DoD specifications against the requirements stated in Table 2-1. No measurable increase in attenuation or damage to the cable occurred in any of these tests.

The combination of cable design and material selection outlined above enabled the TFOCA cable to perform well during mechanical testing. The yarns not only provide the tensile strength for the cable but also cushion and protect the buffered fibers from impact and radial loads. The four glass rods reinforce the sheath to resist

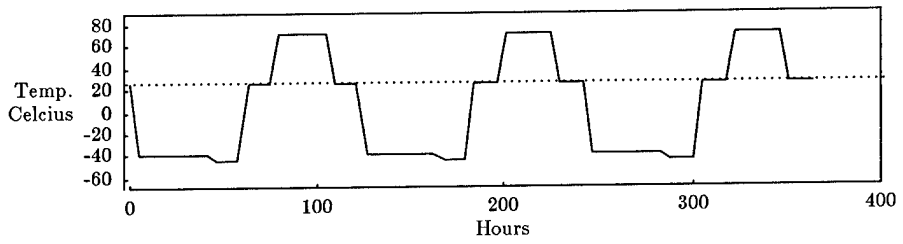



Figure 4.1a. Temperature Cycle

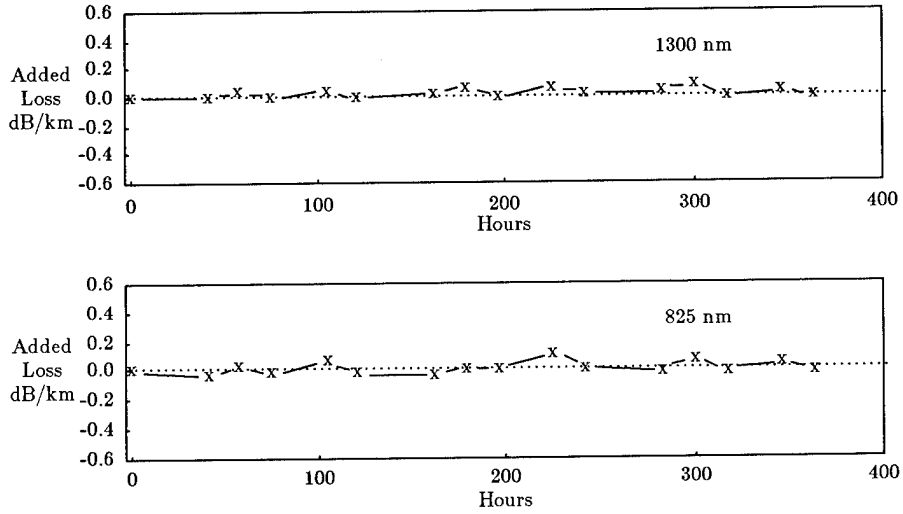



Figure 4.1b. Average Added Loss Performance

**Figure 4.1. Tactical Cable Performance at Extreme Temperatures**

compressive loads and to prevent large sheath deformation due to impact, flexure, lateral compression and cold bending. Finally, the polyurethane jacket resists tearing and splitting due to mechanical abuse.

*4.3 Flammability*

The TFOCA cable is required to be flame retardant per DoD-STD-1678 method 5010. A flame-retardant polyurethane was selected with a limiting oxygen index of 29.5 and minimal drip when burned. Three 600-mm cable samples were tested during which a gas flame over 1000 ° C was applied perpendicular to a sample mounted on an angle 60 ° to the horizontal for 30 seconds. According to method 5010, such a sample must not continue to burn for more than 30 seconds or ignite tissue located below the sample.

The cable passed this test easily, all samples self-extinguishing within 6 seconds after removal of the flame with no flaming drips. The flame-retardant polyurethane jacket contributes most to the cable design's flammability performance, charring when burned rather than dripping. This material also retains the mechanical properties of non-flame-retardant polyurethanes required for overall durability.

*5. CONCLUSION*

AT&T Bell Laboratories has completed the development of a two fiber all-dielectric cable that provides a range of physical characteristics required for tactical deployment while maintaining good optical performance. The 2200-newton rated cable is 6.0 mm in diameter and weighs about 30 kg/km.

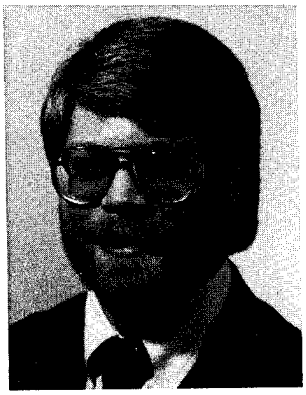
The cable design has less than 0.2 dB/km added loss over the -46 ° C to 71 ° C temperature range. Mechanical testing proved the ruggedness of the design as prototypes passed all required tests with no increase in attenuation.

*6. ACKNOWLEDGEMENTS*

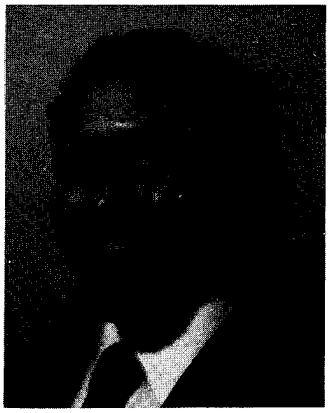
The authors gratefully acknowledge the contributions of the following: Olinda Mascarenhas for TFOCA documentation and helpful advise; Lou Tate for manufacturing early cable design iterations; Brian Adams and Ron Partain for fiber buffering; members of the AT&T Bell Laboratories' Lightguide Cable Group for testing assistance; the Lightguide Measurement Group for optical performance evaluation; and the Product Engineering Control Center of AT&T Network Systems for their construction of final design prototypes.



Artis C. Jenkins joined AT&T Bell Laboratories in Norcross, Georgia in 1980. His responsibilities include military cable design, nonmetallic sheath design, cable testing and cable termination. He received his BSME degree in 1976 and worked as a design engineer at Eastman Kodak in Kingsport, Tennessee from 1976 through 1978. He received his MS and Ph.D. from Georgia Institute of Technology in 1980 and 1984 respectively from the School of Mechanical Engineering. He is an associate member of the American Society of Mechanical Engineers.



Mickey R. Reynolds joined AT&T Bell Laboratories in Norcross, Georgia in 1978 as a Member of Technical Staff. His current responsibilities include military cable design, lightguide sheath design, and lightguide cable process characterization. He previously worked in lightguide splicing as project engineer for the Single-Mode Bonded Splice, and prior to that in copper cable mechanical characterization. He received his BS and MS degrees in Engineering Mechanics from Georgia Institute of Technology in 1978 and 1979 respectively.



Charles R. Lovelace is a Senior Technical Associate at AT&T Bell Laboratories in Norcross, Georgia. His current work in the Lightguide Design and Measurement Group involves optical fiber characterization and diagnostic measurements. Previous assignments have included high precision interferometric measurement techniques and fiber coating processing. He received his A.S. degree from Devry Institute of Technology and continues his education at DeKalb Community College.



Mr. Kalomiris is currently a project leader responsible for fiber optic cables, connectors, and fiber optic system development. He served for three years as chairman of the Tri-Service Group on fibers, cables and connectors. He is a member of EIA P6.7 Working Group on Fiber Optic Cables. He is also involved in the establishment of a test facility. Most recently, he worked for ITT-EOPD as a project engineer for the air layable cable which he designed. Prior to joining ITT-EOPD, Mr. Kalomiris was associated with General Cable Corp. R&D as a research engineer for 6 years. While at General Cable he was involved with the design, development and manufacture of the prototype superconductive power cable with flexible core. Before joining General Cable he spent a year working for the Hellenic Telecommunications Organization as a communications engineer responsible for planning and designing microwave links. While in Greece he translated "Mathematical Methods for Science Students" by G. Stephenson, Imperial College University of London. He is a member of IEEE and the Technical Chamber of Greece (Society of Professional Engineers). Education: B.A. in Mathematics, New York University; B.S. in Electrical Engineering, New York University; and an M.S. in Electrical Engineering, New York University.

# Low Temperature Fiber Optic Tactical Cable Without the Use of Antibuckling Members

John Chamberlain and Teresa Clarke

Siecor Corporation
P.O.Box 489
Hickory, North Carolina 28603

## Abstract

A duplex fiber optic cable has been developed for the military field environment. Cable requirements include less than 2.0 dB/km attenuation change over the -55°C to +85°C temperature range, flexibility without degradation of the optical properties and 1800 Newton pull strength without fiber breakage. All of these requirements have been met in a low cost cable with an outer diameter equal to 5.2 mm. The low cost jacketing materials meet VW-1 indoor flame standards, so that the cable can be used for both indoor and outdoor applications.

## Introduction

The military field environment requires rugged, flexible cables with good optical performance at low temperatures. Since these are somewhat contradictory from a design standpoint, a new approach was necessary.

Loose tube cables typically incorporate a free space window into their design in order to mechanically decouple the fiber from the cable and thus achieve good low temperature performance. Tight buffered fiber cables are flexible and easily handled because of the direct application of protective layers. The cable described here combined these assets to meet the requirements of the military environment.

## Cable Design

The cable design specifications call for two multimode fibers with 550 μm ± 50 μm outer diameters. Two 50 μm core diameter fibers with 125 μm cladding diameters are used, which are obtained coated to 500 μm with dual layers of UV cured acrylates. These fibers are color coded using a thermal cure wipe die system.

The target requirements of the cable design, listed in Table 1, include an operating temperature range of -55°C to +85°C, and tensile loading strength of up to 1800 Newtons without the fibers breaking. These parameters are considered the most difficult to obtain with the 5.2 mm limit on the cable outer diameter.

A dual jacket design is used (see Figure 1). The inner jacket consists of a polyurethane material (which meets VW-1 flammability stand ards) selected for ruggedness and low temperature flexibility. The inner jacket contains the two optical fibers stranded with two aramid strength elements, and is designed to allow free space around the fibers. The strength elements enable the outer layer of aramid strength elements and the second polyurethane jacket (using the same material grade used above) to be applied without excessively straining the fibers.

Two factors are considered in the initial cable design. They are (1) the coefficient of thermal expansion of the inner jacket material, and (2) the free space contained within the inner jacket. It is assumed that the manufacturing of the inner jacket does not strain or stretch the fibers. Thus, the fiber length is equivalent to the jacket length. At low temperatures the jacket contracts more than the optical fibers; so, due to the different thermal coefficient of the jacket material and the fibers, the fibers become relatively longer.

The length change, $\Delta\ell$ , due to a change in temperature $\Delta T$ is

$$\Delta\ell = \alpha_\rho \cdot \Delta T \qquad (1)$$

where $\alpha_\rho$ is the thermal expansion coefficient of the inner jacket material. It is assumed that the expansion coefficient is constant across the operating temperature range and is dependent only upon the type of plastic used.

Experiments have shown [1] that the attenuation change, , for an optical fiber within an unstranded tube can be calculated as

$$\Delta\alpha = 1.5\times10^{5}\ \omega^{2.6}\ e^{\frac{-20}{\sqrt{\eta}}} \cdot \left(\frac{d}{d_o}\right)^{2} \cdot \left(\frac{NA_o}{NA}\right)^{5} \quad (2)$$

Here, $\omega$ is the free space (the jacket inner diameter less the fiber diameter), $\eta$ is the fiber excess length in %o (1/1000), d is the fiber core diameter, and NA is the fiber numerical aperture. The subscript "o" implies reference fiber values.

An approximate value for $\omega$ can be found from equation (2) by an iterative procedure. Substituting

$\alpha_\rho = 8.3*10^{-5}$ /°C
$\Delta T = 80°C$,
$\eta = 6.6$%o,
$\Delta\alpha = 2.0$ dB/km,
$d = 50\ \mu m$,
$NA = 0.21$
$d_o = 62.5\ \mu m$
and
$NA_o = 0.16$,

into formulas (1) and (2), $\omega$ is found to be 1.3 mm. Hence, the inner jacket diameter is 1.8 mm.

The second pass applies an additional 14 strands of aramid strength elements and the outer polyurethane jacket over the inner jacket, increasing the cable diameter to 5.2 mm.

## Results

Approximately one kilometer of cable was fabricated using the above design. After the inner jacket was completed, attenuation change versus temperature testing was performed, per DOD-STD-1678, procedure 4020. This resulted in a total attenuation change of 0.2 dB/km through three cycles of the temperature range -55°C to +85°C. All attenuation change measurements were made by overfilling the fiber with 850 nm light so that worst case results would ensue.

The cable was finished by applying the strength elements and the outer jacket. This process caused no degradation to the optical fibers' performance. The finished cable was then temperature cycled, using the aforementioned procedure and test setup. An average attenuation increase of 0.7 dB/km was observed at -55°C. No increases were found at +85°C, or, after cycling was completed, at room temperature.

A tensile test was performed with a long length tensile tester built for optical fiber cable characterization (see Figure 2). 150 meters of prototype cable was set up around the rotating sheaves. The ends of the cable were brought to a monitoring device similar to the one used in temperature cycling described above, and any fiber attenuation changes were recorded. One fiber showed a 0.9 dB/km increase at 1113 Newtons load, while the second fiber showed no corresponding change.

Room temperature impact testing, cyclic flexing, low temperature flexibility, cable twist-bend and compressive strength tests were performed using DOD-STD-1678, procedures 2030, 2010, 2020, 2060 and 2040 respectively. At an energy of 1 Newton-meter, and at temperatures of -55°C, +25°C and +85°C, the cable survived 200 impacts without fiber breaks. Additionally, the cable survived 2000 cyclic flexing cycles with a ten kilogram load. Finally, the cable was tightly wrapped 20 times around a 25 mm diameter mandrel at -55°C, resulting in no attenuation increases or obvious jacket defects.

Some problems were encountered in the remaining tests. The cable survived only 900 twist-bend test cycles, 1100 cycles less than targeted. At 36 Newtons/cm, crush testing resulted in a 1.8 dB attenuation increase, which was larger than initially targeted. However, the cable ultimately withstood 8500 Newtons/cm without permanent fiber damage, far beyond expectation.

## Final Design

To correct the mechanical sensitivity difference between the two fibers, a more controlled payoff system was used during manufacture to ensure equal fiber tension. The crush test failures were reversed by using a more microbend insensitive silicon/acrylate hybrid fiber coating. The final cable design test results are also displayed in Table 1.

A final design cable was connectorized to detect any residual problems. A bifurcation technique developed for a similar datacomm duplex cable was implemented. A 66 kilogram load connector pull test resulted in no cable/connector interface damage. Finally, this connectorized sample showed less than 0.1 dB/km attenuation increase over the specified operating temperature range.

Future cable design refinements include (1) improving the cable performance to meet other military tests, (2) cost reduction, thereby making the cable more attractive to datacomm markets, and (3) an increase to four or six

fibers per cable. Also, single mode optical fiber may be included in this design.

## Summary

A fiber optic cable has been developed for the military field environment that maintains good fiber performance at low temperatures without antibuckling elements. It was successfully connectorized using standard procedures.

This cable also has definite possibilities in indoor datacomm applications because of its VW-1 flame retardant materials, handling ease, mechanical stability and relative low cost.

## Acknowledgments

Special thanks are due to Jennifer Gage for her technical input and especially to Dr. Bruce Hellmann for his assistance in editing this paper.

## Reference

[1] Zeidler, G., Hasselberg, A., Schicketanz, D., "Effects of Mechanically Induced Periodic Bends on the Optical Loss of Glass Fibers", Optics Communications, Vol. 18, Number 14, September 1976.

Figure 1

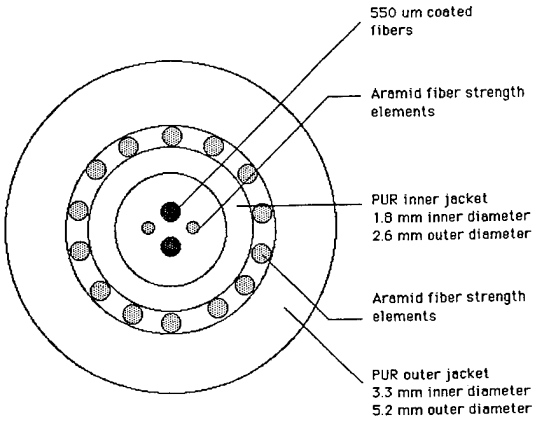
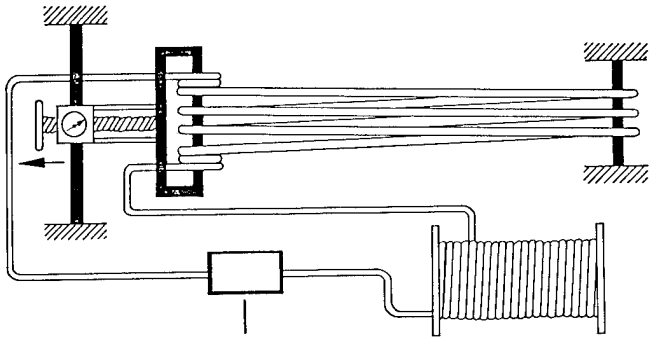



Figure 2

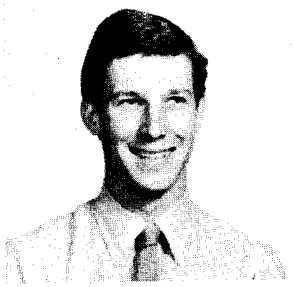


## APPARATUS FOR CABLE TENSILE AND BEND RESISTANCE TESTS

TABLE I

Testing Results for Two Fiber Tactical Cable
(all measurements made @ 850 nm)

| Test Parameter | Final Test Cable Performance | Target Specifications |
|---|---|---|
| Operating Temperature Range | -55°C to 85°C<br>0.3 dB/km | -55°C to +85°C<br>2 dB/km |
| Cable Outer Diameter | 5.2 mm | 4.8 ± 0.4 mm |
| Cable Weight | 25 kg/km | 22.6 kg/km |
| Compressive Strength | 1500 N/cm<br>2.0 dB/km @ load | 36 N/cm<br>1.5 dB |
| | 8500 N/cm<br>0.3 dB/km residual | 245 N/cm<br>no breaks |
| Cold Bend | -55°C/25 mm<br>0 dB/km | -55°C/25 mm<br>1 dB/km |
| Twist Bend | 750 cycles/10kg/30mm<br>2000 cycles/5kg/30mm | 2000 cycles/10kg/30mm |
| Impact Resistance | 500 cycles/1 Nm<br>50 cycles/3.3 Nm | 200 cycles/1 Nm |



John Chamberlain

Siecor Corporation
489 Siecor Park
Hickory, NC 28603

John Chamberlain was born in Detroit, MI, in 1961. He received his B.S. degree in Electrical Engineering from The Georgia Institute of Technology in 1983. Since graduation, he has been employed by Siecor Corporation in the Research, Development and Engineering Department.



Teresa Clarke

Siecor Corporation
489 Siecor Park
Hickory, NC 28603

Teresa Clarke graduated from North Carolina State University with a B.S. in Mathematics in 1978. She is presently the Product Development Laboratory Supervisor for the Research, Development and Engineering Department of Siecor.

# LONG-TERM RELIABILITY OF OPTICAL FIBER COMPOSITE GROUND WIRE

M. Ogai, H. Hiramatsu, M. Oda, Y. Kamata, Y. Miyajima and M. Ieshige

The Furukawa Electric Co., Ltd.,
No.6 Yawata-Kaigan, Ichihara, Chiba, 290, Japan

## Abstract

Optical fiber composite ground wire is subjected to high temperature. Hydrogen could evolve from coating material and diffuse into silica fiber to form OH radicals more actively at high temperature. Special attention has to be payed on the selection of dopant material as well as coating material. Acceleration tests on the complete cable have been carried out to find long-term reliability of the fiber for a special application.

## 1. Introduction

New information transmission system has been required for electric power transmission and disribution networks. In addition to data transmission for automatic power supply systems, network stabilizing systems and remote monitor and central control systems, new channels are required for office automation(OA), and factorory automation (FA) to operate and maintain associated facilities. Wideband video signals are included in these new requirements. Considering there expanding transmission capacity, new integrated digital communication network based on optical fiber transmission and packet switching system have been planned to be inplemented by electric power company.

Optical fiber is ideal transmission medium because of its low transmission loss, wide band width, immunity to electromagnetic interference, etc. Various cables have been developed to find out new possibilities around power transmission facilities such as pole, duct, tunnel, composition to electric power cable, et al and overhead ground wire seems to be the most promissing cable for intergrated digital communication network systems of electric power companies.

Many types of design have been experimentally tried to find suitable design for OPGW. Since the ground wire is subjected to high temperature and its elongation is large, special attention have to be payed not only on coating material selection and strain of fiber but also dopant selection of fiber itself.

## 2. Cable Design

### 2.1 Fundamental Requirements for OPGW

The optical fiber cable combined with a overhead ground wire is exposed to sever circumstances such as wide temperature variations, large strain. The temperature of ground wire is increased by ohmic loss. Umbalance of phase in power conductor lines induces electric current in ground wire. The maximum temperature rise caused by such umbalance current is generally limitted to be less than 100°C in most cases and less than 150°C in special cases.

Short circuit causes sharp temperature rise up to 300 ∿ 450°C in short period. These temperature rises can be estimated and the ground wire is designed so as to keep temperature rise under specified values. The optical fiber cable must withstand such a high temperature and cable materials have to be carefully selected.

In addition to the high temperature resistivity such as melting point et al, hydrogen evolution is required to be small. Thermosetting silicone is one of promissing candidates for coating materials that can withstand high temperature, but speciall rearangement of material is required to minimize hydrogen evolution. Such minimization is not always sufficient to garantee long term stability and suitable dopant material selection is required to minimize reaction of hydrogen in fiber.

### 2.2 Basical Design of Optical Cable

Considering the above mentioned requirements, the optical fiber cable composed to ground wire is designed. Two types of cable have been developed and the cross sections are shown in Fig. 1. In type A design, silicone coated optical fibers are stranded and soft silicone rubber is filled in interspaces of these fibers to form a basical unit. This unit is jacketed by FRP[1] (fiber reinforced plastics). Detail dimension of this cable is listed in Table 1. The number of fibers can be increased from six to ten with the increase of outer diameter from 2.0mm to 2.5mm. This type of cable is loosely housed to move longitudinally with small friction. Therefore the stress of the fiber can be reduced from that of ground wire and the cable can be replaced with a new one by pulling operation even after installation. High Youngs modulus and high melting point of FRP are essential for this design.

In another design, type B, optical fibers are housed in spiral groves of an aluminum spacer. In basical design, the coated fiber with special grade of silicone is jacketed by teflon that has melting point over 300°C and individually spaced into a groove. In modified design, after silicone coated fibers are stranded and jacketed by teflon, they are spaced into a groove to increase the number of fibers within limited space. Details of this design are added in Table 1.

## 2.3 Design of Ground Wire

These cables are placed in the center space of ground wire. Special segment is applied to minimize the increase of outer diameter after arranging center space. When the type A cable is used, aluminum pipe is not always essential and can be elliminated to get larger space for smooth movement of the cable.

Fig 1 Section of OPGW

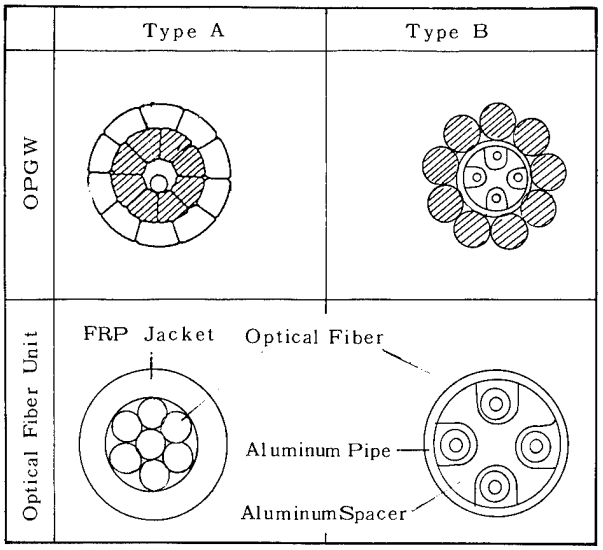



Table 1. Optical Fiber Cables

| ITEM | | SPECIFICATION | | |
|---|---|---|---|---|
| Optical Fiber | Fiber Material | Doped Sillica, Graded-Index Type | | |
| | Core Diameter (μm) | 50 ± 3 | | |
| | Surface Diameter (μm) | 125 ± 3 | | |
| | Numerical Aperture | 0.21 ± 0.03 | | |
| | Primary Coating Diameter (mm) | 0.4 | | |
| Unit | Type | A | B | B′ |
| | Number of Fibers | 6 | 1 | 3 |
| | Unit Sheath | FRP | Teflon | Teflon |
| | Outer Diameter (mm) | 2.0 | 0.7 | 1.1 |

## 3. Hydrogen Induced Loss

### 3.1 Basical Mechanism

Hydrogen evolved from coating and cable materials has been pointed out to cause transmission loss increase in infrared wave-length region[2]. Stability against hydrogen can be tested by heating fibers in hydrogen atmosphere at elevated temperature of 100∿200°C[3]. Heating test of jacketed fiber containing hydrogen source such as silicone rubber is another simple way to evaluate both stability of fibers and hydrogen evolution from coating material relatively with each other[4]. Minimization of phosphorus co-doping in G.I. fiber with $SiO_2$ - $GeO_2$ composition is very useful to improve stability against hydrogen[2].

### 3.2 Acceleration Tests

Hydrogen partial pressure estimation in practical cables offers the prediction for hydrogen induced loss increase in long-term[5],[6]. Hydrogen evolution from individual cable materials can be found using gas-chromatography but combination of these materials could cause excess hydrogen evolution in practical cables. In this meaning, acceleration tests on practical complete cables are very important. Japanese standard cables with tight silicone buffur structure were subjected to heat-cycling and continuous heating tests to know the hydrogen effects in practical cables. G.I. fiber 50μm core diameter, 125μm outer diameter, 1% refractive index difference with different dopant compositions, silicone coating and nylon jacketing were stranded into cables.

### 3.3 Experimental Results

Heat-cycling of the whole cable in a large chamber in -40∿80°C temperature range caused remarkable loss increase in infrared wavelength range. Transmission loss at 1.55μm increased almost linearly with time and one tenth of the loss increase was found at 1.3μm as shown in Fig.2. Larger loss increase was found in more sensitive fiber against hydrogen and close correlation was found as shown in Fig.3 where the loss increase after heating test in hydrogen atmosphere at 200°C is taken as a measure of sensitivity of fiber against hydrogen. To find temperature dependency of these loss increase, some other cables were continuously heated in chamber with about 100 times larger loss increase than the cable left inside the factory.

From these data, activation energy of the loss increase was found to be around 27 Kcal/mol and it is larger than that of loss increase after heating tests in hydrogen atmospher reported to be 10∿15 Kcal/mol over 100°C. Utilizing these results, first-order loss estimation in long term can be made in practical cables after acceleration test of the whole cable.

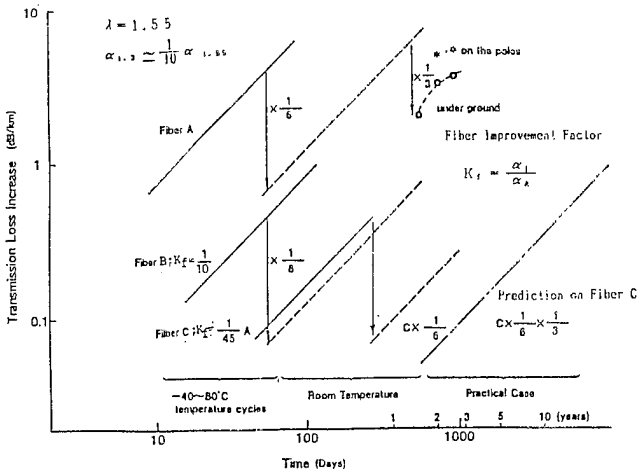



Fig.2 Acceleration Test Results by Heat Cyclings

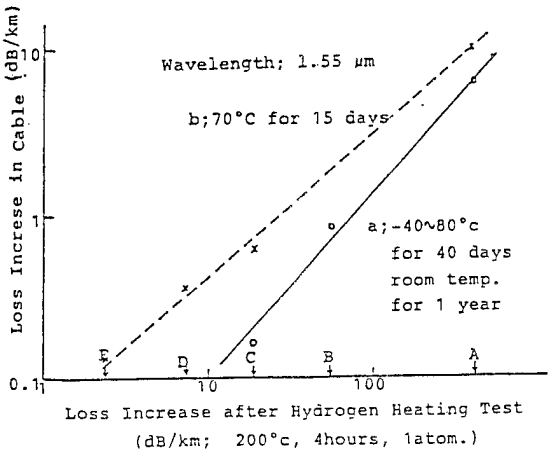



Fig.3 Transmission Loss Inclease of Cable versus Loss after Hydrogen Heating Test

## 4. Long-Term Stability of OPGW

### 4.1 Continous heating tests of OPGW

Two types of optical cables for OPGWs shown in Fig.1. were subjected to high temperature heating tests at 70 ∿150° in ambient atmospher in the chamber. Various types of silica fiber with different grade of thermosetting silicone were made into these cables. The sensitivity of these fibers was tested by heating in hydrogen atmospher and hydrogen evolution of silicone resin was also checked using gas-chromatography in advance of heating test of the whole cable.

### 4.2 Test result of type A cable

Type A cables containg GI fibers of 50μm core diameter, 125μm outer diameter and 1% refractive index difference were heated at 70°C ∿ 150°C and the results are plotted in Fig.4. Transmission losses increased very rapidly in the first stage and gradients of increase then came down to small level. It can be understand that hydrogen evolution and diffusion into fiber is very active in the first stage and the evolution speed decreases and out diffusion of hydrogen starts in the following stage. The saturated loss level of individual fiber was found to have a close relationship with loss increase after heating in hydrogen atmosphere for a certain period. It means that suitable dopont composition and manufacturing process can be relatively found from the results of acceleration test in hydrogen atmosphere. Further first order rough estimation of loss increase of suitably designed fiber can be made by knowing loss increase of hydrogen sensitive fiber in practical environment in addition to such sensitivity.

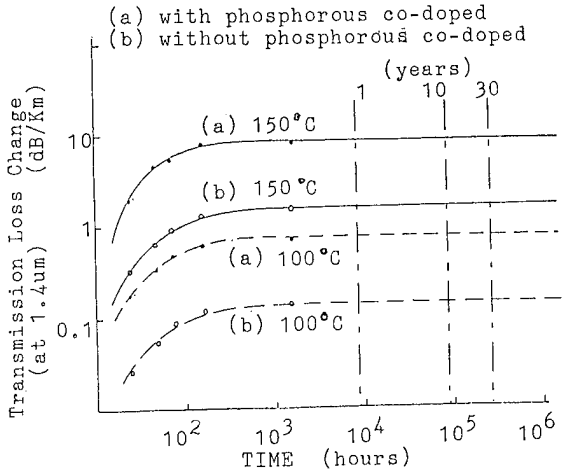



Fig.4 Transmission Loss Increase in Continuous Heating test(Type A)

### 4.3 Test results of type B cable

Graded index fibers of 50μm core diameter, 125μm outer diameter and 1% refractive index difference were made from the normal VAD process including jacketing of natural silica tube and made into type B cables after coating of thermosetting silicone and jacketing teflon with the outer diameter of 0.4mm and 0.7mm respectively. On to the fibers in type B1 cable, standard silicone resin was coated. It had a large amount of silicone hydrides in cross linker to promote the cross linking with vinyl and the residual of silicone hydrides disolved to generate hydrogen after getting OH radicals from moisture in the jacket. On to the fibers in type B2 cable, improved silicone resin was applied. The amount of silicone hyrides was reduced in shortned chain in cross linker and more vinyl were added in the improved main silicone polymer.

These cables were subjected to continuous heating tests at 100°C and 150°C for more than one month and the transmission loss was periodically checked. Since the transmission loss change at 1.3μm was negligibly small, the change of OH peak loss around 1.4μm was plotted in Fig.5. From the acceleration tests on this type of fiber in hydrogen atmosphere, loss increase at 1.3μm can be estimated to be one-thirtyth of OH peak loss increase around 1.4μm. A large difference can be found between cables "B1" and "B2" and usefulness of suitable selec-

tion of coating material can be easily made. The gradients of loss increase can also be found to reduce and the extrapolation of loss can be made. The loss increase caused by OH radicals around 1.4μm is estimated to be 1 dB/km at 100°C and 8 dB/km at 150°C. From these estimations, type B2 cable can be judged sufficiently stable for more than 30 years. In practical cases, the temperature does not continue at such a high level and it reaches to the specified maximum value only in some part of the whole time. In this meaning, the above estimation is safety.

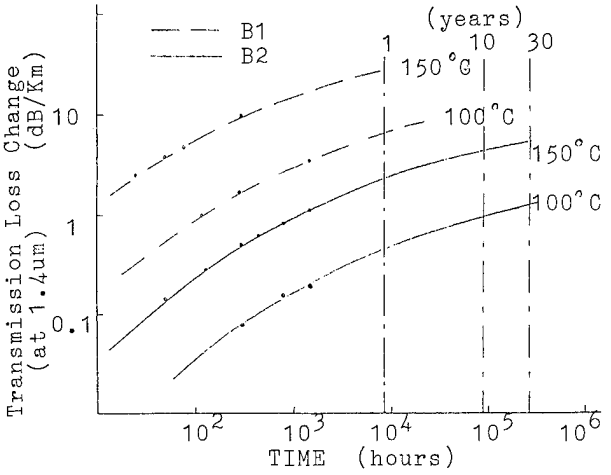



Fig.5 Transmission Loss Increase in Continuous Heating Test(Type B)

## 4.4 Temperature dependency of transmission loss after continuous heating tests

The cables subjected to high temperature continuous heating tests were cooled down to -20°C repeatedly a few times during the tests to find out deterioration of transmission loss at low temperature. Both types of the cables showed no remarkable degradation. Typical results are shown in Fig.6.

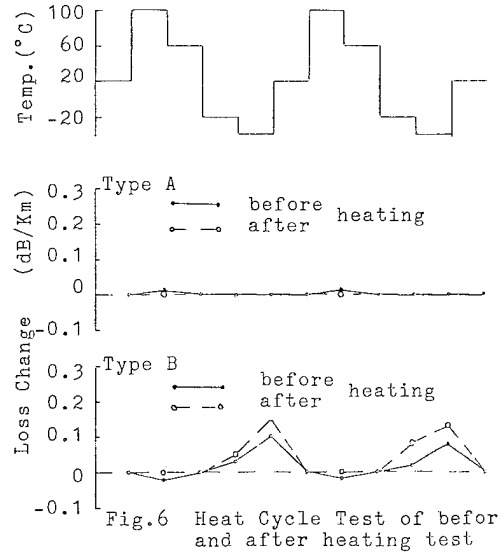



Fig.6 Heat Cycle Test of before and after heating test

## 4.5 Mechanical strength after continuous heating test

Mechanical tests were done on the cables before and after continuous heating tests. Initial mechanical performance was found to be kept even after continuous heating test.

## 5. Conclusion

Continuous heating tests at higher than 100°C were carried out on OPGWs to find out long-term stability of transmission loss and mechanical strength. Through these tests, the following points have been charified.

(A) Hydrogen induced transmission loss at 1.3μm in practical conditions after 30 years, can be estimated to be less than 0.1 dB/km.

(B) Degradation of temperature dependency of transmission loss was found negligibly small even after 150°C continuous heating tests.

## 6. Reference

(1) K. Fuse et al., The Furukawa Electric Review No. 74, 1983

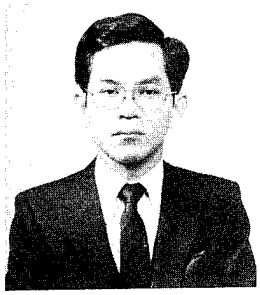
(2) N. Uchida et al., in Technical Digest, 9 th ECOC, 1983 PD Paper

(3) M. Ogai et al., in Post Deadline Papers, OFC '84 WI12

(4) N. Uesugi et al., Apply. Phys. Lett. 43, No. 4, 1983

(5) P. Lemaire et al., OFC '85 TUI1, 1985

(6) N. Uesugi et al., OFC '85 TUI2, 1985



Mikio OGAI

The Furukawa Electric
Co., Ltd.
6 Yawata-Kaigan-Dori,
Ichihara, Chiba, Japan

Mr. Ogai graduated from Tokyo Univ. 1970 with a B. Sc. in electrical engineering. Then he joined The Furukawa Electric Co., Ltd. and he engaged in research and development on millimetric wave guide line. He is presently working on research and development of optical fiber cables.

Mr. Ogai is now a manager of Optical Fiber Transmission Group, Chiba Research Laboratory, Research & Development Division at The Furukawa Electric Co., Ltd. and he is a member of the institute of Electronics and Communication Engineers of Japan.

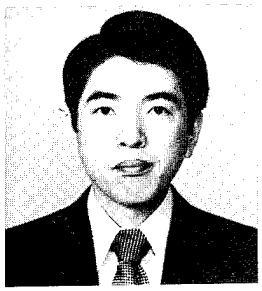


Hideyo HIRAMATSU

The Furukawa Electric
Co., Ltd.
6 Yawata-Kaigan-Dori,
Ichihara, Chiba, Japan

Mr. Hiramatsu graduated from Kyoto Univ. 1984 with a B. Sc. in electric engeeniring then joined The Furukawa Electric Co., Ltd. and has been engaged in development of the optical fiber cable.

Mr. Hiramatsu is now a staff engineer of Optical Fiber Transmission Group, Chiba Research Laboratory, Research & Development Division and a member of the Institute of Electronics and Communication Engineers of Japan.

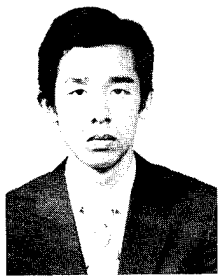


Mikio ODA

The Furukawa Electric
Co., Ltd.
6 Yawata-Kaigan-Dori,
Ichihara, Chiba, Japan

Mr. Oda graduated from Osaka Univ. with a B. Sc. in chemical engineering in 1971. Then he joined The Furukawa Electric Co., Ltd. and has been engaged in research and development of plastic material and manufacturing methods for telophone cables. He is presently working on development of the optical fiber cables.

Mr. Oda is now a assistant manager of the Production Engineering Section of Optical Fiber Telecommunication Division at The Furukawa Electric Co., Ltd.

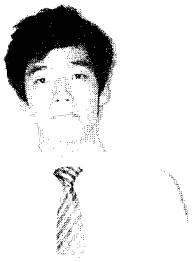


Yoshiyuki KAMATA

The Furukawa Electric
co., Ltd.
6 Yawata-Kaigan-Dori,
Ichihara, Chiba, Japan

Mr. Kamata graduated from Chiba Univ. 1983 with a B. Sc. in electronics engineering then joined The Furukawa Electric co., Ltd. and has been engaged in development of the optical fiber cable.

Mr. Kamata is now a staff engineer of Optical Fiber Transmission Group, Chiba Research Laboratory, Research & Development Division at The Furukawa Electric Co., Ltd. and a member of the Institute of Electronics and Communication Engineers of Japan.

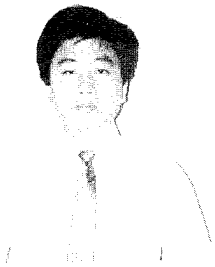


Yukio MIYAJIMA

The Furukawa Electric
Co., Ltd.
6 Yawata-Kaigan-Dori,
Ichihara, Chiba, Japan

Mr. Miyajima graduated from Tokyo Institute of Technology in 1983 with a B. Sc. in production engineering then joined The Furukawa Electric Co., Ltd. and has been engaged in development of the optical fiber cables.

Mr. Miyajima is now a staff engineer of the Production Engineering Section of Optical Fiber Telecommunication Division at The Furukawa Electric Co., Ltd.



Makoto IESHIGE

The Furukawa Electric
Co., Ltd.
6 Yawata-Kaigan-Dori,
Ichihara, Chiba, Japan

Mr. Ieshige graduated from Univ. of Electro communication 1982 with a B. Sc. in mechanical engineering then joined The Furukawa Electric Co., Ltd. and has been engaged in development of the telecommunication cable.

Mr. Ieshige is now a staff engineer of Telecommunications Group, Product Engineering Department at The Furukawa Electric Co., Ltd. and a member of the Japan Welding Society.

# OPTICAL STABILITY OF SINGLE MODE FIBER IN LOOSE-TUBE CABLE DESIGNS

**Keith A. Emig**
**Robert A. Modavis**
**John R. Sicotte**

**Corning Glass Works**
**Corning, New York**

**David O. Bostrom**
**Eugene W. Riley**
**David W. Williams**

**Ericsson, Inc.**
**Overland Park, Kansas**

## ABSTRACT

This paper reports on what effect the process of cabling fiber in a loose-tube design has on the properties of step-index single mode fiber manufactured by the outside vapor deposition (OVD) process.

Complete optical measurements were made on six randomly selected fibers prior to cabling. Routine optical characteristics of the fibers were evaluated during each step of the manufacturing process. Once the fibers were in finished cable form, complete optical measurements were again made.

In making the final analysis of the data, the post-cabling measurements of each fiber were compared to the pre-cabling measurements. As expected, the intrinsic glass properties, i.e., chromatic dispersion and mode field diameter, were unchanged. Additionally, there was no quantifiable effect on the total attenuation of the fiber over a wide spectral region. A discussion on the functionality of the effective cutoff wavelength with respect to measurement condition is included as well.

## INTRODUCTION

During the latter half of the 1970's, glass optical fibers proved to be both a technical and economic challenge to the traditional metallic-based transmission media for medium distance voice and data transmission. These early applications used graded-index, multimode optical fibers operating at wavelengths of 850 and 1300 nanometers.

Although multimode fibers remain the media of choice in many applications, the pulse dispersion and signal loss present in systems configured with these fibers limits transmission capacity to an extent which makes long distance, high data rate systems economically impractical.

Open competition in the long distance communications market in the early 1980's gave impetus to the development of the more efficient single mode fiber and associated electronics. Pulse dispersion and signal loss in systems employing single mode fibers are substantially less than in systems using multimode fibers, allowing much higher transmission rates over significantly increased repeaterless distances. Single mode fiber is considerably different from multimode fiber in both design and propagation characteristics. Hence, some new parameters, different from those typically used for multimode fiber, are necessary to describe the transmission characteristics of single mode fiber.

The objective of the work reported herein was to determine which of the single mode fiber transmission parameters, if any, would be affected by the cable process and design.

## SAMPLE AND PROCEDURE

**Single Mode Fiber**

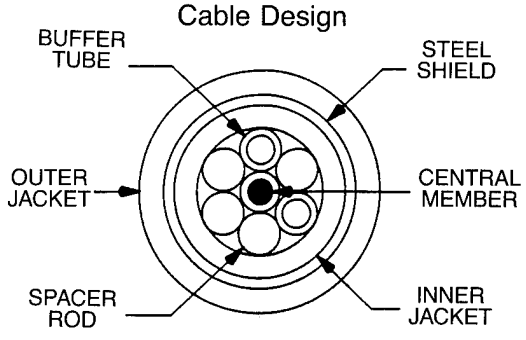
Six commercially available telecommunications grade single mode fibers manufactured by the OVD process were randomly selected for use in this experiment. The characteristics of the fiber used are as follows:

| | | |
|---|---|---|
| Index Profile | : | Matched Clad, Step Index |
| Cut-off Wavelength, [ $\lambda_c^t$ ] | : | 1200 ±70 nm |
| Refractive Index Difference [ $\Delta$ ] | : | 0.30 ± 0.04% |
| Mode Field Diameter [$2W_0$] | : | 10 ± 1 $\mu$m |
| Zero Dispersion Wavelength [ $\lambda_0$] | : | 1310 ± 15 nm |
| Attenuation [ $\alpha$ ] @ 1300 & 1550 nm | : | ≤0.5 dB/km |
| Dispersion [ $\sigma$ ] | | |
| @ 1285 – 1330 nm | : | ≤3.5 ps/nm·km |
| @ 1550 nm | : | ~17 ps/nm·km |
| Cladding Diameter | : | 125 ± 3 $\mu$m |
| Acrylate Coating Diameter | : | 250 ± 15 $\mu$m |
| Proof Stress Level | : | 0.35 GN/m² |

**Loose-Tube Cable**

The basic cable design used in this experiment is commonly employed in long distance communication systems installed in the United States today. The specific configuration used, shown in Figure 1, consists of two filled buffer tubes containing six single mode fibers each and four solid spacer rods helically stranded around a coated steel central strength member. A high molecular weight polyethylene inner jacket, polymer coated steel armor and a high molecular weight polyethylene outer jacket are applied for mechanical protection. [1]

**FIGURE 1**
Cable Design



The cable was manufactured using 5 kilometer fiber lengths. Only three fibers from each of the two buffer tubes were utilized for this experiment. This sample size of six fibers was sufficient to produce statistically valid experimental results since a matched pair sampling technique was used.

### Parameters Evaluated

The four parameters evaluated in this study and generally recognized as most germane to transmission in single mode fiber today are shown in Table 1.[2,3,4]

**TABLE 1**

Measurement Program Summary

| PARAMETER | MEASUREMENT STAGE | | | | | TEST METHOD |
|---|---|---|---|---|---|---|
| | INITIAL | | AFTER BUFFERING | AFTER STRANDING | FINAL | |
| | SHORT LENGTH | FULL LENGTH | | | | |
| ATTENUATION | X | X | X | X | X | 2 POINT CUT-BACK |
| CHROMATIC DISPERSION | | X | | | X | 5 POINT PULSE DELAY |
| MODE FIELD DIAMETER | X | X | | | X | VAMFF |
| CUT OFF WAVELENGTH | X | X | | | X | TRANSMITTED POWER |

### Measurement Procedures

Table 1 also indicates the cable manufacturing stages preceding each measurement and the test methods used. The standard techniques used to measure spectral attenuation (i.e., 2 point cut-back) and chromatic dispersion (i.e., 5 point pulse delay) utilize the full length of fiber which allows for the direct evaluation of the effects of cabling. However, the standard techniques which were employed to measure mode field diameter (i.e., variable aperature method in the far-field designated VAMFF), and cutoff wavelength (i.e., transmitted power) require the measurements to be performed on short lengths (2 meters) of fiber. Therefore, although not standard procedure, to permit isolation of the effects of the cable process and design on these parameters, full length (5 kilometer) measurements were also made prior to cabling. In addition, the short length measurements were made on samples taken from both ends of the fiber and the results averaged for use in the analysis reported in this paper.

Each parameter was measured multiple times on a sample of the fibers to verify adequate precision of the measurement benches.

## THEORETICAL BACKGROUND

The desired transmission characteristics of an optical fiber are determined by the design of the index profile and geometrical structure, and the selection of materials used in its manufacture. The ensuing discussion primarily concentrates on identifying the possible effects on the transmission characteristics through changes in the optical and physical design structure of the fiber due to its packaging in a loose-tube cable. However, it is best to first establish the relationship between the transmission characteristics and fiber design parameters.

### Attenuation

The principle intrinsic loss mechanisms contributing to the total attenuation in a single mode fiber manufactured by the OVD process today are scattering losses. These intrinsic scattering losses, said to be "refractive index fluctuations frozen in the glass at the time of manufacture," [5] vary with wavelength as $A/\lambda$, where A is a material constant and $\lambda$ is the operating wavelength.[6]

### Chromatic Dispersion

Chromatic dispersion in a single mode fiber is due to the sum of two components, material dispersion and waveguide dispersion.

The material dispersion is a function of the inherent refractive index of the glass composition used to manufacture the fiber. It results from the spectral variation in the refractive index given by $\lambda/c\ (d^2n/d\lambda^2)$, where c is the speed of light in a vacuum and n is the group refractive index.[6]

Waveguide dispersion occurs in single mode fiber because, as opposed to multimode fiber, some of the power propagates in the cladding region surrounding the core. The result is that the effective speed of the light in the fiber is somewhere between that of the higher refractive index cladding and the lower refractive index core varying with wavelength as a function of $a/\lambda$, where a is the core radius.[6,7]

### Mode Field Diameter

Since, as mentioned above, the distribution of power in a step-index single mode fiber is not confined to the core diameter, as in multimode fiber, the functional parameter used to characterize the mode power distribution is known as the mode field diameter.

The following theoretical formula [8] expresses the mode field diameter of a step-index single mode fiber in terms of its core radius and refractive index characteristics:

$$2W_o = a\,[0.65 + 1.169V^{-1.5} + 2.379V^{-6}]$$

where,

$$V = (2\pi a n_1/\lambda)(2\Delta)^{1/2}$$
$$\Delta = (n_1^2 - n_2^2)/2n_1^2$$
$$n_1 = \text{core refractive index}$$
$$n_2 = \text{cladding refractive index}$$

### Cutoff Wavelength

The cutoff wavelength also can be theoretically expressed in terms of the core radius and refractive index characteristics of the fiber:

$$\lambda_c = (2\pi a n_1/V_c)(2\Delta)^{1/2}$$

with the normalized cutoff frequency $V_c = 2.405$

However, the theoretical cutoff wavelength has proven difficult to measure directly and therefore impractical to specify. Alternatively, industry standards organizations have settled upon an arbitrary operational definition which lends itself to more reproducible measurements, i.e., only a single mode propagating at the end of a 2 meter length of fiber containing one complete loop with a 25 centimeter diameter.

For the single mode fiber used in this experiment, the theoretical cutoff wavelength is 50 – 100 nm higher than the cutoff wavelength value obtained using the standard test procedure. Since the specified cutoff wavelength range, 1130 – 1270 nm, is representative of cutoff wavelength values obtained by the standard test procedure, the theoretical cutoff wavelength is oftentimes higher than the operating wavelength.

The measured cutoff wavelength has been shown to vary dramatically with bending and length conditions of the fiber under test. Both decreasing the bend diameter and increasing the length of the fiber will reduce the measured cutoff wavelength.[9] The equivalent bend diameter of the fiber in the cable, as a result of helical stranding, was 9 cm, which is considerably less than the 25 cm bend diameter used under standard test conditions. While this smaller bend diameter would expectedly result in a measured cutoff wavelength lower than that obtained by the standard test procedure, the decrease due to length when measuring the full 5 kilometers of fiber should be much greater. For these reasons, it has been noted that the "effective" cutoff wavelength of an operating cable span may be significantly lower than the value

measured under the standard test conditions. Although the current specified wavelength range, 1130 – 1270 nm, has proven satisfactory, discussion has ensued in standards organizations with respect to allowing the upper limit of the range to extend beyond the operating wavelength, under certain circumstances.[10]

**Cabling Effects**

It is now clear that the transmitting characteristics of the fiber are highly interdependent. Consequently, the fiber manufacturer must strike a balance between the refractive index properties and core diameter to produce a single mode fiber which will operate at high transmission rates over long distances and can be easily spliced.

Although it is theoretically possible that the refractive index properties of the glass and the physical structure of the fiber could change due to temperature and stress effects, the temperatures required to soften and deform the glass are orders of magnitude higher than those experienced during the cabling process. Therefore, the possibility of permanent thermally-induced change occuring during cabling is non-existant. Also, because the objective of this experiment is to study only the effects of cabling on the fiber, the impact of enviromental temperature variations on fiber transmission characteristics will not be discussed here. Moreover, many publications have already addressed this topic.

The intent of the loose-tube cable design is to minimize the application of any stress on the fiber. Fiber stress during cabling generally occurs as a result of either longitudinal or compressive force. Both longitudinal and compressive stress cause changes in the refractive index of the glass which produce changes in the transmitting characteristics of the fiber.[11] Because the loose-tube design allows the fiber to reach a relaxed state, the possibilities of stress-induced changes in the intrinsic glass properties is insignificant. Thus, the possibility of change in the transmitting characteristics which are directly related to the intrinsic properties of the glass, namely chromatic dispersion, mode field diameter, theoretical cutoff wavelength and the intrinsic contributions to attenuation, is also insignificant.

An interesting stress-optic effect does exist that can result in an increase in the extrinsic contributions to total attenuation in a cabled fiber. It is difficult, in the practical packaging of fibers through cable design and fabrication, to avoid the introduction of small bends. As the refractive index of a fiber becomes small, as in a single mode fiber, it becomes increasingly more difficult for the transmitted wave to negotiate such small bends without some power being radiated away through the cladding. Such losses are referred to as induced cabling losses due to microbending. In single mode fiber, microbending manifests itself as a "microbending edge" where, beyond some critical wavelength the loss rapidly increases. It is the intent of the fiber manufacturer and cabler to keep the microbending edge beyond the intended operating range of wavelengths, i.e., greater than 1550 nm.

Therefore, one area that received considerable attention during the early stages of product development was control of microbend-induced loss through careful consideration of cable design. After the basic cable design was established, a mathematical model was developed to predict the magnitude of expected induced loss using empirical data taken on a prototype cable manufactured with specially developed highly-microbend-sensitive single mode fibers. The mathematical model was based on an expression derived by Furuya and Suematsu [12] for the incremental loss due to random bends. The basic cable design was refined until the mathematical model predicted no cabling-induced microbending effect on commercial grade single mode fiber.

## EXPERIMENTAL RESULTS

**Attenuation**

Although a very wide spectral range was studied, Table 2 shows the effects of cabling on attenuation at only the relevant wavelengths of 1300 and 1550 nm including the average attenuation [ $\bar{\alpha}$ ], and the standard deviation [ $S_{\bar{\alpha}}$ ] of the results on the six fibers. The average difference [ $\bar{\Delta}$ ] between the initial results and those obtained after subsequent cabling operations and the standard deviation of the differences [ $S_{\bar{\Delta}}$ ] show no statistically significant change throughout the manufacturing process.

It is clear that the cable design employed prevents the microbending edge from impinging on the 1550 nm operating window.

### TABLE 2

Effect of Cabling on Attenuation (dB/km)

| λ | MEASUREMENT STAGE | $\bar{\alpha}$ | $S_{\bar{\alpha}}$ | $\bar{\Delta}$ | $S_{\bar{\Delta}}$ |
|---|---|---|---|---|---|
| 1300 nm | INITIAL | 0.37 | 0.016 | * | * |
| | AFTER BUFFERING | 0.34 | 0.021 | -0.03 | 0.021 |
| | AFTER STRANDING | 0.35 | 0.008 | -0.02 | 0.014 |
| | FINAL | 0.36 | 0.027 | -0.01 | 0.027 |
| 1500 nm | INITIAL | 0.22 | 0.019 | * | * |
| | AFTER BUFFERING | 0.21 | 0.017 | -0.01 | 0.021 |
| | AFTER STRANDING | 0.21 | 0.008 | -0.01 | 0.026 |
| | FINAL | 0.22 | 0.019 | 0.00 | 0.015 |

* The differences are expressed relative to the initial values.

The data presented in subsequent Tables 3, 4 and 5 utilize the same statistical notations as used in Table 2 for attenuation.

**Chromatic Dispersion**

The fact that there was no movement in the zero dispersion wavelength [ $\lambda_o$ ], as shown in Table 3, confirms the insensivity of the dispersive characteristics of the fiber to the loose-tube cable design and processing.

### TABLE 3

Effect of Cabling on Zero Dispersion Wavelength (nm)

| MEASUREMENT STAGE | $\bar{\lambda}_o$ | $S_{\bar{\lambda}_o}$ | $\bar{\Delta}$ | $S_{\bar{\Delta}}$ |
|---|---|---|---|---|
| INITIAL | 1310 | 1.44 | — | — |
| FINAL | 1310 | 0.75 | -0.5 | 1.14 |

Table 4 summarizes the dispersion [ $\sigma$ ] measurement results over the optimized operating window, 1285 – 1330 nm, as well as the potential second operating window, 1550 nm. Consistent with the absence of effect on the zero dispersion wavelength, no changes were observed over a broad range of wavelengths evaluated, including those reported here.

### TABLE 4

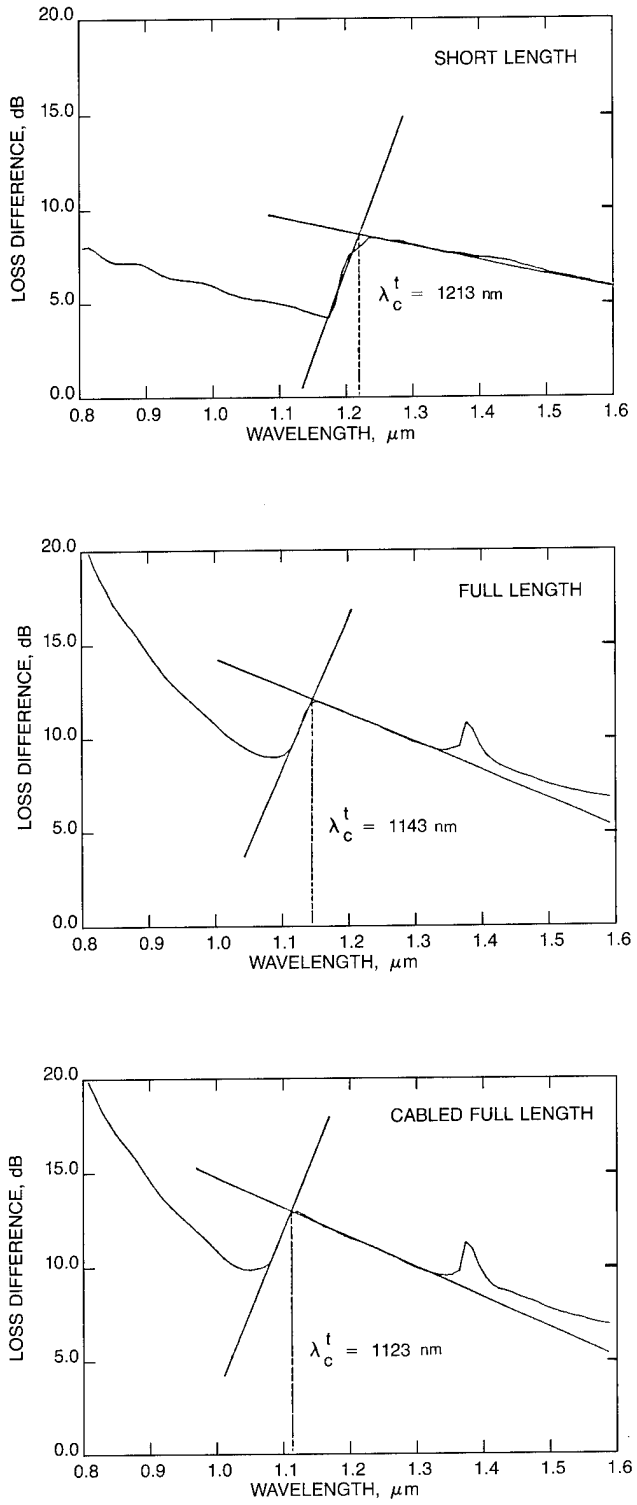
Effect of Cabling on Dispersion (ps/nm·km)

| λ | MEASUREMENT STAGE | $\bar{\sigma}$ | $S_{\bar{\sigma}}$ | $\bar{\Delta}$ | $S_{\bar{\Delta}}$ |
|---|---|---|---|---|---|
| 1285 nm | INITIAL | -2.30 | 0.132 | * | * |
| | FINAL | -2.29 | 0.075 | 0.01 | 0.110 |
| 1330 nm | INITIAL | 1.72 | 0.137 | * | * |
| | FINAL | 1.78 | 0.084 | 0.06 | 0.117 |
| 1550 nm | INITIAL | 16.88 | 0.173 | * | * |
| | FINAL | 17.06 | 0.141 | 0.18 | 0.135 |

* The differences are expressed relative to the preceding value.

## FIGURE 2

Effects of Cabling on Cutoff Wavelength (nm)




**Mode Field Diameter**

Mode field diameter [$2W_0$] results are reported in Table 5. As is to be expected, identical values were obtained from initial short and full length fiber measurements which verified the technical suitability of using a short length to characterize the mode field diameter of long commercial lengths of fiber. In addition, the equivalence of results from the initial full length and cabled full length measurements substantiates the theory that the mode field diameter is unaffected by the processing or design of the cable.

## TABLE 5

Effect of Cabling on Mode Field Diameter ($\mu m$)

| MEASUREMENT STAGE | LENGTH | $\overline{2W_0}$ | $S_{\overline{2W_0}}$ | $\bar{\Delta}$ | $S_{\bar{\Delta}}$ |
|---|---|---|---|---|---|
| INITIAL | SHORT | 10.3 | 0.15 | * | * |
| | FULL | 10.3 | 0.14 | 0.0 | 0.04 |
| FINAL | FULL | 10.3 | 0.10 | 0.0 | 0.05 |

* The differences are expressed relative to the preceding value.

**Cutoff Wavelength**

Figure 2 clearly shows the predicted impact of the measurement condition on cutoff wavelength [$\lambda_c$]. The mean difference between measurements on a short fiber length and a full fiber length was -70 nm. Comparison of the cutoff wavelengths measured on the full fiber length before and after cabling show an average difference of -20 nm. As was expected the change due to length was far greater than the change caused by cabling. Additional studies need to be conducted to determine what results would be obtained using the transmission method to determine cutoff wavelength in fiber of different lengths and other cable designs.

## CONCLUSIONS

The experimental data confirms the theoretically expected results. The filled loose-tube cable design has proven to be a highly efficient way to package single mode fiber.

The stability of the intrinsic functional transmission parameters, particularly chromatic dispersion and mode field diameter, throughout the loose-tube cabling process has been successfully demonstrated. Clearly, the reliable and readily predictable performance of the single mode fiber makes it redundent to recharacterize these parameters of the fiber in the final cable product, as confirmed by the successful installation of over a hundred thousand kilometers of fiber in the loose-tube configuration.

The absence of induced loss due to microbending demonstrates that the cable design insures the ability to upgrade to the inherently lower loss 1550 nm window as suitable lasers become available.

It is shown that the effective cutoff wavelength when measured in long lengths of cable is significantly lower than when measured by the standard test procedure. The implications of this phenomena are currently a topic of discussion in industry standards organizations.

## REFERENCES

1. K. Cornelison, M. Fleck, "Applications and Comparative Performance of Lightwave Cable Sheaths," Proceedings of 33rd International Wire and Cable Symposium, 1984.

2. G. Copa, B. Costa, P. Di Vita, U. Rossi, "Characterization of Single Mode Optical Fibres," CSELT Technical Reports, December 1984.

3. G. Bonaventure, U. Rossi, "Standardization Within CCITT of Optical Fibres for Telecommunication Systems," CSELT Technical Reports, December 1984.

4. C. Lemrow, P. Reitz, "Single-Mode Optical Waveguide Specifications," Telecommunications Magazine, May 1984.

5. D. Keck, "Transmission Properties of Optical Fiber Waveguides," SPIE Vol. 63 — Guided Optical Communications, 1975.

6. P. Bocko and J. Gannon, "Optical Waveguide Materials," Technical Report — Corning Glass Works, August 1983.

7. D. Keck, "Fundamentals of Optical Waveguide Fibers," IEEE Communications Magazine, May 1985.

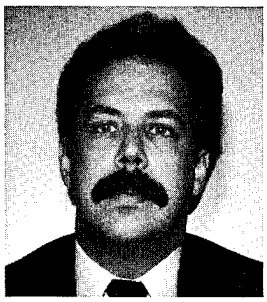
8. D. Marcuse, "Loss Analysis of Single Mode Fiber Splices," Bell System Technical Journal — Vol. 56, May - June 1977.

9. D. Eccleston and J. Dick, "Industrialized Measurement System for Single Mode Fibers," Proceeding of SPIE — Vol. 425, August 1983.

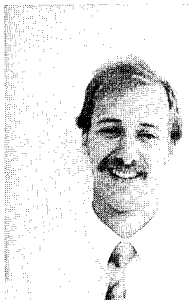
10. CCITT VIIIth Plenary Assembly — Malaga — Torremolinas, 1984, Document 103, Study XV — Report R48, Recommendation G.652, Section 1.5.

11. K. Hafemeister, T. Clark and E. Buonopane, "Automated Differential Fiber Strain Measurement System for Single and Multimode Fiber," Symposium on Optical Fiber Measurements, NBS, October 1984.

12. K. Furuya and Y. Suematsu, "Random - Bend Loss in Single Mode and Parabolic - Index Multimode Optical Fiber Cables," Applied Optics, May 1980.



*Keith A. Emig is a Senior Measurements Equipment Development Engineer at Corning Glass Works' Waveguide Product Engineering Laboratory in Corning, New York. He received a A.A.S. degree in Electronics from the Williamsport Area Community College in 1978 and a B.T. degree in Electrical Engineering from the Rochester Institute of Technology in 1982.*



*Robert A. Modavis has been in Research and Development at Corning Glass Works, Corning, New York, for three years. He received his B.S. and M.S. in Optics from the University of Rochester in 1981 and 1982, respectively.*



*John R. Sicotte is a Senior Applications Engineer with the Telecommunications Products Division of Corning Glass Works in Corning, New York. He received a B.S. — Civil Engineering degree from the University of Rhode Island in 1978 and an M.B.A. from Syracuse University in 1983.*



*David O. Bostrom is a graduate of the College of Wooster in Wooster, Ohio with a degree in chemistry and economics. He has held several positions within Ericsson, Inc., or its predecessor since 1970 including his present position, Director of Quality Assurance.*



*Eugene W. Riley is Chief Engineer at the Ericsson, Inc. TelecomCable Product Engineering Center in Overland Park, Kansas. He received the B.E.E. degree from the University of Delaware in 1958 and the M.S. degree in mathematics from Northern Illinois University in 1968.*



*David W. Williams is Supervisor of the Optical Measurements Laboratory at the Ericsson, Inc. TelecomCable Products Engineering Center in Overland Park, KS. He received a B.S. in Engineering Technology from Central Missouri State University in 1979. After graduation he joined what is now Ericsson, Inc. and has been involved in the development of fiber optic measurements.*

# PREDICTION OF OPTICAL CABLE LOSSES DUE TO HYDROGEN

S.R. Barnes, N.J. Pitt

Standard Telecommunication Labs.,
Harlow, Essex, England, UK.

S. Hornung

British Telecom Research Labs.,
Martlesham Heath, Suffolk, England, UK.

## Summary

This paper outlines a simple model which can be used to predict hydrogen levels in optical cables. From this the optical attenuation can be predicted from isobarometric degradation data. A further advantage of the method is that only hydrogen evolution rate data is required rather than elevated temperature measurements which are prone to error.

## Introduction

The effect of hydrogen on the optical properties of waveguides has been extensively reported[1,2], but cable design thus far has been on an 'ad hoc' basis. This paper outlines a simple model that can be used to predict hydrogen levels in optical cables. From this the optical attenuation can be predicted from available degradation data.

This paper is an extension of the approach of Hornung et al[3] and is illustrated by reference to single mode optical fibre, but the principle can be used with any fibre type.

## Sources of Hydrogen

There are three major sources of hydrogen in optical cables; polymer degradation, metallic outgassing and galvanic corrosion.

### Polymer Degradation

In extensive tests hydrogen has been shown to evolve from the majority of commercially available polymers, often with little or no thermal excitation. Because they are by no means homopolymers the specific nature of the reactions cannot normally be identified, although oxidation and hydrolysis are known to produce hydrogen in specific instances[4]. Complex formulations, as found in many acrylate primary coating materials, are almost impossible to analyse.

### Metallic Outgassing

Hydrogen is retained in metals in a variety of trapping sites such as grain boundaries and dislocations. The amount of hydrogen is strongly dependent on the original manufacturing process but can be significantly altered by subsequent processing, cold working for instance.

The majority of hydrogen is tightly bound and will not be released even at moderately elevated temperatures. The lowest loosely bound site in steel is, for instance, the ferrite-carbide interface where the peak evolution rate occurs around 120°C.

### Galvanic Corrosion

Hydrogen will be produced in cable structures containing dissimilar metals and an electrolyte such as ionised water. The electrochemical reactions of interest are:

i) Anode reaction

$$\text{Metal} \longrightarrow \text{Metal}^{n+} + ne^{-}(\text{electrons})$$

ii) Cathode reaction

$$H_2O + e^{-} \longrightarrow H^{+} + OH^{-}$$
$$2H^{+} + 2e^{-} \longrightarrow H_2$$
$$O_2 + 2H_2O + 4e^{-} \longrightarrow 4OH^{-}$$

### Degradation of Single Mode Optical Fibres

The loss increment $\alpha$ (dB $km^{-1}$) in optical fibres can be divided into three separate components:-

$\alpha_1$ Interstitially dissolved hydrogen loss,
$\alpha_2$ Hydroxyl formation loss,
$\alpha_3$ Wavelength dependent loss.

The following empirical relationship has been derived for STC single mode optical fibres.

$\alpha_1$ can be described in terms of pressure, P(at), absolute temperature, T(K) and a scaling factor $S_\lambda$ values of which are shown in Table 1

$$\alpha_1 = 1.4 \times 10^{-2} \rho S_\lambda \exp \frac{1550}{RT}$$

| $\lambda$ | 1290 | 1300 | 1310 | 1320 | 1330 | 1550 |
|---|---|---|---|---|---|---|
| $S_\lambda$ | 1.8 | 1.3 | 1.0 | 0.8 | 0.7 | 2.7 |

Table 1 Scaling factor $S_\lambda$ as a function of $\lambda$

Experimental results show that, within the 1300 nm window $\alpha_2$ and $\alpha_3$ exhibit a similar time and pressure dependence and appear to be related. Furthermore the effect of $\alpha_3$ is one or two orders of magnitude greater than that of $\alpha_2$. Therefore for the purpose of this analysis we can combine these two components as $\alpha_{2+3}$.

$$\alpha_{2+3} = 10\sqrt{P}\ \ 1 - \frac{1}{[1 + 2.33 \times 10^{11} t\sqrt{P} \exp(-26100/RT)]}$$

where t is time (s) and R is the gas constant.

The total loss increment can be calculated by combining equations (1) and (2).

$$\alpha_{TOT} = \alpha_1 + \alpha_{2+3}$$

Using these equations Fig. 1 shows the loss increment at 1310 nm for an STC single mode fibre after 25 years, as a function of hydrogen pressure.

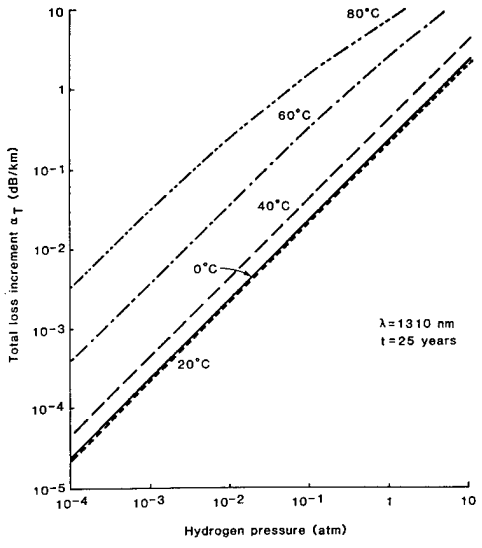



Fig. 1 Total Loss Increment as a Function of Hydrogen Pressure

## Partial Pressure of Hydrogen in Cables

Most cables can be reduced to two elements; a barrier (generally cylindrical) which envelops a core. The barrier may be located at any part of the cable and is considered to be the component which prevents hydrogen diffusing away from the waveguide.

Ignoring solubility effects the partial pressure of hydrogen in the cable is given by (Ref. 3)

$$P = H/Q\ [1 - (1 - P_o Q/H) \exp(-Qt/V_o)]$$

where $P_o$ = Original partial pressure of hydrogen (at)
$P$ = Partial pressure of hydrogen (at)
$H$ = Hydrogen evolution rate ($cm^3\ cm^{-1} s^{-1}$)
$Q$ = Hydrogen transmission rate through barrier ($cm^3 cm^{-1} s^{-1}$)
$V_o$ = Free volume per unit length of cable ($cm^3 cm^{-1}$)

This is illustrated in Fig. 2.

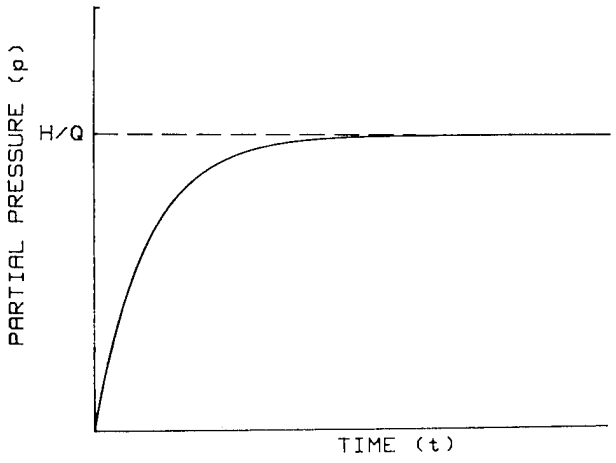



Fig. 2 Partial Pressure of Hydrogen as a Function of Time for a Typical Cable Sample

Assuming that H is constant and the time constant $V_o/Q$ is short compared with the lifetime of the cable the hydrogen level for the service period will asymptotically tend to:

$$P = \frac{H}{Q}$$

In general the hydrogen evolution rate decreases with time so that if the initial value is selected for H this will be suitably pessimistic for the purposes of cable design. The partial pressure P can now be applied to the hydrogen degradation data to predict the loss increase for single mode and multimode fibres.

## Transmission Rate - Q

The transmission rate through a cylindrical barrier is given by the following relationships[5]:

i) Cylindrical metallic barrier

$$Q = \frac{K\ 2\pi\ P^{1/2}}{\ln r_1 - \ln r_2}$$

ii) Cylindrical polymeric barrier

$$Q = \frac{K\ 2\pi\ P}{\ln r_1 - \ln r_2}$$

iii) Glover barrier (non-cylindrical - see Fig. 3).

$$Q = \frac{K\ P\ D}{W}$$

where K = Permeability constant
$r_1$ = Outside radius of cylinder
$r_2$ = Inside radius of cylinder
D = Thickness of laminate layer
W = Width of overlap layer

Hornung[3] has measured Q for a Glover barrier and found it to be well above its theoretical value indicating incomplete sealing in many cases.

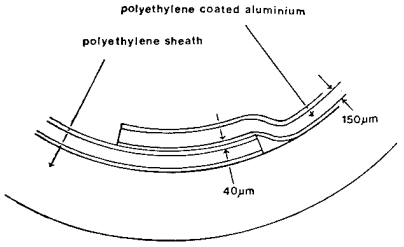



Fig. 3 Glover Barrier

## Hydrogen Evolution Rate - H

The hydrogen evolution rate can be determined in a number of ways:

Flushing tests Complete cables can be analysed by purging out resident gases through hydrogen measuring equipment[3] provided that they have low pneumatic resistance, for instance open channel cables (see Fig. 4). Because the hydrogen is seldom evenly distributed the average hydrogen is considered to be the most relevant for predicting the optical degradation.

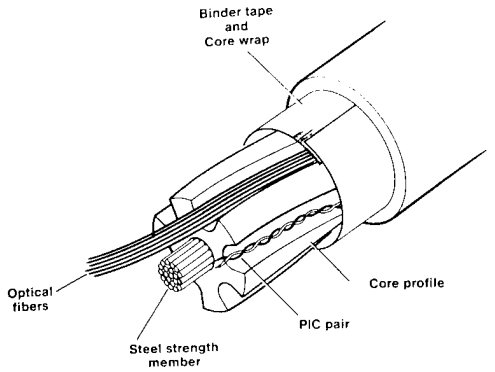



Fig. 4 Open Channel Cable

Individual elements Outgassing tests can be carried out on each cable element[5]. The rates can then be added together to give the total hydrogen evolution rate.

Composite samples To reduce the cost of testing composite sampling has been assessed. Here the entire core of the cable is tested in a 'cocktail' form. A further advantage of the test compared to the testing of individual elements is that synergistic effects are accounted for. The major drawback is that 'bad actors' will not be identifiable and further measurements will be required where the total hydrogen evolution rate is too high.

The temperature of testing is also important. Polymer degradation rates are strongly influenced by second order thermal transitions, e.g. glass transition temperature. Testing should be carried out at the maximum services temperature wherever possible.

The three tests have been compared for two cables. The results are shown in Table 2.

The results show that there is good agreement between the three regimes.

| Cable | Temperature (°C) | Individual Elements | Core Sampling | Flushing Test |
|---|---|---|---|---|
| 1 | 20 | - | $3.9 \times 10^{-10}$ | $1.2 \times 10^{-10}$* |
| | 40 | - | $5.6 \times 10^{-10}$ | - |
| | 50 | - | - | $4.0 \times 10^{-10}$ |
| | 80 | $1.4 \times 10^{-8}$ | $1.9 \times 10^{-8}$ | $3.4 \times 10^{-8}$ |
| 2 | 20 | - | $3.3 \times 10^{-11}$ | - |
| | 40 | - | $9.0 \times 10^{-11}$ | - |
| | 80 | $1.6 \times 10^{-9}$ | $6.8 \times 10^{-10}$ | $1.1 \times 10^{-9}$ |

Table 2 Hydrogen outgassing rate ($cm^3cm^{-1}s^{-1}$) for various testing regimes (* Approximate temperature)

## Discussion

The level of optical degradation can now be predicted (see Table 3 below).

| Cable | Temperature(°C) | Monomode | Multimode* |
|---|---|---|---|
| 1 | 20 | $1 \times 10^{-3}$ | $3.5 \times 10^{-2}$ |
| | 80 | 1-5 | - |
| 2 | 20 | $1 \times 10^{-4}$ | $1.2 \times 10^{-2}$ |
| | 80 | 0.2-0.4 | - |

Table 3 Predicted hydrogen degradation (dB $km^{-1}$) after 25 years (*Multimode fibre data ex reference 7(=1%$P_2O_5$))

An attempt has been made to estimate the effect of changing the barrier by using the core in Cable 2 in two simulated constructions; a welded steel tape and a thermoplastic jacket.
By comparing the above core with a Glover barrier, the importance of the barrier material in cable design can be ascertained. The results are shown in Table 4.

It is likely that the welded metallic result is a gross overestimate because the hydrogen evolution rate has been shown in separate experiments to reduce greatly with increasing levels of background hydrogen. However from the cable design aspect polymeric barriers will give lower partial pressures of hydrogen than welded metallic tubes.

Where high losses are predicted from high partial pressures this is generally due to high evolution rates. Further tests must be conducted to verify this. These will generally take the form of expensive non-cumulative tests.

It should be noted that all the above tests refer to undamaged cables. We anticipate that a damaged cable flooded with water may suffer higher rates of corrosion resulting in significantly higher levels of hydrogen.

## Conclusions

This paper outlines a simple model which can be used to predict hydrogen levels in cables due to the competing mechanisms of hydrogen evolution within the core and outward permeation. From this the optical attenuation can be predicted from isobarometric degradation data.

We have also shown that a number of tests can be successfully used to determine the hydrogen evolution rate and that core sampling compares favourably with more expensive flushing and elemental testing.

| | Glover barrier | 0.5 mm Welded Steel Tape | 3 mm Polyethylene Jacket |
|---|---|---|---|
| K ($cm^3cm^{-1}s^{-1}at^{-1}$) | - | $2.6 \times 10^{-12}$*(Ref. 8) | $5.0 \times 10^{-5}$(Ref. 9) |
| H/Q (at) | $7 \times 10^{-3}$-$2 \times 10^{-2}$ | 0.2-2.5 | $1.0$-$1.5 \times 10^{-3}$ |
| $\alpha_{TOT}$ (dB $km^{-1}$) | 0.2-0.4 | 5 | $2 \times 10^{-2}$ - $3 \times 10^{-2}$ |

Table 4 Hydrogen degradation for differing barrier materials for cable stored at 80°C (* Units $cm^3cm^{-1}s^{-1}at^{-1/2}$)

## References


1. Philen D.L., Gartside C., 33rd IWCS, Reno, Nevada (1984)

2. Abe K, Lowe R. and Thornson E., 33rd IWCS, Reno, Nevada (1984)

3. Hornung S., Cassidy S.A., Reeve M.H., 3rd Boulder Symposium on Optical Fiber Measurements, Boulder, Colorado (1984)

4. Gunderson and Hart, 'Silicone Lubricants' (Chapman and Hall)

5. Barnes. S.R., Riley. S.P. and Wolfe S.V., IEE Colloquium on Implementation and Reliability of Optical Fibre Links, Digest Number 1984/74, London (1984)

6. Crank. J., Mathematics of Diffusion, Oxford University Press (1975)

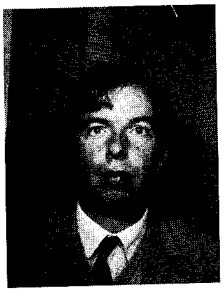
7. Rush J.D., Beales K.J., Cooper D.M., Duncan W.J., Rabone N.H., British Telecom. Tech. J. 2 pp 84-93 (1984)

8. Louthan M.R., and Derrick R.G., Corrosion Science 15, pp.567-577, (1975)

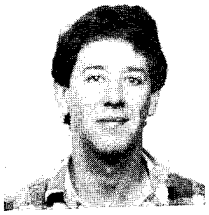
9. Engineering Design for Plastics. (Ed. E. Baer) Van Nostrand Reinhold (1964)


## Acknowledgements


The authors wish to thank the Directors of Research, British Telecommunications plc., and the Directors of STL for permission to publish this paper.

Stuart Robert Barnes was born in Worksop, England, and received a B.Sc. (Eng.) and Ph.D. from Queen Mary College, University of London. Since joining STL he has been involved in many aspects of cable design and development, in particular, cables for submarine applications.



Nicholas Pitt was born in Warwickshire, England, in 1954. He graduated in Materials Science from Sheffield University in 1975 and received a Ph.D. from the same university in 1979 for work on hydrogen and water in vitreous silica. He joined STL in 1981 to work on fibre optic materials and processing, and is currently engaged in development of new fibre materials for transmission in the mid infra-red waveband.



Stephen Hornung graduated from the University of Exeter, Exeter, England in 1975. In 1980, he received the D.Phil. from the University of Oxford, Oxford, England for work in low-temperature nuclear orientation of some neutron-light isotopes of iridium.

Since 1979, he has worked for British Telecom Laboratories on optical-fibre communications research, specializing in measurements on optical fibres with particular interest in cabling aspects.

# OVERCOMING THE HYDROGEN PROBLEM IN OPTICAL FIBERS

P. ANELLI (*), G. GRASSO (*), E. MODONE (**), B. SORDO (**), F. ESPOSTO (***)

(*) SOCIETA' CAVI PIRELLI, MILANO (ITALY) - (**) CSELT CENTRO STUDI LABORATORI COMUNICAZIONI,TORINO (ITALY) - (***) SIP D.G.,ROMA (ITALY)

## ABSTRACT

Hydrogen impairs transmission properties of both monomode and multimode fibers. The three mechanisms contributing to the fiber loss increase are identified and their effects are quantitatively characterized as a function of composition, structure, time, hydrogen pressure and temperature. The actual effect of hydrogen on fibers inside optical cables depends on the design and type of the material used as well as on the environmental conditions. An effective way of overcoming the hydrogen problem without imposing heavy restrictions on cable design, based on the use of hydrogen chemical getters as cable components is illustrated. A hydrogen absorbing material,suitable to be included in the cable structure as sealing compound has been developed and fully tested.Experimental results and absorbing properties are given. Industrial application to actual cables is illustrated.

## INTRODUCTION

Since the first evidence of damage to optical fibers due to the presence of hydrogen in a cable was found in 1982, intensive activity was started in many research centers with the aim of elucidating the mechanisms of such optical damage and to provide effective counter-measures The results obtained made possible the clarification of many aspects of this hydrogen related degradation of optical fibers so as to provide basic criteria for the development of possible remedies. In principle, two different approaches could be adopted to prevent hydrogen damages in fibers, i.e. suppressing the hydrogen in the environment or using fibers that are insensitive to it.
As will be shown in the paper, none of the known types of fibers was found to be immune from hydrogen effects, although different fibers showed different sensitivity, either quantitative or qualitative. Similar results are found in literature with the only exception of fibers with ceramic (silicon oxynitride) coating,which are reported to be protected against hydrogen permeation for an exceedingly long time. The other approach, i.e providing a hydrogen free environment around the fibers was the one adopted by Societa' Cavi Pirelli where intensive investigation was especially focused on the development of an effective "hydrogen getter" suitable for use in optical cables.
We report here on the extensive testing and the fully successful results obtained by the use of a polymer based composition containing a selective hydrogenation catalyst,which has found its first industrial application in a cable designed in cooperation with SIP, the Italian telephone operating company, and installed in Venice in mid 1985.

## HYDROGEN IN FIBERS

As it is now widely recognized, exposure to a hydrogen atmosphere produces three distinct effects on the optical properties of silica glass fibers, i.e.: a) a reversible loss increase due to absorption of molecular hydrogen. b) an irriversible loss increase due to chemical reaction of atomic hydrogen with glass constituents to form hydroxyl (-OH) groups. c) a wide band loss increase,which is probably due to the formation of color centers (background loss).
All the effects contributing to the fiber optical loss increase depend, although in different ways, on fiber type and composition, hydrogen exposure time, hydrogen pressure and temperature.
An experimental investigation on single mode and multimode fibers having different profiles and core dopant materials (Table I)was carried out in order to quantitatively determine their sensitivity to the different hydrogen effects. Moreover, suitable interpretative models were developed to estimate long term losses for these fibers under the conditions of temperature and hydrogen concentration usually encountered in actual cables. The tests were performed under pure hydrogen atmosphere at pressures below 700 mmHg in order to control possible pollution from the environment by pressure monitoring. As an example, the spectral attenuation curve of a multimode fiber for a hydrogen absorption/desorption cycle at 20°C is shown in Fig.1. The absorption peaks labelled A are due to molecular hydrogen, while those labelled B,C and D are due to -OH vibration. Only a very limited background loss increase is observed in this fiber.

The general results obtained in our investigation can be summarized as follows:

## Molecular Hydrogen Loss Increase

The complete reversibility (Fig.1) of the absorption loss confirms that the phenomenon is related to diffusion and solution of hydrogen in the silica matrix. The optical loss variation can be described by the expression:

$$\Delta\alpha_\lambda = \Delta\alpha_0 \left(1 - \exp\left(-t/\tau\right)\right)$$

where $\Delta\alpha_0$ is the asymptotic value and $\tau$ the diffusion time constant. From the experimental data, a value of $\tau$ at 20 C° of about 200 hours is always obtained, while $\Delta\alpha_0$ seems to depend on fiber type. The effect of molecular hydrogen loss on the transmission wavelengths of 1.3 μm and 1.55 μm is limited, but can be significant in very low loss fibers. In practice, for both multimode and single mode fibers the following approximated expressions can be assumed at 20°C:

$$\Delta\alpha\,(1.3\,\mu m) = 0.25\ db/km \cdot P_{H_2}(atm)$$

$$\Delta\alpha\,(1.55\,\mu m) = 0.60\ db/km \cdot P_{H_2}(atm)\,.$$

## OH related loss

The irreversible peaks labelled B, C, D in Fig.1 are respectively ascribed to OH vibrations in Si-OH, Ge-OH and P-OH groups resulting from the reaction of hydrogen with glass constituents. Such a reaction is strongly dependent on fiber composition and type. For example OH formation is negligible in P-free single mode and multimode fibers but is relevant in 1% $P_2O_5$ doped fibers and is dramatic in more heavily phosphorus doped fibers. Fig.2 shows the behaviour at $\lambda$ = 1.41 μm (wavelength of Ge-OH vibration) for three different types of fibers in an absorption/desorption cycle at 20°C. These results support the general belief, also confirmed by E.S.R. measurements[1], that the OH formation occurs at the site of fiber structural defects, whose number then is thought to determine the asymptotic extent of the phenomenon. No saturation effects could be shown up to now even after long term high temperature tests (Fig.3). On the other hand, the hydroxyl formation rate, which is most important from the application point of view, was found to be strongly dependent on temperature and hydrogen pressure and to follow a time law which is consistent with the theory of chemical reaction rate [2].
Assuming the approximate time dependence shown in Fig.3, which well interpolates the experimental results, extrapolations were made to actual service conditions. The results are given in Table II for multimode fiber with 1% $P_2O_5$ content.

## Background loss

A background loss increase, sometimes referred to as "UV tail" as it is higher at lower wavelengths ($\Delta\alpha \propto 1/\lambda^4$), is observed during accelerated tests at high temperatures (70°C to 100°C). Such effect (which is much larger in single mode phosphorus free than in multimode fibers) is the less known so far, although it seems reasonable to interpret it as the result of color centers formation linked to the presence of germanium. Some of the experimental results of aging tests obtained up to now are represented in Fig.4 and show quantitative differences which are now under investigation, among the various types of fibers. Furthermore the influence of temperature and hydrogen pressure on reaction rate is under study in order to predict optical loss in actual cable environment.

As a conclusion from this investigation on a broad variety of fiber types and from literature data it can be stated that all silica glass fibers are sensitive to hydrogen effects. Therefore the only total solution to the hydrogen problem, as far as the fiber is concerned, seems to be the adoption of a hydrogen impervious coating, as successfully experimented by British Telecom and Hewlett-Packard [3,4]. However, a certain number of problems especially related to coating reliability and economic viability of manufacturing process seem to be not completely solved for a full industrial application of this solution.

## HYDROGEN IN CABLES

Hydrogen enters optical cables either because it is dissolved in constituent materials or is generated by chemical reaction during manufacture or service life. Indicative values of hydrogen amounts expected to evolve from typical cable materials during service life are reported in Table III.
Some of the quoted materials, like aluminium or silicone rubber, can generate even larger hydrogen quantities by chemical reaction with moisture. Furthermore, hydrogen content or more precisely hydrogen partial pressure, also depend on cable structure. This means that the hydrogen problem can be strongly reduced, provided that particular care is taken in the cable design by selecting suitable constituent materials and by prescribing metals heat pretreatment, dry atmosphere, limited degree of filling, gas purging, etc.
In particular situations, such as fully filled cables with metallic sealing, the adoption of such criteria involves very heavy restrictions on the materials choice and on the degree of filling. As a matter of fact, due to the low solubility of hydrogen in the compound, the filling coefficient of a metallic sealed cable has a significant influence in determining the hydrogen partial pressure that is built up inside the cable itself.
As an example, in the cable structure represented in Fig.5, assuming that all the hydrogen contained in the cable components according to the data of Table III is released, the resulting hydrogen partial pressures are 360 and 800 mm of Hg for a coefficient of filling of internal spaces of 65% and 90% respectively. In such a situation a substantially different approach, based on gettering the hydrogen possibly evolved rather than avoiding its

evolution (a "permissive" rather than "repressive" solution) appears very attractive in order to avoid excessive limitations in the materials and cable structure.

## HYDROGEN GETTERS IN OPTICAL CABLES

A broad spectrum investigation into a variety of candidate hydrogen getters, i.e. materials having the capability to absorb hydrogen, was carried out. The major requirements that the hydrogen getters should fulfill were defined as follows:

- High hydrogen absorption in the whole range of temperatures and partial pressures encountered in optical cables.
- Stability of the absorption capacity during all the expected service life of the optical cable.
- Full irreversibility of hydrogen absorption.
- Short absorption time in comparison with the rates of hydrogen diffusion and chemical reaction in optical fibers.
- Possibility of being incorporated in optical cables without significantly modifying cable design and manufacturing process.
- Low cost.

### Physical vs. Chemical "Gettering"

Hydrogen getters can be classified in two well distinct categories depending on whether the mechanism governing hydrogen absorption is essentially physical or chemical.

Physical Getters. Hydrogen, in this case, is absorbed by solids, e.g. Palladium or liquids and maintained in a solution. The phenomenon is based on a thermodynamic equilibrium and is therefore characterized by a non zero residual hydrogen pressure outside the getter and a certain degree of reversibility, mainly due to temperature effects:absorbed hydrogen levels are in fact inversely proportional to temperature.

Chemical Getters. In this case hydrogen is consumed via chemical reaction (as for example an oxide reduction or an addition onto an unsaturated compound). This phenomenon is not an equilibrium process and therefore is potentially able to produce complete and irreversible removal of all ambient hydrogen, the only limit to the total amount absorbed being given by the stoichiometry of the reacting species. The process is strongly activated by temperature according to the well known Arrhenius law. In many cases, when thermal activation is not sufficient for the chemical reaction to take place at ambient temperature, a suitable catalyst must be added. As a matter of fact, extremely active specific catalysts may be used to speed up a particular reaction with hydrogen, and appreciable rates can be reached also at ambient temperature.
Different types of physical and chemical hydrogen getters suitable to be incorporated in a cable have been developed by Societa' Cavi Pirelli.

Results obtained to date have shown that chemical getters are the most atttractive solution, mainly due to irreversibility and to the zero hydrogen residual pressure characterizing their action.
The first chemical getter now undergoing extensive testing is thereinafter referred to as HYDROGETl (patent application pending). It can be prepared in the form of a grease which has an excellent water resistance and is suitable to be incorporated as waterproof filling compound in optical cables.

## CHARACTERIZATION OF PROPERTIES OF HYDROGEN GETTERS

### Physical Properties

HYDROGETl is a greasy compound with a viscosity and a degree of hardness suitable to be processed by conventional pumping devices.These characteristics are substantially stable in the temperature range $-40^{\circ}C$ to $+70^{\circ}C$, which corresponds to actual service conditions of optical cables.
Its water sealing properties have been tested by submitting it to standard IEC 708-1 test and the results were found to be similar to those obtained with usual petroleum jellies used in telecommunication cables.
Compatibility tests with all the cable materials are in progress and up to now no particular evidence of aggressiveness has been found.

### Short term absorption tests

For a preliminary evaluation of HYDROGETl gettering properties, a weighed amount of getter is smeared on the walls of a glass container in order to minimize diffusion time. The container is then evacuated, filled with a metered quantity of hydrogen, connected to a pressure transducer and sealed. From then on, pressure vs. time is recorded, and final atmosphere in the container is checked by gaschromatography for hydrogen traces and/ or air leaks.
Two types of test were carried out using this set-up.

1) Absorption tests in excess of hydrogen atmosphere for measuring asymptotic absorption capacity of HYDROGETl.
2) Absorption test in shortage of hydrogen atmosphere for characterizing reaction kinetics under conditions closer to actual ones.

In Fig.6, the specific hydrogen quantity reacted with HYDROGETl at ambient temperature is shown for two pressure ranges. The initial hydrogen quantity is in excess with respect to HYDROGETl capacity and all the values are corrected for solubility effects.
As can be seen, an asymptotic value of 1.8 $cm^3STP/g$ results. It is independent of pressure and fully irreversible (1 month ageing of fully reacted material at $70^{\circ}C$ in vacuum sealed containers gave no hydrogen in gas chromatographic analysis). This value is actually well consistent with the degree of unsaturation of the polymer and was shown to be independent of temperature in the

range 0°- 70°C.
In Fig.7 reaction curves at different temperatures are shown. The tests are conducted as before, but the hydrogen quantity is short with respect to HYDROGETl capacity. As it can be seen, practically zero pressure (gas chromatographic analysis gave residual hydrogen pressure less than 0.01 mmHg) is reached in times varying between 1000 and 4 hours in the zero to 70°C temperature range. As shown in APPENDIX, these reaction times are short enough compared to hydrogen diffusion time in optical fibers to avoid any impairment of the transmission characteristics.

## Aging tests

In order to obtain some information on long term behaviour of HYDROGETl efficiency, some accelerated aging tests at elevated temperature were carried out assuming 150°C as the maximum temperature allowing to extrapolate the results of the test to service conditions. Material samples were aged in air for 1 month at 150°C, corresponding to 20 years at ambient temperature if a reasonable value of 12 Kcal/mole is assumed for the activation energy of the aging process. The aged samples were then submitted to reaction with excess hydrogen showing only a reduction in the asymptotic value from 1.8 to 1.27 $cm^3$STP/g, which can easily be taken into account in cable design.
The effect of higher temperatures that could be met in some particular applications, as for example optical cables in overhead ground wires, was simulated by submitting material samples to thermal shocks of 0.5 hours at 200°C
The absorption test at 20°C successively performed in shortage of hydrogen atmosphere gave some ten times reduction in reaction rate (Fig.8). However, the effectiveness in reaching zero pressure is maintained and the reaction rate is still competitive with hydrogen diffusion ratio into the fiber as shown in the APPENDIX. Tests of HYDROGETl in contact with all the materials used in optical cables are in progress and the results indicate that no further degradation of gettering properties of HYDROGETl is introduced by the cable materials.

## Tests on fibers and cables

HYDROGETl ability to prevent hydrogen diffusion into optical fibers and to absorb hydrogen in actual cable environment, i.e. with slow continuous generation was experimentally verified.

## Tests on fibers

From the results of reaction kinetics of HYDROGETl previously shown, it appears that hydrogen absorption is fast enough to be competitive with the transient of hydrogen diffusion into optical fibers (see APPENDIX).
These theoretical predictions were verified by carrying out a series of tests on primary coated fibers having a double acrylate jacket of 250 μm outer diameter. A number of fiber lengths of different types were wound on 80 mm radius reel and each layer was smeared with 0.2 g/meter of HYDROGETl and wrapped with paper. Each reel was then sealed in a glass vessel containing a gas mixture of hydrogen (10 mmHg) and air, which simulates the atmosphere of a hydrogen affected cable, and the vessel was aged at 70°C for a month.
Spectral attenuation measurements were performed on the fiber at intervals during the test, together with gas chromatographic analysis of the atmosphere. In all cases the results showed that HYDROGETl offers complete protection against hydrogen until saturation.
Fig.9 shows an example of the spectral attenuation results obtained after 48 hours ageing with and without HYDROGETl of a multimode fiber with high sensitivity to hydrogen (7% $P_2O_5$ content). Analysis of the atmosphere in the glass container with HYDROGETl showed no significant hydrogen content and further ageing for two months did not modify the results.

## Tests on optical cables

To experimentally verify the hydrogen gettering properties of HYDROGETl in an actual cable environment with slow continuous hydrogen generation, two lengths of an optical cable having the structure shown in Fig.10 were manufactured. The main cable components are the optical core made of a grooved element containing 6 loosely deposited single mode fibers with primary coating, a first layer of aluminium shaped segments, then an armour of steel strips and an outer aluminium sheath. The entire cable is filled to a degree of 95% with a water blocking compound consisting of a silicone grease in one case and HYDROGETl (14 g/m) in the other case.
This cable structure was selected to represent a particularly critical case from the point of view of hydrogen, due to the presence of large quantities of metallic materials (more than 1 Kg/m), the high degree of filling and the metallic sealing. Two types of tests were performed on the two cable lengths. Short cable samples of 0.5 meters were cut and sealed in glass containers with reduced air pressure and aged at 70°C. In Fig.11 the quantities of hydrogen detected by gas-chromatographic analysis and the corresponding partial pressures calculated on the basis of the known internal volume are shown as a function of time for the two types of cable samples. These results confirm the exhaustive gettering properties of HYDROGETl in the presence of continuous hydrogen generation inside a cable.
As a further confirmation, the whole cable lengths have been aged at 70°C and the spectral attenuation of the fibers has been continuously checked. After two months no significant loss variation was observed on the length manufactured using HYDROGETl, whilst a distinct absorption peak at 1.24 μm due to molecular hydrogen was detected on the other length (Fig.12).

## INDUSTRIAL APPLICATION OF HYDROGETl

### Cable design

From the experimental data previously shown, it is possible to calculate, for a particular cable structure, the specific quantity of HYDROGETl necessary to avoid the presence of hydrogen during the cable life. As far as the hydrogen evolved by the cable components is concerned, HYDROGETl has enough gettering capacity for practically any cable structure. When hydrogen is continuously generated by electrolytic phenomena (either due to impressed currents or to non-polarizable galvanic cells), the quantity of compound needed to absorb all the hydrogen evolved during cable life could be in excess of cable capability and in this case a different solution should be sought.
Such a situation can arise, for example, when optical cables are contained in submarine power cables connecting off-shore platforms. High hydrogen concentration in the sorrounding water is generated by large size cathodic protections and/or by the Fe-Zn galvanic cell, if galvanized steel wires are used for the cable armour.
Furthermore, the service temperature of this type of cable can be in the 50 to 70 C range, thus enhancing the possible effect of hydrogen on the optical fibers. In this case the solution is a metallic sheath applied on the optical cable to prevent the externally generated hydrogen from entering the optical core. Of course, the internally generated hydrogen is absorbed by a suitable amount of HYDROGETl.

### Cable manufacture

The first industrial application of HYDROGETl was in a cable designed in cooperation with the New Development Sector of the Italian operating telephone company (SIP) and Societa' Cavi Pirelli. The cable was manufactured by Societa' Cavi Pirelli and installed in a partly terrestrial and a partly underwater route connecting San Marco Square and the Lido Island in Venice in mid 1985.
The section of the underwater cable, characterized by a very high mechanical strength is shown in Fig.13.
The main hydrogen source in the cable structure is the possible oxidation of the aluminium sheath due to moisture introduced in the cable components during the manufacturing process.
The hydrogen partial pressure inside the cable is enhanced by the high degree of filling of the optical core, necessary to avoid water penetration in case of damage of the cable protections.
The anticipated maximum hydrogen concentration in the cable was calculated to be 0.6 $cm^3$STP/m and the HYDROGETl quantity required was therefore 0.3 g/m. Taking into account a suitable safety factor, 3 g/m were used.

## CONCLUSION

Silica glass fibers are inherently sensitive to hydrogen effects even if to a different extent.
The industrial on-line application of a fiber coating impervious to hydrogen seems premature. In such a situation optical cable design and manufacture are subject to heavy restrictions.
The use of hydrogen absorbing materials (the so-called hydrogen getters) as cable components represent a total solution to the hydrogen problems in most actual applications.
The extensive tests reported in this paper show that, provided the proper amount of hydrogen getter is incorporated in the cable structure, the hydrogen evolved and/or generated by the other cable components is completely absorbed, with consequent elimination of any detectable effect on fiber transmission properties.
The first cable incorporating a hydrogen getter HYDROGETl, as a filling compound was successfully manufactured and installed in mid 1985.

## ACKNOWLEDGEMENTS

The authors are indebted to Dr. G. Roba (CSELT) for the initiation and encouragement of research, Mr. G. Colombo (Societa' Cavi Pirelli) for accurate measurements, SIP for financial support of this CSELT activity, SIP, Societa' Cavi Pirelli and CSELT managements for authorization to present this paper.

## REFERENCES

1. N. Uchida et al. Conference Paper, 9th ECOC, 1983.

2. J.E. Shelby J., Appl.Phys. 51 (1980) p.2589

3. W.J. Duncan et al. SPIE 506 Fiber Optics in Adverse Environment (1984) p.134

4. R.Hiskes, Topical Meeting on Optical Fiber Communications (1979), Paper WF6

5. H.S. Carslaw, I.C. Jaeger " Conduction of Heat in Solids", Oxford Clarendon Press (1959) p.199

6. K. Noguchi et al. J.Lightwave Tech.LT-3 (1985) p. 236

## APPENDIX

The diffusion into an optical fiber in the presence of a definite quantity of gas has been studied theoretically in two conditions:

a) fiber without hydrogen getter.
b) fiber with hydrogen getter.

Hydrogen concentration in the fiber was in both cases normalized to the saturation hydrogen

content which was assumed to be neglegible with respect to the total amount of hydrogen.
Case a) is then well approximated by an absorption at constant pressure. The quantity of hydrogen getter is assumed to be in excess with respect to the total amount of hydrogen, so that case b) can be represented by an absorption process at a decreasing pressure.
The fiber is assumed to be a solid homogeneous cylinder of radius $a$ submitted to the following boundary conditions:

a) constant hydrogen concentration at the surface in case a)

b) decreasing concentration at the surface, $\phi(t)$ in case b).

Being the concentrantion at the surface proportional to hydrogen pressure, an experimental expression for $\phi(t)$ has been obtained by approximating the ambient temperature absorption curve of Fig. 7 with the sum of two exponential functions, as shown in Fig. 14. As it is well known, the relevant equations in the two cases are [5] :

$$C_a(r,t) = 1 - 2\sum_{m=1}^{\infty} e^{-D\alpha_m^2 t/a^2} J_0(\alpha_m r/a) / \alpha_m J_1(\alpha_m)$$

$$C_b(r,t) = (2D/a^2) \sum_{m=1}^{\infty} e^{-D\alpha_m^2 t/a^2} \left[\alpha_m J_0(\alpha_m r/a)/J_1(\alpha_m)\right] \cdot \int_0^t e^{-D\alpha_m^2 s/a^2} \phi(s)\, ds$$

with

$C_a(r,t)$ ratio of hydrogen concentration (corresponding to the radial position $r$ and to the time $t$ ) to the saturation value for case a).

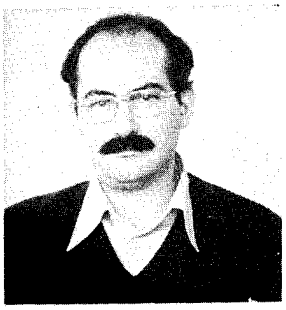
$C_b(r,t)$ as above for case b).

$D$ = $1.1 \times 10^{-11}$ cm$^2$/sec, diffusion coefficient for hydrogen in silica glass [6].

$J_0, J_1$ Bessel function of the first type.

$\alpha_m$ Roots of the equation $J_0(\alpha) = 0$

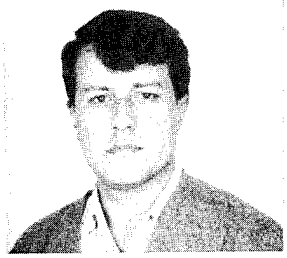
In Fig. 15 are shown the results of calculations performed for $r/a = 0.4$, roughly corresponding to the location of the core-cladding interface in a multimode fiber and for $r/a = 0$, corresponding to the fiber center.
While in case a) an asymptotic curve is found, in agreement with experimental data, in the presence of hydrogen getter only a transient concentration at a very reduced level is obtained, followed by hydrogen desorption from the fiber. In practice, the maximum transient concentration value is around 1% of the saturation value for the core-cladding interface of a multimode fiber and less than 1% for the fiber center. An extreme ageing condition has been also simulated by increasing the time constants of the absorption process by an order of magnitude. The corresponding maximum transient concentration is about 8% of the saturation value for $r/a = 0.4$ and the getter results still competitive with the diffusion process.



Pietro Anelli was born in 1942 in Cremona, Italy. He received his degree in physics from the University of Parma in 1966 and joined Societa' Cavi Pirelli, where he has been involved in metallurgy. electrochemistry and polymer physics at the Central Cable Research Laboratory. At present he is responsible for the chemical laboratory. He is a member of B.N.F.M.R.A.

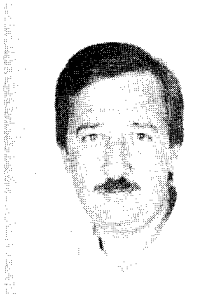


Giorgio Grasso was born in 1949 in Rome, Italy. He received his electronic engineering degree from the University of Bologna in 1972. He joined the Central Cable Laboratory of Societa' Cavi Pirelli in 1973 where he has been involved in the development and design of optical cables and optical fiber measurements.
At present he is responsible for the laboratory for the development of new optical fiber characterization methods.



Eros Modone was born in Torino, Italy, in 1948. He received his doctorate in chemistry from the University of Torino in 1972 and he worked two years as assistant professor in the same University Faculty of Physical Chemistry, in the field of catalysis. In 1979 he joined CSELT where he has been involved in research activity on optical fiber technology.
His activity has regarded some chemical aspects of optical fiber technology such as: chemical analysis of optical fiber constituents, purification of raw materials, study on dopant inplantation and on primary coating polymers.

Presently he is involved in research on single mode MCVD fibers and non-oxide glasses for mid-IR applications.
On these subjects he holds three international patents and is co-author of 15 papers.He has lectured on single mode fiber technology at the Superior School Guglielmo Reiss Romoli.



Bruno Sordo was born in Dogliani (Cuneo), Italy, in 1948. He received his doctorate in physics from the University of Torino in 1972. Since then he has been working at CSELT, where he is currently doing research on optical fiber communication measurement techniques.
In particular, he has been engaged in the characterization of multimode and single more fibers from the point of view of optical parameters. He has improved many measurement techniques with noticeable results on backscattering methods. On this subjects he holds an international patent and is co-author of some 20 papers. He has lectured on optical fiber and cable measurements at the Superior School Guglielmo Reiss Romoli.



Feliciano Esposto was born in Arcevia (Ancona), Italy, in 1948. He received his doctorate in physics from the University of Torino in 1976.
In 1969 he joined CSELT, where he did research on optics and optical communications, particularly holography and optical fiber characterization.
Since 1980 he is with SIP, the Italian telecommunication operating company,which like CSELT belongs to the STET group, where he has been involved in optical fiber transmission system design. At present he is in charge of physical carrier design and development on the "Industrialization of New Technology" division at SIP headquarters in Rome.
Feliciano Esposto is co-author of many papers and lectures at Superior School Guglielmo Reiss Romoli.

| Monomode fibres | Cladding/core composition | Testing temperature (°C) | | |
|---|---|---|---|---|
| type A | $SiO_2$ / $SiO_2$ - $GeO_2$ | 20, | 50, | 100 |
| type B | $SiO_2$ - F / $SiO_2$ - $GeO_2$ | 20 | | 100 * |
| type C | $SiO_2$-$P_2O_5$ - F /$SiO_2$-$GeO_2$ | 20 * | | 100 |
| type D | $SiO_2$ - F / $SiO_2$ | 20 * | | 100 |
| **Multimode fibres** | **Core composition** | **Testing temperature** | | |
| type A | $SiO_2$ - 6.7% $GeO_2$ - 7% $P_2O_5$ | 20 | | 100 |
| type B | $SiO_2$ - 12% $GeO_2$ - 1% $P_2O_5$ | 20 | | 100 |
| type C | $SiO_2$ - 27% $GeO_2$ | 20 | | 100 * |

(*) Test in progress

TABLE I - FIBRES TESTED UNDER 600 mmHg HYDROGEN PRESSURE

| | | Temperature (°C) | | |
|---|---|---|---|---|
| | | 20 | 50 | 70 |
| Hydrogen | 60 | 0.03 | 0.27 | 1.04 |
| pressure | 6 | 0.01 | 0.08 | 0.34 |
| (mmHg) | 0.8 | 0.001 | 0.03 | 0.14 |

TABLE II - LOSS INCREASE (dB/Km) AFTER 20 YEARS AGEING IN DIFFERENT CONDITIONS FOR MULTIMODE FIBRES WITH 1% $P_2O_5$ CONTENT

| MATERIALS | HYDROGEN CONTENT ($cm^3$STP/Kg) | |
|---|---|---|
| Aluminium "soldered sheath" | 0.8 | METALS |
| Aluminium segments | 0.8 | hydrogen extraction |
| Galvanized steel | 4.8 | at 170°C under vacuum |
| Copper-clad steel wire | 0.07 | |
| Copper soldered sheath | 0.02 | |
| Silicon rubber | 14 | PLASTICS |
| Fiberglass | 0.07 | hydrogen extraction |
| Other organic components | 0.01 | at 20°C under vacuum |

TABLE III - HYDROGEN CONTENT IN VARIOUS MATERIALS

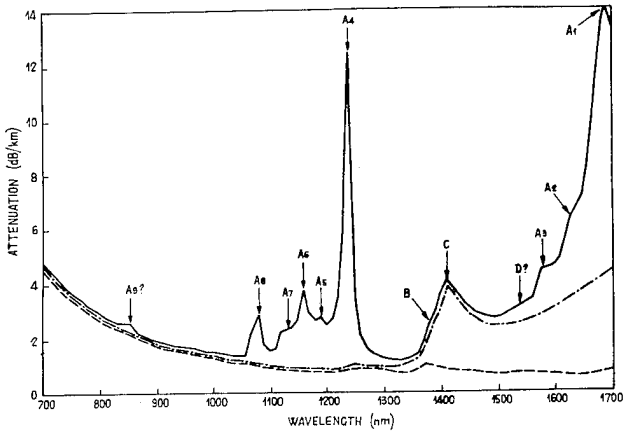



FIGURE 1 Spectral attenuation curve of a multimode fiber with 1% $P_2O_5$ before (- - - - -), after an absorption (————) and a subsequent desorption (— · — · — · —) period of 1260 hours at 20°C and 600 mmHg.

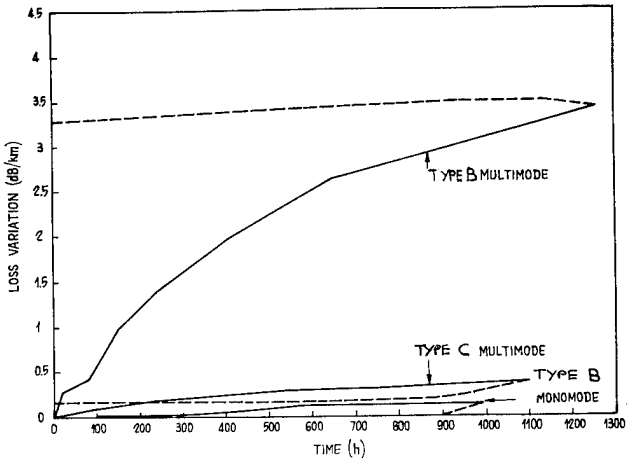



FIGURE 2 Loss variation at 1.41 μ for three different types of fiber during an absorption (————)/desorption (— — — — —) cycle at 20°C and 600 mmHg. For fiber type identification refer to table I.

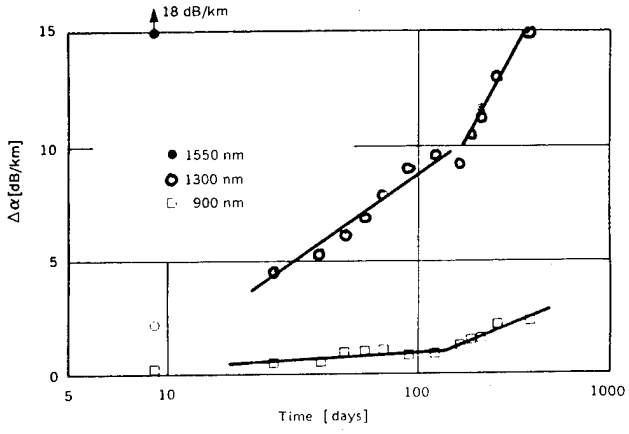



FIGURE 3 Loss increase at different wavelengths in an accelerated ageing test on multimode fibers having 1% $P_2O_5$ content at 100°C and 640 mmHg.

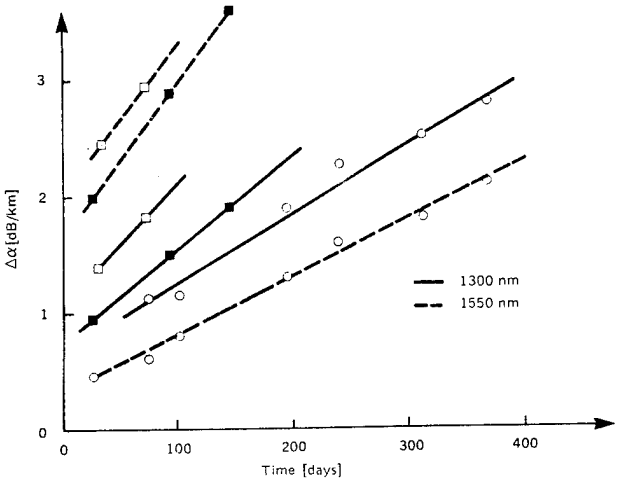



FIGURE 4 Loss increase at different wavelengths in an accelerated ageing test on type A ( ○ ), type C ( ■ ) and type D ( □ ) single mode fibers at 100°C and 640 mmHg.

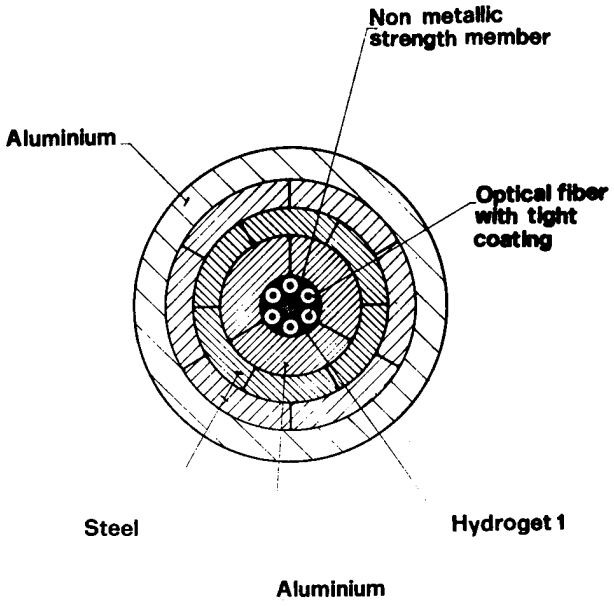



FIGURE 5 Structure of an armoured optical cable incorporating HYDROGET1.

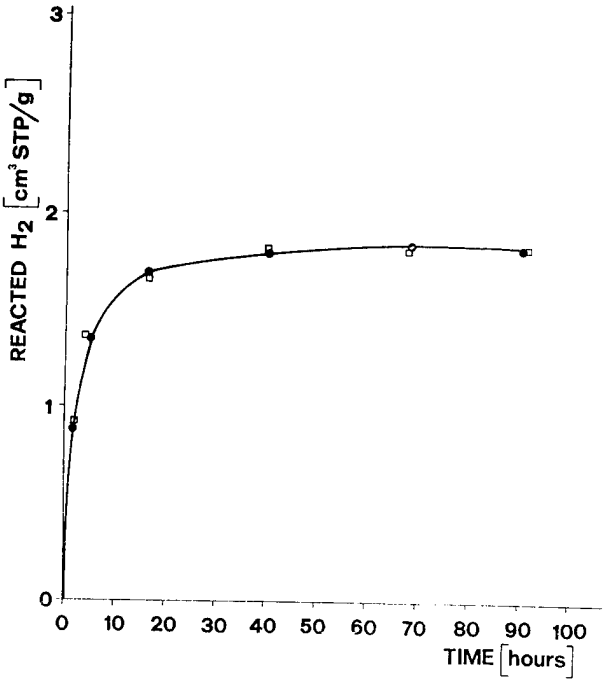



FIGURE 6 Absorption test results in excess of hydrogen atmosphere at ambient temperature within two different pressure ranges: 760 to 640 mmHg ( ● ) and 300 to 180 mmHg ( □ ).

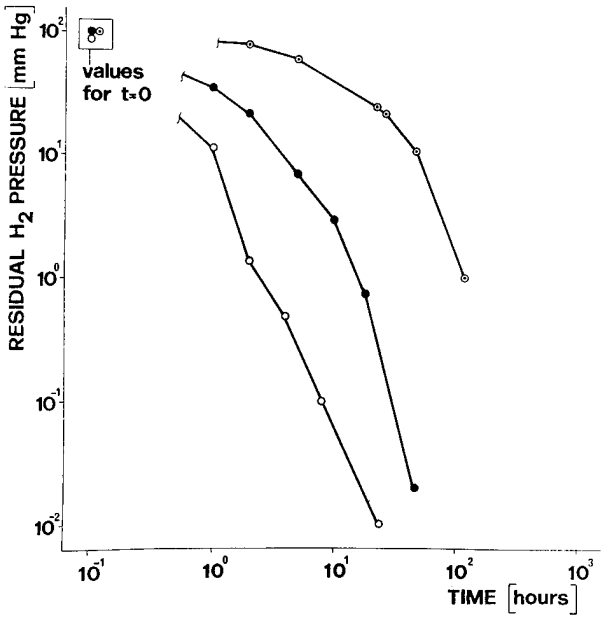



FIGURE 7 Absorption test results in shortage of hydrogen atmosphere at 0 ( ⊙ ), 25 ( ● ) and 70 ( ○ )°C. Initial pressure 100 mmHg. An activation energy of 11 Kcal/mole can be estimated for the absorption process.

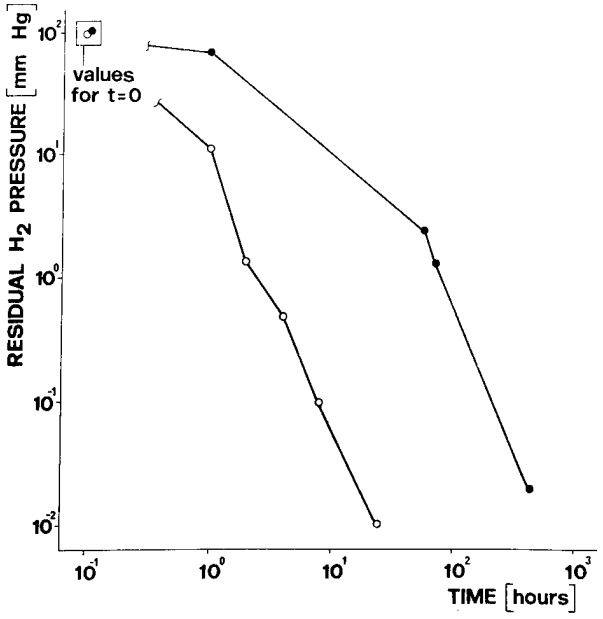



FIGURE 8 Absorption test results in shortage of hydrogen atmosphere at 70°C before ( ○ ) and after ( ● ) thermal shock in air ( 0.5 hours at 200°C).

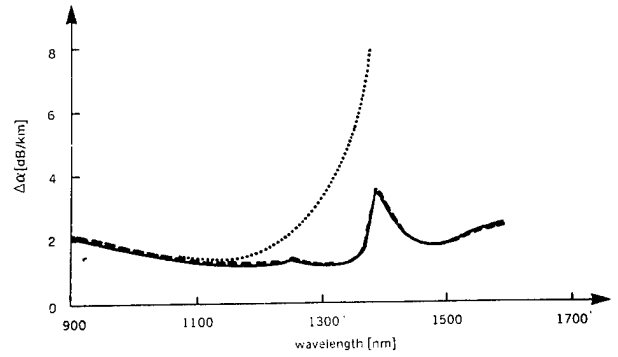



FIGURE 9 Spectral attenuation curves of a multimode fiber having 7% $P_2O_5$ content submitted to a hydrogen pressure of 10 mmHg at 70°C for 48 hours. Initial curve (———), final curve with (– – – –) and without (·····) hydrogen absorber.

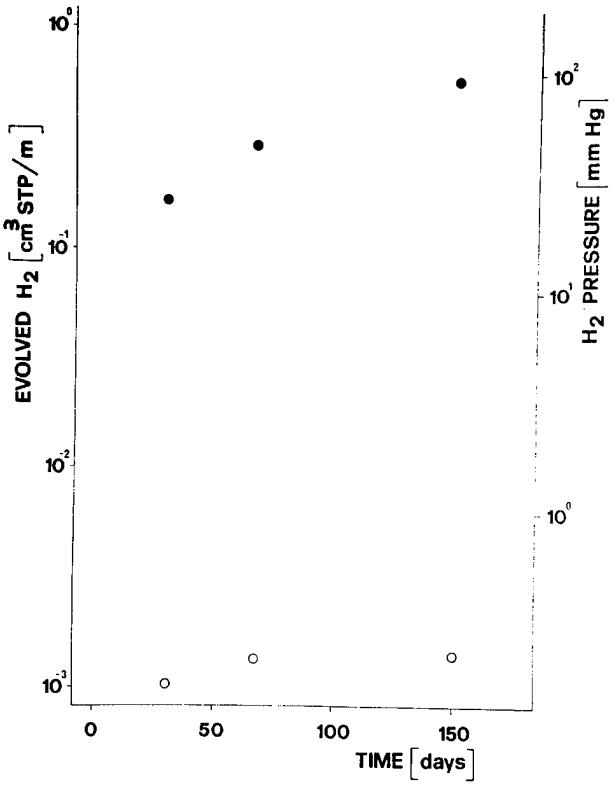



FIGURE 11 Evolution of hydrogen from samples of the cable of figure 10 at 70°C with ( O ) and without ( ● ) HYDROGET1 in optical core.

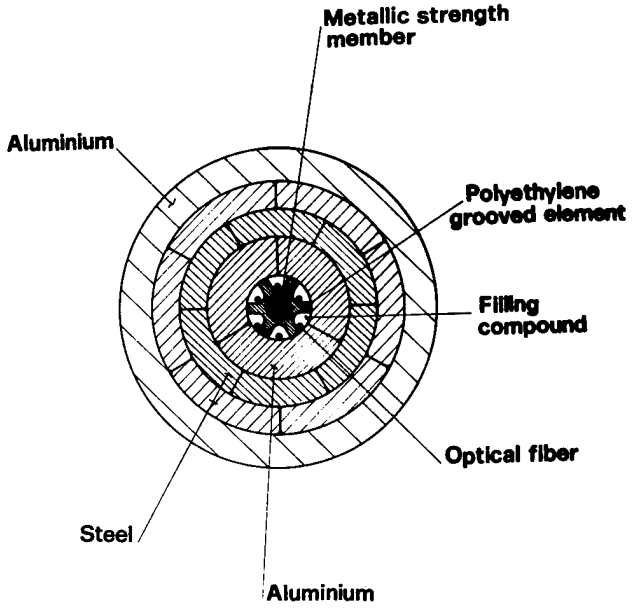



FIGURE 10 Structure of an armoured optical cable with grooved central element.

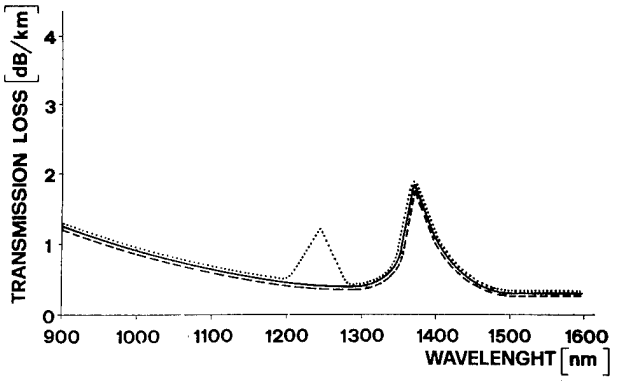



FIGURE 12 Attenuation curve of a monomode fiber contained in the cable of figure 10 with (– – – –) and without (·····) HYDROGET1 after 1 month ageing at 70°C. Initial curve (———) in also shown.

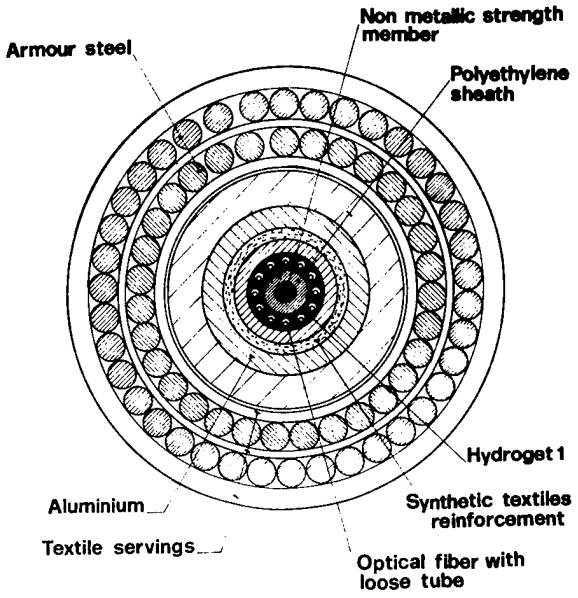



FIGURE 13 Section of the underwater armoured cable installed in Venice.

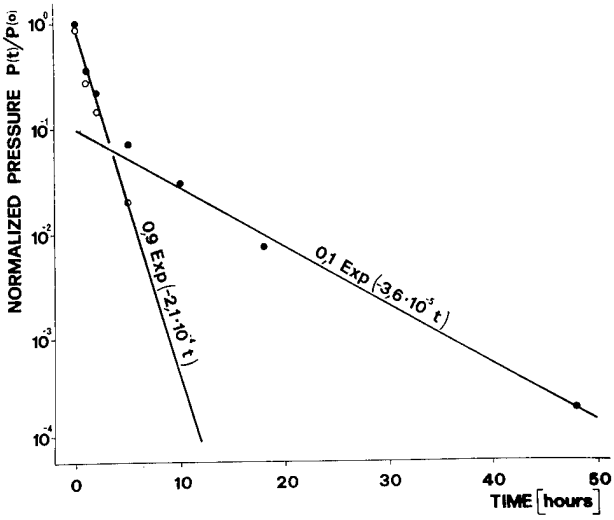



FIGURE 14 Approximation of the ambient temperature absorption curve of figure 7 by two exponential functions. Experimental ( ● ) and interpolating ( O ) points are shown.

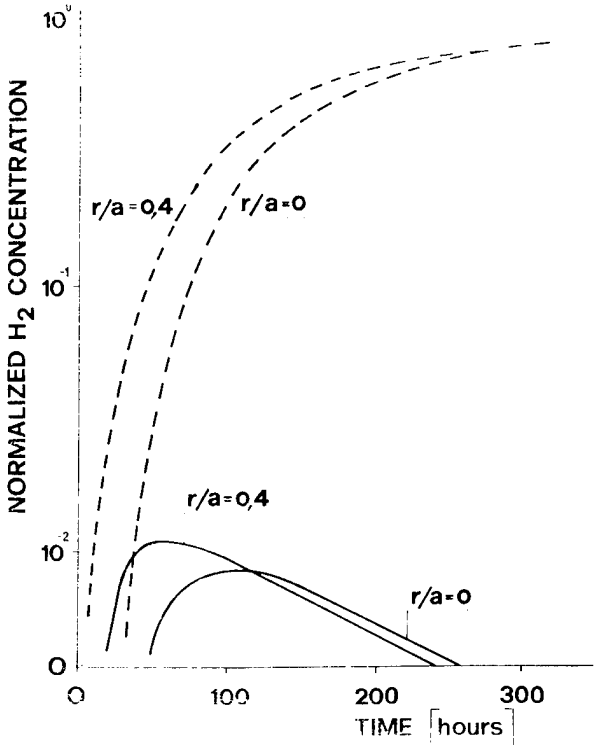



FIGURE 15 Computed hydrogen concentration versus time for a fiber with (——) and without (— — —) HYDROGET1. Results for two values of the radial coordinate are shown.

# EVALUATION OF TEMPERATURE CONDUCTIVITY IN OPTICAL FIBER CABLES

Satoshi MOCHIZUKI*, Koji ARAKAWA** and Takamasa YASHIRO*

*NTT Ibaraki Electrical Communication Laboratories
Tokai, Ibaraki-ken, 319-11 Japan

**NTT Musashino Electrical Communication Laboratories
Musashino-shi, Tokyo, 180 Japan

## Abstract

A new method has been proposed for evaluating temperature conductivities of optical cable constituent layers with complex structures, by using the heat conduction equation and measured temperatures at surfaces of the layers. The temperature conductivities have been evaluated for a corrugated-steel (CS) sheathed optical cable, and the values are found to be quite useful for explaining the temperature change characteristics of the cable. To study the fire-resistant properties of the CS-sheathed optical cable, heat test has been carried out in accodance with the JIS-A-1302 heating curve simulating a house fire. The measured values are in good agreement with those calculated using the evaluated temperature conductivities. Excellent fire-resistance and optical loss stability characteristics of the CS-sheathed cable have been confirmed.

## 1. Introduction

In order to design heat and flame resistant optical fiber cables, it is important to evaluate the temperature conductivities of cable constituent layers. However, it is difficult to evaluate them theoretically for a cable with a complex structure, taking into account the structural dimensions and the constituent material parameters. Temperature changes of the individual layers in a cable due to heating can be measured directly using thermocouples inserted in the layers. Further, they can be described by the heat conduction equation, which contains the individual layer temperature conductivities as key parameters. Therefore, it is expected that the numerical calculation of the equation using the measured temperature changes can lead the evaluation of the temperature conductivities.

This paper studies temperature characteristics of a corrugated-steel (CS) sheathed optical fiber cable to examine the usefulness of this proposed method. As a result, the temperature rise characteristics of the cable constituent layers are found to be well explained using the evaluated temperature conductivities. Furthermore, heat-resistance properties of CS-sheathed and LAP-sheathed cables have been investigated in accordance with the JIS-A-1302 heating curve[1] simulating a house fire. The measured and evaluated results have revealed the excellent heat-resistance and optical loss stability characteristics against heating for the CS-sheathed cable.

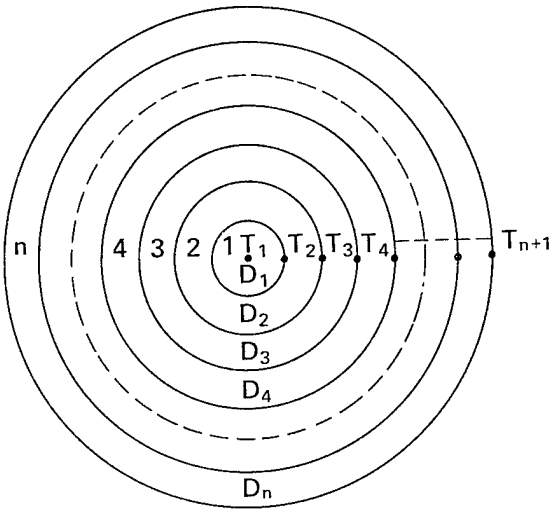
## 2. Numerical Calculation Method of Temperature Conductivity in Cable

Temperature distribution in a long, uniform column is determined by solving the heat conduction equation for a given boundary condition. The heat conduction equation is given by

$$\frac{\partial T}{\partial t} = D \cdot \left( \frac{\partial^2 T}{\partial r^2} + \frac{1}{r} \cdot \frac{\partial T}{\partial r} \right) , \qquad (1)$$

where T is the temperature in a column, r the distance from the center of the column, t the time, and D the temperature conductivity. Optical fiber cables usually consist of many layers with different temperature conductivities and thicknesses, and a simple model is considerd as shown in Fig.1. Here, the cable is composed of n layers, and the i-th layer temperature conductivity is denoted as $D_i$. The surface temperature of the i-th layer is represented by $T_{i+1}$. Temperature changes of individual layers in a cable are given by solving Eq.(1). However, it is difficult to obtain analytical solution of Eq.(1). Therefore, Eq.(1) is studied using a difference equation.

When the i-th layer is divided into many thin concentric cylindrical sub-layers of thickness $\Delta r_i$, the following difference equation is obtained from Eq.(1) for the i-th layer.




$D_i$ : Temperature conductivity of the i-th layer

$T_i$ : Surface temperature of the (i−1)-th layer

Fig.1 Optical fiber cable structure model from the viewpoint of temperature conductivity.

$$T_i(r_j, t+\Delta t) = \frac{1}{M_i} \cdot \left\{ \left(1 + \frac{\Delta r_i}{2r_j}\right) \cdot T_i(r_j + \Delta r_i, t) + (M_i - 2) \cdot T_i(r_j, t) + \left(1 - \frac{\Delta r_i}{2r_j}\right) \cdot T_i(r_j - \Delta r_i, t) \right\} , \quad (2)$$

where $T_i(r_j, t+\Delta t)$ is the temperature after small increment of time $\Delta t$ at j-th point when the i-th layer is divided into $\Delta r_i$ and the numbers are given in order at divided points, $r_j$ is the distance between the center of the cable and the j-th point, and $M_i$ is written by

$$M_i = \frac{(\Delta r_i)^2}{D_i \cdot \Delta t} . \quad (3)$$

Therefore, the temperature changes of individual layers in a cable can be obtained by substituting the temperature conductivities of individual layers into Eq.(2).

A flow chart to determine the temperature conductivity of each layer by giving temperatures at boundaries between layers is shown in Fig.2. If temperature $T_{i+1}$ and temperature conductivity $D_i$ are given, temperature $T_i$ is obtained by using Eq.(2). The temperature conductivity $D_i$ is determined so that the calculated temperature agrees well with the measured one.

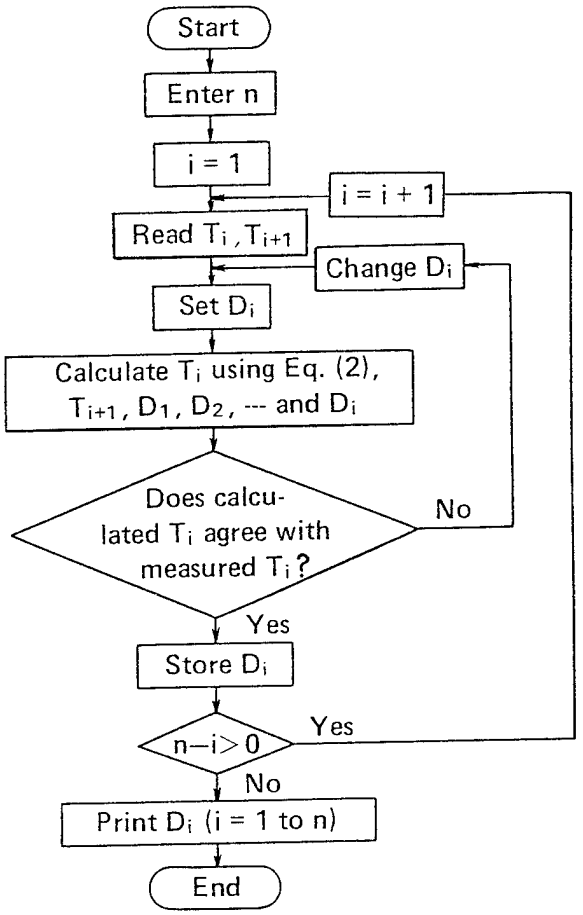



Fig.2 Flow chart to determe the temperature conductivity of each layer.

## 3. Measurement of Temperature Conductivity

### 3.1 Optical fiber cable structure

Figure 3 shows the structure of a CS-sheathed optical fiber cable. The cable consists of a conventional LAP-sheathed optical cable[2] and a CS-sheath with a welded steel seam. The main specifications of the cable are summarized in Table 1. Single-mode optical fibers operating at 1.3-μm wavelength are used.

Since a CS-sheathed optical cable has a complex structure, as shown in Fig.3, It is difficult to evaluate the temperature conductivities of each layer theoretically. Therefore, in accordance with the layer model shown in Fig.1, the cable are divided into five groups for simplicity; CS-sheath layer, LAP-sheath layer, wrapping tape layer, optical unit layer, and central tension member layer. Copper-constantan thermocouples are inserted between each layer in the cable to measure the temperature changes.

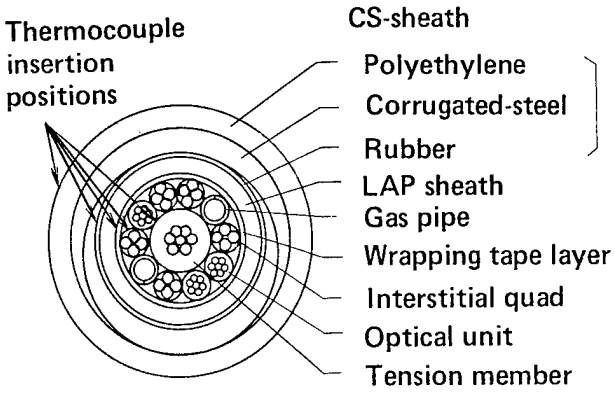



Fig.3 CS-sheathed optical fiber cable structure.

Table 1 Main specifications of CS-sheathed optical fifer cable.

| Item | Specification |
|---|---|
| Mode field diameter ( $\mu$m) | 10±1 |
| Cladding diameter ( $\mu$m) | 125±3 |
| Effective cutoff wavelength ( $\mu$m) | 1.10～1.29 |
| Optical loss (dB/km at 1.3 $\mu$m) | Less than 0.5 |
| Coating materials | Silicone and Nylon |
| Coated fiber diameter (mm) | 0.9±0.1 |
| Standard cable diameter (mm) | 34 |
| Standard cable weight (kg/m) | 1.2 |

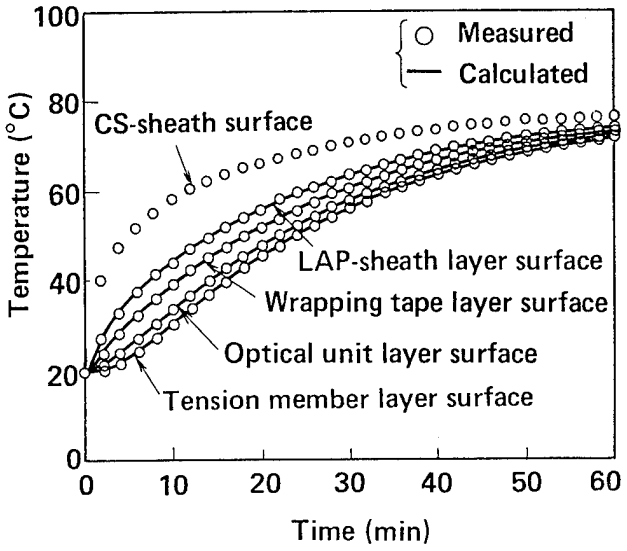



FIG.4 Temperature rise characteristics of each layer.

Table 2 Evaluated Temperature conductivities of CS-sheathed optical fiber cable.

| Layer | Temperature conductivity * |
|---|---|
| CS-sheath | 5.2 |
| LAP-sheath | 7.2 |
| Wrapping tape | 2.2 |
| Optical unit | 4.5 |

* $\times 10^{-4}$ $m^2$ /h

3.2 Evaluation of temperature conductivities

The CS-sheathed optical cable with thermocouples was laid in a thermostatic chamber. The temperature of the chamber was changed from 20 °C to 80 °C, and the temperature change at each layer surface was measured using the thermocouples. Measured temperature rise characteristics of each layer are shown in FIg.4 by circles.

It is possible to evaluate the temperature conductivities of each layer by using the method described in Chap.2, because the temperatures at individual layer surfaces are measured. Evaluated temperature conductivities of the layers are summarized in Table 2. The solid curves in Fig.4 are the temperature rise characteristics of the layers calculated by the above-mentioned procedures. It is clear from Fig.4 that calculated and measured values for each layer agree quite well at all measured points. Therefore, it is concluded that temperature characteristics of the cable are explained by the layer model, where each layer with a complex structure has an equivalent temperature conductivity.

In Table 2, the temperature conductivity of a LAP-sheath is higher than that of polyethylene ($5.0\times10^{-4}m^2/h$). This is because the LAP-sheath consists of polyethylene and aluminium, and aluminium has a high temperature conductivity. On the other hand, the temperature conductivity of a CS-sheath is lower than that of steel. This is because the polyethylene and rubber contribute to the reduction of the equivalent

temperature conductivity of the CS-sheath. Therefore, it is reasonable to consider that the evaluated temperature conductivities represent the equivalent temperature conductivities of individual layers with complex structures.

## 4. High Temperature Test of Optical Fiber Cables

### 4.1 Experimental procedure

It is important that an optical fiber cable preserves its signal transmission ability when the cable is laid in severe high temperature circumstances due to a fire. To examine the ability, heat tests were carried out for a CS-sheathed cable and a LAP-sheathed cable. The tests simulated a house fire, where the aerial cable was laid 1 m apart from the house. The mean temperature change of the outer surface of the cable is approximated by the JIS-A-1302 heating temperature curve (the maximum temperature 840°C). A furnace that could simulate the heating temperature curve was prepared. A structure of the furnace is shown in Fig.5. In order to even the temperature distribution, a number of burners are inserted in the furnace through openings. The cables are laid across the upper part of the furnace, and are fixed by an adiabatic frame. A cover made of silisic acid calcium was laid on the frame when the cables were heated. The heated length of each cable was 2.1 m. Thermocouples were laid near the cables to measure the cable surface temperatures, and the heating power of the burners was controlled so that the temperature near the cables followed the JIS-A-1302 heating temperature curve. A thermocouple was also inserted in the cable to measure the temperature change on the surface of the optical unit.

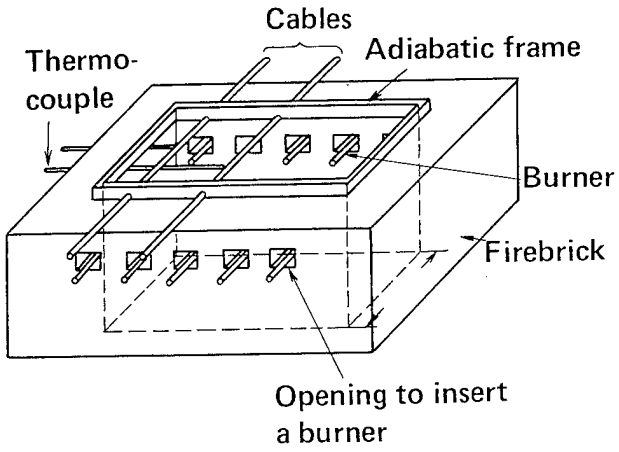



Fig.5 Structure of furnace.

Four coated fibers in one optical unit were spliced at the cable end, and the optical loss change was monitored using an LED light source operating at 1.3-μm wavelength.

### 4.2 External appearance of heated cables

Figure 6 shows a photographic view of the cables after heating. As for the CS-sheathed optical cable, the bare CS tube maintained the original shape throughout the heating, although the outer polyethylene layer was melted away. On the other hand, as for the LAP-sheathed optical cable, polyethylene and a part of aluminium of the LAP-sheath, and plastic materials of the cable core were melted away, and only metallic materials remained.

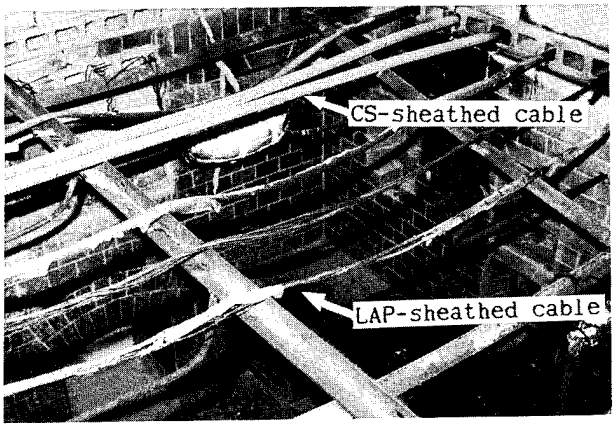



Fig.6 Photographic view of cables after heating.

### 4.3 Temperature changes in cables

The temperature changes in the cables were measured on the surface of the optical unit layer for the CS-sheathed and the LAP-sheathed optical cables. The measured temperature changes are shown in Fig.7. Temperature changes for the CS-sheathed optical cable are represented by the open circles, and those for the LAP-sheathed optical cable are indicated by the filled circles. The measured temperature change at the cable sheath surface is also shown by the dashed curve in Fig.7. This temperature change coincides well with the JIS-A-1302 heating curve.

When the temperature change on the sheath surface and the temperature conductivities of individual layers are given, the temperature change in the cable is calculated easily by using Eq.(2). The solid curves in Fig.7 represent the calculated temperature changes at the optical unit layer surface for the CS- and

LAP-sheathed cables. In this calculation, the temperature conductivity values shown in Table 2 are used. The calculated and measured values for the CS-sheathed optical cable agree well up to the maximum temperature point. However, the measured temperature is lower than the calculated one in the decreasing temperature region. This is mainly caused by burning out the outer polyethylene layer of the CS-sheath, resulting in temperature lowering inside the cable. In spite of the small discrepancy, it is confirmed that temperature characteristics are well explained by the evaluated temperature conductivities even at high temperatures, and that the maximum temperature in a cable involved in a house fire is estimated as far as the cable does not lose its original shape.

On the other hand, for the case of the LAP- sheathed optical cable, temperature measurement was possible only for the initial increasing region, because the structure of the cable is strongly damaged by the heating.

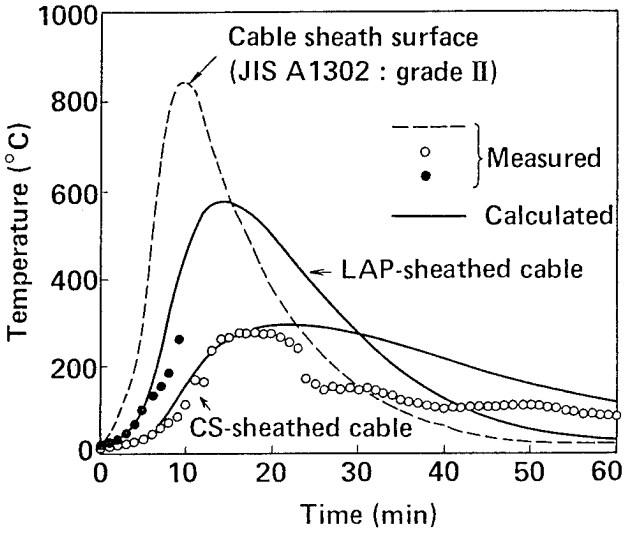



Fig.7 Temperature change at optical unit layer surface.

## 4.4 Optical loss characteristics

Measured optical loss increases in the CS-sheathed and the LAP-sheathed optical cables due to heating are shown in Fig.8. Optical loss for the LAP-sheathed cable rapidly increases and reaches the large loss increase of 20dB/8.4m after about 12 minutes. Then, it is observed that the fiber is broken.

While, optical loss for the CS-sheathed cable begins to increase slowly after 15 minutes of heating. The loss increase does not exceed 0.18 dB/8.4 m. It is noted that the loss increase occurs

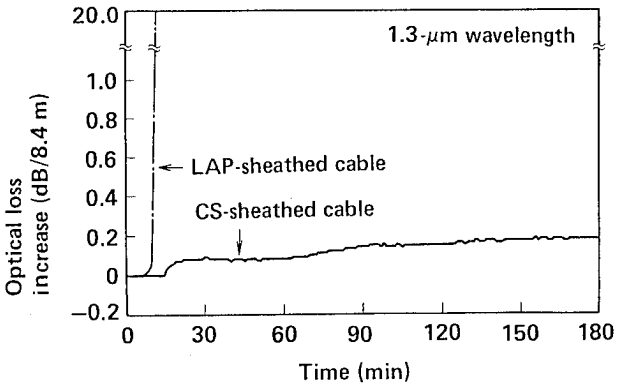



Fig.8 Measued optical loss increase.

after the temperature begins to decrease. After the heating experiment was finished, the optical loss in the CS-sheathed cable was measured by the cut-back method. No additional loss increase was observed. Therefore, it is concluded that the CS-sheathed optical fiber cable has excellent optical loss stability characteristics against heating even when it is involved in a house fire.

## 5. Conclusion

A new method for evaluating temperature conductivities of cable constituent layers with complex structures was proposed. Based on the temperatures of the layer surfaces measured using thermocouples, the temperature conductivities of the layers were evaluated using a difference equation of the heat conduction. By using the method, temperature increase characteristics were evaluated for a CS-sheathed optical fiber cable, where the five layers, i.e. CS-sheath, LAP-sheath, wrapping tape, optical unit, and tension member, were considered. As a result, it was found that the equivalent temperature conductivities of the layers thus evaluated were fully useful for describing the temperature characteristics of the cable.

Next, temperature changes in the CS-sheathed and LAP-sheathed optical cables were investigated, assuming that the cables were involved in a house fire. The calculated temperatures of the CS-sheathed cable using the evaluated temperature conductivities agreed well with the measured temperatures up to the point where the polyethylene layer of the CS-sheath melted. It was clarified that the evaluation of the maximum temperature in a cable exposed to a house fire is possible as far as the cable does not lose its original shape. Furthermore, it was found that a CS-sheathed optical cable has excellent optical loss stability

characteristics against heating even when it is involved in a house fire.

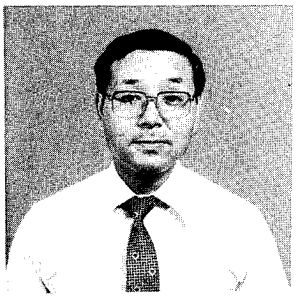

## Acknowledgments

The authors would like to thank N.Uchida and Y.Ishida for carefully reviewing the manuscript, and providing helpful discussions and suggestions. They would also like to thank H.Fukutomi and N.Kojima for their encouragement.


## References


(1) "Method of Fire Test For Noncombustible Structural Part of Building", JIS A 1302

(2) Y. Ishida, et al., "Performance of Field-installed 1.3-μm band single-mode optical cable", Appl. Opt. 22, 3079 (1983)

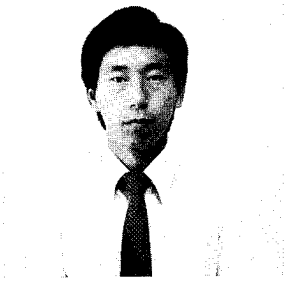




Satoshi MOCHIZUKI

NTT Ibaraki Electrical Comunication Lab., Tokai, Ibaraki-ken 319-11, Japan


S. Mochizuki, Assistant Chief of Cable Facility Section, Outside Plant Development Division, NTT Ibaraki ECL, has been engaged in research and development on metallic and optical communication cables since he joined ECL in 1971.

He was born in 1946 and received B.E. and M.E. degrees from Shinshu University in 1969 and 1971, respectively. He is a member of the Institute of Electronics and Communication Engineers of Japan , and the Japan Society of Mechanical Engineers.

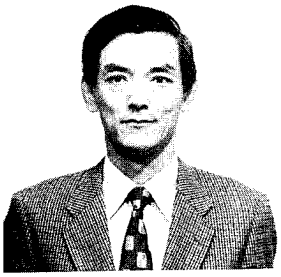



Koji Arakawa

NTT Musashino Electrical Comunication Lab., Musashino-shi 180, Japan


K. Arakawa, Engineer of Outside Plant Engineering Section, Engineering Division, NTT Musashino ECL, has been engaged in research and development concerning anti-creepage cable and flame resistant cable. Presently, he is engaged in research on optical fiber cable reliability.

He was born in 1954 and received a B.E. degree from Osaka Prefecture University in 1978. He is a member of the Institute of Electronics and Communication Engineers of Japan.




Takamasa YASHIRO

NTT Ibaraki Electrical Communication Lab., Tokai, Ibaraki-ken 319-11, Japan


T. Yashiro, Senior Staff Engineer of Optical Transmission Line Facility Section, Outside Plant Development Division, NTT Ibaraki ECL, has been engaged in research and development involving new materials and design for optical fiber cables.

He was born in 1941 and received B.E. and M.E. degrees from Keio University in 1966 and 1968, respectively. He is a member of the Institute of Electronics and Communication Engineers of Japan , and the Society of Polymer Science, Japan.

# THE FUTURE OF OPTICAL TIME DOMAIN REFLECTOMETRY: UTILIZATION OF THE COHERENT DETECTION TECHNIQUE

S. Heckmann[+], J. Rybach[+], E. Brinkmeyer[x], R. Knoechel[*]

[+] Philips Kommunikations Industrie AG
Cologne, West Germany

[*] Philips GmbH Forschungslaboratorium Hamburg, Hamburg, West Germany

[x] Technische Universität Hamburg-Harburg
Hamburg, West Germany

## Summary

At first a comparison of state of the art techniques for backscatter signal processing is given. As examples, the advantages and disadvantages of the correlation technique, the photon-counting technique, the laser preamplification and the coherent detection technique will be discussed.

The comparison shows that the coherent detection technique should be used to obtain the necessary dynamic range of long wavelength backscatter reflectometers.

Thereafter the principle of such a reflectometer is explained using a simple block diagram. Practical solutions are presented regarding
- getting a light source with a sufficient coherence length
- and finding an optical system design with a sufficient small insertion loss.

In addition results of corresponding experiments are presented.

## Introduction

If a short light pulse is coupled into a fiber, a small part of this light propagates in backward direction and can be detected at the near end of the fiber.

This signal is composed of two contributions:

- The first part are fresnel reflections from the fiber near and far end or from breaks within the fiber. The latter can be used for fault location.
- The second part stems from Rayleigh backscattering and has a much smaller level. This part is responsible for the exponential decay in signal amplitude, is a measure for fiber attenuation and allows to determine splice loss.

Therefore optical time domain reflectometry has become an important tool, which is used to measure the attenuation or to detect faults during manufacture, installation and maintenance of optical cables and systems. The main advantage of this technique is that anomalies, defects, and other influences on the transmission quality can be located from one end of the fiber by non-destructive means.

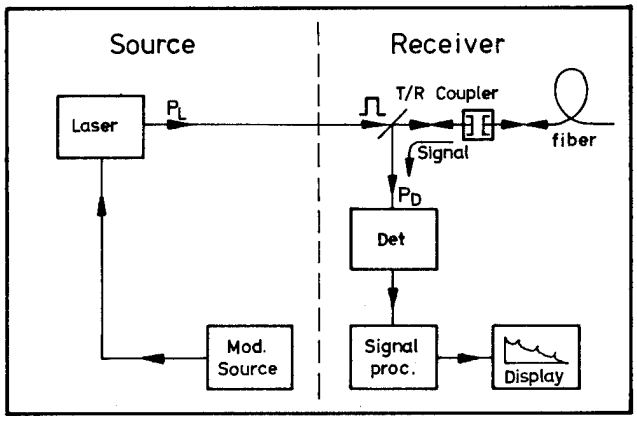



Fig. 1 General block-circuit diagram for a conventional OTDR

An Optical Time Domain Reflectometer (OTDR) is basically constructed as presented in Fig. 1.

It contains a direct modulated (pulsed) laser source, preferably a semiconductor laser, a transmit-receive coupler, a direct detection receiver, a signal processing unit and a display unit.

Optical time domain reflectometry at the wavelength of 850 nm in multimode fibers is

now well established and there are many useful equipments commercially available on the market using this technique.

But future optical communication systems will operate with single-mode (SM) fibers at the wavelengths 1300 nm or 1550 nm in order to obtain better transmission channel properties. Then repeater spacings of 30 km and more will be realized, so that a one way dynamic range of 30 dB is required for OTDRs taking into account splice losses, connector losses, and so on. The dynamic range realizable today can be estimated as shown in Fig. 2.

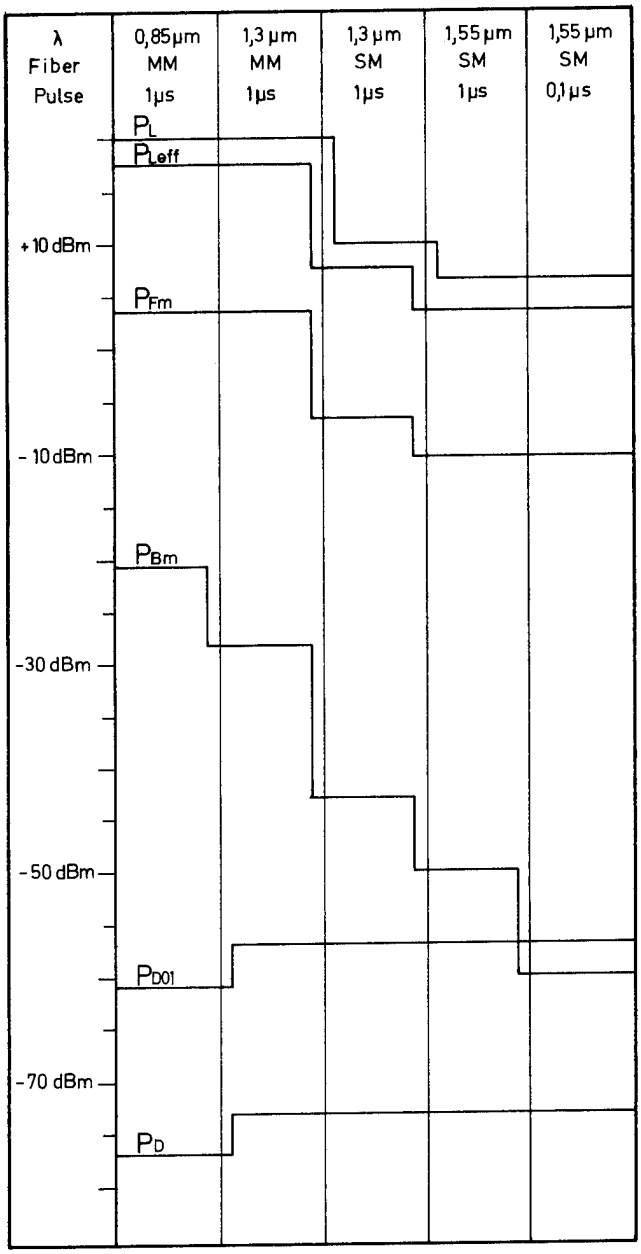



Fig. 2 The fundamental levels in the Optical Time Domain Reflectometry

The upper limit in this diagram is given by the maximum laser peak power $P_L$ coupled into the laser pigtail fiber. This power is reduced by the optical system loss. If an acousto-optic modulator (AOM) is used as transmit-receive coupler, this loss will be approximately 2.5 dB. The resulting power is named effective laser power $P_{Leff}$. At the lower end the diagram is limited by the minimum detectable power $P_D$. The employed value of $P_D$ for long wavelengths is the best one realized up to now without cooling for a bandwidth of 1 $MHz^{-1}$. The value of $P_D$ for 850 nm represents a commercially available receiver module. If the allowable noise is restricted to 0.1 dB then the lower limit is represented by $P_{D01}$. Both power values $P_D$ and $P_{D01}$ can be improved by averaging in the signal processing unit. The maximum backscatter power $P_{Bm}$ and the maximum fresnel power $P_{Fm}$ were calculated by the well known corresponding formulas.

Now the dynamic range can be determined from the figure: To obtain the one way dynamic range for backscatter measurements the difference between $P_{Bm}$ and $P_D$ ($P_{D01}$) has to be divided by 2. The difference between $P_{Fm}$ and $P_D$ ($P_{D01}$) divided by 2 is the one way dynamic range for fault location if ideal fresnel reflections are assumed.

Maximum dynamic ranges of 15 dB or 11,5 dB are realizable in SM-OTDRs with 1.3 µm or 1.55 µm operating wavelength. Assuming acceptable processing times, an additional improvement of 10 dB is possible by signal averaging. But if a better local resolution (pulselength: 0.1 µs) or the possibility to check splices ($P_{D01}$) is required the maximum dynamic ranges will decrease again (Fig. 2).

As shown before OTDR-measurements in single-mode fibers at 1300 nm or 1550 nm are much more difficult due to

- the decreased Rayleigh backscatter level,
- the decreased detector sensitivity,
- and the less powerful optical sources.

The estimation given and results of reflectometers commercially available indicate that there is a gap of 5 - 10 dB one way dynamic range, so that it is not possible e.g. to check future fiber lines in full length between repeaters from only one end of the line using a conventional direct detecting reflectometer.

Thus solutions are required to improve OTDRs concerning future requirements of local resolution and dynamic range.

1. Different ways to improve the properties of OTDRs

If the dynamic range of a reflectometer is to be enhanced this can principally be achieved in two different ways:

On the one hand, the energy of the laser pulse source per backscatter signal can be increased. As an alternative, the sensitivity of the receiver may be improved.

a. Increasing the pulse energy

The signal scattered back by the fiber is proportional to the pulse energy, i.e. to the product of the pulse power times the pulse length.

This means that the dynamic range can, on the one hand, be enhanced by increasing the duration of the pulse. And indeed, reflectometers are taking use of this method. Most of the conventional reflectometers allow for a switch-over of the pulse duration between typically 50 ns corresponding to a resolution of 5 m, and a value of typically 1 µs which corresponds to a local resolution of 100 m.

A further increase in the pulse duration is not useful because of the increasing deterioration of the local resolution.

Instead of the pulse duration, the pulse power can be increased also.

In this context, it has to be noticed that fibers above a certain light power show a non-linear transmission response (e.g. stimulated raman scattering).

If a linear parameter of the fiber, the attenuation is to be measured this certain light power must not be exceeded.

In the course of corresponding laboratory experiments, power values of up to + 36 dBm (4 Watt) were coupled into the single-mode fiber to be measured by means of high-power lasers[2].

When comparing this power to the best semiconductor lasers commercially available ($P_L$ = + 10 dBm), the one-way dynamic range can be increased in this way by more than 13 dB.

The disadvantage of the high-power lasers clearly lies in the costs, the dimensions of these lasers and in the energy requirements for these lasers. Thus, by increasing the power of the optical source, the dynamic range can only be enhanced in laboratory set-ups. If, however, a portable field reflectometer is to be used other conceptions must be considered.

An alternative way to increase the exciting energy can be achieved by means of the correlation technique as it is well known from the microwave radar technique. For this purpose, instead of a single pulse a pulse train with certain statistical properties is coupled into the fiber to be measured.

Backscatter signal and pulse train will be fed to a correlator within the receiving system. In the simpliest case, the latter consists of an adjustable delay line by means of which the exciting pulse train is delayed and of a multiplier (switch) which processes both backscatter signal and pulse train. In case of a fixed delay time, a signal is obtained at the output of the correlator to which all pulses have contributed and which is the measure for the backscatter level of a certain site of the fiber to be measured.

By varying the delay time, the entire fiber line can be measured.

As the corresponding publications[3] to this conception show, the correlation technique offers advantages in case of short-range high resolution OTDRs, whereas a dynamic range improvement of long-range OTDRs has not yet been achieved by this method.

b. Increasing the sensitivity of the receiver

If the receiver sensitivity is to be improved it should be determined which receiver sensitivities can be obtained at present.

Under the condition that today's most essential noise source for long-wave length receivers is the shot noise caused by dark current, the smallest detectable power $P_D$ of a direct detection receiver is given by:

$$P_D = \sqrt{2 \cdot e \cdot I_D \cdot B}/r$$

with
electron charge e (= $1.6 \cdot 10^{-19}$ As)
Dark current of the detector $I_D$
(typ. 1 nA - 10 nA)
Bandwidth of the receiver system B
(typ. 1 MHz)
conversion factor of the detector r
(typ. 0.7 A/W)

When applying above values to the formula, the result is a power of $P_D$ = - 71 dBm to - 76 dBm. These values are in good agreement with the best value of - 73 dBm[1] obtained so far. Between this value so far obtained and the value being theoretically realizable under the condition that the

dark current of the diode is negligible and that the shot noise is caused by the signal itself, there is a gap of about 20 dB. In a direct detection receiver this gap can only be decreased by deteriorating the local resolution or by using other receiver conceptions:

Normally, avalanche photodiodes in optical receivers are operated below their breakdown voltage so that by one photon only a finite number of free charge carriers is generated. In case of the photon-counting technique, however, the avalanche diode is operated above its breakdown voltage so that by one photon a full breakdown of the diode occurs which would destroy the latter if the breakdown would not be interrupted by means of a limiter. The breakdown of a diode causes a current pulse which can be detected. Proceeding from the most simple case, the pulses can be detected by means of a digital counter with the number being a measure for the respective backscatter level.

With this technique, $P_D$-values of - 80 dBm and thus an improvement of the sensitivity by 7 dB was obtained[4].

The disadvantage of this technique can be put down to the facts

- that the diode must be cooled considerably (e.g. to 77°K) in order to prevent its thermal breakdown
- that suitable diodes must be selected and
- that actually only a small dynamic range can be processed, since only one photon per recovery time of the detector circuit can be detected.

Furthermore, the sensitivity of a detector may be increased by connecting an optical amplifier in series with the photodiode.

In principle, normal lasers amplifying the signal light on its path through the cavity may be used. For an improvement of the dynamic range, however, not only the laser amplification must be taken into consideration but also the additional optical insertion loss of the amplifier and the additional noise being generated during the amplification. These two influences lead to a deterioration of the attainable dynamic range. In the course of a corresponding experiment[5], the laser amplification amounted to 16 dB. Due to the insertion loss and the additional noise, however, an extension of the dynamic range of not more than 1.5 dB (one way) was obtained.

If we take into account the given requirements for reflectometers, i.e. a dynamic range of $> 30$ dB, a resolution of $< 100$ m as well as field usability, such an equipment cannot be realized with the above mentioned conceptions alone.

2. Coherent Optical Time Domain Reflectometry

In the receivers up to now a receiving technique is used which corresponds to the direct detection receivers from the beginning of the radio engineering. In the radio engineering a drastical improvement of the sensitivity was obtained as the first superhet receiver was realized. This technique also can be used to improve the sensitivity of optical receivers. As known for coherent, specially heterodyne detection a local oscillator (LO) generating $E_{LO}(t)$ has to be applied to the detector together with the signal $E_{SIG}(t)$.

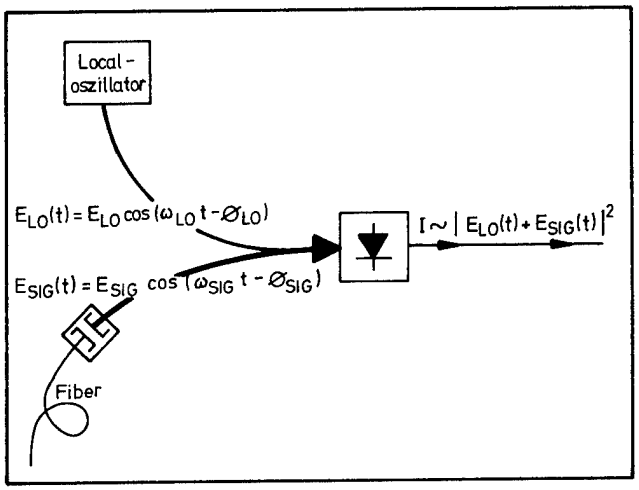



Fig. 3 Opto-electric conversion of coherent signals with photodiodes

The detector current I is given by

$$I \sim \frac{1}{2} \cdot E_{LO}^2 + \frac{1}{2} \cdot E_{SIG}^2 + E_{LO} \cdot E_{SIG} \cdot \cos(\omega_{IF} \cdot t - \varphi_{IF})$$

$$\sim \frac{1}{2} \cdot P_{LO} + \frac{1}{2} \cdot P_{SIG} + \underbrace{\sqrt{P_{LO} \cdot P_{SIG}} \cdot \cos(\omega_{IF} \cdot t - \varphi_{IF})}_{\text{Beat frequency}}$$

with $\omega_{IF} = |\omega_{LO} - \omega_{SIG}|$

$\varphi_{IF} = \varphi_{LO} - \varphi_{SIG}$

Both waves differ in frequency by some ten MHz. Because of the square relationship between the optical amplitudes and the detector output current a beat frequency is produced at the intermediate frequency $\omega_{IF}$.

If a sufficient high LO-power is used, the output noise is now mainly shot noise of the current due to the LO-wave. The other noise sources, e.g. shot noise due to the dark current, due to the signal can be neglected. Since the output signal and the output noise of the detector depend on the LO-power linearly, the signal-to-noise ratio and consequently the minimum detectable power $P_D$ are independent of the LO-power.

The minimum detectable power is given by

$$P_D = 2 \cdot e \cdot B/r$$

$$= 2 \cdot h \cdot f \cdot B/\eta$$

with
Planck's Constant times optical frequency $h \cdot f$
$(= 1.53 \cdot 10^{-19}$ Ws$(\lambda = 1.3$ µm$))$
Quantum efficiency $\eta$ (typ 0.7)

The factor 2 takes into account a 3 dB mixing penalty because the backscatter signal polarization is random. Using the above given practical values the minimum detectable power $P_D$ can be estimated to - 93 dBm.

As a disadvantage, we have to note, that heterodyne detection is polarization and phase sensitive (different backscattering elements interfere with each other), and the following signal processing requires some kind of frequency stabilization for the input signals.

| Direct | Heterodyne |
|---|---|
| Detector current depends linearly on $P_{SIG}$ | Detector current depends linearly on $\sqrt{P_{SIG}}$ |
| Min. det. Power - 73 dBm △ (Typical value) | Min. det. Power - 93 dBm △ (Typical value) |
| Polarization, Phase — independent | Polarization, Phase — dependent |
| No special laser | Line narrowed laser (<1 MHz) |

Fig. 4 Comparison between direct and heterodyne detection

In Fig. 4 a comparison is summarized between direct and heterodyne detection.

- The first difference is in the signal current at the detector output. The output current for direct detection depends linearly on the optical power $P_{SIG}$ whereas the heterodyne detection output shows a linear dependence on the optical amplitude $E_{SIG}$ and consequently a linear dependence on the square root of the optical power.

  This demonstrates the much better dynamic range of heterodyne detection.

- Secondly, using typical values for detectors at 1.3 µm, we note that heterodyne detection has an advantage of 20 dB in sensitivity compared to direct detection.

- In comparison to direct detection, heterodyne detection is complicated a little bit by the fact, that the beat signal now depends on polarization and phase of the optical wave.

- And finally, and this is the most important disadvantage: Heterodyne detection requires a line-narrowed laser source. Using 1 µs-pulse as OTDR excitation signal, a linewidth of less than 1 MHz is required.

A general block-circuit diagram for a heterodyne OTDR is shown in Fig. 5.

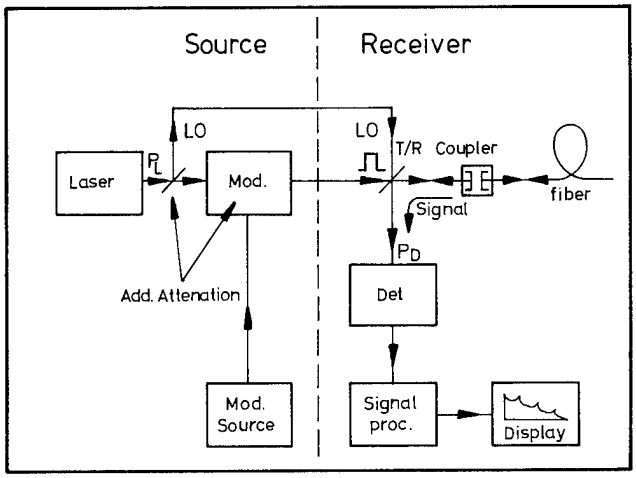



Fig. 5 General block-circuit diagram for a heterodyne OTDR

On the optical receiver side, the transmit-receive coupler is not only used to separate the excitation and backscatter signal but simultaneously combines the backscatter signal and the LO-wave. The IF-signal now requires a second detection in the signal processing electronic before the signal can be averaged.

The requirement of a LO-wave and the demand for a narrow laser linewidth result in the need for an external power splitter and an additional modulator to provide the frequency shift between the backscatter signal and the LO-wave and to pulse the excitation signal. The higher complexity of the circuit arrangement causes an additional attenuation which will lower the effective launch power into the fiber, thus deteriorating the advantage of heterodyne detection.

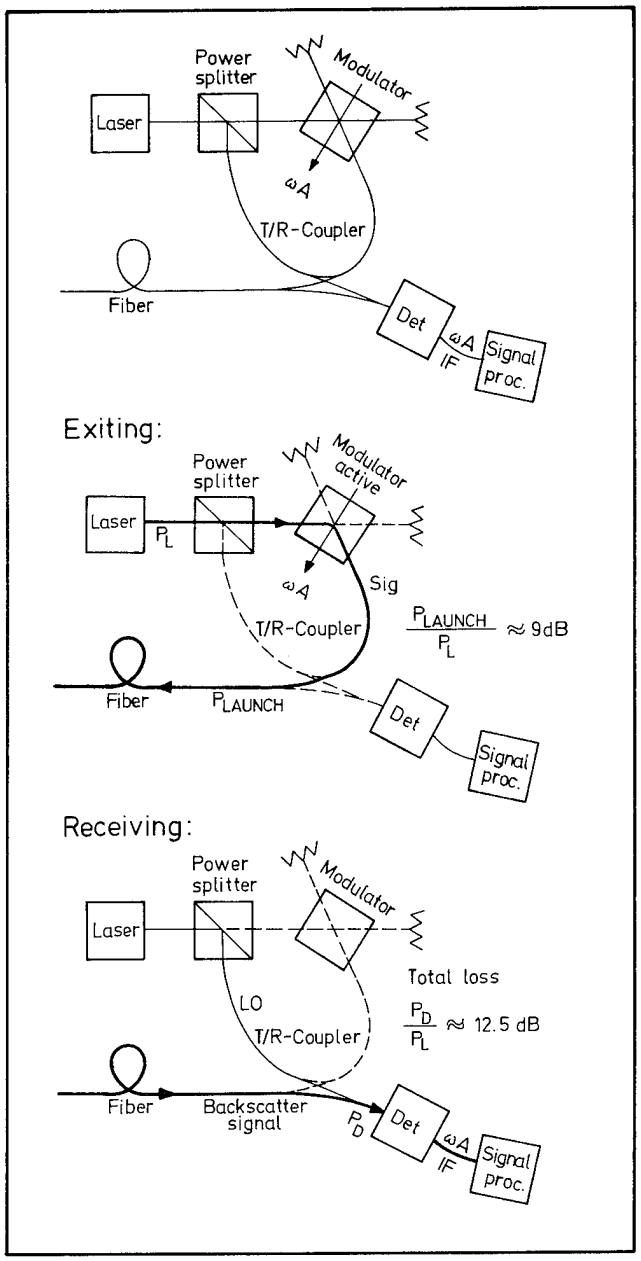



Fig. 6 First realization of a heterodyne OTDR

In Fig. 6 the first realization of a heterodyne OTDR which was made by British Telecom in 1982 and then refined by the British company STC in 1983[6] is presented. They used a HeNe gas laser at 1.5 µm as the optical source because of the short term coherence properties. The LO-wave was coupled out by a power splitter. An acousto-optic modulator was used for gating and frequency shifting the excitation signal. The transmit-receive coupler was a fused fiber coupler.

In the exciting mode the acousto-optic modulator is active. It then deflects the excitation signal into the transmit path. At the same time it gates the pulse width and produces a frequency shift on the light wave by the acoustical frequency $\omega_A$, which later will be the intermediate frequency $\omega_{IF}$. If we collect the internal system attenuation on the excitation signal, say 3.5 dB in each coupler and 2 dB in the acousto-optic modulator, then we find, that the launch power into the fiber is reduced by 9 dB compared to the laser output.

In the receiving mode, the modulator is off. The backscatter signal is now combined with the LO-wave by the transmit-receive coupler and fed into the detector. By passing the transmit-receive coupler, the backscatter signal suffers another 3.5 dB attenuation, so that the total system loss from the laser output to the detector input is about 12.5 dB, and this value deteriorates the system sensitivity.

Compared to a good direct detection system, which uses an acousto-optic modulator as transmit-receive coupler, the internal attenuation of the present heterodyne system is about 10 dB higher due to the more complicated optical arrangement, resulting in a loss of 5 dB in the one way attenuation range.

Additionally a HeNe laser is not useful in a portable equipment because its properties, e.g. the coherence length, are very sensitive to shock or vibration.

## 3. A practical Heterodyne Optical Time Domain Reflectometer

In the heterodyne OTDR described above the main problems are the unsuitable optical source and the internal optical system attenuation. In the following solutions for both problems will be presented.

The optical excitation source has to generate a sufficient stable and narrow optical spectrum and on the other hand its properties have to be independent on temperature, shocks, vibrations, and other environmental factors.

The second requirement can be satisfied by the use of a temperature stabilized semiconductor laser source.

However, difficulties are caused by the unsufficient coherence properties of these lasers.

In Fig. 7 is illustrated what happens, if the laser linewidth and hence the detected IF-signal does not fit into the IF-bandwidth.

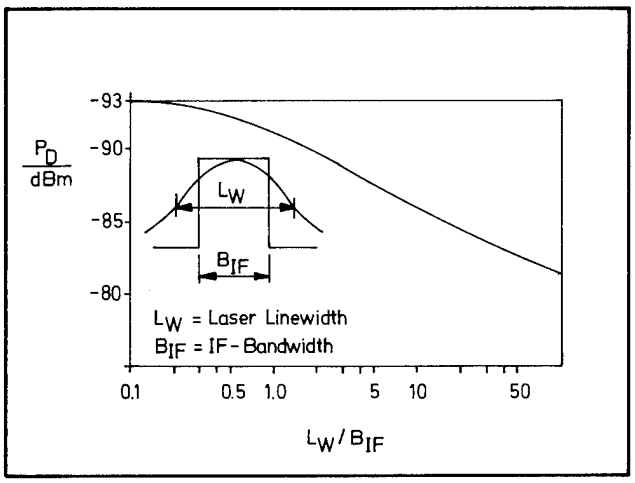



Fig. 7 Influence of the laser linewidth on the minimum detectable power $P_D$

Then all the power outside the bandwith $B_{IF}$ is lost, and the minimum detectable power $P_D$ deteriorates. So for instance an IF-bandwidth of 1 MHz and a laser linewidth of 50 MHz would lead to a penalty of more than 10 dB in the detectable power $P_D$. Hence the advantage of heterodyne detection is lost. This illustrates the importance of laser linewidth narrowing for heterodyne OTDR. In our example, laser linewidths of less than 1 MHz are required.

Laser linewidth narrowing can be obtained for example by selective feedback of optical power into the laser using an external grating (Fig. 8).

Using this approach linewidths of less than 1 MHz were achieved. But it is known, that such external gratings are difficult to adjust, and stable and reliable operation can only be obtained under laboratory conditions up to now. Therefore it is questionable, if this method can be developed in order to arrive at a field portable stable laser source.

Another attractive solution for laser linewidth narrowing has recently been published by the British company STC[7]. The semiconductor laser is coupled to a length of optical fiber (Fig. 8). The output power is extracted from the end of that fiber. Then the backscatter signal of that fiber acts to line-narrow the laser. As reported[7,8], we have found in our laboratory that linewidths smaller than 50 kHz can be obtained with this method. Simultaneously, the laser

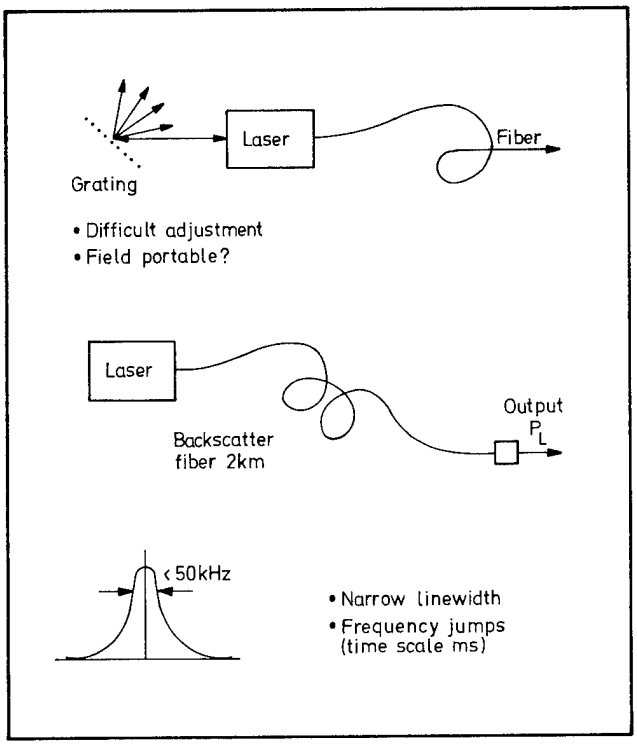



Fig. 8 Laser linewidth narrowing by optical feedback

center frequency is permanently jumping by some hundred MHz on a time scale of some jumps per second.

In Fig. 9 and Fig. 10 typical measurement results are presented.

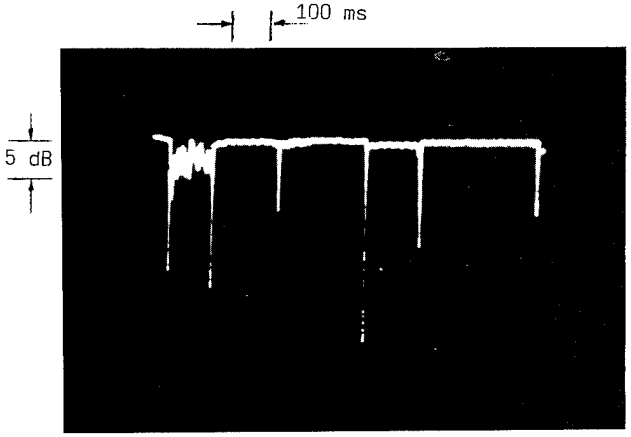



Fig. 9 Stability time measurement of a laser linewidth with a self-heterodyne set-up and a bandpass

To obtain Fig. 9 and Fig. 10 the output light of the line-narrowed laser was processed in a self-heterodyne set-up[9]. At first the spectrum of the output signal of the self-heterodyne set-up which is essentially the frequency shifted laser spectrum was transmitted by a bandpass. The

bandpass center frequency was equal to the acoustical frequency of the used acousto-optic modulator. Its bandwidth was 30 kHz.

Fig. 9 shows that the laser spectrum was typically stable for some hundred ms and unstable for very short times which were ascertained to be typically one ms.

To obtain Fig. 10 the output signal of the self-heterodyne set-up was processed by a radio frequency spectrum analyzer. If the analyzer scanned very slowly both the stable and the unstable spectrum were displayed. In the stable mode only the center line of the displayed spectrum existed.

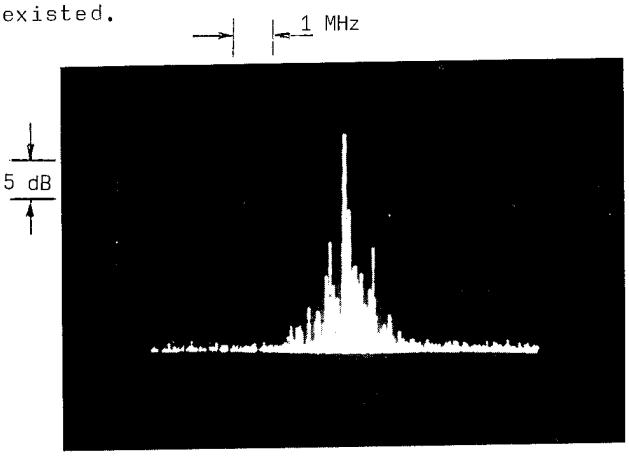



Fig. 10 Time averaged frequency spectrum of a line narrowed semiconductor laser

The jumping of the laser frequency is not a disadvantage for an OTDR, because it is only required, that the whole backscatter signal returns until a frequency jump occurs. This signal needs less than one ms to be detected by the receiver.

The disadvantage of this stabilization method is, that the stabilization mechanism is not yet completely understood.

Certainly laser linewidth narrowing will remain a future main working field in heterodyne optical time domain reflectometry.

A solution for the second problem, a new design for a heterodyne OTDR set-up is presented in Fig. 11.

This system allows a significant reduction of the additional system loss. It can be achieved by using two acousto-optic modulators in the system, which act to switch the light between the different ray paths. Both modulators are driven with different acoustic frequencies. The first AOM acts simultaneously to pulse the signal and to couple out the LO-wave. The second is the transmit-receive coupler.

When launching the excitation signal into the fiber only the first modulator is active, the second is off. Then the laser output is deflected and frequency shifted by $\omega_{A1}$. This signal then enters the fiber. Because there is only the attenuation in the first AOM due to the limited deflection efficiency, the launch power is only reduced by 2 dB compared to the laser output power.

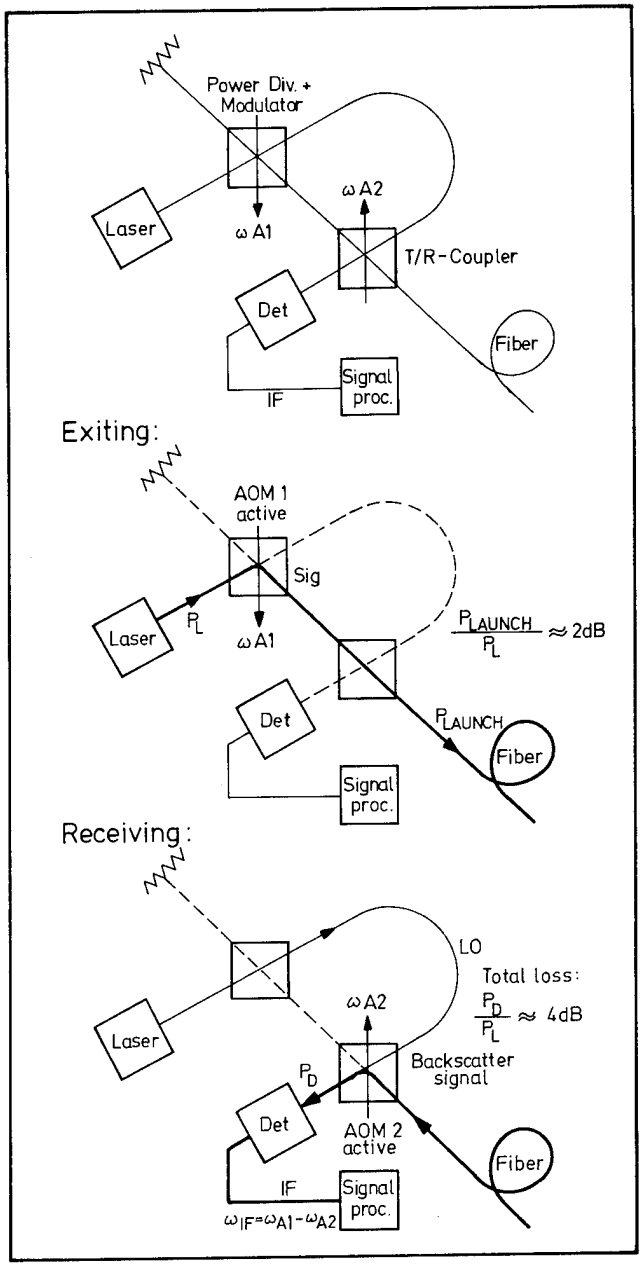



Fig. 11 New design for a heterodyne OTDR

When the OTDR is switched in the mode to receive the backscatter signal, the second AOM is activated. It then deflects the backscatter signal to the detector, pro-

ducing another 2 dB loss, so that we have a total system loss of 4 dB. Compared to the direct detection system, the penalty for the complicated heterodyne system arrangement is only 2 dB, hence making most of the heterodyne detection advantage available for the sensitivity improvement.

Since the first AOM is off during reception, the undeflected laser output can be used as LO-wave. The LO-wave is fed through the second AOM onto the detector. Because the second AOM is active, the LO-wave suffers a power loss, but this is not very important as the reduced power is sufficient to drive the detector into shot noise limited operation.

The second AOM produces another frequency shift for the backscatter signal until it reaches the detector. If the AOMs are adjusted in the right way, then the IF can be arbitraryly chosen as the difference between $\omega_{A1}$ and $\omega_{A2}$.

So the signal processing electronic can operate at the most convenient frequency, allowing a lot of flexibility in the design.

Another important feature is, that the optical system is mainly composed only of two equal components, which simplifies the production of such reflectometers.

## Conclusions

Heterodyne detection in OTDR is an attractive means to improve sensitivity and dynamic range. However, the heterodyne advantage of about 20 dB in detector sensitivity will only lead to an increase in measurable one way attenuation range, if a reliable and field portable solution for laser stabilization is found and if the system insertion loss is minimized. Solutions for these critical points were presented.

## Acknowledgement

We gratefully acknowledge financial support from the German Bundesministerium für Forschung und Technologie (BMFT).

## References

1 P. Healey, D. R. Smith, Electron. Lett., vol. 18, pp. 959 - 961, 1982

2 M. Nakazawa et al, Optics lett., vol. 9, pp. 312 - 314, 1984

3 J. J. Bernard et al, Proc. 10th European Conference on Optical Communication, pp. 84 - 85, 1984

4 P. Healey, Electron. Lett., vol. 17, pp. 751 - 752, 1981

5 K. Suzuki, Electron. lett., vol. 20, pp. 714 - 716, 1984

6 S. Wright, K. Richards, Proc. 9th European Conference on Optical Communication, pp. 177 - 180, 1983

7 R. E. Epworth et al, Proc. 10th European Conference on Optical Communication, pp. 132 - 133, 1984

8 R. Knoechel et al, Proc. Laser '85 Opto-Elektronik, 1985

9 T. Okoshi et al, Electron. lett., vol. 16, pp. 630 - 631, 1980



Siegfried Heckmann studied at the University of Bochum and graduated in 1978 in electrical engineering. 1983 he obtained his doctorate at the University of Wuppertal on the basis of his thesis on a subject taken from the field of communication engineering. Since 1983 he has been active as group leader with F&G Telecommunication Cables and Systems, a member of Philips Kommunikations Industrie AG, where he is responsible for the development of optical measuring equipment.



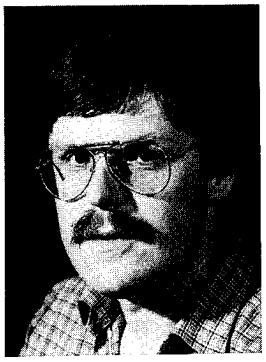
Johannes Rybach studied at the Universities of Cologne and Düsseldorf and received the Diplom degree in 1976, the Dr. rer. nat. degree in 1982, both in physics.
From 1976 to 1984 he was a Research and Teaching Assistent at the Physikalisches Institut in Düsseldorf where he worked on lasers and optical diagnostic methods. Since 1984 he has been with F&G Telecommunication Cables and Systems, a member of Philips Kommunikations Industrie AG. There he is engaged in R&D on spectral line-narrowed laser diodes and optical measuring equipment.



Ernst Brinkmeyer received the Diplomphysiker and the PhD-degree from the Faculty of Physics of the University of Göttingen, Germany, in 1973 and 1976, respectively. Up to that time he worked on problems concerning shock waves and cavitation.

Subsequently, he joined the Electrical Engineering Department of the University of Wuppertal, where he was involved in experimental and theoretical work on optical waveguides.

Since 1983 he is a Professor for Technical Optics at the Technische Universität Hamburg-Harburg.



Rheinhard Knoechel received the Dipl.-Ing. degree and the Dr.-Ing. degree from the Technical University Braunschweig, West Germany, in 1975 and 1980, respectively. He joined Philips Forschungslaboratorium, Hamburg, in 1980, where he is currently involved in research on Optical Time Domain Reflectometry and in the development of microwave identification systems. He was engaged in industrial and medical applications of microwaves before.

From 1975 to 1980 he was with the Institut für Hochfrequenztechnik, Braunschweig, where he worked on oscillator theory and on microwave and millimeterwave integration.

# Automated Multi Fiber Attenuation Change Measurement System

K. Hafemeister, A. Garg, B. Hellmann,
D. Schicketanz, D. Vokey

Siecor Corporation
Hickory, North Carolina

## Abstract

This paper describes an automated system to measure attenuation changes on installed optical fiber cables. It is designed for use on single mode fibers and for long-term unattended operation.

The measurement system is currently used to monitor the attenuation change on two self-supporting aerial cables of different design, for use on high tension lines. A newer version of this system includes transmitter, coupling and receiver improvements as well as size reductions.

## Introduction

Fiber optic cables, using either buffer tubes or slotted core designs, are usually constructed to have an operating window allowing for cable expansion or contraction without stressing the fibers. For all cables, this window must be verified to assure performance after installation and during the expected lifetime. Self-supporting aerial cables [1], for example, must endure not only installation forces, but also stresses due to ice loading, high winds and temperature extremes.

To test the performance of two prototype aerial fiber optic cables, a system was developed to monitor the output power of the encased single mode fibers given a reference input power. Automatic measurement of fiber delta-attenuation was incorporated so that operation would be possible over extended time periods. The system was to be of modular construction for easy assembly, modification or repair.

## Theory

By stressing or straining a fiber, its attenuation characteristics can be changed. Within the operating window of the cable, the fiber moves freely inside the cable. If these window limits are exceeded, microbending effects cause measurable attenuation changes [2].

The attenuation change suffered by an optical fiber is defined as

$$\Delta \alpha = \frac{10}{L} \log \frac{P_m}{P_o},$$

where $\Delta \alpha$ is the attenuation change in dB/km, L is the fiber length in kilometers, $P_o$ is the fiber output power in arbitrary units at the start of the measurement period, and $P_m$ is the fiber output power at any later time. For an ideal cable operating within its window, $\Delta \alpha$ is zero. The allowed values of $\Delta \alpha$ are determined by the system's loss budget, including a safety factor.

## Measurement System

The measurement system consists of transmitter(s), a receiver for each fiber, and a data acquisition/storage unit. The power supplies, the computer and the analog-to-digital converter are commercially available.

Each transmitter consists of a tungsten ribbon lamp, an optical filter, and a 400 Hz tuning fork chopper. The bulb is operated below its published ratings to increase its expected life. The fibers being tested are spliced to the transmitter via a multifiber single mode pigtail. The pigtail is illuminated using one-to-one optics.

Each receiver consists of a photodiode, a high gain transimpedance amplifier, a 400Hz active bandpass filter, and a peak detector. The DC output voltage is proportional to the receiver input power, and is linear over the necessary operating range. The bandpass filter width is approximately 10 Hz. Parts for each receiver are assembled on a small printed circuit board and are mounted in an aluminum cabinet. (See figure 1.)

All receiver output voltages are measured by a multichannel analog-to-digital converter. Each voltage is sampled for 50 seconds, ten readings per second. The computer averages this data to obtain a resolution of approximately ±0.1 dB and an accuracy of approximately 0.2 dB

over a one year operating period. This produces an overall signal-to-noise ratio of approximately 20 dB optical, with a dynamic range of over 10 dB.

A prototype of this measurement system is currently being used in the Cascade Mountains of Oregon. The temperatures at this site vary between -35°C and +45°C; winds up to 100 mph and one inch radial ice loading on power conductors have been reported in this area. The two units under test are self-supporting, entirely dielectric aerial cables of different designs containing twelve single mode fibers each [1], and are suspended across two spans of high tension towers.

All electronics are located in a test hut into which both cables enter through an underground duct. (See figure 2.) As the other end of the cable is inaccessible, the fibers are spliced so that a return trip is made through the same cable. The total round trip length is 2.06 km per fiber.

The reference loops consist of short lengths of fibers connected to individual receivers. Their purpose is to both verify transmitter operation and to provide a reference number for relative power calculations. These fibers are contained entirely within the hut.

This particular measurement system consisted of two transmitters, one at 1300 nm and one at 1550 nm, and fourteen receivers, along with the associated power supplies, computer, etc. (See figure 1.) This system has been in continuous operation since December 1984.

## System Options

Several measurement system modifications are planned. The tungsten ribbon lamp will be changed to a halogen lamp, decreasing not only the noise but the size of the associated power supply. The pigtail illumination scheme will be modified for better uniformity, and a turning wheel chopper will be used for increased stability. With these revisions, the size of the transmitters will be reduced to one-quarter of the original size.

For multiple wavelength measurements, a spectral transmitter mounted on a monochromator is available.

Receiver modifications include a newly designed fiber coupling for easier assembly. Either a capillary as a bare single mode fiber adapter, a multiple V-groove unit for bare multimode fibers, or a connectorized photodiode for single or multimode fibers is available.The bandpass-peak detector circuit has been changed to a synchronous detector-low pass filter circuit, resulting in a 40 dB dynamic range and improved signal-to-noise ratio.

The measurement system has application in either laboratory or field environments and can be used efficiently in Quality Control when either temperature or tensile tests are performed. Any long-term testing of either multimode or single mode fiber cables resulting in attenuation change can also utilize this system.

## Summary

The measurement system described herein has been in operation for over nine months without a failure. It is easy to use and can be tailored to fit almost any attenuation measurement need.

## Acknowledgement

The authors would like to thank Barry Cline and Teresa Clarke for their support and technical expertise.

## Reference

[1] H. Goldman, E. Mayr and U. Oestreich, "Improved Fiber Optic Aerial Cables in Power Lines," IEEE Global Telecommunications Conference, Vol. 1, see 2.4.1, November 1984.

[2] N. Sutor, "Testing the Mechanical and Thermal Characteristics of Optical Cables," Telecom Report, Vol. 6. pp 183-187, October 1983.

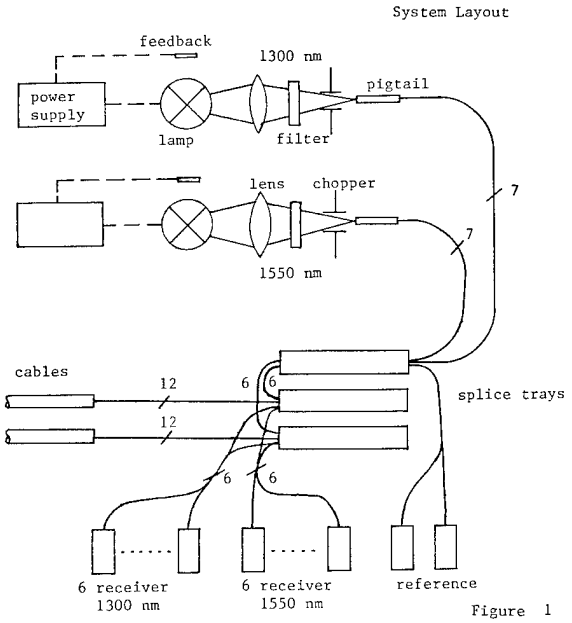



Figure 1

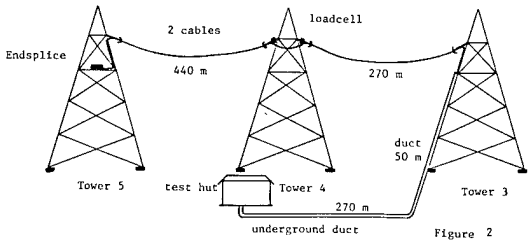
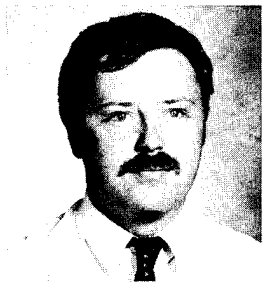


Figure 2



Bruce Hellmann was born in Westbury, NY, in 1950. He received the B.S. degree in Physics (cum laude) from NY Institute of Technology in 1973, the M.S. degree from the University of Mississippi in 1978, and the Ph.D. from The Florida State University in 1984, where he was the last student of the late Nobel laureate P.A.M. Dirac.

Dr. Hellmann joined the R,D&E staff of Siecor Corporation in January, 1985 and is currently a Senior Product Development Engineer.



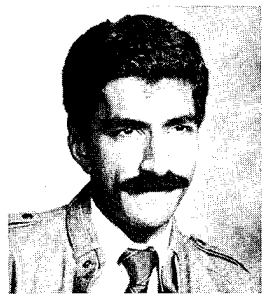
Klaus Hafemeister was born in Duisburg, West Germany in 1955. He received the M.S. degree in electrical engineering from the University of Duesseldorf in 1980. He then joined the Communications Development Department of the Quality Control Division of Siemens Corporation, where he was mainly involved in the design and implementation of fiber optic test equipment.

Mr. Hafemeister has been working for Siecor Corporation since 1984 and is currently a Senior Development Engineer.



Dieter Schicketanz was born in Puerto Montt, Chile, in 1943. He received the Ingeniero Civil in Electrical Engineering from the University of Chile, Santiago, Chile in 1968 and the Ph.D. in Physics from the University at Graz, Austria, in 1974. He joined Siemens Research Laboratory, Munich in 1970, where he has worked on several different areas of optical communications.

Dr. Schicketanz has been working for Siecor Corporation since 1984 and is currently a Senior Scientist. He has authored many papers on optical related areas.



Avinash Garg received the BS degree in Physics from St.Xavier's College, Bombay (India) in 1978, the M.S. degree from the University of Bombay in 1980, and the M.S.E.E. degree from Virginia Tech, VA, in 1982.

Mr. Garg has been working for Siecor Corporation since 1982 and is currently a Senior Development Engineer. He has co-authored six technical papers on nondestructive testing and evaluation using differential interferometry.



David Vokey was born in Winnipeg, Canada in 1946. He received the Dipl. Tech from the Manitoba Institute of Technology in 1969, the B.S.E.E in 1973, and M.S.E.E. in 1984, both from the University of Manitoba.

Mr. Vokey was Manager of Design and Development at Canada Wire and Cable. He joined Siecor Corporation in 1982, where he is the Manager of Product Development.

# HIGH ACCURACY MEASUREMENT OF OPTICAL FIBRE LENGTH

O.R. Andersen, P. Hoejergaard, P. Hornung, G. Mogensen, and E. Hornung

NKT Elektronik, Denmark

## Abstract

Highly accurate determination of the length of an optical fibre is an extremely useful tool in the development of optical fibre cable construction as well as during regular production and in many cases also during installation.

All known techniques rely on the pulse transit time - or the equivalent frequency domain technique.[1-5] An improved version of the technique is presented in this paper. The improvement is due to the employment of a so-called window-sampling technique, whereby the conventional sampling technique is combined with digital control of the sampling gate as well as digital post processing. The technique has allowed the construction of a complete self-contained, portable test equipment, which is much more compact than the hitherto used gatherings of standard laboratory equipment.

## Measurement Method

The measuring principle is based on a time domain technique and is shown schematically in fig. 1.

The set-up consists of an optical pulse transmitter and a wide-band optical receiver connected to the two arms on one side of a 2 x 2 fibre directional coupler. The directional coupler may be multimode or single mode, as appropriate. In single ended measurements the near end is connected to one of the free ends of the directional coupler, and the far end shall be prepared to ensure a sufficient level of reflectivity, depending on round trip loss. Double ended measurements can also be made by connecting the two ends of the fibre to the two free ends of the coupler.

For each pulse transmitted, the directional coupler provides two received pulses. The first to be received is caused by a reflection at the near end connector, while the last pulse received, furthermore, has made the distance to and fro the end of the test fibre. The time, in which those pulses are separated, is, therefore, exactly twice the transit time of the test fibre (single ended measurement).

As the two pulses, furthermore, run through the same electronics, any influence of introduced delay is eliminated.

To avoid ambiguity, only one light pulse is allowed in the test fibre at a time; this leads to a low pulse repetition frequency (PRF) and increased measuring time.

In the actual case, PRF is set to $\frac{1}{163.84\ \mu s} \approx 6.10$ kHz corresponding to a maximum fibre length of 16 kms (single ended measurement).

In order to relate an optimal time-of-arrival definition to the involved pulses, the pulse transmitted has to be narrow, and a detailed knowledge of the pulse shape, before and after propagating through the fibre, is required.

The high bandwidth and low repetition rate of the pulse signal call for a special application of the sampling technique. The window-sampling technique uses repetitive sampling in a narrow window (40 ns), positioned in the period by a 14 bit word on the timing modules bus. The window can be moved in increments of 10 ns as indicated, by using 14 bit and a period time of 163.84 µs

$$163.84\ \mu s \cdot 2^{-14} = 10\ ns \qquad (1)$$

Exclusion of the uninteresting parts of the signal gives a corresponding processing time reduction. To take full advantage of this reduction, a first-hand knowledge of the pulse positions has to be acquired. A fast hard wired digital processor carries out this task with a resolution of 40 ns by means of digital signal averaging.

The output of the low-pass filter, which is a low frequency copy of the selected

part of the signal, is then digitized and fed to the CPU for further calculation.

The measuring cycle is controlled by a microprocessor, and the system features several read-out facilities. It is, however, also possible to step the window manually, which could be of interest in certain applications.

The measuring time is about ten seconds and includes coarse pulse position determination (by the digital processor), analog sampling in the immediate vicinity of the near and far end reflections, transit time calculation based on the center of gravity definition, and finally, presentation of the result according to the selected display mode (abs., rel., or o/oo).

## Window-Sampling

A block diagram showing the principle of the window-sampling is presented in fig. 2. From this it appears that the timing signals are generated from two crystal oscillators, a stable reference source operating at 100 MHz, and a voltage controlled oscillator locked to the first one with an offset of -40 Hz. False lock at 100 MHz +40 Hz is prevented by implementing an image-rejecting PLL.

The window generator is essentially a 14 bit 100 MHz programmable synchronous counter, implemented by nine ECL circuits. The fourteenth output of the counter provides the transmitter trigger signal, and the "window" output gives a precisely 40 ns wide ECL pulse placed in the period according to the 14 bit combination.

This "window-pulse" is used to gate the 24.99999 MHz signal, and consequently, the sample gate will only be activated within the selected timeslot. The 24.99999 MHz signal and the window pulse width are in accordance with the desire of a repeated sampling of the selected timeslot.

The equivalent sampling rate $f_s$ can be calculated from the 24.99999 MHz signals phase displacement $\Delta T$ from one period to the next:

$$\Delta T = 2^{14}/99.99996 \text{ MHz} - 163.84 \text{ µs} = 65.536 \text{ ps} \rightarrow f_s = \frac{1}{\Delta T} \approx 15 \text{ GHz} \qquad (2)$$

This is more than sufficient to observe Nyquist's sampling theorem, as the receiver bandwidth is approximately 800 MHz. The analog signal processing sampling - low-pass filtering - gives the low-frequency duplication a better signal to noise ratio than the high-frequency original. It can be shown that the SNR improvement in the ideal case equals $(2 \cdot B \cdot \Delta T)^{-1}$, where B is the bandwidth of the high-frequency signal. In the actual situation the improvement is

$$20 \cdot \log (2 \cdot B \cdot \Delta T)^{-1} \approx 20 \text{ dB}.$$

Sampling can be described as a time stretching process, and the stretching factor is

$$\left(1 + \frac{T}{\Delta T}\right) = 1 + 163.84 \text{ µs}/65.536 \text{ ps} = 2.5 \cdot 10^6. \qquad (3)$$

The period of the low-frequency timeslot copy is, therefore, 40 ns $\cdot$ $2.5 \cdot 10^6$ = 100 ms = 1/10 Hz.

## The Digital Processor

As mentioned before, the digital processor roughly estimates the pulse positions. This is done by splitting up the period in 4096 timeslots, and relating every pulse received to one of those. Then by averaging several periods, a better decision can be taken, due to the noise reduction effect.

Collecting and processing of all 4096 signal values from one period demand the use of a fast and expensive logic and memory circuit. Due to the non-correlative nature of noise a compromise between technology and processing time can be arranged.

In the implemented digital processor, two counters, CI and CII, select the actual timeslots and point out a related memory cell in a 2 K x 8 RAM. As the internal states of the window generator equal the counter states, a window pulse is generated. This pulse is used to sample the signal value in the actual timeslot and to update the related memory cell by activating a read-write cycle.

Within one period the counter CI is incremented by a window pulse to point out the next timeslot, and the use of 7 bit indicates that 128 samples are taken in each period. These 7 bit are the most significant bit, so the time between two samples is 1.28 µs and is spent on accessing and updating the RAM cell.

During the next period all samples will be taken in the subsequent timeslots, as the counter CII is incremented by the "trig laser" signal. The processor is hard wired and stops automatically, when one RAM cell is full, i.e. a minimum of 255 periods will be averaged.

One period is formed from 32 succeeding real time periods, as only 128 samples

are taken from the 4096 available time-slots. Therefore, to average 255 periods will last

$$32 \times 255 \times 163.84\ \mu s = 1.34\ sec. \qquad (4)$$

## Result

The resolution of the system must be divided in two contributions, jitter at the low-pass filter output and variations in the fundamental clock's period time. 50 psec (HF equivalent) jitter was measured independently of the window position. Temperature tests showed $\pm 5$ ppm variation over normal operation range. Jitter sets the resolution limit, when measuring short fibres, whereas clock frequency variations determine the resolutions for long fibre measurements.

The digital processor's ability to find noise hidden pulses limits the dynamic range of the system to 34 dB. Therefore, a fibre with 34 dB one way attenuation can be measured using double-ended technique, whereas practicable fibre length is given by the applied far-end-reflection, when using the single-end measurement.

The principles described herein have been submitted for patent applicant.

## Acknowledgement

The author wishes to thank Hans Damsgård, NKT Fibre and Cable R & D Department, as well as Gregers Mogensen and Peter Højergaard, both NKT Elektronik R & D Department, for many fruitful discussions.

## References

1. R. Kashyap, M.H. Reeve and S. Hornung: "Measurement of Strain Relief in an Experimental Optical Fibre Cable" Electronics Letters, 18th March 1982, vol. 18, No. 6, pp. 263-265

2. S. Tanaka, M. Hoshikawa, N. Kurauchi, Y. Katsuyama, and T. Horiguchi: "Precise Measuring Method of Elongation and Residual Strain of Optical Fiber Due to Cabling Processes" 7th ECOC

3. M. Johnson, and R. Ulrich: "Fibre-Optical Strain Gauge" Electronics Letters, 6th July 1978, Vol. 14, No. 14, pp. 432-433

4. Helmut F. Schlaak, and Michael Gwiazdowski "Optical Fiber Length Measurement by Pulsereflectometry" Frequenz, Vol. 35, 1981, No. 9, pp. 243-246

5. R. Yamauchi, K. Inada, Y. Sugawara, and T. Kobayashi "Elongations of Optical Fibers in an Optical Cable Under Installation" 4th ECOC

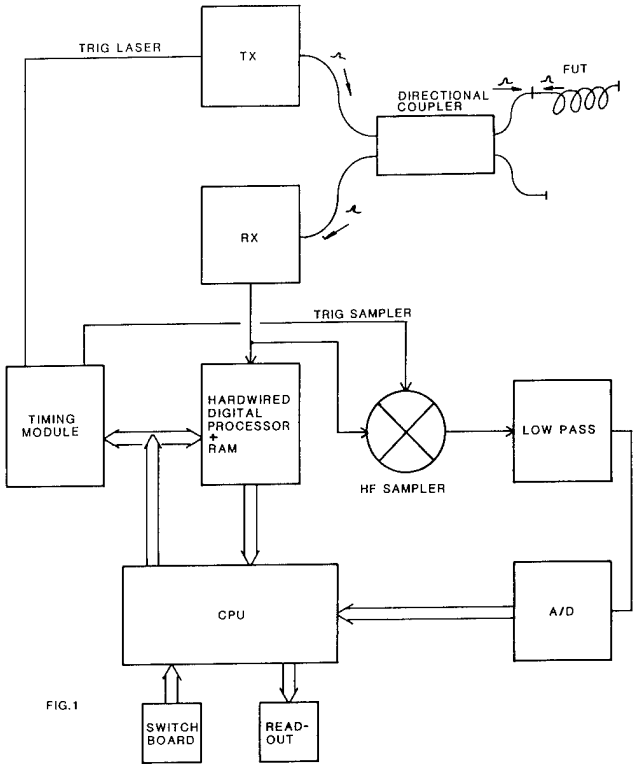
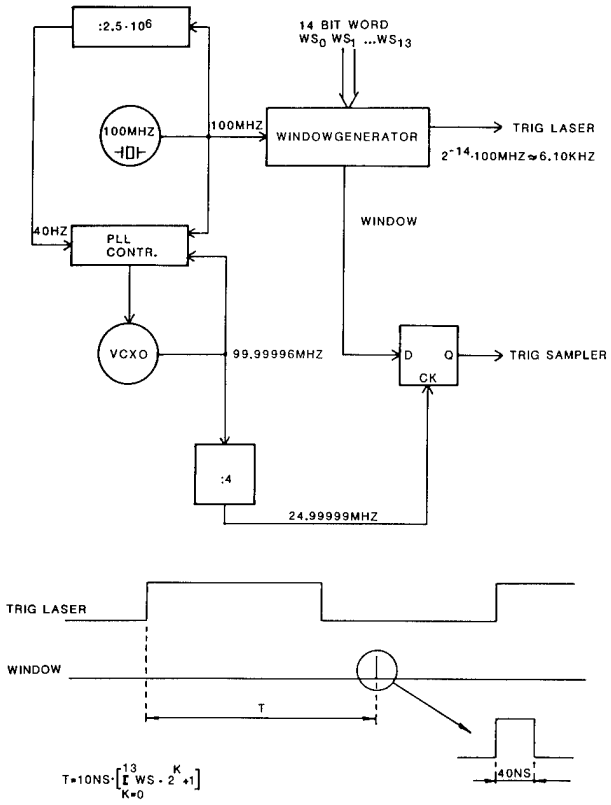



FIG.1

WINDOWSAMPLING

FIG.2



# New Field Measurement System for Single Mode Fiber Dispersion Utilizing Wavelength Division Multiplexing Technique

W. H. Hatton*, M. Nishimura*, W. Haltiwanger**

* Sumitomo Electric Research Triangle Inc.,
Research Triangle Park, NC 27709
** South Carolina Electric and Gas,
Columbia, SC 29218

## ABSTRACT

A new field dispersion test system has been developed to qualify the performance of installed single mode fiber cables. This new measuring system uses the modulation phase / multiple laser diode technique to determine dispersion values within a range of 1200 to 1330 nm. However, it eliminates the reference laser and fiber, common to this method, by the use of wavelength division multiplexing.

A detailed laboratory evaluation was conducted onto this system in order to examine the dynamic range, accuracy, and repeatability of this method. A series of field test were also conducted to verify the laboratory results, and to demonstrate the ease of working with this system in the field.

## INTRODUCTION

Chromatic dispersion, as well as attenuation, is a major factor in determining the transmission handling capability of a single mode fiber communication system. With the increasing need for high bitrate systems; field measurements of chromatic dispersion on installed single mode fibers are becoming more and more important.

Two techniques have been reported for field use; the modulation phase technique[1][2][3], and the swept frequency technique[4]. Of these two methods, the modulation phase technique is believed to be highly accurate (better than 0.1 ps/km/nm )[2]. Coupling this method with the multiple laser diode technique, enables dispersion to be measured over a broad band of wavelengths.

The principle of this method is to measure the group delay by detecting the modulation phases of sinusoidally modulated laser diodes, however, the drawback to this method is the requirement of a extra laser diode and fiber necessary for transmitting a reference signal.

In this paper, a new field chromatic dispersion system that incorporates the modulation phase method/multiple laser diode technique will be presented. The advantage of this new system is that the extra (reference) laser diode is eliminated by alternatively coupling the different wavelengths into the test fiber by the use of wavelength division multiplexing. Laboratory and field results will also be presented.

## SYSTEM DESCRIPTION/THEORY OF OPERATION

The new system was designed around the commercially available Ando AQ-7501 chromatic dispersion measurement system. This modified version is schematically shown in Fig. 1. Four laser diodes with different wavelengths ( 1.21, 1.27, 1.30 and 1.33 um ) are incorporated into this system. All four lasers are sinusoidally modulated by a synthesized signal generator. Four different modulation frequencies ( 6, 30, 200, 800 MHz ) can be selected depending on the stage of measurement.

Relative phase shift between the different wavelengths are determined by combining the 1.21 um wavelength light signal with one of the other three light signals ( alternatively selected by an optical switched ) through a single mode optical fiber coupler. The combined signals are then launched into the test fiber.

At the output end of the test fiber, the two light signals of different wavelengths are divided by a wavelength division demultiplexer and converted into electrical signals. Total phase shift ( system + test fiber ) between the two signals can be measured by a phase meter. The contribution to

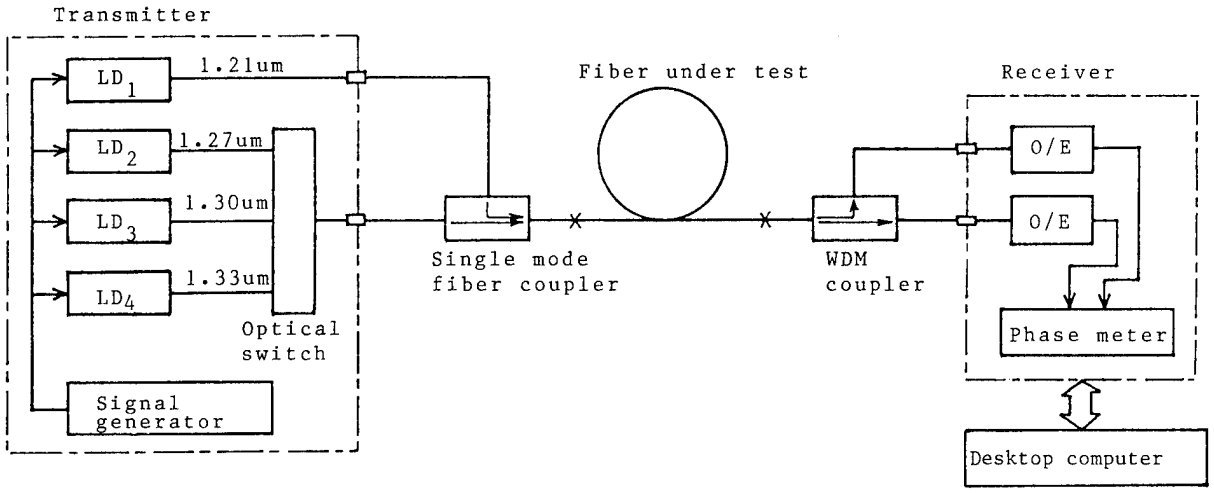



Fig. 1 Measuring system

total phase shift from the test fiber can be determined if system phase shift is known.

$$\theta_{\text{test fiber}} = \theta_{\text{total}} - \theta_{\text{system}}$$

This can be accomplished by measureing system phase shift prior to the measurement ( $\theta$ system can be determined by measuring a 1-2m fiber sample )

By coupling the different lasers into the test fiber, relative group delays between the 1.21 um signal and the three longer wavelengths can be determined.

Since higher modulation frequencies produce greater resolution in the measured group delay [2], the system was designed to operate at either 200 MHz or 800 MHz ( the modulation frequency used would depend on fiber length ).

The phase meter used in this system has a measurement range of 180°. Depending on the delay time of the test fiber, high modulation frequencies could produce a phase shift greater than 360°. To compensate for this problem, the lower frequencies are used to determine how many multiples of 360° must be added to the measured phase shift.

Relative group delay between the different wavelengths is calculated from the measured phase shift by using;

$$\tau\,(\text{ps/km}) = \frac{\theta_{TEST} \times 10^{12}}{360 \times F(\text{MHz}) \times L(\text{km})}$$

A Sellmeier representation is then used to fit the calculated data into a group delay curve;

$$\Delta\tau = A\lambda^2 + B + C\lambda^{-2}$$

where $\Delta\tau$ denotes the group delay as a funciton of wavelength, and the constants A, B, and C are determined by a least square means technique. Figure 2a shows a typical group delay curve obtained using this procedure.

Dispersion characteristics of the test fiber are determined by differentiating the fitted equation with respect to wavelength;

$$S(\lambda) = 2a\lambda - 2c\lambda^{-3}$$

where $S(\lambda)$ denote the dispersion as a function of wavelength. A representative dispersion curve can be observed in Fig. 2b.

## ERROR ANALYSIS

The modulation phase technique has been shown to be highly accurate[2], however, an examination on the error induced into the measured phases by wavelength division multiplexing was conducted to insure this level of accuracy.

For an ideal wavelength demultiplexer, each decoupled wavelength would be totally isolated, from the other wavelengths, at the output ports (Fig. 3a). Since commercially available demultiplexers are not ideal, each output port would include the desired decoupled wavelength plus a small fraction of the

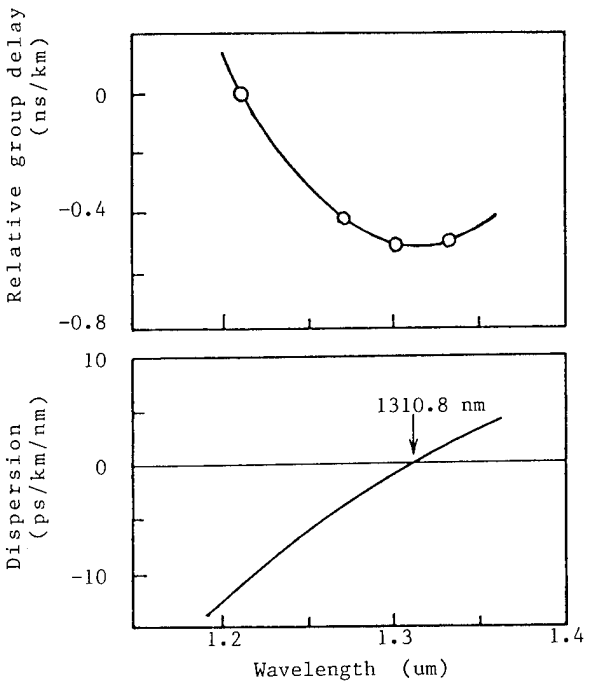



Fig. 2 Measurement result of a 9.2 km Single mode fiber

other decoupled wavelengths (Fig. 3b). The fraction of signal crosstalk is determined from the coupling efficency of the demultiplexer. If these unwanted signals are sufficiently large then a crosstalk induced phase shift will occur in the output signals. (Fig. 3c) This phase shift must be kept low to insure accurate dispersion measurements.

To determine the induced error, a theoretical analysis was conducted to observe the effects of wavelength isolation on phase error. The isolation between the output signals was effected by three factors.

$$R = P_{01} - P_{02} - (\alpha_2 - \alpha_1)L - \gamma$$

where R is the isolation or attenuation difference between wavelengths 1 and 2 at port 1, L is the total length of the test fiber, $\gamma$ is the demultiplexer decoupling efficiency, and $P_{01}$ , $\alpha_1$ and $P_{02}$ , $\alpha_2$ are the input power level and fiber attenuation of wavelengths 1 and 2 respectively.

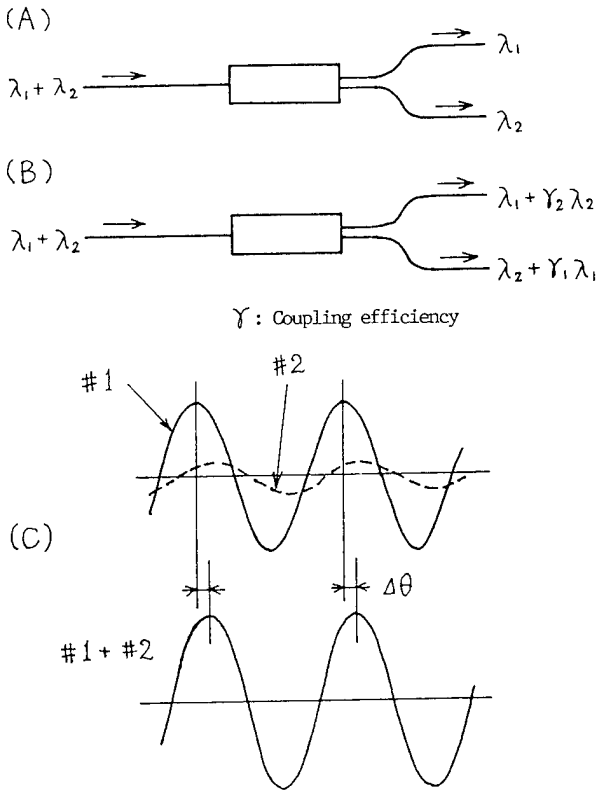



Fig. 3. Analysis of signal crosstalk
(A) Ideal demultiplexer
(B) Typical demultiplexer
(C) Crosstalk error

The phase error induced in wavelength 1 can be determined from

$$\theta = -\arctan\left(\frac{P_{21} \times \sin\theta}{P_{11} + P_{21} \times \cos\theta}\right)$$

where $P_{11}$ is the power level of wavelength 1 at output port 1, $P_{21}$ is the fraction of wavelength 2 at output port 1, and $\theta$ is the phase difference between the two wavelength ( $\theta = 90^\circ$ for worst case ). The relationship between phase error and wavelength isolation is shown in Fig. 4.

The systematic phase error was determined from measured wavelength isolations ( attenuation differences between the four (1.21, 1.27, 1.30, 1.33 um ) wavelengths at the output ports of the demultiplexer ). The lowest isolation was observed for the 1.27 um signal. The absolute value of this isolation was dependent on the test fiber length ( Fig. 5 ), however, for worst case analysis, wavelength crosstalk would induce a phase shift of .23° into the 1.27 um signal. This error would have negligible effect on dispersion measurements[2].

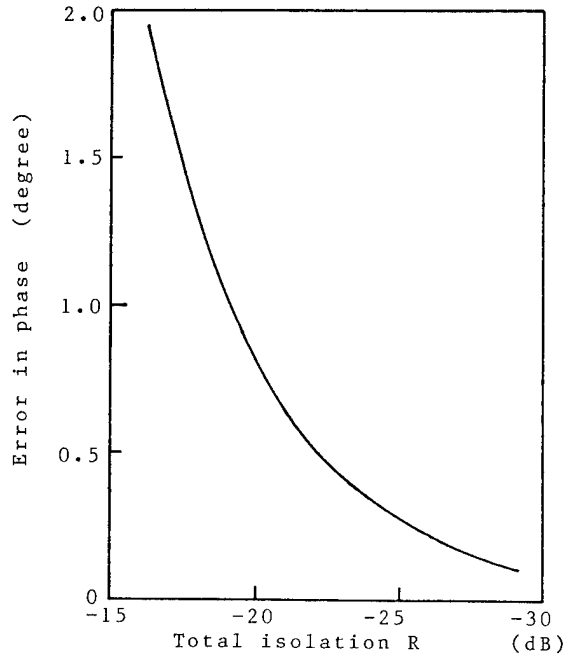



Fig. 4 Crosstalk error vs total isolation

## DYNAMIC RANGE

Field measurement systems designed to characterize installed single mode fibers must have the ability to operate over extremely long distance, therefore, it was imperative to verify the system's dynamic range. To obtain this information a sequence of test were conducted onto a 13.4 km section of fiber (total attenuation of -7 dB ). Measurements were conducted at both 200 and 800 MHz, and between each measurement, the total system attenuation was increased by the insertion of a series of inline attenuators.

Results obtained from this experiment are shown in Figure 6 and 7. For total attenuation less than or equal to -30 dB, a deviation of less than .01 ps/km/nm and .1 nm was observed in the measured dispersion values and zero dispersion wavelength respectiely.

When attenuation was increased above -30dB, a small error was observed in the measurements conducted at 800 MHz, however , higher stability, and a larger dynamic range ( -35 dB ) was obtain when the 200 MHz signal was employed.

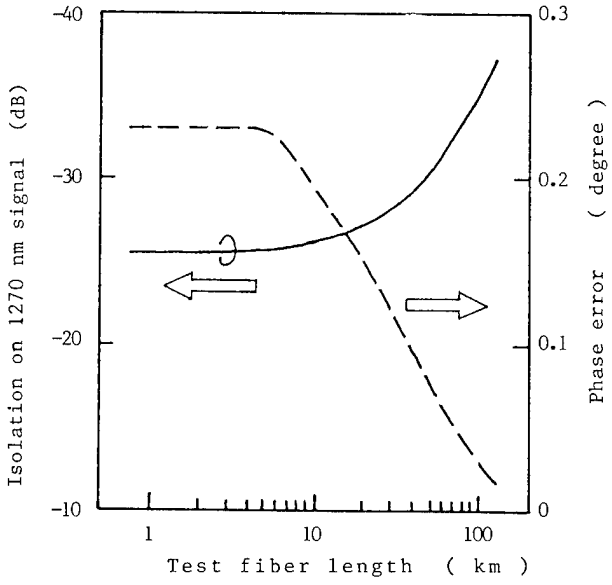



Fig. 5 Plot of estimated 1270 nm signal isolation and maximum phase error vs. test fiber length.

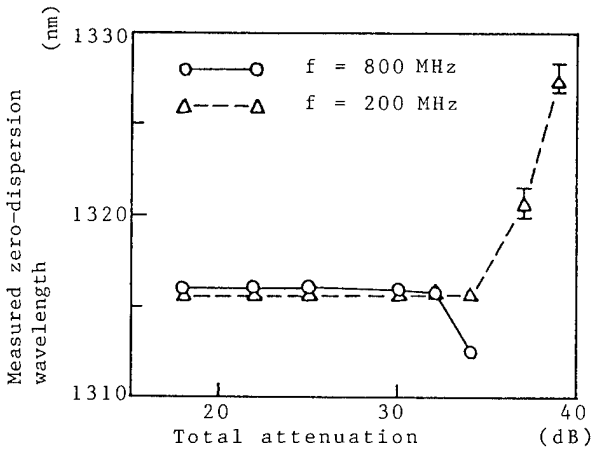



Fig.6 Measurement results of a 13.4 km fiber with different attenuators(1)

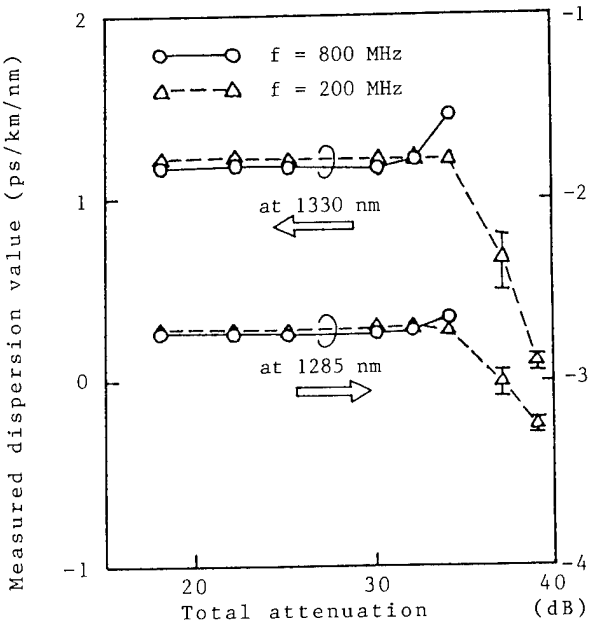



Fig. 7 Measurement results of a 13.4 km fiber with different attenuators (2)

## LABORATORY MEASUREMENTS

Before far end chromatic dispersion measurement could be made in the field, it was necessary to verify the repeatability and accuracy of this test system.

This was achieved by conducting measurements in the laboratory on a selected set of primary coated (silicone buffer ) single mode fibers. These fiber were selected so that the systems' performance could be evaluated over a wide range of dispersion values and lengths. Table 1 summarizes the result obtained from these fibers.

High repeatability was observed between measurement conducted on each fiber; a variation of less than .02 ps/km/nm and .03 nm was observed in the measured dispersion values and zero dispersion wavelength respectively.

To further characterize this system, several of the previously mentioned fibers were fusion spliced together to produce a total fiber length of 81.1 km, and total attenuation of -34.5 dB. ( including splice losses ). Dispersion measurements were conducted, and the results were compared to the predicted total dispersion .

Predicted dispersion of the spliced section was obtained from

$$\text{Spred.} = \frac{\Sigma S_i L_i}{\Sigma L_i}$$

where Si and Li were the measured dispersions and lengths of the individual fibers respectively.

Results obtained from this experiment are summarized in Table 2. A discrepancy of less than .02 ps/km/nm was observed between the predicted and measured values.

| Fiber # | Length (km) | Dispersion (ps/km/nm) 1285 nm #1 | 1285 nm #2 | 1330nm #1 | 1330nm #2 | Zero Dispersion Wavelength (nm) #1 | #2 |
|---|---|---|---|---|---|---|---|
| 1 | 13.3 | -3.90 | -3.90 | -.8 | -.8 | 1331.0 | 1331.0 |
| 2 | 5.9 | -1.64 | -1.63 | 2.34 | 2.33 | 1303.3 | 1303.2 |
| 3 | 8.0 | -2.37 | -2.37 | 1.57 | 1.57 | 1312.1 | 1312.1 |
| 4 | 9.8 | -2.43 | -2.43 | 1.43 | 1.43 | 1312.8 | 1312.8 |
| 5 | 9.2 | -3.17 | -3.17 | .74 | .74 | 1321.1 | 1321.1 |
| 6 | 8.0 | -1.55 | -1.56 | 2.34 | 2.35 | 1302.4 | 1302.6 |
| 7 | 8.8 | -4.15 | -4.15 | -.36 | -.36 | 1334.5 | 1334.5 |
| 8 | 7.5 | -2.47 | -2.47 | 1.44 | 1.44 | 1312.8 | 1312.8 |
| 9 | 8.7 | -3.38 | -3.38 | 1.39 | 1.39 | 1313.2 | 1313.2 |
| 10 | 5.1 | -3.66 | -3.65 | .11 | .11 | 1329.1 | 1329.1 |
| 11 | 10.3 | -2.90 | -2.90 | 1.05 | 1.05 | 1318.4 | 1318.4 |
| 12 | 14.2 | -2.54 | -2.54 | 1.12 | 1.12 | 1315.7 | 1315.7 |
| 13 | 8.6 | -2.70 | -2.70 | 1.10 | 1.10 | 1316.5 | 1316.5 |

Table 1 Measured dispersion values obtained from the selected group of primary coated single mode fibers. Each fibers was measured twice.

| Wavelength (nm) | Predicted Dispersion (ps/km/nm) | Measured Dispersion (ps/km/nm) |
|---|---|---|
| 1285 | -2.91 | -2.88 |
| 1300 | -1.57 | -1.57 |
| 1330 | .92 | .94 |

Table 2 Comparison between predicted and measured dispersion values for 81.1 km of fusion splice primary coated single mode fibers.

The laboratory evaluation thus showed the accuracy and repeatability of this test system. This analysis also demonstrated the ability to measure very long lengths of single mode fiber. The 81.1 km section of spliced fiber is the longest length to have had dispersion measurements conducted on to date.

## FIELD MEASUREMENTS

To demonstrate the practicality of this system, the performance of an installed 30.5 km section of Sumitomo OPGW ( Composite Fiber Optic Overhead ground wire ) was evaluated. Cable construction consisted of two buffer tubes, each containing six single mode fibers, stranded around the central strength member of the ground wire (Fig. 8).

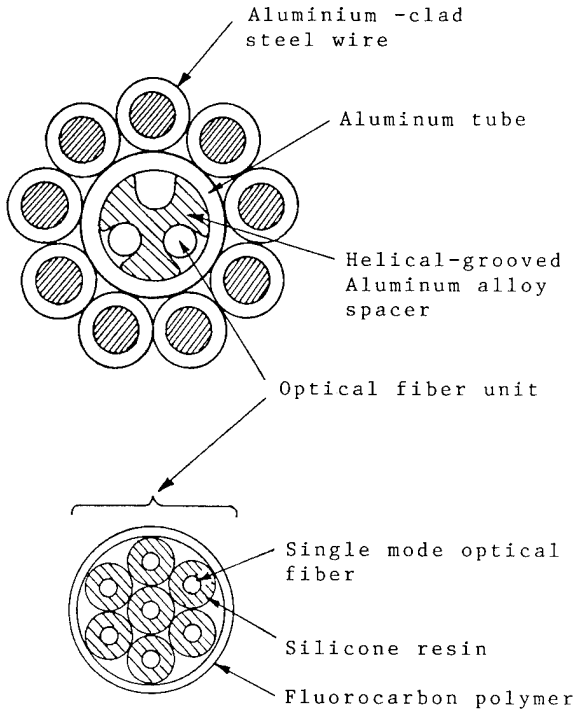



Fig. 8 Structure of OPGW

This particular span was located near St. George S.C. , and forms a part of the fiber network that South Carolina Electric and Gas are currently installing between Charleston and Columbia S.C. The installation route and splice point information of the St. George section is shown in Fig. 9. Once completed, the system will operate at a bitrate of 405 Mb/s.

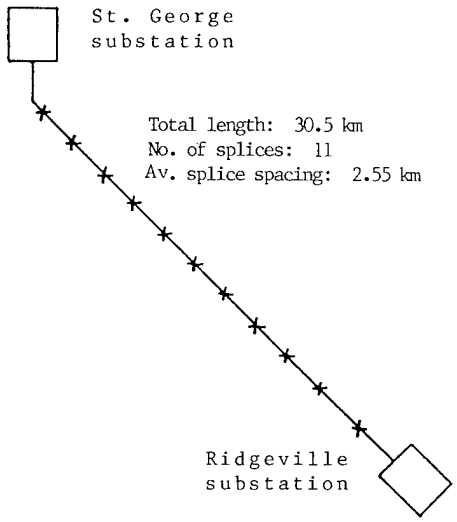



Fig.9 OPGW link tested in field trial of the dispersion measurement system.

The field dispersion equipment was arranged according to Fig. 1. With an operator at the transmitter side and one at the reciever side, chromatic dispersion of each fiber was measured. The measured dispersion characteristics of the installed cable are summarized in Table 3. Each fiber was measured twice, and a discrepancy of less than .02 ps/nm/km was obsereved.

| Fiber # | Measured Dispersion (ps/km/nm) | | | | Zero Dispersion wavelength (nm) | |
|---|---|---|---|---|---|---|
| | 1285 nm | | 1330 nm | | | |
| | #1 | #2 | #1 | #2 | #1 | #2 |
| 1 | -3.21 | -3.21 | .58 | .58 | 1322.8 | 1322.8 |
| 2 | -3.37 | -3.37 | .43 | .43 | 1324.7 | 1324.7 |
| 3 | -3.15 | -3.15 | .67 | .67 | 1321.8 | 1321.8 |
| 4 | -3.12 | -3.12 | .68 | .69 | 1321.6 | 1321.5 |
| 5 | -3.02 | -3.02 | .77 | .77 | 1320.4 | 1320.5 |
| 6 | -3.14 | -3.14 | .67 | .67 | 1321.8 | 1321.8 |
| 7 | -3.31 | -3.30 | .48 | .48 | 1324.0 | 1324.0 |
| 8 | -3.14 | -3.14 | .66 | .66 | 1321.8 | 1321.8 |
| 9 | -3.55 | -3.55 | .24 | .24 | 1327.0 | 1327.0 |
| 10 | -3.23 | -3.23 | .59 | .59 | 1322.8 | 1322.7 |
| 11 | -3.28 | -3.28 | .52 | .52 | 1323.5 | 1323.5 |
| 12 | -3.08 | -3.08 | .72 | .72 | 1321.1 | 1321.1 |

Table 3 Field results obtained on 30.5 km section of installed 12 fiber OPGW. Each fiber was measured twice.

This field evaluation was conducted prior to construction of the repeater stations, therefore, measurement conditions were less than ideal ( i.e. high humidity, high temperature, and cramped conditions ). Even with these extreme conditions, system set-up and operation was conducted without any problems. The dispersion measurement, including computer time, took less than 10 minutes per fiber.

## CONCLUSION

A new system for measuring chromatic dispersion in the field was described. This new system uses the modulation phase / multiple laser diode techniques, however, with the use of wavelength division multiplexing, the reference laser and fiber, common to these techniques, was eliminated.

Laboratory tests demonstrated that no significant error was introduced into the measured signals when wavelength division multiplexing was used, and that very long lengths of installed single mode fibers could be measured.

Field measurements demonstrated that this system could be used in the field, even when adverse conditions were experienced, and produce accurate and repeatable results. Set-up and measurement time was calculated to be less than 10 minutes per fiber.

Future requirements suggest the need for dispersion information around 1550 nm. This can be easily accomplished by adding one extra laser diode, operating around 1550 nm, to the existing system. With a small modification in the software used to curve fit the measured data, dispersion information for a wavelength range between 1200 to 1550 nm can be obtained. Laboratory results for this extended range will be presented at the conference.

## REFERENCE


(1) Vella P.J., Garel - Jones P. M., and Lowe R.S.: "Measurement of Chromatic Dispersion Long Spans of Single - Mode Fibre: A Factory and Field Test Method ", Electron. Lett., 1984, 20, pp. 167-168.

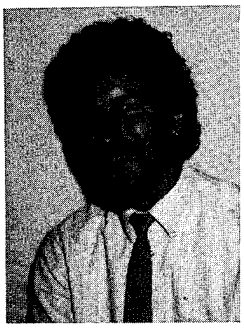
(2) Tanaka Shigeru, and Kitayama Yoshinobu: " Measurement Accuracy of Chromatic Dispersion by the Modulation Phase Technique " IEEE J. Lishtwave Technol., 1984, Vol. LT-2, pp. 1040-1044.

(3) Horiguchi Tsuneo, Tokuda Masamitsu, and Negishi Yukiyasu: " Chromatic Dispersion Measurements Over 50-km Single - Mode Fiber ", IEEE J. Lightwave Technol., 1985, Vol. LT -3, pp. 51-54.

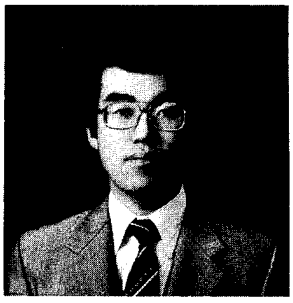
(4) Rao R.: " Field Dispersion Measurements - A Swept Frequency Technique ", Technical Digest of Symposium on Optical Fiber Measurement, 1984, pp. 135-138.



William Hatton was born in 1958 and recieved a M. S. degree in Electrical Engineering from North Carolina State University in 1983. He joined Sumitomo Electric Research Triangle Inc. in 1984, and has been engaged in the research and development of new measurement techniques for the characterization of optical fibers. He is a member of the Optical Society of America.



Wayne Haltiwanger was born in 1956 and has recieved Associate Degrees in Electrical and Electronic engineering and a Bachelor of Science degree in Electronic Engineering. He has been employed by South Carolina Electric and Gas for 7 and one half years where he is currently the telecommunication engineer responsible for the integrity of a 120 mile span, including local loops, of optical fiber.



Masayuki Nishimura was born in 1956 in Sapporo, Japan and received a M.S. degree in electronics engineering from the University of Tokyo in 1981. He joined Sumitomo Electric Industries, Ltd. in 1981 and moved to Sumitomo Electric Research Triangle, Inc. in 1984. He has been engaged in research and development of optical fibers and cables. He is a member of the Optical Society of America.

# INSERTION LOSS AND VSWR ANALYSIS OF COAXIAL CABLE

Arnold J. Daniels

TRW Inc.

ABSTRACT

This paper is based on IL (Insertion Loss) and VSWR (Voltage Standing Wave Ratio) test results for four (4) popular coaxial cables through a wide frequency range (5 MHz through 3.5 GHz), and an analysis of the data.

The data analysis includes:

a. Location of major impedance steps.
b. Calculation of VSWR at the connector interfaces.

Figure 1 contains a plot of IL versus frequency for RG-400/U, RG-402/U, SR-390 and double-shielded RG-316/U.

## INTRODUCTION

The computer age has brought a major change in the use of test data. BCTD (Before Computerized Test Data) the personnel responsible for test evaluation would spend hours analyzing the very limited data and could, based on practically nothing, generate volumes of conclusions.

Today, through the use of complex test equipment supported by a computer-controlled brain, we push the ON button and obtain volumes of test data. A very limited portion of the data is then used to extract the desired information. The remainder, although of little interest, is not destroyed. It is used to fill file cabinets, floppy discs, or whatever. To make matters worse, the user, who formerly had to be able to understand the inner workings of transmission lines to derive some intelligence from the limited data, is busy sorting through the voluminous amounts of data.

The analysis contained in this paper is not a new approach. It is the method used BCTD. It is hoped that, by reappearance in a 1985 publication, the sequence of application of basic transmission line theory will aide today's computer-oriented cable engineer in his/her examination of the electrical performance of a coaxial cable assembly.

## TEST

Four cable types were evaluated. Two of them are flexible coax--double-shielded RG-316/U and RG-400/U. Two of them are semi-rigid coax--RG-402/U (sometimes called SR-141) and SR-390.

The testing was done on an ANA (Automatic Network Analyzer). IL and VSWR measurements were made. Frequency range was 5MHz to 3.5 GHz in 5MHz steps. All test cable assemblies were 10 feet long. They were tested in a straight condition. Temperature was a nominal 23°C. Humidity was less than 30%.

The three smaller assemblies were terminated with compatible SMA's. The SR-390 connectors were TNC.

Scanning through the complete frequency range required four different equipment arrangements.

## DATA ANALYSIS

The analysis includes use of the data to:

a. Determine the location of major impedance steps.
b. Calculate the VSWR values at the connector interfaces.

Cable impedance (for 50 ohm cables ) is typically specified in MIL-C-17 as 50 $\pm$ 2 ohms, or 50 $\pm$ 1 ohm. This tolerance, however, is applicable to multiple production. Within the limited length of a typical cable assembly, the absolute value of cable impedance may range from 48 ohms to 52 ohms (for a 50 $\pm$ 2 ohm cable) but the total variation in impedance rarely varies more than several tenths of an ohm. Manufacturing controls are usually tight enough to prevent major deviation within short fncrements of cable length. It can therefore be assumed that the major impedance steps in a coaxial cable assembly occur at the interface between the cable and the connectors. Since total insertion loss of a coaxial cable assembly is primatily due to power dissipated (attenuation) within the cable, plus the reflection losses at the terminations, one typically expects to see the cable length as the distance between major impedance steps. TDR (Time Domain Reflectometer) measurements can be used to directly view impedance steps, but until fairly recently were frequency limited. Determining the distance between impedence steps at gigaherz frequencies can be accomplished by analysis

of the incremental VSWR data. This paper explains a relatively simple math procedure. It also demonstrates the method of extracting the nominal values of VSWR for the connector/cable mis-match at each end of a cable assembly, based on the min/max VSWR values at any frequency.

a. Determination of major impedance steps.

As previously noted, incremental cable impedance variation is small compared to the impedance steps at or adjacent to the connectors. In other words, it can be assumed that the VSWR peaks on plots of VSWR versus frequency are caused by termination reflection.

Analysis of the VSWR chart for RG-402/U:

There are 45 peaks between 2GHz and 3.5 GHz. 3.5 −2.0/45 = 33.333 MHz = average frequency delta between peaks.

$Vp = 3 \times 10^{10}$ cm/sec. for propagation in air.

$Vp$ in Teflon = $3 \times 10^{10} / \sqrt{e} = 3 \times 10^{10} / \sqrt{2.1} = 2.069 \times 10^{10}$ cm/sec.

The frequency $\Delta$ of 33.333 MHz represents a span of $180^{\circ}$. F = 2 X 33.333 = 66.667 MHz = the resonant frequency for the sample length.

$$\lambda = VP/F = 2.069 \times 10^{10}/66.667 \times 10^{6} =$$

$.0310 \times 10^{4}$ cm. = 310 cm. = 10.17 ft.

This is close enough to the cable assembly length of ten feet to substantiate the basic assumption that the terminations are the prime source of the impedance steps.

The RG-316 is in agreement. It has about 46 peaks from 2000 to 3500 MHz.

The SR-390 has only 34 peaks, but its dielectric is primarily air. The e value is 1.28 rather than 2.1. Its Vp therefore is $3 \times 10^{10} / \sqrt{e} = 3 \times 10^{10} / \sqrt{1.28} = 2.65 \times 10^{10}$ cm/sec.

Frequency $\Delta$ = 1500/34 = 44.11 MHz for 180° so F = 2 X 44.11 = 88.22 MHz.

$$\lambda = Vp/F = 2.65 \times 10^{10}/88.22 \times 10^{6} =$$

$.030 \times 10^{4}$ cm. = 300 cm. = 9.84 ft.

Similar to the analysis of RG-402 and RG-316/U, results are close enough to substantiate that the terminations are the prime source for the impedance steps.

The RG-400, however, is not in accord. It has 41 peaks, suggesting a much shorter overall length, or impedance steps within the cable that are similar to those at the termination. Subjecting the RG-400 to a TDR analysis is warranted.

NOTE: The values for Vp in air and cable dielectric constant are nominal. They suffice for purposes of this analysis.

b. VSWR determinations at cable terminations.

The test data identifies the combination effect of all the impedance steps. If it is assumed that each assembly has only two VSWR steps (one at each termination) then simple mathematics can be used to calculate the termination VSWR's.

Let $VS_{max}$ = Any peak VSWR

$VS_{min}$ = An adjacent valley VSWR

$VS_A$ = VSWR at one end = $VS_{max} \times VS_{min}$

$VS_B$ = VSWR at other end = $VS_{max} / VS_{min}$

$VS_{max} = VS_A \times VS_B$

$VS_{min} = VS_A / VS_B$

For low values of VSWR:

$VS_{max} = VS_A + VS_B - 1$

$VS_{min} = VS_A - VS_B + 1$

Combining these two equations:

$$VS_A = \frac{VS_{max} + VS_{min}}{2}$$

$$VS_B = \frac{VS_{max} - VS_{min} + 2}{2} \text{ or } VS_{max} - VS_A + 1$$

These equations were applied to the test results at locations that have a large $VS_{max}$ to $VS_{min}$ delta. The results are itemized in Table 1. Note: The formal identification of VSWR-- (Ex. 1.23:1) has been abbreviated to 1.23 to save space.

Table 1--VSWR Values

| CABLE TYPE | FREQ MHz | VS MAX | VS MIN | VS A | VS B |
|---|---|---|---|---|---|
| RG-316 | 2525 | 1.23 | 1.09 | 1.16 | 1.07 |
| RG-400 | 2450 | 1.45 | 1.09 | 1.27 | 1.18 |
| RG-402 | 2830 | 1.16 | 1.025 | 1.09 | 1.07 |
| SR-390 | 3260 | 1.20 | 1.01 | 1.10 | 1.10 |

## SUMMARY AND CONCLUSIONS

The RG-316 VSWR values, (see Table 1) indicate that since $VS_B$ termination has a VSWR of 1.07, and both terminations are the same type, then the $VS_A$ should be capable of much better performance.

The RG-400 VSWR values show that one termination is better than the other. However, even if both ends were 1.18, there would be a peak value at 2450 MHz of 1.39 -- (1.18 X 1.18).

The RG-402 and SR-390 VSWR values are indicative of well-made assemblies. Both terminations have low VSWR and are almost equal.

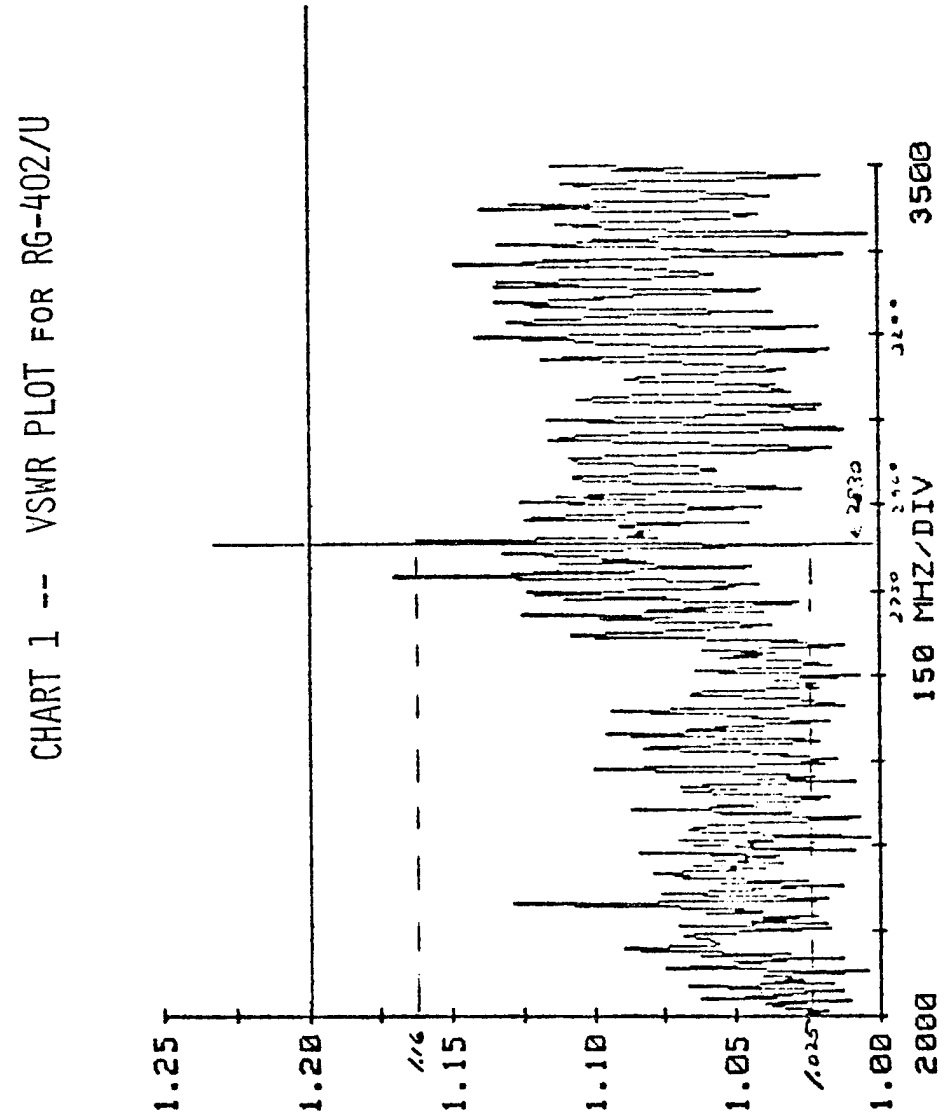
As noted for the analysis used to substantiate that, if there are major impedance steps, they typically occur at the terminations, the RG-400 assembly data suggests faulty cable. The other three cables performed well.

## REFERENCES

The Microwave Engineer's Handbook and Buyer's Guide, 1963.

Arnold Daniels is a Member of the Technical Staff in the RF Cable and Harness Engineering Department, TRW Inc. His experience in cable and connector technology encompasses ground, shipboard, aircraft and aerospace.

Note: The original computer printout data has been re-packaged into 15 pages of tables. It will be made available upon request.


CHART 1 -- VSWR PLOT FOR RG-402/U
1.25
1.20
1.15
1.10
1.05
1.00
2000
150 MHZ/DIV
3500

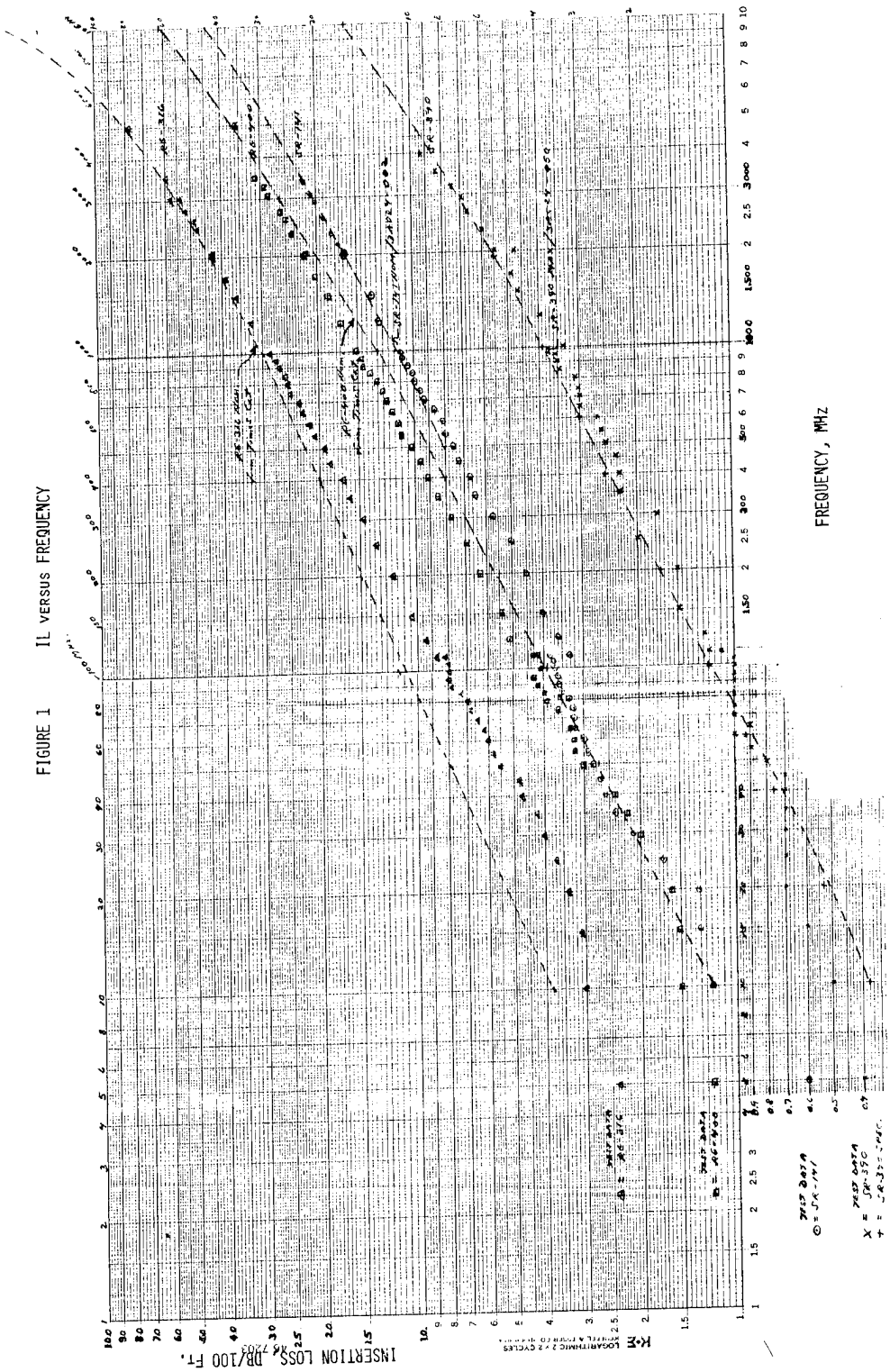



FIGURE 1 IL versus FREQUENCY

# QUALITY ASSURANCE APPROACH FOR FIBER OPTIC CABLE

P. A. Link B. R. Rapacki

Bell Communications Research, Inc.
Holmdel, New Jersey

## ABSTRACT

The capabilities of optical fiber as a transmission medium make it an attractive resource for meeting present and future needs for telecommunications services. Meeting these needs effectively and efficiently requires an effective means of assuring the quality of optical fiber cables. Traditional lot-by-lot acceptance inspection plans are insufficient or inefficient owing to their focus on only the end product and the limitations of the attributes information generated. Testing of the end product is partially destructive and time consuming for some parameters and infeasible for others. The approach described in this paper consists of an on-going surveillance program to verify implementation of effective controls by the manufacturer. Emphasis is placed on a new variables data analysis technique that obtains effective results from a minimum of samples. By comparing the manufacturer and customer test results on a small sample of in-process and final product, this technique allows for testing at the most economical points in the process as well as verifying manufacturer data, measuring the degree of process control and providing a conventional comparison with specified requirements. Examples are given that illustrate the differences between this and traditional quality approaches and describe the benefits to the customer and the manufacturer.

## INTRODUCTION

The capabilities of optical fiber as a transmission medium make it an attractive resource for meeting present and future telecommunications needs. Because of the high cost of replacing fiber optic cable and the even higher cost of an in-service failure, these needs can only be achieved with a high quality product. Thus it is important for a telephone company to have an effective means of assuring the quality of the fiber optic cables they purchase. This is particularly true in the present day environment of high demand, rapid evolution and many new manufacturers of fiber optic cable.

The quality assurance approach developed by Bell Communications Research (Bellcore) for fiber optic cable consists of an in-depth analysis of a manufacturer's process and quality controls and an on-going surveillance program. The analysis effort is a key factor in the overall approach because it provides the user with information that identifies those manufacturers that build quality into the product rather than attempt to test it into the product. However, once purchase decisions are made by a telephone company, there is a strong need to efficiently and effectively assure the on-going implementation of the manufacturer's controls and thus the quality of the cable. The surveillance program provides this assurance through a variety of activities, including a new variables data analysis technique that will be the focus of this paper.

## SURVEILLANCE PROGRAM

The surveillance program is the means by which the customer is assured of product quality by verifying a manufacturer's consistent, on-going implementation of process and quality controls. As described in this paper, it is a non-traditional quality assurance program because it assures product conformance without dependence on intensive product retest. However, to use this approach the customer must first determine that effective process and quality controls exist. This is achieved by an activity called a Quality Program Analysis (QPA), which examines a manufacturer's process controls in detail with respect to documented criteria.[1] Overall, fourteen major aspects of the process and quality program are reviewed. These elements are listed in the table below.

| | |
|---|---|
| 1. | Management Commitment & Organization |
| 2. | Documentation of the Quality System |
| 3. | Control of Design Changes |
| 4. | Control of Procured Material |
| 5. | Manufacturing Controls (In-Process) |
| 6. | Completed Item Inspection |
| 7. | Equipment Calibration & Maintenance |
| 8. | Control of Nonconforming Material |
| 9. | Storage, Handling & Packaging |
| 10. | Corrective Action Program |
| 11. | Product Identification |
| 12. | Periodic Product Qualification |
| 13. | Quality Information |
| 14. | Collection & Analysis of Field Data |

**Table 1.** The Fourteen Elements of a QPA.

The surveillance program uses two primary activities to provide a full scope of assurance to the customer. The first is called Periodic Product Qualification (PPQ). A manufacturer's PPQ program is originally reviewed as an element of a QPA, and then is continually reviewed as a part of the surveillance program. It involves periodic stress/environmental testing to protect against unforeseen problems caused by changes of design, materials, processes, or manufacturer's inspection philosophies. PPQ tests are performed by the manufacturer and witnessed by the customer. They should include environmental, mechanical and electrical stress tests that represent installation, maintenance, and environmental stresses. A list of recommended PPQ tests and corresponding EIA test procedures is shown in the table below.

| | |
|---|---|
| *ENVIRONMENTAL:* | Compound Flow (FOTP 81)<br>Low/High Temp. Bend (FOTP 37)<br>Temperature Cycling<br>Fluid Penetration |
| *MECHANICAL:* | Macrobending (upgradability to 1550 nm)<br>Tensile Loading/Bending (FOTP 33)<br>Cyclic Flex (FOTP 104)<br>Impact (FOTP 25)<br>Compressive Load (FOTP 41)<br>Twist (FOTP 85)<br>Jacket Elongation/Tensile (FOTP 89) |
| *ELECTRICAL:* | Dielectric Strength<br>Lightning Conduction |

**Table 2.** Recommended PPQ Tests.

The second activity of a surveillance program is called product/process verification. It is an activity that assures ongoing product quality by verifying both the contractual requirements to specifications and the manufacturer's test process controls and test data.

## PRODUCT/PROCESS VERIFICATION

### The Approach

The traditional approach to assuring the ongoing product quality consists of the customer inspecting samples of the product ready for shipment and making an accept/reject decision. The decision is usually based on attributes results (pass/fail) relative to the specified requirements. Because this approach considers only the end product and uses attributes data, the sample sizes required to obtain enough information to make an accurate decision are relatively large. The actual sample size required depends on the sampling plan used and whether decisions are made on a lot-by-lot, skip-lot or a time period basis. The most widely used attributes sampling plan today is MIL-STD-105D. A new skip-lot attributes plan that has some improvements over MIL-STD-105D is named Bellcore-STD-100.[2] Both will be compared later in this paper with a new variables sampling plan.

A more efficient approach to assuring ongoing product quality is to measure the degree of process control as well as product conformance to requirements. Good process control as demonstrated by low variability, allows supplier data to be used to help assess shipped quality, reflects on all product shipped rather than just the samples inspected and supports the customer moving away from lot-by-lot inspection towards time period decisions about the process and product (e.g. monthly). When done using variables data instead of attributes (i.e. using the actual test results instead of pass/fail results), the number of samples required to have enough information to make a decision is significantly less than that required by the lot-by-lot or skip-lot attributes plans.

While the more traditional attributes approach is still being used for the physical aspects of fiber optic cable, the process/product verification approach is now being used to assure a number of the optical parameters. A special, variables sampling plan, BELLCORE STD-400, was developed for use with this approach. It will be compared with the more traditional plans later in this paper.

### Application to Fiber Optics

Techniques such as the variables data approach described here are particularly useful in fiber optics because the uncommon nature of fiber optic cable make it impractical to focus on the end product alone. For example, it is not feasible to test for some performance parameters in finished product. Sometimes testing requires destruction of a piece of the cable or fiber and access to limited test facilities. Methods for testing some of the performance parameters are not consistent across the industry, and test sets are not always calibrated with traceable standards. Telephone company purchasing strategies also make it necessary to be able to verify parameters such as attenuation over an entire section of many cables as well as for individual cables.

The variables data approach represents an innovative quality assurance technique that responds to many of the challenges presented by fiber optics. It is simple in concept but powerful in the result it produces. It provides a means of testing a minimum of samples to compare the product with specified requirements, verify the manufacturer's results and measure the effectiveness of the process controls at the same time. It allows testing of samples at the most efficient point in the manufacturing process and inspires manufacturer attention to the precision of the testing and stability of the product between measurements. It reduces the number of cables that must be prepared, yet allows the verification of span loss requirements without measuring all or most of the cables in the span. Since it attains results with a minimum of samples and allows more efficient testing, it lowers the cost of verifying manufacturer's results and thus helps to maximize the payoff to a telephone company from receiving high quality cables made in an efficient process. This procedure is also a promising tool for future savings since it can be applied to most all performance parameters.

There are three major goals for the variables data technique.

- Make the manufacturer responsible for the quality of his product. Independently verify that he is doing it properly.
- Inspire processes and controls that build quality into the product rather than inspecting it in.
- Maximize the cost benefits of high quality to the customer. Excessive quality verification activities can be a significant burden on the manufacturer and will be reflected back in the cost of the product to the customer. Insufficient quality verification activities provide poor assurance that contract requirements are being met and little protection against expensive field problems and the associated customer dissatisfaction and loss of revenue.

### How It Is Done

The activity associated with this technique is a direct comparison and then statistical analysis of manufacturer and customer testing results on the same fibers. How repeatable is the test process? Can the customer use the manufacturer's results for engineering and planning or for comparison purposes if a field problem arises? How well-controlled is the test process? These questions are answered by the following:

1. Compare the manufacturer's (M) and customer's (C) readings on a fiber.
2. Determine the impact of the difference (M-C) by squaring it to get a *penalty* (P). (The rationale for using a quadratic penalty function is the topic of the next section.)
3. Compare (P) for each fiber sampled with a previously developed standard (S) that represents the average amount of variability one would expect to see in a well-controlled test measurement process. This creates an index (I) for each fiber with the desired level being 1.0 or less.
4. Summarize the results over a month's time to obtain enough data to decide about the process controls.
5. Statistically analyze the data to produce a quality rating.

This process is illustrated in the figure below.

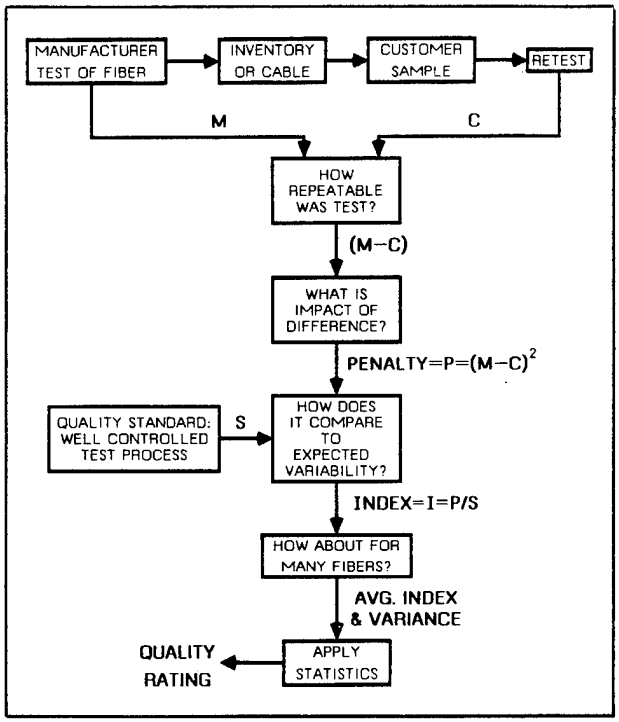



**Figure 1.** Flow Chart - Variables Data Analysis Plan.

The two test readings on a single fiber are obtained using the same test measurement process i.e., they are each made using a test set and operator from the group of test sets and test personnel available for the measurement in question. In this manner the repeatability of the overall test process is measured - including variability within test sets, between test sets and due to the operators and test procedures.

The first reading (M) is the one taken by the manufacturer as a normal part of the quality control or quality assurance program. For the case of an attenuation measurement, it is usually made after the fiber has been placed in a cable. For the case of a bandwidth or zero dispersion wavelength measurement, the reading is usually taken in the fiber spool stage before cabling. The second reading (C) is also made by the manufacturer, but witnessed by the customer. This is done on the customer's sample of the spooled or cabled fibers after the manufacturer has completed tests for the parameter under study.

### The Penalty Function

A quadratic penalty function was selected for this approach because, at this time, it most appropriately reflects the impact of poor test process repeatability on the customer. As illustrated by the following figure, the quadratic function assesses little penalty for small deviations between manufacturer's (M) and customer's (C) measurements. Small deviations in the measurements indicate a well-controlled process and have a small impact on the customer. Thus they should receive small penalties.

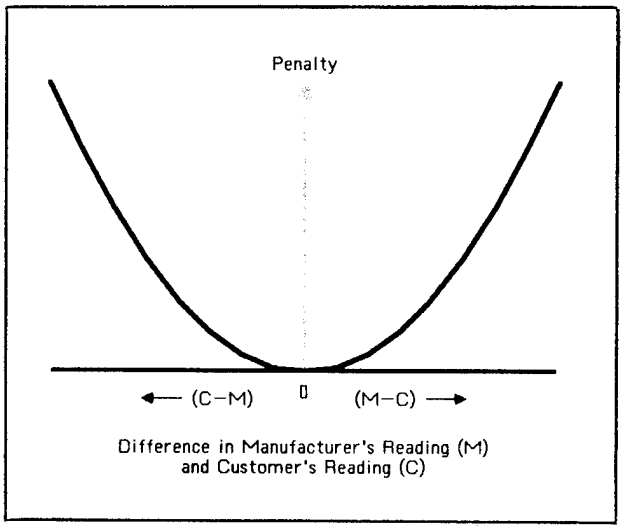



**Figure 2.** Quadratic Penalty Function.

When the differences between the manufacturer's and customer's measurements increase, the impact increases. While the impact increases slowly at first, there is a point at which the probability of a number of undesirable effects builds very rapidly. Manufacturer data may no longer be suitable to assess product quality, resulting in additional costs to the customer from doing quality assurance on a more traditional, sampling intensive basis. The product may not meet the maximum attenuation requirements as ordered. The customer has no accurate reference to determine if installation resulted in increased attenuation. Finally, assumed system margins may no longer be valid.

A linear penalty function does not accurately reflect the lack of impact on the customer of small differences in measurements. A cubic or higher order penalty function would accelerate the penalty more rapidly than can be presently supported by the potential effects of the uncertainty in the data. The quadratic function is the most representative of the situation at this time. Additional work is being done to better quantify the nonlinear effects and more precisely define the penalty function.

### Quality Standards

The quality standard (S) represents the expected amount of penalty when the test process has acceptable variability. Given that there is a test process variation of $\sigma^2$,

$$S=E[P]$$

$$S=E[\,(M-C)^2\,]$$

Using standard statistical techniques it can be shown that:

$$S=2\sigma^2$$

This is based on the assumptions that

1. There is no bias in the measurement process
2. The manufacturer's and customer's readings come from the same distribution since they are made using the same process.

The standard calculates to be two times the variance of a well controlled test process. Thus, to set the quality standard, one must define the variance typical of or desired of the test process for each

parameter. Using a standard of $2\sigma^2$ makes no assumptions about the underlying distribution of the test process (e.g., it doesn't assume normality).

To establish the desired variance of the test process one must consider both the capability of a well controlled process and the needs of the customer. Let us use attenuation as an example. A survey of the industry showed that laboratory test processes are capable of good repeatability with standard deviations as low as a couple of hundredths of a dB (0.02 dB). However, when multiple test sets and personnel are involved in a manufacturing environment, the capability can increase to 0.07 to 0.09 dB. Thus a quality standard equivalent to a standard deviation of 0.1 dB (a variance of 0.01 dB) would be reasonable with respect to process capability.

If one assumes an ordered loss of 0.5 dB/km, a reel length of 2.0 km and a normal distribution for the test process, some interesting statistics can be generated. If the allowed process standard variation is 0.1 dB, then about one third of the manufacturer's test results could be off by more than 10%. Virtually all readings will be within ±30% of the true value (i. e., ±0.3 dB). However, if the variability reaches three to five times this level, about one third of the manufacturer's readings could be off by more than ±20%. All readings will be within ±50% of the true value.

These results show that, even at present process capabilities, the customer may have to tolerate a small number of cables with sizeable errors in the data. Significant deviations from the present manufacturer capability could result in sizeable errors on significant portions of production, and could be considered unacceptable by the customer. The strategy used in introducing this plan was to start by setting the standard at the level equivalent to a $\sigma$ of 0.1 dB. Then, the objective is to better quantify the industry capability through data collection and analysis, help identify the reasons for the process variability and, finally, move the standard downward as appropriate.

### Sampling Plan for Variables Data

The final step in the variables data analysis technique is to apply statistics and come up with a quality rating. To do this, a sampling plan[3] was developed. BELLCORE-STD-400 not only may be used to detect shifts in variability of data (although this paper is limited to that aspect) but also to detect a shift in product quality.

If we assume that measurements of a particular parameter have been made by the manufacturer on each fiber, two things are possible under the variables data technique. First, we can review these measurements to see if they conform to specifications set by the customer. If they do not, the cable is rejected and supplier corrective action is generated. Second, we can remeasure a small sample of fibers and, using BELLCORE-STD-400, determine if we have confidence in the readings.

BELLCORE-STD-400 (as do the other BELLCORE-STD sampling plans) takes into account factors such as inspection costs, costs of field failures, and available resources (inspection personnel). Using BELLCORE-STD-400 formulas, one computes the recommended sampling frequency, $f$, and the number of consecutive units (fibers, in our case) on which to take measurements, $n$. Thus, the product $f \times n$ is the sample size over a given period of time. As will be shown in the next section, the sample size is low relative to attributes sampling plans such as MIL-STD-105D and BELLCORE-STD-100.

### Advantages

To summarize, the variables sampling technique has the following advantages over the traditional attributes sampling plans:

- *It results in lower sample sizes.* This thereby reduces the cost of personnel and material in preparing samples for inspection, reduces the time that the inspection equipment is used, and reduces personnel costs (both to the manufacturer and the customer) in performing the inspection. This is illustrated by an example shown later in this section.
- *BELLCORE-STD-400 reacts faster to changes in quality.* It will be shown that BELLCORE-STD-400 reacts to changes in process quality faster than the traditional MIL-STD-105D attributes sampling plan.
- *It provides sensitivity to problems in process and end product.* Since all data measurements are known, trends in quality can be identified more quickly. Therefore, there will be faster identification and resolution of problems and less defective product in the field.
- *It allows testing at the most efficient point in the manufacturing process.* Some manufacturers may choose to take measurements at the fiber stage for those attributes that normally do not change during the cabling process (such as bandwidth and zero dispersion wavelength). If this is the case, variables data may also be taken at this point and a sample need not be taken on the finished cable.
- *It retains the ability to reject product.* If a manufacturer's reading does not conform to contractual specifications, a nonconformance can be generated. Also, a nonconformance can be generated if a customer's retest measurement does not meet requirements.
- *The customer has access to all data measurements.* In traditional attributes sampling plans, the customer only has information on the portion of product that was selected as the sample. With all data measurements known, changes in attenuation caused by the installation process can be determined.
- *The true readings are known.* Attributes data provide only a indication of pass/fail. A "failure" could be a measurement that was only slightly outside specifications, or one that could be orders of magnitude defective.
- *Span requirements can be verified.* Since all attenuation measurements are known, span loss measurements can be calculated and compared to requirements.

### Examples

The following example shows the advantage of lower sample size and increased detection power over traditional attributes sampling plans. For this example, the following parameters were assumed:

- A monthly production of 90 cables.
- An average of forty fibers per cable. Therefore, production is assumed to be 3600 fiber lengths per month.
- Weekly accumulation of product into lots. Therefore, 840 fiber lengths per lot.
- A standard of 0.01 (1.00 Defects Per Hundred Units [DPHU]).

First let us compute the sample sizes that would be used if MIL-STD-105D were the sampling plan. At level II, normal inspection, a lot size of 840 and a standard of 1.00 DPHU results in a sample size of 80. Similarly, at reduced inspection (as a result of good quality history), the sample size would be 32, and at tightened inspection (as a result of bad quality history),the sample size would be 80. At 4.286 weeks per month (30/7), this would be 137, 343, and 343 samples per month, respectively, for reduced, normal, and tightened.

Sample sizes for both BELLCORE-STD-100 and BELLCORE-STD-400 depend not only on past quality history, but also on other

factors such as cost of inspection, cost of a field failure, and available resources. If we make reasonable estimates for costs and resources, we can compute sample sizes for good, average, and poor quality history (corresponding to reduced, normal, and tightened inspection under MIL-STD-105D, respectively) as shown in the below table.

| | SAMPLING INTENSITY | | |
|---|---|---|---|
| SAMPLING PLAN | RED. | NORM. | TIGHT. |
| MIL-STD-105D | 137 | 343 | 343 |
| BELLCORE-STD-100 | 85 | 170 | 255 |
| BELLCORE-STD-400 | 36 | 72 | 104 |

NOTE: The sample sizes shown for the variables data sampling plan represent theoretical minimums. In practice, a higher minimum may have to be set to assure that enough data would be available to provide statistical significance over the monthly rating period.

**Table 3.** Monthly sample sizes.

Other monthly production examples would produce similar reductions in sample size per month.

To show that the BELLCORE-STD plans react faster than MIL-STD-105D to changes in quality, consider another example. Assume that the production level and standard were as before, and further assume the following time sequence (no prior history known):

- Excellent quality for 14 lots (zero defects).
- A "bust" on the 15th lot (number of defects found is greater than allowed).
- Another "bust" on the 19th lot.
- Excellent quality on the next 8 lots.

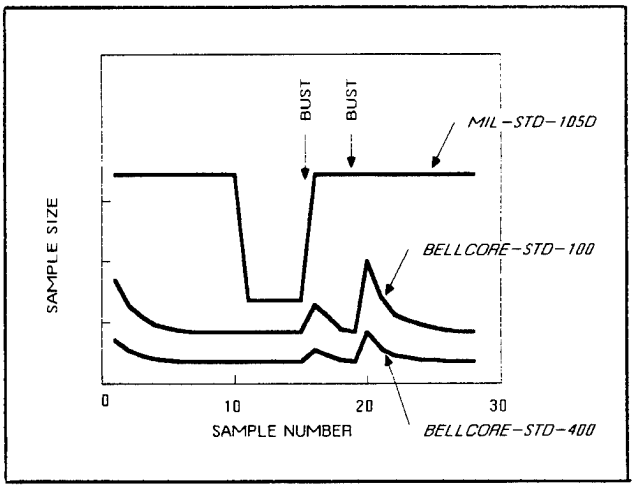



**Figure 3.** Effect of Quality Changes on Sample Size.

As shown in the above figure, after 10 lots, MIL-STD-105D would shift from normal inspection to reduced. The bust at the 16th lot would shift from reduced to normal under MIL-STD-105D. The second bust at the 20th lot would shift from normal to tightened, and shift again from tightened to normal at the 25th lot, under MIL-STD-105D. Using the BELLCORE-STD plans, sample sizes would be adjusted downward and upward more quickly.

The variability of sample sizes under BELLCORE-STD-400 is smaller than the other two sampling plans shown. This is because the power of the variables approach keeps the sample size at a low level regardless of the quality.

Although not shown in the figure, both BELLCORE-STD-100 and BELLCORE-STD-400 would still result in a decrease in sample size over MIL-STD-105D in a situation of continued poor quality.

**Analysis of Data**

Data have been collected and analyzed for the following three parameters:

- Attenuation (both single mode and multimode)
- Zero dispersion wavelength (single mode).
- Bandwidth (multimode).

Attenuation is probably the single, most important optical parameter to a telephone company. The level of attenuation determines if the transmission system will work initially as expected and if there is enough margin to allow for aging, maintenance and planned upgrades or expansions over the life of the cable. It is the one optical parameter that can change during cable manufacture, installation and use. Attenuation is also one of the more troublesome parameters to measure. It requires destruction of a small piece of cable during each test and a lengthy preparation of the cable end for testing.

Zero dispersion wavelength is included in this activity because it is not readily measured in the final product. Zero dispersion wavelength is now measured using a expensive, sophisticated test set-up that requires special safety precautions. It is usually measured in the fiber spool stage because of the need to use long lengths of fiber to achieve accurate results. Thus, it is more efficient to use the new variables approach to verify the manufacturer's measurements than to attempt measurements in the final product.

Bandwidth is included because it is an important parameter for multimode fiber. It is also the parameter that has the most variability in measurement, primarily because of variability in launching conditions.

Almost 8400 data comparisons in attenuation measurements have been analyzed. A total of four manufacturers have been included in the analysis, and measurements have been taken for both single mode and multimode fibers and at two wavelengths (800 and 1300 nm for multimode and 1300 and 1550 nm for single mode). Measurements have also been analyzed for zero dispersion wavelength and bandwidth.

Some interesting conclusions can be drawn regarding attenuation, zero dispersion wavelength and bandwidth results:

1. Test process repeatability for attenuation is about the same regardless of wavelength. While additional variability was expected at 1550 nm compared to 1300 nm, the data show no difference.
2. There is no bias in the test processes analyzed to date. Differences are due to variability within test sets, between test sets and between operators.
3. Due to the sensitivity of the test process, small problems can lead to large variations in measurements. This is an excellent

tool to monitor the process.

4. Suppliers can readily meet the original standards set on the basis of process capability.
5. Data are well behaved as represented by symmetrical, unimodal distributions.
6. Causes of random errors can be identified and repeatability can be substantially improved.

One of the ways that data are analyzed is to plot differences in manufacturer's and customer's readings versus observation number, as shown in Figure 4.

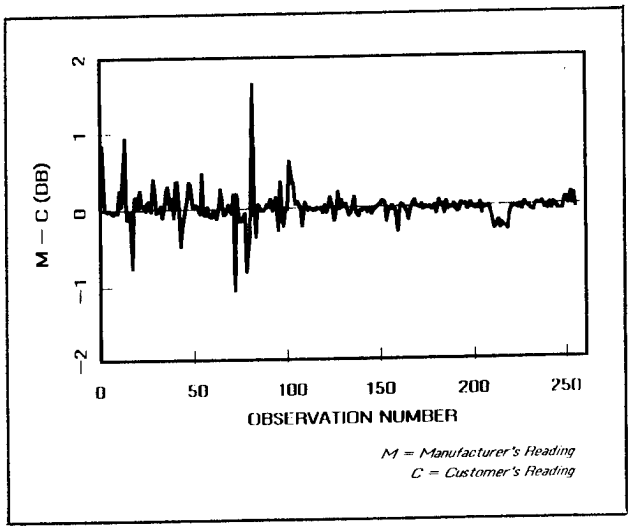



**Figure 4.** Differences in fiber attenuation measurements.

The figure shows two things of note. First, it shows sensitivity of the variables data to a temporary problem created in one process and the resolution of that problem. Second, it shows an average difference over the 255 readings of near zero difference. That is, one reading is, on the average, neither consistently higher or lower than the other. This indicates no bias in the test process and is typical of all processes analyzed to date. The lack of test repeatability is due to random variability in the process.

Another way in which the data are analyzed is to plot a histogram of differences in readings versus number of occurrences. A typical plot is shown in Figure 5, which is a composite of all data readings collected. Data are grouped into 0.03dB differences in manufacturer's and customer's readings. Hence, the center bar, labeled "0.00", would contain readings of -0.01, 0.00, and +0.01dB. Data outside the range ±0.56dB have been truncated for this figure.

Figure 5 shows a well behaved, symmetrical, unimodal distribution centered at close to zero difference. The average of the nearly 8400 data points on attenuation was only +0.0089dB. Had there been a substantial bias in the differences, a plot of this type would have readily shown it. Similar analyses have been done using data on zero dispersion wavelength and bandwidth.

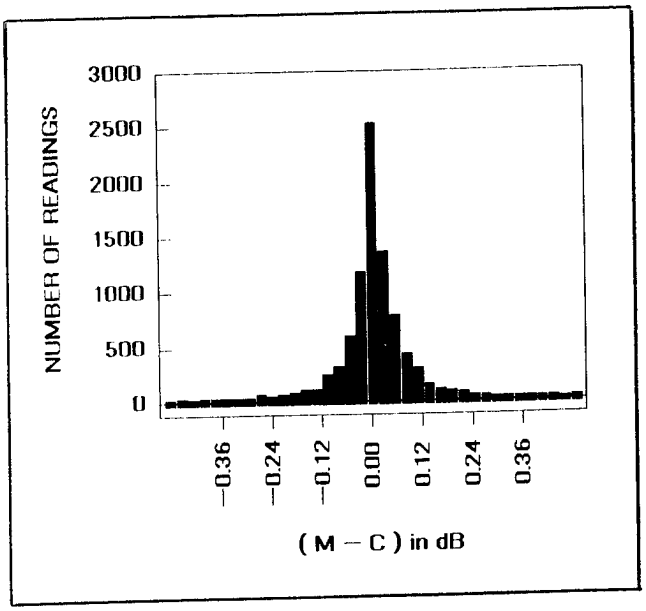



**Figure 5.** Histogram of attenuation readings.

One additional data analysis tool is used in the data analysis process. To show a manufacturer's quality history over a period of time, Bellcore generates *trend charts*, which contain:

- *Long Run Averages:* The circle is the long run process quality average and is calculated by averaging sample data over the five previous rating periods and the current period.
- *Current Index:* The "x" on the chart represents the index for the current rating period.
- *Best Measure:* The bar is the best measure of quality, and is the weighted average of the long run average and the current period's sampled data.
- *Interval Estimate:* The vertical bar is the 90% confidence limits of the current period's quality.

An example of a trend chart (purely hypothetical) is shown in Figure 6.

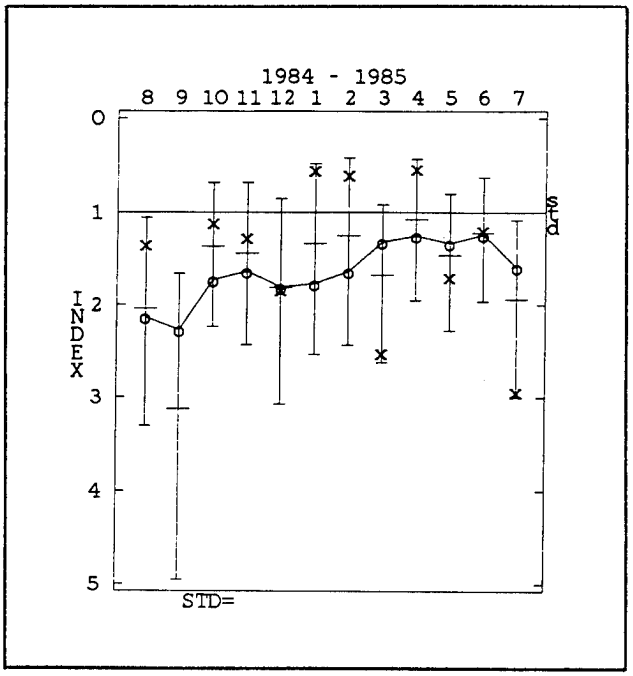



**Figure 6.** Typical trend chart.

## FUTURE GOALS

Data have also been collected on the following dimensional and optical parameters:

- Cladding Diameter
- Macrobending Loss
- Cutoff Wavelength

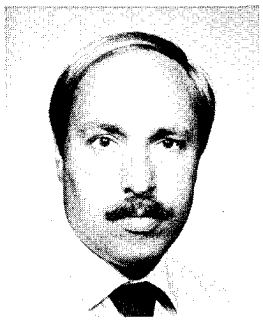
Plans are to start collecting data on mode field diameter.

Although data on these attributes are sparse, enough data have been collected to show that these attributes, as well as other optical and dimensional attributes, could be sampled using the new variables data analysis technique. Expansion to include additional parameters would increase the effectiveness of the new variables data sampling technique.

Also planned are refinements to the existing quality standards. Standards were originally set to those attainable by a number of manufacturers. Since then, a review of the data shows that reductions of the standards are in order because of refinements in the state of the art for the manufacture and measurement of optical fiber. A redefinition of standards would better represent the needs of the customer by representing the lower costs to the customer from improved product quality.

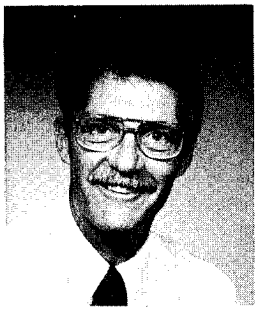
## REFERENCES

1. Bellcore Technical Reference TR-TSY-000039, *Quality Program Analysis,* Issue 1, March 1985.
2. Bellcore Technical Reference TR-TSY-000016, *BELLCORE-STD-100 & BELLCORE-STD-200,* To Be Issued.
3. Bellcore Technical Reference TR-TSY-XXXXXX, *BELLCORE-STD-400 - A Variables Sampling Resource Allocation Plan,* DRAFT.



P. Allen Link
Bell Communications Research
Crawfords Corner Road
Holmdel, NJ 07733

P. Allen Link received a BSEE degree from Lafayette College in 1968 and an MS degree in Systems Engineering and Operations Research from the University of Pennsylvania in 1970. From 1968 through 1983 he was in the Bell Laboratories Quality Assurance Center where he developed quality assurance procedures and standards for wire and cable, fiber optic, microwave radio, PBX and digital carrier products. Since 1984, Mr. Link has been with the Quality Assurance Technology Center in Bell Communications Research where he is the District Manager responsible for quality and reliability criteria, anaylses and surveillance program development for fiber optic and digital terminal products.



B. R. Rapacki
Bell Communications Research
Crawfords Corner Road
Holmdel, NJ 07733

B. R. Rapacki received a BSEE degree from Fairleigh Dickinson University in 1965 and an MSEE degree from Polytechnic Institute of Brooklyn in 1968. He joined Bell Telephone Laboratories in 1963. From 1965 to 1974 he was a Member of Technical Staff in the Reliability Engineering Center and worked on a variety of military projects. In 1974, he transferred to the Quality Assurance Center. His activities included product performance survey development on PBXs and quality surveillance on customer premise equipment. In 1984, he joined Bell Communications Research and had responsibility for quality engineering on a variety of switching equipment. He now has responsibility for quality and reliability efforts on optical fibers and fiber optic cable.

# ADVANCES IN THE OPTIMIZATION OF MULTI-LAYER SHIELD DESIGNS

John W. Kincaid Jr.

James A. Krabec

Belden Technical Research Center
Geneva, Illinois

## ABSTRACT

Empirical results for the optimization of multi-layer shields are presented. The surface transfer impedance characterization is utilized as the primary optimization parameter. Results for single layer braid and foil shields are discussed in the diffusion and inductive coupling frequency zones. Considerations for double braid and foil plus braid designs are given. Practical examples of three layer designs (foil/braid/foil) for local area network (LAN) and CATV cabling are presented.

## INTRODUCTION

In cable shield design, optimization is the process of adjusting mechanical and electrical design parameters to achieve maximum performance. The number of descriptors needed to define performance is a function of the many variables in any given application. These variables include mechanical handling characteristics such as weight, flexibility, connectorization and flex life, operating temperature range and chemical reactivity. Also included are the cable transmission path characteristics associated with the shield and the decoupling role the shield plays in isolating the transmission path circuit from external circuits. Elaboration of the shields decoupling role makes prominent such factors as frequency of interference (audio, video, VHF, UHF) type of interference (predominately E, electric field, predominately H, magnetic field, combined E and H near field effects, and traveling wave type electromagnetic fields) and circuit impedance levels. Practical cable shields are optimized in some sense with respect to cost and all of the above performance factors which are pertinent to the cables end use environment.

In retrospect, standard flexible cable shield design procedures used over the years have specified additional layers of shielding when more shielding effectiveness has been required. Gains achieved by optimizing single layers such as braid or foil are not comparable to the gain achieved by simply adding an additional layer. Optimization of single layer braid or foil designs is based on approximate theoretical models and empirical results.

Theoretical models of multi-layer foil/braid (tinned copper braid, aluminum foil) designs are not available and design schemes have relied on an apparent direct proportionality between the number of shielding layers and the amount of shielding effectiveness. By simply employing multiple foil/braid layers it is possible to practically realize shielding effectiveness in excess of 100 decibels and satisfy most applications.

However, this approach has been fully exploited due to the increased importance of cable shielding caused by such factors as FCC regulations, proliferation of local area network metallic cabling systems and the generally increased awareness of the importance of EMC (Electromagnetic Compatibility). Beyond a certain point, the small gains in shielding effectiveness yielded by simply adding another layer are quickly offset by the added burden in cable size, weight, connector incompatibility, installation problems and cost.

This paper focuses on one aspect of the "decoupling role", or shield effectiveness function. Development work has primarily utilized the surface transfer impedance[1], $Z_t$, characterization of a cable shield for definition of optimized performance. The design with lowest $Z_t$ provides maximum decoupling and is optimal. The work has been primarily empirical. A computer automated transfer impedance set-up was used[2]. Optimization of single layer braid and foil shields is discussed in the diffusion and inductive coupling frequency zones, Empirical results are presented. Next, optimization considerations of double braid and foil plus braid two layer shields are discussed. The paper concludes with an example of how optimized three layer shields can be used to good advantage over four layer shields currently used for local area network cabling and CATV drop cable.

## SURFACE TRANSFER IMPEDANCE CHARACTERISTICS

The $Z_t$ versus frequency characteristic of flexible cable shields may be thought of as having two zones; the low frequency or diffusion coupling limited zone and the high frequency or inductive coupling limited zone. This is illustrated in figure 1 along with the $Z_t$ characteristics of a seamless tubular shield.

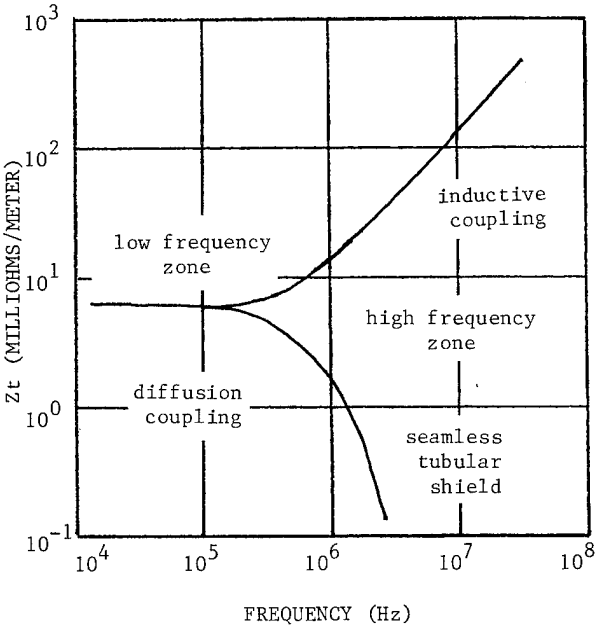



Fig. 1 - Components of transfer impedance vs. frequency.

The seamless tubular shield exhibits decreasing transfer impedance in the high frequency zone whereas flexible shields composed of one or more layers of foil or braid exhibit an increasing transfer impedance characteristic. Of course, seamless tubular shields are too inflexible and unwieldy for many applications; however, the $Z_t$ characteristic of this shield type provides a benchmark for flexible shields.

In the low frequency zone the transfer impedance is forced to be non-zero because of the finite conductivity of all metals. In this zone $Z_t$ is equal to the DC resistance of the shield. Thus, optimal performance implies lowest possible DC resistance. For braid shields this implies large cross sectional area braid wires, low wrap angle measured with respect to the cable longitudinal axis, and high percent optical coverage. Likewise for foil shields, the low DC resistance criteria implies cigarette wrap of foils with large cross sectional area.

In the high frequency zone two factors force the transfer impedance to be non-zero. First, finite conductivity imposes a non zero $Z_t$ even for seamless tubular shields. Second, braid and foil shields have built-in characteristics which allow them to be flexed but also permit inductive coupling and the increasing $Z_t$ characteristic.

## OPTIMAL BRAID

The braid shield has been studied by many workers [3, 4, 5] and today there is a very good general understanding of how coupling takes place through the braid. Nonetheless, the braid is sufficiently complex to make optimization on empirical art. Figure 2 is a plot of $Z_t$ at 100 MHz versus braid angle ($\alpha$) and percent coverage (K) for the braid constructions detailed in table 1. The existence of optimal $\alpha$ and K combinations is evident in the data points and fitted second order surface. These optimal combinations are not predicted by know engineering models of the braid shield [6]. Figure 3 compares the fitted second order surface of figure 2 with the engineering model surface.

The optimal angle/percent coverage combinations are understood to arise when the inductive coupling mechanisms partially cancel each other.

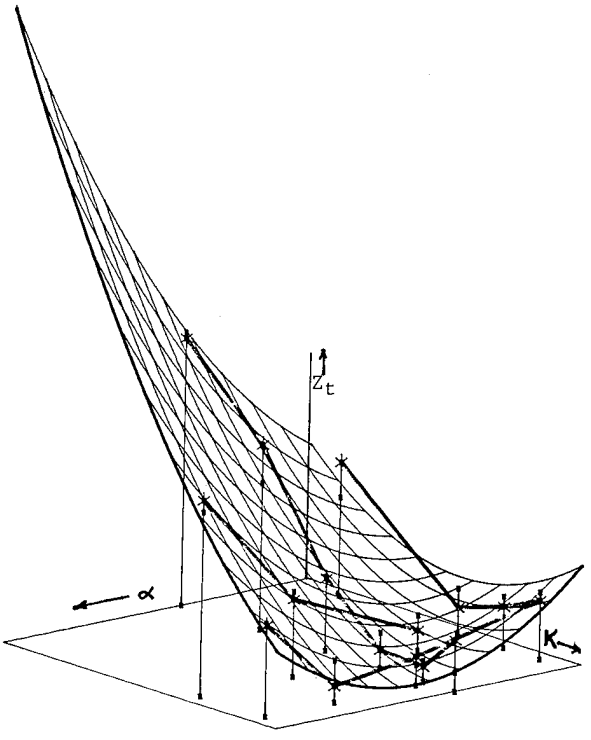



Fig. 2 - Surface fitted to transfer impedance data from Table 1 braid designs, at $10^8$ Hz.

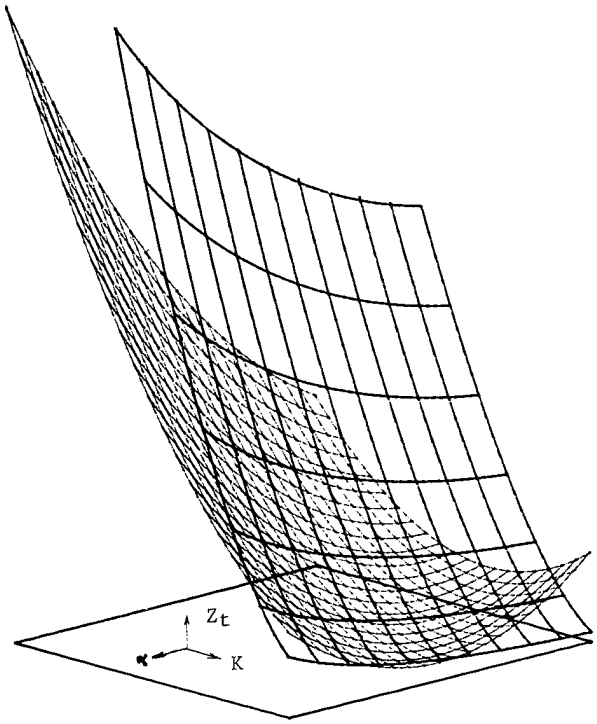



Fig. 3-Comparison of fitted second order surface with engineering model.

Table 1 - Braided Shield Designs

Material: Tin Plated Copper
Strand Diameter: .005 inch (36 AWG)
Diameter Under Braid: .143 inch
Number of Carriers: 16
Conductivity: 5.8 x $10^7$ mhos/meter
Optical Coverage: K (% covg. = 100K)
Braid Angle: $\alpha$
Number of Ends/Carrier: N

| Curve No. | 100K (%) | $\alpha$ (Degrees) | N | $Z_t$ @ 100MHz (mohm/m) |
|---|---|---|---|---|
| 1 | 90.8 | 17.0 | 8 | 570 |
| 2 | 90.8 | 33.2 | 7 | 280 |
| 3 | 90.6 | 43.9 | 6 | 160 |
| 4 | 90.5 | 53.0 | 5 | 880 |
| 5 | 95.3 | 31.8 | 8 | 500 |
| 6 | 90.1 | 31.8 | 7 | 150 |
| 7 | 83.0 | 31.8 | 6 | 180 |
| 8 | 73.9 | 31.8 | 5 | 700 |
| 9 | 63.0 | 31.8 | 4 | 1,800 |
| 10 | 50.1 | 31.8 | 3 | 2,600 |
| 11 | 79.7 | 24.5 | 6 | 200 |
| 12 | 79.8 | 40.9 | 5 | 750 |
| 13 | 80.0 | 53 | 4 | 1,900 |
| 14 | 84.7 | 17 | 7 | 400 |
| 15 | 77.2 | 17 | 6 | 250 |
| 16 | 57.5 | 17 | 4 | 1,300 |

For the braid designs given in Table 1, the empirical data in figure 4 show that there can be up to an order of magnitude difference in $Z_t$ between two 91% coverage braids with different braid angles. Likewise figure 5 shows the importance of braid angle selection for 80% coverage braids. Figures 6 and 7 show the variation in transfer impedance with % coverage when braid angle is held constant at 17° and 32° respectively. The data suggests the optimal percent coverage/optimal angle relationship given in figure 8. Here the optimal 91% coverage braid exhibits lower transfer impedance than the optimal 80% coverage braid. There is some evidence that the optimal braid designs are quite sensitive to small changes in braid construction. For example, the 90% coverage/32° angle construction is significantly better than 91% coverage/33° angle construction in figure 4. The data were obtained for the same braiding machine at different times with slightly different gearing ratios.

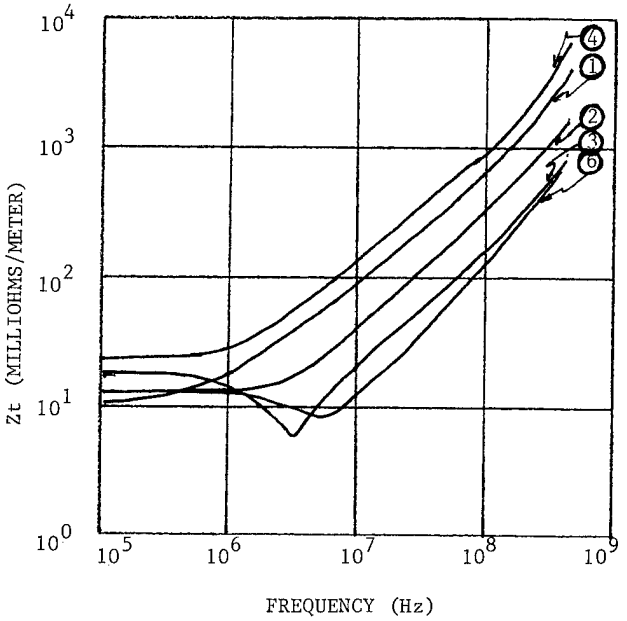



Fig. 4 - Variation in transfer impedance vs. braid angle for K = .91. (Re: Table 1)

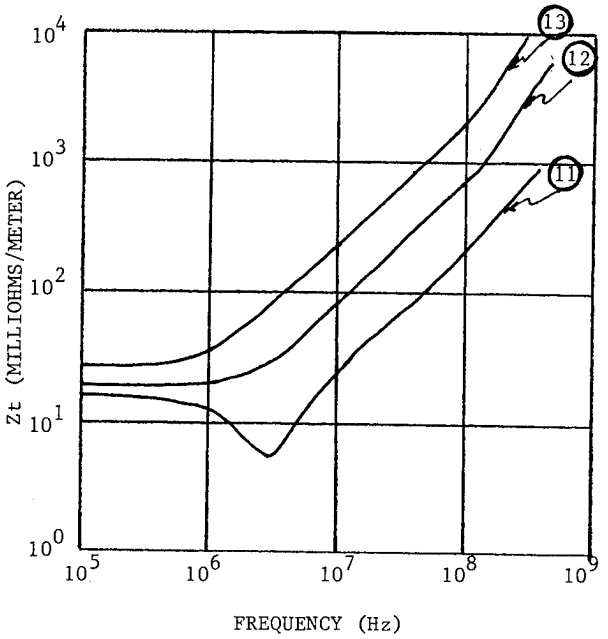



Fig. 5 - Variations in transfer impedance vs. braid angle for K = .8. (Re: Table 1)

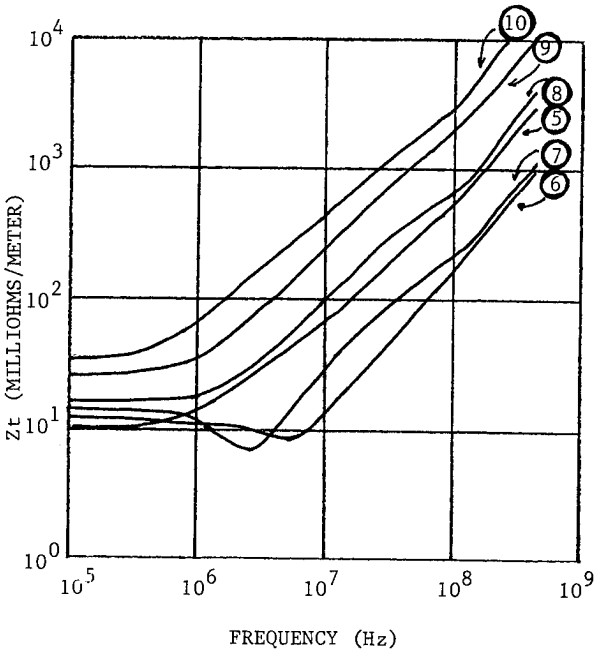



Fig. 7 - Variation in transfer impedance vs. braid coverage for $\alpha$ = 32°. (Re: Table 1)

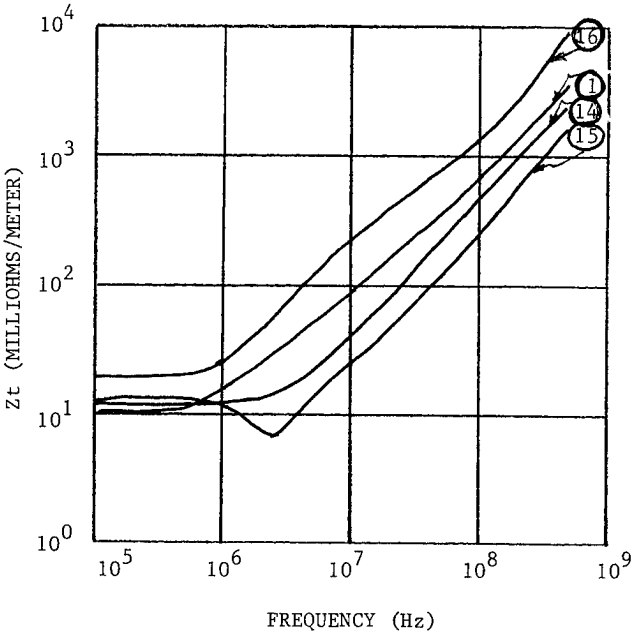



Fig. 6 - Variation in transfer impedance vs. braid coverage for $\alpha$ = 17°. (Re: Table 1)

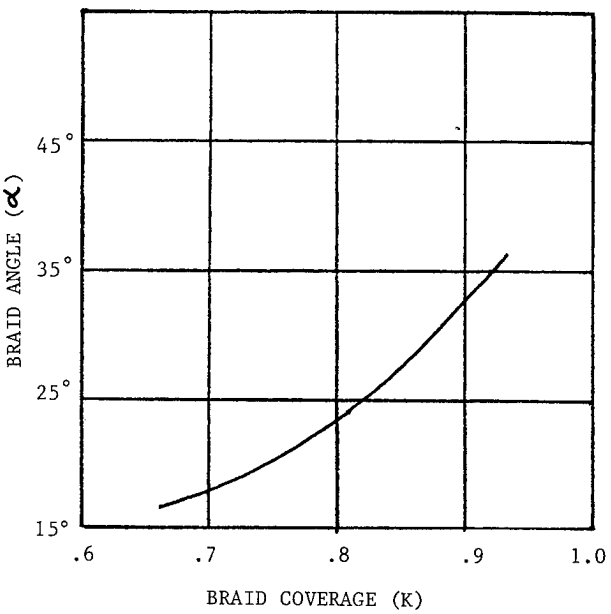



Fig. 8 - Empirical behavior of optimum shield transfer impedance vs. K and $\alpha$

## OPTIMAL FOIL

The parameters associated with foil design are given in table 2. For optimal $Z_t$ the "cigarette" wrap is required.

Data in figure 9 shows that the cigarette wrap design with shorting fold has three orders of magnitude less $Z_t$ at 100 MHz than the spiral wrap with a 34° angle. Applying a shorting fold to the spiralled tape is seen to yield a slight improvement. With cigarette wrap the amount of overlap is important. Figure 10 compares 62%, 36%, 9% overlap with a 17% slot. The 17% slot gives two orders of magnitude increase in $Z_t$ at 100MHz. The data suggests that too much overlap can be counter productive. Finally the data in figure 11 compares overlap and shorting fold performance. The effect of the shorting fold is minimal at low frequencies. Its effectiveness above 100 MHz is limited by oxide/lubricant films on the foil surface. In this range the data show the maximum improvement to be a factor of 5.

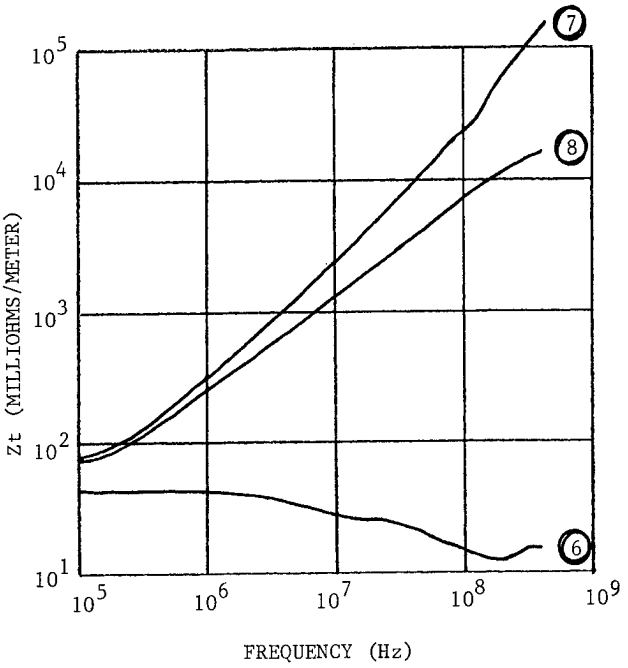
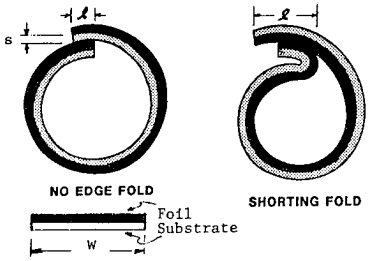



Fig. 9 - Variation in transfer impedance for a spiral vs. longitudinal ($\alpha$ =0°) wrap angle. (Re: Table 2)

Table 2 - Taped Shield Designs




Material: Aluminum

Conductivity: 3.5 x $10^7$ mhos/meter
Diameter Under Tape: .143 inches
Note: All dimensions listed in inches. The S-fold tapes were folded back for a width of .125 inches.

s = substrate thickness
$\ell$ = length of overlap
t = foil thickness

| Cable No. | $\ell$ | % Overlap | s | t | $\alpha$ (Deg.) | w |
|---|---|---|---|---|---|---|
| 1 | -.08 | -17 | -- | .001 | 0 | .375 |
| 2 | .04 | 9 | .002 | .001 | 0 | .5 |
| 3 | .17 | 36 | .002 | .001 | 0 | .625 |
| 4 | .29 | 62 | .002 | .001 | 0 | .75 |
| 5 | .17 | 36 | S-fold | .001 | 0 | .75 |
| 6 | .29 | 62 | S-fold | .001 | 0 | .875 |
| 7 | .24 | 52 | .002 | .001 | 34 | .625 |
| 8 | .24 | 52 | S-fold | .001 | 34 | .75 |
| 9 | .17 | 36 | .001 | .001 | 0 | .625 |
| 10 | .17 | 36 | .001 | .00033 | 0 | .625 |

Comparison of single foil $Z_t$ (figure 11) with single braid (figures 4, 5, 6, 7) $Z_t$ reveals that in the high frequency zone the foil provides approximately an order of magnitude less transfer impedance than the braid. However in the low frequency zone the relatively thin layer of foil gives higher DC resistance and higher $Z_t$ than exhibited by the braid. Performance of the foil in the low frequency zone is improved with increasing foil thickness. Figure 12 compares $Z_t$ for .00035" thick aluminum foil and .001" thick foil.

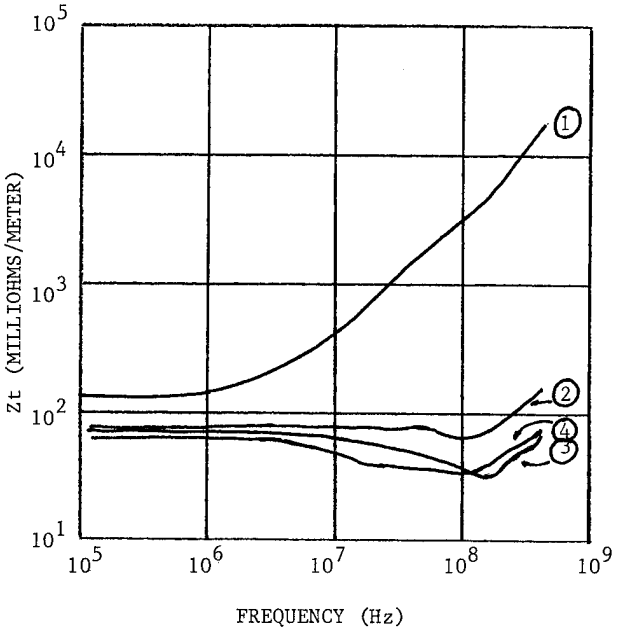



Fig. 10 - Transfer impedance vs. amount of tape overlap "S". (Re: Table 2)

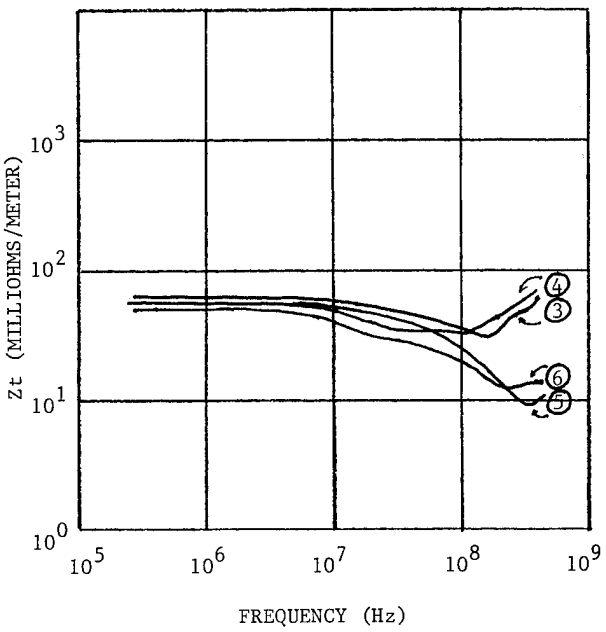



Fig. 11 - Transfer impedance vs. separation "S" at overlap showing effect of shorting fold. (Re: Table 2)

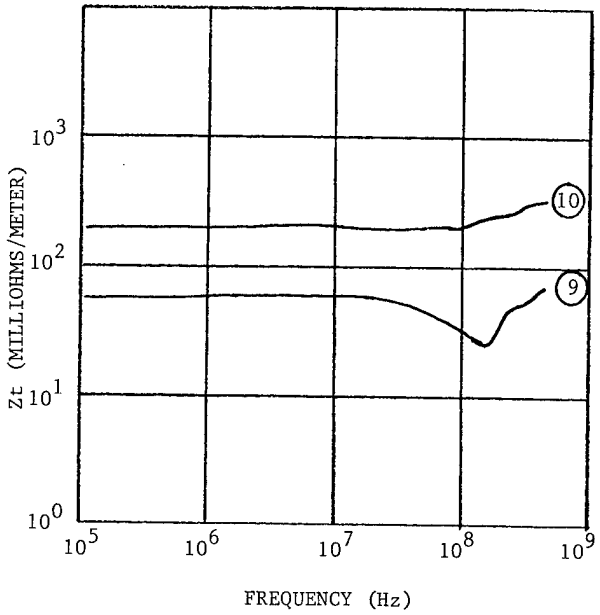



Fig. 12 - Transfer impedance vs. foil thickness. (Re: Table 2)

## OPTIMAL FOIL-BRAID

The above analysis of single foil and braid shields suggests that the combined foil-braid shield will have the low DC resistance characteristics of the braid in the low frequency zone and the reduced inductive coupling characteristics of the foil in the high frequency zone. This is illustrated by the $Z_t$ data in figures 13 and 14. The shield constructions are given in table 3.

The foil-braid design gives roughly two orders of magnitude reduction in $Z_t$ at 100 MHz compared to braid alone. Selection of braid parameters is still important in the foil-braid design with the variation in performance less than an order of magnitude. However, in the frequency range from 100 MHz to 500 MHz performance converges for all braids measured. This would not be expected from the single braid performance data. The optimal foil-braid design is constructed with the optimal single layer foil and single layer braid designs.

Table 3 - Foil/Braid Shield Designs

| Inner Foil On All Cables: Longitudinally applied .001 inch aluminum; $\ell$ = .17, s = s-fold | | | |
|---|---|---|---|
| | Braid Design | | |
| Cable No. | 100K | $\alpha$ (deg.) | N |
| 1 | 71.9 | 33.2 | 5 |
| 2 | 81.0 | 33.2 | 6 |
| 3 | 88.3 | 33.2 | 7 |
| 4 | 93.8 | 33.2 | 8 |
| 5 | 88.5 | 18 | 8 |
| 6 | 89.1 | 34.7 | 7 |
| 7 | 89.3 | 45.5 | 6 |
| 8 | 89.6 | 54.6 | 5 |

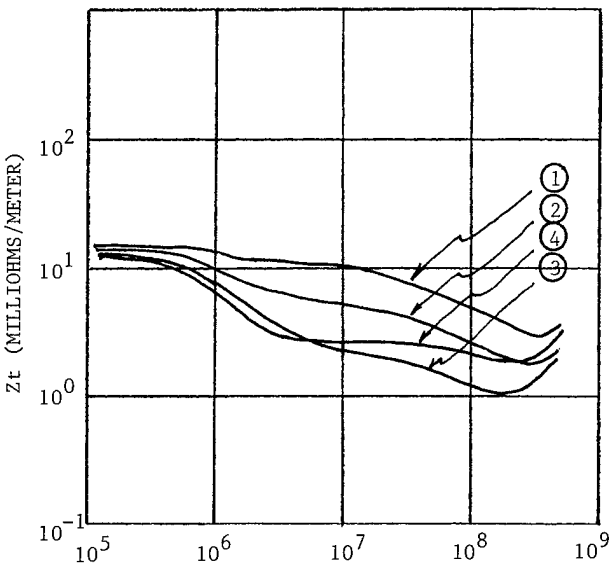



Fig. 13 - Transfer impedance for foil/braid shields in Table 3: $\alpha$ = 33°; K varies.

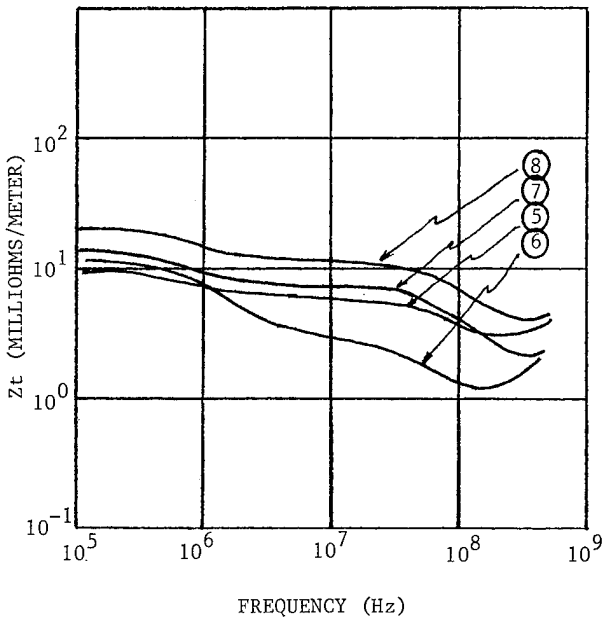



Fig. 14 - Transfer impedance for foil/braid shields in Table 3: K = .88, $\alpha$ varies.

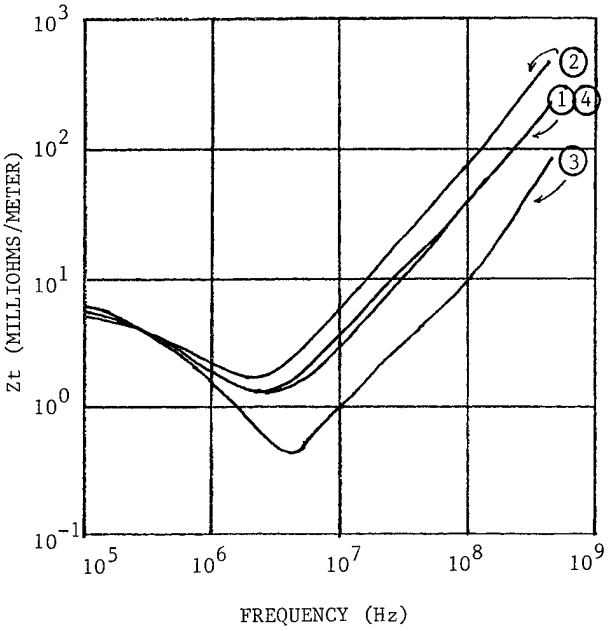



Fig. 15 - Transfer impedance of double braids combining single layers of optimum and non-optimum braid designs. (Re: Table 4)

Table 4 - Double Braid Shield Designs

| Material: Tin Plated Copper | | | | Diameter Under Inner Braid: .143 inch | | |
|---|---|---|---|---|---|---|
| Conductivity: 5.8 x $10^7$ mhos/meter | | | | Diameter Under Outer Braid: .163 inch | | |
| Braid Wire Diameter: .005 inch | | | | Number of Carriers: 16 | | |
| | Inner Braid | | | Outer Braid | | |
| Cable No. | 100K | $\alpha$ (deg.) | N | 100K | $\alpha$ (deg.) | N |
| 1 | 90.8 | 17 | 8 | 90.8 | 42.3 | 7 |
| 2 | 90.8 | 17 | 8 | 91.1 | 19.1 | 9 |
| 3 | 90.6 | 43.9 | 6 | 90.8 | 42.3 | 7 |
| 4 | 90.6 | 43.9 | 6 | 91.1 | 19.1 | 9 |

## OPTIMAL DOUBLE BRAID

$Z_t$ data for four double braid constructions is given in figure 15. The shield design data is given in table 4. The data suggests that the optimal double braid design is constructed with optimal single layer braids. However, double braids will generally have uncontrolled aperture orientations, and the $Z_t$ performance will be distributed. Figure 16 gives the variation in four random orientations of the optimal double braid. Vance's[3] formula for double braid does not take aperture orientation into account and differs by up to an order of magnitude with empirical results.

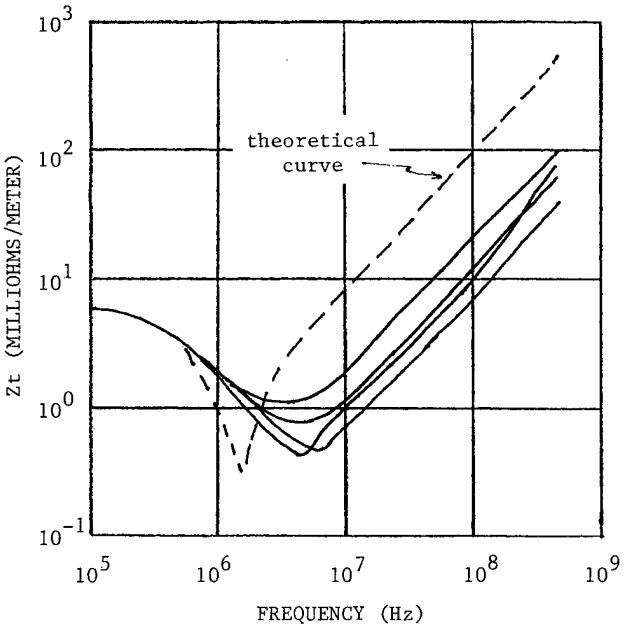



Fig. 16 - Cable No. 3, Table 4 with randomized orientation between the braid layers.

## OPTIMIZED THREE LAYER SHIELD

Figure 17 presents, layer by layer, the $Z_t$ performance of the Ethernet(TM) coaxial trunk cable. The shields four layers provide an effective $Z_t$ which is less than the Ethernet systems $Z_t$ limits. These are also plotted in figure 17. This standard design is relatively expensive. Two braids and two foils are utilized. (See table 5). The second braid adds cost due to materials and processing as well as added cost for jacket material due to the increased cable diameter. Elimination of one braid would result in a smaller, more cost effective cable. The inductive coupling contribution of three layers (curve 3) is small enough to pass the Ethernet requirements. However, $Z_t$ values between .6 MHz and 7 MHz are greater than allowed. Since this frequency range corresponds to the high frequency zone of a seamless tubular shield it is not expected that shorting folds would allow much improvement. Rather, an increase in thickness of the shield would be expected to lower $Z_t$ here.

Figure 18 presents $Z_t$ performance for three layer shield designs also described in table 5. The 61% braid design is clearly not optimal, but comes close to the Ethernet requirements. The 95% #34 AWG braid design with .002" short folded foil outside does meet the requirements. Surprising enough, the thicker 95% braid with .001" short folded foil outside has lower DC resistance but does not drop off rapidly enough to meet the Ethernet requirements.

Ethernet is a Trademark of Xerox Corporation.

Table 5 - Multilayer Shield Designs - Ethernet

(All Dimensions In Inches)

| Cable No. | Inner Foil | Inner Braid | Outer Foil | Outer Braid |
|---|---|---|---|---|
| 1 | .002 Aluminum<br>Overlap = 37%<br>s = .002<br>Bonded | | | |
| 2 | .002 Aluminum<br>Overlap = 37%<br>s = .002<br>Bonded | Tinned Copper<br>d = .0063<br>K = .93<br>= .43° | | |
| 3 | .002 Aluminum<br>Overlap = 37%<br>s = .002<br>Bonded | Tinned Copper<br>d = .0063<br>K = .93<br>= .43° | 2-Layer Aluminum<br>Laminate<br>t = .00033/layer<br>Overlap = 25% | |
| 4 | .002 Aluminum<br>Overlap = 37%<br>s = .002<br>Bonded | Tinned Copper<br>d = .0063<br>K = .93<br>= .43° | 2-Layer Aluminum<br>Laminate<br>t = .00033/layer<br>Overlap = 25% | Tinned Copper<br>d = .0063<br>K = .93<br>= 43° |
| 5 | .002 Aluminum<br>Overlap = 28%<br>s = s-fold<br>Bonded | Tinned Copper<br>d = .0063<br>= 43°<br>K = .61 | .001 Aluminum<br>Overlap = 36%<br>s = s-fold | |
| 6 | .002 Aluminum<br>Overlap = 28%<br>s = s-fold<br>Bonded | Tinned Copper<br>d = .0071<br>= 38°<br>K = .95 | .001 Aluminum<br>Overlap = 36%<br>s = s-fold | |
| 7 | .002 Aluminum<br>Overlap = 28%<br>s = s-fold<br>Bonded | Tinned Copper<br>d = .0063<br>= 43°<br>K = .93 | .002 Aluminum<br>Overlap = 36%<br>s = s-fold | |

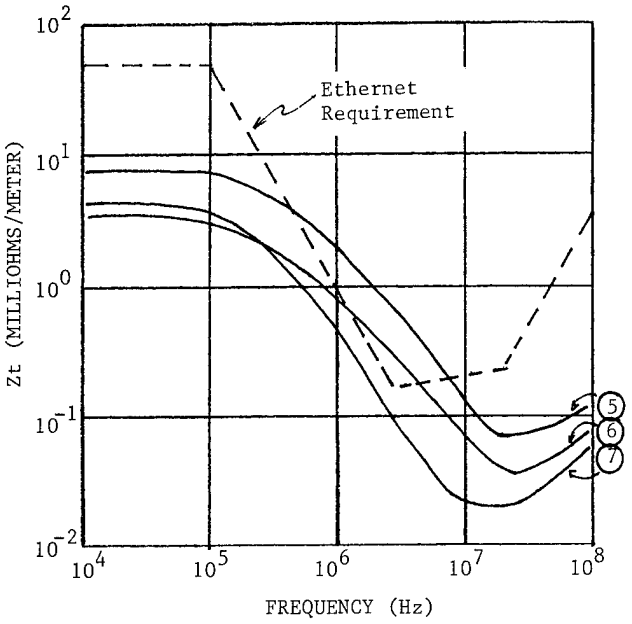



Fig. 18 - Transfer impedance of 3-layer Ethernet shields - Table 5.

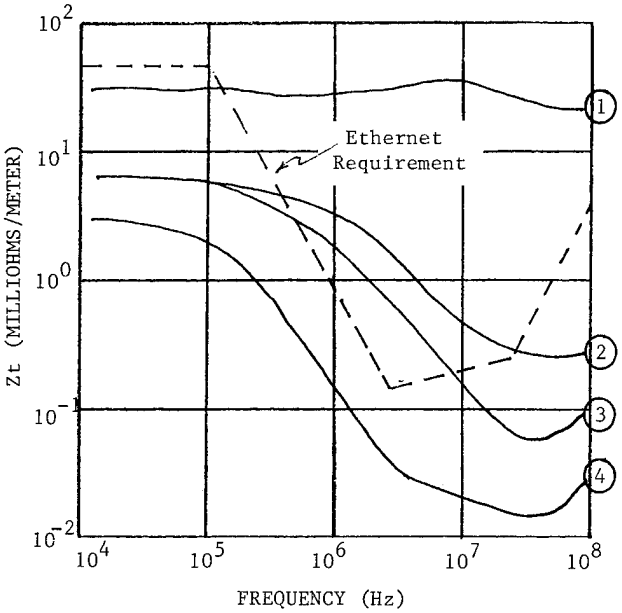



Fig. 17 - Transfer impedance data for Ethernet 4-layer shield as individual shield layers are removed - Table 5.

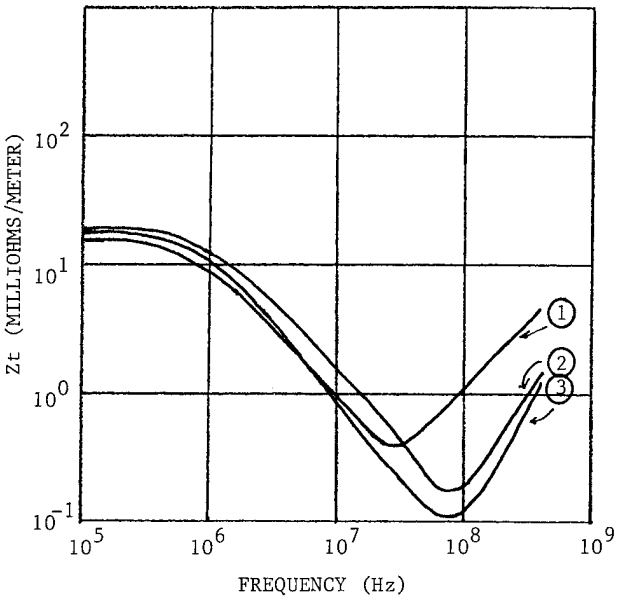



Fig. 19 - Transfer impedance data for 3-layer vs. 4-layer shields - Table 6.

The RG-59 type coaxial cable commonly used for feed-in from main distribution trunk cables (Community Antenna Television) uses combinations of foil plus braid shielding. Currently these RG-59 type shields are not required to conform with transfer impedance limits. Nonetheless, transfer impedance is used as a basis of comparison among these shield types. Figure 19 compares $Z_t$ performance for the three designs given in table 6. Curve 1 is for a four layer shield (quad). This design results in a bulkier, heavier cable, which requires special connectors. Curves 2 and 3 are for optimized 3 layer shields. The shorting fold reduces inductive coupling above 25 MHz. Although the quad shield is thicker than the 3 layer shield it is not dense enough to cause $Z_t$ to decrease more rapidly (compared to the 3 layer shield) in the high frequency diffusion zone. Optimized 3 layer shields are smaller, and more economical than the quad shield.

Table 6 - Multilayer Shield Designs - 59/U

(All Dimensions In Inches)

| Cable No. | Inner Foil | Inner Braid | Outer Foil | Outer Braid |
|---|---|---|---|---|
| 1 | 2-Layer Aluminum Laminate<br>t = .00033/layer<br>Overlap = 36% | Aluminum<br>d = .0063<br>= 18°<br>K = .57 | 2-Layer Aluminum Laminate<br>t = .00033/layer<br>Overlap = 36% | Aluminum<br>d = .0063<br>= 36°<br>K = .37 |
| 2 | 2-Layer Aluminum Laminate<br>t = .00033/layer<br>Overlap = 36% | Aluminum<br>d = .0063<br>= 17°<br>K = .66 | .001 Aluminum<br>Overlap = 36%<br>s = s-fold | |
| 3 | 2-Layer Aluminum Laminate<br>t = .00033/layer<br>Overlap = 36% | Aluminum<br>d = .0063<br>= 17°<br>K = .77 | .001 Aluminum<br>Overlap = 36%<br>s = s-fold | |

## CONCLUSIONS

This paper has just touched the surface of multi-layer shield optimization. More work is warranted on both the empirical and theoretical issues. Such work will yield cable shields which allow systems shielding objectives to be met most economically.

## ACKNOWLEDGEMENTS

The authors express their appreciation of the efforts by their co-workers in making this paper possible. In particular thanks to Glen Greissler whose work with the automated transfer impedance set-up was superb.

## REFERENCES

1. S. A. Schelkunoff, "The Electromagnetic Theory of Coaxial Transmission Lines and Cylindrical Shields", Bell System Tech. J., Vol. 13, pp. 532-579.

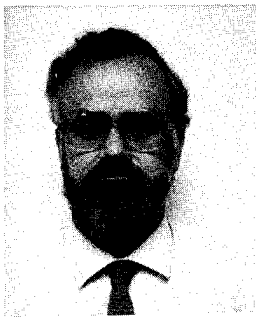
2. A. Tsaliovich, "The Transfer Impedance Test Clamp, Improvements In Electronic Cable Shielding Effectiveness Measurement Techniques", 1982 Symposium Proceedings On Electromagnetic Compatibility, IEEE Catalog #82 CH 1718-6.

3. E. F. Vance, "Coupling to Shielded Cables", Wiley - Interscience, John Wiley & Sons; New York, 1978.

4. P. J. Madle, "Contact Resistance and Porpoising Effects In Braid Shielded Cables", IEEE Transactions Electromagnetic Compatibility, Vol., EMC-9, pp. 206-210, 1980.

5. M. A. Dinallo, "Theoretical and Experimental Transfer Impedance For Concentric Layers of Coaxial Shielding", 1982 Symposium Proceedings on Electromagnetic Compatibility, IEEE Catalog #82 CH 1718-6.

6. A. Tsaliovich, "Braided Shield Engineering Model: Shielding and Transmission Performance, Optimal Design", 1981 International Wire & Cable Symposium Proceedings, Cherry Hill, PA.



John Kincaid received the MSEE and BSEE degrees from the University of Oklahoma in 1967 and 1966, respectively. He joined Belden in 1972 as a Product Development Engineer with our Electronic Division. John is presently Manager - Advanced Electronic Product Development at Belden's Technical Research Center in Geneva, Illinois. Mr. Kincaid is a member of EIA Subcommittee TR 30.1.



Jim Krabec received his BS and MS degrees in Physics from the University of Illinois in 1966 and 1968, respectively. He joined Belden in 1978 as a Product Development Engineer at the Belden Technical Research Center. Prior to joining Belden, Jim was involved in the design and application of electronic and CATV cables.

# CRUSHING METALLIC SHIELDED TELECOMMUNICATIONS CABLES WITH DYNAMIC MAGNETIC FIELDS


| Prakash U. Bakhru | Kenneth E. Bow | Dave Fischer | Edward Schrom |
|---|---|---|---|
| Dow Chemical USA<br>Granville, Ohio | Dow Chemical USA<br>Granville, Ohio | Superior Cable Corporation<br>Atlanta, Georgia | Consultant<br>Valatie, New York |



Physical damage to metallic sheathed telecommunications cables has been achieved by subjecting cable samples to dynamic magnetic fields characteristic of lightning transients. The resulting "magnetic crush" causes varying degrees of damage as a function of transient field amplitude and duration, cable shield or armor conductivity and thickness and specific construction or design. Results dramatically show that cables with shields or armor with circumferential conductivity are subject to severe damage while those without suffer little or no damage. Thus, bare metallic tapes or solid tubes used for shield or armor functions in telecommunications cables may be very poor performers in the natural environment, while shields and armor made from longitudinally applied plastic coated metal tapes having dielectric coatings will be virtually undamaged.


## Introduction

Historically, metallic shielded telecommunications cables buried in earth have been damaged by transient energy associated with lightning discharge. The most susceptible and first reported cables to suffer crushing effects are coaxial cables with air dielectric used in long haul transcontinental routes. With these cables, the damage can be so severe that the metallic circuit becomes shorted rendering the facility inoperable. In the 1950s, the long haul coaxial routes suffered considerable damage due to this phenomena. So, studies were undertaken to ascertain the mechanisms at work and cable designs were developed based upon the results of such work and tests.

The standard test, which exists today, for modeling such lightning damage is termed the "sandbox test": a cable is buried in a box containing wet sand and soil, compacted to a degree, and subjected to discharge from a high current generator with a wave shaped to provide a wave form and amplitude characteristic of a natural lightning discharge. Typically, the high current generator probe is buried in the box of soil in close proximity to the cable at a point at which a small circular hole has been made in the cable jacket exposing the metallic shield or armor. Discharge from the generator causes an arc to form, terminating on the cable resulting in considerable heat damage and quite often a hole results in the cable shield. On occasion, additional damage occurs to the cable in the vicinity of the arc: denting or crushing of the cable shield or the entire cable. The classical and acceptable explanation for this phenomenon has been termed the "steamhammer" effect[1]. It is thought that a high pressure steam front of sufficient magnitude and short duration is generated by the discharge along the arc path and this causes the denting or crushing.

This paper presents evidence that the actual crushing mechanism is due to magnetic field energy. The authors strongly hold that the "steamhammer" is effectively inoperable as a plausible mechanism for crush under natural lightning phenomena.

The popular belief that lightning striking a tree causes the tree to split by the "steamhammer" has recently been subject to great suspicion as well[2]. The actual mechanism at work under this condition is acoustic shock which is remotely recognized as thunder. A further but coarse analysis of the energy required to generate a steam front in soil of sufficient magnitude and short duration to crush a telecommunications cable renders the required energy level to be far in excess of that contained in the most severe lightning discharge known to exist in nature.

As a result of the work that follows, the "sandbox" test is seen to be one in which a hole is merely burned in a buried cable by an electrical arc. Such a test could be performed in air and characterized with equal, if not improved, validity. The authors presume the popular belief that lightning discharge to earth in proximity to a buried cable axiomatically arcs or discharges to that cable is the fundament upon which the "sandbox" test was conceived. We shall demonstrate that this fundament is not axiomatic, but conditional with low apriori probability of direct discharge. Lightning is more likely to pass by, over or under the cable. The results of this paper clearly show that cable damage still results under such "bypass" conditions and that the "sandbox" test does not clearly identify the effects of these phenomena.

## Theory

The fundaments of electromagnetics show that if a linear filamentary current flows obliquely to a linear conductor at Angle A, then the magnetic field generated as a result of the

electron flow is orthogonal to the linear filament. Figure 1 demonstrates this simple relationship and shows that the orthogonal field can be broken into tangential and orthogonal field components with respect to the linear conductor, viz: H(0) and H(90). The most ubiquitous instantiation of this model is the power line (filamentary current) and telecommunications cable (linear conductor) couple in the operating environment. The power line electric (E) field can be neglected if the cable is buried in the earth. The magnetic field, however, cannot be neglected in this case since it permeates the earth with equal ease as it does air. Under the usual conditions, the orthogonal component of the magnetic field, H(90), induces longitudinal current flow along the buried linear conductor through its terminating longitudinal impedances. The question asked is: "How much current can the usual cable shields and armor carry without cable damage?" This paper provides definitive answers with respect to lightning discharge.

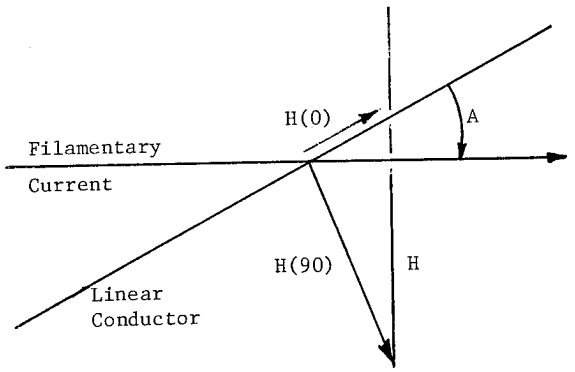



Figure 1. Magnetic Field Components

The remaining magnetic field component, H(0), is tangential to the linear conductor. This component causes currents to flow circumferentially about the linear conductor, provided the conductor has circumferential continuity. Fundamental electromagnetics show that if electron current flow occurs under these conditions, an additional phenomenon is present: a radial force is exerted on the electrons directed orthogonally to the longitudinal axis of the conductor. The fundamental equation for this force is:

$$\bar{F} = q\bar{v} \times \bar{B} \qquad (1)$$

where $\bar{F}$ is force (newtons) exerted on elemental or aggregate charge $q$, $\bar{v}$ is the charge velocity (meters/second) and $\bar{B}$ is magnetic flux density (weber/meter$^2$). For the materials and media of interest here, we also have:

$$\bar{B} = \mu\bar{H} \qquad (2)$$

where $\mu$ is scalar permeability (henry/meter) and $\bar{H}$ is magnetic field intensity (ampere/meter). For free space, and effectively for our case, $\mu = 4 \times 10^{-7}$. Hence, EQS (1,2) render:

$$\bar{F} = \mu q \bar{V} \times \bar{H} \qquad (3)$$

which shows that a free charge at rest ($v = 0$) in a constant static field $\bar{H}$ experiences no forces upon it from the magnetic field. However, if either $v \neq 0$ or $\bar{H}$ is time-variant, then $\bar{F}$ is non-zero.

Consider now a conductor forming a closed circuit that is linked by dynamic, time-varying, magnetic flux. If the closed circuit impedance is Z (ohms), then from Maxwell's Equation, as derived from Faraday's Laws in integral form, the current flowing in the circuit is given by:

$$I = \frac{V}{Z} = -\left(\frac{1}{Z}\right) \iint \frac{\partial \bar{B}}{\partial t} \cdot d\bar{s} = -\left(\frac{\mu}{Z}\right) \iint \frac{\partial \bar{H}}{\partial t} \cdot d\bar{s} \qquad (4)$$

where I is measured in amperes and $\bar{s}$ is the surface vector for that surface defined by the boundaries of the closed circuit. This is referred to as the transformer effect, or transformer induction.

It follows at once, from EQS (1,4) that for circuits of fixed geometry intersecting identical time-varying magnetic fields, the magnetic forces imparted to the conductor will be larger for those conductors with higher conductivities (thus lower Z, higher I). Hence, with mechanical properties set aside, copper and aluminum shields will suffer greater crushing forces than steels under identical field and geometric conditions.

Although the general problem is complex in nature, since stroke currents are distributed in soil with geometrics not always filamentary or linear in dimension, we can, nevertheless, demonstrate the fundamental encounter between cable and stroke fields by analyzing the effect of the magnetic components generated in the medium. Earth seldom has effect upon magnetic field distribution or structure: earth permeability is not significantly different from that of air in most cases. So, consider a buried linear conductor C terminated in man-made "grounds" $Z_1$ and $Z_2$, interacting with a stroke current I as depicted in Figure 2. Taking the geometry of the earth current I to be nearly filamentary and reasonably linear in extent, we can assume the associated magnetic field $\bar{H}$ to be effectively normal to I as shown in Figure 2. Thus, $\bar{H}$ can always be decomposed into tangential and orthogonal components [H(0) and H(90), respectively] pointwise with respect to conductor C. See Figures 1 and 2.

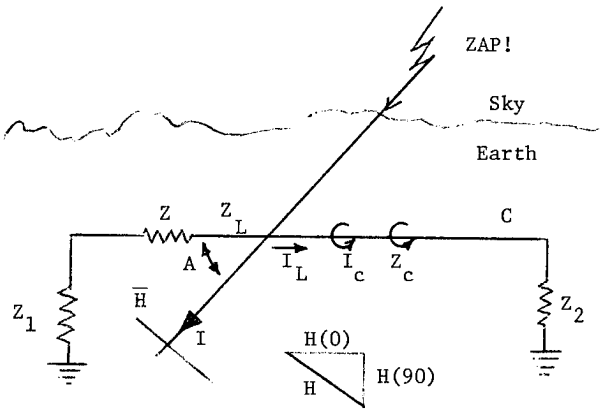



Figure 2. Schematic of a Lightning Stroke to Earth in the Vicinity of Cable

These two components of magnetic intensity cause currents to flow both longitudinally and circumferentially in conductor C: H(90) generates currents flowing along the conductor axis (longitudinal current) while H(0) induces currents to flow around the conductor axis (circumferential current). Thus, we need to consider two separate circuital impedances, $Z_L$ and $Z_c$. $Z_L$ is the longitudinal circuit impedance comprised of distributed service impedances along the conductor, the man-made ground impedance $Z_1$ and $Z_2$ and the impedance of the earth-return path. $Z_c$ is the circumferential impedance around the conductor per unit length. For bare metals, apriori observations give $Z_c \ll Z_L$, in the general, practical case. Under these conditions, under dynamic magnetic induction, both longitudinal ($I_L$) and circumferential ($I_c$) currents flow on conductor C for a filamentary current flowing near the cable at arbitrary angle A.

Kraus[3] gives the most general case for induction:

$$I = \frac{V}{Z} = \oint \bar{E} \cdot d\bar{\ell} - \iint \frac{\partial \bar{B}}{\partial t} \cdot d\bar{s} \qquad (5)$$

where $\bar{E}$ is the electric field intensity (volts/meter) and $\bar{\ell}$ is a line vector along the longitudinal path.

From EQS(1,2,3) we may write:

$$\bar{F}/q = \bar{v} \times \bar{B} = \mu \bar{v} \times \bar{H} \qquad (6)$$

which is the force per unit charge or $\bar{E}$ = field intensity (volts/meter). Hence, $\bar{E} = \bar{F}/q$ and EQ(5) becomes:

$$I = \frac{V}{Z} = \oint (q\bar{v} \times \bar{B}) \cdot d\bar{\ell} - \iint \frac{\partial \bar{B}}{\partial t} \cdot d\bar{s}$$

$$= \mu \left[ \oint (q\bar{v} \times \bar{H}) \cdot d\bar{\ell} - \iint \frac{\partial \bar{H}}{\partial t} \cdot d\bar{s} \right] \qquad (7)$$

Currents $I_L$ and $I_c$ can be determined from EQ(7) with $Z = Z_L$ or $Z_c$ and $\bar{H}$ = H(90) or H(0), respectively, along with the requisite conductor geometry.

Of primary interest here is the force exerted on the conductors due to induced charge movement within the conductor boundaries by the tangential component of the incident stroke current's magnetic field, namely H(0).

The tangential component H(0) causes currents to flow around the conductor, if the conductor has some degree of circumferential continuity. Application of EQS(1,3) again show the plane containing charge velocity v and magnetic field $\bar{H}(0)$ to contain the longitudinal axis of C. Hence, again, the resulting forces on the conductor must exist radially or normal to the conductor axis. However, quite interesting here, is the fact that these radial forces are directed inward, thus exerting pressure to crush the conductor. This renders an apparent "reverse" skin effect as well.

The above explanations of field and force effects are quite elemental, the authors acknowledge greater analysis and detail is necessary to fully explain all the phenomena at hand and that such work is beyond the present intent of this paper.

This paper clearly demonstrates that even under the worst case, excessive-valued H(90) and $I_L$, longitudinal current, there is no damage or fault that occurs to cables employing the metallic armors and/or shields used by the industry today. Longitudinal stroke currents directly impressed on cable samples show no damage. Yet, it appears that historically the main concern in design has been to expect damage in this mode. On the other hand, small-valued H(0) or circumferential currents, $I_c$, have been demonstrated in this paper to cause considerable shield/armor/cable damage - the "magnetic crush" is a most effective fault generator!

## Definition of Tests

Numerous cable types and designs were subjected to two tests: 1) longitudinal current surge and 2) magnetic crush.

The list of cables and cable components tested are as follows.

A. Aluminum tubing used in CATV cables.
B. Air core, disc-insulated coaxial cables.
C. Foam dielectric coaxial cables.
D. Jacketed tubes, constructed from longitudinal tapes of copper.
E. Twisted pair copper cables -- copper shields.
F. Twisted pair copper cables -- coated aluminum shields.
G. Twisted pair copper cables -- coated aluminum shield/coated steel armor.
H. Loose tube fiber optic cables -- coated steel armor.

I. Open channel fiber optic cables -- coated steel armor.
J. Loose tube fiber optic cables -- copper shield/stainless steel armor.
K. Fiber optic cable -- helically applied steel wire armor.

All samples were approximately 12 inches in length. Each sample placed under test was subjected to the effects of generator discharge and photographic documentation of the waveform and amplitude was recorded. These tests were performed at the General Electric High Voltage/ High Current Laboratory in Pittsfield, MA.

The longitudinal current surge tests were performed by connecting the sample directly across the generator terminals as depicted in Figure 3.

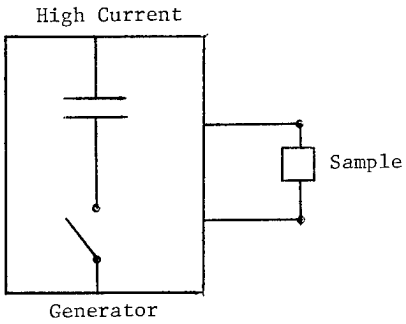



Figure 3. Schematic for Longitudinal Current Tests

This direct connection eliminates any effect associated with arcing to the sample and the full current capacity of the generator flows through the sample. This configuration then represents the case for longitudinal current flow directly through the sample and can be considered a worse case current condition.

Tests for the magnetic crush were performed by placing a 3.5 turn coil wound on a fiberglas core of sufficient diameter to allow insertion of the cable sample within. The coil was connected directly across the generator as depicted in Figure 4.

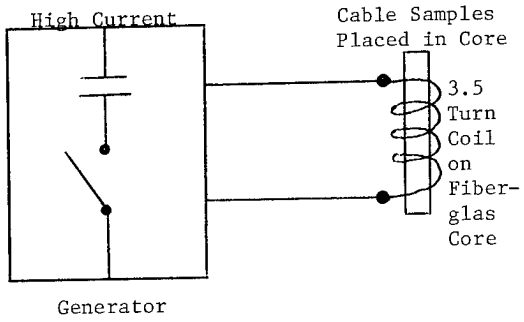



Figure 4. Schematic for Circumferential Current Tests

Photo 1 shows the actual coil used in the experiment. The length of this coil is approximately 4 inches. The solenoidal field produced by the coil places a strong magnetic field component parallel to the sample's metallic shield or armor. Measurements of the coupling between coil and sample show a coefficient of coupling in the range of 0.25 to 0.5 as a function of sample material and diameter, and as a placement of test piece. Larger internal diameters of the coil reduces the coupling efficiency to the test piece when its diameter is smaller in relation to the primary coil. Coupling efficiency will vary inversely with the specific resistance of the metallic component.

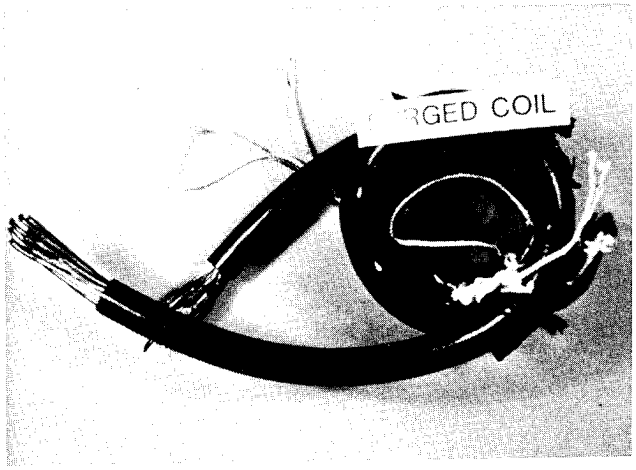



Photo 1

The high current generator tends to act as a constant current source as does natural lightning. Current amplitudes from 5,000 to 150,000 amperes were obtained in these tests. A typical example of the current waveform is shown in Figure 5.

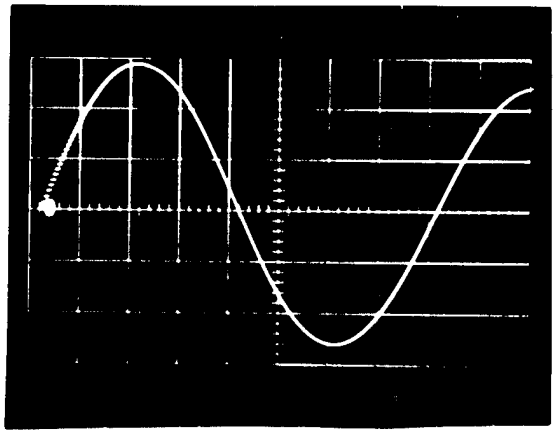


Figure 5. Typical Lightning Waveform (Magnitude 2.9 cm x 5 V/div. = 14.50 or 145 KA)

The waveform depicts a rise time to peak value of approximately 20 microseconds and an oscillatory frequency near 12.5 kilohertz. Thus, the generator seems to be producing waveforms quite characteristic of the phenomena of natural lightning. Lightning amplitude distributions have been studied and reported often in the literature[4]. Typical cumulative distributions show that 50 percent of all strokes are less than 40,000 amperes, that 80 percent are less than 60,000 amperes, that 95 percent are less than 100,000 amperes, that 98 percent are less than 130,000 amperes, and that 99.98 percent are less than 220,000 amperes. Thus, the tests performed here represent at least the applications for cables by which 99.8 percent of all strokes to earth might pass within an inch or so of the cable. Thus, these results are most representative of the natural condition.

## Test Results -- Longitudinal Surge

Table I and the following photographs show the results of the longitudinal current surge test. Photo 2 shows a hollow aluminum tube with 25 mil (1 mil = 0.0254 mm) wall and 495 mils diameter that was subject to three consecutive surges of 46, 66 and 90 kiloamps. The tube suffered no damage or excessive heating due to the longitudinal current. The crushing at the left end was the result of the type of clamp used. This clamp has a hollow cylindrical portion through which the tube passed before making clamp contact with the generator. Current flowing around this cylindrical shell induced circumferential crushing currents which resulted in the damage shown. This is an excellent example in which very large longitudinal currents were carried by the sample without harm and relatively small current crushed the sample nearly flat. The clamp was changed to another type for the remaining longitudinal tests.

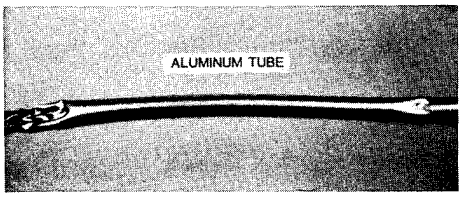



Photo 2

Photo 3 shows a foam dielectric coaxial cable through which 70, 90, 110 and 125 kiloamperes were passed. No crushing or thermal damage were caused. The sample has been dissected and sectioned for clearer viewing. Photo 4 shows fiber optic cables of loose tube design with coated steel armor which were subjected to 60, approximately 90 and 117.5 kiloamperes respectively as shown from top to bottom in the photo. Sample 3 in Photo 4 exhibited a quick flaming at the cable ends which promptly extinguished. The armor darkened, yet no apparent damage occurred to the fiber optic core. Photo 5 shows fiber optic cables, loose tube design, with an inner shield of bare copper and outer armor of stainless steel which were subjected to 48 and 68 kiloamps respectively. Photo 6 shows the same samples opened and no metallic damage of any kind is apparent.

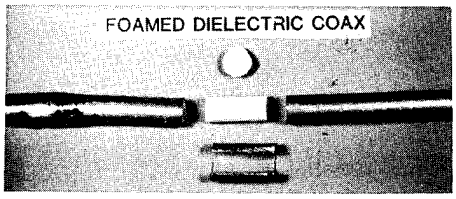



Photo 3

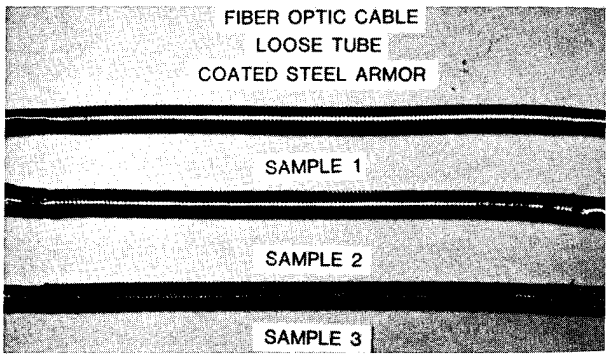



Photo 4

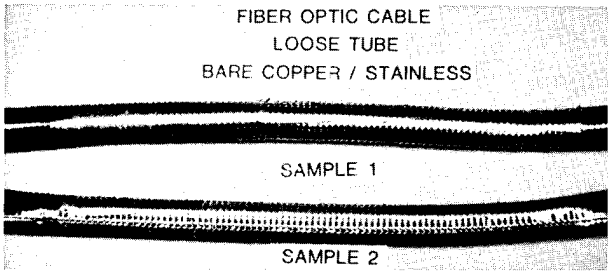



Photo 5

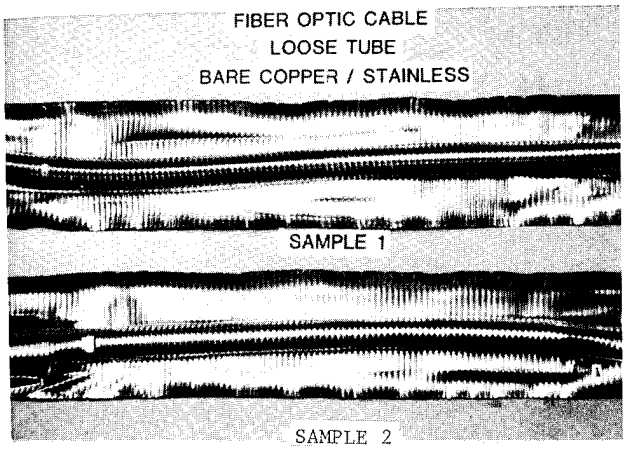



Photo 6

The authors did not measure component temperatures of surged samples since one author had previously surged similar coated steel armored cables successively[5]. In the most severe case wherein a 6 foot sample sustained 12 consecutive surges of 70,000 amperes, the jacket temperature did not exceed 105°F.

Other samples were also tested involving copper, aluminum and stainless steel. The results were similar, no damage to the core was sustained. However, as shown in Table I, cables incorporating highly conductive shields were able to withstand the higher thermal energy generated by the longitudinal surge. These data and samples clearly show that the standard designs of the industry for shields and armors are more than sufficient to sustain longitudinal currents characteristic of the extreme majority of lightning strokes, even under direct hit conditions, save for the ubiquitious hole burning arc. Such arcing is as likely to occur in aerial construction as in buried. Few will argue the impracticality of a cable design to withstand such energy conversion without damage under arc conditions.

## Test Results -- Magnetic Crush

Of the numerous samples tested, the authors have selected those which best represent the range of crushing which occurred with respect to cable designs presently employed by the industry. Again, it should be clearly noted that such damage can occur to cables even though there is no direct conduction (arcing) present. When the stroke currents, either in filamentary or sheet form, pass in near proximity to exposed telecommunication cables containing metallic shields or armors, induced currents could result in the crushing effects.

The tables and the following photographs present the test results in detail.

Photo 7 shows samples of aluminum tubes with 25 mil walls which have been magnetically crushed. Samples 5, 6 and 7 were subjected to 39, 42 and 47 kiloamperes of coil current respectively. (Note: actual current in the sample is determined by the coupling efficiency of the coil which is estimated at 0.25 to 0.5 times the coil current. This means the actual current in the sample is lower than the coil current.) These tubes are 498 mils in diameter. Sample 7 has a 2.2 inch long crushed area with final maximum diameter of 51 mils. The samples fail beginning at the weakest metallic point and the crush continues until contact is made with the inner metallic surface, thus resisting further inward movement. Photo 8 shows the cross-section of a foamed dielectric coaxial cable after a coil current of 125 kiloamperes. Photo 9 demonstrates the effect of magnetic crush on air core, disc-insulated coaxial cables. Coil currents on the order of 100 kiloamperes caused this damage. Photo 10 shows a cross section from a sample of such crushed coaxial cables; the metallic circuit is completely short circuited.

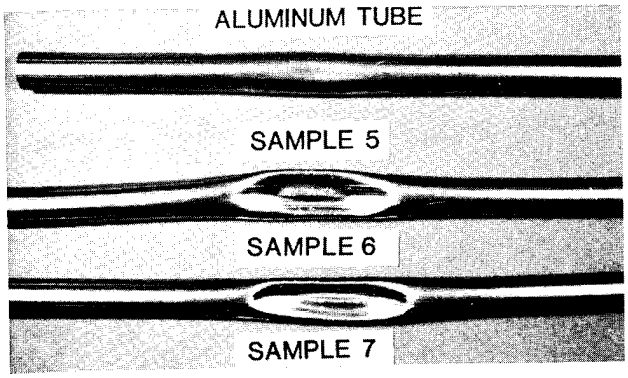



Photo 7

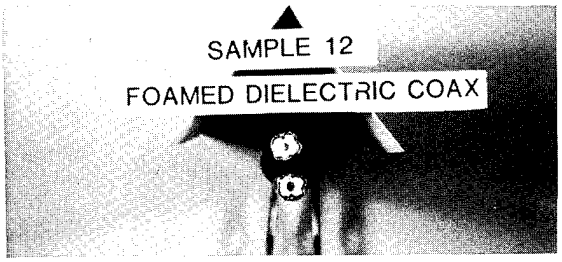



Photo 8

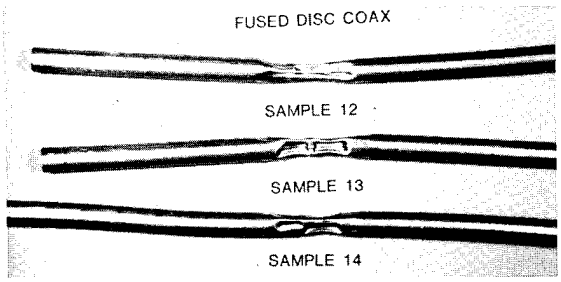



Photo 9

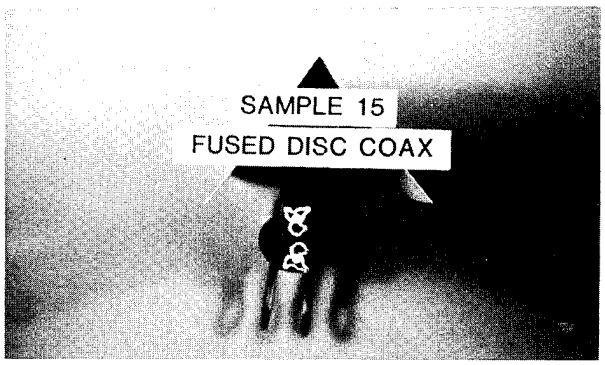



Photo 10

Photo 11 shows the results with 5 mil copper, 0.555 inch diameter jacketed tubes. Currents here are in the vicinity of 100 kiloamps. It is to be noted that these tests were conducted with jacketed tubes constructed from bare metallic tapes longitudinally folded into a cylinder, and no core was present. During the test, the magnetic force causes the overlapped metallic portions to separate, thus partially mitigating the degree of crush. However, in an actual cable, the cable core prevents such motion of the overlap and crushing occurs.

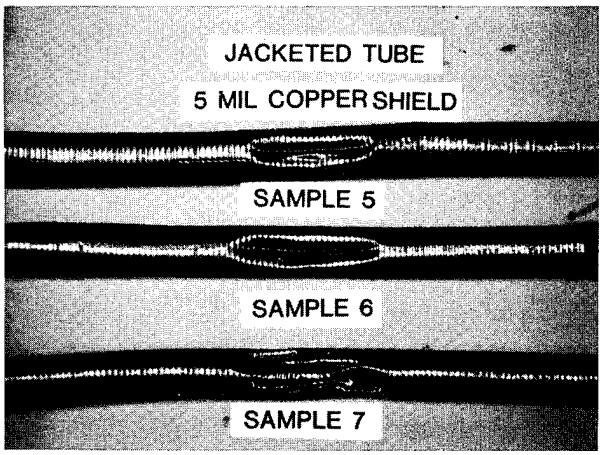



Photo 11

Photo 12 shows a twisted pair copper cable with a 5 mil copper shield. Clearly, heating and burning have occurred. Photo 13 shows that arcing has occurred along the overlap of sufficient magnitude to burn portions of the copper away. The coil current in this sample was 125 kiloamperes and a small amount of core crush is visible but no apparent core damage is evident. Photo 14 is that of a similar cable except with a 10 mil copper shield. This sample was subjected to 2 coil surges of approximately 140 kiloamperes.

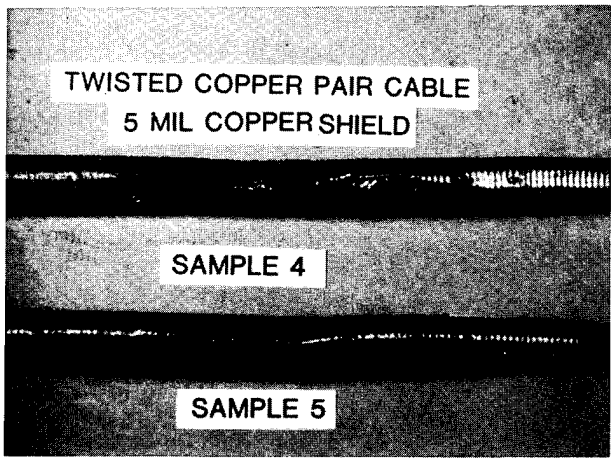



Photo 12

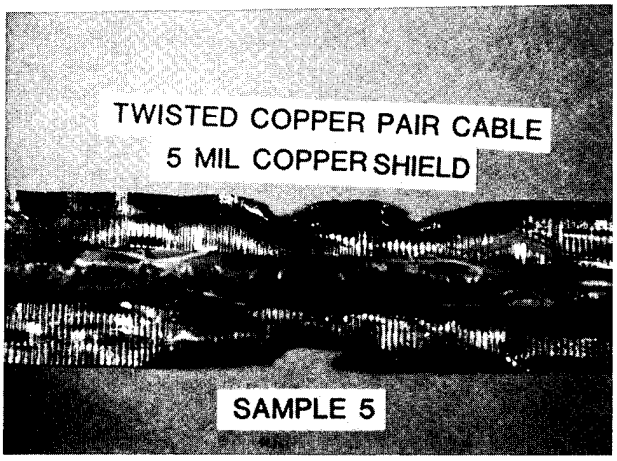



Photo 13

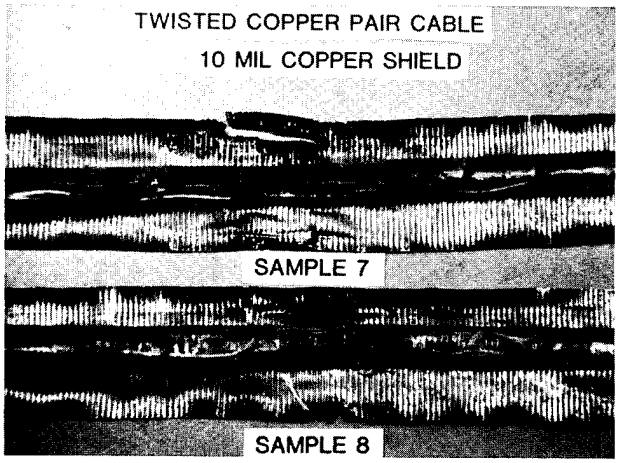



Photo 14

Of the actual telecommunications cables tested, one was subject to greater failure than all the others. This is a fiber optic cable, loose tube design, with 2 metal circumferential components: a bare copper inner shield and a stainless steel armor both constructed from longitudinally applied tapes. The cable is constructed so that the overlaps of the two tapes are 180° apart. Crushing and denting are evident, even at coil currents as low as about 50 kiloamperes. An interesting phenomena occurs with this design. The copper appears to arc at the overlap; and as a secondary effect, the stainless steel adjacent to it is physically burned through at the point above the edge of the copper tape.

Photo 15 shows a dissected sample having been exposed to a coil current of 85 kiloamperes. Copper has been deposited on the inner core. Photo 16 is another sample of this cable having been subjected to a coil current of 147.5 kiloamperes. The slit burned in the stainless steel at the bottom of the photo is nearly 2.5 inches in length and 140 mils in width and the copper shield, center, is severely crushed. Photo 17 clearly shows the burnt core and the corrugations of the copper shield are embossed in the inner cable jacket.

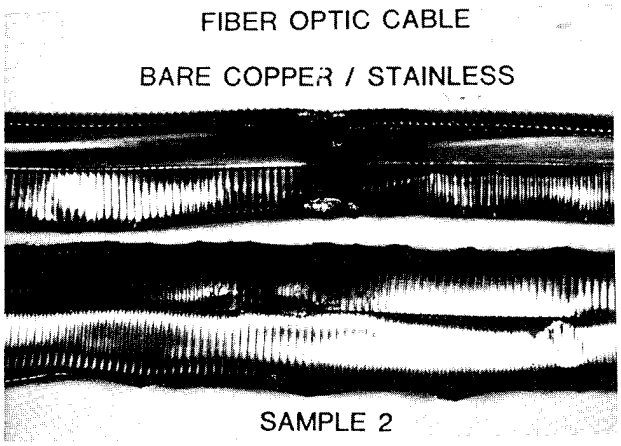



Photo 15

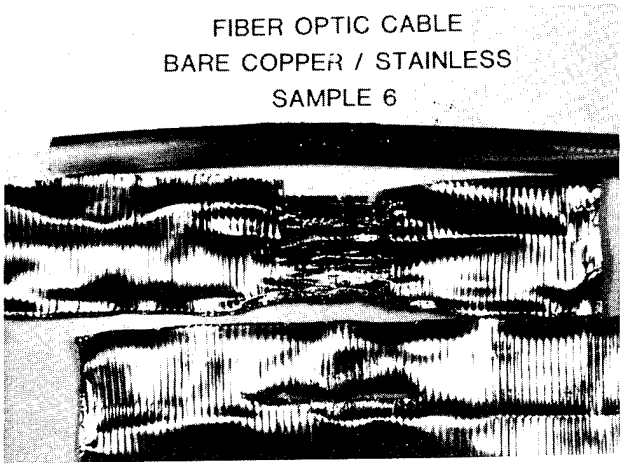



Photo 16

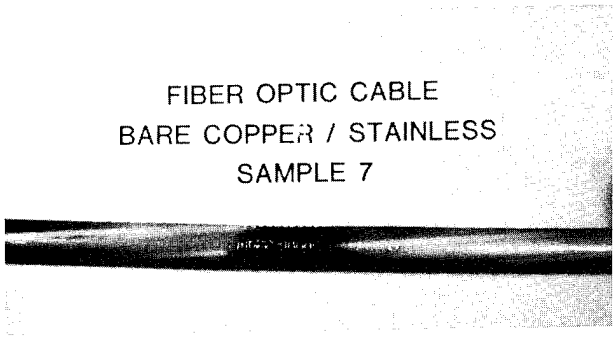



Photo 17

There were cables tested which survived the full range of coil currents without any real physical damage; no burning, crushing or denting. The common characteristic of these cables is that they have metallic shields or armors made from longitudinal tapes which have been coated with copolymer coatings of high dielectric strength. Cables with such coated metals are in common use by many telephone companies today. Cables utilizing these tapes therefore do not have or allow circumferential continuity. Thus, the impressed voltages do not dissipate in heat via current discharge and therefore no circumferential or circulating current flows and the magnetic crush is effectively mitigated. Photos 18, 19, 20, 21, 22 and 23 are self-explanatory. No effective damage is visible. Photo 21 shows some discoloring along the inner surface of the steel tape beyond the overlap. This discoloration appears to be a fine powder which was caused by mechanical abrasion due to magnetic flexing of the shield. Also, the ripchord in this cable apparently aggravated the condition, but no physical damage was apparent to the cable core.

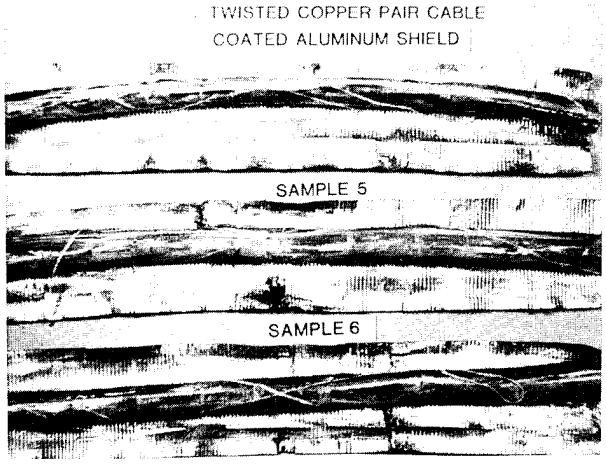



Photo 18

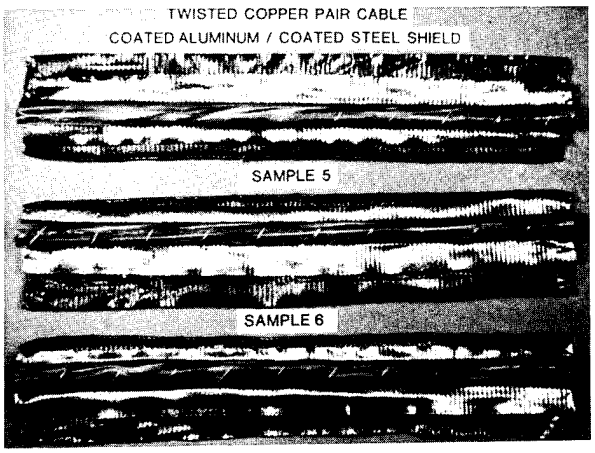



Photo 19

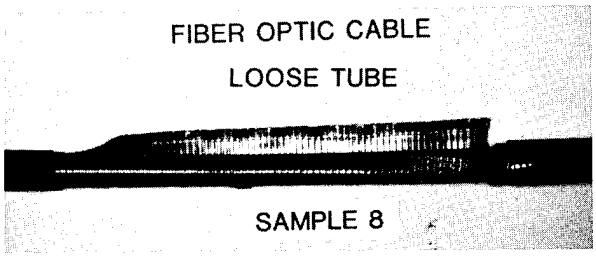



Photo 20

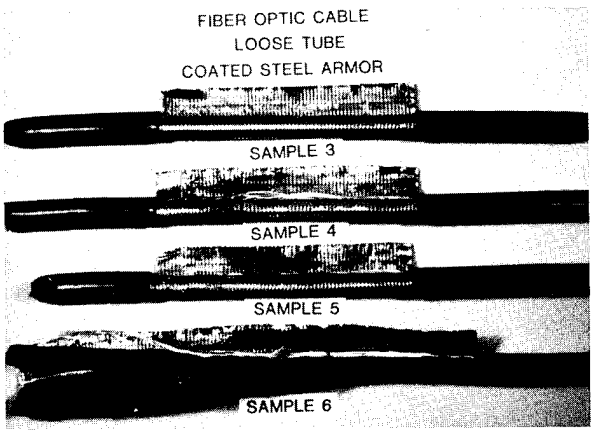



Photo 21

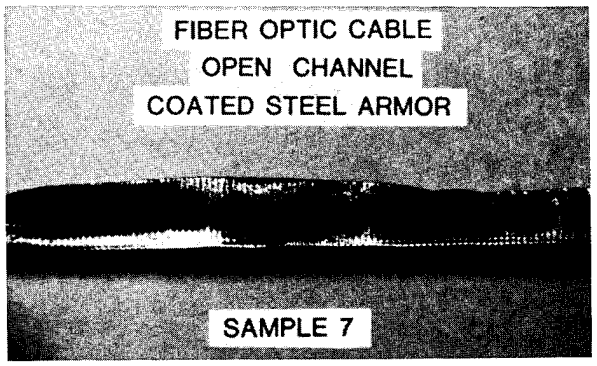



Photo 22

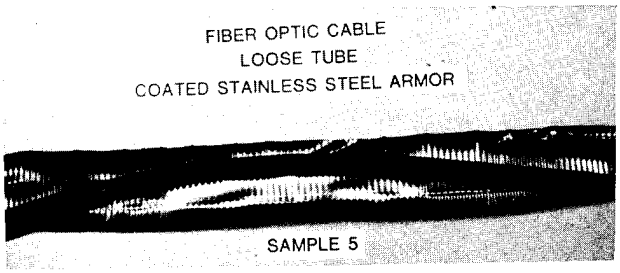



Photo 23

## Discussion

The correlation between physical damage and coil currents has been made and is described as follows.

Table II shows the data generated on the effects of circulating currents in hollow cylindrical tubes. These data show that physical damage to these tubes is in proportion to the coil currents and increases as the magnitude of these currents increases. One may also notice that larger diameter aluminum tubes crushed at lower coil currents and had a greater degree of physical damage than tubes of a smaller diameter. This table also shows that the lower the specific resistance of the shield, the greater the susceptibility for it to crush. The 25 mil aluminum tubes crushed at lower coil currents than 5 and 10 mil copper longitudinally corrugated shields; and 10 mil copper crushed at lower currents than 5 mil copper.

Table III shows the relationship between the physical damage and the coil currents for coaxial cables. Again, these data show that the degree of physical damage increases as the magnitude of the coil currents increase. Also, as expected, the air core fused disc coaxial cable crushed at lower coil currents than foamed dielectric coaxial cable and sustained a greater degree of physical damage.

Table IV shows the relationship between the physical damage and the coil currents for twisted pair cables. Several distinct observations can be made from this table.

1. Cable utilizing a highly conductive shield of 10 mil copper showed a greater propensity for crushing.

2. Cables utilizing shields of lower thermal capacity, such as 5 mil copper, showed a greater degree of damage due to burning as a result of arcing at the overlap.

3. Cables utilizing an aluminum shield protected by copolymer coatings of high dielectric strength (6,000 volts per mil) withstood much higher coil currents. However, slight arcing effects and minor crushing was noticed when subjected to maximum currents (145 KA).

4. The cable utilizing dual shields of copolymer coated aluminum and copolymer coated steel did not show any signs of physical damage due to arcing or induced magnetic fields in the full range of coil currents and at repeated shots at maximum currents. The copolymer coatings of high dielectric strength on both aluminum and steel totally protected the cable.

Table V shows the relationship between the physical damage and the coil currents for fiber optical cable. As these data show, no damage to fiber optical cables (both loose tube and open channel core configurations) utilizing copolymer coated steel or stainless steel was found even at a maximum coil current of approximately 140 kiloamperes.

The cables utilizing steel wires also survived the full range of coil currents without any apparent damage to the cable. Fiber optical cable utilizing dual shields of bare copper and stainless steel experienced a high degree of physical damage from circulating currents. The copper shield showed signs of crushing at coil currents as low as 50 kiloamperes. Burning of copper and crushing of copper was also noticed as shown in Photos 15, 16 and 17.

Based on the data generated on the dual shield of coated steel and coated aluminum (Table V), it is expected that the physical damage to fiber optical cables utilizing copper and stainless steel can be prevented by coating both shields with coatings of high dielectric strength. A high performance sheath for the protection of fiber optical cables can then be achieved which will totally handle the longitudinal currents and prevent magnetic crush from circumferential currents.

## Conclusions

Magnetic crush is indeed a real phenomenon and characterizable. It is far more plausible than the classical "steamhammer" effect. Cables with bare metallic shield or armor members are subject to severe crushing and denting as well as very high heating, sufficient to vaporize and deposit copper and stainless steel. The effective mechanism for mitigation is to use plastic coated shields and armors which exhibit no circumferential conductivity. This is clearly demonstrated by the test results. The authors have no suggestions for improvement of those cables, such as coaxial, which demand circumferential conductivity for necessary shielding.

The authors entered into these tests with the clear intent to provide information to this industry that magnetic crush is the effective mechanism whereby non-arcing damage occurs to communications cables in the natural environment. We sincerely desire that others find our work of sufficient interest to put forth continued effort to further analyze and detail the phenomenon and to devise new and improved tests whereby better cables can be designed for the telecommunications industry.

Acknowledgement: The authors would like to thank Don Caverly, Donna Shoults, Don Gromacki, and Colene Sayers for their help in the preparation of this paper.

## References

[1] WCL Weinraub, DD Davis, MD Kinard, "A Rodent and Lightning Protective Sheath for Fiber Optic Cables", International Wire and Cable Symposium Proceedings, 1983, p. 243-249.

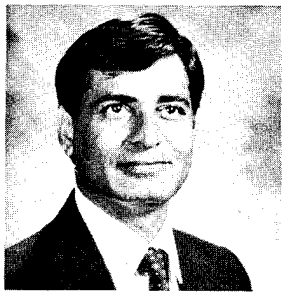
[2] RH Lee, Industrial and Commercial Power Systems Technical Conference, May 13-16, 1985, p. 86-89.

[3] JD Kraus, Electromagnetics, McGraw-Hill, 1953.

[4] DA Douglas, "Lightning Induced Current Surges on a Buried Multicoaxial Cable System", International Wire and Cable Symposium Proceedings, 1971, p. 293-308.

[5] D Fischer, "High Current Surge Performance of Metallic Components in Valtec Fiber Optic Cables", unpublished report.

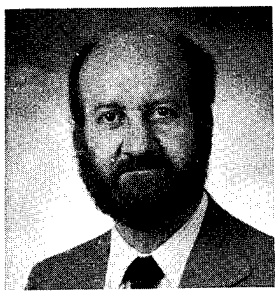
Biography



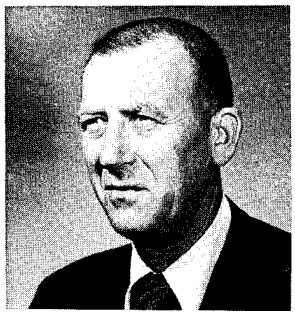
Prakash (Buck) U. Bakhru is a Development Leader with Dow Chemical USA in Granville, Ohio. He joined Dow in 1973, working on magnesium process research. He is currently engaged in the application development of coated metals for the Fiber Optical Cable Industry. Mr. Bakhru holds a Bachelors degree in Metallurgical Engineering from Nagpur University, India, and a Master's degree from the University of Missouri-Rolla.



Kenneth E. Bow is an Associate Development Scientist with Dow Chemical USA, Granville, Ohio. He has been involved in the research and development of materials for the wire and cable industry for over 20 years. He is currently responsible for the development of coated metal shielding and armoring tapes for applications in cables. Mr. Bow graduated with a B.S. E.E. degree from Michigan State University in 1962.



Dave Fischer is presently Director of Engineering for Superior Cable Corporation. His background is mathematics, electromagnetics and antennas, physics, telecommunications and radio astronomy. He had held faculty positions at the University of Kansas, the University of Nebraska, Earlham College, and the University of Indiana (Richmond). He served as a Project Engineer and Chief Technical Consultant for HyGain Electronics, Lincoln, Nebraska, and was Transmisssion Engineer for Lincoln Telephone and Telegraph. He held the engineering positions of Transmission Engineer, Group Engineering Manager: Systems Planning, New Product Development Manager, and Technical Director for Superior Continental Corporation, Hickory, North Carolina, and was Technical Director, Superior Cable Corporation. His experience with Continental Telephone (Contel) included Noise and Protection Specialist, Manager: Technical Support, Director Broadband Transmission Systems, and Director Technical Analysis. His experience in fiber optic cables and systems included Senior Staff Engineer and Manager, Applications Engineering with Valtec (later ITT-EOPD). He is also active in long haul radio communication and ionospheric studies.



Edward C. Schrom is currently a consultant, having recently retired from the General Electric Company after 38 years of service. At General Electric, Mr. Schrom worked in various laboratories in Schenectany, New York, and Pittsfield, Massachusetts. He has been engaged in activities associated with high voltage testing and high energy pulse discharges aided by stored energy. He received a number of management awards for his work on pulse power. In the last 11 years of his career with General Electric, Mr. Schrom was the Manager of High Voltage Laboratory. He is a member of the IEEE.

TABLE I. Observation of Samples Subjected to Longitudinal Current Surge

| Sample | Shield | Surge Current KA | Observations |
|---|---|---|---|
| Tube | Aluminum 0.025" | 46 | No damage |
| | | 66 | No damage |
| | | 90 | Possible crushing at the ends as a result of clamps used, see photo 2 |
| Foamed Dielectric Coaxial Cable | Aluminum 0.025" | 70 | No damage |
| | | 90 | No damage |
| | | 110 | No damage |
| | | 125 | No damage, see photo 3 |
| Fiber Optic Cable (loose tube) | Copolymer Coated Steel, 0.006" (steel) 0.0105" (total) | 60 | No damage |
| | | 90 | Melting of copolymer coatings |
| | | 117.5 | Flaming of cable jacket at the ends; no apparent damage to core, see Photo 4 |
| Fiber Optic Cable (loose tube) | Copper/Stainless Steel Armor | 48 | No damage |
| | | 68 | No damage, see Photo 5 and 6 |
| Fiber Optic Cable (loose tube) | Copolymer Coated Stainless Steel | 40 | No damage |
| | | 50 | Melting of copolymer coatings |
| Twisted 25 Pair Copper Cable | Copper 0.005" | 46 | No damage |
| | | 68 | Burning of copper at cable ends |
| Twisted 25 Pair Copper Cable | Copolymer Coated Aluminum (0.0121) (Aluminum 0.0075") | 46 | No damage |
| | | 68 | No damage |
| | | 70 | No damage |

TABLE II. Observation of Samples Exposed to Simulated Lightning Currents - Hollow Cylindrical Tubes

| Sample | Wall Thickness Inches | Coil Currents | Initial Tube Diameter Inches | Physical Damage Crushed O.D., in. | Physical Damage Crushed Length, in | Observations |
|---|---|---|---|---|---|---|
| Aluminum | 0.025 | 35 | 0.498 | -- | -- | No Damage |
| | | 39 | | 0.40 | 1.3 | Crushing first observed |
| | | 42 | | 0.05 | 2.2 | Crushed |
| | | 47 | | 0.05 | 2.2 | Crushed, see Photo 7 |
| Aluminum | 0.025 | 36 | 0.860 | -- | -- | No Damage |
| | | 38 | | 0.76 | 1.4 | Crushing first observed |
| | | 40 | | 0.60 | 1.9 | Crushed |
| | | 43 | | 0.39 | 2.4 | Crushed |
| Jacketed Copper | 0.005 | 55 | 0.555 | -- | -- | No visible damage |
| | | 60 | | 0.50 | 0.95 | Crushing observed |
| | | 70 | | -- | -- | Severe crush |
| | | 75 | | -- | -- | Severe crush; see Photo 11 |
| | | 85 | | -- | -- | Severe crush |
| Jacketed Copper | 0.010 | 45 | 0.555 | -- | -- | Crushing first observed |
| | | 50 | | -- | -- | Opening of overlap - 4.3" crushed |
| | | 60 | | -- | -- | Crushed |

TABLE III. Observation of Samples Exposed to Simulated Lightning Currents - Coaxial Cables

| Sample | Shield Thickness Inches | Coil Currents KA | Cable Diameter Inches | Physical Damage Crushed O.D., in | Physical Damage Crushed Length, in | Observations |
|---|---|---|---|---|---|---|
| Fused Disc Coaxial | 0.025 | 85 | 0.510 | -- | -- | No damage |
| | | 89 | | 0.49 | -- | Crushing first observed with slight neck down |
| | | 93 | | 0.45 | 0.70 | Crushed |
| | | 97.5 | | 0.44 | 1.50 | Crushed |
| | | 101.5 | | 0.42 | 1.61 | Crushed |
| | | 105 | | 0.41 | 1.54 | Crushed |
| | | 115 | | 0.36 | 1.83 | Crushed |
| Foamed Dielectric Coaxial | 0.025 | 96 | 0.510 | -- | -- | No crush |
| | | 100.5 | | 0.41 | 0.99 | Crushing first observed |
| | | 117.5 | | 0.38 | 1.53 | Crushed |
| | | 125 | | 0.36 | 1.89 | Crushed |

TABLE IV. Observation of Samples Exposed to Simulated Lightning Currents - Twisted Pair Telephone Cable

| Sample | Shield Thickness, in | Coil Currents KA | Observations |
|---|---|---|---|
| 25 Pair Cable Copper Shield | 0.005 | 75 | Minor arcing at the bottom side of overlap. |
| | | 105 | Arcing at overlap, pinhole and cracks at overlap. |
| | | 115 | Massive arcing & burning of copper; slit in the copper was 4.7" long; crushing observed opposite of overlap. |
| | | 125 | Burning of copper due to arcing. Cable crushed and twisted, embossing of corrugations and copper into core, see Photo 12. |
| 25 Pair Cable Copper Shield | 0.010 | 65 | Discoloration due to arcing. |
| | | 85 | Pinhole in the metal observed. |
| | | 105 | Crushing observed. |
| | | 125 | Distinct crushing; Embossing of corrugations of copper into core. |
| | | 145 | Crushing and twisting of cable; arc length - 6.3"; slit in metal - 1.2". |
| 25 Pair Cable Coated Aluminum Shield | 0.121" (0.0075 Aluminum coated with 0.0023 of copolymer coatings) | 105 | No damage. |
| | | 115 | Some fusion of copolymer; no arcing; no crushing. |
| | | 125 | Very minor arcing, fusion of flooding compound. |
| | | 125 | Two repeated shots of simulated lightning currents. |
| | | 125 | Crushing appeared to have begun, reduction in diameter - 0.060". |
| | | 145 | Arcing damage, some burning of aluminum; affected area 1.6 to 2.8 inch. |
| 25 Pair Coated Aluminum - Coated Steel | 0.0121 & 0.0105 (Aluminum 0.0075 coated with 0.0023 Copolymer coatings. Steel 0.006 coated on both sides with copolymer coating Dual Shield Armor) | 85 | No damage. |
| | | 125 | Two repeated shots of simulated lightning currents with no damage. |
| | | 140 | No damage |

TABLE V. Observation of Samples Exposed to Simulated Lightning Currents - Fiber Optic Cable

| Core, Type | Sheath Type | Coil Currents KA | Observations |
|---|---|---|---|
| Loose Tube | Coated steel; Steel - 0.006" steel coated with copolymer coatings | 85 | No damage. |
| | | 145 | No damage. |
| Loose Tube | Bonded sheath; Coated steel; rip chord between coated steel and the jacket | 85 | No damage. |
| | | 125 | No physical damage. |
| | | 140 | Some discoloration of flooding compound used between coated steel and the inner jacket. This appears to be due to powder from mechanical abrasion caused by magnetic flexing of the shield. Rip chord apparently aggravated this condition. |
| Open Channel | Bonded sheath; Coated steel | 85 | No damage. |
| | | 145 | No damage. |
| Loose Tube | Bonded sheath; Coated stainless steel; Stainless steel - 0.005" with 0.0023" copolymer coatings. | 90 | No damage. |
| | | 127.5 | Two repeated shots of simulated currents with no damage. |
| | | 132.5 | No physical damage. |
| Ribbon Fiber | Steel Wire Armor | 107.5 | No damage. |
| | | 142.5 | No damage. |
| Loose Tube | Copper inner shield, stainless steel outer shield (0.66" outside diameter) | 50 | Crushing of copper observed; slight plating of copper at inner surface of stainless steel; no damage to stainless steel. |
| | | 85 | Crushing of copper; arcing (length 0.64") at overlap of copper; plating of copper on the inner surface of the stainless steel; several holes in the stainless steel due to arcing of copper; embossing of copper on core. |
| | | 120 | Crushing of copper, arcing (length 1.43") at the overlap of copper; slit in stainless 1.4" long due to burning of copper at the overlap, width of slit 0.040" - 0.050"; no crushing of stainless steel. |
| Loose Tube | | 122.5 | Crushing of copper and core; crushed diameter of core - 0.615"; deep embossing of corrugations in core; slit in the stainless steel. |
| | | 125 | Two repeated shots of simulated lightning currents. Severe burning and crushing of copper causing slit 2.4" long to be burned in the stainless steel. |
| | | 130 | Burning of copper at overlap causing severe damage to stainless steel - slit 2.1" long and 0.043 to 0.079" wide burned in the stainless. |
| | | 147.5 | Burning and severe crushing of copper; slit burned in stainless steel with length of 2.442". |

# AN INITIAL INVESTIGATION ON THE ACCELERATED AGING AND LIFETIME PREDICTIONS OF WIRE AND CABLE INSULATIONS USED FOR LOCAL NETWORK INSTALLATIONS

G.L. Grune and T.L. Talarico

Polymers (E79) and Analytical Chemistry (E62) Groups
IBM Corporation
Research Triangle Park, NC 27709

## I. ABSTRACT

The effect of elevated temperature on various wire and cable insulations has been well studied and understood[1 and 2] for approximately 40 years[3], since the adoption of the use of vinyls and other thermoplastics by the National Electrical Code in 1940. In this study, the combined environmental stresses of elevated temperature and humidity on various "non-plenum" materials including; flexible grade poly(vinyl chloride), radiation-cured solid and foamed (or "air-blown") polyethylene, and poly(ethylene terephthalate) (PET) films, were evaluated. All insulation materials were subjected to elevated temperatures in 98-100% RH environments. After accelerated environmental exposure, "isothermally" aged samples were tested for physical properties, and gel permeation chromatography (GPC) was performed to determine any corresponding molecular weight changes. Thermogravimetric analysis (TGA — or "dynamic" analysis) correlated well with expected degradation mechanisms for each insulation system.

The information collected, using both isothermal and dynamic techniques, was useful in determining endpoint criteria for lifetime predictions. Arrhenius plots derived from several sets of data yielded apparent energy of activation (Ea) values which correspond with both previous outdoor exposure and accelerated aging studies. This correlation provided further confidence in our "useful lifetime" predictions for these insulations and, subsequently, the overall cabling system.

## II. INTRODUCTION

In a previous article[4], the design and material requirements for the local network cabling system was discussed in detail. Since 1983, the IBM Cabling System has been available and is currently being installed for both inter- and intra-office use. The cable design has also progressed, and now includes a fourth pair of telephone conductors or voice grade media (VGM) for both the plenum and non-plenum versions. A diagram of the new "Type 2" cable is shown below in Figure 1.

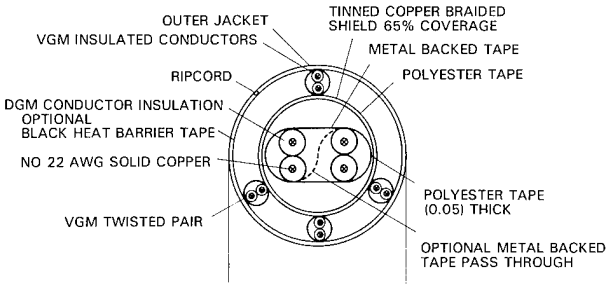



**Figure 1**
**Current Design of the Type 2 Non-Plenum Cable for the IBM Cabling System**

The only difference between the plenum and non-plenum design remains the selection of materials required to pass the stringent Underwriters Laboratories (UL) 910 flame and low smoke test requirements, which all but dictates the continued use of fluoropolymer jacket and conductor insulations for plenum cables. Mechanisms of aging and its effects on the thermal, chemical, environmental, and electrical stability of fluorocarbon insulations are well understood[5]. With the possible exception of jackets which may crack at sub-zero temperatures, these insulation materials should perform satisfactorily over the design life within the required $-40$ to $+80$ C temperature range.

It is the use of the materials required for the non-plenum cables which came under careful scrutiny in terms of the potential life expectancy of the designs previously described[4]. The current cable design still includes at least a 15 year life requirement, and it was a goal of this study to determine both a test for this design need and a method for evaluating the cable system's longevity.

In developing test methods to determine the useful lifetime of this cabling system, a multitude of severe environments were considered. Initially it was hoped that the wire and cable insulations could be subjected to accelerated aging under extreme individual exposures of UV light, heat, moisture, and artificially created ozone ($0_3$) using destructive test techniques. In addition, non-destructive electrical testing of the total cable construction was planned. Time constraints limited the study to determining the effects of a multiple stress environment, consisting of elevated heat and humidity.

It was thought that long term storage or transport in warehouses which are not air-conditioned (hot, humid environments), was the most hazardous exposure that these cables (with the exception of the indoor/outdoor fiber optic cable) would experience prior to office installation. The installation of these cables under extremely cold conditions will occur, but lifetime predictions using cryogenic or temperature cycling techniques for wire and cable insulations leads to several different failure modes, and therefore, uncertain conclusions. The employment of both destructive (physical testing) and non-destructive (electrical testing) methods was retained. The destructive testing results, and implications for predicting both insulation and eventual system failure, are the subject of this paper.

## III. EXPERIMENTAL

Three sets of wire and cable insulations were prepared for exposure to elevated temperature and humidity in three separate chambers. Each set of insulation included 8" lengths of poly(vinyl chloride) (PVC) jackets from both Type 6 (office type) and Type 2 cables, ASTM D 638[6] tensile and elongation dumbell specimens, 8" lengths of foamed polyethylene (PE) insulation from which the 26 AWG copper conductors were stripped, 6" lengths of solid, irradiated (cross-linked) PE insulation from which the 22 AWG copper conductors were stripped, and 8" x 1" x .001" polyethylene terephthalate (PET) film samples, some of which were aluminum backed. In addition, full cable constructions measuring at least 30' in length were coiled in approximately 1' diameters and added to

the back of each chamber for non-destructive testing purposes. The actual configuration of wire and cable samples within the environmental chambers is as shown below in Figure 2.

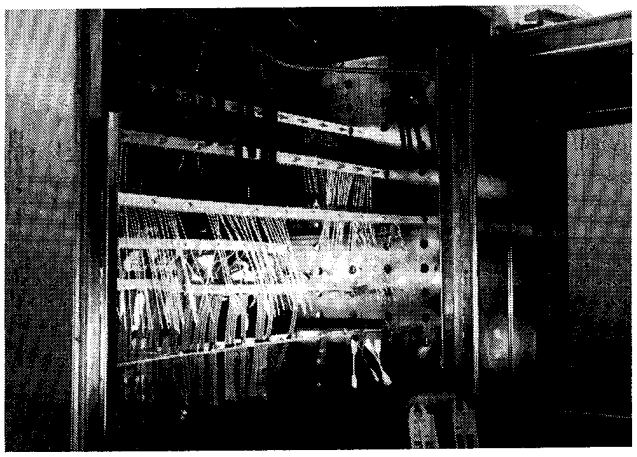


**Figure 2**
**Non-Plenum Wire and Cable Insulations and Total Cable Constructions Exposed to Elevated Temperature and Humidity in an Environmental Chamber**

The three chambers were set to operate at 70, 85, and 100 C and 98-100% RH and to maintain these conditions within ±2 C and 2% RH. These conditions were maintained and monitored by continuous wet and dry bulb temperature readings, and in the case of the 100 C oven, continuous steam injection insured the 100% RH condition. The three chambers, although somewhat larger than the "working chamber volume" (25 ft.$^3$) allowed by ASTM D 2436[7], all met the requirements of between 100 and 200 air changes/hour. It should also be recognized that ASTM D 2436 is a standard which was written for conventional air-oven aging of electrical insulation materials. Although calibration to this standard was not performed, it was thought that the overwhelming presence of moisture in these chambers would mask any temperature fluctuation or air-flow restriction non-uniformities. Sherwood and Boronski[8] devised a technique for more proper diffusion using wire mesh screens for improving air-oven flow patterns. This technique would have improved the reliability of our test data. More importantly for this study, however, is that the polymers would not be susceptible to substantial thermal degradation at these relatively low temperatures. This presumably allowed for degradation via hydrolysis and oxidation mechanisms to dominate.

3.2 Destructive Physical/Mechanical Testing of Wire and Cable Insulations

*(A) PVC Homopolymer Jackets and White ASTM Dumbells (80 C and 105 C Rated)*

To determine changes in tensile strength and elongation (at break), 5 sets of both actual cable jacketing and ASTM dumbell specimens were taken from the environmental chambers after the first 24 hours of exposure, and then every 7 days thereafter as required until a specified endpoint was reached. The ASTM dumbell PVC specimens were prepared by extruding strips of the 80 C rated material on a Brabender using the following standard set of conditions: 15:1 L/D ratio, compression ratio of 2:1, and a short head barrel with settings of 380, 350, and 340 C for the barrel head and final two zones, respectively. The dumbells were then cut from these extruded strips using standard small D 638 dies.

The main difference between the jackets and the dumbells is that the dumbells were extruded without the use of carbon black pigment. All the tested dumbells were from the 80 C, UL rated compound. The tested jackets were both 80 C, and 105 C UL rated compounds, and both contained between 1.5-2% carbon black. The 80 C rated compounds were extruded over Type 6 office cables and included a grooved design, while the 105 C rated compounds were extruded over Type 2 cables using the standard extrusion die allowing for the jacket's smooth appearance. The three specimen types used are pictured in Figure 3. Other distinguishing features between the UL 80 and 105 C rated PVC compounds are listed in Table 1. Finally, it was determined via Energy Dispersive X-ray (EDX) analysis that the 80 C rated PVC compound contained lead salts and titanium dioxide for heat stabilization and oxidation inhibition. The 105 C rated compound does not include either additive, and the only inorganic filler which appeared in its EDX spectra was $CaCO_3$.

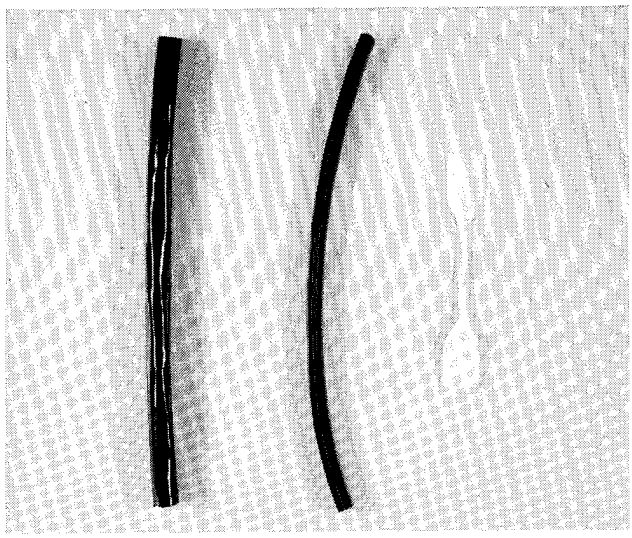


**Figure 3**
**PVC Jackets and ASTM Dumbell Specimen Used for Destructive Testing. (From Left to Right, Smooth 105 C Rated Compound Jacket, Grooved 80 C Rated Compound Jacket, and ASTM, 80 C Rated Compound Dumbell)**

**Table 1**
**Typical Physical Parameters of PVC Homopolymer Compounds Used for Destructive Testing**

| Property | 80 C UL Rated Compound | 105 C UL Rated Compound |
|---|---|---|
| Specific Gravity | 1.36 | 1.26 |
| Hardness, Durometer A | 80 | 76 |
| Tensile Strength, PSI | 2300 | 2170 |
| Elongation % | 325 | 380 |
| Brittle Temperature (ASTM D-746) | −30 C | −40 C |
| % Retention of Elongation | 77 (7 days at 113 C) | 62 (7 days at 136 C) |
| Oxygen Index, Volume% | 24 | 26 |
| Residual Vinyl Chloride Monomer (Test sensitivity to 1 PPM) | Non-Detectable | Non-Detectable |

Figures 4A and 4B picture the Instron Model 1125 set-up used to find tensile and elongation values for the PVC jackets and ASTM dumbells respectively. For the jackets, a special jaw configuration, using fine mesh sandpaper attached to each face, was employed. This allowed for less slippage of the jacket as the jaws were pulled apart during testing. The jaws were preset to a gauge length of 45 mm, and elongation measurements were made by determining the change in length of the jaws from the original 45 mm setting. This was found to be a more precise method than the use of the strain gauge. Tensile strength measurements were made by determining the load required to break each specimen and dividing this value by the cross-sectional area of the approximately .030" - .035" (thickness) jacket. The variability in cross-sectional area of different sample sets of the same jacketing was determined to be less than 3%, so a standard value was used for both jacket types. The Instron Model 1125 was equipped with a 200 lb tensile load cell for all testing, and all samples were broken using a set crosshead speed of 500 mm/min.

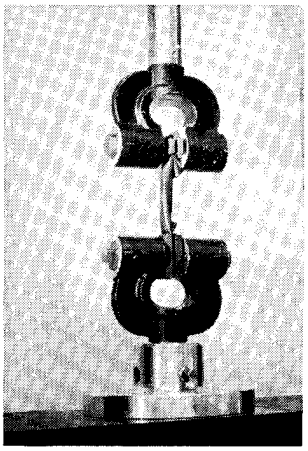


**Figure 4A**
**Laboratory Apparatus for Destructive Testing of PVC Jackets**

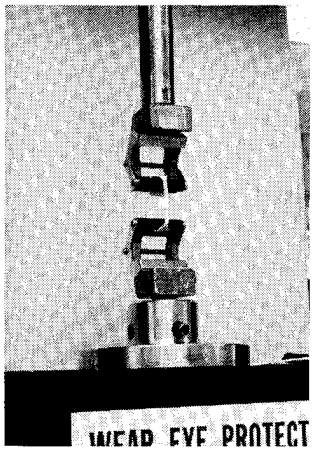



**Figure 4B**
**Laboratory Apparatus for Destructive Testing of ASTM PVC Dumbells**

The PVC dumbells were tested using a set of elastomeric jaws normally employed for rubber specimens. Again, fine mesh sandpaper was used on each jaw face to prevent slippage. The preset gauge length for dumbell testing was 35 mm, and final elongation values were determined at the point of specimen rupture. Each dumbell was premeasured for thickness with a micrometer to insure proper calculation of cross-sectional area.

*(B) Foamed Polyethylene Data Grade Media (DGM) Insulation*

Three different sets of PE conductor insulations were exposed in the three aforementioned environments. These included two sets of foamed PE insulated "tubes" extruded over the same 22 AWG solid copper conductor. The only difference in these two sets were the manner in which they were marked — one with a black helical stripe, the other with an orange helical stripe. Special care was taken in stripping the insulation off the conductor so the inner portion of the tube would not be "scaved". The technique employed, although not 100% successful, produced extremely reliable results, with standard deviations ( $\sigma_{n-1}$ ) of .08% for loads and 2.9% for extensions of unaged specimens subjected to tensile testing.

The third set of insulations exposed to the elevated temperature and humidity conditions contained smaller diameter tubes which had been extruded over 26 AWG stranded copper conductors. The average cross-sectional area of this insulation system was .00209 $in^2$, while the insulation for the 22 AWG conductors typically measured .00474 $in^2$ — or approximately twice that of the 26 AWG set. The purpose for exposing both sets of insulation was to evaluate whether diffusion mechanisms had any influence in the accelerated weathering of this insulation system.

The apparatus used to break these and all other tubular insulations, was a specially designed set of jaws, which are pictured in Figure 5 below. This allowed for an initial gauge length between the bottom and top of the round discs of 50 mm.

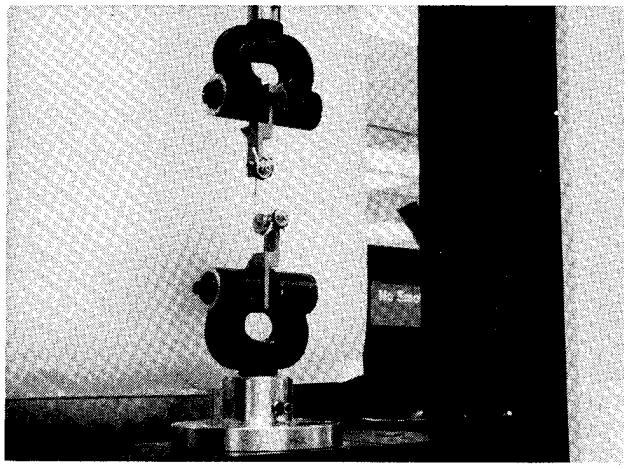


**Figure 5**
**Laboratory Apparatus for Destructive Physical Testing of Tubular Polyethylene Insulations**

The polyethylene used is of the high density variety ( $\varphi$ = 0.95 ) and incorporates a small percentage of high density polypropylene ( $\varphi$ = 0.90 ). A chemical blowing agent (azodicarbonamide) is used to accomplish a 50-55% air containing dielectric insulator.

*(C) Polyethylene Terephthalate (PET) Films*

The PET films subjected to accelerated aging in this study included .001" thick samples, both with and without aluminum backing. The same elastomeric jaws test fixture as shown in Figure 4B, used for the ASTM PVC dumbells, was used to pull these samples until rupture occurred. An initial gauge length of 100 mm was used for this sample set. Most of the testing was performed on the PET films without the aluminum backing, as it was soon obvious that the initial mode of degradation for the aluminum backed films was delamination between the polyester and the aluminum due to adhesion loss. This was not thought to be an alarming mode of failure for the cabling system; however, further work to predict the life of the aluminum backed films continues. The cross-sectional area of the PET film used to determine tensile strength was .00110 $in^2$. Figure 6 depicts the apparatus used for destructive testing of the PET films.

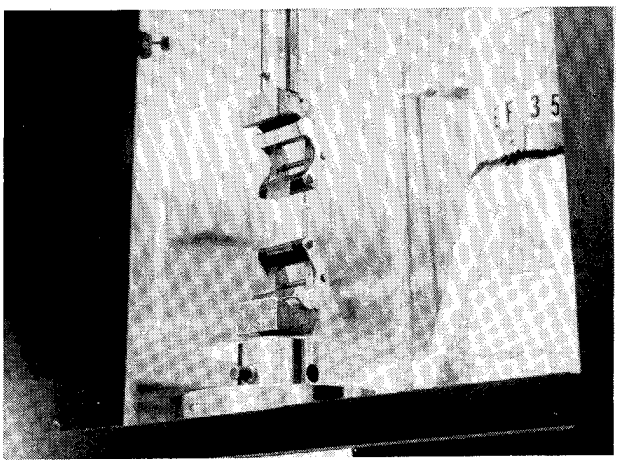


**Figure 6**
**Laboratory Apparatus for Destructive Physical Testing of PET Films**

*(D) Radiation Cured Cross-Linked Polyethylene Insulations and ASTM Dumbells*

As previously mentioned, only three pair of telephone wires were initially included in the Type 2 cable design; however, further development of the IBM Cabling System required the addition of a fourth pair. The accelerated aging of cables began with subjecting the original three pair of solid, cross-linked PE telephone or Voice Grade Media (VGM) wire to the elevated stress environments. The original three pair were colored solid blue, green, or orange, with the second wire of the twisted pair bearing the same color helically striped around the "natural" pastel white pigmented surface.

Destructive testing of the solid PE insulation was performed in an identical manner as that of the foamed PE tubular samples (see Figure 5). The exception for the VGM insulation (stripped away from the 22 AWG solid conductor) was that each conductor diameter was individually measured with a micrometer. This was necessary due to the 7-10% diameter variation found for these as-extruded tubular insulations. All six of the available VGM conductor insulations were subjected to accelerated aging and subsequent tensile testing.

The ASTM dumbell PE specimens were also prepared by extrusion of strips on a Brabender using the following set of conditions; 25:1 L/D ratio, compression ratio of 3:1, and head temperature of 180 C with settings of 170, 160 and 150 C from the barrel head back toward the hopper. Dumbells were then cut in the same manner as their PVC counterparts. These samples were prepared to determine if great differences occur merely by varying the type and form of extrusion. The base, high density, polyethylene resin's specific gravity is 0.95 gm/cm$^3$ prior to electron beam irradiation. After irradiation, the density is increased to 1.26-1.27 gm/cm$^3$, dramatically increasing thermal resistance.

*(E) Endpoint Determination For Wire and Cable Insulations*

A review of the literature and recommended procedures[9-14] for accelerated aging of insulation materials indicates that when making physical test measurements, an endpoint associated with failure criteria often used is 50% of the original value. Although there is some resistance to the use of this criterion, both on a national and international level, the fact remains that many lifetime predictions of various insulating materials have been published using this "specified endpoint". The problem occurs when one begins to compare polymeric insulations on the basis of tensile and elongation values. An insulation system which unaged, exhibits 3500 psi tensile strength and reduces to 1750 psi after 5,000 hours at 100 C may be considered "better than" a similar insulation system which begins at 1500 psi tensile strength and reaches 50% of its original value in 15,000 hours. Clearly, this incongruency illustrates the need to decide on a particular value for the endpoint (rather than some arbitrary percentage of the original value) which has some bearing on the functionality of either the insulation or component system.

For PET films and the foamed PE insulation, endpoint selection was a fairly simple matter, with a specific value of % elongation correlating with embrittlement of the material. The value determined for PET film was 20% elongation — any handling of this insulation not capable of this much stretching would result in physical tearing. For foamed PE, any value less than 70% elongation was found to be unsatisfactory due to embrittlement and physical cracking.

Determination of an endpoint for PVC and cross-linked PE insulations was a much more difficult problem. In the absence of extreme heating in dry atmospheres (> 120 C), the expected mechanism of degradation was unknown, and the possibility existed that even under the accelerated environmental conditions, endpoints would not be reached within a reasonable time frame. Determination of apparent energies of activation (Ea) via the conventional "isothermal" technique could not be performed based on physical test data alone.

3.3 Thermogravimetric Analysis of Wire and Cable Insulations and ASTM Dumbell Specimens

In addition to determination of the apparent energy of activation (Ea) by plotting tensile and elongation endpoint values via the conventional Arrhenius or "isothermal" method, it was deemed necessary to obtain corresponding values of Ea using the thermogravimetric analysis (TGA) or "dynamic" technique as detailed in ASTM E698[15]. This technique involves heating the sample material at several heating rates in the range from 1 to 20 K/min. For our testing purposes, four heating rates (1, 2, 5 and 10 C/min.) were run for each insulation sample. Temperatures at which the reaction peak maxima occurred were recorded and linearized and values of the apparent energy of activation (Ea) calculated from the following equation:

$$\text{Energy of Activation (Ea)} = \frac{R\,d\ln(\beta/T^2)}{d(1/T)} \qquad \text{Equation (1)}$$

where $\beta$ is the heating rate
T is the linearized "corrected" peak temperature maxima

Equation (1) represents the slope of the line when one plots $(\beta/T^2)$ versus (1/T) and is based on the assumptions that the reaction kinetics are first order and that the mechanism of the degradation for the reaction will not change as time and temperature are increased. The ASTM procedure outlines a method to confirm these assumptions using isothermal test methods to determine the kinetic rate constant from the general form of the Arrhenius equation:

$$k = Ae^{-Ea/RT} \qquad \text{Equation (2)}$$

where A is the pre-exponential factor
k is the kinetic rate constant
Ea is the apparent activation energy
R is the gas constant
T is the temperature

Once the value of k is known, then the time to endpoint can be determined assuming first order reaction kinetics from the equation:

$$t = 0.693/k \qquad \text{Equation (3)}$$

where t is the time required to reach a specified endpoint
k is the same kinetic rate constant

To finish the procedure, one selects a temperature at which a sample will reach half of its specified endpoint value, then performs TGA and records its reaction peak. Next, one performs the same TGA on an unaged sample and records its reaction peak. "On an equal weight basis, the peak area or displacement from the baseline of the aged sample should be one half that of the unaged sample. If so, the reaction kinetics are confirmed for the temperature range explored."[13]

The TGA was performed with the aid of a DuPont 990 Thermal Analyser coupled with a 951 TGA plug-in module. The standard procedure followed for the insulation samples included loading of the sample pan with 5-7 mg, followed by a 99.99% pure $N_2$ purge (45-50 ml/min. flow rate) at 70 C for 1 hour. The TGA unit was then heated at the four rates to 600 C. This technique was required after review of earlier weight loss data indicated more than one significant weight loss peak occurred without nitrogen purge of the cell. A sample of a set of four TGA analyses (run at the 1, 2, 5, and 10 C/min. rates) performed for an unaged PVC jacket is shown in Figure 7.

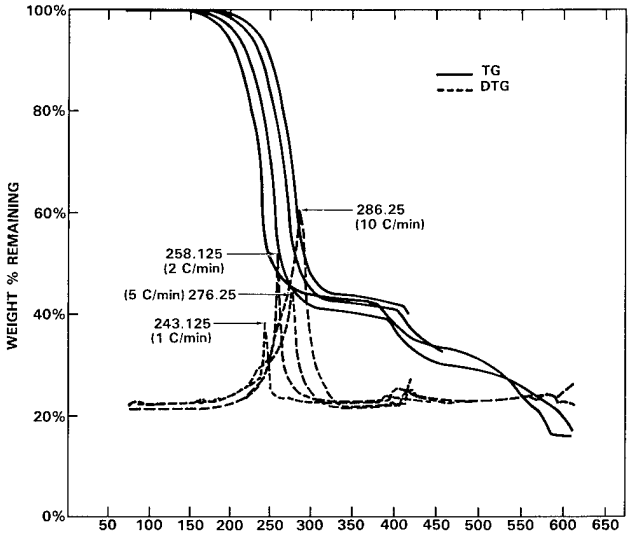



**Figure 7**
**Weight Loss Data Illustrating Reaction Peaks for Unaged 80 C Rated Grooved PVC Jacket at Four Different Rates of Heating (1, 2, 5, and 10 C/min.) Using $N_2$ Purge**

A similar set of analyses is shown in Figures 8 and 9 for unaged foamed PE and unaged PET film, respectively.

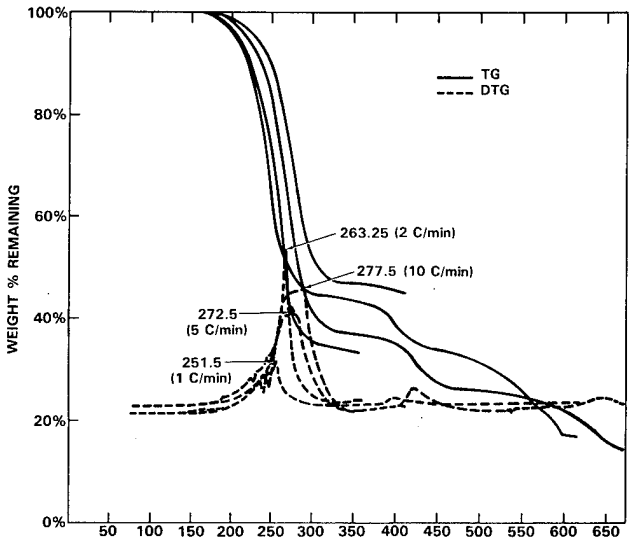



**Figure 8**
**Weight Loss Data Illustrating Reaction Peaks for Unaged Foamed PE Tubular Insulations at Four Different Rates of Heating (1, 2, 5, and 10 C/min) Using $N_2$ Purge**

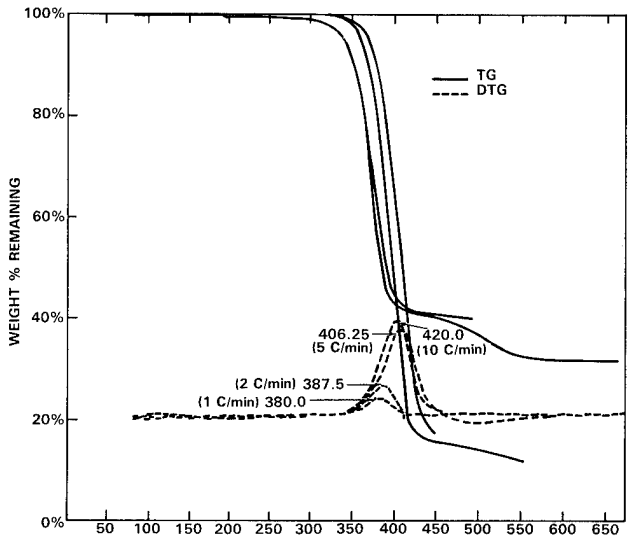



**Figure 9**
**Weight Loss Data Illustrating Reaction Peaks for Unaged PET Film at Four Different Rates of Heating (1, 2, 5, and 10 C/min.) Using $N_2$ Purge**

3.4 Gel Permeation Chromatography (GPC) Analysis of Wire and Cable Insulations

Gel permeation chromatography (GPC) is a technique used to separate molecules on the basis of hydrodynamic volume (or size in solution). This technique was used to generate two types of analyses on cable insulations. Initially, GPC was used to separate the polymer from the additives and thus determine if plasticizer loss was a mode of degradation. Secondly, molecular weight distributions were determined to examine structural changes in the polymer backbone of poly(vinyl chloride) (PVC), polyethylene (PE) and polyethylene terephthalate (PET) insulations.

A basic chromatography system includes a pump for solvent delivery, an injection port for sample introduction, a column to effect separation, and some mode of detection to visualize changes in the sample concentration. The key to obtaining a separation with the maximum amount of useful information is choosing the proper column set. In the analysis of PVC, all columns used were Ultra Styragels® available commercially from Waters Associates. The columns are packed with porous cross-linked styrene divinylbenzene beads. They are typically hydrophobic and are available to separate molecular weight ranges from about 500 to 50,000,000. The columns used for characterization of PE were Shodex A80's. As for characterization of PET films, silica based GPC columns, known as Bondagels®, were used.

GPC columns are packed with porous gels suspended in solvent. Solvent molecules move freely in and out of these pores as well as down the length of the column. As an analysis is initiated and a sample is introduced onto the head of the column, solute molecules permeate the pores of the gels as their size permits. Larger molecules enter very few pores and spend most of their time in the interstitial space surrounding the gels. Since these large molecules do not enter many pores, movement down the column is rapid. During this time, smaller solute molecules are able to diffuse in and out of the pores and therefore move down the length of the column less rapidly. As a result of this difference in column retention, a chromatogram such as that pictured in Figure 10 is generated. One notices the high molecular weight material elutes at the left hand side of the chromatogram and the lower molecular weight material to the far right.

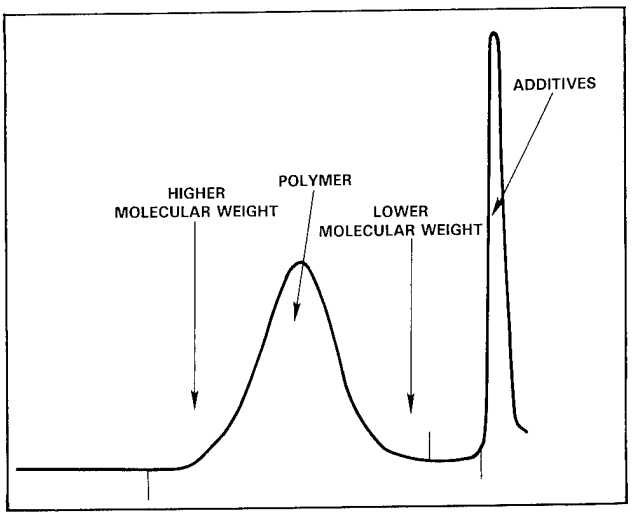



**Figure 10**
**Sample Chromatogram of PVC Insulation (Columns — $10^6$, $10^4$, 500 A° Ultrastyragel® )**

It is possible through column selection to change the shape and separation power of the system. In the case of determining plasticizer loss from poly(vinyl chloride) insulations, it was desirable to choose columns which would yield two fairly narrow peaks to distinguish differences between samples. This separation may be obtained by using one 500 A° Ultrastyragel® column. A sample chromatogram is shown in Figure 11. All of the larger polymer molecules are excluded from the pores and thus elute as one peak at the front of the chromatogram. Likewise, all of the smaller additive molecules are able to permeate the pores and elute as a single peak at the end of the chromatogram.

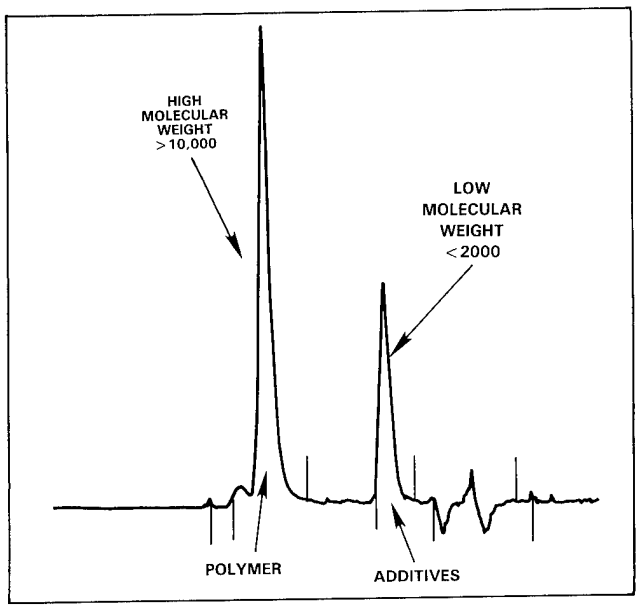



**Figure 11**
**Sample Chromatogram of PVC Insulation (Narrow Range of Pore Size Column — 500 A° Ultrastyragel® )**

A more typical GPC separation, like that shown in Figure 10, is obtained by using a set of columns which possess a wider range of pore sizes. Sample molecules are separated in a continuous range due to the wide size of available pore sites for diffusion. In this separation, the distribution is more bell shaped and calculation of molecular weight averages is possible.

Reproducibility of results is an important factor in any analytical technique. As an example of reproducibility in GPC, two sequential injections of filtered sample from a white ASTM dumbell were made separately. The calculated molecular weight averages are as follows:

| | Mn | Mw | Mz | Polydispersity |
|---|---|---|---|---|
| | 69141 | 132330 | 222658 | 1.32 |
| | 68672 | 132143 | 222808 | 1.32 |
| % difference | 0.7 | 0.1 | 0.1 | — |

The differences between the calculated averages are very low, leading one to believe that results generated by this method are reasonably precise and reproducible.

*(A) PVC Homopolymers*

A Waters Associates 150 C chromatograph and 740 Data Module combination was used for analysis on all PVC samples. In each run,

a differential refractometer was the sole mode of detection. All standards and samples were run in HPLC grade tetrahydrofuran (THF), stabilized with 2,6-di-tert-butyl-p-cresol to prevent peroxide buildup. The columns were standardized with narrowly dispersed polystyrene standards available from the Pressure Chemical Company.

Samples were prepared to 0.25% (weight to volume) in solution. These samples were then filtered through a Millex SR five A° filter to remove any particulates. Injections were made in duplicate with 350 ml of the filtrate. A flow rate of 1 ml/min. was used throughout the analysis. The column set used in this analysis matched that depicted in Figure 10.

*(B) Foamed Polyethylene Data Grade Media (DGM) Insulation*

Tubular PE samples were dissolved and filtered in HPLC grade trichlorobenzene. The instrumentation used was a Waters 150 C liquid chromatograph operated at 145 C in the injector compartment and 135 C in the column compartment. Sample concentration was 0.15% weight to volume. The flow rate through the system was 1 ml/min. One Shodex-A80 column was used for the separation.

*(C) PET Films*

Samples were dissolved in hexafluoroisopropanol to 0.25% weight to volume. Samples were then filtered through a 5 micron filter to remove any particulates present. Injections were made with 50 ml of filtered sample.

The columns used in the chromatographic system were one E125 and one E1000 Bondagel® from Waters Associates. An I60 diol column was then added to aid in the low end resolution of the chromatogram. The mode of detection employed was a differential refractometer coupled with a UV detector. Flow through the system was 0.3 ml/min.

3.5 Solubility of PVC in Tetrahydrofuran (THF)

During the GPC analysis of PVC insulations, it was discovered that after exposure to the elevated temperature and humidity environments, certain specimens became insoluble in THF. This insolubility point, which will later be shown to correspond with "gelation" or crosslinking of the polymer chain, was considered as a possible endpoint for the useful life of the jacket insulations. This chemically determined endpoint took on even greater meaning as it was determined that no gross changes in measurable physical/mechanical properties were observed within the accelerated aging time period (up to 274 days).

A 0.04 gram sample was cut from the insulations which had been exposed to high temperature and humidity conditions. This sample was then placed in a test tube with 7 ml of THF. Each tube was capped with a rubber stopper and placed in a sonic bath for five minutes. The tubes were then removed and allowed to stand at ambient temperature overnight (16 hours).

Tubes were then shaken and observed with the aid of a lightbox. Samples which had PVC "backbones" remaining were considered insoluble. Other samples which had a uniform appearance were carefully examined for any remaining solids in solution before being declared "soluble".

## IV. RESULTS

4.1 Destructive Physical/Mechanical Testing Data and Endpoint Determination for Wire and Cable Insulations

*(A) PVC Homopolymer Jackets and White ASTM Dumbells (80 and 105 C Rated)*

Destructive physical/mechanical testing of the aged PVC jackets (and other insulations) as described in Section 3.2, was normally performed within 48 hours after removal of the samples from the environmental chambers. Data recording consisted of documenting the peakload and elongation at break for all PVC samples. A sample of the typical stress-strain curve generated in this test procedure is given in Figure 12. The aged PVC specimens yielded almost identically shaped curves throughout the aging period.

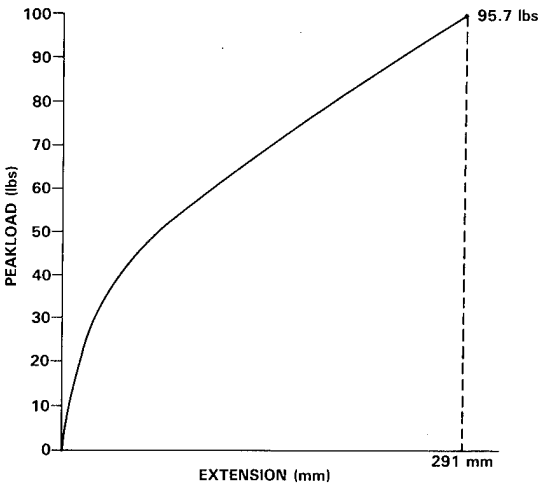



**Figure 12**
**Typical Stress-Strain Curve Generated in Destructive Physical-Mechanical Testing of Grooved PVC Jacketing (Unaged) From Type 6 80 C Rated Office Cable**

With the aid of a statistical analysis package (SAS-Statistical Analysis System) a program was written which generated mean values for both elongation and tensile strength at each temperature over a specified time period, using the three dimensional bar chart form as shown in Figures 13A and 13B. These figures illustrate the same typical trends associated with flexible PVC which has been exposed to *air-oven aging*. First, there is a gradual increase in elongation, followed by a fairly consistent decrease in this property value. Also, there is a steady increase in tensile strength until the composition begins to degrade beyond recognition due to either excessive temperature or age. Increased tensile strength values correlated with increased stiffness of the samples. For samples which have been exposed to dry-heat aging, this phenomenon is normally associated with loss of plasticizer in the PVC compound. As will be shown,

although the same general changes in physical properties occurred when PVC was exposed to elevated temperature and humidity, cross-linking mechanisms in the main chain of the polymer were responsible for the shifts in physical properties.

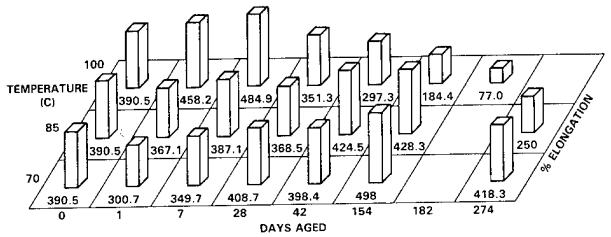



**Figure 13A**
**Loss of Elongation for "Grooved" 80 C Rated PVC Jacketing from Type 6 Office Cable**

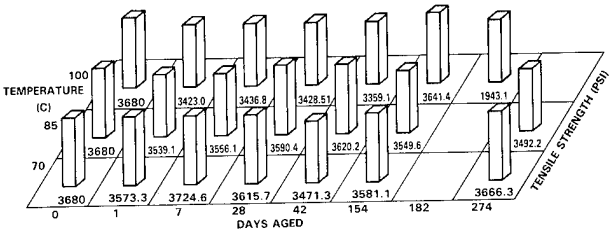



**Figure 13B**
**Loss of Tensile Strength for "Grooved" 80 C Rated PVC Jacketing from Type 6 Office Cable**

Figure 14 has been included to illustrate that the white PVC ASTM dumbells, which are composed of the same resin as the grooved jackets but which did not contain carbon black, yielded almost identical results in the same accelerated aging environments. This was an expected result as the carbon black loading is added to stabilize PVC in the presence of light rather than heat.

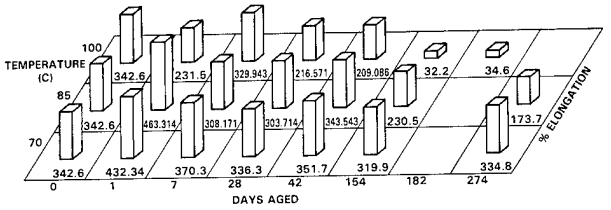



**Figure 14**
**Loss of Elongation for White PVC ASTM Dumbells (Base Resin for Jacketing of Type 6 Office Cable - see Figure 13)**

Figure 15 indicates that the use of a different heat stabilizing system in the UL 105 C rated PVC compound, also guarded the system from oxidative and hydrolytic degradation. The rather large changes in elongation seen for the 80 C rated compounds are not evident here. Notice that the values for loss of tensile strength are not reported in Figures 14 and 15. As indicated by Mathes[16], the usefulness of tensile strength property data as an indicator of life expectancy of most insulation systems is suspect. The flexible grade PVC's investigated for this study actually showed increases in tensile strength with time, which correlated with GPC results (Section 4.3) indicating corresponding increases in molecular weight. The increases in molecular weight coincided with decreases in solubility in THF for these same samples.

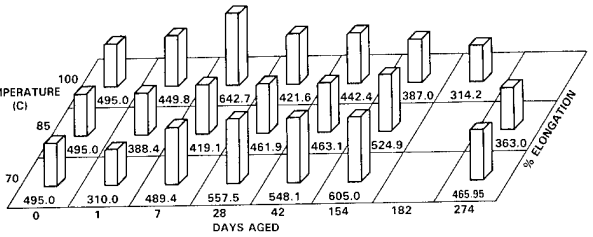



**Figure 15**
**Loss of Elongation for "Smooth" 105 C Rated PVC Jacketing for Type 2 Non-Plenum Cable**

*(B) Foamed Polyethylene Data Grade Media (DGM) Insulation*

The tubular foamed PE insulations, which were tested as shown in Figure 5, exhibited some surprising physical changes during environmental exposure. Within the first week, even at the lowest temperature exposure, an immediate increase in tensile strength values for both thicker tubular insulations (from which the 22 AWG copper conductors were removed) occurred (see Figure 16). This trend continued for at least the first 154 days of exposure at all three temperatures and was evident to an even greater extent for the thinner foamed tubular samples as depicted by Figure 17. It was theorized that this phenomenon was due to an increase in density of the PE which may have occurred because of a change in both crystallinity and % cross-linking during the course of exposure. The fact that increases in tensile strength were more dramatic for the thinner (26 AWG) insulations may be a result of a higher rate of diffusion of moisture through less (by weight, volume, and cross-sectional area) insulation.

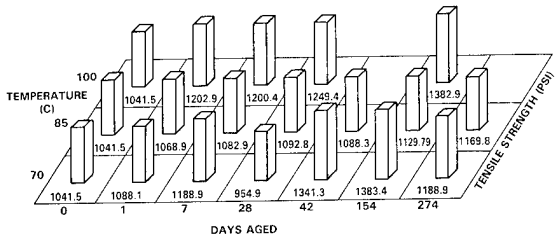



**Figure 16**
**Change in Tensile Strength for Tubular "Foamed" PE 22 AWG Conductor Insulations With Black Helical Stripes**

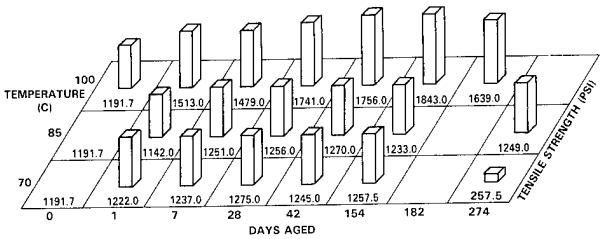



**Figure 17**
**Change in Tensile Strength for "Foamed" Tubular PE 26 AWG Conductor Insulation**

Trends in % elongation loss for the three foamed tubular PE insulations tested were more difficult to analyse. Except for the change which occurred between the 154 and 274 days aged data at 70 C, Figure 18 illustrates the expected decrease in ability to stretch under load of the 22 AWG foamed PE insulation with time. As the insulation neared the 70% elongation mark, an associated change in durability, due to physical embrittlement and cracking, was noticed. Figure 19 illustrates the fact that similar trends occurred for the thinner (26 AWG), but otherwise identical, insulation. Figures 20 and 21 illustrate the differences which occurred in the shape of the stress-strain curves generated as the material was aged in an accelerated environment. An explanation for these results is attempted in Section 5.1.

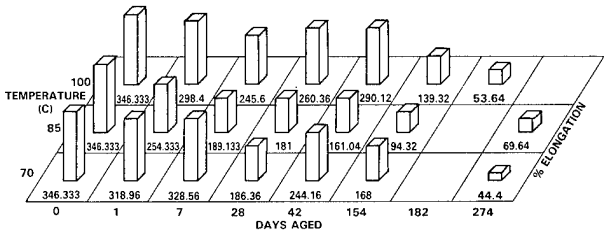



**Figure 18**
**Loss of Elongation for**
**"Foamed" Tubular PE 22 AWG Conductor Insulation**
**(Orange Helically Striped)**

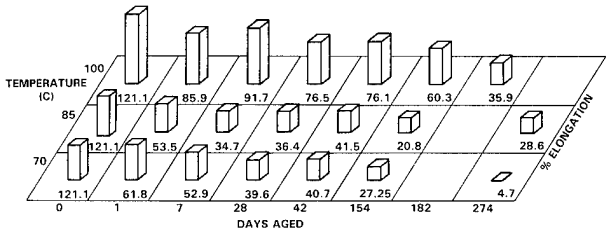



**Figure 19**
**Loss of Elongation for**
**"Foamed" Tubular PE 26 AWG Conductor Insulation**

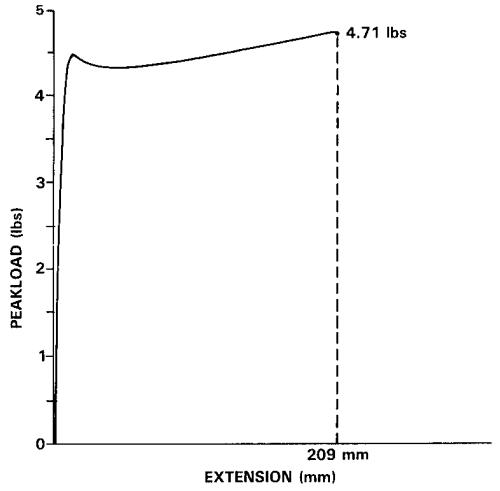



**Figure 20**
**Typical Stress-Strain Curve For**
**Tubular Foamed 22 AWG (Orange Helically Striped)**
**PE Insulation - Unaged**

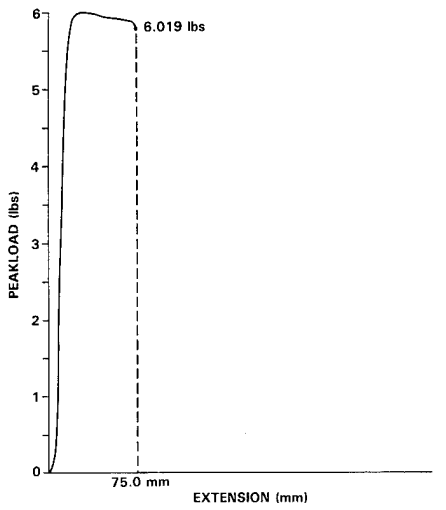



**Figure 21**
**Stress-Strain Curve For**
**Tubular Foamed 22 AWG (Orange Helically Striped)**
**PE Insulation Aged 154 Days in 100 C/98%+ RH Environment**

*(C) PET Films*

The overwhelming presence of moisture combined with extreme temperatures caused the poly(ethylene terephthalate) films to deteriorate in a characteristic manner. A sample of the typical stress-strain curve generated during tensile testing is given in Figure 22, the shape of which did not change throughout the aging period. Figures 23A and 23B illustrate the loss in both elongation and tensile strength with time. Careful inspection of Figure 23B shows that the loss of tensile strength properties due to oxidative and hydrolytic degradation were not quite as rapid or severe as the loss in elongation (Figure 23A). It is interesting to note that loss of tensile strength in PET films, however, is the property most often reported in the literature. Also interesting, were the slight increases in both elongation and tensile properties at 70 C after 2 weeks of aging. One can only theorize that perhaps a reorganization in the crystalline structure of the film allowed for better orientation in the uniaxial direction in this specific temperature region after aging. Certain x-ray diffraction techniques would be neccessary to determine if this theory has any validity.

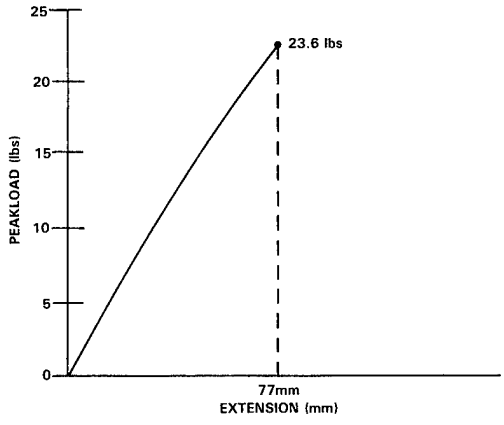



**Figure 22**
**Typical Stress-Strain Curve**
**Generated in Destructive Physical-Mechanical Testing**
**of PET Film (Unaged)**

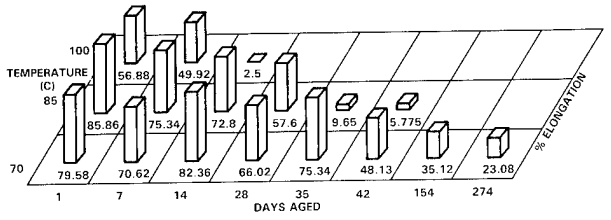



**Figure 23A**
**Loss in Elongation for PET Films**
**With Time and Temperature in a 98%+ RH Environment**

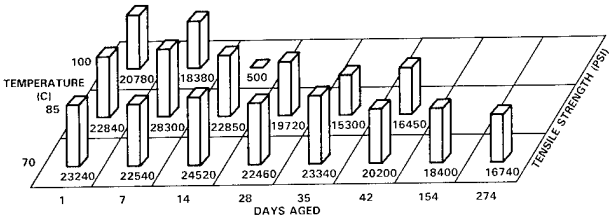



**Figure 23B**
**Loss of Tensile Strength for PET Films**
**With Time and Temperature in a 98%+ RH Environment**

*(D) Radiation Cured Cross-Linked Polyethylene Insulations and ASTM Dumbells*

The most important result which can be ascertained from the large amount of data collected for both the tubular and dumbell specimens of the cross-linked PE insulation is that there were no significant changes in any of the physical properties as time progressed. Figure 24, the stress-strain curve for the solid tubular radiation cured cross-linked PE samples, is typical of that of other cross-linked polyethylenes, and did not change at all during the aging period. The other interesting result is dramatically shown by comparison of Figures 25 and 26, illustrating that no differences in tensile or elongation values occurred for either solid colored or naturally pigmented cross-linked PE.

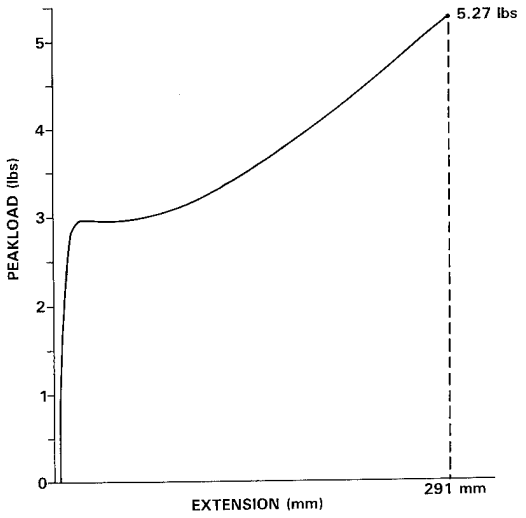



**Figure 24**
**Typical Stress-Strain Curve**
**Generated in Physical-Mechanical Testing of**
**Cross-linked Solid Polyethylene (22 AWG) Insulation (Unaged)**

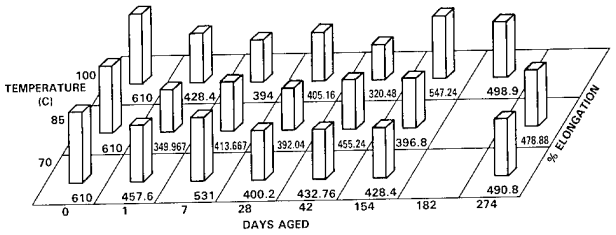



**Figure 25**
**Change in Elongation for**
**Solid Tubular Cross-Linked PE (22 AWG) VGM Insulation -**
**Blue with a White Helical Stripe**

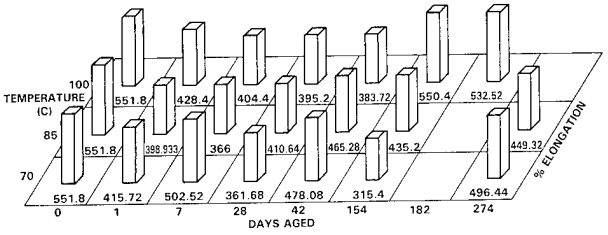



**Figure 26**
**Change in Elongation for**
**Solid Tubular Cross-Linked PE (22 AWG) VGM Insulation -**
**White with a Blue Helical Stripe**

Because of the lack of change in the physical properties of the cross-linked PE insulations over the same length of exposure which caused all other cable insulations to deteriorate in some manner, further efforts to predict the life of this system were discontinued. An Arrhenius model, representing an estimated life based solely on thermal aging is included and discussed in Section 4.5.

*(E) Endpoint Determination For Wire and Cable Insulations*

Endpoint determination, using the data of aged insulation samples, was accomplished by graphical means in a manner similar to that developed by Nelson[17, 18 and 19] and Hahn.[20] First, the probable average value for elongation at each time interval desired was determined using Gaussian distribution paper. For a large percentage of the data, the Gaussian distribution fit well. Another technique, not yet performed, would be the use of Weibull distribution paper.

Next, multi-cycle semilog paper was used to plot % elongation (on the abscissa) values versus log-time (along the ordinate). This technique usually illustrates a dramatic drop in properties which occur within a very limited time region, allowing for a more precise estimate of the time at which the endpoint occurs. This "time-to-endpoint" value is then used for obtaining the curve in the conventional 1/temperature vs. log-time plot often referred to as the "Arrhenius Model". The usefulness of this endpoint determination will become more apparent in the discussion involving Arrhenius modeling found in Section 4.5.

4.2 Thermogravimetric Analysis (TGA) and Apparent Energy of Activation (Ea) Values Generated from both Aged and Unaged Insulation Specimens

*(A) PVC Homopolymer Jackets and White ASTM Dumbells*

Section 3.3 describes the techniques used to determine values for the apparent energy of activation (Ea) for the various wire and cable insulations. Thermogravimetric analyses (TGA) at the four separate rates of heating (1, 2, 5, and 10 C/min) were run for 11 different

samples of the black pigmented, grooved 80 C rated, PVC jackets. An additional TGA run was performed to determine the reproducibility of results. Figure 7 illustrated the weight loss curves for an unaged PVC grooved jacket insulation. Three additional Figures, 27-29, indicate that the mechanism of degradation, for samples which had been aged for 154 days (22 weeks) at each temperature, and then were subsequently submitted to thermal analysis, did not change appreciably with time. The curves indicate major weight loss (approximately 50%) in the 200-300 C temperature region, followed by a more minor loss (approximately 10%) of weight in the 425-460 C temperature regime. Energy of activation values were calculated based on peak maxima temperatures associated with the major weight loss portion of the curves only. All runs were performed with the $N_2$ purge and therefore should indicate weight loss solely based on thermal degradation. It is emphasized here, that this form of accelerated aging (or heating) of the samples is of a completely different mode than that of the isothermal aging performed in the high humidity environments.

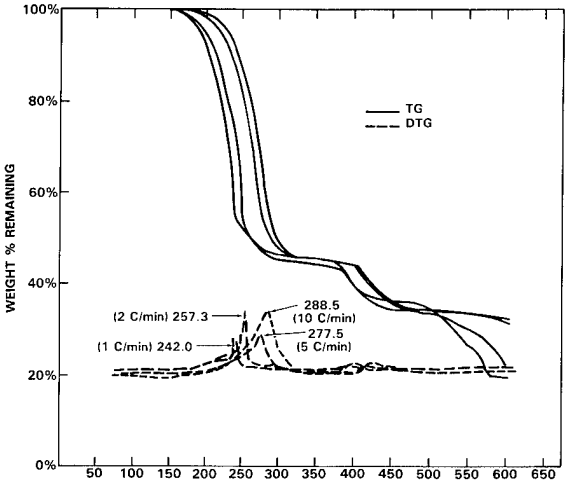



**Figure 27**
**Thermogravimetric Analysis (TGA) of**
**80 C Rated PVC Jacket Insulation Aged 154 Days**
**in 70 C/98%+ Environment**

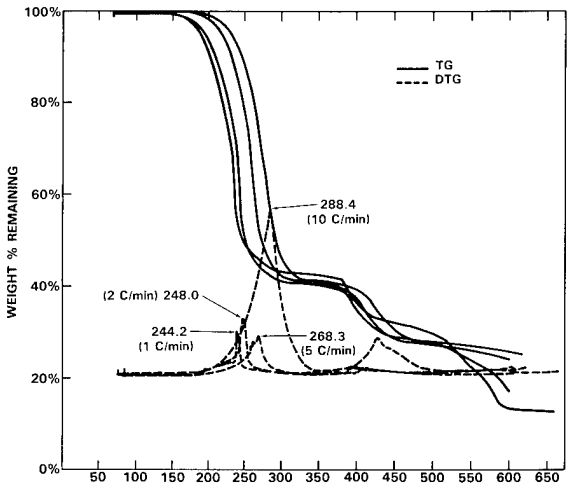



**Figure 28**
**Thermogravimetric Analysis (TGA) of**
**80 C Rated PVC Jacket Insulation Aged 154 Days**
**in 85 C/98%+ RH Environment**

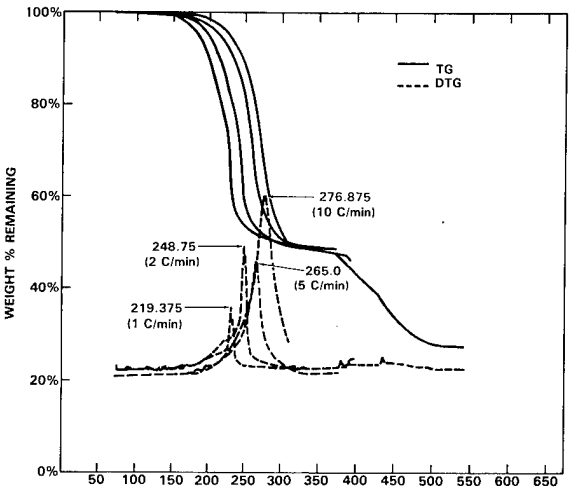



**Figure 29**
**Thermogravimetric Analysis (TGA) of**
**80 C Rated PVC Jacket Insulation Aged 154 Days**
**in 100 C/98%+ RH Environment**

Ea values calculated for each sample are 25.80, 25.80, and 20.97 Kcal/mol for Figures 27, 28, and 29, respectively. The difference in Ea for the TGA curve shown in Figure 29, which was aged for 154 days at 100 C, indicates that perhaps the onset of thermal degradation had already begun in earnest after that period of time in the most severe environment. This theory took on further meaning when it was determined that the Ea value for the same insulation aged for only 126 days in the same environment yielded a higher Ea value of 24.42 Kcal/mol., indicating less physio-chemical deterioration.

Reproducibility of the thermal analysis data obtained for the grooved 80 C rated PVC specimens was only within 20% based on subsequent runs of unaged specimens. This was the poorest result found for reproducibility of any of the insulations tested via TGA. ASTM white dumbells in both an aged and unaged condition were submitted to thermal analyses; however, inconclusive results were obtained based on limited sample size.

*(B) Foamed Polyethylene Data Grade Media (DGM) Insulation*

Figure 8 illustrates the weight loss curves for an unaged tubular (22 AWG sized) PE insulation. Inspection of this figure indicates a much different result than that of the curves shown below in Figures 30-32. Indications are that the foamed HDPE increased in both density and crystalline morphology almost immediately after exposure to elevated temperature environments. A value of 23.50 Kcal/mol for the Ea of the unaged sample was calculated from the weight loss curves of Figure 8. Meanwhile, the values for samples aged 154 days are 50.92, 52.76, and 44.47 Kcal/mol for TGA calculations made from Figures 30, 31, and 32, respectively. It should be noted that after only 2 weeks at even the lowest temperature exposure (70 C), there was a tremendous increase in the calculated Ea, based on an 80% weight loss within the extremely high temperature range (for PE) of 400-475 C. Again, all runs were made with $N_2$ purge, and therefore, Ea values should be based solely on thermal degradation mechanisms. All aged samples exhibited the same basic weight loss characteristics. Thus a mean value of 52.07 Kcal/mol was found for the 10 aged samples evaluated, with a standard deviation between samples of no greater than 12%. This was again indicative of the fact that the mechanism of aging was constant during the accelerated environmental exposure time.

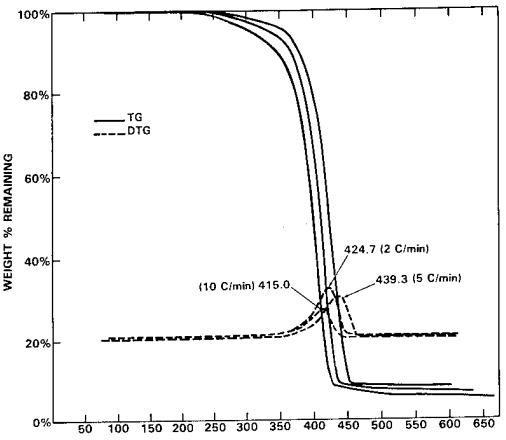



**Figure 30**
**Thermogravimetric Analysis (TGA) of Foamed PE Insulation Aged 154 Days in 70C/98% + RH Environment**

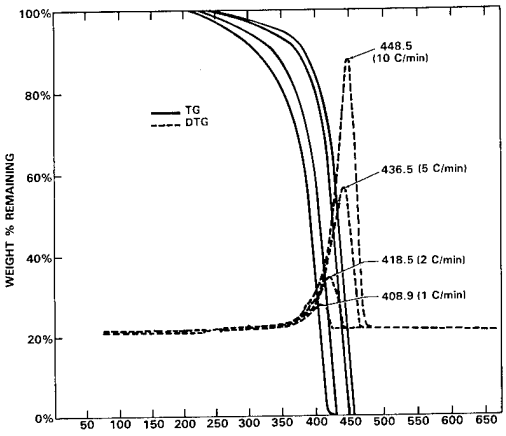



**Figure 31**
**Thermogravimetric Analysis (TGA) of Foamed PE Insulations Aged 154 Days in 85 C/98% + Environment**

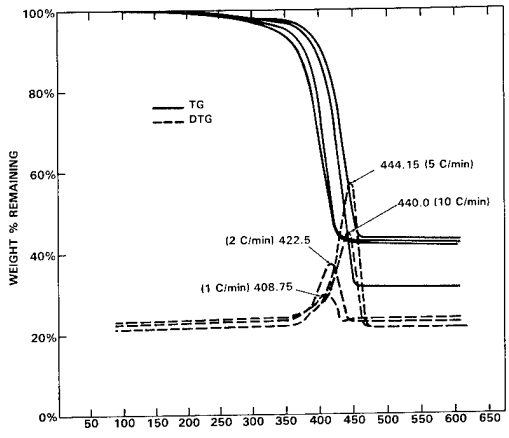



**Figure 32**
**Thermogravimetric Analysis (TGA) of Foamed PE Insulation Aged 154 Days in 100 C/98% + RH Environment**

*C. PET Films*

Figure 33 below illustrates the importance of developing the previously discussed $N_2$ purge technique. TGA, for an unaged PET film without the purge, indicated other lower temperature weight loss peaks (most likely due to oxidation and possibly some hydrolysis related reactions) which made calculation of activation energies nearly impossible.

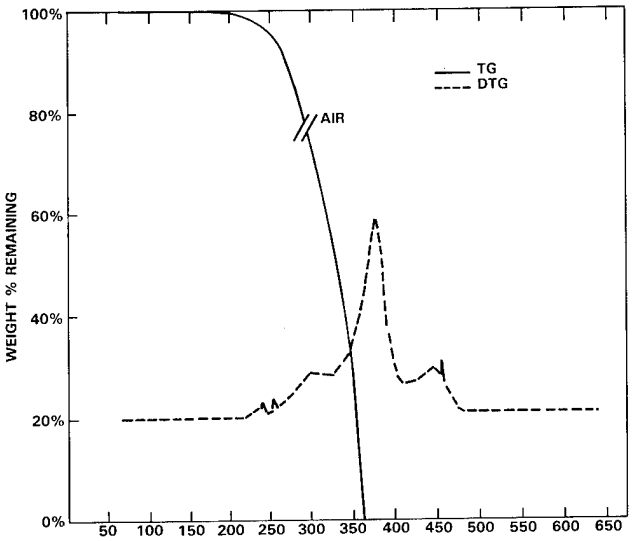



**Figure 33**
**Thermogravimetric Analysis (TGA) of Unaged PET Film Without $N_2$ Purge (in Air with 45-50 ml/min. flowrate) Heated at 5 C/min.**

Re-inspection of Figure 9 indicates the absence of any pre-thermal degradation mechanisms, due to the use of inert carrier gas which provided a nitrogen atmosphere. Due to this informative procedural study on PET films, all subsequent TGA runs were performed with $N_2$ purge. For PET films, this was required so a single mechanism of thermal degradation could be studied. It is assumed that the same technique was required for the same purposes with the other insulation systems under study. Peak maxima temperatures were associated with approximately 45% weight loss of each sample.

The data for 13 different samples indicate that PET films aged in a 98 ± 2% RH environment within a 70 - 100 C temperature range degrade in a like manner when subjected to thermal decomposition in an inert atmosphere. The fact that the values of Ea for each set of samples aged for different times at different temperatures are within good agreement (less than 1% standard deviation) gives further creedance that this method can be used to establish life criteria for certain materials if the mechanism of degradation remains constant. The applicability of thermal analysis techniques to determine lifetimes of materials has been very controversial and is well documented.[21-27] In this case, the mechanism of thermal degradation of PET film overwhelms the effect of hydrolytic and oxidative degradation which occurred while these samples were subjected to accelerated aging within the environmental chambers. The values for Ea also decrease for PET film subjected to the higher temperature environments, from 45.78 to 44.60 to 44.54 Kcal/mol for the 70, 85 and 100 C exposure levels, respectively.

4.3 Results of Gel Permeation Chromatography (GPC) Analysis

*(A) PVC Homopolymer Jackets and White ASTM Dumbells*

Loss of plasticizer affects the physical properties of poly(vinyl chloride). In the past, it has been shown that plasticizer loss can

be traced by a variety of methods[39]. Turi[28] has documented thermal methods for analysis of plasticizer loss in an 121 C circulating air oven. Table 2 contains the results of that study. To qualify GPC as a viable method for tracking plasticizer loss, samples of 105 C rated insulation were placed in a 100 C oven for varying periods of time. These samples were removed from the 100 C oven and analyzed by GPC as sited previously. Table 3 lists the exposure time and peak area ratio for the PVC and plasticizer peaks. A sample chromatogram is shown in Figure 34. Fractions were collected and analyzed by infrared spectroscopy to confirm the presence of polymer and plasticizer. The concentration of volatile plasticizer in insulations had undergone a 19% decrease within 196 hours of oven exposure. This data confirms GPC's effectiveness in tracking changes in plasticizer content for flexible PVC compounds.

**Table 2[28]**
**Estimation of Di-iso-decylphthalate (DIDP) Lost From PVC During Oven Aging At 121 C**

| Time at 121 C (Days) | Plasticizer lost (wt %) | Concentration DIDP calculated (phr) | $T_g$ (K) | Conc. DIDP estimated (phr) |
|---|---|---|---|---|
| 0 | 0 | 30.0 | 275 | 28 |
| 3 | 12.8 | 26.2 | 287 | 24 |
| 6 | 18.1 | 24.6 | 290 | 23 |
| 10 | 23.1 | 23.1 | 299 | 20 |
| 14 | 35.6 | 19.3 | 305 | 18 |
| 24 | 54.0 | 13.8 | 315 | 14 |

**Table 3**
**Relative Plasticizer Content in 80 C Rated PVC Insulations Aged at 100 C in a Circulating Air-Oven**

| Hours in Oven | Area Percent | |
|---|---|---|
| | PVC | Additives |
| 0 | 69.6 | 30.4 |
| 8 | 70.8 | 29.2 |
| 24 | 71.1 | 28.9 |
| 48 | 72.1 | 27.9 |
| 96 | 73.4 | 26.6 |
| 144 | 74.8 | 25.2 |
| 196 | 75.3 | 24.7 |

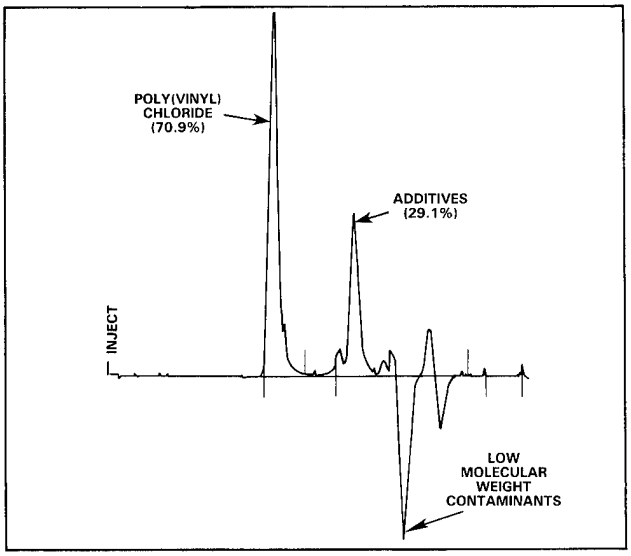



**Figure 34**
**Sample Chromatogram of Air-Oven Aged 80 C Rated Grooved Jacket PVC**

Samples were selected from insulations exposed to the high temperature/high humidity environments and run in the same fashion as those from the 100 C oven. Table 4 lists the results from the analysis of samples exposed to 85 C and 98% ± 2% RH. After an initial 8% decline in plasticizer content, no further change in concentration can be detected. A sample chromatogram from this analysis is included in Figure 35. Analysis of 80 C rated insulations and white ASTM Dumbells aged in the same environment yielded similar results.

**Table 4**
**Relative Plasticizer Content in Cable Insulations (105 C Rated Insulations Aged at 85 C)**

| Weeks in Chamber | Area Percent | |
|---|---|---|
| | PVC | Additives |
| 0 | 67.7 | 32.3 |
| 5 | 70.9 | 29.1 |
| 15 | 70.3 | 29.7 |
| 23 | 70.3 | 29.7 |

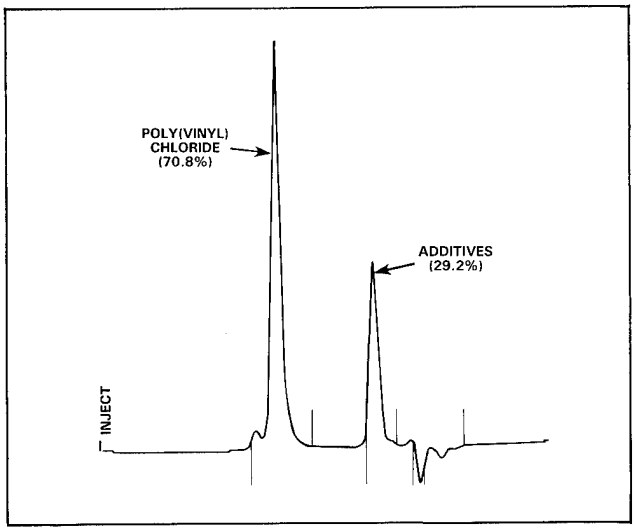



**Figure 35**
**Sample Chromatogram for 105 C Rated PVC Insulations Exposed to 85 C/98+% RH Environment**

Base polymer resin of insulations which were not exposed to high temperature/high humidity conditions were analyzed by GPC. An overlay of chromatograms from 105 C and 80 C rated insulations as well as white ASTM dumbells are included in Figure 36. The molecular weight averages as listed in Table 5, indicate the white base resin has just slightly lower molecular weight averages than the 80 C rated and 105 C rated insulations. These differences, however, are well within the expected experimental error of 10% normally associated with GPC techniques. In other words, there are no discernable differences between the molecular weight distributions and any of the base resins.

**Table 5**
**Comparison of "As Received" Polymers**

| Insulation | Mn | Mw | Mz |
|---|---|---|---|
| 105 C Rated | 73676 | 145993 | 264561 |
| 80 C Rated | 73853 | 146962 | 261381 |
| White Base Resin | 72408 | 143378 | 252970 |

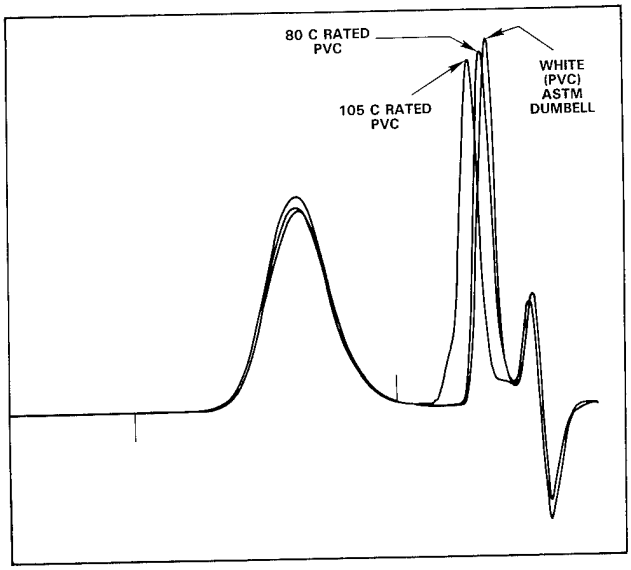



**Figure 36**
**Overlay of Chromatograms from Unaged 80 C, 105 C Rated PVC, and White PVC ASTM Dumbells**

Grooved PVC jacket (80 C rated) insulations removed from the 100 C, 85 C, and 70 C / high humidity environments were analyzed by GPC methods. Insulations exposed to the 100 C, high humidity environment show rapid increases in Mn, Mw, and Mz. After two weeks of exposure, the Mw of the insulation increased 77% as can be seen in Table 6. In Figure 37, a comparison may be made of subsequent chromatograms. A "shoulder" has formed on the sample with a two week exposure, indicating the buildup of higher molecular weight material. The molecular weight distribution has also broadened and shows an increase in polydispersity.

**Table 6**
**Calculated Molecular Weight Averages for Grooved PVC 80 C Rated Insulations Exposed to a 100 C/98%+ RH environment**

| Exposure Time (days) | Mn | Mw | Mz | Polydispersity |
|---|---|---|---|---|
| 1 | 72148 | 139138 | 233470 | 1.9 |
| 4 | 72315 | 141775 | 243273 | 2.0 |
| 14 | 81426 | 246435 | 674377 | 3.0 |

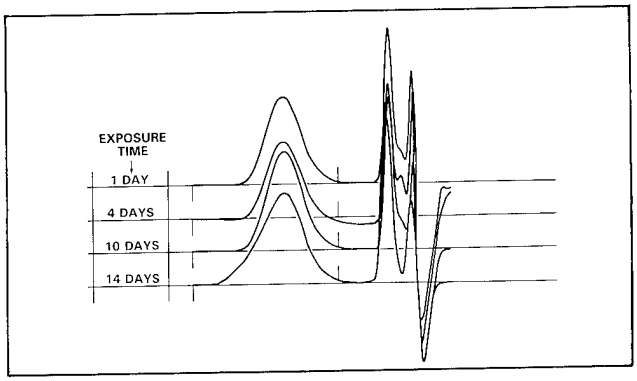



**Figure 37**
**80 C Rated Grooved PVC Jacket After Exposure to 100 C/98+% RH for an Increasing Length of Time**

After exposure to the 85 C environment, 80 C rated jacket insulations show a significant increase in weight and z-average molecular weights. Table 7 includes molecular weight calculations for four analyses through 14 weeks of exposure. One may also note an increase in dispersity of the sample. This increase in dispersity indicates an increase in the width of the distribution defined as:

$$\text{Dispersity} = Mw/Mn$$

A comparison of chromatograms may be seen in Figure 38. Notice the development of the high molecular weight end of chromatograms after 10 weeks of exposure. Also, the distribution broadens and flattens due to the changing dispersity. Figure 39 is an overlay of insulations which were in both as received condition and after exposure to the 85 C environment for 14 weeks. This view enhances the ability to see the changes in molecular weight distributions mentioned previously.

**Table 7**
**Molecular Weights of Grooved 80 C Rated PVC Jacketed Insulations After Exposure to 85 C/98% RH Environment**

| Exposure Time (weeks) | Mn | Mw | Mz | Polydispersity |
|---|---|---|---|---|
| 0 | 66235 | 145936 | 297568 | 2.2 |
| 4 | 72904 | 236386 | 800101 | 3.2 |
| 10 | 70832 | 334360 | 1736240 | 4.7 |
| 14 | 64836 | 353126 | 2004210 | 5.4 |

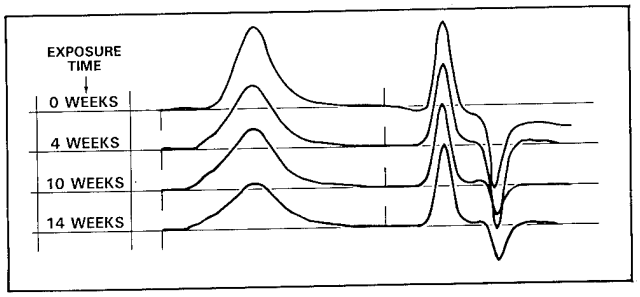



**Figure 38**
**80 C Rated PVC Grooved Jacketed Insulations After Exposure to 85 C/98+% RH Environment**

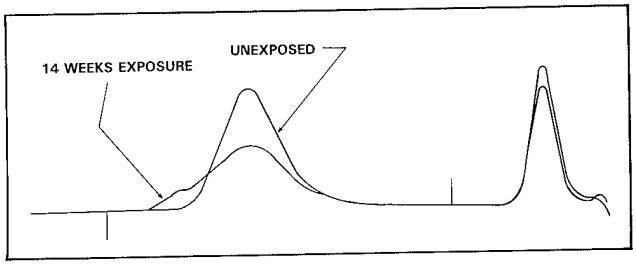



**Figure 39**
**80 C Rated Grooved Jacket Insulations Exposed to 85 C/98+% RH Environment**

At this point, one may compare the results for insulations exposed to both 100 C and 85 C conditions. The physical changes are very similar although the higher the exposure temperature, the more quickly an increase in molecular weight can be detected.

Insulations exposed to the 70 C environment show similar changes in their molecular weight distributions, although changes do not

occur as rapidly. Table 8 lists molecular weight averages for five samples exposed to the 70 C environment. There is an initial "jump" in molecular weight occurring until 10 weeks of exposure. Following 10 weeks exposure, changes occur much less rapidly. The increases are still not of the same order of those samples exposed to 85 or 100 C, indicating further increases in molecular weight are still possible with longer exposure times.

**Table 8**
**Molecular Weights of Grooved 80 C Rated PVC Jacket Insulations After Exposure to 70 C/98+% RH Environments**

| Exposure Time (weeks) | Mn | Mw | Mz | Polydispersity |
|---|---|---|---|---|
| 0 | 54684 | 126328 | 219701 | 2.3 |
| 10 | 62059 | 199700 | 514650 | 3.2 |
| 15 | 59563 | 200159 | 526103 | 3.4 |
| 23 | 62435 | 199507 | 508497 | 3.2 |

Smooth 105 C rated PVC Jackets insulations which were exposed to the 100 C high humidity environment all exhibit changes in their molecular weight distribution over time. Table 9 contains molecular weight data for 105 C rated insulations after exposure to 100 C/98+% RH.

**Table 9**
**Calculated Molecular Weight Averages for Smooth 105 C Rated Insulations Exposed to 100 C/98+% RH Environment**

| ExposureTime (weeks) | Mn | Mw | Mz | Polydispersity |
|---|---|---|---|---|
| 0 | 66508 | 139217 | 247039 | 2.1 |
| 2 | 66896 | 143517 | 260753 | 2.2 |
| 3 | 68982 | 163980 | 326728 | 2.4 |
| 4 | 70445 | 185731 | 400082 | 2.6 |

In this case, a noticable increase can be detected in number, weight, and z-average molecular weights along with dispersity. These results indicate a 33% increase in the weight average molecular weight of the PVC after only four weeks of exposure. A visual comparison of the chromatograms may be made in Figure 40. Again, note the change in the high molecular weight end as time of exposure increases.

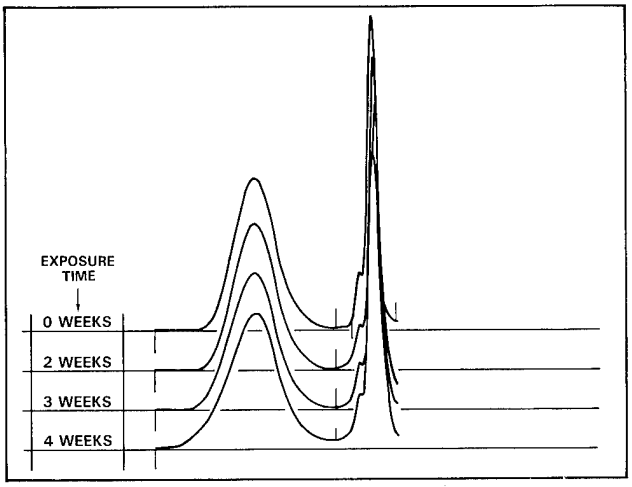



**Figure 40**
**Comparison of 105 C Rated PVC Jacket Insulations After Exposure to the 100 C/98+% RH Environment**

After exposure to the 85 C environment, a molecular weight increase is detected, but the increase is much less rapid than that observed after exposure to 100 C as can be seen in Table 10. The chromatograms show no major differences in the high molecular weight end. The results observed after exposure to the 70 C environment are similar to those noted after exposure to 85 C. In this case, longer exposure times are required to detect changes in the molecular structure of these insulations.

**Table 10**
**Calculated Molecular Weight Averages for Smooth 105 C Rated Insulations Exposed to 85 C/98%+ RH Environment**

| Exposure Time (weeks) | Mn | Mw | Mz | Polydispersity |
|---|---|---|---|---|
| 0 | 67176 | 129712 | 221392 | 1.9 |
| 5 | 67319 | 129903 | 222140 | 1.9 |
| 23 | 68547 | 150209 | 302188 | 2.2 |

The white PVC D-638 ASTM dumbells were exposed to environments identical to those used for 105 C and 80 C rated jacket insulations. After exposure to 100 C, dumbells underwent a molecular weight increase as was observed for these insulations.

A comparison of day 1, day 7, and day 14 chromatograms exposes a slight increase in the number of high molecular weight molecules present in a sample subjected to 100 C for 14 days. This overlay can be seen in Figure 41. There is a 25% increase in Mw over the same 14 day period as indicated in Table 11.

**Table 11**
**Calculated Molecular Weight Averages for PVC White ASTM Dumbells Exposed to 100 C/98%+ RH Environment**

| Exposure Time (days) | Mn | Mw | Mz | Polydispersity |
|---|---|---|---|---|
| 1 | 71782 | 139589 | 237339 | 1.9 |
| 7 | 71825 | 141942 | 247140 | 2.0 |
| 14 | 76529 | 174195 | 361485 | 2.3 |

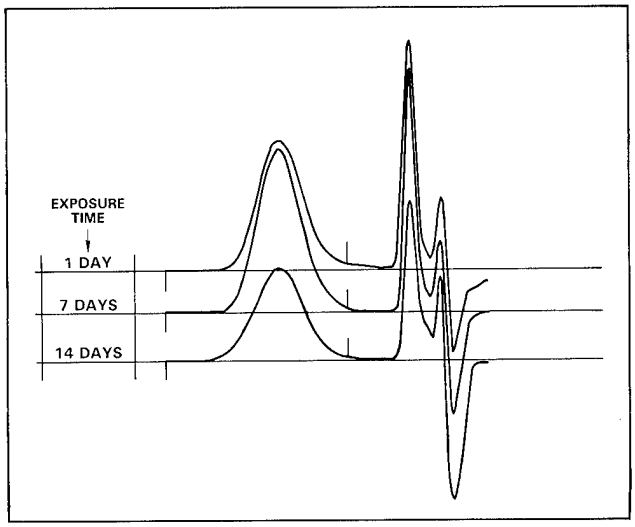



**Figure 41**
**Comparison of White ASTM Dumbells After Exposure to the 100 C/98+% RH Environment**

Dumbells exposed to an 85 C environment undergo a molecular weight increase at a much slower rate. Table 12 lists calculated molecular weight averages of the dumbells. One can see the increases are of lower magnitudes than their 100 C counterparts and that much more exposure time is required to achieve the same molecular weight gains.

**Table 12**
**Calculated Molecular Weight Averages for PVC White ASTM Dumbells Exposed to an 85 C/98%+ RH Environment**

| Exposure Time (weeks) | Mn | Mw | Mz | Polydispersity |
|---|---|---|---|---|
| 0 | 66811 | 142638 | 256369 | 2.1 |
| 5 | 71138 | 143509 | 259434 | 2.0 |
| 14 | 70539 | 157565 | 311205 | 2.2 |

*(B) Foamed Polyethylene Data Grade Media (DGM) Insulation*

Insulations from two environments, 70 C and 85 C, were analyzed by GPC. An initial increase in molecular weight is observed in all samples exposed to the elevated temperature/humidity environment. After this initial change, however, no trends can be mapped. Results for a few insulations are listed in Table 13. One can see from this data that results show initial increases, but then become random and show no further increase in molecular weight. This lack of correlation was most probably due to insoluble, highly cross-linked portions of the aged tubular polyethylene insulation.

**Table 13**
**Molecular Weight Averages for Foamed Polyethylene Insulations**

| Sample | Mn | Mw | Mz | Polydispersity |
|---|---|---|---|---|
| 0 Weeks | 38,606 | 198,403 | 1,503,883 | 5.14 |
| | 36,379 | 196,592 | 1,408,632 | 5.40 |
| 85 C | 39,128 | 374,957 | 4,252,935 | 9.58 |
| 2 Weeks | 37,724 | 377,813 | 4,147,428 | 10.02 |
| 85 C | 37,180 | 315,306 | 3,690,639 | 8.48 |
| 10 Weeks | 36,855 | 292,165 | 3,737,465 | 7.93 |
| 85 C | 29,606 | 265,623 | 2,917,250 | 8.97 |
| 23 Weeks | 28,314 | 260,662 | 2,871,949 | 9.21 |
| 85 C | 39,119 | 331,758 | 4,044,125 | 8.48 |
| 28 Weeks | 38,861 | 334,454 | 4,097,017 | 8.61 |
| 70 C | 37,813 | 410,835 | 5,602,361 | 10.87 |
| 5 Weeks | 34,493 | 391,518 | 5,431,964 | 11.35 |
| 70 C | 28,966 | 403,008 | 5,813,669 | 13.91 |
| 23 Weeks | 29,634 | 366,206 | 5,547,166 | 12.36 |
| 70 C | 31,164 | 442,553 | 6,027,854 | 14.20 |
| 28 Weeks | 30,443 | 449,272 | 5,861,832 | 14.76 |

*(C) PET Film*

After five weeks of exposure to the 70 C, 98% +RH environment, PET film shows small decreases in molecular weight averages (see Table 14). As time of exposure increases, the amount of molecular weight degradation increases more rapidly. The weight average molecular weight undergoes a 17.2% decrease over a 23 week exposure. A steady increase in polydispersity occurs in PET, indicating the peaks are broadening with increased exposure time.

An overlay of chromatograms of PET exposed to the 70 C environment may be seen in Figure 42. Note that in the degradation of PET film, the peaks shift downfield. This shift is interpreted as a reduction in molecular weight. These results are in direct contrast with the results shown for PVC insulations, in which an increase in molecular weight is detected.

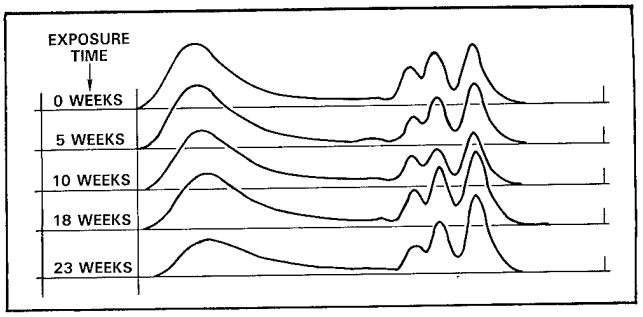



**Figure 42**
**Polyethylene Terephthalate After Exposure to 70 C, 98%+ RH**

A sample exposed to 85 C and 98% RH for 35 days was also analyzed by GPC. The number average molecular weight for this sample was 15,100 with a weight average of 31,600. This may be compared to the 5 week aged sample in Table 14, exposed to 70 C, with a number average of 22,000 and a weight average of 46,300. The PET film which was exposed to 85 C for the same period shows the corresponding greater *decrease* in molecular weight.

**Table 14**
**Results of GPC Analysis of PET Film Aged at 70 C/98%+ RH**

| Time In Chamber | Mn | Mw | Mz | Polydispersity |
|---|---|---|---|---|
| 0 weeks | 22600 | 46500 | 64100 | 2.06 |
| 5 weeks | 22000 | 46300 | 64800 | 2.11 |
| 10 weeks | 20100 | 43400 | 60200 | 2.17 |
| 18 weeks | 18300 | 40000 | 54900 | 2.19 |
| 23 weeks | 17300 | 38500 | 52900 | 2.23 |
| NOTE: All molecular weights are relative to Nylon 6,6 | | | | |

PET film exposed to 100 C and 98%+ RH undergoes a decrease in molecular weight averages at a more rapid rate than its 70 C and 85 C counterparts. For this reason, a PET sample which was exposed for only 7 days to the high temperature environment was analyzed. The number average of this PET sample was 11,800 and the weight average was 22,500. Referring again back to Table 14, note that this sample is degraded more than that of the sample exposed for 23 weeks at 70 C.

4.4 Solubility of PVC Insulations to Determine "Gel Points"

PVC 80 C rated grooved jacket insulations from all three environments were tested for solubility in tetrahydrofuran (THF) to determine a relative endpoint for useful life predictions. Figures 43, 44, and 45, illustrate 80 C rated insulations in solution. Samples from the 100 C environment reached "gel point" between 2 and 4 weeks of exposure (Figure 43). Those from the 85 C environment reached the same point between 18 and 23 weeks (Figure 44). There is no data for any points in time between 23 and 39 weeks of sample exposure. In the 70 C environment, these insulations reached an endpoint in this region, between 23 and 39 weeks (Figure 45), and thus a specific point in time was estimated for endpoints (i.e., gel point) criteria.

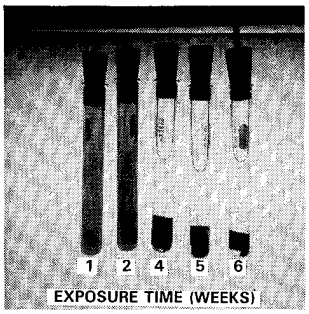



**Figure 43**
**Solubility of 85 C Rated PVC Insulations After Exposure to 100 C/98%+ Environment**

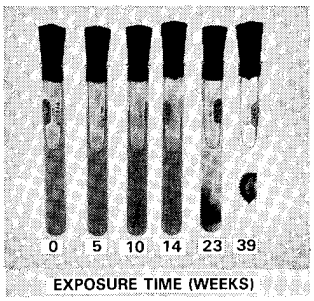



**Figure 44**
**Solubility of 85 C Rated PVC Insulations After Exposure to 85 C/98%+ Environment**

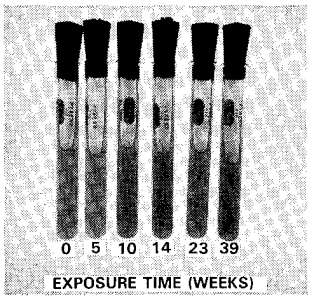



**Figure 45**
**Solubility of 85 C Rated PVC Insulations After Exposure to 70 C/98%+ Environment**

White ASTM Dumbells, (the base resin for the 80 C rated black grooved jackets), which were removed from the 100 C environment became insoluble between 2 and 3 weeks of exposure. Samples hung in the 85 C environment were insoluble at a point between 23 and 39 weeks of exposure. Since the 39 week sample did not retain its shape when placed in solution, the endpoint may be assumed to be near the upper end of this time interval. The insulations exposed to 70 C had not yet achieved an endpoint after 39 weeks. Photographs of these samples are included in Figures 46 and 47. This correlates well with the data for the black, grooved jacket insulations, and indicates that the presence of carbon black may actually hinder thermal and/or hydrolytic stability.

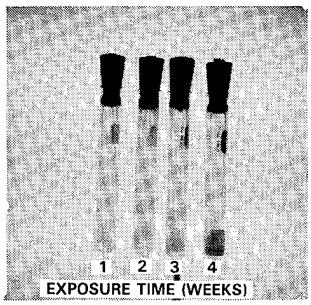



**Figure 46**
**Solubility of White PVC ASTM Dumbells After Exposure to 100 C/98%+ Environment**

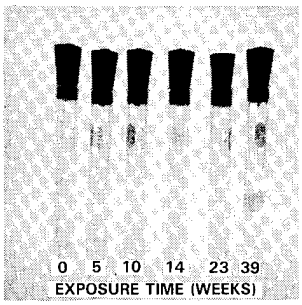



**Figure 47**
**Solubility of White ASTM Dumbells After Exposure to 85 C/98%+ Environment**

Poly(vinyl chloride) 105 C rated jacket insulations from the 100 C environment did not dissolve after 7 weeks of exposure. Since there is no shape retention and the carbon black loading is diffusing, this point may be considered the endpoint. Samples which were placed in the 85 and 70 C environments had not yet reached an endpoint after 39 weeks of exposure. These results are illustrated in Figures 48 and 49.

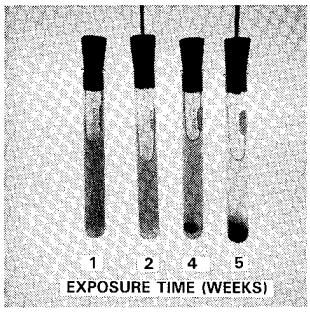



**Figure 48**
**Solubility of 105 C Rated PVC Insulations After Exposure to 100 C/98%+ Environment**

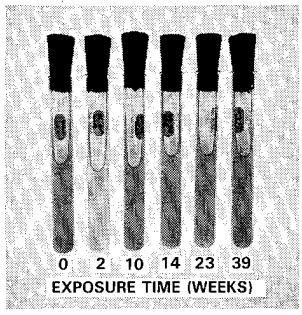



**Figure 49**
**Solubility of 105 C Rated PVC Insulations After Exposure to 85 C/98%+ Environment**

4.5 Arrhenius Modeling Techniques and Results for Physical/Mechanical and Thermogravimetric (TGA) Data

The Arrhenius equation (2) described in Section 3.3 is a general kinetic rate expression which applies to several different reactions within specific limitations. Beginning with equation (2):

$$k = Ae^{-Ea/RT}$$

and simply applying the natural logarithm to the equation yields:

$$\ln k = \ln A - Ea/RT \qquad \text{Equation (4)}$$

which is in point-slope form and can be easily converted to the more convenient log equation for plotting 1/temperature vs. log time on semi-log paper:

$$\log t = \log A - 2.303\ Ea/RT \qquad \text{Equation (5)}$$

where the slope of the line is equivalent to $-2.303\ Ea/R$. The major assumptions are that the degradation reaction is first order and that the mechanism of degradation does not change over the temperature range of interest.

*(A) Arrhenius Modeling for PVC Insulations*

As shown in Figures 13-15 (Section 4.1), the effect of the accelerated environmental stress on the PVC homopolymer insulations included increases in tensile strength and only slight decreases in elongation after as much as 274 days aging. This presented a problem in that no endpoint determination could be made for PVC on the basis of tensile testing. As outlined in Sections 3.5 and 4.4, however, a solubility technique using THF which correlated with physical stiffness (and presumably the mechanisms of dehydrochlorination and subsequent cross-linking) was determined while solutions were prepared for GPC analysis. The time of exposure until the PVC insulation became insoluble was then used as an endpoint, which due to its chemical correspondance with gelation was thought to represent a constant mechanism of degradation. The three data points at which PVC was no longer soluble in THF in the 70, 85 and 100 C environments were then plotted on semi-log paper, and linear regression analysis was performed to determine the best straight line and slope approximation. For the grooved PVC jacket (UL 80 C rated) samples, the Arrhenius model of Figure 50 indicates that the mechanism of degradation is indeed constant over the

temperature range tested with a linear regression coefficient of (r = .979). This value was found based on "endpoints" of 4, 18 and 39 weeks aging at temperatures of 70, 85 and 100 C, respectively. In the Arrhenius model of Figure 50, the prediction that could be made if it were known that the mechanism of degradation remained constant down to room temperature is that the 80 C rated PVC jackets would not stiffen appreciably for approximately 57 years. Using the "rule-of-thumb" technique which establishes an extrapolation of 25 C from the lowest isothermal point (70 C in this case), the predicted insulation life would be approximately 15 years if exposed to 40 C and 98%+ RH continuously. The value for the energy of activation (Ea) determined from the slope of the line of Figure 50 is 19.19 Kcal/mol. The calculated values for the same PVC resin without carbon black loading, in the shape of ASTM dumbells, yields an even more optimistic prediction of useful service life. Figure 51 shows that it would take 15 years under a continuous environment of 55 C and 98%+ RH before the insulation would stiffen past an acceptable level. This plot was based on a theoretical endpoint reached in 45 weeks at 70 C and yielded an apparent energy of activation (Ea) of 31.93 Kcal/mol.

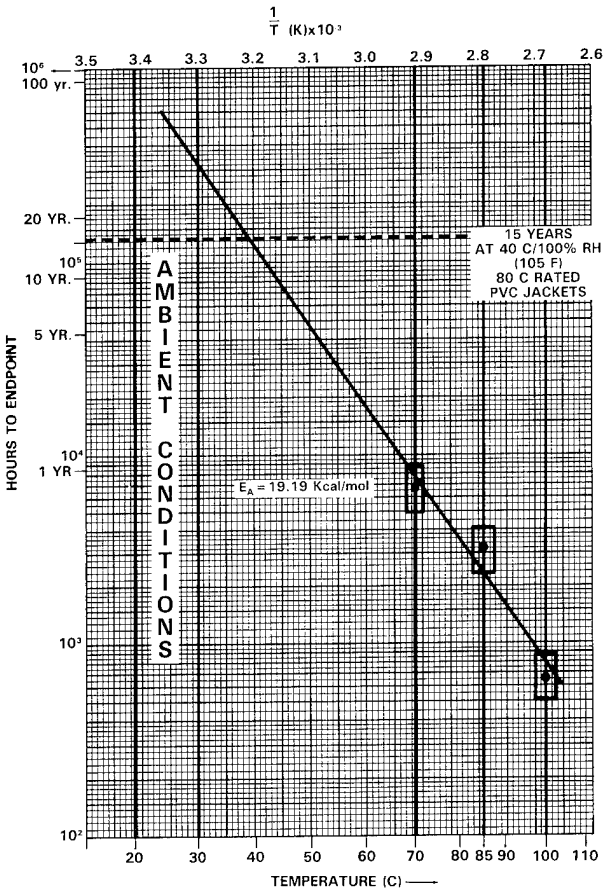



**Figure 50**
**Arrhenius Model of 80 C Rated Grooved PVC Jacket Aged in 98%+ RH Environment Using Solubility as End-of-Life Criteria**

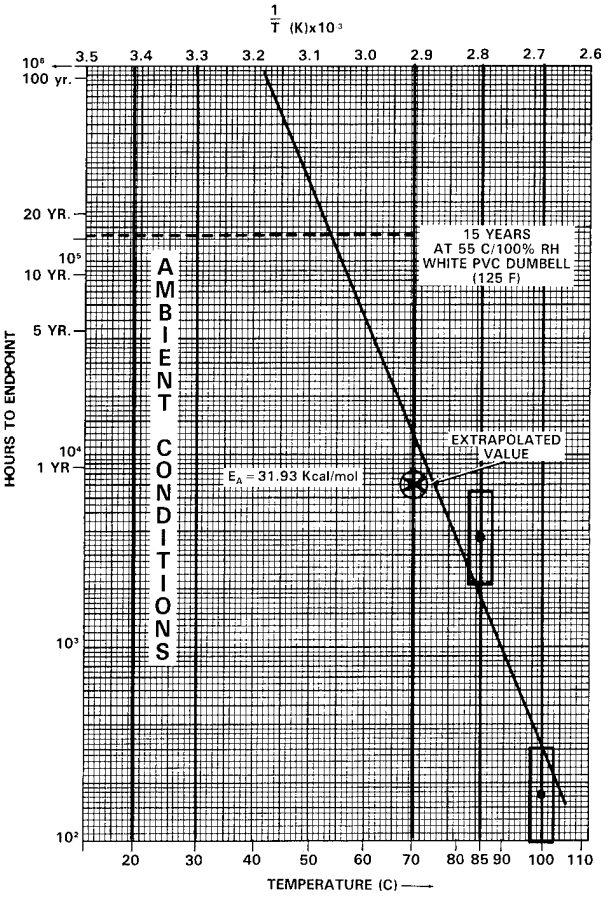



**Figure 51**
**Arrhenius Model of 80 C Rated White ASTM Dumbells Aged in 98%+ RH Environment Using Solubility As End-of-Life Criteria**

Finally, the 105 C rated smooth PVC jackets behaved as expected in the elevated temperature environments. Stiffness occurred with these samples as well, but the only isothermal endpoint experimentally determined was in the 100 C environment. As detailed in Section 4.4, the insolubility point was reached after 7 weeks. Predictions for the longevity of this insulation system is, therefore, even more optimistic than for either of the 80 C rated compound specimens tested.

*(B) Arrhenius Modeling for Foamed (DGM) Polyethylene Insulations*

Using the data generated from the destructive physical/mechanical testing performed on orange helically striped thicker (22 AWG) foamed PE insulations in the Instron (Figure 5), an endpoint (in terms of days) at 70% elongation for each of three temperatures was determined as outlined in Section 4.1. Figure 52 depicts the three experimentally determined endpoints and clearly indicates an order of magnitude difference in the prediction of anticipated life for these tubular insulations using this endpoint criteria compared with the PVC systems. The predicted insulation life would be approximately 2 years at 25 C/98%+ RH or only 1.4 years at the 45 C/98%+ RH environment allowed by the aforementioned rule-of-thumb 25 C extrapolation. The apparent energy of activation (Ea) value calculated from the slope of the line equaled 2.81 Kcal/mol. Two

important issues must be realized about the extremely conservative values found for the orange helically striped foamed DGM (22 AWG) samples. First, the confidence level that the mechanism of degradation is constant throughout the 70-100 C temperature range is low; after careful review of all three insulation data sets. Second, the 70% elongation value as an endpoint was somewhat arbitrary in that some samples which exhibited less than 70% elongation were not visibly cracked. GPC results did not allow for making life estimates based on chemically determined endpoints for reasons stated in Section 4.3.

*(C) PET Films*

Again, using data from the destructive physical/mechanical testing performed for PET films (Figure 6), an endpoint (in terms of days) at both 20% elongation and 14,000 PSI tensile strength for each of the three temperatures was determined as before. In Figures 53 and 54, endpoint determination for the PET film aged in the 100 C, high humidity environment was difficult, in that deterioration of the film was extremely rapid.

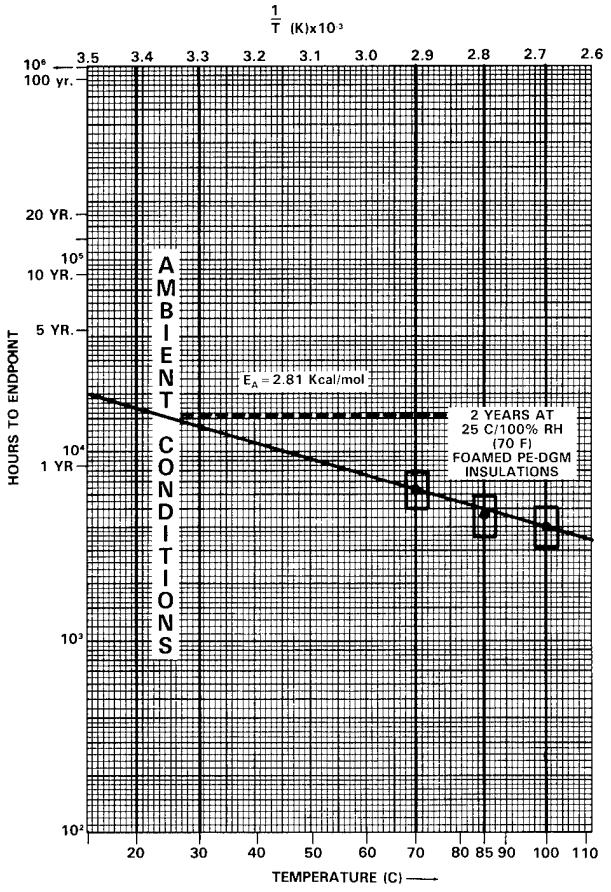



**Figure 52**
**Arrhenius Model of Tubular Foamed PE-DGM (22 AWG) Insulations Aged in 98%+ RH Environment Using 70% Elongation As End-of-Life Criteria**

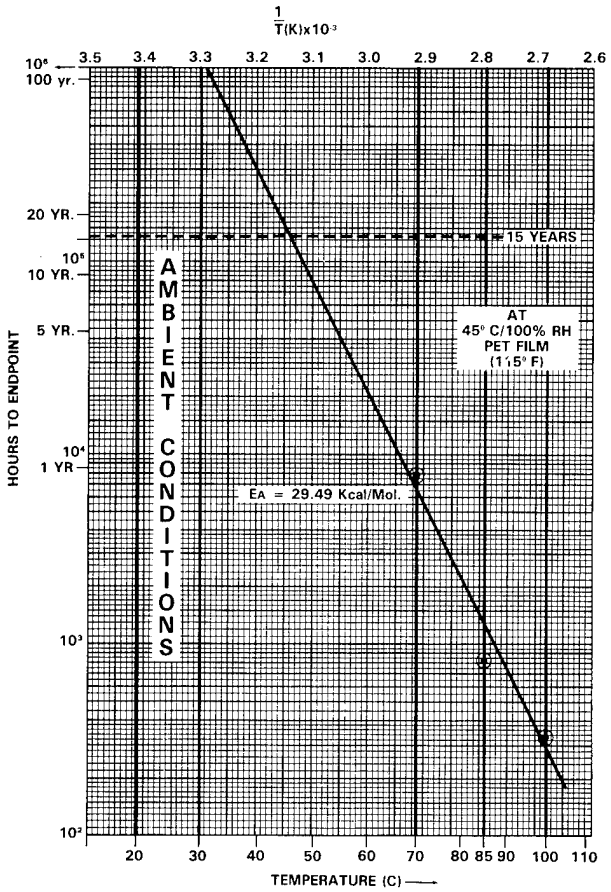



**Figure 53**
**Arrhenius Model of PET film in 98 + 2% RH Environment Using 20% Elongation as End-of-life Criteria.**

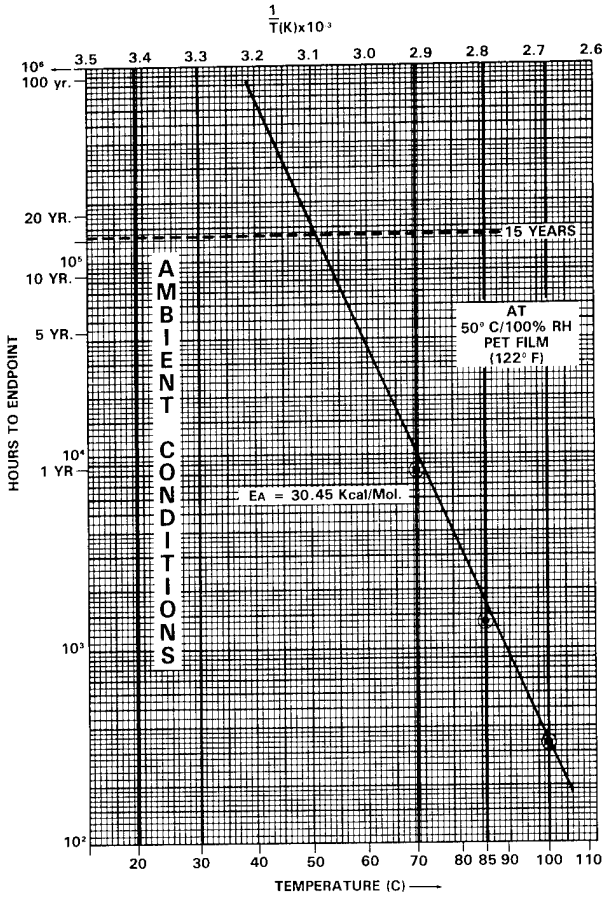



**Figure 54**
**Arrhenius Model of PET Film in 98 + 2% RH Environment Using 14,000 PSI Tensile Strength as End-of-life Criteria.**

In the Arrhenius model of Figure 53, the predictions that could be made if it were known that the mechanism of degradation remained constant down to room temperature, is that the PET film would not degrade beyond the 20% elongation point for greater than 100 years. The value for the energy of activation (Ea) determined from the slope of the line of Figure 53 is 29.49 Kcal/mol. Similar predictions, using Figure 54 are even more optimistic. The value for Ea of Figure 54 is 30.45 Kcal/mol.

*(D) Arrhenius Modeling for Cross-Linked PE (VGM) Insulations*

As stated previously and shown in Figures 25 and 26, physical changes in cross-linked PE insulations within the stressed environments of this study were essentially indetectable. GPC analysis could not be performed due to the highly cross-linked state of the insulation and subsequent insolubility. The only indication of life expectation for this insulation compound is given by the "Arrhenius" plot shown in Figure 55. This plot was obtained by testing insulations in air-ovens at excessive temperatures, and it is obvious that above 136 C, the mechanism of degradation changes. Therefore, the application of an Arrhenius-type model for this insulation system using elevated temperature in the range of 130 C -150 C is without any scientific validity. It is sufficient to state that this insulation system is perhaps the most indestructable non-plenum material found to date, based on the environmental stresses to which it has been exposed.

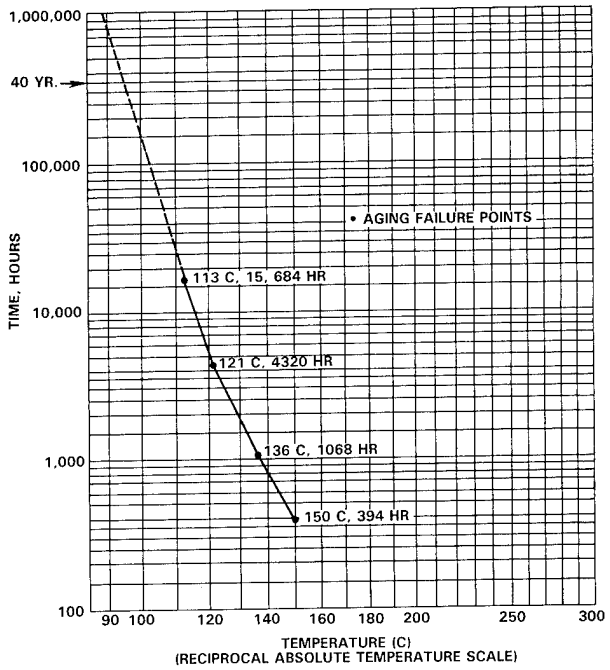



**Figure 55**
**Arrhenius Model for Solid Cross-linked PE-VGM Insulation (Air-Oven Aging)**

## V. DISCUSSION

5.1 Comparison of Environmental (Isothermal) Data with Both Thermogravimetric (Dynamic) Analysis and With Previous Studies

*(A) PVC Homopolymer Jackets and White ASTM Dumbells*

The major difference between aging the insulations in an isothermal manner versus using the dynamic analysis of TGA is the humid environment in which the insulations were placed. Initially, it was not known how the overwhelming presence of humidity would alter the mechanism of aging as compared with the standard air-oven environments normally used by both Underwriter Laboratories (UL) and the majority of the wire and cable industry. Common practice in UL Subject 758[29] rating of PVC insulations is to subject 80 C rated compounds to 113 C for 7 days in a standard air oven (as per ASTM D 2436) and 105 C rated insulations to 136 C for 7 days, and then test for both tensile strength and elongation of the aged samples. The insulations are "blessed" with these ratings if samples are capable of at least 70% and 65%, respectively, of the values for the original unaged samples. The pitfalls associated with this method of evaluating expected lifetimes of insulation systems has already been discussed.

Because of this standard practice used to evaluate PVC and other insulation compounds, a compendium of information[30-35] is available concerning both the common degradation mechanisms of flexible PVC homopolymers and copolymers (with vinyl acetate) in dry, heated atmospheres and different formulations which can help retard this degradation. Only a small group of investigators

have studied the influence of moisture or water on these PVC insulations[36-38]. These studies, however, focused primarily on the effects of moisture for power cables.

Studies involving dry heat aging of PVC insulation for communications wire and cable involve the loss or migration of highly volatile plasticizers, which can occur at much lower temperatures than the rated service temperature. Specifically, Warren[39], and Loadholt and Kaufman[40] studied the loss of plasticizer from wire insulations. Warren[39] concluded that the rate of volatile loss of plasticizer coincided with an activation energy of 15-20 Kcal/mol within a reasonably well defined dry thermal stress.

As stated in Section 4.3, GPC analysis showed conclusively that the environment of elevated heat and humidity did not cause excessive plasticizer evolution. This is theorized to be as a result of the elevated vapor pressure in each chamber set at 98%+ RH, which did not allow for the highly volatile plasticizer to diffuse into the already moisture saturated environment.

Instead, the mechanism of degradation associated with the elevated temperature and humidity conditions of this study seems to be more along the lines of dehydrochlorination followed by unsaturation, chain scission and/or oxidation and chain branching as summarized by Winkler[33]. The point of this discussion is that the values for Ea (19.19-31.27 Kcal/mol) determined for the 80 C rated compounds based on insolubility in THF are most likely based on degradation of PVC via dehydrochlorination in the absence of plasticizer evolution. The formation of a gelation point occurs, which corresponds with cross-linked portions of the polymer as a result of both dehydrochlorination and unsaturation. Confirmation of the fact that unsaturation occurs, is that a darkening in color of the white ASTM dumbells (turning brown) was visible after aging in the 85 and 100 C environments. Energy of activation (Ea) values determined with TGA (20.97-25.80 Kcal/mol) are in agreement with the published values of Warren[39], and support the concept that in the presence of an inert atmosphere and heat, plasticizer evolution is the initial mode of destabilization.

Even more interesting to note, is that PVC insulations aged outdoors in Avon Lake, demonstrated trends in changes of tensile and elongation properties quite similar to those exhibited by our samples exposed to elevated temperature and humidity environments. Table 15 indicates actual changes in the tensile strength and % elongation at rupture for outdoor weathering of PVC compounds as a 1/32" wall on #14 AWG wire. Many of the compound recipes have not changed since the early 1950's.

**Table 15**
**Changes in Physical Properties of Flexible PVC Compounds Aged Outdoors in Avon Lake, Ohio**

| Date Recipe Issued | 5/28/52 | 5/21/52 | 12/19/52 | 12/8/52 |
|---|---|---|---|---|
| Compound Color | (A) Black | (B) Black | Natural | Transparent |
| **Tensile, PSI** | | | | |
| Original | 1715 | 1140 | 1540 | 2675 |
| Aged Avon Lake, 2 yrs. | 1430 | 1000 | 1760 | 2390 |
| Aged Avon Lake, 5 yrs. | 1800 | 1650 | 1970 | 1750 |
| Aged Avon Lake, 10 yrs. | 1930 | 1695 | 2220 | 1610 |
| Aged Avon Lake, 20 yrs. | 3175 | 2350 | 2550 | Too Brittle |
| **Elongation %** | | | | |
| Original | 185 | 175 | 215 | 240 |
| Aged Avon Lake, 2 yrs. | 170 | 175 | 190 | 180 |
| Aged Avon Lake, 5 yrs. | 166 | 189 | 131 | 85 |
| Aged Avon Lake, 10 yrs. | 166 | 203 | 112 | 61 |
| Aged Avon Lake, 15 yrs. | 154 | 207 | 98 | No Data Possible |

With the exception of only the transparent PVC compound, all samples exhibited increases in tensile strength, as was the case for samples exposed to our accelerated aging environment (as documented in Section 4.1). Changes in % elongation, however, varied according to the compound recipe and seemed to correspond with durometer hardness. Softer samples (like that of the 105 C compound of this study) such as compound (B) in Table 15, exhibited steady increases, while their harder counterparts, (compound (A)) exhibited steady losses in "stretchability". These data serve to re-emphasize the difficulty associated with using physical/mechanical techniques to demonstrate the life expectancy of PVC insulations. As a final note, Clark[41], based on data compiled by Nowak[42], describes the life value of a "typical" poly(vinyl chloride) insulation, based strictly on thermal aging of a compound composed of suspension type PVC (70%) and pthalic acid ester as the plasticizer (30%). The formation of hydrogen chloride during heat aging, determined by the pH value of a water solution of the effluent gases was accepted as the gauge of polymer life. Based on this standard, a significant decrease in the life of the poly(vinyl chloride) at temperatures higher than 100 C was noted. The estimated Ea value for this study of 14 Kcal/mol indicates that life estimates for thermal degradation of the vinyl chloride backbone are worse than those for estimates based on plasticizer evolution. For at least the 105 C rated PVC compound of this study, the value for Ea, which would be determined by the solubility methods outlined in Section 3.5, predicts a much longer lifetime than that calculated from Nowak's[42] study.

*(B) Foamed Polyethylene Data Grade Media (DGM) Insulation*

The physical characteristics of polyethylene are intimately tied to its density. An increase in the density of the polyethylene corresponds with an *increase* in; degree of crystallinity, load at yield point, crystalline melting point, and hardness, but a *decrease* in; percent deformation under load (creep), percent elongation, and abrasion resistance. These property changes also correspond with changes in % crystallinity which occur when heating polyethylene. The differences in change of % crystallinity are shown in Figure 56 below.

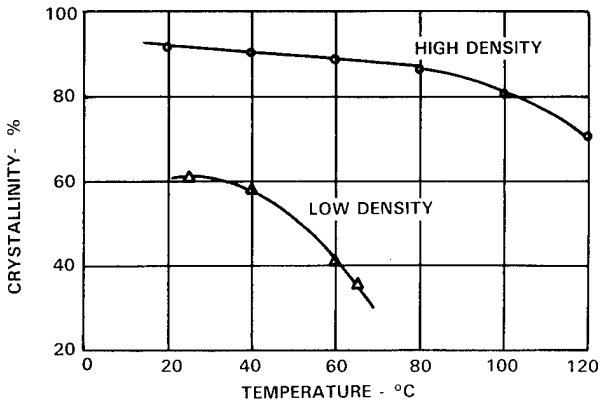



**Figure 56[43]**
**The Effect of Heat Treatment on the Crystallinity of Polyethylene**

Figure 56 illustrates that, even for high density polyethylene, a loss of approximately 10% crystallinity occurs within the 70-100 C temperature range to which our samples were exposed. Another morphological effect which may have altered the thermal and physical property determinations for our foamed HDPE samples (containing a small percentage of PP) is that the cooling rate (or quench) from a high temperature determines the size of crystalline spherulites in the polymer matrix. The relatively slow rate of cooling, combined with the presence of PP in the foamed HDPE tubular insulation, most probably caused large crystalline spherulites to form.

How these changes in the morphological structure of the HDPE samples under test affected the thermal stability of the insulation remains in question; however, heat embrittlement of polyethylene is known to occur when the material is exposed to continued high temperature slightly below the crystalline melting point. It is also known that the period of time necessary to develop this heat embrittlement decreases exponentially with an increase in the melt index value. Again, this fact favors the use of HDPE rather than the low density variety.

The Ea value of 2.81 Kcal/mol determined for the HDPE of this study (as reported in Section 4.5) is associated with the heat embrittlement phenomenon previously alluded to, but may actually be more closely tied to the mechanism of oxidation. In a comprehensive study to determine the oxidative stability of HDPE cables, Bernstein and Lee[44] found that the Arrhenius plot of the air oven aging behavior for HDPE is linear between 105-150 C and was calculated to be 23.4 Kcal/mol.

The dynamic, thermal analysis technique which employs either DSC or TGA techniques in the presence of oxygen yields Ea values which are extremely close to the 23.4 Kcal/mol reported using isothermal aging techniques. The thermal analysis work for polyethylenes was pioneered by Bair and has more recently been reviewed by Cassel[45] and by Gilroy and coworkers[46]. This information suggests that the overwhelming presence of moisture in our isothermal aging experiment, greatly accelerated the thermal and/or oxidative degenerative mechanisms. An abundance of studies[47-49], concerning the oxidative stability of polyethylene insulations exists in the literature. Many authors investigated the use of copper deactivators[50-52], due to the ability of copper to catalyze the oxidation reaction, for stabilizing these insulation systems. Several of these chemical "deactivators" have performed adequately in both laboratory test and actual field exposure since the cracking disasters associated with certain telephone wire insulations in outdoor pedestal installations which occurred in the early 1970's. Pusey and coworkers[49] indicated that actual white-colored field samples, which visibly cracked and caused early failure, were highly loaded with $TiO_2$. They continued their study by exposing samples to 100% RH conditions by hanging sets of white specimens in tightly closed jars over water and concluded that the presence of moisture (while limiting oxygen concentration) enhances service life of polyethylene insulation. This study, in which the presence of atmospheric $O_2$ not limited, indicates just the opposite effect is true for air-blown white pigmented HDPE.

Finally, in trying to comprehend the extremely large values found for the *apparent* energy of activation (Ea) via TGA (as reported in Section 4.2) for these same HDPE insulations, it must be understood that, initially, the value of 23.5 Kcal/mol coincides with that reported by Bernstein and Lee[44] (23.4 Kcal/mol). It was only after exposure to the elevated temperature and humidity environments that the PE insulations exhibited dramatic increases in Ea values. The only cause for this change which can be theorized to date (based on GPC and physical test results) is that these insulations became highly cross-linked during exposure and therefore developed extreme heat resistance. It is important to realize that this high heat resistance occurred in the *absence* of oxygen.

*(C) PET Films*

Thermal degradation and hydrolysis of both PBT resins and PET films has been previously studied[53-58]. Physical testing involving the effect of relative humidity on PBT resins illustrates that hydrolysis is a primary degradation mechanism for both filled and unfilled polymer systems. Kinetic analysis of these same systems yielded values of between 23 and 27 Kcal/mol in 50-100% RH environments aged at temperatures from 66-93 C. As expected, the filled systems (including flame retardants and glass) exhibited lower Ea's and therefore shorter lifetime predictions. The degradation was attributed to ester hydrolysis which creates hydrophillic acid endgroups, and as a result, water adsorption continues to increase as the polymer degrades.

This same degradation effect is seen for PET films and also is enhanced in the presence of elevated temperatures and air. Results of the PET film studies for 0.0005" and .0100" thick specimens correlate well with this study of 1 mil specimens. PET films aged in an unspecified manner at 100% RH were determined to have an apparent energy of activation (Ea) of 18.5-25.0 Kcal/mol increasing with increased film thickness. This compares favorably with the value of 29.49 Kcal/mol determined for the .001" thick film of this study and indicates that the reaction which leads to oxidative/hydrolytic degradation is somewhat limited by diffusion.

The degradation mechanisms for poly(ethylene terephthalate) in air and moisture are quite different from those occurring when the material is thermally decomposed in an inert atmosphere. Hydrolysis of PET constitutes initial cleavage of endgroups such as hydroxyl (OH) and carboxyl radicals (COOH). Hergenrother[53] reported that thermal decomposition of PET yarns containing up to 4% poly(diethylene glycol) terephthalate (PDEGT) showed only slight changes in hydroxyl and carboxyl endgroup concentrations upon heat aging. The same article[53] reports the energy of activation (Ea) of 100% PET as 47.3 Kcal/mol. This compares favorably with the value of 44.5-45.8 Kcal/mol as found via TGA reported in Section 4.2.

It becomes obvious from this and previous studies that polyester resins and films are susceptible to rapid deterioration in the combined presence of moisture, heat, and air. Lee and Hodges[59] recognized this problem and tried the use of isocyanate coatings to improve both moisture and heat resistance of PET films with some success.

*(D) Radiation Cured Cross-Linked Polyethylene Insulations*

For the sake of completeness, a discussion concerning the aging of the solid x-linked HDPE is included. It is generally agreed that this type of insulation is extremely heat resistant and exhibits excellent service life up to 105 C continuous use temperatures (as required in some nuclear power applications). The main concern with regard to the accelerated aging of this insulation system is that the already pastel solid-colored 22 AWG conductors, faded with time, such that potential problems with detection may result in future installations. Of the many studies involving cross-linked PE for wire and cable insulations, only one[60] attempts to provide a value for the apparent energy of activation (Ea). The value of 13 Kcal/mol is based on the rate of moisture uptake vs. time for cylindrical XLPE samples. Exactly how this information can be related to the expected service life of XLPE, however, is not currently known.

## 5.3 Discussion of Gel Permeation Chromatography Results

Initial examination of tensile and elongation, as well as thermal properties, indicated plasticizer loss from PVC cable insulations was the main mode of degradation. Chromatographic studies confirm literature results[28] of plasticizer evolution from PVC upon exposure to high temperature (100 C) environments. In experiments involving PVC insulations which were exposed to high temperature (100 C), coupled with high humidity (98$^+$ %), there was no significant plasticizer loss detected after 23 weeks of exposure. It was concluded therefore that plasticizer loss from insulations was not the main mode of degradation and that some other reaction was influencing the mechanical properties of PVC.

GPC analysis of 80 C and 105 C rated PVC jackets, as well as white ASTM dumbells from three environments, indicated trends of molecular weight change. Specifically, an increase in molecular

weight averages occurred as insulations were exposed to high temperature/humidity conditions. These increases occurred over the shortest time when exposed to the 100 C environment. For each different type of insulation, the extent of molecular weight gain over the same range of exposure time decreased as exposure temperature was reduced. In other words, the 100 C environment was more severe than the 85 or 70 C environment and the 85 C environment was more severe than the 70 C environment. The 80 C rated jacket (grooved) insulations underwent molecular weight gains more rapidly than their 105 C rated and ASTM dumbell counterparts. The 80 C rated grooved PVC jacket base resin is of the same formulation as the ASTM dumbell material, but has been shown to "degrade" more rapidly in terms of molecular weight change. The extrusion of 80 C rated insulation aligns polymer chains and could permit small molecular weight gains before high temperature/humidity exposure begins.

The 105 C rated insulation exhibits the most resistance to large gains in molecular weight with time. This material is known not to contain lead heat stabilizers (80 C rated jackets and dumbells have lead present as shown by EDX analysis), but instead may contain trimellitate plasticizer and/or some other stabilizer which retards molecular weight increases more efficiently than additives present in 80 C rated PVC insulations.

Chain scission and dehydrohalogenation have been shown to occur in flexible PVC composites[33]. Mechanisms in which a free radical is formed have also been postulated. In a situation in which free radicals are formed, backbiting, or attacks between chains, occur and crosslinking results. Crosslinking of the PVC backbone through intermediate radical formation in flexible PVC insulations appears to be the mode of degradation in cases where insulations are exposed to both high temperature and high humidity conditions. This crosslinking results in an increase of high molecular weight PVC and a widening of the distribution as determined by GPC.

PET film undergoes a decrease in molecular weight upon exposure to high temperature/humidity environments. Film exposed to the 100 C environment underwent the most degradation in the shortest time period. Likewise, insulations exposed to 70 and 85 C environments undergo degradation, but at much reduced rates. The degradation, in this case, indicates a loss of molecular weight, presumably due to loss of endgroups as contrasted with PVC which undergoes increases in average molecular weight.

Polyethylene degradation is not as well understood as that of PET or PVC. Initially, PE undergoes a dramatic increase in average molecular weight in all environments. It is impossible to distinguish between samples exposed to one or ten weeks in the harsh environment. After examining the filtrate of samples, it was found that not all material in the samples exposed to a high temperature/humidity environment permeates the small pores of the filter. The PE molecular weight is too great, indicating that crosslinking or crystallization has occurred prior to GPC analysis. In this experiment, a limit to the range of molecular weights injected onto the system occurred and the data cannot be used comparatively among environments. The only conclusion based on GPC results is that PE undergoes a dramatic increase in molecular weight upon exposure to high temperature/humidity environments.

### 5.4 Discussion of Solubility Results

Solubility of insulations in THF was useful for determining endpoint criteria. UL 80 C rated insulations were found to become crosslinked and insoluble much earlier than their 105 C rated counterparts, as expected, after examining GPC data. White ASTM dumbells, which contained the same base resin as the grooved jacket insulations, became insoluble at much longer times than the office jackets. PVC jacket insulations rated at 105 C showed the most resistance to crosslinking, and endpoints for the 70 and 85 C environments had not been found after 39 weeks of exposure. This resistance may be due to the use of stabilizers, which are more adept at scavaging free radicals after formation than the lead used in the 80 C rated insulations. The time to endpoint, in ascending order, is then; 80 C rated insulation, white ASTM dumbell, 105 C rated insulation. Solubility of PVC can be used for relative endpoint determination and lifetime predictions of insulations. These predictions should be valid over a wider temperature range than those made by dry heat aging of flexible grade PVC, which is based primarily on plasticizer volatility. The mechanism of degradation due to dehydrochlorination and crosslinking is consistent over the 70-100 C temperature range in extremely moist environments, thus allowing for proper use of the Arrhenius model.

## VI. CONCLUSIONS AND RECOMMENDATIONS FOR FUTURE STUDY

An exhaustive study to determine the expected life of various insulations for a local network wire and cable system has been undertaken. A worst case scenario for the environmental exposure hazard was approximated by subjecting the insulations to nearly 100% RH conditions and temperatures lower than those used for conventional air-oven aging. Because of the wealth of information regarding "dry" thermal aging of various insulating materials, a comparison with activation energies (Ea) determined in this manner with the values found for aging similar materials in the combined presence of elevated heat and humidity is of interest.

For flexible PVC jacketing compounds which are UL rated at 80 C, a solubility technique (in THF) was developed to determine endpoint criteria associated with cross-linking of the polymer backbone. This mechanism of degradation was consistent over the temperature range (70-100 C) of study and met the other criteria required for use of an Arrhenius model, such that a value for the apparent energy of activation (Ea) of 19.19 Kcal/mol (Figure 50) could be determined. This value compares favorably with that of the dry thermal aging of a "typical" PVC compound in which only HCl evolution was measured and yielded an Ea of approximately 14 Kcal/mol. These values correspond with a predicted service life of 10-15 years in a constant 40 C/100% RH environment. Ea values for the 105 C rated PVC compounds were estimated to be much higher than those of the 80 C rated materials, and therefore even longer service lives are predicted. Actual long term outdoor exposure of similar PVC compounds aged in a manner which closely followed the changes in physical properties of the PVC aged in the humid environment used in our laboratories. A convenient consequence of all this work is that measurement of loss of plasticizers from the same type of PVC compounds yielded Ea values of 15-20 Kcal/mol, again allowing for very similar lifetime predictions. Gel permeation chromatography (GPC) analysis was performed for these insulation systems to confirm a consistent mechanism of molecular weight increase which leads to stiffness in the poly(vinyl chloride) backbone. Thermogravimetric analysis (TGA) reconfirmed that the Ea value found for the PVC compounds for weight loss in a dry (in this case - inert) atmosphere correlates with loss of plasticizer rather than degradation of the polymer chain.

High density polyethylene compositions used to insulate data grade conductors were not as simple to analyse for reliable service life predictions. Physical/mechanical analysis revealed that problems occur with the loss in % elongation of this foamed dielectric, and using this property as an end-of-life criteria, yielded the lowest Ea value of any of the insulation systems of this study - 2.8 Kcal/mol. This value was determined from the Arrhenius model (Figure 52) and predicts a short service life. Fortunately, solid PE skin over the HDPE foamed conductors apparently increases the service life by at least an order of magnitude. Previous studies[44 and 45] predicted much longer service life based on thermal aging in an oxygen containing atmosphere, using heat embrittlement as endpoint criteria, with Ea values of 20-25 Kcal/mol. Gilroy[60], in a recent

article, indicated that actual field failures (cracking insulation) occurred within 4-5 years for low density PE insulations, but that high density PE insulations, combined with phenolic antioxidants and a metal deactivator, shifted the life-expectancy curves back to 40 year service at 40 C (predictable with Ea values of greater than 20 Kcal/mol). GPC analysis was inconclusive in predicting what mechanism of degradation for PE predominates in our high humidity atmospheres. Thermal analysis yielded Ea values approximately 2.0-2.5 times greater than that of the values reported for oxidative degradation, as expected due to the pure $N_2$ atmosphere employed during testing.

It has been shown conclusively, that the combined effect of oxidation and hydrolysis causes PET film to degrade more rapidly than that of thermal degradation in the absence of earth's atmosphere. By Arrhenius modeling techniques, it was concluded that 1 mil PET film will maintain its physical integrity for approximately 15 years in a continuous 45 C/98+% RH environment. This same modeling technique yields an apparent energy of activation (Ea) value of 29.5 Kcal/mol, which is almost half of the value found when degrading the film thermally (48 Kcal/mol). Therefore, a much less conservative estimate of 25-30 years life in a continuous 45 C (0% RH) environment, could be made for PET film aged in a "dynamic" manner (via thermogravimetric analysis). This work reconfirms results of earlier studies[53-58].

As expected, the effect of elevated humidity at the relatively low temperatures of exposure for the radiation-cured HDPE used for voice grade media insulation, was negligible. No reliable life-expectancy data could be ascertained based on these results; however, it was found that this insulation system should yield useful service life longer than any of the other insulations involved in the manufacture for these cables. In all, no devastating failures are anticipated over the 15 year life requirement for this cabling system.

Future work will include the correlation of these chemical and physical changes in the cable insulations with changes in electrical properties during exposure to the same accelerated stress environments. Comparisons with standard air-oven aging techniques used for the same insulations would also be valuable. Non-destructive test techniques including the measurement of changes in mutual capacitance and dissipation factor for both voice grade and data grade transmission media, continues. Work required to determine actual mechanisms of degradation for PVC and especially PE in extremely humid environments is still warranted. Use of thermal analysis to determine actual changes in glass transition temperatures (Tg) of PVC and x-ray diffraction techniques to monitor crystalline morphology differences in HDPE as these insulations are aged in an accelerated manner, would provide much needed information. Also, the use of IR to determine if oxidation occurs at a more rapid pace in the presence of moisture for the same HDPE insulations could provide a better insight into the aging mechanism of foamed HDPE insulations. Finally, these changes should be correlated with "real-life" outdoor weathering of these same insulation systems to provide further confidence in our predictions.

## LIST OF SOURCES CITED


1. "Polymeric Materials—Long Term Property Evaluations," Underwriters Laboratories (UL) 746 B (1982) pp.1-26.
2. "Guide for the Determination of Thermal Endurance Properties of Electrical Insulating Materials," Part 2—List of Materials and Available Tests, IEC Document 216-2 (1974) pp. 1-15.
3. Greisser, E.E., and Higgins, W.T., "Development of Weather-Resistant Vinyl Jackets," Proc. of Fourth Annual Signal Corps Wire and Cable Symposium, Dec. 7 (1955).
4. Grune, G.L., "Material Requirements for Multimedia Communications Cable," Proc. of 33rd International Wire and Cable Symposium (1983) pp. 255-67.
5. Bro, M.I., McCabe, D.I., Allen, D.B., and Reed, J.C., "Perfluoroalkoxy Fluorocarbon Resin Properties Relating to Electrical and Electronic Applications". Proc. of the 29th International Wire and Cable Symposium (1980) pp. 94-100.
6. ASTM D 638, "Standard Test Method for Tensile Properties of Plastics," Revised (1982) pp. 250-61.
7. ASTM D 2436, "Standard Specification for Forced-Convection Laboratory Ovens for Electrical Insulation," Revised (1980) pp. 470-73.
8. Sherwood, R.M., and Dornski, S.J., "An Improved Oven for Accelerated Aging of Polyvinyl Chloride Compounds," Proc. of 16th International Wire and Cable Symposium (1967).
9. ASTM D-2307, "Standard Test Method for Relative Thermal Endurance of Film-Insulated Round Magnet Wire," Revised (1984) pp. 270-79.
10. "IEEE Standard for the Preparation of Test Procedures for the Thermal Evaluation of Solid Electrical Insulating Materials," IEEE Std. *98* (1984) pp. 1-19.
11. "Polymeric Materials—Long Term Property Evaluations," Underwriters Laboratories (UL) 746 B (1982) pp. 1-26.
12. Daikin T.W., "Electrical Insulation Deterioration Treated as a Chemical Phenomenon," Transactions AIEE *67* (1948) pp. 113-18.
13. "A Review of Equipment Aging Theory and Technology," EPRI Report NP-1558, Project 890-1 Sept. (1980) Final Report.
14. "Guide for the Determination of Thermal Endurance Properties of Electrical Insulating Materials," Part 1—General Procedures for Determination of Thermal Endurance Properties, Temperature Indices and Thermal Endurance Profiles, 216-1 (1974) pp. 1-27.
15. ASTM E-698 "Arrhenius Kinetic Constants for Thermally Unstable Materials" (1979) pp. 1-8.
16. Mathes, K.N., "Thermal Aging of Electrical Insulation—Technology and Standardization," IEEE Elec. Insulation Mag. 1 (1985) pp. 29-35.
17. Nelson, W., "Graphical Analysis of Accelerated Life Test Data with the Inverse Power Law Model," IEEE Trans., R-21, *1* (1972) pp. 2-11.
18. Nelson, W., "Analysis of Accelerated Life Test Data—Part I: The Arrhenius Model and Graphical Methods," IEEE Trans., EI-6, *4* (1971) pp. 165-81.
19. Nelson, W., "Analysis of Accelerated Life Test Data—Part II—Numerical Methods and Test Planning," IEEE Trans., EI-7, *1* (1972) pp. 36-55.
20. Hahn, G.J., and Nelson, W., "Graphical Analysis of Incomplete Accelerated Life Test Data," Insulation/Circuits Sept. (1971) pp. 79-84.
21. Lindley, D.W., Greenwood, D.D., and Yow, J.R., "Arrhenius Methodology of Aging for Nuclear Environmental Qualification," Corp. Cons. & Dev. LTD. Internal Report (1980) pp. 1-32.

22. Duswalt, A.A., "The Practice of Obtaining Kinetic Data by Differential Scanning Calorimetry," Thermochemica ACTA, *8* (1974) pp. 57-68.

23. Gyulai, G., and Greenhow, E.T., "Non-Isothermal Analysis: A Critical Examination of Some Recent Theories," *Talanta, 21* (1974) pp. 131-39.

24. Krizanovsky, L., and Mentlik, V., "The Use of Thermal Analysis to Predict the Thermal Life of Organic Electrical Insulating Materials," J. of Thermal Analysis, *13* (1978) pp. 571-80.

25. Toop, D.J., "Theory of Life Testing and Use of Thermogravimetric Analysis to Predict the Thermal Life of Wire Enamels," IEEE Trans., EI-6, *1* (1971) pp. 1-13.

26. Paloniemi, P., "Isothermal Differential Calorimetry as a Means to Measure Insulation Aging Rate Down to the Operating Temperatures," IEEE Trans., EI-7, *3* (1972) pp. 126-32.

27. Randino, J.P., and Andreotti, T.R., "Differential Thermal Analysis As Applied to the Deterioration of Electrical Insulation," Insulation (1964) pp. 24-32.

28. Turi, E.A., "Thermal Characterization of Polymeric Materials," Academic Press, N.Y. (1981) p. 883.

29. UL Subject 758, "Appliance Wiring Material," Underwriters Laboratories (UL) Subject 758, revised 1980, pp. 32-33.

30. Wuerth, H.L., "Improved Polyvinyl Chloride Insulation for 105 C Service," Proc. of Fourth Annual Signal Corps Wire and Cable Symposium Dec. 7 (1955).

31. Hamilton, C.W., Leininger, R.I., and Sommerman, G.M.L., "The Natural and Artificial Aging of Wire Jackets," Proc. of Third Annual Signal Corps Wire and Cable Symposium Dec. 7-9 (1954).

32. Boyd, R.C., "Quality Control of Vinyl and Polyethylene Electrical Insulating and Jacketing Materials," Proc. of Third Annual Signal Corps Wire and Cable Symposium, Dec. 7-9 (1954).

33. Winkler, D.E., "Mechanism of Polyvinyl Chloride Degradation and Stabilization," J. of Poly. Sci., *35* (1959) pp. 3-16.

34. Summers, J.W., Rabinovitch, E.B., and Booth, P.C., "Measurement of PVC Fusion (Gelation)," SPE ANTEC '85 (1985) pp. 1027-30.

35. Payne, M.T., and Renshaw, J.T., "A Monomeric Plasticizer for High Temperature Applications," SPE ANTEC '85 (1985) pp. 1060-67.

36. Graham, R.C., "Moisture Resistance of Insulated Conductors—A General Review," Proc. of 1st Symposium on Technical Progress in Communication Wire and Cables Dec. 8-10 (1952) pp. 2-9.

37. Ashworth, G.W., Darby, J.R., Koerner, W.E., and Munch, R.H., "The Testing of Polyvinyl Chloride Electrical Formulations," Proc. of 16th International Wire and Cable Symposium (1967).

38. Marsal, M., and Slaninka, P., "Aging Mechanism of 1 KV Plastic Insulated Power Cables, ACTA Technica CSAV (1973) pp. 207-26.

39. Warren, P.C., "Plasticizer Evaporation from Vinyl Insulated Wires," Proc. of 29th International Wire and Cable Symposium (1980) pp. 66-75.

40. Loadholt, J.T., and Kaufman, S., "Development of a Flame Resistant Non Contaminating PVC Jacket for Coaxial Cable," Proc. of 29th International Wire and Cable Symposium (1980) pp. 245-52.

41. Clark, Frank M., "Insulating Materials for Design and Engineering Practice," (1962) pp. 566-68.

42. Nowak, P., "Stability of Organic Synthetic Materials," ETZ *80* (1959) pp. 692.

43. Clark, Frank M., "Insulating Materials for Design and Engineering Practice," (1962) p. 472.

44. Bernstein, B.S., and Lee, P.N., "Oxidative Stability of High-Density Polyethylene Cables," Proc. of 23rd International Wire and Cable Symposium (1974) pp. 202-12.

45. Cassel, B., "Recent Advances in Thermogravimetric Analysis of Polymer and Elastomer Formulations," Presented at Sixth No. American Thermal Analysis Society Conf., June (1976) pp. 1-26.

46. Howard, J.R., Gilroy, H.M., and Korta, E., "Rapid Isothermal DTA Testing for Control of Stability in Polyolefins," Proc. of 23rd International Wire and Cable Symposium (1974) pp. 46-52.

47. Chan, M.G., "High Density Polyethylene for PIC Insulation: Oxidative Stability," Proc. of 23rd International Wire and Cable Symposium (1974) pp. 34-41.

48. O'Rell, D.D., and Patel, A.D., "Oxidative Stability Studies on Cellular High Density Polyethylene Insulation for Communications Wire," Proc. of 23rd International Wire and Cable Symposium (1974) pp. 231-33.

49. Pusey, B.B., Chen, M.T., and Roberts, W.L., "Evaluation of Thermal Degradation in Polyethylene Telephone Cable Insulation," Proc. of 20th International Wire and Cable Symposium (1971) pp. 209-16.

50. Chan, M.G., Gilroy, H.M., Johnson, L., and Martin, W.M., "Copper Deactivators for Polyethylene Insulation," Proc. of 27th International Wire and Cable Symposium (1974) pp. 99-115.

51. Sato, M., Nakagawa, S., Hatta, T., Noda, H., and Kawawata, S., "Development of New Copper Deactivator for Polyolefin Insulations," Proc. of 27th International Wire and Cable Symposium (1974) pp. 107-15.

52. Kiss, K.D., and Malawer, E.G., "Oxidative Stability of High Density Polyethylene," Proc. of 28th International Wire and Cable Symposium (1979) pp. 68-82.

53. Hergenrother, W.L., "Influence of Copolymeric Poly (Diethylene Glycol) Terephthalate on the Thermal Stability of Poly (Ethylene) Terephthalate," J. of Poly. Sci., *12* (1974) pp. 875-83.

54. Gardner, R.J., and Martin, J.E., "Effect of Relative Humidity on the Mechanical Properties of Thermoplastic Polyesters," SPE ANTEC, Tech. Papers *25* (1979) pp. 831-34.

55. Kishore, K., and Sankaralingam, S., "Kinetic Analysis of the Data on the Effect of Humidity on the Stability of Poly (butylene terephthalate)," J. Poly. Engr. and Sci., *24*, No. 13 (1984) pp. 1043-46.

56. Harrington, J.F., and Ward, R.J., "Polyester Film Insulation for Hermetic Motors," ASHREA, *1* (1959) pp. 74-78.

57. McMahon, W., Birdsall, H.A., Johnson, G.R., and Camilli, C.T., "Polyester Film," Materials Des. Engr., *49* Feb. (1959) pp. 94-95.

58. Lee, M.M., and Hodges, R.D., "Resistance to Thermal Embrittlement and Hydrolysis Improved with Isocyanate Treatment for Mylar Polyester Film," Insulation, 5 Oct. (1959) pp. 18-25.

59. Chan, J.S., and Jaczek, S.M., "The Moisture Absorption of XLPE Cable Insulation Under Simulated Service Conditions," IEEE Trans. Electr. Insul., Vol. EI-13, No. 3 (1978) pp. 194-97.

60. Gilroy, H.M., "Polyolefin Longevity for Telephone Service," Proc. of ANTEC '85 (1985) pp. 258-60.

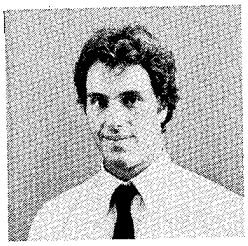
61. Lebok, F.J., "Thermal Endurance Data for Solid Insulating Materials," IEEE Trans., EI-15, 4 (1980) pp. 53-63.

62. Dixon, R.R., "Thermal Aging Predictions from an Arrhenius Plot with Only One Data Point," IEEE Trans., EI-15, 4 (1980) pp. 331-34.



G.L. Grune
IBM Corp.
Polymers Group (E79)
Research Triangle Park, N.C. 27709

Guerry L. Grune obtained his B.S.M.E. from Duke University, 1978 (graduation with distinction) with a double major (A.B.) in Chemistry the same year. After working for Fiber Industries Incorporated, a subsidiary of Celanese and ICI of Great Britain, from 1978-1980 in the heavy denier polyester filament and liquid crystal high modulus organic fiber groups, he returned to graduate school at the University of Massachusetts. There, he obtained his M.S.Ch.E. (1982) from the Departments of Chemical Engineering and Polymer Science and Engineering working under Dr. Robert W. Lenz in the area of thermotropic liquid crystals. Upon finishing his M.S. degree requirements in May 1982, he joined IBM-Raleigh and has been associated with materials selection and development for the IBM Cabling System, fiber optics and the connector systems which will be used for the project.



T.L. Talarico
IBM Corp.
Analytical Chemistry
Research Triangle Park, NC 27709

Todd L. Talarico obtained his B.S.Ch.E. from the Pennsylvania State University in 1983. After working for LCS Laboratories Incorporated, a contract chromatography lab, he came to IBM in 1984. Todd is presently involved in chromatographic analysis along with accelerated aging studies of subassemblies in IBM.

## ACKNOWLEDGMENTS

The authors wish to thank Mr. Kenneth Mathes for his willingness to share his experience and knowledge of insulation systems with us. Mr. Mark Young is also to be congratulated for his diligent efforts involving the physical testing of these insulations and the reproducibility of the results he was able to generate. Along with Mr. Young, Messrs. R.R. Witska, M. Blankenship, G. Oyler, S. Needham, and J. Blom aided in further destructive testing.

Thermal analysis was performed with the aid of Corporate Consulting and Development, Apex, NC, and special thanks are in order for Messrs. D. Hatmaker, D. Greenwood, and C. Kehr. Some Gel Permeation Chromatography analysis was performed at Jordi Associates, Millis, MA. EDX and IR analysis by several members of the Chemical Analysis Group (EG2) during the course of the 3-year study is appreciated.

Finally, other members of the IBM-RTP Materials Lab including L.D. Hobgood, B.L. Chow, T.W. Cochran, R.C. Sanwald, and D.M. Preiss are acknowledged for support of this program along with Messrs. J.L. Carson, O.C. King, R.B. Hobgood, L.S. Stumbough, and A. Overby, for financial and technical assistance. Also, several members of the Brand-Rex Corp., including Messrs. R. Crouch, Wm. Wood, L. Roberts, and R. Brunnelle receive our thanks.

Valley Design, Durham, NC, is responsible for typesetting and artwork.

# FULL-SCALE FIRE TESTS TO SIMULATE AN ELECTRICAL CABLE FIRE IN THE CONTROL ROOM OF AN INDUSTRIAL PLANT

R. M. Eichhorn and J. J. Pickering

Union Carbide Corporation, River Road, Bound Brook, New Jersey 08805

## Abstract

Current requirements for approval of industrial power cables include limitations on flame spread but do not address the generation of smoke or the liberation of gases. To demonstrate that improvements in safety could be achieved with a new, reduced emissions cable design, a full-scale industrial fire situation has been simulated. The ignition source was chosen to provide the heat output of a wastebasket fire which, in the authors' opinion, is realistic and conservative. Test results show that practical and available improvements reduce the generation of smoke and the emission of some gases generally considered toxic.

## Introduction

If electrical wires or cables become sufficiently hot due to short circuits, prolonged current overloads, or proximity to accidental small-area fires, the insulations or jackets used with them may smolder, giving off gases and smoke, or even ignite, with similar emissions plus heat and visible light. If the insulations are sufficiently flammable that they continue to burn in air, after removal of the ignition source, and if fire protection devices are ineffective or missing, the cables may act to spread fire, smoke, and gases. There have been enough well publicized examples that this hazard is acknowledged. Therefore, for certain critical cables, particularly those used in open cable trays, raceways, and risers, modern versions of solid, extruded, polymeric, fire-retardant and low emissions materials have been developed for insulation and jacketing.

To investigate the fire hazards of multiconductor cables in a commercial setting, a full-scale simulation of a control room cable fire has been carried out. The simulation was conducted in a cement block room typical of modern, well designed, industrial construction using a vertical, open cable tray.

Four different cable types, three of them conventional and one new, have been tested. The results of smoke density, gas concentration, and temperature measurements are presented, as well as observations of the operating times of smoke detectors and sprinklers, and the obscuration time for an Exit sign.

The study has shown that there are substantial differences in fire properties among conventional cables and that the new design offers advantages in terms of reduced smoke generation and gas emission which deserve further consideration.

Some of the observations were unexpected. For example, in tests where (1) the smoke density completely obscured vision within the room, (2) ionization type smoke detectors were activated within 20 seconds and photoelectric smoke detectors within 3 minutes, and (3) the ceiling temperature in the room exceeded 200°F for over 4 minutes and reached 250°F, the three 165°F sprinklers in the room did not operate.

## Fire Test Facility

After a survey of modern, well designed commercial and industrial construction in power plants, manufacturing facilities, hospitals and shopping centers which were in compliance with appropriate fire codes, a full-scale fire test room was built. The room, 12 by 23 feet and 11 feet high, with 6-foot corridors on each side for observation, instrumentation, and gas collection, partially simulates the control room in a large industrial plant. It is of concrete block and mortar construction with a roof/ceiling of hollow core prestressed concrete slabs, 2 feet wide by 8 inches thick. Access to the room is provided by a large door, while a window on the same long wall provides visual observation of tests. Figure 1 shows a diagram of the room with the cable tray for specimen mounting, burner, exit sign, and light beams for optical density determination in place. The ignition source, a 15 by 15 inch sand burner

which produces a flame plume 1.5 to 3 feet in height and radiant heat flux of about 20 kW/m$^2$, was chosen to simulate a waste-basket fire.[1,2] It is large enough to produce measurable smoke obscuration from all cable samples but not large enough to prevent distinction between them. It was not intended to be a significant fire by itself. The burner is located 3 inches in front of the cables in the tray so the flame will not impinge upon them.

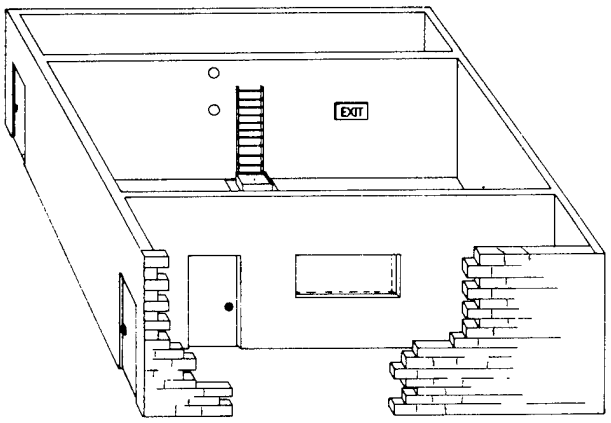



FIGURE 1

FULL SIZE CONTROL ROOM TEST
SHOWN WITH CEILING REMOVED
12' x 23' x 11' + END CORRIDORS

The cable tray is a standard open ladder type, 18 inches wide, 10 feet long and 4 inches deep, made from 0.065-inch galvanized steel. It is mounted vertically, 6 inches from the back wall. The electroluminescent exit sign is 9 by 15 inches and mounted 8 feet from the floor. There is a 20-inch wide by 12-inch high opening at floor level behind the tray, and a 12-inch high curb surrounding the tray and burner to simulate the effect of a cable tray passing into the room from an adjacent area. The natural convection from this opening provides the only ventilation for the room except for minor leakage around the door. Excessive ventilation to force burning was not provided.

Two UL listed smoke detectors, one photoelectric and one ionization, were installed on the ceiling along the center line of the room and 8 feet from the cable tray. In addition, three sprinkler heads were installed 12 inches below the ceiling along the center line of the room. One was directly in front of the cable tray, the others were 8 feet to either side. The sprinkler heads were pendant type with standard 1/2 inch orifices and rated for 165°F. They were not connected to water piping, but the links were connected to electrical circuits for recording the time of fusing.

Fifty-three thermocouples were installed to measure air and surface temperatures at various locations in the test room. A calorimeter was used to measure the heat flux of the sand burner and the flaming cables. Gas analyzers and sampling equipment consisting of glass tubing, electric pumps, and aspirators were used to collect gas samples at two locations in the room. Concentrations of $O_2$, CO, and $CO_2$ were measured continuously, while determinations of HCl, HBr, HCN, and $NO_2$ were made four times during the 30-minute test.

## Cable Samples Tested

Four different UL Type TC constructions designed to satisfy the UL-1277 requirements were tested. They are described in Table 1. The first four cables listed were chosen on the basis of commercial usage as tray cable in the U.S. in 1982. The fifth represents a new construction which offers more desirable fire properties.

For fire testing, cable samples were mounted in trays in two solid layers. The larger 9 conductor 12 AWG cables were tested 48 at a time in the tray while the smaller 7 conductor 14 AWG cables were tested 66 at a time. Each sample was

Table 1
Constructions of Cables Tested

| | | Insulation | | | Wrap | Jacket |
|---|---|---|---|---|---|---|
| Cable | Size+ | Type | Material | Jacket | Tape | Material |
| THHN/FRPVC | 9/12 | THHN/THWN | FRPVC | Nylon | Polyester | FRPVC |
| THHN/FRPVC | 7/14 | THHN/THWN | FRPVC | Nylon | Polyester | FRPVC |
| RHW/CSPE | 7/14 | RHW | EPR | None | Polyester | CSPE |
| XHHW/PCP | 7/14 | XHHW | XLPE | None | Polyester | PCP |
| XHHW/NHXLP/RE* | 9/12 | XHHW/RE* | XLPE | None | Glass | NHXLPE** |

+All conductors were stranded copper.
*Proposed designations for REDUCED-EMISSIONS insulation and jacket.
**Halogen-free XLPE.

secured to the rungs with ties at two positions.

The reason that two sizes were used was that all cables were not available in either size. For this reason the 7c/14ga size was selected as the conservative option and the common THHN/FRPVC was used in both sizes to indicate any difference due to geometry.

## Test Procedure

After filling each cable tray with two full layers of specimens, the tray was weighed and mounted vertically in position in the test room. The burner was adjusted into position, ignited, and all analytical instruments were started. During the test, visual observations were made and recorded through the window from the corridor as shown in Figure 1. Observations included ignition of the cables, the character and development of the fire, smoke development, and time to obscuration of the exit sign. After 7 minutes the burner was extinguished, although observations and measurements were continued until the end of the 30-minute test period. After removing the tray from the room at the conclusion of the test it was weighed again to give the mass loss of the specimen.

During the test period, temperatures, heat fluxes, smoke densities, and concentrations of $O_2$, CO, and $CO_2$ were recorded every 20 seconds. Gas samples of HCl, HBr, HCN, and $NO_2$ were collected four times during the test for subsequent analysis.

## Analytical Methods

Samples of the gases in the room were taken from two levels in the center of the room directly in front of the cable tray. One was 4 feet from the floor, the other 10 feet, one foot below the ceiling. The 4-foot level is the height of a seated person's head while 10 feet represents the likely level of greatest concentration. Separate sampling lines were provided from each point for HCl, HBr, HCN, and $NO_2$. Another line was used for $O_2$, CO, and $CO_2$.

One-quarter inch diameter glass tubing was used for the gas sampling lines which passed from the sampling points through holes in the back wall to the measuring instruments and collecting bottles in the rear corridor shown in Figure 1. The tubes were wrapped with electrical heating tape which maintained approximately 100°C to prevent condensation on their inner surfaces. Small gas pumps were installed in each line to provide gas flow at a steady and controlled rate. Where necessary, lengths of glass tubing were joined by short lengths of Tygon tubing.

Concentrations of $O_2$, CO, and $CO_2$ were determined continuously using a Beckman Model 755 paramagnetic analyzer for oxygen, and Horiba P1R-2000 fixed wavelength infrared analyzers for CO and $CO_2$. These instruments are direct reading and their analogue outputs were accumulated by an Accurex Autodata 10 Data Logger. The instruments were calibrated before each test with certified purge gases which were introduced at the sampling points to ensure that the entire sampling system was functioning properly.

Quantitative determinations of HCl, HBr, and HCN were made by drawing 10 liter samples, and use of ion specific analyzers, according to NIOSH methods S246, S175, and P&CAM 116, respectively. $NO_2$ was measured by use of 250 ml samples and NIOSH method P&CAM 108--"Evacuated Bottle Method." Interferences between halide ions were investigated and it was observed that bromide interfered positively with chloride but the reverse was not true. This proved of no importance, however, since no cable contained components such that it could liberate both chlorine and bromine.

## Test Results

### Visual Observations

Certain of the fire parameters were recorded by visual observation through the window in the room, and by the event recorder which marked the time at which a given event occurred. This information is presented in Table 2. In the table the times to ignition, to activation of the second smoke detector, and to obscuration of the exit sign are in seconds, the maximum flame height is in feet, and the weight loss is in pounds (+/- 0.1 lb). The value used for peak optical density was measured horizontally at the 6-foot level.

### Heat Flux

The radiant heat flux from the burner and the cables, after ignition, was measured by a single HyCal calorimeter which was mounted at the front edge of the sand burner. The calorimeter had a viewing angle of 180 degrees, a flat black surface, a water-cooled copper body, and a full-scale range of 170 $kW/m^2$ (13.2 $BTU/ft^2$-sec) at 10 mV output.

Figure 2 shows the variation of heat flux with time. Note that the flux decreases abruptly when the burner is extinguished after seven minutes. The only significant difference among the

Table 2
Events Recorded Visually During Fire Tests

| Cable | Size | Time to Ign. | Smoke Det's Act'd | Max Flame Hgt | Wt Loss | Peak OD/Ft (X100) | Exit Sign Obsc'd |
|---|---|---|---|---|---|---|---|
| THHN/FRPVC | 9/12 | 92 | + | 5.5 | 5.0 | 33.33 | 155 |
| THHN/FRPVC | 7/14 | 125 | 94 | 5.5 | 3.0 | 33.33 | 157 |
| RHW/CSPE | 7/14 | 100 | ++ | 4.5 | 0.5 | 26.29 | 180 |
| XHHW/PCP | 7/14 | 180 | 165 | 4.0 | 1.2 | 33.33 | 280 |
| XHHW/NHXLP/RE | 9/12 | 305* | 209 | 1.0 | 0.0 | 6.48 | Never |

*One of two specimens did not ignite at all.
+Time not recorded.
++Photoelectric detector inoperative, ionization detector activated in 15 sec.

Physical damage to the sample cables was as follows:

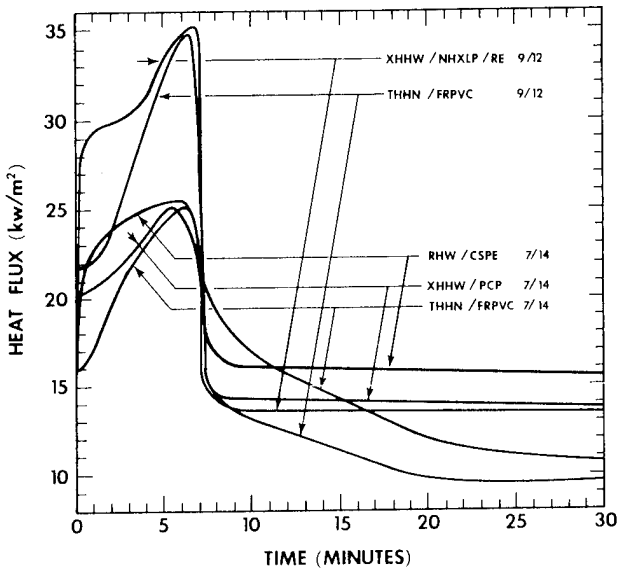
| | | |
|---|---|---|
| THHN/FRPVC | 9/12 | Bare cond. 2 to 4 ft, char and blister 4 to 6 ft. |
| THHN/FRPVC | 7/14 | Bare cond. 2 to 4 ft, char and blister 4 to 6 ft. |
| RHW/CSPE | 7/14 | Heavy char 2 to 3 ft, char and blister 3 to 4 ft. |
| XHHW/PCP | 7/14 | Bare cond. 2 to 3 ft, char and blister 3 to 4.5 ft. |
| XHHW/NHXLP/RE | 9/12 | Some cracking, char and blister 2 to 3 ft. |

All cable samples showed no damage below 2 ft, which was the level of the base of the ignition flame.

curves seems to be that the heavier cables get hotter early in the test and are cooler than most at the end. It is apparent that none of these cables, which were designed to satisfy the UL 1277 Type TC flame test requirements, will propagate flame or continue burning under the conditions of this test without a continuous supply of energy.

FIGURE 2

TOTAL RADIANT HEAT FLUX
FROM BURNER AND CABLES




## Room Temperatures

Fifty-three thermocouples were installed in the room at various locations to measure the temperatures of gas/air and surfaces. The air temperatures were determined at five levels, 1, 6, and 10 feet above the floor, and 1 and 6 inches below the ceiling. Eight such thermocouples in each layer were radially disposed as shown in Figure 3. Figure 4 shows the variation of air temperature with time at the 6-foot level and 6 feet from the cables while Figure 5 shows it at the 10-foot level.

FIGURE 3

INSTRUMENTATION OF TEST ROOM

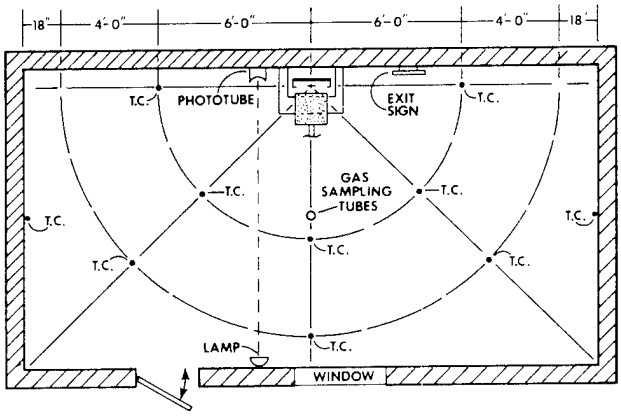


FIGURE 4

AVERAGE AIR TEMPERATURE AT 6-FOOT LEVEL
AT 6-FOOT RADIUS FROM BURNER POSITION

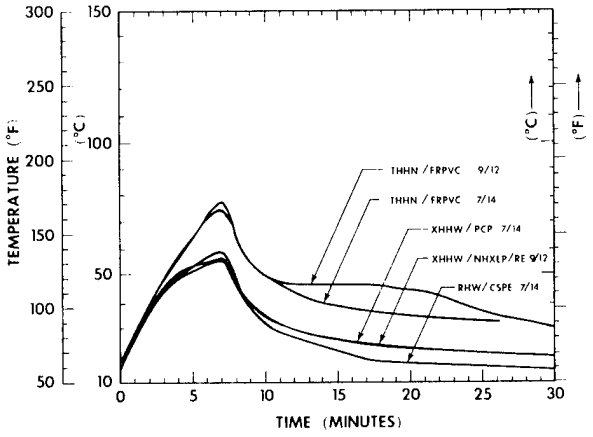
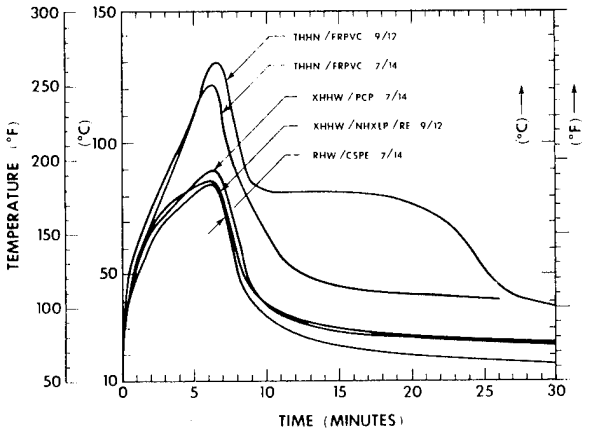



FIGURE 5

AVERAGE AIR TEMPERATURE AT 10-FOOT LEVEL
AT 6-FOOT RADIUS FROM BURNER POSITION



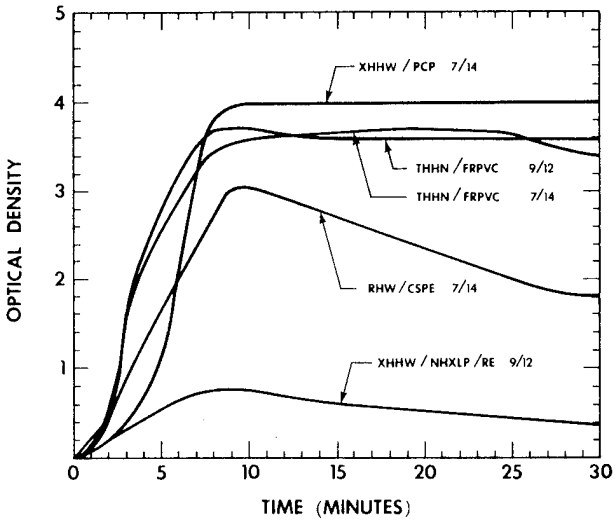

The scales are the same to facilitate comparison and the indicated temperatures are the averages of the five thermocouple responses at each level. As expected, the ceiling temperature is higher than that at 6 feet and the shapes and relationships of the curves are the same. While the curves are divided into high and low groups, the groups are not the same as in the heat flux data.

## Optical Density

Two light beams were installed to shine across the room in the short direction near the site of the burner and cables, as shown in Figure 3. The light sources were GE Model 4405 sealed beam spotlights; the detectors were Weston Model 856BB photocells. Measurements of light transmission, converted to optical density, are plotted with respect to time in Figure 6. If the times measured to obscuration of the exit sign (see Table 2) are compared with these curves, the data are found to be consistent and obscuration occurs at 0.9 OD or 0.075 OD/ft. The curves clarify the earlier observation that the new cable design was the only one which did not cause complete obscuration of vision in the room and permitted an observer to read the exit sign during the complete 30-minute test.

FIGURE 6

OPTICAL DENSITY AT 6-FOOT LEVEL




## Fire Gases

Since combustion is an oxidation reaction, when anything burns oxygen is consumed, and its concentration in a room with limited ventilation will decrease. This was the situation in the test room since it was designed to simulate fire safe construction where in the event of fire the HVAC systems would shut off to limit fire spread.

Figure 7 shows the variation of oxygen concentration with time during the burning of each of the test cables. In this situation there would be no great hazard due to oxygen depletion, which is usually considered to exist when $O_2$ concentration decreases by about 5%.

There are many gases liberated when organic materials undergo combustion or thermal decomposition and they have been the subject of investigations and publications too numerous to list here. A few of those which are considered hazardous have been measured in this experiment. Carbon monoxide is usually considered the most serious threat and Figure 8 shows its liberation with time. The hazard

suggested by the two highest curves is probably greater than the others for two reasons. First is the greater concentration, second is the rapid rate at which it seems to appear.

FIGURE 7

OXYGEN CONCENTRATION AT 4-FOOT LEVEL

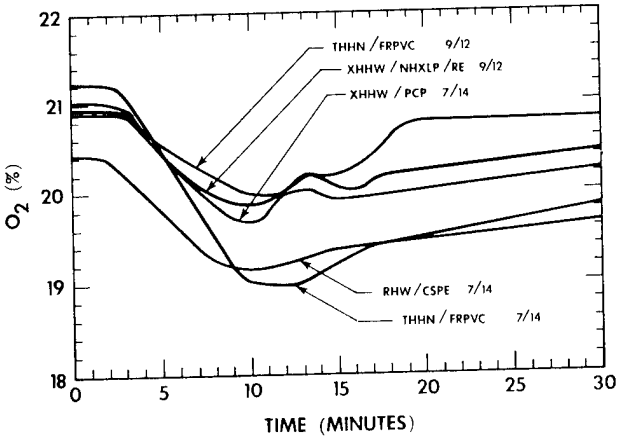
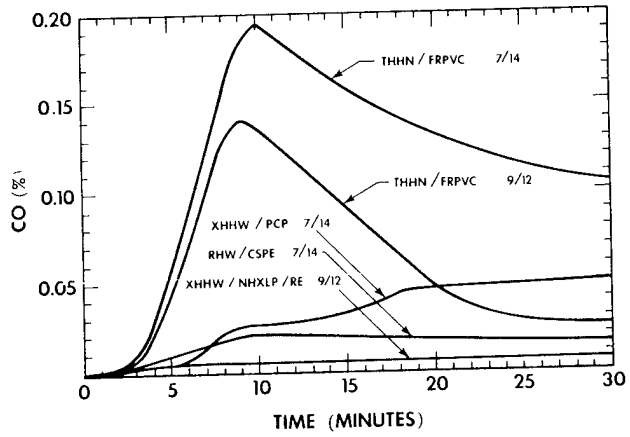



FIGURE 8

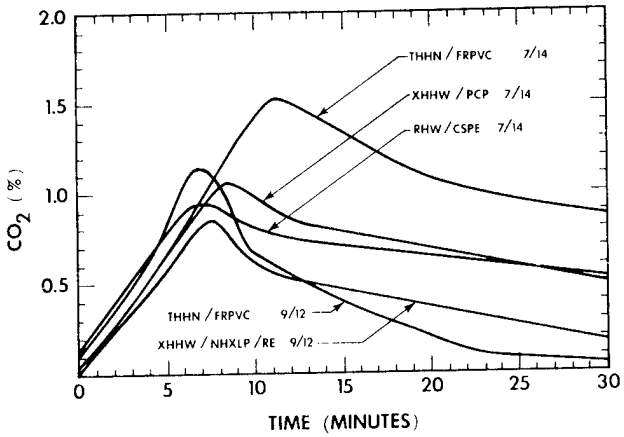
CARBON MONOXIDE CONCENTRATION AT 4-FOOT LEVEL




Carbon dioxide has generally been considered much less noxious than CO but recently has been the subject of work which suggests interactions between the two in terms of toxicity. However, these results are not yet published. Figure 9 shows the variation in concentration of $CO_2$ with time.

FIGURE 9

CARBON DIOXIDE CONCENTRATION AT 4-FOOT LEVEL




Other gases hazardous to health are HCN, nitrogen oxides, HCl, and HBr. The last two are also corrosive and can cause damage to metal parts such as switches, conductors, machines, etc. The maximum concentrations of these gases which were found to exist during the test are presented in Table 3. It is apparent that in terms of the gases measured in this test the new cable design appears to offer an improvement in safety.

## Conclusions

Experiments have been made to determine the relative behaviors of four different tray cable constructions when exposed to the radiation from a small simulated wastebasket fire in a large room where the conditions are similar to those in a modern industrial control room. It was found that a cable design which uses a new reduced-emissions XLPE insulation and a halogen-free jacket offered the following advantages with respect to the other cables tested:

1. longer time to ignition under test conditions

Table 3
Maximum Concentration of Fire Gases at 4-Foot Level*

| | | CO | $CO_2$ | HCl | HBr | HCN | $NO_2$ | $CO/CO_2$ |
|---|---|---|---|---|---|---|---|---|
| THHN/FRPVC | 9/12 | 1,460 | 11,400 | 1,960 | 199 | 143 | 28 | 0.128 |
| THHN/FRPVC | 7/14 | 1,950 | 15,100 | 1,720 | 545 | 46 | 7 | 0.129 |
| XHHW/PCP | 7/14 | 500 | 10,500 | 16 | 1 | <1 | 2 | 0.048 |
| RHW/CSPE | 7/14 | 200 | 9,400 | 24 | 1 | <1 | 2 | 0.021 |
| XHHW/NHXLP/RE | 9/12 | 65 | 8,500 | <1 | <1 | <1 | 1 | 0.008 |

*Tabulated in ppm.

2. less burning and cable damage
3. substantially less smoke
4. significantly lower concentrations of CO, $CO_2$, HCN, $NO_2$, HCl, HBr
5. much lower $CO/CO_2$ ratio

Other observations were that both photoelectric and ionization smoke detectors worked well while standard commercial sprinklers did not operate under the conditions of this fire.

The information presented here is not intended by either of the authors or by Union Carbide Corporation to predict or reflect the performance of any of the cables or materials in a real fire. The results of test programs like this one, although attempting to simulate practical conditions, are only relative and are limited in significance to conditions exactly as used in the test.

## References


1. V. Babrauskas, "Upholstered Furniture Heat Release Rates: Measurements and Estimation," J. OF FIRE SCIENCES 1, 1, p. 9 (1983).

2. "Flammability Studies of Cellular Plastics and Other Building Materials Used for Interior Finishes," UL Report, June 1975, p. 23.


## Biographies

Robert M. Eichhorn is a Research Associate (Physics) in the Polyolefins Division of Union Carbide Corporation which he joined in 1954. His responsibilities are in the field of measurements and research on dielectric materials used for electrical insulation. He is a member of the American Physical Society, the American Institute of Physics, CIGRE, and a senior member of the IEEE. He is currently a committee chairman of the Electrical Insulation Society, a member of the AdCom and has served as an Assistant Editor of the IEEE TRANS EI.

James J. Pickering is Manager of Wire and Cable Product Applications in the Polyolefins Division of Union Carbide which he joined in 1962. He is responsible for interfacing with various end-users and specifying agencies. Previous to his present assignment, he spent 12 years in Research and Development working in the area of wire and cable compound development, and 8 years in sales where he called on major wire and cable accounts in the Midwest as an account representative. Mr. Pickering is a member of the Society of Plastics Engineers, the Institute of Electrical and Electronics Engineers, The National Fire Protection Association and the Wire Association.

# DEVELOPMENT OF LOW SMOKE, HALOGEN FREE, FLAME RETARDANT CABLES FOR SHIPS

Y.Shingo, T.Mathuda, M.Murayama, S.Yoshikawa, M.Hasegawa, A.Yoshino

FUJIKURA LTD.
Tokyo, Japan

## 1.Abstract

New types of low smoke,halogen free,flame retardant cables have been developed for the purpose of applying to ships.Kinds of cables for purposes of data transmission (optical fiber cable),instrumentation,control, low voltage power and trailing cable are now available.

And a composite optical fiber/power cable for data transmission and low voltage power,functional and satisfactorily safe even if at fire condition,was developed.

## 2. Introduction

In recent years, fire outbreaks in the multistoried hotels,warships, and the subway facilities have injured and killed many people due to the formation of exessive toxic gases and smoke which prevent occupants to escape from the burning structures and impeding fire-fighting activities.

The biggest problem is due to organic polymers containing halogens(chlorine,bromine and fluorine) are commonly used as building materials and cable materials in recent years.In case of fire,polymers such as polyvinyl chloride(PVC) give off highly toxic and corrosive gases,liquid and much smoke.

Ironically, cable manufactures use materials that contain halogens to make cable flame retardant,while retaining good electrical and mechanical performance.

From the viewpoint of fire safty, cables used at power plants,multistoried building,ships,subways and so on must improve performance requirements not only in terms of flame retardancy but also with respect to low levels of generation of smoke,toxic substances,and corrosive gases.The authers have made efforts to find ways of producing flame retardant cables without resorting to these halogen containing polymers,and have succeed in new flame-retardant,low-toxic and non-corrosive cables for data transmission, instrumentation,control,low voltage power and trailing cables.

In this paper, specific safety properties of materials and finished cable of HF cable are described.

## 3. Cable Requirements

Efforts to impart flame retardant properties to cables were started at an early period. Most of cables have been rendered flame retardant by using halogenated polymers and additives, but the use of these cables leads to generation of smoke,corrosive and toxic gases in case of a fire.

Thus,the basic requirements of new types of flame-retardant cables to be developed are as follows;

(1) flame retardancy
(2) low toxicity
(3) low corrosiveness
(4) low smoke generation

## 4. Construction and general characteristics of HF cables

### 4-1 Construction

Shipboard cable are classified into four types of cables as shown in Tabel 1 and the selection of of the constructional types and materials are determined to meet to the applications.In addition to the properties mentioned in Section 3,cables must meet the following requirements;

(1) general properties to be as similar in quality to conventional cables compling with IEC 92-3,
(2) cost performance to be as similar to conventional one.

Materials composing the cable,insulation,filler,tapes and sheath,are all halogen-free.

The combination of a flame barrier layer and a specially formulated polyolefine compound for the sheath,make HF cables flame-retardant.

A specially formulated halogen-free elastomer compound with good abrasion resistance for a trailing cable are developed.

All types of cables have a galvanized steel wire braid armouring, except for the trailing cable.

### 4-2 Properties of materials

The properties of materials used in HF cables are shown in Table 2.

Conventional XLPE or EPDM is used for insulation, therefore HF cables have electrical properties that are as good as those of conventional cables. For trailing cables, flame-retardant, halogen-free materials are developed for the insulation with keeping electrical properties.

The flame-retardant polyolefine compound(FR-PO) and

Table 1 Types and constructions of cables

| | Power cable | Telecommunication cable | Data transmission cable | Trailing cable |
|---|---|---|---|---|
| Conductor | Tinned annealed copper wires | Annealed copper wires | · Tinned annealed copper wires<br>· Optical fibers | Tinned annealed copper wires |
| Insulation | EPDM | XLPE | EPDM | FR-EPDM |
| Filler | Kraft paper | Kraft paper | Kraft paper | — |
| Flame barrier layer | · Kraft paper<br>· PET laminated aluminum tape | · Kraft paper<br>· PET laminated aluminum tape | Glass laminated mica tape | — |
| Sheath | FR-PO [1] | FR-PO | FR-PO | FR-EL [2] |
| Amouring | Galvanized steelwire braid | Galvanized steelwire braid | Galvanized steelwire braid | — |

1) Halogen free polyolefine compound
2) Halogen free elastomer compound

Table 2 Properties of cable materials

| | | | Power cable | Telecommunication cable | Data transmission cable | Trailing cable |
|---|---|---|---|---|---|---|
| Insulation | Tensile strength<br>Elongation | kg/mm²<br>% | 0.72<br>708 | 2.10<br>570 | 0.68<br>675 | 0.65<br>700 |
| | After aging<br>TS %retained<br>EL %retained | %<br>% | 96 (1)<br>101 | 95 (2)<br>96 | 100 (3)<br>96 | 95 (4)<br>92 |
| | Oxygen index | - | 20 | 18 | 20 | 25 |
| | Insulation resistance | MΩ·km | 1300<br>(60mm²) | 10000<br>(1.25mm²) | 1300<br>(60mm²) | 1250<br>(60mm²) |
| Sheath | Tensile strength<br>Elongation | kg/mm²<br>% | 1.20<br>357 | | | 0.93<br>230 |
| | After aging<br>TS %retained<br>EL %retained | %<br>% | 98<br>96 | | | 108<br>103 |
| | Oil resistance<br>TS %retained<br>EL %retained | %<br>% | 85 (5)<br>75 | | | 92 (6)<br>86 |
| | Halogen asid gas generation(IEC754) | % | non detectable | | | non detectable |
| | Smoke generation (NBS) | — | 72 | | | 95 |
| | Copper mirror corrosion test (ASTM D2671) | — | pass | | | pass |
| | Oxygen index | | 32 | | | 31 |

(1):135°C for 168h (2):120°C for 96h (3):100°C for 24 h (4):100°C for 168h
(5): 70°C for 4h(ASTM#2oil) (6):121°C for 18h(ASTM#2oil)

Table 3 Test results of the Vertical Tray Flame Test

| Cable | | Power cable | | Telecommunication cable | | Data transmission cable | Trailing cable |
|---|---|---|---|---|---|---|---|
| Size | | 3cx14mm² | | 7cx1.25mm² | | 3cx3.5mm² optical fibers | 3cx22mm² |
| | | HF | Conventional | HF | Conventional | HF | HF |
| Combustion length (cm) | Insulation | 38 | > 180 | 80 | > 180 | 60 | 44 |
| | Sheath | 80 | > 180 | 105 | > 180 | 95 | 70 |
| Judgement | | pass | fail | pass | fail | pass | pass |
| Smoke density (D) | | 0.04 | 0.21 | 0.06 | 0.72 | 0.04 | 0.08 |
| Gas generation (ppm) | Hcl | 0 | 130 | 0 | 250 | 0 | 0 |
| | $SO_2$ | 0 | 30 | 0 | 35 | 0 | 0 |
| | CO | 25 | 60 | 25 | 250 | 20 | 25 |
| | $CO_2$ | 1200 | 3000 | 1000 | 3500 | 1100 | 1600 |

flame -retardant elastomer compound(FR-EL), for the sheath materials, have a good flame retardancy equivalent to a high LOI in excess of 30,and low smoke generation properties.

A materials used for the HF cables have passed the copper-mirror corrosion test specified in ASTM D-2671 so that they generate no toxic gases.

FR-EL is outstanding in flexibility,oil resistance and abrasion resistance, promising to replace conventional polychloroprene.

## 5. Properties of flame barrier layer

Flame retardancy of HF cables is due to the combination of the flame barrier and flame retardant sheath.

Electrical properties are given the great emphasis in HF cables, while the insulation materials are same as those of conventional cables.

In general,the combustion of polymers is initiated by the formation of flammable gases by pyrolysis from the melted surface of polymer with exothermic reaction taking place as these gases burn. The continuous propagation of fire is due to the repetition of these process.

Thus,for HF cables, it is of paramount importance that the flame barrier layer should be effective in preventing the melted insulation materials from gushing out and flammable gases from being released.

### 5-1 Efficiency of the flame barrier layer

The efficiency of the flame barrier layer ( airtightness ) of typical kinds of tapes,kraft paper, glass laminated mica tape and PET laminated aluminum tape,were evaluated.

Cellulose materials such as kraft paper are found to be suitable for as the tape materials as they don't melt by heat, and they form a adiabatic layer even on carbonization in reduced oxygen condition.

To evaluate the airtightness of the tapes, leakage measurements on each tape were carried out at different air pressures. For the measurements, an air pressure as similar to the combustion gas pressure of cable during a fire are applied.

The results are that PET laminated alminum is the best tape in terms of airtightness and showed minimum leakage, followed by PET laminated aluminum tape > glass laminated mica tape > kraft paper.

### 5-2 Relation between the efficiency of flame retardant barrier and flame retardancy/ smoke generation

Cables with kinds of flame barrier layers have been evaluated for flame retardancy by the vertical tray flame test (VTFT) specified in IEEE Std.383.

These results and the airtightness of tapes mentioned in Section 5-1 above are compared.

It appears that the cable with a better airtight barrier shows a shorter combustion length. At the same time,the rate of smoke generation from cables was measured,using the photometric system(0.25m length of optical path), set in the VTFT room.

Smoke density (D) is obtained from the following formula;

$$D = 1/L \log (Io/I) \quad \text{-------(1)}$$

Io: light intensity without smoke
I : light intensity through smoke
L : length of optical path (m)

Smoke generation from cables is consistent with the efficiency of the flame barrier layer.

Thus, the best choise of flame barrier layer can be determined.

### 5-3 Flexibility

The flexibility is one of important properties in cable installation.

The construction of the flame barrier layer affects flexibility of a cable.Cables with better airtightness shows poorer flexibility. Cables,whose flame barrier layer consist of a PET laminated aluminum tape, showed the best flame retardancy,but the poorest flexibility.

After considering the relations between the construction of flame barrier layer and flammability, smoke generation,and flexibility, the combination of kraft paper and PET laminated aluminum tape was finally selected.

## 6. Cable properties

### 6-1 Flame retardancy

The flame retardant properties of HF cables were evaluated in accordance with IEEE Std.383(VTFT). The test results are shown in Table 3. HF cables satisfactorily passed the VTFT but conventional shipboard cables burnt out.

### 6-2 Smoke generation

The smoke generating properties of HF cables during the VTFT were evaluated by the same method as that mentioned in Section 5-2. The results are shown in Table 3. The smoke density (D) of HF cable is extremely low as compared with conventionl shipboard cables.

The reason is that smoke generation from any of the HF cable material are low enough and the length of combustion in the VTFT is short due to its high flame retardancy.

### 6-3 Toxicity

The gases generated during the VTFT have been measured with gas detected tubes. The concentration of four typical gases (HCL,SO2,CO,CO2) are given in Table 3.

In the HF cables the gases considered harmful to the living body (HCl,SO2) are not detectable.

Toxicity tests on gases generated from HF cables and conventional ones were conducted using mice.This method is specified in Notification No.1231 of the Ministry of Construction, Japan.

The test equipment is as shown in Figure 1.

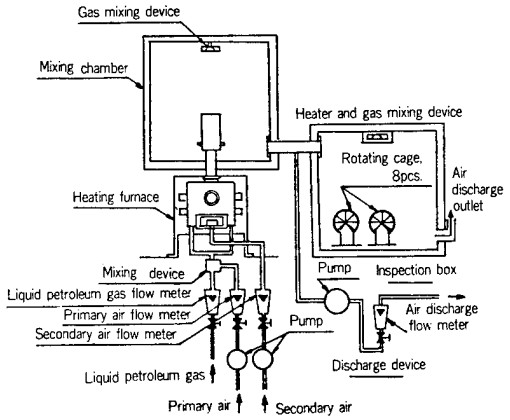



Figure 1 Typical equipment for testing toxicity of the gas, using mice (Notification No.1231 of the Ministry of Construction,Japan)

Cable samples of 9 pieces, 22cm long, are closely arranged a pearlite plate (22cm x 22cm), burned by a gas burner and an electric heater for 15 minutes.

The behavior of eight mice in the combustion gases was recorded. Toxicity of the samples was evaluated by survival time.

The charts recording the behavior of the mice ( Figure 2)show that,in case of conventional flame-retardant CV (XLPE insulated PVC sheathed) cable, all of the eight mice ceased to move after about 9 minutes, whereas in case of HF cable,all continued to move even after 15 minutes exposure.

From the test results obtained, the gases generated during the burning of HF cables substantially contain no elements toxic to living animals.

## 6-4 Fire resistant property

For data transmission cable,composite construction of optical fibers for data transmission and low voltage power cores is designed to impart with fire-resistant properties in addition to flame-retardancy, low smoke generation and low toxicity.

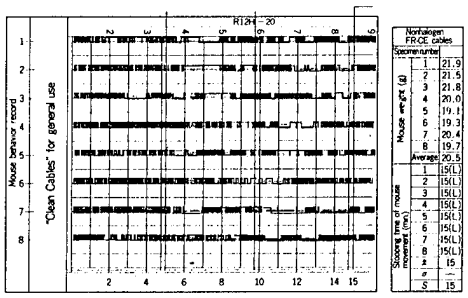
The cable was put to a fire-resistant test based on Notification No.7 of the Ministry of Fire Defence Agency ,Japan as shown in Figure 3.

A cable sample of 1.3m long is set on a pearlite plate and heated for 30 minutes in accordance with a temperature curve as shown in Figure 4.

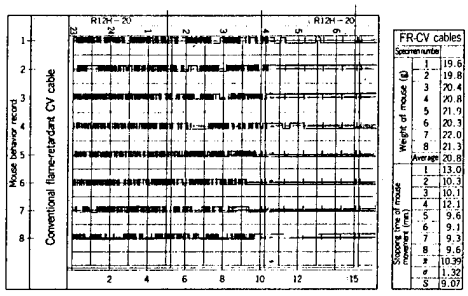
The cable was tested under the fire at the rated voltage, after heating the high-voltage endurance test was carried out.

At the same time, the changes in transmission loss of optical fibers were recorded during the test. The test results are shown in Figure 4.

The low voltage power cores satisfactorily withstood not only to the rated voltage of 600v at 840°C for 30 minutes but also to high voltage of 1500V for 1 minute after heating. While the change in transmission loss for optical fibers was only 0.05 dB/m during the test, it returned to initial level after the test.




A) HF cable




B) Conventional flame-retardant CV cable

Figure 2 Mouse behavior records during combustion of cables

Thus, it appears that this cable also has good fire-resistant properties.

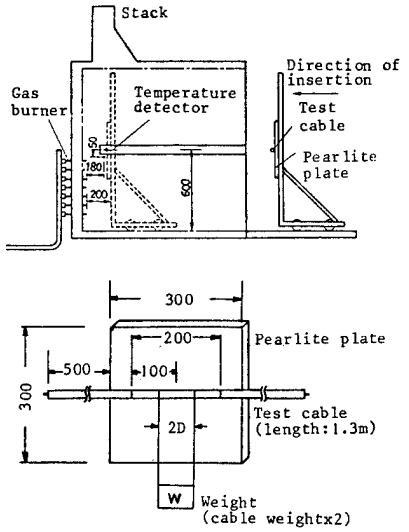



Figure 3 Equipment of fire resisting test

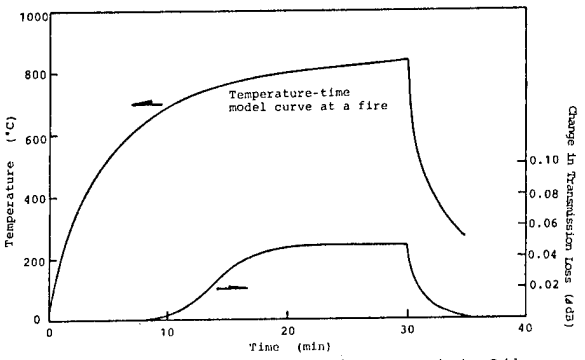



Figure 4 Fire resistant properties of Data Transmission Cable

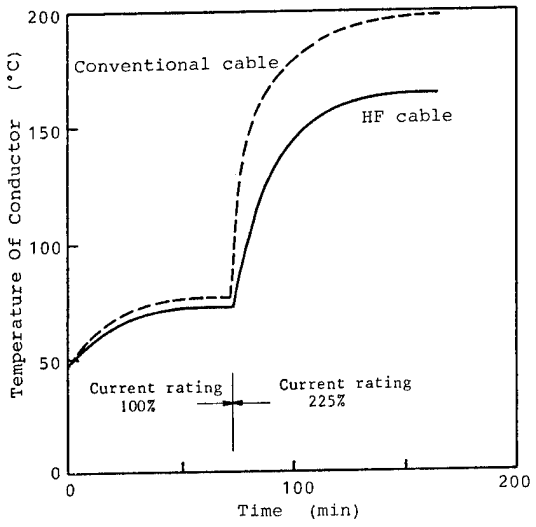



Figure 5 Temperature Rise Curve

## 6-5 Mechanical properties

The conventional cables must endure the rated tension and side wall pressure during installation, while a trailing cable must endure the specified tention,side wall pressure and repeated bending.

The mechanical tests shown in Table 4 were conducted and the test results are **also shown in Table 4.**

It is clear therefore that HF cables have good mechanical properties.

## 6-6 Temperature rise test

The temperature rise test was conducted on HF cables and conventional shipboard cables.The test results are shown in Figure 5 and Table 5.

In case of HF cables, the temperature rise of conductor was lower than conventional shiboard cables.

The thermal resistance was evaluated only 82% of conventional one.

It appears that HF cables have better thermal properties than conventional ones.

Table 5 Temperature rise test (cable:3c×14mm²)

| cable | Current rating | Thermal resistance | Temperature of conductor |
|---|---|---|---|
| HF cable | 100% | °C/W/cm 167.6 | 72°C |
| | 225% | 130.7 | 164°C |
| Conventional cable | 100% | 204.0 | 76°C |
| | 225% | 156.0 | 198°C |

## 7. Proposal of Smoke Density Index (D̄)

From the viewpoint of the safty design of cables, it's very important to estimate the amount of smoke generated from a cable in case of fire.

It is difficult to predict the smoke-generation properties of cables because each material forming part of the cable has different smoke-generation properties.

Up to now, smoke generation of cables have been measured by tests according to the London Transport exective 3m cube smoke emission test, the Steiner tunnel test specified in ASTM E 84 and so on.

Table 4 Mechanical properties

| Item | Method | Power cable | Telecommunication cable | Data transmission cable | Trailing cable |
|---|---|---|---|---|---|
| Side wall pressure test (100Ckg/m) | non-rotating pulley; Pulley diameter :550mm | no damage | no damage | no damage; no change in transmission loss | no damage |
| Compression test (800kg) | 25mm | no damage | no damage | no change in trsnsmission loss | no damage |
| Bending test (100000 cycles) | | — | — | — | no damage |
| Impact test (1 time) | 90° weight R10 | — | — | no damage at 18kgm | no damage at 14kgm |

It is useful to estimate the smoke generation from a cable without any cable test. We propose a value for the Smoke Density Index ($\bar{D}$), which is a measure of smoke generation of cable, using smoke generation data for various materials composing cable.

This value ($\bar{D}$) means the smoke density when the cable with unit length burns in space with unit volume.

Smoke generation data taken in the NBS smoke chamber were used to detarmine the value $\bar{D}$.

$$\bar{D} = \frac{Vn\ Ao}{Vo} \sum Dsi \cdot Ai \quad \text{------- (2)}$$

Vn : volume of NBS smoke chamber
Vo ; volume of sample at NBS test
Ao : cross sectional area of cable
Dsi: specific optical density of material i in NBS smoke chamber
Ai ; cross sectional area ratio of material i in cable

Table 6 Smoke Density Index ($\bar{D}$)

| Cable ($3^C$x5.5$mm^2$) | $\bar{D}$ |
|---|---|
| PVC/PVC*cable | 62.1 |
| XLPE/PVC cable | 55.4 |
| FR-XLPE/FR-PVC cable | 68.5 |
| HF cable | 25.7 |

* Insulation/Sheath

The Smoke Density Indexes ($\bar{D}$) calculated by formula(2) are shown in Table 6. The value D of HF cables are much smaller than conventional shipboard cable. The smoke generation from cables will be calculated by using the following formula;

$$Dcal = \frac{n\ L}{V} \bar{D} \quad \text{-------- (3)}$$

n : number of cables
L : combustion length
V : Volume of combustion room
$\bar{D}$ : smoke density index

In this formula,combustion length L can be predicted by using the concept of the average oxygen index ( $\overline{OI}$ ) of a cable.[1)]

The value Dcal obtained from the formula(3) and the smoke density (D) from the cable test were compared.

The smoke density (D) was taken as the measured value by the formula (1) using the LTE smoke emmision test equipment.

The relation of Dcal and D is shown in Figure 6.

It appears that the calculated value (Dcal) is in good correlation with the value (D) from the results of the cable test.

Thus, the smoke generation from cables under a fire condition will be presumed by the formula (2) and (3).

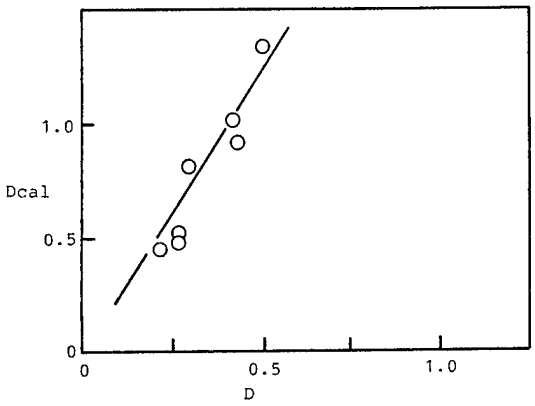



Figure 6 Relation between Dcal and D

## 8. Conclusion

New types of low smoke, halogen free, flame retardant cables have been developed for application to ships. Cable types used for data transmission (optical fiber cable),instrumentation ,control,low voLtage power and trailing cable are now available.

(a) The cables have successfully passed the vertical tray flame test in accordance with IEEE Std.383.
(b) It appears that the cables are low smoke generation and low toxic gas emission through the NBS smoke chamber test,LTE 3m cube smoke emission test and biological test using mice.
(c) Optical fiber cable has passed a fire test of 840 C for 30 minutes without break of the fibers,while the change of transmission loss was practically negligible during the test.
(d) Temperature rise of the cables were as lower than corresponding conventional shipboard cables.

The smoke density index ($\bar{D}$)was proposed to predict the smoke generation from cables.

This value $\bar{D}$ is calculated from the specific optical density Ds of the materials in the NBS smoke chamber.

This value $\bar{D}$ is correlated with the results of the cable test. It may be useful for the cable design that smoke generation from a cable is easily estimated by this concept.

These HF cables with their greater safty, are availa ble to prove the outstanding properties in other application such as power generating stations,plants, subways,tunnels and large buildings.

## 9.Reference

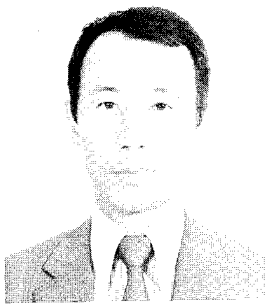
1) T.Yamamoto,et al;"Development of flame resistant cables for instrumentation and communication", Proceedings of the 28th International Wire and Cable Symposium,1979.



Yoshioki Shingo

FUJIKURA LTD.
9-1 Futaba-Cho,
Numazu-City,
Shizuoka,Japan

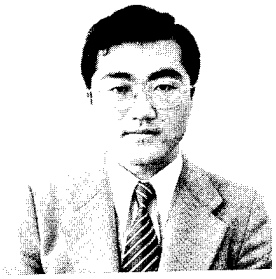
Mr.Shingo received the B.E.degree in electrical engineering from Chiba University in 1965. He joined FUJIKURA LTD. in 1965 and has been engaged in development and manufacturing of insulated wires and cables. He is now a Manager of cable engineering section in production engineering department. He is a member of the Institute of Electrical Engineer of Japan.



Takao Mathuda

FUJIKURA LTD.
9-1 Futaba-Cho,
Numazu-City,
Shizuoka,Japan

Mr.Mathuda received the M.S.degree in chemistry from Kwansei Gakuin University in 1972. He joined FUJIKURA LTD.in 1972 and has been engaged in development and manufacturing of insulated wires and cables.



Motohisa Murayama

FUJIKURA LTD.
1-5-1 Kiba,
Koto-Ku,
Tokyo,Japan

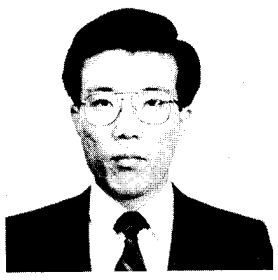
Mr.Murayama finished the course of electrical engineering at Kitatoshima Technical High School in 1967. He joined FUJIKURA LTD.in 1967 and has been engaged in engineering of insulated wires and cables.



Satoru Yoshikawa

FUJIKURA LTD.
1800 Kishioka-Cho,
Suzuka-City,
Mie,Japan

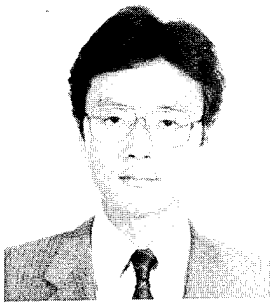
Mr.Yoshikawa received the B.E.degree in electrical engineering from Tohoku University in 1974. He joined FUJIKURA LTD.in 1974 and engaged in development and manufacturing of cables.



Masatake Hasegawa

FUJIKURA LTD.
1-5-1 Kiba,
Koto-Ku,
Tokyo,Japan

Mr.Hasegawa received the B.E.degree in applied chemistry from Osaka University in 1978. He joined FUJIKURA LTD. in 1980 and has been engaged in research and development of plastic and rubber materials.



Akira Yoshino

FUJIKURA LTD.
9-1 Futaba-Cho,
Numazu-City,
Shizuoka,Japan

Mr.Yoshino received the M.E.degree in polymer engineering from Tokyo University of Agriculture and technology in 1979. He joined FUJIKURA LTD.in 1979 and has been engaged in development and manufacturing of insulated wires and cables. He is a member of the Society of Polymer Science,Japan.

# A NEW NON-HALOGENATED FLAME RETARDANT COMPOUND AND ITS JACKETED TELECOMMUNICATION CABLES

K. Nakano T. Ishikawa H. Suzuki M. Sakasai N. Sato

Fujikura Ltd. Sakura-shi, Chiba-ken, 285, Japan

## SUMMARY

A non-halogenated flame retardant compound is generally considered to be a defective material for telecommunication cables, although possessing inherent no toxic residues and low smoke generation. The main reasons are the poor resistance to the low temperature brittleness and mechanical handling under installation.

We have developed a remarkable non-halogenated flame retardant compound and the jacketed telecommunication cables.

The resultant telecommunication cables meet the requirements of the standard IEEE 383 Vertical Tray Flame Test.
From the results of mechanical tests and severe installation tests at from low temperature to high temperature, it has been proved that the telecommunication cables using the new non-halogenated flame retardant compound are very stable to mechanical handling of practical use.

## 1. Introduction

Recently, non-flammable cables have been developed for power plants, factories, and tonnels, etc., in order to prevent the propagation of fire. Particularly so-called non-gas emission performance is strongly required to prevent the creation of large volume of smoke or toxic gases, etc., during fire outbreak. Although halogenides have been mainly used as flame retarder conventionally, these materials should be completely eliminated for the purpose above. However, if inorganic compounds such as hydroxide of metal are used instead of using halogenides, the additive quantity will become larger and a base polymer has to be soft. Consequently, this completed cable used to suffer from the poorer mechanical characteristics and resistivity against damage, etc.. Because of these effects, non-halogenated retarder was not used in large and heavy telecommunication cables.

The authors studied to improve these defects and successfully developed the new compound of higher contents of hydroxide of metal with good physical characteristics including much better resistivity against damage. The compound was applied to telecommunication cables while proving satisfactory performance of practical use.

## 2. Features of new compound

### 2-1. Features

In the conventional methods, using non-halogenated flame retarder, olefinic thermoplastic elastomer was based on and mixed with a large amount of the retarder. Therefore, the foregoing defects were resulted. The authors have revealed that these defects can be effectively improved by adding a polymer which contains -COOH functional group. This would be because hydrogen or ion bonding is created between polymer molecules having -COOH functional group or the polymer and filler agent or via metal ion.

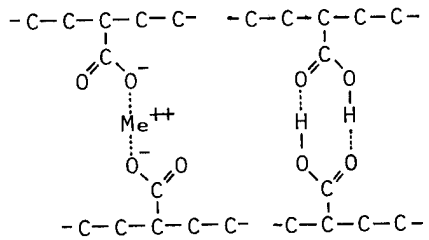



Figure 1 Ion and Hydrogen Bonding

### 2-2. Properties of the new compound

The properties of the new compound are shown in table 1. The compound consists of a base of olefinic thermoplastic elastomer and the additives of non-halogenated flame retarder, stabilizer and polymer with -COOH functional group. The compound shows excellent characteristics also in smoke emission. According to the measurment in the non-flaming method of NBS, Ds is smaller than those of halogenide and neat PE material. Ds (Specific Optical Density) is calculated in the following manner:

$$Ds = 132 \log (100/T)$$

T = % Transmittance

Table 1 Properties of Compound

| Property | Unit | Test Method | Typical Value |
|---|---|---|---|
| Tensile Strength | $Kg/mm^2$ | ASTM D 638 | 1.3 |
| Elongation at Break | % | ASTM D 638 | 500 |
| Melt Index | g/10min | ASTM D 1238 | 0.3 |
| Limited Oxygen Index | - | ASTM D 2862 | 30 |
| Environmental Stress Crack Resistance | $F_0$,hrs | ASTM D 1693 | 1000 |
| Brittleness Temperature | $F_0$, °C | ASTM D746 | -40 |
| Smoke Density | Ds | NBS(NF) | 120 |
| Density | $g/cm^3$ | ASTM D 1505 | 1.4 |
| Volume Resistivity | ohm·cm | ASTM D 257 | $1x10^{16}$ |
| Hardness, Shore D | - | ASTM D 2240 | 50 |

Fig. 2~4 show the long-time reliability against heat, water, and ultra violet. The new compound is not problematic in all of these characteristics at all.

## 2-3. Resistance to damage

The use of a large amount of non-halogenated flame retarder resulted in softer base polymer. Thereby, the mechanical characteristics of completed cables used to become poorer especially in the resistance to damage. Howevr, the new non-halogenated flame retardant compound can successfully eliminate these defects by adding polymer, having -COOH functional group.

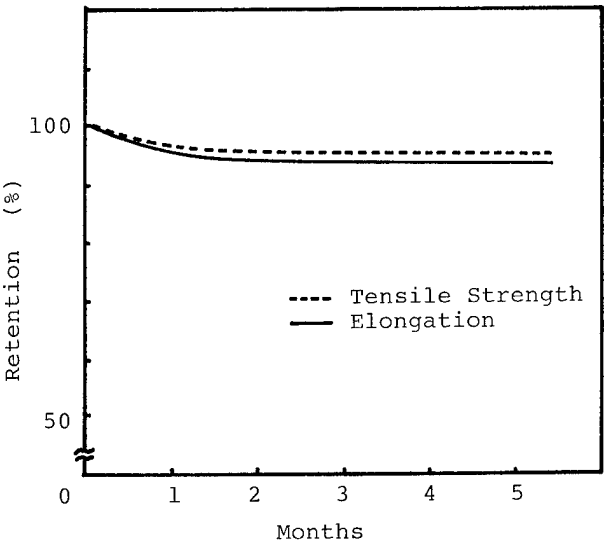



Figure 2 Heat Aging at 100°C

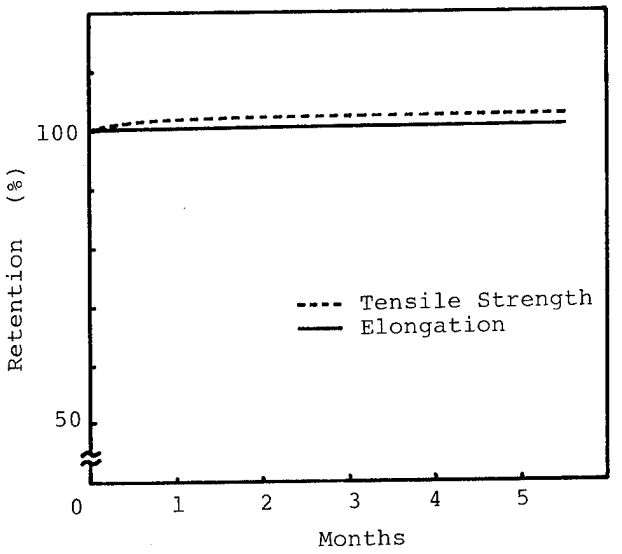



Figure 3 Immersion in Water at 50°C

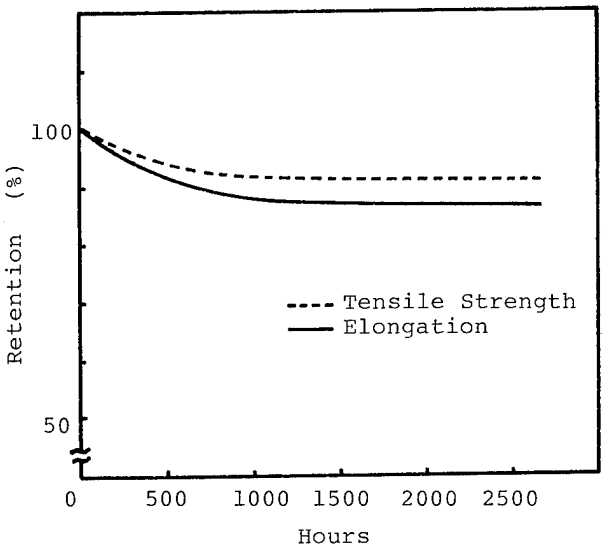



Figure 4 Ultra Violet Resistance

The resistance to damage was assessed by 2 methods (1) edge method and (2) abrasion test. In (1) the edge method, a blade of 90° edge was set up on a sample as shown in Fig. 5, the sample was pulled at a speed 50 mm/min and degree of damage created at that time was visually compared. However, this method has a defect that the degree of damage cannot be evaluated quantitatively. To assist this defect, the abrasion test was performed. This method

is based on MIL-5438 in principle, in which a sand paper is used and the quantity of abrasion is measured.

A sample without -COOH fuctional group is napped at part contacted with the edge in the test (1), showing less resistance to damage. On the other hand, the sample with -COOH functional group is less napped with the edge. This tendency became more obvious as the content of -COOH functional group was increased. In abrasion test(2), samples were compared in the same way. Those without -COOH functional group showed the shorter distance of a sand paper abrasion up to penetrated conduction. With a larger content of -COOH functional group, the distance of sand paper abrasion becomes longer.

We assessed resistance to damage by these methods and selected the compounds.

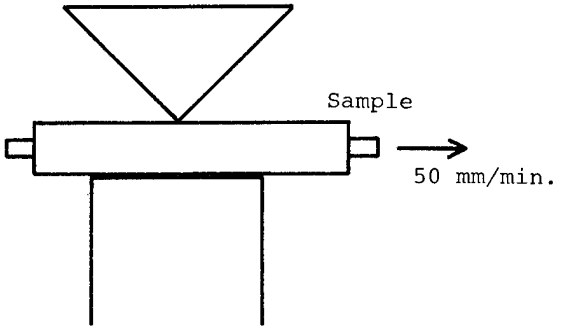



Figure 5 Edge Method

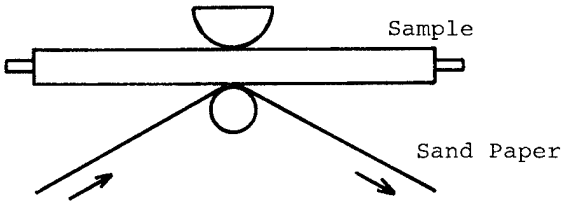



Figure 6 Abration Test

## 3. Characteristics of completed cables

The jacket of test cables is laminated Aluminum non halogenated flame retardant compound previously described, and the insulation is neat PE. The cable diameters range in 3 levels of 20, 50, and 70 mm , while maintaining weights of 750, 4500, and 8500 kg/km respectively.

### 3-1. Pulling test

The pulling test was carried out to simulate the damage occurring when the

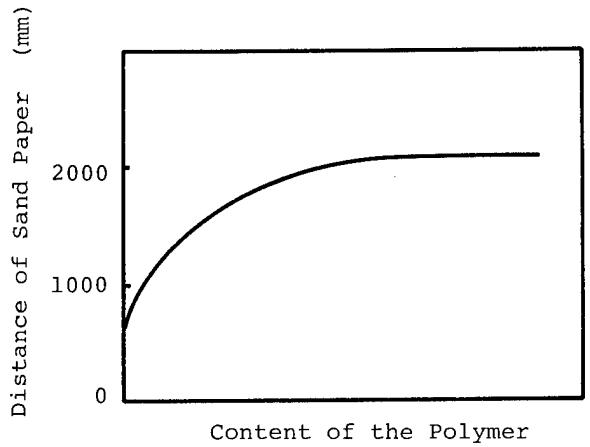



Figure 7 The Effect of the Polymer Having -COOH Functional Group on Abration Test

cable is actually installed. The outer sheath of the cable is abraded with a 90° metal edge so that the test would be more rigorous than the actual installation. The pulling test is detailed in the following:

(1) Test method

A sample is set up as shown in Fig. 8 and the wire is pulled at a certain tension to abrade the sample onto a fixed pulley. The metal edge is attached to part of a fixed pulley, where the sample is in contact with. The sample is abraded by this edge, and the degree of damage on the surface of the cable is visually observed. The sample is maintained longer than 10 hours in a constant temperature chamber (-30°C and 40°C) before the test. After taken out from the constant temperature chamber, the sample is set up as shown in the figure and is immediately tested.

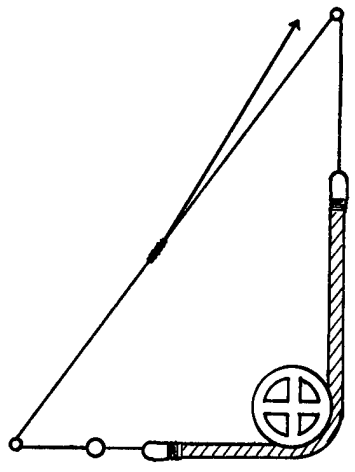


Figure 8 Pulling Test

(2) Result

Like the result in the section of resistance to damage, the sample without -COOH functional group is easily napped at the sheath. The tendency becomes more obvious at higher temperature. In the test at 40°C, the napping was so serious that the sheath was often penetrated. Samples with -COOH functional group show similar trends in temperature changes but their napping conditions were much better, in which the sheath surfaces were slightly damaged.



Photo. 1 The Surface of the Sample Without -COOH Functional Group

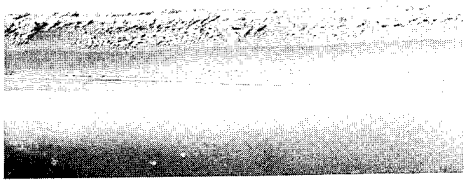


Photo. 2 The Surface of the Sample With -COOH Functional Group

## 3-2. Flaming test

(1) Test method

The non-flammability of completed cable was tested by the standard IEEE 383.

(2) Result

Halogenated non-flammable compound was also tested to compare with our new non-halogenated compound.

Although a sample using the halogenated compound could pass the VTFT, smoke was emitted such that the sample could not be seen during the test as shown in Photo. 3. On the other hand, the sample using the non-halogenated compound did not emit much smoke so that the sample could be clearly seen up to the end of the test, while complying with the VTFT as shown in Photo. 4. In the VTFT, a sample is more easily burned when the sample diameter is smaller. However, our new compound can satisfy the specification even with a small diameter (20mm). However, the non-flammability of completed cable is largely influenced by, not only the material of sheath, but binder, filler, and sheath thickness, etc., so that these factors should be thoroughly considered during the cable design.

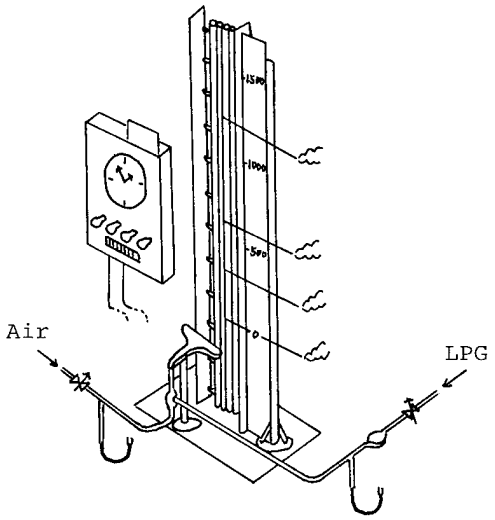



Figure 9 Arrengement of Vertical Tray Flame Test

## 3-3. Duct installation test

Telecommunication cable is installed by pulling in the cable from a manhole and passing in a duct. At that time, the cable comes in contact with a duct wall, and pulley, etc., while abrating the outer sheath of the cable. Assume this condition test was performed.

(1) Installation test

The cable was installed with the route in Fig. 10. The diameter of the

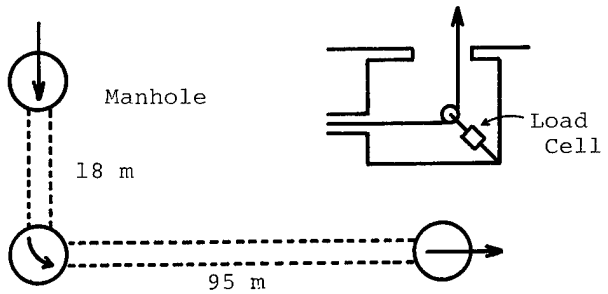



Figure 10 Route of Duct

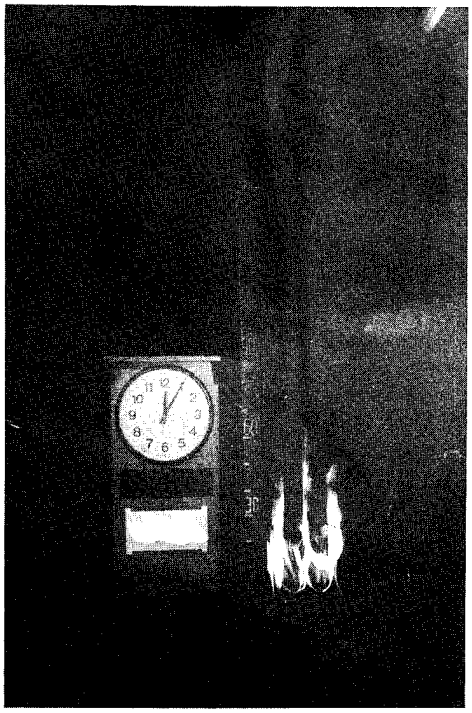


Photo. 3 The Sample Using the Halogenated Compound

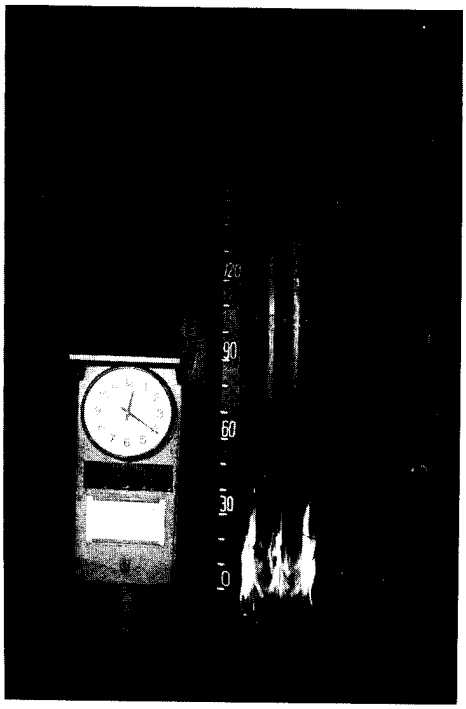


Photo. 4 The Sample Using the Non-Halogenated Compound

cable and duct are 70 and 75 mm respectively and the cable length is about 150m. The cable is filled with the air at 2 kg/cm pressure. The electrical characteristics of the cable were measured before and after the installation. The cable tension was also measured.

(2) Result

The maximum tension during the installatiton was 800kg, and there were no problems when the cables were installed. There was not too much damage on the surface of the cable jacket, and also the electrical characteristics and gas pressure were not influenced.

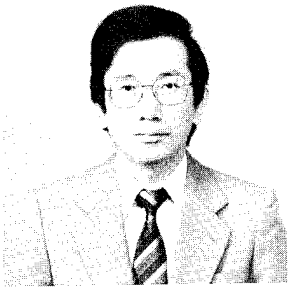
These tests proved that our new non-halogenated flame retardant compound can be used for the practical applications.

## 4. Conclusions

Our new compound contains a large amount of hydoroxide of metal as flame retardant agent. Nevertheless, their physical characteristics are not much deteriorated while maintaining good resistance to damage by means of adding polymer with -COOH functional group. In addition, smoke emission is very low with maintaining non-flammability conforming to the VTFT of the standard IEEE 383.

## 5. Acknowledgements

Many members in Fujikura Ltd. have made important contributions to our study. The autuors wish to acknowledge them and especially express deep appreciations for much advise of Mr. Y. Sekiguchi and Dr. K. Inada.



Kousaku Nakano

Senior Engineer

Telecommunication Cable Reserch & Development Department. Fujikura Ltd.
1440, Mutsuzaki, Sakura-shi, Chiba-ken, 285, Japan

Mr. Nakano received the M. S. degree in polymer chemistry from Gunma University in 1975 and joined Fujikura Ltd.. He has been engaged in research and development of plastic materials and manufacturing method for electric and telecommunication cables. Mr. Nakano is a member of The Chemical Society of Japan.



Toraichi Ishikawa

Engineer

The Materials Department Research & Development Center. Fujikura Ltd.
1-5-1, Kiba, Koto-ku, Tokyo, 135, Japan

Mr. Ishikawa graduated from Tokyo University of Agriculture and Technology in Department of textile and polymer science in 1984. Then he joined Fujikura Ltd. and has been engaged in research and development of non-halogenated flame retardant telecommunication cables and its accessory. Mr. Ishikawa is now a member of The Chemical Society of Japan.

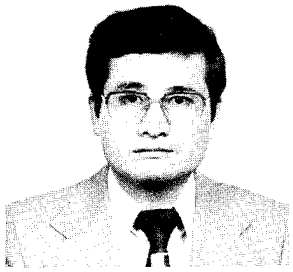


Hideo Suzuki

Assistant Chief

Telecommunication Cable Reserch & Development Department. Fujikura Ltd.
1440, Mutsuzaki, Sakura-shi, Chiba-ken, 285, Japan

Mr. Suzuki received the B. E. degree in polymer chemistry from Gunma University in 1971 and joined Fujikura Ltd.. He is responsible for the development of plastic materials and polymer processings. He is a member of The Society of Polymer Science, Japan.

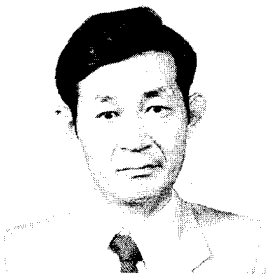


Michio Sakasai

Assistant Cheif

Telecommunication Cable Manufacturing Engineering Section. Sakura Plant. Fujikura Ltd.
1440, Mutsuzaki, Sakura-shi, Chiba-ken, 285, Japan

Mr. Sakasai received the B. E. degree in metallurgical engineering from Ibaraki University in 1972 and has been engaged in manufacturing engineering section of telecommunication cables. He is a member of The Institute of Electronics and Communication Engineers in Japan.



Nobuyasu Sato

Chief

Telecommunication Cable Research & Development Department. Fujikura Ltd.
1440, Mutsuzaki, Sakura-shi, Chiba-ken, 285, Japan

Mr. Sato received the B. E. degree in Telecommunication Engineering from Tohoku University in 1966 and has been engaged in development of telecommunication cables. He is a member of The Institute of Electronics and Communication Engineers of Japan.

# FIRE-RESISTANT CHARACTERISTICS OF AERIAL OPTICAL CABLES

TAKASHI KONNO*, SHYOICHI HASEGAWA*, KIYOHIRA SUGAWARA*, YUSUKE TABATA*
KOJI NIIKURA**, HIROAKI HORIMA**, YUICHI YAMADA*** AND AKIRA KUROSAWA***

* TOHOKU ELECTRIC POWER CO., INC. 3-7-1, ICHIBAN-CHO, SENDAI 980, JAPAN
** SUMITOMO ELECTRIC INDUSTRIES, LTD. 1, TAYA, TOTSUKA-KU, YOKOHAMA 244, JAPAN
*** KITANIHON ELECTRIC WIRE CO., LTD. 1-2-1, KORIYAMA, SENDAI 982, JAPAN

## Abstract

In evaluating the total reliability of the optical communications system using aerial optical cables, the possibilities of fire accidents have also to be taken into consideration.
For this purpose, we studied the past cases of the fire accidents in actual optical cables, focusing our interest on the changes in the transmission characteristics of optical cables and copper telecommunication cables. Then, for better understanding the phenomena, various experiments were carried out.
As a result, it has been found that the transmission characteristics of optical cables in case of fire tends to be quite stable, compared to copper telecommunication cables.

## 1. Introduction

Tohoku Electric Power Co., Inc. is introducing optical cable as communication line in the electric power utilities positively since 1980. As of 1985, the total length of optical cable has become about 750 km.

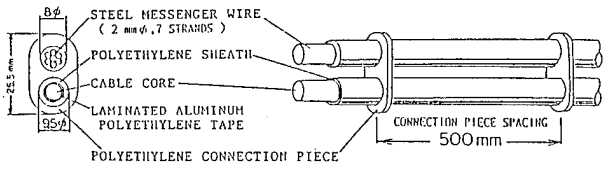
Almost all of these optical cables are installed along power distribution lines. Since many of them are installed at locations near private houses, there is the need to consider the fire accident of optical cable in order to evaluate the reliability of optical communication system.

We have experienced 3 cases of fire from neighboring private houses so far spreading the flames to optical cables jointly installed along power distribution lines. The result of analysis of these 3 cases of fire inflicted on optical cables and the result of experimental study conducted to grasp the phenomenon at the time of sustaining fire are explained hereinafter.

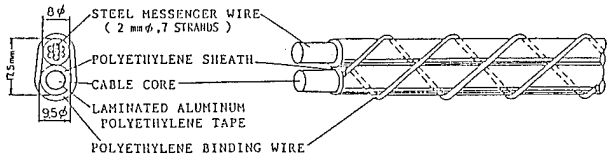
## 2. Examples of fire damage on optical cables

### 2.1 Summary of fire damage on optical cable

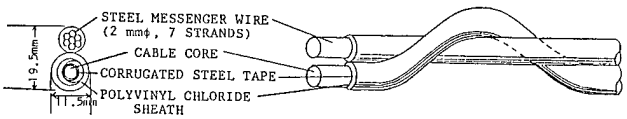
Fire damages on optical cables that we have experienced are all due to the spread of flame from the fire of houses neighboring the optical cables. The configurations of optical cables that sustained fire damage are of 3 kinds shown in Fig. 1. All of these cables are of the self-supporting type construction. The 2 cases amoungst the 3 cases of examples of fire damages were for those that optical cables and copper communication cable shown in Fig. 2 were jointly installed on the same power distribution line and both of these cables sustained fire damage.




(a) Pre-hanger type




(b) Lashing type




(c) Stranded type

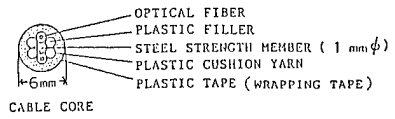



Fig. 1 Structure of optical cable for aerial use

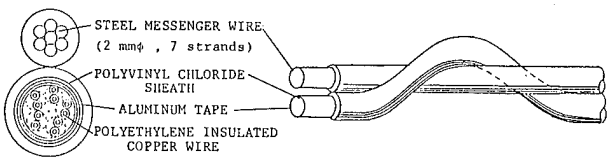



Fig. 2 Structure of copper communication cable 0.9 mm 10 pairs CPEV-SSS
(Polyethylene insulated polyvinyl chloride sheathed self-supporting cable)

The summary of fire damage sustained by these cables is shown in Table 1. Also Photo 1 shows an example of situation of fire damage.

All optical cables that sustained fire damage had outer PE (polyethylene) sheath melted.
In the pre-hanger type and lashing type optical cables that use PE sheath, although the PE was melted and dropped, aluminium tape as well as steel messenger wire were scarcely exposed with the PE retaining the original shape approximately.

Also in the stranded type optical cable with corrugated steel armour, the outer sheath of PVC ( polyvinyl chloride) was dropped and hung down and both corrugated steel tape and steel messenger wire exposed considerable.

On the other hand, in the copper communication cable that sustained fire damage likewise, PVC sheath was melted and aluminium tape was exposed indicating the same situation for both 2 cases. Also the PE insulation was melted and copper wires indicated the condition of being short-circuited.

Table 1 Summary of fire damage sustained by cables

| Fire Example | A | | B | | C |
|---|---|---|---|---|---|
| Date of fire occurrence | Aug. 2, 1983, AM 11:05 | | Nov. 14, 1983, AM 9:43 | | March 24, 1984, PM 11:35 |
| Continuing time of fire | 3 hours 10 minutes | | 35 minutes | | 31 minutes |
| Weather, wind velocity etc. | fine, 26°C, wind of 4 m/s | | fine, 9°C, wind of 5 m/s | | fine, 12°C, breeze |
| Scale of fire | One story factory of steel beam, steel sheet siding 264 $m^2$ completely burnt, plastic products 30t and plastic raw material 80t were completely burnt. | | Wood structure, mortar siding 2 story house 176 $m^2$ completely burnt. | | Wood structure one story, wood structure working house 182 $m^2$ and warehouse 49 $m^2$ completely burnt. Wood structure 2 story mortar siding 121 $m^2$ completely burnt. Wood structure one story warehouse 275 $m^2$ completely burnt. |
| Kind of cable that sustained fire damage (configuration) | Optical cable (pre-hanger type) refer to Fig.1 (a) | Copper communication cable refer to Fig.2 | Optical cable (lashing type) refer to Fig.1 | Copper communication cable refer to Fig.2 | Optical cable (stranded type) refer to Fig.1 (c) |
| Cable height above ground | 8 m | 6.7 m | 7 m | 7 m | 8 m |
| Horizontal distance from the house that had the outbreak of fire | 1 m | 1 m | 5 m | 4 m | 1 m |
| Length of fire damage sustained | 100 m | 100 m | 16 m | 16 m | 8 m |
| Situation of fire damage of cable sustained | PE sheath did not have gloss indicating rather soot condition. PE connection piece was melted. At the middle part of damage sustained, the entire PE connection piece covering 30 m was melted and the main cable was separated from the messenger wire. At the part where the PE connection piece melted, aluminium tape was exposed. | PVC sheath was melted and aluminium tape was exposed covering 50 m. PE insulation inside aluminium tape was melted and copper wires were short-circuited. | Although PE sheath was melted, the original shape was maintained. No break of binding wire. No exposure of aluminium tape and steel messenger wire. | PVC sheath was melted and aluminium tape was exposed. PE insulation inside aluminium tape was melted and copper wires were short-circuited | PVC sheath was melted. Corrugated steel tape and steel messenger wire were exposed. |



Photo 1 Example of fire situation

## 2.2 Situation of communication during fire

The change of transmission characteristics of communication cable that sustained fire damage is shown in Table 2. At the time of encountering 3 cases of fire accident, optical cable maintained the stable transmission characteristics posing no problem to communication. Although increase of optical transmission loss presumed to stem from heating was produced in the fire example C, a small valve was available that had no impact on the transmission performance.

On the other hand, in the copper communication cable that sustained fire damage, communication was stopped completely in 20 plus a few minutes after the occurrence of fire because of the short-circuit of copper wires for both 2 cases.

In the fire example A, the continuous measurement of the change of transmission quality before and after the fire damage sustained was made possible for both optical cable and copper communication cable. As shown in Fig. 3, the deterioration of error rate was quite unable to be observed in the optical cable.

Table 2 The change of transmission characteristics of the cables that sustained fire damage.

| Fire example | Kind of cable (configuration) | Change of transmission characteristics |
|---|---|---|
| A | Optical cable (pre-hanger type) | No change for both optical loss and transmission quality. |
| | Copper communication cable | Because of the short-circuit of copper wires, circuit was disconnected in 23 minutes after occurrence of fire. |
| B | Optical cable (lashing type) | No change for both optical loss and transmission quality. |
| | Copper communication cable | Because of the short-circuit of copper wires, circuit was disconnected in 21 minutes after occurrence of fire. |
| C | Optical cable (stranded type) | Optical loss increased by 0.5 dB. No change of transmission quality. |

However, the copper communication cable indicated the rapid deterioration of transmission performance immediately after the occurrence of fire and the condition of circuit disconnection continued until the completion of restoration work of copper communication cable that sustained fire damage.

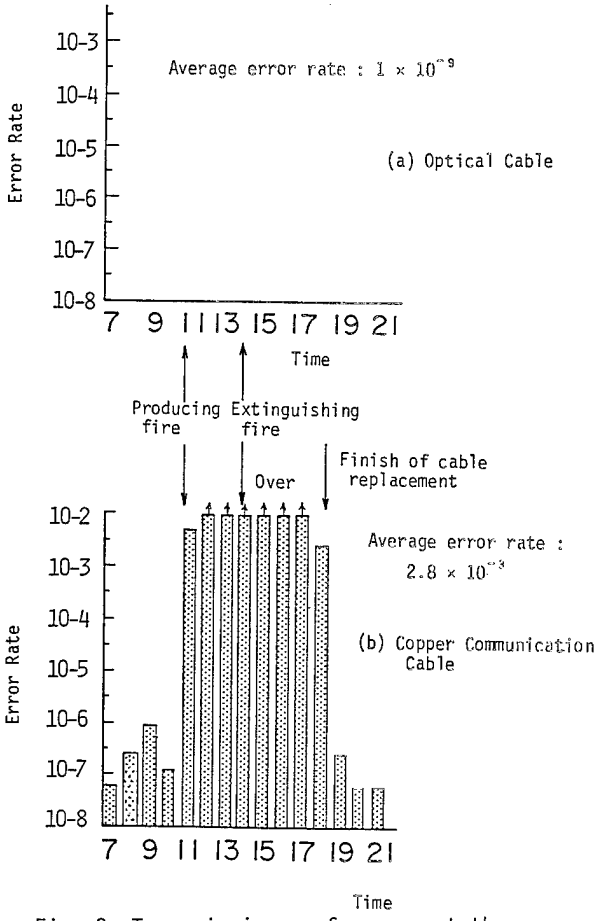



Fig. 3 Transmission performance at the time of sustaining fire

## 2.3 Restoration of cables that sustained fire damage

The situation of restoration work of cables that sustained fire damage is shown in Table 3.

In the case of optical cable, since there was no deterioration of transmission characteristic for all 3 cases being possible to serve the purpose of communication continually even after the fire damage, there was no need of urgency in conducting the cable restretch for restoration.

On the other hand, since the copper communication cable that sustained fire damage encountered the short-circuit of its copper wires hence resulting in communication interruption, urgency was required to cope with restoration. Awaiting the extinguishment of fire therefore, the restretch operation for restoration was undertaken and the communication after restoration was commenced within that day.

Table 3 Situation of operation for restoration

| Fire example | A | | B | | C |
|---|---|---|---|---|---|
| Kind of cable (configuration) | Optical cable | Copper communication cable | Optical cable | Copper communication cable | Optical cable |
| Situation of restoration | After 2 days from the day of fire, restretch of the part that sustained fire. | Restretch and restoration the same day. (4.5 hours after fire extinguishment) | After 31 days from the day of fire, restretch of the part that sustained fire. | Restretch and restoration the same day 5 hours after fire extinguishment. | After 31 days from the day of fire, restretch of the part that sustained fire. |
| Restretching length of cable | 130 m | 130 m | 100 m | 70 m | 250 m |
| Time of communication stoppage by fire | None | 7 hours 30 minutes | None | 5 hours 30 minutes | None |

## 3. Experimental investigation

To grasp the phenomenon at the time of fire damage sustained by optical cable and to investigate the impact of heating on optical cable, burning test was conducted simulating the condition of the line installed on-site.

### 3.1 Burning test

First, we conducted the heating of optical cable based on the fire-temperature curve of Fig. 5 by the test method shown in Fig. 4 and observed the condition of impairment by burning at that time and the change of optical loss was observed.

The condition of impairment by burning for each heating hour elapsed is shown in Table 4. When comparing the condition of impairment by burning of cable sheath, the surface temperature of optical cable at the actual time of fire damage sustained can be presumed as below 350°C.

Also when the cable surface is heated to about 200 °C in the experiment, it was observed that PP ( Polypropylene) buffer material of core interior started to contract by heating, on the contrary, the impact of heating on the core interior was not recognized in an example of accident from fire sustained. In this case, at the condition optical cable is installed along power distribution line, it can be conceived that since the diffusion of heat applied on the optical cable spacewise was large, compared to the experiment room set up, there was the difference due to the restriction of heat conduction to the core interior.

The situation of transmission loss variation against heating is likewise shown in Table 4. It was confirmed experimentally for optical cable that transmission loss almost did not change and stable transmission characteristic was maintained against heating up to 420°C.

### 3.2 Temperature distribution in the longitudinal direction of cable

In order to obtain the use criteria of the optical cable that sustained fire, we studied the longitudinal cable core situation.

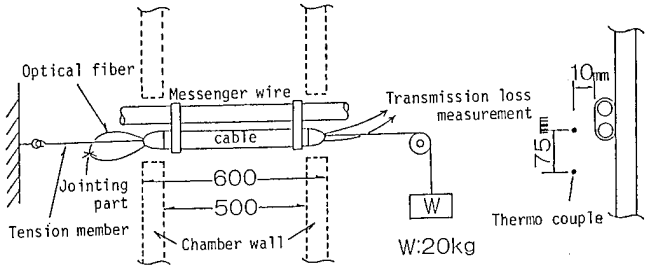



Fig. 4 Method of heating test
(The construction of heating furnace is in compliance with Japanese industrial standard JIS A 1305)

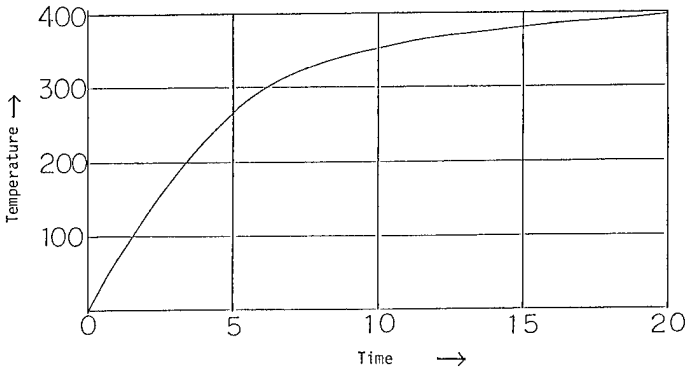



Fig. 5 1/2 fire-temperature curve
(Temperature curve complying to Japanese industrial standard JIS A 1304)

Table 4 Situation of impairment by burning of cable and variation of optical loss in the burning test

| Kind of cable (configuration) | | Transition of the degree of burning impairment of cable | | | Variation of optical loss |
|---|---|---|---|---|---|
| | | 270°C (5 minutes) → | 353°C (10 minutes) → | 380°C (15 minutes) | |
| Optical cable | Pre-hanger type | Cable surface indicates gloss.<br>PE connection piece starts to melt. | PE sheath is carbonized.<br>PE connection piece melts and cable separates from messenger wire. | PE sheath is ignited at 370°C (13 minutes).<br>Aluminium tape is exposed. | Against heating up to 420°C, there is no break of fiber.<br>After a few minutes from the time of starting heating, there is the case that transmission loss increases temporarily. (Max. 1.5 dB)<br>Residual optical loss after test is 0-0.5 dB. |
| | Lashing type | Cable surface indicates gloss.<br>Jacket of binding wire starts to melt. | PE sheath is carbonized. | PE sheath is carbonized.<br>Lashing condition can not be discriminated. | |
| | Stranded type | PVC sheath is melted and starts to hang down. | PVC sheath is carbonized.<br>Corrugated steel tape is exposed at some locations. | PVC sheath is carbonized.<br>Corrugated steel tape is exposed. | |
| Copper communication cable | | PVC sheath is melted and starts to hang down. | PVC sheath is cabonized. | PVC sheath is carbonized.<br>Aluminium tape is exposed. | Copper wires are short-circuited at 340-365°C. |

As shown in Fig. 6, by applying heat of 180-240°C to optical fiber cable using ribbon gas burner, temperature rise of respective points in the core was observed. Test result is shown in Table 5.

Despite being in the core of optical cable heated, at the location parted over 50 cm from the heat source, it was clarified that its temperature was close to room temperature. Hence, in the case optical fiber is heated, it can be presumed that the range of effect due to heat is sufficient by considering about several meters ahead from the position where the heated trace remains by seeing the cable sheath surface.

### 3.3 Physical characteristic after burning

Furthermore, a variety of mechanical tests were conducted against the speciments heated to 350°C in compliance with the fire - temperature curve of Fig. 5. And while focussing attention to the variation of transmission loss, comparison with the optical cable not heated was conducted. Test result is shown in Table 6.

From Table 6, although the optical cable heated had the physical characteristics dropped a little for sure compared to the one before heating, in the normal installed condition, its extent of characteristic deterioration is considered acceptable to fall in the range posing no rpblem for transmission. Therefore, it was judged that the remedial measures to conduct the restretch and restoration of optical cable that sustained thermal impairment, in general did not necessitate the urgency.

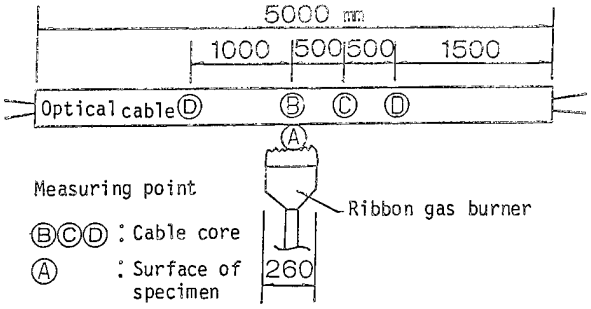
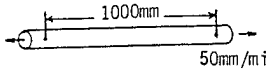
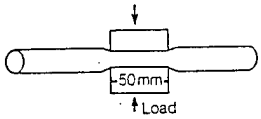
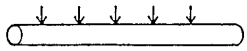
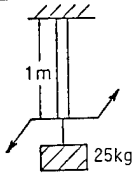
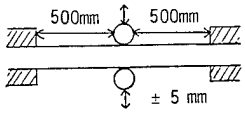



Fig. 6 Measurement of temperature distribution

Table 5 Condition of burning impairment of cable

| Cable type | Lapse of time | A | B | C | D |
|---|---|---|---|---|---|
| pre-hanger type | 0 min. | 20°C | 20°C | 20°C | 20°C |
| | 5 | 180-240 | 170-200 | 27 | 20 |
| | 30 | 180-240 | 170-200 | 27 | 20 |
| Corrugation | 0 min. | 20°C | 20°C | 20°C | 20°C |
| | 5 | 180-240 | 160-200 | 27 | 20 |
| | 30 | 180-240 | 160-200 | 27 | 20 |

Table 6 Result of mechanical test

| No. | Test item | Test condition | Test result |
|---|---|---|---|
| 1 | Tension |  <br>(1) Distance between standard points: 1,000 mm<br>(2) Pulling speed: 50 mm/min.<br>(3) No. of samples: 3 | After heating, break load dropped somewhat.<br>(30~40% lower than the break load before heating) |
| 2 | Bending |  <br>(1) Mandrel diameter: 200 mmϕ<br>(2) No. of times of bending: 20 times of reciprocating bending<br>(3) No. of samples: respectively 2 | When bending 180° after heating a large increase of transmission loss was produced and transmission loss remained despite restoring to straight line. |
| 3 | Compression |  <br>(1) Flat plate compressed: 50 mm × 50 mm<br>(2) Compressive load: Max. 100 kg<br>(3) No. of samples: 3 | No difference before and after the heating. |
| 4 | Impact |  <br>(1) Impact load: 3 kg<br>(2) Height (drop): 0.3 m<br>(3) Impact body: metal body of 25 mmϕ<br>(4) Location of drop: 5 different locations<br>(5) No. of samples: 3 | No difference before and after the heating. |
| 5 | Torsion |  <br>(1) Sample length: 1 m<br>(2) Load: 25 kg<br>(3) Torsion angle: 360°/m<br>(4) No. of samples: 2 | Variation of transmission loss increases max. 0.6 dB after heating. |
| 6 | Vibration |  <br>(1) Amplitude: ± 5 mm<br>(2) No. of vibration: 10 Hz<br>(3) No. of times of vibration: $10^6$ times<br>(4) No. of samples: 3 | No difference before and after the heating. |

## 4. Conclusion

As the result of conducting the accident analysis of 3 cases of fire of optical cables experiment thereafter, the fire-resistant characteristics of aerial optical cables was possible to be clarified as described below.

(1) The heating temperature to the aerial optical cables due to the burning spreaded from the fire of houses nearby can be presumed to be below 350°C in general.

(2) Aerial optical cables are possible to maintain the extremely stable transmission characteristics compared to those of copper communication cables.

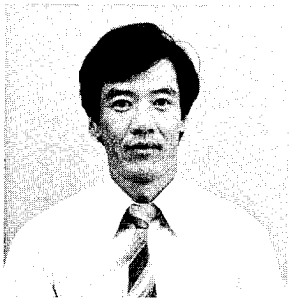
(3) The change of physical characteristics of aerial optical cables by heating is of the extent posing no trouble for transmission. Therefore, the remedial measures of restretch and restoration of optical cables that sustained fire damage do not necessitate the urgency, compared to those of copper communication cable.

From the above the self-supporting type optical cables that we are using at present possess fire-resistant property in spite of non-fire-resistive structure beyond our expectations. And it is presumed that there are many cases where the aerial cables can withstand the use at times of fire accident.



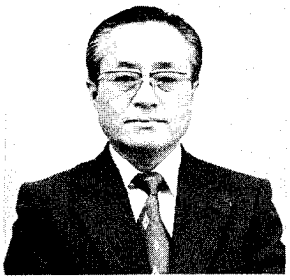
Takashi Konno
Tohoku Electric
Power Co., Inc.
7-1, 3-chome,
Ichibancho,
Sendai, Japan

Takashi Konno was born in 1956 and received the B.A. degree from Tohoku University in 1979. He then joined Tohoku Electric Power Co., Inc., and has been engaged in the section of communication and electronics engineering.
He is now an engineer of the Communication and Electronics Engineering Section of Tohoku Electric Power Co., Inc.



Syoichi Hasegawa
Tohoku Electric
Power Co., Inc.
7-1, 3-chome,
Ichibancho,
Sendai, Japan

Syoichi Hasegawa was born in 1947 and graduated from Taira Technical School in 1966. He then jointed Tohoku Electric Power Co., Inc. and has been engaged in the section of communication and electronics engineering. He is now an engineer of the communication and Electronics Engineering Section of Tohoku Electric Power Co., Inc.



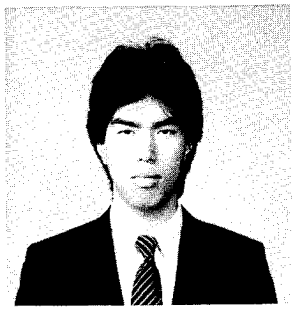
Kiyohira Sugawara
Tohoku Electric
Power Co., Inc.
7-1, 3-chome,
Ichibancho,
Sendai, Japan

Kiyohira Sugawara was born in 1937 and graduated from Miyagi Technical School in 1957. He then joined Tohoku Electric Power Co., Inc., and has been engaged in the section of distribution engineering. He is now a senior staff member of the Communication and Electronics Engineering Section of Tohoku Electric Power Co., Inc.



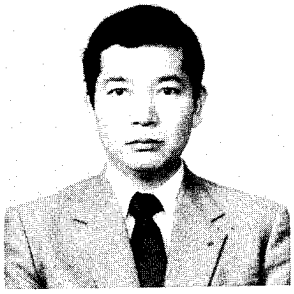
Yusuke Tabata
Tohoku Electric
Power Co., Inc.
7-1, 3-chome,
Ichibancho,
Sendai, Japan

Yusuke Tabata was born in 1934 and received the B.A. degree form Akita University in 1957. He then joined Tohoku Electric Power Co., Inc., and has been engaged in the section of communication and electronics engineering. He is now a Manager of the Communication and Electronics Engineer and a member of the Institute of Electrical Engineers of Japan.



Koji Niikura
Sumitomo Electric
Industries, Ltd.
1, Taya-cho,
Totsuka-ku, Yokohama
Japan

Koji Niikura was born in 1961 and received the B.S. degree for engineering from Waseda University in 1984. He jointed Sumitomo Electric Industries, Ltd. in 1984, and has been engaged in development and design of optical fiber cables. He is a member of Fiber Optics Division in Sumitomo Electric Industries Ltd.



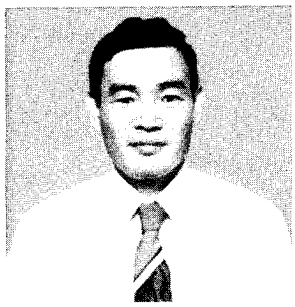
Hiroaki Horima
Sumitomo Electric
Industries, Ltd.
1, Taya-cho,
Totsuka-ku, Yokohama
Japan

Hiroaki Horima was born in 1947. He received the M.S. degree for engineering from Osaka University in 1972. He joined Sumitomo Electric Industries Ltd. and worked on the development of CATV coaxial cables, multi-pair PEF-insulated junction cables and low loss unbalanced type cables.
Thereafter he concentrated on the development of optical fiber cables. He is a section manager of Fiber Optics Division in Sumitomo Electric Industries Ltd. He is a member of the Institute of Electronics and Communication Engineers of Japan.



Yuichi Yamada
Kitanihon Electric
Wire Co., Ltd.
1-2-1, Koriyama
Sendai 982
Japan

Yuichi Yamada was born in 1952.
He joined Kitanihon Electric Wire Co., Ltd. and has been engaged in design and development of communication cables, power cables and accessories for these cables. He is a member of the Institute of Electronics and Communication Engineers of Japan.



Akira Kurosawa
Kitanihon Electric
Wire Co., Ltd.
1-2-1, Koriyama
Sendai 982
Japan

Akira Kurosawa was born in 1947.
He received the B.E. degree from Tohoku University in 1970. He joined Kitanihon Electric Wire Co., Ltd. and has been engaged in design and development of communication cables. He is a member of the Institute of Electronics and Communication Engineers of Japan.

# THE OVERALL SAFETY OF WIRE AND CABLE MATERIALS IV: A TEST REGIMEN FOR MEASURING CABLE FIRE AND HAZARD

Frederic B. Clarke and Irwin A. Benjamin

Benjamin/Clarke Associates, Inc.
Kensington, Maryland

Summary

A test regimen is presented which addresses the ease of ignition and mass loss rate of cables exposed to a fire in a compartment. This test regimen was implemented for five cable samples and the results are reported. A formalism for ranking cable fire performance is suggested, and its significance discussed.

## Introduction

The past decade has seen a new perspective established in how fire hazard is conceptualized and measured. Historically, one or two fire tests were used to determine whether or not a material was acceptable in given use, but have provided the means whereby a material's expected full-scale fire performance can be envisioned, accounted for mathematically, and the outcome of its involvement in a real fire estimated. It is natural that this technology be extended to wire and cable flammability. Where it had been customary to characterize cable flammability by a simple flame test. This is no longer adequate. Not only are there other aspects of fire hazard than flammability, but in fact modern insulation materials often do not ignite readily from small ignition sources. A simple pass-fail flammability test is useful in distinguishing those materials at the lower end of the flammability scale: they separate those that spread flame readily from those that do not. However, they provide little information beyond that fact.

In the first paper of this series, we pointed out that there were observable differences among materials which pass the same flammability test (IEEE 383), and that this difference could be expected to have consequences when cables were exposed to actual fires (1). In subsequent papers, we and other workers have identified additional measurement techniques, including rate of heat release calorimetry, which would be helpful in elucidating this overall fire performance (2). As important as these measurement techniques are, they provide by themselves no information on what one would expect the actual fire conditions to be which a cable encounters in actual use. For this information, one must depend on full-scale fire tests or, alternatively, one must compute expected fire conditions from the foreseeable conditions of an actual fire using mathematical modeling techniques (4). From these two considerations arises the conceptual framework of an overall fire safety test regimen, based on expected full-scale exposure conditions, which can be used as a practical means of evaluating cable fire safety. The first such approach, to our knowledge, was developed by a series of fire experts at a conference sponsored by Benjamin/Clarke Associates, at the University of Maryland, in 1984 (4).

This paper provides the first experimental data on the overall test regimen proposed by the Maryland Roundtable. It will demonstrate that the performance characteristics of wire and cable can be differentiated by existing test methods, and that this method is both feasible and rational as a routine fire hazard evaluation tool.

## Rationale of the Test Regimen

### A. Background

The current interest in cable fire

performance, especially in the mass transit industry and in defense applications, prompted Benjamin/Clarke Associates, Inc., to invite 17 experts in fire safety to a 1 1/2 day roundtable held at the University of Maryland. The focus of the roundtable was to suggest how the fire hazard of cable should be assessed, not to review or critique any proposed specifications. The emphasis was on "why" a given fire property should be measured in a specification and what it meant, and far less on "how" the measurement should be made, i.e., what test method should be used.

B. Summary of Roundtable Recommendations

The roundtable had three objectives:

1. To identify the most important components of fire hazard;

2. To suggest how these elements can best be combined and used in performance specifications for current purchasing; and

3. to suggest the nature and type of development applicable to more advanced material specifications for the future.

The panel identified a number of aspects of cable fire hazard which should be addressed. They are:

1. Ignitability

2. Flame spread along cable

3. Contribution to total fire load

4. Contribution to fire buildup

5. Smoke* as a vision-obscuring agent

6. Smoke* as an incapacitating or lethal agent

7. Smoke* as a corrosive agent to equipment

In some cases, test methods exist for evaluating these properties directly. In the others, data from several different tests most be combined to yield an estimate of how cable will perform.

An abbreviated summary schematic of the resulting fire safety evaluations scheme is presented in Figure 1.**

The logic of the scheme is, first to avoid use of cables which are easily ignited, or decomposed by a small ignition source (i.e., in the absence of another major fire source.) Once this is accomplished a cable's contribution to hazard is governed by the degree to which it contributes to the smoke and heat buildup of a fire in which it is one participant. While it is impossible to foresee all possible fire scenarios, reasonable assumptions can be made regarding the need for human tenability in the environment, escape time, corrosion protection and the like. The needed level of protection can thus be identified and criteria set for fire and smoke development; and these parameters can in turn be related to small-scale test performance.

The principal features of the roundtable's recommended approach which distinguish it from traditional specifications are: 1) criteria for performance are related to the fire scenarios; and 2) several tests have no pass or fail level associated directly with them -- instead the data they provide are ingredients of more physically realistic hazard parameters, and it is these which are controlled.

C. Test Regimen

1. Ignitability: It is important to avoid fires caused by cable ignitions and exacerbated by rapid spread along cables, and so an ignitability test is needed. The panel preferred the Factory Mutual Flammability Apparatus or Cone Calorimeter for this purpose because they provides results in the form of the thermal energy needed for ignition. This in turn is relatable to the intensity of exposure fire needed for ignitions. For example, a minimum ignition flux ($q_c''$) of 1.5-2.0 $W/cm^2$ would keep the cable from igniting below approximately 400°C.

At present, ignition and flame spread along cables are both dealt with by IEEE-383. As an interm ignitability measure, this may be acceptable; since it seems to fail cables which ignite below about 1.5 $W/cm^2$

* Smoke herein means all the products of combustion: both gaseous and particulate.

** Copies of the full report are available from: Benjamin/Clarke Associates, Inc., 10605 Concord Street, Suite #501, Kensington, Maryland 20895

2. Rate of Burning: How much a cable bed will contribute to the buildup of fire in a compartment depends on its rate of burning. (The same quantity is needed to determine the buildup of smoke and its effects). However, no single test currently measures this quantity: it can be estimated by knowing both the burning rate per unit area of cable and the rate at which a cable bed becomes involved in flame. The former is a heat release/mass loss measurement for which there are several available methods; the latter is a linear flame spread measurement. The flame spread value could be developed on the flooring radiant panel, ASTM E-648, with some modification. Alternatively, UL-910 could also be adopted for this use. Both heat-release-rate and flame-spread should be determined at elevated flux level, e.g. 2-3 $W/cm^2$, typical of a developing fire. In this work, another flame spread apparatus was used because of its ready adaptability to cable flame spread measurement (see below).

3. Smoke Production - The Mass Burning Rate: The smoke production rate is the product of the smoke produced per gram of cable and the rate of burning of the cable, expressed as weight loss in grams/sec. The smoke obscuration provided per gram of cable is given by its mass optical density. This can be measured on either the FM Flammability Apparatus, or in a smoke cabinet (e.g. the NBS smoke chamber) can easily be equipped to measure it as well.

4. Production of Toxic and Corrosive Products: The mass burning rate controls the amount of smoke produced. For a given cable multiplying the mass burning rate by the toxicity or corrosivity of smoke gives a relative measure of the potential for doing human or material damage.

Criteria for smoke corrosivity and smoke toxicity depend first on the units of the corrosion and smoke toxicity measurement (e.g. smoke toxicity might be expressed in lethal dose, toxicity index, or some incapacitation measure) and, the panel believes, can be derived rationally. However, the specifying authority needs to define the tenability limits for machines or men before they can be quantified. Once this is accomplished, it is simply a matter of determining the smoke concentration to which these limits correspond.

## Application of Theory to Smoke Hazard

The rate of mass loss, $\dot{m}''$ per unit area of cable exposed to a heat load, $\dot{q}''$, is:

$$\dot{m}'' = \frac{\dot{q}''_e - \dot{q}''_c}{L}, \quad \text{where} \qquad (1)$$

$\dot{q}''_e$ = external heat flux imposed

$\dot{q}''_c$ = critical ignition flux, i.e., below which no significant mass loss occurs

$L$ = apparent heat of gasification of cable insulation or jacket

The total mass lost by the cable per unit time is then the mass loss per unit area times the area involved, A.

$$\dot{m}_t = \dot{m}''A$$

If there is sufficient insulation and jacketing on the cables that the spread of flame is significantly faster than the burn-through rate,

$A = \dot{a} \times \text{time}$, where

$\dot{a}$ = linear flame spread rate down the cable bed

The quantity $\dot{a}$ is a function of the imposed flux, here assumed to be linear above $\dot{q}''_c$.

The total rate of mass loss of the cable is therefore

$$\dot{m}_t = \frac{\dot{q}''_e - \dot{q}''_c}{L}\, \dot{a}(\dot{q}'')\,[t - t_{(\dot{q}''_e = \dot{q}''_c)}] \qquad (2)$$

The quantities $\dot{q}''_c$, L, and $\dot{a}(\dot{q}''_e)$ are measured in the laboratory, using the Factory Mutual Flammability apparatus or the cone calorimeter for the first two and a suitable flame spread apparatus for $\dot{a}(\dot{q}''_e)$. The external flux, $\dot{q}''_e$, and the time at which the sample is exposed to the critical flux, $t(\dot{q}''_e = \dot{q}''_c)$, are

determined by the fire conditions to which the cable is exposed.

For a rapidly-developing fire, such as a fuel spill, $t(q'' = q'') = 0$, so in such cases the relative mass loss rates of a series of cables at any given flux can be predicted solely on the basis of laboratory measurements.

$$\dot{m}_{rel} \quad \frac{(\dot{q}''_e - \dot{q}''_c)a(\dot{q}''_e)}{L} \qquad (3)$$

For a slower fire, the relative loss rates will also depend on the time interval before the various cables ignited: $t(\dot{q}''_e = \dot{q}''_c) > 0$.

As discussed above, mass loss rate is important because it, in combination with appropriate smoke density, toxicity, or corrosion measures, allows one to predict the actual relative threat of cable due to these characteristics.

Amount of visible smoke/sec. $\sim \dot{m} \cdot (\alpha\ \chi)$, where

$\alpha\ \chi$ = mass optical density (light-obscuring power per unit mass)

Smoke Toxicity/sec. $\sim \dot{m} \cdot T$, where

T = smoke toxicity per unit mass 1

Smoke Corrosivity/sec. $\sim \dot{m} \cdot C$, where

C = smoke corrosive power per unit mass

All three of these smoke properties can be measured in the laboratory (although measuring smoke toxicity is fraught with difficulties of its own (5)). Hence, it is possible to rank order cable smoke hazard based on laboratory measurements alone.

## Experimental Results

### A. Test Samples

This paper reports the results of components of this test regimen when applied to five cable assemblies. The cables used are described in Table 1. Cables number 1 and 2 typify the kind of assembly used in many military applications up until very recently. Cable 3 is an electronics cable composed entirely of fluoropolymer materials. Cable 4 an example of the cross-linked polyolefin technology currently gaining prominence in many "non-halogen" applications and Cable 5 is a modern construction containing a low halogen jacket and fluoropolymer insulation.

All of the cables pass IEEE-383. All were obtained from commercial suppliers and all except for Cable 3, which is a coaxial electronics cable, all the cables were multiconductor type, similar to those which meet the electrical and mechanical requirements set forth recent military specifications.

### B. Flammability Tests

The bulk of the flammability parameters were obtained using the Factory Mutual Flammability Apparatus (6) or the Cone Calorimeter developed by the Center for Fire Research at the National Bureau of Standards (7). Both devices are similar in concept: they measure rates of mass loss and heat release of the test material on exposure to a well-characterized radiant heat load. By varying the radiant heat flux to the sample, two important parameters can be deduced. They are:

1. The critical ignition flux ($\dot{q}''_e$), which is the minimum imposed radiance level under which a sustained ignition of the cable will occur;

2. The apparent heat of vaporization (L), which is the amount of energy required to convert unit mass of polymeric solid to fuel vapor.

The latter quantity is obtained by monitoring the rate of mass loss of the sample as a function of flux, as is shown in Figure 1, and taking the slope of the resulting plot.

Flame spread rates were obtained using the International Maritime Organization Flame Spread Apparatus, developed by Robertson (8) at the National Bureau of Standards. This device imposes a radiant flux gradient on a vertically-mounted sample and the lateral flame spread rate across the sample is monitored: see Figure 2.

Details of the experimental techniques used and a close comparison of similar data obtained from different instrument prototypes will be reported elsewhere.

### B. Smoke Density and Corrosivity

Both the Factory Mutual Device and the Cone Calorimeter are equipped with a

light source and photo-multiplier for measuring smoke obscuration as a function of mass loss. The values reported in this paper are those taken with the Factory Mutual apparatus.

The corrosivity of the smoke was measured by the resistance of a carefully-calibrated copper film which had been exposed to smoke for a fixed period of time, one hour. The method is that of Rio and, at Centre National pour L'Etude Telecommunications (CNET) the French National Center for the Study of Telecommunications. The percent change in resistance after one hour is reported.

C. Results

The results of the measurements are reported in Table 2. The table also contains a tabulation of the relative mass loss per unit area, m", discussed in the previous section, as a measure of the proclivity of the cable jacketing and insulation to decompose. The values range over a factor of approximately 50.

Table 3 shows the relative smoke and corrosion producing qualities of the five cable samples. The smoke results, expressed in optical density units per second, are proportional to the rate at which a given volume becomes obscured by smoke from the burning cable bed.

The range of values is approximately 300. The relative corrosivity values vary over a range of approximately 100.

## Discussion

The approach just described is very different in concept from traditional methods of specifying cable fire/smoke properties. The advantages it offers are: 1.) it permits one to estimate how cables will respond to one set of real fire conditions; and 2.) to the extent that any set of fire conditions can be anticipated quantitatively, it is usually possible to infer how a given cable will perform under those conditions as well.

Consider, for example, a case in which a cable bed is exposed to a developing fire in a compartment. The initial fire need not involve the cable at all, but might begin in a piece of machinery, accumulated combustibles such as found in an office space, or in any of an almost infinite number of other ways. The fire will heat up its surroundings and, if it is in the compartment proper, a sizable layer of hot smoke will accumulate in the upper part of the room. This hot layer can ignite items well removed from the original fire source if they are sufficiently ignition-prone. The minimum ignition flux, as measured by either the FM apparatus or the cone calorimeter, is a good indicator of how readily a cable will ignite. Values obtained in this work range from 18 kW/sq.m. to 48 kW/sq.m. For comparison, the radiant energy transmitted to the horizontal surfaces from a fire burning in a typical compartment (10'x15'x8', 30 inch doorway) is plotted as a function of fire size in Figure 3. A cable bed located in the room, and not located in near proximity to the fire, would experience a radiant heat load no greater than that shown in the figure. A two foot diameter fuel fire produces approximately 1000 kW, so that any cables having a critical ignition flux above about 25 kW/sq. meter would not be expected to ignite from such a fire unless it is located very near the cable bed. Cables having a higher critical ignition flux require a correspondingly larger ignition source.

The measurement of mass loss and flame spread also permits one to estimate the cable's contribution to the total fire and smoke once ignition has occurred. Consider, for example, an exposure fire which eventually grows large enough to ignite any of the cables under discussion. As the fire grows, so does the radiant flux to the horizontal surfaces. When the heat load to a horizontal surface reaches the value of the critical ignition flux of a cable, the cable begins to burn. The rate of flame spread along the cable is given by the flame spread parameter, a, and the amount of mass loss per unit cable area by the parameters, q, q , and L. The expected mass loss rate for the exposure fire and each of the 5 cable samples can be calculated, as can the total smoke mass produced by the exposure fire and each cable. These are important considerations in determining how cable will perform under actual conditions, and will be expolored more fully in the near future.

## References

1. Clarke, F., Benjamin, I., and DiNenno, P., "Overall Fire Safety of Wire and Cable Materials:, Proceedings of the 32nd IWCS, 390, 1983.

2. Clarke, F., and DiNenno, P., "Fire Safety of Wire and Calbe Materials, Part III: An approach to Estimating Cable Fire Hazard", Proceedings of the 33rd IWCS, 40, 1984.

3. C.F. Jones, W., "A Review of Compartment Fire Models", National Bureau of Standards (U.S.), NBSIR 83-2684, April, 1983.

4. Clarke, F., "Report on the Maryland Roundtable on Cable Fire Safety", in Fire Safety Through Use of Flame-Retarded Polymers, Joint Conference of Fire-Retardant Chemicals Association and the Society of Plastics Engineers, Houston, TX, March, 1985.

5. Clarke, F., "Toxicity of Combustion Products: Current Knowledge", NFPA Fire Journal, p. 84, September, 1983.

6. Tewarson, A., Lee, J., and Pion, R., "Categorization of Cable Flammability-Labroatory Evaluation of Cable Flammability Parameters", Electric Power Research Institute, EPRI NP-1200, Project 1165, October, 1979.

7. Babrauskas, V., "Development of a Cone Calorimeter - A Bench-Scale Heat Release Apparatus, Based on Oxygen Comsumption, "Fire and Materials, 8, 81 (1984).

8. Robertson, A., "A Flammability Test Based on Proposed ISO Spread of Flame Test", Third Progress Report, Integovernmental Maritime Consultative Organization (now International Maritime Organization), IMCO FP/215, 1979.

TABLE 1

Cables Used in Test Regimen

| Number | Description (Insulation/Jacket) |
|---|---|
| 1 | PVC / Polyethylene |
| 2 | Silicone Rubber / PVC |
| 3 | Fluoropolymer / Fluoropolymer Coaxial |
| 4 | Cross-linked Polyethylene (XLPE) / Cross-Polyolefin (XLPO) |
| 5 | Ethylene-tetrafluoroethylene (ETFE) / Ethylene-acrylic Copolymer |

TABLE 2

Results of Laboratory Flammability Tests

| Cable | L, kJ/g | $\dot{q}''_c$ (kW/m) | $\dot{a}$ (mm/sec) $^2$ | | $\dot{m}''_{rel}$ at 50 kW/m$^2$ |
|---|---|---|---|---|---|
| | | | 25 kW/m$^2$ | 50 kW/m$^2$ | |
| 1 | 2.4 | 14 | 5 | 15 | 221 |
| 2 | 4.5 | 11 | 7 | 24 | 119 |
| 3 | 1.3 | 40 | - | 0.5 | 4 |
| 4 | 10.5 | 17 | 1.6 | 10.8 | 34 |
| 5 | 8.3 | 24 | 0.7 | 3.2 | 10 |

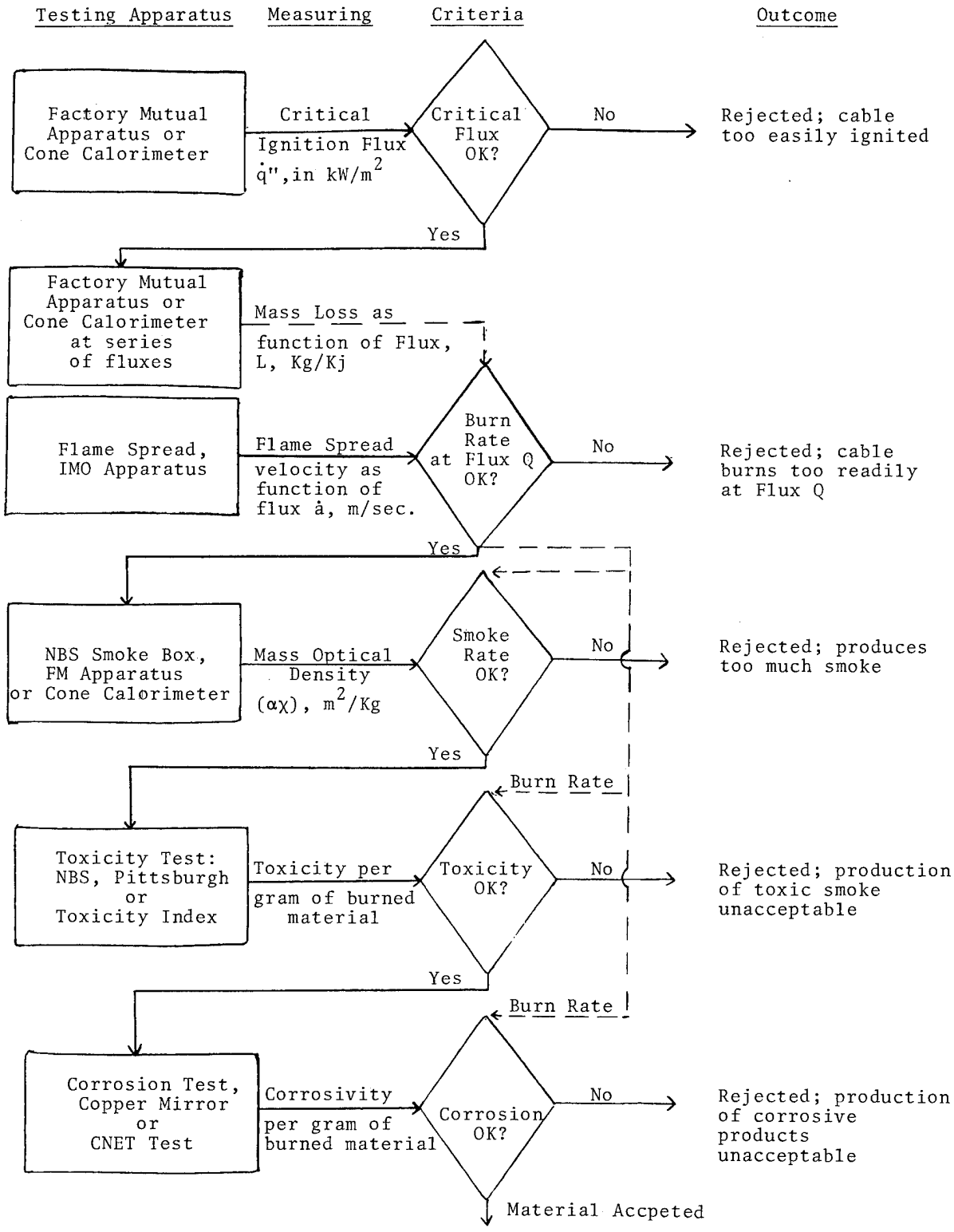
TABLE 3

Relative Production of Smoke and Corrosive Products

| Cable | $\alpha X$, m$^2$/g | $\Delta R$, % | Visible Smoke/sec | Corrosivity/sec |
|---|---|---|---|---|
| 1 | .76 | NA | 168 | NA |
| 2 | .54 | 40 | 64 | 4760 |
| 3 | .01 | NA | .04 | NA |
| 4 | 1.34 | 4 | 46 | 136 |
| 5 | .54 | 3 | 5.4 | 30 |

NA = Not Available

FIGURE 1


Testing Apparatus
Measuring
Criteria
Outcome
Factory Mutual Apparatus or Cone Calorimeter
Critical Ignition Flux q", in kW/m2
Critical Flux OK?
No
Rejected; cable too easily ignited
Yes
Factory Mutual Apparatus or Cone Calorimeter at series of fluxes
Mass Loss as function of Flux, L, Kg/Kj
Flame Spread, IMO Apparatus
Flame Spread velocity as function of flux à, m/sec.
Burn Rate at Flux Q OK?
No
Rejected; cable burns too readily at Flux Q
Yes
NBS Smoke Box, FM Apparatus or Cone Calorimeter
Mass Optical Density (αχ), m2/Kg
Smoke Rate OK?
No
Rejected; produces too much smoke
Yes
Burn Rate
Toxicity Test: NBS, Pittsburgh or Toxicity Index
Toxicity per gram of burned material
Toxicity OK?
No
Rejected; production of toxic smoke unacceptable
Yes
Burn Rate
Corrosion Test, Copper Mirror or CNET Test
Corrosivity per gram of burned material
Corrosion OK?
No
Rejected; production of corrosive products unacceptable
Material Accpeted

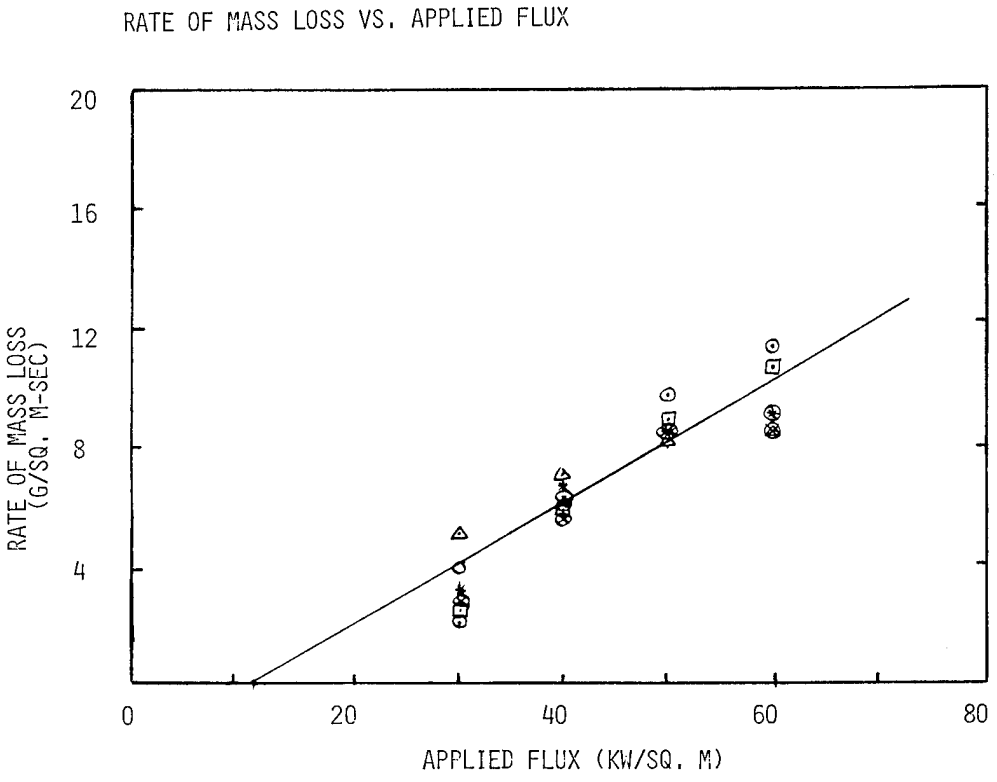



FIGURE 2

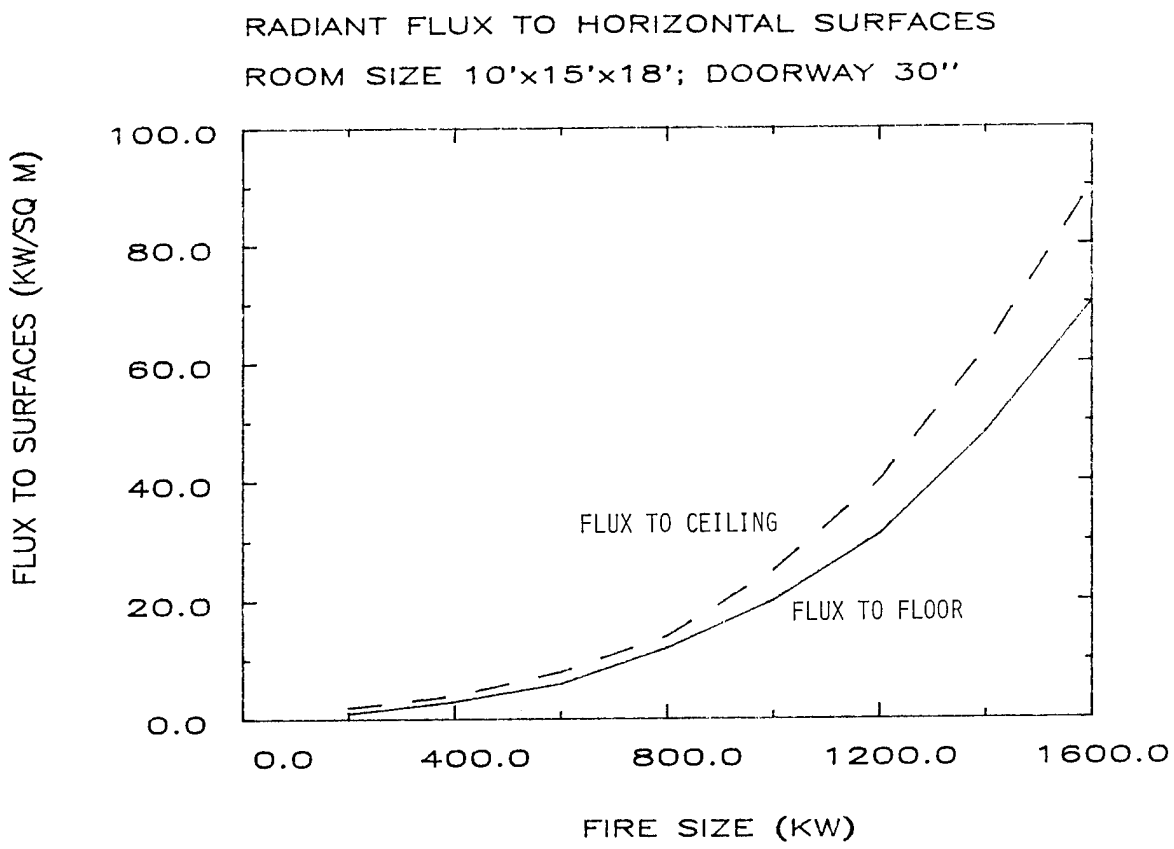



FIGURE 3

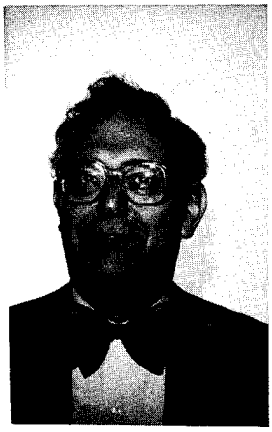


FREDERIC B. CLARKE, III, Ph.D.

Frederic Clarke is President of Benjamin/Clarke Associates, Inc., a firm specializing in the characterization and analysis of fire safety problems. Until fall, 1981 he was director of the National Bureau of Standards' Center for Fire Research, the Nation's principal Federal fire laboratory. He was also Science Advisor to the United States Fire Administration. He is currently a member of the National Academy of Sciences Committee on Fire Toxicity.

From 1976-1977, he served as legislative assistant to Senator John Culver (D.-Iowa), specializing in economic and product liability legislation; and a staff assistant to Congressman Jim Wright (D.-Texas), the House Majority Leader.

He holds a Ph.D. in chemistry from Harvard University.



IRWIN A. BENJAMIN, P.E.

Irwin Benjamin is Vice President of Benjamin/Clarke Associates, Inc., a firm specializing in the characterization and analysis of fire safety problems. Until fall, 1981, he was Chief of the Fire Safety Engineering Division, Center for Fire Research, National Bureau of Standards. In that capacity, he supervised the development of systems for evaluating fire risk in buildings including the extension of analytical fire modeling to the solution of practical fire problems, and the development of a toxicity protocol for screening materials.

He holds a B.S., Civil Engineering, Illinois Institute of Technology, and an M.S., Structural Design, Kansas State University. He is a Graduate, Federal Executive Institute, and holds the Department of Commerce Silver Medal.

# "LIGHT WEIGHT POLYIMIDE FILM/MICA MARINE CABLE"

Cutter D. Palmer David B. Allen William J. Kopish

E. I. Du Pont de Nemours & Co. Inc.
Polymer Products Department
Specialty Polymers Division

## Abstract

An advanced shipboard cable insulated with polyimide film* and glass reinforced mica tape has been developed for the United States Navy's Aegis cruiser and other vessels for the Navy of the future. The polyimide/mica cable, MIL-C-24640/19 thru 24, combines the best features of MIL-C -915E and PMS-400-881. It offers the same high performance, water tightness and circuit integrity in a fire of MIL-C-915E, and the light weight, flexibility and very low smoke and corrosive gas generation of PMS-400-881.

## Introduction

As vessels for the United States grow more sophisticated in operational capabilities and weapons systems, so must cable technology.
In the past, certain MIL-C-915E cable constructions adequatedly met the performance requirements of shipboard cable. They offered two major advantages: circuit integrity in fire conditions and watertightness in the event of a flooded compartment. But, they also had two major drawbacks: heavy weight and high smoke and corrosive gas generation in a fire.
These drawbacks led to the development of PMS-400-881, a light weight cable construction. It offers significant reductions in size and weight over MIL-C-915E and provides superior fire retardancy, including reduced smoke and corrosive gas generation. But, it too, has two major deficiences: no circuit integrity in a fire and no watertightness.
Now a unique new, advanced cable using water-blocked conductors, a glass reinforced mica tape and polyimide film has been developed to fill the gap between certain MIL-C-915E constructions and PMS-400-881.
This paper will explore the design and makeup of the three cable constructions and review the battery of test results that demostrate the superiority of the new mica/polymide cable.

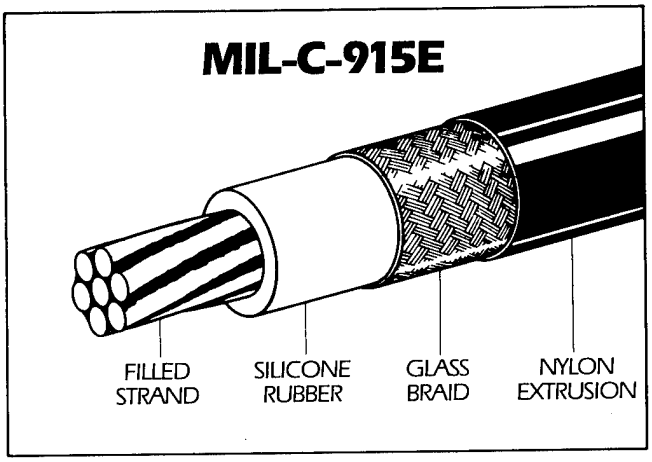
*Du Pont's Kapton® Polyimide Film

## MIL-C-915E

MIL-C-915E has long been the standard for performance in maintaining physical, thermal, electrical and mechanical properties of marine cable.
Certain MIL-C-915E constructions are designed to maintain circuit integrity in fire conditions and water tightness to prevent axial water flow.
Figure 1 shows a cutaway view of a Typical MIL-C-915E construction. The interstices of the stranded conductor and component wire members are filled with a waterblocking compound to prevent axial water flow through the conductors in the event of a flooded compartment.
The silicone rubber insulation, a good insulating dielectric, performs well under fire conditions. It forms a non-conductive ash so the cable will continue to operate in a fire until the cable becomes saturated with water.
The glass braid is applied to mechanically protect the relatively fragile silicone rubber during manufacture, installation and use. It also

contains the ash in event of a fire. The extruded nylon covering provides additional insulation as well as a mechanical protection to prevent the glass braid from fraying. It also adds chemical resistance.

Figure 1




The polyvinyl chloride (PVC) outer jacket gives the insulated conductors protection from physical stress, moisture and chemical exposure.

Although MIL-C-915E has performed well from a circuit integrity standpoint, it is being phased out because of its shortcomings in fire protection and size. When exposed to fire MIL-C-915E generates a great deal of smoke and corrosive gas. Smoke hampers evacutation and fire fighting. Corrosive gas can damage shipboard electronic systems. Its large size adds substantial weight to a vessel and takes up valuable space.

PMS-400-881

PMS-400-881, with MIL-W-81044/12 component wire, offers several advantages over MIL-C-915E. The cable is about half the weight and one-third the cross sectional area. It also reduces smoke and corrosive gas generation during a fire. But, because it is not watertight and lacks circuit integrity during a fire, it is designed only for applications above the water line.

Figure 2

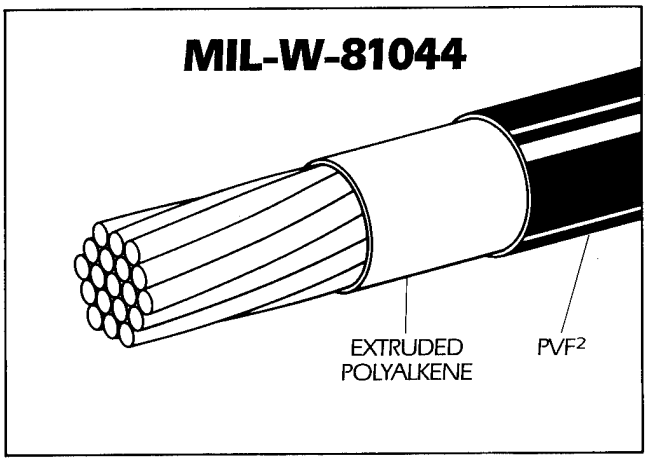


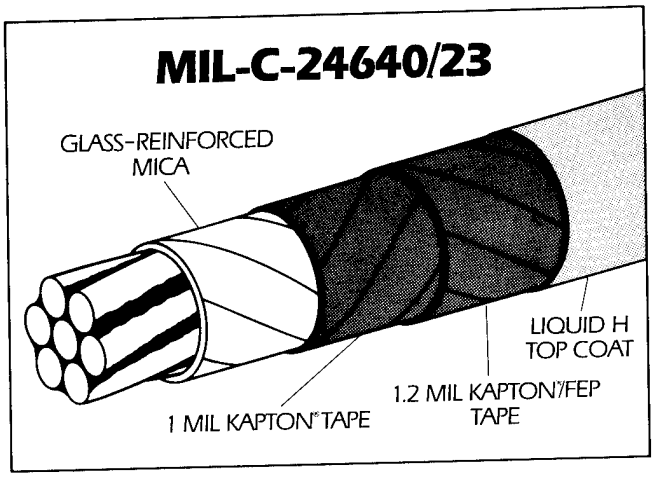

Figure 2 shows a cutaway view of a typical MIL-W-81044/12 construction. The insulation consists of 4 mils of cross-linked polyalkene, jacketed with 3 mils of polyvinylidene flouride (PVF). Polyalkene provides a high dielectric insulation and the polyvinylidene flouride gives added mechanical protection and a degree of flame retardancy. The outer jacket of the PMS-400-881 cable is a flame retardant, cross-linked polyolefin with exceptional mechanical properties and very low smoke generation in a fire.

MIL-C-24640/19-24

A cooperative effort between a wire and cable manufacturer and materials suppliers resulted in a construction utilizing water blocked conductor, a glass reinforced mica tape and two polyimide tapes that combines the best features of MIL-C-915E and PMS-400-881.

The construction is called out in MIL-C-24640 slash sheets 19 through 24.

Figure 3




The polyimide film/mica construction provides several benefits, including:

Low smoke generation that facilitates evacuation and permits fire fighters to more readily locate the fire source.

Low corrosive gas generation that reduces damage to electronic systems and reduces costly, time consuming repairs.

Improved circuit integrity that ensures continuous power, control and data transmission even if the cable becomes fully engulfed by fire. The results of the gas flame test for maintaining circuit integrity under the most challenging conditions, such as vibration, show polyimide/mica insulated cable superior to MIL-C-915E.

Watertightness that prevents flow of water from a flooded compartment to other parts of the ship.

Lower Weight that increases ship maneuverability and stability. Mica/polyimide cable is approximately 1/2 the weight and 1/3 the cross sectional area of MIL-C-915E. This weight and space savings can also mean fuel savings, increased payload and increased growth margin.

MIL-C-24640/19-24 component wire is tape wrapped rather than extruded. Extrusion of mica and polyimide film is not possible because these materials do not melt. Tape wrapping allows precise thickness control for excellent concentricity of insulation and low variation from specified weights and diameters.

A typical polyimide/mica wire construction begins with the application of water blocking compound to a seven strand bare copper conductor.

The blocked conductor is then wrapped with a glass reinforced mica tape, providing an initial layer of insulation. The mica/glass tape is wrapped with 50% overlap, effectively providing two layers of protection.

The mica/glass tape is covered with a 1 mil polyimide tape, 50% overlapped, and a 1 mil polyimide tape coated on both sides with 1/10 mil "Teflon FEP", also 50% overlapped.

After the tapes are heat sealed, the construction is coated with Liquid H, an aromatic polyimide resin topcoat, applied with a dip process to produce a smooth surface, pigmented to provide a background for printed identification. The individual conductors are 100% inspected with an electrical impulse dielectric tester to insure freedom from insulation flaws.

The insulated conductors are cabled with additional waterblocking compound applied under pressure. The cable core is then wrapped with a "Mylar" binder tape and jacketed with a low smoke, low flame spread, cross linked polyolefin. The finished cable is dielectrically tested while immersed in water to insure its overall integrity, as is required of all United States Navy cable.

The polyimide/mica cable is subjected to a battery of tests and results show that it meets or exceeds the performance levels of both MIL-C-915E and PMS-400-881 constructions.

In fire tests, the polyimide/mica construction exhibits very low smoke and corrosive gas generation. It also meets the gas flame circuit

integrity test of MIL-C-915E, which is three hours exposure to 1600°F.+ flame with zero current leakage, conductor to conductor with 100 volts impressed phase to phase. In addition, the polyimide/mica cable maintained zero leakage even during vibration.

In watertight tests, the polyimide/mica cable proves effective in stopping axial water flow. It is also tough and abrasion resistant to withstand rigors of installation. In spite of the wall thickness reduction, ruggedness has not been sacrificed, according to results of dynamic cut-through tests performed on an Instron tensile tester, showing the polyimide/mica construction to be equivalent to the much thicker MIL-C-915E construction (Table 1).

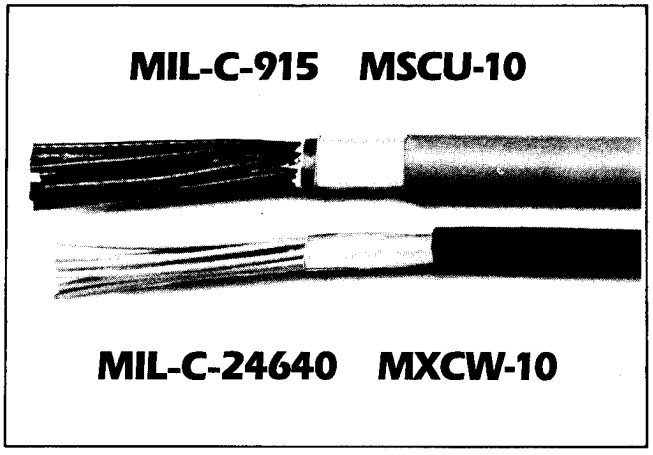
TABLE 1

Cut Through Resistance

| | |
|---|---|
| MIL-C-915E | 35 lbs. |
| MIL-C24640/19-24 | 35 lbs. |

Although the polyimide/mica insulation has high cut-through resistance, it can be readily stripped using commercially available hand-held wire strippers. Also the cables increased flexibility, coupled with low weight and small cross sectional area, make it easier to handle and install than MIL-C-915E constructions.

Figure 4




The mica/polyimide cable, though new to the marine industry, is based on proven technology. Most major commercial and military aircraft, space vehicles and missiles depend on the high performance characteristics of wire insulated with polyimide film. Millions of air miles of virtually fault free operation have made polyimide film the standard for aerospace wire insulations. Glass reinforced mica tape and water-blocked conductors have been added to the airospace construction to bring this high performance record to shipboard cable. This should be particularly important for power and control systems installed below the water line, such as ship steering and other systems vital to the completion of a mission under adverse conditions.

## Conclusion

Wire & Cable constructions on mica/polyimide film of MIL-C-24640/19-24 combine the best features of MIL-C-915E and PMS-400-881 constructions.

They offer the high performance tradition of MIL-C-915E with the lightweight flexibility of PMS-400-881 in a single, complete package of performance characteristics essential for shipboard applications.



Cutter D. Palmer
Consultant

Recently retired from the DuPont Company as Senior Development Programs Manager in the Specialty Polymers Division of the Polymer Products Department. He was with DuPont over 35 years, with many years as an electrical design engineer working with the wire and cable industry on the application of "Mylar" a polyester film and "Kapton" a polyimide film in a wide variety of cable constructions.

Mr. Palmer received a BSEE from the University of Nebraska.

He is a member of several industry committees, namely:

- Insulated Conductor Committee of IEEE
- NEMA High Temperature Wire Tech Com
- Electrical Section of NFPA
- The Wire Association
- Institute of Printed Circuits
- ASTM Comm. D-9 Electrical Ins. Mat'ls
- American Defense Prepardness Assoc.



David B. Allen
Development Program Mgr.
Specialty Polymers Div
Polymer Products Dept
DuPont Company

Mr. Allen has been with DuPont for the past 31 years in various technical and marketing assignments.

His present assignment involves development of new markets and uses for wire and cable made from high performance resins and films.

He is a member of several wire and cable committees, namely:

- Society of Automotive Engineers
  Aerospace Council
  AE 8D Subcommittee on Wire & Cable
- NEMA High Temperature Wire Section
- EIA (Electronics Industry Assoc.) C83.3
  Committee on Coaxial Cable for MIL-C-17



William J. Kopish
Development Specialist
Specialty Wire & Cable Gp

His present responsibilities include development of wire and cable applications for high performance resins and films for shipboard and military electronics.

Mr. Kopish has been with DuPont for 22 years in positions primarily associated with market and product development.

He is a member of the American Chemical Society and the Society of Automotive Engineers.

# RAPID RIBBON SPLICE FOR OPTICAL FIBER FIELD SPLICING

N. E. Hardwick, III and S. T. Davies

AT&T Bell Laboratories
Norcross, Georgia 30071

## Abstract

The ribbon-based cable design used in many multimode fiber installations makes it practical to rapidly splice ribbons for LAN applications or to rapidly resplice ribbons for field restoration. A Rapid Ribbon Splice that uses mechanically-held, molded piece-parts has been developed for this purpose. This splice has long-term stability over a wide temperature range (-40°F to 170°F), produces service restoral in as little as twenty minutes (1.75 minutes/fiber), and provides permanent, low loss splices ($x_{mean} < 0.3$ dB). This design is ideal for LAN applications because the splice design is permanent, low cost and relatively easily accomplished.

## Introduction

A significant advantage of ribbon-based cable designs is that multifiber splicing is practical. Both multimode and single-mode optical fibers are now being used extensively in 12-fiber ribbon cables with factory-connectorized silicon chip arrays. Field fabrication of silicon chip arrays can also be done, when required for repair or service restoral; this typically requires two hours for the first ribbon and one hour for each additional ribbon. The Rapid Ribbon Splice (RRS) described in this paper allows quick field service restoral of multimode ribbons in twenty minutes (1.75 minutes/fiber) with permanent low loss splices (mean loss < 0.3 dB). This molded plastic splice has long-term stability over a wide temperature range (-40°F to 170°F).

## Comparison of Restoration Splicing Times

The importance of multifiber splicing can be emphasized using Figure 1. Expected fiber joining times for service restoral, as a function of fiber count, are shown for preconnectorized ribbon arrays, rapid ribbon splicing, field-fabrication of factory-type arrays, and individual fiber splicing techniques such as fusion welding. These curves are based on the most recently available data for ribbon joining and an optimistic estimate of 15 minutes per splice for individual fiber splicing. The ribbon ends (or existing connectorized arrays) are assumed to be already accessible.

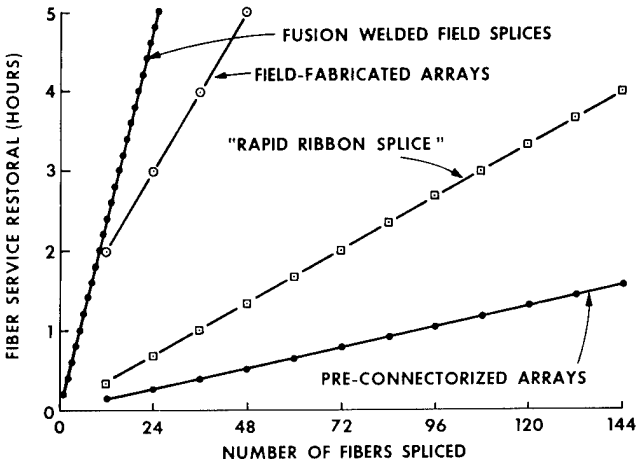



**FIGURE 1. FIBER JOINING TIME FOR RESTORATION (After Access to Ribbon Ends)**

The plots in Figure 1 indicate dramatic differences in fiber joining rates for the four methods. Preconnectorized array splicing is the fastest temporary restoration method but requires replacing the cable section. Rapid Ribbon Splicing provides slightly slower restoration but results in a permanently repaired cable section and is significantly faster than the field-fabricated array method. Field-fabricated arrays are now expected to be appropriate only for rebuilding damaged "halves" of array splices during initial installation.

All the multifiber splicing methods provide significantly faster restoration than individual fiber splicing.

For service restoral of one 12-fiber ribbon, the Rapid Ribbon Splice method takes less than one-half hour, and saves at least two hours and three hours compared to using field-fabricated arrays and fusion splicing, respectively. For 36 fibers, the RRS method takes approximately one hour and saves six hours compared to individual fiber splicing (three hours compared to field-fabricated arrays). As the number of fibers to be joined increases the time savings using multifiber joining techniques increase even more dramatically.[1]

## Continuous Groove Concept

The RRS is based on the continuous groove concept in which butt joints of all twelve pairs of mating ribbon fibers are formed simultaneously in twelve adjacent grooves of a common substrate (see Figure 2). The continuous grooves insure precise alignment of the mating fibers, independent of the lateral spacing of adjacent grooves.

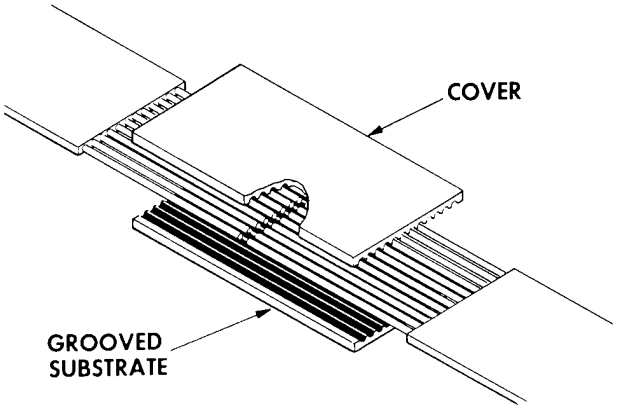



FIGURE 2. CONTINUOUS GROOVE CONCEPT USED IN RAPID RIBBON SPLICE

To take advantage of the continuous groove concept, a number of subtle difficulties must be overcome to achieve low splice loss for all 12 fibers that is stable over extreme temperature excursions. These difficulties include (1) fiber pullback tendencies, (2) thermal expansion stresses and (3) fiber and groove dimensional variations.

## Rapid Ribbon Splice Configuration

The materials and geometry of the RRS were analytically optimized to resolve the above problems and provide a stable splice. An expanded view of the RRS splice is shown in Figure 3. The molded plastic substrate has vacuum openings to facilitate fiber seating.[2] The cover has a slot so index matching gel can be applied (to reduce Fresnel reflections at the fiber junction) after the cover is clamped into position. The spring fasteners provide mechanical gripping so no epoxy or adhesives are required. A molded plastic strain relief is attached to each end of the splice to minimize stress transfer caused by ribbon movement.

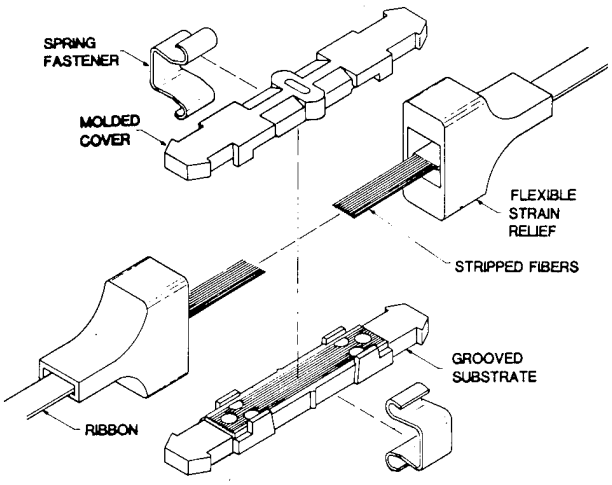



FIGURE 3. EXPLODED RAPID RIBBON SPLICE

## RRS Splice Assembly

The Rapid Ribbon Splice is completed in the following five straightforward steps:

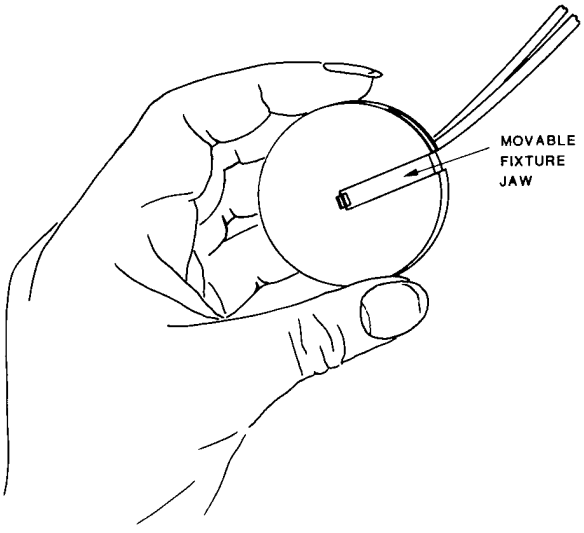



FIGURE 4. TOOL SETUP TO POLISH RIBBON ENDS SIMULTANEOUSLY

1) The ribbon ends are prepared and simultaneously polished (See Figure 4). Traditionally, bare fiber ends are prepared for repair splicing by scoring and breaking. The Rapid Ribbon Splice uses a unique grinding and polishing procedure which results in perpendicular ends of equal fiber length on all 24 fibers.

2) The twelve fiber butt joints are formed in the substrate grooves, Figure 5.

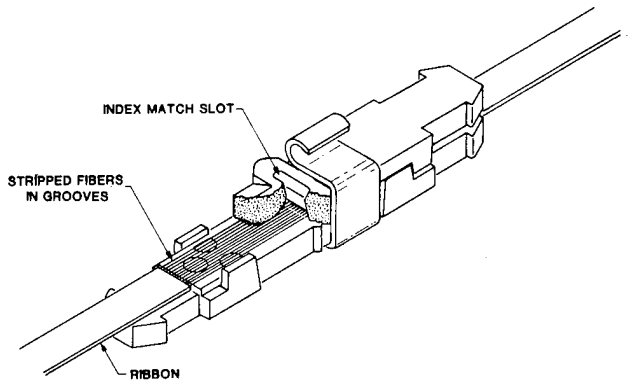



FIGURE 5. CUTAWAY VIEW SHOWING CONTINUOUS GROOVE SPLICE JOINT

3) The cover is clamped in position to seat the fibers with the spring clips as shown in Figure 5. The assembly tool shown in Figure 6 aids in these two steps.

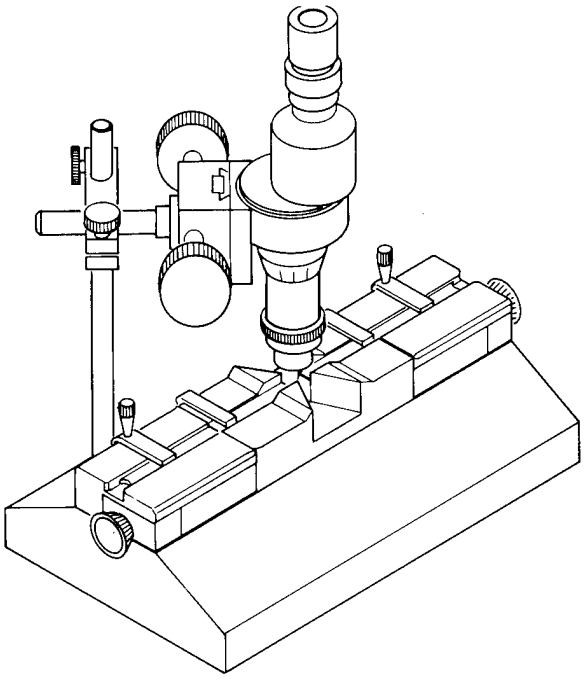


FIGURE 6. RAPID RIBBON SPLICE ASSEMBLY TOOL

4) The refractive-index matching material is applied at the fiber joints. As shown in Figure 7, the index matching material is dropped into the index match slot which also allows viewing of the seated fibers.

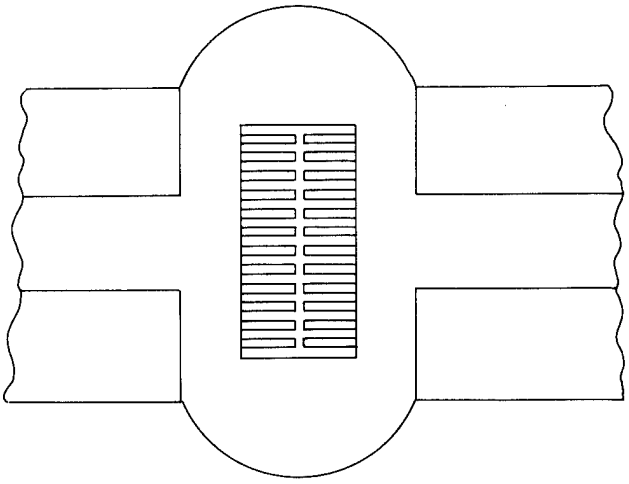


FIGURE 7. MAGNIFIED VIEW OF INDEX MATCH SLOT

5) Finally, the strain reliefs are pushed onto each end to complete the splice as shown in Figure 8.

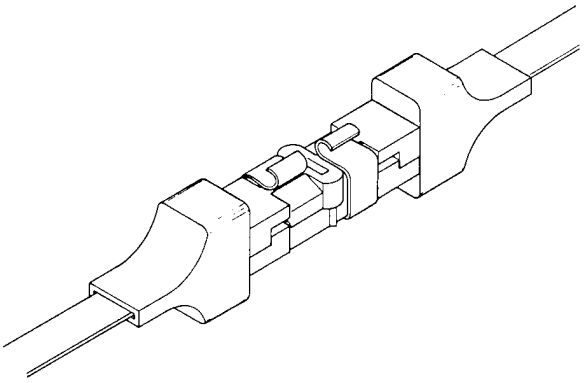


FIGURE 8. LIGHTGUIDE RAPID RIBBON SPLICE

## Environmental Testing

The Rapid Ribbon Splice has remained stable during harsh environmental cycling tests for long periods of time. Figure 9 shows a portion of the mean added loss data (12-fiber ribbon) for a typical RRS during 230-234 daily cycles between -40°F and 170°F. The same pattern (i.e., daily loss variations between -0.05 dB and +0.05 dB) shown over this period occurred throughout the environmental test. (The initial room temperature loss on this splice was only

$x_{mean}$ = 0.1 dB). There was no net added loss after the testing was completed.

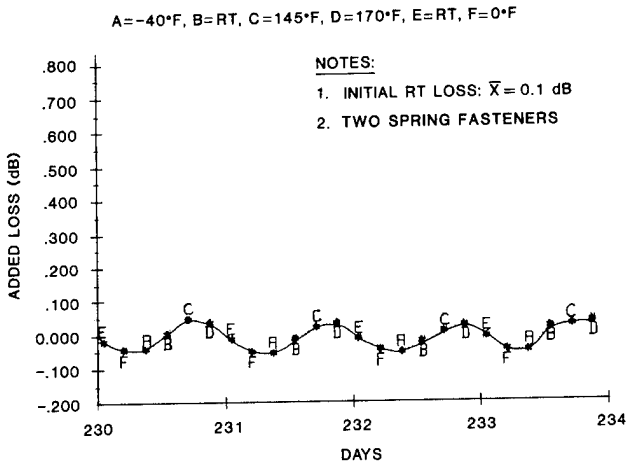



FIGURE 9. ADDED LOSS TO RRS DURING THERMAL CYCLING BETWEEN -40°F AND 170°F (UP TO 234 DAYS).

## Splice Features

The salient features of the Rapid Ribbon Splice are listed in Table I. The RRS design provides a rapid, permanent ribbon splice with low splice loss. The assembly time from access to the ribbon ends until service is restored is 20-25 minutes. The splice is environmentally stable over a wide temperature range (-40°F to 170°F). The assembly tools and procedures are designed so the splice assembly is easy to learn. The RRS fulfills the need for a quick repair splice for ribbon-based cable. This splice can also be used for installation splicing in Local Area Networks where extremely low losses are not required.

## TABLE I

## RAPID RIBBON SPLICE FEATURES

- RELIABLE, LOW-LOSS FIELD SPLICE
- RAPID SERVICE RESTORAL (~2 MIN/FIBER)
- LONG TERM STABILITY (-40°F TO 170°F)
- PERMANENT
- EASY TO LEARN
- REPAIR OR INITIAL INSTALLATION USE

## Field Application Experience

Splice data from field repair splices on cables in service confirm the expected low loss restoration results. The Rapid Ribbon Splice has been used for restoration or rerouting of several sections of working cable. Splice Loss data from a typical repair of a damaged cable is given in Figure 10. Fiber splice loss measurements on the four repaired ribbons gave an overall mean loss of 0.18 dB which is excellent. No individual fiber loss was greater than 0.8 dB.

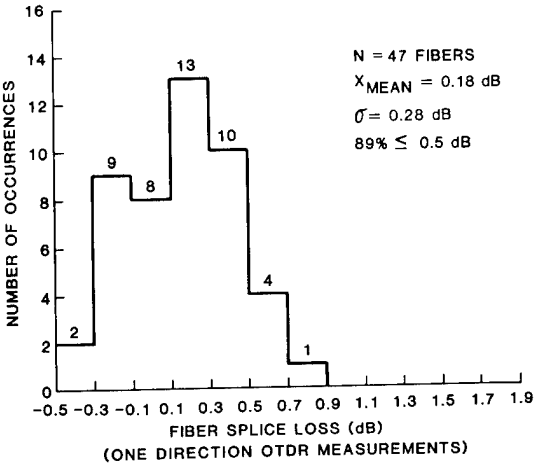



FIGURE 10. INITIAL FIELD RESTORATION RESULTS USING RRS TO REPAIR A WORKING CABLE (4 RIBBONS)

## Conclusions

A molded plastic Rapid Ribbon Splice has been developed that is low cost, easy to assemble, and provides a low loss, permanent ribbon splice. This mechanical splice requires no adhesives, is reenterable and has long-time stability over a wide temperature range.

The RRS has been used for repairing multimode fiber systems in several field restorals. The splice has sufficiently low loss to make it practical as a splice for LAN multimode fiber installations. The Rapid Ribbon Splice may also have application with single-mode ribbon cable.

## Acknowledgements

The authors wish to acknowledge P. F. Gagen, Jr., as a co-inventor of the RRS, C. M. Miller and E. I. Brame for their contributions to the ribbon polishing process, C. J. Aloisio and R. R. Cammons for overseeing the mold designs and molding the pieceparts, as well as A. H. Cherin and P. J. Rich for

their early work on vacuum-assisted plastic splices.

## References


1. N. E. Hardwick III, C. F. Cottingham, P. D. Patel, and A. L. Hale, "Design for Rapid Lightguide Restoration," IEEE Global Telecommunications Conference, GLOBECOM '82 Miami, Florida, November 29-December 2, 1982.

2. A. H. Cherin, P. J. Rich, C. J. Aloisio, and R. R. Cammons, "A Vacuum-Assisted Plastic Repair Splice for Joining Optical Fiber Ribbons," Bell Syst. Tech. J., Vol. 58, No. 8 (October 1979), pp. 1825-1838.





Nathan E. Hardwick III
AT&T Bell Laboratories
2000 Northeast Expressway
Norcross, Ga. 30071


Nathan E. Hardwick, III, has received B.S. and M.S. Degrees in Mechanical Engineering from the University of South Carolina and a Ph.D. in Mechanical Engineering from Lehigh University. After joining Bell Laboratories in 1965, he initially designed and thermally characterized ceramic integrated circuit packages. Later work included responsibility for the design and the initial installation of the outside plant hardware system for FT3 lightguide cable. Currently, Nate is a member of the Lightguide Joining Group where he is working on multifiber splicing and splice mechanisms analyses. Dr. Hardwick spent one year as a Bell Laboratories Visiting Professor at N.C. A&T State University.




Scott T. Davies
AT&T Bell Laboratories
2000 Northeast Expressway
Norcross, Ga. 30071


Scott T. Davies is a Senior Technical Associate at AT&T Bell Laboratories in Norcross, Georgia. Since joining AT&T Bell Laboratories in 1980, he has been engaged in various types of optical fiber splicing and environmental testing. His present responsibilities include the design and development of the Rapid Ribbon Splice. Mr. Davies received an AAS Degree from Richmond Technical College in North Carolina.

# FIELD MOLDED SPLICE CLOSURE SYSTEM FOR COPPER AND FIBER CABLES USING LOW PRESSURE MOLDING

I.H. Miller J.L. Horton J.R. Scott L.J. Charlebois

BELL CANADA

BELL NORTHERN RESEARCH

## Abstract

Northern Telecom, Bell Northern Research and Bell Canada are jointly developing and introducing a reliable and cost effective new splice closure system called Low Pressure Molding (LPM). LPM is the process of low pressure injection of liquid plastic into an aluminum mold placed around a taped splice bundle. The plastic quickly cools and hardens forming a water and pressure tight closure. To date, buried service wire terminations and buried non-pressurized copper cable splices have been successfully encapsulated in the field. Pressurized copper and fiber optic splices have been built in a lab environment and are currently being field trialed. Additional applications of this technology are being studied.

## Introduction

The key factors that telephone industry management are looking for when evaluating a splice closure system are:

1) reduced labour costs
2) reduced material costs
3) long term reliability resulting in decreased maintenance costs.
4) low craft sensitivity
5) completely integrated system that can be used in all outside plant construction.
6) air pressure retention and re-enterability in air core plant
7) safe method of installation

With these concerns in mind Northern Telecom, Bell Northern Research and Bell Canada have developed a new closure system. This unique system of molding protective closures in the field may be the final solution for all splice closure requirements.

## Field LPM Closure System

The field LPM system is a method of transporting liquid plastic to a jobsite and using the plastic to mold a splice closure around a specially prepared splice bundle in an aluminum mold. The plastic is carried in a thermal storage cannister called an injector. Two splice closures have been developed with applications for non pressurized and pressurized copper and fiber optic cables in the buried and underground Outside Plant environment. Development work is underway to use LPM for all splice closures in telephone plant.

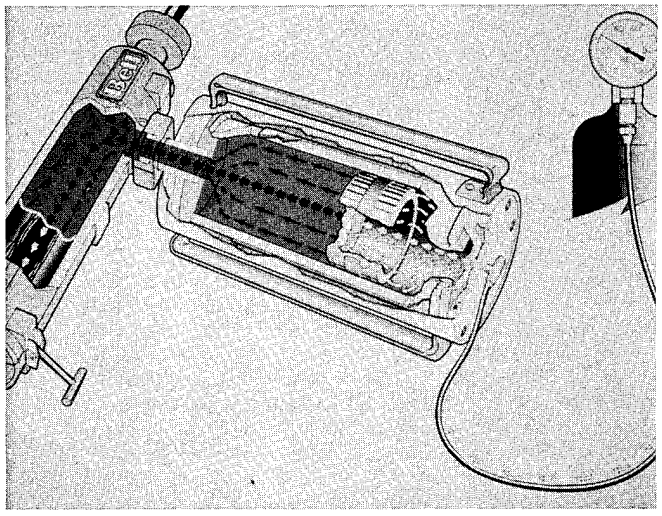



figure 1 LPM Closure System

The integrated LPM closure system provides many advantages over other splice closure systems. LPM is cost effective with savings approaching 75% of initial costs when compared to other closure systems. It has also proven to be more reliable than other systems in both the lab and field environments. The system is extremely flexible and is compatible with the existing material and tools currently in use in most telephone companies. It offers improvements in productivity and decreased long term maintenance costs. The system will ultimately fulfill all splice closure requirements.

## Background

LPM technology was developed because of recurring service problems experienced by Bell Canada with its buried plant. Investigations showed that the penetration of water into cable splices caused most of the failures in buried closures. Several different methods were tried to combat this problem; however, in all cases the long term reliability of each method was a major obstacle.

Bell Canada and Bell Northern Research personnel developed the LPM factory pretermination method. This technique has proven that it can provide the reliability demanded by Bell Canada.

The procedure for building these closures is straight forward. The wire splices and protective closures are made under controlled factory conditions. Service wires are spliced to the cable at predetermined points. The splice connectors are placed between layers of non-conductive ethylene polypropylene rubber (EPR) tape. Liquid plastic is injected from an extruder into an aluminum mold surrounding the splice bundle. As the plastic cools it shrinks forcing the EPR tape around the connectors providing a watertight seal. The plastic closure provides mechanical protection for the splice.

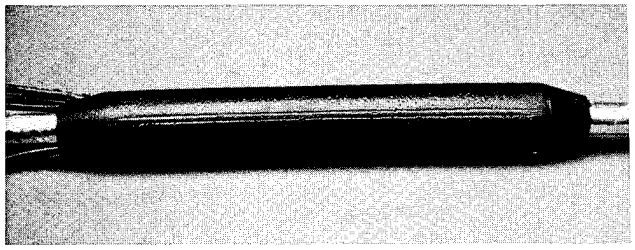


figure 2 LPM Preterminated Cable Splice

Since the technology was introduced in 1981 factory assembly lines have been established in three locations by Bell Canada and Northern Telecom to manufacture custom distribution cable. Approximately 45,000 splice closures have been placed without any service problems. This success lead to a joint research and development program between to devise a method to use this technology in the field.

## Equipment

Three special purpose tools have been developed to use LPM technology to mold splice closures in the field. They are injectors, extruders and aluminum molds. The injector is used to transport liquid plastic to the field splice location and to inject the plastic into the mold. The extruder liquifies the plastic and is one method of filling the injectors. The aluminum molds are placed around the prepared splice bundle and form the outer closure for moiding.

The injector consists of an insulated aluminum barrel with a free floating sealed piston housed in a protective outer shell. Each unit has thermostatically controlled heater bands which maintain the plastic in a liquid state and are capable of melting solid plastic charges. In some injector models additional heating capacity for the unit is provided by a centre core heating element. All injectors are equipped with a high temperature cut-off control as a safety backup for the thermostat. The injectors are designed to use 1500 Watts at 110 Volts AC and are compatible with house current or portable generators. A maximum of nine kilograms of plastic can be transported in a single injector.

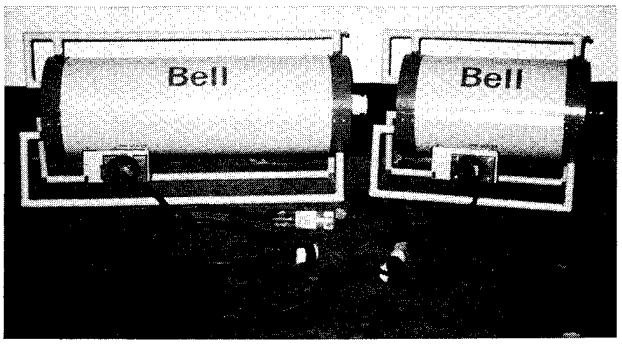



figure 3 Injectors

There are two methods of filling the injectors with plastic. The hot charge method requires an extruder. In this case the injector nozzle is connected to the extruder outlet. The extruder melts plastic pellets to a liquid state and extrudes it into the injector. Extruders are usually located in work centres where there are several injectors. The second method is to fill the injector with solid one kilogram plastic charges through a hinged cover. The injector heaters melt the plastic charges to the correct operational temperature in three hours.

The injector is equipped with indicators to show the amount of plastic in the injector, the heating time required and a plastic ready indicator. Work centres are equipped with injector storage cabinets where the plastic termperature is controlled by a seven day timer. The injectors which are cold charged at the end of the day by the technicians are turned on during the night ensuring that the plastic is ready for use in the morning.

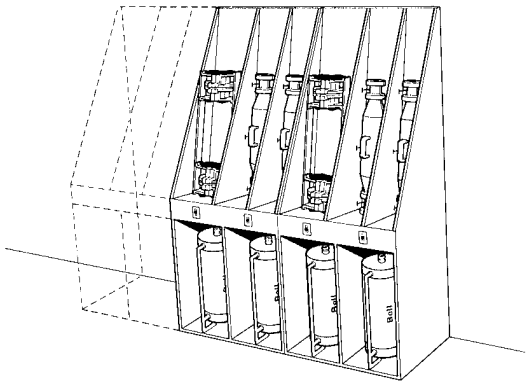


figure 4 Injector Storage Cabinet

Once the injector is transported to the jobsite the plastic is kept warm by the truck generator until all cable splicing operations are complete. The insulation in the injector will keep the plastic at a temperature suitable for molding for one and a half hours without any power being applied to the injector. This allows a great deal of flexibility in use.

After all the splicing operations have been completed the injector is connected to the aluminum mold and using air pressure 276 $kN/m^2$ gauge, the piston is advanced forcing the plastic into the mold. The injector is equipped with a safety pressure relief valve that operates at 345 $kN/m^2$ gauge preventing accidental over pressuring. The mold is filled until plastic comes running out the overflow port. The molds are then allowed to cool for approximatley fifteen minutes before they are removed exposing the completed splice closure.

A family of cast aluminum molds has been developed to cover the full range of cables used by Bell Canada. There are two basic mold configurations. One configuration is a light weight cast mold that forms a solid one piece closure for non pressurized applications. The other configuration is required for pressurized applications and consists of a pair of end disk molds.

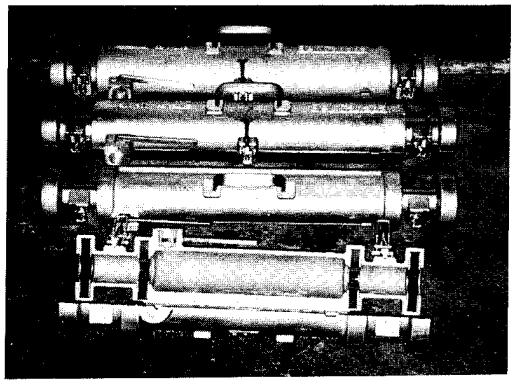


figure 5 Cast Aluminum Molds For Non-pressurized Splices

## Current Applications

Two applications have been developed for the LPM field closure system and a third application is currently under development.

The first application is the termination of buried service wires. This closure is prepared in the same way as the factory encapsulation. To prevent water from entering the splice from the unfilled buried service wire an EPR water dam is placed on the service wire. The connectors are buried in layers of EPR tape which is both moisture proof and non-conductive. A metal support bar is added to the splice to reduce the cable flexibility during molding. The LPM plastic contracts as is cools creating pressure forcing the EPR mastic around the connectors preventing the ingress of water. This closure is placed on 25 to 400 pair distribution cables. A maximum of six buried service wires and a ground wire can be terminated in one splice.

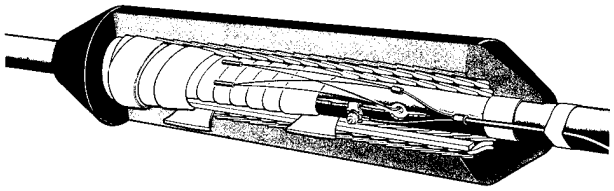


figure 6 Cross Section Of Buried Service Wire Splice

The second application developed is for buried non-pressurized splice closures. The major concern of Bell Canada Management was to prevent the penetration of water into the splice. Water enters the cable at sheath damage locations and migrates along the core of the cable to the splice. The use of filled core cable greatly reduces the migration of water along the cable but does not fully stop it. To obtain better performance against water penetration a trade off has been made with re-enterability.

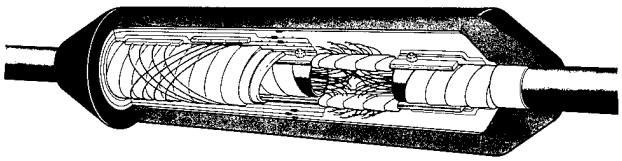


figure 7 Cross Section Of Buried Non-pressurized Splice

The preparation of the non-pressurized buried splice is similar to the buried service wire encapsulation. Two support bars are placed on either side of a small sheath opening 50 to 75 mm. The bars provide support and the electrical continuity of the cable sheath. As the cable is spliced the connectors are distributed along the splice opening to form a uniform splice bundle. Each layer of connectors is wrapped in a layer of EPR tape. After the final layer of EPR tape is placed the splice is wrapped completely in vinyl tape and molded. The heat of the LPM plastic softens the EPR tape. The liquid plastic contracts as it cools forcing the mastic around the connectors forming a watertight seal ensuring the integrity of the connectors.

A reenterable pressurized closure is the third application currently being developed. The pressurized design consists of a set of LPM end discs molded in place on the cables, manufactured sleeve, sealing interface and end disc support bars.

The pressure seal between the end disc and cable is formed by an EPR/DR tape wrap. When the end disc is molded the liquid plastic softens the EPR tape causing it to flow. As the LPM plastic cools it shrinks applying pressure to the contained tape and forming a pressure tight cable to end disc interface. Two metal fittings are molded into the discs to provide a ground lug and a pressure test valve. The molded end disc has three advantages over other cable to disc seals.

1. A single solid disc is formed for all multiple cable configurations.

2. The disc to cable seal is not dependent on the outer sheath of the cable being perfectly round.

3. A strain relief device is molded into each end disk. The strain relief device provides axial pull strength up to 5300 N that exceeds field requirements. This will eliminate sheath pull out problems.

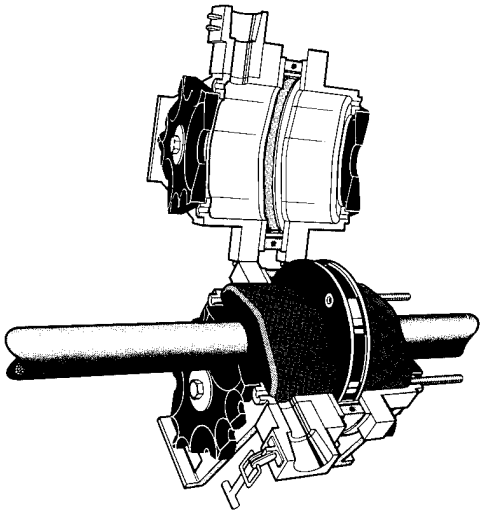


figure 8 LPM End Disc Mold

Four closure sizes are being developed; they are 115mm, 140mm, 200mm and 255mm diameters . These will accomodate the full range of pressurized copper cables up to 3600 pairs and as all fiber optic splice organizers.

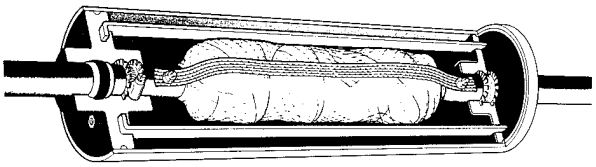


figure 9 LPM Pressurized Closure

Lab Test Program

Each LPM application has undergone an extensive lab test program before it was field trialed and introduced into general operations. Test samples were prepared at various temperatures between -10°C and 45°C. Table I is an outline of the major mechanical test parameters.

TABLE I

| Test | Criteria |
|---|---|
| Temperature Cycling | 50 cycles from -40°C to 60°C allowing the closure to stabalize at the temperature extreme. |
| Water Immersion | 50 cycles under 1m of water. |
| Freeze Thaw Cycling | 50 cycles in water. |
| Static Load | 1 $kN/5cm^2$ for 10 minutes. |
| Vibration | 5-500 hz for 2 hours on two planes. |
| Axial Pull | A static load is placed on cable to a maximum of 2750 N. |
| Impact | Weight is dropped with 20 joules of energy over full temperature range. |
| Static Pressure | 83 $kN/m^2$ gauge for 24 hours. |

The most rigorous test for non pressurized closures is the water immersion cycling test. The closure is immersed in 1 meter of water with the cable sheath removed adjacent to the closure to ensure that water penetrates the core of the cable. The temperature of the water is cycled so that the temperature of the closure varies between 2°C and 20°C. Insulation resistance between pairs must exceed $10^8$ ohms at all times.

The most rigorous test for pressurized closures is the dry temperature cycling test. The environmental chamber is cycled 50 times between -40°C and +60°C. The closure is allowed to reach the temperature extreme of each cycle before the temperature is reversed. There must be no loss of air pressure during this test.

## Economics

A detailed economic analysis of the field LPM system was conducted by Bell Canada. The study evaluated the net effect over ten years of introducing LPM technology. The applications evaluated were non-pressurized buried closures, pressurized copper closures, pressurized fiber optics closures and aerial terminals. Initially there is a large capital cost for tools; however, the overall system has savings of $14 million dollars (1984 dollars). The major savings result from lower initial material and labour costs and the long term reduced maintenance costs. The capital cost of the tools is recovered within 3 years.

## Future Applications

The economic and technical feasibility of several other applications for this system are currently being examined. Potential uses include aerial terminals, aerial closures, pressure plugs for fiber and copper cable, sheath to strand binds and building closures. These applications are being designed to use the exisiting sets of molds.

## Conclusion

There are many benefits associated with the LPM closure system. When fully developed LPM will provide a simplified closure system applicable to all splicing environments.

The solid non-pressurized closure provides protection for the connectors from water ingress that is superior to all other closure systems. The long term reliability of the non pressurized system will build confidence in the construction of completely out-of-sight plant. The pressurized closure combines reliability with ease of re-entry. Overall the system provides significant economic savings and a rapid payback of the initial capital investment.

## Authors



Ian H. Miller graduated from Queen's University at Kingston, Ontario with a B.Sc (Engineering Physics) in 1978. He joined Bell Canada in July 1978. He has worked in the Installation and Repair, Outside Plant Engineering, Outside Plant Construction, Regional Support and Regional Budget departments. Since January 1985 I. Miller has been working in the Headquarters Technology Development group on the LPM project. He is a member of the Association of Professional Engineers of Ontario, the Society of Management Accountants and the Canadian Association of Physicists.



J.L. (Jim) Horton received his BASc degree in Civil Engineering from the University of Waterloo in 1981. After graduation he joined Bell Canada in Toronto where he initially became involved with Outside Plant Structures Provisioning. He subsequently joined the Corporate Outside Plant Technology Development group originally assuming responsibility for structures design and is presently responsible for splice closure development. Jim is a member of the Association of Professional Engineers of Ontario.



J.R. (Jim) Scott graduated as a Mechanical Technologist from the Eastern Ontario Institute of Technology, Ottawa in 1964. Initially he worked in a manufacturing engineering capacity for Canadian General Electric before joining the Northern Electric R & D Division (now Bell-Northern Research) in 1966. Jim has worked on the design of the MINIBAR Switch, the LD4 Outside Plant System and various fiber optic projects. Jim presently manages the Splicing Systems department at BNR involved in design and evaluation of Outside plant hardware for both copper and fiber systems. Presently his major responsibility is the development of the LPM family of splice closures. Jim is a member of the Association of Professional Engineers of Ontario.



L.J. (Len) Charlebois joined the Northern Electric R & D Division (now Bell-Northern Research) in 1964 and has been responsible for the design & development of many Outside Plant products. Len has been instrumental in the evaluation and development of the complete family of splice closures using low pressure molding technology and presently holds over 14 patents on the system. Len is presently the LPM project leader and is a member of scientific staff at BNR.

# OPTICAL FIBER CABLE WITH PREMOUNTED MULTI-FIBER CONNECTOR

S. Tachigami, A. Ohtake, Y. Obara, S. Nakai, R. Yuguchi, Y. Kamata

The Furukawa Electric Co., Ltd., Chiba, Japan

## Summary

Small diameter and one touch quick connection assembly for the whole optical cable has been developed using multiple fiber connector to cut down installation cost drastically.

The successful installation and connection were confirmed in the field. Individually jacketed multiple fibers are terminated in a plastic molded plug in one plane with a specified pitch. These plugs are protected by connector housing and protection cover screwed on to the housing during installation and a pair of plugs and housings are mated at one time to complete a connection. "O" rings fitted in the housing keep inside of connector perfectly water-proof.

Eleven pieces of this type of connector premounted 8 fiber cables were applied to a field test. These were installed on to the poles and partially into duct. Most of the connection were completed within 3 minutes. Some of the connections were done before hunging on to the messenger wire almost at the middle of pole span. Some of the connected parts were pulled after connection to adjust the cable excess length at the poles. One connector assembly were attached to the cable in the field after installation.

Connection loss of each connection was measured by insertion loss measurment method during installation. Average connection loss were 0.16 dB.

After installation the total span loss including connections and cables was measured by OTDR method. No span loss change between just after and 6 months after installation was occured.

## 1. Introduction

It is widely known that the inefficiency in optical fiber cable joining is counted as one of the obstacles in constructing a public communication system using optical fibers.

For instance, when joining optical fiber cables with the fusion splicing, each optical fiber must be spliced by fusion splicing and the splice points must be accommodated in the sleeve together with their excess length, and further the cable sheath must also be joined. Consequently this mehtod of joining involves various defects such as that it requires skill and takes a long time.

Therefore, we have developed a optical fiber cable with premounted multi-fiber connector.

Features of the optical fiber cable with premounted multi-fiber connector (the connector premounted cable) in the connection work are considered as follows:

(1) Reduced work time and man power required.
(2) Non-skilled work with no special tools.
(3) Small work space required.
(4) No limitation to the location of connecting points.
(5) No need for connection loss measurement.

## 2. Constitution and Applications of the Connector Premounted cable

### 2-1 Basic constitution

The multi-fiber plug used in this study is shown in Fig.1. Up to eight optical fibers can be connected at one time using this plug. The plug is an extension of the low loss 5-fiber plug.[1,2,3] Detailed construction of the plug will be described in the following section.

Following two types are considered as connector premounted cables using this plug.

(1) Housing accommodated type (Fig.2-(a))
In this type, a multi-fiber plug is accommodated in a waterproof housing at the factory. It is used mainly for those cables with eight or less fibers.

(2) Sleeve accommodated type (Fig.2-(b))
Only the multi-fiber connectors are attached to the cable at the factory and the connectors are acommodated in a protection sleeve at the site. It is applied mainly to those cables with nine or more fibers.

As the features separately applicable to each type, type (1) allows one-touch connection as well as achieving a small diameter of the joint and type (2) can cope with multi fiber cables while facilitating branching.

Because either type of cable has connectors at both ends, the cable length can be uniformed.

The detailed constructions are as described in the following section.

## 2-2 Applications of the connector premounted cable

An example of the application of the connector premounted cable is shown in Fig. 3. Straight connection of the cable is very easy.

Branching and connection to the transmitter at the cable end can be achieved also easily using a split cable as shown in Fig.3.

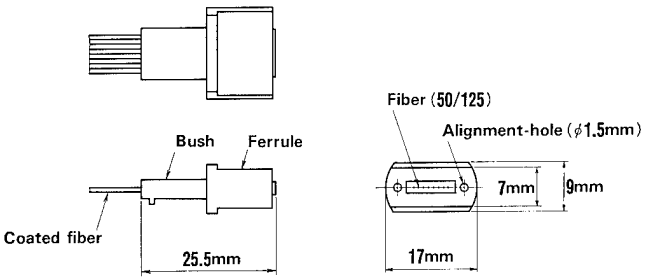
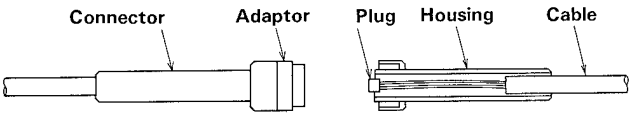
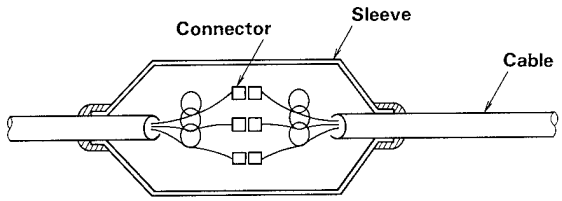



Fig.1
**Construction of Multi Fiber Plastic Plug**




**(a) Housing type**




**(b) Sleeve type**

Fig.2
**Fiber Connector Premounted Cable**

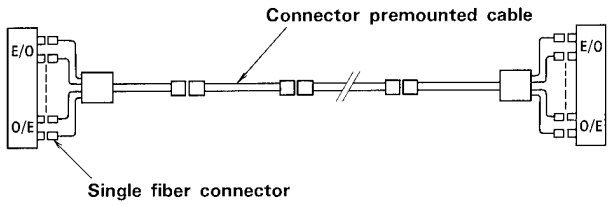



Fig.3
**Application of Connector Premounted Cable**

## 3. Structures of the Connector

### 3-1 Multi-fiber plug

The structure of the plug is shown in Fig.1.

The end face of the plug is 7 mm (t) X 17 mm (W), which has two alignment holes with a diameter of 1.5 mm for inserting aligning guide rods. Up to eight optical fibers are arranged at fixed pitches on the line that connects the centroids of these holes. A 0.9 mm pitch is used considering the applicaiton to those fibers with 0.9 mm outer diameter that are used in Japan as the standard. Since the alignment holes and the fibers are positioned in a high accuracy, eight fibers can be connected at a time by using this plug.

This plug is made from plastics (epoxy resin) through high accuracy molding, in which, the mold has a V-groove with sub-micron accuracy, a transfer molding is performed with the fibers and guide rods placed into these grooves. The end face of the optical fibers are polished as a mirror surface after curing the resin.

### 3-2 Housing and sleeve

#### (1) Housing accommodated type

The connector of this type is consisted of the multi fiber plug and its housing. The plug is accommodated in a housing, and the housing can join the cable sheath. So, connecting the connectors can complete joining the cables. Further, the housing acts as a pulling eye.

The structure of the housing type is shown in Fig.4.

The multi-fiber plug described in the above is accommodated in the inner housing and further this inner housing is accommodated in the outer housing in a manner where it can slide freely via a spring. To enable one touch connection, sub-guide rod is attached to the inner housing and such a method is employed where the connector guide rod is inserted along this sub-guide rod.

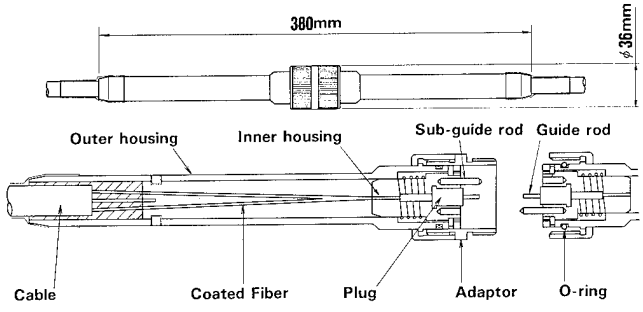



Fig.4 **Construction of Housing Type**

The tension-member and cable sheath are fastened to the outer housing using resin to give the outer housing a function to join the cable sheath.

The connectors are connected using an adaptor to eliminate their male and female discrimination. It is also waterproofed with an O-ring.

Using this housing, the cable joining can be completed easily within a short time by inserting the plug and screwing a protection cover on to the adaptor. The state where the connectors are connected has such a small diameter as a maximum outer diameter of 36 mm and a total length of 380 mm as shown in Fig.4.

(2) Sleeve accommodated type

The sleeve and housing used for the sleeve accommodated type is shown in Fig.5. In this type only the multi-fiber connectors are premounted to the cable at the factory and connectors are accommodated in a protection sleeve at the site. The multi-fiber plug which is shown in Fig.1 is connected by using a housing, and accommodated in the sleeve together with the fiber excess length at the site. The housing is made in a small size so as to be accommodated in the sleeve. The sleeve can join the cable sheath and is waterproofed.

As a few connectors are accommodated in one sleeve, joining of those cables with nine or more fibers and branching can be easily made.

## 4. Evaluation of the Connector

Table 1 shows the evaluation test items and their test conditions.

### 4-1 Results of plug evaluation

(1) Connecting loss

The setup for measuring the connecting loss of the multi-fiber plugs is shown in Fig.6. The result of measurement are shown in Fig.7.

The GI type optical fiber with a core diameter of 50 μm and outer diameter of 125 μm is used. Connecting loss measured using matching grease for 62 plug samples (496 optical fibers) was 0.16 dB as an average. Even the maximum value was 0.6 dB, which is considered to cause no problem in actual uses.

(2) Heat cycle test

The multi-fiber plug was attached to the end of eight fibers with 5 m length, and it was exposed to the heat cycles of -30° to 60°C, 4 cycles/day for 20 days. The variation in loss are shown in Fig.8. It can be understood that the variation during the heat cycle cause no practical problem.

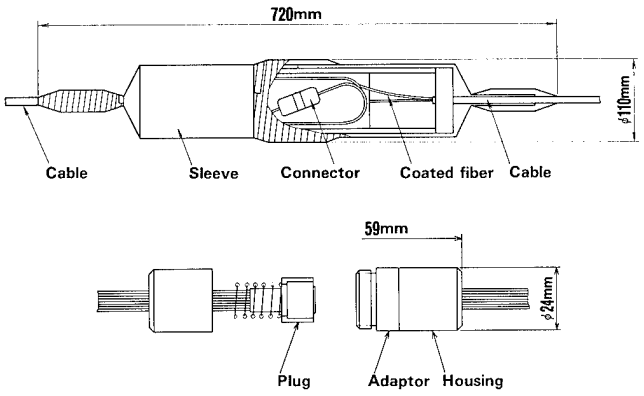



Fig.5 **Construction of Sleeve Type**

Table 1 **Reliability Test Condition**

| Item | Condition | The Number of Samples | Estimation Method |
|---|---|---|---|
| Heat Cycle | −30℃~60℃ 4 Cycle/day | 6 (3 couples) | Loss Increase |
| Humidity | 60℃×95%RH | | |
| High Temperature | 80℃ | | |
| Low Temperature | −20℃ | | |
| Vibration | Frequency : 10 Hz<br>Amplitude : 10 mm<br>Direction : Radius<br>Time : 30 hrs. | | |
| Tensile test | Chucking span : 400 mm | | Tensile Strength |
| Squeezing | Radius : 250 mm<br>Tension : 100 kg | 4 (2 couples) | Loss Increase |
| Water proof test | Submerging in water | 6 (3 couples) | |
| Connecting and Disconnecting | 200 times | | |

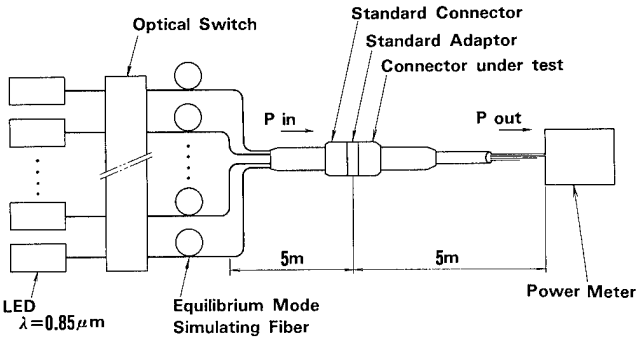



Fig.6
**Mesurement Setup of Multi Fiber Connector**

(3) Humidity test

The same samples used for the heat cycle test was put into a humidity test chamber with 60°C x 95%RH. The variation of loss before and after the humidity test is shown in Fig.8. It can also be understood that the variation under the himidity cause no problem.

(4) High- and low-temperature tests

The same samples as used in the above is used for these tests. The samples exposed to the high temperature of 80°C for 20 days and a low temperature of -20°C for 20 days. The results are shown in Fig.8. Both results show that there is no problem.

## 4-2 Evaluation of the plug and housing

The evaluation on the characterisics of the housing accommodated type, in particular, is performed in this section.

(1) Vibration test

A vibration test was made by attaching the multi-fiber plug and housing to the end of the cable as shown in Fig. 9 and joined via an adaptor.

The result is shown in Fig.8. It can be seen that the variation of the connecting loss is on a level which causes no problem.

(2) Tensile strength test

Fig.10.shows the method for the tensile strength test. The cable used is the same as in Fig.9. The tension member used in this test is galvanized steel wire with an outer diameter of 2.6 mm. It has been proved to have a 150 kg tensile strength, which is considered enough for installation.

(3) Squeezing test

Fig.11.shows the method of the squeezing test.

A metal wheel with a radius of 250 mm was used for this test, and five times of round-trip squeezings were made with an angle of 135° and a tension of 100 kg.

The variation in loss after the test is as shown in Fig.8 and considered to causes no problem in cable installation.

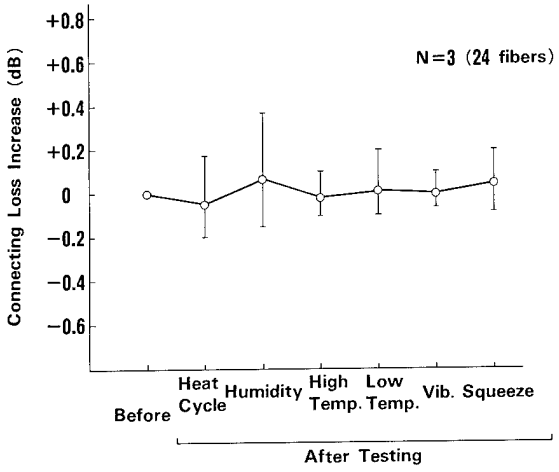



Fig.8 **Connection Loss Chage Before and After Reliability Test**

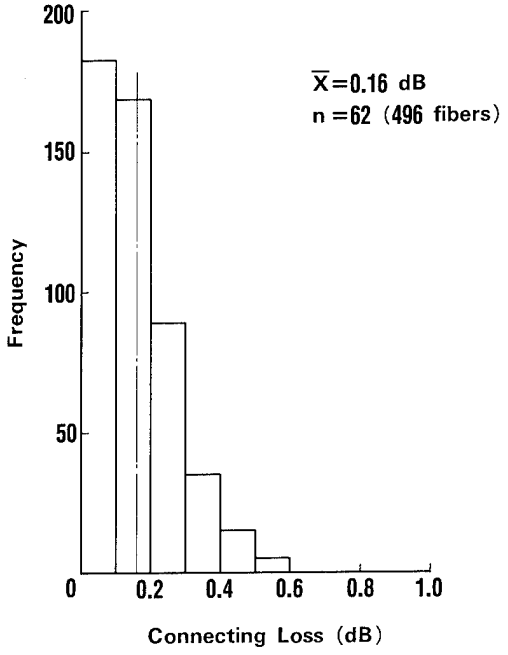



Fig.7 **Connecting Loss**

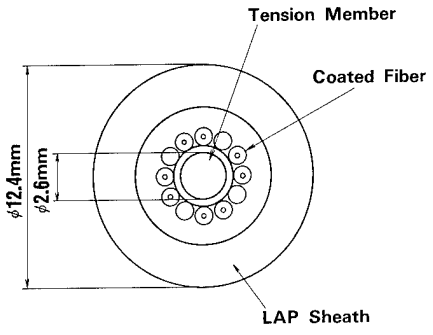



Fig.9 **Optical Fiber Cable**

(4) Waterproof test

A pair of connectors was connected and was soaked into a water tank of 50 cm depth for 5 days. No water intrusion into the connector was detected and also no variation in loss was caused. Therefore the waterproof characteristic at the time of connection is considered sufficient.

(5) Repetitive connecting and disconnecting test

The muiti fiber plug and housing were attached to an end of 5 m cable and connecting and disconnecting were repeated 200 times while measuring the loss in the manner as shown in Fig.6. The result is shown in Fig.12.

The variation in the connection loss was less than 0.1 dB and confirmed to cause no problem in practical use.

4-3 Field test

As described in the items above, a satisfactory result was obtained from the evaluations in the laboratory. Then the field test was performed.

(1) Installed cables

The structure of the installed cable is the same as that in Fig.9. It is a 8 fiber cable.

A housing accommodated type connector was used and the plug and the housing were premounted at the factory.

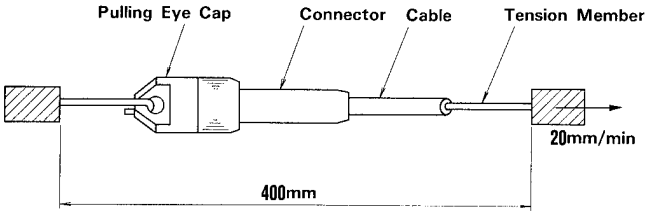



Fig.10 **Tensile Test Method**

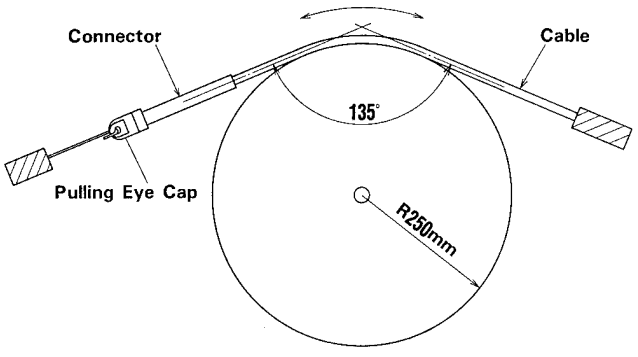



Fig.11 **Squeezing Test Method**

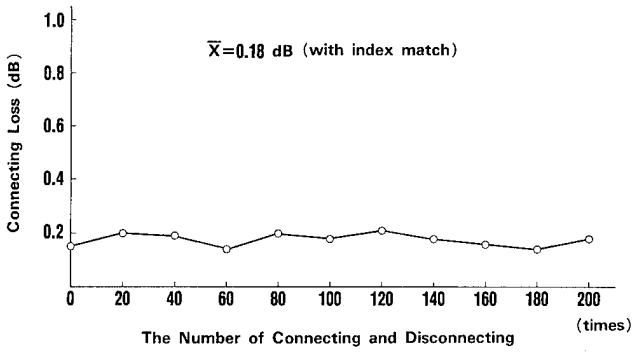



Fig.12

**Result of Connecting and Disconnecting Test**

(2) Field test

The route for installation is as shown in Fig.13. Eleven pieces of cables were installed. Some of them installed into duct, and most were on to the poles. Though almost all connectors were the housing accommodated type as stated in the above, only one connector was attached at the site using the sleeve accommodated type at the point (A) in the Fig.13. Though some of the joints were connected before they were hung on to the messenger wire and their joints were located between the poles, they caused no problem due to relatively a small outer diameter of the joints.

Connecting work even using the matching grease completed within a 3 minutes at most points and the work efficiency at the site was thus proved.

Incidentally, also the tension applied to the cables and connectors after installation to adjust the cable excess length caused no problem.

The connecting loss was measured at each joint with the insertion loss measuring method and the results of measurements are shown in Fig.14. The average connecting loss was 0.16 dB, which was on the same level as that obtained in the laboratory. Incidentally, the total loss after installation including connections and cables can be

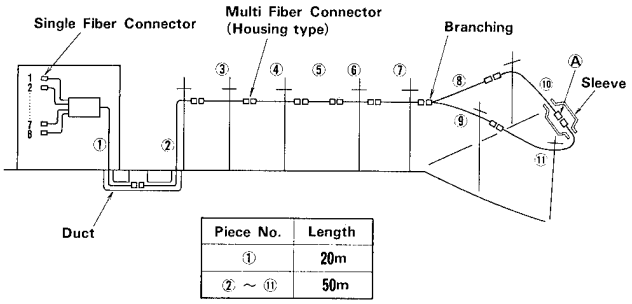



Fig.13 **Installed Cables**

measured with also the OTDR method.
The variation in the total loss within 6 months after installation are shown in Fig.15. It shows that stable characteristics can be obtained over a long period.

## 5. Other Applications

### 5-1 Application to another types of cables

As described in the above, we evaluated by using one type of optical fiber cable. However, the connector premounted cable is applicable to all optical cables irrespective of their structures. For instance, it is applicable to Ny, UV and FRP coated fibers, applicable to galvanized steel and FRP rod as the tension member.

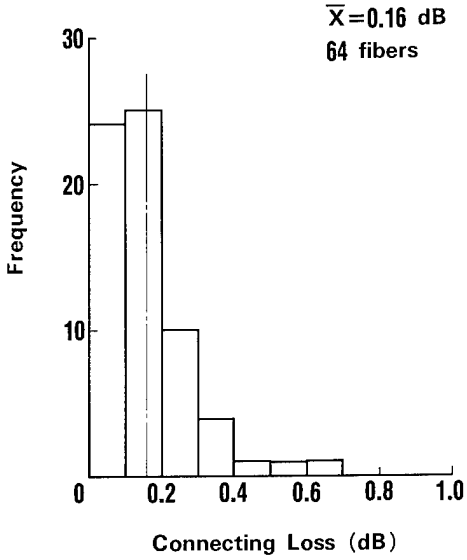



Fig.14
**Connecting Loss of Installed Cables**

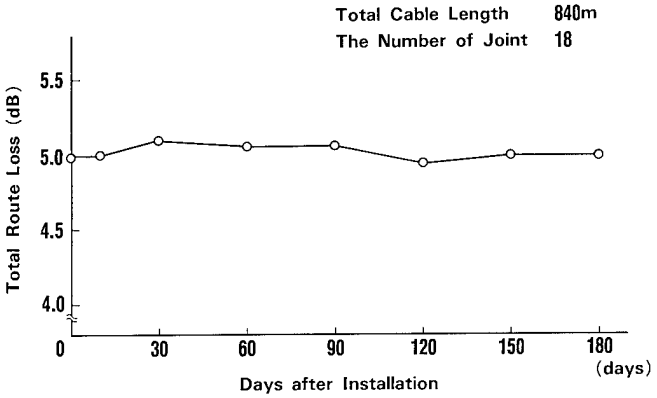



Fig.15 **Loss Change After Installation**

### 5-2 Application of a cable in which optical fibers and metal cores are combined

Though the connector premounted cables described in the above are all those where only optical fibers are contained, this connector premounted cable can also be applied to an optical metal complex cable, where the metal cores for power transmission are contained together with optical fibers.

A prototype of the connector for use with an optical metal complex cable is shown in Fig.16. The multi fiber plug used here is the same as that shown in Fig.1. The maximum outer diameter and total length of a joint are 39 mm and 380 mm respectivly. By the use of this connector, two pairs of metal cores and eight optical fibers can be easily connected at a time in a compact manner.

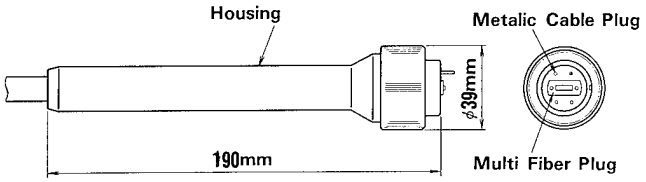



Fig.16
**Optical-metal Complex Connector**

## 6. Conclusion

We have developed an optical fiber cable with premounted multi-fiber connectors that facilitates cable joining at the site. The results of examinations are as described below.

1) We have proposed two types of connector premounted cable: housing accommodated type and sleeve accommodated type. In comparison with the conventional splicing method, the cable can be joined very easily and the joining work time is reduced so much. The joint of the housing accommodated type is such a small size as a maximum outer diameter of 36 mm and a total length of 380 mm.
2) The connecting loss was 0.16 dB with the matching grease. It satisfied various reliability test and a sufficient strength for installation was also confirmed.
3) An installation test was performed using the housing accommodated type and it proved its characterisics that cause no problem in installation as well as its high work efficiency. The average connecting loss was 0.16 dB for each joint (with matching grease). It was proved to facilitate cable joining with a low level of loss.
4) This connector premounted cable can be applicable to all types of optical fiber cables and optical metal complex cables.

## 7. Acknowledgement

We would like to express our appreciation to Mr. M. Azuma and Mr. S. Inao of Chiba Research Laboratory of the Furukawa Electric Co., Ltd. for valuable guidance and advice in this developing project. We are also gratefull to Mr. T. Iso, Mr. T. Hayashi, and Mr. K. Motai of the company for many helpful contribution in manufacturing and evaluation of the connector premounted cable.

## 8. References

(1) T.Satake, et al., "Low-Loss Plastic Molded Optical Fanout", J. Lightwave Technol. vol-LT-3, 1985 (to be published)
(2) M. Oda, et al., "Nylon Extruded Fiber Ribbon and its Connection", OFC, 1982.
(3) S. Tachigami, et al., "Fabrication and Evaluation of a High Density Multi Fiber Plastic Connector", IWCS, 1983.

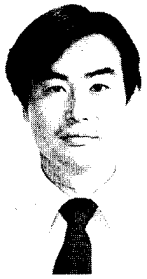


Shigeru TACHIGAMI

The Furukawa Electric Co., Ltd.
6 Yawata-Kaigan-Dori,
Ichihara, Chiba, Japan

Mr. Tachigami graduated from Tohoku Univ. 1970 with a B. Sc. in mechanical engineering. Then he joined The Furukawa Electric Co., Ltd. and has been engaged in research and development to telephone cable and the accessories. He is presently engaged in research and development of accessories of optical fiber cable.

Mr. Tachigami is now a manager of Fiber Optics Apparatus Group, Chiba Research Laboratory, Research & Development Division. He is a member of the Institute of Electric Engineers of Japan.

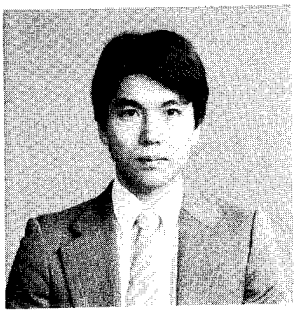


Akihiro OHTAKE

The Furukawa Electric Co., Ltd.
6 Yawata-Kaigan-Dori,
Ichihara, Chiba, Japan

Mr. Ohtake graduated from Tohoku Univ. 1974, and joined The Furukawa Electric Co., Ltd. in 1974 and has been engaged in development of coaxial cables, optical fiber cables, and now development of accessories of optical fiber cables.

Mr. Ohtake is now an assistant manager of Fiber Optics Apparatus Group, Chiba Research Laboratory, Research & Development Division at The Furukawa Electric Co., Ltd. and a member of the Institute of Electronics and Communication Engineers of Japan.

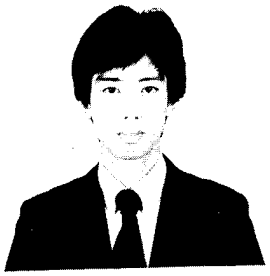


Yuichi OBARA

The Furukawa Electric Co., Ltd.
6 Yawata-Kaigan-Dori,
Ichihara, Chiba, Japan

Mr. Obara graduated from Keio Univ. 1974 with a B. Sc. in phyisical engineering then joined The Furukawa Electric Co., Ltd. and has been engaged in research and development of the accessories for the telecommunication systems.

Mr. Obara is now an assistant manager of Electronics Eguipments Research Section, Chiba Research Laboratory, Research & Development Division at the Furukawa Electric Co., Ltd. and a member of the Institute of Electronics and Communication Engineers of Japan.

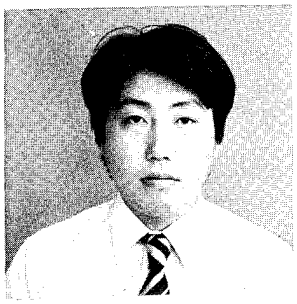


Renichi YUGUCHI

The Furukawa Electric Co., Ltd.
6 Yawata-Kaigan-Dori,
Ichihara, Chiba, Japan

Mr. Yuguchi graduated from Tokyo Institute of Technology 1984 with a M. Sc. in mechanical engineering. Then he joined the Furukawa Electric Co., Ltd. and has been engaged in research and development of fiber optics apparatus.

Mr. Yuguchi is now a staff engineer of Fiber Optics Apparatus Group, Chiba Research Laboratory, Research & Development Division at The Furukawa Electric Co., Ltd. and a member of the Institute of Electronics and Communication Engineers of Japan and also a member of the Japan Society of Mechanical Engineers.

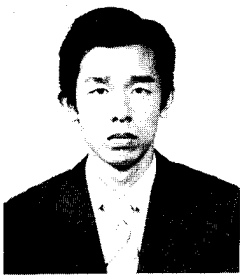


Shinichiro NAKAI

The Furukawa Electric Co.. Ltd.
2-5-1, Okano,
Nishi-ku,
Yokohama, Kanagawa,
Japan

Mr. Nakai graduated from Toyohashi University of Technology 1983 with a M. Sc. in information engineering, then joined The Furukawa Electric Co., Ltd. and has been engaged in research and development of fiber optics apparatus.

Mr. Nakai is now a staff engineer of Optical-Electronic Devices & Components Department, Electronics & Communications Systems Division at The Furukawa Electric Co., Ltd. and a member of the Institute of Electronics and Communication Engineers of Japan.



Yoshiyuki KAMATA

The Furukawa Electric Co., Ltd.
6 Yawata-Kaigan-Dori,
Ichihara, Chiba, Japan

Mr. Kamata graduated from Chiba Univ. 1983 with a B. Sc. in electronics engineering then joined The Furukawa Electric Co., Ltd. and has been engaged in development of the optical fiber cable.

Mr. Kamata is now a staff engineer of Optical Fiber Transmisson Group, Chiba Research Laboratory, Research & Development Division at The Furukawa Electric Co., Ltd. and a member of the Institute of Electronics and Communication Engineers of Japan.

# High Strength Splice with Restoration Coat of Optical Fiber for Cabling

T. Kakii, Y. Suetsugu, S. Tanaka

Sumitomo Electric Industries, Ltd.
1, Taya-cho, Totsuka-ku, Yokohama, Japan

## Summary

Arc fusion splice with restoration coating up to the nominal coating diameter is proposed in the submarine cable field to obtain the super-long length fiber. Applicability of this technology to the terrestrial cables is studied, where more severe environmental conditions are encountered such as wide temperature range from -40 °C to 80 °C, small bending radius etc. In conclusion, the developed high strength (average 450 kpsi) arc fusion splice of fibers with mold reinforcement showed sufficient mechanical and environmental performances for the practical application. Predicted longterm reliability is of equivalent quality to that of unspliced fibers. The experimentally fabricated cables containing the proposed splices showed the sufficient performance. This technology will promise the stable mass production of ultra-long fiber cables.

## 1. Introduction

High strength fiber splicing with restoration coating is commonly used in the field of submarine cables [1][2]. This is because the optical submarine cables require high strength fibers and continuous long cable lengths. Thus fibers of limited length after high level screening are spliced together to form a continuous long length fiber. The spliced sections of the fibers in the submarine cables usually experience mild conditions. For example, the cable temperature in the operation condition is approximately 0 °C, neither at the extreme high temperature nor at the extreme low temperature. During cable installation the cable rarely experiences the abrupt bending which is often the case with terrestrial cables.

In this paper, we examine the performance of high strength fiber splices with mold coating when applied to the terrestrial cables. First, we describe the structure and characteristics of high strength fiber splicing with mold recoating. Then these splices are applied to the typical terrestrial cables, and cable performance is examined with thermal cycling experiments and installation simulation. Throughout the experiments the fiber splices with mold recoating showed satisfactory performances.

The technology described in this paper promises improved productivity in the field of ultra-long length cables.

## 2. High strength splicing

### 2-1 Reinforcement structure [3]

Figure 1 shows the developed structures of fusion splice with mold reinforcement. For the mold reinforcement, three structures have been developed. Figure 1(a) shows a structure for the UV curable resin coated fiber [type-A]. Figure 1(b) shows a structure for the first coated fiber splice and continuous secondary coat extrusion [type-B]. Figure 1(c) shows a structure for the splice of already primary and secondary coated fibers [type-C]. Each molded material is chemically compatible with the original coated layer. Furthermore, the molded diameter is essentially equal to that of the original coated fiber. Therefore, the high strength splicing structure can withstand bending stress exerted on the coated optical fiber and prevent the concentration of any stress in the spliced portion. The continuity of flexibility and diameter between the spliced segment and the original coated fiber provides high reliability of the spliced segment.

For structures of type-A, the diameters and lengths of the molded segments are typically 0.4 mm and 15 mm, respectively. For type-B structures, the molded portions are the same as type-A with the continuous extrusion applied as reinforcement. The final molded length after double reinforcement for the first and second coatings is 30 mm, in type-C structures.

With the above described mold reinforcements, it is possible to generate a long coated optical fiber from spliced sections, without seriously altering the original coating structure.

### 2-2 Procedure of high strength splicing

Figure 2 and Figure 3 show the procedure of high strength splicing for types A, B and C.

For type-A splices, a UV curable coated fiber of 0.4 mm diameter is prepared. In the first step, the coated fiber is cleaved through coated layer using an automatic cleaving machine. Next, the UV curable coated layer is removed by immersion in a hot concentrated sulfuric acid bath. The final bare fiber length is about 7 mm. Fibers are then spliced together by arc fusion using the splicing machine. During fusion splicing procedure the fibers are secured by clamping only the coated areas in order to avoid mechanical damage to the bare glass surface. After high strength splicing, two-pieces-split-type mold is used to apply a UV curable coating to the bare fiber portion. This restores the diameter to that of the original coated fiber. Finally, the spliced portion with mold reinforcement is subjected to a 2.5 % elongation strength proof test to ensure the minimum strength. Furthermore, with respect to type-B splices, continuous secondary coat extrusion is provided over the above described fiber containing type-A splices. For type-C splices, the nylon coated layer and the silicone buffered layer are removed by using a wire stripper and by immerising in hot concentrated sulfuric acid, respectively. After high strength splicing, double mold reinforcement, using silicone and nylon, is applied. The mold reinforcement lengths of silicone and nylon are 15 mm and 30 mm, respectively. Finally, the spliced portion is subjected to a 2.5 % elongation strength proof test to ensure the minimum strength.

## 2-3 Characteristics of high strength splicing

### 2-3-1 Cleaving for high strength splicing

To avoid mechanical damage to the bare glass surface, the fiber is cleaved by gripping coated fiber and cracking the glass surface through the coated layers. Figure 4 shows the cleaving angle distribution achieved by the high strength splicing automatic cleaving machine. The average cleaving angle is approximately 1 degree. This is significant because the cleaved angle greatly affects single-mode fiber splice loss. This automatic cleaving machine allows for splicing loss less than 0.2 dB even for the single-mode fiber.

### 2-3-2 Removing the coating layer

Contaminants on glass surfaces induce degradation of splice strength at the melting joint. Consequently, complete removal of the coating is required. In order to avoid mechanical damage to bare glass surfaces, two methods of coat removal: (i) chemically, using hot concentrated sulfuric acid, and (ii) mechanically, using special equipment; have been developed. The mechanical device is shown in Figure 5. This equipment consists of two felt rollers dampened with acetone. The contact force of these rollers is regulated by a spring to prevent cracking of the fiber surface. Uncoated fibers of as high as 5 % elongation strength have been obtained by keeping the stripping force along the fiber axis less than about $5 \times 10^{-2}$ N [4]. The choice of chemical or mechanical stripping methods is dependent on individual circumstance.

### 2-3-3 Splicing

After coat removal, each uncoated fiber is set on a "splicing machine of coat clamping type". It is important for the uncoated fiber to avoid contact with other objects and to be spliced in a clean atmosphere. The tested fibers were single-mode and multi-mode fibers, coated in-line with UV curable acrylate to a nominal 0.1375 mm thickness. Figure 6 shows splice loss distributions of single-mode and multi-mode fibers. The average splice losses of single-mode and multi-mode fiber were approximately 0.1 dB and 0.05 dB, respectively.

### 2-3-4 Mold reinforcement

After high strength splicing, the spliced portion is molded with the material which is chemically compatible with the original coating layer. Tyep-A splices are finished using a UV curable resin molded onto the spliced bare fiber. The split type mold consists of two pieces, one of which is of metal and the other one is of glass. After UV curable resin molding, UV radiation is applied to the molded resin through the glass portion of the mold. Molding accuracy is determined by the diameter of the mold and the shirinkage of the resin. The resultant diameter is typically within ± 0.01 mm of the original coating. To produce type-B splices, nylon is extruded over a type-A fiber splice, yielding a continuous nylon coated optical fiber. The final diameter of the spliced region is within ± 0.05 mm of the nominal diameter. On the other hand, in type-C mold reinforcement, double reinforcement of silicone and nylon is provided to the spliced area using the proper molds. The diameter of the double reinforced portion is found to be within a range of 0.9 mm plus or minus 0.05 mm. After reinforcement, 2.5 % elongation proof testing of the reinforced portion ensures the minimum strength. Figure 7 shows an example of the strength distributions of type-A. The mean strength of type-A is about 455 kpsi.

## 2-4 Reliability

A number of tests have been performed to confirm the long term reliability of spliced portions. Essentially, the same performance was obtained for all three types of fiber splice. In the following sections, test results for type-A are described as examples. Proof testing at 2.5 % elongation strength was performed for all samples.

### 2-4-1 Initial tensile strength

Figure 8 shows the initial tensile strengths used in the reliability tests. The average measured tensile strength of 10 high strength splice

portions, all having passed the minimum proof tests, were about 446 kpsi. The tensile speed and the length were 100 mm/min and 200 mm, respectively.

### 2-4-2 High temperature/humidity test

During the high temperature/high humidity tests were subjected to temperatures of 60 °C and 95 % R.H. for 30 days. Figure 9 shows the distribution of tensile strength after 30 days. Average measured tensile strength were approximately about 432 kpsi. There was no significant degradation in tensile strength over in the circumstances of high temperature and high humidity.

### 2-4-3 High temperature test

Considering the high temperature encountered during the cabling process, sometimes as high as 150 °C, the performance at the extreme high temperature was examined. The splices were tested at a temperature of 150 °C for one half hour. Figure 10 shows the distribution of tensile strength after the test. The average measured tensile strength of the 10 spliced portions was approximately 472 kpsi. There was no degradation by the 150 °C high temperature test. The experimental results indicated that the cabling temperature is not serious problem for spliced segments.

### 2-4-4 Low temperature test

To simulate cable installation in cold climates, low temperature tests were carried out at a temperature of -40 °C for 30 days. Figure 11 shows the distribution of tensile strength. Average measured tensile strength of the 10 spliced segments was approximately 442 kpsi. Therefore, experimental results indicate that there was no significant degradation by low temperatures.

### 2-4-5 Thermal cycling test

The thermal cycling test consists of cycling the fibers between -40 °C and 80 °C, for 100 cycles at 6 hours/cycle. Figure 12 shows the distribution of the tensile strength after the thermal cycling test. Average measured tensile strength of the 10 spliced segments was approximately 468 kpsi. Therefore, experimental results indicate that there was no significant degradation in tensile strength due to thermal cycling. The relationship between reinforced splice loss and temperature variation was also measured during this test. Figure 13 shows the experimental results. The reinforced splice loss varied by only 0.02 dB/splice in the temperature range from -40 °C to 80 °C. The experimental results indicate that the reinforced splices have a stable structure for temperature change.

### 2-4-6 Repetitive bending and torsion test

Repetitive bending and torsion tests were performed to confirm the mechanical stability of spliced segments. Table-1 shows the test condition of 7 samples for each test. No fiber breakage was found in under $10^6$ twists or bends.

### 2-4-7 Minimum bending radius

In conjunction with the tensile strength, minimum bending radius is one of the most important parameters for cabling the spliced portion. The minimum bending radius has been examined by winding several turns of fibers containing spliced segments. Figure 14 shows the experimental results of minimum bending radius test with 12 samples. The results confirmed that the minimum bending radius of spliced segments is not a serious problem for cabling spliced fibers.

### 2-4-8 Water immersion test

Water immersion tests have been performed at a depth of 5 cm in room temperature water for 30 days. Figure 15 shows the distribution of the tensile strength after the test. The average measured tensile strength of the 10 spliced segments was about 438 kpsi. Experimental results indicate that there was no significant degradation in tensile strength.

### 2-4-9 Dynamic fatigue test

In order to confirm the long term reliability of spliced segments dynamic fatigue tests have been performed at five levels of strain rate 5 %/min, 10 %/min, 25 %/min, 50 %/min and 250 %/min. Figure 16 shows the experimental results of the dynamic fatigue test of the spliced sections. The fatigue parameter N value was found to be about 28, which is almost equal to that of original unspliced fibers. The results show that the long term reliability of spliced portion is very similar to that of unspliced fiber for fatigue characteristics.

## 3. Fabrication of cables with proposed fiber splice

### 3-1 Cable structure

Based on the preliminary study on the splice structure, two optical fiber cables shown in Figure 17 and Figure 18 were experimentally fabricated. Figure 17 shows the structure of the fabricated 4-fiber spacer cable which contains 4 UV curable resin coated fibers of 0.4 mm diameter stranded into grooves of the spacer. Two fibers are single-mode fibers and two are multi-mode fibers. Each fibers contains 10 serial type-A splices in its length. The fiber parameters of the single-mode fiber are as follows; the mode-field radius at 1.3 μm wavelength $W_0$=5 μm ; effective cutoff wave-

length λce=1.2 μm; and the fiber diameter D=125 μm. The multi-mode fiber is a graded-index multi-mode fiber. The core diameter is 50 μm, outer diameter is 125 μm and relative refractive index difference is 1%. The spacer of 3.5 mm diameter contains a steel wire of 1.3 mm diameter as a central strength member. The cable diameter is 7.6 mm.

Figure 18 shows the structure of the fabricated 14-fiber cable in which 14 nylon coated fibers of 0.9 mm diameter are stranded around a central strength members. The glass fiber of 125 μm diameter is coated with a UV curable resin to 400 μm diameter and with nylon to 900 μm diameter. The central strength members consists of a steel wire of 2.4 mm diameter with polyethylene steath of 3.3 mm diameter. The 7 of the fibers are single-mode and 7 are multi-mode. Each fiber contains 10 serial splices of tyep-A or C in its length. The parameters of the fibers are the same as those in the 4-fiber spacer cable. The cable diameter is 14 mm.

## 3-2 Transmission characteristics

### 3-2-1 Transmission loss changes during cabling process

Figure 19 and Figure 20 show measured transmission loss changes during cabling process of the 4-fiber spacer cable and the 14-fiber cable, respectively. Optical transmission loss changes at 1.3 μm wavelength of single-mode and multi-mode fibers, each of them having the 10 serial splices in its length, were examined during the cabling process and found to be less than ± 0.03 dB/km. The measured cable length of both types were 100 m. Taking into account the accuracy of the cut back measurement method, it is concluded that no loss change was incurred during the cabling process.

### 3-2-2 Transmission loss changes due to temperature

The tested cable length of both types was 100m. The two single-mode fibers and two multi-mode fibers in the cable, respectively, each containing 10 serial splices, were spliced to form a 200 m long optical fiber link. The optical transmission loss was continuously monitored at 1.3 μm wavelength. Figure 21 and Figure 22 show the measured optical transmission loss changes due to temperature of the 4-fiber spacer cable and the 14-fiber cable, respectively.

Transmission loss changes due to temperature for the fibers in the fabricated cables proved to be less than 0.015 dB/splice over the temperature range from -40 °C to 60 °C.

## 3-3 Mechanical characteristics

### 3-3-1 Tensile strength test

To simulate mechanical forces affecting the installed optical fiber cable, the two cable types were subjected to a tensile strength test. A schematic representation of the tensile strength test system is shown in Figure 23. The 100 m long sample optical cables, in which each fiber has 10 serial splices of type-A or C in its length, were stretched between two poles by universal wire stretchers set between the cable and the poles. The cable tension was monitored by tension meters at both ends of the tested cable. The 4-fiber spacer cable was continuously loaded with a tension of 500 N and the 14-fiber cable was loaded with 2,000 N for one day. After the tensile strength test, no fiber break was found in either cable. The tension loads of each cable were chosen to simulate disign parameters.

It is concluded that the fabricated cables using spliced fibers have tensile strengths comparable to cables using unspliced fibers.

### 3-3-2 Installation simulation

Optical fiber cables experience many kinds of external forces during installation. The most severe condition occurs while squeezing inside the duct because the optical fiber in the cable is subjected to simultaneous tension and bending moments at the same time. Therefore, in order to evaluate the squeezing effect, the installation simulation must be considered. Schematic drawing of the installation simulation system is shown in Figure 24. A movable truck, with three curved guides, moved from one end of the test cable to the other end to squeeze the cable. As shown in the Figure, the optical fiber cable was subjected to three bends. The bending radius of the cable was 200 mm.

Figure 25 shows the monitoring system used in this installation simulation. Both types of cable the 4-fiber spacer cable and the 14-fiber cable, were used for the installation simulation. The cable length was 100 m. Two single-mode fibers and two multi-mode fibers in the test cables, respectively, each having 10 serial splices, were spliced to form a 200 m long optical fiber link at one end of the cable. The optical transmission loss was monitored at a wavelength of 1.3 μm.

The 4-fiber spacer cable and the 14-fiber cable were squeezed twice under a tension of 500 N and 2,000 N, respectively. Each tension was chosen as a designed value. During the squeezing no change in optical transmission loss was observed including impulsive fluctuations, for both types of fibers and for both types of fiber splice A and C. The performance of the fabricated cable during installation simulation was equal to that of the cables using unspliced fibers.

### 3-3-3 Bending test

The two types of the fabricated cables were wraped around a mandrel of specified diameters as showsn in Figure 26. The mandrel diameters for the 4-fiber spacer cable and the 14-fiber cable were chosen to be 90 mm and 170 mm, respectively, so that the bending radii would be six times as large as the cable diameter. The cable components as well as the fibers were fixed with epoxy resion at the end in order to obtain the maximum fiber strain. A schematic representation of the bending test under applying is shown in Figure 26. It was found that no fiber break occured in both types of test cables.

## 4. Conclutions

High strength (average 450 kpsi) arc fusion splice of fibers with restoration coating showed sufficient mechanical and envionmental performances for the practical application. Predicted longterm reliability is of equivalent quality to that of unspliced fibers. The experimentally fabricated cables containing the proposed splices showed the sufficient performance. The proposed splice was shown to meet the severe environmental conditions encountered in the actual fiber cables, including the wide temperature range -40 °C to 80 °C. This technology will promise the stable mass production of ultra-long length fiber cables.

## References


[1] Y. Miyajima., et al., "Lon-length fiber containing high strength splices", Electron Lett., 1981, vol.17, No.18, pp.670-671

[2] T. Kakii., et al., "New reinforcement method of fusion spliced fiber for long length cable manufacturing", OFC '82, 1982, paper THAA4.

[3] C. Tanaka, et al., "Joining method to obtain elongated coated optical fiber", U.S. Patent, No. 4475935.

[4] T. Haibara, et al., "New fiber coat stripping method for high-strength splicing", Appl. Opt., vol.22, No.19, pp.2945-2947.

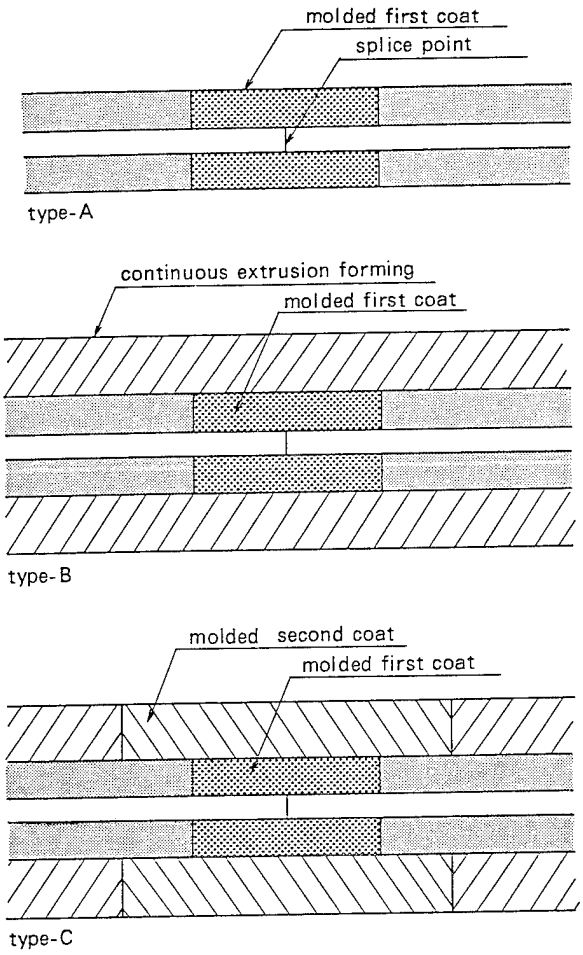



Figure 1 Structures of fusion splice with mold reinforcement

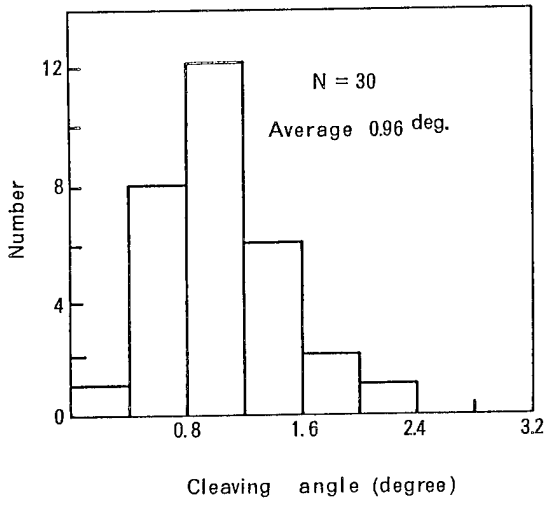



Figure 4 Histogram of cleaving angle

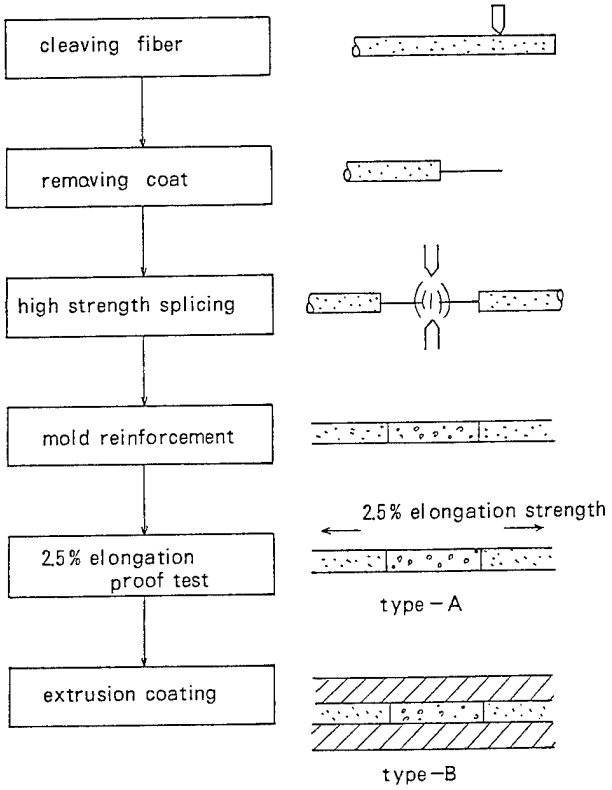



Figure 2 Procedure of high strength splicing for type-A and type-B

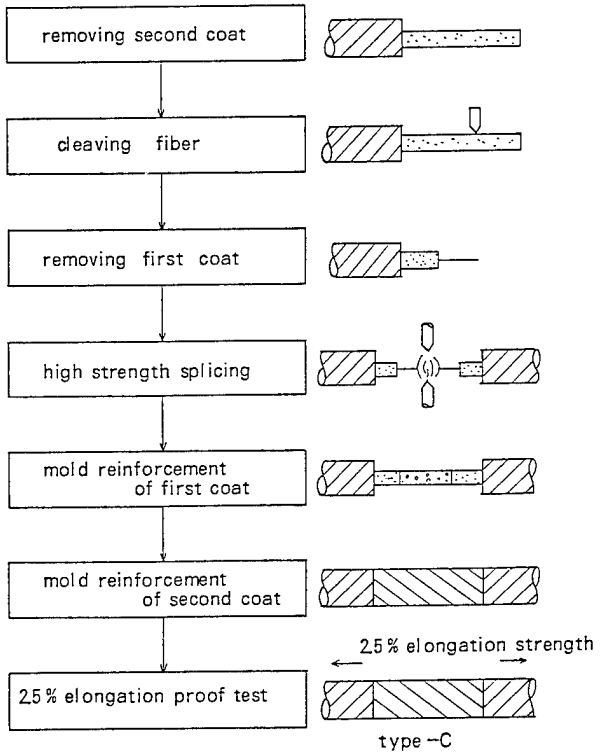



Figure 3 Procedure of high strength splicing for type-C

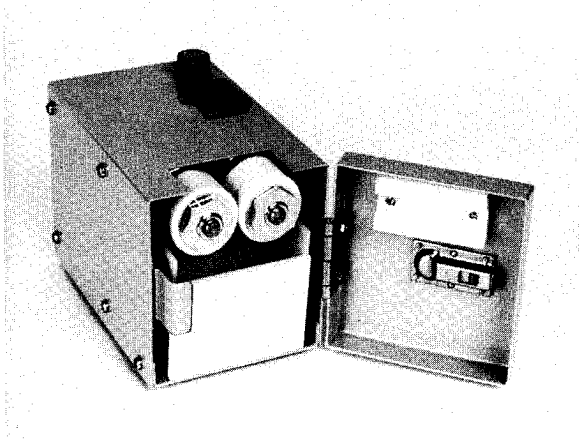


Figure 5 Coat removing equipment

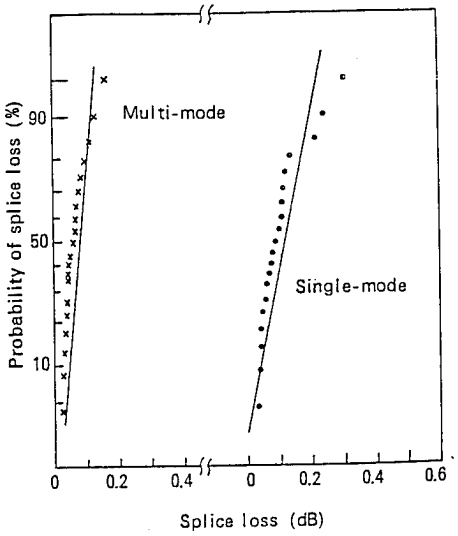



Figure 6 Splice loss of high strength splicing

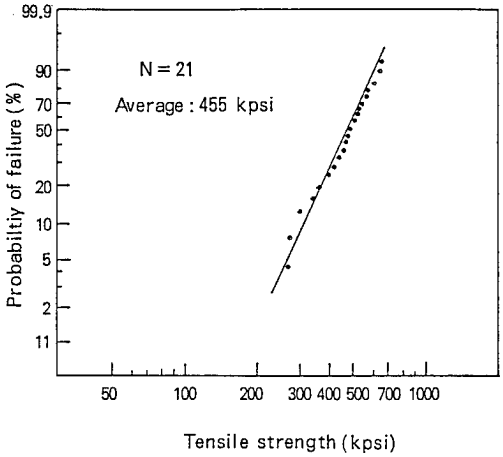



Figure 7 Tensile strength of high strength splice

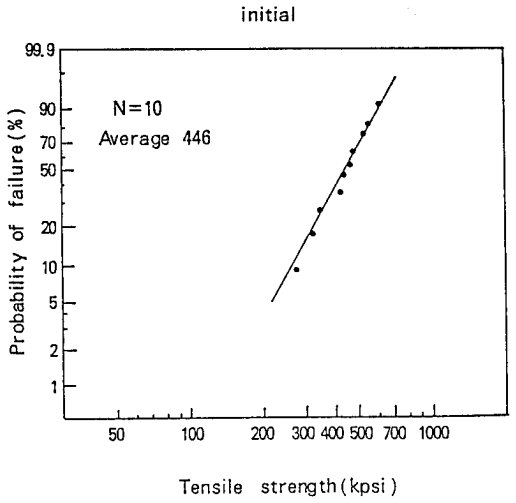



Figure 8 Initial tensile strength

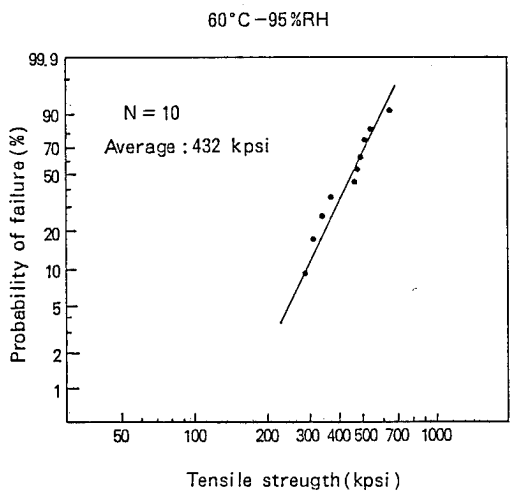



Figure 9 Tensile strength after high temperature/ humidity test

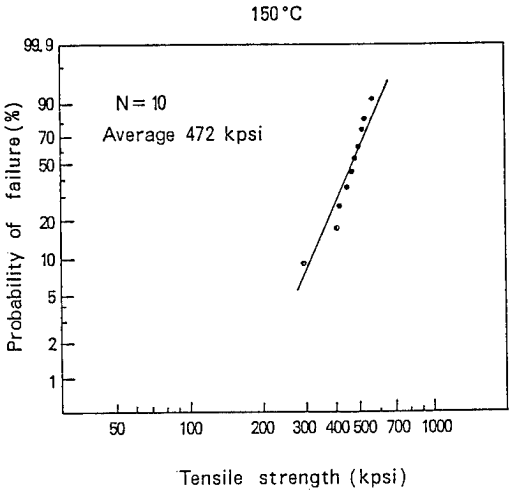



Figure 10 Tensile strength after high temperature test

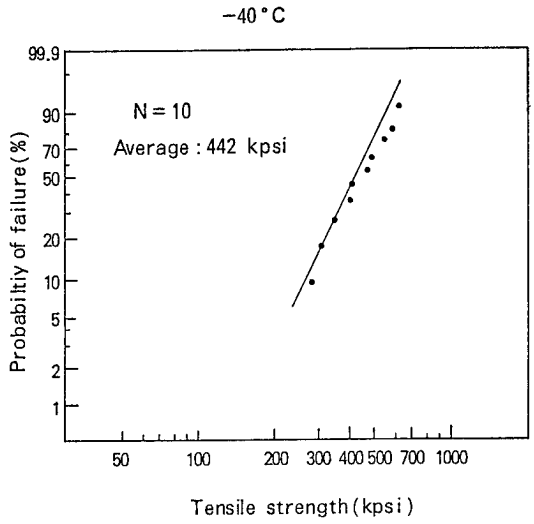



Figure 11 Tensile strength after low temperature test

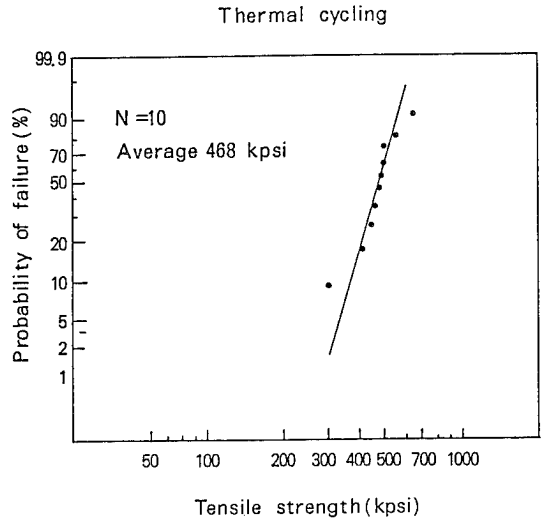



Figure 12 Tensile strength after thermal cycling test

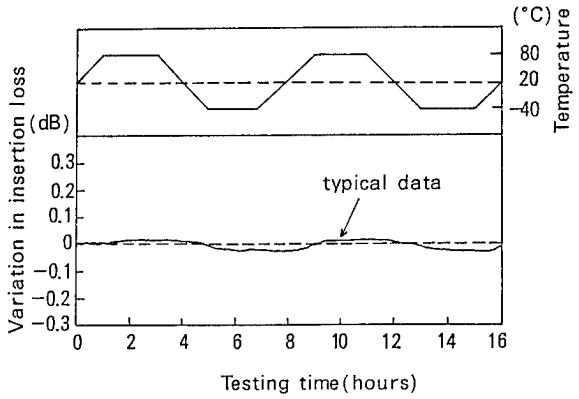



Figure 13 Relationship between splice loss and temperature

Table 1 Repetitive bending and torsion test

| Item | Test condition | Result |
|---|---|---|
| Repetitive bending | radius 4mm<br>angle 120°<br>tension 20kpsi<br>frequency $10^6$ | No fiber break |
| Repetitive torsion | ±360° deg/500mm<br>tension 20kpsi<br>frequency $10^6$ | No fiber break |

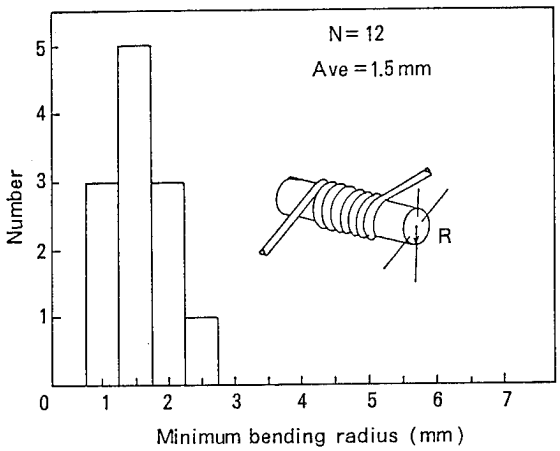



Figure 14 Minimum bending test

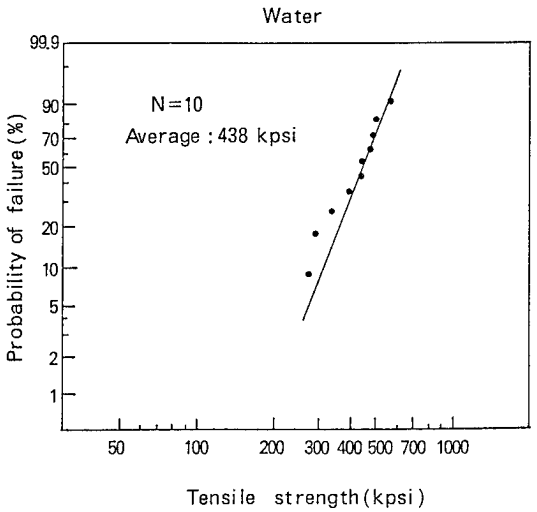



Figure 15 Tensile strength after water immersion test

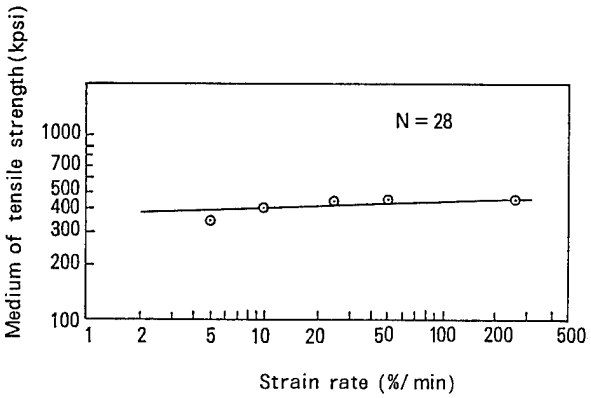



Figure 16 Dynamic fatigue test

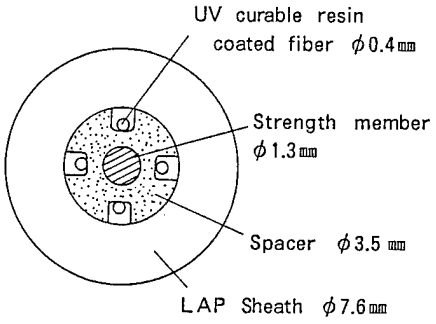



Figure 18 Structure of 4-fiber spacer cable

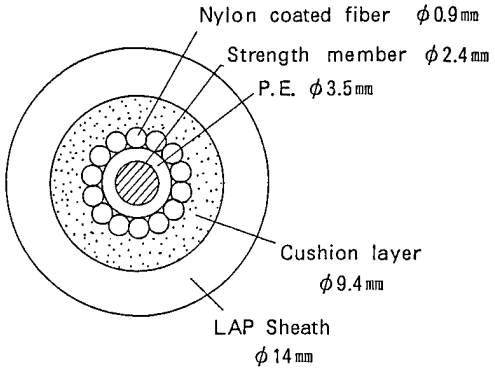



Figure 18 Structure of 14-fiber cable

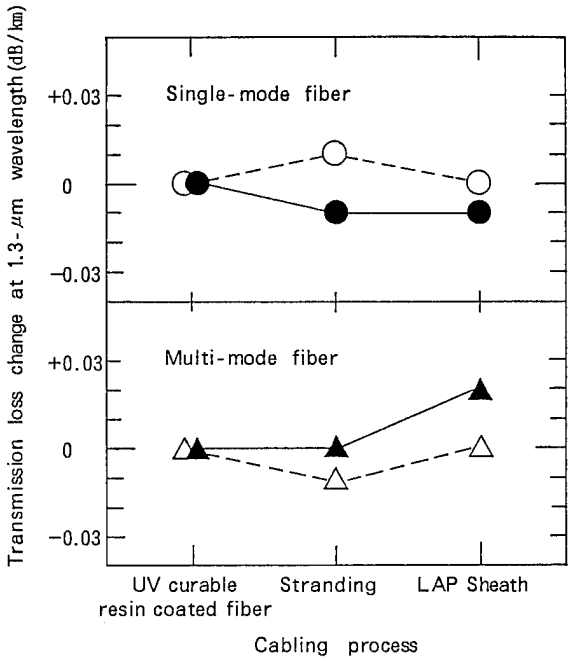



Figure 19 Transmission loss changes during cabling process for 4-fiber spacer cable

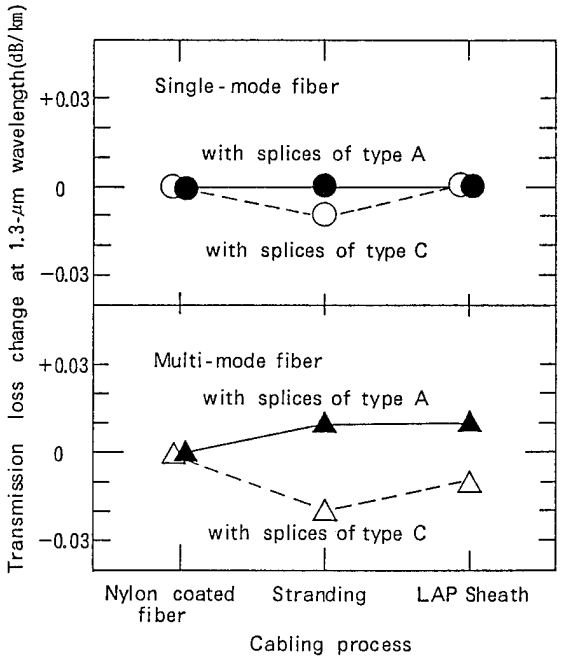



Figure 20 Transmission loss changes during cabling process for 14-fiber cable

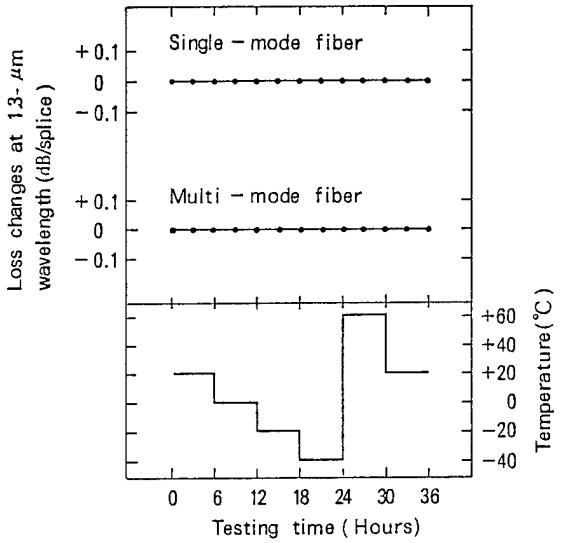



Figure 21 Transmission loss changes due to temperature of 4-fiber spacer cable

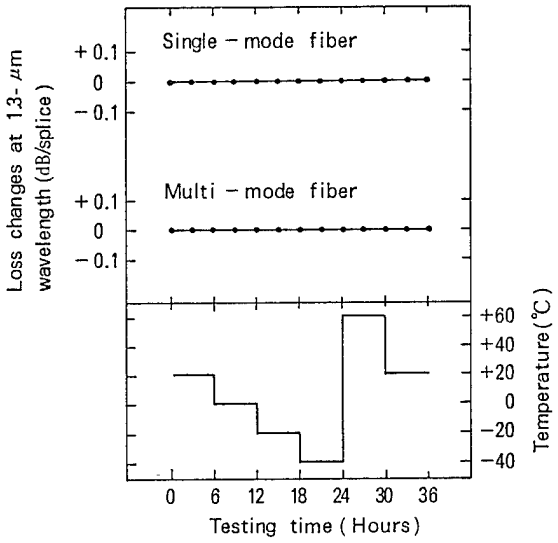



Figure 22 Transmission loss changes due to temperature of 14-fiber calbe

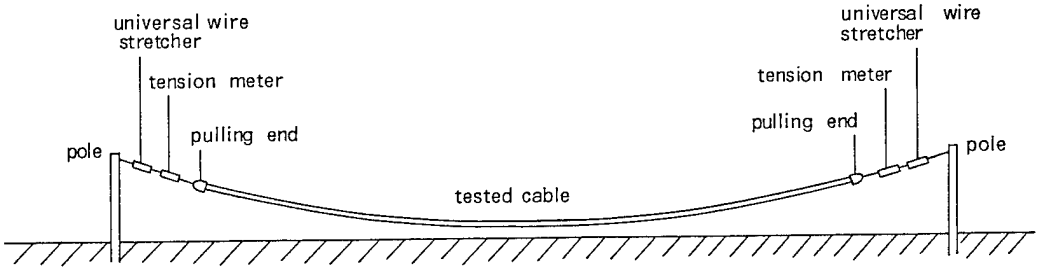
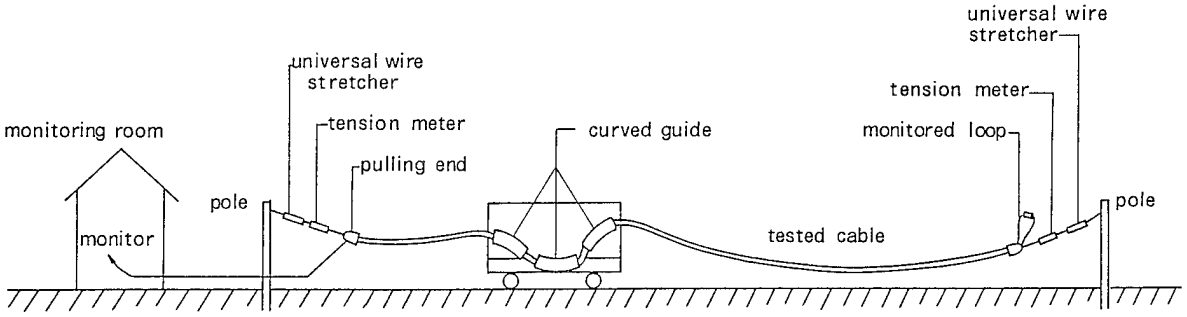



Figure 23 Tensile strength test system




truck moving velocity ; approx. 10 m / min.

Figure 24 Installation simulation system

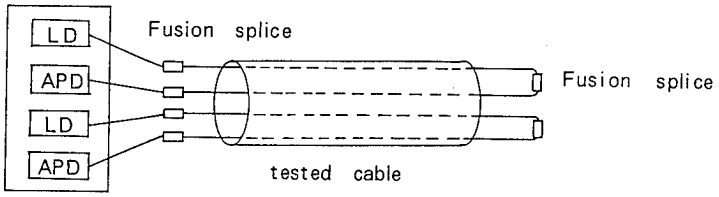



Figure 25 Monitoring system used in the installation simulation

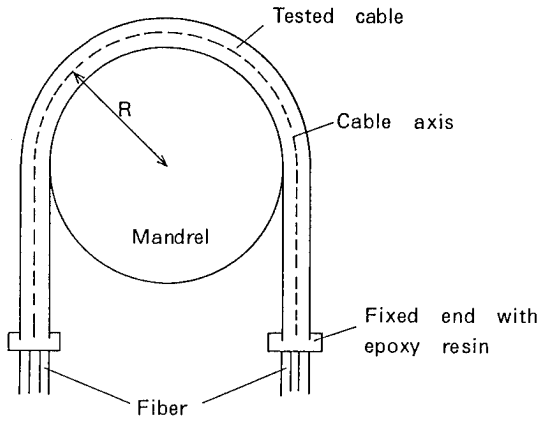
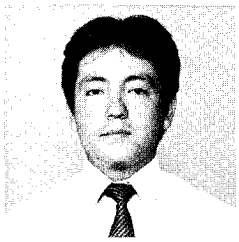



Figure 26 Cable bending test



Yoshiyuki Suetsugu

Sumitomo Elctric
Industries, Ltd.
1, Taya-cho,
Totsuka-ku,
Yokohama, Japan

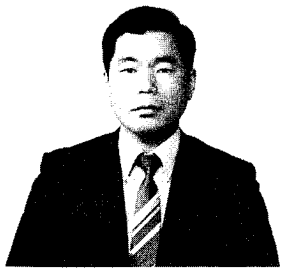
Yoshiyuki Suetsugu was born in 1961 and received a B.S. degree from Tsukuba University in 1984. He joined the Sumitomo Electirc Industries Ltd. in 1984, and has been engaged in the design and characterization of optical fibers and fiber cables. He is a member of Institute of Electronics and Communication Engineers of Japan.



Toshiaki Kakii

Sumitomo Electric
Industries, Ltd.
1, Taya-cho,
Totsuka-ku,
Yokohama, Japan

Toshiaki Kakii was born in 1955 and received the B.E. and M.E. degrees from Keio University in 1978, and 1980, respectively. He joined Sumitomo Electric Industires, Ltd. in 1980 and has been engaged in research and development of optical fiber jointing method. He is a member of the Institute of Electronics and Communication Engineers of Japan.



Shigeru Tanaka

Sumitomo Electric
Industries, Ltd.
1, Taya-cho,
Totsuka-ku
Yokohama, Japan

Shigeru Tanaka was born in Tokyo, Japan, on December 2, 1951. He received the B.S. and M.S. degrees from Tokyo University in 1974 and 1976, respectively. He joined the Sumitomo Electric Industries Ltd. in 1976, and has been engaged in the design and characterization of opital fibers and fiber cables. He is a member of Institute of Electornics and Communication Engineers of Japan.

# A TWO-FIBER TACTICAL FIBER-OPTIC CONNECTOR

J. M. Anderson, B. V. Darden, B. G. LeFevre and V. E. Kalomiris

AT&T Bell Laboratories and US Army Communications-Elec. Com.
Norcross, Georgia 30071 Fort Monmouth, New Jersey 07703

## Abstract

Design features and performance characteristics of a connector and bulkhead receptacle for a tactical fiber-optic cable assembly are presented.

The connector is a hermaphroditic duplex embodiment of the biconic connector. It is joined to the cable by capturing the cable's tensile-strength members between self-tightening locking tapers. This stainless-steel cable-retention assembly requires no special tools, and typically yields pull-out strengths exceeding 900 pounds.

The sealed connector-insert assembly is made from an impact-resistant thermoplastic providing ample float and isolation to achieve, without duplex penalty, the consistent high performance that is characteristic of the biconic connector in its simplex configuration. The mating alignment surfaces of both the biconic plugs and sleeve are accessible for cleaning in the field.

## Introduction

The tactical fiber-optic connector discussed in this paper is a hermaphroditic duplex embodiment of AT&T's biconic connector. Large-scale manufacture and installation of this connector in several simplex configurations began in 1979. Since then it has been used to join nearly two million cable ends. Many connections have been in stable continuous operation since 1979 in a variety of environmental circumstances. The following is a brief historical perspective of the biconic connector blended with a discussion of its basic design and definition of some dimensions whose careful control is crucial to the connector's performance.

## Biconic Connector

The simplex biconic connector illustrated in Figure 1 consists of a plug on each cable end, an alignment sleeve and some peripheral hardware to contain and mount the sleeve and to hold the assembly together under load. The plug ends have the shape of truncated cones, and the sleeve has two corresponding internal tapers. The design of the connector was based on the observation that transverse offset of fiber ends contributes about twenty times more loss in a lightguide connection than longitudinal end separation of the same amount. A taper was chosen for the aligning surface so that lot-to-lot isotropic variations in nominally identical molding materials would not manifest themselves in transverse offset but in the less critical end separation. A taper also provides for easy insertion with low abrasion.

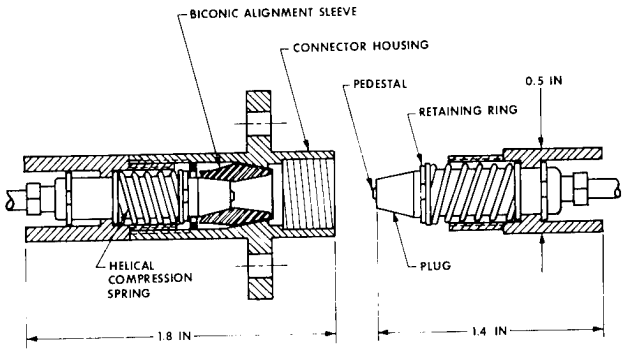



Figure 1. Biconic Connector

In the 1977 Atlanta fiber experiment conducted by AT&T Bell Laboratories,[1] anticipated variations in end separation were accommodated through elastic contact of index matching cushions which adhered to each plug tip and provided a protective covering for protruding fiber ends. The alignment sleeves used in the Atlanta experiment were machined from brass and had eccentricities as great as 5 μm. Shortly after Atlanta, a lapping and polishing procedure was adopted which produced fiber ends flush with a small pedestal at the end of each plug. This permitted precise adjustment of taper length by comparing the protrusion of a plug from a steel taper with that of a gauge ball as depicted in Figure 2. Moreover, W. C. Young concur-

rently developed a molded biconic sleeve whose dimensions could be held more closely

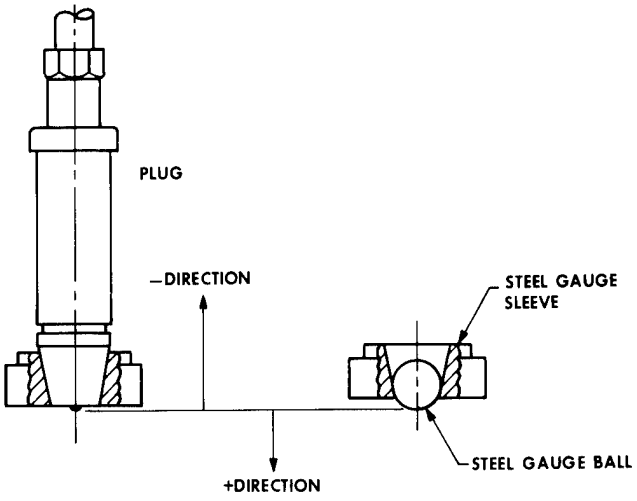



Figure 2. Plug Taper Length

than those of machined sleeves. In particular, eccentricities were less than 2 μm, and tighter length control as determined by the separation of two truncated gauge balls shown in Figure 3 was achieved.

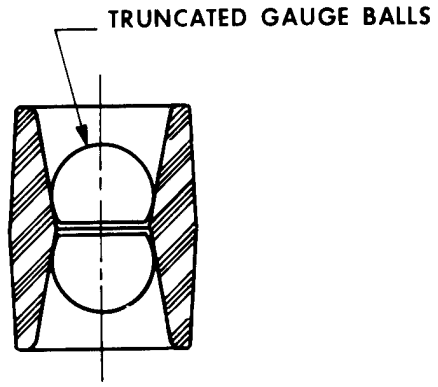



Figure 3. Sleeve Ball Separation

Following these improvements, the nominal separation between fiber ends in a connection was reduced to a 25-μm air gap. A comparison of mean loss and standard deviation obtained without index matching cushions with the loss associated with Fresnel reflections at an air gap suggested that some connections must have had contacting fiber ends. In 1980, W. C. Young, P. Kaiser, et al reported mean connector losses of just over 0.20 dB with standard deviations less than 0.10 dB by purposely selecting plug and sleeve lengths to insure contact of plug ends in the assembled connector.[2] Impressive figures like these have driven the evolution of connector specifications in a direction corresponding to contacting fiber ends.

Given the reality that some manufacturing tolerance must be allowed on plug taper length and sleeve ball separation, it is geometrically obvious that the biconic design cannot achieve seated alignment and contacting fiber ends in all connections without some compliance in the connector components. A nonlinear finite-element analysis has quantified this requisite compliance and found it to be shared between an overall expansion of the sleeve and local deformation at the plug-sleeve interface. In Figures 2 and 3 the indicated cone angle of the plug is specified somewhat smaller than that of the sleeve. This predisposes alignment to occur nearest the fiber ends and promotes the necessary deformation by intensifying the contact stresses at the interface between the plug and sleeve.

## Tactical Fiber-Optic Connector

In the duplex-configured connector, one of the two fiber channels terminates with a biconic alignment sleeve and the other with a plug. The connector is rugged, waterproof and resistant to the stringent environment typical of tactical military applications. A companion bulkhead receptacle developed for the system differs from the connector in external features but shares a common hermaphroditic interface assembly. Hence any cable end will mate with any other or with a receptacle.

The sealed connector-insert assembly shown in Figure 4 contains two plugs and an alignment sleeve. It is made from an

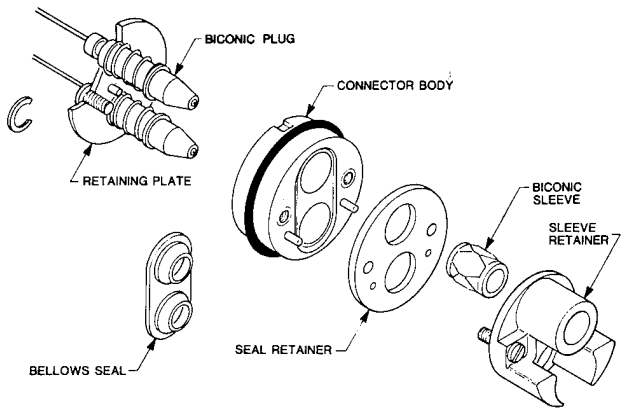



Figure 4. Connector-Insert Assembly

impact-resistant thermoplastic and comprises the heart of the tactical connector and receptacle. The spring-loaded plugs must be free to move axially and radially to align with their counterparts in a mated connector. A fluorosilicone bellows seal allows the necessary float and prevents water entry around the plugs. The insert assembly provides ample isolation to achieve without duplex penalty the consistent performance characteristic of the biconic connector in its simplex configuration.

The sleeve retainer is the forwardmost part of the insert assembly. Geometric alignment and orientation features preclude mismating connectors, provide a hermaphroditic profile and protect the biconic components during impact. A cylindrical boss on the retainer holds the sleeve, and two protruding lobes partially encircle and shroud the plug. The boss and lobes are of stout proportions to insure positive engagement and to withstand the impact if the connector is dropped on its end.

Figure 5 shows in section the complete tactical connector assembly. A metal shell encloses the insert assembly described above. It also provides storage space for enough slack fiber to reterminate the ends and retains the cable- termination hardware. A free-turning threaded coupling nut tightens the joint between two connectors or between a connector and receptacle. The coupling threads are a modified 60° stub for strength with a double lead for easy engagement. The connector shell and coupling nut are designed to elastically withstand 400-pounds tension across a connection.

An insert-molded bend limiter at the rear of the connector compresses a seal which blocks the water-entry path along the cable and mechanically isolates inner parts of the connector against cable twist. Other leak paths are blocked by a face seal and an O-ring.

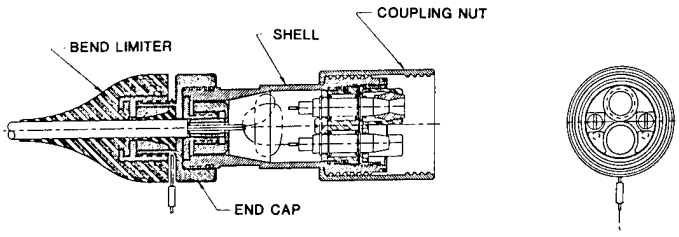



Figure 5. Tactical Fiber-Optic Connector

A dust cover is provided to prevent water or dust entry into an unmated connector. The dust cover contains a mounted sleeve retainer identical to the one comprising the front face of the connector-insert assembly. This assists in mating the cover and connector by bringing them into proper alignment. A short coupling nut on the cover screws onto the connector shell to secure the cover and to compress the face seals. The cover is also hermaphroditic so that when two connectors are mated, their respective dust covers can be similarly joined to prevent contamination. A flexible stainless-steel lanyard prevents inadvertent separation of the connector and cover.

Cleanliness is essential to a repeatable low-loss lightguide connection, and a significant attribute of the tactical connector is that it is easy to clean. After soaking an uncovered connector in mud, it is merely necessary to rinse it in a pail of water and to wipe the biconic components dry in order to restore unaffected optical transmission. No special cleaning kit is required. If mud encrustation is particularly severe, the sleeve retainer's captive screws permit its removal in the field to gain greater access to the plugs and sleeve for a more thorough cleaning.

With regard to size and weight, a mated connector pair is less than 4 cm in diameter, measures 15.25 cm in length excluding bend limiters, and weighs 581 grams including dust covers.

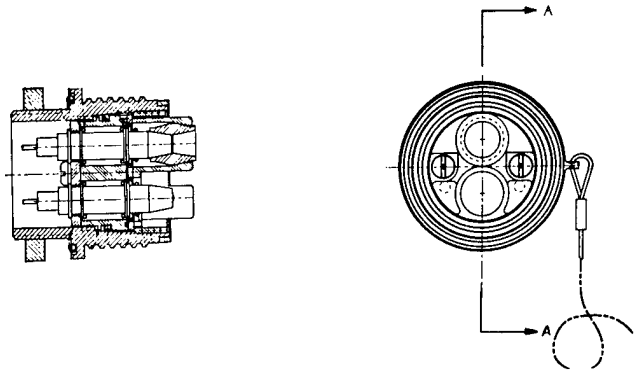



Figure 6. Tactical Fiber-Optic Receptacle

## Receptacle

The forward end of the receptacle shell and the connector-insert assembly shown in Figure 6 are identical to corresponding parts of a connector. Hence, any cable end will mate with the bulkhead receptacle. The receptacle assembly terminates with short buffered-fiber pigtails

emanating from the rear of the biconic plugs. These are for splicing to internal cables, and no strain relief is provided. The receptacle may be mounted through a D-hole in panels up to 6.4 mm thick with a standard AN-series jam nut. As the jam nut is tightened, an O-ring under the mounting flange is compressed and seals the panel-receptacle interface. The receptacle protrudes less than 2.5 cm from the bulkhead and measures about 4 cm in diameter at the mounting flange. An unmated receptacle is protected by a lanyard- attached dust cover identical to the one provided for the connector.

## Materials

The connector and receptacle shells are aluminum die castings. The connector end cap, dust-cover shell and both coupling nuts are machined from wrought aluminum. All aluminum components are given a black-anodize finish for appearance and corrosion resistance. The cable-retention assembly and other internal metal items are passivated stainless steel; the dust-cover lanyard is a stainless-steel stranded cable. Except for the biconic components, the connector-insert assembly is injection molded from filled resins having excellent dimensional stability, high impact strength, and good chemical and heat resistance. Seal materials are neoprene and fluorosilicone.

## Tactical Connector Tests

The primary design objectives of the tactical connector are low coupling loss and field ruggedness. The assembly is required to remain optically and mechanically functional under environmental and mechanical exposures typical of tactical field applications. To assess progress toward these goals, tests were conducted at critical intervals on prototype connectors to evaluate performance with respect to: coupling loss, thermal cycle, shock drop, vibration, shock, cable retention, flex life, water immersion, and mud immersion. These tests are reviewed and the results summarized in the following paragraphs.

## Coupling Loss

The coupling loss was measured at 825 and 1300 nm with the test set-up shown schematically in Figure 7. LED sources with over-fill launch conditions were used in conjunction with large-area PIN detectors and Equilibrium Mode Simulators consisting of 3-turn 20-mm diameter mandrel-wraps.

The initial coupling loss measurements were made to compare the tactical connector with the standard multimode biconic (Figure 1) which has a well-characterized laboratory and field performance average under 1 dB on jumper-quality fiber. Differential loss measurements were made by first connecting standard product in the configuration shown in Figure 7* and, after zeroing the test set, replacing all hardware components (except the biconic) with the tactical-connector hardware. In a series of 3 tests the average differential (added) loss was 0.05 dB.

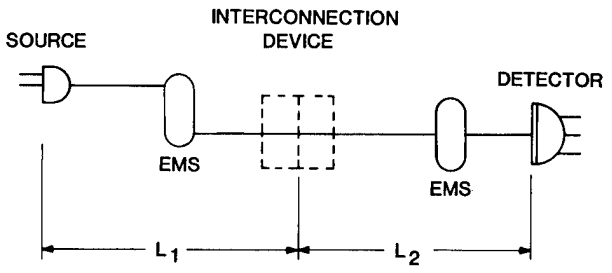



Figure 7. Coupling-Loss Test Schematic

In a series of 30 reconnection tests (multiple insertions) the standard deviation was 0.03 dB. The above results indicate that, with the tactical-connector hardware, highly repeatable connections can be made and no measurable loss is added to that achievable with standard biconic fixtures.

Absolute coupling-loss measurements were made with the tactical connector by the cut-and-insert method of EIA Fiber Optic Test Procedure #34. Biconic plugs of single-mode and multimode fiber quality were used to terminate TFOCA cable samples with fiber meeting the following requirements: core diameter 50 ± 1.5 μm; eccentricity ≤ 3 μm. The results yield a mean loss of 0.81 dB with a standard deviation of 0.40 dB - slightly higher than that typical of jumper-grade cable.

Additional coupling-loss measurements were made by concatenating pairs of plug-terminated 1-km cables randomly selected from a group of 24 design models. The coupling loss was derived by subtracting the cabled-fiber attenuation from that of the measured assembly. For 32 couplings (64 channels) the mean loss and standard deviation were 0.66 and 0.19 dB.

*The terminated ends were made and checked under factory conditions before assembling the two-cable concatenation.

## Thermal Cycle

Two mated plug samples were exposed to three thermal cycles ranging from ambient to -46°C to 71°C. The maximum added loss was 0.11 dB.

## Shock Drop

This test was conducted to determine if the connector terminations can withstand accidental drops without damage. Four unmated plug samples were dropped without dust covers from a height of 10 feet twenty times onto a wood slab over concrete. No physical damage, loose parts or mechanical malfunction occurred as a result of the impacts. The test was repeated with one mated pair while optical transmission was monitored. No added loss resulted from the impacts.

## Vibration

A mated plug-receptacle sample was subjected to dynamic vibrational stresses characteristic of those incurred during transport by ground vehicle (MIL STD 810C). Sinusoidal cycling was used with a 15-minute logarithmic frequency sweep of 5 to 500 Hz at 4.2g. The sample was vibrated in three mutually perpendicular directions. The added (transient) loss was less than 0.05.

## Shock

A mated plug-receptacle sample was subjected to dynamic shock stresses simulating those encountered during handling and transport. The sample was shocked an 11 millisecond sawtooth pulse of 40g's in three mutually perpendicular directions a total of 18 times. The added transient loss was less than 0.05 dB.

## Cable Retention

The cable retention assembly was tested for its load bearing-capability when connected to prototype cable samples. Short (36 cm) cable lengths were terminated on each end with retention fixtures and loaded axially to failure at room temperature in an Instron tensile machine. All twenty-five such samples exceeded the minimum 1780-newton requirement. The average, low and high failure loads were 4280, 3204 and 5874 newtons respectively. The failure mechanism was separation of the aramid yarn. An additional five samples were subjected to thermal shock cycling between -61°C and +71°C before testing at room temperature. The load bearing capacity was not measurably changed by thermal exposure.

## Flex Life

The purpose of the flex test is to determine the likelihood of damage at the cable/connector-interface region as a result of cable flexure during handling. One connectorized cable sample was flexed as shown in Figure 8 for 2500 cycles of ± 90° at room temperature. The maximum loss change was less than 0.05 dB and no physical damage occurred in any part of the connector/cable assembly.

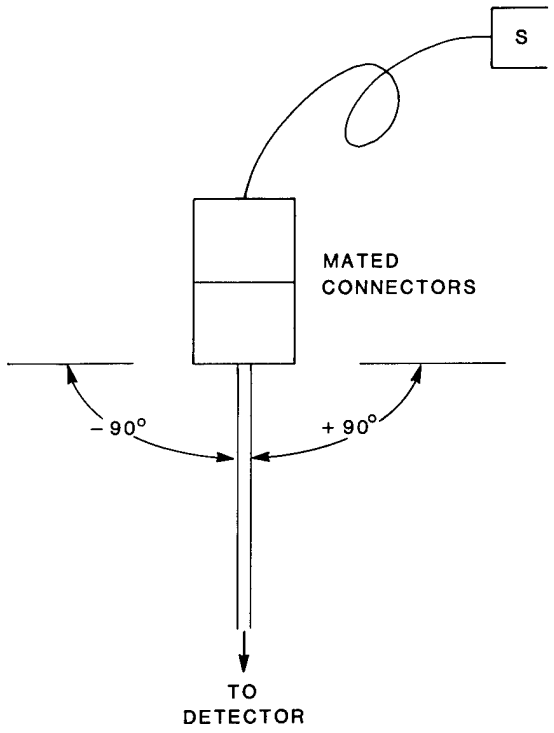



Figure 8. Flex-Test Schematic

## Water Immersion

This test is used to determine the susceptibility of mated connectors to leakage when under water. The effectiveness of the assembly's watertight seals was evaluated by submerging the coupled ends of plug-terminated cable samples under two meters of water for 24 hours. Attenuation measurements were taken at 12 and 24 hours. No added loss was observed. The connectors were then decoupled, disassembled and examined for evidence of leakage. Condensate was found on some assembly parts but there was no evidence of leakage.

## Mud Immersion

The tactical connector was designed to allow easy access to the precision alignment parts so that they can be easily cleaned after mud immersion. This aspect of the design was evaluated by subjecting a plug connector pair to 10 cycles of the following sequence:

a. decouple and immerse each end in a mud bath for 5 minutes;

b. water rinse, wipe clean, air dry;

c. recouple and measure loss change.

The maximum observed loss change was 0.05 dB.

## Conclusion

The two-fiber tactical fiber-optic connector described herein meets all the requirements set forth by the contract sponsor, the U.S. Army CECOM. The product design effort considered not only performance but also cost. Existing technology developed by AT&T for commercial lightguide products aided in maintaining a low design to unit production cost.

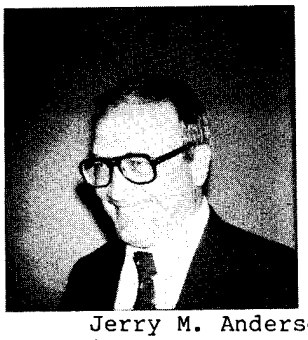
## Acknowledgements

The authors acknowledge the assistance of H. R. Lunde, L. C. Hotchkiss, R. R. Richardson and T. E. Simmons, Jr., in the testing and evaluation of the connector.

## References

1. P. K. Runge and S. S. Cheng, "Demountable Single-Fiber Optic Connectors and Their Measurement on Location," The Bell System Technical Journal, Vol. 57, No. 6, July-August 1978.

2. W. C. Young, P. Kaiser, N. K. Cheung, L. Curtis, R. E. Wagner and D. M. Folkes, "A Transfer-Molded Biconic Connector with Insertion Losses Below 0.3 dB Without Index Match," Sixth European Conference on Optical Communication-Conference Publication Number 190.



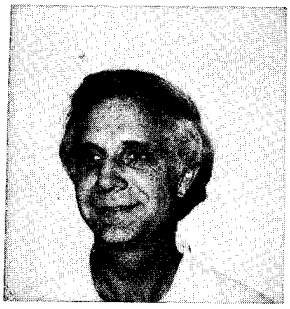
J. M. Anderson
AT&T-Bell Laboratories
2000 N.E. Expressway
Norcross, GA 30071

Jerry M. Anderson has been a Member of Technical Staff at AT&T Bell Laboratories in Atlanta since 1979. Before joining AT&T Bell Laboratories, he was a member of the faculty of Georgia Institute of Technology from 1967 to 1979 and consulted continually with the Lockheed-Georgia Company from 1972 to 1979. He received a BSME and MSME from Auburn University and a PhD in Mechanics from Stanford University in 1967.



B. V. Darden
AT&T-Bell Laboratories
2000 N.E. Expressway
Norcross, GA 30071

Bruce V. Darden is a Member of Technical Staff at AT&T Bell Laboratories, Norcross, Georgia. He received a B.S. Degree in Engineering from North Carolina State University in 1951, and held engineering positions with Western Electric Company until 1960 when he joined AT&T Bell Laboratories. He is currently a member of the Connector Systems Development Group.



B. G. LeFevre
AT&T-Bell Laboratories
2000 N.E. Expressway
Norcross, GA 30071

B. G. LeFevre (Bruce) is a Member of Technical Staff at AT&T Bell Laboratories, Norcross. He received his B.S. (Colorado School of Mines) and PhD (University of Florida) in Physical Metallurgy. He joined AT&T Bell Laboratories in 1976 after ten years on the faculty of Georgia Institute of Technology. He has been involved in the study of metals and alloys used in the manufacture of cables and connectors. He is currently working with lightguide connectors.



V. E. Kalomiris
US Army Communications
Electronic Command
Fort Monmouth, NJ
07703-5202

Mr. Kalomiris is currently a project leader responsible for fiber optic cables, connectors, and fiber optic system development. Served for three years as chairman of the Tri-Service Group on fibers, cables and connectors. Member of EIA P6.7 Working Group on Fiber Optic Cables. He is also involved in the establishment of a test facility. Most recently, he worked for ITT-EOPD as a project engineer for the air layable cable which he designed. Prior to joining ITT-EOPD, Mr. Kalomiris was associated with General Cable Corp. R&D as a research engineer for 6 years. While at General Cable he was involved with the design, development and manufacture of the prototype superconductive power cable with flexible core. Before joining General Cable he spent a year working for the Hellenic Telecommunications Organization as a communications engineer responsible for planning and designing microwave links. While in Greece he translated "Mathematical Methods for Science Students" by G. Stephenson, Imperial College University of London. He is a member of IEEE and the Technical Chamber of Greece (Society of Professional Engineers). Education: B.A. in Mathematics, New York University; B.S. in Electrical Engineering, New York University; and an M.S. in Electrical Engineering, New York University.

# AN UPDATE ON PRACTICAL FUSION SPLICING OF MULTIMODE AND SINGLE-MODE FIBERS

S. L. SAIKKONEN, M. J. HACKERT

CORNING GLASS WORKS
CORNING, NEW YORK 14831

## ABSTRACT

Arc fusion splicing is a well accepted means of providing permanent joints between optical fibers. Previous work in this area has provided a process for reclamation of short multimode fiber lengths and the ability to provide long link lengths having low loss, high strength splices with fiber and coating geometries indistinguishable from unspliced fiber. With the rapid increase in popularity of long length single-mode fiber, continued development of a fiber splicing process to include this product was needed.

In this paper, previously unreported fiber bandwidth and in-cable test results for factory spliced multimode fiber will be presented. An updated splicing process accommodating both multimode and single-mode fibers will be discussed, and optical, mechanical and environmental test results for spliced single-mode fiber given.

## INTRODUCTION

Current state-of-the-art arc fusion splicing equipment provide a means for producing stable, reliable, low loss interconnection of both multimode (MM) and single-mode (SM) optical waveguide fibers. Current equipment is capable of repeatedly achieving splice losses of less than 0.1 dB for homogeneous SM and MM fiber splices, i.e. a fiber simply broken then spliced back together. Previous work has defined and quantified the fiber parameters affecting intrinsic splice loss as well as define the methods of fiber end preparation, fusion splicing, splice restrengthening and recoating to produce spliced multimode fiber meeting the same optical, mechanical and environmental standards as unspliced fiber[1,2]. The purpose of this paper is to present a simplified procedure for fiber selection and splicing which yields consistent results regarding splice attenuation, strength and geometric tolerances. The splicing process accommodates an array of both multimode and single-mode products, providing excellent splice performance without major changes or adjustment of the process or equipment. Fiber bandwidth and in-cable test data for spliced multimode fiber will be presented. Splice attenuation, fiber dispersion, static and dynamic fatigue, mechanical test and environmental test results for spliced single-mode fiber will also be given.

A Monte Carlo simulation of theoretical intrinsic splice losses in heterogeneous (fibers from different preforms) single-mode joints will be presented including empirical data to support this theory.

## SPLICING PROCEDURE

### A. Fiber End Preparation

To consistently produce both MM and SM fusion splices having low extrinsic splice loss and high strength, certain fiber preparation and handling procedures must be followed. The UV-cured acrylate fiber coating is mechanically stripped using a tool designed to ensure no mechanical damage occurs to the cladding glass. Residual coating particles are removed by pulling the bare glass through a clean cotton pad. The fiber ends are cleaved at a short distance from the point of coating termination to minimize the amount of exposed glass as well as eliminate any contact between the exposed glass and the clamping surfaces in this and subsequent steps of the splicing procedure. Cleaved fiber ends should show approximately one half degree or less of angle and have a flat surface with no protruding lips. A small chip at the outside edge created by the cleaving blade is acceptable provided the damaged

area does not extend toward the center of the fiber more than approximately one tenth of the fiber diameter.

Because residual coating particles and other contaminants can contribute to high extrinsic splice loss and low tensile strength, the bare fiber ends must be scrupulously cleaned just prior to the fusion operation.[1] The bare glass is submerged in an ultrasonic bath containing clean isopropyl alcohol to remove all surface contaminants.

B. Fusion Splicing

The basic process of fusion splicing consists of two steps: precision alignment of the fibers to achieve maximum power coupling and proper fiber end gap spacing, then an automated arc fusion cycle. The splicing machine must maintain precise angular fiber alignment, have suitable lateral core axis alignment resolution, and must provide automated timing and positioning of the fiber ends along the longitudinal axis during the fusion cycle. Our studies show that an optimum setting for the fusion arc current, duration and electrode spacing can be achieved whereby various types of MM and SM fibers may be spliced having consistently low splice loss and high tensile strength. Lateral fiber core alignment is achieved prior to fusion by utilizing an optical time domain reflectometer (OTDR) having the appropriate operating wavelength and launch for the type of fiber being spliced, and a high resolution, real-time display.

C. Splice Recoating

The spliced joint must be recoated to provide similar mechanical and environmental protection to the bare glass as provided by the existing coating material. It is important to maintain the same geometric tolerances in the recoated area as found on the existing coating such that the recoated section is transparent to subsequent cable manufacturing operations and cabled fiber performance. The spliced (bare) fiber is recoated with a UV-cured acrylate, similar to the existing coating, by utilizing a molding technique.

D. Splice Loss Measurement

Since the splice loss measurements must be non-destructive, an OTDR is utilized for loss measurement. Precautions must be taken when interpreting the results of this technique. Because the scattering properties of two different fibers may vary, a splice between such fibers may indicate a "negative insertion loss" when measured in one direction with and OTDR. A measurement from the opposite direction will indicate a positive insertion loss which is greater than the previous "negative insertion loss." Splice loss measurements for SM fibers should be taken from both ends of the fiber then averaged to yield the actual insertion loss.[3] For MM fiber splices an averaged bi-directional OTDR loss measurements only provides a range in which an actual one-way insertion loss will lie. Here the actual insertion loss in either direction will be greater than 0 decibel (dB) but less than two times the averaged bi-directional loss measurement.[4] To ensure accuracy a cutback measurement technique utilizing a stabilized source and detector operating at the appropriate wavelength was used to obtain the splice loss measurements provided in this paper.

E. Strength Testing

Each splice must be proof tested to assure a minimum tensile strength. The spliced area is tensile loaded at a 4% strain rate, held at the established proof stress level for a minimum of 0.7 seconds then released. Test specimens are progressively loaded to failure to provide ultimate strength data. Strength data from many hundreds of MM and SM arc fusion splices indicate the ultimate tensile strength of the splice will generally be approximately one third of the original unspliced fiber strength.

## HOMOGENEOUS SPLICE PERFORMANCE

The flexibility and repeatability of the splicing system is demonstrated by preparing homogeneous splices using various types of fiber. Extrinsic splice loss, that attributed to the splicing process only, is determined by simply breaking then splicing a fiber while recording before and after system

power. Table 1 illustrates the extrinsic losses for both MM and SM fiber splices using the aforementioned preparation procedures and no changes to the fusion procedure or fusion splicer settings. Table 1 also shows the tensile strength of the various spliced fibers.

| Fiber Type | # Of Samples | Splice Loss $\bar{X}$ (dB@λ) | Splice Loss $\sigma$ (dB) | Ultimate Strength $\bar{X}$ (GN/m$^2$) | Ultimate Strength $\sigma$ (GN/m$^2$) |
|---|---|---|---|---|---|
| 50/125 Double Window | 20 | 0.05 @ 850 | 0.02 | 1.54 | 0.31 |
| 100/140 Short Distance | 20 | 0.04 @ 850 | 0.01 | 1.71 | 0.53 |
| 85/125 Data Band | 20 | 0.02 @ 850 | 0.008 | 1.42 | 0.36 |
| 10/125 Single-Mode | 80 | 0.04 @ 1300 | 0.04 | 1.41 | 0.47 |
| 9/125 Dispersion Shifted Single-Mode | 30 | 0.06 @ 1300 | 0.04 | 1.28 | 0.38 |

Table 1. Homogeneous Splice Performance

## SINGLE-MODE SPLICE LOSS ANALYSIS

The two major contributing factors to intrinsic splice loss in SM fiber splices are mode field diameter mismatch and lateral offset of the fiber cores. A theoretical study, utilizing a Monte Carlo simulation technique was used to calculate splice loss for 10,000 randomly paired fibers.[5] The fiber parameters were chosen to reflect typical industry specifications for mode field diameters (10 μm ± 1 μm) and core/clad concentricity (± 1 μm). Results of the simulation show the mean loss due to the mode field diameter mismatch contribution is 0.008 dB and the 99th percentile of 10,000 pairs is less than 0.05 dB. An experiment was conducted in which fibers with various measured mode field diameters were fusion spliced and the joint loss measured. It can be seen in Table 2 the measured losses are very close to the theoretical losses provided an extrinsic loss value of approximately 0.04 dB is added to the theoretical values.

| MFD (μm)[1] | MFD (μm)[2] | Avg. Loss[1] (dB @ 1300nm) | Theoretical Loss (dB @ 1300nm) |
|---|---|---|---|
| 10.70 | 8.90 | 0.192 | 0.146 |
| 10.70 | 9.50 | 0.102 | 0.060 |
| 10.70 | 10.02 | 0.060 | 0.019 |
| 10.24 | 10.02 | 0.034 | 0.002 |

Table 2. Experimental Loss vs. Theoretical Loss

[1] Avg. of 10 splices.

In the case of lateral core offsets, the Monte Carlo simulation took into consideration two possible extremes of core offset at a joint which may occur if fibers are aligned by reference to the cladding diameters. Figure 1 illustrates these two conditions of core offset. The mean joint loss for the 10,000 randomly paired fibers for minimum offset ($\delta_1 - \delta_2$) is 0.015 dB while maximum offset ($\delta_1 + \delta_2$) produced a mean of 0.14 dB. The 99th percentile for minimum and maximum offsets are attenuation <0.095 dB and < 0.45 dB respectively.

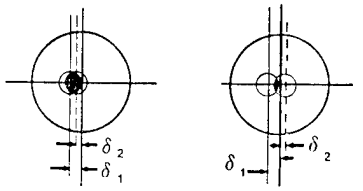



Fig. 1. The Contribution of Fiber Orientation to Lateral Offset

Since the fusion splicing procedure aligns the fiber cores by power peaking, only the effects of cladding surface tension during the fusion process will disturb the optimized core alignment. Experiments were conducted in which maximum core offsets ($\delta_1 + \delta_2$) of up to 2.0 μm were fusion spliced using the prescribed technique. Here the contribution to splice loss due to core offset was < 0.01 dB.

## EXPERIMENTAL DATA - MULTIMODE

In addition to previously published optical, mechanical and environmental testing of spliced MM fibers[1], the effects of fusion splices on fiber bandwidth and in-cable test results were examined.

### Spliced Fiber Bandwidth

In order to evaluate the effect of fusion splicing on multimode fiber bandwidth, an experiment was performed consisting of measuring a fiber's bandwidth at 850 nm and 1300 nm before and after fusion splicing. The sample set consisted of five 50/125 double window fibers, 2.2 km in length, chosen with a range of bandwidths (155 Mhz to 1063 Mhz) and a range of peak bandwidth wavelengths ($\lambda\rho$). The resultant biases ranged from -5.3% to 5.2% and the

average bias was 2%. Although examination of the resultant pulse and frequency plots from the measurements consistently show a reduction in power in the higher order modes, it can be concluded from these results that the effect on the bandwidth of moderately well tuned fibers is fairly small (i.e. almost insignificant).

In - Cable Testing

Cables of the tight buffer and loose tube designs were fabricated containing both non-spliced fiber (control) and fibers having numerous splices. Both cables were tensile tested in the areas containing the splices, as the output power of each fiber was monitored. Maximum design tensile load as well as 150% and 200% maximum loads were applied for one hour in three separate cycles. The spliced fibers behaved very similar to the unspliced controls under tension and after release of the loads.

## EXPERIMENTAL DATA - SINGLE-MODE

As with the spliced MM fibers, splices for SM must perform to the same specifications as unspliced fiber. Geometries, optical performance and protection of the recoat area for a series of spliced fibers have been evaluated. The spliced pairs were randomly selected from fibers produced by one specific manufacturing process, but drawn from different preforms.

A. Recoating Geometry

The spliced and recoated fiber must have the same diameter and geometry as the unspliced fiber. The recoated section should be nominal ± 15 μm in diameter and have a concentricity ≥ 0.7. Measurements on ten spliced fibers are shown in Table 3. Both parameters are well within the stated specifications.

| Overall Dia. (μm) | Concentricity Min. Coating Thickness / Max. Coating Thickness |
|---|---|
| 248 | 0.91 |
| 250 | 0.89 |
| 242 | 0.92 |
| 244 | 0.92 |
| 243 | 0.91 |
| 244 | 0.86 |
| 243 | 0.94 |
| 245 | 0.90 |
| 248 | 0.94 |
| 250 | 0.90 |

Table 3. Coating Geometry. 250μm Nominal Diameter.

B. Attenuation Discontinuity

The attenuation step at a splice as determined utilizing an averaged bi-directional OTDR measurement should be < 0.2 dB. The average value for 35 fusion spliced SM fibers is 0.064 dB. Figure 2 illustrates the cumulative distribution for the measured splice losses.

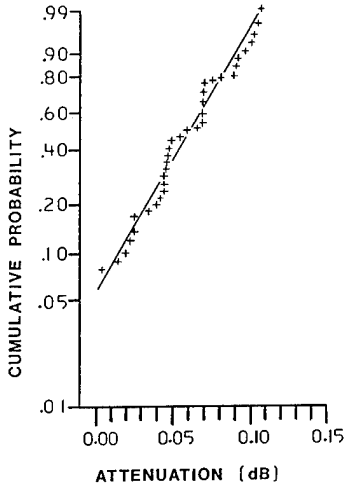



Fig. 2. Cumulative Distribution for Splice Losses of SM Fibers.

C. Dispersion

The total dispersion for spliced SM fibers should meet the standard specification of ≤ 3.5 psec/nm-km in the 1285-1330 nm wavelength range and ≤ 6.0 psec/nm-km between 1260 and 1365 nm. Figure 3 shows the mean, maximum and minimum total dispersion measurements at these wavelengths for ten 2.2 km long fibers containing one splice near mid-span.

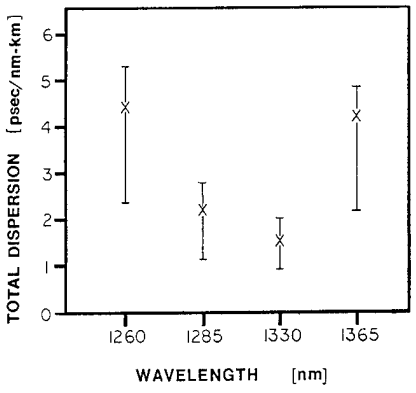



Fig. 3. Total Dispersion for Spliced Fibers.

D. Strength

The specification of tensile strength requires the spliced section pass a proof stress of 0.69 GN/m² (100 KPSI). Average measured tensile strengths of 20 fusion spliced and recoated sections is 1.41 GN/m² (198 KPSI). A cumulative distribution of the 20 measured samples is shown in Figure 4.

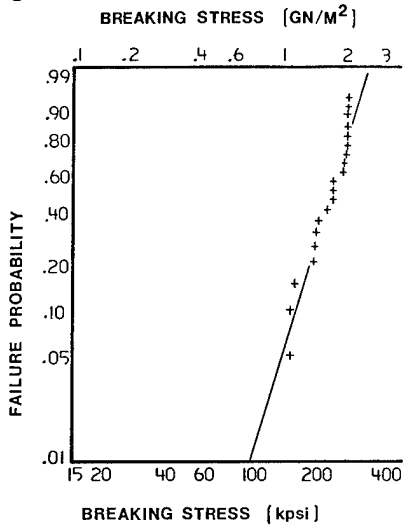



Fig. 4. Cumulative Distribution for Tensile Strength of Spliced Fibers.

E. Static and Dynamic Fatigue

One meter sections of SM fiber containing one recoated splice at mid-span were tested for static fatigue by subjecting four sets of fibers to four different static loads over a three month period. The time to failure was recorded for each broken fiber. Four similar sets of spliced fibers were tested for dynamic fatigue by subjecting each set to a different strain rate. The breaking stress was recorded for each sample. The fatigue constant (n) was calculated using the classic regression on log (stress)/log (time) for the static test and log (strength)/log (rate) for the dynamic test. The distribution of "n" values calculated from equal ranked data points is shown in Figure 5. The best fit "n" for all data points is 16 and 17 for the static an dynamic tests respectively. When compared with previous fatigue data for unspliced fibers it may be concluded the splicing operation does not change the fatigue characteristics of the waveguides.

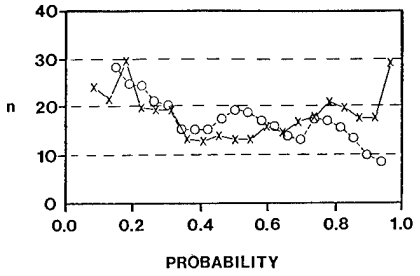



Fig. 5. Distribution of Static (o) and Dynamic (x) Fatigue Constant "n" for Spliced Fiber.

F. Abrasion Resistance

The material used to recoat the stripped and fusion spliced area should provide the fiber the same level of resistance to mechanical abrasion as the original coating. A measure of this resistance is done by tensioning the fiber and dropping sand on the recoat area until failure occurs. The average amount of sand required to cause failure in 10 spliced and recoated sections is 25 kg. These results are comparable to the resistance demonstrated by the original UV-curable acrylate coatings.

G. Microbend Resistance

The increase in attenuation as measured on a fusion spliced and recoated section should not exceed that of an adjacent unspliced section. For this test, 1.635 m of SM fiber was placed upon 150 grit silicon carbide sandpaper and loaded with flat steel plates to induce microbending. A plot of attenuation versus load is shown in Figure 6. The maximum average attenuation was seen to be 0.51 dB. These results are comparable to the microbend resistance of the unspliced fiber.

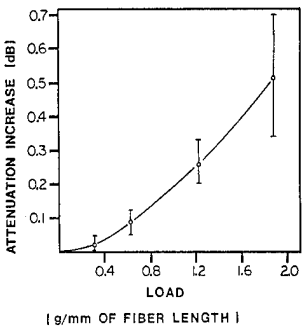



Fig. 6. Microbend Loss

H. Temperature Dependence - Cold

The maximum allowable increase in attenuation at 1300 nm shall be ≤ 0.05 dB/km over the temperature range of 25°C to -40°C. The average increase in attenuation for five 2.0 km fibers containing one splice per length is 0.01 dB/km, with a 0.017 dB/km standard deviation, and a maximum of 0.04 dB/km.

I. Temperature Humidity Cycling

Figure 7 shows the change in attenuation for three 2.0 km SM fibers containing one splice at mid-span when subjected to temperatures from 65°C to -10°C and relative humidities from 98% to 4% in 24 hour cycles. The induced attenuation is well within the specification of ≤ 0.05 dB/km.

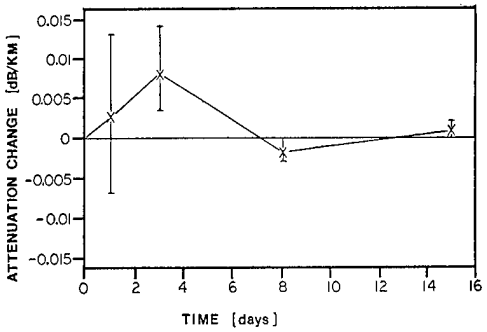



Fig. 7. Temperature Humidity Cycling

J. Water Soak at 23°C

The change in attenuation for three spliced fibers soaked in room temperature water is shown in Figure 8. Again, the induced attenuation is considerably less than the specification of ≤ 0.05 dB/km.

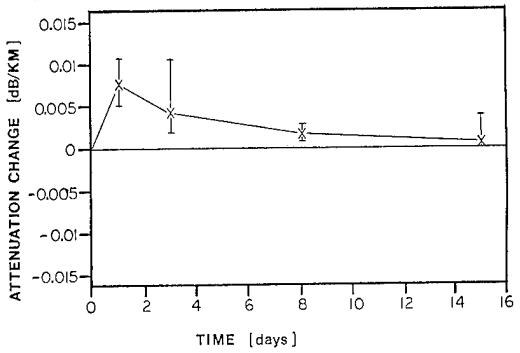



Fig. 8. $23^{O}$ Water Soak

CONCLUSIONS

It has been demonstrated that various types of both MM and SM fibers may be fusion spliced using the same fiber end preparation, fusion splicing and splice recoating equipment and settings, with the only necessary change being the operating wavelength and launch conditions of the OTDR. High strength, low loss splices can be repeatedly achieved by utilizing careful fiber end preparation techniques and close control of the fusion process. The spliced SM fibers meet the same optical standards as unspliced fiber. The recoated section meets the same geometric tolerances and provides the same mechanical and environmental protection as the existing coating.

ACKNOWLEDGEMENTS

The authors thank D. A. Wait and R. C. Daeffler for the fabrication, testing and documentation of many hundreds of spliced fibers. They express their appreciation to all members of the Corning Waveguide Product Engineering Laboratory for their valuable assistance in the exhaustive testing procedures performed. They also acknowledge Siecor Corporation for their cooperation in the fabrication and testing of the cabled fibers.

REFERENCES

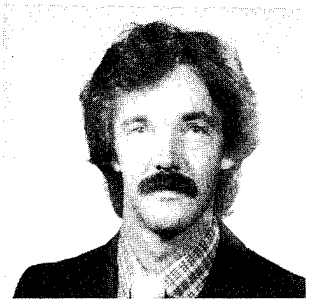
1. Taylor, D. H., Saikkonen, S. L., "Factory Splicing of Optical Waveguide Fiber", International Wire and Cable Symposium Proceedings, 1983, pp. 63-69.

2. Miller, C. M., Mettler, S. C., "A Loss Model for Parabolic - Profile Fiber Splices", The Bell System Technical Journal, Vol. 57, No. 9, Nov. 1978, pp. 3167-3181.

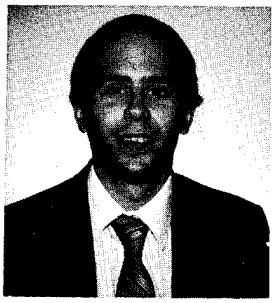
3. Heckmann, S., et al., "Long-Range Backscattering Experiments in Single-Mode Fibers", Optics Letters, Vol. 6, No. 12, Dec. 1981, pp. 634-635.

4. Danielson, B. L., "Backscatter Signature Simulations", (U.S.) National Bureau of Standards, Report No. NBS TN-1050, Dec. 1981.

5. Hevey, L. M., Saikkonen, S. L. and Taylor, D. H., "Theoretical Splice Loss Study of Single-Mode Fibers", Proceedings of SPIE, Vol. 479, May, 1984, pp.48-52.



Stuart Saikkonen is currently a Senior Mechanical Engineer with Corning Glass Works' Telecommunications Products Division. His present responsibility covers process development, equipment design and product testing for Optical Waveguide fiber splicing. He received his Bachelor's degree in Mechanical Engineering from Rochester Institute of Technology in 1981. He has been granted one patent for fiber splice recoating, and is a member of SPIE.



Michael Hackert began his work at Catholic University from which he received his BSEE in 1980. He went on to do his graduate work under Dr. C. C. Cutler and Dr. H. J. Shaw at the Ginzton Applied Physics Lab at Stanford University. He received his MSEE in 1982. Since then he has been working at the Waveguide Product Engineering Lab of Corning Glass Works in Corning, New York developing fiber measurements.

# Power and Communication Cables Designed for Later Insertion of Optical Fibers

Albert Gyger

C a b l e x S.A., Route de Lonay 3,
CH-1110 Morges, Switzerland

**Summary**

In the field of optical information transmission in electric utility networks different kinds of cables are used: combined high-voltage cables with integrated optical fibers, heavily armoured optical cables or optical cables drawn in a separate plastic tube.
We present a novel kind of combined cables. Thin plastic tubes are stranded in the interspaces of the electrical cables. With the technique described in this paper it is possible to introduce an optical fiber after it has been laid.
This technique is feasible on cable lengths up to 1000 m.
Typical applications are signal transmission in medium voltage networks (e.g. remote control of transformers) and temperature monitoring of high voltage cables.

## Optical fibers in power distribution networks

### Why optical fibers?

In recent years optical fibers have found a broad field of application due to the technical and economical advantages of this product.
While the large bandwidth and the low attenuation have lead to a broad application in telephone and data transmission networks, optical fibers have also other qualities so that their application in other fields is of great interest.
The small dimensions, the electromagnetic compatibility and the electric insulation qualities of the optical fibers lead to many applications in electric utility networks.

### Transmission systems for electric utilities networks.

Today, for most transmission problems suitable terminal equipment is on the market. We will present two examples.

Distance protection relay: In high voltage networks cable sections are monitored and, in case of failure, separated off the network.
We have developed a remote control unit for optical transmission of the signals of the relays. The unit is shown in fig. 1.

Multi-purpose transmission system: Electric utilities often have many kinds of different signals to be transmitted: telephone signals as well as data, control and measurement signals have to be transmitted on one line.
Fig 2. shows the block diagram of a fiber optic transmission system designed for the needs of electric utilities. By choosing the appropriate plug-in unit, up to six different signals can be transmitted on the same fiber pair.

### Cable types and installation

Provided that a high-voltage cable and an optical cable has to be laid in the same duct, at least four different solutions can be chosen:

1. Combined cable. An optical cable can be built in the spaces of a three-core high-voltage cable. This solution has already been applied by many cable manufacturers.

2. Common pulling. The high-voltage cable and the optical cable can be pulled in together. This solution calls for a heavy armouring of the optical cable for mechanical protection. An example of such a cable is shown in fig. 3. This optical cable has been pulled in a duct together with three one-core high-voltage cables.

3. Common pulling of a plastic tube. Together with the high-voltage cable a plastic tube is pulled in the duct. In this tube (inner diameter approx. 30 mm) an optical cable can be pulled in. An armouring of the optical cable is not needed. Dielectric cables with a central strength member of FRP have been pulled on lengths exceeding 1000 m.

4. Cables with built-in tubes for later insertion of optical fibers.
We have developed a technique which permits optical fibers to be inserted in a cable after it has been laid, provided it contains spare tubes for this purpose. It is also possible to remove the fibers at a later date.
This paper will explain this technique in more details.

## Technique for inserting optical fibers in existing cable installations

### Advantages of this technique

Many potential users of fiber optics, in particular electrical utilities, know that they will need optical communication in the near future, due to their technical and economical advantages.
In many cases an immediate use is not possible, maybe because the appropriate terminal equipement is not yet on the market, maybe because an existing network of copper cables cannot be replaced immediately.
To overcome this problem we propose to use cables with spare tubes.

Our technique has a number of advantages:

- At virtually no extra cost a facility can be included in a cable which permits an optical link to be added at any date in the future.
- the optical fibers only need to be purchased when they are actually required.

By inserting the optical fibers in the conventional cable

- the cost of cable laying is reduced since only one cable has to be laid
- better use is made of the space in the cable duct, which is usually limited
- separate protection of the optical fibers is not necessary as the mechanical strength of the conventional cable is sufficient.
- no danger of fiber quality deterioration during cabling and laying exists since the fibers are introduced only after the cable is laid.

A similar technique has been proposed by BTRL (Ref. 1). Introduced fiber length up to 300 m have been reported to have been introduced. With our technique lengths of up to 1000 m have been successfully introduced.

### Description of the technique

Fibers. We use step- and graded-index fibers with tight coating. The outer diameter is 0.5 ÷ 1.0 mm. To increase the friction with the flowing air, cotton yarns are braided around the fibers.

Tubes. We use pressure-resistant available commercially plastic tubes, e.g. Polyamide 6/6. The outer and inner diameter are 5 and 3 mm for cable lengths up to 700 m and 6 and 4 mm for cable length up to 1000 m. For special applications metal tubes can be used as well.

Cables. The tubes can be stranded in the interspaces of a three-core high-voltage cable (fig. 4) or in the place of a quad in a telephone cable. The achieved length of 1000 m is sufficient for most applications.
In the cable joints the tubes can be connected (if the total length is less than 1000 m) or the fibers can be spliced (fig. 5).

Insertion of the fibers. The insertion of the fiber is not done by traction, but by the continuously distributed force of the air flow through the tube. Thus the longitudinal force on the fiber remains very low and the tube may be almost arbitrary bent.
Fig. 6 shows a schematic view of the insertion process. The reel with the fiber is mounted in the insertion device and approx. 1 m of fiber is manually pushed into the tube. The apparatus is now closed and set under pressure. The pressure is set to a value at which the fiber glides in the tube with an easy movement of the handwheel.
The speed of the fiber is held at 1 ÷ 3 m/s, a fiber length of 1000 m can thus be inserted within a few minutes.
To permit the sliding of the fiber, an air flow of approx. 15 l/min (at atmospheric pressure) is required. This means that the following pressures are needed:

| Tube length | air pressure |
|---|---|
| 100 m | 6 bar |
| 700 m | 30 bar |
| 1000 m | 50 bar |

Fig. 7 shows the measured dependence of air pressure, air flow and fiber tension at the beginning of the fiber.

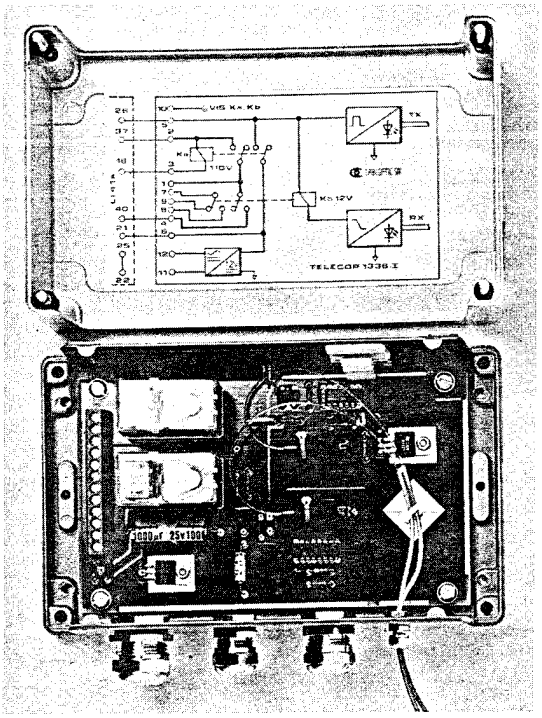
No degradation of the optical characteristics after insertion has been detected up to now.

### Application of the technique

Signal transmission in the medium-voltage network. In Switzerland, for many electric utilities it has become a common practice to equip all new medium voltage cables with spare tubes. Later on, these tubes can be equipped with optical fibers in order to transmit signals for remote control and monitoring of substations.

Temperature monitoring of high voltage cables. In the city of Zurich a concrete duct (inner diameter 130 cm) crossing a river has been built. This duct carries 3 systems of 150 kV cables and 19 systems of 20 kV cables. This concentration leads to a heat accumulation so that monitoring of the cable temperature is a necessity.
A measuring system with electric temperature sensors would hardly work in this electromagnetically harsh environment.
Recently, passive optical sensors have become available. These sensors can be mounted at the end of an optical fiber and they are not thicker than

the fiber itself. The system works on a fiber length up to 500 m (see Ref. 2).
For mechanical reasons it was not possible to integrate these fibers and sensors in the one-core 150 kV cables. In addition the manufacturer can not give a warranty on the lifetime of the sensors.
We have overcome the problem by stranding a layer of tubes and fillers on the cable.
With our technique this fibers can easily be inserted in the tubes an the sensors positioned to the desired place. In case of failure of a sensor it can be replaced with the same technique.



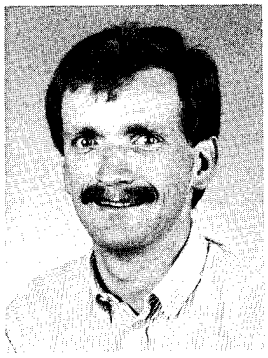

## Acknowledgments

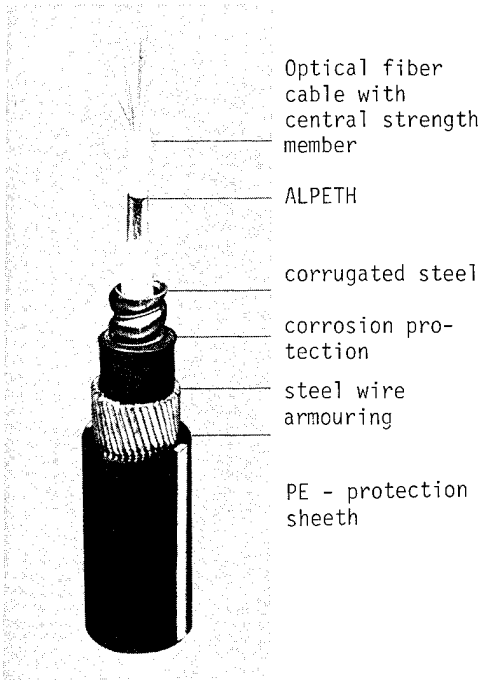
The author wishes to express his thanks to **Cableworks BRUGG Ltd., CH-5200 BRUGG,** for making possible the development of this technique, and to **MM. Kamber** and **Hirt** of Flugzeugwerke Emmen, who carried out the aerodynamical calculations.


## References


Ref. 1. Installation of optical fiber units using viscous drag of air.
M. Reeve and S. Cassidy, BTRL, ECOC 83, Geneva.

Ref. 2. Fiber-Optic Systems for Temperature and Vibration measurements in industrial applications.
C. Oven, M. Adolfsson and B. Hök, ASEA.
Int. Conf. on Opt. Techniques in Process Control 1983, The Hague.




**Albert Gyger** was born in 1955 and received his degree of Electrical Engineer from the Swiss Federal Institute of Technology (ETHZ) in 1979. In 1981 he joined Cableworks Brugg Ltd. where he was engaged in design an testing of symmetrical cables. He is now working on optical and combined electrical/optical cables projects.

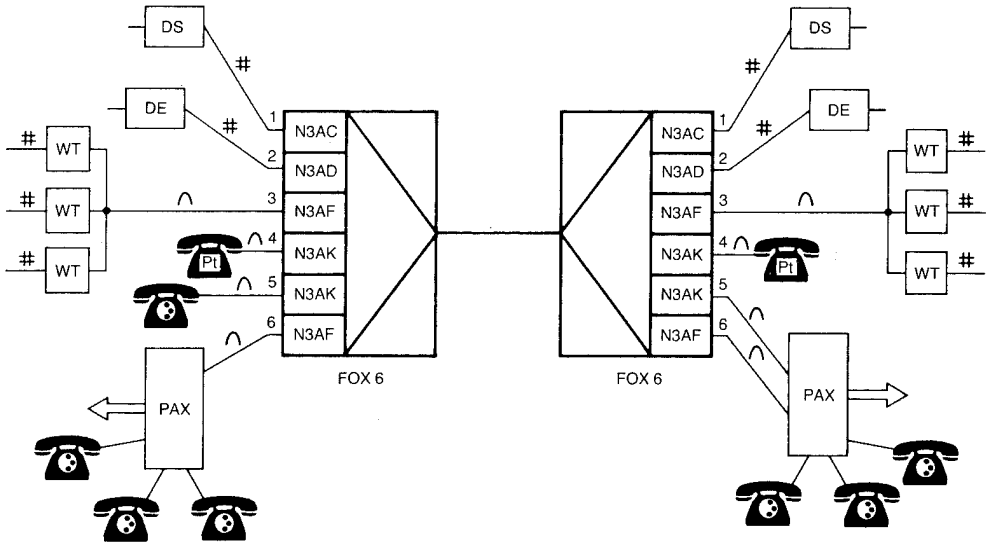
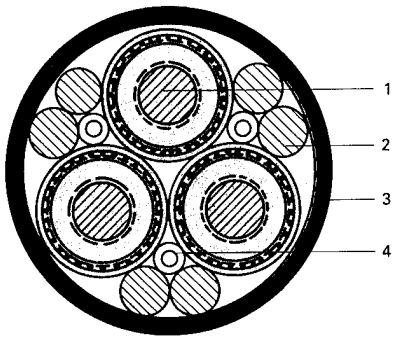



Fig. 2 – Possible applications of the compact optical fibre transmission system FOX 6

| | | | |
|---|---|---|---|
| DS | Distance protection relay | N3AC | Digital protection interface |
| DE | Data terminal equipment, e.g. of a telecontrol system | N3AD | Asynchronous data interface |
| WT | Voice frequency telegraphy channel | N3AF | PAX-PAX interface |
| PAX | Telephone exchange | N3AK | Subscriber-PAX interface |
| Pt | Point-to-point telephony | # | Digital |
| | | ∩ | Analog |



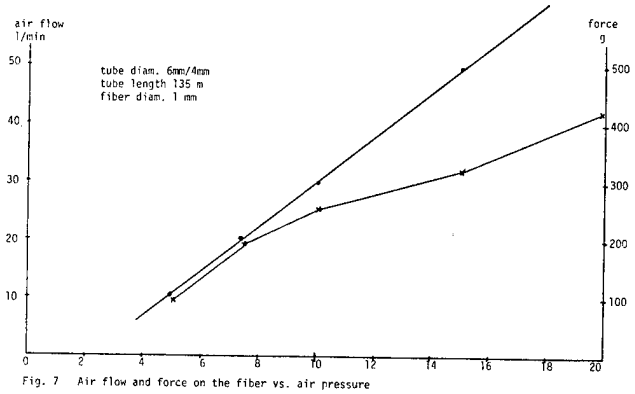
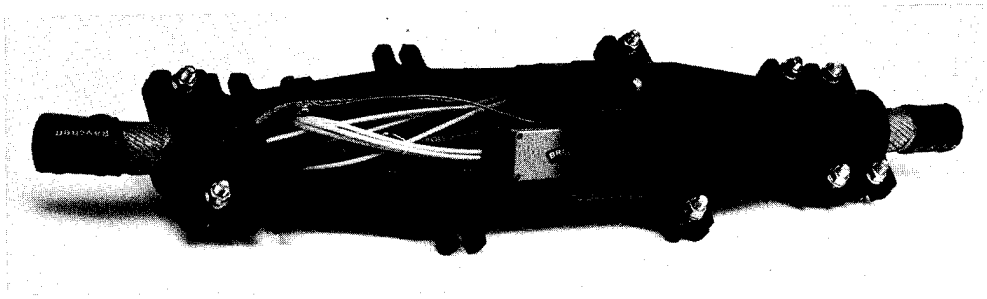




Fig. 7 Air flow and force on the fiber vs. air pressure



SCHEMATIC LAYOUT OF FIBRE INSTALLATION

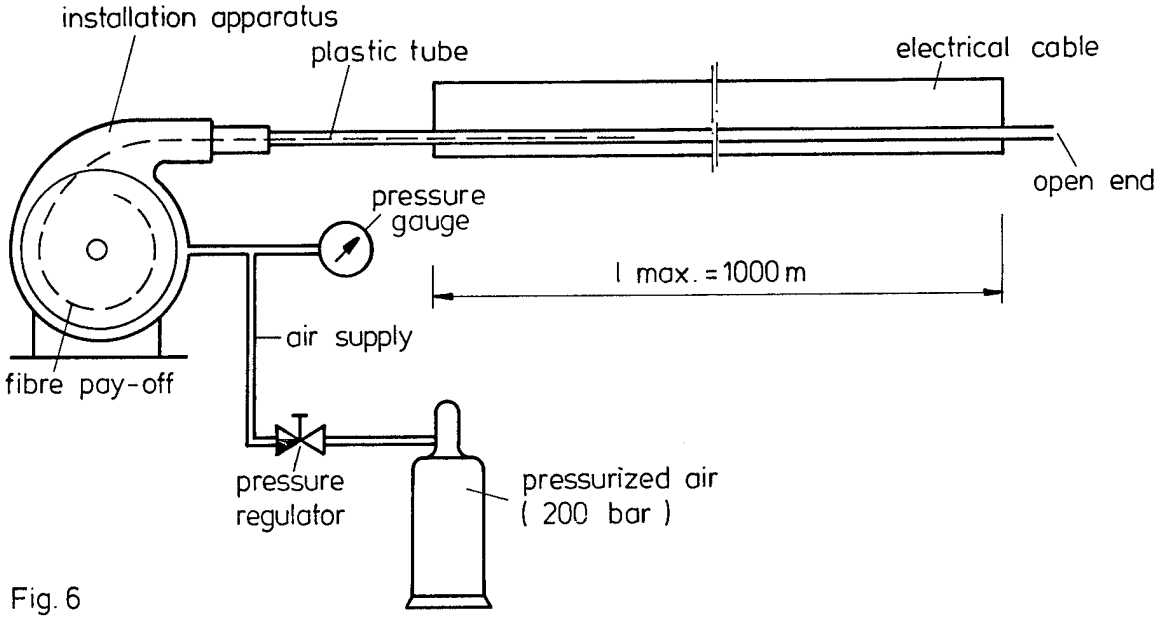



Fig. 6

# ETHERNET AND THINNET UNDERCARPET COMPATIBLE LOCAL AREA NETWORK WIRING SYSTEM

Kenneth P. Blum
Conrad W. Ponder

Thomas & Betts Corporation
Raritan, New Jersey

## ABSTRACT

Ethernet is a trademark for a local area network which provides a communication facility for high speed data exchanges among computers and other digital devices. Ethernet, developed by Xerox Corporation, DEC and Intel in 1980, was the basis for the 10 Mbps CSMA/CD baseband standard of the IEEE 802.3 Standards Committee. The Ethernet network can link equipment manufactured by a variety of vendors and cover a fairly large geographic area with high performance characteristics.

The primary goal of the Cheapernet standards committee was to develop and propose an economical network. A secondary goal was to develop a network that would easily be implemented with products readily available today and also would be acceptable to the industry. Cheapernet and Thinnet are synonymous and will be used interchangebably.

This paper discusses the design and implementation of an undercarpet Ethernet/Thinnet distribution and interconnection system. This system was developed to address the cabling and connection issues present when integrating the bus network design into the modern office landscape. Moves and changes, appearance, and installation costs are advantages of the undercarpet system in the open office environment as compared to the conventional round wire distribution system.

## 1. INTRODUCTION

Undercarpet wiring systems have been used to meet various data and communication transmission requirements in the commercial office as an alternative to conventional practices. The Ethernet/Thinnet compatible systems have been developed to achieve maximum flexibility in installations where aesthetics are of prime importance in the office. It is versatile and convenient because it installs inconspicuously under commercial carpet tiles. There are no unsightly cables and office design changes can be easily accomplished.

The Ethernet/Thinnet undercarpet system was developed to provide a local area network segment that is completely compatible with the present Ethernet and Thinnet round wire distribution systems. The standards for this system are the same as for the conventional round coaxial cable. For Ethernet applications, the limiting specification is the DC loop resistance of 5.0 ohms per segment which limits the maximum cable run distance.

Undercarpet coaxial cable is completely compatible to meet or exceed the specifications of Cheapernet (IEEE 802.3 10/Base/2). An undercarpet transceiver cable, which connects the transceiver to the data terminal, is also available to complete the undercarpet Ethernet/Thinnet cabling network.

The connectorization of this system is completely field installable without the use of any special tooling. The installation of this system provides the user with a cost-effective method in the initial installation and when moves, changes and rearrangements in the office are necessary.

## 2. DESIGN CRITERIA

The design criteria for this system were the following:

1. Achieve performance characteristics to meet IEEE 802.3 requirements.
2. Offer a complete cabling and interconnection system (Taps, BNC's, "D" Connectors).
3. Offer a system that can be installed in the office environment without additional distribution facilities (i.e., raceway, duct, etc.).
4. Ease and flexibility of installation without special tools or factory preconnectorized cables.
5. Ease and flexibility of rearrangements with minimal disruption to network operation.

## 3. PERFORMANCE CHARACTERISTICS

### 3.1 Coaxial Cable

A comparison of the differences of the IEEE 802.3 Standard CSMA/CD and Thinnet local area networks are shown in Table 1.

**Ethernet is a registered trademark of Xerox Corporation.**

TABLE 1
Comparison of Thinnet with
Standard CSMA/CD LAN

| PARAMETER | ETHERNET | THINNET |
|---|---|---|
| Data Rate | 10Mbit/s | 10Mbit/s |
| Segment Length | 1,600 ft. | 600 ft. |
| Network Span | 8,000 ft. | 3,000 ft. |
| Nodes per Segment | 100 | 30 |
| Nodes per Network | 1,024 | 1,024 |
| Node Spacing | At 2.5 meter intervals (on cable marker bands) | 0.5 meter min. separation |
| Segment Cabling System | 0.4" dia. 50 ohm Coax w/N-Series connectors | 0.25" diameter 50 ohm Coax w/BNC conn. |
| Transceiver Interface | 0.38" dia. Multiway cable w/15 pin D-Series connectors (length up to 165 ft.) | (Optional) |
| Coaxial Cable Loop Resistance | 5 ohms | 10 ohms |

The Ethernet IEEE Standard 802.3 was developed to be a high performance system and cover a large geographic area. Thinnet, however, was proposed to be a high performance network that would be operational over a moderate or reduced geographic area as compared to Ethernet. The Thinnet system utilizes an RG58 cable medium and BNC connectors for connectorization of the networking system. Thinnet then basically utilizes a thinner and cheaper cable which is much easier to install with a connectorization system that is well known in the industry.

Since the primary environment of undercarpet cabling covers the open office landscape and there was not the need for a 1600 foot length, we developed a system that was compatible with the Standard CSMA/CD for limited segments and met the Thinnet Specification. Table 2 shows the coaxial cable characteristics and specifications for the Ethernet, Thinnet and the Undercarpet Cabling System which provides the main bussing medium for the system.

As shown in the table, the major difference from the Standard Ethernet and Thinnet is the DC loop resistance which impacts the length of run.

## 3.2 Transceiver Cable

The transceiver cable is used to interface Data Terminal Equipment to the coaxial cable medium via the transceiver. The undercarpet cable is a four pair 78 ohm impedance cable using 15 pin D connectors. Each pair of conductors are individually shielded and separated from each other and contain a drain wire. The cable construction and the electrical characteristics are shown in Table 3 and in Figure 1.

TABLE 3
TRANSCEIVER CABLE CHARACTERISTICS

| | | |
|---|---|---|
| Impedance | | 78 ± 5 ohms |
| Capacitance | | 17 pf/ft. |
| Attenuation: | 5 Mhz | 2.4 db/100 ft. |
| | 10 MHz | 3.3 db/100 ft. |
| Velocity of Propagation: | % | 68 |
| | NS/ft. | 1.5 |
| Center Conductors | | 26 AWG |
| D.C. Resistance | | 40 ohms/1000 ft. |
| Insulation | | Polyethylene |
| Shield | | Aluminum Foil; 100% Coverage |
| Drain Wire | | 26 AWG, Silver plated |
| D.C. Resistance | | 20 ohms/1000 ft. |
| Outer Jacket | | PVC |
| Flammability | | UL 94 Horizontal Burn<br>UL 83 Vertical Burn |
| Near End Crosstalk: | 1.0 KHz | 120 db |
| | 1.0 MHz | 73 db |

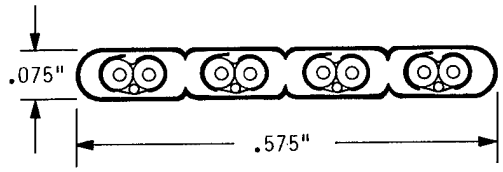



FIGURE 1
TRANSCEIVER CABLE CONSTRUCTION

The limiting factor of meeting the specification while meeting all of the parameters is the D.C. resistance per conductor which has to be less than 1.75 ohms. The undercarpet transceiver cable therefore can be used with lengths up to 50 feet.

TABLE 2
COMPARISON BETWEEN ETHERNET/THINNET SPECIFICATION AND UNDERCARPET COAXIAL CABLE

| CHARACTERISTIC | ETHERNET | REQUIREMENTS THINNET | UNDERCARPET CABLE |
|---|---|---|---|
| Zo, (impedance) ohms | 50 ± 2 | 50 ± 2 | 50 ± 2 |
| Capacitance picofarad/ft. | 26.0 | 26.0 | 25.0 |
| Velocity of Propagation: | | | |
| % | 78 | 65 min. | 78 |
| NS/ft. | 1.3 | 1.55 | 1.3 |
| Attenuation: | | | |
| @ 5 MHz | 6.0 db/1600 ft. | 6.0 db/600 ft. | 4.0 db/600 ft. |
| @ 10 MHz | 8.5 db/1600 ft. | 8.5 db/600 ft. | 6.5 db/600 ft. |
| Center Conductor | Copper (Tinned) | Tinned Copper | Copper, Silverplated |
| Wire Size: AWG | #11 | #20 Stranded | #19 |
| Nominal D.C. Resistance (ohms) | 1.42/1000 ft. | 10.8/1000 ft. | 7.5/1000 ft. |
| Nominal cond. diam. | 0.086" | 0.032" | 0.035" |
| Insulation: | | | |
| Core | Polyethylene | Solid Polyethylene | Cellular Polypropylene |
| Outer Jacket | Yellow PVC<br>Orange Teflon | PVC or Teflon | Yellow PVC |
| Shield | Braid & Foil | Braid or Foil | Copper Foil |
| FCC Docket 20780 | Pass | Pass | Pass |
| Drain Wire: | | | |
| Size -- AWG | N/A (Braid) | N/A (Braid) | #26 Copper, Silverplated |
| Shield Coverage | 100% | ≥95% | 100% |
| Resistance shield, ohms | 1.42 ohms/1000 ft. | 4.1 ohms/1000 ft. | 7.5 ohms/1000 ft. |
| Resistance, ohms: | | | |
| Center Conductor | 1.42/1000 ft. | 6.14/600 ft. | 4.5/600 ft. |
| Shield and Drain | 1.52/1000 ft. | 2.5 /600 ft. | 4.5/600 ft. |
| D.C. Loop - Resistance ohms/600 ft. | ≤5.0 | ≤10 | 9.0 |
| Flammability | UL VW-1 | UL VW-1 | UL 94 Horizontal Burn<br>UL 83 Vertical Burn |
| Shape | Round | Round | Trapezoidal |
| Dimensions | 0.400" | 0.200" | Height - 0.115"<br>Width - 0.475" |
| |  |  |  |

3.3 Physical Requirements

Because Undercarpet Wiring is a relatively new concept, the following mechanical and environmental tests have been developed and performed in addition to the basic electrical tests. These tests are:

1. Mechanical Abuse Test
2. Compressive Load
3. Resistance to Environment
   a) Chemical
   b) Water
   c) Steam
   d) Concrete
4. UL94 Horizontal Flame
5. UL83 Vertical Flame

Shown in Figures 2, 3, 4 and 5 are the test methods and results required.

3.3.1 Mechanical Abuse Test

This test was devised to determine the performance of undercarpet cables to perform reliably when located near a desk as found in commercial and industrial offices. Shown in Figure 2 is the Mechanical Abuse Test procedure. The cable is secured to floor with tape. The entire area is covered with carpet tiles and a 300-pound weight (on 9 casters) is rolled over the carpet (100 cycles in 4 directions). Upon completion of the mechanical abuse, the electrical parameters of impedance, capacitance, velocity of propagation, and sinusoidal attenuation are measured. In addition, the cables are subjected to 1500 Vac for one minute without breakdown between conductors and shield and between shield and water.

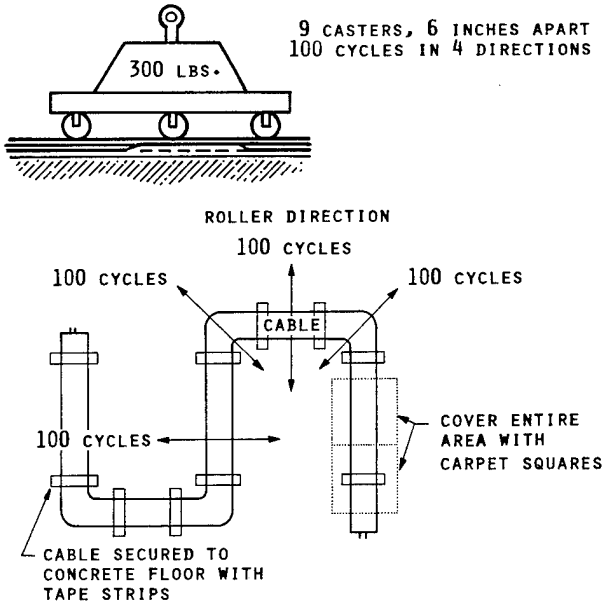
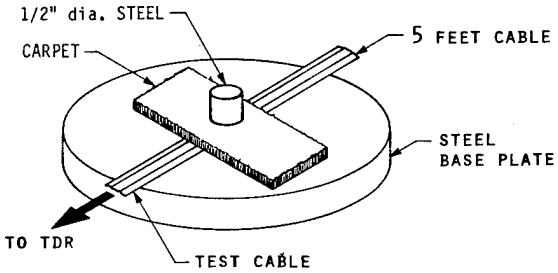



FIGURE 2
MECHANICAL ABUSE TEST

3.3.2 Compressive Load

The purpose of the Compressive Load test is to see what force is required to change the cables impedance 5.0 ohms. This test method was devised to determine the ability of undercarpet cable to perform reliably when located in areas such as under filing cabinets. It is performed by securing a five foot length of cable to the steel base plate. A carpet square is placed on top of the cable and a force is applied to the carpet above the cable with a 1/2 inch diameter rod, at a rate of 0.1 inches per minute. The force required to cause a 5.0 ohm change in the cable impedance is recorded and also the percent change of the impedance from the nominal value when the force is removed. Typical results are shown in Table 4.




CABLE PLACED DIRECTLY BETWEEN BASE PLATE AND CARPET

FIGURE 3
COMPRESSIVE LOAD TEST

TABLE 4
Compressive Load Test Results

| SAMPLE | INITIAL Zo | Zo UNDER LOAD | FORCE (LBS.) | % DIFFERENCE AFTER LOAD REMOVAL |
|---|---|---|---|---|
| 4 Pair Cable | 78 ohms | 73 ohms | 1,000/1/2" dia 5,100/in$^2$ | 1.7 |
| Coaxial Cable | 50 ohms | 45 ohms | 750/1/2" dia 3,827/in$^2$ | 1.5 |

3.3.3 Resistance to Environment

Environmental resistance requirements are placed on the cable to insure that it will provide maintenance free service when exposed to carpet cleaning materials.

Carpet Cleaning Fluids. Cable samples are placed in a 5% solution of acetic acid and water, a 5% solution of sodium phosphate with a .01% non-ionic detergent for 30 days. Periodic insulation resistance measurements are made between conductors and shield. A minimum of $10^9$ ohms is required at the end of the test and cannot decrease by more than a factor of 10 from the original value. In addition, the cable shall withstand 1500 Vac for one minute.

Water. Cable samples are immersed in water for 30 days and the same test criteria as used for Carpet Cleaning Fluids are required.

Steam. Cable samples are immersed in hot water 180°F (82.6°C) for five minutes and observed for apparent damage. Passing measurements for insulation resistance and dielectric breakdown are required.

Concrete Exposure. Cable samples are immersed in a saturated solution to Calcium Hydroxide Ca $(OH)_2$ for 72 hours. Samples must pass a 1500 Vac dielectric test between conductors and also between conductors and shield.

3.3.4 UL 94 HB Flammability Test

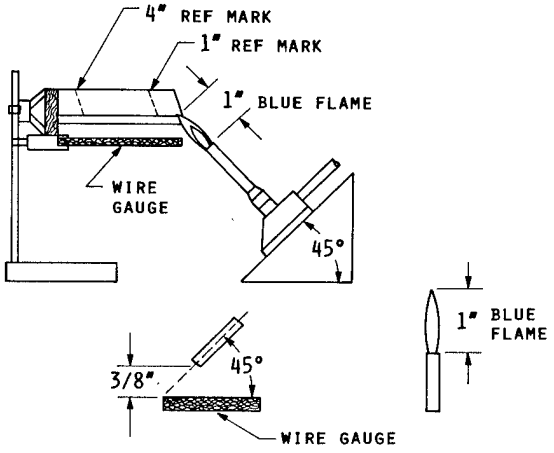



FIGURE 4
HORIZONTAL FLAME TEST

The purpose of this test is to determine whether the cable meets the UL 94 Standard for Flammability of Plastic Materials. Shown in Figure 4 is the test procedure. The cable is subjected to flame for 30 seconds. Passing criteria is that the burning rate shall not exceed 3 inches per minute or that the cable ceases to burn before the flame reaches the 4 inch reference mark.

3.3.5 UL 83 Vertical Flame Test

The purpose of this test is to determine whether the cable will convey flame along its length or to combustible materials in its vicinity when tested to UL83, UL Standard for Thermoplastic Insulated Wires.

UL 83 Vertical Burn Test for Flammability

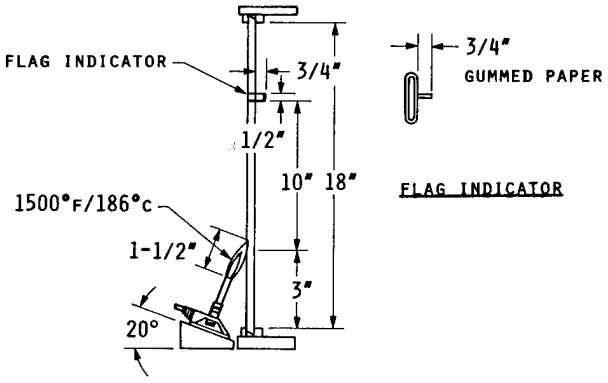



FIGURE 5
UL 83 VERTICAL FLAME TEST

TEST REQUIREMENT: A finished cable shall not flame for more than 1 minute following five 15 second applications. The cable specimen is considered unacceptable if more than 25% of the indicator flag is burned away or charred after 5 applications of flame or the flame burns longer than 60 seconds after the fifth application of flame.

4. INTERNCONNECTION COMPONENTS

The system interconnection components for the 50 ohm undercarpet cable consist of coaxial cable clamps or more commonly referred to as taps, male and female BNC coaxial connectors, 50 ohm BNC terminators and optional use of BNC "Tee" adaptors. For the undercarpet transceiver cable interface, a shielded 15-pin "D" male and female connector are used.

The taps and BNC coaxial connectors are completely field installable without the use of special tools. The 15-pin "D" connectors can be installed using a standard crimping tool.

Depending on user requirements and system design, either taps or coaxial connectors or a combination of both may be used to interconnect the system. The tap utilizes Insulation Displacement Technology (IDC) and eliminates cutting of the 50 ohm coaxial cable or using factory pre-connectorized coaxial cables.

## 4.1 Coaxial Cable Clamp (Tap) Construction

Shown in Figure 6 is the mechanical construction of the coaxial cable clamp.

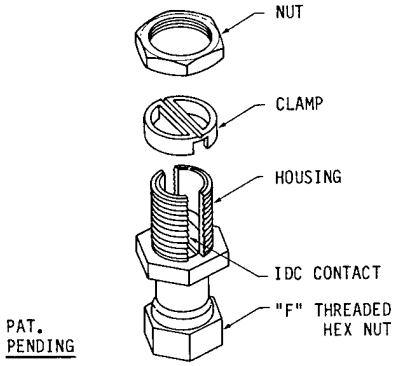



FIGURE 6
COAXIAL CABLE CLAMP

Depending on system transceiver design and whether it is used internal or external, the "F" threaded hex nut, which attaches the transceiver to the coaxial cable clamp, can also be available with a male BNC connector. Shown in Figure 7 is how a typical coaxial cable clamp would be attached to the cable and transceiver.

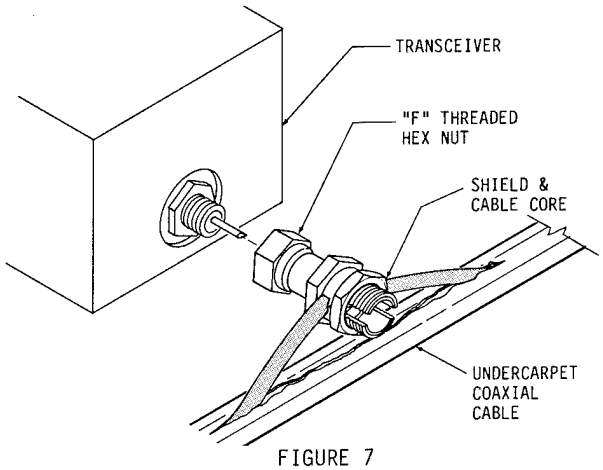



FIGURE 7
"F" THREADED TAP CONNECTION METHOD

The coaxial cable clamp (tap) is designed for an impedance matched low capacitance connection to the coaxial cable. It includes a conductive housing which supports in electrical isolation the insulation displacing electrical contact. The clamping element forces the center conductor of the coaxial cable down onto the insulation displacing portion contact for electrical termination. The assembly nut maintains that the drain wire and shield of the undercarpet coaxial cable are in direct electrical contact with the clamp housing. This feature also provides a permanent electrical connection between the coaxial cable center conductor and the insulation displacement contact and has very low contact resistance.

## 4.2 BNC Coaxial Connector Construction

Shown in Figure 8 is the mechanical construction of the Male and Female BNC coaxial connectors.

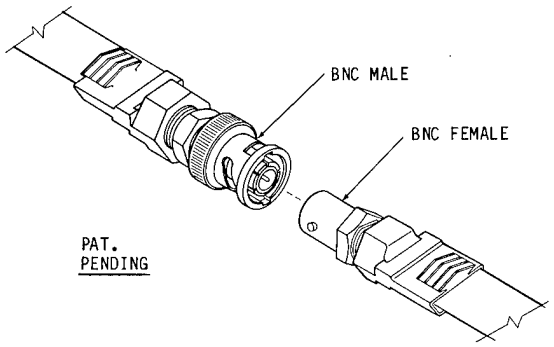



FIGURE 8
MALE AND FEMALE COAXIAL CONNECTORS

These BNC coaxial connectors for undercarpet wiring provide flexible and reliable connections. They are completely field installable with standard pliers and a cutter. One of the main advantages of their use is that bulk reels of cable can be used instead of preconnectorized lengths. This results in an easier design and layout and provides more flexibility in installing the system. Any future additions, moves and rearrangements let the user make changes with minimal cost.

## 4.3 15-Pin "D" Connectors

Male and Female 15-pin "D" connectors with shielded backshells and proper lockposts and sliding latch are used to interface the transceiver and data terminal equipment. They are connected to the undercarpet transceiver cable shown at bottom of Table 3 in Figure 1

using a standard crimping tool. A connector assembly is shown in Figure 9.

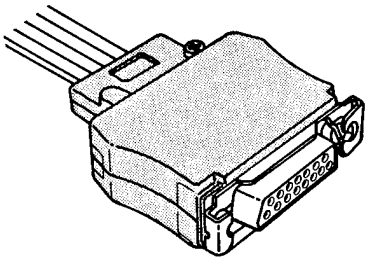


FIGURE 9
15-PIN "D" & UNDERCARPET TRANSCEIVER CABLE

## 5. SYSTEM INSTALLATION

The undercarpet Ethernet/Thinnet System can either be a standalone system or integrated into a conventional round cable network. Installation as a segment in the conventional round cable system is accomplished via a transceiver/repeater interface. Figures 10, 11 and 12 show typical networks in the standalone and integrated network mode.

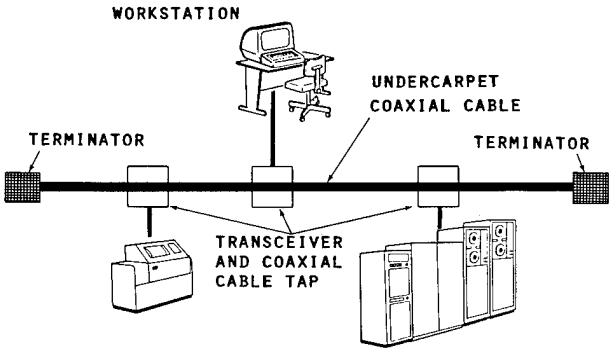



FIGURE 10
STANDALONE ETHERNET NETWORK

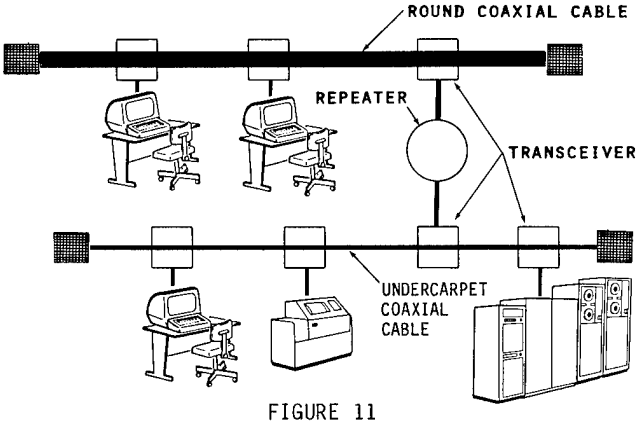



FIGURE 11
UNDERCARPET ETHERNET INTERFACE
WITH STANDARD ETHERNET NETWORK

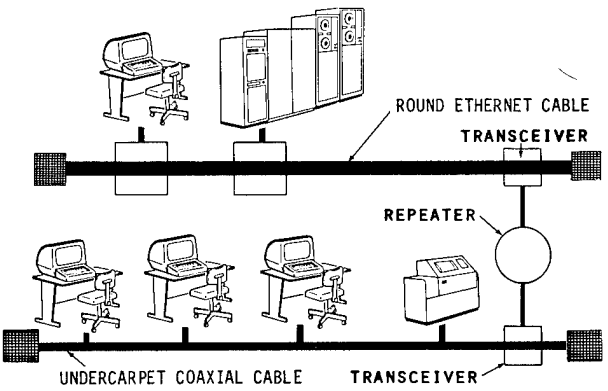



FIGURE 12
UNDERCARPET THINNET INTERFACE
WITH STANDARD ETHERNET NETWORK

Installation is accomplished by laying the cable directly onto the floor in an "S" pattern. This method of installation is used to provide spare cable for moves and rearrangements. Modular carpet tiles are not mandatory for this type of installation although flexibility for moves and changes are enhanced when carpet tiles are used instead of broadloom carpeting.

Once the cable is in place, either the non-obstrusive tap or BNC connector system is installed at the work space location. Figure 13 shows a BNC connection method. The advantages of the nonobstrusive tap is that the cable is not cut and can be restored

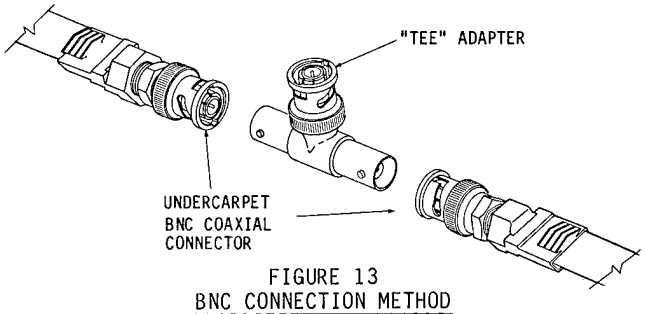



FIGURE 13
BNC CONNECTION METHOD

once a tap is moved. Pedestal housings shown in Figure 14 are used to protect and secure the transceiver at the terminal location.

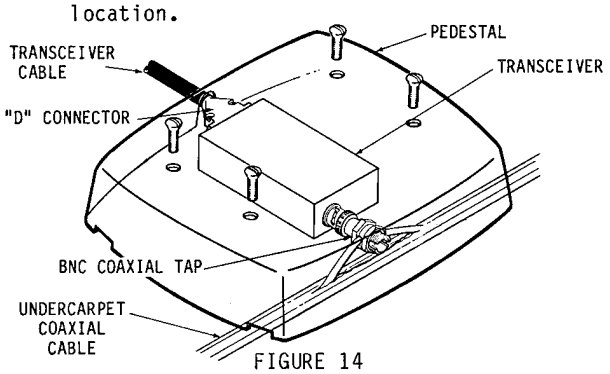



FIGURE 14
BNC MALE TAP CONNECTION METHOD

Undercarpet transceiver cable is also available in the event that the transceiver is located in areas other than floor locations. This cable is terminated with 15-pin "D" connectors and has a maximum distance of fifty feet.

## 6. CONCLUSION

The undercarpet Ethernet/Thinnet distribution system has been developed to enhance the application of conventional bus networking systems in the commercial office environment. Flexibility and cost effectiveness are achieved through the use of undercarpet cable and its associated interconnection components.

The undercarpet system was designed to meet the IEEE 802.3 specification for electrical performance characteristics. It has been subjected to rigorous mechanical and environmental tests to function satisfactorily undercarpet.

Implementation of the system in either a standalone or hybrid configuration enhances the functionality of the Ethernet/Thinnet networking concept.

## 7. REFERENCES


1. IEEE 802.3 Standards Committee, "CSMA/CD Access Method and Physical Layer Specifications," 1982, IEEE Press

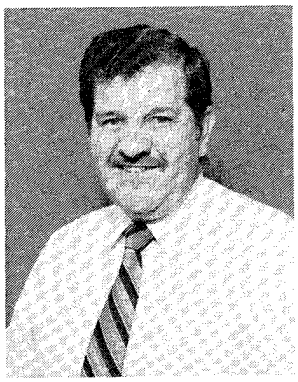
2. Architecture Technology Corporation, "The Ethernet-Type Local Networks Report," 1985, Minneapolis, Minnesota

3. Digital Equipment Corporation, "Introduction to Local Area Networks," 1982

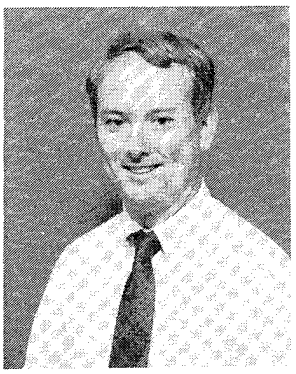
4. Flatman, Dr. A. V., "Cheapernet - A Low Cost Open System LAN"

5. IEEE 802.3, Section 10, Standards Committee, "Medium Attachment Unit and Baseband Medium Specifications for TYPE 10 BASE 2," Draft E, November, 1984, IEEE Press


©1985 Thomas & Betts Corporation. All Rights Reserved.



Kenneth P. Blum is a Senior Engineer for Research and Development in the Wiring Systems and Components Division. He received his BSEE from New Jersey Institute of Technology in 1973. He has been involved with the cable industry since 1975 and joined Thomas & Betts Corporation in 1978.



Conrad W. Ponder, PE, is the Telecommunications Product Manager in the Wiring Systems and Components Division. He received a BIE from Georgia Institute of Technology in 1969 and a MBA from Georgia State University in 1976. He has been involved in the communications industry since 1974 and joined the Thomas & Betts Corporation in 1984. He is a member of IEEE and BICSI.

# VERY LIGHT-WEIGHT, FIELD-USE PORTABLE FIBER OPTIC CABLE WITH CONNECTOR

T. OHSUGI T. YAMAZAKI Y. KITAYAMA T. KAKII

SUMITOMO ELECTRIC INDUSTRIES, LTD.
1, TAYA-CHO,TOTSUKA-KU,YOKOHAMA JAPAN (TEL) 045-851-1281

## Summary

A very light weight, non-metallic, flame-retardant, field-use portable optical fiber cable with connector has been newly developed. Two tight-buffer-coated optical fibers and two tensile strength members are housed in helical grooves of a flame-retardant plastic spacer. The cable weight is 14.5kg/km and its outer diameter is 4.3 mm. The cable has excellent mechanical and temperature characteristics in adverse conditions. An optical connector developed for the cable is characterized by its compact and waterproof structure, low connections loss and sufficient durability for repeated connection (> 1,000 times ).

## 1. Introduction

Communication cables which are portable and deployable in the fields are necessary in some situations like TV broadcasting of outdoor events. The currently used copper cables for these purposes suffer from problems such as heavy weight, small information capacity and susceptibility to electromagnetic interference (EMI). Use of optical fiber cable is now being considered as an effective means to solve these problems. In order to replace the currently used portable copper cables, optical fiber cable must be able to withstand repeated deployment and retrieval in rough terrain and in adverse conditions.

Y.saitoh, et al. developed a field-use optical fiber cable [1] which housed optical fibers and steel wires within the spiral grooves of a spacer. This cable was confirmed to have excellent mechanical and thermal properties. However, as this kind of cable is used in the field, it is preferable to reduce its size and weight as much as possible.

In this paper the design and properties of a newly developed non-metalized field-use optical fiber cable are described.

## 2. Properties required of the cable and connector

Field-use optical fiber cables must be able to be easily carried by human force alone and must have sufficient mechanical and thermal properties to withstand repeated deployment and retrieval. Therefore this cable and connector need the following qualifications.

1. Transmission loss of the optical fiber cable should be stable over the temperature range from -40°C to +70°C.
2. The optical fiber cable should withstand various mechanical forces in the field such as tensile strength, compressive force, impact force and repeated bending.
3. The cable should be light in weight and small in diameter to be carried and handled easily.
4. The connector should be compact and have sufficient durability for repeated connection and disconnections.

## 3. Cable Design

The cross section of the newly developed non-metalized field-use optical fiber cable is shown in Fig.1 and its outside view in Photo 1. The construction parameters of the cable is shown in Table 1. This cable is entirely dielectric and contains two tight-buffer-coated optical fibers. A spacer, which is made of flame-retardant polyethylene, has two kinds of spiral grooves; larger grooves for a very high density Kevlar® bundle to be housed tightly, and smaller grooves for optical fibers. The spacer is wrapped with plastic tape and then covered with low specific-gravity flame-retardant polyethylene.

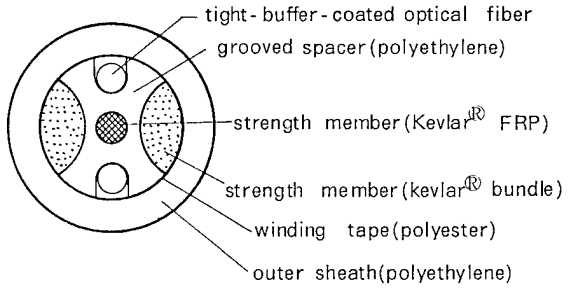



Figure 1. Cross section of new field-use optical cable

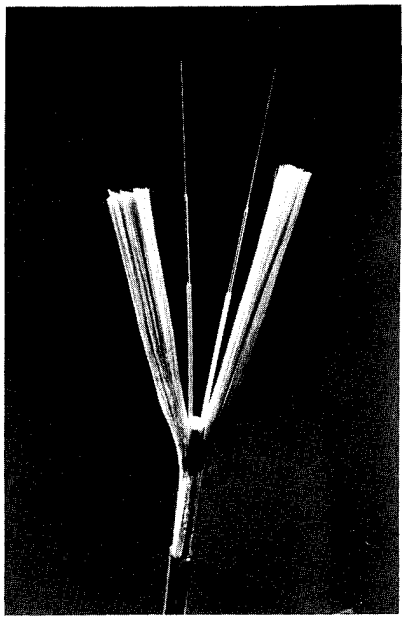


Photo 1. Outside view of new field-use optical cable

Table 1. Construction parameters of new field-use optical cable.

| Item | | | Typical value |
|---|---|---|---|
| Optical fiber | Core diameter | | 50 μm |
| | Outer diametr | | 125 μm |
| | NA | | 0.20 |
| | Coating | Material | Silicone and Fluorocarbon polymer |
| | | Outer diameter | 0.7 mm |
| Spacer | Number of fibers | | 2 |
| | Diameter | | 3.0 mm |
| | Material | | flame-retardant PE |
| Strength Member | | | 0.65 mm kevlar® FRP and kevlar® bundle |
| Sheath | Material | | flame-retardant PE |
| | Thickness | | 0.65 mm |
| | Diameter | | 4.3 mm |
| Cable weight | | | 14.5 kg/km |

The design philosophy of this cable is as follows:

Highly resistant to compression: The optical fibers of field-use cable should withstand high compressive force. The deformation of spacer type optical fiber cables under compressive force is generally less than that of non-spacer type optical fiber cables. Therefore, a spacer structure was used for this cable. Fig.2 shows transmission loss increase against compressive force for the spacer type and the non-spacer type optical fiber cable for comparision. In the non-spacer optical fiber cable, the transmission loss of the optical fiber starts increasing when compressive force of 120 kgf is applied to a 5cm portion of the cable. On the other hand, the spacer type optical fiber cable provides rigid protection against lateral pressure. It withstands compressive force as much as three to four times large as that of the non-spacer type.

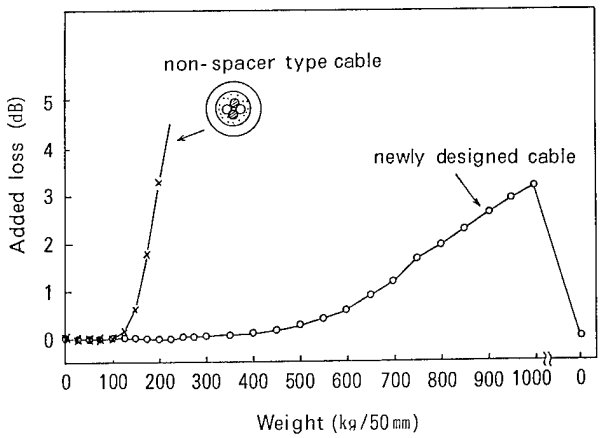



Figure 2. Compression property

High tensile strength: Kevlar® bundles are utilized as strength members in the non-metalized high strength cable. The elongation of non-twisted Kevlar® under tensile force is generally less than that of twisted Kevlar®(Kevlar® rope). Therefore, very high density non-twisted Kevlar® bundles are tightly housed in spiral grooves of the spacer. Fig.3 indicates the cable elongation against tensile load. Though the portion of the cable where it is fixed in the test breaks under the tensile load of 250 kgf, it is confirmed that the elongation of the cable is less than 0.5% under a tensile load of 70 kgf and that the breaking point of the cable is above 250 kgf.

Small diameter: It is preferable to reduce the diameter of the spacer to obtain small-diameter cable. However, the compression property would be worse with the smaller diameter. Furthermore, the larger grooves necessary under this arrangement would also deteriorate the compression property. Fig.4 shows the maximum allowable compressive force at which transmission loss increase does not occur for two types of the spacer, a small-grooved type and a large-grooved type. Though the spacer with larger grooves has less compression resistance than that with smaller grooves, a highly rigid spacer with larger grooves which has a diameter of 3.0 mm and the maximum allowable compressive force of 75 kg / 50 mm was successfully developed by means of using high Young's modulus polyethylene.

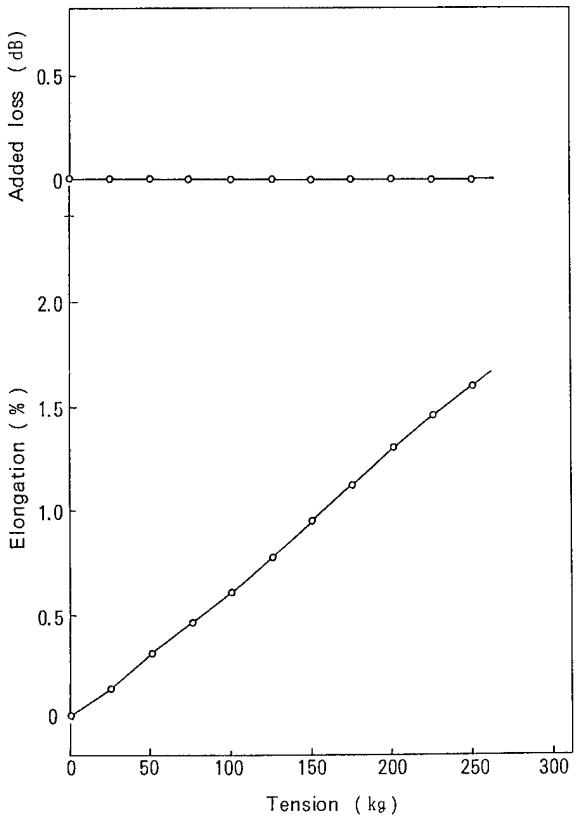



Figure 3. Tensile strength property

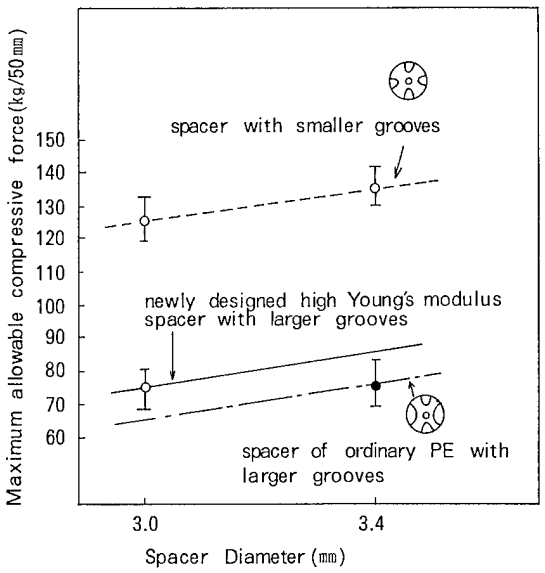
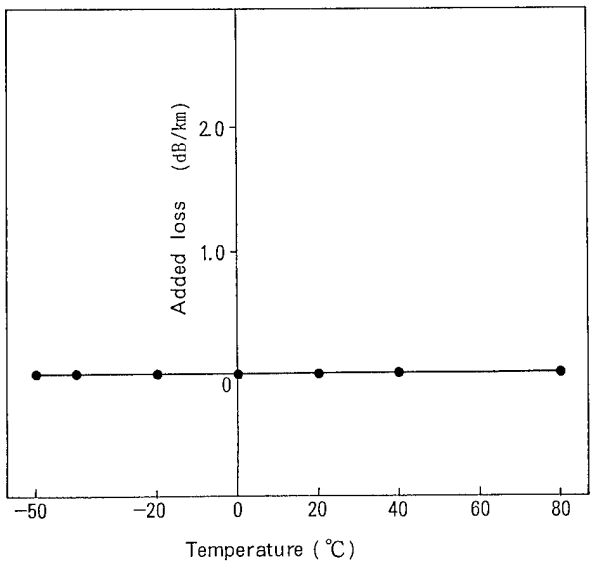



Figure 4. Compression property of spacer

## 4. Cable characteristics

### Temperature characteristics

Fig.5 shows transmission loss fluctuation of the optical fiber cable at -50°C ~ +80°C. The change, which was measured with and LED light source of 0.85μm wavelength, was within 0.1 dB/km for -50°C ~ +80°C.




Fibure 5. Temperature-transmisson loss property

### Mechanical characteristics

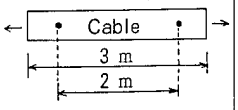
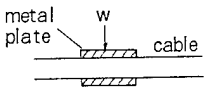
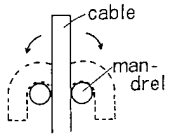
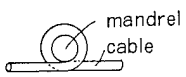
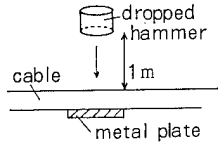
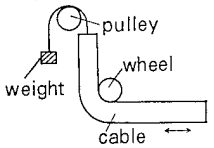
Mechanical characteristics were examined against tensile strength, compressive force, impact force, flexure, bending and scrape abrasion. Table 2 shows testing methods and results for various mechanical tests. Measurement of transmission loss was made with an LED light source of 0.85 μm wavelength. Tensile strength and compression tests have been already described in section 3 in detail.

(a) Flexure: The cable was bent 180 degrees to the right and left repeatedly around a mandrel of 20mm diameter. After 30 cycles there was neither breakage of fiber nor transmission loss increase.

(b) Bending test: To confirm the flex resistance of the cable, it was bent 360 degrees around various mandrels. As shown in Table 2, the minimum permissible bending diameter was 50mm, at which no transmission loss increase occurred, and even at the bending diameter of 40mm, the change in transmission loss was within 0.02 dB/km.

(c) Impact test: A hammer was dropped 5 times onto the same portion of the cable for a given impact energy, which is equal to the product of drop height and hammer weight. As shown in Table 2, no breakage of the fiber was observed even at 3kg·m of impact energy.

Table.2 Mechanical characteristics and inflammability

| Mechanical test | Test method | Result |
|---|---|---|
| Tensile strength | sample length : 3 m<br>measuring length : 2 m<br>hold time at each load : 1min.<br>  | <0.5 % elongation at 70 kgf<br>breaking load >250 kgf |
| Compression | plate length : 50 mm<br>compressive load :<br>0→1000 kgf (25kgf step)<br>  | no loss increase at 200 kgf. |
| Flexure | mandrel dia.:20 mm<br>  | no loss increase after 30 cycles |
| Bending | bending angle : 360°<br>  | no loss increase at the bending diameter of 50 mm |
| Impact | dropped hammer dia. : 25 mm<br>impact energy : 3 kg・m<br>  | no breaking after 5 dropped times |
| Scrape abrasion | wheel dia. : 40 mm<br>weight : 80 kgf<br>  | no breaking after 5 cycles |
| **Flame test** | **Test method** | **Result** |
| VW − 1 | temperature of the tip of flame : 836℃ or higher<br>combustion time : 15sec.×5 times | passes the spec. of VW−1 |

(d) Scrape abrasion: The cable was scraped by means of the wheel shown in Table 2 with weight applied. The scraping action was done in both directions along with the longitudinal axis of the cable for 5 cycles (10 strokes). No breakage of the optical fiber was observed at 80 kgf of applied weight.

In these tests, no cracks on the cable sheath were observed until breakage of the cable.

Inflammability

This test was based on VW-1 (Vertical Wire) flame test. Combustion was conducted 5 times for 15 seconds; however, the fire self-extinguished within 1 second each time.

Given these results, the newly developed optical fiber cable is expected to withstand harsh weather conditions and mechanical forces in actual use.

## 5. Cable connector

Cable connector structure

The appearance of a newly developed cable connector is shown in Fig.6. The connector is for two fiber cables and jointing is carried out using two connector plugs and an adapter. Each connector plug has two standard FC-type ferrules[2] of 2.499 mm outer diameter. The maximum outer diameter of the cable connector is only 18mm and the total connected length is 180mm. In order to fix the connector plug to the cable, the cable's Kevlar® tension member is clamped onto the inner part of connector by tightening clamping screws. Rubber rings inside the connector make it waterproof. In addition, ferrules are held in place in the insertion-guide by means of a spring for each of the two ferrules. The finished cable has a connector plug on both ends. Because an adapter is attached to each plug of the cable, it is very easy to connect cable in the field without bringing an adapter.

Experimental results

The measured insertion loss of the cable connector is shown in Fig.7. The measurement set up is shown in Fig.8. The insertion loss was measured for steady state mode distribution at 0.85 μm wavelength. The multi-mode fiber used had a 50 μm core and 125μm diameter. The average insertion loss was 0.54 dB, which is as low as that for an ordinary code-type single connector. Furthermore, an insertion loss test was performed by disconnecting and connecting the cable, 200 times. Experimental results are shown in Fig.9. Maximum insertion loss variation range was less than 0.2 dB, which is almost equal to that of ordinary code-type single connector. Vibration tests were conducted during 5 hours in 2 directions (vertical and horizontal). As shown in Fig.10,

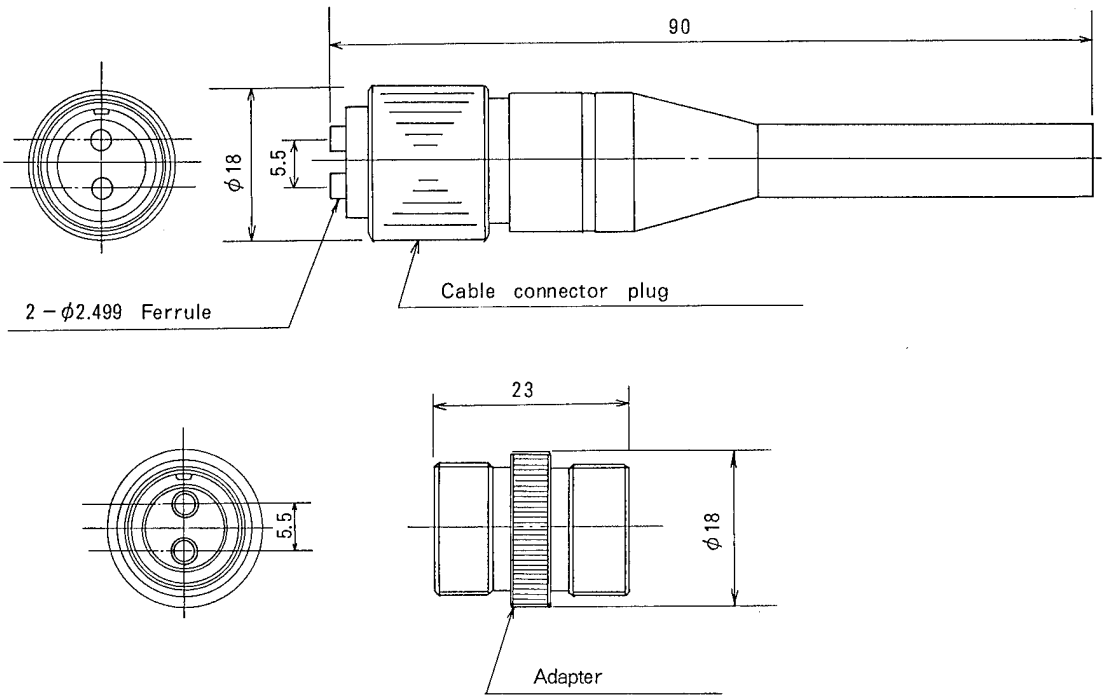



Figure 6. Structure of cable connector

there was no degradation due to vibration. With respect to temperature characteristics, joined connectors have been subjected to a thermal cycle test under the conditions of temperature ranging from -40°C to +70°C over 20 days. The relation between insertion loss and temperature is shown in Fig.11. Variation in insertion loss was less than only 0.2 dB. Then, impact tests were conducted by dropping the connector from a height of 1m. The experimental set up is shown in Fig.12. Measured insertion loss variation was ploted with respect to falling times. Over the course of 20 consecutive falls, the variation of insertion loss was less than 0.2 dB and there was no degradation on the connector end-face observed with a microscope. Furthermore, in order to confirm the waterproof property, the joined cable connector was submerged under water about 5cm deep for 20 days. There was no variation in insertion loss, and no water was detected inside of the connector. Finally, a tensile strength test of the cable connector was performed with 9 joined connectors. Fig.13 shows the distribution of tensile strength. Average measured tensile strength of 9 cable connectors was about 145 kg. And measured tensile strength was more than 100 kg for each of joined connectors. These results indicate that clamping of the Kevlar® was successful in fixing the cable to the connector plug.

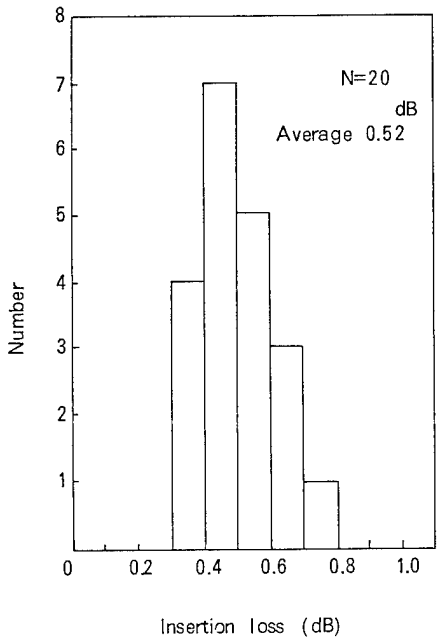



Figure 7. Distribution of insertion loss

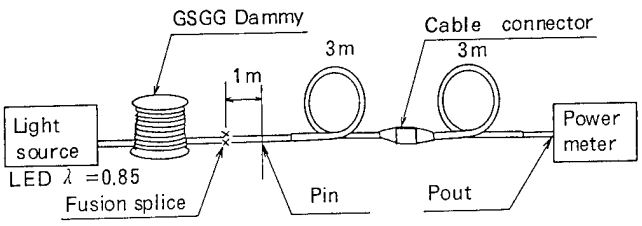



Figure 8. Measurement set up

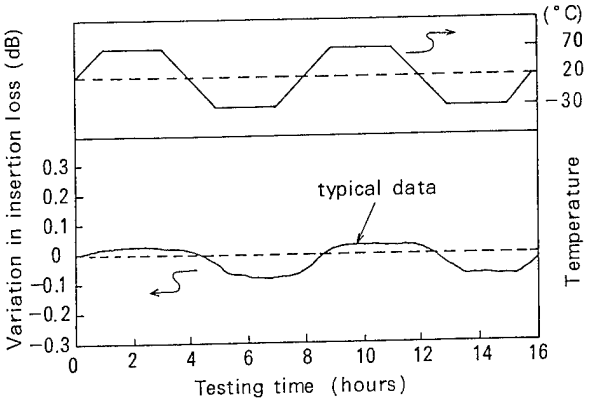



Figure 11. Thermal dependence

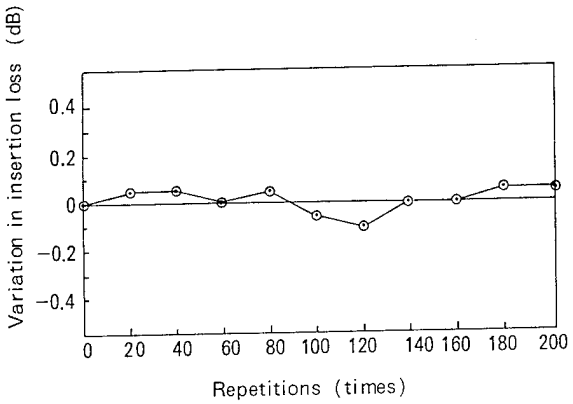



Figure 9. Repeatability test

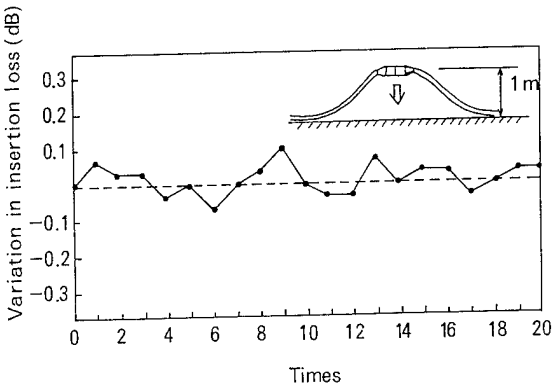



Figure 12. Impact test

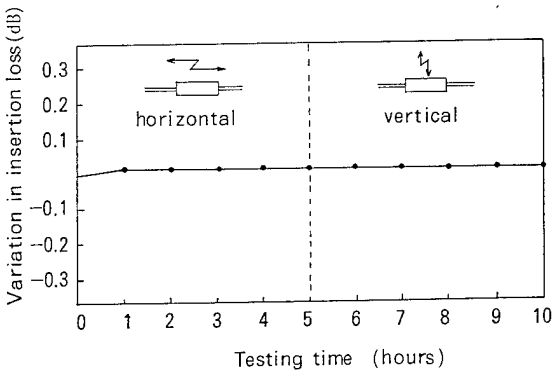



Figure 10. Vibration test

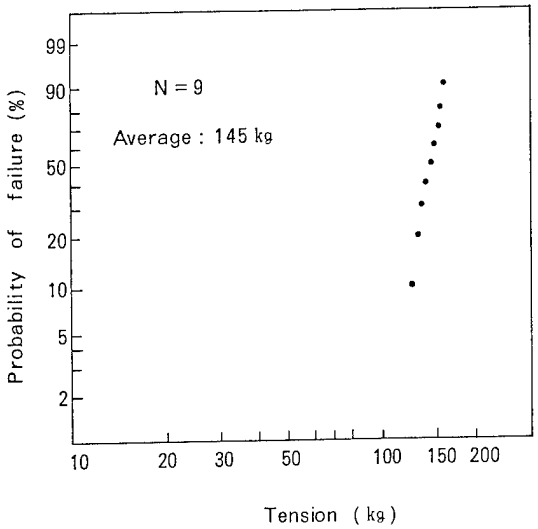



Figure 13. Tensile strength

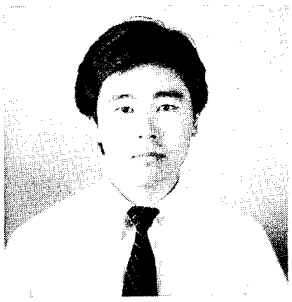
## 6. Conclusion

A very light weight, non-metallic, flame-retardant, field-use portable optical fiber cable with connector has been developed, fabricated and tested. The cable is very small in diameter (4.3mm) and very light in weight(14.5kg/km). Average connection loss of an optical connector developed for the cable is approximately 0.5dB and its diameter is only 18 mm.

It was confirmed that the cable and connector have excellent mechanical and temperature characterisitcs in adverse conditions.

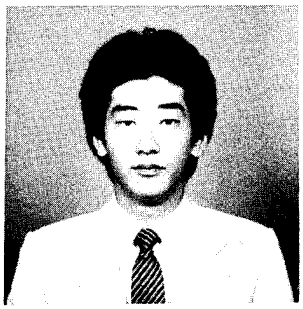
## 7. References


1. Y. Saitoh et al., "Development of Field Optical Fiber Cable with Connector ", Sumitomo Electric Technical Review, Sep., 1984
2. N. Suzuki et al.,Electron. Leff., Vol.15, P.809,Dec. 1979.


Tetsuya Ohsugi
Sumitomo Electric
Industries, Ltd.
1, Taya-cho,
Totsuka-ku, Yokohama,
Japan


Tetsuya Ohsugi received his B.S. degree in physical engineering from science university of Tokyo in 1984. He then joined Sumitomo Electric Industries and has been engaged in research and development of optical fiber and cables. Mr. Ohsugi is a member of Communication R&D Department in Yokohama Research Laboratories, and a member of the Institute of Electronics & Communication Engineers of Japan.




Yoshinobu Kitayama
Sumitomo Electric
Industries, Ltd.
1, Taya-cyo,
Totuska-ku
Yokohama, Japan


Yoshinobu Kitayama received his M.S. degree in Electrical Engineering from Kyoto Univ. in 1982. He then joined Sumitomo Electric Industries and has been engaged in research and development of optical fiber and cables. Mr. Kitayama is a member of Communication R&D Department in Yokohama Research Laboratories, and a member of the Institute of Electronics & Communication Engineers of Japan.




Toshiaki Kakii
Sumitomo Electric
Industries, Ltd.
I, Taya-cho,
Totsuka-ku,
Yokohama, Japan


Toshiaki Kakii was born in 1955 and received a M.E. degree from Keio University in 1980. He joined Sumitomo Electric Industries, Ltd. in 1980 and has been engaged in research and development of optical fiber jointing method. He is a member of the Institute of Electronics and Communication Engineers of Japan

# Underground Fiber Optic Cable Placement - Cable Pulling Tensions Helically Wrapped Cables in Straight and Curved Conduit Sections

P. B. Grimado

Bell Communications Research

Fiber optic cables are presently placed in underground conduit systems through innerducts or subducts. It has been reported that in certain instances these innerducts or subducts have a tendency to bend and curl when they are installed, forming a helical path through which the fiber optic cable passes. Any deviation from a straight path will increase the tension required to pull the fiber optic cable through an underground conduit route. Therefore, in this regard, fiber optic cable pulling tensions through straight and curved helical sections have been computed. Appropriate formulae and graphical aids are presented to aid the Outside Plant engineer in determining, for a given conduit route, the maximum continuous length of fiber optic cable that can be placed without damage.

## 1. Introduction

Fiber optic cables are smaller in size and weigh less than their copper wire cable counterparts. These characteristics enable long lengths of fiber optic cable to be wound on cable reels. Consequently, it is possible to place long cable lengths in one continuous piece thus eliminating costly multiple cable pulling set-ups and minimizing splicing, which is a time consuming difficult operation at best. It turns out, however, that in many instances the length of continuous fiber optic cable that is eventually placed is not limited by the maximum number of cable feet wound in a cable reel, but on the mechanical stress and strain properties of the cable design. Fiber optic cables available today are capable of transmitting between 600 and 1000 pounds of tensile force before irreversible mechanical damage to the optical fibers ensues. Therefore, these cables must be pulled through underground systems without exceeding this mechanical limit. The pulling force required to place cables depends on the weight of the cable, the friction force between the cable sheath and duct wall and, most importantly, the geometrical variations of the conduit route.

In practice before any underground cable pull is performed, the engineer surveys the conduit route and calculates the cable pulling tensile forces required. Many engineering aids are available for use by the engineer in estimating these cable pulling tensions along the length of conduit [1,2]*. These graphical and/or computerized aids are capable of handling a wide variety of horizontal and vertical changes in cable pulling direction. They, however, do not account for situations where the cable or winch line is either helically wrapped around other cable, or the innerduct through which fiber optic cable passes is helically shaped.

It has been reported on a number of occasions that the innerducts after placing in conduit have a tendency to curl back into the duct upon release of the pulling tension forming, to first approximation, a helical configuration. On the other hand, to increase the utilization of available conduit space and to decrease the time expended for cable placement, investigations are underway to explore methods for placing cable without innerducts. This cost reducing technique can also lend itself to consideration of pulling cable through a helical configuration, since in certain instances it is not hard to envision the winch line helically wrapped around previously placed cable. This phenomena, which tends to increase the required pulling tension, was not previously addressed because the mathematical models employed reflected copper wire cable technology where these affects do not occur since innerducts and multi-occupied ducts are non-existent. It is only with these two cable placement configurations that this helical geometry is possible.

In this paper, equations are derived for computing fiber optic cable pulling tensions for conduit placement when the cable is pulled through either straight or curved helical sections. Pulling tension computations for several parameter variations are graphically presented. The derived tension equation is simple enough to be easily exercised on most hand calculators.

## 2. Geometric Considerations

Consider the toroid with coordinate system as shown in Figure 1. The equation of a helix mapped onto the surface of the toroid has been considered by Lutchansky [3] and Zhadnov [4] and therefore can be presented using their results in terms of the cartesian coordinate system illustrated in Figure 1 as:

$$x = (\rho + R \cos\theta) \sin\frac{k\theta}{\rho} \quad , \tag{1a}$$

$$y = \rho(1 - \cos\frac{k\theta}{\rho}) + R(1 - \cos\theta \cos\frac{k\theta}{\rho}) \, , \tag{1b}$$

$$z = R \sin\theta \quad , \tag{1c}$$

where

$k = \ell/2\pi$ (Ft.), the lay length or pitch of the helix divided by $2\pi$,

$\theta$ = the angular cylindrical coordinate,

$\rho$ = the radius of curvature of the toroid as well as the conduit system (Ft.),

$R$ = the cross-sectional radius of the toroid (Ft.).

Depending on the problem being considered, the toroid radius R represents the curl radius of the innerduct, and for the case of the helically wrapped cable, this quantity is the radius of the cable bundle around which the cable passes. In any event, R cannot

* Numbers in brackets are keyed to the list of references contained in the back of the paper.

exceed the cross-sectional radius of the duct section.
Note that when the toroid assumes the shape of a cylinder, represented by $\rho \to \infty$, eqs. (1) pass in the limit to:

$$x = k\theta\ , \tag{2a}$$

$$y = R(1-\text{Cos}\theta)\ , \tag{2b}$$

$$z = R\ \text{Sin}\ \theta\ , \tag{2c}$$

which is the equation of a simple helix. The angular variation along the length of the toroid or the bend angle is given by, [3]:

$$\phi = \frac{k\theta}{\rho}\ . \tag{3}$$

Equations (1) and (2) can be used to describe the geometry assumed by fiber optic cables when pulled through innerducts or when wrapped around other cables in curved and straight conduit sections, respectively. With this description of the geometry completed the cable pulling tension equation is derived in the next section 3.

## 3. Fiber Optic Cable Pulling Tension Equation

Consider a cable helically wrapped over the surface of a toroid or a cable passing through a small diameter tube (innerduct) which is helically wrapped. The equations describing this helix are given by eq. (1). It is assumed, without loss of generality, that the fiber optic cable has negilible bending stiffness and can only support tensile forces. In addition, fiber optic cables are very light, on the order of .1 lb/ft, and therefore in many practical situations the effect of the weight is small with respect to, for example, the tail load which can be of the order of say, 50 pounds. Consequently, in the following analysis, the fiber optic cable weight is neglected. Equilibrium of the forces generated during the cable placing operation dictates the satisfaction of the following vector differential equation, Figure 2:

$$N\hat{n} - \tau\hat{t} + \frac{d}{dS}(T\hat{t}) = 0 \tag{4}$$

where

$N$ = the principal normal reaction force applied to the cable (lb/ft),

$\hat{n} = \frac{1}{K}\frac{d\hat{t}}{dS}$, the principal unit normal vector,

$K$ = the curvature ($Ft^{-1}$)

$\tau = \mu|N|$, the coulomb friction or shear force acting on the cable in the tangential direction opposite to the cable pulling motion (lb/ft),

$\mu$ = the coefficient of friction,

$\hat{t}$ = the unit tangent vector,

$S$ = the arc length of the cable measured from the origin of the cartesian coordinate system x=y=z=o, Figure1,

$T$ = the cable pulling tension along the cable (lb).

There are 3 unknown forces to be resolved the cable reaction forces N, $\tau$ and the cable tension force, T. The vector differential equation (4) provides 2 scalar equations while the third comes from the Coulomb friction law which linearly relates the shear or friction force, $\tau$, to the normal force N, i.e. $\tau = \mu|N|$. The arc length S can be expressed in terms of the cylindrical coordinate, $\theta$; this result is explicitly given in the Appendix. The three required equations for N, $\tau$ and T are from eq. (4) and the Coulomb friction law:

$$N = -KT, \tag{5a}$$

$$\tau = \mu|N| \tag{5b}$$

$$\frac{dT}{d\theta}(\theta) = \tau\left(\frac{dS}{d\theta}\right)\ . \tag{5c}$$

Substituting (5a) and (5b) into (5c) the equation for the cable pulling tension is:

$$\frac{dT}{d\theta}(\theta) - \mu K(\theta)\frac{dS}{d\theta}(\theta)T(\theta) = 0\ , \tag{6a}$$

with the boundary condition,

$$T(0) = To\ . \tag{6b}$$

The tension To is generally called the tail load. Equation (6) is linear and, therefore, by separation of variables, the solution is simply obtained in the form:

$$\frac{T(\theta)}{To} = \text{Exp}\left[\mu\int_o^\theta K(\theta')\frac{dS}{d\theta'}(\theta')\,d\theta'\right]\ . \tag{7}$$

The expression for the product $K(\theta)\frac{dS}{d\theta}(\theta)$ is given in the Appendix. It can be observed in eqs. (12)-(14) given in the Appendix, that this expression contains a parameter $R/\rho$ which is very small. The radius R cannot exceed the duct radius which is typically 2 inches while for practical underground systems the radius of curvature of conduit $\rho$ is typically greater than 10 feet, therefore $R/\rho << .0167$. Since $R/\rho$ is small, the right hand side of equation (7) can be expanded in a Taylor series about $R/\rho = o$. Retaining terms up to first order, eq. (7), after considerable algebra, is finally cast into the form:

$$T(\theta)/To = \text{Exp}(\mu\beta\theta)\left\{1+\frac{\mu}{\beta}\left[2\left(\frac{k}{\rho}\right)\theta\text{Sin}\gamma\text{Cos}^5\gamma + 3\left(\frac{k}{\rho}\right)^2 \text{Sin}^2\gamma\text{Cos}^6\gamma\text{Sin}\theta + \text{Sin}^4\gamma\ \text{Sin}\theta\right]\left(\frac{R}{\rho}\right)\right\} + O\left(\frac{R}{\rho}\right)^2\ , \tag{8}$$

where

$\gamma$ = the helix lay angle , shown in Figure 3,

$$\text{Sin}\gamma = \frac{R}{\sqrt{R^2+k^2}}\ , \tag{9a}$$

$$\text{Cos}\gamma = \frac{k}{\sqrt{R^2+k^2}}\ \text{and} \tag{9b}$$

$$\beta = \sqrt{\left(\frac{k}{\rho}\right)^2\text{Cos}^6\gamma + \text{Sin}^2\gamma}\ . \tag{9c}$$

The form of equation (8) is similar to the simple capstan result in that the cable pulling tension is exponentially increased as one moves down the length of conduit. In fact, not unexpectedly, the capstan equation is obtained from eq. (8). Setting, the helix lay

angle $\gamma=0°$ and recalling that from eq. (3), the bend angle is given by $\phi=\frac{k}{\rho}\theta$ the capstan equation results:

$$\frac{T|\phi|}{To} = Exp[\mu\phi] . \qquad (10)$$

The exponential growth in eq. (8) depends very strongly on the parameter $\beta$ which contains the radius of curvature and helix parameters $(\frac{k}{\rho})$ and $\gamma$. For the case of a straight conduit section $(\frac{k}{\rho}) = 0$ the solution, eq. (7) can be integrated exactly with the value of $\beta = Sin\gamma$. The variation of $\beta$ with lay angle, $\gamma$, is an interesting one and worthy of discussion. The $\beta$ versus $\gamma$ curve takes on two fundamentally different shapes for specific ranges of the parameter $(k/\rho)$. In each instance, $\beta(o)=k/\rho$ and $\beta(90°)=1$, but for numerical values of $k/\rho \le [1/3]^{1/2} = .577$ $\beta$ increases monotonically with increasing $\gamma$. While, on the other hand, when $k/\rho > [1/3]^{1/2}$, $\beta$ has a minimum value at the lay angle $\gamma_{min} = Cos^{-1}\left\{\left[1/3(\frac{k}{\rho})^2\right]^{1/4}\right\}$.

An infinite number of combinations of $(\frac{k}{\rho})$ and the lay angle $\gamma$ will produce the same value of $\beta$; the only exceptions are the extremes $\gamma=o,\pi/2$, $(k/\rho)=o$ and $(k/\rho)\to\infty$. This property could be useful for experimentally investigating cable pulls in configurations that are more conveniently accessible than the actual conduit system located in the field. Notice, however, since $\phi = (\frac{k}{\rho})\theta$ the actual bend angle in the simulated curved configuration will be different.

A point should be made regarding the relationship between parameters. From the definition of $\gamma$ given by eqs. (9a) and (9b) we have:

$$Tan\,\gamma = (R/\rho)/(k/\rho) , \qquad (11)$$

and, therefore, only two of these parameters can be chosen arbitrarily. The third must come from eq. (11). In fact, the range of these parameters is further constrained by the previously invoked requirement that $(R/\rho)<<1$; at least to the extent that the simplified solution given by eq. (8) is used. If it is further stipulated that any value of $(R/\rho) \le .05$ does not invalidate the applicability of eq. (8); a plot of $(k/\rho)$ versus $\gamma$ with $R/\rho=.05$ is given in Figure 4 to aid in ascertaining the appropriate range. In this figure the region bounded and including the axes and the curve contains compatible $(k/\rho)$, $\gamma$ pairs. For values outside this domain the cable pulling tension must be obtained through numerical integration of eq. (7).

Calculations of the cable pulling tension in curved conduit sections are shown graphically in Figures 5 to 9 for several values of the parameters $\mu$ (.1, .15, .2, .3, .4), $k/\rho$ (.1, .08, .05, .02, .01) and a range of lay angles, $\gamma$ (0°, 5°, 10°, 15°).

In practical conduit systems, it is expected that $k/\rho < 1$ and the lay angle, $\gamma$ should not be too large; these considerations dictated the range of parameters presented in the figures. In addition, of the chosen parameters only the values of $(k/\rho)$ and $\gamma$ producing at least a twofold increase in tension at $\phi = 90°$ are plotted. The curves labeled $\gamma = 0°$ represent the simple capstan equation (10). Notice, for example, in Figure 5 that the curves for $k/\rho=.02$, $\gamma=10°$ and $k/\rho=.01$, $\gamma=5°$ coincide; this occurs because the ratio of $\beta/(k/\rho)$ is equal. From these figures the following trends for a given bend angle are evident:

a. the simple capstan equation represents a lower bound,

b. for a given lay angle, the cable pulling tension increases with decreasing $(k/\rho)$,

c. for a given $(k/\rho)$, the cable pulling tension increases with increasing lay angle.

Stated more concisely, any change in parameter that increases the overall wrapped cable length will increase the cable pulling tension. This conclusion can be demonstrated by observing the helical arc length equations (20b) and (20c) given in the Appendix. For a given distance along the axis of the helix, the overall length of cable in curved and straight sections is increased when the lay angle, $\gamma$ increases. The lengthening of cable also occurs in curved sections by reducing the parameter $k/\rho$ which has the effect, as seen through eq. (11) and Figure 4, of increasing the lay angle, $\gamma$ or for a given lay angle, increasing the radius of curvature, $\rho$. Intuitively, this is what one would expect, and in fact the solution obtained supports and quantifies this conclusion.

In Figures 10-12 the cable pulling tension in straight helical sections is plotted. In these plots the tension is shown varying with length along the conduit section. Once again, it is seen that the tension increases with increasing lay angle.

In Figures 13-15, plots are given for determining the maximum allowable conduit length with a central bend when the fiber optic cable pulling tension and tail load ratio T/To = 20. This can correspond, for example, to a fiber optic cable rated at 600 pounds with a tail load of 30 pounds. The curves are computed for several variations of the parameters; bend radius of curvature, $\rho$, helix lay angle, $\gamma$ and coefficient of friction, $\mu$.

## 4. Conclusions

A fiber optic cable pulling tension equation has been developed for situations where either the cable passes through innerduct or subduct that forms a helical path or when the cable itself is helically wrapped around previously placed cable. The conduit sections can either be straight or curved. The resulting equation exhibits a dominant exponential increase in tension with increasing distance along the conduit reminiscent of the simple capstan formula which is shown to yield a lower bound. In this case, the argument of the dominant exponential is dependent on two helix parameters $(k/\rho)$ and the lay angle, $\gamma$. The results of calculating the tension for several variations in the parameters are presented for convenience, although the equation which contains only elementary functions is simple enough to be exercised on most hand calculators.

The analyses and results presented herein should be useful to the Outside Plant engineer responsible for specifying the length of continuous fiber optic cable that can be placed in a given conduit section. Although some of the helical parameters are difficult to measure, parameter studies can be easily conducted to increase the engineers' degree of confidence in their final determination.

## References


[1] *Conduit System Design*, Bell System Practices, Section 919-240-100, Issue 3, October 1977.

[2] J. Macaulay, "Computerized Method of Predicting Cable Pulling-in Tensions", Proc. of the 33rd International Wire and Cable Symposium, November, 1984, pp. 372-375.

[3] M. Lutchansky, "Axial Stresses in Armor Wires of Bent Submarine Cables", Journal of Engineering for Industry, NO. 68-WA/DE-1, pp. 1-5.

[4] G. P. Zhadnov, "Bending Stresses in Steel Wire Ropes", Nauchnye Trudy Karkov, Gornogo Inst. 2, 1955, pp. 127-135.

## Appendix

The explicit expressions of $K(\theta)$, $\frac{dS}{d\theta}(\theta)$, $S(\theta)$ and the Taylor series expansion of the exponential $\mathrm{Exp}\left[\mu\int_0^{\theta} K(\theta')\frac{dS}{d\theta'}(\theta')\,d\theta'\right]$ in the small parameter $R/\rho$ are documented here. The algebraic details which were indeed considerable, are not included and only the final results are presented.

Consider the position vector

$$\hat{r} = x\,\hat{i} + y\,\hat{j} + z\,\hat{k}\,, \tag{12}$$

where x,y,z are the cartesian coordinates and $\hat{i},\hat{j}$ and $\hat{k}$ are the unit vectors in these directions, respectively. The unit tangent vector appearing in equation (4) is then given by the relation:

$$\hat{t} = \frac{d\hat{r}}{dS}\,, \tag{13}$$

or more explicitly by,

$$\hat{t} = \frac{d\theta}{dS}\left[\frac{dx(\theta)}{d\theta}\,\hat{i} + \frac{dy(\theta)}{d\theta}\,\hat{j} + \frac{dz(\theta)}{d\theta}\,\hat{k}\right], \tag{14}$$

where $S(\theta)$ represents the arc length and $x(\theta)$, $y(\theta)$ and $z(\theta)$ are equations of the helix given in (1). The principal unit normal vector, $\hat{n}$ and the associated curvature, K are also obtained by operating on the position vector in the following manner:

$$\hat{n} = \frac{1}{K}\frac{d^2\hat{r}}{dS^2}\,, \tag{15}$$

or

$$\hat{n} = \frac{1}{K}\left\{\left[\frac{d^2x(\theta)}{d\theta^2}\,\hat{i} + \frac{d^2y(\theta)}{d\theta^2}\,\hat{j} + \frac{d^2z(\theta)}{d\theta^2}\,\hat{k}\right]\frac{d\theta}{dS} + \left\{\left[\frac{dx}{d\theta}(\theta)\,\hat{i} + \frac{dy}{d\theta}(\theta)\,\hat{j} + \frac{dz}{d\theta}(\theta)\,\hat{k}\right]\frac{d^2\theta}{dS^2}\right\}. \tag{16}$$

Now since $\hat{n}$ is a unit vector the curvature is simply given by:

$$K(\theta) = \left[\left(\frac{d^2x(\theta)}{d\theta^2}\frac{d\theta}{dS} + \frac{dx}{d\theta}\frac{d^2\theta}{dS^2}\right)^2 + \left(\frac{d^2y(\theta)}{d\theta^2}\frac{d\theta}{dS} + \frac{dy(\theta)}{d\theta}\frac{d^2\theta}{dS^2}\right)^2 + \left(\frac{d^2z(\theta)}{d\theta^2}\frac{d\theta}{dS} + \frac{dz}{d\theta}\frac{d^2\theta}{dS^2}\right)^2\right]^{1/2} \tag{17}$$

or more explicitly,

$$K(\theta) = \frac{\left[A^2 + B^2 + C^2\right]^{1/2}}{\left[(R^2+k^2) + k^2\left(\frac{R}{\rho}\right)\left(2+\frac{R}{\rho}\mathrm{Cos}\theta\right)\mathrm{Cos}\theta\right]^{3/2}}\,, \tag{18}$$

where

$$A^2+B^2+C^2 = k^4\left(1+\frac{R}{\rho}\mathrm{Cos}\theta\right)^2\left[2R\frac{R}{\rho} + \frac{k^2}{\rho}\frac{R}{\rho}\left(2+\frac{R}{\rho}\mathrm{Cos}\theta\right)\mathrm{Cos}\theta\right]^2 + 2k^2\frac{R}{\rho}\left(1+\frac{R}{\rho}\,\mathrm{Cos}\theta\right)\left[2R^2+k^2+k^2\frac{R}{\rho}\left(2+\frac{R}{\rho}\mathrm{Cos}\theta\right)\mathrm{Cos}\theta\right]\left[k^2\left(1+\frac{R}{\rho}\mathrm{Cos}\theta\right)+R^2\right]\mathrm{Cos}\theta + \left\{k^3\frac{R}{\rho}\left(1+\frac{R}{\rho}\mathrm{Cos}\theta\right)^2 - 2k\frac{R}{\rho}\left[R^2+k^2+\frac{k^3}{\rho}\left(2+\frac{R}{\rho}\mathrm{Cos}\theta\right)\mathrm{Cos}\theta\right]^2\right\}\mathrm{Sin}^2\theta + R^2\left[k^2\left(1+\frac{R}{\rho}\mathrm{Cos}\theta\right)+R^2\right]^2. \tag{19}$$

The variation of helical arc length with the independent variable, $\theta$ is obtained in the form:

$$\frac{dS}{d\theta}(\theta) = \left[R^2+k^2+k^2\frac{R}{\rho}\left(2+\frac{R}{\rho}\mathrm{Cos}\theta\right)\mathrm{Cos}\theta\right]^{1/2}. \tag{20}$$

To find the helical arc length $S(\theta)$ expand eq. (20) in a Taylor series about $R/\rho=0$ and integrate with respect to the variable $\theta$:

$$S(\theta) = R\left[\theta/\mathrm{Sin}\gamma + \left(\frac{k}{\rho}\right)\mathrm{Cos}\gamma\mathrm{Sin}\theta + \left(\frac{k}{\rho}\right)^2\mathrm{Sin}^3\gamma/4\,(\theta + \mathrm{Sin}\,2\theta/2) + \ldots\right]. \tag{20a}$$

The arc length of the helix descrbed by eq. (20a) can be alternately expressed in terms of the bend angle, $\phi$. Substituting eqs. (3) and (11) into (20a) we obtain:

$$S(\phi) = \rho\phi/\cos\gamma + \ldots\,, \tag{20b}$$

and for a straight section with $\rho\to\infty$ we have the arc or cable length in terms of the linear distance, X in the axial direction, expressed simply as:

$$S(X) = X/\cos\gamma\,. \tag{20c}$$

The Taylor series expansion of the exponential $\mathrm{Exp}\left[\mu\int_0^{\theta} K(\theta')\frac{dS}{d\theta'}(\theta')d\theta'\right]$ in terms of the small parameter $R/\rho$ follows:

$$\mathrm{Exp}\left[\mu\int_0^{\theta} K(\theta')\frac{dS}{d\theta'}(\theta')d\theta'\right] = \mathrm{Exp}\left[\mu\int_0^{\theta} K(\theta')\frac{dS}{d\theta'}(\theta')\right]_{R/\rho=0} d\theta' + \mu\int_0^{\theta}\frac{d}{d(R/\rho)}\left[K(\theta')\frac{dS}{d\theta'}(\theta')d\theta'\right]_{R/\rho=0}(R/\rho) + \cdots\Bigg\}, \tag{21}$$

where

$$K(\theta)\frac{dS}{d\theta}(\theta)\Big]_{R/\rho=0} = \left[\left(\frac{k}{\rho}\right)^2 Cos^6\gamma + Sin^2\gamma\right]^{1/2} \equiv \beta\,, \qquad (22)$$

$$\frac{d}{d(R/\rho)}\left[K(\theta)\frac{dS}{d\theta}(\theta)\right]_{R/\rho=0}$$

$$= \frac{\left[3\left(\frac{k}{\rho}\right)^2 Sin^2\gamma Cos^6\gamma + Sin^4\gamma\right] Cos\theta + 2\left(\frac{k}{\rho}\right) Sin\gamma Cos^5\gamma}{\beta}\,. \qquad (23)$$

Finally, after performing the indicated integrations, eq. (21) becomes:

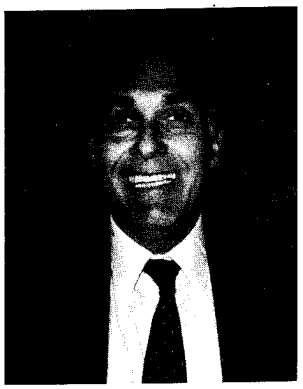
$$Exp\left[\mu\int_0^{\theta} K(\theta')\frac{dS}{d\theta'}(\theta')d\theta'\right] = Exp(\mu\beta\theta)\Big\{1 +$$

$$+ \frac{\mu}{\beta}\left[2\left(\frac{k}{\rho}\right) Sin\gamma Cos^5\gamma\,\theta\right.$$

$$+ 3\left(\frac{k}{\rho}\right)^2 Sin^2\gamma Cos^6\gamma Sin\theta$$

$$\left. + Sin^4\gamma\, Sin\theta\right]\left(\frac{R}{\rho}\right) + 0\left(\frac{R}{\rho}\right)^2\Big\}\,, \qquad (24)$$

This expression appears in eq. (8).



BIOGRAPHY

PHILIP B. GRIMADO, B.S. (Civil Engineering), 1961, City University of New York; M.S. (Applied Mechanics), 1962, Columbia University; Ph.D. (Applied Mechanics), 1968, Columbia University; Bell Laboratories, 1968-1983. Responsibilities include vulnerability studies of antiballistic missile systems, fire protection studies involving fire risk analyses, heat-transfer calculations, development of standard fire testing methods for telephone company equipment, and development of algorithms for optimum control of building environmental equipment. Bell Communications Research 1983-present, engaged in outside plant activities concerned with fiber optic cable placement, restoration and damage assessment.

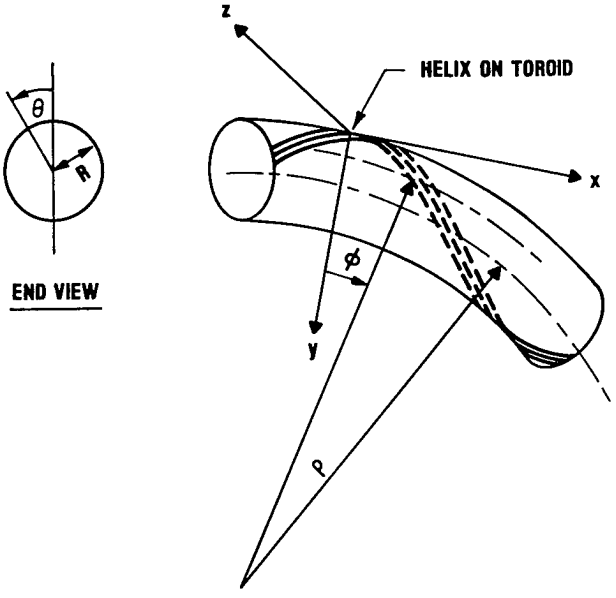



FIGURE 1 - HELIX ON TOROID

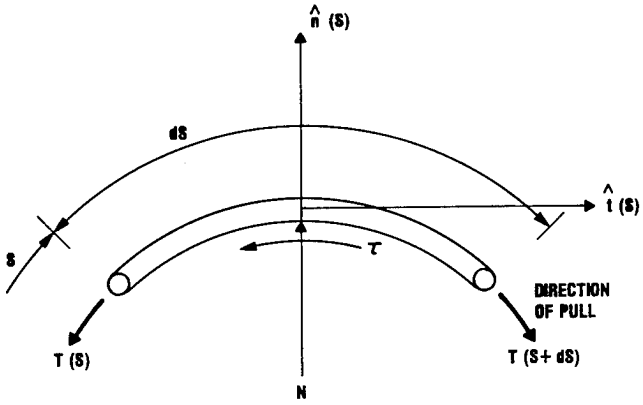



FIGURE 2 - PULLING FORCES ACTING ON A DIFFERENTIAL ELEMENT OF CABLE

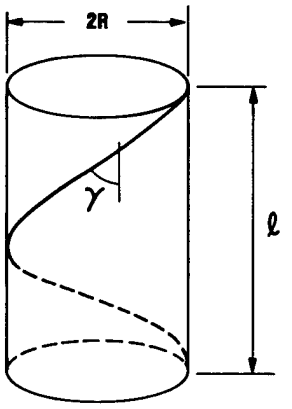



FIGURE 3 - HELIX LAY ANGLE, $\gamma$.

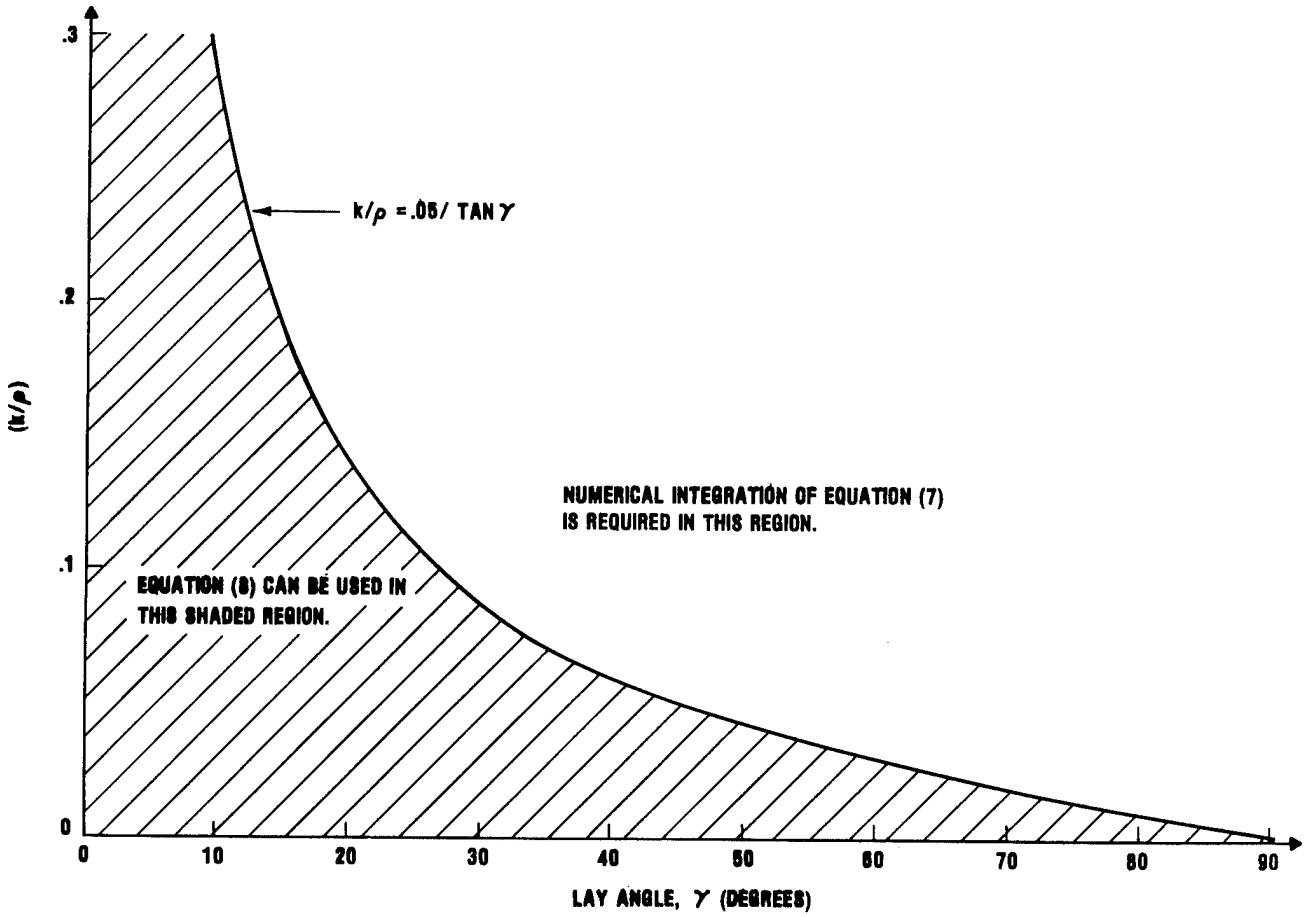



FIGURE 4 - RANGE OF PARAMETERS ($k/\rho$ ) AND $\gamma$ FOR USING EQUATION (8)

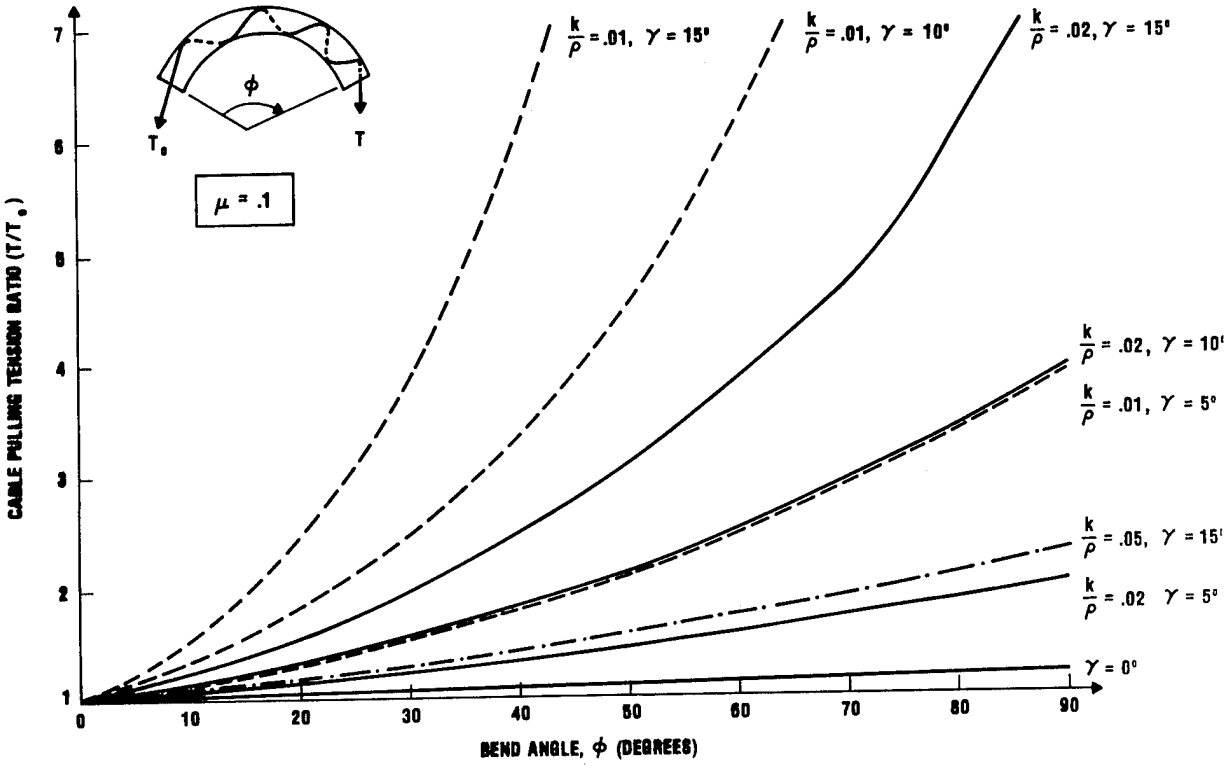



FIGURE 5 - CABLE PULLING TENSION THROUGH CURVED HELIX

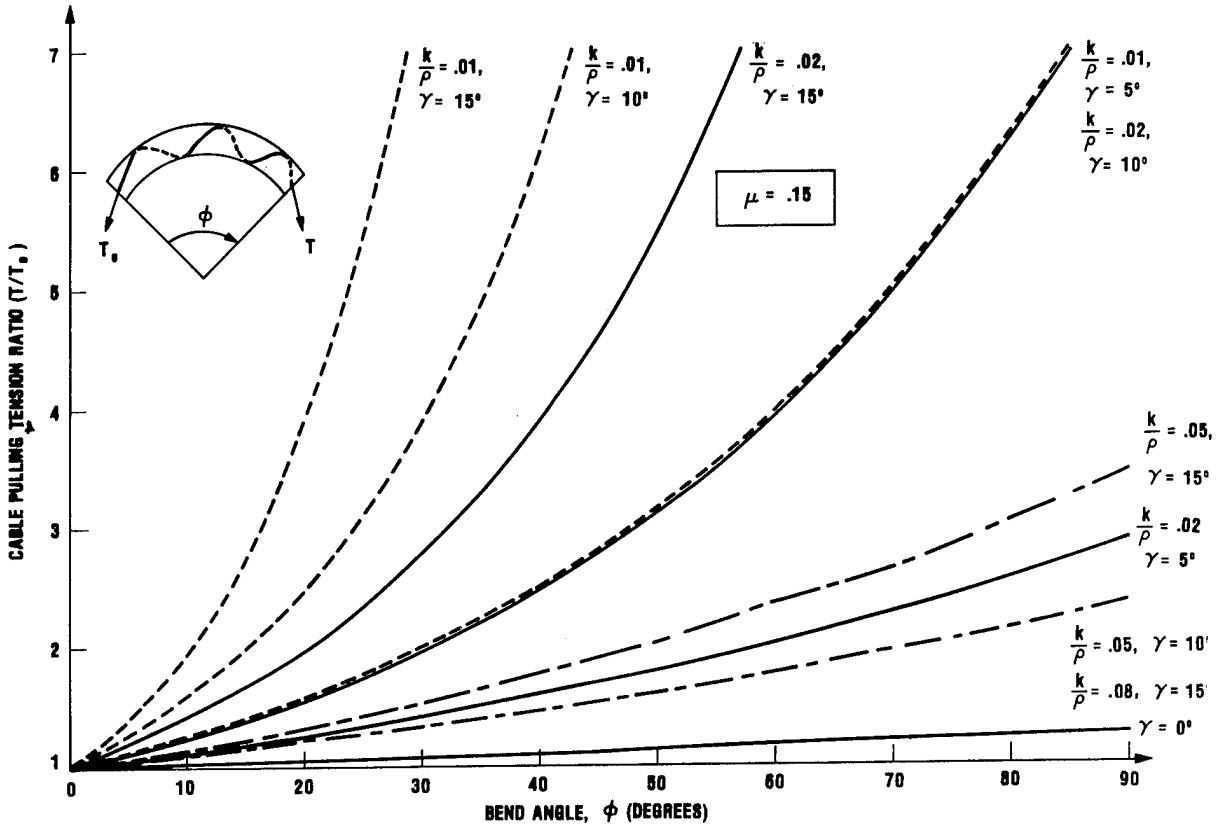



FIGURE 6 - CABLE PULLING TENSION THROUGH CURVED HELIX

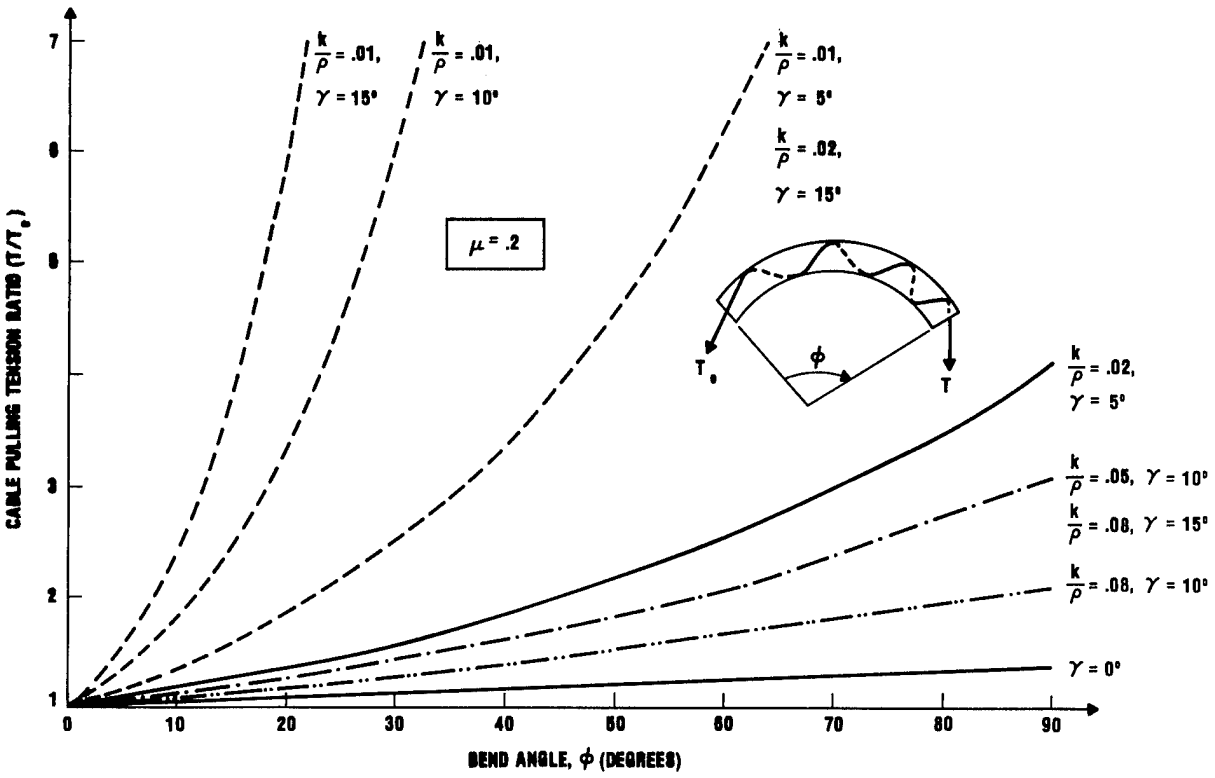



FIGURE 7 - CABLE PULLING TENSION THROUGH CURVED HELIX

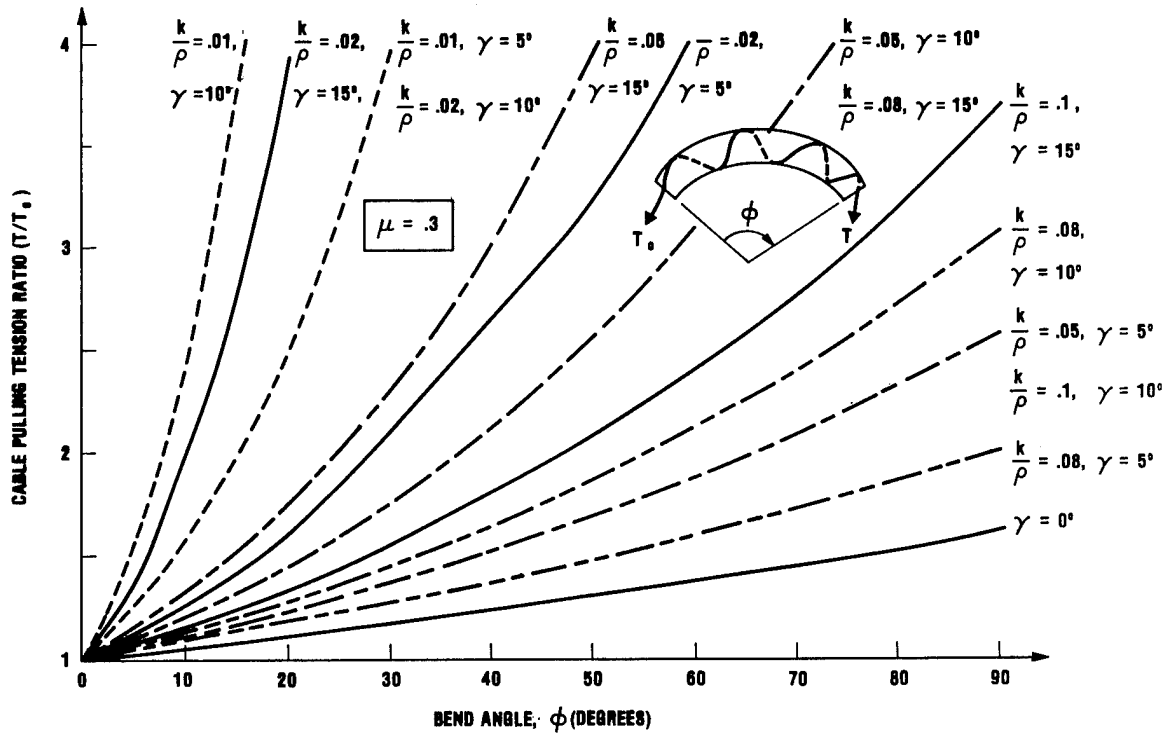



FIGURE 8 - CABLE PULLING TENSION THROUGH CURVED HELIX

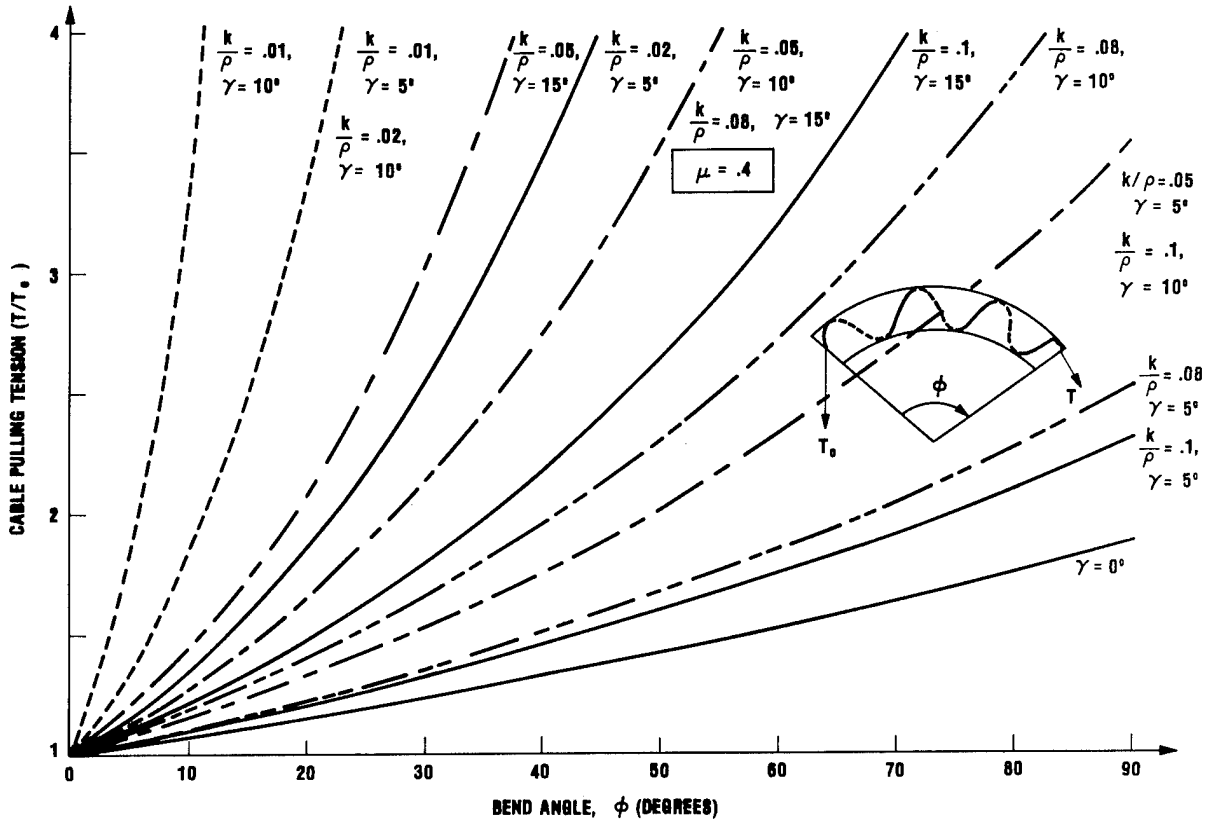



FIGURE 9 - CABLE PULLING TENSION THROUGH CURVED HELIX

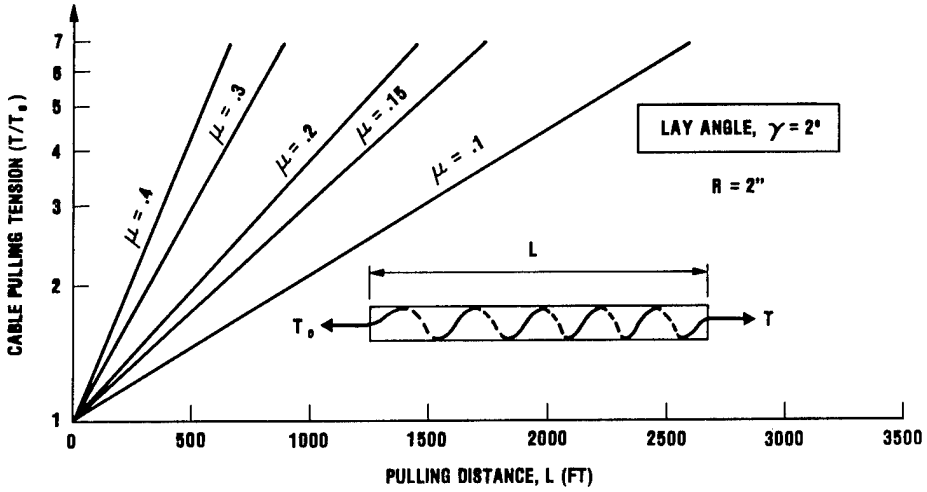



FIGURE 10 - CABLE PULLING TENSION FOR STRAIGHT HELIX SECTION, LAY ANGLE, $\gamma = 2°$

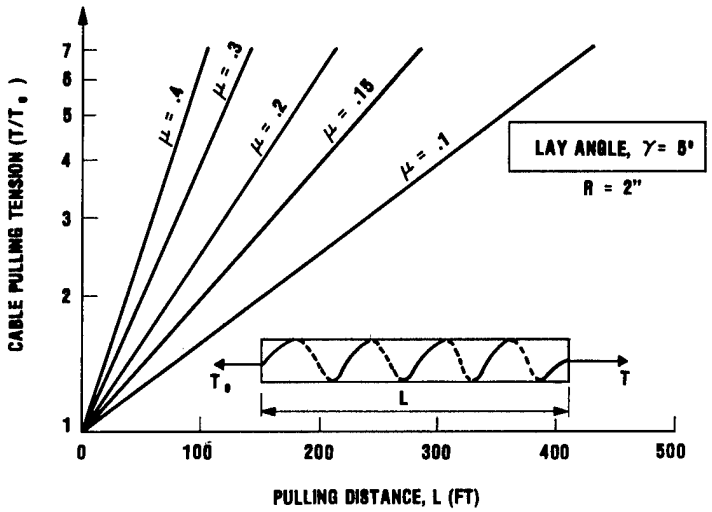



FIGURE 11 - CABLE PULLING TENSION FOR STRAIGHT HELIX SECTION, LAY ANGLE, $\gamma = 5°$

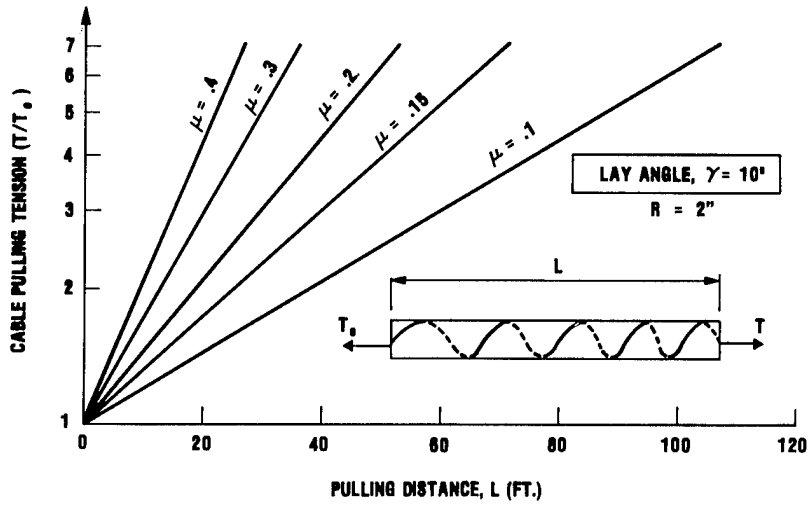



FIGURE 12 - CABLE PULLING TENSION FOR STRAIGHT HELIX SECTION, BY ANGLE, $\gamma = 10°$

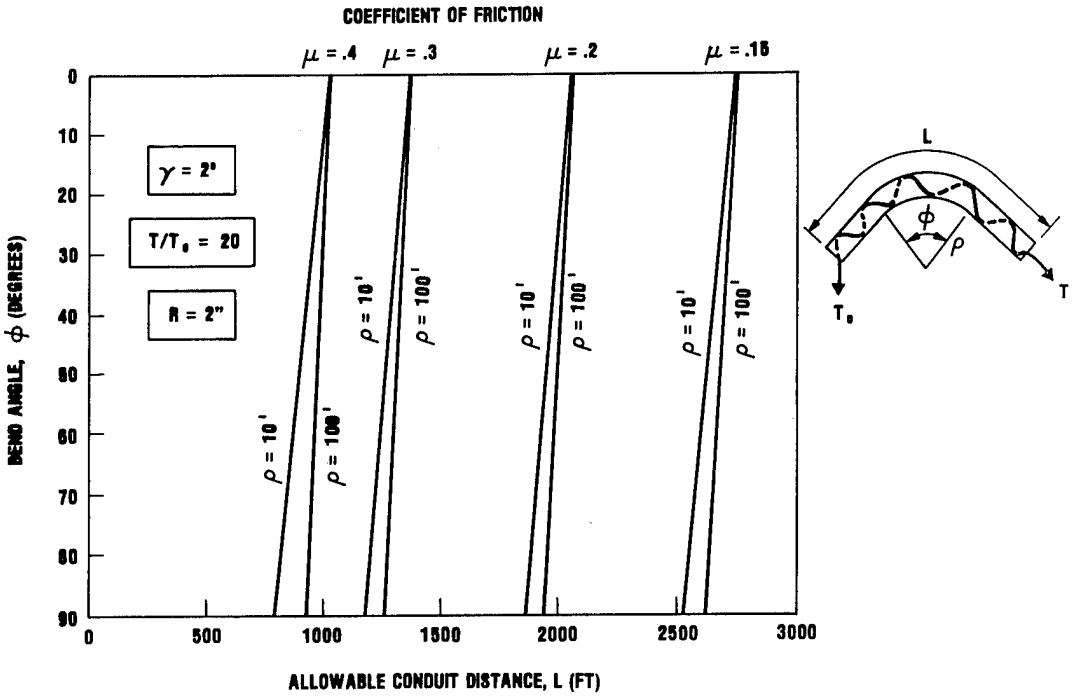



FIGURE 13 - ALLOWABLE CONDUIT LENGTH FOR CENTRAL BEND, $T/T_0 = 20$, $\gamma = 2°$

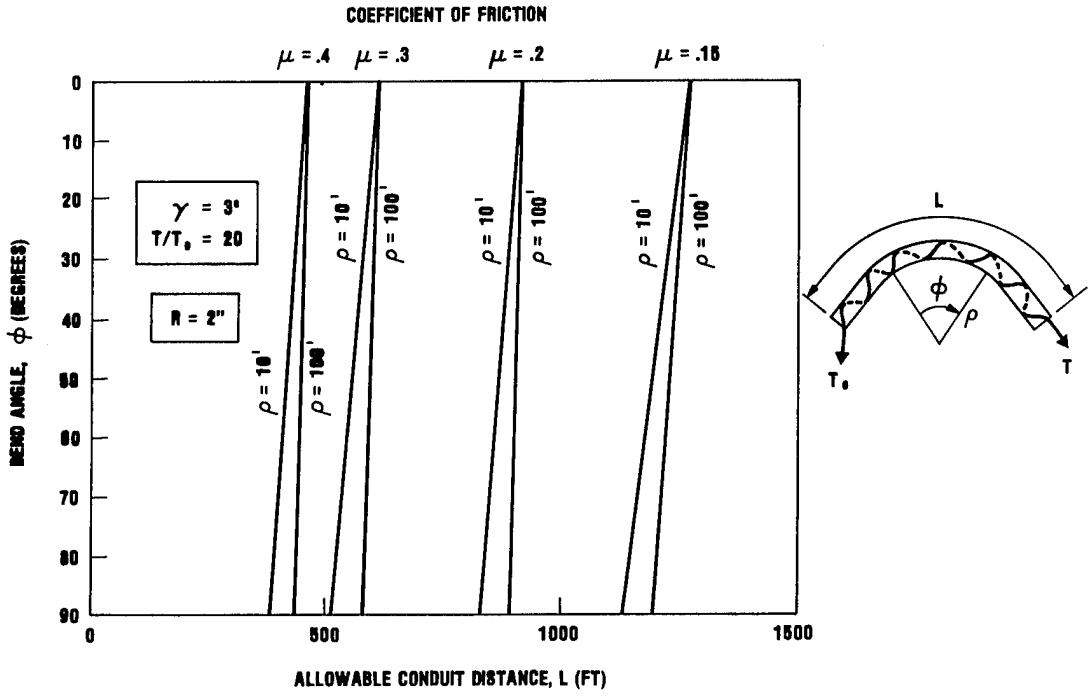



FIGURE 14 - ALLOWABLE CONDUIT LENGTH FOR CENTRAL BEND, $T/T_0 = 20$, $\gamma = 3°$

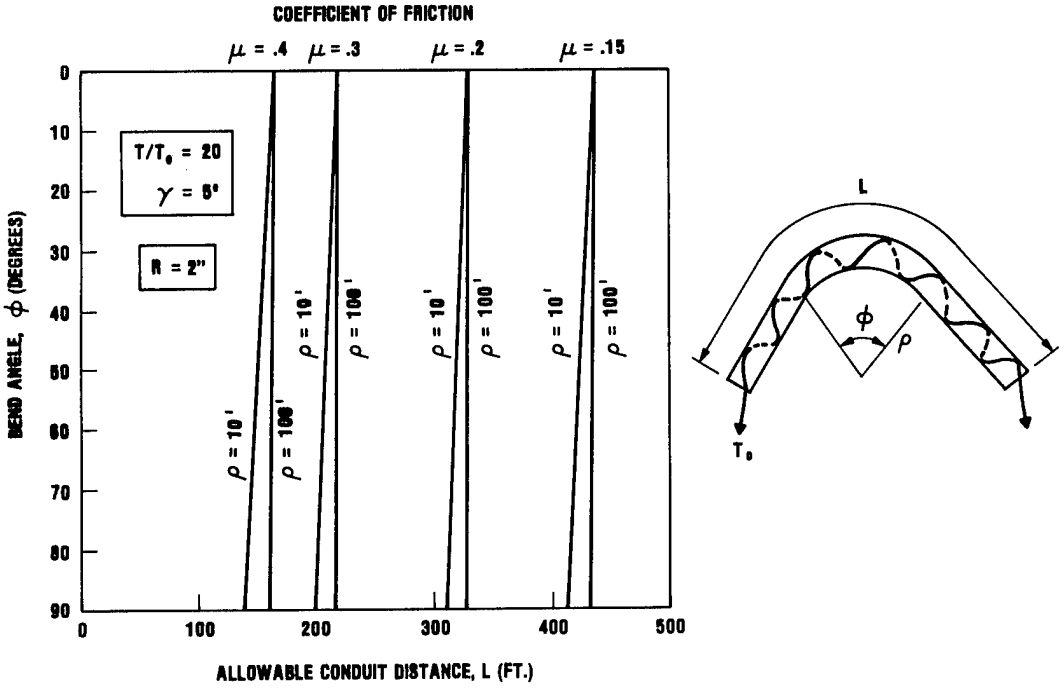



FIGURE 15 - ALLOWABLE CONDUIT LENGTH FOR CENTRAL BEND, $T/T_0 = 20$, $\gamma = 5°$

# Optical Fibre/Copper Conductor Composite LAN Cable for Mining Application

Paul Gregor, Georg F. Hög, Waldemar Gläsel, Helmut G. Haag

AEG KABEL Aktiengesellschaft, Mönchengladbach, Fed. Rep. of Germany

## 0. Summary

The increasing demand for digital information and the increasing distances in the mining area requires an improvement of the existing symmetrical mining cables. This led to the development of mining cables with foam skin insulated copper conductors and individual shielded units. Taking into account the typical mining field topology various cable design performances are necessary. The obtained advantages in comparison to the conventional cables respecting electrical and mechanical behaviour are commented. To evaluate also the next generation for digital LAN application, optical fibres are incorporated in the cables. The results for the transmission parameters of the optical fibres are reported in this contribution. The paper includes the laying procedure and the jointing technique, particular for the shaft cable. It is shown, that the electrical characteristics are appropriate for digital applications and that the optical characteristics are not changed during cabling and laying.

## 1. Introduction

In the range of primary energy coal takes worldwide the leading position regarding existing sources as shown in figure 1.
The quantities of the West Germany area exclusively do fulfil the future industrial demands far into the next millenium. Haulage of this natural raw material is set into an extremely high importance.

Consequently mining activities to be carried out need adcanced technology. Data exchange and communication between conveying equipments below ground on the one hand and to the commanding central station above ground on the other hand via distances up to 20 km become necessary. The existing telecommunication plants within mining area are not able to meet requirements of modern data processing systems. In fact of their design performance conventional cables mainly used within telephone links cannot serve as transmission medium for the new digital systems to be erected [1], [2].

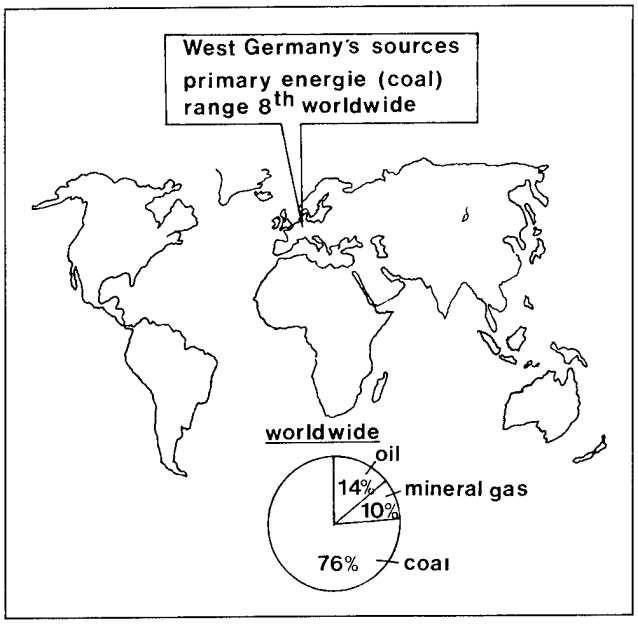



Fig. 1: Worldwide existing primary energy

## 2. Task

High demands compared to conventional cables have to be realized on the mechanical and electrical behaviour of this new cable generation in order to meet the overall concept.

Determination and design of stranding elements have to be made in such a way that electromagnetic field influences are kept to a sufficient low level. According to the

inherent topology within coal mining area 3 different types of cable design performances are required to complete the transmission link in total.

In order to investigate the capability for optical fibres to be used in the robust mining environment regarding mechanical stresses and loads and to realize copper stranding elements for broadband data transmission to build up a LAN network [3], [4], [5] a composite cable as described here has been created.

## 3. System Configuration

Between a master station above ground and so-called slave stations below ground digital datas employing various types of modulations shall be transmitted bitseriel. The individual slave station is adapted to the transmission circuit via a bus coupling device. Regarding data systems up to 19,2 kBaud corresponding to a pulsed frequency of 100 kHz copper conductors shall be used within this local network in bus configuration. In order to realize systems up to a transmission rate of 1 MBaud optical fibres are provided. Instead of and in addition to a bus configurated network point-to-point connections and star configurations are under consideration.

Within the semi duplex operating SEAB® system (SEAB = Serieller Anlagenbus) the master station contacts the individual slave stations rhythmically by transmitting a telegram signal, the slave stations response by applicating the same signal in reversal direction, as long as there is no particular information. However, in the event of an information at the slave station, the latter is reacting by transmitting a special signal. After each polling step (call/response) the master is able to send an order, which is to be marked by the relevant slave station. The self assured SEAB® system enables a network performance up to 127 adressable stations.

The LAN structure and the relevant cable constructions are shown in principle in figure 2. The cable connections at site are performed within cabinets (MDC, C, SDC), where the individual circuits are assembled via disjoinable clamps in order to achieve branching points for future network extension or supplements. The flexible tail cables are adapted to the sub distribution cabinet (SDC) by using mining-proof connecting plugs [9]. The optical fibres are terminated in the SDC, where the optical signal is changed into an electrical one and then branched off via flexible copper tail cables. Moreover optical fibres can be used for seperate trunk links connecting two adjacent coal mines (figure 3).

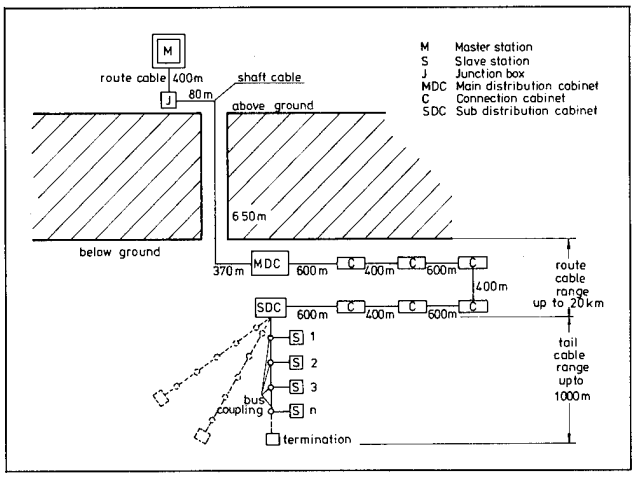



Fig. 2: LAN structure in coal mining range

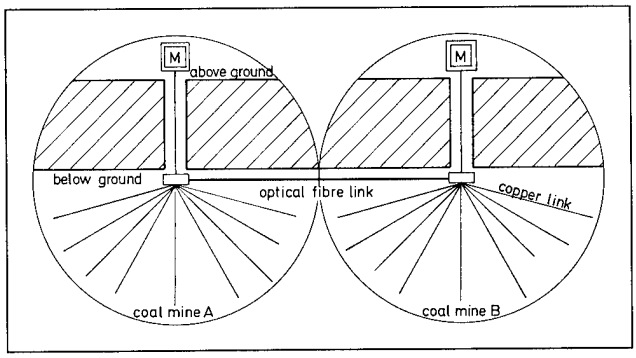



Fig. 3: Optical fibre link between coal mines within LAN structure

## 4. Cable Design and Manufacture

Installing a LAN-system within coal mining area means actually entering into a new cable generation. Consequently there are some major changes in cable components respecting relevant design principles different to conventional mining cables, as listed up in figure 4.

| parameter | conventional cables | LAN cables | achieved advantages |
|---|---|---|---|
| copper conductor diameter | 0,8 mm | 1,2 mm | lower line attenu- |
| insulation | solid-PE | foam skin-PE | ation |
| stranding | pairs in concentric layers | pairs in units | homogenous electrical characteristics low capacitance unbalances |
| shielding | non | shielding of units | higher crosstalk attenuation |
| optical fibres | non | yes | additional transmission capacity, noise immunity |

Fig. 4: Design Principles for LAN Cables

With respect to the typical european mining structure 3 various cable constructions are necessary: shaft, route and tail cables below ground. The cable core consists of a combination of symmetrical copper stranding elements and optical fibres being designed respectively selected regarding broadband transmission obtaining low line attenuation, high crosstalk attenuation, and sufficient noise immunity.

### 4.1 Shaft cable

Solid copper conductors of 1,2 mm diameter have been insulated by a dual foam skin polyethylene material. To achieve a remarkable low cylinder capacitance of insulated core the insulation material consists of high foamed cellular PE covered by solid PE resulting in a mechanical robust element to meet the particular requirements within mining industry. Two of these insulated conductors are twisted together to form a pair. Four pairs are stranded together forming a basic unit. Such units are covered by a multilayer wrapping consisting of a copper tape and plastic foils to form the shielded unit of about 13 mm cuter diameter [6], [7].
The lay of pairs and the wrapping performance are chosen in such a way that units keep their natural flexibility inspite of wrapping, aiming finally in a stranding assembly of segmented units presenting a relatively high pair density.

Comparing the so constructed cable core with an individual screened pair assembly a diameter decrease of about 20% is achieved for a 12 pair cable. Regarding design with individual screened pairs moreover it should be noted that line attenuation increases in fact of higher vicinity influence of the screen itself.

Within a concrete project 3 basic units and two optical fibres have been stranded together to build up the cable core. Over the wrapping a PVC sheath is extruded. A double layer of heavy galvanized flat steel wires has been applied in opposite stranding direction gaining a fairly torsion-free behaviour during installation of the cable. The two steel wire layers have been finally kept together by a steel tape helix. The outer protection of cable is again formed by an extruded PVC sheath

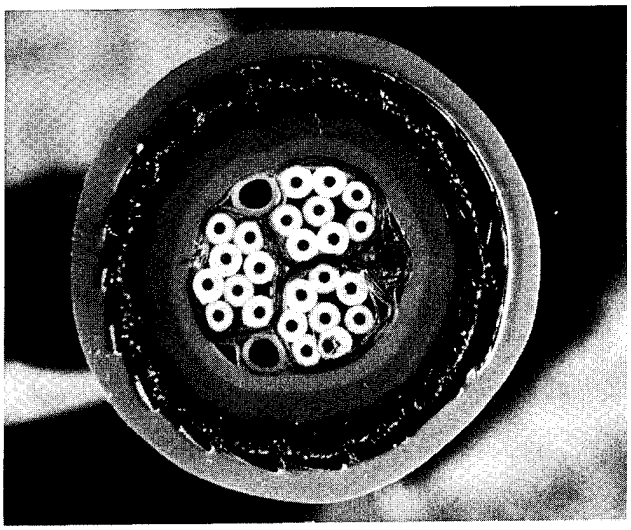


Fig. 5: Cross section of Shaft Cable

4.2 Optical fibre element

The optical fibre element contains two filled loose buffered fibres and four dummies. These components are stranded around a central strength member of fibre reinforced plastic (FRP) to form the finally wrapped cable core. The dimensions and the pitch length of the elements are chosen in such a way, that the fibre element fits into the interstices, and that the necessary length compensation of the fibre length due to expansion and constraint of the cable is possible without any mechanical stress on the fibres themselves.

Graded index fibres 50/125 µm with an attenuation of 2.7 dB/km at a wavelength of 850 nm and a bandwidth of 200 MHz related to 1 km are chosen for information transmission. By using the same bandwidth and an attenuation of 0,7 dB/km the transmission at 1300 nm is also possible. The numerical aperture of these fibres is to 0.20 ± 0.02 [8].

Such fibres combined with cost effective LED's as transmitters can bridge distances up to 14 km without any regenerator at 850 nm. Using laser diodes the distance can be extended up to 19 km. Beyond this, the distance without regenerator can be increased by another 10 km in changing to 1,3 µm techniques.

4.3 Route cable

The cable core for the route cable is of the same configuration as for the shaft cable. In contrary to the shaft cable the sheath design has been performed metal-free. Instead of steel wires a glassyarn reinforcement in connection to the PVC outer sheath according to figure 6 has been used [9]. The glass yarn reinforcement consists of a lattice as a combination of individual glass yarns applied axially and transversally, where the axial running components serve as tensile strength members, particular for the laying process and the transversal performed components present a certain impact resistivity (figure 6)

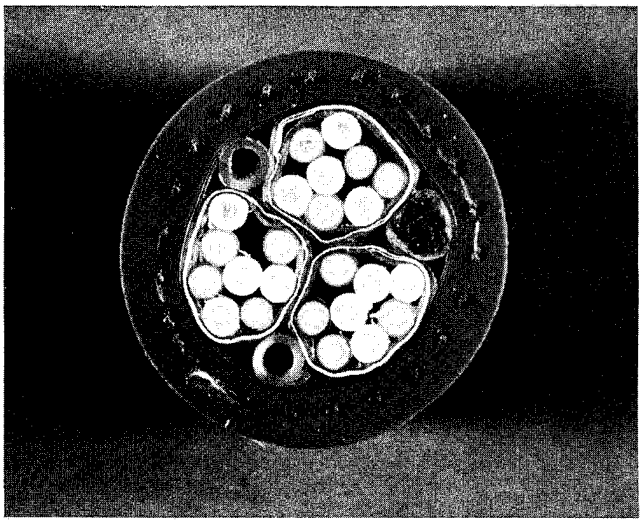


Fig. 6: Cross section of Route Cable

4.4 Tail cable

This cable is designed without optical fibres. Taking into account a necessarily higher

flexibility four stranded copper conductors of 1 $mm^2$ cross section with cellular polyethylene insulation have been stranded together to form a star quad. Above plastic core wrapping a thin copper foil is applied longitudinally acting as an additional flame barrier. The outer sheath made out of PVC exhibits as well glass yarn incorporated elements.

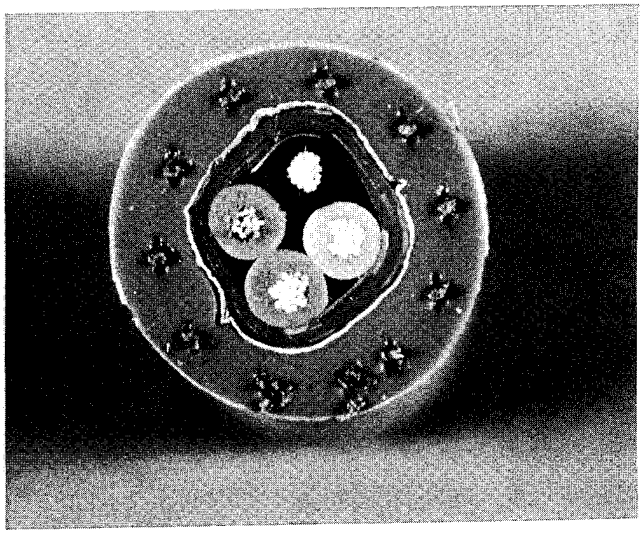


Fig. 7: Cross Section of Tail Cable

Some of the substantial mechanical cable datas are described in figure 8

| Mechanical datas | | | |
|---|---|---|---|
| cable / characteristic | Type 1<br>G-02YSYbbY<br>12X2X1,2 BdiMF<br>2650/125<br>(shaft cable) | Type 2<br>G-02YSY(Zg)Y<br>12X2X1,2 BdiMF<br>2650/125<br>(route cable) | Type 3<br>L-02Y(ST)Y(Zg)Y<br>2X2X1,0 $mm^2$<br>(tail cable) |
| outer diameter (mm) | 46 | 36 | 12 |
| cable weight (kg/km) | 3100 | 1100 | 160 |
| bending radius (mm) | 460 | 360 | 120 |
| tensile strength (N) | 32000 | 4000 | 1500 |
| properties of materials | | | |
| PE-insulation<br>PVC-sheath | VDE 0207 | VDE 0207 | VDE 0207 |

Fig. 8: Mechanical Datas of LAN Cables

## 5. Characteristics

### 5.1 Electrical characteristics

The electrical characteristics of cables are shown in figure 9

| current No. | parameter | frequency | dimension | characteristics (at 20 °C) cable with copper conductors ⌀ 1,2 mm | flexible wire copper conductors = 1,0 $mm^2$ | test method according to VDE 0472/ part |
|---|---|---|---|---|---|---|
| 1 | loop resistance | D. C. | Ohm/km | ≤ 31,8 | ≤ 31,8 | 501 |
| 2 | conductor resistance unbalance | D. C. | Ohm/km | ≤ 0,2 | - | 501 |
| 3 | insulation resistance | D. C. | MOhm-km | ≥ 10.000 | ≥ 10.000 | 502 |
| 4 | mutual capacitance | 800 Hz | nF/km | ≤ 36 | ≤ 36 | 504 |
| 5 | capacitance unbalance | 800 Hz | pF/1000 m | ≤ 70 within unit | ≤ 210 | 506 |
| 6 | attenuation | 100 kHz | dB/km | 2,2 | 2,6 | 515 |
| 7 | characteristic impedance | 100 kHz | Ohm | 130 ± 12 % | 130 ± 12 % | 516 |
| 8 | crosstalk within unit<br>NEX<br>FEX | 108 kHz | <br>dB<br>dB/km | <br>≥ 70<br>≥ 70 | <br>≥ 70<br>≥ 70 | 517 |
| 9 | dielectric strength<br>conductor/conductor<br>conductor/screen | 50 Hz | V | <br>1000<br>1000 | <br>1000<br>1000 | 509 |

Fig. 9: Electrical Characteristics of LAN Cables

A typical distribution of capacitance unbalance in function of the length respecting a tail cable L-02Y(St)Y(Zg)Y 2x2x1,0 $mm^2$ is shown in figure 10. The maximum peaks herein are below 5 pF/1000 m.

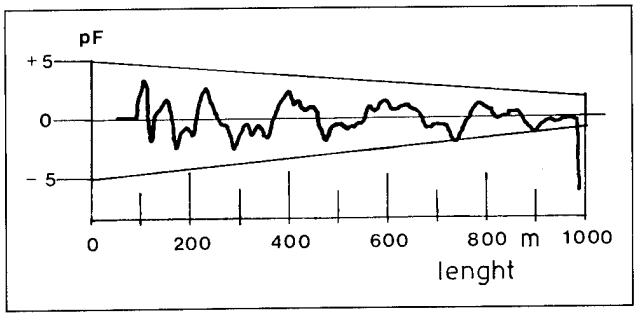



Fig. 10: Distribution of Capacitance Unbalance over a Tail Cable Length

Mutual capacitances and capacitance unbalances of LAN-cables are compared with conventional mining cables G-2YYbY 100x2x0,8 in following diagramms figures 11 and 12.

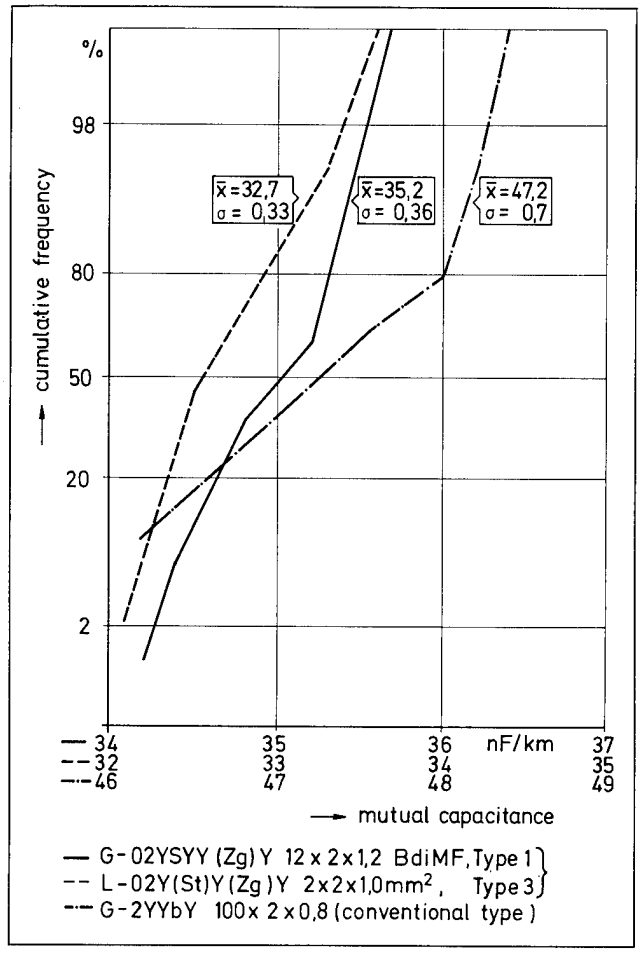



Fig. 11: Comparison of Mutual Capacitance between LAN Cables and Conventional Types

As a result one can point out that for the unit technique of composite cables the standard deviation of mutual capacitance is marching to smaller tolerances. Consequently transmission rate is independent from the chosen pair of composite cable cross-section. This is contrary to the behaviour of a cable made up in concentric layers. A homogenous rate level is an important characteristic for cables within LAN-bus-systems.

The characteristics of line attenuation and characteristic impedance of the composite LAN cable G-02YSY(Zg)Y 12x2x1.2 are compared with standard cable G-2YYbY 100x2x0.8 in figures 13 respectively 14

By the use of thicker copper conductors together with the foam skin insulation the obtained line attenuation for instance at 100 kHz has been reduced by approximately 40 %.

Therefore the repeaterfree cable links are substantially extendable by using this new cable design.

The conventional hauling cables have been provided only for VF-systems. Within the desired bus transmission data link the need of a frequency band utilisation up to 100 kHz has been demanded. Therefore certain requirements regarding crosstalk attenuation particular the near end crosstalk have to be met. The

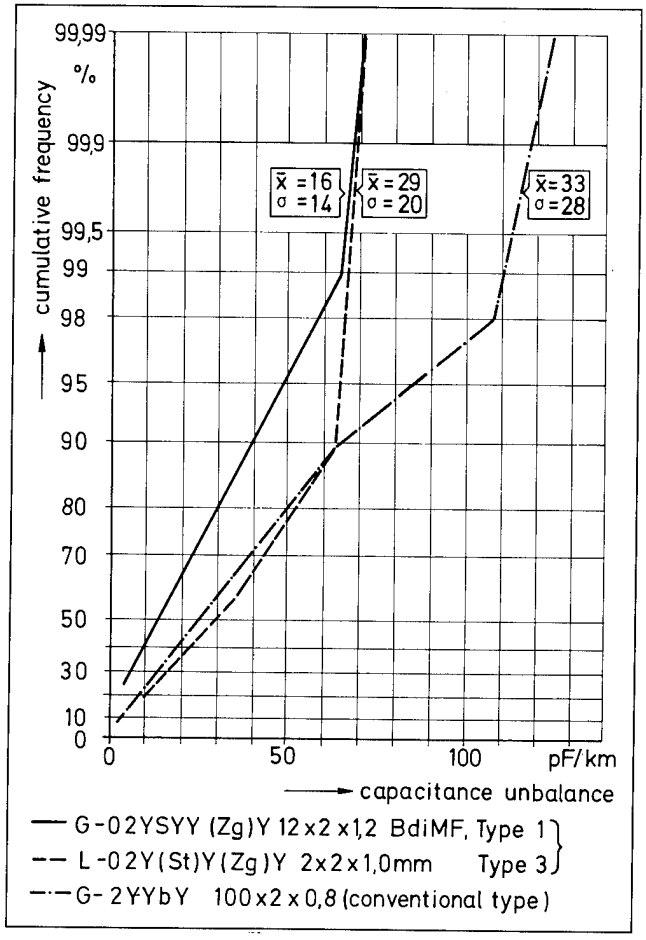



Fig. 12: Comparison of Capacitance Unbalance between LAN Cables and Conventional Types

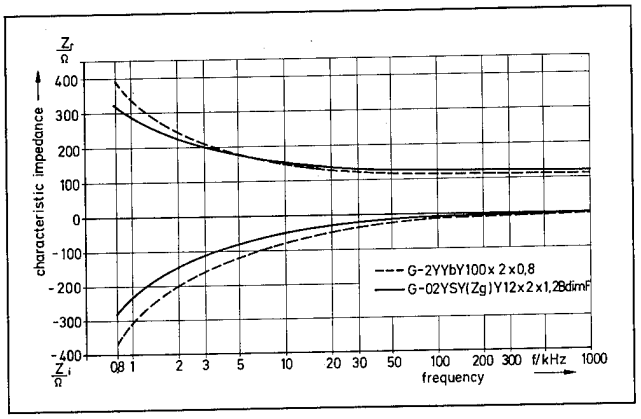



Fig. 13: Characteristic Impedance of LAN Cable

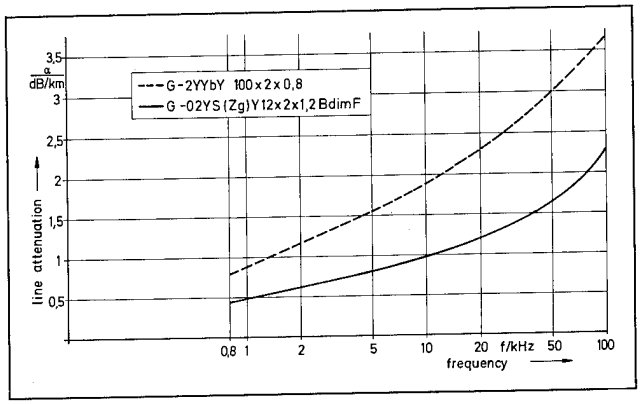



Fig. 14: Line Attenuation of LAN Cable

cumulative probability for crosstalk within screened units of delivery lengths is shown in figure 15.

Crosstalk FEX and NEX between adjacent units have been measured at 100 kHz being better than 90 dB/km. In using different units for the both transmission directions the maximum possible repeaterless cable distance will be limited only by the line attenuation. There is no restriction by crosstalk. Typical NEX values in function of frequency within units are shown in figure 16.

## 5.2 Noise immunity

The before mentioned systems have been

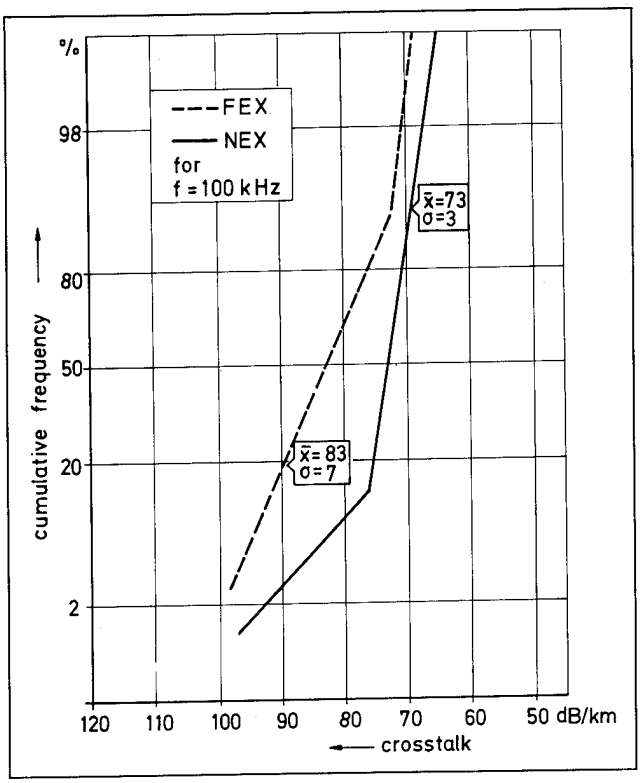



Fig. 15: NEX and FEX level of LAN cables

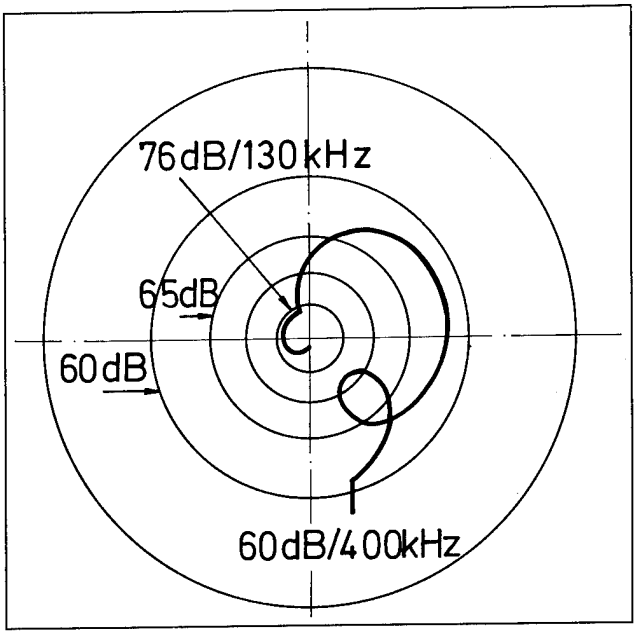



Fig. 16: Typical NEX Level of LAN Cable within Unit

determined for use in a frequency range basically up to 100 kHz, in a future step up to 400 kHz. Thus the behaviour of cable with respect to noise immunity shall be investigated.

Existing noise sources can influence the transmission in the data cable. The possible noise sources in the vicinity are summarized in figure 17.

| type of noise source | frequency |
|---|---|
| power cable/flexibles (break down) | 50 Hz |
| thyristor harmonics | up to 20 kHz |
| radio channels for railway operation | 70 - 130 kHz |
| emergency signalling system | 1 - 250 kHz |

Fig. 17: Electromagnetic noise sources below ground

Transfer impedance as well as reduction factor measured over the frequency upon delivery lengths have been registered in figure 18 respectively figure 19.

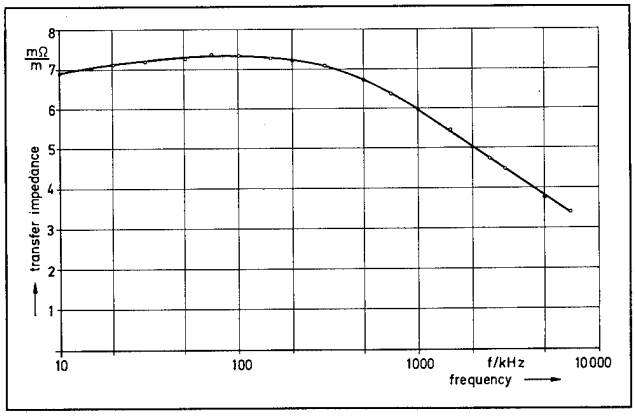



Fig. 18: Transfer Impedance of LAN Unit

In order to examine the immunity of these new composite cables to electromagnetic noise sources a complete LAN-circuit of 5 km length

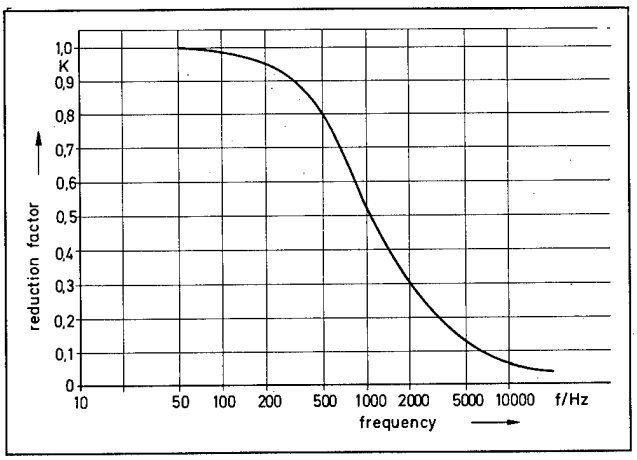



Fig. 19: Reduction Factor of LAN Unit

was examined over a period of 24 hours. Maximum recorded peaks have been found up to 75 µV for the mentioned cable section.

## 6. Installation

### 6.1 Installation and Mounting of cables

The configuration of cables within the cable route in total and the distribution of lengths including jointing sleeves have been shown in figure 2.

The shaft cable length has been put down by using a shifting wheel with a diameter of 2.2 m positioned directly to the 650 m deep shaft (figure 20).

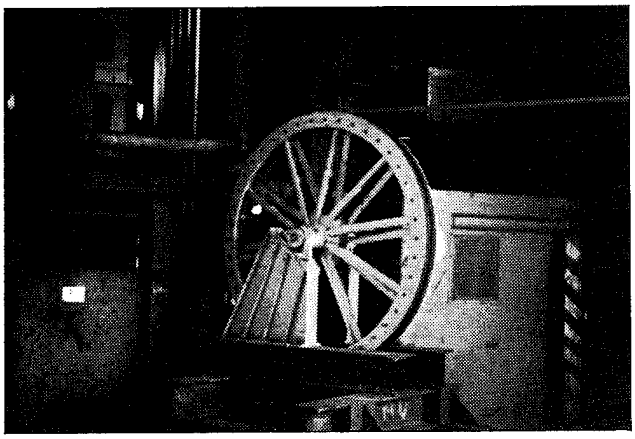


Fig 20: Shifting Wheel for Shaft Cable Installation

The cable was coiled in 6 layers, each covered by a protection layer on a special drum, 10 m length in total including transporting device with a total weight of 30 tons (figure 21).

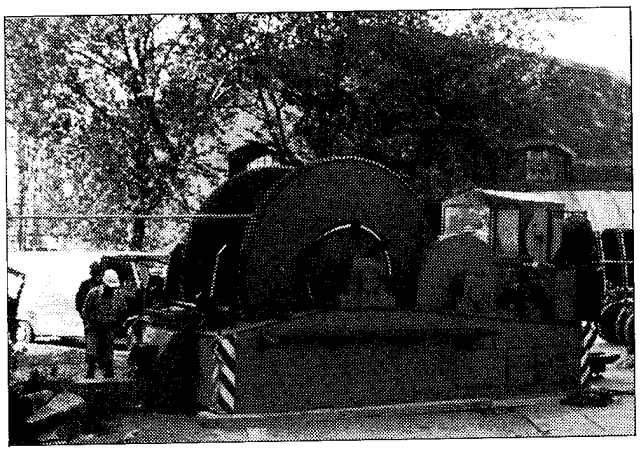


Fig. 21: Shaft Cable Drum

The drum diameter was 1.25 m. The distance between drum and shifting wheel has been about 45 m. The cable head has been connected to a 30 kg weight during hang down operation in order to center the cable within the shaft.
From this special drum equipped with a brake, the cable was put down into the shaft via the shifting wheel with a speed of 8m/min.

During the installation of the shaft cable no rotation of the latter has been registered as a result of particular armouring performance. After finishing the hang down procedure the cable has been fastened every 6 m to the firm shaft construction by utilization of special clamps.

After completion of installation measurement results of backscatter measurements on the optical fibres have clarified that there are no deteriorations due to the laying process. Route cables below ground have been mounted on to steel shells, being arranged in regular intervalls.

6.2 Accessories for jointing

Route cables have been jointed together within mining proof cabinets (C), as shown in figure 22.

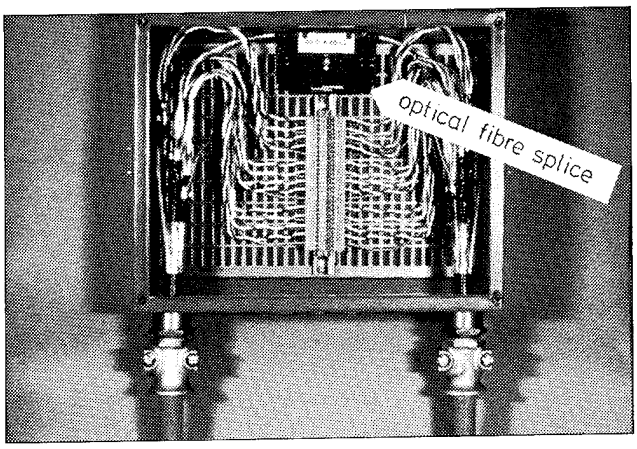



Fig. 22: Cabinet for Connecting/Distributing

Such steel cabinets, sized 300x400 mm, have been constructed under consideration of firm inputs and outputs, and the conductors have been switched together along the line by using screwed connections. The individual jointing technique permits in fact of the screw performance a separate interruption with regard to later distribution or branching of certain circuits.

The screening per unit has been switched via the link separately in order to avoid undesired noise interferences by vagabonding current flow.

The unit configuration as well as the pair twisting make up has been approached as far as possible to the screw connection. The lay-out of cabinets provide several closed cable in- and outputs, simplifying future extensions. Splices for optical fibres elements have been located with additional length in a separate protected frame beyond the copper circuit switches, as shown in figure 22.

## 7. Conclusion

A new cable generation to be used within LAN systems of coal mining industry has been realized. The suitability of compents of these composite cables have been proofed within a realistic field. In fact of unit stranding transmission characteristics exhibit a homogenous level for all elements. a necessary condition for digital data links. All results reported show that the possible field distance without repeater to be installed is relatively high, for instance 20 km regarding a 19,2 kBaud system. Particular care has been taken by determination of stranding elements respecting noise immunity. This cable design solution presents a high transmission capacity both regarding copper elements and optical fibres for future system performances.

## 8. Literature


|1| K. Pistor — IKOS, ein lokales Netz für die Prozeß-Kommunikation

|2| R. Kersten — Signalarten und Signalfarben bei der Übertragung von PCM-Signalen auf symmetrischen Fernsprechkabeln

|3| CCITT — Yellow Book Volume III - Fascicle III.3 Digital Networks

|4| CCITT - Rec. I 430 Abschnitt 2.1

|5| DBP TL 1 R 230 T12 Dez. 83

|6| DIN VDE 0816/2.79 — Außenkabel für Fernmeldeanlagen

|7| DIN VDE 0817/4.84 — Leitungen mit Litzenleitern für erhöhte mechanische Beanspruchungen

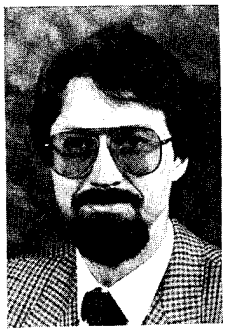
|8| DIN VDE 0888, Teil 2, Entw. März 1985 — Lichtwellenleiter für die Nachrichtentechnik Fasern, Einzeladern, Bündeladern

|9| H. G. Dageförde/ P. Gregor/ G. Thoenessen — PIC-Trunk Cable assembled with connecting plugs




Paul Gregor (44) (Speaker) is head of the Technical Sales Group for Telecommunication Cables. He reached his Ing. from the Ingenieurschule Duisburg in 1966 and jointed Kabelwerk Duisburg, now a part from AEG KABEL. He was engaged in the development of Telecommunication Cables and hold his present position since 1980.

Georg F. Hög (35) is head of the Development Group for Optical Fibre Cables. He reached his Dipl.-Ing from the University of Aachen and jointed AEG KABEL in 1977. After being engaged in the development of symmetrical telecommunications cables he get the responsibility for this group in 1980. Since spring 1985 he covers his present position.



Waldemar Gläsel (34) is head of the Technical Sales Group for Optical Fibre Cables. He reached his Dipl.-Ing. in Communication Engineering 1975. After being engaged in different development, planing and sales division in the AEG Group he jointed AEG KABEL in 1981 to take his present position.



Helmut G. Haag (37) is head of The Technical Sales Division for Telecommunications. After reaching his Dipl.-Physiker from the University of Stuttgart he jointed AEG KABEL in 1975 for the development of coaxial cables. Later he was also responsible for the development of optical fibre cables. From 1980 to 1983 he built up the production plant for these cables. In autumn 1983 he took his present position.

# "MANUFACTURE AND PERFORMANCE OF FIBRE UNITS FOR INSTALLATION BY THE VISCOUS DRAG OF AIR".

S Hornung, S A Cassidy, P Yennadhiou and M H Reeve

British Telecom Research Laboratories
Martlesham Heath
IPSWICH, UK

## Abstract

Fibre units containing 7 fibres each have been manufactured to be installed by the viscous flow of air. The manufacture was characterised by loss measurements on optical fibres. The performance over a wide temperature range was investigated, during which both attenuation and fibre strain were measured. In multi-mode fibre the attenuation increased by only 0.2dB/km between -10 and +30°C. The total change of strain between -15 and +30°C was 0.12%. Four fibre units were successfully installed in operational ducts with no increase in attenuation.

## Introduction

Two years ago a radically new approach to optical fibre cable design and installation was reported at I.W.C.S (1) Units containing a number of fibres were drawn into pre-installed empty bores (tubes), using the viscous drag of air. The drag force acting on the fibre unit is distributed along it's length, which makes it possible to introduce fibres into complicated routes, with low strain.

The fibre units each containing seven fibres are "blown into" previously installed empty polyethylene bores, pulled into the ground using traditional techniques and with no special care. Each bore has an inside diameter of 6mm and an outside diameter of 8.3mm. Seven such bores are assembled in a "six round one" configuration to form a cable with an outer diameter of 29mm including an outer sheath of polyethylene. Using a seven fibre unit, the capacity of this cable is 49 fibres.

In this paper we will look at this cable in terms of two important parameters governing the performance of any cable. These are fibre attenuation and fibre strain. These are important in three areas of cable performance, dealt with separately, which are Manufacture, Temperature performance and Installation.

## The fibre unit

The fibre unit is a miniature fibre optic cable, made up from an expanded polyethylene coated bundle of seven straight laid optical fibres in a "six-round-one" configuration. It contains a mixture of materials (ranging from polymer to silica) with different thermal properties. As fibre optic cables experience a range of different temperatures during storage and after installation in the ground, the materials within them engage in constant "trials of strength" as the various materials try to expand by different amounts. This can result in microbending loss or even in excessive strains.

## Measurements

Measurements were made on both single-mode and multi-mode fibres incorporated into fibre units.

The classical technique for the measurement of fibre loss is the cut-back method. This technique was used for a small number of measurements on single-mode fibres. Since after installation only one fibre end is available, the other being typically 1km removed, the bulk of measurements were made using an Optical Time Domain Reflectometer (O.T.D.R.).

For single-mode fibres a serious limitation to this technique arises from the fibres' scatter coefficient which may be different depending on the direction of measurement. This is no problem if fibre ends are labeled, and only changes of loss are required. Alternatively fibre can be measured in both directions and averaged.

In multi-mode fibre the large number of modes launched ensure that this is not a problem. A problem will arise however, if the launch distribution varies from measurement to measurement. To overcome this we used a connectorised tail between the O.T.D.R and the fibre under test. Many repeated measurements have shown a standard deviation for the repeatability of the measurement of ±0.1dB.

Changes in strain were detected by the now well known method of "phase delay" (2), which measures small changes of fibre propagation delay in the frequency domain.

## Manufacture of fibre units

A number of fibre units containing multi-mode fibre were made by directly extruding expanded

polyethylene onto a straight laid bundle of 7 fibres. Fibre loss was measured by O.T.D.R. at 904nm, before and after the manufacture. To improve accuracy each fibre was measured in both directions. The average change in loss after manufacture is +0.15dB/km with a standard deviation of ±0.21dB/km.

A fibre unit was made containing two single-mode fibres. Fibre attenuation was measured using the cut-back method in the 1.3μm and 1.55μm windows before and after the unit was manufactured. No increase of loss was apparent to within the accuracy of the measurement of ±0.03dB/km.

## Temperature Performance

An unit containing multi-mode fibre was temperature cycled between+40 and -40°C. Using two of the seven fibres we simultaneously monitored strain changes in one fibre and attenuation in the other. The change in attenuation was less than +0.2dB/km between +40 and -10°C. Severe microbending loss is apparent at lower temperatures. Fig.1.

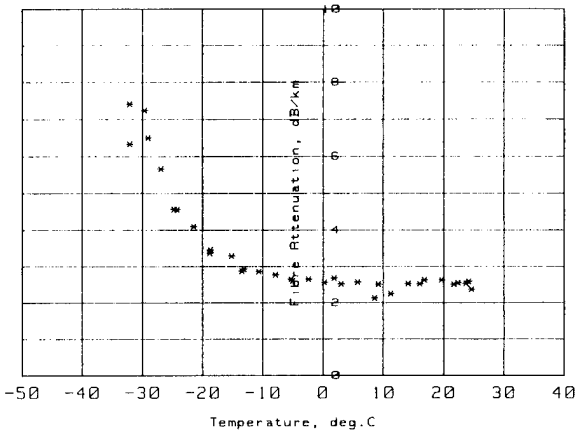



Fig.1. Attenuation of multimode fibre, measured by O.T.D.R. as function of temperature.

The measurement of strain (propagation delay) in the fibre reveals that the fibre is compressed as the temperature is lowered. This is quite reasonable, as the polymer has a coefficient of linear expansion of ~$10^{-4}$, whereas the fibre' is only $2*10^{-7}$.

For a composite structure of fibre with polymer coating, the change in propagation delay is affected by several competing phenomena, including changes of group index as function of temperature and strain and physical changes of fibre length. We can express the coefficient of expansion of the polymer coating ( $\alpha_c$) as (3):

$$\alpha_c = \frac{(1+K_f/K_c)}{(1+\frac{E_f}{N}\frac{dN}{d\sigma})}\left[\frac{1}{t}\frac{dt}{dT} + \frac{E_f \alpha_f}{N}\frac{dN}{d\sigma} - \frac{1}{N}\frac{dN}{dT}\right] - \frac{K_f \alpha_f}{K_c}$$

Where $\alpha_f$ and $\alpha_c$ are coefficients of expansion of fibre and coating respectively. $K_f = A_f E_f \alpha_f$ and $K_c = A_c E_c \alpha_c$, with $A_f$ and $A_c$ the cross-sectional areas of fibre and coating respectively, and $E_f$ and $E_c$ the Young's moduli of fibre and coating respectively. N is the fibre's group index, dN/dT and dN/dσ are directly measured coefficients (2).

Using the above expression and the experimentally measured values of dt/dT, we calculate $\alpha_c$ as a function of T. This is plotted in Fig. 2 and compared with directly measured $\alpha_c$ (4). The agreement is very good. From this analysis it appears that at all times there is no overall slippage between the various fibre unit elements, and that there is no buckling of fibre. This is in agreement with the conclusions of reference (5), regarding the stiffness of a seven fibre bundle.

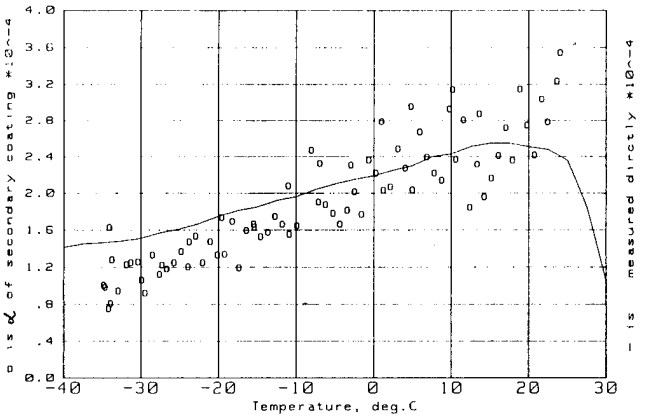



Fig.2. Comparison of coefficient of expansion of fibre unit coating, measured directly and calculated from measured fibre strain as function of temperature.

We can also infer from this, that the observed increase in loss is not due to microbending associated with buckling, but is rather caused by microbending due to radial compression of the polymer coating.

In the absence of buckling, we can use the measured values of α and E to calculate the total change of strain experienced by the fibre on warming from -15 to +30°C, as 0.12%. However, as the fibre unit is coated with polymer at an elevated temperature, on cooling to room temperature the fibre will be in a compressed state. Any change after installation is most likely to be a lowering of temperature which will result in further compression. Therefore the only possible threat of strain to the fibre may come from the unit's installation.

## Installation

Three fibre units were manufactured and installed into a trianglular network of outer tube units (Fig.3). Multimode fibre was used throughout to connect two LANs in two BT buildings

to the main telephone exchange. Each fibre unit contained 7 fibres of which only 4 were terminated with optical connectors. All outer tube units were installed by local teams using standard practices. The fibre units were "blown in", each in two sections from a central manhole, always fleeting half of the fibre unit in a "figure of eight".

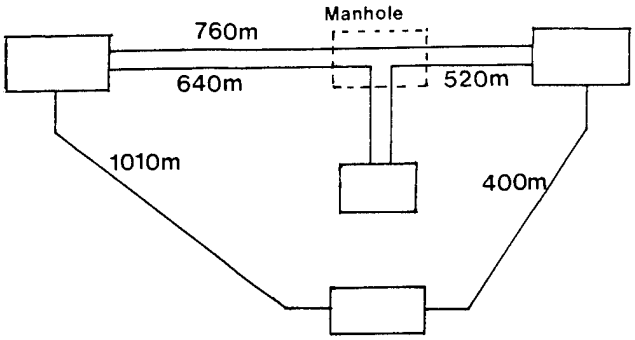



Fig.3. Diagram of trial route.

Fibres were measured by the O.T.D.R. before the installation, and four months after it. Fig.4 shows the histogram of measured changes in loss. The mean value is 0dB, with a standard deviation of 0.17dB. The null change of loss is consistent with the strain-free installation technique, and the standard deviation is consistent with the measurement accuracy.

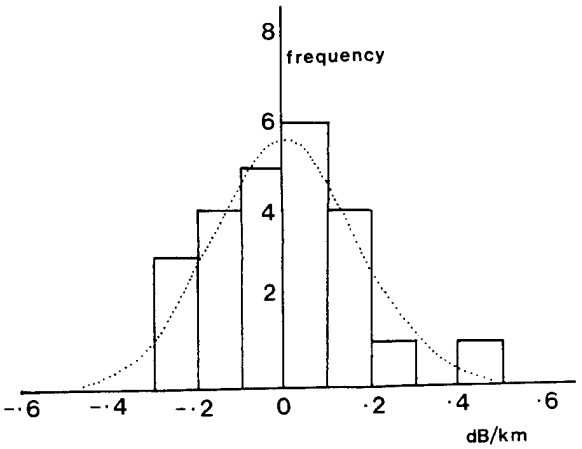



Fig.4. Histogram of multimode fibre loss change due to installation measured by O.T.D.R.

Two further links were added to this network at a later date.

Using the theory from Ref. 1, and experimental measurements (6), the maximum strain experienced by a 500m fibre unit at the end of an installation will be 0.08% at one end of the unit, and 0 at the other. The average is therefore 0.04%, most of which will relax out as soon as the installation process is stopped.

## Conclusions

We have described the manufacture, temperature and installation performance of a simple fibre unit for installation by the blown fibre technique. The unit can be made and isntalled with no significant changes in loss in both single-mode and multi-mode fibre. Multimode change in loss remains below 0.2dB/km between -10 and +30°C.

The strains associated with installation are negligible, as are those likely to arise from temperature changes. From this we may infer that fatigue breaks will be very unlikely in the 20 year fibre lifetime (7).

## Acknowledgements

The authors would like to thank their many colleagues for their help, in particular Mr S Haig and Mr P Constable for polymer properties measurements. The authors gratefully acknowledge the head of Local and Junction Network Operations and the Director of British Telecom Research Laboratories for permission to publish this work.

## References

1. A radically new approach to the installation of optical fibres using the viscous flow of air. S A Cassidy and M H Reeve, IWCS 1983.

2. Single-ended fibre strain and length measurements in frequency domain. R Kashyap, M H Reeve, Elec Lett, 16, No 18, p689-690, August 1980.

3. Temperature desensitisation of delay in optical fibres for sensor applications. R Kashyap, S Hornung, M H Reeve and S A Cassidy, Elec Lett, 19, No 24 p1039-1040, November 1983.

4. S J Haig, 1984, Private communication.

5. A fibre unit for blown fibre cable, S A Cassidy S Hornung, IEE colloquium on "Implementation and reliability of optical fibre cable links", London, June 1984.

6. Optical characterisation of a trial link using blown fibre cable. S A Cassidy, S Hornung, P Yennadhiou M H Reeve, ECOC Venice 1985.

7. Effect of service environment on proof test of optical fibres. W Duncan et al. 7th ECOC, Copenhagen 1981.



Stephen Cassidy graduated from Oxford University in 1980 with a degree in Natural Sciences. Since joining British Telecom Research Laboratories, he has worked on various aspects of optical cable research. These have included studies of fibre strain during several coating and cable fabrication processes and in cable installation.



Michael Reeve graduated from Durham University in 1973 with a degree in applied physics and joined the British Telecommunication (then Post Office) Research Department at Martlesham in Suffolk. He has worked on a number of aspects of optical fibre communications including fibre scattering and mode cut-offs, fibre strength and cabling. He is currently head of a group concerned with optical cable research.



Stephen Hornung graduated from the University of Exeter, Exeter, England in 1975. In 1980, he received the D.Phil from the University of Oxford, Oxford, England for work in low-temperature nuclear orientation of some neutron-light isotopes of iridium.

Since 1979, he has worked for British Telecom Laboratories on optical-fiber communications research, specializing in measurements on optical fibres with particular interest in cabling aspects.



Peter Yennadhiou received the B.A. degree in natural sciences from Girton College, University of Cambridge, England in 1984.

Since then he has worked for the British Telecom Research Laboratories within the optical fibre cabling group.

# MECHANICAL ARCHITECTURE OF A 147 KILOMETER REPEATERLESS FIBER OPTIC UNDERSEA CABLE SYSTEM

Tek-Che Chu, Louis J. Marra and Robert K. Stix

AT&T Bell Laboratories
Undersea Systems Laboratory
Holmdel, New Jersey 07733

*Abstract*

AT&T has designed, built, and will soon install an undersea 147 KM repeaterless fiber optic cable to serve as a data link between an offshore platform and a shore terminal. Data is transmitted at a rate of 3 Mb/s using a signal wavelength of 1.55μm. One-half kilowatt of power is also delivered to the platform. This paper will detail the mechanical architecture and components of this system, including cables, spliceboxes, and end couplings. A final section will discuss the manufacture and optical performance of the integrated system.

*Introduction*

AT&T has designed and built, and is currently under contract to install, an undersea repeaterless fiber optic system. A diagram of the complete system is presented in Figure 1. AT&T's commitments for this project are:

1. Supply a 147 Km, 3 Mb/s repeaterless fiber optic cable to serve as a data link between a shore terminal building and a moored offshore platform, operating in the 1.55μm wavelength range. In addition, the cable will supply 0.5 kilowatts of power to the platform with the current return through an ocean ground.
2. Supply the equipment to transmit and receive the digital optical signals, as well as equipment to deliver the power.
3. Install the cable and associated equipment.

The scope of this paper is limited to a discussion of the system's cable elements, the hardware used in joining cable sections together, and the anchoring assembly used to attach the cable to the offshore platform. The paper will give an overview of the design of each of these components and the specifications which guided the design work. In addition, a final section will discuss the optical performance of the cable during manufacture and integration of the system.

A schematic of the system's mechanical architecture is shown in Figure 2. The system can be broken down into the following components:

1) *Fiber Core.* This is the central member common to both types of cables used in the system. It is the structure which contains the optical fibers.
2) *Trunk Cable.* The portion of the system from the ocean-bottom touchdown point to the shore (Figure 1) is composed of sections of a trunk cable design known as SL.
3) *Riser Cable.* A section of the system forms a catenary from the ocean floor to the offshore platform. Here a cable known as the riser is utilized (see Figure 1).
4) *Cable-to-Cable Splicebox.* Due to manufacturing limitations, the SL trunk cable section could not be manufactured in one continuous length. A splicebox is utilized to join the sections together. A special version of the splicebox, known as a junction box, is used to join the SL deepwater cable to the riser cable.
5) *End Coupling.* The two ends of the system are terminated in mechanical assemblies known as end couplings. These assemblies anchor the riser cable to the platform, the trunk cable to the terminal station, and break out the cable's fibers and power.

The design of these components is discussed in the following sections.

*Fiber Core*

A schematic of the fiber core design is shown in Figure 3. The central member of the core is a steel wire known as the kingwire. The kingwire serves as the starting element around which the balance of the core is built. The kingwire is surrounded by a buffering elastomer known as Hytrel.[1] Embedded in this material are the 4 single-mode optical fibers needed for the system. The fibers are stranded within this structure, with a lay length of about nine inches. The buffering material is visco-elastic, and protects the fibers from impingement on any hard surface (such as the kingwire) which could cause micro bending losses.

Extruded over the elastomer/fiber matrix is a nylon sheath which prevents the matrix from distorting or kinking, another possible cause of microbending. In addition, the sheath makes the core more rugged and easier to handle during subsequent cable manufacturing operations.

*SL Cable*

The functions of the trunk, or SL cable are:

1. Protection of the optical fibers against the high pressure of the ocean bottom.
2. Protection of the fibers against excessive strain during laying and recovery.
3. Provision of a powering path.
4. Provision for a 25 year service life.

Additionally, the installation of ocean-bottom cable places

several constraints on the design as explained previously by Gleason et al. [1]

The SL cable, designed to meet the above goals, is illustrated in Figure 4. The cable consists of the lightguide core protected by two layers of high strength steel stranded wires, a copper sheath, and a low-density polyethylene extruded jacket. The steel-and-copper structure act as a pressure vessel to protect the core. In addition, the copper furnishes a low resistance power path in the cable. The polyethylene provides high-voltage insulation and environmental protection.

Extensive testing and at-sea trials [2] have been performed to demonstrate that the SL cable maintains its optical and mechanical integrity under the conditions of low temperature, high pressure, and high tension. Results from all of these tests indicate that no significant permanent mechanical or optical degradation is induced.

As Figure 1 and 2 illustrate, the SL cable is overarmored in certain sections with either a single layer of steel or two layers of steel. Figures 5 and 6 show details of these two cable designs.

*Riser Cable*

The riser cable must protect the fiber core from the forces associated with the undersea environment in much the same way as the SL cable does. However, the placement of this cable in the system also generates the following additional specifications on its designs:

1. A 10 year service life.
2. Nominal torque-balancing under tension to prevent knotting.
3. Protection of the insulation from sharkbite damage.
4. A design rugged enough to withstand repeated flexures without increased optical attenuation or fatigue of its steel strength members and electrical insulators. This flexure will arise in the section of cable underneath the platform due to wave action and movement of the structure.

The design of the riser cable is shown in Figure 7. The design consists of three layers of steel wire stranded about the core, a branched low-density polyethylene electrical insulation sheath, and a medium density sharkbite protection sheath.

The first two layers of steel wire are very similar in design to the SL cable. The third layer, consisting of smaller but more numerous wires, is counterwound with respect to the first two, giving the cable the torque-balanced properties which are required. Between the second and third layers, and between the third layer and the low-density polyethylene sheath, a polyester/fiberglass tape is applied. This tape is applied to keep the strand package intact during subsequent manufacturing operations.

In deference to fatigue considerations, there is no copper power conductor in the riser cable. The steel wires provide the power path. Because of the riser cable's short length, the increase in total system resistance is not significant. The thickness of the low-density polyethylene is sufficient to insulate the cable.

The function of the medium-density polyethylene sheath is solely to protect the electrical insulation from sharkbite. Established procedures [3] were used to test the effectiveness of this sheath. The tests demonstrated that the medium-density polyethylene provides sharkbite protection of almost a factor of two greater than required. The medium density polyethylene is injected with carbon black for protection against degradation due to the ultraviolet radiation of the sun. In addition, a black cable is less susceptible to shark attack [3].

The riser cable was successfully tested under a program similar to that used for the SL cable. The cable's mechanical, electrical, and optical properties were checked after it had undergone various conditions of temperature, pressure, and tension loading to simulate the static undersea condition. Results of a 50 meter cable subjected to tensions up to 20,000 lbs. showed no increase in optical attenuation.

In addition to the static tests, special dynamic tests were run in order to verify that requirement 4 above had been met. In one test, the flexural loading on the cable was magnified in order to accelerate the testing so that it could be finished in a reasonable time frame. Using Miner's equation [4], and the results of this test, it was shown that the steel wire members of the cable would meet the design goal. In addition, measurements of the cable's optical attenuation before and after the test revealed no significant change. Tests were also undertaken to ensure the reliability of the polyethylene materials utilized.

The riser cable is overarmored at various points with either a single layer of wires or a double layer. The armoring design is virtually the same as shown for the SL cable, with some dimensional variations.

*Cable-to-Cable Splicebox*

The requirements for cable joints are similar to those for the cable. They must provide optical, mechanical, and electrical continuity while satisfying the following requirements [2]:

1. Usable in ocean depths to 7.5 km
2. Capable of being assembled easily and safely
3. Compatible with tension, torsion, and bending characteristics of the cable
4. Capable of being handled with normal cable machinery, and of being stored in cable tanks.
5. Reliable for 25 years.

Armorless cable joints which satisfy these requirements consist of five basic components. These include a strength termination, splice shelf, pressure housing, electrical insulation and bend limiters. The assembly of these components is illustrated in Figure 8.

The strength terminations are assembled onto the cable ends to be joined. Termination of the cable is accomplished through the use of a copper sleeve which cold flows and work hardens about the steel strands [2]. The terminations transfer tension and torsion from the cable to the pressure housing. They also establish electrical contact between the cable power conductors and both the splice shelf and the pressure housing. The shelf and housing form the power transmission path between the terminations.

The splice shelf, which is fastened to each termination, provides storage for excess fiber under controlled conditions and protects the fiber splices from being damaged during handling and installation. The shelf is enclosed in a housing which forms a pressure vessel that isolates it and the fibers from the sea. The housing and terminations are overmolded with polyethylene which then forms the high-voltage insulation from sea ground. It also inhibits water ingress to the fibers. Finally, elastomeric bend limiters are attached at each cable-to-joint interface to protect the cable from being bent severely during handling.

When armored cables are joined, the outer armor wires are relaid so that the wires from one cable lay over the joint and

1 Hytrel is a tradename of E.I. duPont Co., Wilmington, Delaware.

overlay the armor wires on the other cable. This technique establishes tension and torsion coupling across the joint.

The junction box which connects the SL cable to the riser cable is virtually identical to the SL splice box. However, some dimensional variations in the riser end termination and bend limiter exist.

Reliability and performance of joints is checked by subjecting them to a wide range of mechanical, optical, and electrical tests. These included tension-bending-torsion, pressure-temperature, shock-vibration, optical transmission, high voltage and handling-assembly. The results of both laboratory and factory tests, and of field tests in deep-ocean environments during 1982 and 1983 show that cable joints exhibit stable behavior under all operating conditions.

*End Coupling*

An end coupling is applied on both ends of the system. This assembly was designed with the needs of the riser end in mind, since the requirements at the shore end are a subset of the riser's. Figure 9 shows a rendering of the assembly, with the housing cut-away at points. The design goals for this assembly are:

1. Mechanical anchoring of the riser cable.
2. Break out of the fibers from the core so that they can be spliced to single-fiber, jacketed, connectorized cables. This design goal negates the need for fiber splicing on the platform.
3. Termination of the cable's power in a socket connector and insulation from the platform.
4. Housing of the end coupling in a canister which is watertight to 500 psi. This allows for an installation scenario where the end coupling is snaked up to the platform.

The housing is composed of three cylinders secured together by clamp rings. At each junction there is a bulkhead which divides the interior into three chambers. These chambers correspond to successive stages of assembly and serve different functions.

The housings of the two chambers closest to the cable, the splicing and anchor/mold chambers, are kept intact both during deployment and installation. The tension is transferred from the cable anchor to the platform through these housings. The housing of the chamber where the jacketed fiber optic cable is stored is clamped on during installation (to keep the assembly watertight) but is removed once the coupling is secured to the platform.

In the anchor/mold chamber, the steel strands of the cable, along with the kingwire from the core are terminated. A small amount of slack fiber is stored in the anchor assembly under controlled conditions in the event of any slippage of the termination. The fibers exit from the assembly in a small tube which also conducts the system power.

The whole anchor assembly, except for the last quarter-inch of the tube, is overmolded with branched low-density polyethylene to form the electrical insulation. The tension is transferred from the termination to the load-bearing plate of the housing through a gasket of polyethylene. With the low tensions involved in this system (600 pounds), cold-flowing of the polyethylene is avoided through careful attention to surface finish of the metallic load-bearing surfaces.

The overmolded tube containing the fiber protrudes into the splicing chamber. The splicing chamber contains a tray where the excess length of fiber needed to reach the fusion splicing equipment is stored under controlled conditions. The power circuit is also completed in the splicing chamber.

As already noted, the storage chamber contains the connectorized, single-fiber cable. Once the housing is removed, the power connector is mounted on the bulkhead for quick hook-up. The storage housing exterior contains a pulling eye to assist in the installation.

*Manufacture And Performance*

The riser cable was fabricated in one span, designated as RO during manufacture. The SL cable was manufactured in six spans, each of different lengths, designated as Y01 through Y06 during manufacture. Figure 10 presents a system map showing the lengths of these sections. Note that the longest span was 57.8 km. Five cable-to-cable spliceboxes were employed, as well as a junction box.

During manufacture, the attenuation of each fiber in the cable was measured after each successive stage. Table I presents this data for the Y05 span. The 4 fibers are identified by the color of their coating. This data is typical, showing a slight rise in attenuation after the fibers are stranded, which is relieved afterward by viscoelastic relaxation of the hytrel. Table II presents a summary of the net cabling loss for the seven spans.

For each transmission path in the system eight splices had to be made; five at cable-to-cable spliceboxes, one at the junction box, and two at the end couplings.

Table III presents the data showing the cumulative losses of these splices as well as that of the whole system. Note that average splice loss data is also presented. Finally, data on the attenuation per kilometer for the integrated system is shown. The numbers listed are well within the range of what is needed to transmit the data over the system length without the use of a repeater.

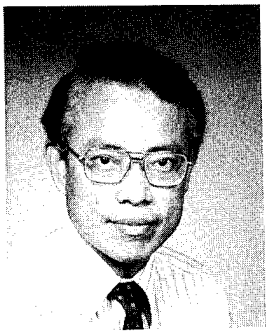
*Conclusion*

An undersea optical cable system has been designed and built by AT&T for a 147 KM repeaterless data link operating in the 1.55μm wavelength range. The mechanical elements of this system have been described both in terms of requirements and performance. In addition, optical performance data is presented indicating that the integrated system has met its design objectives.

*REFERENCES*


1. R. F. Gleason, R. C. Mondello, B. W. Fellows, and D. A. Hatfield, "Design and manufacture of an experimental lightguide cable undersea transmission system", in *Proc. Int. Wire and Cable Symposium* (Cherry Hill, NJ) 1978.
2. A. Adl, T. M. Chien, and T. C. Chu, "Design and Testing of the SL Cable" *IEEE Journal on Selected Areas in Communications*, Volume SAC-2, Number 6, November 1984.
3. B. Prindle, and R. G. Walden, *Deep-Sea Lines Fishbite Manual*, Woods Hole Oceanographic Institution, Woods Hole, Massachusetts, 1975.
4. M. F. Spotts, *Design of Machine Elements*, Prentice-Hall, Inc., Englewood Cliffs, New Jersey, 1978.

**Tek-Che Chu**



Tek-Che Chu received the B.S. degree in 1964 from Cheng Kung University, Taiwan, the M.S. degree in 1967 from Syracuse University, and the Ph.D. degree in aerospace engineering in 1971 from Cornell University.

He joined AT&T Bell Laboratories in 1972 where he initially worked on the physical design of the T4M digital transmission system and the development of an optical fiber connector. Since 1981, he has been working on the design of undersea lightguide cable.

**Louis J. Marra**

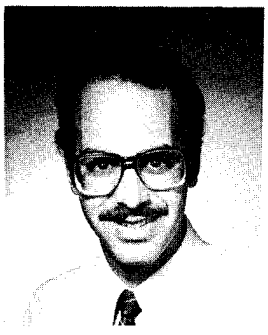


Louis J. Marra received the B.S. degree in 1979 from the Cooper Union and the M.S. degree in mechanical engineering in 1981 from Stanford University.

He joined AT&T Bell Laboratories in 1981, initially working on the design and manufacture of undersea cable repeaters. Since 1983, he has been working on the design of repeaterless fiber-optic cable systems.

He is a member of Tau Beta Pi and Pi Tau Sigma.

**Robert K. Stix**



Robert K. Stix was born in St. Louis, MO. He received the B.S. degree in mechanical engineering in 1980 from Purdue University and the M.S. degree in mechanical engineering in 1981 from Stanford University.

Since joining AT&T Bell Laboratories in 1980, Mr. Stix has worked on the physical design of the SL undersea lightwave cable system. Currently, he is responsible for the design, development, and testing of cable-to-cable joints, SL terrestrial cable-to-cable joints, and cable end seals, both armored and armorless. He has also been involved with the development of shipboard installation and handling techniques for the SL undersea lightwave cable and apparatus.

He is a member of Tau Beta Pi and Pi Tau Sigma.

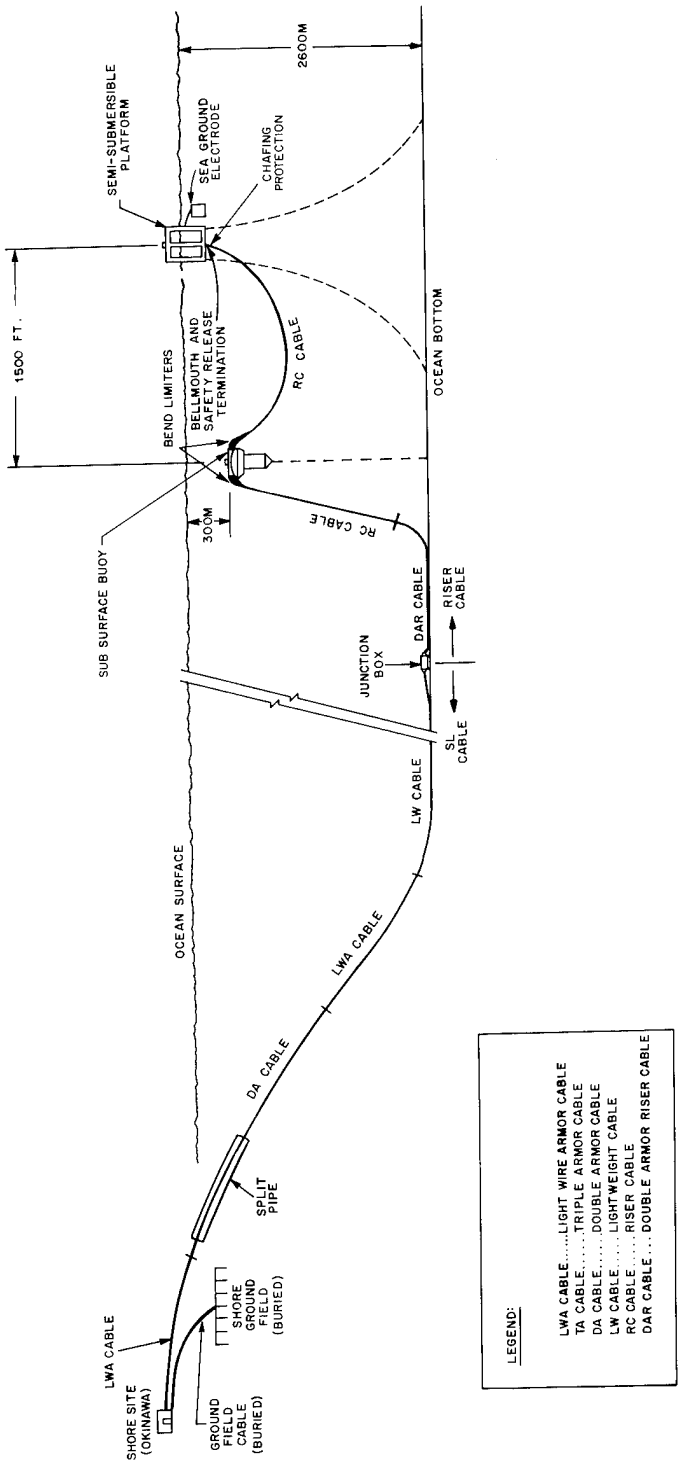



Figure 1
SYSTEM DESIGN

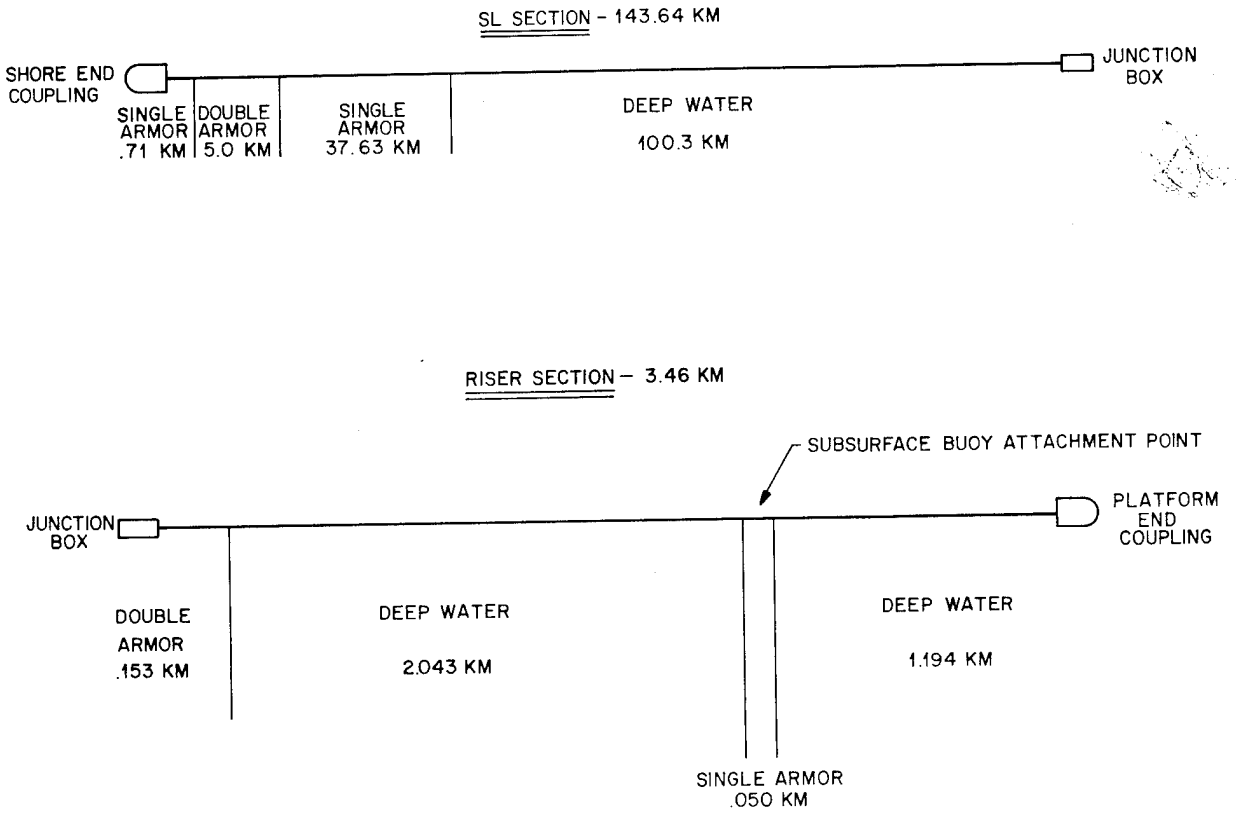
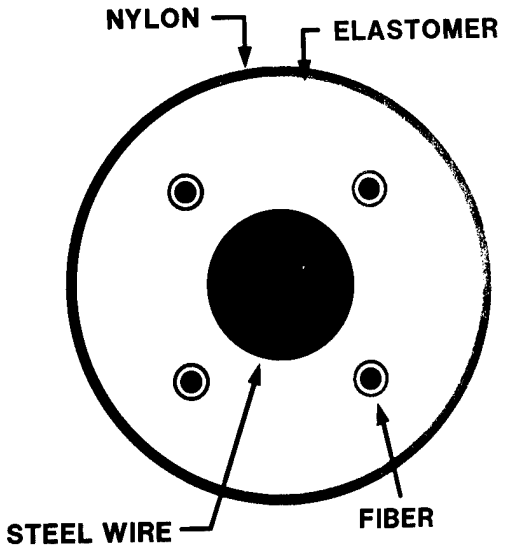



FIGURE 2 - SYSTEM ARCHITECTURE




**CORE DETAIL**

Figure 3

**LIGHTWEIGHT CABLE (LW)**

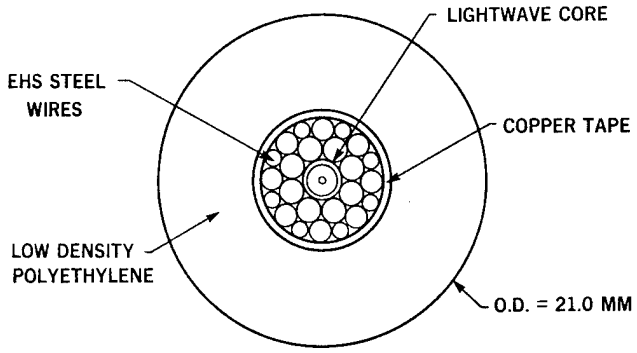



Figure 4

**LIGHT WIRE ARMOR CABLE (LWA)**

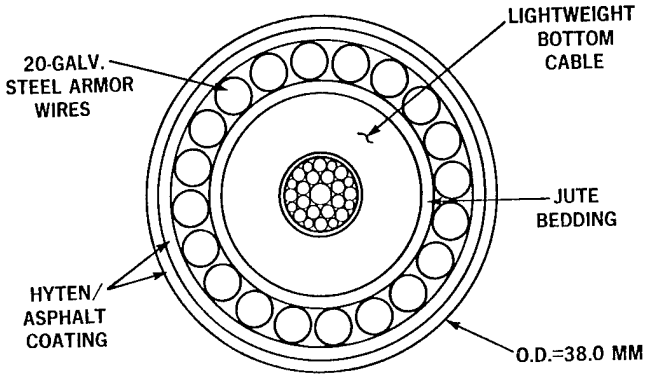



Figure 5

**DOUBLE ARMOR CABLE (DA)**

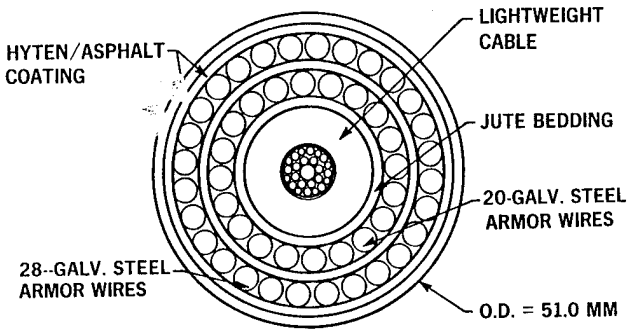



Figure 6

**RISER CABLE**

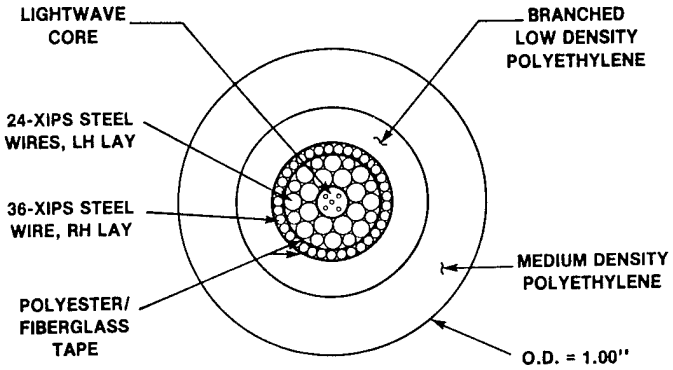



Figure 7

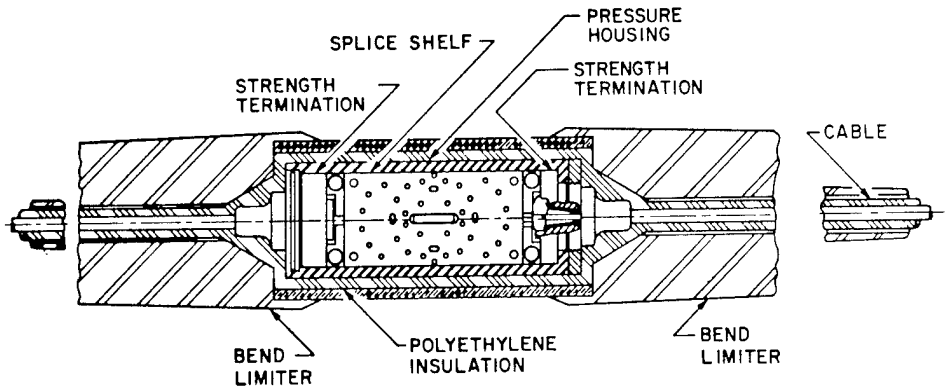



Figure 8 SCHEMATIC OF CABLE JOINT (ARMORLESS)

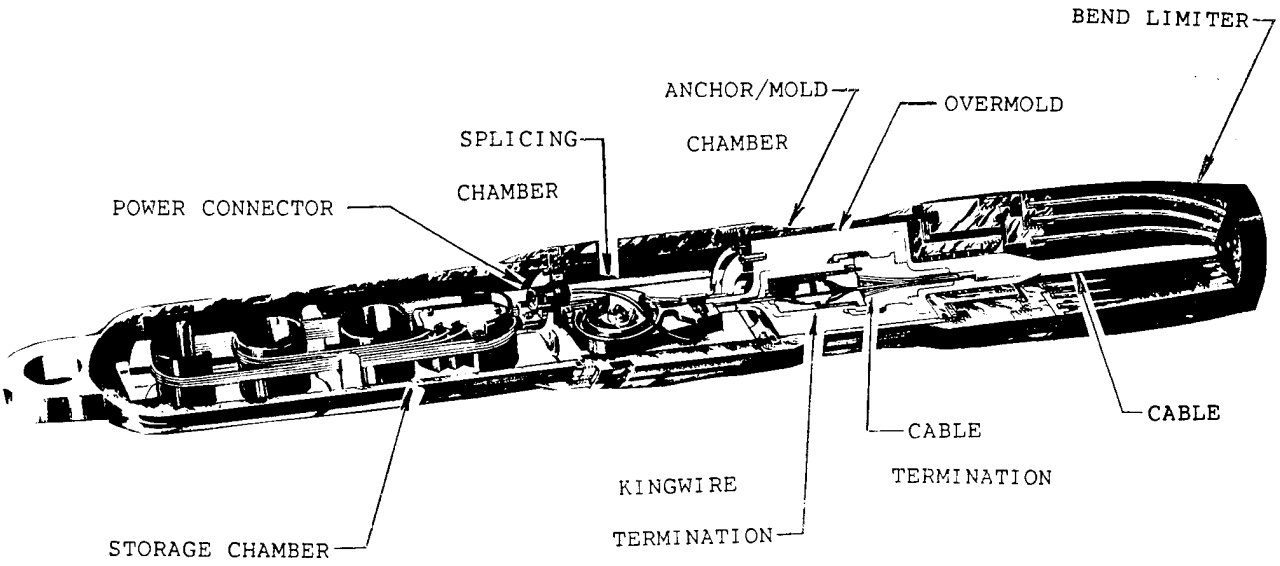



Figure 9 - End Coupling Assembly

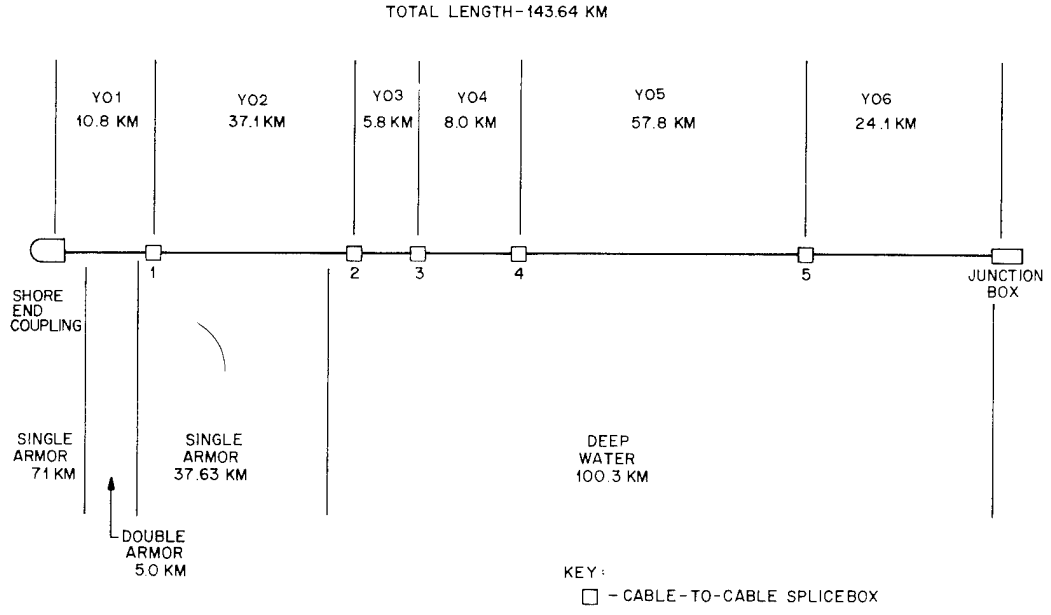



Figure 10 - SL SECTION MANUFACTURE

TABLE I
Y-05 (dB/km at 1.538 um)

| | NATURAL | RED | ORANGE | GREEN |
|---|---|---|---|---|
| As Rec | .216 | .223 | .215 | .225 |
| Hytrel | .212 | .223 | .246 | .215 |
| Nylon | .207 | .217 | .210 | .212 |
| Copper | .199 | .219 | .212 | .215 |
| PE | .213 | .216 | .201 | .213 |

Table II
Cabling Loss
(db/km at 1.538 μm)

| | Orange | Green | Red | Natural |
|---|---|---|---|---|
| Y01 | .047 | .021 | .016 | -.011 |
| Y02 | -.001 | .006 | .001 | -.014 |
| Y03 | .000 | -.009 | -.024 | -.010 |
| Y04 | -.009 | .001 | -.001 | .001 |
| Y05 | .003 | .019 | .013 | .029 |
| Y06 | -.011 | .005 | .000 | .004 |
| R0 | .007 | .004 | -.042 | -.010 |

TABLE III
SYSTEM ATTENUATION
147 km, Loss at 1.55 μm

| | Sum of Cables dB (dB/km) | Sum of 8 Splices dB (dB/splice) | Integrated dB (dB/km) |
|---|---|---|---|
| ORANGE | 35.18 (.239) | 1.55 (.19) | 36.78 (.250) |
| GREEN | 37.32 (.254) | 1.62 (.20) | 38.94 (.265) |
| RED | 36.03 (.245) | 1.84 (.23) | 37.87 (.258) |
| NATURAL | 36.34 (.247) | 1.08 (.14) | 37.42 (.255) |

# Optical Fibre and System Considerations for a Broadband Subscriber Network

Helmut G. Haag, Georg F. Hög, Peter E. Zamzow

AEG KABEL Aktiengesellschaft, Federal Republic of Germany

## 0. Summary

System considerations for an overlay network for broadband communications are undertaken. Out of these assumptions it become clear, that single mode fibres with matched cladding profile are cost effective against graded index fibres. It was experienced that it is possible to construct cables with up to 2000 fibres with good optical and mechanical characteristics. The important problem of connecting and branching in the distribution network is considered and solutions are presented.

## 1. Background

In the mid-seventies of this century it becomes clear worldwide, that the optical fibre and the digital transmission technique are powerful and economic broadband transmission techniques and will succeed the existing communication technique with copper conductors. Also the up to now used coaxial cables for trunk lines will be replaced by optical fibres and communication satellites. All industrial nations took part in this technical development. It becomes clear that finally all present and future smallband and broadband services will be transmitted in a single net, the optical fibre local network as integrated digital services. |1|, |2|. The bidirectional transmission of a 140 Mbit/s broadband channel is projected for picture phone and video conferencing in industry, administration and commercial area. The following system considerations assume that the fully integrated broadband local network will start by an overlay network in island creation strategy |3|, |4|.

It was appropriate that the introduction of optical fibres took place first in the trunk network. Since 1982, in the Federal Republic of Germany, the super trunk line "BIGFERN" from Hamburg, via Hanover and the Ruhr-area up to Munich and Nuremberg is constructed |5|, |6|.

Also in 1982 the "BIGFON"-project for the local network was started, to gain experience over the costs and the services in subscriber cabling with optical fibres |7|, |8|. By these projects it becomes clear that a new digital integrated broadband network will be only economic if mainly subscribers for broadband transmission services like picture phone and video conferencing will be connected.

Later on, smallband services and broadband distribution services can then be added on for economic prices. For these broadband communication subscribers it will be necessary to erect a wide-spread overlay net which covers with low subscriber density the existing copper network. The way to the total integration is done in the steps

1. Overlay network for broadband communication services
2. Integration of other services in the overlay network

3. Extension of the overlay network and absorption of the services of existing networks.

For this conception the net structure and the services as well as the appropriate cable and installation technique will be described.

2. Network Structure

Also the communication network for broadband over optical fibres will be erected as a star network [9]. While for the existing smallband services the network is hierarchically organized in trunk network, junction network and local network with the relevant exchanges which are mashed, the overlay network for the strating phase of the broadband communication traffic will be organized in two hierarchic levels: Trunk network and local network. In the optical fibre trunk network (figure 1) the foreseen broadband exchanges are connected forming a "C". No mashing is provided.
In this trunk network 60 to 160 broadband channels are bundled and transmitted over graded index and single mode fibres.

In the local network, the connection area which is directly connected to the broadband exchanges, the individual broadband subscribers are star-like connected. The subscribers coming mainly from the industrial, business, administration, and banking area are in mean 10 to 12 and in maximum 25 km apart from the exchange. The routing of these subscriber lines follow those of the existing smallband copper network. Therefore the subscriber line goes from the broadband exchange over the subordinated group and local exchanges of the smallband network and from there over the main cable routes and the distribution network to the subscriber (figure 2).

In this subscriber area, precision graded index fibres can be used which transmit one broadband channel of 140 Mbit/s regenerator

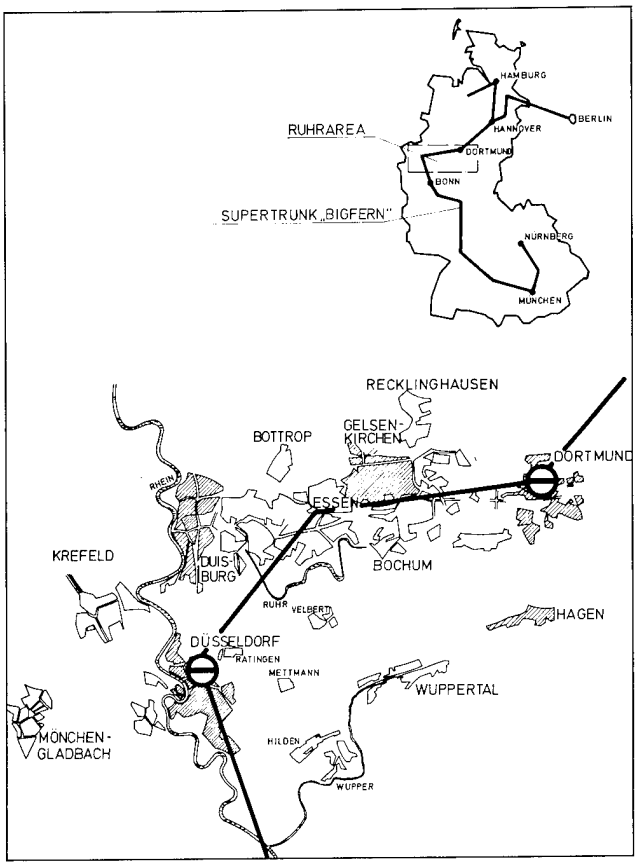



Fig. 1: Backbone of the German overlay network with optical fibres

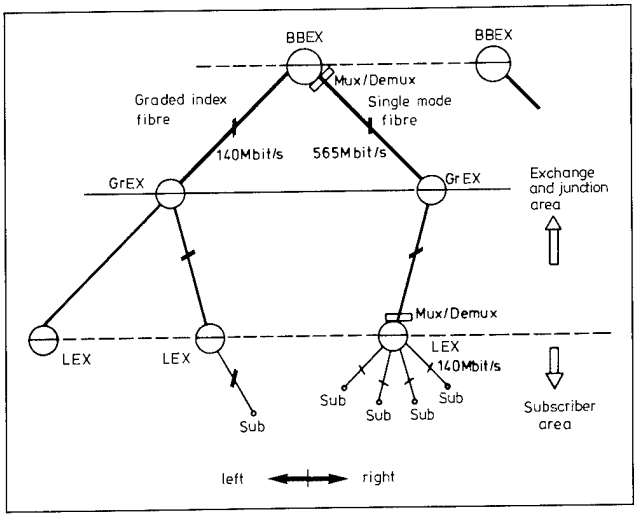



Fig. 2: Connection techniques for the subscribers in the overlay network

free over up to 25 km or single mode fibres which can transmit over equal of greater distances 4 broadband channels. By using graded index fibres the subscriber is connected from the broadband exchange without regenerators directly with two fibres, one for each direction (figure 2, left). Single mode fibres can transmit from the broadband exchange to a subordinated local exchange 4 broadband channels by a 4-fold multiplexer. From there the individual subscribers are connected over maximum 5 km by a single fibre duplex connection (figure 2, right). This connection technique covers the installation of active components in the subscriber network.

The choice between these two connection possibilities is due to the number of subscribers in the direct connection area below the local exchange and the availability and costs of the components. At least for the begin of the erection of this overlay network the precision graded index fibre will be taken.

The future general introduction of optical fibres in the total communication network will make it necessary to extend the previous broadband exchanges to dominating network nods and to mash each other. In the subscriber area relevant digital exchanges for broadband and smallband services will be erected at the place of the existing smallband exchanges. The connecting lines to the subordinated local exchanges will be converted to junction lines and the existing cables will be further used.

The switching points of the overlay network are changed to exchanges and the subscriber lines will be reduced to the well-known distances of 2 km up to a maximum of 7 to 8 km. At this time for the local area high count optical fibre main cables with some hundred fibres will be needed.

To transmit all possible services the single mode fibre will dominate.

3. Services

The introduction of optical fibre systems was in the beginning done under the view point to extend the trunk network for telephone services |10|, |11|. But for the considerations done here, we will concentrate on the possible services in the overlay network and a future optical fibre local network.

The overlay network will transmit picture phone and video-conferencing on a 140 Mbit/s channel. It is advantageous to transmit this bandwidth without any costly bandwidth reduction by redundance operations because the capacity is available on the optical fibre.

For the future integrated optical fibre network on the picture phone channel the services:

- o broadband distribution (TV)
- o high definition TV (HDTV)
- o fast data
- o smallband ISDN

will be added. This will require bandwidths on the subscriber line between 144 kbit/s for ISDN and some hundred Mbit/s for the summation for all services. Even if the subscriber line lengths will be reduced in the fully integrated network high sophisticated fibres will be needed to transmit the bandwidth. To assure a high security for the future the single mode fibre will be preferred.

On the other hand the majority of subscribers will take only the smallband services. This requires a cost-effective transmitter. With a new developed edge-emitting LED a coupling efficiency to a single mode fibre of some

ten µW with a spectral width of 45 nm to 1300 nm can be reached. This allows the transmission of 140 Mbit/s over 30 km.

A power budget under realistical assumptions for fibre attenuation, repair margin and splice loss via the connection length is given in figure 3.

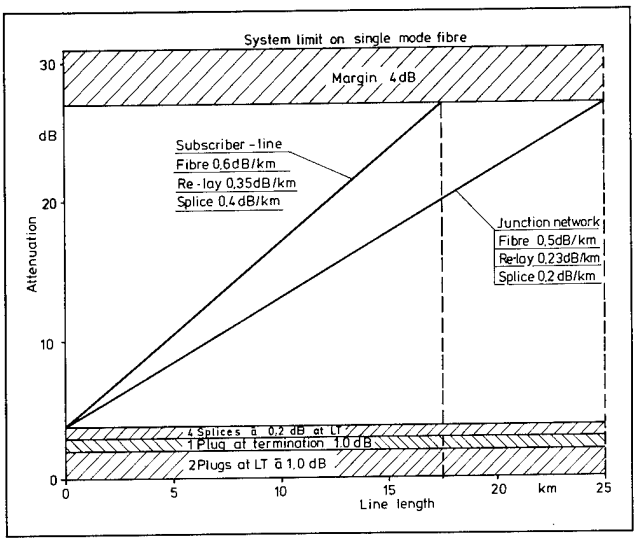



Fig. 3: Power budget for single mode fibre systems in the overlay network

By the permanent increase of splice and connector techniques and the reduced fibre tolerances the splice compatibility in using fibres from different manufacturers can be assured.

Also the adaption to higher hierarchic levels of the PCM-technique is assured by the use of single mode fibres already in the overlay network.

## 4. Transmission media

Constructions of optical fibre cables for the transmission of broadband signals in the trunk network with graded index fibres and with single mode fibres at 1.3 µm are available and are in service for ten years.

The use of single mode fibres has against precision graded index fibres, the advantage of higher achievable bandwidth and lower attenuation, so that transmission rates of 140 and 565 Mbit/s over 25 km and more are possible.

Optical fibre cables with precision graded index fibres and single mode fibres for trunk cables up to 120 fibres are available following the technical specification of the German PTT (FTZ). Local cables with graded index fibres are described in [12], [13]. The use of the single mode fibres in cables for the local network are experienced on the basis of the mentioned experiences.

### 4.1 Fibre

The build-up of an overlay network is not transferable to the final estate of a local network, therefore the choice of the fibre must assure a high flexibility and future possibilities. This will be assured by the use of single mode fibres with low attenuation at 1300 nm and at 1560 nm with the zero dispersion at 1300 nm [14], [15]. The security for future of such a single mode fibre (figure 4) is dominated by the technical specifications for the optical fibre local network and under the viewpoint of economy:

| | |
|---|---|
| fibre design | "matched cladding" |
| mode field diameter | 10 µm |
| fibre attenuation | mean value 0.55 dB/km at 1300 nm and 0.45 dB/km at 1560 nm |
| dispersion coefficient | $\leq$ 4 ps/(nm·km) between 1280 and 1330 nm |
| splice loss | mean value 0.25 dB |

In contrary to this fibre the higher valued single mode fibre with the depressed inner cladding profile for the trunk network [16] is in comparison to this local network single

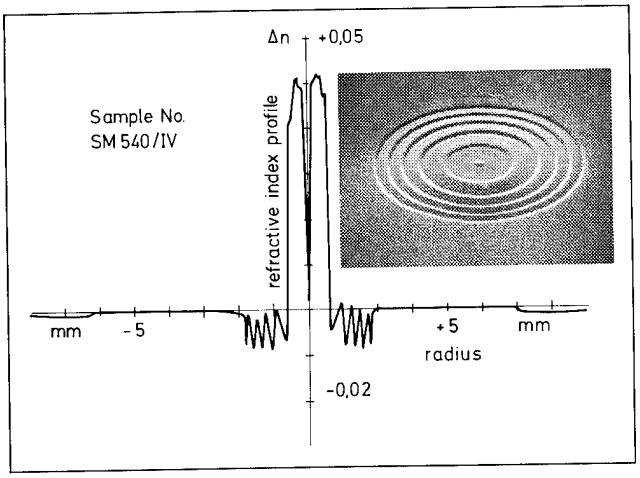



Fig. 4: Profile of a matched cladding SM fibre

mode fibre in the production process considerably more expensive. This economic advantage of the local network single mode fibre and the possible use of LED transmitters makes the advantage of this single mode fibre for the local network [17], [18], [19], [20]. The spectral loss and the dispersion behaviour of such a single mode fibre is shown in figure 5.

4.2 Cable

For the above described network with the 3 hierarchical levels in the final state optical fibre cables with 2 to 2000 single mode fibres are necessary. For the construction of those cables different solutions are possible under the assumption, that cables with many fibres for the local network are not thicker than the existing communication cables with copper conductors.

The relation between cable diameter and number of fibres for the different cable concepts are shown in figure 6. The advantage of a single layer construction with single buffered fibres and multi fibre buffers are their easy access during jointing. But the greatest disadvantage is the fact that even for a low number of fibres thick central elements for the cable core are necessary. Therefore for cables with 80 fibres

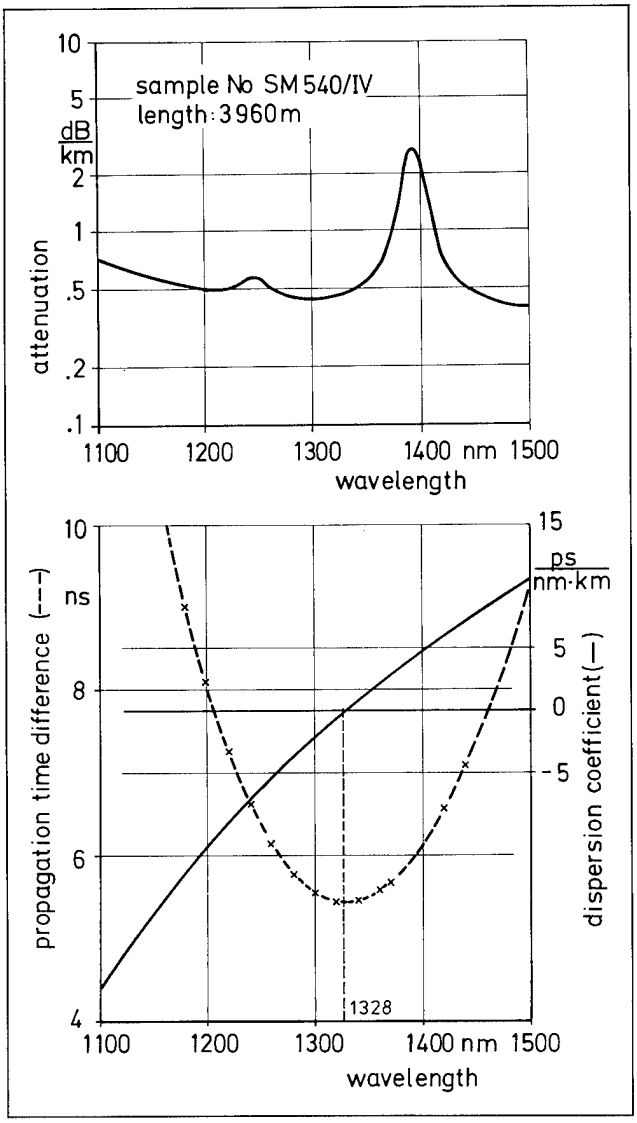



Fig. 5: Attenuation and dispersion of a typical matched cladding SM fibre for the local network

and more the sub bundle construction of the cable core is advantageous. For these bundles normally 20- or 40-fibre-bundles are efficient. Such a sub bundle contains 5 multi fibre buffers with 4 respectively 8 fibres. As it is seen from figure 6 both possibilities are equal in diameter if for the 4-fibre-buffer the buffer diameter is chosen to 2.0 to 2.2 mm respectively 2.8 to 3.0 mm for the 8-fibre-buffer.

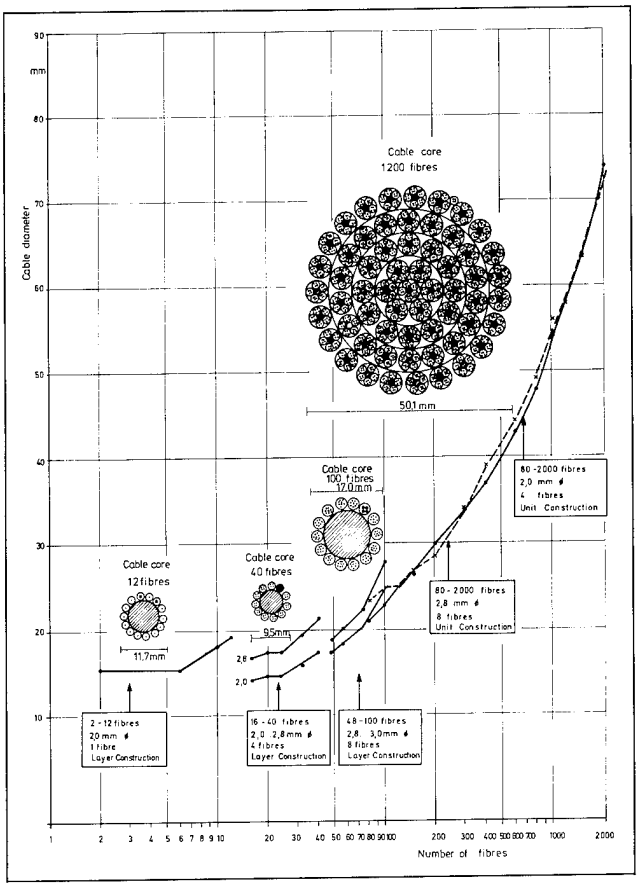



Fig. 6: Cable construction with single mode fibres for the local network

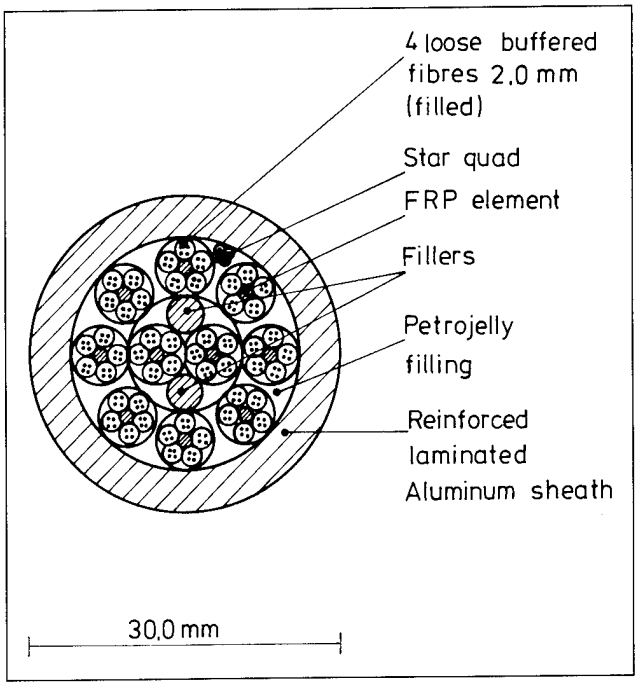



Fig. 7: Cross-section of 200 SM fibre cable for the local network

Investigations on single mode fibres in 4-fibre-buffers with 2.0 mm diameter and 8-fibre-buffers with 2.8 mm diameter have shown, that by the fact of the microbending behaviour of the single fibres the construction of 4-fibre-buffers with 2.0 mm diameter for high count fibre cables are preferable. Figure 7 shows the investigated cable with 200 single mode fibres. The results are summarized in figure 8. During cabling no change in attenuation occurs, which gives the security for a long term stability without degradation by mechanical stresses. Also under climatic conditions and mechanical forces like pulling and bending the optical characteristics stay stable in a wide range.

4.3 Connecting and branching technique

The jointing boxes in the subscriber network are constructed like the jointings in the optical

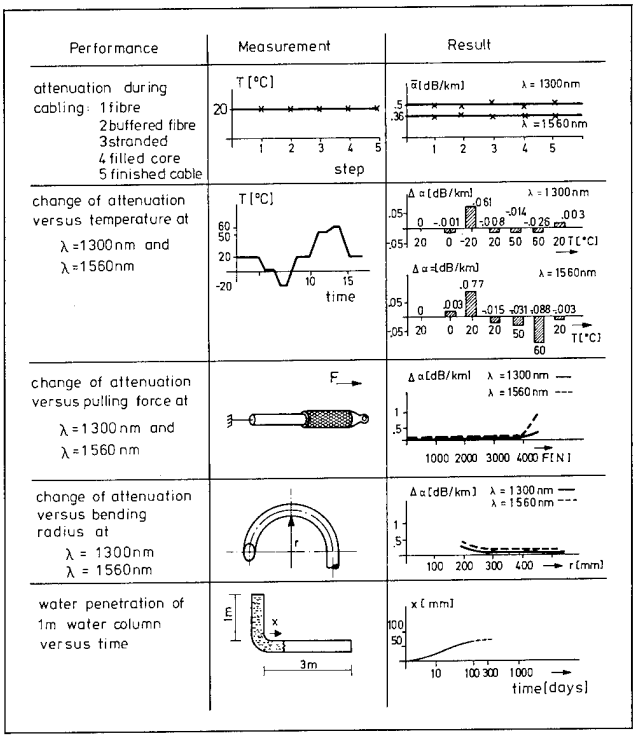



Fig. 8: Tests and results for a 200 single mode fibre cable in sub-bundle techniques

fibre trunk network. The fibres are spliced by the arc fusion technique. The fibres are arranged in cassettes. In dependance from the number of fibres in the cable the size of the jointing box is chosen. This technique will not be discussed in detail here.

In the exchanges respectively in the passed exchange stations the fibres are terminated in fibre distribution cabinets (figure 9). The trunk cables, the indoor cable to the exchange, and the local cables are connected to different termination areas. The fibres of the coming and going cables are connected by shunting fibres and allow by this a high flexibility in the connection built-up. This technique also is derivated from the existing trunk network technique.

But the branching technique in the subscriber area is new. The development of a adequate technique for this is an important condition for a successful connection strategy. For the distribution cables which are normally installed as buried cables it is proposed to choose the numbers of fibres in such a way that the connection of all potential subscribers to this link is possible, also if in the time of installation only one subscriber is connected. The future connection has the to be done by branching from the existing and layed cable the fibres to the new subscriber by minimum effort on burying. To minimize also the splicing, cutting of the whole cable, which is usuable in the trunk cable technique, should be avoided. On one hand the necessary cable overlapping of at least 2 m is not available and on the other hand the connected subscriber lines should not be interrupted. The construction of an adequate branching closure in adhesive splice technique is shown in figure 10 schematically. The sheath of the cable to be branched will be removed on a length which is similar to the closure size. The buffers to be branched are cut and the buffer is removed from the fibres. Also the hub cable to the subscriber is prepared on the necessary length. The fibres of the branching hub cable are mechanically spliced with the subscriber's fibre of the distribution cable. The attenuation of this mechanical splice is of minor importance because this splice only occurs once for one subscriber line. Figure 11 shows a finished branching closure. The "dead" fibres of the ongoing cable can be used for cross switching purposes.

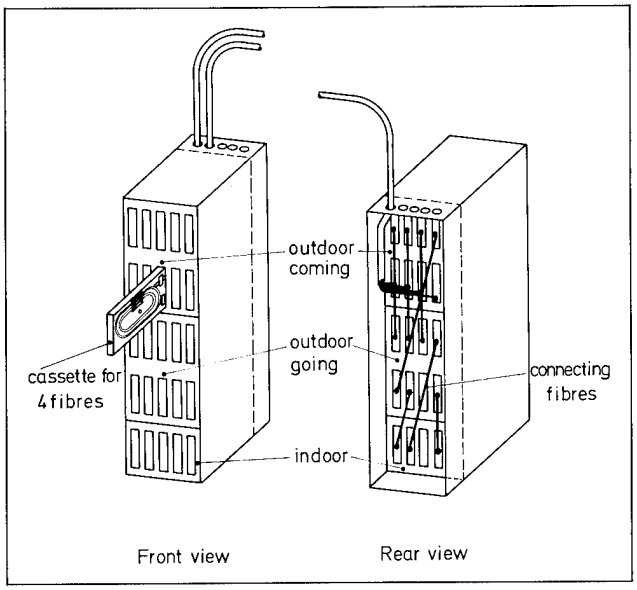



Fig. 9: Termination racket for optical fibres in the overlay network switching stations

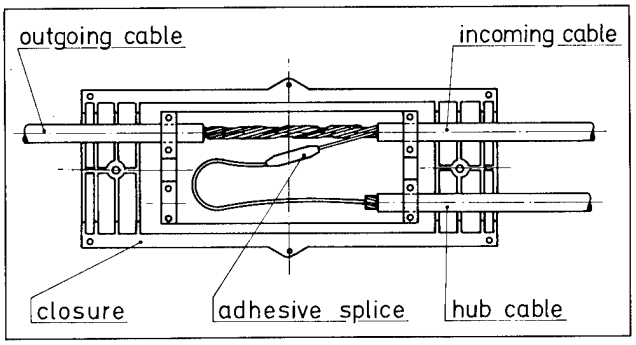



Fig. 10: Branching technique in the subscriber line area

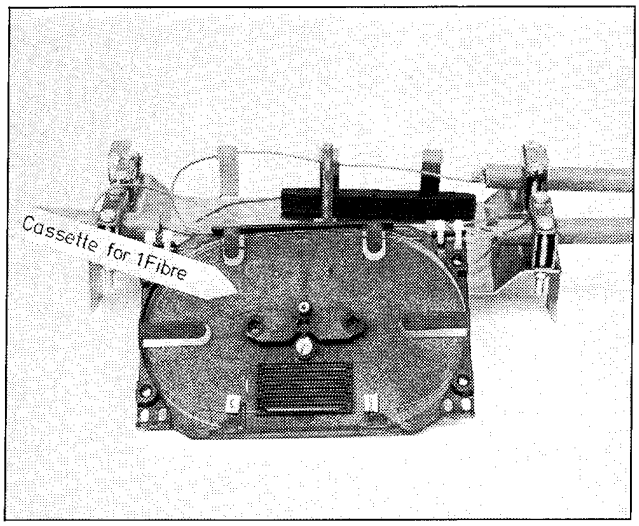



Fig. 11: Branching closure with SM fibres

## 5. Outlook

The network structure which was proposed for the broadband overlay network can be developed without leakage in the network to a fully integrated local network, which covers all broadband communication and distribution services as well as smallband services. To assure the necessary security for future of the subscriber line the single mode fibre with matched cladding profile is proposed which gives in connection with a LED as transmitter an economical solution in near future. Based on the multi fibre buffer technique arranged in main bundles for high count fibre cables with single mode fibres, it has been shown that these cables have comparable diameters to the existing communication cables with copper conductors. Therefore the existing infrastructure of the network can be used for the new network. For those cables it was shown that the optical and mechanical parameters are fully satisfying.

Solutions for the connecting and branching technique are described.

Therefore nowadays starting to build-up an optical fibre network in overlay technique can be conducted to a future fully integrated optical fibre network.

## 6. Literature


|1| Konzept der Deutschen Bundespost zur Weiterentwicklung der Fernmelde-infrastruktur; BPM Stab 202; Bonn, 1984

|2| Kanzow J., Activities of the Deutsche Bundespost towards the introduction of optical fibres in the subscriber line network. Proc 10th ECOC 1894, Stuttgart, pp. 26 - 27.

|3| Haag H. G., et al. Kabel- und Anlagen-konzept für Overlay- und Ortsnetz-anwendungen mit Glasfasern. NTG-Tagung, Bad Nauheim, Okt. 1985

|4| Schüßler H., Einführungsstrategien für Lichtwellenleiternetze, Techn. Mitt. AEG KABEL (Aug. 1984)

|5| Haag H. G., et al., Einmodenfaserkabel und deren Eigenschaften in Kabelanlagen bei Wellenlängen von 1330 nm und 1550 nm. NTZ 38 (1985) 6, pp. 386 - 393

|6| Bambach W., et al., 565 Mbit/s singlemode transmission system with monolithic integrated circuits. Proc 10th ECOC 1984, Stuttgart, pp. 254 - 255.

|7| Schmidt W., Systemversuch zur breit-bandigen Dienstintegration in Glasfaser-Fernmeldeortsnetzen. NTZ 35 (1982) 11, pp. 680 - 684

|8| Gleißner E., H. G. Haag, H.-G.Zielinski, Glasfaser-Kabelanlagen in Düsseldorf und Hannover. Techn. Mitt. AEG KABEL (1984) H. 5, pp. 1 - 11

|9| Haag, H. G., P. E. Zamzow, Überlegungen zur Kabeltechnik in einem künftigen Glasfaser-Ortsnetz, Techn. Mitt. AEG KABEL (1984) H. 5, 12-20

|10| Mazurezyk V. J., et al., 420 Mb/s transmission trough 203 km using silicacore fiber and a vapor phase transported DFB laser. Proc 10th ECOC 1984, Stuttgart, PD-7.

|11| Kasper B. L. et al., A 130 km transmission experiment at 2 Gbit/s using silicacore fiber and a vapor phase transported DFB laser, Proc 10th ECOC 1984, Stuttgart, PD-6

|12| Haag, H. G., P. T. Rautenberg, P. E. Zamzow, High-density optical fibre cables for the local network. Proc 30th IWCS 1981, pp. 259 - 269

|13| Zamzow, P. E., Possibilities for production of communication cables. Wireworld 8 (1985), pp. 152 - 155

|14| Huber H. P., J. Guttmann, R. Rettich. High-rate preform preparation for single-mode fibres by MCVD-process. Conference Proc. IOOC/ECOC. Venezia 1985

|15| Hersener J. H.-P. Huber, J. v. Wienskowski. Semiquantitative X-ray microanalysis on preforms for optical waveguide fibres. J. d. Phys. 45 (1984) H. 2. pp. C2-761-762

|16| Nagel S. R., Reviews of the depressed cladding singlemode fiber design and performance for the SL undersea system application J. Lightwave Techn. LT-2 (1984) H. 6. pp. 792 - 801

|17| Krumpholz O. Subscriber Link using single-mode fibres and LEDs. Proc 11th ECOC 1985. Venezia

|18| Arnold G., O. Krumpholz. Optical Transmission with single-modefibres and edge-emitting diodes Electron. Lett. (1985). 21. pp. 390 -392

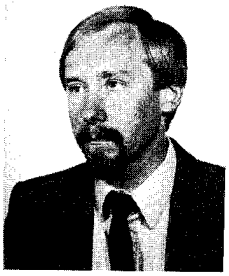
|19| Arnold G., 1.3µm edge-emitting diodes launching 250 µW into a single-mode fiber at 100 mA Electron. Lett. (1985)

|20| Krumpholz O., Teilnehmeranschluß mit Monomodefaser und LED. NTG-Tagung. Bad Nauheim. Okt. 1985



Helmut G. Haag
AEG KABEL
Technical Sales Division
Mönchengladbach. West-Germany

Helmut G. Haag (37) is head of the Technical Sales Division for Telecommunications. After reaching his Dipl.-Physiker from the University of Stuttgart he jointed AEG KABEL in 1975 for the development of coaxial cables. Later he was also responsible for the development of optical fibre cables. From 1980 to 1983 he built up the production plant for these cables. In autumn 1983 he took his present position.



Georg F. Hög (Speaker)
AEG KABEL
Telecommunications Development
Mönchengladbach. West-Germany

Georg F. Hög (35) is head of the Development Group for Optical Fibre Cables. He reached his Dipl.-Ing. from the University of Aachen and jointed AEG KABEL in 1977. After being engaged in the development of symmetrical telecommunications cables he get the responsibility for this group in 1980. Since spring 1985 he covers his present position.



Peter E. Zamzow
AEG KABEL
Telecommunications Development
Mönchengladbach. West-Germany

Peter E. Zamzow (45) is director of the Telecommunications Development Division. After finishing his postgraduate studies in telecommunications at Munich and Graz as Dipl.-Ing. he jointed AEG KABEL in 1970. He has been engaged in development and production of telecommunications cables. In 1980 he became head of the fibre optic division in AEG KABEL and was in 1982 nominated as a senior engineer. Since 1985 he covers his present position.

# DESIGN AND INSTALLATION OF AN OPTICAL FIBRE LOCAL WIDEBAND DISTRIBUTION SYSTEM IN AN URBAN ENVIRONMENT

James W. Reilly

Mercury Communications Ltd.
London, England.

Graham Holden

BICC Telecommunication Cables Ltd.
Prescot, England

## 1. SUMMARY

A local wideband distribution system has been developed to be installed in the City of London, which makes extensive use of a Victorian hydraulic pipe network to carry the cables. This network is a matrix of 150 miles of uni-diameter pipes ($\simeq$ 6 inches diameter) interconnected by 'X' and 'T' joints and valves.

An optical cable system was chosen to make optimum use of the space in the pipe network and to provide the wideband facility. The system offers route diversity to all subscribers, thus ensuring added security against cable breakdowns. A number of Distribution Nodes are evenly spread around the City with approximately 3 km spacing, thus avoiding the need to acquire and set up single large premises to act as the hub of the system -a difficult task for a new telecoms operator in a busy city. Terminal equipment is located only at customers premises and at the Distribution Nodes which have access to the national Trunk Network.

## 2. INTRODUCTION

On completion of the first stage of its nationwide Trunk Network, Mercury Communications, the recently licensed Public Telecommunications Operator in the UK, had an important requirement to provide an efficient and cost effective local wideband facility for the City of London.

Recognising the potential cost of civil engineering and the practical difficulties associated with the construction of a totally new cable distribution system, MCL purchased the defunct London Hydraulic Power Company (LHPC) which owned and maintained an extensive hydraulic pipe network covering the whole of Central London.

A novel approach to cable network design was needed to make best use of the LHP pipe system and, at the same time, achieve the system objectives. This was achieved by using optical fibre cables direct to customers' premises, sub-ducting the hydraulic pipe and adopting a distributed nodal approach.

## 3. NETWORK REQUIREMENTS

i) Ability to connect customers in a quick and cost-effective manner to a wideband cable system that is capable of future expansion.

ii) To evenly distribute the demand for bore space within the uni-diameter duct system. This was essential to minimise the costly civil engineering work required to provide additional ducts in the more congested sections.

iii) To avoid the use of street furniture in keeping with local planning regulations and public opinion.

iv) Ability to recover quickly and cost effectively from unforeseen cable breakdowns.

v) As a standard feature, the ability to provide route diversity to any customer requiring it.

vi) To make the cable network as secure as possible.

These last three items are becoming increasingly important as business users rely more and more on telecoms carriers for the secure transmission of data vital to their day-to-day operations.

## 4. TRANSMISSION MEDIUM

The requirement to provide a local wideband distribution system in an area characterised by a high concentration of large business subscribers and limited duct space, made the choice of optical cable as the transmission medium somewhat obvious.

The specific choice of fibre seemed to be limited to three types - singlemode, 50/125 $\mu$m and 85/125 $\mu$m multimode. Singlemode was rejected on the grounds that optical devices were expensive and difficult to obtain in large quantities. It was also considered that splicing and connectorising would be too laborious and necessitate the use of expensive equipment.

85/125 fibre should have been the logical choice of the two multimode types, ease of splicing and connectorising being its main attributes.

Also, the bandwidth and loss characteristics of 85/125 fibres were considered adequate to support the system objectives over the maximum 4 km range envisaged for this network. However, 85/125 fibre was not available in volume, and consequently was at a price premium.

50/125 fibre is already well established and splicing and connectorising is little more difficult than for 85/125. Relatively cheap optical devices are readily available for this fibre and so it was chosen for the network.

It was further decided that fibre suitable for operation at 850 nm and 1300 nm would be used so that early advantage could be taken of the abundance of 850 nm devices whilst allowing the option to operate at 1300 nm when suitable devices become cheaper and more readily available.

## 5. NETWORK DESIGN

A conventional local network design usually incorporates a radial type of cable distribution where a central switch supplies service to a given catchment area, and is typified by a dense population of large cables close to the central switch, with a gradual thinning of cable density towards the perimeter - a 'taper' distribution. This type of network design does not completely satisfy the requirements outlined earlier in the text. Furthermore, it would require that central premises large enough to cope with future expansion and with suitable access for cable be made available for equipment. The cost of acquiring suitable premises in the ideal location and the difficulties and cost associated with the additional ductwork nearby were regarded as prohibitive.

As with most Central Business Districts, the City of London was considered to have an even distribution of large telecoms users throughout the whole area, so a hybrid 'ring main/taper' network was devised.

### 5.1 Primary Distribution Network - 'Ring Main' Element

The Primary Distribution Network consists of a small number of Cable Distribution Nodes that are interconnected by a web of 160-fibre cables. For the City of London, it was decided that these Nodes would be spaced at intervals of 2-3 kms and the cables would be installed within the hydraulic pipes which were conveniently positioned under the carriageway, away from all the congestion and hazards that exist under the footway. Typically each Node is situated on the periphery of the area to be covered and occupies approx. 100 sq. metres of floor space. The acquisition of such premises is quite straightforward and the amount of civil engineering work for cabling in the vicinity of each is small.

This forms the backbone of the Local Wideband System and is called the Primary Distribution Network (See Fig.1).

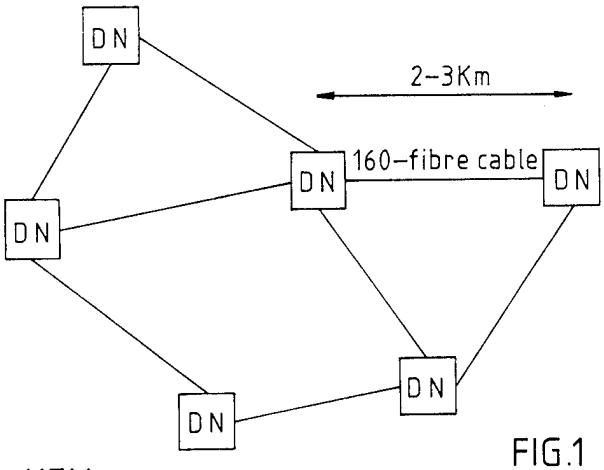



FIG.1

KEY

DN-Distribution Node

Any such network can start from a basic building block of, say, 3 Distribution Nodes and extend outwards to serve a larger urban area as illustrated in Fig.1

It may seem strange at this point that Distribution Nodes containing terminal equipment are interconnected by 160-fibre cables which seem to go nowhere. The reason will become clearer when the Secondary Distribution Network is described.

### 5.2 Secondary Distribution Network - 'Taper' Element

The Secondary Distribution Network provides the connection to the customer by breaking into the 160-fibre cable, at a Primary Flexibility Point (PFP). A number of these PFPs, typically 10 to 12, will be located on each 160-fibre cable installed between two Distribution Nodes. (See Fig.2).

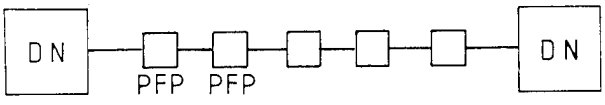



FIG.2

KEY

DN-Distribution Node

PFP-Primary Flexibility Point

By careful selection of primary cable routes, an even distribution of PFP's throughout the coverage area can be achieved.

At each PFP, the 160-fibre cable passes through a sealed re-enterable housing with its sheath removed inside the housing. The cable, which is made up of sixteen 10-fibre tubes, is treated as a duct containing sixteen, 10-fibre cables. Inside the PFP housing, a 10-fibre unit can be cut and the two resulting loose ends spliced to a 20-fibre secondary cable. (See Fig. 3).

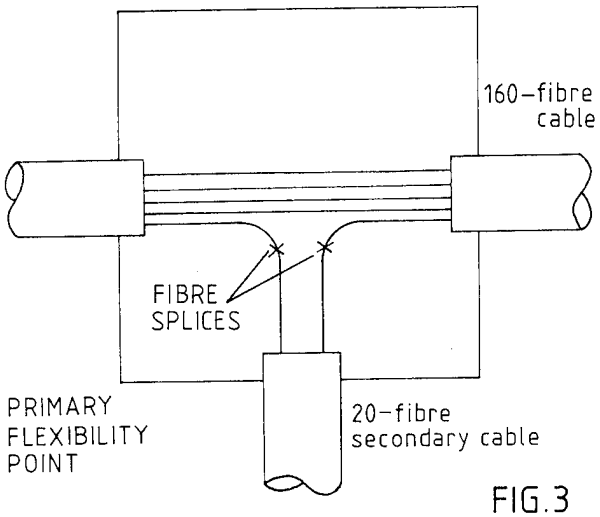



FIG.3

Once spliced to a secondary cable, the tube will not be cut at any other PFP i.e. each tube is dedicated to one secondary cable. Secondary cables can, of course, be spliced into the Primary Network at any point and at any time. This allows any PFP to support a number of secondary cables should demand for service become high in its vicinity. Since there is a typical spacing of approximately 200 m between PFP's it was estimated that no more than four secondary cables would be needed at each, and housings were designed accordingly.

Each 20-fibre cable terminates at a Secondary Flexibility Point in another sealed, re-enterable housing (See Fig.4). Customer Distribution Cables radiate from each SFP into the customers premises, where a simple termination box is used to splice to internal connectorised leads.

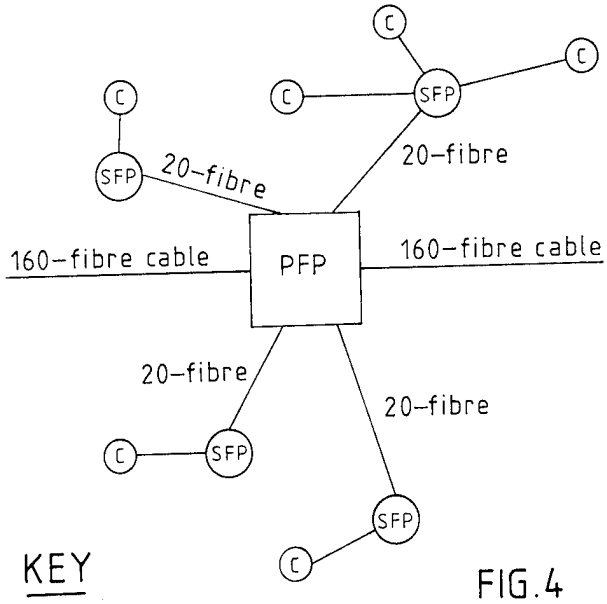



FIG.4

Housings for the PFP and SFP have been designed to allow an extension to be made to any secondary cable leg. This may be done by breaking two 10-fibre tubes in the PFP and splicing to a 40-fibre secondary cable. Two tubes in the 40-fibre cable are spliced straight through the first SFP. In this way, each SFP is fed by one tube from the primary cable. (See Fig.5).

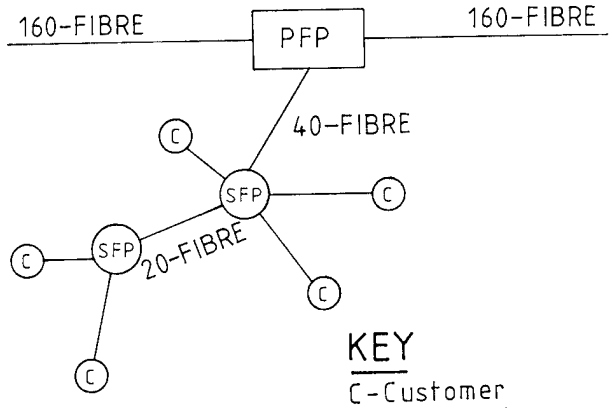



FIG.5

## 6. SECURITY

It can be seen from Figures 1 to 5 that a customer can, if he so wishes, be provided with two independent fibre connections to different Distribution Nodes. This kind of connection will ensure that the customer remains in service should there be a failure of the primary cable at any point between that particular customer's PFP and one of the Distribution Nodes. Equally, service interruption due to a catastrophic failure at a Distribution Node can be circumvented by simply re-splicing affected customers into adjacent Distribution Nodes.

There is still a risk, however, that the secondary cable carrying both links is damaged, although this is quite minimal since the secondary link will be typically less than 100 m. However, the risk can be removed by the addition of a secondary link from a different primary cable (See Fig.6). This back-up link can be arranged to enter the customer's premises by a different route for the ultimate protection.

The facility to offer a diverse route is beneficial in recovering from cable breakdown and during maintenance operations. Customers without a diverse route can be temporarily supplied with one in such instances.

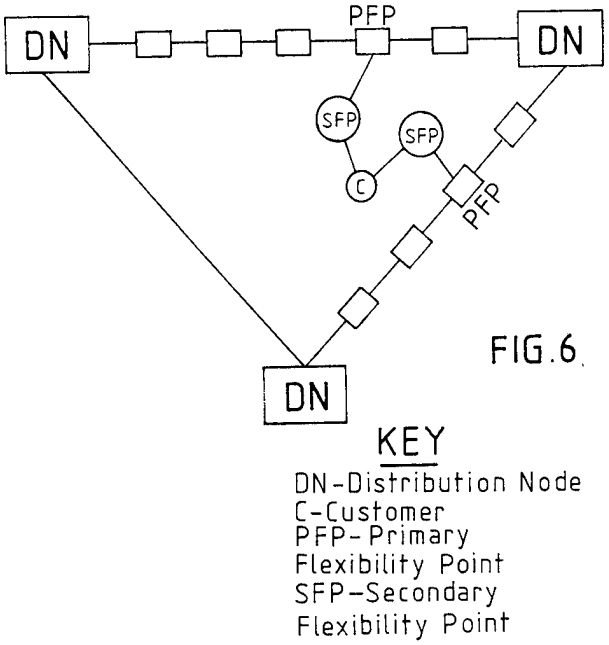



FIG.6

In the City of London, the hydraulic pipe network was installed many years ago beneath the carriageway and, as a result, the Primary Distribution Network including the manholes containing the PFPs is installed in the carriageway. Although this poses some problems during installation due to the presence of heavy vehicular traffic, it is thought that there will be some additional security benefit in that the primary cables and PFPs will be physically divorced from all the congestion and inevitable hazards that exist in the footway.

For this reason, it is expected that the Primary Network of future installations in major UK centres will also be in the carriageway.

In terms of mechanical protection, the LHP pipes provide an ideal duct route since they consist of steel and cast-iron sections with wall thicknesses of upto $1\frac{1}{2}$ inches.

## 7. NETWORK EXPANSION

The network can be expanded in a number of ways to cope with the various demands placed on it in the future.

i) Careful choice of fibre performance will ensure that the long term needs of most business customers will be satisfied by simply upgrading the terminal equipment.

ii) Increased penetration of customers connected will be accommodated by installing further primary cables and PFPs within the initially constructed manhole and duct network. Sub-ducting techniques are employed to facilitate additional cable installation, and care is taken at the outset to ensure that all carriageway chambers are large enough to accommodate 2-3 PFPs.

iii) Increased traffic levels will dictate the need for more equipment space at each Distribution Node. At that time, new Distribution Nodes will be introduced by intercepting the Primary Distribution Network at any convenient PFP.

## 8. INSTALLATION

Prior to actual installation, a small model of the proposed network was constructed, including full size versions of the individual components used -i.e. Primary and Secondary Flexibility Points, Joint Chambers etc. (see photographs at the end of this paper).

This exercise provided invaluable data such as:

i) Quantity of cable and fibre to be stored at each Primary and Secondary Flexibility Point location.

ii) Manpower required to fit a PFP to a 160-fibre cable to assist in Manpower planning.

The actual installation project entailed four discrete activities -

i) Ductwork civil engineering - i.e. LHP refurbishment work.

ii) Subduct installation.

iii) Primary Distribution cabling - this activity was extended to include some secondary cabling required to connect the first few customers.

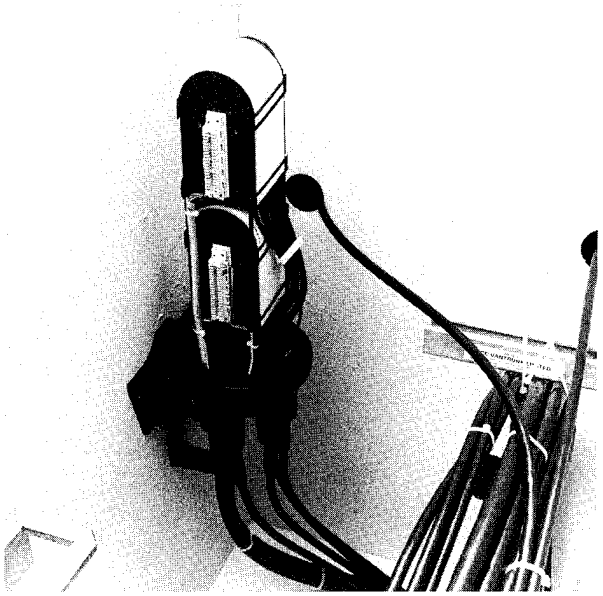
iv) Cable Distribution Nodes established.

Primary Flexibility Points were housed in manholes which were built in place of the 'T' joints and valves that formed part of the hydraulic pipe network. This pipe network was found to be very comprehensive with joints and valves at almost all major road junctions and many smaller ones.

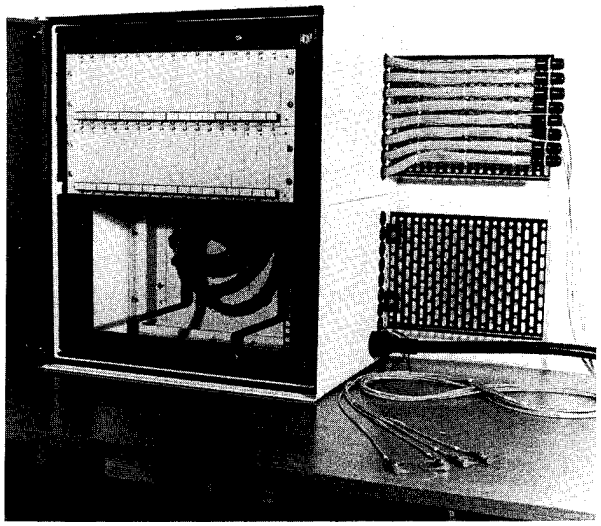
## 9. CONCLUSION

Currently available optical cables and devices have made it possible to design a Local Wideband Network for public use, which makes cost-effective use of the minimal space available in the City of London and, indeed, any other Central Business District.

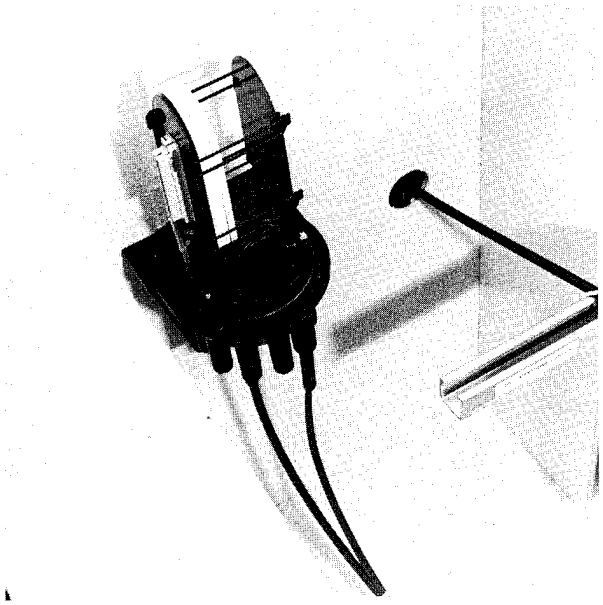
By providing a hybrid 'Ring-main/ Taper' distribution network, various levels of diversity can be made available to ensure the continuity of service demanded by todays business users.



Primary Flexibility Point in a Jointing Chamber



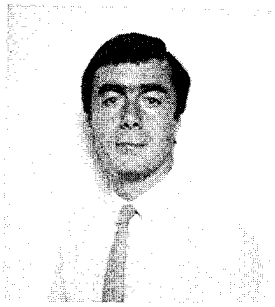
Cable Termination Rack for Two 160-Fibre Cables



Secondary Flexibility Point with one Customer Drop Cable fitted

ACKNOWLEDGEMENT

The authors thank the Directors of Mercury Communications Limited and BICC plc for permission to publish this paper, and colleagues for assistance with development and with preparation of the paper.



James W. Reilly
Mercury Communications
Limited
Ninety Long Acre
LONDON,
WC1N 2BC

James W. Reilly joined Mercury Communications Limited in 1983 and became responsible for the design and planning of Local Cable Networks using Optical Fibres and associated devices. He has previously worked in the Network Planning areas of Trunk and Local Distribution. He is currently Manager of the Local Distribution Department in the Network Operations Division and is responsible for the Company's local microwave and cable planning.



Graham Holden
BICC Telecommunication
Cables Limited
PRESCOT
Merseyside
L34 5SZ

Graham Holden graduated in 1979 from the University of Liverpool, UK with a B.Eng (Hons) in Electronic Engineering. He joined BICC Telecommunication Cables to work on the development of cable splicing techniques and accessories and is currently employed in the development of Local Wideband Systems.

# COST EFFECTIVE OPTICAL SYSTEMS FOR UK JUNCTION NETWORK

C H ROBBINS

BRITISH TELECOM, LONDON, UK

## SUMMARY

In April 1983 British Telecom confirmed plans to accelerate their overall network modernisation with the target date for digital replacement of the associated transmission links from local exchanges, BT's junction network, brought forward to 1995. The economics of an optical solution in this environment where low capacity routes of limited length proliferate have always been unfavourable and a constraint on their use. The paper outlines how BT approached UK Industry with a definition of the prospective optical fibre and equipment market which could be enjoyed if costs could be significantly reduced. This approach has now precipitated volume production of cost effective cable and equipment operating at 8Mbit/s over multimode fibre. However, the price trends in optical fibre production have changed dramatically over the last two years and the paper concludes with a consideration of the factors related to the economic exploitation of single mode fibre in this part of the Network.

## INTRODUCTION

British Telecom's Junction Network provides the transmission links between local exchanges and more importantly, from each local exchange to its parent higher order exchange, nominally the Group Switching Centre (GSC). Traffic is carried over 1.1M circuits currently amalgamated on 63000 traffic routes. In simple terms the Network is configured as individual star networks radiating from each of the 350 GSC sites. In contrast there are some 6500 local exchanges and junction requirements are directly dependent on the distribution of these local exchange types in terms of numbers, switching capacity and distance from the parent GSC site. Over half the traffic originates from a relatively small number (1500) of large local exchanges, the remaining traffic being thinly distributed over the other 5000 small local units. It is therefore not surprising that 'low capacity' transmission systems represent the largest proportion in any potential junction, optical fibre market.

The adoption of an Integrated Digital Network (IDN) strategy 4 years ago heralded the start of a major digital transmission planning and provision programme. The Junction Network (JN) objective was to achieve 100% digitalisation by the year 2000. A task of this magnitude demands a readily available supply of cost effective digital transmission systems in large production volumes. Historically optical fibre systems, particularly at 2 and 8Mbit/s, had failed to satisfy these basic criteria. The major constaint being the high cost of both fibre, cable sheathing and equipment.

## POTENTIAL OPTICAL MARKET

In April 1983 BT confirmed plans to accelerate the modernisation programme based on an increased availability of digital exchange production capacity. The target date for completing Junction digitalisation was brought forward 5 years but more significantly the bulk of work had to be done by 1990. With procurement lead times of typically 2 years this change of strategy highlighted the need for an immediate break-through on optical costs. Any delay in introducing a cost effective "low bit rate" system would clearly reduce the potential market size and leave the network with a higher proportion of conventional systems.

It was therefore essential to act quickly and secure support from UK Industry to ensure volume production in reasonable timescales. To encourage such support it was necessary to define:

i) The potential optical cable and equipment market.

ii) Target prices for the primary elements of the prospective optical systems.

In a network modernisation environment Junction transmission requirements are directly dependent on the distribution of local exchanges by:

i) exchange type

ii) numbers of exchanges in each category

iii) average connection size

iv) distance from the parent exchange

v) digitalisation period.

These parameters are shown in Table 1 together with the typical optical system bit rate appropriate for links in each category.

## DISTRIBUTION OF LOCAL EXCHANGES

| | TXS LARGE | TX E4/ 4A | TXK 1/3 | TXE2 | TXS SMALL | TXS VERY SMALL |
|---|---|---|---|---|---|---|
| AVERAGE CX SIZE | 12,000 | 13,500 | 8000 | 2000 | 1000 | 500 |
| NUMBER OF UNITS | 870 | 330 | 530 | 1500 | 1000 | 1800 |
| DISTANCE FROM PARENT KM. | 7 | 6 | 7 | 13 | 11 | 17 |
| LINKS DIGITAL BY | 1990 | 1990 | 1990 | 1995 | 1995 | 1995 |
| TYPICAL OFS (Mbit/s) | 34/8 | 34/8 | 34/8 | 8/2 | 2 | 2 |

TABLE 1

A simple SBC based network model provided the framework to calculate the longer term requirements for digital line plant, expenditure and manpower. To derive the potential market for OFS the size of the various transmission links were bracketed and related to specific optical system bit rates. The final output provided a theoretical guide to the total potential fibre and equipment market over the modernisation period. The study programme ignored existing digital plant so it is important to stress that the practical market size would be smaller. The results of this study are shown in Tables 2 and 3 against the assumptions that total network demand would be met by:-

a) Full availability of 2, 8 and 34Mbit/s OFS

b) Only 8Mbit/s OFS

c) Only 8 and 34Mbit/s OFS.

## FIBRE MARKET

[F/km (000's/ANNUM)]

| STUDY \ SYSTEM (Mbit/s) | 2 | 8 | 34 | TOTAL |
|---|---|---|---|---|
| 2-8-34 Mbit/s | 75 | 10 | 5 | 90 |
| 8 Mbit/s only | | 50 | | 50 |
| 8-34 Mbit/s only | | 33 | 5 | 38 |

TABLE 2

## EQUIPMENT MARKET

(Equipment ends/annum)

| STUDY \ SYSTEM Mbit/s | 2 | 8 | 34 | TOTAL |
|---|---|---|---|---|
| 2-8-34 Mbit/s | 2000 | 500 | 850 | 3350 |
| 8 Mbit/s only | | 2500 | | 2500 |
| 8-34 Mbit/s only | | 1500 | 850 | 2350 |

TABLE 3

We can see that the fibre market, and to a lesser extent the "equipment end" market are strongly influenced by the availability of a cost effective 2Mbit/s optical system. This simply reflects the proliferation of small routes in the Junction Network. It is equally obvious that there is only a restricted market for 34Mbit/s systems.

If any sizeable optical penetration is to be achieved industry must produce a cost effective 8 and/or 2Mbit/s system. The ultimate choice would largely be dictated by the prevailing system costs.

### SYSTEM ECONOMICS

It will be obvious by now that cost had been the restraining influence on optical penetration in the Junction Network. In the past we have specified the system requirements; placed tenders with Industry and then adjudicated on both technical and cost grounds. Thus costs have been obtained as a by-product of the system requirements.

Because of the necessity to make a rapid break-through in this difficult area it was decided to start by "specifying" the required costs for an optical system that would be competitive with the conventional transverse screen cable based PCM system equivalent. The conclusions derived from an iterative cost analysis to meet this requirement are captured in Table 4. The simple message was that the costs of both cable and equipment had to be half the prevailing proprietary system level if either 8 or 34Mbit/s systems were to be totally cost effective.

TARGET PRICES FOR COST EFFECTIVE SYSTEMS
[DIRECT STORES COST (£)]

| | (8F) CABLE/km | | | L.T.E. | | | 2/8 MUX | 2/8 MUX |
|---|---|---|---|---|---|---|---|---|
| | 34 | 8 | 2 | 34 | 8 | 2 | | |
| POLS 3 | 3500 | 2000 | — | 3400 | 2000 | — | 2400 | 2700 |
| REQUIRED | 1500 | 1400 | 1000 | 1700 | 1000 | 500 | 1200 | 1350 |

TABLE 4

The next step was to predict from the most up to date information what the real system costs might be in say 1985 and then compare these with the required target costs.

**Fibres**

The general pattern of multimode fibre prices at that time can be seen in Fig 1, the information being taken from Cornings 81 catalogue.

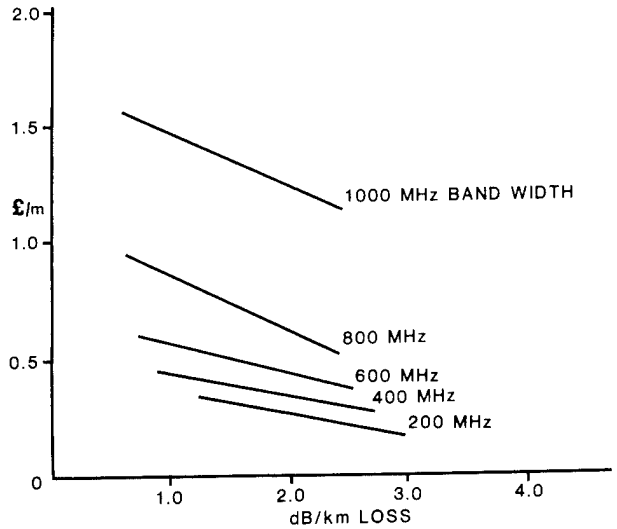



FIGURE 1 - DISTRIBUTION OF FIBRE COSTS (Corning June 1981)

An examination of the market place indicated two important trends.

i) Prices were generally reducing

ii) Those reductions were progressively more marked as fibre quality increased.

These factors have the effect of "closing-up" the lines in Fig 1 such that the price differential in the 1dB/400MHz and 600 MHz would be small.

For the purpose of the study it was predicted that 10 pence/metre provided a challenging but realistic target for 1985 fibre prices assuming significant production volume.

**Cable Construction**

Looking at 1985 when fibre prices should be further reduced it was clear that the cable sheathing element could grossly predominate.

Although there are a myriad of different cable construction designs they were simply categorised according to basic design philosophy. The likely costs for three basic options are given below.

| TYPE | Central Strength member | "high strength" hollow tube | Simple hollow tube |
|---|---|---|---|
| Cost/Km | | | |
| £ | 1500 | 750 | 300 |

It was assumed that option 2 represented a realistic figure for 1985 construction costs.

## Multiplexing

It was fortuitous that during this study a new generation design of 2 to 8Mbit/s multiplex was just being introduced into the network. This equipment capitalised on the advantages offered by Large Scale Integrated (LSI) circuits which made it possible to fabricate the complete multiplex on a "single card" philosophy. This factor and a change towards permitting more commercial freedom in the equipment specification has resulted in significant cost reductions.

Referring back to Table 4, it did not seem unreasonable to assume that the cost target for the 2/8Mbit/s multiplex element of the optical system could be achieved by 1985.

## Optical Line Terminal Equipment

The most interesting components in the OLTE are the optical transmit and receive devices. The optical output power level, receiver sensitivity and operating wavelength are all critical factors in the design and ultimate cost of this "optical package". Commercial security is naturally very evident in this area, a factor which made it difficult to be certain about suppliers and the price levels in the market place. Despite this there was evidence to suggest that the "optical package" represented the major cost element of the OLTE. It was also clear that the cost of the "optical package" was critical to any expectations of future price reductions.

## Conclusions

The study sought to predict anticipated prices prevailing in 1985. The results indicated that the target prices in Table 4 could be achieved for:

i) Fibre

ii) Cable sheath construction

iii) 2/8Mbit/s Multiplex

It appeared that the cost of the optical devices and thus line terminating equipment represented the major constraint to achieving cost effective systems.

## APPROACH TO INDUSTRY

Against the background outlined in the preceeding sections BT formally approached UK cable and transmission equipment suppliers. Industry were advised of the plans to accelerate the network modernisation strategy which in turn offered the prospect for a sizeable fibre market given lower system costs than those currently offered. Individual suppliers were invited to offer likely costs of cables and equipment against a background of their own particular design proposals. They in turn responded to this initiative and in a series of presentations set down their proposals for meeting this need.

In broad terms their response followed a common theme based on a cost effective 8Mbit/s "integrated" terminal design with a supporting multimode fibre cable designed around a "simple" construction theme as anticipated.

## FUNDAMENTAL USER REQUIREMENTS

The primary operational objective was to secure a rapid introduction of cost effective systems in relatively large production volumes. In order to achieve this it was thought essential to give individual suppliers commercial freedom in their equipment realisations whilst recognising the need to establish some basic framework of system philosophy.

The overriding operational interest was to secure a simple system philosophy that minimised planning and installation resources. To this end some initial criteria were established as follows:-

i) The previous practice of tailoring fibre loss and bandwidth to individual section lengths would not be adopted.

ii) The grade(s) of fibre chosen would support upgrade to 34Mbit/s by change of terminal equipment alone.

iii) There would be no underground repeaters thus eliminating the need for power feeding over the cable.

iv) The number of surface repeaters would be limited to one, or two at most, to eliminate the need for sophisticated supervisory systems.

v) The alarm requirements would be no more complex than those for existing copper based systems.

In the event separate statements of user requirements were written for cable and equipment respectively. A summary of these initial requirements is given below.

## Cable

i) The design must be strong enough to require no special cabling restrictions.

ii) The fibre requirements were specifically specified to be 50/125 micron, 1300nm multimode with the following characteristics

400 MHz/km - 1.5dB/km

600 MHz/km - 1.0dB/km

iii) Cables from different manufacturers must be capable of being jointed together.

iv) Cable would be stocked in standard lengths.

**Equipment**

i) The basic requirement was for a 4x2Mbit/s system over a nominal 8Mbit/s optical path.

ii) Terminal equipment must be compatible with BT's TEP-1E rack practice.

iii) Input and Output interfaces must comply to standards specified.

iv) The optical, electrical and mechanical aspects must conform to appropriate safety requirements.

v) The system should operate over a path length of 0-10km with 1.5dB/km fibre and 10-15km with 1.0dB/km fibre ie a common maximum fibre loss of 15dB.

vi) The cabled fibre loss between equipment connections must not exceed 24dB.

The overall system is designed to have an optical dynamic range of $\geq$ 25dB and a typical optical power budget as given below.

| | |
|---|---|
| LED Launch Power | -16dBm |
| Receiver Sensitivity | -49dBm |
| Available Power Ratio | 33dB |
| Fibre loss | 15dB |
| Joint Margin | 5dB |
| Roadworks/Maintenance | 4dB |
| Maximum Cabled loss | 24dB |
| Equipment Design Margin | 2dB |
| Ageing Margin | 4dB |
| Connectors | 3dB |
| Total | 9dB |

**PRODUCTION EQUIPMENT, FIBRE AND CABLE**

In July 1984 sufficient confidence had been established with Industry to permit placing substantial contracts for cable and equipment representing some 20,000km of multimode fibre. The various designs are reviewed below.

**Equipment**

The basic equipment philosophy from all manufacturers follows the trend shown in Fig 2.

Each system end comprises of two cards, one for the optical transmit/receive components plus line coding (1B2B) with the second embracing the 2/8Mbit/s MUX and DE-MUX elements. The standard equipment shelf accommodates up to 4 system ends together with common power and alarm facilities.

TYPICAL EQUIPMENT LAYOUT

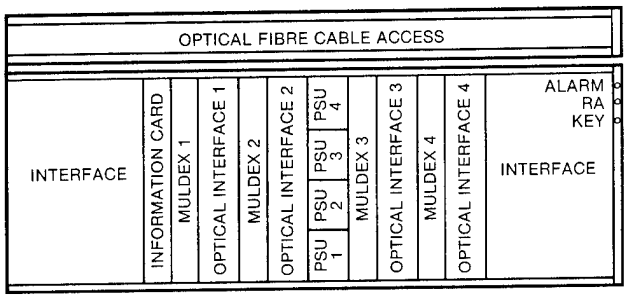
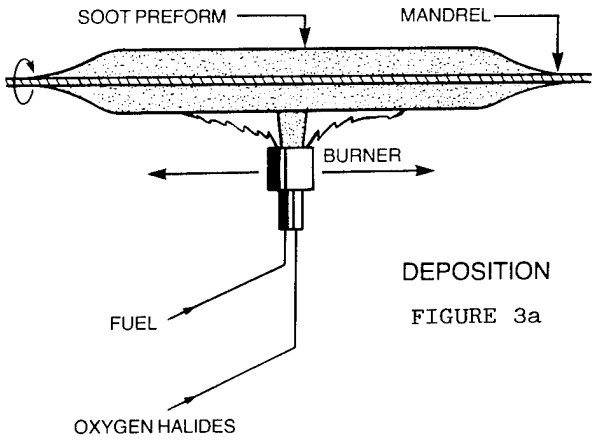



FIGURE 2

**Fibre**

The multimode fibre was specified and design approved separately. The fibre specification called for primary coated 50/125$\mu$m fibre suitable for use in loose tube main cable construction. Secondary coated fibres to the same specification were used in the terminating cable to the equipment interface. The majority of fibre was supplied by a UK company whose production facilities originated from the Corning Glass Works with whom they are in direct partnership. The process uses the outside vapour deposition OVD system. In this method the oxygenated liquid chemical constituents are fed into an enclosed cabinet or "lathe" where they are heated by a burner which traverses latterally depositing the 'soot' on a supporting rod. The input mixture, temperature and the number of passes by the burner are the primary control mechanisms which determine the required index profile. The glass blank of some 0.75m in length and 80mm in diameter made in this deposition process shown in Fig 3a is sufficient to produce some 20-25km of fibre when reheated and "pulled".




DEPOSITION

FIGURE 3a

In this separate pulling process the blanks are mounted at the top of 8m pulling towers, reheated and drawn vertically down to the 125μm size and wound as finished fibre on spools at the base of the tower. This is shown in Fig 3b.

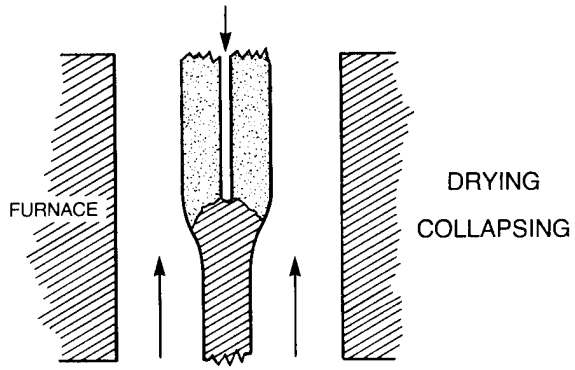



FIGURE 3b

## Cables

The aim of this project was to secure a rapid introduction of cost effective designs by persuing a policy of encouraging maximum commercial freedom coupled with minimum BT constraint in design.

Thus the cable specification used for contract purposes concentrated on the fundamental requirements of size, strength, flexibility and overall optical performance. Because the basic system philosophy was conceived to afford system upgrade to 34Mbit/s and the nature of the network is typified by a preponderance of small routes, fibre counts over a range of 2 to 16 fibres were considered adequate to meet all applications.

A dedicated duct bore policy for optical cable was never considered operationally acceptable and therefore it was necessary to specify that cables had to withstand being handled like any conventional design in a mixed duct environment. To afford adequate protection under cabling conditions a minimum cable size of 15mm was specified to limit the possibility of these relatively small cables wedging under large cables already lying in the duct. The other key factor in this equation related to cable strength and its relationship to any residual strain imparted on the fibres whose life expectancy is rapidly degraded due to stress corrosion when under quite low levels of stress. To this end the specification stated that fibres should not be strained by more than 0.25% when the cable is pulled with a force equal to the weight of 2km of cable. Samples of the fibre are tested in the laboratory to determine the tensile strength (by elongation) and predicted service life due to stress corrosion at the earlier fibre design approval stage. The finished cable must also be flexible enough to permit ease of handling during cabling operations and tests at a minimum bending radius of 12 times the cable diameter were specified.

The optical performance of the fibre was specified at the initial stage of the project as a fundamental system parameter. These factors are outlined in the preceeding section of the paper detailing our "Fundamental User Requirements".

## Production Designs

During the preparatory study phase of this project outlined previously it was suggested that a hollow tube philosophy represented one obvious way forward to achieve a simple cost effective cable construction provided strength requirements could be maintained. However, in the real world of cable manufacture the design, production and performance aspects are complex, varied and exhibit a considerable interdependance between the parameters involved. Not least of the cable makers concerns is the level of investment in new plant required and the depreciation overheads which follow.

In the event our four major UK cable manufacturers offered differing design solutions which can be broadly categorized as follows.

i) Hollow tube with fibre ribbons

ii) Central core with fibre units

iii) Central core with open slot extrusion

iv) Central core with integral slot extrusion

The target diagrams for each cable design have been collated to assist comparison and are illustrated towards the end of the paper. A brief review of each design is given below.

## Hollow Tube with Fibre Ribbon

The concept of this design was to introduce the fibre elements longitudinally into the protective sheath in a single process with adequate stress relief to the combination. The "ribbon" or "tape" array of fibres was developed to allow up to 8 fibres to be laid side by side and bonded together using an acrylate similar to that used for the primary coating of fibres. The ribbon is pre-formed to take on undulating profile along the hollow tube to ensure the required excess fibre length and strain relief is achieved. The "set" of this undulation is achieved using two fine copper wires along the outside edges of the ribbon. In production the ribbon is made off-line to ease manufacture, minimise the consequences of fibre breakages and provide isolation from the slower sheathing process. The corrugation of the ribbon and subsequent sheathing operations are completed as a single production pass. The required longitudinal strength is provided by incorporating bundles of glass fibre elements into the sheath wall providing a flexible cable.

### Central Core with Fibre Units

The supplier of this design was one of the first to develop the hollow tube philosophy in conjunction with secondary coated fibres and these cables have been successfully used in the network in their light armoured version. However the final form of construction chosen for our main cost effective cable orders followed the more traditional central strength member and stranded fibre units approach.

In this particular design four primary coated fibres are loosely packaged in a thermoplastic tube to form the unit. Four such units plus two dummy fillers and the metallic pair are stranded around the central compacted steel strand strength member. The internal diameter of the unit tube and the stranding lay of the units are carefully selected to control the amount of excess fibre and resulting strain relief. In order to reduce the pneumatic resistance the tube fillers each have a longitudinal slot cut in them. The tubes are finally protected with a paper belt and polyethylene sheath containing an aluminium laminate moisture barrier.

### Central Core with Integral Slot Extrusion

This construction provides another basic low cost cable design with potential for a one-shot production process. The design has the same central compacted steel strand strength member around which is extruded a closed integral construction providing 4 slots in which the fibres are contained. The extrusion is laid over the core with an oscillating twist to provide the required excess fibre and strain relief. Selected slots are allocated to carry the pair of insulated copper wires used for the engineering speaker facility. Access to the fibres for jointing purposes is provided by easy tear strips in the periphery of each slot. This part of the production process is followed by the application of the normal aluminium moisture barrier tape and polythene outer sheath. The two parts of the process could be tandemised and considered as a single pass operation.

### Central Core with Open Slot Extrusion

This cable is based on the well proven Northern Telecom design and comprises a central steel strand core around which is extruded an open slotted construction with six channels which follow a reverse helix path along the length of this member. Four of the slots contain the fibres with the remaining two allocated for the insulated copper wires. To hold the fibres and conductors in place during manufacture two binding yarns are applied in opposite directions. A longitudinal wrapping is applied over this "core" followed by the aluminium plastic laminate moisture barrier. The outer sheath in common with all other designs consists of a layer of black polyethylene.

## INSTALLATION PROGRAMME

The overall objective of this project which started in 1983 was to trigger a rapid introduction of cost effective junction network optical systems. In July 1984 BT placed its first main contract for these system comprising 20,000 fibre km of cable and 2500 equipment ends representing approximately 25% of the annual junction provision programme. Follow-on orders for a further 40,000 fibre km and 3000 equipment ends have also been placed.

Cable and equipment from the initial order is now being installed by BT field staff and the first system was successfully brought into service back in January this year. There have been no reports of installation difficulties associated with the cabling of long lengths and the only area of anticipated debate relates to interpretation and analysis of joint loss results.

## FUTURE SINGLE MODE SYSTEMS

During the last three months we have been studying with UK industry and BTRL the implications of moving to single mode fibre based systems. The price of single mode fibre has fallen dramatically over the last three years and this factor coupled with its ability to support system speeds of 140Mbit/s and beyond makes it a very attractive transmission bearer. Unfortunately, the cost of exploiting such bandwidth potential can be significant and directly dependent on the price and availability of suitable optical transmitting devices.

The various aspects of the overall system equation are reviewed as follows.

### Single Mode Fibre

The price of single mode (SM) fibre has fallen quickly in response to world demand and increasing confidence of production. The relative price trends of single and multimode (MM) fibre suggest that equivalence with multimode is anticipated during 1986 with prospect of savings in subsequent years.

It is interesting to note that our major UK fibre supplier now produces three times more SM fibre than MM. With high throughput and simpler processing SM fibre should potentially be the cheaper product.

### Cable Design

There is confidence that our current range of cost effective optical cable designs can be used with SM fibre and thus there is no additional cost penalty anticipated in this area.

### Equipment Philosophy

The primary aim is to introduce SM systems with marginal or nil cost penalty when compared with

the existing MM systems previously described. Our present cost effective 4x2Mbit/s system is based on fibre qualities deliberately chosen to give 40MHz bandwidth with a loss of not greater than 15dB excluding joint losses, allowing a 34Mbit/s capability over 15km. Strategic planning of the network requires that a 15km system reach between regenerators should be maintained.

The lowest cost equipment option is to use the present 4x2Mbit/s LED based optical terminals over new SM fibre sections. Unfortunately the LED devices are supplied with short MM fibre pigtails of 50μm core diameter. When this is coupled to the very much smaller 8μm core diameter of the SM main cable fibre there is a considerable loss of optical power at the transition. In essence this calls into question the distance one can confidently plan without using repeaters and incurring further cost. Present studies indicate that 10km may be a practical limit using this approach but with this constraint a large proportion of our network requirements could still be satisfied.

## Alternative Device Options

For route lengths in excess of 10km at 8Mbit/s and all junction demand at 34Mbit/s higher transmit power devices are essential. There are several options available.

i) Higher power LEDs with MM pigtails

ii) LEDs with SM pigtails

iii) Lasers

The first two options can be obtained at some cost penalty to give a small improvement in system reach. However, the use of lasers offer the most attractive solution providing more than adequate power for all network requirements. Unfortunately the present cost of lasers is prohibitive and a constraint to a more widespread application of SM fibre. As a result we are currently in debate with optical device manufacturers to assess the prospect of obtaining "low cost" laser devices for short haul applications.

## CONCLUSIONS

The overall network objective in 1983 was to precipitate a rapid introduction of short haul junction multimode optical systems that were price competitive with the traditional copper based PCM solutions. In a little over 12 months from the start of this project BT placed contracts for 20,000 fibre km of cable and 2500 terminal ends which are now as complete operational systems being progressively brought into service.

During this period the price trends in optical fibre production have changed dramatically and BT is now actively pursuing the steps necessary to afford a rapid introduction and exploitation of single mode fibres for short haul network applications.

## ACKNOWLEDGEMENTS

Acknowledgement is made to the Director of Engineering of British Telecom Local Communication Services for permission to publish this paper.

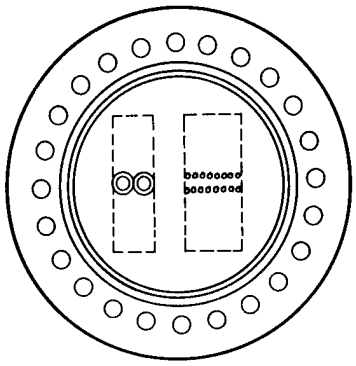


Mr Robbins is Head of the Junction Network Operations Section of British Telecom Headquarters. He is responsible for providing support to forecasting, planning and works staff in the local District offices and identifies the need for, and sponsors the development of new transmission systems. He is a Chartered Engineer and a Member of the Institution of Electronic and Radio Engineers.

C H Robbins
British Telecom
LCS Local Line Services, LLS2.2
Lutyens House
1-6 Finsbury Circus
London EC2M 7LY

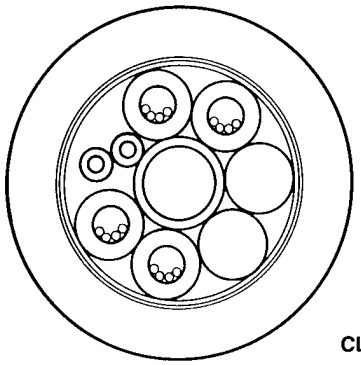
Tel. 01-357 3275

## HOLLOW TUBE-RIBBON DESIGN



- Optical Fibre ribbon(s) of approximate sine wave form with an amplitude (peak to peak) of approx 6mm and wavelength of approx 40mm.
- Two 0.6mm diameter insulated Copper wires applied in the same way as the fibre ribbons.
- Paper tape to nominally 175µm thickness.
- Identification tape.
- Moisture barrier of 150µm thick Aluminium tape coated on both sides with polyethylene.
- Black polyethylene sheath incorporating bundles of glass yarn tension relief elements.

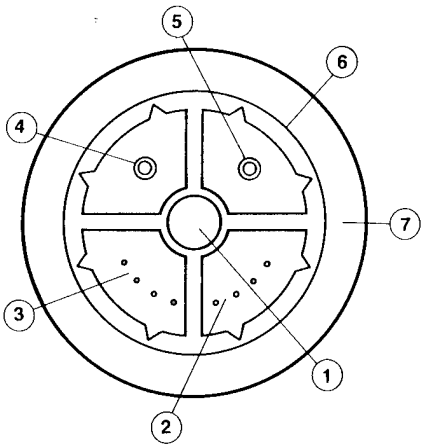
## STRANDED UNIT DESIGN



Units consisting of 4 primary coated graded index fibres within a polypropylene tube, laid up around a polyethylene sheathed high tensile steel strength member, with coloured marker fillers and a Ø.6mm polyethylene insulated pair. Paper tape lapped and polyethylene aluminium laminate sheathed.

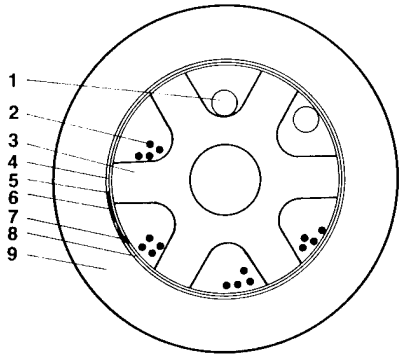
For the 4, 8 and 12 fibre cables, the superfluous fibre units are, replaced by yellow polyethylene fillers.

## CLOSED INTEGRAL CONSTRUCTION




1. Compacted Steel Strand
2. Optical Fibres
3. Optical Fibres
4. Insulated Ø.6mm Copper Wire
5. Insulated Ø.6mm Copper Wire
6. EASY Tear Polymer Extrudate
7. Moisture Barrier Black Polyethylene Sheath

## OPEN CHANNEL DESIGN




1. Insulated copper wire
2. Optical fibre
3. Open Channel Member with central steel strand
4. Binding yarn
5. Wrapping tape
6. Identity tape
7. Ripcord
8. Aluminium plastic laminate
9. Polyethylene sheath

# HIGH-PERFORMANCE OPTICAL FIBER CABLE COVERAGE THROUGHOUT JAPAN

Ichiro YAMANOUCHI

NTT New York Office
Nippon Telegraph & Telephone Corporation
New York, U.S.A.

## Abstract

This paper describes an outline of high-performance optical fiber cable used by NTT and the most recent progress for the Information Network System (INS).

Single-mode optical fiber cable (8400 km) and graded-index cable (1800 km) have already been installed into trunk lines. The major trunk line of single-mode cable extends the length of Japan and is about 3400 km long, including 72 km of submarine cable. Improvements in optical loss were obtained, which lead to a maximum repeater spacing of 40 km. Graded-index cable is introduced into medium-haul intra-city transmission lines.

At Tsukuba Expo'85, subscriber optical fiber cable has been introduced in commercial use. High-density subscriber optical fiber cable of five-fiber ribbon structure and other related technological developments have been advanced. These developments will meet the increasing demand for broadband services, such as video and high-speed digital transmission.

## 1. Introduction

Optical fiber cable has been introduced into many fields of telecommunications because it offers significant advantages, such as low attenuation, wide signal transmission band, light weight and small diameter.

NTT started the study of optical fiber technology since 1966 and introduced the first optical transmission system using graded-index optical fiber cables in 1981. Graded-index optical fiber cable has been introduced mainly in medium-haul intra-city transmission lines. Its total length is about 1800 km.

Single-mode optical fiber cable has such superior optical loss and transmission band characteristics that it has been applied to long-haul large capacity main transmission lines. Large capacity transmission lines using single-mode optical fiber cables have been introduced since the beginning of 1983. In February 1985, the major trunk line was completed. It extends the length of Japan and is about 3400 km long, including 72 km of submarine optical fiber cable. Some side lines, which extend from the major trunk line, have also been laid and the total length of single-mode optical fiber cable is about 8400 km at this time. These transmission lines form the telecommunication highways for the Information Network System (INS).

Field trials of optical fiber cable subscriber loops, started in the Musashino and Mitaka areas in 1982. They lead to the INS Model System which involves a total of 2000 monitors. High-speed digital data and broadband services, such as TV conferencing and color facsimile, are provided in this system. Based on techniques developed in these extensive trials, commercial tests on subscriber optical fiber cable started in April 1985 at the site of Tsukuba Expo'85 and at other exibition sites throughout Japan. Subscriber optical fiber cable has also been placed into commercial use for digital transmission services at up to 6.3 Mb/s and for video transmission services at 4 MHz.

This paper describes the status of optical fiber cable technology at NTT, including commercial test results, the most recent progress, and future trends towards the realization of INS.

## 2. High Performance Transmission Lines Running through Japan

### 2.1 History of High Performance Optical Transmission Line Development

The introduction of optical fiber cable started with trunk networks because they have relatively simple network structures as well as economical advantages due to long repeater spacing and large transmission capacity.

The first optical fiber cable put into practical use in Japan was for transmission systems such as the F-32M and F-100M. It featured graded-index optical fiber. Its commercial tests started in the spring of 1981 and since the spring of 1983 it has come into regular use. Graded-index cable has also been used in the F-6M

transmission system, which employs wavelength division multiplexing technology, since 1983.

Single-mode optical fiber cable is expected to be used in long-haul, large capacity transmission lines. NTT started commercial tests on single-mode optical fiber cable for the F-400M transmission system in February 1983. This system was introduced as the main transmission route extending the length of Japan from Asahikawa in Hokkaido to Kagoshima in Kyushu.[1] In February 1985, this route was completed and will be the backbone of INS.

In the submarine sections of this route, a non-repeater submarine transmission system was introduced. Submarine optical fiber cable must have higher reliability than land cable. For this purpose, proof tests are carried out for submarine optical fiber cable under the condition of 1.0% elongation distortion, although proof tests are done for land cable under the condition of 0.5% distortion.

During commercial tests on single-mode cable, NTT investigated a variety of optical fiber cable performances, including the influence of installation on its optical characteristics and the efficiency of its installation work. As shown in Fig. 1, optical loss after installation was found to be sufficiently low at an average loss of 0.70 dB/km including splicing losses. The loss increase caused by installation was negligibly small, and showed an average loss increase of less than 0.01 dB/km. In single-mode optical fiber splicing, the power monitoring method was used to allign core axes. Using this method, a 0.11 dB average splicing loss and a 22 minute average splicing time were realized. The results of the commercial tests on optical fiber splicing can be seen in Fig. 2.

During these commercial tests, improvements in optical fiber loss and in emitted power of the optical devices were obtained. These allowed extending the maximum repeater spacing from 34 km to 40 km. Moreover, an optical fiber splicing machine using the direct core observation system has been developed. The appearance of the machine is shown in Photo. 1. In this system, the optical fibers are monitored by a TV camera installed in the splicing machine and the core is identified by visual analysis and the core areas are aligned by micro-computer control. This method requires only one working point in the splicing manhole, compared to the conventional power monitoring method which requires three working points; one in the telephone office, another in the splicing manhole and the other in the power receiving manhole.

As the application area of single-mode optical fiber cable has extended into that of graded-index optical fiber cable, the specifications of graded-index optical fiber were modified in February 1985. Three grades of graded-index optical fiber cables, which have 500, 300 and 100 MHz·km bandwidths, have been introduced for medium-haul intra-city transmission lines. Conventional 900 and 700 MHz·km grade cables were displaced by single-mode cables. 500 and 300 MHz·km grades of graded-index cables are used for the F-32M system and 100 MHz·km grade cables are used for the F-6M system.

Up to now, more than 10,000 km of optical fiber cable have already been installed into trunk networks throughout Japan. The introduction status of optical fiber cable in NTT is shown in Fig. 3.

## 2.2 Optical Fiber Specifications and Applications

Graded-index and single-mode optical fiber parameters are the same as CCITT Recommendation G651 and G652. Three grades of bandwidth characteristics such as 500, 300 and 100 MHz·km are specified for graded-index optical fiber to establish economical intra-city networks. In both the F-32M and F-6M systems, 20 km repeater spacing can be realized using these kinds of graded-index optical fiber cables. This repeater spacing can cover more than 95% of their application routes. 500 MHz·km grade cables are also used for the short distance F-100M system.

Single-mode optical fiber cable has such superior bandwidth characteristics that only its optical fiber loss characteristics are specified. Two grades of optical loss characteristics are prepared. Recently, single-mode optical fiber, which has an about 0.4 dB/km average loss, has been efficiently produced due to the progress in fiber fabrication technique. As a result, high grade single-mode optical fiber guarantees optical loss to be within 0.5 dB/km for 90% and 0.65 dB/km for 100% of the fibers. The 90% loss value of low grade single-mode optical fiber is 0.8 dB/km and the 100% loss value is 1.0 dB/km. These grades of single-mode cables are applied to the F-400M and F-100M systems according to the total loss requirement of the route. The most suitable light wavelength for single-mode optical fiber has been determined by optical loss and chromatic dispersion characteristics. The lowest optical loss is obtained at about 1.30 μm and the minimum chromatic dispersion is obtained at about 1.32 μm. Based on these characteristics, the most suitable wavelength has been determined as 1.31 μm.

The specifications of graded-index and single-mode optical fiber cables are shown in Table 1. Fig. 4 sums up the application of optical fiber cables in NTT.

## 3. Large Scale Introduction into Subscriber Loops

### 3.1 History of Subscriber Optical Fiber Technology Development [2]

The first application area of subscriber optical fiber cable was small-scale leased lines between two points for broadband and/or high-speed digital services. This network structure resembled that for trunk networks. Consequently, the technology for trunk networks could be applied to suscriber optical fiber cable of this application area. In 1982, graded-index subscriber optical fiber cable was introduced into commercial use to provide video transmission services over broadband leased lines.

The second stage development is leading toward optical subscriber networks between telephone offices and unspecified customers. For expanded introduction into subscriber networks, the following characteristics must be taken into consideration.

(1) Low grade optical fiber is applicable as the lengths of subscriber lines are shorter than those of trunk lines.
(2) Optical fibers must reach all subscribers, without any repeaters although signal multiplication technology can easily be applied to trunk lines.
(3) The network structures are more complex than those of trunk networks and different kinds of subscriber cables are needed in accordance with their application environment.
(4) Easy reconnection techniques are needed to rapidly respond to subscriber demand.

To establish economical and flexible optical fiber cable systems, the technology for cost reduction, higher fiber density, easy cable branching, dropping and splicing, etc., has been advanced.

Following the field trials in the Musashino and Mitaka areas. NTT has devoted great effort to construct the INS Model System covering these areas and the Kasumigaseki area in downtown Tokyo. In 1984, large scale monitor tests involving a total of 2,000 monitors were started. This system provides high-speed digital data and broadband services, such as TV conferencing and color facsimile.

At Tsukuba Expo'85, the international exposition held in Japan since March 1985. NTT has provided diverse advanced telecommunication services for public communications and control operations within the exposition site. For these purposes, commercial tests on subscriber optical fiber cable started in April 1984 at the site of Tsukuba Expo'85 and other exibition sites throughout Japan. Subscriber optical fiber cable has also been introduced for digital transmission services at up to 6.3 Mb/s and for video transmission services at 4 MHz.

### 3.2 Developmental Status for Commercial use [3]

The maximum number of optical fibers required in a commercial cable was determined to be 100 according to predicted optical fiber demand. The transmission rate is expected to be 100 Mb/s from the viewpoint of future video transmission systems (PCM video). In order to economically achieve this transmission rate for 7 km long subscriber lines, two different grades of transmission bandwidth were prepared for subscriber optical fiber cables. Regular (R) grade fibers are applied for subscribers near telephone offices and special (S) grade fibers are used for subscribers far from them.

Aerial optical fiber cable for distribution use, indoor cable, drop wire, and premise wire were also developed. Optical connectors are necessary in subscriber networks to reconnect optical fibers in feeder distribution cabinets and to drop them to subscribers. To meet these requirements, an optical connector for outdoor use has been developed. As shown in Fig. 5, an average splice loss of 0.38 dB was obtained in field splicing work. Furthermore, a closure to easily branch underground cable and an access terminal box for aerial cable have been employed.

### 3.3 Large Scale Introduction

Recently, the demand for high-speed digital transmission services has rapidly increased. And video transmission systems among business centers has caused a centralized demand for optical fibers. To meet the increasing demand for broadband services, high-density subscriber optical fiber cable consisting of a five-fiber ribbon structure is going to be introduced into commercial use. The structure of the high-density cable compared to that of conventional one can be seen in Fig. 6. And related techniques that incorporate a multi-fiber fusion splicing machine and a multi-fiber connector have also been developed. The results of field researches on multi-fiber fusion splicing machines can be seen in Fig. 7.

Since the commercial tests on subscriber optical fiber cables realized the excellent bandwidth characteristics, R grade optical fibers can be applicable to 7 km long subscribers, even if they might be designed for the subscribers near from the telephone offices. NTT is investigating the revision of subscriber optical fiber

specifications, including the unification of R and S grades, as shown in Fig. 8. Besides, connector joining is expected to have wider application, to reduce splicing labor and to enhance network flexibility.

## 4. Future Trends on Fiber Optics

### 4.1 The New Submarine Optical Fiber Cable

A new submarine optical transmission system, the FS-400M, is going to be introduced to expand the 400 Mb/s main transmission lines to all over Japan. This system uses submarine repeaters that enable long-haul transmission across the sea. Repeater spacing for shallow submarine routes and deep submarine routes is to be specified separately, since the operating wavelength change due to the temperature of the water surrounding the repeater affects the repeater spacing because of the dispersion characteristics change.

A conventional submarine cable can be laid only to a depth of 1500 m, higher proof test specification will be needed in order to apply submarine cable to a depth of 8000 m, since the pulling force during the cable laying will increase tremendously.

Investigations for longer repeater spacing and for larger transmission capacity are also being carried out. They indicate that a repeater spacing of about 100 km will be expected for operation at the 1.5 μm wavelength, since optical fiber has a lower loss at 1.5 μm than at 1.3 μm. Adequate optical fiber design for this purpose is being discussed.

### 4.2 The Future of Subscriber Optical Fiber Systems

Subscriber optical fiber networks are expected to rapidly expand, especially in business centers in large cities, because of the increasing demand for broadband services such as videotex (CAPTAIN etc.) and video response system (VRS). To provide diverse broadband services for the future, NTT is engaging in development of higher density optical fiber cable (more than 1000 fibers). The application of single-mode optical fiber cable to subscriber networks is also to be investigated considering the future wider application of digital subscriber transmission systems (i.e. digital video and integrated service systems), cost reduction of optical fibers as well as expansion of optical subscriber areas.

Although it is very difficult to forecast the demand for optical fibers, subscriber telecommunication facilities must rapidly respond to new subscriber demands and facility reinstallation should be avoided. Therefore, flexible optical fiber distribution systems and easy splicing techniques are indispensable. In aerial cable distribution, definite-length cable with connectors on both ends will be applied and any fiber in the cable can be dropped to a subscriber from pre-assigned distribution points. Furthermore, connector joining is intended to be applied at all splicing points to enable fast splicing and reconnection.

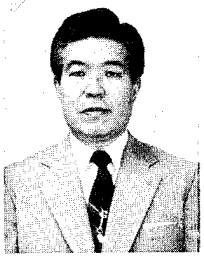
## 5. Conclusion

This paper has described the development story of optical fiber cable technology at NTT, including the most recent progress and advanced investigation. Optical fiber networks will form the physical infrastructure of the entire INS.

The next stage toward the full realization of the INS is the integration of various service networks, using digital signal processing technology. The activities described in this paper will eventually lead to providing economical networks which have enough transmission capacity to deal with the digital signals integrated from many services.

## Reference


1) T. Uenoya, "High Performance Single-mode Optical Fiber Cable Covering Whole of Japan", J.T.R., Vol. 27, No. 2, 1985
2) H. Ishihara, "Subscriber Optical Fiber Cable Technology", J.T.R., Vol. 26, No. 3, 1984
3) H. Ishihara et al, "Optical Fiber Cable Bandwidth Design for Subscriber Loops", ICC'85 Conference Proceedings, Vol. 2, pp537-539


Ichiro Yamanouchi

Deputy General Manager,
NTT New York Office

200 Park Avenue
Suite 2905
New York, N.Y. 10166


Mr. Ichiro Yamanouchi, Deputy General Manager of NTT New York Office is now engaged in the management of NTT oversea office in New York. He used to work for outside engineering, especially maintenance and operation of systems.

He is a member of the Institute of Electronics and Communication of Japan.

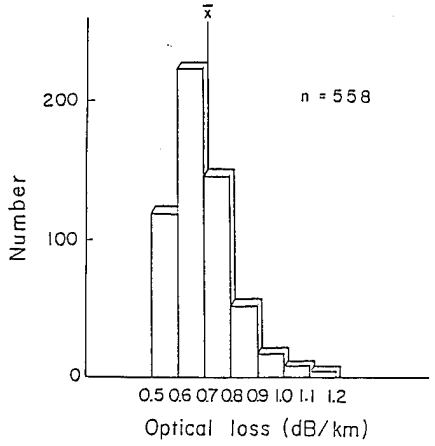



Fig. 1 Optical loss of single-mode optical fibers

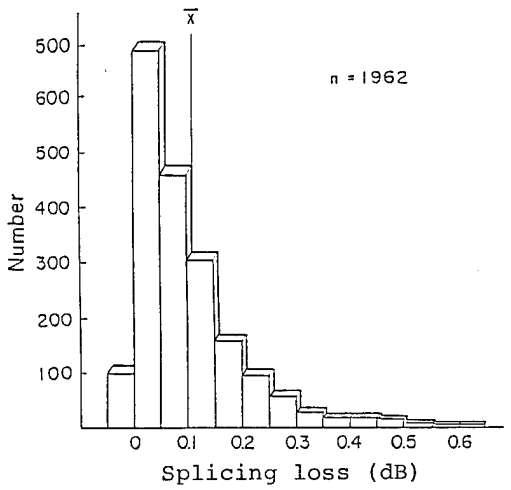



Fig. 2 Splicing loss in single-mode optical fiber fusion splicing

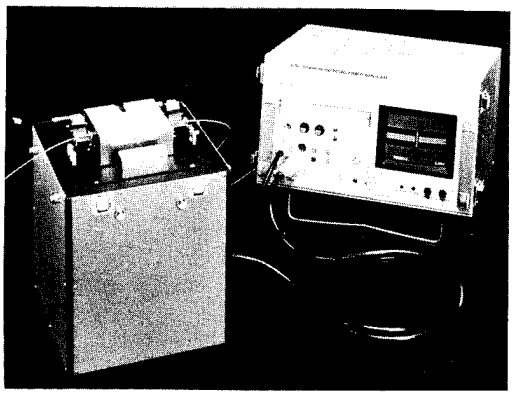


Photo. 1 Direct core observation splicing machine

| Optical Fiber Cable | | System | Commercial Introduction '81 | '82 | '83 | '84 | Route Length (km) |
|---|---|---|---|---|---|---|---|
| Trunk | SM | F-400M | | | ▲ | | 8400 |
| | GI | F-100M F-32M | ▲ | | | | |
| | | F-6M | | | ▲ | | 1800 |
| Submarine | SM | F-400M | | | | ▲ | 80 |
| | GI | FS-6M FS-1.5M | | | ▲ | | 170 |
| Subscriber | GI | FV-4M-P FV-4M-A | | ▲ | | | 530 |

Fig. 3 Introduction of optical fiber cable

Table 1 Specifications of trunk optical fiber cables

| Items | | GI type Optical Fiber Cable | | | SM type Optical Fiber Cable | |
|---|---|---|---|---|---|---|
| Grade | | 500 MHz type | 300 MHz type | 100 MHz type | 0.5 dB type | 0.8 dB type |
| Core Diameter (μm) | | 50 ± 3 | | | 10.0 ± 1.0 * | |
| Cladding Diameter (μm) | | 125 ± 3 | | | 125 ± 3 | |
| Cut off Wavelength (μm) | | — | | | 1.10 – 1.29 | |
| Optical Loss (dB/km) | 90% Value | ≦1.0 | | | ≦0.5 | ≦0.8 |
| | 100% Value | ≦1.3 | | | ≦0.65 | ≦1.0 |
| 6 dB Band (MHz·km) | 90% Value | 500 | 300 | — | — | — |
| | 100% Value | 300 | 200 | 100 | — | — |
| Wavelenghth Used (μm) | | 1.31 ± 0.01 | | | 1.31 ± 0.01 | |

* Mode field diameter

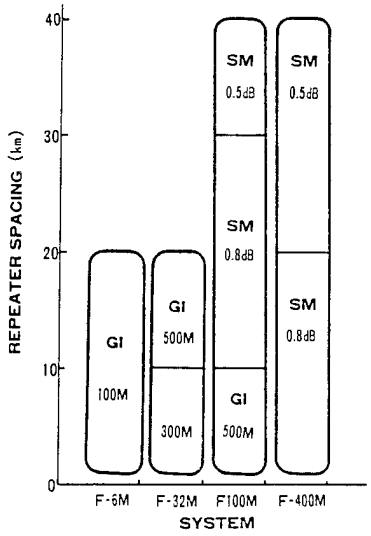



Fig. 4 Application of optical fiber cable systems

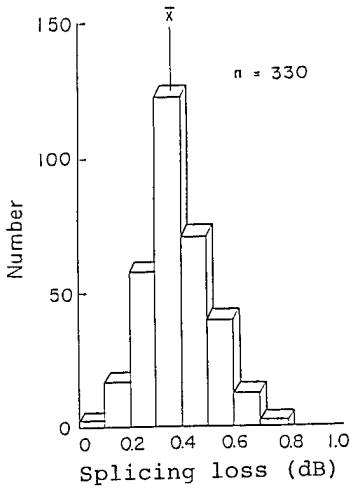



Fig. 5 Splicing loss in optical connector joining

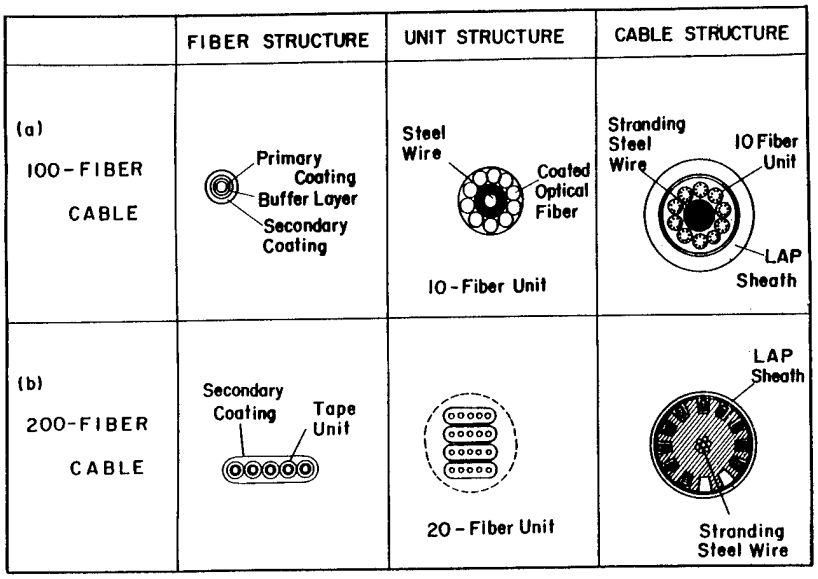



Fig. 6 Subscriber optical fiber cable structure

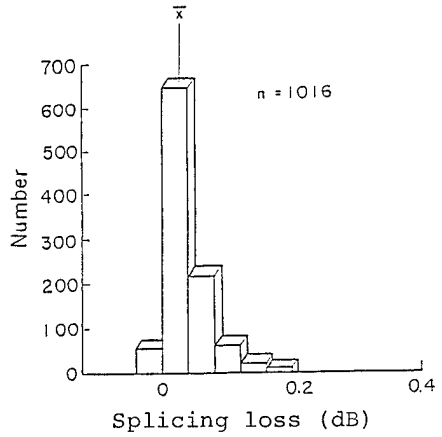



Fig. 7 Splicing loss in multi-fiber fusion splicing

| Characteristics \ Grade | | R grade | S grade |
|---|---|---|---|
| Optical Loss | 90% value | 1.3 dB/Km | 1.3 dB/Km |
| | 100% value | 1.5 dB/Km | 1.5 dB/Km |
| 6 dB Bandwidth | 90% value | 200 MHz·Km | 500 MHz·Km |
| | 100% value | 150 MHz·Km | 300 MHz·Km |

| | | |
|---|---|---|
| Optical Loss | 90% value | 1.0 dB/Km |
| | 100% value | 1.3 dB/Km |
| 6 dB Bandwidth | Average | 500 MHz·Km |
| | Minimum | 150 MHz·Km |

note) Optical fiber parameters are the same as CCITT Recommendation G651.

Fig. 8 Revision of subscriber optical fiber specifications

# CABLE DESIGN AND INSTALLATION TECHNIQUE FOR DIRECT BURIED NON-METALLIC OPTICAL CABLES

B.T. de Boer R.W.A. Ayre R.B. Schuster

TELECOM AUSTRALIA, MELBOURNE, AUSTRALIA.

## ABSTRACT

The use of non-metallic optical fibre cables for long-haul and rural routes has significant advantages in relation to lightning induced damage, and on routes affected by power line proximity or other electromagnetic interference. The preferred installation technique for such cables is direct burial using cable ploughing techniques, however a number of difficulties were observed which were not previously encountered with traditional metallic cables. Detailed experiments and field trials were undertaken using sensitive fibre strain measurement equipment, and the parameters of suitable cable designs and installation equipment were established. As a result of successful developments in this area, Telecom Australia has standardised on non-metallic filled optical cables for all rural and long distance optical fibre installations.

## INTRODUCTION

Like many other Telecommunication Administrations, Telecom Australia is faced with substantial demand for increased digital capacity in its long-haul trunk and rural networks. Single-mode fibre systems have now been established as a cost effective alternative to both coaxial cable and radio systems for these applications, and substantial trans-continental optical fibre links are now planned by Telecom Australia. (Fig. 1).

The use of optical transmission also offers the possibility of a completely metal-free cable that is immune from lightning-induced damage. This is an important consideration over much of the Australian continent, as is the flexibility in route design offered by a cable not subjected to power induction and noise problems associated with power transmission lines. The installation of non-metallic optical fibre cables does however present some problems when compared to the techniques used for their traditional metal conterparts. In rural Australia, as in many other countries, cable ploughing techniques have been established as the most attractive method of installing long-distance directly buried cables. In general however, cable ploughing equipment and techniques have been developed with robust metal cables in mind, and their suitability with the smaller, lighter and more fragile optical cables required detailed assessment.

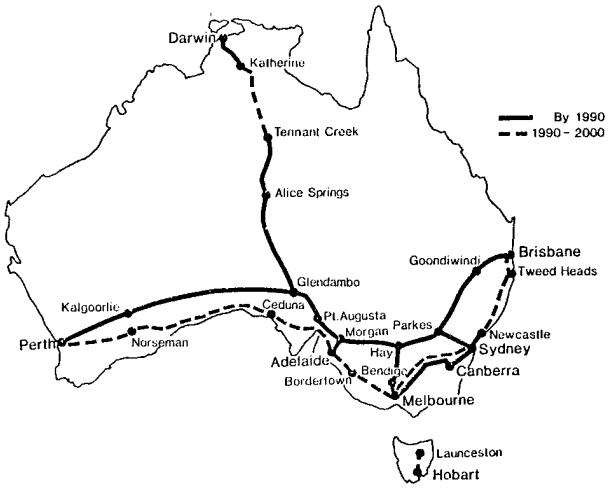



Fig. 1. Optical Fibre Cable Implementation in the Australian Inter-Capital Trunk Network.

## CABLE INSTALLATION TRIALS

The use of conventional cable ploughing equipment and techniques designed for metal cables could impose excessive tensions on optical cables which in turn could lead to excessive short and/or long term strain levels in the fibres. Optical fibres are proof tested during manufacture to strain levels of typically 0.5% to 0.8% and may fail instantaneously if exposed to strain levels in excess of the proof-test value. A more insidious problem also arises, in that optical fibres within a cable are susceptible to failure through static fatigue if they are subjected to even small strain levels over a long period of time. (ref.1.)

Whilst cables with extra strengthening materials and metal sheaths have proved successful for such applications, these items add to the cable cost and negate the attractive non-metallic features of the optical fibres themselves.

A series of trials was therefore conducted covering a range of non-metallic cable designs and using a variety of cable ploughing equipment. The elongation of fibres within each of the cables was continuously monitored during the cable installation period, together with a number of other parameters. The results were then interpreted in terms of the variations in cable structural features and differences in the type of cable ploughing equipment used.

Measurement System : The theoretical basis for the measurement system has been established by other authors. The elongation of an optical fibre can be determined from the change in the propagation time of an optical signal along a fibre. Methods employing phase-delay measurements with sine-wave modulated optical sources (references 2-4), and time delay measurements with pulse modulated sources (references 5-7) have been reported. Due to features of the experimental technique employed, it was found that greater resolution of fibre elongation was achieved with the phase - delay method.

The measurement system (reference 8) is illustrated in Figure 2. A loop is formed by splicing two fibres in the cable at the far end (i.e. on the cable drum). A laser diode produces an optical signal which is coupled to one of the fibres. The optical signal is modulated at 200 MHz by a signal from a frequency synthesiser. The returning signal on the second fibre is detected by an avalanche photodiode, and a vetor voltmeter measures the phase difference between the transmitted and received signals.

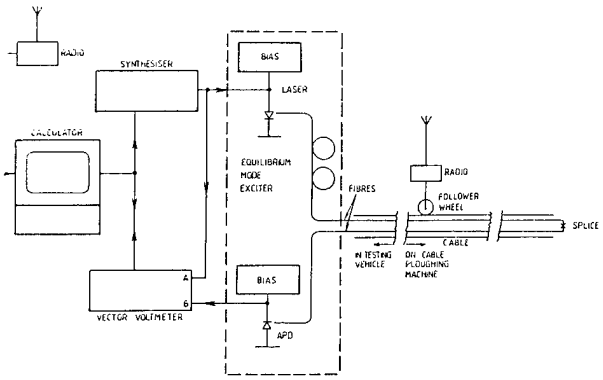



Fig. 2 Fibre Strain Measurement System

The equipment thus described is capable of measuring the fibre elongation relative to its initial state. In order to determine the strain corresponding to this elongation, it is necessary to know the length of cable installed. This was measured by a follower wheel mounted on the cable plough. As each extra metre of cable was ploughed, a data word, representing the cumulative installed length, is relayed by radio from the tractor to the measurement station and entered into the calculator's data record. The stored results can be used to generate a number of records, such as fibre elongation and strain of either residual (steady-state) or transient nature, changes in attenuation, length of cable installed at various times, and cable ploughing speed. In addition, a real-time plot of average strain against length of cable installed can be displayed so that the installation progress can be monitored and installation techniques modified if necessary.

Cables Installed in Trials : Six different cable structures were used in two series of trials in an attempt to establish the effect of cable design parameters on the installation process. The cable structures are shown in Figure 3 and brief details are as follows :

A : Loose tube structure with fibre reinforced plastic (FRP) central strenth member and kevlar peripheral strengthening.

B : Tight stranded structure with six nylon jacketed fibres (0.9mm) and six dummy fillers around a FRP strength member.

C : Spacer-type cable with six nylon jacketed fibres laid loosely in plastic channels between spacers. FRP strength member.

D : Integral type cable with fibres housed in closed slots wihin a polyethylene cartwheel-like structure. FRP strength member.

E : Slotted core structure with FRP strength member.

F : Grooved spacer type cable with FRP strength member.

Most of the cables used on the trials contained filling compounds. All cables were fitted with an additional nylon outer jacket which is traditional in Australia for protection against ants and termites.

Cable Ploughing Equipment: Trials were conducted using various systems and modifications on existing cable ploughing tractors (typically Caterpillar D9 type) to reduce tensions on cables during installation.

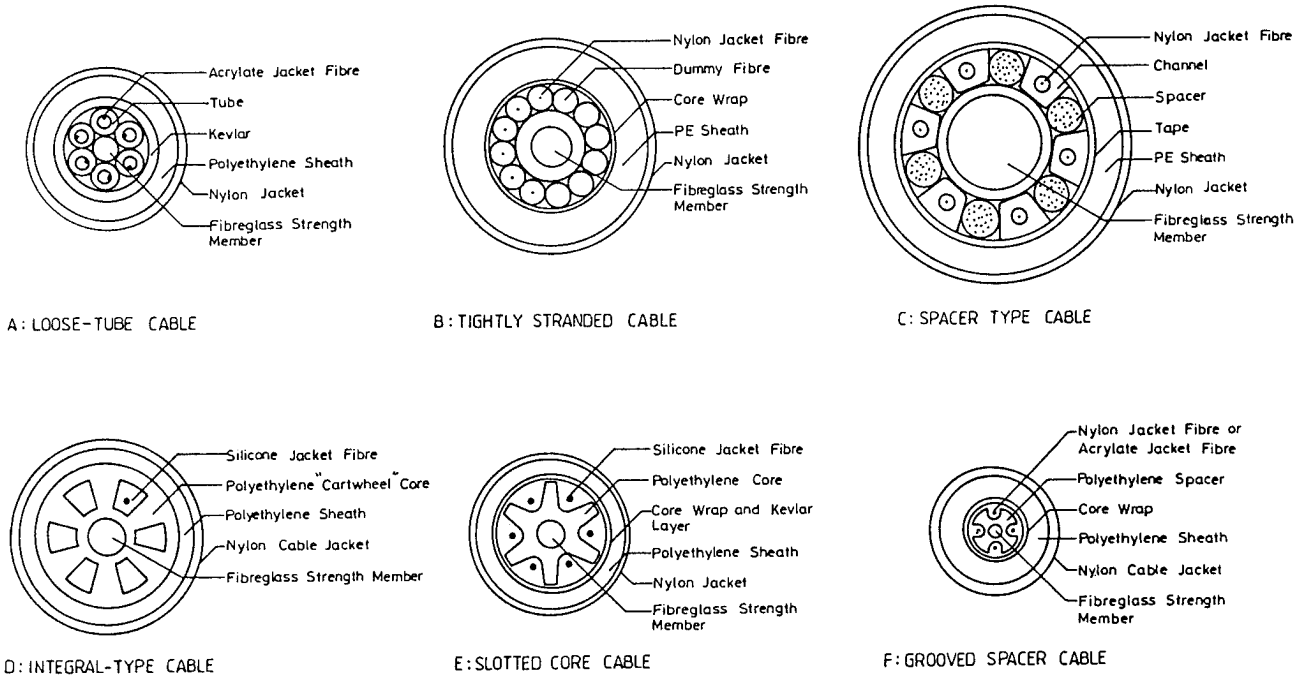



Fig. 3. Cables Installed in Field Trials.

The modifications included:

- Additional tension operated drive capstan at the top of the cable plough box.
- Hydraulic cable drum braking system.
- Automatic Catenary controlled cable drum drive system.
- Teflon lining within the cable plough box.

## RESULTS OF FIELD TRIAL

The field trials demonstrated that optical cables with only minimal strength design can be successfully installed using modified cable ploughing equipment without introducing strain levels that might prejudice the fibre lifetime. Two significant cable design features were identified in the trial :

(a) Cables in which fibres are housed loosely, and which may include some small excess fibre length, provide a degree of protection against transient strains.

(b) Cables with high flexibililty can be installed with smaller residual strain levels than stiffer cables.

With regard to installation equipment, conventional ploughing equipment was found to be less than suitable particularly with cables that did not meet the above criteria. Whilst large residual strains were almost totally attributed to the cable parameters of flexibility and strength, transient strains were heavily dependent on the ploughing equipment. Figure 4 shows the elongation of the spacer-type cable (Figure 3C) plotted against the corresponding length of cable installed. This cable showed the highest residual elongation totalling approximately 600 mm over the 920 metres of cable installed. The observed elongation is considered to arise as a result of the tension required to pull the cable around the 90 degree bend at the lower end of the cable plough-box. This cable was quite stiff and radial reaction forces are produced at points where the cable makes contact with the guiding surfaces of the plough-box. These in turn cause friction forces to act on the moving cable at these points of contact, and in overcoming the friction forces, the cable is left with a residual tension. The use of a more flexible cable, or a plough box with increased radius of curvature, would allow the cable to be placed at a lower tension, and hence a lower strain level. Alternatively additional cable strengthening could be used.

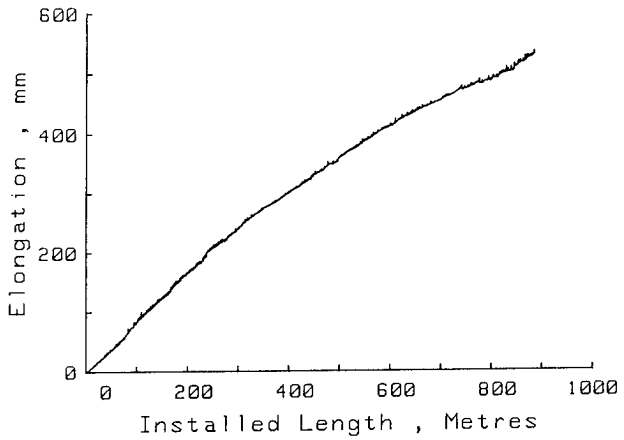



Fig. 4 Elongation versus installed length for Spacer Type Cable 3C

Figures 5 and 6 show the elongation versus time curve for the tightly stranded cable design shown as 3B in Figure 3. Figure 6 provides greater detail showing a 2 minute period starting at approximately the 20 minute mark of Fig. 5. The feature of significance for this cable is the high transient elongations which show as peaks at regular intervals. The installation equipment in this particular experiment did not use any form of drum drive. The peaks occur as tension in the cable increases, and diminish when the tension has reached a level that causes the cable drum to rotate, spilling off excess cable. The elongation values plotted occur basically over the short distance between cable drum and plough box and are values averaged over 2 second measurement intervals. The actual instantaneous elongation values would therefore be higher than those indicated and correspond to a transient strain of up to approximately 0.5%.

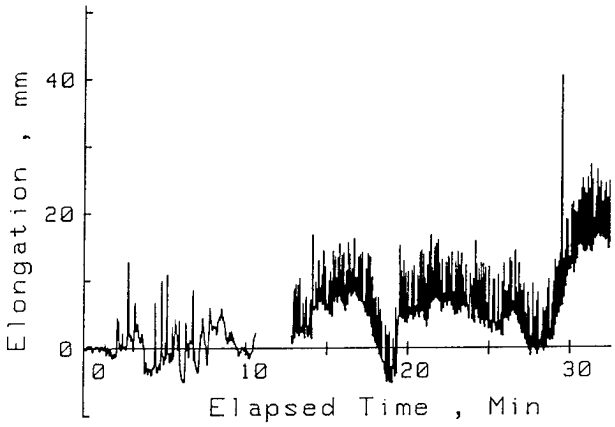



Fig. 5 Elongation versus time for Tightly Stranded Cable

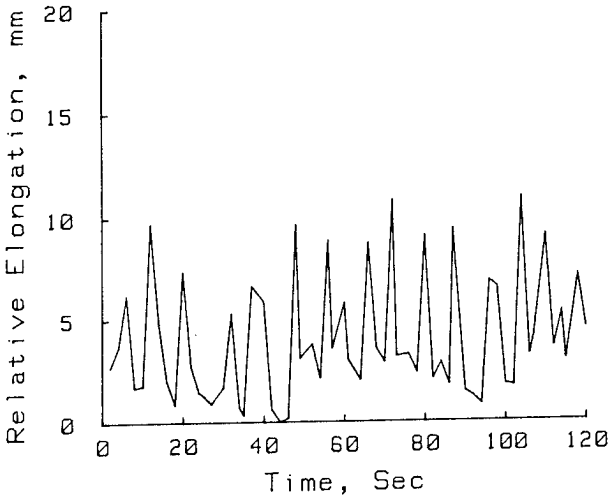



Fig. 6 Expansion of the Figure 5 plot over a two minute interval.

As this level is close to the proof-test level, some action to reduce the transient strain is necessary.

These results indicate the benefits of isolating the cable drum movement and momentum from the installation system. Of significant success in this respect was the automatic catenary controlled drum drive system which was used for the first time in these trials. The use of a reasonable amount of cable slack in the catenary would also assist in diminishing any other effect associated with rapid movements in the tractor itself. Whilst the cable drum brake was of assistance in reducing transient levels, the new catenary controlled drum drive system offered a further improvement in performance to the extent that it effectively concealed any differences in the behaviour of individual designs.

## MODIFIED CABLE INSTALLATION EQUIPMENT

The aims in selecting and developing installation equipment were specifically directed towards absolute strain free installation, should this be possible, rather than accepting small strain values, either long-term or transient. As a result of the trials, and with the above aim in mind, the automatic catenary controlled drum drive equipment was chosen as standard equipment for optical fibre cable installation.

### Cable Feed Control System

The cable drum driving system that was developed monitors cable demand and then adjusts the speed and direction of rotation of the cable drum so that a constant slack loop of cable is always maintained. The overall configuration of the cable feed control system is shown in Figure 7.

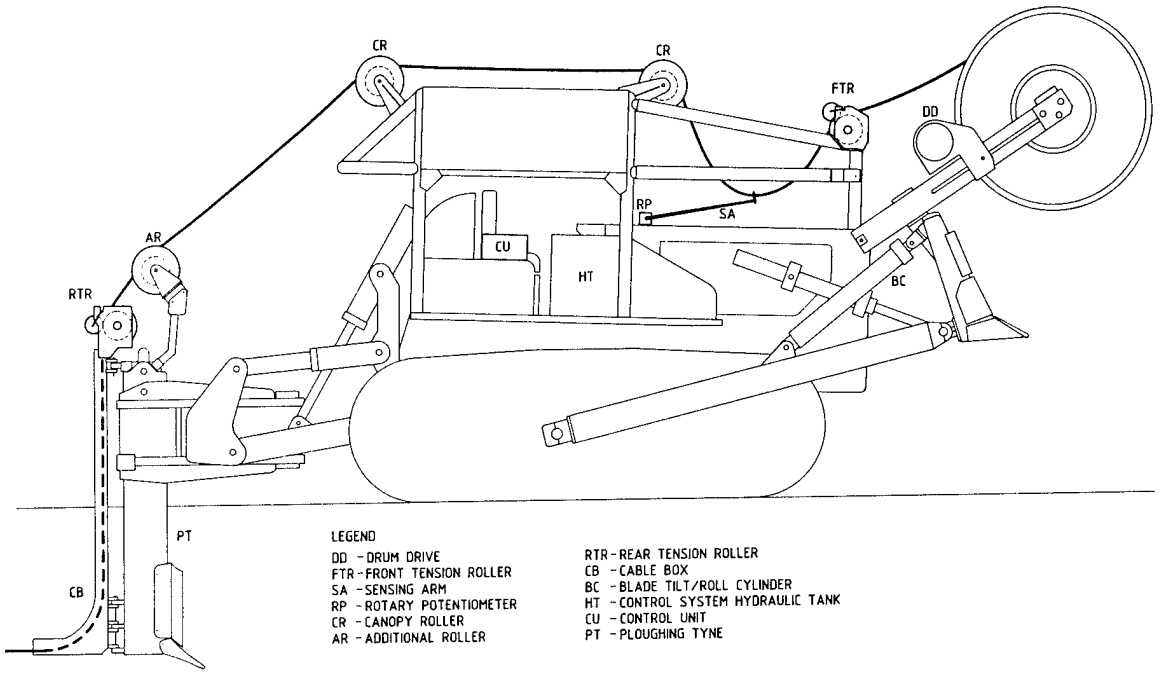



Fig. 7. Schematic Diagram of Modified Cable Ploughing Tractor with Automatic Catenary Drum Drive.

The basic function of the slack catenary loop of cable is to decouple the cable already in the ground and flowing through the cable plough box from the high inertia of the cable drum. The sag in the cable catenary is sensed by a spring-tensioned sensing arm attached to a rotary position transducer which indicates the position of the cable loop. Any deflection of the sensing arm from its normal operating angle results in a signal which causes the electro-hydraulic drum drive to either payout or wind in cable in order to return the sensing arm to its 'normal' angle, and thus maintain the desired sag in the slack loop.

The cable drum, preferably a steel drum, is driven on both flanges via vulcanised rubber wheels. Firm contact between drive wheels and flanges is ensured by two hydraulic cylinders housed within the cable drum carry arms. The control system offers excellent response time between sensing arm deflection and cable payout or wind in. Drum acceleration from 0 to 6 KPH (tractor speed) is possible in only 0.1 seconds through use of the following components:

- A pressure compensated, axial piston pump which is driven off the tractor PTO (Power-Take Off).
- Two high-torque, low speed radial piston motors which rotate the vulcanised rubber drive wheels and thus the cable drum.
- Solenoid operated servo valves mounted directly onto the motor ports. Full hydraulic system pressure is applied to these valves during the cable feed operation, ensuring the fastest possible response of the motors to input control signals.

Overall, this arrangement yields the quickest possible motor reaction to movement of the sensing arm.

The control system has other secondary features:

i. The operator can manually override the system. This is necessary for initial set-up of the cable drum and feeding of the cable through the apparatus.

ii. Tractor autostop. Should the control system malfunction, the tractor transmission is automatically shifted into neutral and the brakes are applied before excessive tension can be applied to the cable.

Other Tractor Modifications: Several other components mounted onto the tractor contribute toward mimimised tension during ploughing of cable:

a. The cable drum is mounted on a hollow spindle rotating on sealed roller bearings.

b. Hydraulically driven rollers in the cable path at the front and rear of the tractor assist the passage of the cable into the plough box. These roller motors develop only a very small torque and are easily stalled. Their overall effect is to keep unwanted slack out of the cable on the tractor, and to balance frictional drag in the feeding path.

c. Stainless steel is used to line the plough box. The expense of teflon lining of the plough box, and the difficulty in securing it to steel, was found not to be warranted.

## CABLE DESIGNS

The requirements of a cable design for use in direct buried long distance and rural applications were set as :

- Non-metallic and filled.
- At least 5km drumlengths.
- Able to be installed by cable ploughing techniques.
- Appropriate crush resistance.
- Minimised cost.

In Australia, metallic sheaths are not required for rodent protection, and as a result the standard sheath on traditional pair type cables has been all plastic. Of major concern however, has been the potential for attack by ants, termites or other insects. It has been found that an additional hard nylon jacket applied over the standard polyethyene sheath offers almost total protection against this problem (reference 9). This same sheath construction is seen as satisfactory for directly buried non-metallic optical cables.

As a result of the field trials, it was shown that high flexibility and a loose cable structure gave the best installation performances. Appropriate designs known to meet those requirements include those based on single slotted core concepts (multiple fibres per slot for higher fibre counts) or loose tube constructions (multiple fibres per tube). These designs have been shown to provide excellent characteristics of flexibility through small cable diameter (ie. high fibre packing densities) and have the ability to provide excellent tensile strength, lateral crush and impact protection.

Relevant Cable Specifications related to cable structure are:

Cable Diameter: In order to maximise cable flexibility and lengths accommodated on limited size cable drums, the overall cable diameter shall be minimal and shall not exceed 20mm for cables up to 60 fibre. Cable lengths in excess of 5km are required.

Tensile Strength: The cable shall have a tensile strength to mass ratio of greater than 5 Newtons/(kg/km). Cables with a mass of less than 100 kg/km require a minimum tensile strength of 500 Newton. The tensile strength is defined as the tension required to produce a strain in the fibres at a level of 30% of the proof-test strain. Designs which include excess fibre length therefore have an advantage.

Minimum Bending Radius: The cables shall be capable of meeting the following minimum bending radius requirements without experiencing cable or fibre damage or attenuation increase:

- 10 times cable diameter at no load
- 20 times cable diameter at maximum tensile strength.

Crush Resistance: Cables must be capable of withstanding a long-term crushing force (ie. statically applied lateral load) of at least 10KN/m, and a short term (1 minute) crushing force of at least 20KN/m without experiencing fibre damage or attenuation increase.

Filling Compound Barrier :

One aspect, which is still under evaluation, is the inclusion of an all plastic barrier material between the cable core and the cable sheath to prevent absorbtion by the sheath of oils and other materials contained in the filling compounds. Several materials show promise for this application through their properties of low permeability to oils, and it is proposed that appropriate laminated plastic tapes made from these materials would be bonded to the inside of the polyethyene sheath in a similar way to existing aluminium moisture barrier laminates.

The requirement for these filling compound barriers arises from concerns that absorbed filling compounds may have a longer term effect on the sheath of the non-metallic optical cable or may leave voids or water paths in the cable core.

## LOCATION OF INSTALLED NON-METALLIC CABLES

Whilst the use of non-metallic cables will have advantages, significant problems may occur when these cables must be located some time after installation.

A number of locating systems have been examined including metallic tapes, wires and cables layed above the optical cable, however none of these has proved satisfactory.

The most successful technique, which will be used on early installations, uses a combination

of marker posts, buried plastic tape, and electronically detectable transponder pegs.

The highly extendable, non-metallic plastic tape is simultaneously ploughed in about 500 mm above the cable. The tape has warning markings, and is designed to attract the attention of anyone digging above the cable.

A marker post system will also be used. Each post will include a sign denoting optical fibre cable, as well as an accurate, permanent sketch plan showing the cable alignment in relation to the post. The sketch is made just after the tractor passes the post location.

In addition, relocatable passive transponder pegs will be buried above the cable at significant changes of direction, and at pre-determined spacings. The pegs can be accurately located to within 50mm, using a special detector.

It is expected that this combination of systems will ensure that the cable is adequately marked and protected, and able to be accurately located after installation.

## CONCLUSION

In countries or areas where metallic cable sheaths are not required for mechanical or rodent protection reasons, non-metallic optical fibre cables can offer significant advantages in relation to lightning damage and on routes affected by electromagnetic induction problems. The costs of these cables could however become excessive if high tensile strengthening elements must be incorporated into the cable designs to cope with the rigours of installation.

As a result of an extensive set of field trials, Telecom Australia has developed cable specifications and installation equipment which will allow low cost non-metallic cables to be installed successfully, and specifically without residual fibre strain. An extensive programme of installation of such cables is now underway and will extend well into the 1990's.

## ACKNOWLEDGEMENTS

Many people rendered valuable assistance in the design and conduct of the experiments and trials and their help is gratefully acknowledged. Special acknowledgement is given to the staff of the Optical Systems Section of the Telecom Research Laboratories and to staff in the Queensland Automotive Plant Section. The permission of the Chief General Manager, Telecom Australia, to publish this paper is acknowledged.

## REFERENCES

(1) S. Tanaka et al. "Lifetime Design of Optical Fibre Cable for Long Term Use", Sumitomo Electric Technical Review, No. 21, January 1982, P. 47-51.

(2) M. Tateda et al. "Thermal Characteristics of Phase Shift in Jacketed Optical Fibres", Applied Optics, Vol. 19 No. 5, 1 March 1980, P. 770-773.

(3) R. Kashyap and M. Reeve, "Single Ended Fibre Strain and Length Measurement in Frequency Domain", Electronics Letters, Vol. 16, No. 18, 29 August 1980, P. 689-690.

(4) S. Tanaka et al. "Precise Measuring Method of Elongation and Residual Strain of Optical Fibre Due to Cabling Process", Seventh European Conference on Optical Communications, Copenhagen, September 1982, P. 6.6.

(5) A.H. Hartog et al. "Variation of Pulse Delay with Stress and Temperature in Jacketed and Unjacketed Optical Fibres", Optical and Quantum Electronics. Vol. 11, 1979, p. 256-273.

(6) O. Kawata et al. "Residual Elongations of Submarine Optical Fibre Cable Laid on the Sea Bottom", IEEE Journal of Lightwave Technology., Vol. LTI, No 1, March 1983, P. 190-194.

(7) T. Kobayashi et al. "Stress in Fibres During Optical Cable Manufacturing Process", Proceedings of the International Wire and Cable Sumposium, November 1978. P. 362-386.

(8) R.W.A. Ayre "Measurement of Longitudinal Strain in Optical Fibre Cables During Installation by Cable Ploughing", Accepted for publication in IEEE Journal of Lightwave Technology.

(9) R.A. Clark & G. Flatau "Development of Nylon Jacketed Telephone Cable Resistant to Insect Attack" 21st International Wire & Cable Sumposium, USA., 1972.

B.T. de Boer
External Plant Inter-
Exchange Networks Branch
Telecom Australia
28/570 Bourke Street
MELBOURNE VIC 3000
AUSTRALIA



Bob de Boer is currently head of the External Plant Inter-Exchange Networks Branch at Telecom Australia. He joined Telecom Australia in 1972 after graduating in Electrical Engineering from Monash University in Victoria. He has had extensive experience in areas of telecommunications cable design, specifications and provisioning, as well as in the installation of External Plant. He currently has full responsibility for all external plant aspects of optical fibre systems within Telecom Australia.

R.W. Ayre
Optical Systems Section
Research Department
Telecom Australia
770 Blackburn Road
CLAYTON VIC 3168
AUSTRALIA



Robert W.A. Ayre received the BS degree in Electronics from the George Washington University, Washington DC in 1967, and the BE and M.E.Sc degrees from Monash University, Melbourne in 1970 and 1972 respectively. In 1972 he joined the Research Laboratories of Telecom Australia, initially working on video signal processing techniques and transmission systems. Since 1977 he has been working on optical transmission systems and optical fibre measurement techniques. He is currently Head, Optical Systems Section, Telecom Australia Research Laboratories, Melbourne, Australia.

R.B. Schuster
Automotive Plant Section
Telecom Australia
54 Postle Street
COOPERS PLAINS
QUEENSLAND 4208
AUSTRALIA



Richard Schuster joined Telecom in 1982 after graduating from the University of Queensland. He has had substantial experience in external plant installation activities associated with cable ploughing equipment and procedures.

# A NEW WIRE CONNECTOR JOINS A PAIR WITH A PINCH

T. C. Cannon and D. T. Smith

AT&T Bell Laboratories
Norcross, Georgia 30071

## Abstract

A new, pair-at-a-time, wire connector has been developed that may be installed with an ordinary pair of pliers. The connectors may be used for making repairs to modular splices, rehabilitating pedestals and splicing small pair count cables. Because of its in-line configuration, it is well suited for splicing with little slack and for making half taps.

## Introduction

A new, pair-at-a-time connector has been developed for splicing outside plant multipair cable. The connector is the latest in a series that began with the B-Wire Connector and includes the 700-type connector. The introduction of waterproof cable and aluminum conductors hastened the development of 700-type connectors for joining individual conductors and somewhat later the 710 Modular Connector for joining 25 pair units with greatly improved joining rates. The new connector, coded the 709 Connector, complements a modular joining system by providing a more space efficient and convenient way of splicing a pair of wires with common tools than using individual wire connectors. The 709 connectors' areas of application, salient features, design details and performance are discussed in the sections that follow.

## Application

The primary use for the connector is for splicing small pair count cables. The new connector is also particularly well suited for making repairs and rearrangements to existing splices.

## Features and Capabilities

A notable feature of the connector is its ability to be installed with commonly available splicers' tools. A pair of snips (for wire trimming) and a pair of long nose pliers (for pressing the connector) are all that is needed. This feature unburdens the splicer from having to transport and maintain a variety of special purpose connector application tools to handle different splicing situations. For splicing larger pair count cables, a magazine type pressing tool is available.

The connector can handle wire sizes from 22 to 26 gauge and comes in either filled or unfilled versions. The arrangement of the contact elements in the connector body allows the wires to be joined in an in-line fashion, thus facilitating splicing with a minimum amount of slack. The connector can also be used for half-tapping.

The connector is extremely space efficient in that it joins two wires in a 0.15"x0.3"x0.95" envelope. The pair-at-a-time feature not only increases space efficiency, but helps preserve tip/ring identity.

## Design Details

The heart of the design of the new connector is its new, low profile, split beam, insulation displacing contact element. The low profile allows the element to accept a broad range of wire sizes, yet fit into a small package. The dimensions of the U-shaped element are tailored to allow elastic energy to be stored in its beams during wire insertion. Unlike other split beam contacts, the low profile contact stores energy in both bending and torsion. This feature gives it the compliance necessary to accept a wide range of wire sizes yet be stiff enough in the wire insertion direction to completely remove the insulation from the wire. The energy stored in the contact elements helps insure long term electrical reliability.

Since the connector body is injection molded from clear plastic, it is easy for splicers to verify proper wire insertion. A center rib which runs the length of the connector body assures that the connector will be properly

closed, even when pressed with tools having non-parallel jaws (as is the case with long nose pliers).

The connector housing is fabricated by assembling two separate plastic parts - the cover and base. The two ends of the connectors' cover are separately hinged and thus permit wires entering one end to be pressed independent of wires entering the opposite end. This has a strong positive influence on wire handling efficiency since one pair of wires can be inserted, pressed finger tight and kept under control while the splicer performs a similar operation with the remaining pair of wires. Final connector pressing with the pliers can then be done without the splicer having to contend with positioning the wires. Internal features of the housing provide dielectric separation between the two contact elements, strain relief gripping of the wires and latching that holds the housing parts together.

Half-tapping is done by first terminating the cut or tap pair in one end of the connector. The opposite end of the cover is then removed by twisting it off with ones' fingers or pair of pliers. In its place is inserted a half-tap adapter, through which the through wires have been routed and temporarily secured in place. The half-tap adapter is then pressed in place with pliers thereby forcing the through wires into the contact elements and automatically completing the electrical bridge.

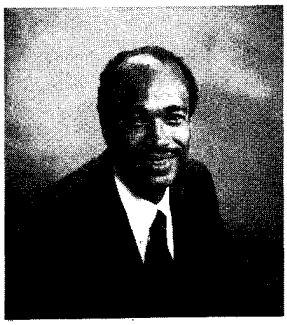
The connector contains two thin walled dimples on its underside to facilitate penetration by test probes. Such penetration permits direct contact with the contact elements.

## Performance

The 709 Connector has been subjected to a barrage of tests to characterize its performance. It has been tested to both AT&T standards and REA PE-52. These tests are summarized in Table I. The connector meets all specifications.

## Summary

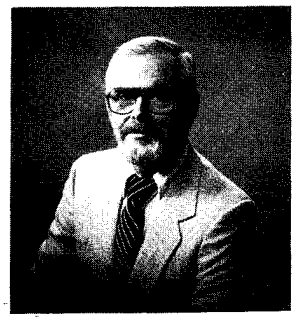
In a cable joining system dominated by modular connectors, the new 709 Connector provides a quick, inexpensive means for joining small pair count cables and making repairs without the need for special application tools. Its full pair capability helps maintain tip-ring identity and keeps the connector size per pair small. It can be used for making both in-line splices and half-taps.



T. C. Cannon (Tom) is supervisor of the Connector Systems Development group. This group has responsibility for developing standard connectors and tools for splicing electrical and lightguide communication cables.

Tom joined AT&T Bell Laboratories in 1970 and worked in the Safeguard Laboratory. His initial assignment dealt with modeling the behavior of missiles in a tactical nuclear environment. Since that time Tom has worked in Ocean Systems and in Loop Transmission. Some of his activities in Loop Transmission have included analytical modeling of lightguide cables and design of lightguide cable splicing hardware.

Tom did both his graduate work and undergraduate work at Purdue University. He received his Ph.D. in Aeronautical, Astronautical and Engineering Sciences in 1970, with a major in solid mechanics.



Donald T. Smith is a Member of Technical Staff in the Connector Systems Development group of AT&T Bell Laboratories. He is a graduate of Wentworth Technical Institute and has been associated with the development of connector systems from 1960 to present.

TABLE I
Testing the 709 Connector

| Test | Source | Method | Requirement | Results |
|---|---|---|---|---|
| Wire Pullout | AT&T | Tension applied at 2"/min | > 60% of Unjoined 22 ga wire strength | Pass |
| | | | > 70% of Unjoined 24 ga wire strength | Pass |
| | | | > 80% of Unjoined 26 ga wire strength | Pass |
| Wire Twist | REA | 90° twist left and right while measuring resistance | < 2% resistance variation (includes 4.8 inches of wire) | Pass |
| Vibration | REA Modified | Vibrate sample in 3 planes, 20 min. ea., 10 to 55 Hz | No momentary opens | Pass |
| | | | < 2 milliohm change at 99.99 percent | Pass |
| Dielectric Strength (wet) | REA | Immerse sample. Increase voltage 500 V rms/sec | > 2500 Vrms | Pass |
| Dielectric Strength | AT&T | Withstand 60 Hz One minute. | > 3000 Vrms | Pass |
| Insulation Resistance (wet) | AT&T | Immerse sample 3 days, dry 3 days - repeat 5 times | > $10^8$ ohms | Pass |
| | | Measure resistance to water @ 100 V DC | | |
| Insulation Resistance (High Humidity) | AT&T | 95% R.H. 30 days cycle temp 32° to 140°F. Sample in lead shot | > $10^8$ ohms | Pass |
| | | Measure resistance to shot | | |
| Contact Resistance (Temp Cycle) | AT&T | 1024 cycles - -40 to 140°F Measure resistance change | < 2 milliohm change at 99.99% | Pass |
| Contact Resistance (Thermal Shock) | REA Modified | 100 cycles liquid nitrogen to 180°F | < 2 milliohm change | Pass |
| | | Measure resistance to change | | |

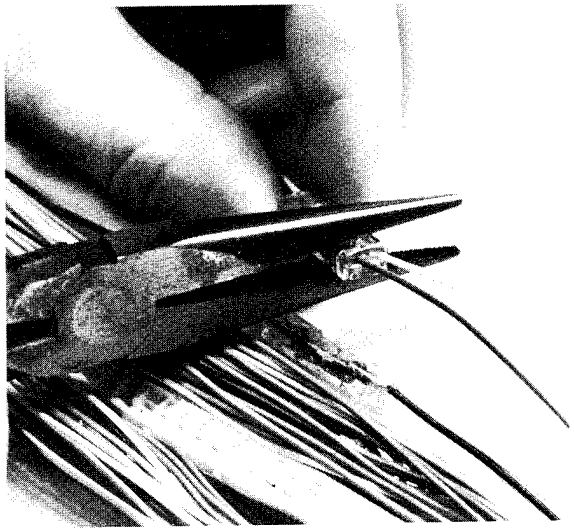


FIGURE 1. THE 709 CONNECTOR IS DESIGNED TO BE PRESSED WITH PLIERS. IT IS SHOWN HERE IN A REPAIR APPLICATION.

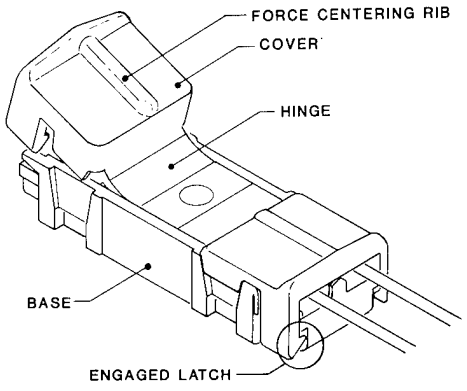



FIGURE 2. THE 709 CONNECTOR HAS TWO INDEPENDENTLY CLOSING ENDS. THIS AIDS WIRE HANDLING.

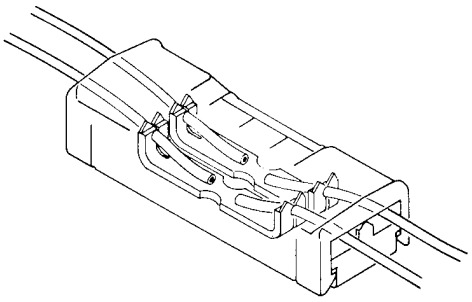


FIGURE 3. TWO LOW PROFILE CONTACTS SHOWN IN A COMPLETED CONNECTION. MOLDED RIBS BETWEEN THE CONTACTS (NOT SHOWN) MAINTAIN DIELECTRIC STRENGTH.

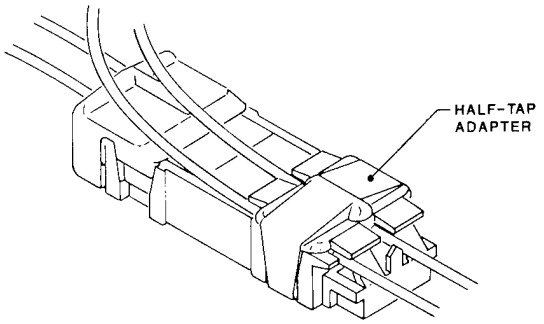



FIGURE 4. THE 709 CONNECTOR IS USED FOR HALF-TAPPING BY REPLACING ONE OF THE HINGED ENDS WITH AN ADAPTER.

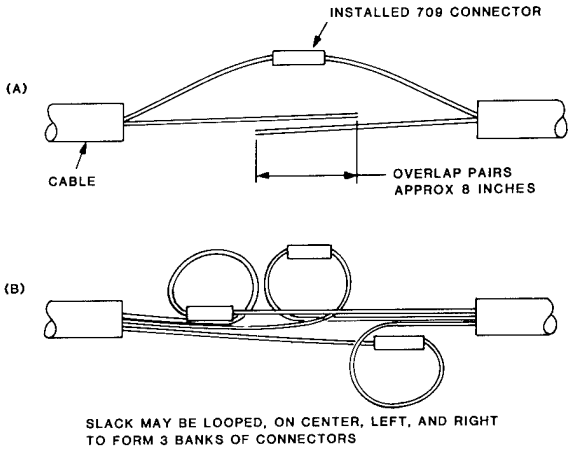



FIGURE 5. A SUGGESTED METHOD FOR AN IN-LINE SPLICE WITH THE 709 CONNECTOR.

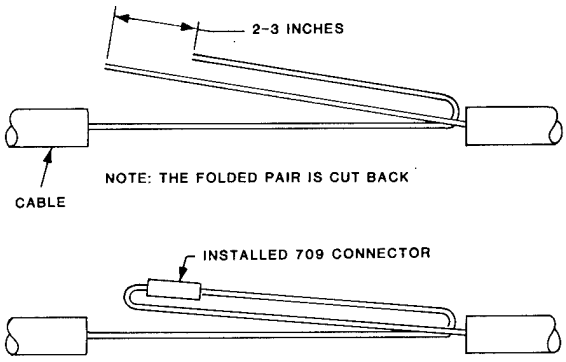



FIGURE 6. THE 709 CONNECTOR MAY BE USED IN FOLDBACK SPLICES.

# LOCAL LAUNCH AND MONITOR FOR SINGLE-MODE SPLICING

R. HUGHES, V. SO, & P.J. VELLA

BELL NORTHERN RESEARCH

## ABSTRACT

A novel evanescent field coupling technique of injecting light into and out of jacketed single-mode fiber core is described. This technique couples enough light into the guided mode for the alignment during splicing of color-coated fiber. Splice loss of less than 0.2 dB is readily available in the field by this one-man splicing technique.

## INTRODUCTION

The last few years have demonstrated a major trend to the utilization of single-mode fiber cables in toll and trunk applications. As a result, there is a need for an efficient method of splicing single-mode fibers. Unlike multimode fiber, single-mode fiber splicing requires a precise core to core alignment to ensure low loss. This is due to the small core diameter, core/cladding eccentricity, and mode-field diameter mismatch. Until recently this alignment was achieved in the field using a straight forward method.

The three station method requires one operator to launch light at the link origin, another at the far end of the cable being spliced onto the link, and of course the splicer. The operator at the far end connects the fiber being spliced to a detector and the optical power level is transmitted to the splicer via order wire. This method is labour intensive, time consuming, and there are the attendant communication problems.

Recent efforts to improve this situation have resulted in two separate approaches. These are visual core alignment and local launch/detect. Examples of the former are the use of core fluorescence (1), the insertion of a beam splitter (2), phase contrast microscopy (3), and vidicon /T.V. monitoring (4). The latter involves bending one fiber to locally launch light and bending the other fiber to locally detect the signal (5).

In order to achieve minimum splice loss the fibers must be aligned to give maximum optical throughput. Local launch/detect methods ensure maximum optical throughput whereas it is not necessarily the case with visual core alignment.

In this paper we are presenting a novel technique utilizing evanescent field coupling to launch light locally into the fiber resulting in a 10 dB improvement in coupling efficiency over conventional bending methods.

## THEORY

When a fiber section is bent into an arc of radius R there exists in the plane of the fiber arc a radius $R_c$ (> R) at which the wave vector of the guided mode is just equal to the wave vector k of a plane wave. For distances greater than $R_c$ the field of the guided wave is coupled to the radiation field. The radius R is given by

$$R_c = R\ \beta/k$$

for typical situations (eg. R = 1 mm, $\beta/k$ = 1.47, $R_c$ = 1.47 mm) $R_c >> a$, where 'a' is core radius of the fiber, and the field strength of the guided mode is small. Therefore, coupling between the guided mode and the radiation field is small. To improve the coupling efficiency the evanescent microbending coupling technique is used.

The fiber is bent and simultaneously pressed against the hypotenuse of a right-angled glass prism (Figure 1). The wave vector paralled to the fiber axis is now given by $k_{11} = nk \cos \Theta$,

where n is the refractive index of the glass prism, and $\Theta$ is the angle between the incident beam and the fiber axis. By judiciously choosing n and $\Theta$, one can get $k_{11} \cong \beta$, making the coupling most efficient near the fiber core, where the field strength of the guided mode is maximum. In this fashion about 10 dB improvement in the coupling efficiency is obtained.

## DESIGN AND USE

A prototype local launch monitor (LLM) was designed and built based on the evanescent field coupling technique described above. A schematic of the launch block is shown in Figure 2. A modulated laser diode operating at a center wavelength of 840 mm is focussed onto the bend in the launch block. The core light of this fiber is detected via the core of the second fiber positioned in the detect block (Figure 2). A phase sensitive detection scheme provides a net dynamic range of 25 dB and an alignment sensitivity of ± 0.05 dB. The current LLM can be used with most conventional single-mode fusion sets as depicted in Figure 4. It is modular in design consisting of a launch module, detect module and a control unit (Figure 7). Light level during alignment is displayed to one hundredth of a dB on the LCD of the control unit.

## TESTS AND RESULTS

The LLM was tested with the Northern Telecom fusion test set to determine its sensitivity to lateral fiber displacement. Once the fibers were aligned to a maximum throughput power, the fibers were displaced by 10 microns in an axis orthogonal to the core axis. One fiber was then scanned along this orthogonal axis through the power peak and 10 microns to the opposite side. The results are presented in Figure 5 where it can be seen that fiber alignment to better then half a micron is achievable.

Both prototype and production units were subjected to technical and field trials. During these trials LLM readings were recorded just prior to and immediately after fusion. It was found that a positive change generally corresponded to a low loss splice.

Figure 6 represents data on splices done with the LLM and an NT fusion splicer. In the case where the pre/post fusion readings decreased, the splice was redone. All the other splices were then measured using the cut-back method. It can be seen on Figure 6 that about 80% of the splices are better then 0.2 dB (in fact, 54% are better than 0.1 dB), and the average splice loss is 0.12 dB. These results confirm that the LLM can give a very good qualitative indication of splice quality.

## SUMMARY

The use of evanescent field coupling technique results in a 10 dB improvement over conventional bending local launch methods. Therefore, the LLM can be used for the accurate alignment of color-coated fibers. Technical and field trials have shown that the splice loss achieved is equal or better than the conventional 3 station method. Furthermore, a qualitative indication of splice loss is given by the pre/post fusion readings.

## REFERENCES


1) K. TAKETURA, H. YAMAMOTO and M. NUNOKAWA, "Novel Core Alignment Method For Low-Loss Splicing of Single-Mode Fibers Utilizing UV-Excited Fluorescence of Ge-doped Silicon Core". Electron Lett. Vol. 18, No. 16, pp. 712, 1982.

2) K. ZMON, and M. TOKUDA, "Axis-Alignment Method for Arc-Fusion Splice of Single-Mode Fiber Using a Beam Splitter". Opt. Lett. Vol. 8, No. 9, pp. 502, 1983.

3) T. HAIBARA, M. MATSUMOTO, T. TANIFUJI and M. TOKUDA, "Monitoring Method For Axis Alignment of Single-Mode Optical Fiber and Splice Loss Estimation". Opt. Lett. Vol. 8, No. 4, pp. 235, 1983.

4) O. KAWATA, K. HOSHINO, Y. MIYAJIMA, M. OHNISHI, and K. ISHIHARA, "A Splicing and Inspection Technique for Single-Mode Fibers Using Direct Core Monitoring". Journal of Lightwave Technology, Vol. Lt. 2, No. 2, pp. 185, 1984.

5) C.M. DeBLOK and P. MATTHIJSSE, "Core Alignment Procedure for Single-Mode Fiber Jointing". Electron. Lett., Vol. 20, No. 3, pp. 109, 1984.

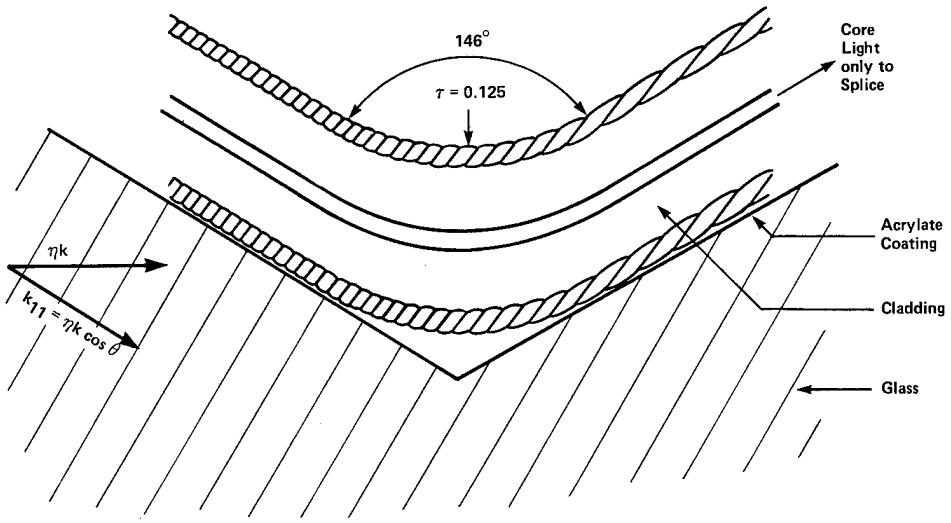



Figure 1 Principle of Operation – Local Launch and Detect

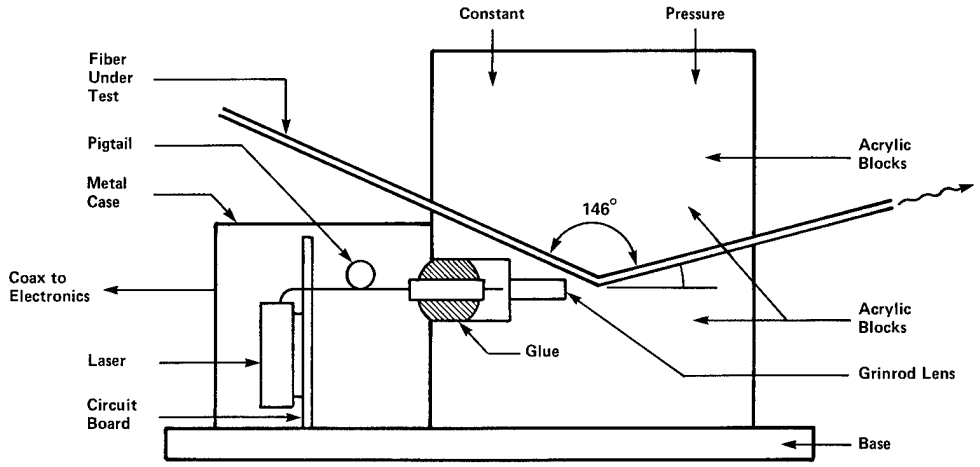



Figure 2 Schematic of Launch Block

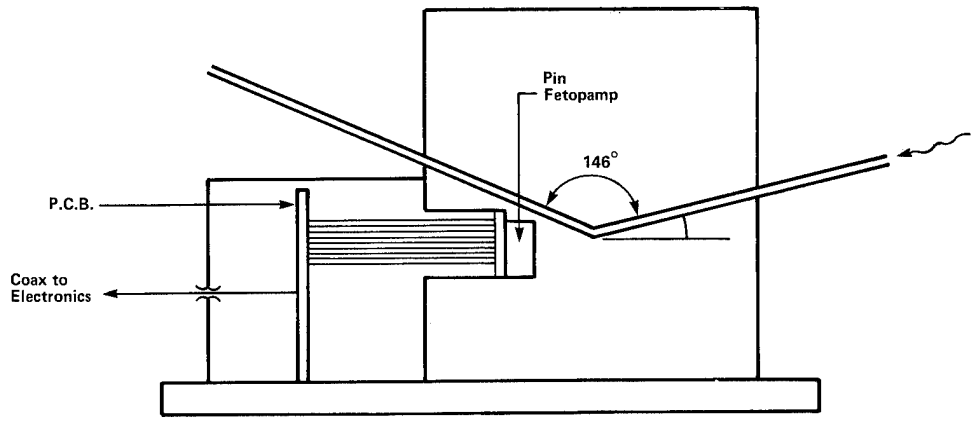



Figure 3 Schematic of Detect Block

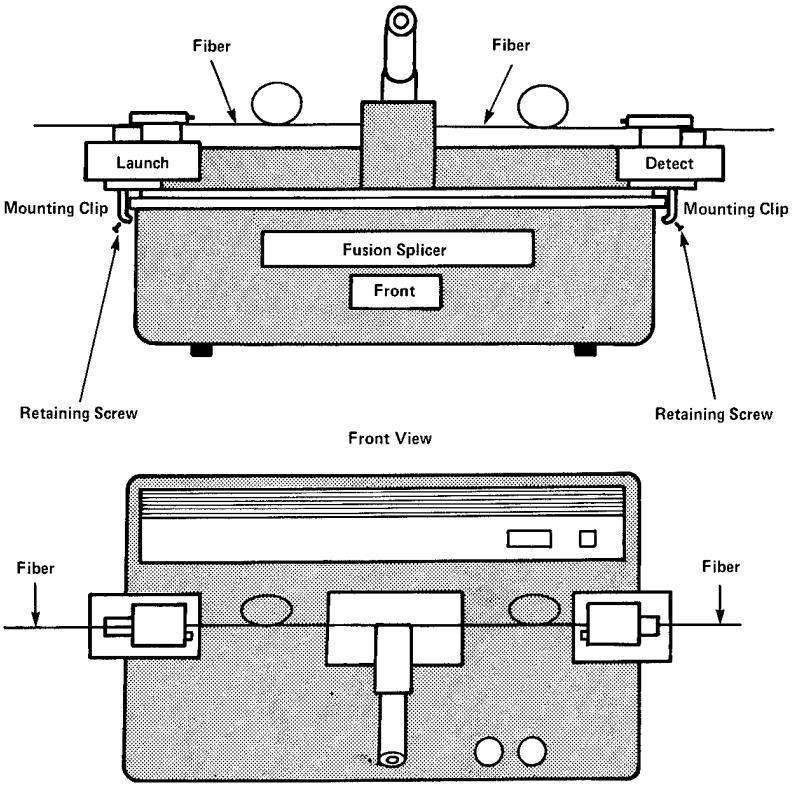



Figure 4 Splicing with LLM and Fusion Set

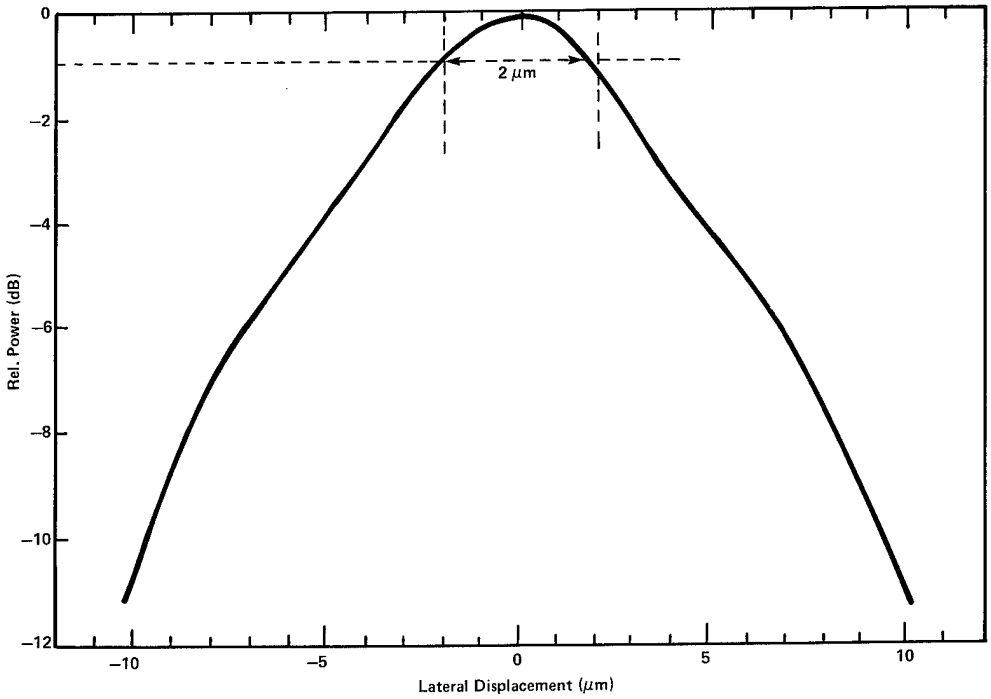



Figure 5 Optical Power Through Splice

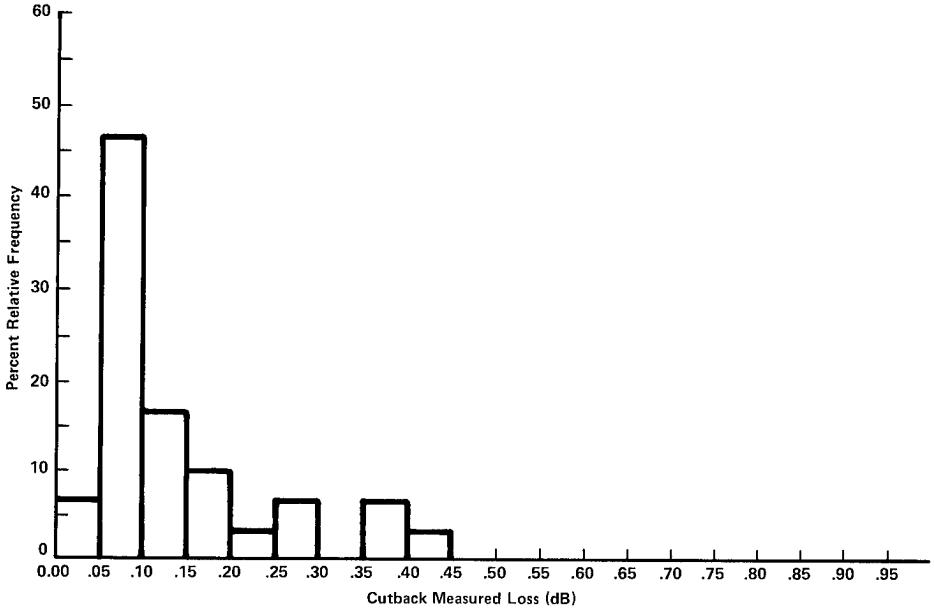



Figure 6 Splice Loss Using the LLM

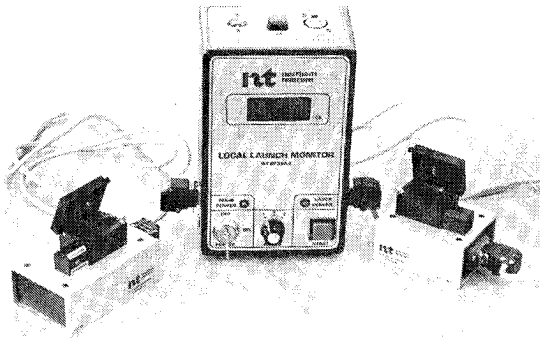
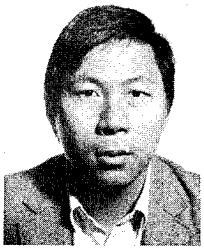


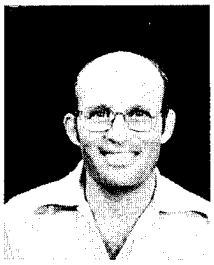

Figure 7



Vincent So received his Ph.D. in Physics from the University of Toronto in 1981, and joined the National Research Council of Canada. In 1984 he joined Bell Northern Research. Currently he is working on fiber characterization, and advance fiber link products.



Richard Hughes received his B.Sc. Physics Degree in 1977 from Concordia University in Montreal. That same year he joined Westinghouse Industrial Products Division where he worked as a Technical Co-ordinator. In 1979 he was employed by Canada Wire and Cable where he was engaged in Fiber Optics Research and Development in the areas of cables and fiber optic couplers. Since joining Bell Northern Research in 1984, Mr. Hughes has been a member of Scientific Staff in the Fiber Transport Link Technology Group.



Paul J. Vella received a Ph.D. in Physics from the University of Toronto in 1974. He joined Bell Northern Research in Ottawa in 1980 and was involved in high frequency fiber system research and fiber characterization techniques. After a brief stay at Northern Telecom where he worked on numerical techniques for characterizing single-mode fiber, he joined the Bell Northern Research Fiber Lab in Edmonton where he currently manages the Fiber Link Products Research.

# THE ROLE OF RE-ENTERABLE ENCAPSULANTS IN WATERPROOF CLOSURES ON METALLIC TELECOMMUNICATIONS CABLES

K. Dawes

Raychem Manufacturing Corp.
Fuquay-Varina, NC

T. E. McNeal

Bell South Services
Birmingham, AL

The use of re-enterable urethane encapsulant for the waterproofing of metallic telecommunication cable has been required in the industry for over a decade. However, both petroleum jelly and Flexgel cables have shown oily interfaces when in contact with the current encapsulants, which can potentially lead to water leak paths and subsequent failure of the closure. The need for an encapsulant which eliminates the interfacial oils became apparent.

This paper describes a range of experiments used to determine the parameters that a new encapsulant must satisfy to give enhanced performance in a buried closure system.

## Introduction

A major requirement for telecommunication links is a reliable operation for at least 20 years. The reliability of the system can be greatly influenced by water ingress, either down the cable or at a cable splicing point. The splice closure can often be a vulnerable section and the practice of using a re-enterable urethane encapsulant for the waterproofing of metallic telecommunications cable splice closures has been required in the industry for over a decade. The main application being in the area of buried closures which are most susceptible to water entry and migration problems.

The presence of water in a copper system will inevitably lead to a deterioration in transmission properties. The new Bell South specification, which addresses the buried closure system and not just the closure itself, has highlighted several areas where urethane encapsulants currently used by the Bell Operating Company are weak.

Over the past 12 months, several new re-enterable urethane encapsulants have been produced. The discussion will review some of the properties in general and describe the functional testing of these second generation re-enterable urethane encapsulants.

In accessing the properties of a re-enterable encapsulant, a successful candidate should

-Be compatible with the filling compound in the cable,

-Have good penetration of the cable core to ensure blocking,

-Be readily and easily re-entered, and

-Be as craft insensitive as possible.

## D-Encapsulant

D-Encapsulant is the most commonly used encapsulant at the present time and has been in use for almost a decade. The encapsulant is prepared by mixing an isocyanate prepolymer with a polyol, and applied to the splice closure by either gravity pouring or by a forced encapsulant system. The latter method has gained a large amount of acceptance within the industry, since good cable core penetration cannot be achieved by gravity poured encapsulation.

The evaluation of splice closures using D-Encapsulant in the Bell South specification showed that water ingress in a splice closure was present when the complete closure was subjected to a temperature excursion of >54°C, and then was immersed in 3 feet of water and/or 8 ft. waterhead applied down the core of the cable for 30 days. Water was detected via measurement of the insulation resistance during applied waterhead and dissection.

When left at ambient temperature or temperatures <54°C, the closure was dry after the normal 8 ft. waterhead. This phenomena was observed irrespective of the type of filling compound used in the cable. Both petroleum jelly and flexgel filled cables showed water ingress down the core at temperatures >54°C.

On re-entering the closures, the encapsulant was not dry but had an oily consistancy. Petroleum jelly filled cable had considerable amounts of oil present. The work of Sabia and Mitchell (Table I[1]) in developing Flexgel showed that petroleum jelly coated conductors have a weak pull out strength when embedded in D-Encapsulant. Flexgel, on the other hand, has a much stronger pull-out force. Flexgel is clearly shown to have some compatibility with D-Encapsulant at room temperature.

Table I[1] (Sabia, Mitchell)

PULL OUT STRENGTH OF INDIVIDUAL CONDUCTORS EMBEDDED IN D-ENCAPSULANTS

| Filling Compound | Pull-Out Strength (lbs.) Uncleaned | Cleaned |
|---|---|---|
| Flexgel | 2.47 | 2.84 |
| Petroleum | 0.27 | 3.96 |

Experiments were conducted in which D-Encapsulant was allowed to cure in contact with petroleum jelly and Flexgel. An oily film was very visible in the core of petroleum jelly and traces of oil were found on the case of Flexgel. The differences in pull-out strengths found by Sabia and Mitchell can be explained by the presence of interfacial oily layers, petroleum jelly being the dominant oily interface.

In order to understand the water ingress after a temperature excursion of >54°C, an attempt to measure the pull-out strengths at elevated temperatures (60°C) was carried out. Samples of air core, petroleum jelly, and flexgel coated conductors were embedded in D-Encapsulant in a test tube, allowed to cure, and then placed in an oven at 60°C. After a period of 30 minutes, the conductors coated with filling compound were observed to be "extruding" from the encapsulant, and measurement of the pull-out strength was zero.

The summary of results shown in Table II indicate that although Flexgel has some compatibility at room temperature, elevation of the temperature level leads to a complete loss of adhesion. Further evidence of oily interfaces with petroleum jelly and Flexgel is shown in Table III; measurement of weight gain or loss of the curing encapsulant in direct contact with the filling compound was carried out. Accelerated aging by placing a sample of sured D-Encapsulant in contact with the filling compound for 7 days at 60°C is shown in Table IV.

Table II

PULL-OUT STRENGTHS OF CONDUCTORS IN D-ENCAPSULANT

| Filling Compound | Pull-Out Strength (lbs.) 23°C | 60°C |
|---|---|---|
| Air Core | 5.28 | 3.30 |
| Flexgel | 2.64 | -- |
| Petroleum Jelly | 0.22 | -- |

Table III

% WEIGHT LOSS/GAIN OF D-ENCAPSULANT ON CURING IN CONTACT WITH FILLING COMPOUND AT RT

| Filling Compound | % Wt. Gain/Loss | Oily Layer |
|---|---|---|
| Petroleum Jelly | -10.4 | Yes |
| Flexgel | - 4.9 | Yes |

Table IV

% WEIGHT LOSS/GAIN OF CURED D-ENCAPSULANT ON CURING IN CONTACT WITH FILLING COMPOUND ( 7 Days @ 60°C)

| Filling Compound | % Wt. Loss/Gain |
|---|---|
| Petroleum Jelly | -22.3 |
| Flexgel | - 8.6 |

Tables III and IV show that D-Encapsulant looses oil when in contact with either petroleum jelly or Flexgel. The generation of oily interfaces, when D-Encapsulant is in contact with a coated conductor, can lead to potential leak paths and allow water ingress from the cable into the splice area.

## NEW GENERATION RE-ENTERABLE URETHANE ENCAPSULANTS

Numerous new re-enterable encapsulants have been evaluated in comparison to D-Encapsulant. The initial evaluations centered on

-Good pull-out strength on coated conductors at 60°C, and

-The ability to absorb filling compounds.

Table V summarizes the experimental results for a series of encapsulants. The results clearly show a major enhancement of adhesion properties of the coated conductors. Significant filling compound absorbing properties were also noted. All of the new generation encapsulants have high pull-out strength at 60°C when compared to D-Encapsulant; all readily absorb Flexgel.

When cured in contact with the filling compound, all the new encapsulants absorb both Flexgel and petroleum jelly. When left in contact with cured encapsulant, petroleum jelly is absorbed by one encapsulant (W), however, the other encapsulants show substantial improvement over "D".

The oil absorbancy increase by the new encapsulants is reflected in the substantial increase in pull-out strength, especially at high temperatures. In fact, all the new encapsulants have a pull-out strength at 60°C with petroleum jelly, that is higher than D-Encapsulant at 23°c. Many have a pull out strength in petroleum jelly at 60°C approaching that of D-Encapsulant with Flexgel at 23°C. Better adhesion between the conductor and encapsulant can lead to a better performing encapsulant since a potential leak path has been eliminated.

All the encapsulants have superior properties to D-Encapsulant when the oil absorbing properties are evaluated. However, several other factors are important in choosing a replacement for D-Encapsulant. Viscosity of the urethane mix prior to curing, and the rate of cure are also are important considerations.

Table V

COMPARATIVE STUDIES OF ENCAPSULANTS

| | "D" | W | X | Y | Z |
|---|---|---|---|---|---|
| Pull-Out Strength (lbs. @23°C) | | | | | |
| Air Core | 5.28 | 5.72 | 4.18 | 1.98 | 5.06 |
| Flexgel | 2.64 | 8.58 | 4.84 | 4.62 | 8.14 |
| Petroleum Jelly | 0.22 | 4.18 | 2.86 | 2.86 | 4.18 |
| Pull-Out Strength (lbs. @60°C) | | | | | |
| Air Core | 3.30 | 11.20 | 6.82 | 5.72 | 11.22 |
| Flexgel | -- | 5.28 | 2.42 | 3.08 | 5.50 |
| Petroleum Jelly | -- | 2.42 | 0.88 | 1.54 | 2.20 |
| % Wt. Loss/Gain of Curing In Contact | | | | | |
| Flexgel | -4.9 | +7.0 | +4.3 | +6.8 | +6.4 |
| Petroleum Jelly | -10.4 | +0.7 | +0.9 | +0.8 | +1.2 |
| % Wt. Loss/Gain For 7 Days Contact At 60°C | | | | | |
| Flexgel | -8.6 | +8.4 | +4.5 | +6.8 | +4.5 |
| Petroleum Jelly | -22.3 | +0.4 | -6.9 | -7.7 | -4.5 |

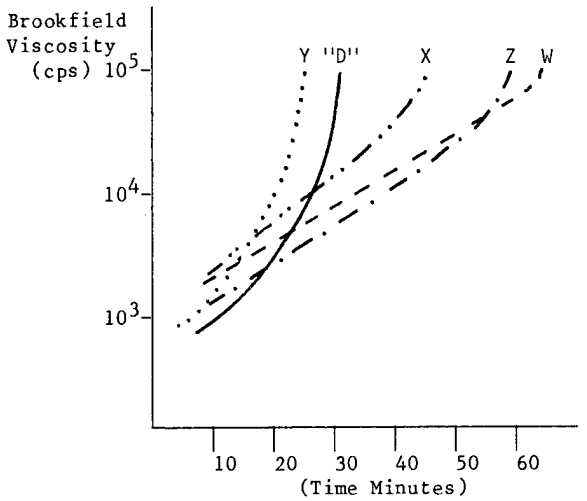
Figure 1 shows the viscosity increase with time for "D" compared to the new generation encapsulants. "D" and Encapsulant Y have a very rapid viscosity increase with time. The other three have a different behavior in that although the initial viscosity is higher that "D", the increase in viscosity is not as rapid as "D". In fact, the viscosity increase profile is much flatter. Encapsulants X, Z, and W have much longer cure times in comparison to "D".

A slow viscosity increase with time is an advantage in using encapsulants in a buried splice closure. In the case of large pair count cables, penetration of the core is difficult. As the viscosity increases, the degree of penetration will decrease. In hot climatic conditions, very rapid curing (i.e. rapid increase in viscosity) will be problematic during installation. The craft person must work rapidly, and any unforseen delay could lead to a mix too

viscous to allow good penetration. Even with a forced encapsulation system which applies pressure to force encapsulant into the core, craft sensitivity can be important.

Figure 1

BROOKFIELD VISCOSITY MEASURED AT RT




The encapsulants with a longer cure time and flatter viscosity profile allow more time for penetration at low viscosities. The craft sensitivity should be greatly reduced, especially in hot climatic conditions.

## Functional Testing

The small scale laboratory experiment discussed previously has identified several encapsulants with properties superior to "D", notably, enhanced adhesion and removal of oily interfaces at the conductors. Functional testing of the encapsulants was carried out on

(a) a typical gravity poured closure, and

(b) a heat shringable closure using a forced delivery system.

### Gravity Poured Closure

Splices assembled on a non-cleaned, 400 pair, filled cable were immersed in 3 feet of water, and subjected to an 8 ft. waterhead for 30 days. In all cases, the closures failed by having a considerable amount of water present in the closure. The penetration of the core was poor, thereby allowing water ingress.

The sealing areas around the cable/closure also allowed the ingress of water.

### Heat Shrinkable Closure With Forced Encapsulant Delivery System

Splices assembled on a non-cleaned, 400 pair, filled cable after immersion and waterhead at the previously mentioned conditions, all passed (i.e. no water present in the closure).

Closures assembled similarly, but cycled from -40°c to +60°C for 15 cycles, and then subjected to immersion and waterhead showed passes in the cases of the Encapsulants W, X, Y, and Z. "D", however, showed the presence of water. On dissection, the absence of oily interface was clear with the new generaton encapsulants; the penetration of the core was good.

The final selection for good replacements for "D" was made by evaluating the re-entry properties of the new encapsulants. All encapsulants had different re-entry characteristics.

"D" Easy to re-enter.
Oily interfaces leave "greasy" connectors.
Breaks in lumps.

W Easy to re-enter.
Clean on re-entry.
Breaks in lumps.
No oily interfaces

X Very hard to re-enter.
Soft and very elastic.
Too tacky.
No oily interfaces.

Y Easy to re-enter, but elastic.
Clean on re-entry.
Breaks in lumps.
No oily interfaces.

Z Easy to re-enter.
Clean re-entry.
Tends to crumble.
No oily interfaces.

Table VI shows the physical properties of the cured encapsulants. The encapsulants with easy re-entry have ultimate elongation of <200%. Y is far too elastic to allow good re-entry; the connectors do not break away cleanly.

Table VI

| | T.S. (psi) | | | U.E. (%) | | |
|---|---|---|---|---|---|---|
| | -10°C | 25°C | 60°C | -10°C | 25°C | 60°C |
| "D" | 12 | 13 | 10 | 150 | 130 | 90 |
| W | 14 | 14 | 10 | 90 | 80 | 40 |
| X | 6 | 8 | 4 | 370 | 390 | 180 |
| Y | 16 | 12 | 10 | 200 | 130 | 180 |
| Z | 21 | 15 | 15 | 50 | 50 | 20 |

## CONCLUSIONS

Laboratory and functional testing have shown that three of the new generation encapsulants are acceptable as replacements for D-Encapsulant. All these show improvement over "D" in terms of removal of oily interfaces when in contact with filled conductors.

The use of a high temperature pull-out strength test is highly indicative of the absorbancy /compatibility of the filling compound and encapsulant.

The new encapsulants will offer a more reliable encapsulated splice closure, and allow a workable system that does not require cleaning of the coated conductors prior to encapsulation.

## Acknowledgements

The authors would like to thank the following people for their contributions to the paper: C. Debbaut, T. Hunter, and S. Roberts; and also B. Wasserman for her help in preparing the manuscript.

## References

1. Mitchell, D. M. and Sabia, R., Proceeding of the Twenty-Nineth International Wire and Cable Symposium, p. 15, 1980.



Keith Dawes received a first class honours B.Sc. degree in Chemistry from University of Newcastle-upon-Tyne in 1966 and obtianed his Ph.D. from the University of Manchester in 1969. After post-doctoral fellowships at Columbia University and Oxford University, he worked at the Malaysian Rubber Producers Research Association. He joined Raychem Corporation in 1979 working in Corporate R & D at Swindon, England. He is now Development Manager for Raychem Telecommunications Division in North Carolina.



Thomas E. McNeal joined the Bell System in 1966 in the outside plant department. He is presently a staff manager with Bell South User Technical Staff in Birmingham, Alabama and is involved in the evaluation and selection of outside plant products.

# A FORCED ENCAPSULATION SYSTEM FOR SPLICE CLOSURES

C. E. Angel
F. J. Mullin
W. C. Reed

AT&T Bell Laboratories
2000 Northeast Expressway
Norcross, Georgia 30071

## ABSTRACT

A Forced Encapsulation Splicing System, comprised of a new encapsulant and a new closure, has been developed for buried and underground, re-enterable encapsulated splice closures. The encapsulant is forced into the organized splice geometry of the closure by a method that controls both encapsulant pressure and encapsulant volume during cure time. This method assures thorough encapsulation with a minimum volume of encapsulant and locks the closure shell into a strong vessel which compressively reinforces the encapsulant against water ingress and isolates the encapsulated splice from mechanical stresses.

This system will survive known worst case placing and backfilling conditions without additional protection and still provide waterhead resistance in excess of existing requirements. It is constructed with few parts, using traditional methods and tools. It does not require flame or other energy sources and can be installed anywhere cable is placed. The installed product can be quality inspected by non-destructive visual examination.

## I. INTRODUCTION

Splice closures have evolved along with cable designs, construction methods and materials. The goal has always been a reliable closure with maximum water resistance at a reasonable cost which can be safely, efficiently and effectively constructed.

Lead sleeves and galvanized cast iron closures containing compressed air protected the pulp and paper insulated cable splices. Later, plastic closures performed the same function for pressurized cable systems. In the mid-1960s, plastic closures filled with hard polyurethane were used for buried splices of plastic insulated conductors in air core cable. In the early 1970s, plastic splice closures with grease encapsulant were introduced for filled cable. During the mid-1970s, a two part polyurethane encapsulant and a plastic shell were developed to protect the larger pair count cables. It should be noted that in the past non-destructive quality inspection has been possible only for air pressurized closures.

This paper describes the forced encapsulation system for re-enterable splices which comprises a new encapsulant and a new closure. Recent studies of closure performance, encapsulation theory, encapsulants and assembly and placement sensitivities guided development of the system and are discussed below.

## II. CLOSURE FAILURE MODES

A study of closure performance confirmed the known failure modes and revealed others that had not previously been apparent. These failure modes are directly related to modes of water entry and can result in electrical faults (see Figure 1). A discussion of these modes follows:

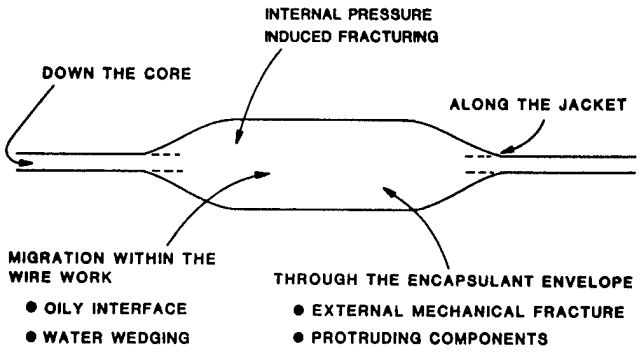



FIGURE 1. MODES OF WATER ENTRY

A. Along Cable Jacket - Water surrounding the closure is forced along the outside of the cable jacket by the pressure of the local water table. Entry is usually through improperly installed or deteriorated blocking collars wrapped or shrunk over a scuffed section of cable jacket.

B. Down Cable Core - Water which has entered a cable at mechanical or lightning damage points may seep along the core and under the sheath

and may penetrate the splice area. Well filled cables are an aid in preventing water entry via this path, but even a trickle will develop a pressure head equal to the elevation difference between the damage point and the splice closure.

C. Through The Encapsulant Envelope - Once inside the closure shell, water can enter the splice through fractures in the encapsulant or along protruding components. Encapsulant fracture may be caused by movement of the unsupported cable relative to the splice or by impact during handling and backfill operations.

D. Within The Wire Work - Once inside the encapsulant envelope, water may migrate within the wire work along any splice components which do not adhere to the encapsulant. Such a condition occurs at an oily interface between conductors and encapsulant that results from improper cleaning of the cable filling compound from the conductors if cleaning is required. As water pressure increases, such an interface may be wedged open causing failure in a short time.

E. Through Pressure Induced Fractures - Water may be wedged into interfaces at pressures as low as 5 psi and fracture some unsupported reenterable encapsulants causing rapid failure of the splice.

## III. ENCAPSULATION THEORY[1]

A study was made to determine the factors affecting the penetration of the encapsulant into the splicework that it is designed to protect. The encapsulant is forced by pressure, developed by gravity or other means, into voids in the splice. Depending on the channel structure leading to these voids, air may be trapped or allowed to escape.

Pressure on the encapsulant will reduce the size of bubbles of trapped air. This pressure, $P_o$, will cause a volume of air, $V_{air}$, trapped in the fluid encapsulant at an initial pressure, $P_{air}$, (essentially atmospheric pressure) to be compressed to a volume, $V_o$, where

$$P_o V_o = P_{air} V_{air} = K \qquad (1)$$

and K is a constant (Boyle's Law).

Pressure will force encapsulant through connecting channels to a void within the cable or splice work of volume, $V_{air}$, and initial pressure, $P_{air}$, to achieve the condition described in Equation (1) after a time. This time dependent process has a time constant, $\tau_t$, (see Appendix A):

$$\tau_t = \frac{K\eta}{G P_o^2} \qquad (2)$$

where K is the Boyle's Law constant,
$\eta$ is the viscosity of the encapsulant,
G is a collection of geometrical terms describing the channel and
$P_o$ is the pressure over the encapsulant (plus the small hydrostatic contribution of depth of the encapsulant which is neglected).

Equation 2 clearly indicates that such voids can be filled more quickly by spreading the splice work to open the connecting channels (G), using a low viscosity fluid encapsulant ($\eta$) and employing a pressure over the encapsulant ($P_o$). These three factors in combination with the gel time of the encapsulant (related to $\tau_t$) may be optimized for forcing encapsulant into these voids.

Pressure over the encapsulant has no effect on filling voids which have a number of passages which allow encapsulant to enter and air to escape. Voids of this type are common in splices as long, horizontal air cavities in the wire bundles. The process for filling these voids is also time dependent with a time constant $\tau_f$, (see Appendix B):

$$\tau_f = \frac{V_f \eta}{\sum G_j \rho h_{max}} \qquad (3)$$

where $V_f$ is the volume of the air cavity,
$\eta$ is the viscosity of the encapsulant,
$G_j$ is the collection of geometrical terms describing the jth inlet channel,
$\rho$ is the density of the encapsulant and
$h_{max}$ is the vertical position of the air outlet port referenced to the lowest inlet port.

Equation 3 shows the means of optimizing the filling of this type of void. The splice work may be spread to increase the cross section and number of connecting channels ($G_j$) leading to a given volume ($V_f$). Removing barriers and clutter, e.g., using a tray and a liner with large perforations, have a similar effect ($G_j$). A low viscosity encapsulant is advantageous ($\eta$). Increasing the pressure difference between encapsulant inlet and air outlet ports ($\rho h_{max}$) is helpful in moving air into the fluid encapsulant where it floats away. This may be accomplished by tilting the closure (and voids) or slanting the wire work; however, increasing the pressure on

the encapsulant has no effect on this pressure difference ($\rho h_{max}$). These factors in combination with the gel time for the encapsulant (related to $\tau_t$) may be adjusted for optimum fill, but pressure on the encapsulant does not aid filling this type of void which vents air.

## IV. ENCAPSULANT

A study of encapsulants was made to guide the development of the closure system and to develop a formulation with significantly improved water resistance compared to existing encapsulants. The study confirmed that the encapsulant must have increased fracture resistance, be optimized for efficient splice penetration, make intimate contact with cleaned and uncleaned filled cable conductors without forming oily interfaces and meet existing encapsulant criteria. Significantly, viscosity and gel time should be optimized for efficient splice penetration and initial encapsulant setup during the time the craftsperson tends to normal duties. In addition, the fracture resistance must be as large as possible but still allow the encapsulant to be re-entered. Re-entry of test closures illustrated the advantages of a clear view of the splice through a transparent encapsulant and closure liner. Such an encapsulant was developed and is described in the accompanying paper by Chapin and Sabia.[2]

## V. ASSEMBLY AND PLACEMENT STUDY

A study of the assembly and placement of a closure examined the impact of human interaction on closure reliability. This study was aimed at the elimination of assembly errors and omissions, the avoidance of damage during placement and the assurance of work safety.

The study indicated that successful assembly is achieved by a logical, sequential building-block procedure requiring a minimum of craft decisions, having no opportunities for omissions and providing immediate feedback of proper assembly. Decision-sensitive operations like wrapping tape, building collars or judging encapsulant volume should be avoided. Operations such as wiping, washing, scuffing and installing of loose parts where incorrect procedure or omission could not be observed in the inspection of the completed closure should also be avoided.

Assembly of the ideal closure should be accomplished with a minimum of components. The assembly procedure should automatically establish dimensional and organizational control of the splice, employ traditional methods and indicate successful completion of each assembly step. Various cable sizes and splice combinations should be accommodated without cutting and fitting of parts.

The placement portion of this study, consisting of investigations of common field conditions for buried and underground installations and soil mechanics research (see Appendix C), also showed the impact of human activity on reliability. Closures, which were designed to be encapsulated in place, were being built at the sides of trenches or a convenient location in a manhole and forced into position. Some buried closures were rotated 180° in the horizontal plane before positioning to take up cable slack, thus transmitting stress into the encapsulated wirework. Large rocks were allowed to impact closures during burial. High cable tensile loads were developed in buried closures from the combination of splice pit dimensions, closure support and backfill methods and in underground closures from improper closure support.

To survive these conditions, closures must prevent encapsulant fracture or movement of splice components, as these would lead to water ingress or broken connections. The encapsulated splice must be isolated from mechanical stresses caused by cable twisting, bending and pulling, including impulsive cable tensile loads as great as 250 lbs (see Appendix C). To meet the requirements of some telephone companies, the encapsulated portion must be protected against impact up to 300 in-lbs and compressive loads up to 500 lbs.

Although complete safety cannot be assured, every opportunity to reduce risk was considered. Material selection and methods of construction were dictated by craftsperson safety. Manual tools were selected over power tools with their attendant wires, hoses and tanks. Torches, which could set off gas explosions or ignite flammable materials in the work space, were excluded. Pressure generation by direct application of force on the fluid encapsulant was employed to avoid the risk of compressed gas.

## VI. SYSTEM DESCRIPTION

A system, comprising an encapsulant and closure, was designed to meet all existing criteria[3] as well as additional performance requirements developed from these recent studies. The system, shown schematically in Figure 2, employs controlled pressurization to force the encapsulant into an organized splice which is spaced inside a water barrier or bladder sealed to the cables. The pressurized encapsulant contained by the bladder and shell during and after cure is forced against surfaces to which it bonds and seals. The encapsulant is formulated to seal to uncleaned con-

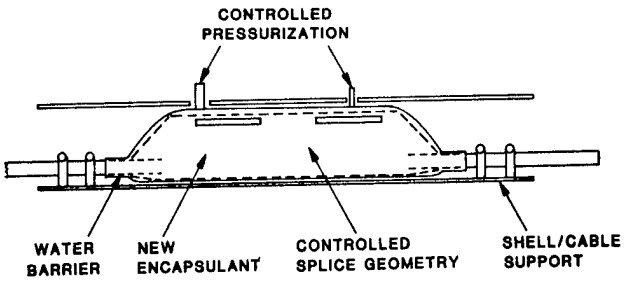



**FIGURE 2. FORCED ENCAPSULATION SYSTEM SCHEMATIC**

ductors and is fracture resistant. For additional fracture protection, the encapsulated portion of the splice is reinforced by an embedded structure, isolated by the outer shell from mechanical stresses and compressed by this shell. A more detailed examination will now be made of the elements required for this system. Parts and procedures will be discussed for one embodiment in the sequence of assembly as follows:

Step 1. Assemble Splice Organizer

The splice organizer is designed to establish the splice opening, restore sheath continuity, support the splice work, control the splice geometry and reinforce the cured encapsulant. It consists of a tray, a liner and attaching ties mounted on a bond bar to which bonding braids are attached (see Figure 3).

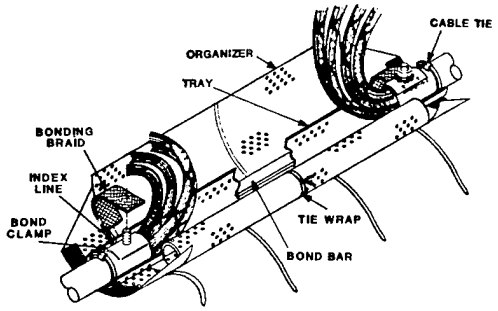



**FIGURE 3. SPLICE ORGANIZER**

The organizer is prepared for assembly by scrolling and temporarily tying the liner flaps to either side of the tray. The prepared unit is secured to the cables with cable ties and the sheath opening is established by index lines on the tray. Cable sheath continuity is then restored through the bonding braids at either end of the bond bar. Splice support during construction is provided by the tray which is supported on the bottom by the bar and at the sides by the scrolls.

The splice is built in a normal fashion and organized naturally with the connectors at the top. In this position, the connectors have an extra margin of protection should water be forced by high pressure into the wire bundles below.

Upon completion of the splice, the liner is released from the temporary scroll ties, wrapped around the splicework and latched to a predetermined diameter. This diameter fits within the shell but does not compact the splice bundle thus insuring maximum encapsulant penetration. The liner and tray are perforated to aid encapsulant penetration and allow air to escape.

The liner wraps into a cylinder with conical ends to completely envelope the splice work and control the splice geometry (see Figure 4). The cured encapsulant bonds to

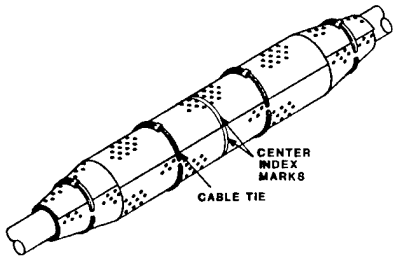



**FIGURE 4. ASSEMBLED ORGANIZER**

the liner and acts as embedded reinforcement against fracture. A continuous enveloping layer of encapsulant is insured by liner dimples which space the lined splice array from surrounding walls. This geometry allows thorough encapsulation with a minimum volume of encapsulant.

To facilitate re-entry the liner and encapsulant are transparent. This transparency allows a clear view of the splicework to guide re-entry and rapid location of the liner edges which are color marked for this purpose. The overlapped edge is lifted to peel the liner and outer layer of encapsulant and to access the splice work.

All parts necessary to assemble the organizer over the splice are included as an integral part of the unit. Complete and proper assembly is indicated by all cable ties being latched and pulled to a stopped position.

Step 2. Seal Bladder

The bladder serves both as a containment for the fluid encapsulant during the forced encapsulation process and as a water barrier for the completed closure. It may also be used for temporary protection of incomplete splices. The bladder is a tough elastomeric sheet with two spouts and a paper protected mastic around its perimeter (see Figure 5).

The bladder surrounds the splice and is

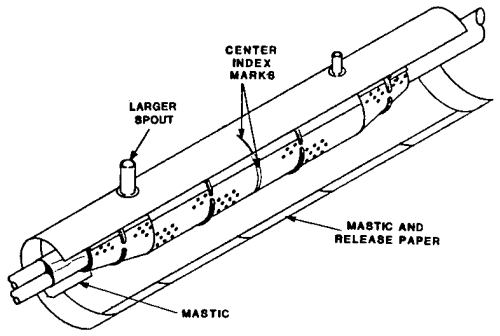



**FIGURE 5. BLADDER**

sealed to itself and to the cables by the mastic. The protective release paper is removed as sealing progresses. The mastic is formulated to stick to cable sheath without scuffing. An extra strip of mastic is supplied to build a seal around branch cables before the bladder is placed. A cable tie and vinyl tape reinforce each seal to the cables (see Figure 6). Later,

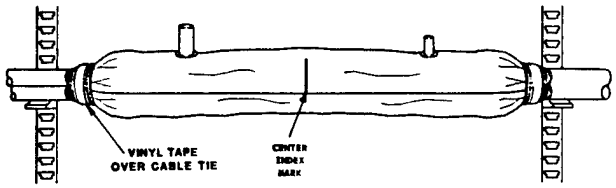



**FIGURE 6. ASSEMBLED BLADDER**

the splice is filled and pressurized with encapsulant through the larger of the two spouts while air is vented through the smaller spout.

The bladder alone will not hold pressurized encapsulant since the elastomeric material will stretch and the mastic seams will peel. Therefore it is contained in a vessel formed by the outer shell and two end supports.

Step 3. Install End Supports

An end support is wrapped over each end of the bladder to form a cone which axially supports the pressurized bladder (see Figure 7). Each support is a strong,

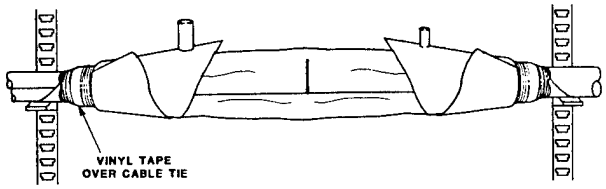



**FIGURE 7. END SUPPORTS**

shaped, fabric sheet and is held in position by a cable tie and vinyl tape so that the flared edges of the cone can be forced by the pressurized bladder to couple frictionally to the outer shell.

Step 4. Mount Outer Shell

The outer shell radially supports the pressurized bladder, isolates the encapsulated splice from mechanical stress and compressively reinforces the cured encapsulant. It is a rugged, cylindrical, plastic tube split longitudinally into upper and lower shells which lock together (see Figure 8).

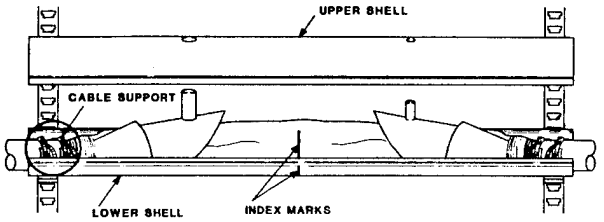



**FIGURE 8. OUTER SHELL**

The lower shell mounts under the splice by unique cable clamps built into each end of the shell. These clamps fix the cables firmly to the shell and prevent movement in all directions. The upper shell with holes for the bladder spouts is joined to the lower shell by sliding clamps along each joint.

Under the action of the pressurized encapsulant, the shell halves lock into a rigid cylinder to which the cables have been firmly fixed external to the encapsulated portion of the splice. This isolates the encapsulated portion from stresses due to cable twisting, bending or pulling thereby preventing encapsulant fracture. The tough shell, now radially reinforced by the pressurized bladder, protects the splice against encapsulant fracture from impact or compressive loads.

The outer shell, end supports and bladder contain the pressurized encapsulant. Pressurization forces the fluid encapsulant against surfaces to which it bonds or seals. The shell continues to compressively load the encapsulant after curing to hold the bonds and seals against high water heads thereby preventing water wedging and pressure induced fracturing of the encapsulant.

Step 5. Force Encapsulant

After the organizer, bladder, end supports and shell are installed, forced encapsulation of the assembled closure can begin (see Figure 9). The encapsulant is mixed and poured into the closure through the

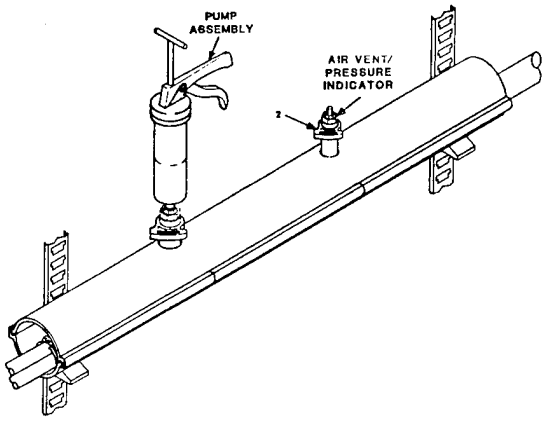



**FIGURE 9. PUMPING ENCAPSULANT**

large spout until encapsulant appears in the small spout. A check valve is then inserted into the larger spout and an air vent/pressure indicator into the smaller spout. A cartridge gun is connected to the check valve, filled with encapsulant and used to force encapsulant into the closure until the pressure indicator shows 15-18 psi.

During pumping, air is automatically vented through the air vent/pressure indicator which passes air but blocks encapsulant. This minimizes air voids which are potential paths for water ingress and spoil the compressive reinforcement of the cured encapsulant by the shell.

After pumping, the craftsperson periodically checks the pressure indicator while tending to normal cleanup duties. Encapsulant is pumped as needed to maintain pressure. When the pressure has stabilized, the pump is removed and a protective cap is placed over the air vent/pressure indicator.

Control of encapsulant pressure and volume during cure is vital. Encapsulant is forced out of the closure and into cable fill defects causing a reduction of the pressure and its encapsulation advantages (see Equation 2). Adding encapsulant restores the pressure to the desired level and insures a sufficient volume to protect the splice.

Step 6. Inspect Completed Closure

It is a simple matter for the craftsperson to inspect the completed closure during or following the forced encapsulation. The inspection consists of a visual examination of the pressure indicator for proper reading and the open closure ends for leaks.

Since the splice geometry has been established within the bladder, this simple inspection checks the proper assembly of remaining components and provides a go/no go indication of successful splice closure construction and encapsulation to the craft. This same inspection can be performed by quality inspectors at anytime in the future. After inspection, the open closure ends are closed with plastic foam blocks to keep out dirt and debris.

## VII. WATERHEAD RESISTANCE OF COMPLETED SYSTEM

Forced encapsulated system closures as described above were assembled and each was subjected to the sequence of Appendix D tests concluding with separate water immersion and sheath injection waterhead tests of 3 feet and 8 feet respectively which exceeds present requirements.[3] Present requirements conduct the 3 foot immersion and 8 foot sheath injected waterheads simultaneously which yields an effective sheath injected waterhead of only 5 feet for many closure systems. The results verified that this closure system passes the more severe tests and demonstrated that waterhead resistance improvements are possible with compressive reinforcement of the encapsulant. In laboratory tests, closures have routinely resisted waterheads of 16 feet and have been built to resist 23 feet for more than 30 days.

Gravity filled encapsulated closures of the past would hold back a 5 foot head (sheath injected waterhead of 8 feet less a water immersion head of 3 feet), if constructed carefully and handled properly. The new pressurized system automatically guarantees the proper assembly and handling protection and employs the new encapsulant[2] so that a separately applied 8 foot sheath injected waterhead resistance is assured.

The total waterhead resistance for the system is achieved by both the new encapsulant and the pressure maintained on the encapsulant and is empirically defined as:

$$\text{Waterhead Resistance} \approx 8 \text{ feet} + \text{Encapsulant Pressure} \quad (4)$$

This relationship is depicted in Figure 10 and has been verified over the range of 0 to 23 feet.

For the water immersion case, the surrounding water contributes to encapsulant pressure by loading the void free encapsulant sealed inside the water barrier (bladder). This contribution increases with immersion depth so the present 3 foot immersion criteria is no challenge.

For the sheath injection case, water forced through a cable does not significantly contribute to the encapsulant pressure and is blocked by the encapsulant as pressurized by the closure.

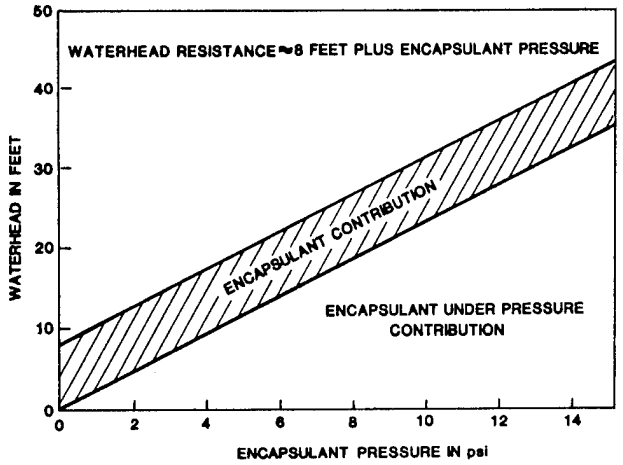



FIGURE 10. WATERHEAD RESISTANCE PLOT

## VIII. Performance and Advantages

This closure system meets or exceeds all existing requirements. It will withstand compressive loads of 500 lbs., impact of 300 in-lb and cable tensile loads of 150 lbs. per inch of cable diameter up to 250 lbs. and still survive a separately applied sheath injected waterhead of 8' and more. This data indicates that the closure system will survive difficult placing and backfilling conditions without additional protection and can even be spliced above ground and buried later.

The system has been successfully installed in buried and underground plant and can be used if desired in aerial applications. Less than ten closure sizes will accommodate all splice combinations of all cable sizes with no cutting or fitting of parts. Since installation requires no external power sources such as compressed air, electricity or flame, the system may be safely installed in manholes, oil refineries or chemical plants and placed jointly with natural gas lines.

The system is constructed from a few major parts using traditional methods. No concealed wrappings, cable collar build up, cable sheath scuffing or conductor cleaning are required. Splice dimensions and organization occur naturally and automatically without craft decision.

A non-destructive visual examination of a completed splice and its indicated pressure shows whether it was constructed satisfactorily. This provides a go/no go indication to the craft so corrective action can be taken before leaving the worksite. It allows management to perform a non-destructive quality inspection at any time in the future.

## IX. SUMMARY

A closure/encapsulant system has been designed which meets or exceeds all existing requirements. The robustness of the new closure enables it to survive the rigors of handling and backfilling during the placement process and still provide water resistance superior to all previous design concepts. Proper construction is assured by a non-destructive, visual quality inspection that can be performed during and after assembly. The closure system has been tested in buried and underground installations and has demonstrated performance superior to other closure designs. All of this is achieved in a reliable system at a reasonable cost which can be safely and efficiently constructed.

## X. ACKNOWLEDGEMENTS

The work described in this paper represents the efforts of many people. Acknowledgement is made of the contributions of the following:

AT&T Bell Laboratories:

Cable and Wire Group
Connector Systems Group
Material and Chemistry Group
Sheath Joining Group
Operation and Training Group

AT&T Technologies:

Product Engineering Control Center
Product Planning
Omaha Manufacturing Engineering

In addition, the cooperation of several Bell Operating Companies that agreed to try the system in actual applications is appreciated.

## REFERENCES

1. W. C. Reed, "A Short Term Water Resistance Test for Filled Service Wire," 28th International Wire and Cable Symposium, November 1979.

2. J. T. Chapin and R. Sabia, "Laboratory Performance Tests and Criteria for Re-enterable Encapsulants," Paper to be presented at the 34th International Wire and Cable Symposium, November 1985.

3. Bell System Technical Reference, PUB55004, Issue 1, "Waterproof Splice Closures," 1981.

## APPENDIX A
## VOIDS WHICH TRAP AIR[1]

Consider a void of volume, V, within a cable, connector or splice work which has access to fluid splice encapsulant through a small passage (see Figure 1a). At some time the cavity will contain some air, $V_{air}$, and some encapsulant, $V_{enc}$, so that

$$V = V_{air} + V_{enc} \qquad (1)$$

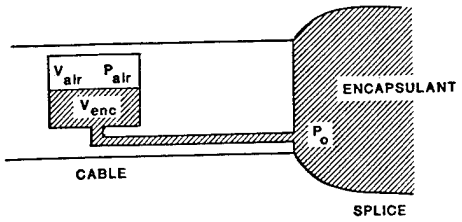



Figure 1a. Encapsulant Flow Into a Cable Void Which Traps Air.

Pressure on the splice encapsulant at the passage entry, $P_o$, forces encapsulant into the cavity and compresses the trapped air to a pressure $P_{air}$. Encapsulant moves into the cavity until $P_{air} = P_o$ (neglecting hydrostatic pressure contributions of the encapsulant) at which time $V_{air} = V_o$. Assuming the compression to be isothermal

$$P_{air}\, V_{air} = P_o\, V_o = K \quad \text{(Boyle's Law)} \qquad (2)$$

The volume rate of flow, Q, of encapsulant into the cavity is determined by the pressure difference, $P_o - P_{air}$, the viscosity of the encapsulant, $\eta$, and the geometry of the passage, G. From Poiseuille's Law, Q may be expressed as

$$Q = \frac{G\,(P_o - P_{air})}{\eta} . \qquad (3)$$

G for laminar flow through a cylindrical passage of radius, R, and length, L, is

$$G = \frac{\pi R^4}{8 L} \qquad (4)$$

but such simple geometry is not to be expected for passages in splices and cables. Fortunately G is considered constant in the following mathematical development and comparisons so that exact geometry need not be known.

By definition Q is

$$Q = \frac{dV_{enc}}{dt} \qquad (5)$$

Combining Equations (2), (3), and (5), the volume rate of flow may be expressed as

$$\frac{dV_{enc}}{dt} = \frac{G}{\eta} P_o - \frac{P_o V_o}{V_{air}} \qquad (6)$$

From Equation (1), Equation (6) may be rewritten as

$$\frac{dV_{enc}}{dt} = \frac{G P_o}{\eta} \frac{V-V_{enc}-V_o}{V-V_{enc}} \qquad (7)$$

and

$$\frac{V-V_{enc}}{V-V_{enc}-V_o}\, dV_{enc} = \frac{G P_o}{\eta}\, dt \qquad (8)$$

To determine the volume of encapsulant, $V_{enc}$, in the cavity at any time, t, Equation (8) is integrated.

$$\int_o^{V_{enc}} \frac{V-V_{enc}}{V-V_{enc}-V_o}\, dV_{enc} = \int_o^t \frac{G P_o}{\eta}\, dt \qquad (9)$$

which yields

$$\ln|V_{enc}-V-V_o| - \ln|-(V-V_o)| = -\frac{G P_o}{\eta V_o} t + \frac{V_{enc}}{V_o} \qquad (10)$$

Equation (10) is simplified by substituting an expression for the maximum volume of encapsulant which may enter the cavity at $P_o$, $V_{enc\ max}$,

$$V_{enc\ max} = V-V_o \qquad (11)$$

and the constant from Boyle's Law

$$K = P_o V_o \qquad (12)$$

With these substitutions, Equation (10) may be written in exponential form as

$$\frac{V_{enc\ max} - V_{enc}}{V_{enc\ max}}\, e^{\frac{-V_{enc}}{V_o}} = e^{\frac{-G P_o^2}{K\eta} t} \qquad (13)$$

The right hand term has the form $e^{-t/\tau_t}$ where $\tau_t$ is the time constant. Thus, the time constant for the flow of encapsulant into a cavity in a splice or cable which traps air is

$$\tau_t = \frac{K\eta}{G P_o^2}$$

## APPENDIX B
## VOIDS WHICH DO NOT TRAP AIR[1]

Consider a void of volume, $V_f$, within a bundle of wires which is accessed by a number of passages such that air may escape. (See Figure 1b.)

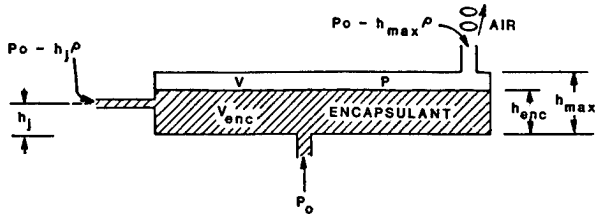



Figure 1b. Encapsulant Flow Into a Wire Bundle Void Which Does Not Trap Air.

The volume rate of flow, Q, of the water into this cavity is the sum of the volume rate of flow for each passage, $Q_j$,

$$Q = \sum_{j=1}^{n} Q_j \qquad (1)$$

where n is the number of passages.

The volume rate of flow for each passage is now expressed as

$$Q_j = \frac{G_j \left(P_{oj} - P - h_{enc}\rho\right)}{\eta} \qquad (2)$$

where $h_{enc}$ is the hydrostatic pressure of the encapsulant within the cavity. $h_{enc}$ is the vertical height of the encapsulant within the cavity referenced to $h_j = 0$, $\rho$ is the density of the encapsulant and $\eta$ is the viscosity of the encapsulant.

$P_{oj}$ is the sum of the outside pressure and the hydrostatic pressure of the encapsulant

$$P_{oj} = P_o - h_j\rho \qquad (3)$$

where $h_j$ is the vertical height of an entrance port referenced to $h_j = 0$.

Since air escapes the cavity from some escape port, the pressure of the air in the void automatically adjusts to the pressure of the encapsulant at the escape port.

$$P = P_o - h_{max}\,\rho \qquad (4)$$

where $h_{max}$ is the vertical position of the escape port referenced to $h_j = 0$.

Combining Equations (2), (3), and (4), the volume rate of flow for each passage is

$$Q_j = \frac{G_j \left(h_{max} - h_j - h_{enc}\right)\rho}{\eta} \qquad (5)$$

and the total volume rate of flow Q is

$$\frac{dV_{enc}}{dt} = \sum_{j=1}^{n} \frac{G_j \left(h_{max} - h_j - h_{enc}\right)\rho}{\eta} \qquad (6)$$

$h_{enc}$ may be approximated in terms of $V_{enc}$ as

$$h_{enc} = \frac{V_{enc}}{A} \qquad (7)$$

where A is the cross sectional area of the cavity.

Equation (6) can now be solved to determine the volume of encapsulant, $V_{enc}$, in the cavity at any time, t. The solution is

$$\int_0^{V_{enc}} \frac{dV_{enc}}{\sum \frac{G_j \left(h_{max} - h_j\right)\rho}{\eta} - \sum \frac{G_j\, \rho\, V_{enc}}{\eta\, A}} = \int_0^t dt \qquad (8)$$

which simplifies to

$$\frac{\sum G_j \left(h_{max} - h_j\right) - \sum G_j \frac{V_{enc}}{A}}{\sum G_j \left(h_{max} - h_j\right)} = e^{-\sum \frac{G_j \rho}{\eta A} t} \qquad (9)$$

Thus the time constant for filling the cavity with encapsulant, $\tau_f$, is

$$\tau_f = \frac{A\eta}{\sum G_j \rho} \qquad (10)$$

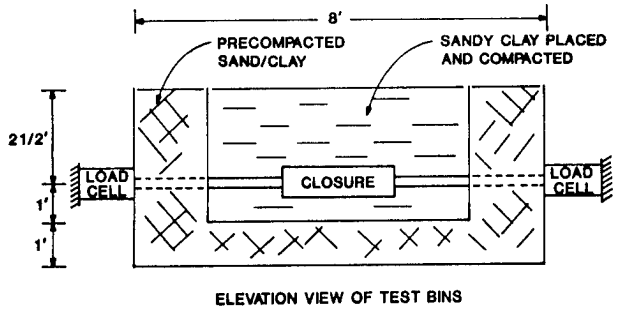
or, since $Ah_{max}$ is the volume of the cavity $V_f$,

$$\tau_f = \frac{V_f\, \eta}{\sum G_j \rho\, h_{max}} \qquad (11)$$

## APPENDIX C
## SOIL MECHANICS STUDY

A study was made to determine the kind of treatment that a closure is subjected to during the process of placement and burial. This study confirmed that some of the existing requirements for buried closures were realistic. However, cable tensile loads during fill were found to be more severe than anticipated in existing requirements. A single size closure was used in the evaluation.

To accurately evaluate the conditions involved, a simulated pit was constructed. This pit was instrumented to monitor the tensile loads applied to the closure during the backfill operation. This pit is illustrated in Figure 1c. A load cell was placed on the cable to measure the loads during backfill. The tensile load measurements obtained are shown in Figure 2c. The chart indicates a maximum peak load of 300 pounds. When the preload of 50 pounds is subtracted, then 250 pounds tensile load is applied to the cable when the first load of dirt is dumped on the closure. Subsequent loads are less severe. Loading similar to that obtained by tamping and rolling with a backhoe are also shown.




ELEVATION VIEW OF TEST BINS

FIGURE 1c. SOIL MECHANICS STUDY

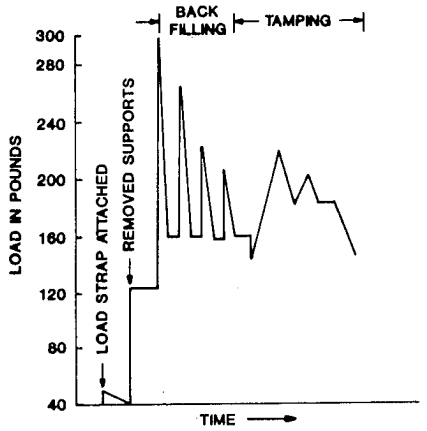


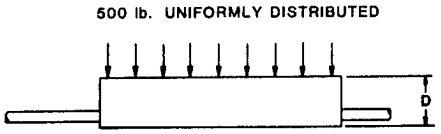

FIGURE 2c. TENSILE LOAD DURING BACKFILL

## APPENDIX D
## CLOSURE TESTS

Forced encapsulation system splice closures were sequentially subjected to compression, impact, cable pull out and water tests to verify that end use and long term reliability requirements were met. These tests are described below.

### A. Compression Test

A 500 pound uniformly distributed load is applied for five hours at temperatures of 0°F (-18°C) and 100°F (38°C). The deformation shall be less than 10% of the original closure diameter. This test is illustrated in Figure 1d.

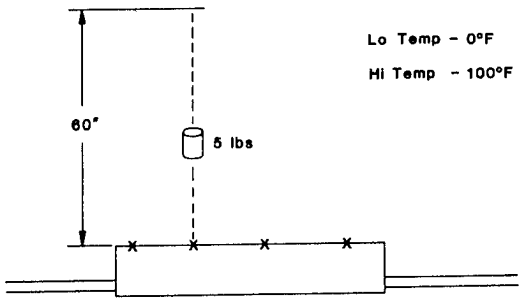



CRITERIA: DEFORMATION, D ≤10%

FIGURE 1d. COMPRESSION TEST

### B. Impact Test

The closure is subjected to an impact of 300 inch pounds at temperatures of 0°F (-18°C) and 100°F (38°C). Neither the closure shell nor the encapsulant shall be damaged. This test is illustrated in Figure 2d.

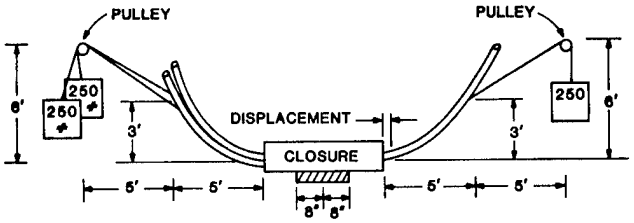



CRITERIA: NO DAMAGE

FIGURE 2d. IMPACT TEST

### C. Cable Pullout Test

A dead weight tensile load is applied to each cable entering the restrained closure. The load applied to each cable is 150 pounds per inch of cable diameter not to exceed 250 pounds. The load is applied for five hours. The displacement of the cable relative to the closure shall be less than 1/8 inch. The test arrangement used is illustrated in Figure 3d.

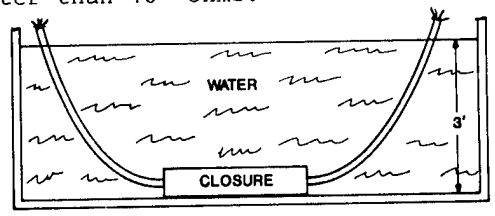



CRITERIA: DISPLACEMENT LESS THAN 1/8 INCH
(NO ENCAPSULANT FRACTURE)

FIGURE 3d. CABLE PULLOUT TEST

D. Water Tests

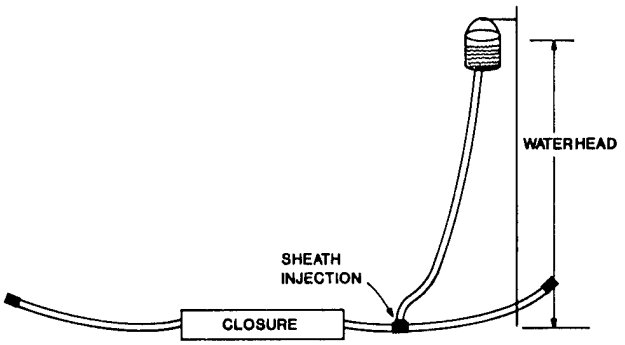
The existing water resistance test[3] requires simultaneous immersion of a closure in three feet of water and sheath injection of an eight foot waterhead. Since these waterheads counteract each other for some closures, an effective sheath injected waterhead of only 5' is possible. For this reason, these tests are done separately. The closure is submerged in three feet of water as shown in Figure 4d for 30 days. After this time there shall be no water inside the splice and all pairs shall maintain an insulation resistance (IR) of greater than $10^9$ ohms.




CRITERIA: IR $\geq 10^9\Omega$
NO WATER INSIDE

FIGURE 4d. WATER IMMERSION TEST

The closure is then subjected to a waterhead applied to the cable core through a prepared opening in the sheath. The waterhead is applied for 30 days. An insulation resistance greater than $10^9$ ohms shall be maintained with no water in the splice. The test is illustrated in Figure 5d.




CRITERIA : IR $\geq 10^9\Omega$
NO WATER INSIDE

FIGURE 5d. SHEATH INJECTION WATERHEAD TEST



C. E. Angel is a member of the Connector System Group of AT&T Bell Laboratories in Norcross, Georgia. He joined AT&T Bell Laboratories in 1950 and has been concerned with the design of a number of military systems. He has also been responsible for the physical design of business telephone station sets, the design of connector splicing tools for outside plant equipment and a new encapsulated closure system for buried and underground use. Mr. Angel received the Bachelor of Mechanical Engineering degree from North Carolina State University in 1949.



F. J. Mullin is a member of the Transmission Media Laboratory, AT&T Bell Laboratories, Norcross, Georgia. He attended John Hopkins University and joined AT&T Bell Laboratories in 1955. During this time he has worked in the outside plant area developing mainframe protection; aerial, buried and building cable terminals, closures and connectors; color coded key closets; Buried Waterproof System; SAI concept and customer trouble report reduction. His present responsibilities include outside plant, copper and fiber transmission media.



William C. Reed is a member of the Transmission Media Laboratory, AT&T Bell Laboratories, Norcross, Georgia. He received a BA in mathematics and physics from Wittenberg University in 1959 and an MA in physics from Wake Forest University in 1969. He joined AT&T Bell Laboratories in 1970 and has worked on the design and development of military power equipment, maintenance test sets and test methods, copper and fiber splicing equipment, buried wire, and encapsulated closures. His present responsibilities include outside plant, copper and fiber transmission media.

# LABORATORY PERFORMANCE TESTS AND CRITERIA FOR REENTERABLE ENCAPSULANTS

J. T. Chapin and R. Sabia

AT&T Bell Laboratories
Norcross, Georgia 30071

## Abstract

Encapsulated splice closures are widely used to protect a splice from water entry. In this paper, failure modes are briefly reviewed. Assuming water entry down the cable core, closure failures due to oily interfaces and wedging are identified as being strongly encapsulant dependent. A splice simulation test has been developed which assumes that a water head acts directly on the splice. In this worst case situation, variables such as cable filling compounds, splice wire work density, connectors, water head, and encapsulant gel time and viscosity are investigated. Data are presented on how these factors influence performance. The result is that a new encapsulant has been formulated which exhibits significant improvements in performance over other commercial encapsulants.

## Introduction

The goal of a reliable, low maintenance telephone plant led to the development of filled cables in the late 1960's.[1,2] This development was followed by the introduction of filled connectors, filled service wire and filled splice closures. The weak link in this filled system has been the splice closure[3] as it is highly vulnerable to water ingress due to system incompatibilities and/or improper installation procedures under field conditions.

A splice closure is intended to restore the cable integrity by acting as an extension of the cable sheath. A brief historical review of splice closure development is presented in the accompanying paper at this symposium by Angel, Mullin and Reed.[4] The preferred closure filling compound is a two part oil extended reenterable polyurethane, commonly referred to as D encapsulant,[3,5,6] although high density oils, soft greases, thermoplastic mastics and hydrophobic powders have been used.

In this paper, filled closure failure modes[4] will be reviewed. Then, criteria for the development of an improved, two part encapsulant will be presented. Standard test data will be listed for a new encapsulant that meets these criteria. The paper will then focus on specific compatibility tests and introduce new performance tests. The data will show that the new encapsulant is a very important step towards improving the reliability of new closure designs such as the one described by Angel, Mullin and Reed.[4]

Other papers at this and earlier symposia attest to the crucial importance of encapsulants and closures to the cable plant. A theme emerges: the encapsulant and closure system must work together to restore the electrical and mechanical properties of the cable.[6]

## Closure Failure Modes

Angel, Mullin, and Reed[4] report closure failure modes that are directly related to water entry and which usually result in electrical faults. These are summarized in Figure 1. It is difficult to separate these failure modes as being primarily closure design dependent or encapsulant dependent. The interdependence of these two factors dictate that encapsulants be developed using closure test data. As closure tests require significant lead time and are very expensive, it was necessary to develop the closure simulation test described below.

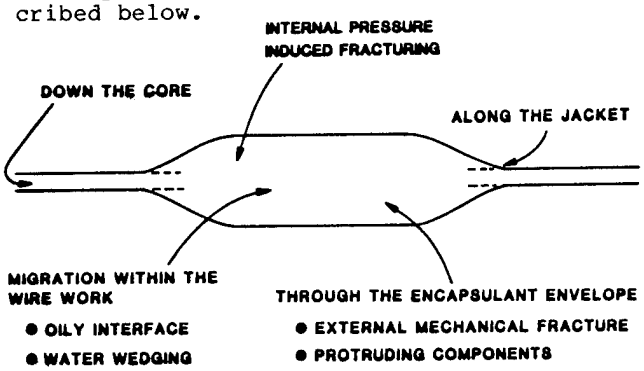



FIGURE 1. MODES OF WATER ENTRY

## Criteria For An Improved Encapsulant Formulation

After examining failure modes, assuming a poorly filled cable core which offers little or no resistance to water entry into the splice area, and characterizing properties of existing encapsulants, the properties of materials required for an improved encapsulant were identified.

Thus, improved compatibility of the encapsulant with cable and closure components (filling and sealing compounds, mastics, tapes, etc.) became a goal. Another goal was to increase the pot life (the time in which the viscosity increases above a critical value, e.g., too viscous to flow readily) of the encapsulant to insure complete penetration of the splice bundle regardless of the field temperature and degree of splice congestiveness. Lastly, the fracture strength of the encapsulant was identified for improvement. The first goal is critical to any successful closure design. The goals of complete penetration and fracture toughness are enhanced by closure design and are covered also in the accompanying paper by Angel, Mullin and Reed.[4] These goals were accomplished while maintaining or exceeding the proven, satisfactory properties of D encapsulant[3,5] such as:

1) safety
2) shelf life
3) reenterability
4) stress cracking effects on plastics
5) hydrolytic stability

## Existing Encapsulant and Performance Specifications

Bell System Technical Reference on "Waterproof Splice Closures", PUB 55004, and Bellcore CA08735 D Encapsulant Specification address compositional and cure properties of a two part, polyurethane encapsulant, compatibility of the encapsulant with closure components, and full scale performance testing of filled closures. In our work, we emphasized testing for compatibility with closure materials while meeting or exceeding other encapsulant properties. The full scale closure tests were replaced by simulated splice tests in which the ability of an encapsulant to maintain high insulation resistance of spliced conductors in the presence of external water pressure is measured.

## Materials Properties

Materials requirements from CA08735 are listed in Appendix A, along with data obtained on an encapsulant developed as a result of this work. Some CAO requirements, such as elongation, are purposely broad to allow for innovation in encapsulant development. Other requirements, such as hydrolytic stability, are necessarily restrictive. The new encapsulant meets these requirements and in most cases exceeds them. An increase in component viscosity at 40°F and gel time were necessary to attain improved closure performance.

## Compatibility Properties

Out of the materials requirements in Appendix A, selected compatibility requirements will be discussed in the following sections. Specifically, compatibility of the encapsulant with cable filling compounds and connectors will be discussed. Compatibility with sealing tapes, mastics, liners, etc. has also been addressed but will not be discussed since these are more closure-design specific. It is sufficient to state that compatible closure materials are readily selected once the compatibility of the encapsulant with cable filling compounds is established.

### Conductor Pullout Force

The compatibility of an encapsulant with cable filling compounds is highly desirable since cleaning insulated conductors under field conditions cannot be assured. The conductor pullout test is a quantitative measure of the interaction between the encapsulant and insulated conductors in the presence of cable filling compounds. The preparation and testing of samples is described in CA08735. In our tests, 22 AWG conductors from aircore and FLEXGEL† and petrolatum filled cables[7,8] were potted in the encapsulant and, after the encapsulant had cured, the force to pull out the insulated conductor was measured. The polyurethane formulation and the gel time of the encapsulant were varied. For the formulations in Table I, there is a good relationship between polyurethane content and conductor pullout force with aircore and FLEXGEL coated conductors. Petrolatum coated conductors show less of a dependence on polyurethane content. Extending the gel time as in Table II did not increase the conductor pullout force. A weak relationship is shown in Table II between the pullout force and tear strength (a measure of encapsulant reenterability). Thus, the data show that it is

†A trademark of AT&T Technologies.

possible to improve the compatibility between an encapsulant and FLEXGEL and petrolatum filling compounds without degrading reenterability.

Although a difference in pullout force is apparent in Table II between FLEXGEL and petrolatum coated conductors, dissection of D1000 encapsulated closures show that FLEXGEL and petrolatum coated conductors are absolutely free of oil syneresis, indicative of excellent compatibility. However, it is important to note that the pullout force does not necessarily provide insight into the performance of the encapsulant, for example, where compacted wire bundles exist. In this area, encapsulant penetration is dependent on the closure design.

TABLE I

Conductor Pullout Force[a] as a Function of Encapsulant Polyurethane Content

| % Polyurethane[b] | Insulated Conductor Coating | | |
|---|---|---|---|
| | Aircore | Petrolatum | FLEXGEL |
| | Pullout Force, lbs | | |
| 30 | 8.4 | 2.9 | 5.1 |
| 35 | 11.0 | 3.3 | 6.2 |
| 40 | 13.0 | 3.1 | 11.0 |

[a]Test based on CA08735.

[b]The encapsulant components are the same, only the polyurethane content is varied. The balance is composed of extender oils and/or compatibilizers.

TABLE II

Conductor Pullout Data as a Function of Gel Time

| Encapsulant | Gel Time | Insulated Conductor Coating | | | Encapsulant Tear Strength,[e] lbs/in |
|---|---|---|---|---|---|
| | | Aircore | PJ | FLEXGEL | |
| | | Pullout Force, lb | | | |
| D[a] | 30 min. | 7.5 | 0.4 | 2.4 | 3.2 |
| D[b] | 17 hrs. | 7.1 | 0.7 | 2.4 | - |
| D1000[c] | 55 min. | 13.0 | 3.1 | 11.0 | 4.2 |
| D1[d] | 17 hrs. | 13.0 | 2.4 | 10.1 | - |

[a]This material is commercially available as D encapsulant.

[b]This material is an uncatalyzed version of D encapsulant.

[c]The properties of this encapsulant are listed in Appendix A.

[d]This material is an uncatalyzed version of D1000.

[e]CA08735.

## Stress Cracking Activity

The stress cracking activity of encapsulants is important. Polycarbonate, used in connector designs, is sensitive to stress cracking by esters commonly used in encapsulants. Other closure materials are more forgiving in contact with encapsulants and will not be discussed. The standard method for determining the stress cracking resistance of polycarbonate to encapsulants is described in CA08735. The test involves encapsulation of annealed, injection molded polycarbonate bars stressed to 0.75% strain using a three point fixture. After 30 days at room temperature, no cracks or crazes of the bars are allowed. The assumption in this test is that a good connector design will stress polycarbonate at lower strain levels. The test is of greater benefit to connector designers than to connector users who during closure reentry apply high pull forces to wires spliced into connectors as well as high flexure forces directly to the connectors. Thus, in the current effort, in addition to the bar test, existing end-product connector tests were modifed to determine the degradation if any, of aged, encapsulated modular connectors.

Using modular connectors, spliced with 19 AWG insulated DEPIC conductors, single insulated conductors are pulled out per a modification of the procedure in AT&T's document "Product Criteria for Communications Cable Wire Joining Systems". The force to pull conductors out of the connectors was measured with a tensile testing machine at 2 in/min. at room temperature after 0, 15 and 31 days for specimens encapsulated and aged at room temperature and at 40 and 60°C. Modular connectors manufactured by AT&T Technologies and coded 710 SB1-25 were used. Data for D encapsulant, D1000 encapsulant and a nonencapsulated control are reported in Table III. Theoretically, values corresponding to the strength at break for insulated 19 AWG wire (37.5 lbs) would indicate no degradation of the connectors. Since the wires broke in our tests, rather than pulling out, encapsulation does not significantly affect the strength of the wire joint.

TABLE III

Conductor Pullout Data for Encapsulated, 25 Pair Modular Connectors[a]

| | Aging Time, Days | Pullout Force, lbs[b,c] | | |
|---|---|---|---|---|
| | | 23°C | 40°C | 60°C |
| Control (not encapsulated) | 0 | 37.5 | -- | -- |
| | 15 | 37.5 | 37.5 | 37.5 |
| | 31 | 37.5 | 37.5 | 37.5 |
| D Encapsulant | 15 | 35.3 | 35.3 | 35.3 |
| | 31 | 35.3 | 35.3 | 35.3 |
| D1000 Encapsulant | 15 | 35.3 | 37.5 | 37.5 |
| | 31 | 35.3 | 37.5 | 35.3 |

[a]AT&T Technologies, 710 SB1-25 modular connector.

[b]Average of 4 samples.

[c]The theoretical value should be the tensile force at break for the insulated wire, 37.5 lb.

The other test, also conducted to failure, is a flexure test following the procedure outlined in ASTM D 790. The connectors were prepared and tested following the procedure and schedule outlined above and tested on a tensile machine at a crosshead speed of 2 in/ min. The data in Table IV show a reduction in the flexure force on aging at 60°C for connectors encapsulated with D and D1000 encapsulant. However, the residual flexure force is sufficient to allow reentry of encapsulated splices.

TABLE IV

Flexure Force to Failure of Encapsulated 25 Pair Modular Connector[a] After Aging at Various Temperatures

| | Aging Time, Days | Breaking Force, lbs[b] 23°C | 40°C | 60°C |
|---|---|---|---|---|
| Control (not encapsulated) | 0 | 136 | -- | -- |
| | 15 | 148 | 139 | 130 |
| | 31 | 130 | 130 | 119 |
| D Encapsulant | 15 | 125 | 112 | 92 |
| | 31 | 121 | 123 | 84 |
| D1000 Encapsulant | 15 | 141 | 123 | 70 |
| | 31 | 125 | 108 | 75 |

[a]AT&T Technologies, 710 SB1-25 modular connector.

[b]Average of 2 samples.

## Splice Simulation Test (SST)

Until now, the only method for evaluating encapsulant performance in a closure was to construct and test full-scale splices. Although valuable information regarding the electrical and mechanical performance of the encapsulant/closure system can be obtained in these tests, the number of experimental variables such as cable pair size, cable core preparation, splicing methods, closure construction methods, etc. make the procedure labor and time intensive - not suited for encapsulant development. To reduce the number of variables and the time required to obtain relevant data, a splice simulation test was devised.

With reference to Figure 1, it was decided that the simulation test would address the more difficult water entry problems, i.e., down the core and within the wire work due to oily interfaces and wedging, leading to insulation resistance failure and to encapsulant fracture at high water heads. The other modes, which are strongly coupled to closure design and are more easily blocked, were not simulated.

Water entry along the core assumes a poorly filled core and was simulated by using wire units pulled out of standard manufacture cables. An oily interface was made probable by not cleaning the insulated conductors. The conditions for wedging of water along the wire work were established by ensuring that the water head on the splice was not restricted and placing it within one inch of the modular splice connector.

Details regarding the materials and construction of SST units are included in Attachment B and in Figures 2 and 3. Briefly, the test cell contains a spliced 25 pair modular connector. The "splice" is surrounded by a liner and secured with cable ties. The splice assembly, along with a ground wire is placed inside a 2" diameter Plexiglas tube with conductors projecting out both ends (see Figure 2). The encapsulant is poured into the "splice" with the tube positioned vertically. Time is allowed for encapsulant to cure (2-3 days). Then, a cable pressure cap with a valve assembly is secured to one end of the test cell in order to apply a water head.

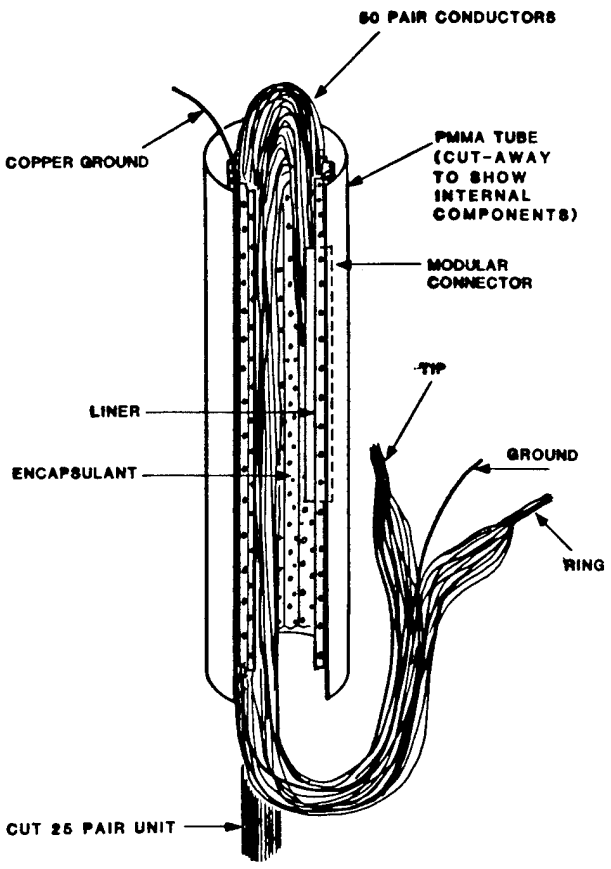



FIGURE 2. ENCAPSULANT TEST CELL

Finally, the SST is attached to a manifold system where water pressure is applied (see Figure 3).

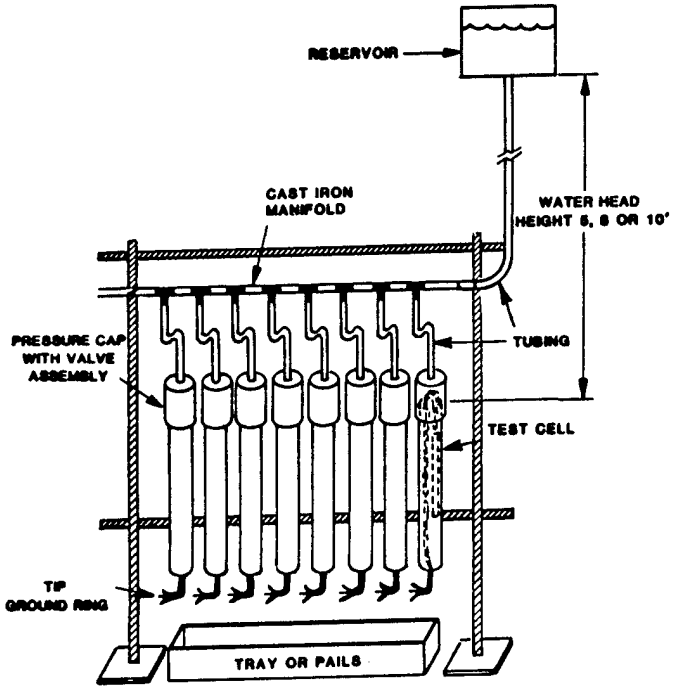



**FIGURE 3. BATTERY OF ENCAPSULANT TEST CELLS**

In carrying out the test, all tip and all ring conductors are twisted together. Failure was defined as insulation resistance (tip-ring, tip-ground, and ring-ground) readings of $< 10^9$ ohm/cm and/or leakage through the splice. Significantly, water has to travel only one inch along the wire work to reach a splice point and cause failure.

Having designed the splice simulation test, factors which impact on the performance of an encapsulant/closure system were investigated. These factors not only include material properties such as viscosity and gel time but closure considerations such as conductor density as well as external factors such as water head height. The following discussion illustrates selected SST data. These results and other data were used to develop the encapsulant reported in Appendix A.

## Effect of Conductor Density

One can readily postulate that as conductor density in a splice increases, encapsulation becomes more difficult. Material properties such as viscosity and gel time can be used to mitigate the problem as discussed below. Similarly, external factors such as encapsulant injection pressure, discussed by Angel et al.[4], can be used advantageously. In order to arrive to the conductor density in the SST design, several experiments were conducted as reported in Table V. The data show a high sensitivity to conductor density. As a result the SST conductor density was standardized to 50 pairs (100 wires, see Appendix B), which is allowed by features in the modular connector used.

TABLE V

SST Results - Effect of Conductor Density

| Encapsulant[b] | Height, Ft | Conductor | Number of Conductor Pairs | Days to Failure |
|---|---|---|---|---|
| F-1 | 8 | FG[a] | 5 | 70+[c] |
| F-1 | 8 | FG | 25 | 62 |
| F-1 | 8 | FG | 50 | 22 |

[a]FLEXGEL coated.

[b]Experimental formulations.

[c]Test terminated before failure occurred.

## Effect of Water Head

The ideal closure is one which can withstand any water head. Such a goal is not cost effective. SST data presented in Table VI show a strong dependence on water head. As a result, the standard SST water head is 10 feet (see Appendix B).

The enhanced performance of D1000 over D encapsulant is apparent. Significantly, the use of aircore conductors show only a slight improvement and suggest that benefits derived from solvent cleaning of conductors prior to encapsulation will be similarly slight.

TABLE VI

SST Results - Effect of Water Head

| Encapsulant | Conductor | Water Head, Ft. 5 | 8 | 10 |
|---|---|---|---|---|
| | | Days to Failure | | |
| D | FG[a] | 2 | -- | -- |
| D | AC[b] | 180+[c] | 4 | -- |
| F[d] | FG | 42 | 4 | -- |
| F-1[d] | FG | 121 | 22 | -- |
| N-6XL[d] | FG | 59 | 14 | -- |
| D-1[d] | FG | -- | 303 | 6 |
| D1000 | FG | -- | 325+ | 282+ |

[a]FLEXGEL coated.

[b]Aircore cable.

[c]Test terminated before failure occurred.

[d]Experimental formulations.

## Effect of Connector

As indicated in the introduction, filled connectors have been used in the filled cable applications. The experimental data presented in Table VII show no clear advantage of filled over aircore connectors. As a result, the standard SST connector is an aircore modular connector (see Appendix B).

TABLE VII

SST Results - Effect of Connector Type

| Encapsulant | Conductor[a] | Water Head, Ft | Modular Aircore Connector Days to Failure | Modular Filled Connector Days to Failure |
|---|---|---|---|---|
| D | FG | 5 | 2 | 3 |
| D | AC | 8 | 180+[b] | 149+ |
| F-17B[c] | FG | 8 | 151+ | 151+ |

[a]FG - FLEXGEL coated, AC - aircore.

[b]Test terminated before failure occurred.

[c]Experimental formulation.

## Effect of Encapsulant Gel Time

Penetration of an encapsulant is strongly dependent on the conductor density of the splice. The encapsulant gel time is normally considered by the user as the time available for the encapsulant to penetrate the splice. The data in Table VIII show that an improvement in performance is possible by increasing the gel time but that more significant improvements can be realized by proper formulation of the encapsulant. This follows because the pot life of the encapsulant is not the gel time but a fraction of it. For example, the pot life could be the time the encapsulant viscosity after mixing increases to 3000 cps. The assumption being that at higher viscosities the degree of penetration in the splice area is significantly reduced. Among other factors which are important is the viscosity-time profile as the encapsulant gels.

TABLE VIII

SST Results - Effect of Catalysis

| Encapsulant | Water Head, Ft | Conductors | 30-60 Min. Gel Time Days to Failure | 17 Hours Gel Time Days to Failure |
|---|---|---|---|---|
| D | 5 | FG[a] | 2 | 6 |
| F[b] | 8 | FG | 4 | 143 |
| F-1[b] | 8 | FG | 22 | 190+[c] |

[a]FLEXGEL coated.

[b]Experimental formulation.

[c]Test terminated before failure occurred.

## Effects of Encapsulant Viscosity

The viscosity of an encapsulant is dependent on its composition. Composition can have a strong influence on performance. To separate the effect of viscosity and composition, an experiment was designed in which the encapsulant was mixed and held until the viscosity increased to a specified level and then poured. By partially precuring the encapsulant, the pot life is significantly reduced. This corresponds to the performance of an encapsulant packaged in a dark container and left in the noonday sun prior to mixing. SST results are reported in Table IX. The implications are clear to the formulator and to the user. The viscosity must be controlled to insure a satisfactory pot life at temperatures encountered in the field. Improper use can defeat the best formulation.

TABLE IX

SST Results - Effect of Encapsulant Viscosity

| Encapsulant[a] | Water Head, Ft | Conductor | Viscosity, cps ~ 1000 Days to Failure | Viscosity, cps ~ 4000 Days to Failure |
|---|---|---|---|---|
| F[c] | 5 | FG[b] | 40 | 3 |
| F-1[c] | 5 | FG | 121 | 1 |

[a]Formulas gel in approximately 30-60 min.

[b]FLEXGEL coated.

[c]Experimental formulation.

## Effect of Filling Compounds

Telecommunication filled cable suppliers use a multitude of filling compounds - primarily oils gelled with microcrystalline waxes (petrolatum) or styrene block copolymers (FLEXGEL) in combination with polyolefins and variations thereof. The development of an encapsulant compatible with this variety of filling compounds constituted the biggest challenge in this development as shown by SST data in Table X. The performance of the D1000 encapsulant after 200+ days under a 10 foot head of water is not sensitive to whether the conductor is aircore or petrolatum or FLEXGEL coated. These results are a significant improvement over D encapsulant.

TABLE X

SST Results - Effect of Cable Filling Compound

| Encapsulant | Water Head, Ft | Days to Failure PJ[a] | FG[b] | AC[c] |
|---|---|---|---|---|
| D | 5 | <<1 | 2 | 180+[d] |
| F[e] | 5 | <<1 | 42 | -- |
| F-1[e] | 8 | <<1 | 22 | 190+ |
| D1000 | 10 | 228+ | 282+ | 303+ |

[a]Petrolatum coated conductors.

[b]FLEXGEL coated conductors.

[c]Aircore conductors.

[d]Test terminated before failure occured.

[e]Experimental formulations.

## Conclusion

Encapsulated splice closures are widely used to protect a splice from water entry. Failure modes have been briefly reviewed. Assuming water entry down the cable core, closure failures due to oily interphases and wedging have been identified as being strongly encapsulant dependent. A splice simulation test has been developed which assumes that a water head acts directly on the splice. In this worst case situation, variables such as cable filling compounds, splice wire work density, connectors, water head, and encapsulant gel time and viscosity have been investigated. Data have been presented on how these factors influence performance. The result is that a new encapsulant has been formulated which exhibits significant improvements in performance over other commercial encapsulants.

## Acknowledgement

The authors wish to express sincere appreciation to their colleagues at AT&T Bell Laboratories and AT&T Technologies for their support and help. In particular, we wish to express our thanks to D. M. Mitchell and D. W. Lemke for their help in devising and carrying out the splice simulation test.

## References

1. Dean, N. S., "The Development of Fully Filled Cables for the Telephone Distribution Network," Seventeenth International Wire and Cable Symposium, Proceedings, December 1968.

2. Biskeborn, M. C., and Dobbin, D. P., "Waterproof Plastic Insulated Multipair Telephone Cable," Seventeenth International Wire and Cable Symposium, Proceedings, December, 1968.

3. Brauer, M., and Sabia, R., "Design Considerations, Chemistry and Performance of a Reenterable Polyurethane Encapsulant," Twenty-Fourth International Wire and Cable Symposium, Proceedings, 1975.

4. Angel, C. E., Mullin, F. J. and Reed, W. C., "A Forced Encapsulation System for Splice Closures," Paper to be presented at the Thirty-Fourth International Wire and Cable Symposium, Cherry Hill, New Jersey, 1985.

5. Bellcore CA08735 D Encapsulant Specification, Issue 1.

6. Bell System Technical Reference, PUB 55004, Issue 1., "Waterproof Splice Closures" 1981.

7. Mitchell, D. M., and Sabia, R., "Development, Characterization, and Performance of an Improved Cable Filling Compound," Twenty-Ninth International Wire and Cable Symposium, Proceedings, 1980.

8. McCann, J. P., Sabia, R., and Wargotz, B., "Characterization of Filler and Insulation in Waterproof Cable," Eighteenth Wire and Cable Symposium, Proceedings, 1969.

ATTACHMENT A

D1000 Encapsulant Test Results
Based on Bellcore CA08735 Encapsulant Specification

CHEMICAL REQUIREMENTS:

| Chemical Property | Requirement | D1000 Encapsulant Results |
|---|---|---|
| 1. Isocyanate Content | 6.5 - 8% NCO | * 7.3% |

PHYSICAL REQUIREMENTS:

| Physical Property | Requirement | D1000 Encapsulant Results |
|---|---|---|
| 1. Corrosion of Copper | Noncorrosive to copper | * Noncorrosive, no visual change observed |
| | | * $1.04 \times 10^{10}$ ohms after 4 hours |
| 2. Hydrolytic Stability | Specimen shall not disintegrate, noticeably swell, or revert to a liquid. The weight shall not change by -10%, +5% | * 0.85% loss |
| | | * no visual changes |
| | | * tack free |
| 3. Peak exotherm | 120°F | * 10°F rise from 75°F |
| 4. Water Absorption | Weight increase after 7 days in 75 ± 2°F distilled water. Average of two specimens, shall be 0.8% maximum | * 0.05% |
| 5. Dry Heat Aging & Weight Loss | Specimens shall not char or revert to a liquid 4% maximum loss at 212°F. | * 1.50% gain |
| 6. Fungi Resistance | "0" rating: No growth permitted | * No growth observed |
| 7. Gel Time[1] | 25 ± 10 minutes at 75°F, | * 55 ± 10 minutes at 75°F |
| | 110 ± 15 minutes at 40°F | * 150 ± 15 minutes at 40°F |
| 8. Volumetric Expansion | Change not to exceed +2% | * No change (<0.2% observed) |
| 9. Stress Cracking of Polyethylene | Only 2 specimens can fail | * No failures observed |
| 10. Viscosity,[1] cps | | |
| a) prepolymer: | 1500 max. at 40°F | * 6,100 cps (0.3 rpm, #18 spindle @ 38°F) |
| b) polyol: | 1500 max. at 40°F | * 3,900 cps (0.3 rpm, #18 spindle @ 38°F) |
| 11. Tensile Strength | 6-30 psi | * 27.3 psi |
| 12. Elongation | 50% min. 250% max. | * 92% |
| 13. Tear Strength | | |
| a) at 25°C | 6.0 lbs/in max. 3.0 lbs/in min. | * 4.2 lbs/in |
| b) at -18°C | 10.0 lbs/in max. | * 9.0 lbs/in |
| c) after dry heat aging, at 25°C | 6.0 lbs/in max. 3.0 lbs/in min. | * 2.4 lbs/in |
| 14. Stress Cracking of Polycarbonate | No stress cracking by mixed material during or subsequent to cure | * No effect |

[1]As indicated in the text, an increase in value was necessary to attain improved closure performance.

[2]See CA08735 Specification.

Physical Requirements cont'd:

| Physical Property | Requirement | D1000 Encapsulant Results |
|---|---|---|
| 15. Water Sensitivity | Change not to exceed, 2% | * No shrinkage or expansion observed |
| 16. Pour point | | |
| a) prepolymer: | -5°F max. | * <-5°F |
| b) polyol | -5°F max. | * -27°F |
| 17. Compatibility | See Par. 6.09[2] | * Compatible, good adhesion |
| 18. Shelf life | See Par. 6.10[2] | * After 12 weeks at 60°C the components and mix viscosities as well as the gel time did change significantly. It is assumed that all other properties also did not change significantly. |
| 19. Colors | See Par. 6.11[2] | * Clear solution when mixed |
| 20. Bond to liner | See Par. 6.12[2] | * 100% adhesion |
| 21. Bond to DR tape | See Par. 6.13[2] | * 100% adhesion |
| 22. Odor | Essentially odorless | * Essentially odorless |
| 23. Phase stability | See Par. 6.15[2] | * No striations, clear |
| 24. Coated Conductor Pull-Out Test | | |
| a) Flexgel | Min. 0.5 kg | * 5.1 kg |
| b) petrolatum | Min. 0.5 kg | * 1.8 kg |
| 25. Liquid Compatibility | See Par. 6.17[2] | * Complete bonding, no adverse effects observed |

ELECTRICAL DATA:

| Electrical Property | Requirement | D1000 Encapsulant Results |
|---|---|---|
| 1. Insulation Resistance | | |
| mixed, cured encapsulant | $1 \times 10^{10}$ ohms minimum after 28 days | * $3.5 \times 10^{10}$ ohms |

ATTACHMENT B

Assembly and Encapsulation Procedure

Note - Refer to Figure 2 for reference.

1. Remove a 25 pair unit from the test cable and remove binder ties.

2. Splice 50 conductors to the 25 pair modular connector so that 25 pairs exit on the index strip side and 25 pairs exit on the cap side. Adhere to the color code. The bridge module is not used in this test.

3. Dress the conductors to one end of the connector as is done in normal practice. Two inches after the end of the connector, bend the 25 pair units back over themselves forming a two inch loop.

4. Place a bare copper ground wire along the conductors with the end 2 inches longer than the end of the loop.

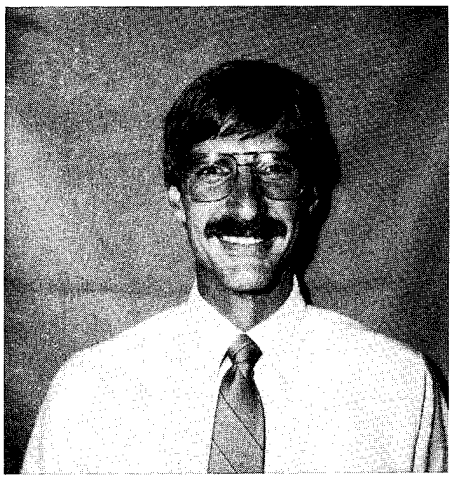
5. Wrap the liner around the splice with the 2 inch loop of conductors and 4 inch ground wire projecting out of one end. The loop end of the modular connector should be 0.5 inches inside the end of the liner. Secure the liner with the three cable ties; one at each end and one in the middle.

6. Insert the wrapped splice into 2 inch I.D. Plexiglas tube (14 inches long), and position the loop end of the liner 0.5 inches from the end of the tube. At this position, the loop end of the modular connector should be 1 inch inside the top of the tube.

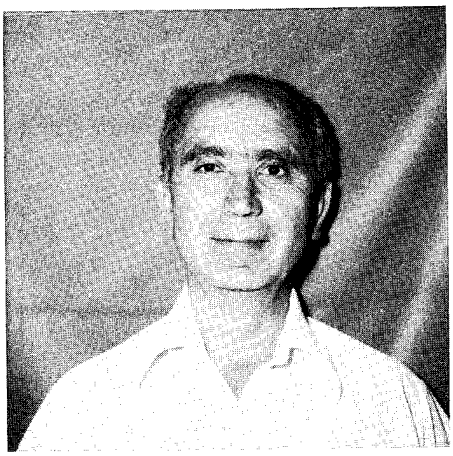
7. Identify one of the two 25 pair units extending out of the tube. Cut it off 3-4 inches from the end of the tube and secure the conductors with a cable tie. Make sure that when the end is cut the conductor ends are "cleared", that is, there are no contacts between conductors. On the remaining unit, separate and strip the tip and ring conductors and twist the stripped ends together. Secure the ground wire and conductors with two cable ties.

8. A seal is made in the bottom of the tube (with encapsulant), and after it has cured, the tube is filled with encapsulant with the tube positioned vertically.

9. After the encapsulant has cured, a pressure cap with valve assembly is attached to the tube and attached to the manifold for testing (see Figure 3).



J. Thomas Chapin, a graduate of the University of Connecticut Institute of Materials Science (B.S. Chemistry, Ph.D. Polymer Chemistry), was employed by the Polymer Chemical Division of the Upjohn Company prior to joining the Transmission Media Laboratory of AT&T Bell Laboratories in 1980. Since 1980 he has been active in the research and development of materials for application in telecommunications.



Raffaele Sabia, a graduate of St. Francis College of Brooklyn (B.S.) and Polytechnic Institute of Brooklyn (Ph.D.), was employed by the Polymer Chemical Division of W. R. Grace prior to joining AT&T Bell Laboratories in 1963. Since 1963 he has been active in the research and development of materials for application in the wire and cable area. Since 1967 he has been supervisor of the Chemical Engineering Group in the Transmission Media Laboratory.

# Authors Index


Akasaka, N. ..... 28
Allen, D. B. ..... 250
Andersen, O. R. ..... 138
Anderson, J. M. ..... 286
Anelli, P. ..... 107
Angel, C. E. ..... 407
Aoki, T. ..... 28
Arakawa, K. ..... 119
Ayre, R. W. A. ..... 385
Bakhru, P. U. ..... 61, 173
Barnes, S. R. ..... 102
Benjamin, A. ..... 241
Blum, K. P. ..... 305
Bostrom, D. O. ..... 97
Bow, K. E. ..... 51, 61, 173
Brinkmeyer, E. ..... 125
Bury, J. R. ..... 38
Cannon, T. C. ..... 393
Cassidy, S. A. ..... 342
Chamberlain, J. ..... 88
Chapin, J. T. ..... 418
Charlebois, L. J. ..... 260
Chu, Tek-Che ..... 346
Clarke, F. B. ..... 241
Clarke, T. ..... 88
Daniels, A. J. ..... 150
Darden, B. V. ..... 286
Davies, S. T. ..... 255
Dawes, K. ..... 402
Dazai, M. ..... 16
de Boer, B. T. ..... 385
Eichhorn, R. M. ..... 213
Emig, K. A. ..... 97
Esposto, F. ..... 107
Fischer, D. ..... 173
Fuse, K. ..... 33
Garg, A. ..... 135
Gartside, C. H., III ..... 21
Gläsel, W. ..... 332
Grasso, G. ..... 107
Gregor, P. ..... 332
Grimado, P. B. ..... 320
Grosser, B. K. ..... 51
Grune, G. L. ..... 187
Gyger, A. ..... 300
Haag, H. G. ..... 332, 355
Hackert, M. J. ..... 293
Hafemeister, K. ..... 135
Hagans, P. L. ..... 61
Hale, P. G. ..... 9
Haltiwanger, W. ..... 142
Hamaguchi, M. ..... 16
Hardwick, N. E., III ..... 255
Hasegawa, M. ..... 220
Hasegawa, S. ..... 233
Hatton, W. H. ..... 142
Heacock, J. F. ..... 44
Heckmann, S. ..... 125
Hellmann, B. ..... 135
Hiramatsu, H. ..... 92
Hög, G. F. ..... 332, 355
Hoejergaard, P. ..... 138
Holden, G. ..... 364
Horima, H. ..... 16, 233
Hornung, E. ..... 138
Hornung, P. ..... 138
Hornung, S. ..... 102, 342
Horton, J. L. ..... 260
Hughes, R. ..... 397
Ieshige, M. ..... 92
Ishikawa, T. ..... 227
Jenkins, A. C. ..... 82
Joiner, D. A. ..... 38
Kajiwara, M. ..... 33
Kakii, T. ..... 275, 313
Kalomiris, V. E. ..... 286
Kamata, Y. ..... 92, 267
Katayose, H. ..... 1
Kikuchi, T. ..... 76
Kincaid, J. W., Jr. ..... 162
Kitayama, Y. ..... 313
Knoechel, R. ..... 125
Konno, T. ..... 233
Kopish, W. J. ..... 250
Krabec, J. A. ..... 162
Kurosawa, A. ..... 233
LeFevre, B. G. ..... 286
Lovelace, C. R. ..... 82
Marra, L. J. ..... 346
Mathuda, T. ..... 220
Matsumura, Y. ..... 76
McNeal, T. E. ..... 402
Miller, I. H. ..... 260
Miura, K. ..... 33
Miyajima, Y. ..... 92
Mochizuki, S. ..... 119
Modaris, R. A. ..... 97
Modone, E. ..... 107
Mogensen, G. ..... 138
Mullin, F. J. ..... 407
Murayama, M. ..... 220
Nakai, S. ..... 267
Nakano, K. ..... 227
Nükura, K. ..... 233
Nishimura, M. ..... 142
Obara, Y. ..... 267
Oda, M. ..... 92
Ogai, M. ..... 92
Ohno, R. ..... 76
Ohsugi, T. ..... 313
Ohtake, Y. ..... 267
Palmer, C. D. ..... 250
Patel, P. D. ..... 21
Pickering, J. J. ..... 213
Pikula, D. G. ..... 51
Pitt, N. J. ..... 102

Ponder, C. W. ..... 305
Punderson, J. O. ..... 44
Ramsay, M. M. ..... 9
Reed, W. C. ..... 407
Reeve, M. H. ..... 342
Reilly, J. W. ..... 364
Reynolds, M. R. ..... 82
Riley, E. W. ..... 97
Robbins, C. H. ..... 370
Rybach, J. ..... 125
Sabia, R. ..... 418
Saikkonen, S. L. ..... 293
Sakasai, M. ..... 227
Sato, N. ..... 1, 227
Schrom, E. ..... 173
Schuster, R. B. ..... 385
Scott, J. R. ..... 260
Seto, K. ..... 1
Seto, M. ..... 33
Shadoff, L. ..... 61
Shingo, Y. ..... 220
Sicotti, J. R. ..... 97
Smith, D. T. ..... 393
So, V. ..... 397
Sordo, B. ..... 107
Stix, R. K. ..... 346
Suetsugu, Y. ..... 275
Sugawara, K. ..... 233
Sugawara, Y. ..... 1
Sutehall, R. ..... 9
Suzuki, F. ..... 28
Suzuki, H. ..... 227
Tabata, Y. ..... 233
Tachigami, S. ..... 267
Talarico, T. L. ..... 187
Tanaka, S. ..... 275
Vella, P. J. ..... 397
Williams, D. W. ..... 97
Yamada, Y. ..... 233
Yamamoto, S. ..... 33
Yamanouchi, I. ..... 379
Yamazaki, T. ..... 313
Yashiro, T. ..... 119
Yennadhiou, P. ..... 342
Yokosuka, H. ..... 1
Yoshikawa, S. ..... 220
Yoshino, A. ..... 220
Yuguchi, R. ..... 267
Zamzow, P. E. ..... 355




# International Wire & Cable Symposium

**SPONSORED BY U.S. ARMY COMMUNICATIONS-ELECTRONICS COMMAND (CECOM)**
**FORT MONMOUTH, NEW JERSEY**
**18, 19 and 20 November 1986**
**MGM GRAND HOTEL, RENO, NEVADA**

Please provide in the space below a 100-500 word abstract (25 copies) of proposed technical paper on such subjects as design, application, materials, and manufacturing of communications and electronics wire and cable of interest to the commercial and military electronics industries. Such offers should be submitted no later than 7 April 1986 to the Headquarters, US Army Communications-Electronics Command, ATTN: AMSEL-COM-D-4, Fort Monmouth, New Jersey 07703-5202.

TITLE:_____

AUTHORS:_____

COMPANY:_____

ADDRESS:_____

Staple

Fold here

Stamp

Commander
US Army Communications-Electronics Command
ATTN: AMSEL-COM-D-4
Fort Monmouth, NJ 07703-5202

Fold here